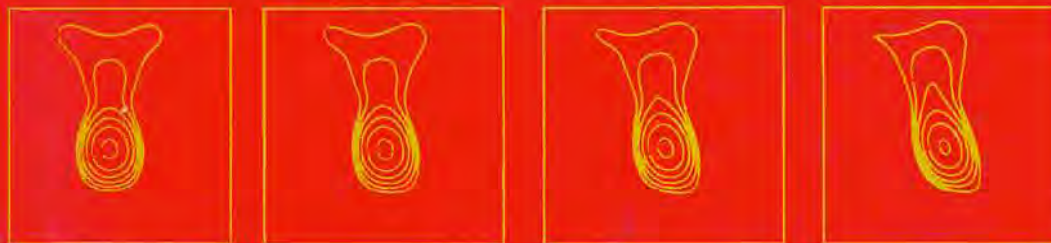
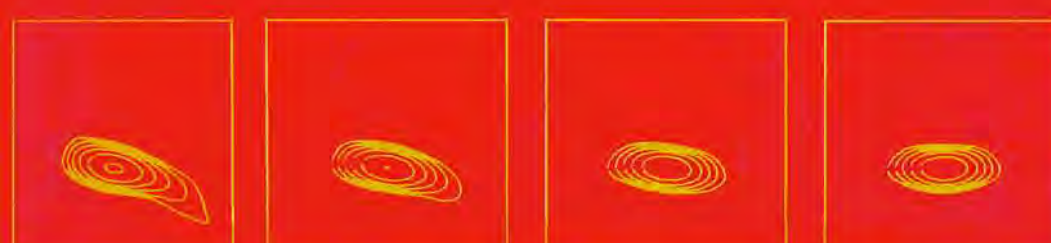
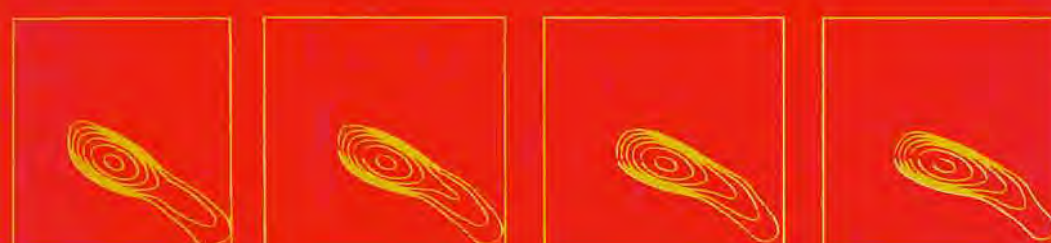


H.-J. Bunge



Texture Analysis in Materials Science

Mathematical Methods



Texture Analysis in Materials Science

Mathematical Methods

Professor Dr H.-J. Bunge

Institut für Metallkunde und Metalphysik, Technische Universität Clausthal

Translated by

Dr Peter R. Morris

Principal Research Physicist, Armco Inc., Middletown, Ohio, USA

In a polycrystalline material such as a metal or ceramic the orientations of the crystal axes in the different grains are often distributed randomly, so that the material as a whole behaves in an isotropic manner. In some cases, however, the individual grain orientations may be grouped closely around a mean value throughout or in parts of a processed material, and as a result anisotropy in mechanical and physical properties is developed. Such preferred orientations or textures are developed by the deformation and the recrystallization of materials, as in the production of wire or sheet in cubic metals, and are dependent on the type of deformation, the crystal structure and the presence of alloying additions in solution.

The development of texture, and thus anisotropy, may be maximized under control for such purposes as directional magnetic properties (as in 3% silicon-iron for transformers) and for drawability (as in sheet low-carbon steel) where strength in the through-thickness direction should be high as compared to that in the plane of the sheet. It is clear, therefore, that the analysis and control of texture in fabricated polycrystalline materials is a very important scientific aspect of the fabrication technology. There are several ways of describing preferred orientation in a material, and modern computational facilities have made it possible to utilize crystallographic data with mathematical methods to improve the quantitative concepts and definition of the phenomenon in the orientation distribution function (ODF). Professor Bunge's work covers this area of texture data calculation and interpretation for a wide range of materials and affected properties.

Texture Analysis in Materials Science, which in its first edition was available only in German, has been revised thoroughly and updated for the English translation.

Contents:

Introduction • Orientation of Individual Crystallite • Orientation Distributions • Expansion of Orientation Distribution Functions • Fibre Textures • Methods not Based on the Series Expansion • Special Distribution Functions • Texture Transformation • A System of Programs for the Texture Analysis of Sheets of Cubic Materials • Estimation of the Errors • Some Results of Texture Analysis • Orientation Distribution Functions of Other Structural Elements • Physical Properties of Polycrystalline Materials • Mathematical Aids • Numerical Tables • Graphic Representations • References • Index • Appendixes

Texture Analysis in Materials Science

Mathematical Methods

Professor Dr H.-J. Bunge

Institut für Metallkunde und Metallphysik, Technische Universität Clausthal

Translated by

Dr Peter R. Morris

Principal Research Physicist, Armco Inc., Middletown, Ohio, USA

Preface

This book is the revised and extended English version of *Mathematische Methoden der Texturanalyse* published in the former German Democratic Republic by Akademie-Verlag, Berlin, in 1969.

English edition first published in 1982
by Butterworth & Co (Publishers)
ISBN 0-408-10642-5

Paperback Reprint

© CUVILLIER VERLAG, Göttingen 1993
ISBN 3-928815-81-4

Digital Edition

© Helga and Hans-Peter Bunge, Wolfratshausen 2015
This digital edition is free for non-commercial use.

All rights reserved. No part of this publication may be reproduced or transmitted in any form or by any means, including photocopying and recording, without the written permission of the copyright holders. Such written permission must also be obtained before any part of this publication is stored in a retrieval system of any nature.

By application of counting techniques it is possible to obtain quantitative information about the orientation distribution of crystallites in polycrystalline materials. This has created a need for the mathematical treatment of the orientation distribution function, and the relationships between various functions, such as pole figures, inverse pole figures, three-dimensional orientation distribution functions and directionally dependent physical properties. In the present book an effort will be made to give a unified presentation of these relationships. It is shown that the representation of the orientation distribution function as a series expansion is a very useful aid for its numerical calculation. The relations between the single crystal properties and texture and the corresponding polycrystal properties also follow particularly simply and logically in this representation. For these reasons I have restricted myself almost exclusively to this form of representation.

Textures have been studied chiefly in metallic materials. They are in principle of importance, not only for these, but also for all polycrystalline materials. The relationships between the various orientation distribution functions and the methods of their treatment are largely independent of the particular material. They are therefore applicable to ceramic materials or partially crystalline synthetics in a manner completely analogous with that for metals.

This book is intended for those who are concerned with the orientation distribution of crystallites. It seeks to provide some mathematical aids for the quantitative treatment of such problems.

At this point I should like to express my sincere thanks to several of my colleagues for their support during, writing and correction of the manuscript. Professor BOLL-DORNBURGER has undertaken a critical review of the manuscript. Dr H. SCHMITTLER displayed particular interest in the writing of the book. She has contributed many valuable suggestions in numerous discussions during drafting of the manuscript and has called my attention to a number of errors. She has very intensively examined the manuscript and corrections. I should also like to thank Mr J. TOBISCH and Mrs U. SCHLÄFER for their help with the corrections.

HANS-JOACHIM BUNGE

Preface to the English Edition

Since the first appearance of this book in 1969 quantitative texture analysis has developed very rapidly. Since large enough computers have become easily accessible in recent years, the calculation of the orientation distribution function (ODF) from experimentally determined pole figures or even incomplete (back-reflection) pole figures can be regarded as a routine procedure which is carried out by available computer programs. The user of this method does not need to be concerned with the mathematics involved. Several brief reviews directed mainly towards the practical use of the ODF method are available^{51,52,57,59,62–64,171,233,236}.

The result obtained, the ODF, is much easier to interpret because it is an unambiguous representation of the texture data compared with pole figures which cannot distinguish by themselves between crystal orientations rotated about the normal of the reflecting lattice plane. Thus, in recent years a large number of texture investigations have been presented in the form of ODF, while in the first edition of this book reference could be made only to a very small number of actual numerical calculations. Chapter 11, dealing with some results of texture analysis, has therefore been completely rewritten. Changes have also been made in Section 2.1, which describes the various orientation parameters used by different authors and the relations between them.

Only very recently have the implications of the centre of inversion as a symmetry element been considered in greater detail. This has led to extending the considerations to polycrystalline materials containing right- and left-handed crystals which must thus be looked at as being two-phase materials which are to be described by two independent texture functions. The description of the sample symmetries thus requires black–white point groups instead of the ordinary ones. Also, in many cases the odd terms of the series expansion have to be taken into account. These problems have been considered in the additional Sections 4.11 for general textures and 5.10 for fibre textures. The implications of the odd part of the texture function have not yet been considered in most of the numerical calculations carried out thus far, but this particular aspect of ODF analysis is in a very effervescent state of development at present.

The concept of the texture transformation by means of an orientation relation function had been treated among other problems in the first edition, Section 10.1, in connection with the development of recrystallization textures from deformation textures. However, exactly the same formalism holds also for phase transformation if the product crystals have the same symmetry as the parent crystals, as

is the case, for example, in the $\gamma \rightarrow \alpha$ transformation in steels or the $\alpha \rightarrow \beta$ transformation in brasses. Because of its great importance in texture formation a special chapter has been devoted to texture transformation (Chapter 8), including also the general case of change of crystal symmetry.

In the first edition, Section 4.9, a system of ALGOL programs was mentioned by which ODF of cubic-orthorhombic symmetry had been calculated. These programs have been used for quite a number of ODF calculations but they have not been published in detail. On the basis of these programs, however, a set of FORTRAN programs has been developed which have been published in the full text.¹⁷¹ In Chapter 9 we therefore give these FORTRAN programs along with the library program by WAGNER, ESLING and BARO.²⁹²

Although a comprehensive error analysis of the mathematical procedure leading from pole figures with their experimental errors to ODF has not yet been developed, a number of different error estimations have been used. Some of them have been described in reference I, Chapter 7, along with the experimental examples. With increasing experimental accuracy, e.g. by the application of neutron diffraction, and with increasing demand for ODF's as accurate as possible, the error analysis becomes more and more important. Hence, a special section was devoted to the estimate of errors. In Chapter 13, dealing with the anisotropy of physical properties, some additions have been made, especially with respect to the plastic properties. In Chapter 14 on mathematical aids the sign convention of the associated LEGENDRE functions has been changed with respect to that used in reference I. Furthermore, Section 14.3 has been changed according to the FOURIER coefficients Q_l^{ms} , which seem to be the most economic way of representing the generalized spherical harmonics.

Finally, Chapter 15, the numerical tables, and Appendix A.4, the graphic representations, have been changed. The coefficients Q_l^{mn} and $B_l^{m\mu}$ are the fundamental quantities by which all the other quantities can easily be expressed. Tables of these quantities have therefore been given up to $l = 34$, which is assumed to be a reasonable upper limit for practical texture calculations. (The value $L = 100$ as given in some of the tables in reference I seems much too high compared with the experimental accuracy and the obtainable resolving power.) Tables of the deduced quantities are given only up to an l of much lower degree, just for checking purposes, since it is assumed that these quantities will never be used as primary data. The Q_l^{ms} and $B_l^{m\mu}$ of Tables 15.1.1 and 15.2.1 might be used as primary data for texture calculations (although it is recommendable to produce them by the library program inside the computer). The numerical tables have been calculated by Dr C. ESLING and Mme Ing. E. BECHLER, Metz. The computations were carried out in the computer centre IRSID, Maizières-les-Metz under the supervision of Mr J. C. FILLER, whose helpful support is gratefully acknowledged. The tables have been recalculated from the very beginning without making use of any primary numerical data. The tables given are photoreproductions of the computer outputs so that typing errors as they occurred in the hand-set tables in reference I have been avoided.

The main part of the book, Chapters 4 and 5, remained nearly unchanged. It should be mentioned that in equations (2.17) and (2.20) in reference I a symmetry assumption according to the cubic symmetry was made which is not correct for the lower symmetries. Thus, in equation (4.35) in the case of lower symmetries the complex conjugate notation is required. I am very much indebted to Dr C. ESLING for making me aware of this error. He also read carefully the whole manuscript and drew my attention to several mistakes. In numerous valuable discussions he contributed much to the finishing of the book.

I also wish to express my gratitude to P. R. MORRIS. He not only carried out the laborious task of the translation, but also as an experienced worker in ODF analysis made many valuable comments on the contents, especially Section 4.10, the comparison between the two notations used in the series expansion method.

Finally, I should like to acknowledge many helpful discussions with Dr J. POSPIECH, who especially contributed to the methods of numerical calculations and provided the numerical example given in Section 9.6.

Contents

List of Symbols Used	xv
1. Introduction	1
2. Orientation of Individual Crystallites	3
2.1. Various Representations of a Rotation	3
2.1.1. EULERIAN Angles	4
2.1.2. Rotation Axis and Rotation Angle	8
2.1.3. Crystal Direction and Angle	10
2.1.4. Sample Direction and Angle	10
2.1.5. Representation of the Orientation in the Pole Figure	14
2.1.6. Representation of the Orientation in the Inverse Pole Figure	15
2.1.7. Representation by MILLER Indices	15
2.1.8. Matrix Representation	16
2.1.9. Relations between Different Orientation Parameters	19
2.1.10. The Invariant Measure	31
2.2. Some Properties of Rotations	36
2.3. Ambiguity of Rotation as a Consequence of Crystal and Specimen Symmetry	36
2.4. Orientation Distance	38
2.5. Orientation for Rotational Symmetry	39
3. Orientation Distributions	42
4. Expansion of Orientation Distribution Functions in Series of Generalized Spherical Harmonics (Three-dimensional Textures)	47
4.1. Determination of the Coefficients $C_l^{\mu\nu}$	49
4.1.1. Individual Orientation Measurements	50
4.1.2. Interpolation of the Function $f(g)$	51
4.2. The General Axis Distribution Functions $A(\mathbf{h}, \mathbf{y})$	53
4.2.1. Determination of the Coefficients $C_l^{\mu\nu}$ by Interpolation of the General Axis Distribution Function	54
4.2.2. Pole Figures $P_{\mathbf{h}}(\mathbf{y})$	57
4.2.2.1. Determination of the Coefficients $C_l^{\mu\nu}$ from Pole Figures	61
4.2.2.2. Separation of Coincidences	63
4.2.2.3. Maximum Resolving Power	66
4.2.3. Inverse Pole Figures $R_{\mathbf{y}}(\mathbf{h})$	69
4.2.4. Comparison of the Representations of a Texture by Pole Figures and Inverse Pole Figures	71
4.3. The Angular Distribution Function $W_{\mathbf{h}\mathbf{y}}(\Theta)$	73

4.3.1. Integral Relation between Pole Figures and Inverse Pole Figures	76	5.10. The Role of the Centre of Inversion	142
4.3.1.1. The Method of HARRIS	77	5.10.1. Right- and Left-handed Crystals	142
4.4. Determination of the Coefficients $C_l^{\mu\nu}$ by the Method of Least Squares	78	5.10.2. Centrosymmetric Sample Symmetries	145
4.5. Measures of Accuracy	79	5.10.3. Centrosymmetric Crystal Symmetries	146
4.5.1. A Special Accuracy Measure for Pole Figures of Materials with Cubic Symmetry	80	5.10.4. Friedel's Law	146
4.5.2. A Method for the Adaption of Back-reflection and Transmission Range	82	5.10.5. Black—White Sample Symmetries	147
4.6. Truncation Error	82	5.10.6. Determination of the Odd Part of the Texture Function	152
4.6.1. Decrease of the Truncation Error by Smearing	84	6. Methods not Based on the Series Expansion	154
4.7. Determination of the Coefficients $C_l^{\mu\nu}$ from Incompletely Measured Pole Figures	85	6.1. The Method of PERLWITZ, LÜCKE and PITSCHE	154
4.8. Texture Index	88	6.2. The Method of JETTER, MC HARGUE and WILLIAMS	157
4.9. Ambiguity of the Solution	90	6.3. The Method of RUER and BARO	161
4.9.1. Non-random Textures with Random Pole Figures	91	6.4. The Method of IMHOF	167
4.9.2. The Refinement Procedure of KRIGBAUM	93	7. Special Distribution Functions	169
4.9.3. The Extremum Method of TAVARD	96	7.1. Ideal Orientations	169
4.10. Comparison with ROE's Terminology	97	7.2. Cone and Ring Fibre Textures	173
4.11. The Role of the Centre of Inversion	100	7.3. 'Spherical' Textures	176
4.11.1. Right- and Left-handed Crystals	100	7.4. Fibre Axes	176
4.11.2. Centrosymmetric Sample Symmetries	104	7.5. Line and Surface Textures (Dimension of a Texture)	178
4.11.3. Centrosymmetric Crystal Symmetries	105	7.6. Zero Regions	179
4.11.4. Friedel's Law	106	7.7. Gaussian Distributions	180
4.11.5. Black—White Sample Symmetries	107	7.8. Polynomial Approximation (Angular Resolving Power)	183
4.11.6. Determination of the Odd Part of the Texture Function	116	8. Texture Transformation	188
5. Fibre Textures	119	9. A System of Programs for the Texture Analysis of Sheets of Cubic Materials	194
5.1. Determination of the Coefficients C_l^{μ}	121	9.1. The Subroutines	195
5.1.1. Individual Orientation Measurements	121	9.2. The Mainline Programs	200
5.1.2. Interpolation of the Function $R(\mathbf{h})$	122	9.3. The Library Program	200
5.2. The General Axis Distribution Function $A(\mathbf{h}, \Phi)$	122	9.4. Calculation Times and Storage Requirements	204
5.2.1. Pole Figures $P_{\mathbf{h}}(\Phi)$	123	9.5. Supplementary Programs	204
5.2.1.1. Determination of the Coefficients C_l^{μ} from Pole Figures	124	9.6. A Numerical Example	205
5.2.1.2. Separation of Coincidences	125	9.7. Listings of the ODF and Library Programs	211
5.2.2. Inverse Pole Figures $R_{\Phi}(\mathbf{h})$	126	10. Estimation of the Errors	212
5.2.2.1. The Fundamental Equation for Fibre Textures	126	10.1. A Reliability Criterion for Pole Figures of Materials with Cubic Symmetry ..	213
5.2.2.2. The Method of HARRIS	127	10.2. The Error Curve $ \overline{\Delta F_l^{\mu} }$	214
5.3. Determination of the Coefficients C_l^{μ} According to the Least Squares Method ..	129	10.3. The Error Curve $ \overline{\Delta C_l^{\mu\nu} }$	217
5.4. Measures of Accuracy	130	10.4. Error Estimation According to the HARRIS Relation	218
5.4.1. A Special Measure of Accuracy for Pole Figures of Materials with Cubic Symmetry	131	10.5. Comparison of Experimental and Recalculated Pole Figures	218
5.5. Truncation Error	132	10.6. Negative Values	221
5.5.1. Decrease of the Truncation Error by Smearing	133	10.7. Estimation of the Truncation Error by Extrapolation	221
5.6. Determination of the Coefficients C_l^{μ} from Incompletely Measured Pole Figures	135	10.8. The Integration Error	222
5.7. Texture Index	137	10.9. The Statistical Error	224
5.8. The Approximation Condition for Fibre Textures	138	10.10. The Indetermination Error for Incomplete Pole Figures	225
5.9. Calculation of the Function $R(\Phi, \beta)$ for Various Crystal Symmetries	140	11. Some Results of Texture Analysis	226
5.9.1. Orthorhombic Symmetry	140	11.1. Three-dimensional Orientation Distribution Functions (ODF)	226
5.9.2. Cubic Symmetry	141	11.1.1. Determination of the Coefficients $C_l^{\mu\nu}$ from Individual Orientation Measurements	227

11.1.2.	The Rolling Textures of Face-centred Cubic Metals and Alloys	227
11.1.3.	The Theoretical Rolling Texture for $\{111\} \langle 110 \rangle$ Slip	240
11.1.4.	The Rolling Textures of Body-centred Cubic Metals	240
11.1.5.	Textures of Tubes	244
11.1.6.	Orthorhombic Crystal Symmetry	247
11.1.6.1.	The Rolling Texture of Uranium	247
11.1.6.2.	Biaxially Deformed Polyethylene (Separation of Partial Coincidences)	250
11.1.7.	Hexagonal Crystal Symmetry	251
11.1.8.	Trigonal Crystal Symmetry (Separation of Real Coincidences)	254
11.1.9.	Transformation Textures	258
11.1.9.1.	The Transformation Texture in Duplex $\alpha-\beta$ Brass	258
11.1.9.2.	Calculation of the Orientation Relation from Starting and Transformed Textures	258
11.1.9.3.	Calculation of the Initial Texture of a Steel (Austenite) from the Transformation Texture (Ferrite)	261
11.1.10.	Cubic-triclinic Symmetry	263
11.1.11.	Representation of the Orientation Distribution Function by Rotation Axis and Rotation Angle	264
11.2.	Fibre Textures	268
11.2.1.	The Drawing Texture of Aluminium Wires	268
11.2.2.	Transformation Texture in Au—Ge TAYLOR Wires	270
11.2.3.	Hexagonal Crystal Symmetry (Titanium)	272
11.2.4.	Orthorhombic Crystal Symmetry (Separation of Partial Coincidences)	272
11.2.5.	Triclinic Crystal Symmetry (Application of the Refinement Procedure)	274
11.2.6.	Orientation Distribution of the Number of Crystallites and the Mean Grain Size	274
11.2.7.	Shape of the Spread about Preferred Orientations	277
12.	Orientation Distribution Functions of Other Structural Elements	279
12.1.	Orientation Distribution Functions of the Grain Surfaces	279
12.1.1.	Orientation Distribution of the Crystallographic Planes in the Outer Surface of an Arbitrary Section	280
12.2.	Orientation Distribution Functions of the Grain Boundaries	281
12.2.1.	The Distribution Function $f(\Delta g)$ of the Orientation Differences	282
12.2.2.	The Distribution Function $\varphi(y)$ of the Grain Boundaries in the Sample Fixed Coordinate System	283
12.2.3.	The Distribution Function $\varphi'(h)$ of the Grain Boundaries in the Crystal Fixed Coordinate System	288
12.3.	Orientation Distribution Functions of the Grain Edges	290
12.3.1.	The Distribution Function $\psi(y)$ of the Grain Edges in the Sample Fixed Coordinate System	290
12.3.2.	The Distribution Function $\psi'(h)$ of the Grain Edges in the Crystal Fixed Coordinate System	292
13.	Physical Properties of Polycrystalline Materials	294
13.1.	Physical Properties of Single Crystals	294
13.1.1.	Representation by Tensors	295
13.1.2.	Representation by Surfaces	295

13.1.3.	Representation by Functions of the Orientation g	297
13.2.	The Problem of Averaging	299
13.3.	The Calculation of the Simple Mean Values \bar{E}	302
13.3.1.	Tensor Representation	302
13.3.2.	Surface Representation	303
13.3.2.1.	Rotationally Symmetric Properties	305
13.3.3.	Representation by Orientation Functions	306
13.4.	Average Values of Special Properties	308
13.4.1.	Magnetization Energy in a Homogeneous Magnetic Field	308
13.4.1.1.	Magnetization Energy of Cubic Crystals	308
13.4.1.2.	Magnetization Energy of Hexagonal Crystals	311
13.4.2.	The Remanence in Ferromagnetic Materials	313
13.4.3.	Tensor Properties of Second Order	316
13.4.3.1.	Thermal Expansion of Uranium	319
13.4.3.2.	Growth of Uranium During Neutron Irradiation	320
13.4.4.	Elastic Properties	321
13.4.4.1.	Cubic Crystal Symmetry	321
13.4.4.2.	Orthorhombic Crystal Symmetry	327
13.4.5.	Plastic Anisotropy	330
13.4.6.	The Reflectivity of Crystallites for X-rays	338
13.5.	Determination of the Texture Coefficients from Anisotropic Polycrystal Properties	340
13.6.	Determination of Single Crystal Properties from Polycrystal Measurements	342
13.7.	Textures With Equal Physical Properties	343
13.7.1.	Fibre Textures of Ferromagnetic Cubic Materials	344
13.7.2.	Magnetic Anisotropy of an Fe—Si Sheet	346
13.7.3.	Tensor Properties of Second Rank for Fibre Textures	346
13.8.	Physical Meaning of the Coefficients $C_l^{\mu\nu}$	348
14.	Mathematical Aids	351
14.1.	Generalized Spherical Harmonics	351
14.2.	Spherical Surface Harmonics	356
14.3.	FOURIER Expansion of the $P_l^{mn}(\Phi)$	359
14.4.	CLEBSCH—GORDAN Coefficients	362
14.5.	Symmetric Generalized Spherical Harmonics	363
14.5.1.	Transformation of the Coefficients $A_l^{\mu\nu}$	369
14.5.2.	The Fundamental Integral	371
14.5.3.	Convolution Integrals	373
14.6.	Symmetric Spherical Surface Harmonics	376
14.7.	The Symmetric Functions of the Various Symmetry Groups	378
14.7.1.	'Lower' Symmetry Groups (Non-cubic)	382
14.7.2.	'Higher' Symmetry Groups (Cubic)	384
14.7.2.1.	Tetrahedral Groups	385
14.7.2.2.	Octahedral Groups	385
14.7.3.	Subgroups	386
14.7.4.	Explicit Representation of Symmetric Generalized Spherical Harmonics	387
14.7.5.	Representation of the Cubic Spherical Surface Harmonics by Products of Powers of Cubic Polynomials	390

14.7.6. Space Groups in the EULER Space	392
14.7.7. Cubic Symmetry	395
14.8. CLEBSCH—GORDAN Coefficients for Symmetric Functions	401
15. Numerical Tables	404
References	405
Appendix 1 Tables 9.2—9.14	421
Appendix 2 Listings of the ODF and Library Programs	439
Appendix 3 Tables for Chapter 15	455
15.1. FOURIER Coefficients	456
15.1.1. Q_l^{mn}	456
15.1.2. a_l^{mns}	494
15.1.3. a_l^{ms}	498
15.2. Symmetry Coefficients $B_l^{m\mu}$	501
15.2.1. Cubic, Fourfold Axis	501
15.2.2. Cubic, Threefold Axis	505
15.2.3. Tetragonal, Orthogonal to Cubic	509
15.2.4. Cubic, ROE's Notation	615
15.3. Generalized LEGENDRE Functions $P_l^{mn}(\Phi)$	519
15.4. Cubic Surface Harmonics $k_l^\mu(\Phi\beta)$	527
15.4.1. In Steps of Φ and β	527
15.4.2. For Low-index Directions	531
15.5. Cubic Generalized Spherical Harmonics	533
15.5.1. Cubic-orthorhombic $T_l^{\mu n}(\varphi_1\Phi\varphi_2)$	533
15.5.1.1. In Steps of $\varphi_1\Phi\varphi_2$	533
15.5.1.2. At Ideal Orientations	543
15.5.2. Cubic-Cubic $T_l^{\mu\mu'}(\varphi_1\Phi\varphi_2)$	550
15.5.2.1. In Steps of $\varphi_1\Phi\varphi_2$	550
15.5.2.2. For Specific Orientation Relations	555
15.5.2.3. For Rotation Axis and Angle (hkl, ω)	556
Appendix 4 Graphic Representations	561
A4.1. The Generalized LEGENDRE Functions $P_l^{mn}(\Phi)$	562
A4.2. Cubic Spherical Harmonics $k_l^\mu(\Phi\beta)$	566
A4.3. Cubic Generalized Spherical Harmonics	568
A4.3.1. Cubic-orthorhombic Generalized Spherical Harmonics	568
A4.3.2. Cubic-cubic Generalized Spherical Harmonics	582
Subject Index	585
In Memory of Hans Joachim Bunge	594

List of Symbols Used

K_A	Sample fixed coordinate system
$X Y Z$	Coordinate axes in K_A
xyz	Coordinates in K_A
y	Sample direction
$\Phi\gamma$	Spherical polar coordinates in K_A (pole figure)
$\alpha\beta$	Spherical polar coordinates of the crystal direction [hkl] in K_A
γ	Orientation angle measured about [hkl]
K_B	Crystal fixed coordinate system
$X' Y' Z'$	Coordinate axes in K_B
$x'y'z'$	Coordinates in K_B
h	Crystal direction
$h_i hkl$	Direction cosines of the crystal direction in K_B
$\Phi\beta$	Spherical polar coordinates in K_B (inverse pole figure)
$\alpha'\beta'$	Spherical polar coordinates of the sample direction y in K_B
γ'	Orientation angle measured about y
$d\mathbf{h}, dy$	Element of solid angle
g	Rotation (particularly that which transforms K_A into K_B)
dg	Element of orientation
Δg	Orientation distance
a_{ij}	Components of g in matrix representation (transformation coefficients)
$\varphi_1\Phi\varphi_2$	EULER angles (first definition)
$\Psi\Theta\Phi$	EULER angles (second definition)
d	Rotation axis
$\vartheta\psi$	Polar coordinates of the rotation axis
ω	Rotation angle
$\varrho\alpha\beta$	WILLIAMS' orientation parameters
$\omega\varphi\varrho$	RUER'S orientation parameters
$\varrho_1\varrho_2\varrho_3$	LÜCKE'S orientation parameters
$(hkl) [uvw]$	MILLER indices of normal direction and rolling direction
ζ	Orientation parameter $\cos \Phi$
I	The invariant measure

g_A, g_B	Rotations of sample and crystal symmetries	Φ_A, Φ_B	Limiting angles in incomplete figure
G_A, G_B	Groups of rotations of sample and crystal symmetries	a	Matching factor for transmission and back-reflection range
$\mathbf{h}_\alpha, \mathbf{y}_\alpha$	Symmetrically equivalent directions	Z_{lmn}	Augmented JACOBI polynomials
g_α	Symmetrically equivalent orientations	$w(\Psi\Theta\Phi)$	Orientation distribution function (ROE's notation)
Z	Number of symmetrically equivalent orientations (multiplicity)	W_{lmn}	Coefficients of the orientation distribution function (ROE's notation)
$\mathbf{h}_i, \mathbf{h}_j, \mathbf{y}_i, \mathbf{y}_j, g_i, g_j$	Symmetrically non-equivalent directions and orientations	$q(\chi\eta)$	Pole figure (ROE's notation)
$f(g), R(\mathbf{h})$	Orientation distribution function in the case of general texture and fibre texture, respectively	Q_{lm}	Coefficients of pole figures (ROE's notation)
$C_l^{\mu\nu}, C_l^\mu$	Coefficients of the orientation distribution function	$\chi\eta$	Spherical polar coordinates of the pole figure (ROE's notation)
$\Delta C_l^{\mu\nu}, \Delta C_l^\mu$	Errors of the coefficients $C_l^{\mu\nu}$ and C_l^μ , respectively	$\Theta\Phi$	Spherical polar coordinates of the inverse pole figure (ROE's notation)
$A(\mathbf{h}, \mathbf{y}), A(\mathbf{h}, \Phi)$	Generalized axis distribution function	$S(\Phi)$	Scattering function in the neighbourhood of a preferred orientation (ideal orientation in a generalized sense)
$P_{\mathbf{h}_i}(\mathbf{y}), P_{\mathbf{h}_i}(\Phi)$	The pole figure associated with the crystal direction \mathbf{h}_i	a_λ, b_λ	Coefficients of the series expansion of the scattering function in the general case and in the case of fibre textures
$F_l^v(\mathbf{h}_i), F_l(\mathbf{h}_i)$	Coefficients of pole figures	S_0	Value of the scattering function for $\Phi = 0$
$\Delta F_l^v(\mathbf{h}_i), \Delta F_l(\mathbf{h}_i)$	Errors of coefficients of pole figures	Φ_0	The value of the angle Φ , for which $S(\Phi)$ has fallen to $1/e$ of its maximum value
$e_l^v(\mathbf{h}_i), e_l(\mathbf{h}_i)$	Differences between measured and calculated coefficients	M_i	Proportion of the i th texture component (ideal orientation or fibre component)
$R_{\mathbf{y}_j}(\mathbf{h}), R_{\varphi_j}(\mathbf{h})$	Inverse pole figure of the sample direction \mathbf{y}_j and Φ , respectively	$\Psi_1(\Phi_0), \Psi_2(\Phi_0)$	Proportion functions
$H_l^\mu(\mathbf{y}_i), H_l^\mu(\Phi_i)$	Coefficients of the inverse pole figure	$n(g)$	Orientation distribution function of crystal numbers
$W_{\mathbf{h}_i \mathbf{y}_i}(\Theta)$	Angular distribution function	$v(g)$	Orientation distribution function of the average grain size
$G_l(\mathbf{h}_i, \mathbf{y}_i)$	Coefficients of the angular distribution function (As index) random distribution	$r_{\mathbf{y}_0}(\mathbf{h})$	Orientation distribution of the crystallographic planes in a section perpendicular to the sample direction \mathbf{y}_0
r	(As index) observed and calculated quantities	$r(\mathbf{h})$	Orientation distribution of the crystallographic planes in an arbitrarily bent section
obs., cal.	Unnormalized quantities	$\varphi_i^v, \varphi_i'^\mu$	Coefficients of the series expansions of the functions $\varphi(\mathbf{y})$ and $\varphi'(\mathbf{h})$, respectively
\wedge	Normalization factor for the \mathbf{h}_i pole figure	$\varphi(\mathbf{y}), \varphi'(\mathbf{h})$	Orientation distribution of the grain boundary surfaces in the sample fixed and crystal fixed coordinate systems, respectively
N_i	Weighting factor for the \mathbf{h}_i pole figure	$z(\mathbf{y}_0)$	Length of grain boundary lines per unit area for a section perpendicular to the sample direction \mathbf{y}_0
w_i	Number of pole figures and inverse pole figures respectively	z'_l	Coefficients of the series expansion of the function $z(\mathbf{y}_0)$
I_P, I_R	Resolving power	$z'(\mathbf{h})$	Length of grain boundary lines per unit area of grains in \mathbf{h} orientation of a spherical section
$l_{\max.}$	Difference integral of the pole figures	z'^μ_l	Coefficients of the series expansion of the function $z'(\mathbf{h})$
ΔP	Residual errors (R factors)	$\psi(\mathbf{y}), \psi'(\mathbf{h})$	Orientation distribution of the grain boundary lines in sample fixed and crystal fixed coordinate systems
R, R_{hi}	Truncation error of the orientation distribution function, pole figure and inverse pole figure, respectively		
$A_L, A_L(\mathbf{h}_i), A_L(\mathbf{y}_i)$	Texture index (sharpness measure) of the orientation distribution function, pole figure and inverse pole figure, respectively		
$J, J_{\mathbf{h}_i}, J_{\mathbf{y}_i}$	Weighting factor of coincident reflections		
q_i	Weighting factor of multi-phase coincident reflections		
q_{ij}	Non-random distribution function with vanishing pole figure		
$f_0(g)$	Abbreviations used in connection with the generalized axis distribution function		
ABDE, abde			

$\psi_i^r, \psi_i'^\mu$	Coefficients of the series expansion of the function $\psi(\mathbf{y})$ and $\psi'(\mathbf{h})$	q	Contraction ratio
$n(\mathbf{y}_0)$	Number of grain corner points per unit area of a section perpendicular to the sample direction \mathbf{y}_0	M	TAYLOR factor
n_i^r	Coefficients of the series expansion of the function $n(\mathbf{y}_0)$	$m_l^{\mu\nu}$	Coefficients of the series expansion of the TAYLOR factor
$n'(\mathbf{h})$	Number of grain corner points per unit area of grains in \mathbf{h} orientation of a spherical section	α	Angle towards the rolling direction
n_l^μ	Coefficients of the series expansion of the function $n'(\mathbf{h})$	R	Measure of plastic anisotropy
$W(\Delta g)$	Texture transformation function (relating two textures of possibly different crystal symmetries (: and (:))	E_i, E^i	Anisotropy coefficients
$w(r, \Delta g)$	Orientation correlation function	Σ_g	Representation matrix
$E(x)$	Physical properties of a material	$T_l^{mn}(g), S_l^{mn}(g)$	Generalized spherical harmonics
E	Property tensor	$Q_l^{mn}(x)$	Generalized spherical functions
$E_{i_1 i_2 \dots}$	Components of the property tensors	Q_l^{mn}	FOURIER coefficients of generalized spherical functions
$E(\mathbf{h}), E(\Phi\beta)$	Property function dependent on the direction \mathbf{h}	$\chi_l(\Phi)$	Trace of the generalized spherical harmonics
e_l^μ	Coefficients of the series expansion of the function $E(\mathbf{h})$	$\dot{T}_l^{\mu\nu}(g)$	Symmetric generalized spherical harmonics
$E(g), E(\varphi_1 \Phi \varphi_2)$	Property function dependent on the orientation g	$k_l^\mu(\mathbf{h})$	Spherical surface harmonics
$e_l^{\mu\nu}$	Coefficients of the series expansion of the function $E(g)$	$k_l^\mu(\mathbf{h})$	Symmetric spherical surface harmonics
\sim	Denotes a polycrystal value	$P_l^{mn}(\Phi)$	Generalized LEGENDRE functions
$-$	Denotes a simple orientation averaged value	$a_l^{mns}, a_l'^{mns}$	FOURIER coefficients of the $P_l^{mn}(\Phi)$
μ_{im}, v_m	Components of the series expansion of a_{ij}	$\bar{P}_l^m(\Phi)$	Normalized associated LEGENDRE functions
$a_l^{mn}(i_1, \dots, i_r; j_1, \dots, j_r)$	Components of the series expansion of the transformation coefficients of a tensor of rank r	$a_l^{ms}, a_l'^{ms}$	FOURIER coefficients of the $\bar{P}_l^m(\Phi)$
$\bar{a}(i_1, \dots, i_r; j_1, \dots, j_r)$	Averaging coefficients of a tensor of rank r	$\bar{P}_l^0(\Phi), \bar{P}_l(\Phi)$	Normalized LEGENDRE polynomials
$a_l^{mr}(i_1, \dots, i_r; j_1, \dots, j_r)$	Coefficients of the series expansion of the averaging coefficients	$\dot{A}_l^{m\mu}, \dot{A}_l^{n\nu}, \dot{B}_l^{m\mu}, \dot{B}_l^{n\nu}$	Symmetry coefficients
K_2, K_4, K_6	Magnetic anisotropy constants	$M(l), N(l)$	Number of linearly independent spherical surface harmonics of the crystal and sample symmetries, respectively
I_S	Saturation magnetization	\therefore	Symbols for various symmetries
I_R	Remanence	ε_m	Normalization factor
σ_{ij}	Stress tensor	$*$	Conjugate complex quantity
ε_{ij}	Strain tensor	$\langle \rangle$	Angle between
s_{ijkl}, c_{ijkl}	Elastic compliance, stiffness tensor	$(l_1 l_2 m_1 m_2 lm)$	CLEBSCH—GORDAN coefficients
V, R, H	Approximation according to VOIGT, REUSS and HILL	$(l_1 l_2 m_1 m_2 lm)$	Multiplication coefficients of the spherical surface harmonics
s_a, c_a	Elastic anisotropy of cubic crystals	$(l_1 l_2 l)$	Multiplication coefficients of the LEGENDRE polynomials
t_{ijkl}	Anisotropy tensor of cubic crystals	$\{l_1 l_2 \mu_1 \mu_2 l\mu\}$	Symmetric CLEBSCH—GORDAN coefficients
t_{ijkl}	Texture tensor of cubic materials	$\{l_1 l_2 \mu_1 \mu_2 l\mu\}$	Multiplication coefficients of the symmetric spherical surface harmonics
N	Number of counts in X-ray or neutron intensity measurements	A_l^{mn}, B_l^{mn}	Integrals with generalized LEGENDRE functions
M	Magnetic torque	D_l^μ	Integrals with symmetric spherical surface harmonics
P	Magnetic power losses	φ_4, φ_6	Cubic invariants
u_i	Displacement vector	n_4, n_6	Normalization factors for cubic spherical surface harmonics
e_{ij}	Deformation tensor	e	Identical rotation
η	Amount of deformation	\mathbb{E}	Identity matrix

\tilde{g}	Class of conjugate rotations
\oint	Integral over the total spherical surface or over the total orientation space
\oint_w	Integral over the elementary region of symmetry
$F(g', g''), F(g')$	Integral over a specified path
G_E	Convolution integral
	Symmetry group in EULER space

1. Introduction

Very many technically important materials, such as metals, ceramics and some plastics, are polycrystalline. Their properties depend on those of the single crystals and also on parameters characterizing the polycrystalline state. Since some of the properties of the crystals are strongly directionally dependent, the crystallographic orientation of the crystallites within the polycrystalline aggregate — the texture — plays an important role among these parameters. When all possible orientations of the crystallites occur with equal frequency, the orientation dependence will disappear on the average. The polycrystalline material thus behaves isotropically on the whole. A typical example of this is sheet, which is to be used for deep drawing. Here the isotropic condition is desired in order to avoid undesirable earing. If, on the other hand, all crystals are nearly similarly oriented, the behaviour of the polycrystalline material in many respects resembles that of the single crystal. A prominent example of this case is the so-called cube texture in sheets of cubic metals. All crystals are thereby so oriented that a cube face lies nearly parallel to the plane of the sheet and a cube edge points approximately in the rolling direction. Then the transverse direction is naturally approximately a cube edge direction (*Figure 1.1*). This texture is usually desired in magnetic materials which are easily magnetizable in the cube edge direction. In transformer cores thus constructed the magnetic flux proceeds almost exclusively in easily magnetizable directions. Particularly favourable properties are thus obtained.

In addition to the orientation distribution itself, changes of this function during the various working processes of a polycrystal also play a role. In the case of plastic deformation of metals, the deformation of a crystallite is almost always accompanied by a change in its crystallographic orientation. One can therefore draw conclusions about the deformation mechanisms in polycrystalline aggregates from the texture changes. If, finally, in the case of recrystallization, a high-angle

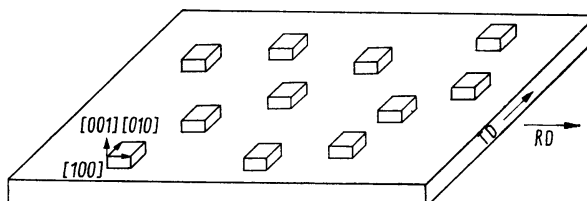


Figure 1.1 Schematic representation of the cube texture in a sheet

2 Introduction

grain boundary is passed through the material, the crystallographic orientation in the region swept out is changed suddenly by a large angle. From the orientation changes one can therefore draw further conclusions about the mechanisms of recrystallization.

These well-known examples show the importance of the orientation and orientation distribution of the crystallites in a polycrystalline material. It is frequently not sufficient to determine that the crystallites possess one or more preferred (ideal) orientations. On the contrary, it is frequently necessary to know the exact distribution function of the crystal orientations. The orientation distribution function is unfortunately not directly measurable by usual X-ray diffraction methods. One obtains experimentally only the well-known pole figures — i.e. integrals of this function. Herein lies the central problem of all texture analysis (see, e.g., reference 130). Its solution, the calculation of the orientation distribution from pole figures, requires mathematical and computational methods which have only recently been developed. Series expansions in spherical surface harmonics and generalized spherical surface harmonics have the advantage in these methods that they also permit treatment of a whole series of different texture problems in a simple and lucid manner, particularly problems of anisotropy of physical properties of polycrystalline materials. In the following I shall try to give a brief summary of the treatment of texture problems by the series expansion method. Other methods, not based on series expansion, will therefore not be considered in detail. It seems, however, appropriate, in addition to the actual texture function (i.e. the orientation of the crystallites), also to consider the orientation distribution of the grain boundaries and grain edges, and orientation distributions of the surfaces and surface intersections, as well as some other distribution functions treated in quantitative metallography. Some practical examples will be cited to illustrate the method. It is not the object of this book to consider the relation between textures and the problems of physical metallurgy, which have been treated in a distinguished series of comprehensive presentations (references 5—9).

2. Orientation of Individual Crystallites

In order to permit description of the orientation of crystallites in a polycrystalline metal, we first define a system of rectangular coordinates K_A in the sample to be investigated. How we select these sample fixed coordinates is, in principle, arbitrary. In general, however, the external shape of the sample will suggest use of a specific coordinate system. Thus, in the case of sheet and foil, we shall as a rule choose a coordinate system whose axes coincide with the rolling direction, transverse direction and normal direction (*Figure 2.1*). For wire and fibres only

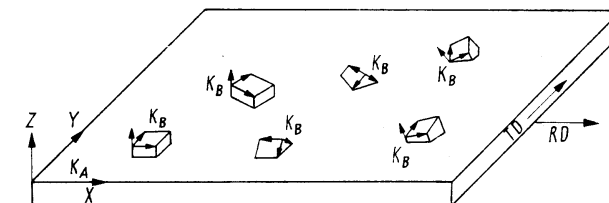


Figure 2.1 The sample fixed coordinate system K_A and the crystal fixed coordinate system K_B in the sheet

one direction, the fibre axis, is distinct. We then place one of the coordinate axes in this direction. As a second coordinate axis one chooses an arbitrary direction perpendicular to the first. The direction of the third axis is naturally thus defined. For each crystallite we then choose an additional coordinate system K_B , which is fixed with respect to the crystal axes. The axes of these coordinate systems can be arbitrary crystallographic directions. They must, however, be the same for all crystallites. As a rule, we shall choose for these crystal fixed coordinate systems, from all possible orientations, one which is appropriate for the crystal symmetry. For cubic crystal symmetry we thus choose as suitable the cube edge directions as axes of these coordinate systems. We describe the orientation of a crystallite within a polycrystalline sample by specification of the rotation g which transforms the sample fixed coordinate system K_A into the crystal fixed coordinate system K_B .

2.1 Various Representations of a Rotation

There are a very large number of possible ways of describing a rotation of two coordinate systems with respect to each other and thereby representing the crystal orientation. All these representations are, in principle, equivalent and can be con-

verted into one another (see Section 2.1.9). One or another may, however, be particularly suitable for various purposes. We shall here consider those which have acquired particular importance for the description of textures (see also reference 144).

2.1.1. Eulerian Angles

We begin with the representation of a rotation almost exclusively used in the following, namely that of EULER's angles. One begins with an orientation of the crystal coordinate system in which the axes are parallel to those of the sample coordinate system. The crystal coordinate system is then first rotated about the Z' -axis through the angle φ_1 , then about the X' -axis (in its new orientation) through Φ and, finally, once again about the Z' -axis (in its new orientation) through the angle φ_2 (Figure 2.2). The rotation g is thus represented by the three EULERIAN angles $\varphi_1 \Phi \varphi_2$.

$$g = \{\varphi_1, \Phi, \varphi_2\} \quad (2.1)$$

If one considers the Z -axes of the two coordinate systems as well as their $X - Y$ planes (Figure 2.3), one thus recognizes that the EULER angles are symmetric with respect to the two coordinate systems. The angle Φ is the angle between the two Z -axes, and φ_1 and φ_2 are the distances of the two X -axes from the line of intersection of the two $X - Y$ planes. With the product notation described in Section 2.2 for two successive rotations one can thus write

$$g = g_{\varphi_2}^{Z'} \cdot g_{\Phi}^{X'} \cdot g_{\varphi_1}^{Z'} \quad (2.2)$$

It is customary to represent the three parameters of the rotation g — namely $\varphi_1 \Phi \varphi_2$ — as Cartesian coordinates in a three-dimensional space, the orientation space or EULER space (Figure 2.4). Each point of the EULER space then corresponds to a particular rotation, and conversely each rotation or crystal orientation leads to a point in the three-dimensional space.

Of course this space has a singularity for $\Phi = 0$. From the definition of the EULER angles (Figure 2.3) one recognizes that for $\Phi = 0$ the rotation is only determined by the sum $\varphi_1 + \varphi_2$ of the other two rotation angles. All points of the line $\varphi_1 + \varphi_2 = \text{constant}$ in Figure 2.4 thus represent the same rotation.

From the definition of the EULER angles it follows that they are periodic with period 2π . The following identity is thus valid:

$$g\{\varphi_1 + 2\pi, \Phi + 2\pi, \varphi_2 + 2\pi\} = g\{\varphi_1, \Phi, \varphi_2\} \quad (2.3)$$

The EULER space represented in Cartesian coordinates is thus three-dimensionally periodic with period 2π in all three axis directions. Moreover, with the aid of Figure 2.3 one can easily verify the following identity:

$$g\{\varphi_1 + \pi, 2\pi - \Phi, \varphi_2 + \pi\} = g\{\varphi_1, \Phi, \varphi_2\} \quad (2.4)$$

This relation represents a reflection in the plane $\Phi = \pi$, with simultaneous displacement through π in the directions φ_1 and φ_2 , and thus a glide plane in EULER

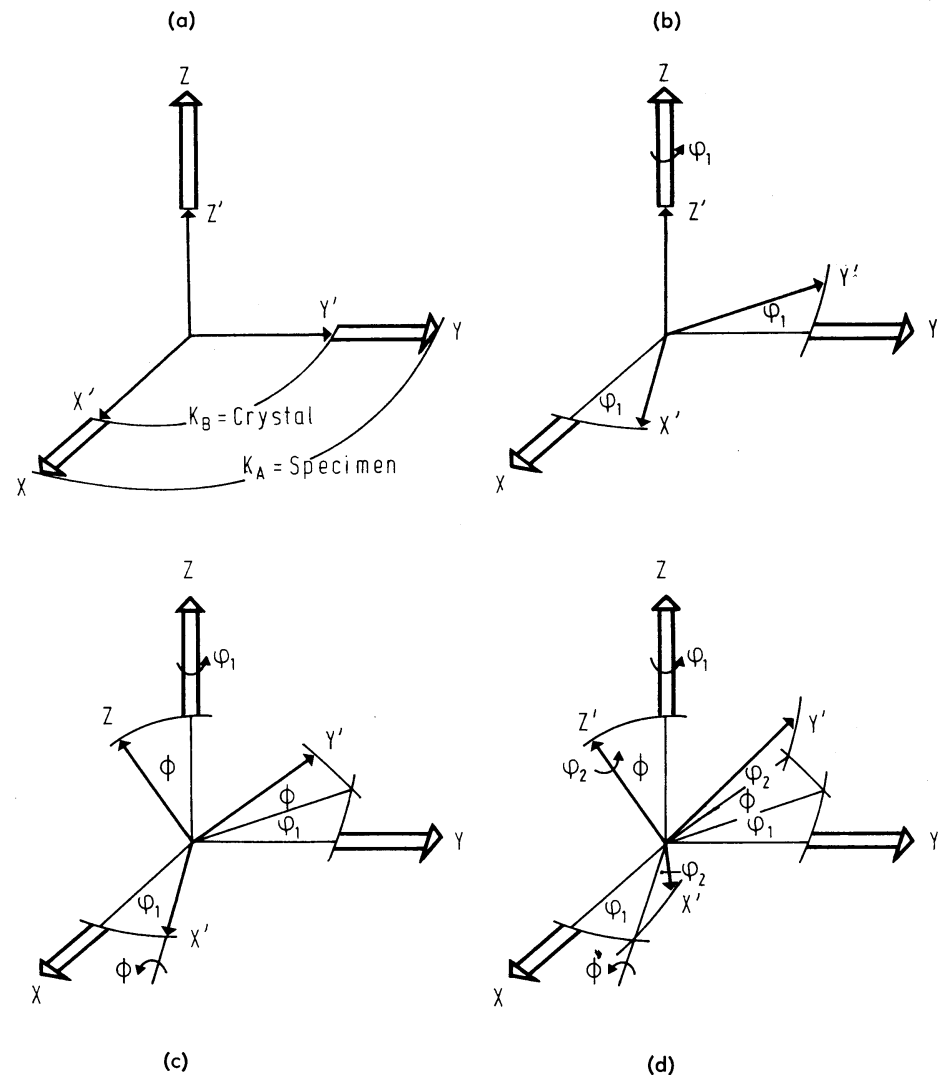
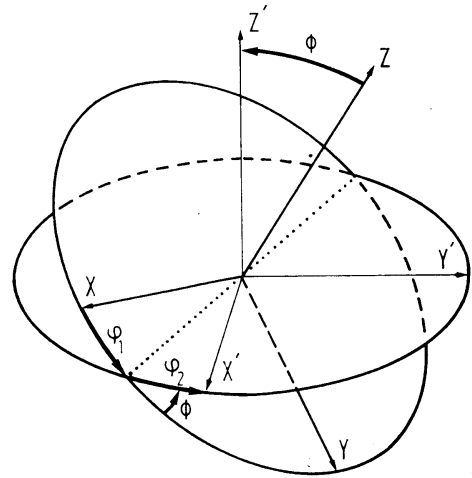
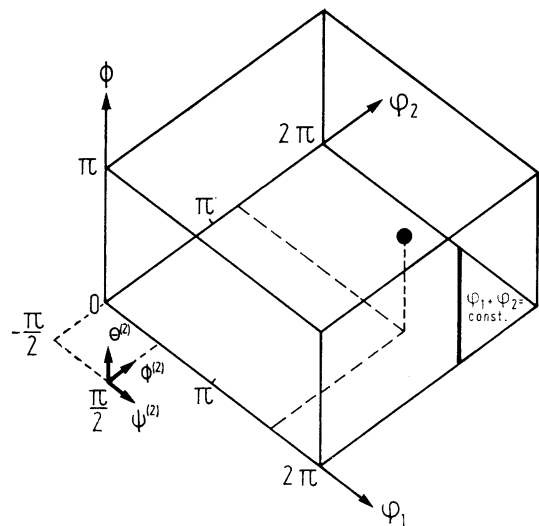


Figure 2.2 On the definition of the EULER angles $\varphi_1 \Phi \varphi_2$: (a) the crystal coordinate system $K_B(X'Y'Z')$ lies parallel to the sample coordinate system $K_A(XYZ)$ (so-called cube orientation); (b) the crystal coordinate system is rotated about the Z' -axis through the angle φ_1 ; (c) the crystal coordinate system K_B is rotated with respect to the orientation (b) around the X' -axis through the angle Φ ; (d) the crystal coordinate system K_B is rotated with respect to the orientation (c) around the Z' -axis through the angle φ_2 .

Figure 2.3 On the definition of the EULER angles $\varphi_1\Phi\varphi_2$ Figure 2.4 The orientation space (EULER space) corresponding to the two definitions of the EULER angles $\varphi_1\Phi\varphi_2$ and $\Psi\Theta\Phi$. Points on the lines $\Phi = 0$, $\varphi_1 + \varphi_2 = \text{const.}$ represent the same rotation or orientation

space. This is represented in Figure 2.5. The EULER space thus forms a three-dimensionally periodic lattice with unit cell $\{2\pi, 2\pi, 2\pi\}$. The asymmetric unit is, however, restricted to the region $\{2\pi, \pi, 2\pi\}$ by a glide plane, as was previously assumed in Figure 2.4. This symmetry corresponds to a space group Pn in EULER space.

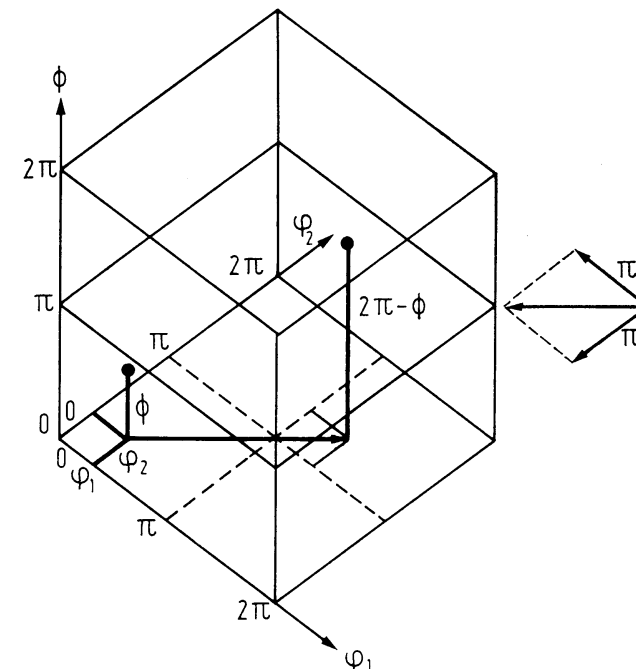
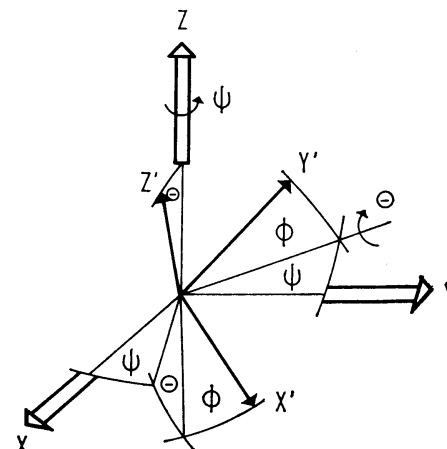


Figure 2.5 Unit cell and asymmetric unit in EULER space

In another variant of EULER angles the second rotation is not carried out about the X' -axis, but about the Y' -axis (Figure 2.6). (The first and third rotations remain, as previously, about the Z' -axis.) It is customary to denote the EULER

Figure 2.6 On the definition of the EULER angles $\Psi\Theta\Phi$ (second variant)

angles thus defined by $\Psi\Theta\Phi$ (see, e.g., reference 246). In order to distinguish them from the EULER angles of the first kind, we shall denote them by a superior (2):

$$g = \{\Psi^{(2)}, \Theta^{(2)}, \Phi^{(2)}\} = g_{\phi^{(2)}}^{Z'} \cdot g_{\theta^{(2)}}^{Y'} \cdot g_{\psi^{(2)}}^{Z'} \quad (2.5)$$

Both kinds of EULER angles stand in a close relationship to each other (see Figures 2.2 and 2.3):

$$\varphi_1 = \Psi^{(2)} + \pi/2; \quad \Phi = \Theta^{(2)}; \quad \varphi_2 = \Phi^{(2)} - \pi/2 \quad (2.6)$$

One obtains another representation of the EULER space if one specifies the orientation of the rolling direction in stereographic projection with respect to the crystal axes (see Figure 2.23) and uses the angle φ_2 as the third orthogonal coordinate (Figure 2.7). This representation of the EULER space was used by IMHOFF¹⁶² in constant φ_2 sections.

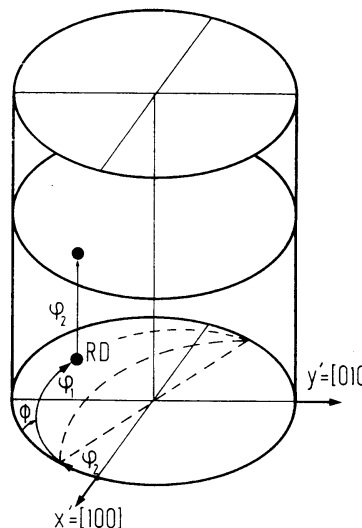


Figure 2.7 Representation of the EULER space according to IMHOFF¹⁶²

2.1.2. Rotation Axis and Rotation Angle

Another representation of the rotation is obtained if one specifies the rotation axis and the attendant rotation angle. The rotation axis can be specified by the unit vector \mathbf{d} , which can be represented by its components d_x, d_y, d_z (direction cosines) or by spherical polar coordinates $\vartheta\psi$. The rotation angle about the direction \mathbf{d} is ω . In this representation one can thus write the rotation g (Figure 2.8):

$$g = \{\mathbf{d}, \omega\} = \{\vartheta, \psi, \omega\} \quad (2.7)$$

This representation of a rotation and thus of the crystal orientation will frequently be obvious.

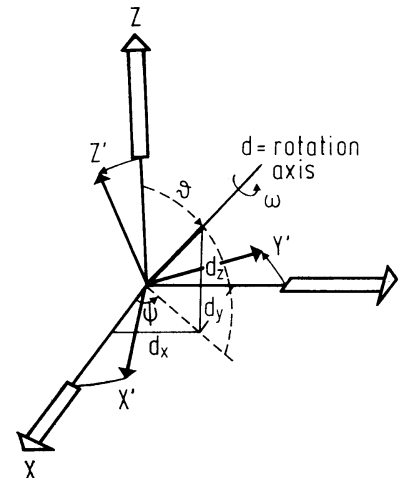


Figure 2.8 Representation of a rotation by the rotation axis \mathbf{d} and the appropriate rotation angle ω . The rotation axis is described either by its direction cosines d_x, d_y, d_z or by polar coordinates $\vartheta\psi$

If one describes the orientation of the rotation axis \mathbf{d} by a point in the stereographic projection (Figure 2.9) and uses the rotation angle ω as the third coordinate,

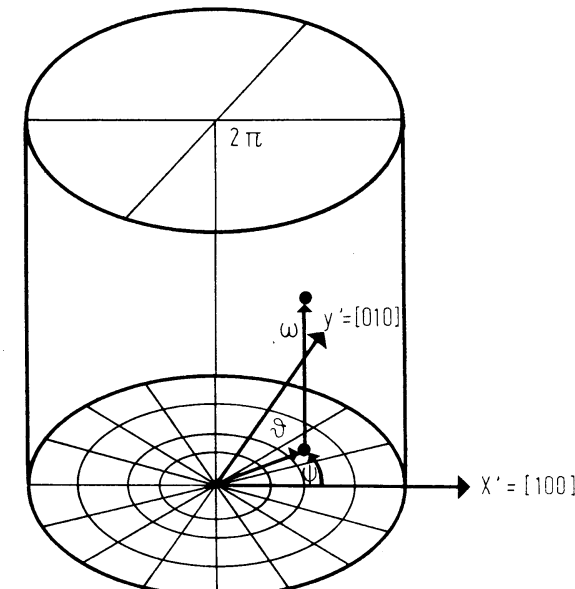


Figure 2.9 Representation of the orientation space by the coordinates $\vartheta\psi\omega$ of the rotation axis and the rotation angle (cylindrical orientation space)¹⁶¹

one thus also obtains a three-dimensional representation of a rotation or crystal orientation^{160,161}. One can, however, also give the spatial orientation of the rotation axis itself (Figure 2.10) and measure the rotation angle ω as distance from the origin. One then obtains a spherical orientation space (see references 160, 161)

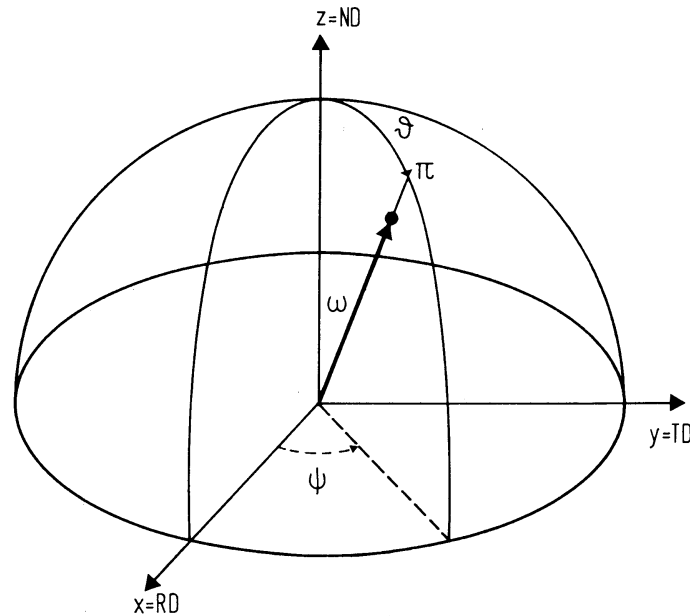


Figure 2.10 Representation of the orientation space by the coordinates $\vartheta\psi\omega$ of the rotation axis and the rotation angle (spherical orientation space)¹⁶¹

2.1.3. Crystal Direction and Angle

One obtains a further frequently used representation of the orientation if one chooses a specific crystal direction $[hkl]$ (and thus a direction fixed in the crystal coordinate system K_B) and gives its orientation in the sample coordinate system K_A by two angles — e.g. spherical polar coordinates α, β (Figure 2.11). The crystal coordinate system is, however, not completely specified by these two angles. It has a degree of freedom, a rotation about the direction $[hkl]$, which must be specified by a third parameter γ . By selection of the crystal direction $[hkl]$ and reference point of the angle γ one in this way obtains a large number of different representations of the orientation.

2.1.4. Sample Direction and Angle

Since the two coordinate systems, the sample coordinate system and the crystal coordinate system, are in principle equivalent, all previously described orientation representations can also be reciprocally used, if one begins with the crystal coor-

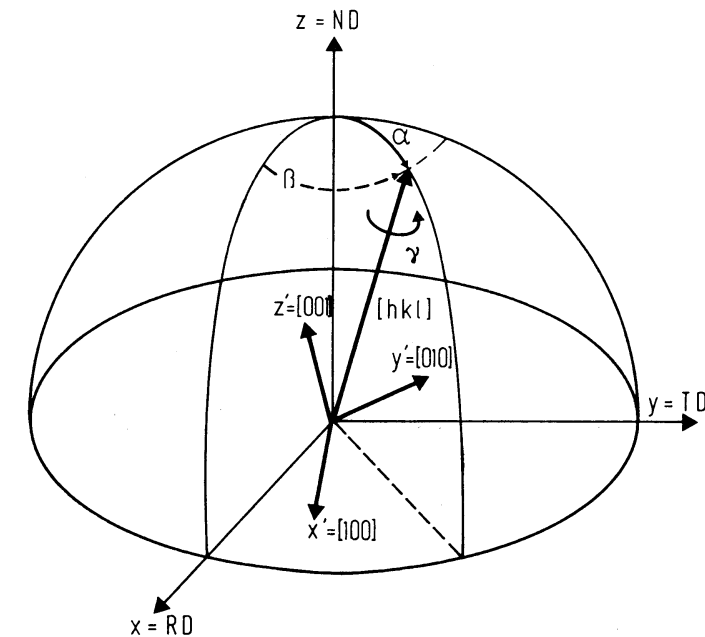


Figure 2.11 The orientation of a specified crystal direction $[hkl]$ relative to the sample coordinate system $K_A = \{XYZ\}$ is described by the polar coordinates α, β . A rotation of the crystal coordinate system about $[hkl]$ is described by a third angle γ

dinate system and specifies the orientation of the sample coordinate system with respect to it.

One then begins with a specific sample direction y , which is fixed with respect to the sample coordinate system K_A (e.g. the sheet normal direction), and describes its orientation relative to the crystal coordinate system K_B by two parameters α', β' (Figure 2.12). The orientation of the sample coordinate system must, however, then be specified by an additional parameter γ' . The choice of sample direction and origin of γ' again results in very many different representations of this kind. The situation will be particularly simple if the sample direction is the Z -direction of the sample coordinate system. (With an appropriate choice of the sample coordinate system this corresponds, for example, to the sheet normal direction.) If one denotes its spherical polar coordinates in the crystal coordinate system (according to R. O. WILLIAMS²⁹⁹) by ϱ and α (Figure 2.13), an additional parameter β is needed in order to completely specify the orientation of the sample coordinate system. It is defined by the angular distance of the rolling direction = X -direction from the line of intersection S of the rolling plane ($X - Y$ plane) and the (100) plane. If one specifies the orientation of the normal direction by its coordinates ϱ, α in stereographic projection and the angle β , which can vary between 0 and 180° , as the third orthogonal coordinate, one thus obtains a representation of the orientation as a point in the volume given in Figure 2.14(a). This

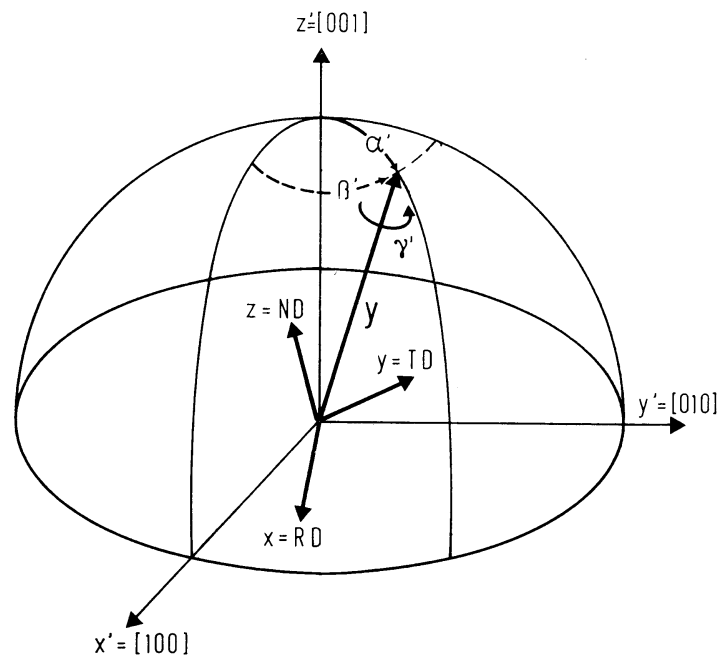


Figure 2.12 The orientation of a specified sample direction y relative to the crystal coordinate system $K_B = \{X', Y', Z'\}$ is described by two angles α', β' . A rotation of the sample coordinate system about y is described by a third angle γ'

representation of orientation has been called the biaxial pole figure by R. O. WILLIAMS (since the orientation is represented by the poles of two directions $X = RD$ and $Z = ND$ in the stereographic projection; Figure 2.13). In this representation it is already assumed that the crystal symmetry is cubic and the sample symmetry is orthorhombic (otherwise, instead of the volume in Figure 2.14(a), a larger volume must be chosen). By consideration of these two symmetries one can also use the volume represented in Figure 2.14(b) in place of that given in Figure 2.14a; this reduces to the R. O. WILLIAMS representation for the cubic-orthorhombic case. This representation has been used in a series of calculations of the orientation distribution function.

A somewhat different representation of this kind was used by D. RUER (Figure 2.15)^{250, 251}. The orientation of the normal direction with respect to the crystal axes is described by the angles ω, φ , which now, however, do not form a spherical polar coordinate system. The rotation about the normal direction is measured by the angle ϱ . One obtains the origin for the angle ϱ if one rotates the sample coordinate system from an orientation parallel to the crystal coordinate system, so that the normal direction follows the shortest path to the point ω, φ — i.e. the rotation takes place about an axis in the (001) plane, which forms the

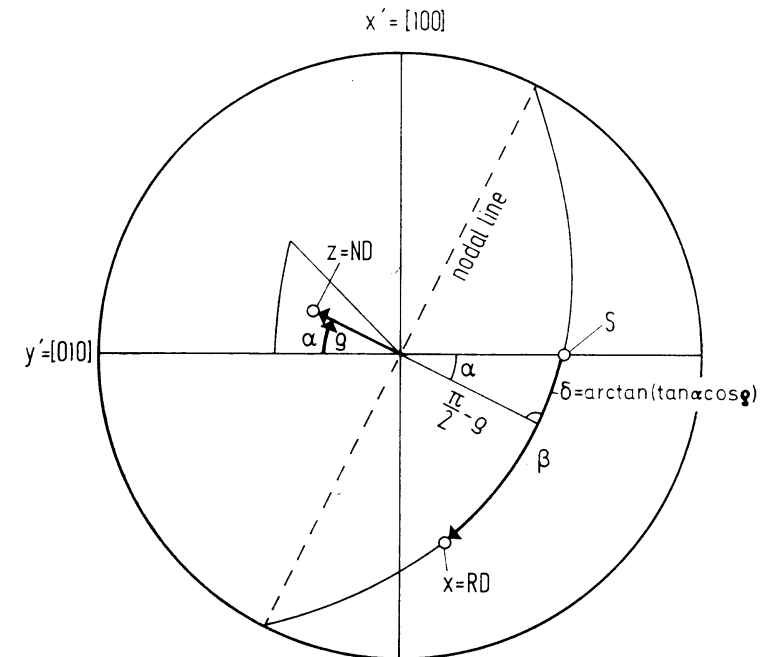


Figure 2.13 On the definition of the biaxial orientation coordinates according to WILLIAMS²⁹⁹

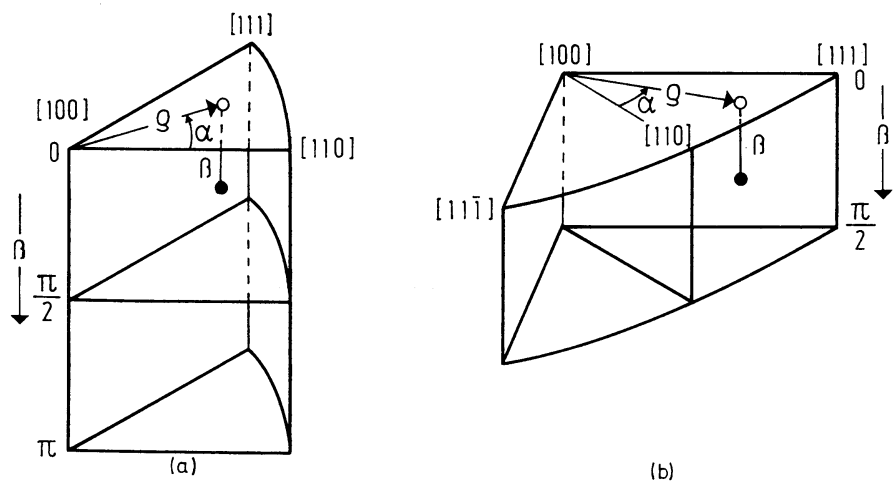


Figure 2.14 Spatial representation of the biaxial coordinates: (a) the asymmetric unit in the case of cubic crystal and orthorhombic sample symmetry is given by one unit triangle and the region $0 \leq \beta \leq 180^\circ$; (b) the asymmetric unit can also be given by two unit triangles and the region $0 \leq \beta \leq 90^\circ$

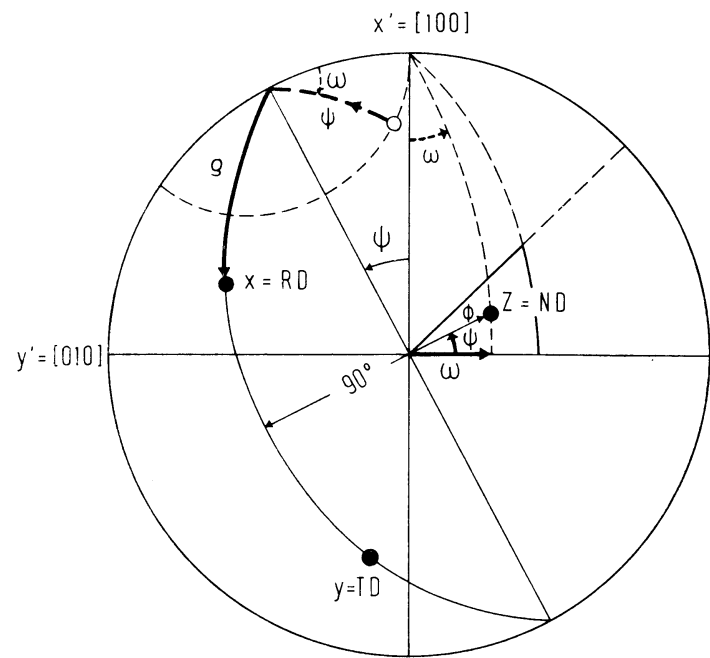


Figure 2.15 On the definition of the orientation coordinates according to RUER²⁵⁰ and RUER and BARO²⁵¹

angle φ with the [100] direction. Thus the rolling direction, which originally lay in the [100] direction, is transformed into the point O, which is the origin for the angle ϱ (Figure 2.15).

A similar representation, which also belongs in this group, was used by PERLWITZ, LÜCKE and PITTSCH^{227,228,231}. They also specify the orientation of the normal direction by spherical polar coordinates; however, they use the [110] direction as pole of the coordinate system (Figure 2.16). The ϱ_1 coordinate is measured from the intersection of the (110) plane, which is the $X'' - Y''$ plane of the polar coordinate system used. These coordinates are thus identical with the EULER angles, if one uses the crystal directions $X'' = \bar{1}\bar{1}1$, $Y'' = \bar{1}12$, $Z'' = 110$ as the crystal coordinate system (see Figure 2.16).

2.1.5. Representation of the Orientation in the Pole Figure

One obtains a frequently used representation of the orientation if one specifies the poles of a specific crystal direction $\langle hkl \rangle$ with respect to the sample coordinates in stereographic projection. For example, a specific orientation is represented in Figure 2.17(a) by its $\langle 100 \rangle$, $\langle 110 \rangle$ and $\langle 111 \rangle$ poles. The orientation of the pole can then be described by the polar coordinates Φ_{hkl} , γ_{hkl} , where $\langle hkl \rangle$ includes all symmetrically equivalent directions. This description is redundant (the Φ_{hkl}

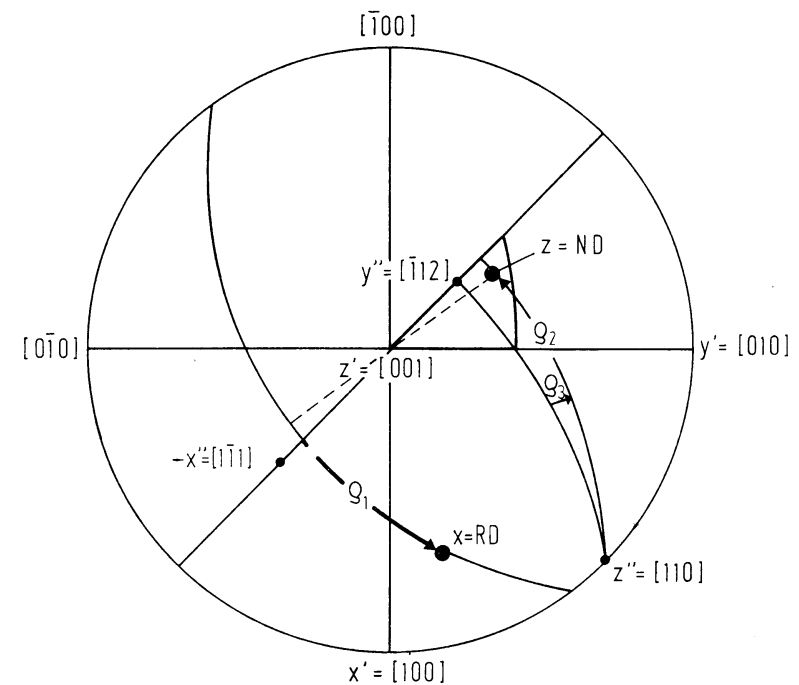


Figure 2.16 On the definition of the orientation coordinates $\varrho_1\varrho_2\varrho_3$ according to PERLWITZ et al.^{227,228}

and γ_{hkl} are not all independent of one another), since the orientation is determined by two of the poles. Such a redundant description is naturally not well suited for representation of orientation distribution functions, since here one requires independent parameters as variables of the orientation distribution function.

2.1.6. Representation of the Orientation in the Inverse Pole Figure

Similarly, one can describe the orientation by specifying the poles of the sample coordinate system with respect to those of the crystal coordinate system in stereographic projection (Figure 2.17b). The orientation is then given by the polar coordinates of three poles Φ_{RD} , β_{RD} ; Φ_{TD} , β_{TD} ; Φ_{ND} , β_{ND} . This representation is analogous to that of Figure 2.17a for the $\langle 100 \rangle$ poles. A representation with poles of directions other than $X = RD$; $Y = TD$, $Z = ND$ is not customary (of course, it is also possible). This representation is also redundant.

2.1.7. Representation by Miller Indices

A frequently used representation of crystal orientations in sheets consists of the specification of the MILLER indices of that crystal plane which is parallel to the

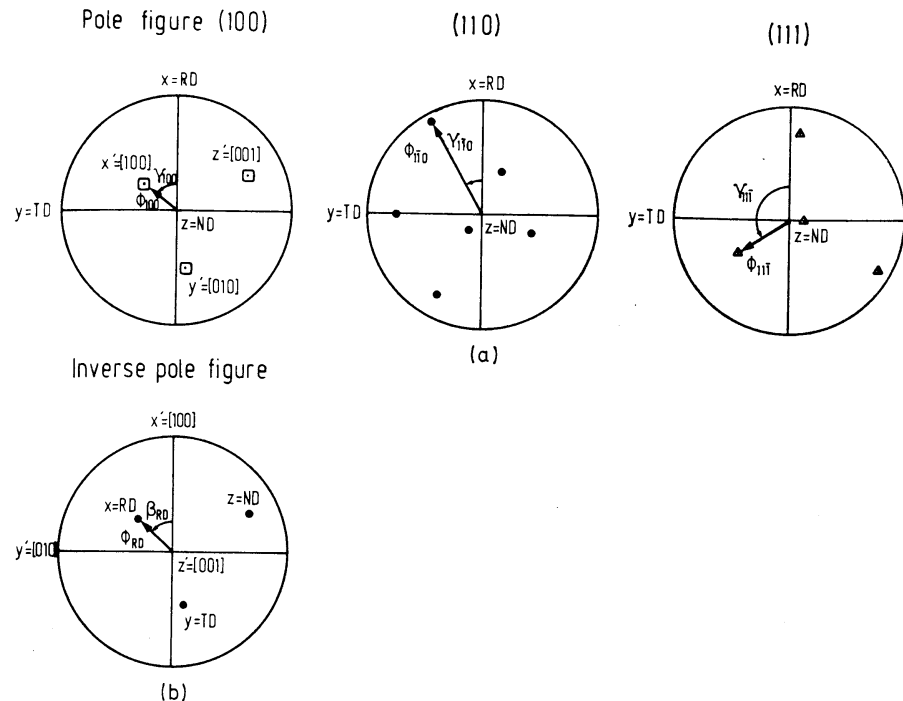


Figure 2.17 (a) The orientation of some crystal directions relative to the specimen coordinate system in stereographic projection (pole figure). The orientation of the poles of these directions can be described by the spherical polar coordinates Φ_{hkl}, γ_{hkl} . (b) The orientation of the specimen directions $X = \text{RD}$, $Y = \text{TD}$, $Z = \text{ND}$ relative to the crystal coordinate axes in stereographic projection (inverse pole figures)

plane of the sheet, as well as the indices of the crystal direction parallel to the rolling direction:

$$g = (hkl) [uvw] \quad (2.8)$$

This representation is closely related to the representation of the inverse pole figure given in Section 2.1.6 (Figure 2.17), if one expresses the orientation of the directions $Z = \text{ND}$ and $X = \text{RD}$ by the corresponding MILLER indices instead of the polar coordinates Φ, β . The representation given by equation (2.8) is likewise redundant.

2.1.8. Matrix Representation

If in equation (2.8) one uses not the integer MILLER indices (hkl) $[uvw]$ but the corresponding direction cosines $h'k'l'$, $u'v'w'$ (normalized to unity) and adds

thereto those of the transverse direction $r's't'$, one thus obtains a representation of the orientation g in matrix form^{144,160,197}:

$$g = \begin{bmatrix} u' & r' & h' \\ v' & s' & k' \\ w' & t' & l' \end{bmatrix} = \begin{bmatrix} a_{11} & a_{12} & a_{13} \\ a_{21} & a_{22} & a_{23} \\ a_{31} & a_{32} & a_{33} \end{bmatrix} = [a_{ij}] \quad (2.9)$$

This is equivalent to the representation of Figure 2.17(b), if one expresses all three directions $X = \text{RD}$, $Y = \text{TD}$, $Z = \text{ND}$ by their direction cosines rather than their polar coordinates Φ, β . The matrix $[a_{ij}]$ is the transformation matrix for the coordinates $x'y'z'$ of an arbitrary point in the crystal coordinate system $K_B = \{X'Y'Z'\}$ expressed by means of the coordinates xyz in the sample coordinate system $K_A = \{XYZ\}$:

$$x' = a_{11}x + a_{12}y + a_{13}z \quad (2.10)$$

$$y' = a_{21}x + a_{22}y + a_{23}z \quad (2.11)$$

$$z' = a_{31}x + a_{32}y + a_{33}z \quad (2.12)$$

If one replaces xyz by x_j and $x'y'z'$ by x'_i , one can write

$$x'_i = \sum_{j=1}^3 a_{ij}x_j \quad (2.13)$$

The column vectors of the matrix $[a_{ij}]$ are by definition unit vectors and are orthogonal to one another; it is therefore true that

$$\sum_{i=1}^3 a_{ij}a_{ik} = \delta_{jk} \quad (2.14)$$

Similarly it is also true for the row vectors that

$$\sum_{i=1}^3 a_{ij}a_{kj} = \delta_{jk} \quad (2.15)$$

For the inversion of equations (2.10)–(2.12) it follows from these two conditions that

$$x = a_{11}x' + a_{21}y' + a_{31}z' \quad (2.16)$$

$$y = a_{12}x' + a_{22}y' + a_{32}z' \quad (2.17)$$

$$z = a_{13}x' + a_{23}y' + a_{33}z' \quad (2.18)$$

The inverse of the matrix is equal to the transpose

$$[a_{ij}]^{-1} = [a_{ji}] \quad (2.19)$$

From equations (2.10)–(2.12) it follows that the columns of the matrix $[a_{ij}]$ are the direction cosines of the directions $X = \text{RD}$, $Y = \text{TD}$, $Z = \text{ND}$ in the crystal coordinate system — i.e. the direction cosines of the directions in the inverse pole figure. From the inversion equations (2.16)–(2.18) it then similarly follows that the rows of the matrix $[a_{ij}]$ are the direction cosines of the directions $X' = [100]$, $Y' = [010]$, $Z' = [001]$ in the pole figure (Figure 2.18).

With the notations $r_x r_y r_z$ for the direction cosines, the orientation matrix can therefore also be written:

$$\begin{bmatrix} r_x^{[100]} & r_y^{[100]} & r_z^{[100]} \\ r_x^{[010]} & r_y^{[010]} & r_z^{[010]} \\ r_x^{[001]} & r_y^{[001]} & r_z^{[001]} \end{bmatrix} = \begin{bmatrix} r_x^{\text{RD}} & r_x^{\text{TD}} & r_x^{\text{ND}} \\ r_y^{\text{RD}} & r_y^{\text{TD}} & r_y^{\text{ND}} \\ r_z^{\text{RD}} & r_z^{\text{TD}} & r_z^{\text{ND}} \end{bmatrix} \quad (2.20)$$

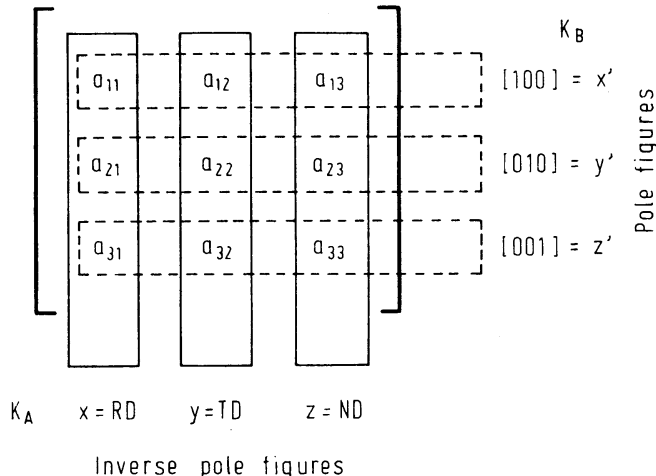


Figure 2.18 Rows and columns of the matrix a_{ij}

The particular advantage of the matrix representation lies in the fact that the result of two successive rotations is given by the product of the two corresponding matrices. (For this reason in Section 2.2 we will speak not of the sum, but of the product of two rotations.)

If one writes the transformation equations (2.13) for two transformations (rotations):

$$x_k'' = \sum_{i=1}^3 a_{ki}^2 x_i'; \quad x_i' = \sum_{j=1}^3 a_{ij}^1 x_j \quad (2.21)$$

one obtains the substitution:

$$x_k'' = \sum_{i=1}^3 \left[\sum_{j=1}^3 a_{ki}^2 \cdot a_{ij}^1 \right] x_i = \sum_{j=1}^3 a_{kj} x_j \quad (2.22)$$

Written in matrix form, these relations are

$$\begin{bmatrix} a_{11} & a_{12} & a_{13} \\ a_{21} & a_{22} & a_{23} \\ a_{31} & a_{32} & a_{33} \\ \vdots & \vdots & \vdots \\ g & = & g_2 & \cdot & g_1 \end{bmatrix} = \begin{bmatrix} a_{11}^2 & a_{12}^2 & a_{13}^2 \\ a_{21}^2 & a_{22}^2 & a_{23}^2 \\ a_{31}^2 & a_{32}^2 & a_{33}^2 \\ \vdots & \vdots & \vdots \\ g & = & g_2 & \cdot & g_1 \end{bmatrix} \cdot \begin{bmatrix} a_{11}^1 & a_{12}^1 & a_{13}^1 \\ a_{21}^1 & a_{22}^1 & a_{23}^1 \\ a_{31}^1 & a_{32}^1 & a_{33}^1 \\ \vdots & \vdots & \vdots \\ g & = & g_2 & \cdot & g_1 \end{bmatrix} \quad (2.23)$$

where the matrix multiplication rule is

$$[a_{kj}] = [a_{ki}^2] \cdot [a_{ij}^1] = \sum_{i=1}^3 a_{ki}^2 \cdot a_{ij}^1 \quad (2.24)$$

The rows of the left-hand matrix (rotation g_2) are thus multiplied by the columns of the right-hand matrix (rotation g_1).

2.1.9. Relations between Different Orientation Parameters

Since different orientation parameters for the description of orientations and orientation distribution functions have been used by different writers, it is frequently necessary to convert the different parameters into one another. This has already been done in Section 2.1.1 for the two variants of EULER angles. In the case of cubic crystal symmetry and orthorhombic sample symmetry, one considers only a portion of orientation space — namely, that for which the angles $\varphi_1 \Phi \varphi_2$ or $\Psi \Theta \Phi$ are smaller than 90° . However, according to equation (2.6) or Figure 2.4, the elementary regions for the two definitions of EULER angles do not agree. It is therefore suitable to include the symmetry relations in EULER space (see Section 14.7.6). For the frequently occurring cubic-orthorhombic case, one thereby obtains

$$\varphi_1 = \frac{\pi}{2} - \Psi^{(2)}; \quad \Phi = \Theta^{(2)}; \quad \varphi_2 = \frac{\pi}{2} - \Phi^{(2)} \quad (2.25)$$

The relations between spherical polar coordinates $\Phi \beta$ and direction cosines $r_x r_y r_z$ of a direction according to Figure 2.19 are

$$r_x = \sin \Phi \cos \beta \quad (2.26)$$

$$r_y = \sin \Phi \sin \beta \quad (2.27)$$

$$r_z = \cos \Phi \quad (2.28)$$

For the orientation matrix $[a_{ij}]$, expressed in terms of the spherical polar coordinates of the sample directions $X = \text{RD}$, $Y = \text{TD}$, $Z = \text{ND}$, in the coordinate system of the crystal directions, one thus obtains

$$g = \begin{bmatrix} \sin \Phi_{\text{RD}} \cos \beta_{\text{RD}} & \sin \Phi_{\text{TD}} \cos \beta_{\text{TD}} & \sin \Phi_{\text{ND}} \cos \beta_{\text{ND}} \\ \sin \Phi_{\text{RD}} \sin \beta_{\text{RD}} & \sin \Phi_{\text{TD}} \sin \beta_{\text{TD}} & \sin \Phi_{\text{ND}} \sin \beta_{\text{ND}} \\ \cos \Phi_{\text{RD}} & \cos \Phi_{\text{TD}} & \cos \Phi_{\text{ND}} \end{bmatrix} \quad (2.29)$$

Correspondingly, for the orientation matrix, expressed in terms of the polar coordinates of the crystal directions $X' = [100]$, $Y' = [010]$, $Z' = [001]$, in the sample coordinate system, one obtains

$$g = \begin{bmatrix} \sin \Phi_{100} \cos \gamma_{100} & \sin \Phi_{100} \sin \gamma_{100} & \cos \Phi_{100} \\ \sin \Phi_{010} \cos \gamma_{010} & \sin \Phi_{010} \sin \gamma_{010} & \cos \Phi_{010} \\ \sin \Phi_{001} \cos \gamma_{001} & \sin \Phi_{001} \sin \gamma_{001} & \cos \Phi_{001} \end{bmatrix} \quad (2.30)$$

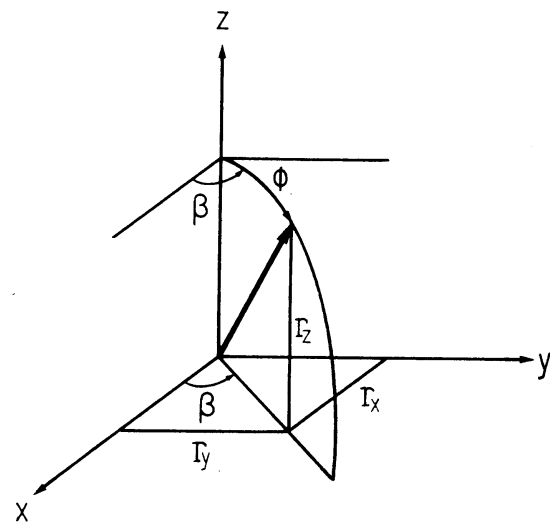


Figure 2.19 Relation between spherical polar coordinates $\Phi\beta$ and the direction cosines $r_x r_y r_z$

The MILLER indices are obtained from the direction cosines by multiplication by a factor which makes them integers. For the MILLER indices of the rolling plane and the rolling direction, defined by equation (2.8), there result

$$h = n \cdot \sin \Phi_{ND} \cos \beta_{ND} \quad (2.31)$$

$$k = n \cdot \sin \Phi_{ND} \sin \beta_{ND} \quad (2.32)$$

$$l = n \cdot \cos \Phi_{RD} \quad (2.33)$$

where

$$n = \sqrt{h^2 + k^2 + l^2} \quad (2.34)$$

$$u = n' \sin \Phi_{RD} \cos \beta_{RD} \quad (2.35)$$

$$v = n' \sin \Phi_{RD} \sin \beta_{RD} \quad (2.36)$$

$$w = n' \cos \Phi_{RD} \quad (2.37)$$

where

$$n' = \sqrt{u^2 + v^2 + w^2} \quad (2.38)$$

The inversion of equations (2.26)–(2.28) yields

$$\Phi = \arccos r_z \quad (2.39)$$

$$\beta = \arcsin \frac{r_y}{\sqrt{1 - r_z^2}} = \arccos \frac{r_x}{\sqrt{1 - r_z^2}} \quad (2.40)$$

If one uses these relations for the MILLER indices of the rolling and normal directions, one obtains

$$\Phi_{ND} = \arccos \frac{l}{\sqrt{h^2 + k^2 + l^2}} \quad (2.41)$$

$$\beta_{ND} = \arcsin \frac{k}{\sqrt{h^2 + k^2}} = \arccos \frac{h}{\sqrt{h^2 + k^2}} \quad (2.42)$$

for the polar coordinates of the normal direction, and

$$\Phi_{RD} = \arccos \frac{w}{\sqrt{u^2 + v^2 + w^2}} \quad (2.43)$$

$$\beta_{RD} = \arcsin \frac{v}{\sqrt{u^2 + w^2}} = \arccos \frac{u}{\sqrt{u^2 + v^2}} \quad (2.44)$$

for the polar coordinates of the rolling direction.

One most easily obtains the relations between the matrix representation and the EULER angles if one begins with the matrices which correspond to the three EULER rotations. The rotation through the angle α in the plane is described by the transformation equations:

$$x' = \cos \alpha \cdot x + \sin \alpha \cdot y \quad (2.45)$$

$$y' = -\sin \alpha \cdot x + \cos \alpha \cdot y \quad (2.46)$$

Thus we obtain for the three EULER rotations

$$g_{\varphi_1}^{Z'} = \begin{bmatrix} \cos \varphi_1 & \sin \varphi_1 & 0 \\ -\sin \varphi_1 & \cos \varphi_1 & 0 \\ 0 & 0 & 1 \end{bmatrix} \quad (2.47)$$

$$g_{\Phi}^{X'} = \begin{bmatrix} 1 & 0 & 0 \\ 0 & \cos \Phi & \sin \Phi \\ 0 & -\sin \Phi & \cos \Phi \end{bmatrix} \quad (2.48)$$

$$g_{\varphi_2}^{Z'} = \begin{bmatrix} \cos \varphi_2 & \sin \varphi_2 & 0 \\ -\sin \varphi_2 & \cos \varphi_2 & 0 \\ 0 & 0 & 1 \end{bmatrix} \quad (2.49)$$

Multiplication of the three matrices according to equation (2.23) yields:

$$g(\varphi_1 \Phi \varphi_2) =$$

$$\begin{bmatrix} \cos \varphi_1 \cos \varphi_2 - \sin \varphi_1 \sin \varphi_2 \cos \Phi & \sin \varphi_1 \cos \varphi_2 + \cos \varphi_1 \sin \varphi_2 \cos \Phi & \sin \varphi_2 \sin \Phi \\ -\cos \varphi_1 \sin \varphi_2 - \sin \varphi_1 \cos \varphi_2 \cos \Phi & -\sin \varphi_1 \sin \varphi_2 + \cos \varphi_1 \cos \varphi_2 \cos \Phi & \cos \varphi_2 \sin \Phi \\ \sin \varphi_1 \sin \Phi & -\cos \varphi_1 \sin \Phi & \cos \Phi \end{bmatrix} \quad (2.50)$$

By comparing the matrix elements of equation (2.50) with the corresponding ones $u'v'w'$ and $h'k'l'$ of equation (2.9) one obtains immediately the relation between the EULER angle representation and the representation of an orientation by MILLER indices (equation 2.8):

$$h = n \sin \Phi \sin \varphi_2 \quad (2.51)$$

$$k = n \sin \Phi \cos \varphi_2 \quad (2.52)$$

$$l = n \cos \Phi \quad (2.53)$$

$$u = n'(\cos \varphi_1 \cos \varphi_2 - \sin \varphi_1 \sin \varphi_2 \cos \Phi) \quad (2.54)$$

$$v = n'(-\cos \varphi_1 \sin \varphi_2 - \sin \varphi_1 \cos \varphi_2 \cos \Phi) \quad (2.55)$$

$$w = n' \sin \varphi_1 \sin \Phi \quad (2.56)$$

By inversion of these relations one obtains the EULER angles, expressed in terms of the MILLER indices (hkl) [uvw]:

$$\Phi = \arccos \frac{l}{\sqrt{h^2 + k^2 + l^2}} \quad (2.57)$$

$$\varphi_2 = \arccos \frac{k}{\sqrt{h^2 + k^2}} = \arcsin \frac{h}{\sqrt{h^2 + k^2}} \quad (2.58)$$

$$\varphi_1 = \arcsin \left[\frac{w}{\sqrt{u^2 + v^2 + w^2}} \cdot \sqrt{\frac{h^2 + k^2 + l^2}{h^2 + k^2}} \right] \quad (2.59)$$

The EULER angles for a series of low-index orientations were calculated with the help of these relations. They are represented in Figure 2.20 for the case of cubic crystal symmetry and orthorhombic sample symmetry. The low-index orientations are represented in orientation space in Figure 2.21. The corresponding representation for the second variant of the EULER angles $\Psi\Theta\Phi$ was originally given by DAVIES, GOODWILL and KALLEND⁹⁵, who also gave the corresponding representation for hexagonal crystal symmetry⁹⁸.

The rotation was expressed by the rotation axis \mathbf{d} and the associated rotation angle ω in Section 2.1.2. This representation can easily be converted into the matrix representation. For this one first carries out a rotation which transforms the Z-axis into the direction \mathbf{d} (the rotation axis); then one rotates about the Z-axis through the angle ω ; and, finally, one performs the inverse of the first rotation:

$$g(\mathbf{d}, \omega) = g^{-1}(Z \rightarrow \mathbf{d}) \cdot g_{\omega}^Z \cdot g(Z \rightarrow \mathbf{d}) \quad (2.60)$$

In matrix notation this relation reads

$$g(\mathbf{d}, \omega) = \begin{bmatrix} \dots & d_1 \\ \dots & d_2 \\ \dots & d_3 \end{bmatrix} \cdot \begin{bmatrix} \cos \omega & \sin \omega & 0 \\ -\sin \omega & \cos \omega & 0 \\ 0 & 0 & 1 \end{bmatrix} \cdot \begin{bmatrix} \dots & \dots & \dots \\ d_1 & d_2 & d_3 \end{bmatrix} \quad (2.61)$$

The rotation which transforms the Z-axis into the \mathbf{d} direction is represented by a matrix in which the last row consists of the components of the vector \mathbf{d} (see Figure 2.18), while the rotation through the angle ω about the Z-axis is given by the matrix of equation (2.47). Since the result can only depend on the components of \mathbf{d} and the rotation angle ω , the six other components of the first and last matrices must not appear in the result. They are therefore not written out. If one

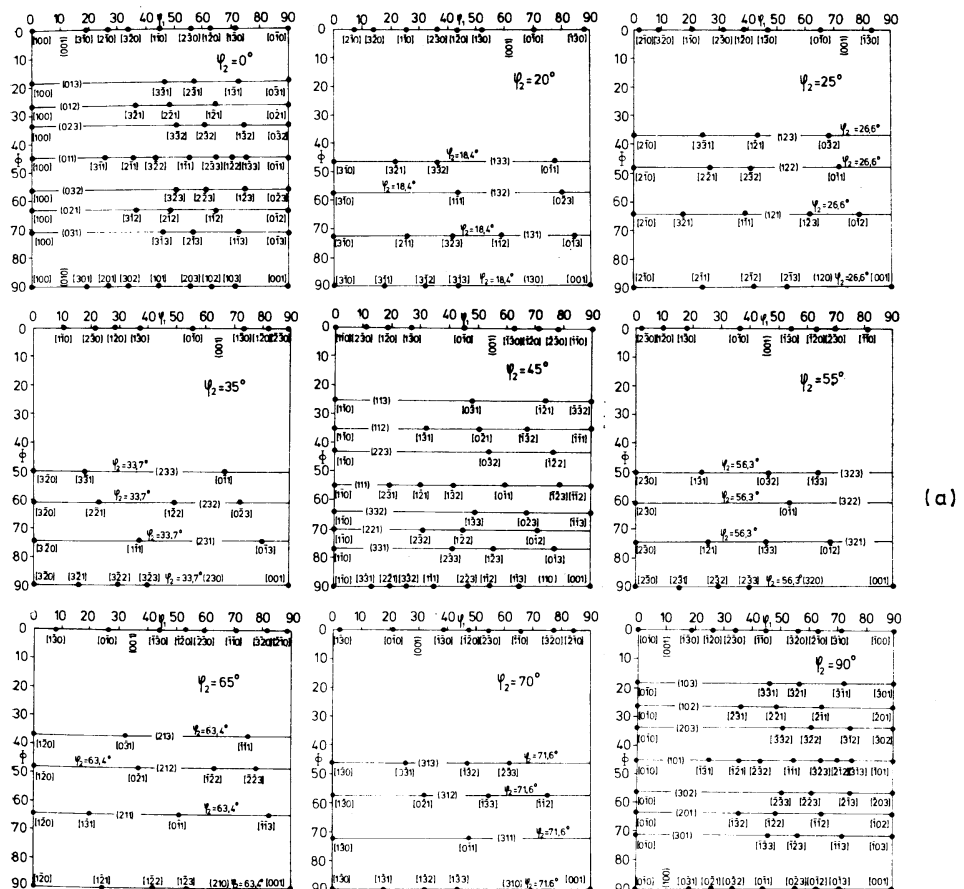
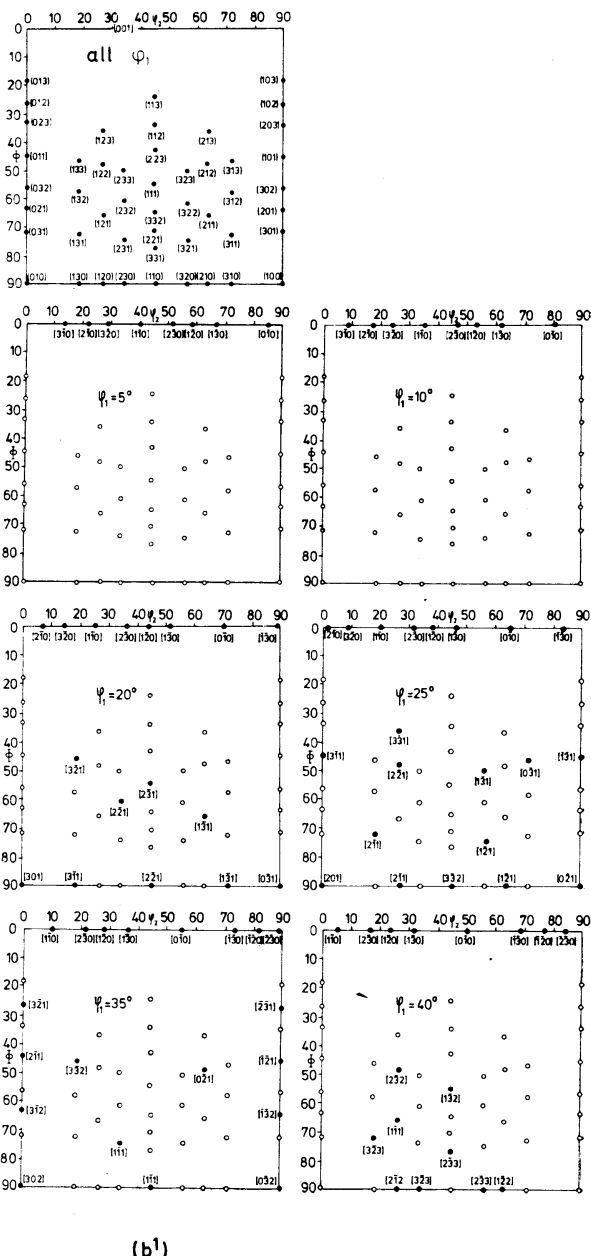
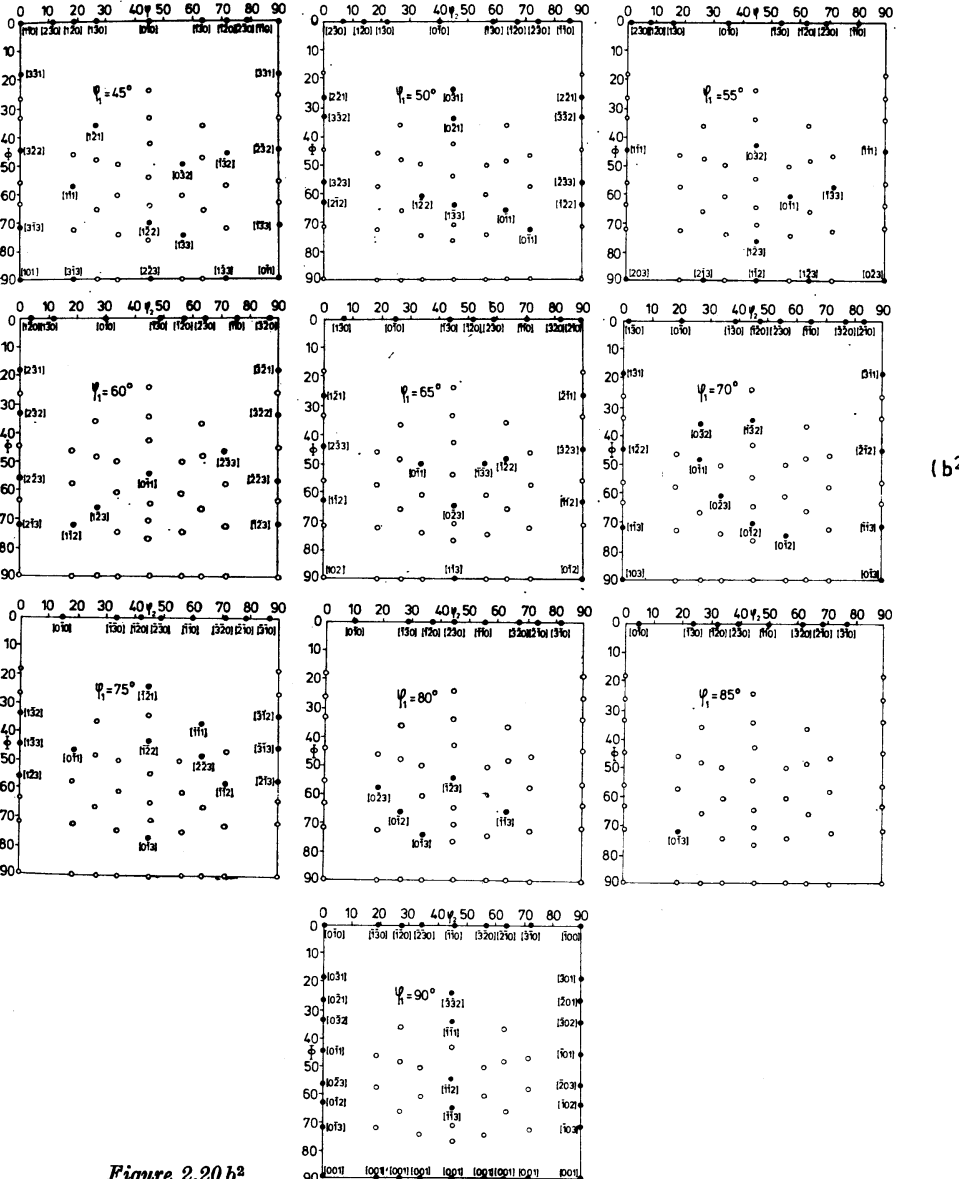


Figure 2.20 The position of some low index orientations in the space of the EULER angles $\varphi_1 \Phi \varphi_2$ ¹⁷¹ (see also reference 95). (a) $\varphi_2 = \text{constant sections}$. Only sections in multiples of $\Delta \varphi_2 = 5^\circ$ are shown. The orientation points are indicated in the nearest neighbouring φ_2 section. The actual φ_2 values are given. (b) $\varphi_1 = \text{constant sections}$. The indices (hkl) of the rolling plane are the same in all φ_1 sections. They are given in the first part of the figure. Only the indices $[uvw]$ of the rolling direction are recorded in the second part of the figure and indeed in their nearest neighbouring φ_1 section. The exact φ_1 values can be taken from the φ_2 sections

(b¹)Figure 2.20 b¹

multiplies the three matrices according to equation (2.23), one thus obtains

$$g(\vartheta\psi\omega) = \begin{bmatrix} (1 - d_1^2) \cos \omega + d_1^2 & d_1 d_2 (1 - \cos \omega) + d_3 \sin \omega & d_1 d_3 (1 - \cos \omega) - d_2 \sin \omega \\ d_1 d_2 (1 - \cos \omega) - d_3 \sin \omega & (1 - d_2^2) \cos \omega + d_2^2 & d_2 d_3 (1 - \cos \omega) + d_1 \sin \omega \\ d_1 d_3 (1 - \cos \omega) + d_2 \sin \omega & d_2 d_3 (1 - \cos \omega) - d_1 \sin \omega & (1 - d_3^2) \cos \omega + d_3^2 \end{bmatrix} \quad (2.62)$$

Figure 2.20 b²

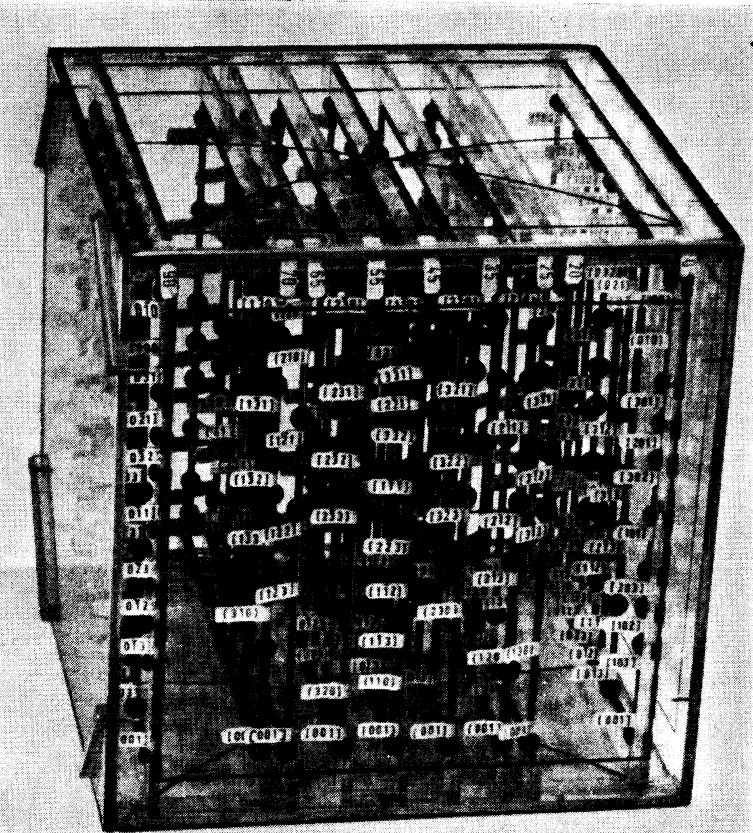


Figure 2.21 Plexiglas model showing some low-index orientations in the EULER space

In equation (2.62)

$$d_1 = \sin \vartheta \cos \psi \quad (2.63)$$

$$d_2 = \sin \vartheta \sin \psi \quad (2.64)$$

$$d_3 = \cos \vartheta \quad (2.65)$$

are the direction cosines of the rotation axis²³². In order to obtain the relations between the EULER angles ($\varphi_1 \Phi \varphi_2$) and the angles $\vartheta \psi \omega$, one equates the rotation equation (2.62) with the rotation equation (2.2) expressed by means of EULER angles:

$$g(\mathbf{d}, \omega) = g_{x_1}^{Z'} \cdot g_{\phi}^{X'} \cdot g_{x_2}^Z \quad (2.66)$$

From this follows directly by multiplication with the corresponding inverse rotations:

$$g_{\omega}^{Z'} = g_{-\Phi}^{X'} \cdot g_{-\omega}^{Z'} \cdot g(d, \omega) \quad (2.67)$$

$$g_{\phi}^{X'} = g_{-\omega_1}^{Z'} \cdot g(\mathbf{d}, \omega) \cdot g_{-\omega_2}^{Z'} \quad (2.68)$$

$$q_{\infty}^{Z'} = q(\mathbf{d}, \omega) \cdot q_{-\omega}^{Z'} \cdot q_{-\Phi}^{X'} \quad (2.69)$$

According to equations (2.47)–(2.49), either one component ($\cos \Phi$) or two components ($\cos \varphi$, $\sin \varphi$) are sufficient for determination of the angles $\varphi_1 \Phi \varphi_2$ from the corresponding matrices. The result was given by POSPIECH²³² in the following form:

$$\sin \frac{\omega}{2} \cdot \sin \vartheta = \sin \frac{\Phi}{2} \quad (2.70)$$

$$\cos \frac{\omega}{2} = \cos \frac{\varPhi}{2} \cos \frac{\varphi_1 + \varphi_2}{2} \quad (2.71)$$

$$\psi = \frac{1}{2} (\varphi_1 - \varphi_2) \quad (2.72)$$

If one compares the orientation matrix (2.30) with that of the EULER angles (equation 2.50), one thus obtains relations between the angles in the (100) pole figure $\Phi_{100} \gamma_{100} \Phi_{010} \gamma_{010} \Phi_{001} \gamma_{001}$ of the three crystal directions [100] [010] [001] and the EULER angles $\varphi_1 \Phi \varphi_2$. Comparison of the third row immediately yields

$$\Phi_{001} = \Phi; \quad \gamma_{001} = \varphi_1 - \frac{\pi}{2} \quad (2.73)$$

From the third column one further immediately obtains

$$\Phi_{100} = \arccos [\sin \varphi_2 \quad \sin \Phi] \quad (2.74)$$

$$\Phi_{010} = \arccos [\cos \varphi_2 \quad \sin \Phi] \quad (2.75)$$

One can obtain corresponding expressions for the angles γ_{100} and γ_{010} by comparison of the remaining four matrix elements. It is, however, simpler to derive them from *Figure 2.22*, which describes the orientation of the poles of the directions $X' = [100]$, $Y' = [010]$, $Z' = [001]$ in stereographic projection (pole figure). By application of the law of sines or cosines of spherical trigonometry to the triangle $AX'Z$ one easily obtains

$$\gamma_{100} = \arcsin \left[\frac{\sin \varphi_2 \cos \Phi}{\sin \Phi_{100}} \right] + \varphi_1 = \arccos \left[\frac{\cos \varphi_2}{\sin \Phi_{100}} \right] + \varphi_1 \quad (2.76)$$

Similarly, from the triangle $AY'Z$ there results

$$\gamma_{010} = \arcsin \left[\frac{\cos \varphi_2 \cos \Phi}{\sin \Phi_{100}} \right] + \varphi_1 = \arccos \left[\frac{\sin \varphi_2}{\cos \Phi_{100}} \right] + \varphi_1 \quad (2.77)$$

From equations (2.73)–(2.75) the inversions of these relations also follow directly, which express the EULER angles in terms of the polar coordinates of the (100) pole figure:

$$\varphi_1 = \gamma_{001} + \frac{\pi}{2} \quad (2.78)$$

$$\Phi = \Phi_{001} \quad (2.79)$$

$$\varphi_2 = \arcsin \left[\frac{\cos \Phi_{100}}{\sin \Phi_{001}} \right] = \arccos \left[\frac{\cos \Phi_{010}}{\sin \Phi_{001}} \right] \quad (2.80)$$

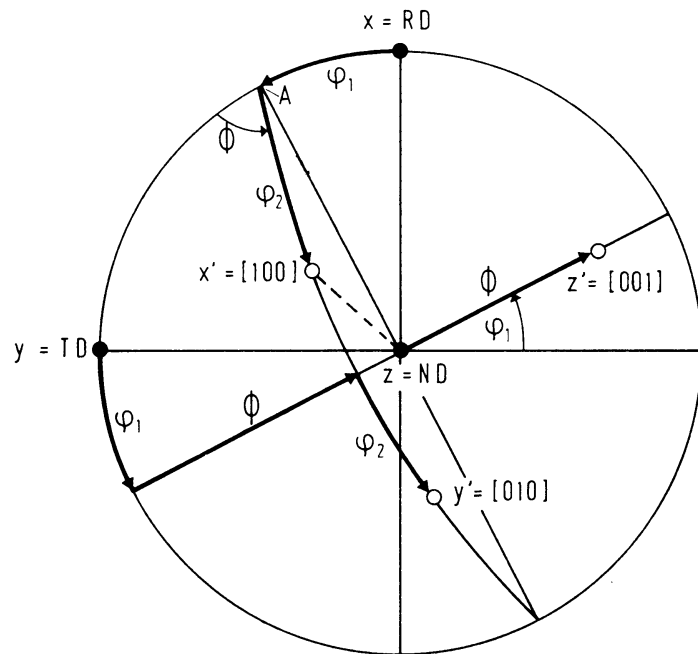


Figure 2.22 The orientation of the crystal directions $X' = [100]$, $Y' = [010]$, $Z' = [001]$ in the stereographic projection in the sample coordinate system (pole figure) expressed by the EULER angles $\varphi_1 \Phi \varphi_2$

The orientation of the sample directions $X = RD$, $Y = TD$, $Z = ND$ in stereographic projection (inverse pole figures) is represented in Figure 2.23(a, b). The relation between the coordinates in the inverse pole figure $\Phi_{RD} \beta_{RD} \Phi_{TD} \beta_{TD} \Phi_{ND} \beta_{ND}$ and the EULER angles similarly results by comparison of matrix (2.29) with that of the EULER angles (equation 2.50). It follows completely analogously that

$$\Phi_{ND} = \Phi; \quad \beta_{ND} = \frac{\pi}{2} - \varphi_2 \quad (2.81)$$

$$\Phi_{RD} = \arccos [\sin \varphi_1 \cdot \sin \Phi] \quad (2.82)$$

$$\Phi_{TD} = \arccos [-\cos \varphi_1 \cdot \sin \Phi] \quad (2.83)$$

The two remaining angles, β_{RD} and β_{TD} , result simply from the triangles $X'Z'A$ and $-X'Z'B$ in Figure 2.24:

$$\beta_{RD} = -\arcsin \left[\frac{\sin \varphi_1 \cos \Phi}{\sin \Phi_{RD}} \right] - \varphi_2 = \arccos \left[\frac{\cos \varphi_1}{\sin \Phi_{RD}} \right] - \varphi_2 \quad (2.84)$$

$$\beta_{TD} = \arcsin \left[\frac{\cos \varphi_1 \cos \Phi}{\sin \Phi_{TD}} \right] - \varphi_2 = \pi + \arccos \left[\frac{\sin \varphi_1}{\sin \Phi_{TD}} \right] - \varphi_2 \quad (2.85)$$

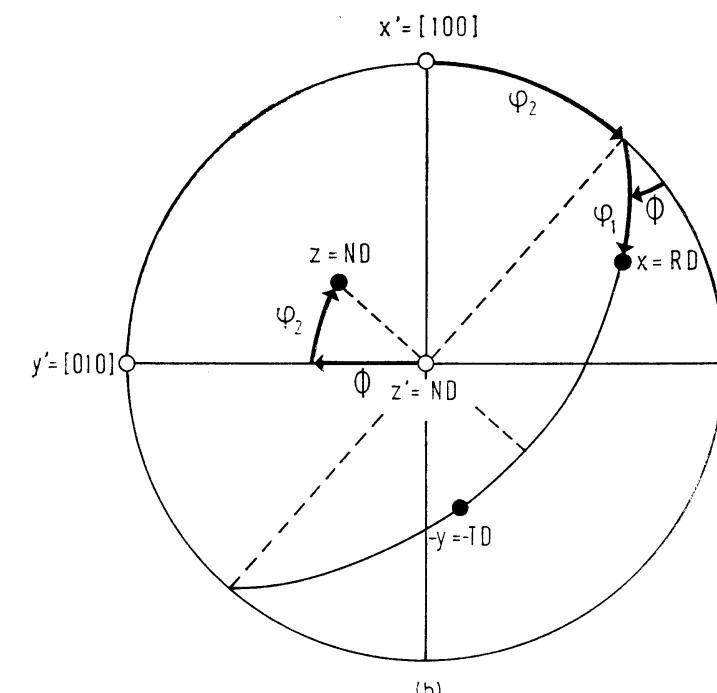
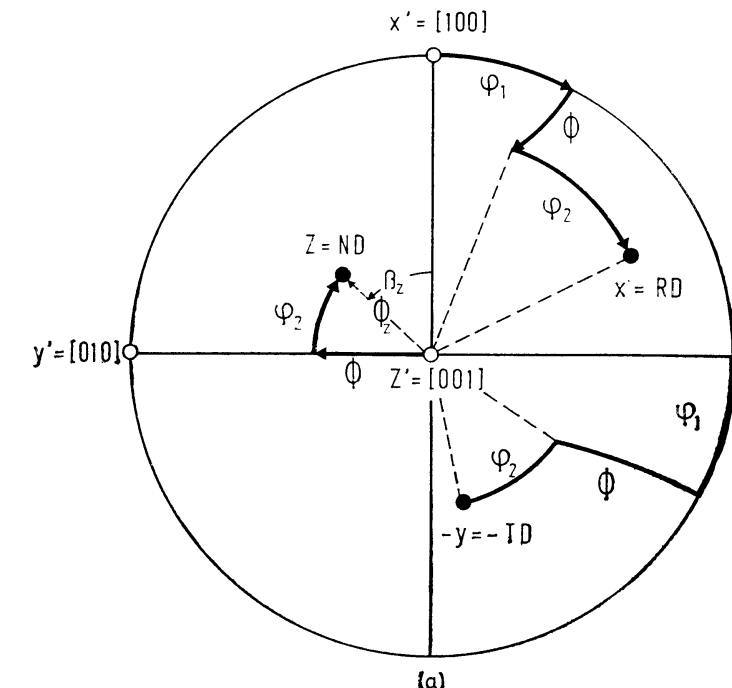


Figure 2.23 The orientation of the sample direction $X = RD$, $Y = TD$, $Z = ND$ in the stereographic projection in the crystal coordinate system (inverse pole figure) expressed by the EULER angles $\varphi_1 \Phi \varphi_2$

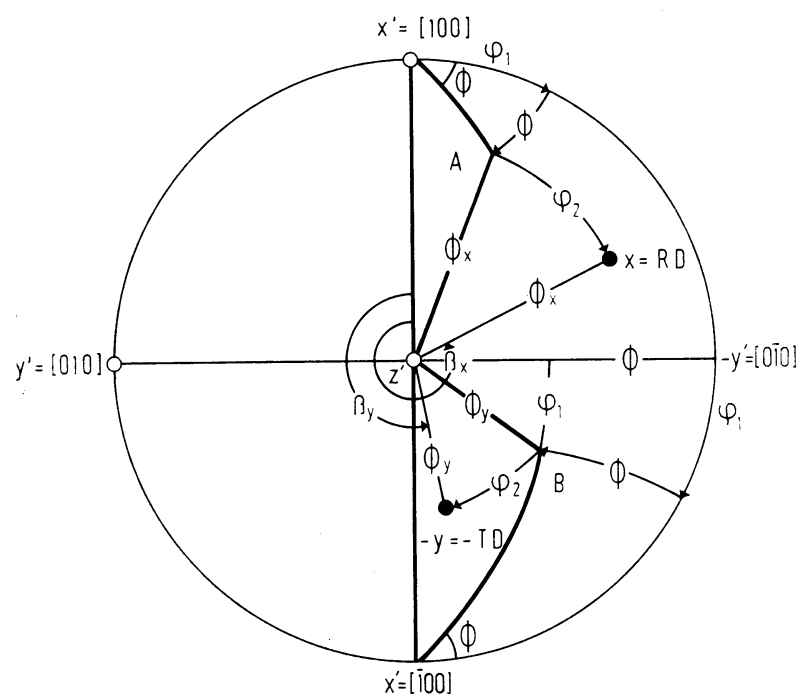


Figure 2.24 Relation of the angles $\Phi_X \beta_X \Phi_Y \beta_Y$ with the EULER angles $\varphi_1 \Phi \varphi_2$

By inversion of equations (2.81)–(2.83) one further obtains the **EULER** angles expressed by means of the polar coordinates of the inverse pole figure:

$$\varphi_1 = \arcsin \left[\frac{\cos \Phi_{RD}}{\sin \Phi_{ND}} \right] = \arccos \left[\frac{\cos \Phi_{TD}}{\sin \Phi_{ND}} \right] \quad (2.86)$$

$$\Phi \equiv \Phi_{ND} \quad (2.87)$$

$$\varphi_2 = \frac{\pi}{2} - \beta_{\text{ND}} \quad (2.88)$$

The representation discussed in Section 2.1.3 of a rotation by specification of the orientation of a crystal direction $[hkl]$ by two angles $\alpha\beta$ as well as a rotation angle γ is related in a simple manner to the EULER angles if one sets

$$[hkl] = [001] = Z' \quad (2.89)$$

The angles denoted there by $\alpha\beta$ are then the angles $\Phi_{001} \gamma_{001}$. According to equation (2.73), they are identical with the EULER angles Φ and φ_1 except for the difference of $\frac{\pi}{2}$. If one further chooses the zero point for the rotation angle γ so that it lies in the point of intersection of the XY plane with the $X'Y'$ plane, it is thus identical with the third EULER angle φ_2 . In this case the representation of a rotation

by a crystal direction $[hkl]$ and the three angles $\alpha\beta\gamma$ is identical with that by means of the EULER angles $\varphi_1\Phi\varphi_2$. The same is true for the representation by a sample direction y and the three angles $\alpha'\beta'\gamma'$, which was discussed in Section 2.1.4. If one chooses

$$y = ND = Z \quad (2.90)$$

the orientation angles $\alpha'\beta'$ of this direction are thus the angles $\Phi_{ND}\beta_{ND}$. According to equation (2.81), they are practically identical with the EULER angles Φ and φ_2 . If, further, one then measures the third angle γ' with respect to the intersection direction of the $X'Y'$ plane with the XY plane, γ' is thus identical with φ_1 and the representation thus specified by a sample direction and the three angles $\alpha'\beta'\gamma'$ is identical with the representation by EULER angles.

WILLIAMS's orientation parameters²⁹⁹ (*Figure 2.13*) belong in the last group, except that the third orientation parameter β is not measured with respect to the $X'Y'$ plane but with respect to the $Y'Z'$ plane. The following relations thereby result for WILLIAMS's coordinates in terms of the EULER angles:

$$\rho^W = \Phi_{ND} = \Phi \quad (2.91)$$

$$\alpha^W = \frac{\pi}{2} - \beta_{ND} = \varphi_2 \quad (2.92)$$

$$\beta^W = \varphi_1 - \frac{\pi}{2} + \arctan(\tan \varphi_2 \cos \Phi) \quad (2.93)$$

One obtains relations between RUER's coordinates ψ^R , ω^R , ϱ^R and the EULER angles from *Figure 2.15*. One obtains the EULER angle Φ from the angles ψ^R and ω^R :

$$\Phi = \arctan \frac{\tan \omega^R}{\cos \psi^R} \quad (2.94)$$

The angle φ_3 results directly by comparison with Figure 2.23:

$$\varphi_2 = \pi - \psi^R \quad (2.95)$$

Finally, the angle φ_1 according to Figure 2.23(b) differs from RUER's angle ϱ by the angle ψ :

$$\varphi_1 = \rho^R - \psi^R \quad (2.96)$$

2.1.10. The Invariant Measure

For the representation of the crystal orientation by the rotation g , we begin with the crystal coordinate system K_B coinciding with the sample coordinate system K_A . It is then brought into the orientation which describes the orientation of the crystal by the rotation g . We can, of course, also begin with an arbitrary different orientation of the crystal coordinate system, which we describe by the

rotation g_0 . From the orientation g_0 we then rotate the crystal coordinate system through g' and describe the orientation of the crystal by g' . This description is related to the original description in terms of the rotation g by the relation (see Section 2.2)

$$g = g' \cdot g_0 \quad (2.97)$$

If we select the same parameters for g and g' — perhaps the EULER angles $\varphi_1 \Phi \varphi_2$ — equation (2.97) thus represents a transformation in the EULER orientation space. A point with the coordinates $g = \{\varphi_1 \Phi \varphi_2\}$ may have the coordinates $g' = \{\varphi'_1 \Phi' \varphi'_2\}$ in the transformed representation. If we consider a volume element which is given by the limits φ_1 to $\varphi_1 + d\varphi_1$, Φ to $\Phi + d\Phi$ and φ_2 to $\varphi_2 + d\varphi_2$, the volume of this element is, in general, not equal to the volume of the transformed element

$$d\varphi'_1 d\Phi' d\varphi'_2 \neq d\varphi_1 d\Phi d\varphi_2 \quad (2.98)$$

The transformation is combined with a distortion. It is therefore appropriate to introduce an invariant measure $I(\varphi_1 \Phi \varphi_2)$ into the orientation space which remains unchanged after an arbitrary transformation

$$I(\varphi'_1 \Phi' \varphi'_2) d\varphi'_1 d\Phi' d\varphi'_2 = I(\varphi_1 \Phi \varphi_2) d\varphi_1 d\Phi d\varphi_2 \quad (2.99)$$

For the EULER angles this measure is

$$I(\varphi_1 \Phi \varphi_2) = \sin \Phi \quad (2.100)$$

If we also add the normalization factor $\frac{1}{8\pi^2}$, for the orientation element in EULER space we can thus set

$$dg = \frac{1}{8\pi^2} \sin \Phi d\varphi_1 d\Phi d\varphi_2 \quad (2.101)$$

This orientation element is transformed by the transformation into

$$dg' = \frac{1}{8\pi^2} \sin \Phi' d\varphi'_1 d\Phi' d\varphi'_2 \quad (2.102)$$

and it is true that

$$dg = dg' \quad (2.103)$$

One obtains a clear idea of the importance of the invariant measure if one thinks of a random distribution of very many orientations. The number of orientations, dn , which fall in a given volume element, $d\varphi_1 d\Phi d\varphi_2$, is then proportional to I (*Figure 2.25*):

$$dn = I(\varphi_1 \Phi \varphi_2) d\varphi_1 d\Phi d\varphi_2 \quad (2.104)$$

One can thus define the invariant measure with the aid of a random distribution

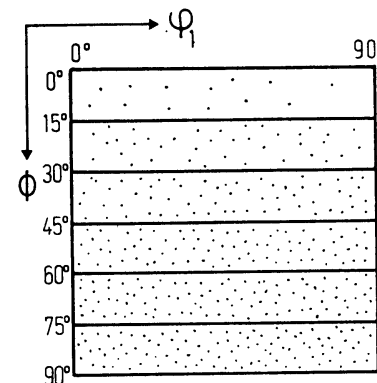


Figure 2.25 On the definition of the invariant measures by a random orientation distribution in the EULER space $\varphi_1 \Phi \varphi_2$

of orientations by the number of orientation points which fall in the interval $d\varphi_1 d\Phi d\varphi_2$:

$$I(\varphi_1 \Phi \varphi_2) = \frac{dn}{d\varphi_1 d\Phi d\varphi_2} \quad (2.105)$$

If we introduce instead of the EULER angle Φ the orientation parameter

$$\zeta = \cos \Phi \quad (2.106)$$

then

$$d\zeta = \sin \Phi d\Phi \quad (2.107)$$

In the orientation space $\varphi_1 \zeta \varphi_2$ the orientation element takes on the form

$$dg = \frac{1}{8\pi^2} d\zeta d\varphi_1 d\varphi_2 \quad (2.108)$$

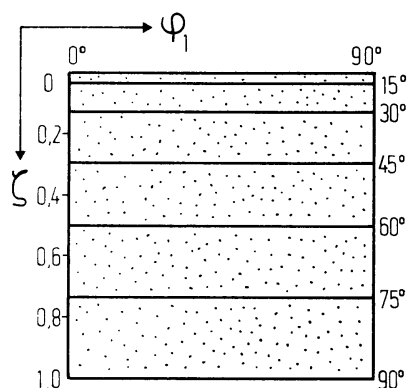
and the invariant measure is

$$I(\varphi_1 \zeta \varphi_2) \equiv 1 \quad (2.109)$$

In this orientation space a random orientation distribution is represented by a constant density of points in each orientation element ($d\zeta d\varphi_1 d\varphi_2$), as is shown in *Figure 2.26*.

If we go from a representation by $\varphi_1 \zeta \varphi_2$ to an arbitrary different representation by three other orientation parameters $\alpha \beta \gamma$, the volume element $d\varphi_1 d\zeta d\varphi_2$ is thus transformed into the volume element $(d\alpha d\beta d\gamma)$, the volume of which is related to the volume of $(d\varphi_1 d\zeta d\varphi_2)$ by the functional determinant

$$(d\alpha d\beta d\gamma) = \frac{\partial(\alpha, \beta, \gamma)}{\partial(\varphi_1, \zeta, \varphi_2)} (d\varphi_1 d\zeta d\varphi_2) \quad (2.110)$$

Figure 2.26 Random orientation distribution in the orientation space ($\varphi_1 \zeta \varphi_2$)

Hence, the invariant measure in the space $\alpha\beta\gamma$ according to equations (2.99) and (2.109) is given by

$$I(\alpha\beta\gamma) = 1 : \begin{vmatrix} \frac{\partial \alpha}{\partial \varphi_1} & \frac{\partial \alpha}{\partial \zeta} & \frac{\partial \alpha}{\partial \varphi_2} \\ \frac{\partial \beta}{\partial \varphi_1} & \frac{\partial \beta}{\partial \zeta} & \frac{\partial \beta}{\partial \varphi_2} \\ \frac{\partial \gamma}{\partial \varphi_1} & \frac{\partial \gamma}{\partial \zeta} & \frac{\partial \gamma}{\partial \varphi_2} \end{vmatrix} = \begin{vmatrix} \frac{\partial \varphi_1}{\partial \alpha} & \frac{\partial \varphi_1}{\partial \beta} & \frac{\partial \varphi_1}{\partial \gamma} \\ \frac{\partial \zeta}{\partial \alpha} & \frac{\partial \zeta}{\partial \beta} & \frac{\partial \zeta}{\partial \gamma} \\ \frac{\partial \varphi_2}{\partial \alpha} & \frac{\partial \varphi_2}{\partial \beta} & \frac{\partial \varphi_2}{\partial \gamma} \end{vmatrix} \quad (2.111)$$

For the representation by the coordinates $\vartheta\psi\omega$ of the rotation axis and rotation angle one obtains (see, for example, reference 232)

$$dg = \frac{1}{\pi^2} \sin^2 \frac{\omega}{2} \sin \vartheta d\vartheta d\psi d\omega \quad (2.112)$$

For these coordinates a representation with constant invariant measure was given by POSPIECH.

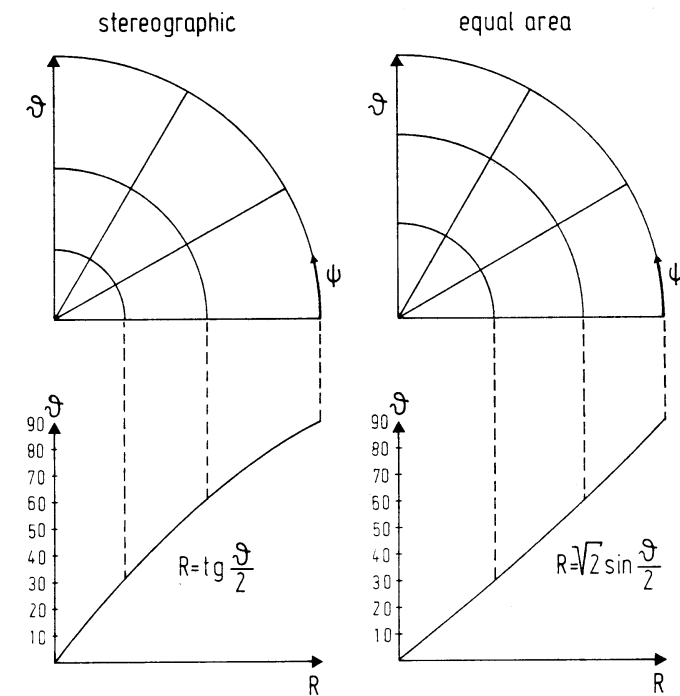
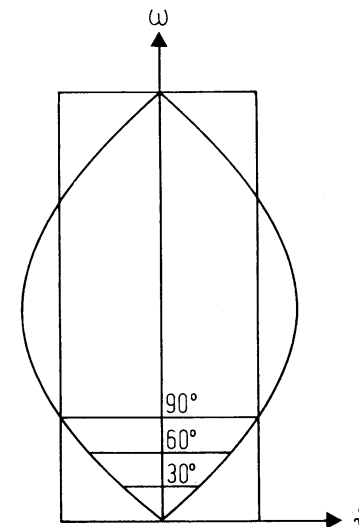
For this purpose the orientation of the rotation axis is shown not in stereographic projection but in equal area projection. In stereographic projection the relation between the angle ϑ and the radius R is given by (Figure 2.27)

$$R \sim \tan \frac{\vartheta}{2} \quad (2.113)$$

while in equal area projection this relation has the form (Figure 2.27)

$$R \sim \sqrt{2} \sin \frac{\vartheta}{2} \quad (2.114)$$

Starting with a cylindrical orientation space similar to that shown in Figure 2.9 but in equal area projection, the radius of the constant $-\omega$ section is multiplied

Figure 2.27 The stereographic and the equal area projections. The scale of the angle ϑ is given by $\tan \frac{\vartheta}{2}$ and $\sqrt{2} \sin \frac{\vartheta}{2}$, respectivelyFigure 2.28 Longitudinal section of the orientation space $\vartheta\psi\omega$ in invariant measure²³²

by the factor $\sin(\omega/2)$ (*Figure 2.28*). Thus the surface element in this section assumes the factor $\sin^2(\omega/2)$ and the orientation space so constructed is a space of constant invariant measure (see reference 232 and *Figure 11.48*).

2.2. Some Properties of Rotations

If two rotations g_1 and g_2 are carried out in succession, the result is also a rotation g . One writes this in the form

$$g = g_2 \cdot g_1 \quad (2.115)$$

In the mathematical sense, the rotations form a group. For each rotation g , the group also contains a rotation inverse to g or counter rotation g^{-1} . This is expressed with the EULER angles as follows:

$$g^{-1} = \{\pi - \varphi_2, \Phi, \pi - \varphi_1\} \quad (2.116)$$

If the three EULER angles are zero, then the coordinate system K_B coincides with the system K_A . The same is true if only $\varphi_1 + \varphi_2$ is zero. Thus the unity element of the rotation group has the form

$$e = \{0, 0, 0\} = \{\varphi_1, 0, -\varphi_1\} \quad (2.117)$$

We have already noted that every rotation can be described by specification of the rotation axis and the appropriate rotation angle ω . The angle ω specifies the absolute value of the rotation. We write this

$$\omega = |g| \quad (2.118)$$

We shall consider later distribution functions which depend only on the absolute value of the rotation. A rotation g may possess a rotation axis d , the rotation angle being ω . A second rotation g' may rotate the space together with the first axis in such a way that the direction d will be transformed into the direction d' . Then

$$g'^{-1} \cdot g \cdot g' = \tilde{g} \quad (2.119)$$

is a rotation through the angle ω , but about the rotation axis d' . If we permit g' to range over all possible rotations, we thus obtain all rotations with the rotation angle ω about arbitrary rotation axes, and thus all rotations, which have the same absolute value of the rotation as the rotation g :

$$|\tilde{g}| = |g'^{-1} \cdot g \cdot g'| = |g| = \omega \quad (2.120)$$

These constitute a class of conjugate rotations.

2.3. Ambiguity of Rotation as a Consequence of Crystal and Specimen Symmetry

The orientation of a crystal in a polycrystalline sample is uniquely characterized by specification of the rotation g . On the other hand, the rotation g is not uniquely fixed by the orientation of the crystal. One recognizes this in the following way. If one has the crystal fixed coordinate system somehow fixed in the crystal, one

can thus carry out a series of rotations, which express the crystal symmetry. The positions thereby obtained can not be distinguished from the initial position because of the crystal symmetry. The coordinate system K_B has, however, different orientations relative to the sample fixed coordinate system K_A . One can also express this as follows: For the determination of the crystal fixed coordinate system many crystallographically indistinguishable possibilities exist. In the cubic system, for example, one can choose for the first coordinate axis any of three cube edges in either of two directions. For the second axis there exist in each case four possibilities, so that in this case one can fix the coordinate system K_B in 24 different, but symmetrically equivalent, ways.

In addition to crystal symmetry, there can also be symmetries in the sample fixed coordinate system. Thus, for sheet the rolling direction, transverse direction and normal direction are generally twofold rotation axes — i.e. crystallites, whose orientations differ from one another by such a rotation, occur with equal frequency. We shall also consider them as symmetrically equivalent orientations (equivalent with respect to the sample symmetry).

In other words, this means that the sample coordinate system can also be chosen in different but symmetrically equivalent ways.

There thus exists a whole series of different rotations, g_α , which lead from one of the possible orientations of the sample coordinate system to one of the possible orientations of the crystal coordinate system. All these rotations represent symmetrically equivalent orientations, which are either completely indistinguishable or which at least occur with equal probability, so that we shall also regard them as equivalent (*Figure 2.29*).

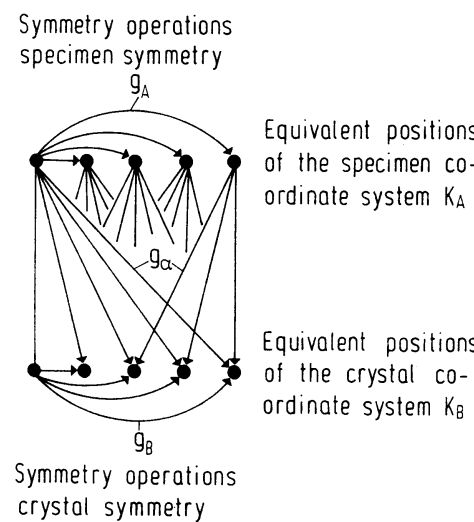


Figure 2.29 On the definition of the symmetrically equivalent rotations g_α , which define the orientation g

One orientation can thus be represented by many points in EULER space, which are all symmetrically equivalent. One can therefore divide EULER space into regions which contain only one of the symmetrically equivalent points (see, e.g., Section 14.7.6, *Figure 14.4*). One thus obtains the so-called asymmetric regions in EULER space. They are transformed into one another by the symmetry elements. Glide planes are also among the symmetry elements in EULER space, as is shown in Section 14.7.6. The orientation path between two points A and B in the EULER space is shown in *Figure 2.30*. If point B is replaced by its equivalent B' within the same asymmetric unit as point A, then the path AB' becomes discontinuous at the glide plane.

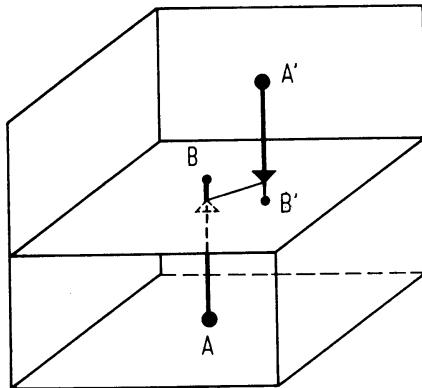


Figure 2.30 Discontinuity of the orientation path AB' which is the equivalent of the continuous path AB crossing the boundary of the asymmetric region in a glide plane

By crossing the region boundaries, closely spaced points are transformed into points widely separated from one another. Recognizing orientation relations can thereby be rendered very difficult. We shall therefore use all equivalent rotations, g_α , to describe an orientation g :

$$g = \{g_\alpha\} = \{g_1, g_2, g_3, \dots, g_z\} \quad (2.121)$$

2.4. Orientation Distance

We now consider two orientations g and g' , which are characterized by the equivalent orientations $\{g_\alpha\}$ and $\{g'_\beta\}$. The orientation difference between g' and g can then be described by the rotations $\Delta g_{\alpha\beta}$, which lead from an orientation g_α to an orientation g'_β :

$$\Delta g_{\alpha\beta} = \{g'_\beta \cdot g_\alpha^{-1}\} \quad (2.122)$$

Among these rotations there is at least one with the smallest rotation angle, ω_{\min} . We shall then denote this smallest rotation angle ω_{\min} as the orientation distance between g and g' :

$$\omega_{\min} = |g' \cdot g^{-1}| \quad (2.123)$$

When we are concerned with large orientation distances, the rotation angles $\omega_{\alpha\beta}$ belonging to different α and β are of the same order of magnitude. The selection of the smallest among them then naturally is somewhat arbitrary. For small orientation distances, to which we will chiefly apply this idea, however, this is not the case. Apart from certain exceptions, in the neighbourhood of a mirror plane, one angle $\omega_{\alpha\beta}$ is then essentially smaller than the rest. If one continuously shifts one of two orientations g or g' into the other, the orientation distance defined by equation (2.123) decreases continuously towards zero. We shall further remark that the orientation difference, as it is defined here, is not identical with that defined by DUNN¹¹⁷.

2.5. Orientation for Rotational Symmetry

In some cases — e.g. for wires and fibres as well as for the orientation distribution of the surface — for the sample fixed coordinate system only a single unique direction, the fibre axis or the surface normal, exists. The choice of the other two axes is completely arbitrary. If, for example, one rotates a crystallite about the surface normal, the same crystallographic plane remains in the sample surface. This rotation thus does not change the ‘surface orientation’ of the crystallites. For wire and fibre textures all orientations which are related by rotations about the fibre axis occur with statistically equal frequency, so that in these cases the orientation distribution is independent of the rotation angle φ_1 about this axis. In these cases only the orientation of the unique sample direction relative to the crystal fixed coordinate system is of importance. It therefore suffices to specify with which crystal direction the unique sample direction coincides. The crystal direction \mathbf{h} can be specified by the components of a unit vector

$$\mathbf{h} = \{h_1, h_2, h_3\} \quad (2.124)$$

It is, however, often convenient to specify it in spherical angular coordinates (*Figure 2.31*):

$$\mathbf{h} = \{\Phi, \beta\} \quad (2.125)$$

The angle Φ is thus measured from the Z-axis of the crystal fixed coordinate system, while the zero point for the angle β is fixed by the X-axis. The angles Φ and β are related in a simple way to the EULER angles. If one places the Z-axis of the sample fixed coordinate system in the unique sample direction, the EULER angle Φ is identical with the angle denoted here by Φ , while the relation between the angles φ_2 and β is (compare *Figures 2.31* and *2.23*):

$$\beta = \frac{\pi}{2} - \varphi_2 \quad (2.126)$$

Finally, there are cases in which one is only interested in the orientation of a single direction of the crystallites relative to the sample fixed coordinate system, while a rotation about this axis plays no part. This is the case for pole figures,

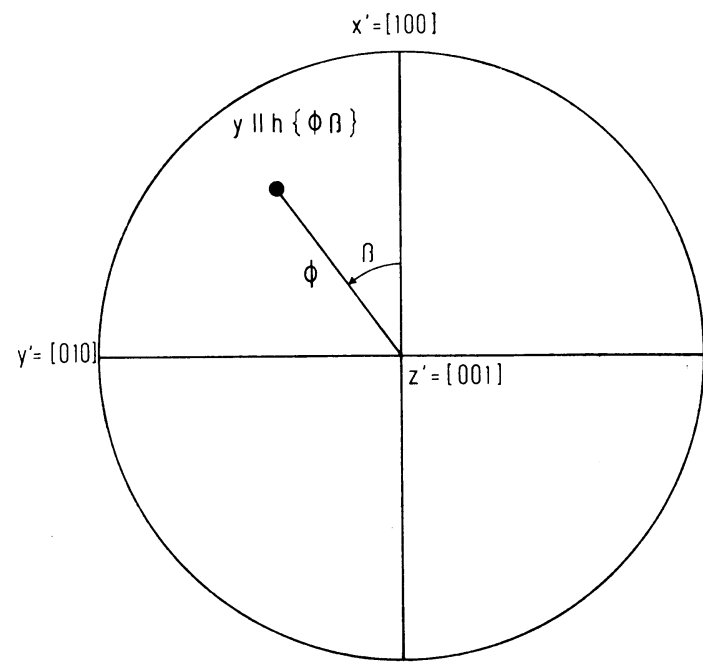


Figure 2.31 Orientation $\Phi\beta$ due to the presence of only one unique sample direction (fibre axis, outer surface normal)

for example, which are distribution functions of an individual crystal direction. We then need only specify the orientation of this direction relative to the sample fixed coordinate system. This can again be done by the components of a unit vector:

$$\mathbf{y} = \{y_1, y_2, y_3\} \quad (2.127)$$

In most cases we will, however, employ spherical angular coordinates (Figure 2.32):

$$\mathbf{y} = \{\Phi, \gamma\} \quad (2.128)$$

The angle Φ will be measured from the Z-axis of the sample fixed coordinate system, and the zero point of the angle γ is given by the X-axis. If we so choose the crystal fixed coordinate system that its Z-axis coincides with the unique crystal direction, the EULER angle Φ thus coincides with the angle here also denoted by Φ , while the relation between the angles φ_1 and γ is (compare Figures 2.32 and 2.22)

$$\gamma = \varphi_1 - \frac{\pi}{2} \quad (2.129)$$

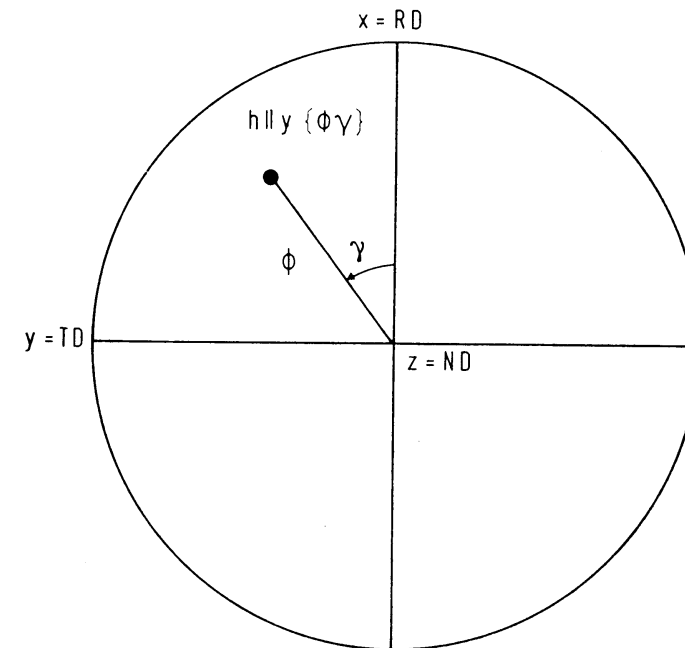


Figure 2.32 Orientation $\Phi\gamma$ of a unique crystal direction \mathbf{h} relative to the sample fixed coordinate system

3. Orientation Distributions

In a polycrystalline material crystallites of different shape, size and orientation are generally present. It can thus also occur that regions of different orientation are not separated from one another by unequivocally defined grain boundaries, but that, on the contrary, the orientation changes continuously from one point to another. If one desires to completely describe the crystal orientation of a polycrystalline material, one must specify the relevant orientation g for each point with coordinates x, y, z within the sample:

$$g = g(x, y, z) \quad (3.1)$$

If one writes g in EULER's angles, this means explicitly

$$\varphi_1 = \varphi_1(x, y, z); \quad \Phi = \Phi(x, y, z); \quad \varphi_2 = \varphi_2(x, y, z) \quad (3.2)$$

One thus requires three functions, each of three variables, which are also discontinuous at the grain boundaries. Such a representation of the crystal orientation is very complicated. We therefore observe that it has as yet been experimentally determined in only a very few cases (see, for example, references 139–141, 200–203), and that its mathematical treatment is so difficult that it is not practically applicable. One must therefore seek a simpler representation. One obtains such a representation if one considers only the orientation but not the position coordinates x, y, z of a volume element in the sample. If one denotes by dV the totality of all volume elements of the sample which possess the orientation g within the element of orientation dg (see equation 4.10), and by V the total sample volume, then an orientation distribution function $f(g)$, in this case the orientation distribution function of the volume, is defined by

$$\frac{dV}{V} = f(g) dg \quad (3.3)$$

If the sample consists of well-defined crystallites in whose interiors in each case exists a uniform orientation, one can thus also specify a similar distribution function for the numbers of crystallites⁴⁶:

$$\frac{dN}{N} = n(g) dg \quad (3.4)$$

One then obtains for the orientation dependence of the average crystallite size

$$v(g) = \frac{dV}{dN} = \frac{V}{N} \frac{f(g)}{n(g)} \quad (3.5)$$

These three orientation distribution functions indeed characterize the polycrystalline state quite well, but still do not completely suffice for all purposes. They do not, for example, take the grain shape into consideration. If there are well-defined grain boundaries, as is the case for recrystallized materials, which are separated by grain boundary surfaces, one can thus describe the shape of the crystals, if one specifies the course of all grain boundary surfaces, perhaps in the form

$$z = f(x, y) \quad (3.6)$$

where x, y, z are the coordinates of points of the grain boundary surface. The function $f(x, y)$ is thus, in general, a very complicated and multivalued function. The detailed description of the courses of the grain boundaries is, like the analogous description of the grain orientations by equation (3.2), generally far too complicated for practical application. One therefore also neglects the position x, y, z of the grain boundaries and specifies the frequency distribution of their orientations. Let the normal vector of a surface element of the grain boundary surface, with respect to a sample fixed coordinate system, be \mathbf{y} . If dF is the portion of the grain boundary surface whose normal vectors lie between \mathbf{y} and $\mathbf{y} + d\mathbf{y}$, and F is the total grain boundary surface, then

$$\frac{dF}{F} = \frac{1}{4\pi} \varphi(\mathbf{y}) d\mathbf{y} \quad (3.7)$$

defines the orientation distribution $\varphi(\mathbf{y})$ of the grain boundary surface in the sample fixed coordinate system.

The two-dimensional grain boundaries intersect one another in one-dimensional grain edges. The complete description

$$y = f_1(x); \quad z = f_2(x) \quad (3.8)$$

of the course of the three-dimensional networks of these edges is also much too complicated. One therefore again neglects the position x, y, z and specifies only the direction distribution. If the direction of an element of length is given by the vector \mathbf{y} in the sample fixed coordinate system, and if dL is the length of all grain edges whose directions lie between \mathbf{y} and $\mathbf{y} + d\mathbf{y}$, and L is the total grain edge length, then

$$\frac{dL}{L} = \frac{1}{4\pi} \psi(\mathbf{y}) d\mathbf{y} \quad (3.9)$$

defines the orientation distribution of the grain edges.

The distribution functions $\varphi(\mathbf{y})$ and $\psi(\mathbf{y})$ describe the orientation distributions of the grain boundary surfaces and grain edges, respectively, relative to the sample fixed coordinate system. One can, however, also specify the orientation of the grain boundaries and grain edges relative to the crystal fixed coordinate systems of the adjoining crystallites. If \mathbf{h} is the normal direction of a surface element of the grain boundary surface in the crystal fixed coordinate system, we thus have,

44 Orientation Distributions

analogous to equation (3.7),

$$\frac{dF}{F} = \frac{1}{4\pi} \varphi'(\mathbf{h}) d\mathbf{h} \quad (3.10)$$

The function $\varphi'(\mathbf{h})$ characterizes the orientation distribution of the grain surfaces in the crystal fixed coordinate system. Analogously, one obtains for the distribution of grain edges in the crystal coordinate system

$$\frac{dL}{L} = \frac{1}{4\pi} \psi'(\mathbf{h}) d\mathbf{h} \quad (3.11)$$

Since the grain boundary surface possesses different crystallographic orientations in the two neighbouring grains, each element of the grain boundary surface in equation (3.10) is to be counted twice. Correspondingly, each length element of the grain edge is to be counted three times in equation (3.11). If the grain boundary surfaces are planes and the grain edges straight lines, one can thus define $\varphi_A(\mathbf{y})$, $\psi_A(\mathbf{y})$, $\varphi'_A(\mathbf{h})$, $\psi'_A(\mathbf{h})$, number distributions analogous to $\varphi(\mathbf{y})$, $\psi(\mathbf{y})$, $\varphi'(\mathbf{h})$, $\psi'(\mathbf{h})$. The average size of the grain boundaries of the orientation \mathbf{y} is then defined by the ratio $\varphi(\mathbf{y})/\varphi_A(\mathbf{y})$. Correspondingly $\varphi'(\mathbf{h})/\varphi'_A(\mathbf{h})$ defines the average size of the grain boundaries of the crystallographic orientation \mathbf{h} . The average length of the grain edges of the direction \mathbf{y} is defined by $\psi(\mathbf{y})/\psi_A(\mathbf{y})$ and finally $\psi'(\mathbf{h})/\psi'_A(\mathbf{h})$ is the average length of the grain edges having the crystallographic direction \mathbf{h} .

The crystallites of different orientations need not be randomly distributed in space. There can, instead, exist a certain ‘short-range order’ between the orientations of neighbouring grains which can be described by a distribution function of the orientation differences of grains in the grain boundary. If the two adjacent grains in a grain boundary have orientations g_1 and g_2 , the orientation difference is thus given by

$$\Delta g = g_2 \cdot g_1^{-1} \quad (3.12)$$

If we denote by dF the grain boundary surface which has an orientation difference Δg within the orientation element $d\Delta g$, and if F is the total grain boundary surface, then

$$\frac{dF}{F} = W(\Delta g) d\Delta g \quad (3.13)$$

defines the distribution function of the orientation difference of the grain boundaries. Since the energy of a grain boundary depends on the orientation difference of the participating grains, these distribution functions play a role in, for example, continuous grain growth. The surface tensions in the grain boundaries are here almost in equilibrium with each other. The orientation-dependent differences of these tensions can, therefore, be indeed significant.

The orientation distribution functions considered so far refer to the interior of the sample. With thin foils, wire or powders, the outer surface can also play an important role. In these cases it is important to know the frequency with which

crystallographic planes lie in the outer surface. Let \mathbf{h} be the crystallographic direction which lies parallel to the surface normal. If dO is the region of outer surface which possesses an orientation between \mathbf{h} and $\mathbf{h} + d\mathbf{h}$, and O is the total outer surface,

$$\frac{dO}{O} = \frac{1}{4\pi} r(\mathbf{h}) d\mathbf{h} \quad (3.14)$$

thus defines the orientation distribution of the outer surface. The outer surface of a sample also plays an important role in a number of methods of measurement where from distributions in the outer surface those in the interior of the sample have to be deduced, as is the case, for example, in metallographic methods.

As previously mentioned, the orientation distribution functions are frequently of interest in the average value construction of orientation-dependent property functions. We first consider here the orientation-dependent energy. Thus, for example, the magnetization energy of ferromagnetic crystals depends on the orientation of the crystal with respect to the magnetic field:

$$E_{\text{mag.}} = E(g) \quad (3.15)$$

In a homogeneous magnetic field the magnetization energy is independent of a rotation of the crystal orientation about the field direction. It depends only on the direction \mathbf{h} of the magnetic field with respect to the crystal axes:

$$E_{\text{mag.}} = E(\mathbf{h}) \quad (3.16)$$

The energy of a grain boundary depends primarily on the orientation difference Δg of the two participating crystallites; to a lesser extent, however, it also depends on the crystallographic orientation of the grain boundary. We thus have for the grain boundary energy

$$E_G = E(\Delta g, \mathbf{h}) \quad (3.17)$$

The outer surface energy can likewise be orientation dependent:

$$E_0 = E(\mathbf{h}) \quad (3.18)$$

For example, the different orientation dependence of the outer surface energy in different atmospheres plays a decisive role in the case of the formation of certain textures in thin foils. Moreover, a whole series of physicochemical properties — e.g. solution rate, electronic work function, potential difference, absorption properties and catalytic properties — are dependent on the crystallographic orientation of the outer surface. Finally, two orientation-dependent quantities which are important in the case of recrystallization will be mentioned. Primary recrystallization is caused by formation of crystal nuclei and migration of grain boundaries thus formed. Both processes can be orientation dependent:

$$\frac{dN}{dt} = \dot{N}(g) \quad (3.19)$$

\dot{N} is the number of crystal nuclei formed per unit time and g is their orientation. The migration rate of a grain boundary, as also its energy, in general, depends both on the orientation difference of the two grains and on the crystallographic directions of their normals. If x denotes the coordinate in the normal direction, then the migration rate is

$$\frac{dx}{dt} = w(\Delta g, \mathbf{h}) \quad (3.20)$$

These examples of the orientation distribution functions, and particularly of the orientation-dependent property functions, should suffice to indicate the importance of the orientation functions.

4. Expansion of Orientation Distribution Functions in Series of Generalized Spherical Harmonics

(Three-dimensional Textures)

A function $f(g)$, which depends on the orientation g , which may or may not possess symmetry properties, can be developed in a series of generalized spherical harmonics^{289,290}:

$$f(g) = \sum_{l=0}^{\infty} \sum_{m=-l}^{+l} \sum_{n=-l}^{+l} C_l^{mn} T_l^{mn}(g) \quad (4.1)$$

If one expresses the orientation g by means of EULER's angles, one thus obtains

$$f(\varphi_1, \Phi, \varphi_2) = \sum_{l=0}^{\infty} \sum_{m=-l}^{+l} \sum_{n=-l}^{+l} C_l^{mn} e^{im\varphi_2} P_l^{mn}(\Phi) e^{in\varphi_1} \quad (4.2)$$

where $P_l^{mn}(\Phi)$ are certain generalizations of the associated LEGENDRE functions. Presentations summarizing the properties of the functions $P_l^{mn}(\Phi)$ as well as $T_l^{mn}(g)$ have been given occasionally (e.g. reference 132). A few of these properties are summarized in the appendix 'Mathematical Aids', as far as we shall require here. If $f(g)$ is an orientation distribution function, then it must be a real quantity

$$f(g) = f^*(g) \quad (4.3)$$

This leads to the following relation between the coefficients C_l^{mn} :

$$C_l^{-m-n} = (-1)^{m+n} C_l^{*mn} \quad (4.4)$$

We have denoted by g the rotation which transforms a sample fixed coordinate system K_A into a crystal fixed coordinate system K_B . We have also seen that there are a series of rotations which transform the crystal from one orientation to a symmetrically equivalent orientation — i.e. not distinguishable from the first. We shall denote these rotations by g_B . They are elements of the point group symmetry of the crystal (precisely, elements of the subgroup G_B , which one obtains by neglecting reflections, which we shall not consider here since they transform a right-hand coordinate system into a left-hand coordinate system). A crystal whose orientation is characterized by g can therefore equally well be characterized by the orientation $g_B \cdot g$. It possesses, as it were, all these orientations simultaneously. Hence follows the symmetry condition

$$f(g_B \cdot g) = f(g) \quad (4.5)$$

In addition to the crystal symmetry, the sample can also possess statistical symmetry of the orientation distribution²⁹⁶. It can happen, for example, that the in-

dividual orientations resulting from rotation about a specific sample direction occur with equal statistical frequency. In this sense the rolling direction, transverse direction and normal direction in a sheet or a foil can be twofold rotation axes. Since the symmetry elements of this sample symmetry are relative to the sample, but not relative to the crystal axes of the individual crystallites, they lead, in general, to crystallographically non-equivalent orientations. The statistical sample symmetry is, consequently, to be strictly differentiated from the crystallographic symmetry. If it is present, however, the distribution function must satisfy a second symmetry condition

$$f(g \cdot g_A) = f(g) \quad (4.6)$$

where g_A are the elements of the group G_A of the sample symmetry.

The series representation (4.1) is valid for arbitrary functions $f(g)$ — i.e. even for those which do not fulfil the conditions of equations (4.5) and (4.6). Therefore not all terms of the series in equation (4.1) can satisfy the symmetry conditions (4.5) and (4.6). If now $f(g)$ must fulfil both symmetry conditions, it is clear that the values of the coefficients C_l^{mn} can no longer be arbitrarily selected. Some of them must be zero; others must be equal to one another. These conditions can, however, be considered relatively easily. Unfortunately, however, in the case of higher crystal symmetries, complicated relations occur between the coefficients, which can not be considered in this simple way. We therefore introduce in place of the series expansion (4.1) a different analogous expression, in which, however, each term of the series separately fulfils both kinds of symmetry conditions, (4.5) and (4.6)^{43,44}:

$$f(g) = \sum_{l=0}^{\infty} \sum_{\mu=1}^{M(l)} \sum_{\nu=1}^{N(l)} C_l^{\mu\nu} \dot{T}_l^{\mu\nu}(g) \quad (4.7)$$

The dots signify that we are dealing with symmetric generalized spherical harmonics. Right-hand dots denote the sample symmetry; left-hand, the crystal symmetry. The different symmetry groups (occurring during the course of the problem at hand) will be distinguished by different numbers of dots. The symmetric functions are all linear combinations of the usual functions (see Chapter 14):

$$\dot{T}_l^{\mu\nu}(g) = \sum_{m=-l}^{+l} \sum_{n=-l}^{+l} A_l^{m\mu} \dot{A}_l^{n\nu} T_l^{mn}(g) \quad (4.8)$$

The coefficients $\dot{A}_l^{n\nu}$ must be so selected that the sample symmetry is fulfilled. This may be done in $N(l)$ linearly independent ways, which can be enumerated in some way or other by the index ν . The coefficients $A_l^{m\mu}$ express the crystal symmetry, where $M(l)$ represents the number of linearly independent solutions, which are enumerated by the index μ . In the cases of ‘lower’ (i.e. not cubic) symmetry, expression (4.8) simplifies quite remarkably, since then, for example, of the coefficients $\dot{A}_l^{n\nu}$ with fixed l and ν , only one is different from zero (or two with opposite n). This can also occur for the coefficients $\dot{A}_l^{m\mu}$, so that the double sum can be reduced to a single term. In these cases we naturally do not have to

introduce new functions $\dot{T}_l^{\mu\nu}$ in place of the T_l^{mn} . It seems, however, appropriate to accomplish the general considerations in the generalized notation by use of the functions $\dot{T}_l^{\mu\nu}$, since one is no longer required to distinguish individual symmetries and symmetry conditions. It need hardly be pointed out that, for numerical calculations, the special cases must naturally be distinguished, so that, for different symmetries, different computer programs must eventually be prepared. Some properties of the symmetric generalized spherical harmonics are summarized in Chapter 14. In particular, the coefficients $\dot{A}_l^{m\mu}$ for the case of cubic symmetry (group \mathfrak{O}_h) are given in Table 15.2.1.

The symmetric generalized spherical harmonics $\dot{T}_l^{\mu\nu}(g)$ form an orthonormal function system like the functions $T_l^{mn}(g)$:

$$\oint \dot{T}_l^{\mu\nu}(g) \dot{T}_l^{*\mu'\nu'}(g) dg = \frac{1}{2l+1} \delta_{ll'} \delta_{\mu\mu'} \delta_{\nu\nu'} \quad (4.9)$$

The asterisk denotes the complex conjugate quantity. The integration ranges over all orientations. The orientation element dg , expressed in EULER’s angles, is given by the following expression:

$$dg = \frac{1}{8\pi^2} \sin \Phi d\Phi d\varphi_1 d\varphi_2 \quad (4.10)$$

We shall normalize the orientation distribution function so that

$$\oint f(g) dg = 1 \quad (4.11)$$

If we denote by f_r the value of the distribution function for random distribution, it follows that

$$f_r \oint \phi dg = 1 \quad (4.12)$$

From here it follows with equation (4.10) that

$$f_r = 1 \quad (4.13)$$

The normalization condition (4.11) is thus identical with the customary normalization in multiples of the random distribution. If we insert the series expansion (4.7) in the normalization condition (4.11), we thus obtain

$$\sum_{l=0}^{\infty} \sum_{\mu=1}^{M(l)} \sum_{\nu=1}^{N(l)} C_l^{\mu\nu} \oint \dot{T}_l^{\mu\nu}(g) dg = 1 \quad (4.14)$$

Because of equation (4.9), for $l \neq 0$ the integral vanishes, while it assumes the value 1 for $l = 0$. Hence results

$$C_0^{1,1} = 1 \quad (4.15)$$

4.1. Determination of the Coefficients $C_l^{\mu\nu}$

If we denote the indices in equation (4.7) by l' , μ' , ν' , multiply both sides of the equation by $\dot{T}_{l'}^{*\mu\nu}(g)$ and integrate over all orientations, we obtain

$$\oint f(g) \dot{T}_{l'}^{*\mu\nu}(g) dg = \sum_{l'=0}^{\infty} \sum_{\mu=1}^{M(l')} \sum_{\nu=1}^{N(l')} C_{l'}^{\mu\nu} \oint \dot{T}_{l'}^{\mu\nu}(g) \dot{T}_{l'}^{*\mu\nu}(g) dg \quad (4.16)$$

Thus follows from equation (4.9)

$$C_l^{\mu\nu} = (2l + 1) \oint f(g) \dot{T}_l^{*\mu\nu}(g) dg \quad (4.17)$$

This relation can serve for determination of the coefficients $C_l^{\mu\nu}$, if the function $f(g)$ is known.

4.1.1. Individual Orientation Measurements

If the ‘orientation distribution’ consists only of a single orientation g_0 , the distribution function is thus different from zero only at the point $g = g_0$ (or possesses there a very narrow and very high maximum). If one considers this in equation (4.17), for the case of a single crystal or ideal orientation, one obtains for the coefficients $C_l^{\mu\nu}$

$$C_l^{\mu\nu} = (2l + 1) \dot{T}_l^{*\mu\nu}(g_0) \oint f(g) dg \quad (4.18)$$

Thus results from equation (4.11)

$$C_l^{\mu\nu} = (2l + 1) \dot{T}_l^{*\mu\nu}(g_0) \quad (4.19)$$

If the texture consists of several different crystals with orientations g_i and volumes V_i , one thus obtains the coefficients as weighted average values from equation (4.19):

$$C_l^{\mu\nu} = (2l + 1) \frac{\sum_i V_i \dot{T}_l^{*\mu\nu}(g_i)}{\sum_i V_i} \quad (4.20)$$

Equation (4.20) serves for determination of the coefficients in cases in which the texture is determined by single orientation measurements — e.g. by LAUE photographs¹²⁰, by electron diffraction^{139–141} or by metallography²⁸⁶. The function $f(g)$ then possesses a form as represented schematically in one dimension in Figure 4.1. If one extends the series expansion to very high, but finite, values of l , the discontinuous function $f(g)$ will be approximated by a continuous function, which in each case possesses maxima where $f(g)$ is different from zero. It will thus reproduce each individual orientation g_i . This, however, is not the main purpose of the application of a series representation of the function $f(g)$. Rather, one would generally like to have a ‘smooth’ function, which represents the ‘distribution density’ of the orientations g_i . In order to accomplish this, one has simply to truncate the series (4.7) at a smaller value $l = L$. With decreasing L , the approximate curve through the individual points will become increasingly smoother and flatter. Finally, the half-widths of the individual maxima become of the same order of magnitude as their mutual separations, so that they can no longer be resolved. The approximation curve is then a ‘smooth’ function, whose values are nearly proportional to the ‘density’ of the original points g_i (Figure 4.1).

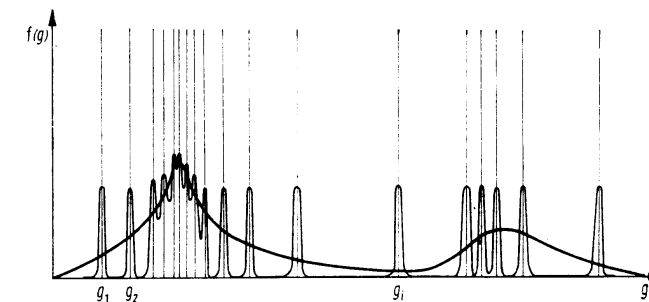


Figure 4.1 Approximation of a discontinuous function $f(g)$ by its ‘density distribution’ (one-dimensional, schematic)

With equations (4.7) and (4.20) we thus obtain for the ‘density distribution’ of individually measured orientations

$$f(g) = \sum_{l=0}^L \sum_{\mu=1}^{M(l)} \sum_{\nu=1}^{N(l)} (2l + 1) \frac{\sum_i V_i \dot{T}_l^{*\mu\nu}(g_i)}{\sum_i V_i} \dot{T}_l^{\mu\nu}(g) \quad (4.21)$$

The value L must therefore, on one hand, be chosen sufficiently large to permit reproducing the essential features of the orientation distribution and, on the other hand, sufficiently small that the individual points g_i are not ‘resolved’, or the casualness of their statistical distribution reproduced. An example of the calculation of an orientation distribution function according to equation (4.21) from electron diffraction single crystal measurements is described in Section 11.1.1. The value $L = 22$ was used there.

4.1.2. Interpolation of the Function $f(g)$

We consider the function $f(g)$ to be already ‘smooth’ and assume it has been measured at the points g_i and has there the values $f(g_i)$ (Figure 4.2). The number of points is I . We approximate the function by a series (equation 4.7) with finite $l = L$. If the number of coefficients $C_l^{\mu\nu}$ of this series is smaller than I , the approx-

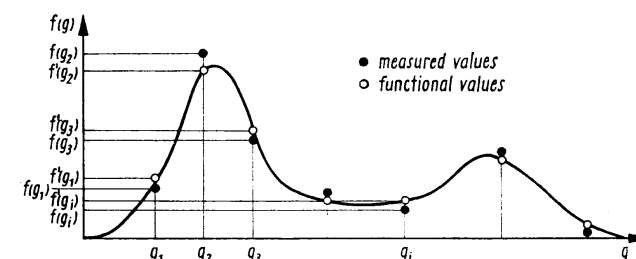


Figure 4.2 Interpolation of the function $f(g)$ by a polynomial approximation (one-dimensional, schematic)

imation function will, in general, at the points g_i not assume exactly the values $f(g_i)$ but the values $f'(g_i)$, with

$$f'(g_i) = \sum_{l=0}^L \sum_{\mu=1}^{M(l)} \sum_{\nu=1}^{N(l)} C_l^{\mu\nu} \dot{T}_l^{\mu\nu}(g_i) \quad (4.22)$$

The coefficients $C_l^{\mu\nu}$ will be determined so that the minimum condition

$$\sum_i w_i [f(g_i) - f'(g_i)]^2 = \min. \quad (4.23)$$

is fulfilled, where w_i are weight factors. From equation (4.23) follows, by differentiation with respect to $C_l^{\mu'\nu'}$,

$$\sum_i w_i [f(g_i) - f'(g_i)] \cdot \dot{T}_l^{\mu'\nu'}(g_i) = 0 \quad (4.24)$$

By consideration of equation (4.22) we obtain

$$\sum_{l=0}^L \sum_{\mu=1}^{M(l)} \sum_{\nu=1}^{N(l)} C_l^{\mu\nu} \sum_i w_i \dot{T}_l^{\mu\nu}(g_i) \dot{T}_l^{\mu'\nu'}(g_i) = \sum_i w_i f(g_i) \dot{T}_l^{\mu'\nu'}(g_i) \quad (4.25)$$

We set

$$\sum_i w_i \dot{T}_l^{\mu\nu}(g_i) \dot{T}_l^{\mu'\nu'}(g_i) = \tau_l^{\mu\mu'\nu\nu'} \quad (4.26)$$

$$\sum_i w_i f(g_i) \dot{T}_l^{\mu'\nu'}(g_i) = q_l^{\mu'\nu'} \quad (4.27)$$

We thus obtain the following system of equations for the determination of the coefficients $C_l^{\mu\nu}$:

$$\sum_{l=0}^L \sum_{\mu=1}^{M(l)} \sum_{\nu=1}^{N(l)} C_l^{\mu\nu} \tau_l^{\mu\mu'\nu\nu'} = q_l^{\mu'\nu'} \quad (4.28)$$

This system contains exactly as many equations as unknowns. Equation (4.22) is an overdetermined system of linear equations. For carrying out the calculation with an electronic computer, in general, standard programs exist for the solution of such systems of equations, frequently providing further information about the probable error of the coefficients $C_l^{\mu\nu}$ so calculated. We shall, therefore, not pursue them here. The interpolation of an orientation function $f(g)$ by a series expression (equation 4.22) is frequently necessary for orientation-dependent property functions. These functions are frequently known from measurement of definite orientations g_i . For calculation of the average value of the property concerned in a polycrystalline textured material, its representation by a series expansion is, however, particularly convenient (see Chapter 13). The coefficients of these series are then to be calculated according to equations (4.22)–(4.28). In the simplest case the weight factors w_i may be set to unity. They may, however, also be set proportional to the volume element Δg_i of the orientation space for which the value $f(g_i)$ is assumed to be representative; or they may be chosen according to any other estimation of the reliability or relative weight of the orientations g_i .

4.2. The General Axis Distribution Function $A(\mathbf{h}, \mathbf{y})$

In addition to the two coordinate systems K_A and K_B , we introduce an additional intermediate coordinate system K . Its Z-axis may have the direction \mathbf{y} in the sample fixed system with spherical angular coordinates Φ_A and γ_A , and the direction \mathbf{h} in the crystal fixed coordinate system with spherical angular coordinates Φ_B and β_B . Then the rotation

$$g_1 = \left\{ \gamma_A + \frac{\pi}{2}, \Phi_A, \psi \right\} \quad (4.29)$$

transforms the coordinate system K_A into K and the rotation

$$g_2 = \left\{ \psi', \Phi_B, \frac{\pi}{2} - \beta_B \right\} \quad (4.30)$$

transforms the coordinate system K into K_B . For the rotation g , which leads from K_A to K_B , it is then true that

$$g = g_2 \cdot g_1 \quad (4.31)$$

We now fix the rotation g_1 , likewise the angles Φ_B and β_B of the rotation g_2 , and permit the angle ψ' to vary. In this way we obtain all those rotations, g , for which the crystal direction \mathbf{h} coincides with the sample direction \mathbf{y} . We form the average value of the orientation distribution function over all these orientations. It is a function $A(\mathbf{h}, \mathbf{y})$ of the directions \mathbf{h} and \mathbf{y} :

$$A(\mathbf{h}, \mathbf{y}) = \frac{1}{2\pi} \int_0^{2\pi} f(g_2 \cdot g_1) \, d\psi' \quad (4.32)$$

In rather abbreviated symbolic notation we may also write for it

$$A(\mathbf{h}, \mathbf{y}) = \frac{1}{2\pi} \int_{[\mathbf{h}\mathbf{y}]} f(g) \, d\psi' \quad (4.33)$$

If we substitute the series expansion (4.7) herein, we thus obtain

$$A(\mathbf{h}, \mathbf{y}) = \frac{1}{2\pi} \sum_{l=0}^{\infty} \sum_{\mu=1}^{M(l)} \sum_{\nu=1}^{N(l)} C_l^{\mu\nu} \int_{[\mathbf{h}\mathbf{y}]} \dot{T}_l^{\mu\nu}(g) \, d\psi' \quad (4.34)$$

For this integral we introduce expression (14.161), derived in the chapter 'Mathematical Aids', and obtain

$$A(\mathbf{h}, \mathbf{y}) = 4\pi \sum_{l=0}^{\infty} \sum_{\mu=1}^{M(l)} \sum_{\nu=1}^{N(l)} \frac{C_l^{\mu\nu}}{2l+1} \dot{k}_l^{*\mu}(\mathbf{h}) \dot{k}_l^*(\mathbf{y}) \quad (4.35)$$

The $\dot{k}_l^{*\mu}(\mathbf{h})$ and $\dot{k}_l^*(\mathbf{y})$ are there symmetric spherical surface harmonics, and the points denote the same symmetries as for the generalized spherical harmonics, for which they were introduced (see also Chapter 14). The coefficients of the series expansion of the function $A(\mathbf{h}, \mathbf{y})$ in products of symmetric spherical surface harmonics are thus, with the exception of the known factor $4\pi/(2l+1)$, identical with those of the orientation distribution function.

It is to be mentioned that usually the general axis distribution function and its specifications, the pole figures and inverse pole figures, cannot be measured unequivocally by polycrystal diffraction experiments. As will be seen in Section 4.11, the experimentally obtained values are always superpositions of $A(+\mathbf{h}, \mathbf{y})$ and $A(-\mathbf{h}, \mathbf{y})$. Because of equation (14.58a) this leads to multiplication by a factor zero of the terms of odd l of the series expansion. Hence, the considerations of the following sections can, in general, only be applied to even orders of l as far as polycrystal diffraction is concerned. For the odd terms see Section 4.11. The considerations concerning individual orientation measurements are to be applied to even and odd values of l .

4.2.1. Determination of the Coefficients $C_l^{\mu\nu}$ by Interpolation of the General Axis Distribution Function

Energy-dispersive X-ray or neutron diffraction methods allow the reflected radiation of a large number of lattice planes to be measured at the same time. Thus the normal directions \mathbf{h}_i are parallel to a specific sample direction which is defined as the bisector of incident and reflected beams^{25,87,133,192,275}. The registered intensity of the reflected beam is thus proportional to the axis distribution function $A(\mathbf{h}_i \mathbf{y}_{ij})$ which specifies the volume fraction of crystals having their \mathbf{h}_i directions parallel to the specimen direction \mathbf{y}_j . The intensity is furthermore proportional to a normalization factor $1/N_i$ which depends on the reflecting lattice plane. Because of this usually unknown factor, we denote the registered intensity by $\hat{A}(\mathbf{h}_i \mathbf{y}_{ij})$, whereby we admit that the sample directions \mathbf{y}_{ij} may be different for different reflecting lattice planes \mathbf{h}_i (see Figure 4.3). We then construct a theoretical axis distribution function $A(\mathbf{h}, \mathbf{y})$ defined by its coefficients $C_l^{\mu\nu}$ in such a way that the sum of the squares of the deviations between experimental and theoretical intensities taken over all measured points \mathbf{y}_{ij} is a minimum. This requires the following relation to be fulfilled⁷¹:

$$\sum_{i=1}^I \sum_{j=1}^{J(i)} w_{ij} [\hat{A}(\mathbf{h}_i \mathbf{y}_{ij}) \cdot N_i - A(\mathbf{h}_i \mathbf{y}_{ij})_{\text{cal.}}]^2 = \min. \quad (4.36)$$

w_{ij} is a weight factor for the measured value at the point ij and N_i is the normalization factor of the i th pole figure. We express $A(\mathbf{h}_i \mathbf{y}_{ij})_{\text{cal.}}$ according to equation (4.35) and obtain

$$\sum_{i=1}^I \sum_{j=1}^{J(i)} w_{ij} \left[\hat{A}(\mathbf{h}_i \mathbf{y}_{ij}) N_i - 1 - \sum_{l=2}^L \sum_{\mu=1}^{M(l)} \sum_{\nu=1}^{N(l)} \frac{4\pi}{2l+1} C_l^{\mu\nu} \dot{k}_l^{*\mu}(\mathbf{h}_i) \dot{k}_l^{\nu}(\mathbf{y}_{ij}) \right]^2 = \min. \quad (4.37)$$

This equation is to be minimized with respect to N_i and $C_l^{\mu\nu}$. This yields the two condition equations

$$\sum_{j=1}^{J(i)} w_{ij} \left[\hat{A}(\mathbf{h}_i \mathbf{y}_{ij}) N_i - 1 - \sum_{l=2}^L \sum_{\mu=1}^{M(l)} \sum_{\nu=1}^{N(l)} \frac{4\pi}{2l+1} C_l^{\mu\nu} \dot{k}_l^{*\mu}(\mathbf{h}_i) \dot{k}_l^{\nu}(\mathbf{y}_{ij}) \right] \hat{A}(\mathbf{h}_i \mathbf{y}_{ij}) = 0 \quad (4.38)$$

$$\sum_{i=1}^I \sum_{j=1}^{J(i)} w_{ij} \left[\hat{A}(\mathbf{h}_i \mathbf{y}_{ij}) N_i - 1 - \sum_{l=2}^L \sum_{\mu=1}^{M(l)} \sum_{\nu=1}^{N(l)} \frac{4\pi}{2l+1} C_l^{\mu\nu} \dot{k}_l^{*\mu}(\mathbf{h}_i) \dot{k}_l^{\nu}(\mathbf{y}_{ij}) \right] \dot{k}_l^{*\mu}(\mathbf{h}_i) \dot{k}_l^{\nu}(\mathbf{y}_{ij}) = 0 \quad (4.39)$$

We introduce the following abbreviations:

$$A_i = \sum_{j=1}^{J(i)} w_{ij} [\hat{A}(\mathbf{h}_i \mathbf{y}_{ij})]^2 \quad (4.40)$$

$$B_{ii}^{\mu\nu} = \sum_{j=1}^{J(i)} w_{ij} \hat{A}(\mathbf{h}_i \mathbf{y}_{ij}) \dot{k}_i^{*\mu}(\mathbf{h}_i) \dot{k}_i^{\nu}(\mathbf{y}_{ij}) \quad (4.41)$$

$$D_i = \sum_{j=1}^{J(i)} w_{ij} \hat{A}(\mathbf{h}_i \mathbf{y}_{ij}) \quad (4.42)$$

$$E_{il}^{\mu\nu\rho\rho'} = \sum_{i=1}^I \sum_{j=1}^{J(i)} w_{ij} \dot{k}_i^{*\mu}(\mathbf{h}_i) \dot{k}_l^{*\rho}(\mathbf{h}_i) \dot{k}_i^{\nu}(\mathbf{y}_{ij}) \dot{k}_l^{\rho'}(\mathbf{y}_{ij}) \quad (4.43)$$

$$G_l^{\mu\nu} = \sum_{i=1}^I \sum_{j=1}^{J(i)} w_{ij} \dot{k}_i^{*\mu}(\mathbf{h}_i) \dot{k}_l^{\nu}(\mathbf{y}_{ij}) \quad (4.44)$$

The condition equations (4.38) and (4.39) thus read

$$N_i A_i - \sum_{l=2}^L \sum_{\mu=1}^{M(l)} \sum_{\nu=1}^{N(l)} \frac{4\pi}{2l+1} C_l^{\mu\nu} B_{ii}^{\mu\nu} = D_i \quad (4.45)$$

$$\sum_{i=1}^I N_i B_{il}^{\mu'\nu'} - \sum_{l=2}^L \sum_{\mu=1}^{M(l)} \sum_{\nu=1}^{N(l)} \frac{4\pi}{2l+1} C_l^{\mu\nu} E_{il}^{\mu'\nu'} = G_l^{\mu'\nu'} \quad (4.46)$$

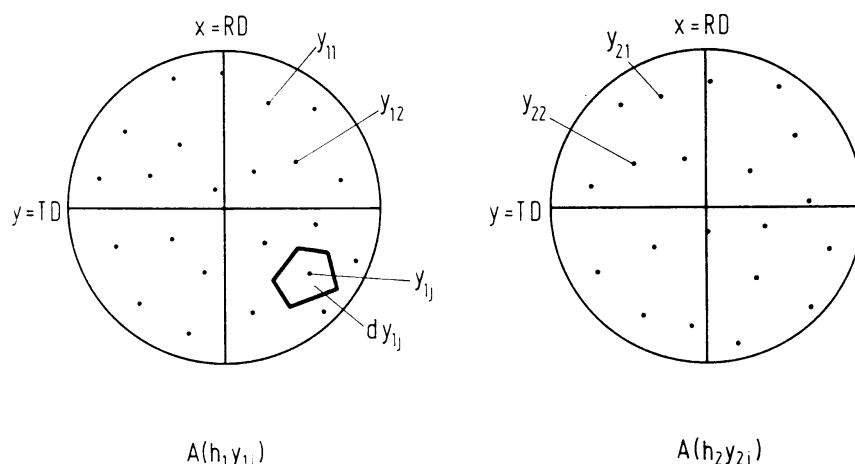


Figure 4.3 Orientation of the measuring directions \mathbf{y}_{ij} for different reflecting lattice planes \mathbf{h}_i (pole figures)

Equations (4.45) always contain only one of the normalization factors N_i . They can therefore be directly solved as follows:

$$N_i = \frac{D_i}{A_i} + \frac{1}{A_i} \sum_{l=2}^L \sum_{\mu=1}^{M(l)} \sum_{\nu=1}^{N(l)} \frac{4\pi}{2l+1} C_l^{\mu\nu} B_{li}^{\mu\nu} \quad (4.47)$$

If one introduces this into equation (4.46), one obtains

$$\begin{aligned} \sum_{i=1}^I \left[\frac{D_i}{A_i} B_{li}^{\mu'\nu'} + \frac{B_{li}^{\mu'\nu'}}{A_i} \sum_{l=2}^L \sum_{\mu=1}^{M(l)} \sum_{\nu=1}^{N(l)} \frac{4\pi}{2l+1} C_l^{\mu\nu} B_{li}^{\mu\nu} \right] \\ - \sum_{l=2}^L \sum_{\mu=1}^{M(l)} \sum_{\nu=1}^{N(l)} \frac{4\pi}{2l+1} C_l^{\mu\nu} E_{li}^{\mu'\mu'\nu\nu'} = G_l^{\mu'\nu'} \end{aligned} \quad (4.48)$$

If, furthermore, one sets

$$a_{li}^{\mu'\nu\nu'} = \frac{4\pi}{2l+1} \left[E_{li}^{\mu'\nu\nu'} - \sum_{i=1}^I \frac{B_{li}^{\mu\nu} B_{li}^{\mu'\nu'}}{A_i} \right] \quad (4.49)$$

$$b_{li}^{\mu\nu} = -G_l^{\mu\nu} + \sum_{i=1}^I \frac{D_i}{A_i} B_{li}^{\mu\nu} \quad (4.50)$$

$$d_{li}^{\mu\nu} = \frac{4\pi}{2l+1} \frac{B_{li}^{\mu\nu}}{A_i} \quad (4.51)$$

$$e_i = \frac{D_i}{A_i} \quad (4.52)$$

one obtains from equation (4.48) the equation system

$$\sum_{l=2}^L \sum_{\mu=1}^{M(l)} \sum_{\nu=1}^{N(l)} C_l^{\mu\nu} a_{li}^{\mu'\mu'\nu\nu'} = b_{li}^{\mu'\nu'} \quad (4.53)$$

the solution of which yields the coefficients $C_l^{\mu\nu}$, and from equation (4.47) there follows for the normalization factors

$$N_i = e_i + \sum_{l=2}^L \sum_{\mu=1}^{M(l)} \sum_{\nu=1}^{N(l)} C_l^{\mu\nu} d_{li}^{\mu\nu} \quad (4.54)$$

The coefficients a, b, d, e are defined by relations (4.49)–(4.52) and (4.40)–(4.44). The selection of the weight factors can be made for different reasons, depending upon estimates of the accuracy and importance of the individual measured values. They depend on the method used. In the simplest case one sets

$$w_{ij} = 1 \quad (4.55)$$

If the pole figures are measured with different total intensities \bar{P}_i , w_{ij} can thus contain a factor which is inversely proportional to the total intensity \bar{P}_i :

$$w_{ij} \sim \frac{1}{\bar{P}_i} \quad (4.56)$$

The individual measured points in the pole figures can be considered with a weight which is proportional to the surface element $d\mathbf{y}_{ij}$ of the pole figure regarded as representative for the measured value $\hat{A}(\mathbf{h}_i \mathbf{y}_{ij})$. One can then set

$$w_{ij} \sim d\mathbf{y}_{ij} \quad (4.57)$$

If the measuring points \mathbf{y}_{ij} for one lattice plane \mathbf{h}_i form a net of equidistant points of interval $\Delta\Phi \Delta\gamma$ one thus can set

$$w_{ij} = w_i \cdot d\mathbf{y}_{ij} = w_i \sin \Phi_j \Delta\Phi \Delta\gamma \quad (4.58)$$

This corresponds to the usual method of measuring pole figures in equidistant angular steps (compare Section 4.2.2). The summation over the points j of a pole figure is then equivalent to an integration over the pole figure, if one considers that an integration is, in general, approximated by a summation over a net of equidistant points. If one therefore introduces equation (4.58) into expressions (4.40)–(4.44) and replaces the sum over j by the integral, one obtains the same expressions as in Section 4.7, which are based on the condition of a minimum integral deviation (4.192) instead of the deviation sum (4.36). Because of the centrosymmetry of pole density values the considerations of this section can generally only be applied to even values of l . For odd values see Section 4.11.

The function $A(\mathbf{h}, \mathbf{y})$ in many regards plays an important role. It gives the volume fraction of the crystals for which the crystal direction \mathbf{h} coincides with the sample direction \mathbf{y} . Thus \mathbf{h} and \mathbf{y} can be completely arbitrary directions. We now consider two particular cases which result when one of the two directions \mathbf{h} and \mathbf{y} is fixed and the other is continuously variable.

4.2.2. Pole Figures $P_{\mathbf{h}}(\mathbf{y})$

We first hold the crystal direction \mathbf{h} fixed and choose it so that it is the normal to a low-index lattice plane with MILLER indices $h_1 h_2 h_3$:

$$\mathbf{h} = \mathbf{h}_i = \{h_1, h_2, h_3\} \quad (4.59)$$

The index i will in some way or other enumerate the different low-index planes, perhaps according to interplanar spacing. We obtain therewith from equation (4.35) when we interchange the sequence of summations over μ and ν

$$A(\mathbf{h}_i, \mathbf{y}) = P_{\mathbf{h}_i}(\mathbf{y}) = \sum_{l=0}^{\infty} \sum_{\nu=1}^{N(l)} \left[\frac{4\pi}{2l+1} \sum_{\mu=1}^{M(l)} C_l^{\mu\nu} k_l^{*\mu}(\mathbf{h}_i) \right] \dot{k}_l^{\nu}(\mathbf{y}) \quad (4.60)$$

To make it clear that the direction \mathbf{h}_i is now no longer continuously variable, but a fixed parameter, in this case we will introduce the new notation $P_{\mathbf{h}_i}(\mathbf{y})$. We set

$$F_l^{\nu}(\mathbf{h}_i) = \frac{4\pi}{2l+1} \sum_{\mu=1}^{M(l)} C_l^{\mu\nu} \dot{k}_l^{*\mu}(\mathbf{h}_i) \quad (4.61)$$

Thus equation (4.60) reads

$$P_{\mathbf{h}_i}(\mathbf{y}) = \sum_{l=0}^{\infty} \sum_{\nu=1}^{N(l)} F_l^{\nu}(\mathbf{h}_i) \dot{k}_l^{\nu}(\mathbf{y}) \quad (4.62)$$

The function $P_{\mathbf{h}_i}(\mathbf{y})$ gives the volume fraction of the sample for which the lattice plane normal $\mathbf{h}_i = \{h_1, h_2, h_3\}_i$ falls in the various sample directions \mathbf{y} . It is therefore none other than the pole figure associated with the direction \mathbf{h}_i . We have therefore already introduced the notation $P_{\mathbf{h}_i}(\mathbf{y})$ for it in equation (4.60). The pole figures will usually be determined by X-ray diffraction. They are generally the experimental results of texture investigations and then form the point of departure for all further considerations. In particular, they represent principally the experimental material from which the coefficients $C_l^{\mu\nu}$ of the series expansion of the orientation distribution function $f(g)$ must be determined. We shall return to it directly.

The function $P_{\mathbf{h}_i}(\mathbf{y})$, as the distribution function $f(g)$, is also normalized in multiples of the random distribution. One sees this as follows:

$$\oint P_{\mathbf{h}_i}(\mathbf{y}) d\mathbf{y} = \sum_{l=0}^{\infty} \sum_{\nu=1}^{N(l)} \left[\frac{4\pi}{2l+1} \sum_{\mu=1}^{M(l)} C_l^{\mu\nu} k_l^{*\mu}(\mathbf{h}_i) \right] \oint k_l^{\nu}(\mathbf{y}) d\mathbf{y} \quad (4.63)$$

Thus

$$d\mathbf{y} = \sin \Phi d\Phi d\beta \quad (4.64)$$

is the element of solid angle. For the symmetric spherical surface harmonics $\dot{k}_l^{\nu}(\mathbf{y})$ the orthonormal condition (14.192) is valid. For $l = l' = 0$ it follows that

$$\dot{k}_0^1 = \frac{1}{\sqrt{4\pi}} \quad (4.65)$$

Thus one obtains from equation (4.63)

$$\oint P_{\mathbf{h}_i}(\mathbf{y}) d\mathbf{y} = 4\pi C_0^{11} \dot{k}_0^1 \oint d\mathbf{y} \quad (4.66)$$

It follows from the normalization condition for the coefficients $C_l^{\mu\nu}$ (equation 4.15) that

$$\oint P_{\mathbf{h}_i}(\mathbf{y}) d\mathbf{y} = 4\pi \quad (4.67)$$

This is exactly the normalization condition which one obtains if one sets the function $P_{\mathbf{h}_i}(\mathbf{y})$ for the case of random distribution equal to 1. From

$$P_{\mathbf{h}_i}(\mathbf{y})_r = 1 \quad (4.68)$$

follows immediately

$$\oint P_{\mathbf{h}_i}(\mathbf{y})_r d\mathbf{y} = \oint d\mathbf{y} = 4\pi \quad (4.69)$$

If we replace the indices l and ν in equation (4.62) by l' and ν' , multiply by $\dot{k}_l^{*\nu}(\mathbf{y}) d\mathbf{y}$ and integrate over all directions \mathbf{y} , we obtain for the coefficients

$$F_l^{\nu}(\mathbf{h}_i) = \oint P_{\mathbf{h}_i}(\mathbf{y}) \dot{k}_l^{*\nu}(\mathbf{y}) d\mathbf{y} \quad (4.70)$$

For the coefficient F_0^1 there results

$$F_0^1(\mathbf{h}_i) = \dot{k}_0^1 \oint P_{\mathbf{h}_i}(\mathbf{y}) d\mathbf{y} = \sqrt{4\pi} \quad (4.71)$$

Now the pole figure $P_{\mathbf{h}_i}(\mathbf{y})$ is known in principle except for an intensity factor dependent on \mathbf{h}_i . For an otherwise arbitrarily normalized pole figure we set

$$\hat{P}_{\mathbf{h}_i}(\mathbf{y}) = \frac{1}{N_i} P_{\mathbf{h}_i}(\mathbf{y}) \quad (4.72)$$

From the normalization condition (4.67) we then obtain

$$\frac{1}{N_i} = \frac{1}{4\pi} \oint \hat{P}_{\mathbf{h}_i}(\mathbf{y}) d\mathbf{y} \quad (4.73)$$

from which results for the coefficients $F_l^{\nu}(\mathbf{h}_i)$

$$F_l^{\nu}(\mathbf{h}_i) = 4\pi \frac{\oint \hat{P}_{\mathbf{h}_i}(\mathbf{y}) \dot{k}_l^{*\nu}(\mathbf{y}) d\mathbf{y}}{\oint \hat{P}_{\mathbf{h}_i}(\mathbf{y}) d\mathbf{y}} \quad (4.74)$$

From equation (4.74) the coefficients $F_l^{\nu}(\mathbf{h}_i)$ of the normalized pole figures can be calculated, without having previously to carry out this normalization. This is important, since the experimental determination of the normalization factors is frequently very difficult. Experimental pole figures are, therefore, frequently only in relative units.

Because of the sample symmetry, the pole figure breaks down into a series of equivalent regions — e.g. octants of the sphere. In these regions the pole figure $P_{\mathbf{h}_i}(\mathbf{y})$ as well as the spherical surface harmonics $\dot{k}_l^{*\nu}(\mathbf{y})$ assume equal values. The integrals over the individual regions are therefore equal to one another. The integration need only be extended over one of these regions, which we shall write in the following way:

$$F_l^{\nu}(\mathbf{h}_i) = 4\pi \frac{\oint \hat{P}_{\mathbf{h}_i}(\mathbf{y}) \dot{k}_l^{*\nu}(\mathbf{y}) d\mathbf{y}}{\oint \hat{P}_{\mathbf{h}_i}(\mathbf{y}) d\mathbf{y}_i} \quad (4.75)$$

The function $P_{\mathbf{h}_i}(\mathbf{y})$ need then also be measured only in this region or one replace it by a function averaged over all regions.

Cases occur in which the pole figure does not appear as a continuous intensity distribution, but is resolved in individual points. This is, for example, the case for metallographic methods, and also for certain X-ray diffraction methods⁴⁶. In this case the arrangement of individual points is not of interest, but only their density distribution. The determination of the coefficients $F_l^{\nu}(\mathbf{h}_i)$ is then possible in a manner completely similar to that previously described for the determination of the coefficients $C_l^{\mu\nu}$ of the orientation distribution function from individual orientation measurements. We assume first that the pole figure is only different from zero at a point

$$\mathbf{y} = \mathbf{y}_0 \quad (4.76)$$

We then obtain

$$F_l^{\nu}(\mathbf{h}_i) = \dot{k}_l^{*\nu}(\mathbf{y}_0) \oint P_{\mathbf{h}_i}(\mathbf{y}) d\mathbf{y} \quad (4.77)$$

Because of the normalization of the function $P_{\mathbf{h}_i}(\mathbf{y})$ there results

$$F_l^{\nu}(\mathbf{h}_i) = 4\pi \dot{k}_l^{*\nu}(\mathbf{y}_0) \quad (4.78)$$

If the pole figure is different from zero at more points

$$\mathbf{y} = \mathbf{y}_i \quad (4.79)$$

and we assign to these points the weights V_j (perhaps the intensity of the corresponding X-ray reflection), we thus obtain for this case

$$F_l^v(\mathbf{h}_i) = 4\pi \frac{\sum_j V_j k_l^{*\nu}(\mathbf{y}_j)}{\sum_j V_j} \quad (4.80)$$

If we substitute this in equation (4.62) and truncate the series at a suitably small value $l = L$, equation (4.62) thus represents the ‘density distribution’ of the points \mathbf{y}_j of the pole figure.

In some cases it is necessary to calculate the coefficients $F_l^v(\mathbf{h}_i)$ of the \mathbf{h}_i pole figure from the values $P(\mathbf{y}_j)$, which the pole figure assumes at the points \mathbf{y}_j . If the number of coefficients is small compared with the number of points \mathbf{y}_j , the approximation function thus assumes there not exactly the values $P(\mathbf{y}_j)$, but some different values $P'(\mathbf{y}_j)$:

$$P'(\mathbf{y}_j) = \sum_{l=0}^L \sum_{\nu=1}^{N(l)} F_l^v(\mathbf{h}_i) k_l^v(\mathbf{y}_j) \quad (4.81)$$

We then require as a condition for the determination of the coefficients $F_l^v(\mathbf{h}_i)$

$$\sum_j w_j [P(\mathbf{y}_j) - P'(\mathbf{y}_j)]^2 = \min. \quad (4.82)$$

From this follows

$$\sum_j w_j [P(\mathbf{y}_j) - P'(\mathbf{y}_j)] \dot{k}_{l'}^v(\mathbf{y}_j) = 0 \quad (4.83)$$

If one substitutes expression (4.81) for $P'(\mathbf{y}_j)$, one thus obtains

$$\sum_{l=0}^L \sum_{\nu=1}^{N(l)} F_l^v(\mathbf{h}_i) \sum_j w_j k_l^v(\mathbf{y}_j) \dot{k}_{l'}^v(\mathbf{y}_j) = \sum_j w_j P(\mathbf{y}_j) \dot{k}_{l'}^v(\mathbf{y}_j) \quad (4.84)$$

We set

$$\sum_j w_j k_l^v(\mathbf{y}_j) \dot{k}_{l'}^v(\mathbf{y}_j) = \alpha_{ll'}^{vv'} \quad (4.85)$$

and

$$\sum_j w_j P(\mathbf{y}_j) \dot{k}_{l'}^v(\mathbf{y}_j) = \gamma_{l'}^v \quad (4.86)$$

we thus obtain for determination of the coefficients $F_l^v(\mathbf{h}_i)$ the following system of equations:

$$\sum_{l=0}^L \sum_{\nu=1}^{N(l)} F_l^v(\mathbf{h}_i) \alpha_{ll'}^{vv'} = \gamma_{l'}^v \quad (4.87)$$

Their solution is the best-fitting solution of the overdetermined system of equations (4.81). The probable error of the solution will frequently be calculated simultaneously with the solution. We shall not, however, go into this. This kind of calculation of the coefficients of pole figures is similar to that for incompletely

measured pole figures, which we shall consider further in Section 4.7. The calculation of coefficients according to equations (4.81)–(4.87) is always recommended when only relatively few terms of the series expansion are required — e.g. for calculation of average values of physical properties and when the pole figures are measured at relatively few points, so that the integral representation is not applicable.

4.2.2.1. Determination of the Coefficients $C_l^{\mu\nu}$ from Pole Figures

In equation (4.62) the pole figures $P_{\mathbf{h}_i}(\mathbf{y})$ appear already developed in a series of spherical surface harmonics of the sample symmetry:

$$P_{\mathbf{h}_i}(\mathbf{y}) = \sum_{l=0}^{\infty} \sum_{\nu=1}^{N(l)} F_l^v(\mathbf{h}_i) k_l^v(\mathbf{y}) \quad (4.88)$$

with the coefficients

$$F_l^v(\mathbf{h}_i) = \frac{4\pi}{2l+1} \sum_{\mu=1}^{M(l)} C_l^{\mu\nu} \dot{k}_l^{\mu}(\mathbf{h}_i) \quad (4.89)$$

If we assume the coefficients $F_l^v(\mathbf{h}_i)$ to be known for a certain number I_P of the pole figures, equation (4.89) for each pair of indices l, ν represents a system of I_P linear equations with $M(l)$ unknown $C_l^{\mu\nu}$ ^{43,246}. (Because of the centrosymmetry of pole figures, the present considerations are only to be applied to even values of l . For odd values of l see Section 4.11.) In order for these equations to have a unique solution, the number of unknowns must be smaller than or at most equal to the number of equations:

$$M(l) \leq I_P \quad (4.90)$$

If the system of equations includes more equations than unknowns, then it can of course occur that it has no solution. We shall, however, at this point suppose that the pole figures were measured without error. The $F_l^v(\mathbf{h}_i)$ then must be so conditioned that the system (4.89) possesses a unique solution, since indeed some orientation distribution $f(g)$ and thus also a certain set of coefficients $C_l^{\mu\nu}$ must exist. If more equations than unknowns are present, not all equations can thus be linearly independent. If the pole figures and thus the coefficients $F_l^v(\mathbf{h}_i)$ are affected by errors in measurement, the equations naturally need no longer be exactly consistent with one another, so that they need not yield an exact solution. How the system of equations can be solved approximately by a method of least squares will be considered in a later chapter. For the moment we shall assume unique solubility.

Now $M(l)$ is a function — in general, increasing with l — which depends on crystal symmetry (Figure 4.4). Therefore, for a given number of pole figures, the system of equations can only be solved uniquely up to a certain degree:

$$l = l_{\max}.(I_P, \text{crystal symmetry}) \quad (4.91)$$

This degree, l_{\max} , which depends on the number I_P of pole figures and the crystal symmetry, we shall call ‘resolving power’³⁸.

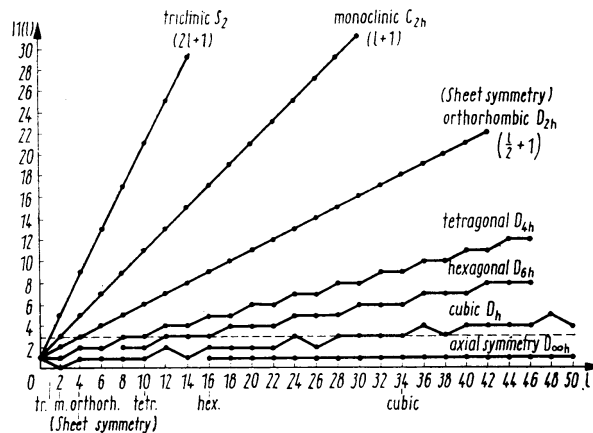


Figure 4.4 Number of linearly independent spherical harmonics of different symmetries as a function of degree l . The points of intersection of the dashed line $M(l)=3$ with the curves give the maximum possible order of the solution which can be obtained for the symmetry in question with three pole figures or with three inverse pole figures (orthorhombic sample symmetry). (Only even orders l are shown. For the odd orders compare Figure 14.1)

If one has sufficient pole figures available, l_{\max} can be comparatively large. For cubic symmetry for four pole figures $l_{\max} = 46$. Since the coefficients C_l^{uv} become smaller with increasing l , and for normal, not too severe, orientation distribution functions ultimately completely vanish, it can occur that below l_{\max} they are already practically zero. One is then permitted to make the plausible assumption that they are also zero or nearly zero above l_{\max} . In this case one is permitted to view the orientation distribution function as uniquely determined by a finite number of pole figures. The pole figures concerned then permit representation to a suitable approximation, thus without noteworthy truncation error, by a series (4.88) with a finite number of terms. The assumption that the texture is determined uniquely by this finite number of pole figures then means that all other unmeasured pole figures are also represented by the same number of series terms with sufficient exactness. This can be the case, but not necessarily. The coefficients of the different pole figures can certainly converge towards zero with different rates. Now the coefficients for large values of l will not, in general, be exactly zero, but only small. The question by how many pole figures a texture is practically uniquely determined therefore depends to a large extent on the accuracy required.

4.2.2.2. Separation of Coincidences

The pole figures $P_{h_i}(y)$ will generally be measured by X-ray diffraction, at a set of lattice planes with the normal direction \mathbf{h}_i . For a given wavelength λ , reflection by the lattice plane \mathbf{h}_i is only possible for a definite angle, which is given by the BRAGG equation

$$\sin \vartheta_i = \frac{\lambda}{2d_i} \quad (4.92)$$

d_i is the interplanar spacing. For example, in cubic crystals it is given by

$$d_i = \frac{a}{\sqrt{h_1^2 + h_2^2 + h_3^2}} \quad (4.93)$$

where a is the lattice parameter and h_1, h_2, h_3 are the MILLER indices. In other crystal systems other, however similar, conditions are valid. One therefore perceives that it can occur that two different lattice planes with different indices possess the same interplanar spacing and therefore the same BRAGG angle. For example, this is the case for cubic symmetry for the lattice planes with indices $\{3, 3, 3\}$ and $\{5, 1, 1\}$. For these one obtains

$$d_{333} = d_{511} = \frac{a}{\sqrt{27}} \quad (4.94)$$

The pole figures $P_{333}(y)$ and $P_{511}(y)$ belonging to these two lattice planes in principle, therefore, can not be separately measured but always only as a sum. If one considers still higher indices, even more than two pole figures can thus be superimposed. In the trigonal symmetry the lattice planes $(hkil)$ and $(khil)$ have systematically the same BRAGG angle, although they are not symmetrically equivalent. Apart from these 'real' coincidences, 'partial' coincidences also may occur if neighbouring reflections are overlapped, as shown in Figure 4.5. In the general case we therefore measure at the BRAGG angle ϑ a linear combination of several pole figures:

$$P_\vartheta(y) = q_1 P_{h_1}(y) + q_2 P_{h_2}(y) + \dots = \sum_{j=1}^{j_{\max}} q_j P_{h_j}(y) \quad (4.95)$$

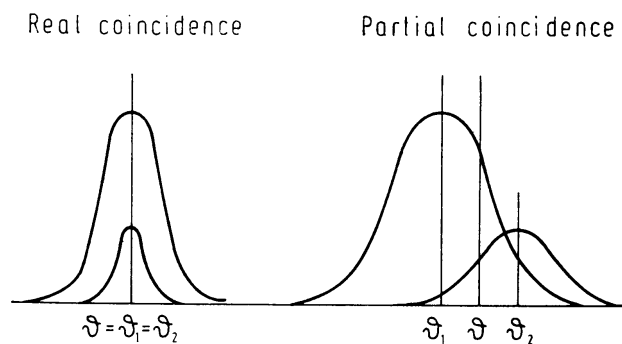


Figure 4.5 Real and partial coincidences

The q_j are factors which can depend on the angle ϑ . We normalize the pole figures $P_{\vartheta}(\mathbf{y})$ in the same way as the pole figures $P_{\mathbf{h}_j}(\mathbf{y})$. Then for the factors q_j it must be true that

$$\sum_{j=1}^{j_{\max.}} q_j = 1 \quad (4.96)$$

If we also expand the pole figures $P_{\vartheta}(\mathbf{y})$ in series corresponding to equation (4.88), an expression similar to equation (4.95) is valid for the coefficients

$$F_l^r(\vartheta) = \sum_{j=1}^{j_{\max.}} q_j F_l^r(\mathbf{h}_j) \quad (4.97)$$

If we substitute for $F_l^r(\mathbf{h}_j)$ expression (4.89), we obtain

$$F_l^r(\vartheta) = \frac{4\pi}{2l+1} \sum_{\mu=1}^{M(l)} C_l^{\mu\nu} \sum_{j=1}^{j_{\max.}} q_j k_l^{*\mu}(\mathbf{h}_j) \quad (4.98)$$

For $j_{\max.} = 1$, equation (4.98) transforms into the corresponding equation (4.89) for non-coincident pole figures.

Real Coincidences

In the case of real coincidences (Figure 4.5a) one can assume that the intensity relations of the overlapping reflections are known and are proportional to the squares of the structure factors of the reflections. The coefficients q_j are then likewise known. In equation (4.98) we can set

$$\sum_{j=1}^{j_{\max.}} q_j k_l^{*\mu}(\mathbf{h}_j) = k_l^{*\mu}(\vartheta) \quad (4.99)$$

The equation system (4.98) is then completely analogous to equation (4.89), except that in place of the coefficients $k_l^{*\mu}(\mathbf{h}_j)$ appear other but according to equation (4.99) likewise known coefficients $k_l^{*\mu}(\vartheta)$.

Partial Coincidences

In the case of partial coincidences (Figure 4.5b) the intensity relations of the overlapping lines depend on the experimental conditions (e.g. width of the lines, their separation and the exact value of the angle, ϑ , of measurement). Then the coefficients q_j can not, in general, be assumed to be known, but must be determined from the calculation.

If one assumes that some non-coincident pole figures can be measured, then one can calculate from these the coefficients $C_l^{\mu\nu}$ up to a certain degree

$$l = l' \quad (4.100)$$

If we substitute these in equation (4.98), we obtain a system of linear equations with $j_{\max.}$ unknown q_j . We can solve these for all coincidences for which $j_{\max.}$ is

smaller than the number of equations — i.e. the number of combinations of l and ν for which the coefficients $C_l^{\mu\nu}$ have previously been determined. If, now, the q_j for some pole figures are known, the corresponding equations from (4.98) are linear equations with known coefficients. We can add these to equations (4.89) for non-coincident pole figures and calculate from this enlarged system the coefficients $C_l^{\mu\nu}$ to a higher degree

$$l = l'' > l' \quad (4.101)$$

Continuing in this way, we can eventually use all equations of the system (4.98) for calculation of the coefficients $C_l^{\mu\nu}$ and the superposition factors q_j . Since the number of measurable pole figures is frequently very limited, this can be very important in the case of texture determination for attainment of the highest possible resolving power.

In order to solve the system of equations (4.98) for the intensity factors q_j of coincident pole figures, at least $j_{\max.}$ non-zero coefficients $F_l^r(\vartheta)$ are necessary. For completely random orientation distribution, however, only one coefficient, namely $F_0^1(\vartheta)$, differs from zero. In this case it is impossible to separate the intensity factors of coincident reflections. However, when the orientation distribution is not random, it suffices, in general, to determine the coefficients $C_l^{\mu\nu}$ of the texture up to a very small degree l , in order to be able to calculate the intensity factors of the coincident reflections. Since the intensity factors depend, among other things, also on the structure factor of the reflection concerned, this fact can be used in the crystal structure analysis of such materials which do not permit preparation of single crystals, but perhaps textured polycrystalline samples^{36,37}.

Multiphase Coincidences

The overlapping of several reflections can also be treated for the case of mixed phases, whereby each phase can have an individual orientation distribution. Actually the separation of coincidences in this case is particularly important, since the probability of overlap naturally increases with the number of reflections present. If we denote the various phases by the index i , equation (4.95) can thus be expanded:

$$P_{\vartheta}(\mathbf{y}) = \sum_{i=1}^{i_{\max.}} \sum_{j=1}^{j_{\max.(i)}} q_{ij} P_{\mathbf{h}_{ji}}(\mathbf{y}) \quad (4.102)$$

$P_{\mathbf{h}_{ji}}(\mathbf{y})$ is the pole figure of the \mathbf{h}_j reflection of the phase i . If the overlapping pole figure $P_{\vartheta}(\mathbf{y})$ is normalized, it must be true that

$$\sum_{i=1}^{i_{\max.}} \sum_{j=1}^{j_{\max.(i)}} q_{ij} = 1 \quad (4.103)$$

From equation (4.102) there results for the coefficients $F_l^r(\vartheta)$ of the overlapping pole figure

$$F_l^r(\vartheta) = \sum_{i=1}^{i_{\max.}} \sum_{j=1}^{j_{\max.(i)}} q_{ij} F_l^r(\mathbf{h}_{ji}) \quad (4.104)$$

If one expresses the $F_l^v(h_{ji})$ in terms of the coefficients $C^{\mu\nu}(i)$, one thus obtains

$$F_l^\nu(\vartheta) = \frac{4\pi}{2l+1} \sum_{i=1}^{i_{\max. M(l,i)}} \sum_{\mu=1}^{j_{\max.(i)}} C_l^{\mu\nu}(i) \sum_{j=1}^{j_{\max.(i)}} q_{ij} k_l^{*\mu}(\mathbf{h}_{ji}) \quad (4.10)$$

For multiphase coincidences one must, in general, assume that the overlapping coefficients q_{ij} are not known. This problem is thus analogous to that of the partial single-phase coincidences. We further assume that for each phase some non-coincident reflection be present from which the $C_l'''(i)$ can be calculated up to a certain value l_{\max} . Equation (4.105) is then a linear equation system for the overlapping coefficients q_{ij} with known coefficients, which can be solved if the total number of overlapping reflections at the angle ϑ is smaller than the number of combinations of the indices l and v up to $l = l_{\max}$. The determination of the overlapping coefficients for multiphase coincidences can thus proceed in complete analogy with the case of the partial single-phase coincidences. If the number of available combinations l, v is greater than the number of unknowns q_{ij} , either some of the combinations can be omitted, or the overdetermined equation system (4.105) can be solved with all l, v combinations according to the method of least squared errors¹⁶⁸.

4.2.2.3. Maximum Resolving Power

The maximum resolving power obtainable by pole figure measurements is given by the number of measurable pole figures associated with different crystal directions. The different reflections for body-centred cubic and face-centred cubic crystals are given in *Tables 4.1* and *4.2* in order of increasing sum of the squares of the indices. Reflections of higher order than the first from the same lattice plane give the same pole figure, and are therefore neglected in consideration of the resolving power. If one uses all reflections up to a specified sum of squares of the indices for solution of the texture, one thus obtains curves given by crosses in *Figures 4.6* and *4.7* for the resolving power. If one only uses the non-coincident reflections the curves represented by the points result. The limiting values of the reflections which can be measured with CuK_α and MoK_α for a lattice parameter of 4 \AA are also given. With MoK_α radiation it is thus possible, in principle, when one uses only the non-coincident reflections, to attain a resolving power of better than 200. From this side practically no limitation of the resolving power is given. On the other hand, the sharp decrease of the intensity of the reflections makes X-ray diffraction measurement difficult. In order to obtain a resolving power of 50, one must thus use reflections whose intensity is less than one-tenth of the intensity of the strongest reflections considered. Thus the time of measurement — for equal accuracy — will be greater by a factor of 10. On this basis it is difficult, for cubic materials and X-ray diffraction measurements of the pole figures, to obtain a resolving power of better than 50. It is to be mentioned that the resolving power so determined concerns only the even part of the texture function. For the odd part see Section 4.11.

Table 4.1 REFLECTING LATTICE PLANES OF THE BODY-CENTRED CUBIC LATTICE
 $(n$ = order of reflection; m = multiplicity of coincidence; \dagger = single reflection first-order)

Table 4.2 REFLECTING LATTICE PLANES OF THE FACE-CENTRED CUBIC LATTICE
(n = order of reflection; m = multiplicity of coincidence; \dagger = single reflection first-order)

hkl	$h^2+k^2+l^2$	n	m	hkl	$h^2+k^2+l^2$	n	m
111	3	1	1†	9 3 1	91	1	1†
200	4	1	1†	8 4 4	96	2	1
220	8	1	1†	7 5 5		1	
311	11	1	1†	7 7 1	99	1	3
222	12	2	1	9 3 3		3	
400	16	2	1	8 6 0	100	1	2
331	19	1	1†	10.0.0		5	
420	20	1	1†	8 6 2	104	1	2
422	24	1	1†	10.2.0		1	
333	27	3	2	7 7 3	107	1	2
511	27	1		9 5 1	107	1	
440	32	2	1	6 6 6		6	
531	35	1	1†	10.2.2	108	2	
442	36	1		9 5 3	115	1	1†
600	36	3	2	8 6 4		1	
620	40	1	1†	10.4.0	116	1	2
533	43	1	1†	10.4.2	120	1	1†
622	44	2	1	7 7 5	123	1	2
444	48	4	1	11.1.1		1	
551	51	1	2	8 8 0	128	4	1
711	51	1					
640	52	1	1†				
642	56	1	1†				
553	59	1	2				
731	59	1					
800	64	4	1				
733	67	1	1†				
644	68	1	2				
820	68	1					
660	72	3	2				
822	72	1					
555	75	5	2				
751	75	1					
662	76	2	1				
840	80	2	1				
753	83	1	2				
911	88	1					
842	84	1	1†				
644	88	1	1†				

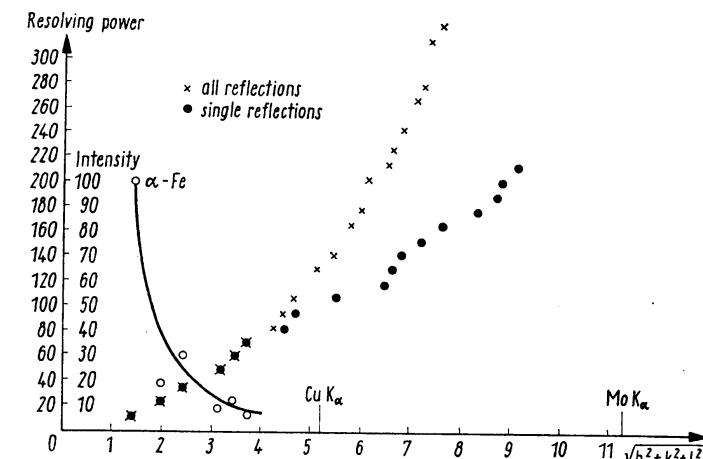


Figure 4.6 The maximum resolving power for texture determination from pole figures of body-centered cubic crystals: \times = all reflections; \bullet = non-coincident reflections. The course of the integrated intensity of X-ray diffraction for α -iron is given for reference

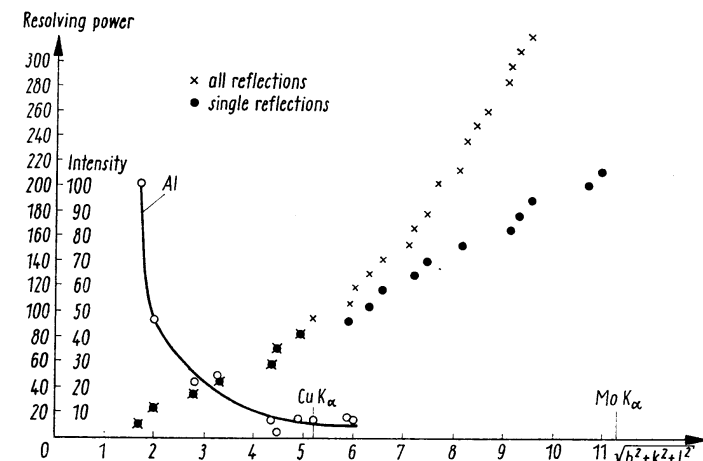


Figure 4.7 Maximum resolving power for texture determination from pole figures for face-centred cubic crystals: \times = all reflections; \bullet = non-coincident reflections. The course of the integrated intensity for X-ray diffraction for aluminium is given for reference

4.2.3. Inverse Pole Figures $R_y(\mathbf{h})$

We now consider the second special case of the function $A(\mathbf{h}, \mathbf{y})$, which results when the sample direction

$$\mathbf{y} = \mathbf{y}_i \quad (4.106)$$

is fixed and the crystal direction \mathbf{h} is allowed to vary continuously. For this case we introduce the notation $R_{\mathbf{y}_i}(\mathbf{h})$:

$$A(\mathbf{h}, \mathbf{y}_i) \equiv R_{\mathbf{y}_i}(\mathbf{h}) = \sum_{l=0}^{\infty} \sum_{\mu=1}^{M(l)} \frac{4\pi}{2l+1} \sum_{v=1}^{N(l)} C_l^{\mu v} \dot{k}_l^v(\mathbf{y}_i) \dot{k}_l^{*\mu}(\mathbf{h}) \quad (4.107)$$

This is a distribution function which gives the frequency with which the various crystal directions \mathbf{h} coincide with a specific sample direction \mathbf{y}_i — perhaps the rolling direction. It is generally called the inverse or the reciprocal pole figure of this sample direction¹⁹. Since expression (4.35) for the function $A(\mathbf{h}, \mathbf{y})$ exhibits complete symmetry with respect to \mathbf{h} and \mathbf{y} , the properties derived for pole figures are also valid in a similar way for inverse pole figures. In particular,

$$\oint R_{\mathbf{y}_i}(\mathbf{h}) d\mathbf{h} = 4\pi \quad (4.108)$$

and this means likewise normalization in multiples of random distribution:

$$R_{\mathbf{y}_i}(\mathbf{h})_r = 1 \quad (4.109)$$

If one writes $R_{\mathbf{y}_i}(\mathbf{h})$ in the form

$$R_{\mathbf{y}_i}(\mathbf{h}) = \sum_{l=0}^{\infty} \sum_{\mu=1}^{M(l)} H_l^{\mu}(\mathbf{y}_i) \dot{k}_l^{*\mu}(\mathbf{h}) \quad (4.110)$$

with coefficients

$$H_l^{\mu}(\mathbf{y}_i) = \frac{4\pi}{2l+1} \sum_{v=1}^{N(l)} C_l^{\mu v} \dot{k}_l^v(\mathbf{y}_i) \quad (4.111)$$

and I_R is the number of different inverse pole figures for the different directions \mathbf{y}_i , for fixed l and μ , equation (4.111) thus represents a system of I_R linear equations with $N(l)$ unknown $C_l^{\mu v}$. This system of equations can likewise be solved up to a certain degree l_{\max} :

$$l = l_{\max}(I_R, \text{sample symmetry}) \quad (4.112)$$

l_{\max} thus depends on the number of inverse pole figures and the sample symmetry. In the case of known inverse pole figures $R_{\mathbf{y}_i}(\mathbf{h})$ the coefficients $H_l^{\mu}(\mathbf{y}_i)$ can be calculated from a relation similar to equation (4.75):

$$H_l^{\mu}(\mathbf{y}_i) = 4\pi \frac{\oint \hat{R}_{\mathbf{y}_i}(\mathbf{h}) \dot{k}_l^{\mu}(\mathbf{h}) d\mathbf{h}}{\oint \hat{R}_{\mathbf{y}_i}(\mathbf{h}) d\mathbf{h}} \quad (4.113)$$

The function $\hat{R}_{\mathbf{y}_i}(\mathbf{h})$, again, need be known only to a constant factor. The integration is now to be extended over an elementary region of the crystal symmetry, in contrast to equation (4.75), where we were dealing with an elementary region of the sample symmetry.

If the inverse pole figure differs from zero only at the points

$$\mathbf{h} = \mathbf{h}_j \quad (4.114)$$

and possesses there the values V_j , one thus obtains for $H_l^{\mu}(\mathbf{y}_i)$

$$H_l^{\mu}(\mathbf{y}_i) = 4\pi \frac{\sum_j V_j \dot{k}_l^{*\mu}(\mathbf{h}_j)}{\sum_j V_j} \quad (4.115)$$

This case occurs, for example, when the crystallographic orientation can be metallographically determined from differently oriented polished faces. If one substitutes expression (4.115) in equation (4.110) and truncates the series at a suitably small value $l = L$, equation (4.110) represents the ‘density distribution’ of the points \mathbf{h}_j in the inverse pole figure.

From the method of HARRIS¹⁴⁶ one obtains values of the inverse pole figure at certain points. We shall denote them by $R(\mathbf{h}_j)$. The inverse pole figure will then be approximated by a series (4.110) with finite $l = L$. If the number of coefficients $H_l^{\mu}(\mathbf{y}_i)$ is smaller than the number of points, then, in general, not the exact values $R(\mathbf{h}_j)$ will be assumed at these points, but some different values $R'(\mathbf{h}_j)$, with

$$R'(\mathbf{h}_j) = \sum_{l=0}^L \sum_{\mu=1}^{M(l)} H_l^{\mu}(\mathbf{y}_i) \dot{k}_l^{*\mu}(\mathbf{h}_j) \quad (4.116)$$

From the requirement

$$\sum_i w_i [R(\mathbf{h}_i) - R'(\mathbf{h}_i)]^2 = \min. \quad (4.117)$$

the equation for determining the coefficients $H_l^{\mu}(\mathbf{y}_i)$ follows:

$$\sum_{l=0}^L \sum_{\mu=1}^{M(l)} H_l^{\mu}(\mathbf{y}_i) z_l^{\mu\mu'} = \gamma_l^{\mu'} \quad (4.118)$$

The values $z_l^{\mu\mu'}$ and $\gamma_l^{\mu'}$ thus have the same meaning as those defined in equations (4.85) and (4.86). Only the spherical surface harmonics of the sample direction $\dot{k}_l^v(\mathbf{y}_i)$ have to be replaced by those of the crystal direction $\dot{k}_l^{*\mu}(\mathbf{h}_j)$.

4.2.4. Comparison of the Representations of a Texture by Pole Figures and Inverse Pole Figures

Pole figures and inverse pole figures are special cases of the generalized axis distribution function $A(\mathbf{h}, \mathbf{y})$, which are an average value of the frequencies of crystals of different orientations. Each point of a pole figure, as also of an inverse pole figure, therefore corresponds to a complete multiplicity of different orientations, which can occur with different frequency. Both kinds of function are, as it were, two-dimensional ‘projections’ of the three-dimensional orientation distribution function. In the general case one is unable directly to read off the frequency of a specific crystal orientation, as from the three-dimensional distribution function. In this respect neither of these kinds of function is preferred over the other. Yet the two are not completely equivalent (see reference 42).

The essential advantage of pole figures consists in their direct measurability by X-ray diffraction. If one allows an X-ray beam to be reflected by a specified set of lattice planes of a crystal, the reflected intensity is thus independent of a rotation of the crystal around the normal to this set of lattice planes. By this reflection process one can obtain information about the orientation of the lattice plane normal in space, but not about a rotation around this normal. By reflection from a polycrystalline sample, one in this way directly obtains the frequency distribution of the lattice plane normals of the kind considered — i.e. the pole figure.

An inverse pole figure indicates the frequencies with which different crystal directions occur in a specified sample direction. Now, since the physical properties of the crystals depend on the crystal direction, one obtains the average value of a property in a specified sample direction, when one multiplies the value of the property in an arbitrary crystal direction by the frequency with which this crystal direction occurs in the sample direction considered, and integrates over all crystal directions. Thus, only the inverse pole figure of the direction considered will be necessary for constructing these average values (see, e.g., references 34 and 35). (We shall return later in detail to what was given in a simplified representation here.) The inverse pole figure thus plays an important role in the calculation or at least estimation of the physical properties of polycrystalline materials. The estimation of the physical properties is frequently the essential, practical objective of a texture analysis. In these cases the pole figures are assumed to be given and the inverse pole figures to be calculated from them. With the series representation used here this requires the calculation of the coefficients $C_l^{\mu\nu}$ of the three-dimensional distribution function $f(g)$. The function $f(g)$ need not be calculated — particularly since, as we shall see later, of the coefficients $C_l^{\mu\nu}$, frequently only very few enter into calculation of the average values.

In the sense just depicted, the inverse pole figures are often the desired goal of a texture investigation¹⁴⁵. It is another question whether one should employ pole figures or inverse pole figures, if one wants to describe a specific texture as well as possible. It is clear that a complete description of a texture is given only by the three-dimensional orientation distribution. Frequently, however, this calculation and indeed its three-dimensional representation are difficult, so that one would like to restrict oneself to two-dimensional functions. One then specifies a certain number (frequently three) of pole figures or inverse pole figures. One now sees immediately that the representations by equal numbers of pole figures and inverse pole figures are equivalent only in some special cases, if the sample symmetry and crystal symmetry are equal. From equations (4.91) and (4.112) one sees that the degree l_{\max} up to which the coefficients $C_l^{\mu\nu}$ can be uniquely determined from pole figures and inverse pole figures depends in one case on the sample symmetry, in the other case on the crystal symmetry. The same resolving power occurs only when the two symmetries are equal. Since the symmetry of the sample for sheet and foil is generally orthorhombic, the two representations are thus only equivalent in the case of orthorhombic crystals. In the case of 'higher' crystal symmetry (e.g. cubic) the resolving power of a representation by pole figures is

higher than for the use of an equal number of inverse pole figures. For 'lower' crystal symmetry the converse of this is true; the inverse pole figures are here superior to the normal ones as far as resolving power and therefore information capacity are concerned (see Figure 4.4). The highest possible sample symmetry in this sense is rotational symmetry, for which

$$N(l) = 1 \quad (4.119)$$

for all l . For this sample symmetry (fibre textures), a single inverse pole figure is thus sufficient for the complete description of the texture (see Figure 4.4). We shall return in more detail to this particularly important special case.

4.3. The Angular Distribution Function $W_{hy}(\Theta)$

We proceed from the pole figure associated with the direction \mathbf{h}_i :

$$P_{\mathbf{h}_i}(\mathbf{y}) = \sum_{l=0}^{\infty} \sum_{\nu=1}^{N(l)} \left[\frac{4\pi}{2l+1} \sum_{\mu=1}^{M(l)} C_l^{\mu\nu} k_l^{\ast\mu}(\mathbf{h}_i) \right] k_l^{\nu}(\mathbf{y}) \quad (4.120)$$

The sample direction \mathbf{y} is thus continuously variable. We now choose an arbitrary sample direction \mathbf{y}_i as the pole of a spherical angular coordinate system Θ, ψ (see

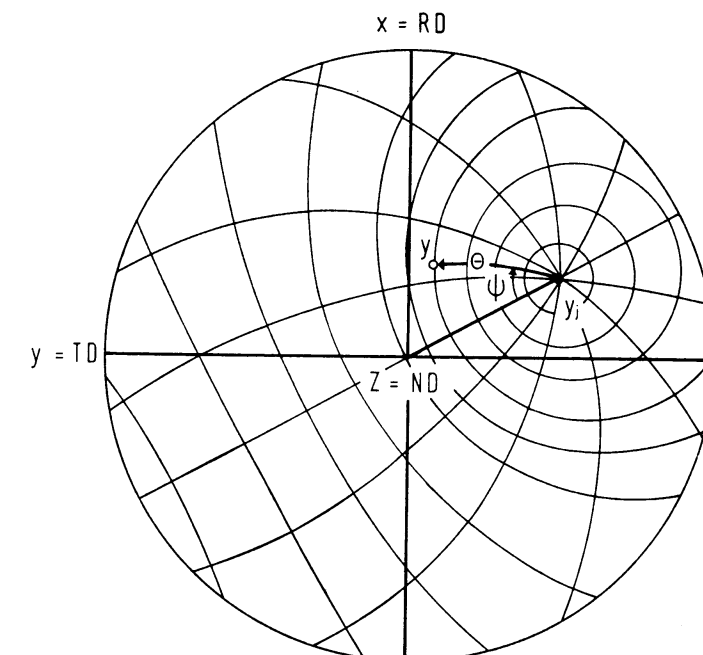


Figure 4.8 The sample direction \mathbf{y}_i as pole of a new spherical polar coordinate system Θ, ψ

Figure 4.8). We can then write the function $P_{\mathbf{h}_i}(\mathbf{y})$ as $P_{\mathbf{h}_i}(\Theta, \psi)$. We now hold the angle Θ fixed and construct the average value of this function over all ψ :

$$W_{\mathbf{h}_i \mathbf{y}_j}(\Theta) = \frac{1}{2\pi} \int_0^{2\pi} P_{\mathbf{h}_i}(\Theta, \psi) d\psi \quad (4.121)$$

One obtains this function, if, for example, one permits the texture sample to rotate rapidly about the sample direction \mathbf{y}_j during the measurement. It thus indicates how frequently the crystal direction \mathbf{h}_i forms the angle Θ with the sample direction \mathbf{y}_j (angle distribution function). If we substitute the series representation (4.120) into equation (4.121), we obtain

$$W_{\mathbf{h}_i \mathbf{y}_j}(\Theta) = \frac{1}{2\pi} \sum_{l=0}^{\infty} \sum_{\nu=1}^{N(l)} \left[\frac{4\pi}{2l+1} \sum_{\mu=1}^{M(l)} C_l^{\mu\nu} \dot{k}_l^{*\mu}(\mathbf{h}_i) \right] \int_0^{2\pi} \dot{k}_l^{\nu}(\mathbf{y}) d\psi \quad (4.122)$$

The index $[\mathbf{y}]$ on the integral means that the spherical surface harmonic $\dot{k}_l^{\nu}(\mathbf{y})$ is first expressed in terms of the new angular coordinates Θ, ψ and the integration over ψ then follows. The integral can be written out from equation (14.200); one then obtains

$$W_{\mathbf{h}_i \mathbf{y}_j}(\Theta) = \sum_{l=0}^{\infty} \left[\sqrt{\frac{2}{2l+1}} \frac{4\pi}{2l+1} \sum_{\mu=1}^{M(l)} \sum_{\nu=1}^{N(l)} C_l^{\mu\nu} \dot{k}_l^{*\mu}(\mathbf{h}_i) \dot{k}_l^{\nu}(\mathbf{y}_j) \right] \bar{P}_l(\Theta) \quad (4.123)$$

The $\bar{P}_l(\Theta)$ here are the normalized LEGENDRE polynomials. If we denote the coefficients of this series by $G_l(\mathbf{h}_i, \mathbf{y}_j)$, we have

$$W_{\mathbf{h}_i \mathbf{y}_j}(\Theta) = \sum_{l=0}^{\infty} G_l(\mathbf{h}_i, \mathbf{y}_j) \bar{P}_l(\Theta) \quad (4.124)$$

with

$$G_l(\mathbf{h}_i, \mathbf{y}_j) = \sqrt{\frac{2}{2l+1}} \frac{4\pi}{2l+1} \sum_{\mu=1}^{M(l)} \sum_{\nu=1}^{N(l)} C_l^{\mu\nu} \dot{k}_l^{*\mu}(\mathbf{h}_i) \dot{k}_l^{\nu}(\mathbf{y}_j) \quad (4.125)$$

This equation, together with equation (4.35), gives

$$A(\mathbf{h}_i, \mathbf{y}_j) = \sum_{l=0}^{\infty} \sqrt{\frac{2l+1}{2}} G_l(\mathbf{h}_i, \mathbf{y}_j) = W_{\mathbf{h}_i \mathbf{y}_j}(0) \quad (4.126)$$

The generalized axis distribution function $A(\mathbf{h}, \mathbf{y})$ is thus given by the summation expression (4.126) over the coefficients $G_l(\mathbf{h}, \mathbf{y})$ of the angular distribution function.

The normalized LEGENDRE polynomials $\bar{P}_l(\Theta)$ satisfy the orthonormal condition (14.49) with $m = 0$. One thus obtains for the coefficients $G_l(\mathbf{h}_i, \mathbf{y}_j)$ of the function $W_{\mathbf{h}_i \mathbf{y}_j}(\Theta)$

$$G_l(\mathbf{h}_i, \mathbf{y}_j) = \int_0^{\pi} W_{\mathbf{h}_i \mathbf{y}_j}(\Theta) \bar{P}_l(\Theta) \sin \Theta d\Theta \quad (4.127)$$

When one substitutes C_0^{11} and \dot{k}_0^1 from equations (4.15) and (4.65), for the coefficients G_0 we obtain

$$G_0(\mathbf{h}_i, \mathbf{y}_j) = \sqrt{\frac{2}{2}} \quad (4.128)$$

With the help of the normalization condition (14.49) of the LEGENDRE polynomials, one obtains from equation (4.124) the normalization condition for the functions $W_{\mathbf{h}_i \mathbf{y}_j}(\Theta)$:

$$\int_0^{\pi} W_{\mathbf{h}_i \mathbf{y}_j}(\Theta) \sin \Theta d\Theta = \int_0^{\pi} G_0(\mathbf{h}_i, \mathbf{y}_j) \bar{P}_0(\Theta) \sin \Theta d\Theta = 2 \quad (4.129)$$

and this is also equivalent to normalization in multiples of the random distribution

$$W_{\mathbf{h}_i \mathbf{y}_j}(\Theta)_r = 1 \quad (4.130)$$

By consideration of expressions (4.61) and (4.111) one can write equation (4.125) as

$$G_l(\mathbf{h}_i, \mathbf{y}_j) = \sqrt{\frac{2}{2l+1}} \sum_{\nu=1}^{N(l)} F_l^{\nu}(\mathbf{h}_i) \dot{k}_l^{\nu}(\mathbf{y}_j) \quad (4.131)$$

$$G_l(\mathbf{h}_i, \mathbf{y}_j) = \sqrt{\frac{2}{2l+1}} \sum_{\mu=1}^{M(l)} H_l^{\mu}(\mathbf{y}_j) \dot{k}_l^{*\mu}(\mathbf{h}_i) \quad (4.132)$$

The coefficients $G_l(\mathbf{h}_i, \mathbf{y}_j)$ are thus expressed, on the one hand, by the coefficients $F_l^{\nu}(\mathbf{h}_i)$ of pole figures and, on the other, by the coefficients $H_l^{\mu}(\mathbf{y}_j)$ of inverse pole figures. If the coefficients $G_l(\mathbf{h}_i, \mathbf{y}_j)$ for a certain number of sample directions \mathbf{y}_j are known, the coefficients $F_l^{\nu}(\mathbf{h}_i)$ of the pole figures up to a certain degree l_{\max} , which is given by the number of rotation directions \mathbf{y}_j and the sample symmetry, can be determined by solution of equation (4.131). If the $G_l(\mathbf{h}_i, \mathbf{y}_j)$ are known for more pole figures, one thus obtains from equation (4.132) the coefficients $H_l^{\mu}(\mathbf{y}_j)$ of the inverse pole figures of the direction \mathbf{y}_j up to a degree l_{\max} , which is given by the number of directions \mathbf{h}_i and the crystal symmetry. The situation is completely analogous to that for the calculation of the coefficients $C_l^{\mu\nu}$ from the coefficients of pole figures. The angular distribution function is a function of only one variable, which is, as it were, a fibre texture with the sample direction \mathbf{y}_j as the fibre axis, artificially produced by a rotation. It is therefore essentially simpler to measure than the two-dimensional pole figures, and also the calculation of the coefficients $G_l(\mathbf{h}_i, \mathbf{y}_j)$ of its series expansion is essentially simpler than in the two-dimensional case. With the aid of relations (4.131) and (4.132) it is thus theoretically possible to reduce every texture determination to the measurement of a certain number of artificially produced fibre textures with the sample directions \mathbf{y}_j as fibre axes. Practically, however, this possibility may be of interest only when comparatively few coefficients $C_l^{\mu\nu}$ of the series expansion are required, as is, for example, the case for the calculation of average values of physical properties of textured materials. For calculation of the elastic properties of cubic materials one requires only the coefficients $C_l^{\mu\nu}$ for $l = 4$. These can be calculated from a single pole figure

and this, in turn, from the $G_l(\mathbf{h}_i, \mathbf{y}_j)$ for three sample directions \mathbf{y}_j . If one is interested only in the property in a single sample direction \mathbf{y}_j , one requires only the inverse pole figure of this direction — i.e. only the coefficients $H_l^\mu(\mathbf{y}_j)$. For cubic crystal symmetry these can be calculated up to $l = 10$ from the $G_l(\mathbf{h}_i, \mathbf{y}_j)$ for a single pole figure \mathbf{h}_i , which is practically sufficient for all physical properties. By application of artificial rotational symmetry, one can thus save expenditures in measurement and calculation in such special cases.

4.3.1. Integral Relation between Pole Figures and Inverse Pole Figures

We also arrive at the same function $W_{\mathbf{h}_i \mathbf{y}_j}(\Theta)$ as in the preceding section if we proceed from the inverse pole figure $R_{\mathbf{y}_j}(\mathbf{h})$ associated with the sample direction \mathbf{y}_j . The crystal direction \mathbf{h} is thus continuously variable. If for \mathbf{h} we now fix a spherical angular coordinate system Θ, ψ' , such that its pole coincides with the direction \mathbf{h}_i (Figure 4.9), we can write the inverse pole figure as $R_{\mathbf{y}_j}(\Theta, \psi')$. If we now also hold the angle Θ fixed and average over all ψ' , we obtain the function

$$W'_{\mathbf{h}_i \mathbf{y}_j}(\Theta) = \frac{1}{2\pi} \int_0^{2\pi} R_{\mathbf{y}_j}(\Theta, \psi') d\psi' \quad (4.133)$$

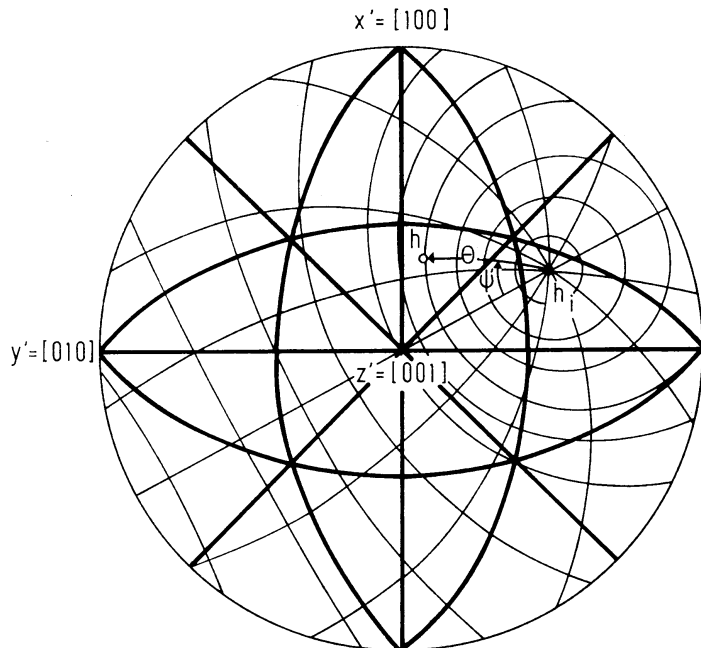


Figure 4.9 The crystal direction \mathbf{h}_i as pole of a new spherical polar coordinate system Θ, ψ'

If we substitute the series expansion (4.107) for $R_{\mathbf{y}_j}(\Theta, \psi')$, we obtain

$$W'_{\mathbf{h}_i \mathbf{y}_j}(\Theta) = \frac{1}{2\pi} \sum_{l=0}^{\infty} \sum_{\mu=1}^{M(l)} \left[\frac{4\pi}{2l+1} \sum_{v=1}^{N(l)} C_l^{\mu v} k_l^v(\mathbf{y}_j) \right] \int_0^{2\pi} k_l^{*\mu}(\mathbf{h}) d\psi' \quad (4.134)$$

If we substitute equation (4.200) for the integral, we finally obtain

$$W'_{\mathbf{h}_i \mathbf{y}_j}(\Theta) = \sum_{l=0}^{\infty} \left[\sqrt{\frac{2}{2l+1}} \frac{4\pi}{2l+1} \sum_{\mu=1}^{M(l)} \sum_{v=1}^{N(l)} C_l^{\mu v} k_l^{*\mu}(\mathbf{h}_i) k_l^v(\mathbf{y}_j) \right] \bar{P}_l(\Theta) \quad (4.135)$$

and one sees that the two functions are identical:

$$W'_{\mathbf{h}_i \mathbf{y}_j}(\Theta) = W_{\mathbf{h}_i \mathbf{y}_j}(\Theta) \quad (4.136)$$

Equation (4.136) with equations (4.121) and (4.133) represent the following integral relation between pole figures and inverse pole figures:

$$\int_{[\mathbf{y}_j]} P_{\mathbf{h}_i}(\Theta, \psi) d\psi = \int_{[\mathbf{h}_i]} R_{\mathbf{y}_j}(\Theta, \psi') d\psi' \quad (4.137)$$

The direction in rectangular brackets on the integral in each case indicates integration around this direction.

4.3.1.1. The Method of Harris

If in equation (4.137) one sets $\Theta = 0$, the two integrands are independent of the angles ψ and ψ' — i.e. of the variables of integration. Since $\Theta = 0$ denotes the sample direction \mathbf{y}_j according to Figure 4.8 and the crystal direction \mathbf{h}_i according to Figure 4.9, it follows from equation (4.137) that

$$P_{\mathbf{h}_i}(\mathbf{y}_j) = R_{\mathbf{y}_j}(\mathbf{h}_i) = A(\mathbf{h}_i, \mathbf{y}_j) \quad (4.138)$$

From this relation one can calculate the values of the inverse pole figure of an arbitrary direction \mathbf{y}_j for all those points \mathbf{h}_i for which pole figures with the indices $\mathbf{h}_i = \{h_1, h_2, h_3\}_i$ can be measured. The pole figures need only be known at the points \mathbf{y}_j for which one wants to ascertain the inverse pole figure. For determination of an inverse pole figure with the help of relation (4.138), one thus needs as many pole figures as possible, but only for a single sample direction \mathbf{y}_j . This method, due to HARRIS¹⁴⁶, for determination of inverse pole figures has frequently been applied to materials with high absorption. Since one only requires the pole figures in one direction, one can cut the sample perpendicular to this direction, whereby the absorption effect will be reduced to a minimum. The application of relation (4.138) assumes previously normalized pole figures. If the pole figures are measured at only one or a few points, normalization with the help of the integral relation (4.67) is not possible. It is then necessary to determine the normalization experimentally, by measurement of a sample with random orientation distribution under the same conditions. Between the few points \mathbf{h}_i , at which the inverse pole figure can be determined in this way, it must then somehow be in-

terpolated. This can be done either graphically or by use of a series, as was described in Section 4.2.3. We shall return to this topic in some special cases for fibre textures.

4.4. Determination of the Coefficients $C_l^{\mu\nu}$ by the Method of Least Squares

For the solution of the system of equations (4.89) for the $C_l^{\mu\nu}$ one must have at least as many equations, and therefore pole figures, as the largest occurring value, $M(l)$. For all l with smaller $M(l)$, one therefore has more equations than unknowns. If the pole figures were measured completely without error, one could thus choose from the corresponding equations as many unknowns as were present in each case, and solve these. The result must then be independent of the choice of equations. Since the measured pole figures are, however, subject to error, this, in general, is not the case. It is then recommended that all equations be used and that the solution be determined by the method of least squares. In the interest of reliability of the coefficients $C_l^{\mu\nu}$ it is therefore recommended in all cases that one use at least one more equation than there are unknowns to be calculated; in other words, not calculate the coefficients up to $l = l_{\max}$, but at most up to $l = l_{\max} - 1$ (see also reference 18).

Because of unavoidable measurement errors, we now have to distinguish between two types of coefficients: those obtained from the measured pole figures according to equation (4.70), which, in keeping with the usual notation in structure analysis, we shall denote by $F_l^v(\mathbf{h}_i)_{\text{obs.}}$, and those which exactly satisfy the system of equations (4.89) for optimum choice of $C_l^{\mu\nu}$. We denote these by $F_l^v(\mathbf{h}_i)_{\text{cal.}}$. We set

$$F_l^v(\mathbf{h}_i)_{\text{obs.}} = F_l^v(\mathbf{h}_i)_{\text{cal.}} + \epsilon_l^v(\mathbf{h}_i) \quad (4.139)$$

The different pole figures can be measured with varying degrees of accuracy. We therefore permit consideration of errors $\epsilon_l^v(\mathbf{h}_i)$ with different weights w_i in the compensation calculations. The $C_l^{\mu\nu}$ then must be determined so that

$$\sum_i w_i [\epsilon_l^v(\mathbf{h}_i)]^2 = \min. \quad (4.140)$$

In this chapter, as in the chapters on measures of accuracy and truncation errors, we shall assume that the function $\dot{T}_l^{\mu\nu}(g)$ as well as the spherical surface harmonics $\dot{k}_l^\mu(\mathbf{h})$, $\dot{k}_l^v(\mathbf{y})$ are chosen to be real. Since all distribution functions occurring must naturally be real, this is also true for the coefficients $C_l^{\mu\nu}$ and F_l^v , as well as the values of error ϵ_l^v . If one substitutes equations (4.139) and (4.89) in equation (4.140), one obtains the condition

$$\sum_i w_i \left[F_l^v(\mathbf{h}_i)_{\text{obs.}} - \frac{4\pi}{2l+1} \sum_{\mu=1}^{M(l)} C_l^{\mu\nu} \dot{k}_l^{\star\mu}(\mathbf{h}_i) \right]^2 = \min. \quad (4.141)$$

If one sets the derivative with respect to $C_l^{\mu\nu}$ equal to zero, one obtains

$$\frac{4\pi}{2l+1} \sum_i w_i \dot{k}_l^{\star\mu}(\mathbf{h}_i) \left[F_l^v(\mathbf{h}_i)_{\text{obs.}} - \frac{4\pi}{2l+1} \sum_{\mu=1}^{M(l)} C_l^{\mu\nu} \dot{k}_l^{\star\mu}(\mathbf{h}_i) \right] = 0 \quad (4.142)$$

For brevity we set†

$$\frac{4\pi}{2l+1} \sum_i w_i \dot{k}_l^{\star\mu}(\mathbf{h}_i) F_l^v(\mathbf{h}_i)_{\text{obs.}} = a_l^{\mu\nu} \quad (4.143)$$

$$\left(\frac{4\pi}{2l+1} \right)^2 \sum_i w_i \dot{k}_l^{\star\mu}(\mathbf{h}_i) \dot{k}_l^{\star\mu}(\mathbf{h}_i) = \alpha_l^{\mu\mu} \quad (4.144)$$

We thus obtain the following characteristic system of equations for determination of the coefficients $C_l^{\mu\nu}$:

$$\sum_{\mu=1}^{M(l)} \alpha_l^{\mu\mu} C_l^{\mu\nu} = a_l^{\mu\nu} \quad (4.145)$$

This contains just as many equations as unknowns — namely $M(l)$. The solution of this system of equations is

$$C_l^{\mu\nu} = \sum_{\mu'=1}^{M(l)} \beta_l^{\mu\mu'} a_l^{\mu'\nu} \quad (4.146)$$

where $\beta_l^{\mu\mu'}$ denote the elements of the inverse of the matrix of $\alpha_l^{\mu\mu'}$.

4.5. Measures of Accuracy

If for the calculation of the coefficients $C_l^{\mu\nu}$ we use more pole figures than unknowns, the overdetermination makes it possible to estimate the experimental errors of the pole figures. One can first compare the pole figures calculated from the coefficients $F_l^v(\mathbf{h}_i)_{\text{cal.}}$

$$P_{\mathbf{h}_i}(\mathbf{y})_{\text{cal.}} = \sum_{l=0}^{\infty} \sum_{\nu=1}^{N(l)} F_l^v(\mathbf{h}_i)_{\text{cal.}} \dot{k}_l^v(\mathbf{y}) \quad (4.147)$$

with the measured pole figures $P_{\mathbf{h}_i}(\mathbf{y})_{\text{obs.}}$ and thereby obtain a qualitative idea of the accuracy of measurement. One can, however, also define different quantitative measures of accuracy — for example, the average value of the difference integral of the pole figures

$$\Delta P = \sum_i w_i \oint [P_{\mathbf{h}_i}(\mathbf{y})_{\text{obs.}} - P_{\mathbf{h}_i}(\mathbf{y})_{\text{cal.}}]^2 d\mathbf{y} \quad (4.148)$$

If one substitutes the series expansion and considers relation (4.139), one thus obtains

$$\Delta P = \sum_i w_i \oint \left[\sum_{l=0}^{\infty} \sum_{\nu=1}^{N(l)} \epsilon_l^v(\mathbf{h}_i) \dot{k}_l^v(\mathbf{y}) \right]^2 d\mathbf{y} \quad (4.149)$$

If one is to remove the brackets, first each series term is to be multiplied by each of the others. In the case of the succeeding integration, however, the mixed terms

† The definition of the quantities $a_l^{\mu\nu}$ and $\alpha_l^{\mu\mu'}$ has been changed with respect to reference I, equations (4.122) and (4.123), in order that the error quantities defined later (equations 4.154 and 4.155) be in better agreement with the usual definitions in the general theory of error analysis (see, e.g., reference 94).

vanish because of the orthogonality of the spherical surface harmonics. Because of the normalization of the spherical surface harmonics, one finally obtains

$$\Delta P = \sum_i w_i \sum_{l=0}^{\infty} \sum_{\nu=1}^{N(l)} |\varepsilon_l^*(\mathbf{h}_i)|^2 \quad (4.150)$$

From the minimum condition (equation 4.140) and the last expression it directly follows that

$$\Delta P = \sum_i w_i \oint [P_{\mathbf{h}_i}(\mathbf{y})_{\text{obs.}} - P_{\mathbf{h}_i}(\mathbf{y})_{\text{cal.}}]^2 d\mathbf{y} = \min. \quad (4.151)$$

With reference to the similar measure of accuracy used in crystal structure analysis, we call the value

$$R_{\mathbf{h}_i} = \frac{\sum_{l=0}^{\infty} \sum_{\nu=1}^{N(l)} |\varepsilon_l^*(\mathbf{h}_i)|}{\sum_{l=0}^{\infty} \sum_{\nu=1}^{N(l)} |F_l^*(\mathbf{h}_i)_{\text{obs.}}|} \quad (4.152)$$

the measure of accuracy (reliability factor) of the pole figure \mathbf{h}_i and the value

$$R = \frac{\sum_i \sum_{l=0}^{\infty} \sum_{\nu=1}^{N(l)} |\varepsilon_l^*(\mathbf{h}_i)|}{\sum_i \sum_{l=0}^{\infty} \sum_{\nu=1}^{N(l)} |F_l^*(\mathbf{h}_i)_{\text{obs.}}|} \quad (4.153)$$

the measure of accuracy for the entire texture.

For the average error ΔF_l^* of the coefficients $F_l^*(\mathbf{h}_i)_{\text{obs.}}$ corresponding to the unit of weight, one obtains (see, for example, reference 94)

$$\Delta F_l^* = \sqrt{\frac{\sum_i w_i [\varepsilon_l^*(\mathbf{h}_i)]^2}{I_P - M(l)}} \quad (4.154)$$

I_P is the number of pole figures and equations used. The average error $\Delta C_l^{\mu\nu}$ of the coefficients $C_l^{\mu\nu}$ therefore amounts to

$$\Delta C_l^{\mu\nu} = \sqrt{\beta^{\mu\mu}} \cdot \Delta F_l^* \quad (4.155)$$

For the practical estimation of the errors of the texture measurement it is found to be useful to average the absolute values of both of the last error values over all values of the indices μ and ν . We then obtain

$$\Delta F_l = \frac{1}{N(l)} \sum_{\nu=1}^{N(l)} |\Delta F_l^*| \quad (4.156)$$

and

$$\Delta C_l = \frac{1}{M(l) N(l)} \sum_{\mu=1}^{M(l)} \sum_{\nu=1}^{N(l)} |\Delta C_l^{\mu\nu}| \quad (4.157)$$

4.5.1. A Special Accuracy Measure for Pole Figures of Materials with Cubic Symmetry

The accuracy measures mentioned in the previous section permit estimation of the accuracy of measured pole figures by considering the compatibility of the pole

figures with one another. It thus requires the measurement of several pole figures and the calculation of the coefficients $C_l^{\mu\nu}$ of the corresponding three-dimensional orientation distribution function. One thus obtains information about possible measurement errors only after carrying out several measurements and an extensive calculation. It is therefore desirable to have an accuracy criterion, which one can obtain from a single pole figure without extensive calculations. Such a criterion exists for materials of cubic crystals.⁴⁵ From Figure 4.4 (p. 62), which gives the number of linearly independent spherical surface harmonics of different symmetries and degrees, one sees that for cubic symmetry

$$M_{\text{cub.}}(2) = 0 \quad (4.158)$$

There thus exist no cubic spherical surface harmonics of degree two — i.e.

$$C_2^{\mu\nu} = 0 \quad (4.159)$$

From equation (4.89), therefore, follows for the calculated coefficients

$$F_2^*(\mathbf{h}_i)_{\text{cal.}} = 0 \quad (4.160)$$

On the other hand, from the measured pole figures one obtains coefficients $F_2^*(\mathbf{h}_i)_{\text{obs.}}$ corresponding to equation (4.74). It therefore follows from equation (4.139) that

$$\varepsilon_2^*(\mathbf{h}_i) = F_2^*(\mathbf{h}_i)_{\text{obs.}} = 4\pi \frac{\oint \hat{P}_{\mathbf{h}_i}(\mathbf{y}) k_2^{*\nu}(\mathbf{y}) dy}{\oint \hat{P}_{\mathbf{h}_i}(\mathbf{y}) dy} \approx 0 \quad (4.161)$$

Expression (4.161) must be exactly zero for pole figures measured completely without error. The disappearance of the values $F_2^*(\mathbf{h}_i)_{\text{obs.}}$ is, however, only a necessary, but not sufficient, condition for the pole figure to be exactly measured. Defective pole figures can exist which make equation (4.161) exactly zero.

For sheets with orthorhombic symmetry we have two linearly independent normalized spherical surface harmonics of second degree:

$$k_2^{*1}(\Phi, \gamma) = \sqrt{\frac{5}{16\pi}} [3 \cos^2 \Phi - 1] \quad (4.162)$$

$$k_2^{*2}(\Phi, \gamma) = \sqrt{\frac{15}{16\pi}} \sin^2 \Phi \cos 2\gamma \quad (4.163)$$

We thus obtain the two measures of accuracy

$$F_2^1(\mathbf{h}_i)_{\text{obs.}} = \sqrt{5\pi} \frac{\int_0^\pi [3 \cos^2 \Phi - 1] \sin \Phi \left[\int_0^{2\pi} \hat{P}_{\mathbf{h}_i}(\Phi, \gamma) dy \right] d\Phi}{\int_0^\pi \sin \Phi \left[\int_0^{2\pi} \hat{P}_{\mathbf{h}_i}(\Phi, \gamma) dy \right] d\Phi} \quad (4.164)$$

$$F_2^2(\mathbf{h}_i)_{\text{obs.}} = \sqrt{15\pi} \frac{\int_0^\pi \sin^3 \Phi \left[\int_0^{2\pi} \hat{P}_{\mathbf{h}_i}(\Phi, \gamma) \cos 2\gamma dy \right] d\Phi}{\int_0^\pi \sin \Phi \left[\int_0^{2\pi} \hat{P}_{\mathbf{h}_i}(\Phi, \gamma) dy \right] d\Phi} \quad (4.165)$$

4.5.2. A Method for the Adaption of Back-reflection and Transmission Range

As will be shown in Section 10.1, the deviation of relation (4.160) is particularly large in the case of pole figures, which are composed of measurements in the transmission and in the reflection regions. This is due in part to the difficulty of matching the two regions to each other. In general, for calculation of the matching factors one uses the values of the pole figures in the overlapping region, in which one requires

$$\int [P_{\mathbf{h}_i}(\mathbf{y})_{\text{trans.}} \cdot a - P_{\mathbf{h}_i}(\mathbf{y})_{\text{refl.}}]^2 d\mathbf{y} = \min. \quad (4.166)$$

If the function values $P_{\mathbf{h}_i}(\mathbf{y})$ in this region are small, the matching factor a is then subject to a large error. For pole figures of cubic materials one can use the accuracy measure (4.160) in place of equation (4.166) to determine the matching factor. We define quantities formally identical with those of equation (4.70) but with the range of integration being only the transmission or reflection range, respectively, instead of the complete pole figure as in equation (4.70):

$$F_{l,\text{trans.}}^v = \int_{\text{trans.}} \hat{P}_{\mathbf{h}_i}(\mathbf{y}) \dot{k}_l^{*v}(\mathbf{y}) d\mathbf{y} \quad (4.167)$$

$$F_{l,\text{refl.}}^v = \int_{\text{refl.}} \hat{P}_{\mathbf{h}_i}(\mathbf{y}) \dot{k}_l^{*v}(\mathbf{y}) d\mathbf{y} \quad (4.168)$$

The requirement of equation (4.160) is then identical with

$$F_{2,\text{trans.}}^v \cdot a + F_{2,\text{refl.}}^v = 0 \quad (4.169)$$

It follows therefrom that

$$a = -\frac{F_{2,\text{refl.}}^v}{F_{2,\text{trans.}}^v} \quad (4.170)$$

Since this requirement for $v = 1$ and $v = 2$ leads, in general, to two different values of a , one can change equation (4.169) to the requirement

$$(F_{2,\text{trans.}}^1 \cdot a + F_{2,\text{refl.}}^1)^2 + (F_{2,\text{trans.}}^2 \cdot a + F_{2,\text{refl.}}^2)^2 = \min. \quad (4.171)$$

This leads to the expression

$$a = -\frac{F_{2,\text{trans.}}^1 \cdot F_{2,\text{refl.}}^1 + F_{2,\text{trans.}}^2 \cdot F_{2,\text{refl.}}^2}{(F_{2,\text{trans.}}^1)^2 + (F_{2,\text{trans.}}^2)^2} \quad (4.172)$$

In expressions (4.170) and (4.172) all measured values of the entire transmission and reflection regions are used to calculate the matching factor.

4.6. Truncation Error

Until now we have formally extended all summations considered up to infinitely large values of the index l . This is, however, not possible for numerical calculations. The series must be terminated at a finite value

$$l = L \quad (4.173)$$

whereby a truncation error occurs. If one determines the coefficients $C_l^{\mu\nu}$ by solution of the system of linear equations (4.89) obtained from the pole figures, they are determined uniquely at most up to $l = l_{\max.}$ as we have seen. In this case the series for the function $f(g)$ (equation 4.7) can only be extended up to a value $L \leq l_{\max.}$. The same is also true for the inverse pole figures, if they can not be directly measured. The series expansion (4.88) for the measured pole figures can theoretically be extended up to infinity. A practical limitation is, however, imposed by the drastically increasing amount of computation time with increasing l .

As a measure of the truncation error of the \mathbf{h}_i -pole figure, we select the quantity

$$A_L(\mathbf{h}_i) = \frac{1}{4\pi} \oint \left[P_{\mathbf{h}_i}(\mathbf{y}) - \sum_{l=0}^L \sum_{\nu=1}^{N(l)} F_l^{\nu}(\mathbf{h}_i) \dot{k}_l^{\nu}(\mathbf{y}) \right]^2 d\mathbf{y} \quad (4.174)$$

If we remove the brackets, in the subsequent integration all terms which are products of spherical surface harmonics with different indices vanish because of the orthogonality of the spherical surface harmonics:

$$A_L(\mathbf{h}_i) = \frac{1}{4\pi} \oint [P_{\mathbf{h}_i}(\mathbf{y})]^2 d\mathbf{y} - \frac{2}{4\pi} \sum_{l=0}^L \sum_{\nu=1}^{N(l)} F_l^{\nu}(\mathbf{h}_i) \oint P_{\mathbf{h}_i}(\mathbf{y}) \dot{k}_l^{\nu}(\mathbf{y}) d\mathbf{y} \\ + \frac{1}{4\pi} \sum_{l=0}^L \sum_{\nu=1}^{N(l)} [F_l^{\nu}(\mathbf{h}_i)]^2 \quad (4.175)$$

By consideration of equation (4.70) one thereby obtains

$$A_L(\mathbf{h}_i) = \frac{1}{4\pi} \oint [P_{\mathbf{h}_i}(\mathbf{y})]^2 d\mathbf{y} - \frac{1}{4\pi} \sum_{l=0}^L \sum_{\nu=1}^{N(l)} [F_l^{\nu}(\mathbf{h}_i)]^2 \quad (4.176)$$

The integral in this expression can be numerically calculated and thereby also the series truncation error $A_L(\mathbf{h}_i)$. From the property of the spherical surface harmonics, to constitute a complete orthogonal system, it follows that

$$A_L(\mathbf{h}_i) \rightarrow 0 \quad \text{for } L \rightarrow \infty \quad (4.177)$$

It is thereby also true that

$$A_L(\mathbf{h}_i) = \frac{1}{4\pi} \sum_{l=L+1}^{\infty} \sum_{\nu=1}^{N(l)} [F_l^{\nu}(\mathbf{h}_i)]^2 \quad (4.178)$$

The possibility of estimating the truncation error hereby results if one plots the values

$$\frac{1}{4\pi} \sum_{\nu=1}^{N(l)} [F_l^{\nu}(\mathbf{h}_i)]^2 \quad (4.179)$$

against l and extrapolates to $l \rightarrow \infty$.

In a completely analogous way we define the truncation error for the function $f(g)$:

$$A_L = \oint \left[f(g) - \sum_{l=0}^L \sum_{\mu=1}^{M(l)} \sum_{\nu=1}^{N(l)} C_l^{\mu\nu} \dot{T}_l^{\mu\nu}(g) \right]^2 dg \quad (4.180)$$

and thereby obtain the two expressions

$$A_L = \oint [f(g)]^2 dg - \sum_{l=0}^L \sum_{\mu=1}^{M(l)} \sum_{\nu=1}^{N(l)} \frac{1}{2l+1} [C_l^{\mu\nu}]^2 \quad (4.181)$$

$$A_L = \sum_{l=L+1}^{\infty} \sum_{\mu=1}^{M(l)} \sum_{\nu=1}^{N(l)} \frac{1}{2l+1} [C_l^{\mu\nu}]^2 \quad (4.182)$$

In the case of calculation of the coefficients $C_l^{\mu\nu}$ from pole figures, the function $f(g)$ is in principle unknown. The truncation error can therefore only be estimated from equation (4.182). For this purpose one can plot the value

$$\sum_{\mu=1}^{M(l)} \sum_{\nu=1}^{N(l)} \frac{1}{2l+1} [C_l^{\mu\nu}]^2 \quad (4.183)$$

against l and extrapolate to $l \rightarrow \infty$.

In Section 4.8 the texture index J will be introduced as a measure of the severity of texture equation (4.212). If we denote by J_L the texture index of the approximation function of L th degree, for the truncation error it is true that

$$A_L = J - J_L \quad (4.184)$$

The truncation error is thus given by the difference between the severity measure of the actual texture and its approximation function.

4.6.1. Decrease of the Truncation Error by Smearing

In practical cases the functions $f(g)$ concerned generally are of small to medium slope. The distance between points of maximum and minimum function values is comparatively large. The terms with $l > L$ omitted in the series expansion represent comparatively 'short wavelength' fluctuations. If, therefore, one 'smears' the function $f(g)$ over a certain region Δg , the short wavelength terms will be eliminated, while the course of the function is retained in the large. By 'smearing' of the function $f(g)$ we shall understand the convolution integral of the function $f(g)$ with a real smearing function $w(\Delta g)$:

$$\tilde{f}(g) = \oint f(g \cdot \Delta g) w(\Delta g) d\Delta g \quad (4.185)$$

This clearly means that we shift the function $f(g)$ in total to different values Δg and superimpose all functions $f(g \cdot \Delta g)$, thus producing a weight distribution $w(\Delta g)$. As will be shown in the chapter on 'Mathematical Aids', for the coefficients of the series expansion of the three functions, it is then valid that

$$\tilde{C}_l^{\mu\nu} = \frac{1}{2l+1} \sum_{\nu'=1}^{N(l)} C_l^{\mu\nu'} w_l^{*\nu\nu'} \quad (4.186)$$

If the smearing function $w(\Delta g)$ depends only on the absolute value of the rotation Δg — i.e. on the rotation angle — it is thus true for the coefficients that (see equations 14.26, 14.27 and 14.15)

$$w_l^{*\nu\nu'} = (2l+1) w_l \delta_{\nu\nu'} \quad (4.187)$$

In this case we obtain

$$\tilde{C}_l^{\mu\nu} = w_l C_l^{\mu\nu} \quad (4.188)$$

The smoother the smearing function — i.e. the more severe the smoothing is — the more quickly the coefficients w_l decrease with l . By choice of a sufficiently rapid smearing function one can thus always ensure that the coefficients $C_l^{\mu\nu}$ will already be approximately zero for $l < L \leq l_{\max}$. The function $\tilde{f}(g)$ then, however, only shows a much smaller truncation error. The accuracy will naturally not be improved by this procedure, since no longer will it be the function that it is sought to be calculated but the smeared function $\tilde{f}(g)$. Multiplication of the coefficients $C_l^{\mu\nu}$ by the factors w_l is analogous to the introduction of an artificial temperature factor in crystal structure analysis. In conclusion, however, it may be noted that, by introduction of coefficients w_l which increase with l , the function $f(g)$ can also be 'sharpened'.

4.7. Determination of the Coefficients $C_l^{\mu\nu}$ from Incompletely Measured Pole Figures

A knowledge of the complete pole figure is a prerequisite to the application of equation (4.74) for calculation of the coefficients $F_l^*(\mathbf{h}_i)$. Frequently, however, pole figures can only be incompletely measured. One thus obtains the pole figures for sheet by the back-reflection method only in a region

$$0 \leq \Phi \leq \Phi_R \quad (4.189)$$

and, by the transmission method, in the region

$$\Phi_D \leq \Phi \leq 90^\circ \quad (4.190)$$

where the angle Φ is measured from the sheet normal (see Figure 4.10). If one combines both methods, one obtains an overlapping region,

$$\Phi_D \leq \Phi \leq \Phi_R \quad (4.191)$$

in which the pole figures can be measured by both methods. With the help of the values of this region one can adapt the two measurements to each other and thereby obtain a complete pole figure. This equalization is, however, frequently uncertain, so that many incomplete pole figures have been given in the literature — i.e. pole figures which are known in only one of the intervals (4.189) or (4.190). If one desires to calculate the coefficients $C_l^{\mu\nu}$ and thereby the orientation distribution $f(g)$ from such pole figures, it is necessary to modify somewhat the methods previously used, since one can no longer make use of the orthogonality relations of the terms of the series.

If we assume the coefficients $C_l^{\mu\nu}$ to be known, we can calculate pole figures $P_{\mathbf{h}_i}(\mathbf{y})_{\text{cal}}$ from equation (4.60). The measured and previously normalized pole figures are $P_{\mathbf{h}_i}(\mathbf{y})_{\text{obs}}$. We shall then propose as a condition for the determination

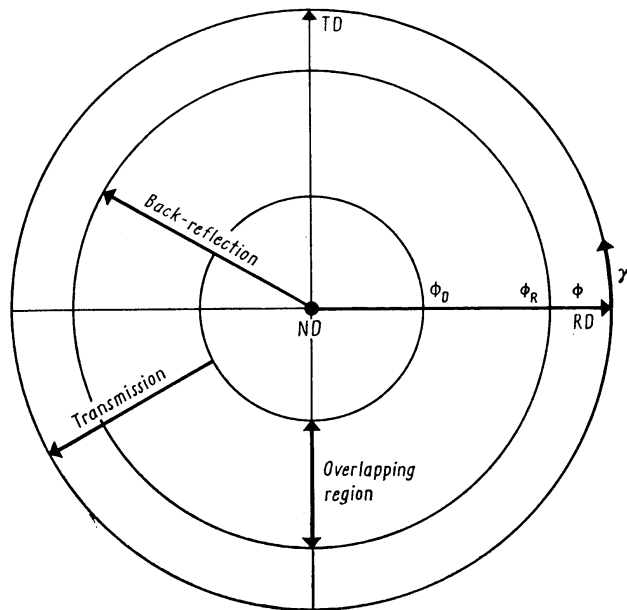


Figure 4.10 Transmission and reflection regions of pole figures (schematic)

of the coefficients $C_i^{\mu\nu}$ that the calculated pole figures deviate as little as possible from the measured pole figures within the available region B . This gives the minimal condition

$$\sum_i w_i \int_B [P_{\mathbf{h}_i}(\mathbf{y})_{\text{obs.}} - P_{\mathbf{h}_i}(\mathbf{y})_{\text{cal.}}]^2 d\mathbf{y} = \min. \quad (4.192)$$

w_i is a weight factor which gives the accuracy of measurement of the \mathbf{h}_i pole figure to be considered. If we express the calculated pole figure according to equation (4.60) and allow the measured pole figure to be present at first with unknown normalization, we thus obtain from equation (4.192)

$$\sum_i w_i \int_B \left[N_i \hat{P}_{\mathbf{h}_i}(\mathbf{y})_{\text{obs.}} - \sum_{l=0}^L \sum_{\mu=1}^{M(l)} \sum_{\nu=1}^{N(l)} \frac{4\pi}{2l+1} C_l^{\mu\nu} \dot{k}_l^{\mu}(\mathbf{h}_i) \dot{k}_l^{\nu}(\mathbf{y}) \right]^2 d\mathbf{y} = \min. \quad (4.193)$$

The $C_l^{\mu\nu}$ and the N_i here are to be so chosen that the expression will be minimized. By differentiation with respect to $C_l^{\mu\nu}$ we first obtain

$$\begin{aligned} & \sum_i w_i \int_B \dot{k}_l^{\mu}(\mathbf{h}_i) \dot{k}_l^{\nu}(\mathbf{y}) \\ & \times \left[N_i \hat{P}_{\mathbf{h}_i}(\mathbf{y})_{\text{obs.}} - \sum_{l=0}^L \sum_{\mu=1}^{M(l)} \sum_{\nu=1}^{N(l)} \frac{4\pi}{2l+1} C_l^{\mu\nu} \dot{k}_l^{\mu}(\mathbf{h}_i) \dot{k}_l^{\nu}(\mathbf{y}) \right] d\mathbf{y} = 0 \quad (4.194) \end{aligned}$$

If one differentiates with respect to N_i , one obtains

$$\int_B \hat{P}_{\mathbf{h}_i}(\mathbf{y})_{\text{obs.}} \left[N_i \hat{P}_{\mathbf{h}_i}(\mathbf{y})_{\text{obs.}} - \sum_{l=0}^L \sum_{\mu=1}^{M(l)} \sum_{\nu=1}^{N(l)} \frac{4\pi}{2l+1} C_l^{\mu\nu} \dot{k}_l^{\mu}(\mathbf{h}_i) \dot{k}_l^{\nu}(\mathbf{y}) \right] d\mathbf{y} = 0 \quad (4.195)$$

We introduce the following quantities for brevity:

$$\int_B [\hat{P}_{\mathbf{h}_i}(\mathbf{y})_{\text{obs.}}]^2 d\mathbf{y} = P_i \quad (4.196)$$

$$\dot{k}_l^{\mu}(\mathbf{h}_i) \int_B \hat{P}_{\mathbf{h}_i}(\mathbf{y})_{\text{obs.}} \dot{k}_l^{\nu}(\mathbf{y}) d\mathbf{y} = a_l^{\mu\nu}(\mathbf{h}_i) \quad (4.197)$$

$$\int_B \dot{k}_l^{\nu}(\mathbf{y}) \dot{k}_l^{\nu'}(\mathbf{y}) d\mathbf{y} = \zeta_{ll'}^{\nu\nu'} \quad (4.198)$$

$$\sum_i w_i \frac{4\pi}{2l+1} \dot{k}_l^{\mu}(\mathbf{h}_i) \dot{k}_l^{\nu}(\mathbf{h}_i) = \alpha_{ll'}^{\mu\nu} \quad (4.199)$$

The condition equations (4.194) and (4.195) thereby become

$$\sum_{l=0}^L \sum_{\mu=1}^{M(l)} \sum_{\nu=1}^{N(l)} C_l^{\mu\nu} \alpha_{ll'}^{\mu\nu} \zeta_{ll'}^{\nu\nu'} = \sum_i w_i N_i a_l^{\mu\nu}(\mathbf{h}_i) \quad (4.200)$$

$$\sum_{l=0}^L \sum_{\mu=1}^{M(l)} \sum_{\nu=1}^{N(l)} C_l^{\mu\nu} \frac{4\pi}{2l+1} a_l^{\mu\nu}(\mathbf{h}_i) = N_i P_i \quad (4.201)$$

If one expresses the normalization factors according to equation (4.201) and substitutes these in equation (4.200), one obtains

$$\sum_{l=0}^L \sum_{\mu=1}^{M(l)} \sum_{\nu=1}^{N(l)} C_l^{\mu\nu} \left[\alpha_{ll'}^{\mu\nu} \zeta_{ll'}^{\nu\nu'} - \frac{4\pi}{2l+1} \sum_i w_i a_l^{\mu\nu}(\mathbf{h}_i) a_l^{\mu\nu}(\mathbf{h}_i) \right] = 0 \quad (4.202)$$

This is a system of linear equations with as many equations as unknowns $C_l^{\mu\nu}$. If the $C_l^{\mu\nu}$ have been calculated from it, the normalization factors thus result from equation (4.201). Since equation (4.202) is a homogeneous system, the $C_l^{\mu\nu}$ are only determined up to a common factor, which is then determined so that the normalization condition (4.15) holds. This is a slightly different description compared with Sections 4.2.1, where the condition $C_0^{11} = 1$ was used from the very beginning. This leads immediately to an inhomogeneous system of equations (4.53) as is obtained from equation (4.202) by setting $C_0^{11} = 1$.

If the normalization factors N_i of the pole figures are experimentally known, the $C_l^{\mu\nu}$ are determined from the inhomogeneous system of equations (4.200). We now consider regions B which are rotationally symmetric about the Z -axis — i.e. those for which the variation of the angle Φ is restricted but not that of the angle γ . If we assume orthorhombic sample symmetry, the spherical surface harmonics $\dot{k}_l^{\nu}(\mathbf{y})$ have the form (see Chapter 14)

$$\dot{k}_l^{\nu}(\mathbf{y}) = \dot{k}_l^{\nu}(\Phi, \gamma) = \frac{\epsilon^{\nu}}{\sqrt{2\pi}} \bar{P}_l^{2(\nu-1)}(\cos \Phi) \cos 2(\nu-1) \gamma \quad (4.203)$$

with

$$\varepsilon^r = \begin{cases} 1 & \text{for } r = 1 \\ \sqrt{2} & \text{for } r \neq 1 \end{cases} \quad (4.204)$$

It thus follows from equation (4.198) that

$$\zeta_{ll'}^{rr'} = \zeta_{ll'}^r \delta_{rr'} \quad (4.205)$$

with

$$\zeta_{ll'}^r = \int_{\Phi_a}^{\Phi_b} \bar{P}_l^{2(r-1)}(\cos \Phi) \bar{P}_{l'}^{2(r-1)}(\cos \Phi) \sin \Phi d\Phi \quad (4.206)$$

The system of equations (4.200) thereby decomposes into a system for each value of r :

$$\sum_{l=0}^L \sum_{\mu=1}^{M(l)} C_l^{\mu r} \alpha_l^{\mu \mu'} \zeta_{ll'}^r = \sum_i w_i N_i a_l^{\mu' r}(\mathbf{h}_i) \quad (4.207)$$

This method has been applied with a pseudo-normalization factor^{177a} which can be improved by an iterative method^{155a}. If, finally, one sets $\Phi_a = 0^\circ$, $\Phi_b = 180^\circ$, equation (4.206) becomes

$$\zeta_{ll'}^r = \delta_{ll'} \quad (4.208)$$

The system (4.207) thus reduces further to

$$\sum_{\mu=1}^{M(l)} C_l^{\mu r} \alpha_l^{\mu \mu'} = \sum_i w_i N_i a_l^{\mu' r}(\mathbf{h}_i) \quad (4.209)$$

In this case the normalization factors result directly from equation (4.73), so that in equation (4.209) only the $C_l^{\mu r}$ are unknown. Equation (4.209) is identical with equation (4.145), as it must be.

4.8. Texture Index

In the preceding section we have seen that a texture can be completely characterized by specification of the coefficients $C_l^{\mu r}$ of its series expansion in generalized spherical harmonics. If one possesses no additional knowledge about the orientation distribution (perhaps the kind which concerns a Gaussian distribution about the ideal orientation — see Chapter 7), all coefficients are then necessary for complete characterization of the texture. The more these coefficients differ from zero, the sharper the texture is.

One is frequently interested only in the severity of the texture without considering the details of the distribution. It is then appropriate to characterize the sharpness of the texture by a single parameter. This can be done, for example, by the integral of the square of the texture function, the so-called texture index J ²⁷¹:

$$J = \oint [f(g)]^2 dg \quad (4.210)$$

If we substitute the series expansion for $f(g)$, we obtain

$$J = \sum_{l,\mu,r} \sum_{l',\mu',r'} C_l^{\mu r} C_{l'}^{*\mu' r'} \oint \dot{T}_l^{\mu r}(g) \dot{T}_{l'}^{*\mu' r'}(g) dg \quad (4.211)$$

Because of the orthogonality of the generalized spherical harmonics, this yields

$$J = \sum_{l,\mu,r} \frac{1}{2l+1} |C_l^{\mu r}|^2 \quad (4.212)$$

In the case of random distribution only the coefficient C_0^{11} is different from zero, and for the normalization used here it has the value 1. Therefore

$$J_r = 1 \quad (4.213)$$

If the texture differs from zero only at the point $g = g_0$ (i.e. we are dealing with an ideal single crystal), the $C_l^{\mu r}$ are thus given by equation (4.19). For this case it therefore follows that

$$J_{\text{ideal}} = \sum_{l,\mu,r} \frac{1}{2l+1} |\dot{T}_l^{\mu r}(g_0)|^2 \rightarrow \infty \quad (4.214)$$

The texture index thus varies between 1 in the case of random orientation and ∞ in the case of one or more ideal single crystals.

We can also define a measure of sharpness of the pole figures analogous to equation (4.210):

$$J_{\mathbf{h}_i} = \frac{1}{4\pi} \oint [\mathbf{P}_{\mathbf{h}_i}(\mathbf{y})]^2 dy \quad (4.215)$$

If we substitute in equation (4.215) the series expansion (4.62), we obtain

$$J_{\mathbf{h}_i} = \frac{1}{4\pi} \sum_{l,\mu} |\dot{F}_l^{\mu}(\mathbf{h}_i)|^2 \quad (4.216)$$

Finally, we obtain for the inverse pole figures

$$J_{\mathbf{y}_j} = \frac{1}{4\pi} \oint [\mathbf{R}_{\mathbf{y}_j}(\mathbf{h})]^2 dh \quad (4.217)$$

and this yields, in terms of the coefficients,

$$J_{\mathbf{y}_j} = \frac{1}{4\pi} \sum_{l,\mu} |\dot{H}_l^{\mu}(\mathbf{y}_j)|^2 \quad (4.218)$$

The measures of sharpness $J_{\mathbf{h}_i}$ and $J_{\mathbf{y}_j}$ are also so normalized that they give the value 1 for random distribution.

By suitable choice of the crystal coordinate system, one can write the pole figure $\mathbf{P}_{\mathbf{h}_i}(\mathbf{y})$ as follows:

$$\mathbf{P}_{\mathbf{h}_i}(\Phi, \varphi_1) = \frac{1}{2\pi} \int_0^{2\pi} f(\varphi_1, \Phi, \varphi_2) d\varphi_2 \quad (4.219)$$

from which we obtain for the measure of sharpness of this pole figure

$$J_{\mathbf{h}_i} = \frac{1}{16\pi^3} \int_0^\pi \int_0^{2\pi} \left[\int_0^{2\pi} f(\varphi_1, \Phi, \varphi_2) d\varphi_2 \right]^2 \sin \Phi d\Phi d\varphi_1 \quad (4.220)$$

Now it is true by a well-known theorem of integral calculus (see reference 92) that

$$\left[\int_0^{2\pi} f(\varphi_1, \Phi, \varphi_2) d\varphi_2 \right]^2 \leq \int_0^{2\pi} [f(\varphi_1, \Phi, \varphi_2)]^2 d\varphi_2 \cdot \int_0^{2\pi} d\varphi_2 \quad (4.221)$$

It follows that

$$J_{\mathbf{h}_i} \leq \frac{1}{8\pi^2} \int_0^\pi \int_0^{2\pi} \int_0^{2\pi} [f(\varphi_1, \Phi, \varphi_2)]^2 \sin \Phi d\Phi d\varphi_1 d\varphi_2 \quad (4.222)$$

This means, from equation (4.210),

$$J_{\mathbf{h}_i} \leq J \quad (4.223)$$

In other words, the measure of sharpness of an arbitrary pole figure can only be smaller than or at most equal to that of the three-dimensional orientation distribution function. It can even be that a sharp orientation distribution function possesses a pole figure with random distribution. One sees this from equation (4.61). If in this equation one sets $F_l^v(\mathbf{h}_i) = 0$ for a specified \mathbf{h}_i and $l \neq 0$, it can yield solutions $C_l^{\mu\nu} \neq 0$ for all l , for which $M(l) \geq 2$ — i.e. a non-constant orientation distribution.

In complete analogy with the above for pole figures, a corresponding inequality also results for inverse pole figures:

$$J_{\mathbf{y}_i} \leq J \quad (4.224)$$

Thus inverse pole figures can not be sharper than the orientation distribution $f(g)$ itself. This result is naturally also clearly evident.

4.9. Ambiguity of the Solution

If in equation (4.61) the number of equations (i.e. the number of pole figures) is smaller than $M(l)$, this system of equations has thus several linearly independent solutions. For a given number I_P of pole figures, according to equation (4.91), this is the case for $l > l_{\max}$. There thus result many different orientation distribution functions $f(g)$, which differ in the coefficients for $l > l_{\max}$, but agree exactly in the selected I_P pole figures. The difference between any two of these functions thus is a function

$$f_0(g) = \sum_{l>l_{\max}}^{\infty} \sum_{\mu=1}^{M(l)} \sum_{\nu=1}^{N(l)} C_l^{\mu\nu} \dot{T}_l^{\mu\nu}(g) \quad (4.225)$$

with coefficients differing from zero for $l > l_{\max}$, which thus can not be zero everywhere, but its first I_P pole figures are identically zero.

Naturally, it is true for the function $f_0(g)$ that

$$\oint f_0(g) dg = 0 \quad (4.226)$$

It must thus also assume negative function value. This function therefore can not be an *orientation* distribution function. If, however, $f(g)$ is an arbitrary orientation distribution function, the function

$$f'(g) = f(g) + f_0(g) \quad (4.227)$$

thus has exactly the same I_P pole figures as the function $f(g)$. The function $f_0(g)$ thus characterizes the uncertainty of the calculation of an orientation distribution function from the I_P pole figures. If $f'(g)$ is an orientation distribution function, it must therefore be true that

$$f'(g) = f(g) + f_0(g) \geq 0 \quad (4.228)$$

The admissible variation region of the coefficients in equation (4.225) will thus be fixed.

The ambiguity of the solution turns out very easily in the series expansion method. It is, however, independent of the specific method employed. Since in methods not based on series expansion (Chapter 6) it is not so easily detected, these methods are sometimes regarded as superior to the series expansion method²⁷⁰. This is, however, an erroneous conclusion.

4.9.1. Non-random Textures with Random Pole Figures

For example, in equation (4.227) we choose

$$f(g) \equiv 1 \quad (4.229)$$

i.e. the random distribution, and $I_P = 1$. $f'(g)$ is thus a non-random distribution, which, however, has a random pole figure. If we assume cubic symmetry, $l_{\max} = 10$. We obtain a special function $f_0(g)$, if in equation (4.225) we assume only the coefficients with $l = 12$ different from zero and choose them so that the \mathbf{h}_i pole figure belonging to $f_0(g)$ is zero. From equation (4.61) it follows that

$$C_{12}^{1\nu} k_{12}^{*1}(\mathbf{h}_i) + C_{12}^{2\nu} k_{12}^{*2}(\mathbf{h}_i) = 0 \quad (4.230)$$

It thus follows that

$$C_{12}^{2\nu} = -C_{12}^{1\nu} \cdot \frac{k_{12}^{*1}(\mathbf{h}_i)}{k_{12}^{*2}(\mathbf{h}_i)} \quad (4.231)$$

The orientation distribution function

$$f'(g) = 1 + f_0(g) = 1 + C_{12}^{1\nu} \left[\dot{T}_{12}^{1\nu}(g) - \frac{k_{12}^{*1}(\mathbf{h}_i)}{k_{12}^{*2}(\mathbf{h}_i)} \dot{T}_{12}^{2\nu}(g) \right] \quad (4.232)$$

thus has a random \mathbf{h}_i pole figure

$$P_{\mathbf{h}_i}(\mathbf{y}) \equiv 1 \quad (4.233)$$

but is itself not random. Since the functions $\dot{T}_l^{\mu\nu}(g)$, and therefore also the expression in brackets in equation (4.232), assume nearly equal maximum negative and

positive values, one can choose the coefficients $C_{12}^{1\nu}$ so that the function $f(g)$ varies in the region

$$0 \leq f'(g) \leq 2 \quad (4.234)$$

while its \mathbf{h}_i pole figure is random according to equation (4.233). One such function is represented in Figure 4.11 for $\mathbf{h}_i = [100]$ and $\nu = 2$. From its \mathbf{h}_i pole figure alone this function cannot be distinguished from the random distribution. It thus



Figure 4.11 An orientation distribution function whose (100) pole figure is random 73b

characterizes the degree of uncertainty of the distribution function calculated from a single pole figure. With the inequality

$$|\dot{T}_l^{\mu\nu}(g)| \leq 1 \quad (4.235)$$

from equation (4.232) one obtains the following estimate for the allowable values of the coefficients $C_{12}^{1\nu}$:

$$|C_{12}^{1\nu}| < \frac{1}{1 + \frac{|k_{12}^{*1}(\mathbf{h}_i)|}{|k_{12}^{*2}(\mathbf{h}_i)|}} \quad (4.236)$$

If in equation (4.225) one assumes several coefficients $C_l^{\mu\nu}$ different from zero, the allowable variation regions of the coefficients satisfying relation (4.228) naturally are interdependent, and they also depend on the selection of the function $f(g)$. If $f(g)$ is already zero at some points, $f_0(g)$ must naturally not be negative there. The estimate of the allowable variation region for the coefficients $C_l^{\mu\nu}$ naturally is then complicated 73b.

4.9.2. The Refinement Procedure of Krigbaum

If the coefficients $C_l^{\mu\nu}$ for $l \leq l_{\max}$ have already decreased to the order of their experimental errors, the uncertainty function $f_0(g)$ is thus of the order of the experimental error and the texture is completely determined within the limit of error from a finite number of pole figures. If, however, this is not the case — i.e. if the coefficients $C_l^{\mu\nu}$ for $l > l_{\max}$ are still larger than their experimental errors (Figure 4.12) — an actual series truncation error occurs, if one neglects them. The truncation

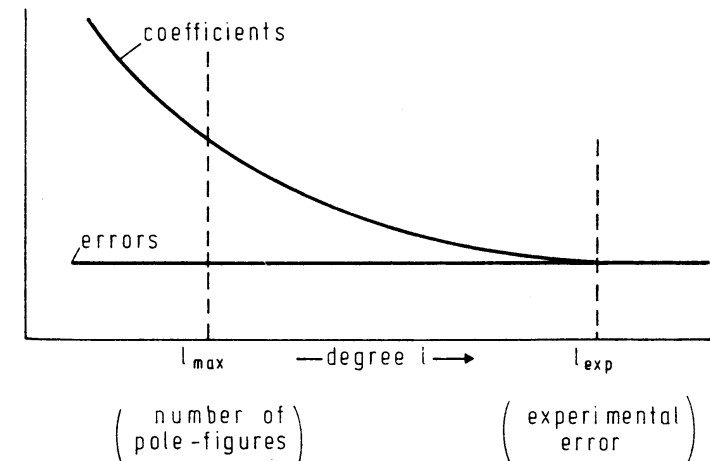


Figure 4.12 Average values of the coefficients $|\bar{C}_l^{\mu\nu}|$ and their errors $|\bar{\Delta C}_l^{\mu\nu}|$ as a function of the index l , as well as the limiting values l_{\max} and l_{\exp} .

error is then of the same order as the uncertainty of the function $f(g)$, owing to the finite number of pole figures. Since in these cases, however, the individual pole figures have a higher accuracy, they can be expanded up to a higher value $l = l_{\text{exp.}}$, which, according to Figure 4.12, is determined by the size of the experimental error. The uncertainty due to $l_{\text{max.}}$ is thus in these cases much greater than the experimental uncertainty of the pole figures. If one only extends the series expansion up to $l_{\text{max.}}$, the experimental information of the pole figures is not completely exploited. One can then ask whether it is not possible further to limit the uncertainty interval of the function $f(g)$ — i.e. to calculate the coefficients $C_l^{\mu\nu}$ beyond $l = l_{\text{max.}}$. Since this is not possible with the use of equation (4.61) alone, one has to add some other information. KRIGBAUM¹⁸² has given a procedure with which, under certain assumptions, this is possible. If one has calculated the coefficients $C_l^{\mu\nu}$ up to $l = l_{\text{max.}}$ from the pole figures \mathbf{h}_i with $1 \leq i \leq I_p$, one can in this approximation calculate further pole figures with $i > I_p$. They have series truncation waves, which correspond to the size of $l_{\text{max.}}$. One now tries to smooth out these waves and thus to construct ‘plausible’ pole figures for $i > I_p$. If one includes the pole figures so constructed in the next calculation, one can calculate the coefficients up to a higher value $l'_{\text{max.}}$. This yields new values for the pole figures constructed which may deviate from those of the first calculation. These new pole figures, again, can be smoothed out and be incorporated into the next step of the calculation. One can continue this process until improvement ceases. The ‘additional information’ which one thus uses to further compress the uncertainty interval of the solution is the ‘smoothness’ or physically ‘plausible’ appearance of non-measured pole figures.

An example of this process was treated by KRIGBAUM and VASEK.¹⁸⁶ They analysed the rotationally symmetric texture (fibre texture) of triclinic polyethylene terephthalate, which had relatively sharp peaks in the pole figures. Because of the low triclinic symmetry, according to Figure 4.4, $M(l)$ is very high. Seventeen pole figures were measured. It results that $l_{\text{max.}} = 8$. If, however, one considers the experimental error, it is necessary to work with a certain overdetermination — i.e. to use more pole figures than unknowns are to be determined. One then arrives at $l_{\text{max.}} = 6$, which corresponds to 13 pole figures. If one now expands the pole figures only up to $l_{\text{max.}} = 6$, one obtains an approximate curve, as is represented in Figure 4.13 by the dashed curve. The pole figures, however, permit a series expansion up to $l_{\text{exp.}} = 16$ to be reasonably obtained (dotted curve). In the approximation $l = 6$, 29 additional pole figures were thus calculated — e.g. the (120) pole figure represented in Figure 4.14 (dashed curve). From the experimental pole figures one can perhaps estimate how sharp the peaks of the non-measured pole figures will be and thus construct a hypothetical (120) pole figure (dotted curve). If one includes the pole figures thus constructed in the calculation, one has 46 pole figures and can extend the calculation up to $l = 16$. The curves of the approximation $l = 16$ after the second refinement cycle are also given in Figures 4.13 and 4.14 (solid curves). One sees that they fit the experimental curves much better than the curves for $l_{\text{max.}} = 6$. With the help of the refinement pro-

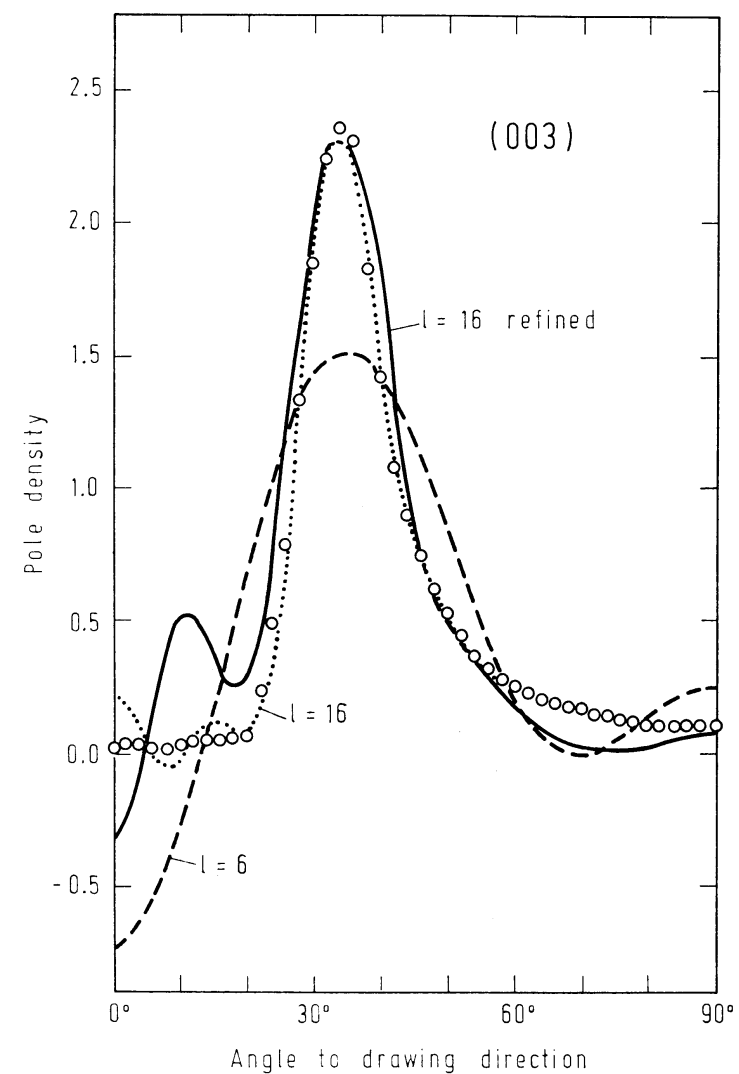


Figure 4.13 The measured (003) pole figure of polyethylene terephthalate (circles), as well as its approximate curves for $l = 6$ (dashed) and $l = 16$ (dotted). The solid curve corresponds to the pole figures recalculated from the coefficients $C_l^{\mu\nu}$ in the $l = 16$ approximation after carrying out a refinement procedure. After KRIGBAUM and VASEK¹⁸⁶

ture the experimental information of the measured pole figures can thus be exploited beyond $l_{\text{max.}}$ and the uncertainty interval be reduced. This method is of particular importance for low crystal symmetries, where very small values of $l_{\text{max.}}$ appear.

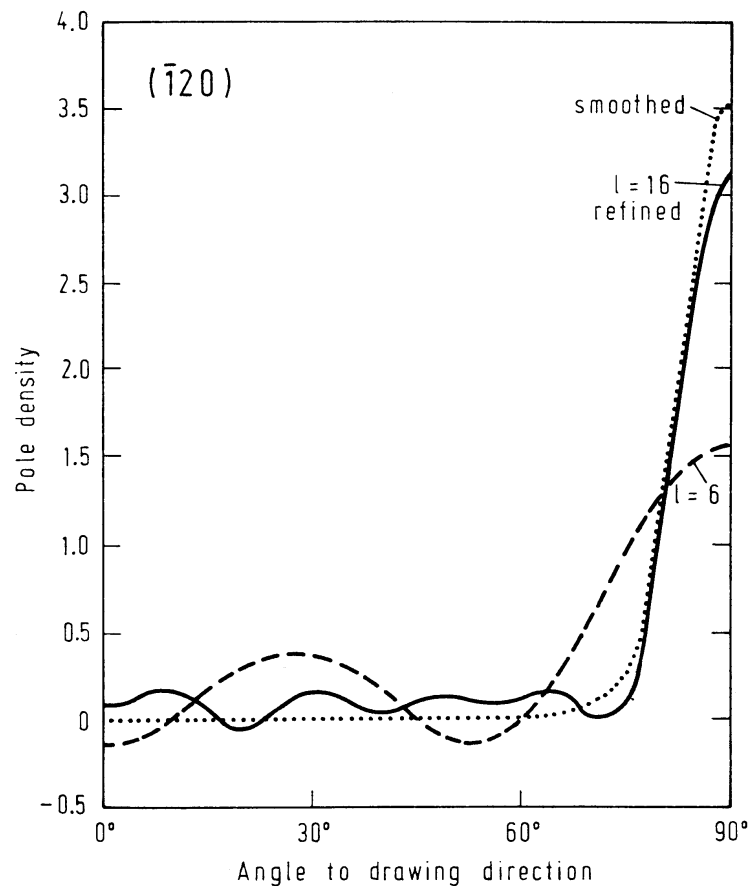


Figure 4.14 The non-measured (1̄20) pole figure. The dashed curve was calculated in the $l = 6$ approximation from the coefficients $C_l^{\mu\nu}$. The dotted curve is the presumed pole figure; the solid curve results from application of the refinement procedure in the $l = 16$ approximation. After KRIGBAUM and VASEK¹⁸⁶

4.9.3. The Extremum Method of Tavard

According to TAVARD and ROYER²⁷⁷, one obtains an unequivocal solution of the equation system (4.60) beyond $l = l_{\max}$, if one determines the coefficients so that, in addition to equation (4.61), the condition

$$\sum_{\mu=1}^{M(l)} |C_l^{\mu\nu}|^2 = \min. \quad (4.237)$$

is fulfilled. As in the process of KRIGBAUM, a requirement of ‘smoothness’ of the function will appear. This serves as additional information to define a function within the uncertainty region.

4.10. Comparison with Roe’s Terminology

The procedure here described for calculation of the orientation distribution from pole figures was described by ROE²⁴⁶ with a different terminology. It is therefore appropriate to compare the quantities with the same meaning in the two terminologies. In place of equation (4.2) the orientation distribution function is described by

$$w(\Psi\Theta\Phi) = \sum_{l=0}^{\infty} \sum_{m=-l}^{+l} \sum_{n=-l}^{+l} W_{lmn} e^{-im\psi} Z_{lmn}(\Theta) e^{-in\phi} \quad (4.238)$$

(Notice that the position of the indices m and n corresponding to the first and third EULER angles is reversed with respect to equation 4.2.) Thus, according to equation (2.6),

$$\Psi^{(2)} = \varphi_1 - \frac{\pi}{2}, \quad \Theta^{(2)} = \Phi, \quad \Phi^{(2)} = \varphi_2 + \frac{\pi}{2} \quad (4.239)$$

The function $w(\Psi\Theta\Phi)$ is so normalized that

$$\int_0^{2\pi} \int_0^{\pi} \int_0^{2\pi} w(\Psi\Theta\Phi) \sin \Theta d\Psi d\Theta d\Phi = 1 \quad (4.240)$$

It follows from this and from equations (4.10) and (4.11) that

$$w(\Psi\Theta\Phi) = \frac{1}{8\pi^2} f(\varphi_1\Phi\varphi_2) \quad (4.241)$$

In particular, it is true that

$$w_{\text{random}} = \frac{1}{8\pi^2}, \quad f_{\text{random}} = 1 \quad (4.242)$$

If one introduces equation (4.241) as well as the relation

$$Z_{lmn}(\Phi) = i^{n-m} \sqrt{\frac{2l+1}{2}} P_l^{mn}(\Phi) \quad (4.243)$$

into equation (4.238) and compares the coefficients with those of equation (4.2), one obtains the relation

$$W_{lmn} = \frac{1}{8\pi^2} \sqrt{\frac{2}{2l+1}} C_l^{-n,-m} \quad (4.244)$$

The pole figures are represented as follows:

$$q_l(\chi\eta) = \sum_{l=0}^{\infty} \sum_{m=-l}^{+l} Q_{lm}^i P_l^m(\chi) e^{-im\eta} \quad (4.245)$$

The following relation thereby exists with the functions used here:

$$P_l^m(\chi) = (-1)^m \bar{P}_l^m(\chi) \quad (4.246)$$

The pole figures are normalized similarly to equation (4.240):

$$\int_0^\pi \int_0^{2\pi} q_i(\chi\eta) \sin \chi d\eta d\chi = 1 \quad (4.247)$$

The angles χ and η correspond to the pole figure angles Φ and γ :

$$\chi = \Phi; \quad \eta = \gamma \quad (4.248)$$

It therefore follows from the normalization condition that

$$q_i(\chi\eta) = \frac{1}{4\pi} P_{\mathbf{h}_i}(\Phi\gamma) \quad (4.249)$$

For the random distribution one obtains

$$q_{\text{random}} = \frac{1}{4\pi}; \quad P_{\text{random}} = 1 \quad (4.250)$$

If one compares equation (4.245) with equation (4.61), one obtains the following relation between the coefficients:

$$Q_{lm}^i = \frac{1}{4\pi \sqrt{2\pi}} F_l^{-m}(\mathbf{h}_i) \quad (4.251)$$

The relation

$$Q_{lm}^i = 2\pi \sqrt{\frac{2}{2l+1}} \sum_{n=-l}^{+l} W_{lmn} P_l^n(\Theta_i) e^{in\Phi_i} \quad (4.252)$$

exists between the coefficients Q_{lm}^i and W_{lmn} , where Φ_i^{Roe} and Θ_i^{Roe} are the polar coordinates of the pole of the reflecting lattice plane i . They correspond to the angles $\Phi_i \beta_i$ used here:

$$\Theta_i^{\text{Roe}} = \Phi_i; \quad \Phi_i^{\text{Roe}} = \beta_i \quad (4.253)$$

If in the sample coordinate system K_A there exists a symmetry according to the symmetry group G_A and in the crystal coordinate system K_B according to G_B , then certain restrictions are imposed on the coefficients W_{lmn} . In the case of 'low' symmetries (non-cubic symmetries) these restrictions may be expressed in the form of 'selection rules', as is described in Section 14.7. This means that some of the coefficients are zero and in certain symmetries the values of W depend only on the absolute values of m or n . For example, in the case of tetragonal crystal symmetry it is²⁴⁸

$$W_{lmn} = W_{lm-n} \quad n = 4k \\ = 0 \quad n \neq 4k \quad (4.254)$$

In the case of high symmetry (i.e. cubic symmetry) the symmetry restrictions cannot be expressed in the form of selection rules. They lead to a system of linear

equations between the coefficients W_{lmn} in the form

$$\sum_{n=-l}^{+l} R_l^{n\mu} W_{lmn}^{(t)} = 0 \quad 1 \leq \mu \leq M'(l) \quad (4.255)$$

where $W_{lmn}^{(t)}$ are the coefficients according to the tetragonal subsymmetry defined by the selection rules (4.254). The coefficients R are independent of m . If $M'(l)$ is the number of linearly independent coefficients in the case of the tetragonal subsymmetry, then equation (4.255) has

$$M(l) = M^{(t)}(l) - M'(l) \quad (4.256)$$

linearly independent solutions. Hence, $M(l)$ of the coefficients W_{lmn} with the lowest n -values may be chosen as linearly independent. The remaining $M'(l)$ can then be expressed by the linearly independent ones in the form

$$W_{lmv} = \sum_{n=1}^{M(l)} R_l'^{nv} W_{lmn} \quad (4.257)$$

The coefficients $R_l'^{nv}$ have been given by Roe up to $l = 22$. In Table 15.2.4 they are given up to $l = 34$.

Equation (4.238) can be written in the form

$$w(g) = \sum_{lmn} W_{lmn} T_{lmn}(g) \quad (4.258)$$

If we introduce the functions T_l^{vm} which are invariant with respect to the crystal symmetry equation (14.122)

$$T_l^{vm}(g) = \sum_{n=-l}^{+l} A_{lnv} T_{lmn}(g) \quad (4.259)$$

then equation (4.258) reads

$$w(g) = \sum_{lmv} W_{lmv}' T_l^{vm}(g) \quad (4.260)$$

where W' are linearly independent coefficients. Comparing equations (4.258) and (4.260), we find

$$W_{lmn} = \sum_v W_{lmv}' A_{lnv} \quad (4.261)$$

where W_{lmn} may be assumed to be the coefficients $W_{lmn}^{(t)}$ corresponding to the tetragonal subsymmetry. With equation (4.255) equation (4.261) leads to

$$\sum_v \sum_n W_{lmv}' A_{lnv} R_l^{n\mu} = 0 \quad (4.262)$$

Since the coefficients W' are linearly independent, they can be so chosen that

$$W_{lmv}' = 1 \text{ for } v = v' \\ = 0 \text{ for } v \neq v' \quad (4.263)$$

Writing again v instead of v' , this leads to the relation

$$\sum_{n=-l}^{+l} A_{lnv} R_l^{n\mu} = 0 \quad (4.264)$$

With equations (4.239) and (4.243):

$$T_{lmn}(g) = \sqrt{\frac{2l+1}{2}} T_l^{-n-m}(g) \quad (4.265)$$

Hence, the symmetry coefficients A_{lnv} in equation (4.259) are related to the symmetry coefficients \dot{A}_l^{nv} previously used by the relation

$$A_{lnv} = \sqrt{\frac{2}{2l+1}} \dot{A}_l^{-nv} \quad (4.266)$$

Taking the tetragonal symmetry into account, we obtain

$$A_{lnv} = \sqrt{\frac{2}{2l+1}} \dot{A}_l^{nv} \quad (4.267)$$

Hence, equation (4.264) reads

$$\sum_{n=-l}^{+l} \dot{A}_l^{nv} R_l^{n\mu} = 0 \quad (4.268)$$

The coefficients $R_l^{n\mu}$ are thus orthogonal to the cubic coefficients \dot{A}_l^{nv} and they are defined according to equation (4.255) in the space of the tetragonal functions. They may thus be identified with the tetragonal coefficients $\dot{A}_l^{n\mu}$ orthogonal to the cubic ones defined in Section 14.7.3:

$$R_l^{n\mu} = \dot{A}_l^{n\mu} \quad (4.269)$$

They are tabulated in Table 15.2.3.

As will be shown in Chapter 11, quite a large number of determinations of orientation distribution functions have been carried out in both these terminologies, so that it will often be necessary to transform the results from one into the other.

4.11. The Role of the Centre of Inversion

In Section 2.3 different but symmetrically equivalent rotations and, hence, equivalent crystal orientations have been considered. Accordingly, the symmetry invariant functions $\dot{T}_l^{nv}(g)$ were introduced in equation (4.8). The symmetry operations thus taken into account are, however, only rotations and not the centre of inversion if it is present in either the crystal or the sample symmetry. Hence, the centre of inversion needs to be considered separately.

4.11.1. Right- and Left-handed Crystals

We consider first crystals without a centre of inversion. They may exist in two equivalent forms, a right- and a left-handed one. A polycrystalline material may

then be considered as a two-phase material consisting of a right- and a left-handed phase which may occur in different proportions and which may each have a texture of its own.

We consider first one of the crystal forms which may be called the right-handed one. We chose for the crystal coordinate system K_B^R three mutually perpendicular crystal directions $\mathbf{h}_1^R \mathbf{h}_2^R \mathbf{h}_3^R$ which form in this sequence a right-handed coordinate system (Figure 4.15a)

$$K_B^R = \{\mathbf{h}_1^R \mathbf{h}_2^R \mathbf{h}_3^R\} \quad (4.270)$$

The crystallographically equivalent directions $\mathbf{h}_1^L \mathbf{h}_2^L \mathbf{h}_3^L$ in the left-handed crystal then form in this sequence a left-handed crystal coordinate system (Figure 4.15b)

$$K_B^L = \{\mathbf{h}_1^L \mathbf{h}_2^L \mathbf{h}_3^L\} \quad (4.271)$$

The system made up of the opposite directions

$$K'_B = \{-\mathbf{h}_1^L - \mathbf{h}_2^L - \mathbf{h}_3^L\} \quad (4.272)$$

then forms a right-handed system in the left-handed crystals but it is not crystallographically equivalent with the right-handed system K_B^R in the right-handed crystals.

A certain crystal direction in the right-handed crystals may be defined by its components

$$\mathbf{h}^R = a_1 \mathbf{h}_1^R + a_2 \mathbf{h}_2^R + a_3 \mathbf{h}_3^R \quad (4.273)$$

or by spherical polar coordinates

$$\begin{aligned} a_1 &= \sin \Phi \cos \beta \\ a_2 &= \sin \Phi \sin \beta \\ a_3 &= \cos \Phi \end{aligned} \quad (4.274)$$

The crystallographically equivalent direction \mathbf{h}^L in the left-handed crystal

$$\mathbf{h}^L = a_1 \mathbf{h}_1^L + a_2 \mathbf{h}_2^L + a_3 \mathbf{h}_3^L \quad (4.275)$$

has the components $-a_1$, $-a_2$, $-a_3$ in the right-handed coordinate system K'_B and its spherical polar coordinates in this system are correspondingly

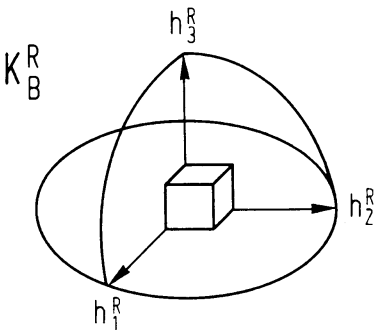
$$\mathbf{h}^L = \{\pi - \Phi, \pi + \beta\} \quad (4.276)$$

The sample coordinate system may be chosen as a right-handed one also, consisting of three mutually perpendicular sample directions (Figure 4.15c)

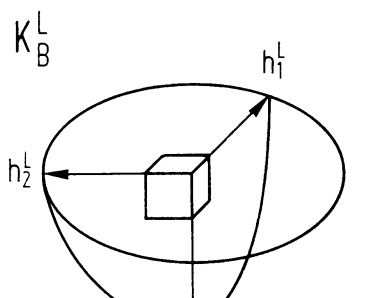
$$K_A = \{\mathbf{y}_1 \mathbf{y}_2 \mathbf{y}_3\} \quad (4.277)$$

With the help of the coordinate system K'_B the orientation g^L of the left-handed crystals can be specified analogously to the orientation g^R of the right-handed crystals. Especially the definition of the EULER angles (Figure 2.2) may be applied to this system.

Right-handed crystals

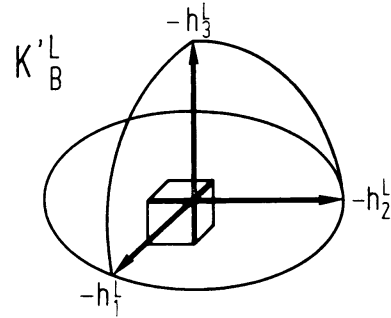


Left-handed crystals

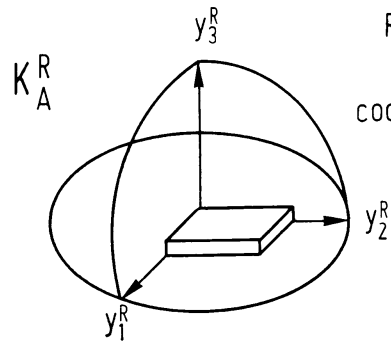


a

b



Right-handed specimen coordinate system



c

Figure 4.15 Coordinate systems in the right- and the left-handed crystals. (a) The right-handed crystal coordinate system K_B^R in the right-handed crystals. (b) The left-handed crystal coordinate system K_B^L and the right-handed coordinate system $K_B'^L$ in the left-handed crystals. (c) The right-handed sample coordinate system K_A^R

The right-handed crystals may be present in the sample with the relative amount M^R and the left-handed ones with M^L , so that

$$M^R + M^L = 1 \quad (4.278)$$

The respective orientation distribution functions may be

$$f^R(g) = \sum_{l=0}^{\infty} \sum_{\mu=1}^{M(l)} \sum_{\nu=1}^{N(l)} C_l^{R\mu\nu} \dot{T}_l^{\mu\nu}(g) \quad (4.279)$$

$$f^L(g) = \sum_{l=0}^{\infty} \sum_{\mu=1}^{M(l)} \sum_{\nu=1}^{N(l)} C_l^{L\mu\nu} \dot{T}_l^{\mu\nu}(g) \quad (4.280)$$

According to equation (4.33), the general axis distribution function was defined by the integral over all those orientations for which a certain crystal direction falls into a certain sample direction. The sample direction may be the direction \mathbf{y} . The crystal direction may be \mathbf{h}^R in the right-handed crystal and the crystallographically equivalent direction \mathbf{h}^L in the left-handed crystals. According to equation (4.35) and taking (4.276) into account, the two general axis distribution functions thus are

$$A^R(\mathbf{h}^R, \mathbf{y}) = 4\pi \sum_{l=0}^{\infty} \sum_{\mu=1}^{M(l)} \sum_{\nu=1}^{N(l)} \frac{C_l^{R\mu\nu}}{2l+1} \dot{k}_l^{*\mu}(\Phi\beta) \dot{k}_l^{\nu}(\mathbf{y}) \quad (4.281)$$

$$A^L(\mathbf{h}^L, \mathbf{y}) = 4\pi \sum_{l=0}^{\infty} \sum_{\mu=1}^{M(l)} \sum_{\nu=1}^{N(l)} \frac{C_l^{L\mu\nu}}{2l+1} \dot{k}_l^{*\mu}(\pi - \Phi, \pi + \beta) \dot{k}_l^{\nu}(\mathbf{y}) \quad (4.282)$$

With relation (14.58a) one thus obtains

$$A^L(\mathbf{h}^L, \mathbf{y}) = 4\pi \sum_{l=0}^{\infty} \sum_{\mu=1}^{M(l)} \sum_{\nu=1}^{N(l)} \frac{C_l^{L\mu\nu}}{2l+1} (-1)^l \dot{k}_l^{*\mu}(\Phi\beta) \dot{k}_l^{\nu}(\mathbf{y}) \quad (4.283)$$

The pole figures of the crystallographically equivalent directions in the right- and the left-handed crystals may thus be defined

$$P_{\mathbf{h}^R}^R(\mathbf{y}) = \sum_{l=0}^{\infty} \sum_{\nu=1}^{N(l)} F_l^{R\nu}(\mathbf{h}^R) \dot{k}_l^{\nu}(\mathbf{y}) \quad (4.284)$$

$$P_{\mathbf{h}^L}^L(\mathbf{y}) = \sum_{l=0}^{\infty} \sum_{\nu=1}^{N(l)} F_l^{L\nu}(\mathbf{h}^L) \dot{k}_l^{\nu}(\mathbf{y}) \quad (4.285)$$

with the respective coefficients

$$F_l^{R\nu}(\mathbf{h}^R) = \frac{4\pi}{2l+1} \sum_{\mu=1}^{M(l)} C_l^{R\mu\nu} \dot{k}_l^{*\mu}(\Phi\beta) \quad (4.286)$$

$$F_l^{L\nu}(\mathbf{h}^L) = \frac{4\pi}{2l+1} \sum_{\mu=1}^{M(l)} C_l^{L\mu\nu} (-1)^l \dot{k}_l^{*\mu}(\Phi\beta) \quad (4.287)$$

The two pole figures belong to crystallographically equivalent directions; hence, they cannot be distinguished in a polycrystal diffraction experiment. Hence, the virtual pole figure

$$\tilde{P}_{\mathbf{h}}(\mathbf{y}) = M^R P_{\mathbf{h}^R}^R(\mathbf{y}) + M^L P_{\mathbf{h}^L}^L(\mathbf{y}) \quad (4.288)$$

must be considered. It may be expressed in the form of a series expansion

$$\tilde{P}_h(y) = \sum_{l=0}^{\infty} \sum_{r=1}^{N(l)} \tilde{F}_l^r(h) k_l^r(y) \quad (4.289)$$

with the coefficients

$$\tilde{F}_l^r(h) = \frac{4\pi}{2l+1} \sum_{\mu=1}^{M(l)} \tilde{C}_l^{\mu r} k_l^{\mu}(h) \quad (4.290)$$

where the coefficients

$$\tilde{C}_l^{\mu r} = M^R C_l^R{}^{\mu r} + (-1)^l M^L C_l^L{}^{\mu r} \quad (4.291)$$

may be regarded as belonging to a virtual texture

$$\tilde{f}(g) = \sum_{l=0}^{\infty} \sum_{\mu=1}^{M(l)} \sum_{r=1}^{N(l)} \tilde{C}_l^{\mu r} \tilde{T}_l^{\mu r}(g) \quad (4.292)$$

Because of the factor $(-1)^l$ in equation (4.291), it is suitable to split the orientation distribution functions into two parts containing even and odd terms only in their respective series expansions

$$f^e(g) = \sum_{l=0(2)}^{\infty} \sum_{\mu=1}^{M(l)} \sum_{r=1}^{N(l)} C_l^{\mu r} \tilde{T}_l^{\mu r}(g) \quad (4.293)$$

$$f^o(g) = \sum_{l=1(2)}^{\infty} \sum_{\mu=1}^{M(l)} \sum_{r=1}^{N(l)} C_l^{\mu r} \tilde{T}_l^{\mu r}(g) \quad (4.294)$$

and it is

$$f(g) = f^e(g) + f^o(g) \quad (4.295)$$

Because of the orthogonality of the generalized spherical harmonics and the normalization condition (equation 4.15), it is

$$\int f^e(g) dg = 1 \quad (4.296)$$

$$\int f^o(g) dg = 0 \quad (4.297)$$

$$\int f^e(g) \cdot f^o(g) dg = 0 \quad (4.298)$$

With the definition of the even and odd part of a texture function (equations 4.293 and 4.294), the virtual texture equation (4.292) may be expressed by the corresponding even and odd parts of the right- and the left-handed texture functions f^R and f^L , respectively

$$\tilde{f}^e(g) = M^R f^{Re}(g) + M^L f^{Le}(g) \quad (4.299)$$

$$\tilde{f}^o(g) = M^R f^{Ro}(g) - M^L f^{Lo}(g) \quad (4.300)$$

4.11.2. Centrosymmetric Sample Symmetries

The sample may be said to exhibit a centre of inversion if the volume fraction of left-handed crystals in the orientation g^L is equal to the volume fraction of right-handed crystals in the orientation g^R . Since this must be true for all orienta-

tions, it follows immediately

$$M^L = M^R = \frac{1}{2} \quad (4.301)$$

and

$$f^L(g) = f^R(g) \quad (4.302)$$

the latter equation being equivalent with

$$C_l^{L\mu r} = C_l^{R\mu r} \quad (4.303)$$

It thus follows for the virtual texture

$$\tilde{f}^e(g) = f^{Re}(g) = f^{Le}(g) \quad (4.304)$$

$$\tilde{f}^o(g) = 0 \quad (4.305)$$

The even part of the virtual texture is thus identical with the even part of the right- and the left-handed crystals, whereas the odd part is being ‘blotted out’.

4.11.3. Centrosymmetric Crystal Symmetries

If the crystals themselves are centrosymmetric, then they can be considered as right- and left-handed *at the same time*, from which it follows immediately

$$M^L = M^R = \frac{1}{2} \quad (4.306)$$

and

$$f^L(g) = f^R(g) = f(g) \quad (4.307)$$

the latter equation being equivalent with

$$C_l^{L\mu r} = C_l^{R\mu r} = C_l^{\mu r} \quad (4.308)$$

The relations in equations (4.306)–(4.308) are similar to those in equations (4.301)–(4.303). There is, however, a physical difference. While the two texture functions $f^L(g)$ and $f^R(g)$ in equations (4.301)–(4.303) are physically distinguished, since they refer to physically distinctive crystals, they are not in equations (4.306)–(4.308). In these latter equations they are but two different descriptions of the distribution of one and the same group of crystals — namely the centrosymmetric ones. Hence, the distribution function $f(g)$ may be written without an index L or R.

The virtual pole figure defined in equation (4.288) — i.e. the superposition of the pole figures of the crystallographically equivalent directions h^R and h^L of the right- and the left-handed crystals — is now the superposition of the pole figures of the $+h$ and $-h$ directions of the centrosymmetric crystals

$$\tilde{P}_h(y) = \frac{1}{2} [P_{+h}(y) + P_{-h}(y)] \quad (4.309)$$

It may be expressed by a series expansion (equation 4.289), with the coefficients of equation (4.290). The coefficients $\tilde{C}_l^{\mu r}$ defining the virtual texture (equation

4.292) take on the form

$$\tilde{C}_l^{\mu\nu} = C_l^{\mu\nu} \frac{1}{2} [1 + (-1)^l] = \begin{cases} C_l^{\mu\nu} & \text{for } l \text{ even} \\ 0 & \text{for } l \text{ odd} \end{cases} \quad (4.310)$$

Hence, the virtual texture, which can be obtained from pole figure measurements of centrosymmetric crystals, is given by

$$\tilde{f}^e(g) = f^e(g) \quad (4.311)$$

$$\tilde{f}^o(g) = 0 \quad (4.312)$$

This means that the odd part of the texture function, which may be different from zero, can not be ‘seen’ by pole figure measurements because of the factor $[1 + (-1)^l]$ in equation (4.310), which vanishes for odd values of l .

4.11.4. Friedel’s Law

Friedel’s law makes the crystal direction $-\mathbf{h}$ indistinguishable from the direction $+\mathbf{h}$ even if the crystal itself is not centrosymmetric. Hence, instead of the pole figure equation (4.284) of the right-hand crystals, the superposed pole figure

$$\bar{P}_{\mathbf{h}^R}^R(\mathbf{y}) = \frac{1}{2} [P_{+\mathbf{h}^R}^R(\mathbf{y}) + P_{-\mathbf{h}^R}^R(\mathbf{y})] \quad (4.313)$$

must be considered. It may be expressed in the form of a series

$$\bar{P}_{\mathbf{h}^R}^R(\mathbf{y}) = \sum_{l=0}^{\infty} \sum_{\nu=1}^{N(l)} \bar{F}_l^R(\mathbf{h}^R) \dot{k}_l^\nu(\mathbf{y}) \quad (4.314)$$

with the coefficients

$$\bar{F}_l^R(\mathbf{h}^R) = \frac{4\pi}{2l+1} \sum_{\mu=1}^{M(l)} C_l^{\mu\nu} \frac{1}{2} [\dot{k}_l^{*\mu}(\Phi\beta) + \dot{k}_l^{*\mu}(\pi - \Phi, \pi + \beta)] \quad (4.315)$$

With equation (4.58a) this is

$$\bar{F}_l^R(\mathbf{h}^R) = \frac{4\pi}{2l+1} \sum_{\mu=1}^{M(l)} C_l^{\mu\nu} \dot{k}_l^{*\mu}(\Phi\beta) \frac{1}{2} [1 + (-1)^l] \quad (4.316)$$

This can be written

$$\bar{F}_l^R(\mathbf{h}^R) = \frac{4\pi}{2l+1} \sum_{\mu=1}^{M(l)} \bar{C}_l^{\mu\nu} \dot{k}_l^{*\mu}(\Phi\beta) \quad (4.317)$$

with the coefficients

$$\bar{C}_l^{\mu\nu} = C_l^{\mu\nu} \frac{1}{2} [1 + (-1)^l] = \begin{cases} C_l^{\mu\nu} & \text{for } l \text{ even} \\ 0 & \text{for } l \text{ odd} \end{cases} \quad (4.318)$$

which may be regarded as belonging to the hypothetical texture $\bar{f}^R(g)$. Because of equation (4.318) we obtain for this texture

$$\bar{f}^{Re}(g) = f^{Re}(g) \quad (4.319)$$

$$\bar{f}^{Ro}(g) = 0 \quad (4.320)$$

Correspondingly, for the left-handed texture

$$\bar{f}^{Le}(g) = f^{Le}(g) \quad (4.321)$$

$$\bar{f}^{Lo}(g) = 0 \quad (4.322)$$

Hence, Friedel’s law ‘blots out’ the odd part of the right-handed as well as the left-handed texture function. Together with equations (4.304) and (4.305) it thus follows for the texture that can be determined from pole figure measurements in the case of right- and left-handed crystals:

$$\bar{f}^e(g) = M^R f^{Re}(g) + M^L f^{Le}(g) \quad (4.323)$$

$$\bar{f}^o(g) = 0 \quad (4.324)$$

Hence, in any case the odd part of the texture function is ‘blotted out’ either by virtue of the centrosymmetry of the crystal itself or by virtue of Friedel’s law. The even part is the superposition of the corresponding parts of the right- and the left-handed textures.

4.11.5. Black—White Sample Symmetries

The direction \mathbf{h}^R of a right-handed crystal is, by definition, *equivalent* with the direction \mathbf{h}^L of a left-handed crystal. This does not imply, however, that the two directions are *indistinguishable*. In Figure 4.16 the directions \mathbf{h}^R and \mathbf{h}^L of a right- and a left-handed crystal are shown along with three other neighbouring directions 1, 2, 3. These neighbouring directions are arranged in the manner of a right-handed screw in the vicinity of \mathbf{h}^R and in the manner of a left-handed screw in the vicinity of \mathbf{h}^L (middle part Figure 4.16). Hence, the two directions or their representing points may formally be distinguished by black and white points, as is shown in the lower part of Figure 4.16.

In Section 4.11.2 we have considered centrosymmetric samples made up of non-centrosymmetric crystals in such a way that each right-handed crystal has its counterpart in a left-handed crystal in the same orientation g . This is shown in Figure 4.17. According to the definition of Figure 4.16, the points representing \mathbf{h}^R and \mathbf{h}^L are thus a black and white one in centrosymmetric position. We can, however, also think of two right-handed crystals having their \mathbf{h}^R -directions in centrosymmetric positions. Furthermore, if we consider all possibilities of how to arrange black and white points at a certain point of the pole figure and its centrosymmetric point, then the five possibilities shown in Figure 4.18 are obtained. The symmetry element $\bar{1}$ thus changes the position of a point into its centrosymmetrical one; the element $1'$ changes the ‘colour’ of the point but not its position; the element $\bar{1}'$ changes colour and position at the same time (it thus corresponds to the case considered in Section 4.11.2). If we do not, at present, take other symmetry elements, being pure rotations, into account, then the sample symmetry is to be described by these five black—white symmetry groups^{219a}.

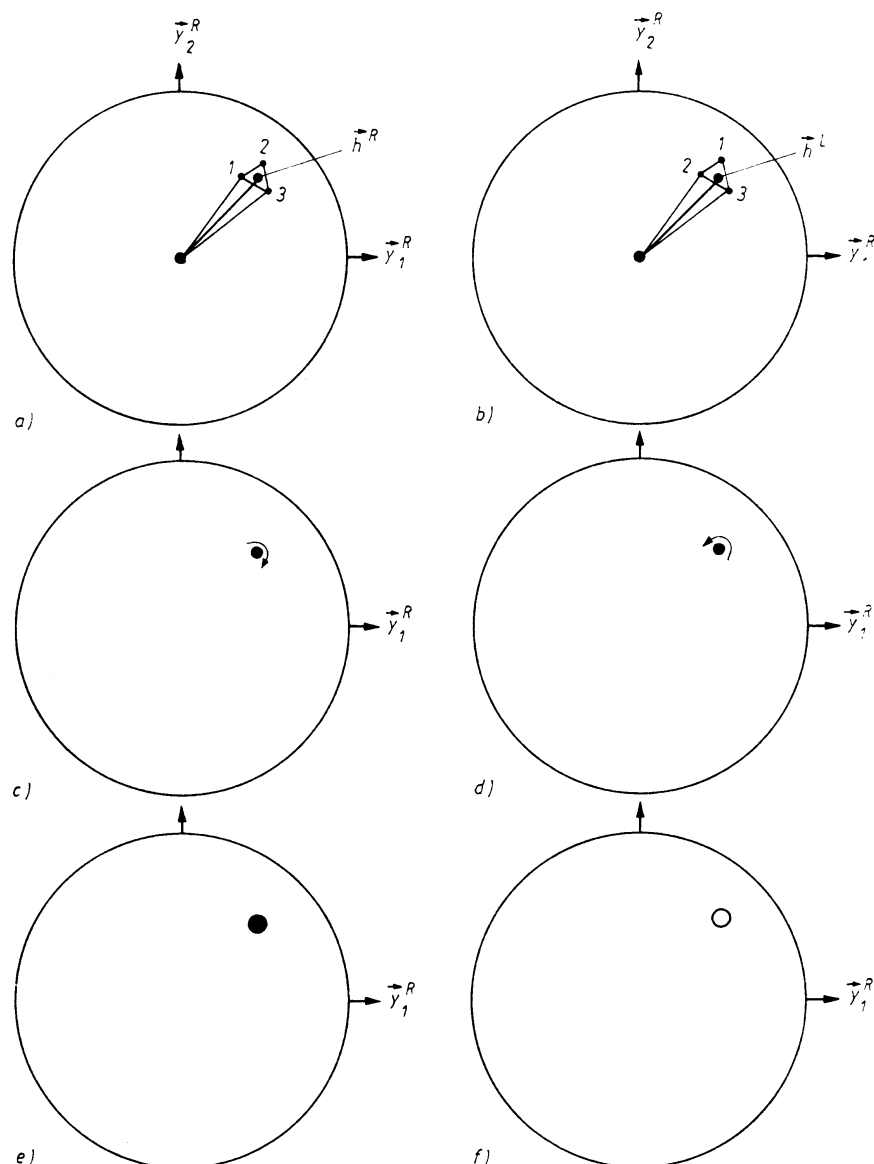


Figure 4.16 A crystal direction \mathbf{h} and its neighbourhood 1, 2, 3: (a) right-handed crystals; (b) left-handed crystals; (c) the directions 1, 2, 3 form a right-handed path about \mathbf{h} ; (d) the directions 1, 2, 3 form a left-handed path about \mathbf{h} ; (e) the direction \mathbf{h}^R with right-handed neighbourhood is represented by a black point; (f) the direction \mathbf{h}^L with left-handed neighbourhood is represented by a white point

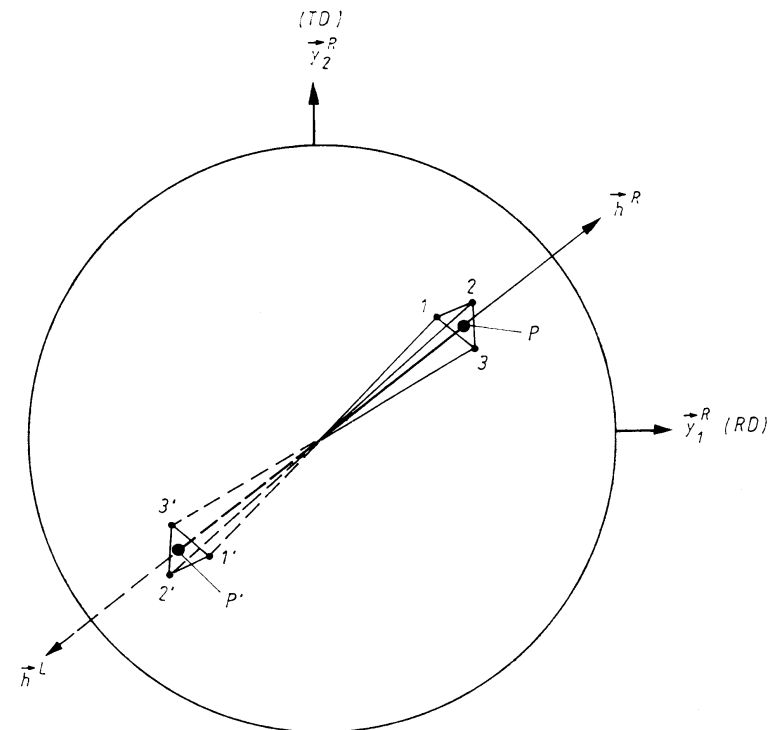


Figure 4.17 The direction \mathbf{h}^R of a right-handed crystal and the direction \mathbf{h}^L of a left-handed crystal (in the same orientation g) are in centrosymmetric positions on the pole sphere. The dashed lines indicate the rear hemisphere

The conditions imposed upon the texture functions of the right- and the left-handed crystals by the symmetry case $\bar{1}'$ (Figure 4.18c) have already been discussed in Section 4.11.2. We shall now consider the case $\bar{1}$ (Figure 4.18b). It describes a centrosymmetry in a sample consisting of right-handed crystals only. The symmetry relation Figure 4.18(b) is assumed to be fulfilled for all points of the pole figure. Hence, it follows from equation (4.284) with (14.58a) that

$$F_l^{R\mu\nu}(\mathbf{h}^R) = 0 \text{ for } l \text{ odd} \quad (4.325)$$

The symmetry relation must also hold for all crystal directions \mathbf{h}^R . Hence, it follows from equation (4.286) that

$$C_l^{R\mu\nu} = 0 \text{ for } l \text{ odd} \quad (4.326)$$

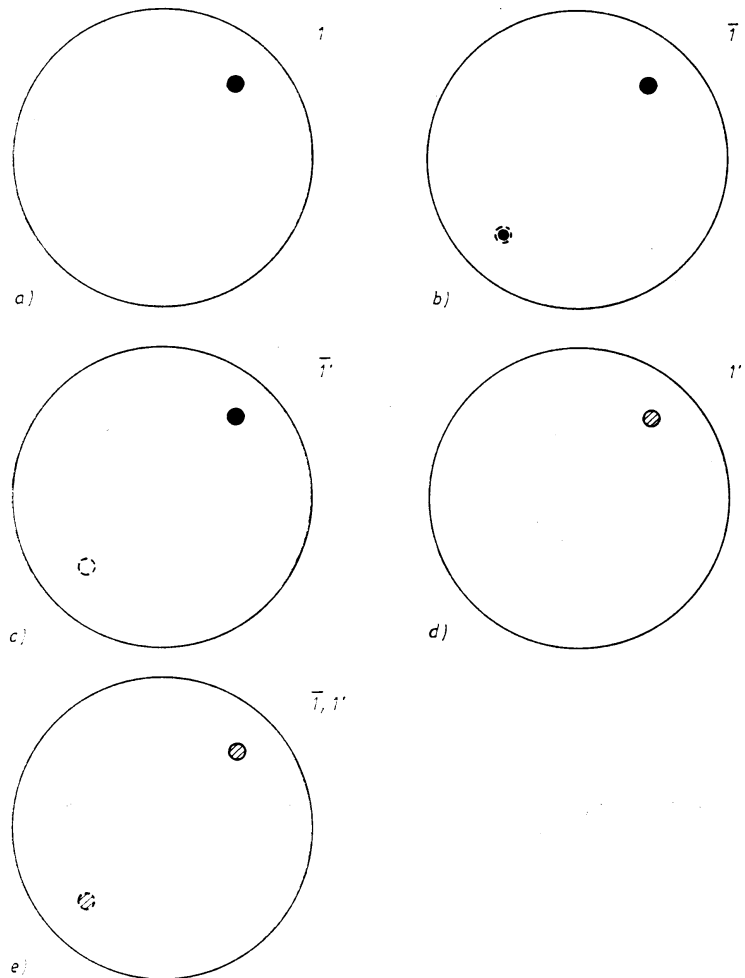


Figure 4.18 The five possible symmetry cases to be obtained by black and white points in centrosymmetric positions (the lower left points are on the rear hemisphere)

Thus, the symmetry element $\bar{1}$ (Figure 4.18b) imposes the selection rule

$$l = 2l' \quad (4.327)$$

If also left-handed crystals are present in the sample, then, correspondingly,

$$C_l^{\text{L}\mu\nu} = 0 \text{ for } l \text{ odd} \quad (4.328)$$

The symmetry case $1'$ (Figure 4.18d) requires a white point in the same place as a black point. This requires

$$M^{\text{L}} = M^{\text{R}} = \frac{1}{2} \quad (4.329)$$

and, according to equations (4.284) and (4.285),

$$F_l^{\text{R}\nu}(\mathbf{h}^{\text{R}}) = F_l^{\text{L}\nu}(\mathbf{h}^{\text{L}}) \quad (4.330)$$

from which follows, with equations (4.286) and (4.287),

$$C_l^{\text{L}\mu\nu} = (-1)^l C_l^{\text{R}\mu\nu} \quad (4.331)$$

The symmetry case $(\bar{1}, 1')$ (Figure 4.18e) finally combines the cases b and d and hence, the conditions of equations (4.301)–(4.303) with equation (4.327).

If the crystals are centrosymmetric, then this requires the symmetry element $\bar{1}'$ — that is, one of the cases Figure 4.18(c or e). Hence, the conditions thus obtained are summarized in Table 4.3.

Table 4.3 SYMMETRY CONDITIONS IN THE FIVE SAMPLE SYMMETRIES FOR CENTRO-SYMMETRIC AND NON-CENTROSYMMETRIC CRYSTALS

		Sample symmetry	1	$\bar{1}$	$\bar{1}'$	$1'$	$(\bar{1}, 1')$
Crystal symmetry	1	$M^{\text{L}} = M^{\text{R}}$	$M^{\text{L}} = M^{\text{R}}$	$M^{\text{L}} = M^{\text{R}}$	$C_l^{\text{L}\mu\nu} = C_l^{\text{R}\mu\nu}$	$C_l^{\text{L}\mu\nu} = C_l^{\text{R}\mu\nu}$	$C_l^{\text{L}\mu\nu} = C_l^{\text{R}\mu\nu}$
	$\bar{1}$	$l = 2l'$	—	—	—	—	$l = 2l'$

The conditions imposed by the five symmetry cases on the pole figures and inverse pole figures or the generalized axis distribution function are to be recognized if we ask for the behaviour of these functions due to a change in sign of either the crystal direction \mathbf{h} or the sample direction \mathbf{y} . Thus, the general axis distribution functions (equations 4.281 and 4.283) are to be considered for the arguments $\pm\mathbf{h}$ and $\pm\mathbf{y}$. In general, it follows with equation (14.58a) that

$$A(\mathbf{h}, \mathbf{y}) = A(-\mathbf{h}, -\mathbf{y}) \quad (4.332)$$

Hence, only two of the four combinations of signs need to be considered. These may be chosen as $\pm\mathbf{y}$, thus considering the $+\mathbf{y}, -\mathbf{y}$ symmetry of the pole figures, or they may be chosen as $+\mathbf{h}, -\mathbf{h}$, thus considering the corresponding symmetries of the inverse pole figures. With the conditions of Table 4.3 the relations shown in Figure 4.19 for the pole figures and in Figure 4.20 for the inverse pole figures are thus obtained. The double arrows indicate values of the arguments $\pm\mathbf{h}, \pm\mathbf{y}$ for which the functions A^{R} and A^{L} take on the same functional value.

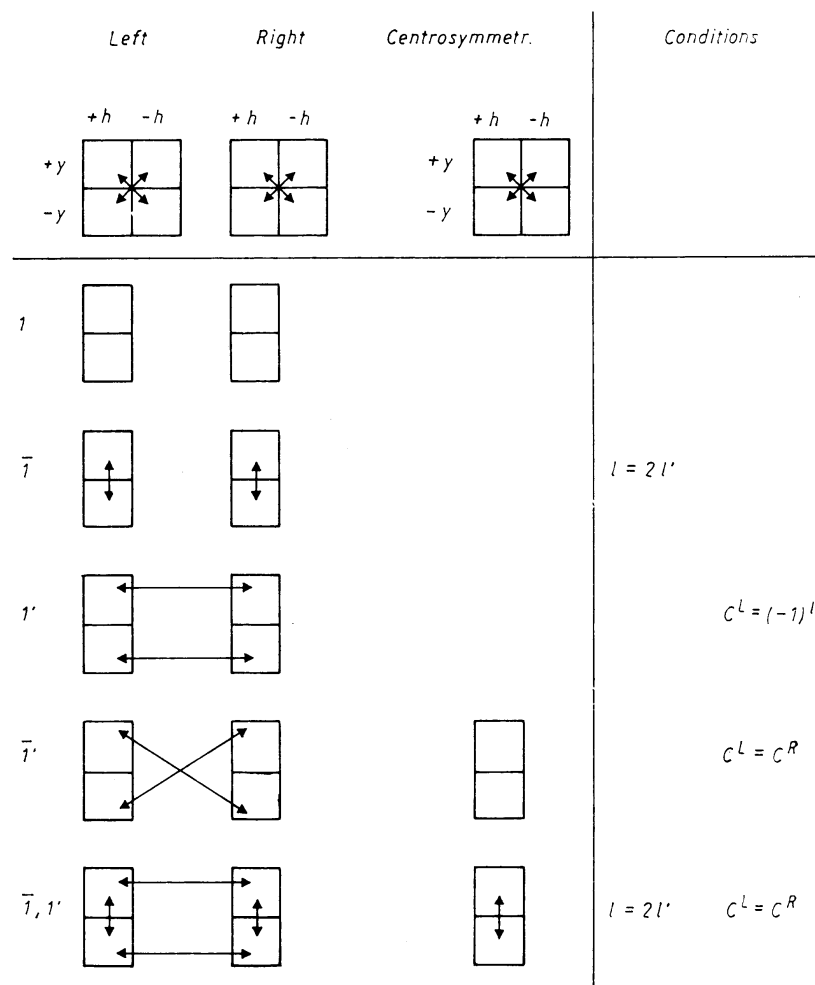


Figure 4.19 Symmetry relations in the generalized axis distribution functions $A^R(\pm\mathbf{h}, \pm\mathbf{y})$ and $A^L(\pm\mathbf{h}, \pm\mathbf{y})$ of the right- and of the left-handed crystals and $A(\pm\mathbf{h}, \pm\mathbf{y})$ of centrosymmetric crystals. Symmetries in the pole figures $P_h^R(\pm\mathbf{y})$, $P_h^L(\pm\mathbf{y})$ and $P_h(\pm\mathbf{y})$

Centrosymmetric crystals may belong to one or the other of the two sample symmetries $\bar{1}'$ or $(\bar{1}, 1')$. As is shown in Figures 4.19 and 4.20, they are distinguished by centrosymmetric or non-centrosymmetric pole figures and inverse pole figures. The pole figure considered in Figure 4.19 is the one of the $+\mathbf{h}$ direction. The pole figure of a symmetric crystal has, however, been generally defined as the superposition of the pole figures of all symmetrically equivalent crystal directions. Hence, in the case of centrosymmetric crystals this is the superposed pole figure of the $+\mathbf{h}$ and the $-\mathbf{h}$ directions, defined in equation (4.309), which is always centro-

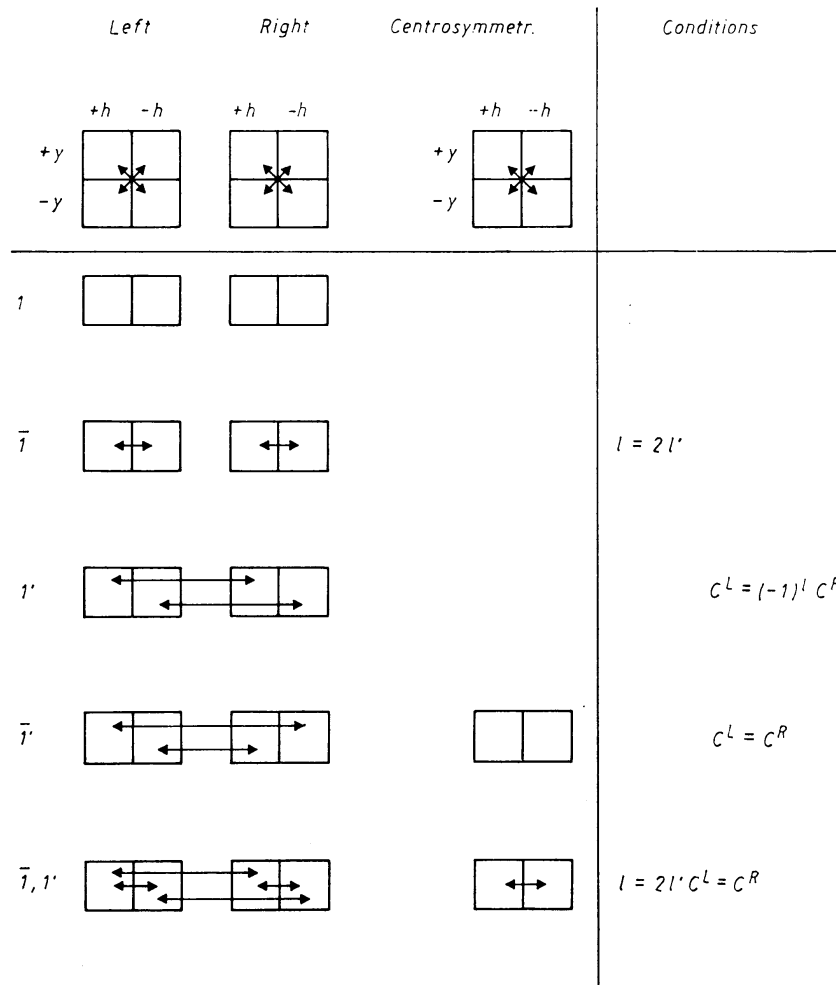


Figure 4.20 Symmetry relations in the generalized axis distribution functions $A^R(\pm\mathbf{h}, \pm\mathbf{y})$ and $A^L(\pm\mathbf{h}, \pm\mathbf{y})$ of the right- and the left-handed crystals and $A(\pm\mathbf{h}, \pm\mathbf{y})$ of centrosymmetric crystals. Symmetries in the inverse pole figures $R_y^R(\pm\mathbf{h})$, $R_y^L(\pm\mathbf{h})$ and $R_y(\pm\mathbf{h})$

symmetric. The inverse pole figure in Figure 4.20 is the one corresponding to the sample $+\mathbf{y}$ direction. It describes the distribution of this direction over all crystal directions \mathbf{h} . According to Figure 4.20, this distribution can be centrosymmetric or not. There is no reason for an additional symmetrization of the inverse pole figure as was the case with the pole figure. Hence, taking the additional symmetrization of the pole figure into account, the symmetry relations of pole figures and inverse pole figures of centrosymmetric crystals shown in Table 4.4 are obtained.

Table 4.4 SYMMETRIES OF POLE FIGURES AND INVERSE POLE FIGURES OF CENTRO-SYMMETRIC CRYSTALS IN THE TWO POSSIBLE SAMPLE SYMMETRIES

Sample symmetry	$\bar{1}'$	$(\bar{1}, 1')$
Pole figure	$P(-y) = P(+y)$	$P(-y) = P(+y)$
Inverse pole figure	$R(-h) \neq R(+h)$	$R(-h) = R(+h)$

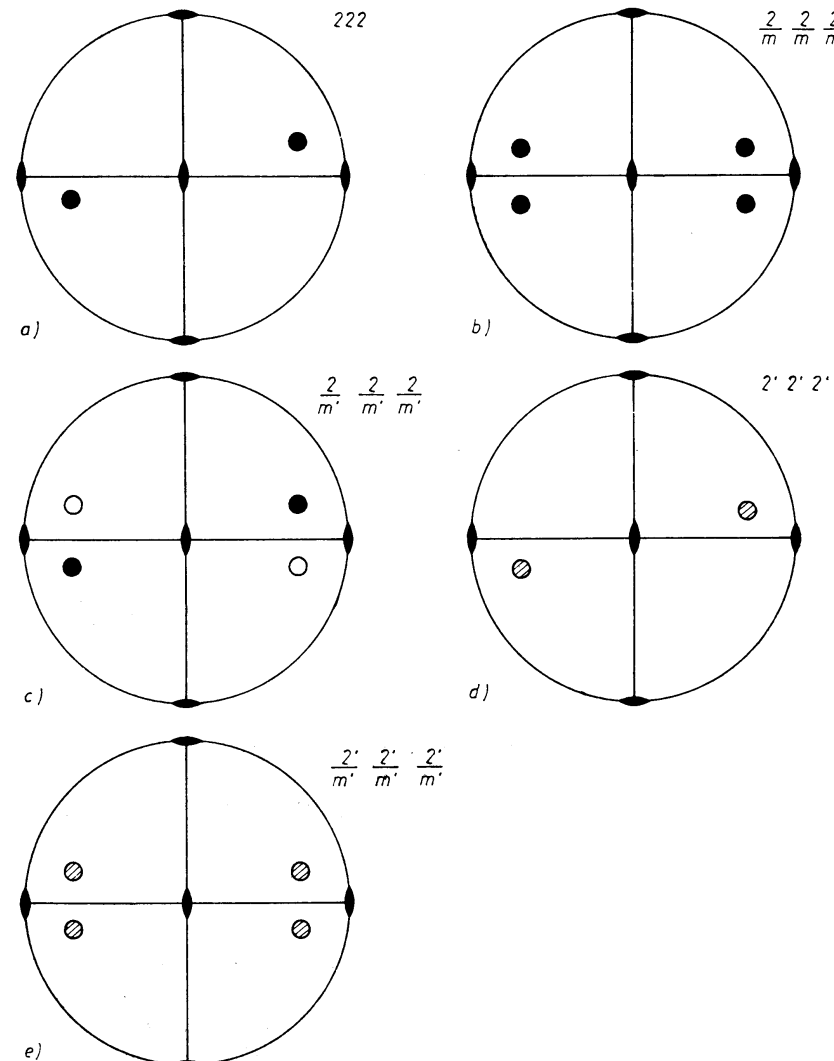


Figure 4.21 The five black–white symmetry groups obtained from Figure 4.18 by addition of the rotation group 222 (only the points on the upper hemisphere are shown)

Symmetry elements which are pure rotations have been fully taken into account in equation (4.7) by using the symmetrized functions \tilde{T}_l^{mn} instead of the ordinary ones T_l^{mn} . The addition of the orthorhombic symmetry group 222 to the sample symmetries of Figure 4.18, for example, thus leads to the black–white sample symmetry groups shown in Figure 4.21. They are thus characterized by the conditions of Table 4.3 and the conditions of equations (14.211) and (14.227). Centrosymmetric crystals may belong to the two cases Figure 4.21 (c and d), which are distinguished according to Table 4.4 by centrosymmetric or non-centrosymmetric inverse pole figures. In equation (14.209a) it has been shown that the spherical harmonics vanish for all those directions which are perpendicular to twofold axes. This means that for these directions y the odd terms in equations (4.281) and (4.283) are zero. Hence, for these sample directions the inverse pole figure does not contain odd terms. The inverse pole figure is thus centrosymmetric for all sample directions perpendicular to twofold axes of the sample symmetry. In the symmetry case Figure 4.21 (c) (with non-centrosymmetric inverse pole figures) these points are shown in Figure 4.22. They are ‘grey’ points in the black–white symmetry group. The black–white notation thus describes very simply the symmetry relations in the inverse pole figure. Black or white points correspond to non-centrosymmetric inverse pole figures, whereas ‘grey’ points belong to centrosymmetric inverse pole figures.

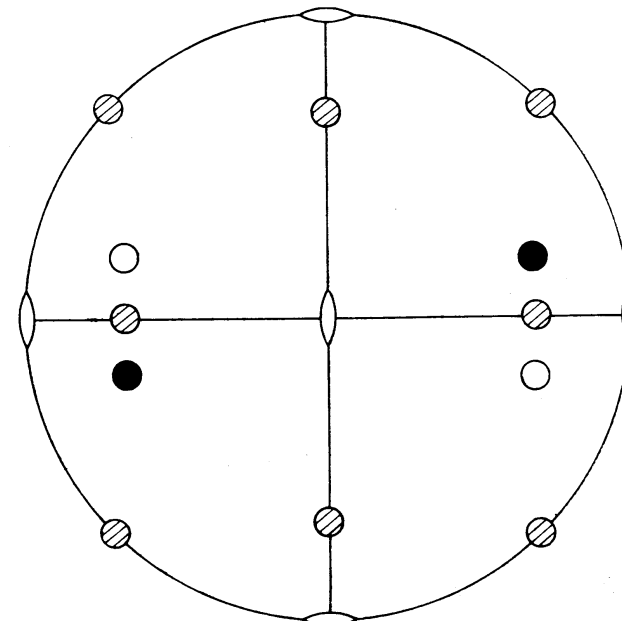


Figure 4.22 The black–white symmetry group $\frac{2}{m'} \frac{2}{m'} \frac{2}{m'}$ and the grey points on planes perpendicular to the twofold axes, corresponding to centrosymmetric inverse pole figures

Similar considerations can also be made for the pole figure, if there are twofold axes in the crystal symmetry. According to *Figure 14.5*, the spherical harmonics $k_l^{*\mu}(\Phi\beta)$ of odd order in equations (4.286) and (4.287) must vanish for these directions. Hence, the coefficients F in equations (4.284) and (4.285) are zero for odd values of l and thus the pole figures are centrosymmetric for these specific crystal directions. Many of the ‘low index’ pole figures belong to this type. They are thus centrosymmetric even in non-centrosymmetric crystals and irrespective of the validity of Friedel’s law.

4.11.6. Determination of the Odd Part of the Texture Function

As has been shown in the preceding sections, the odd part of the texture function cannot be determined directly from pole figure measurements. Nevertheless, the odd part cannot be chosen completely arbitrarily. Being a distribution function of crystals, the function $f(g)$ cannot be negative. Hence, the condition must be fulfilled (see reference 73a):

$$f(g) = f^e(g) + f^o(g) \geq 0 \quad (4.333)$$

As will be shown in Section 7.6, there may be zero ranges z^0 in which

$$f(g) = 0 \quad \text{in } z^0 \quad (4.334)$$

These ranges may be obtained in the way described in Section 7.6 without making use of the series expansion. In the zero ranges,

$$f^o(g) = -f^e(g) \quad \text{in } z^0 \quad (4.335)$$

Since $f^e(g)$ can be obtained from pole figure measurements, $f^o(g)$ is also known in these ranges.

Equation (4.335) may thus be used to determine an approximation to $f^o(g)$. We put

$$f_{L'}^o(g) = \sum_{l=1(2)}^{L'} \sum_{\mu=1}^{M(l)} \sum_{\nu=1}^{N(l)} C_l^{\mu\nu} \dot{T}_l^{\mu\nu}(g) \quad (4.336)$$

and we require

$$\int_{z^0} \left[-f^e(g) - f_{L'}^o(g) \right]^2 dg = \min. \quad (4.337)$$

from which the coefficients $C_l^{\mu\nu}$ can be determined. We put for brevity

$$\int_{z^0} f^e(g) \dot{T}_l^{\mu\nu}(g) dg = -a_l^{\mu\nu} \quad (4.338)$$

$$\int_{z^0} \dot{T}_l^{\mu\nu}(g) \cdot \dot{T}_{l'}^{\mu'\nu'}(g) dg = \alpha_{ll'}^{\mu\mu'\nu\nu'} \quad (4.339)$$

and obtain the condition

$$\sum_{l=1(2)}^{L'} \sum_{\mu=1}^{M(l)} \sum_{\nu=1}^{N(l)} C_l^{\mu\nu} \alpha_{ll'}^{\mu\mu'\nu\nu'} = a_{l'}^{\mu'\nu'} \quad (4.340)$$

This is a system of linear equations which can be solved for the coefficients $C_l^{\mu\nu}$. The quantities $a_l^{\mu\nu}$ are influenced by the experimental errors and by the truncation error of the function $f^e(g)$ which has previously been determined by the series expansion method. Hence, the system of equations (4.240) may not have a unique solution if L' has been chosen too large. On the other hand, the approximation may also be poor if L' is chosen too small. Hence, the optimum choice of L' is an important question which can only be answered by numerical calculations.

Therefore, another approximation procedure may be applied in which only the coefficients $C_l^{\mu\nu}$ of one order l at a time are approximated to the residual function. We put

$$f_{l_0}(g) = -f^e(g) \quad (4.341)$$

where l_0 is the lowest l -value in the series expansion of the odd function (e.g. $l_0 = 9$ for cubic symmetry). The approximation function $f_{L'}^o(g)$ may then be written in the form

$$f_{L'}^o(g) = \sum_{l=l_0} \Delta f_l(g) \quad (4.342)$$

where

$$\Delta f_l(g) = \sum_{\mu=1}^{M(l)} \sum_{\nu=1}^{N(l)} C_l^{\mu\nu} \dot{T}_l^{\mu\nu}(g) \quad (4.343)$$

The following conditions are required from which $\Delta f_l(g)$ will be determined for each degree l separately:

$$\int_{z^0} [f_l(g) - \Delta f_l(g)]^2 dg = \min. \quad (4.344)$$

where

$$f_l(g) = f_{l_0}(g) - \sum_{\lambda=l_0}^{l-2} \Delta f_\lambda(g) \quad (4.345)$$

We put

$$\int_{z^0} f_l(g) \dot{T}_l^{\mu\nu}(g) dg = b_l^{\mu\nu} \quad (4.346)$$

Then equation (4.344) leads to the condition

$$\sum_{\mu=1}^{M(l)} \sum_{\nu=1}^{N(l)} C_l^{\mu\nu} \alpha_{ll'}^{\mu\mu'\nu\nu'} = b_l^{\mu'\nu'} \quad (4.347)$$

which is to be solved for the $C_l^{\mu\nu}$. The quantities α are the same as in equation (4.339). The quantities b may be expressed according to equations (4.345), (4.343) and (4.341) in the form

$$b_l^{\mu\nu} = \int_{z^0} \left[-f^e(g) - \sum_{\lambda=l_0}^{l-2} \sum_{\mu'=1}^{M(\lambda)} \sum_{\nu'=1}^{N(\lambda)} C_\lambda^{\mu'\nu'} \dot{T}_\lambda^{\mu'\nu'}(g) \right] \dot{T}_l^{\mu\nu}(g) dg \quad (4.348)$$

With equations (4.338) and (4.339) this is

$$b_l^{\mu\nu} = a_l^{\mu\nu} - \sum_{\lambda=l_0}^{l-2} \sum_{\mu'=1}^{M(\lambda)} \sum_{\nu'=1}^{N(\lambda)} C_\lambda^{\mu'\nu'} \alpha_{ll'}^{\mu\mu'\nu\nu'} \quad (4.349)$$

whence it follows that

$$\sum_{\mu=1}^{M(l)} \sum_{\nu=1}^{N(l)} C_l^{\mu\nu} \alpha_l^{\mu'\nu'} = a_l^{\mu'\nu'} - \sum_{\lambda=l_0}^{l-2} \sum_{\mu''=1}^{M(\lambda)} \sum_{\nu''=1}^{N(\lambda)} C_\lambda^{\mu''\nu''} \alpha_{l\lambda}^{\mu'\mu''\nu'\nu''} \quad (4.350)$$

The coefficients $C_\lambda^{\mu''\nu''}$ at the right-hand side of this system of equations are already known from the solution of the corresponding system for lower l -values.

In the case that z^0 is the complete orientation space (which is, of course, not possible), the two approximation conditions equations (4.337) and (4.349) are equivalent. In the general case, however, the latter condition allows one better to estimate the convergence of the series expansion.

The approximation function $f_L^0(g)$ obtained in the zero range z^0 is defined according to equation (4.236) in the whole orientation space. It may thus be regarded as an approximation to the odd part of the texture function in the whole orientation space.

Note added in proof

The applicability of the zero range method has been tested in the case of a theoretical texture — i.e. the ideal orientation $\{110\}\langle112\rangle$ with Gaussian spread about it. In this case the odd part, which is to be obtained by the calculation, is already known beforehand. In this calculation better results were obtained with the first method of solution (equations 4.337–4.340). The coefficients $C_l^{\mu\nu}$ so obtained agreed with the theoretical ones within 2 per cent (C. ESLING, E. BECHLER-FERRY and H. J. BUNGE, 1981. Numerical calculation of the odd part of the texture function. *J. Phys. Lett.*, 42, L 141–L 144).

An alternative method, how to determine the odd part of the texture function, has been proposed by K. LÜCKE, J. POSPIECH, K. H. VIRNICH and J. JURA (1981) (On the problem of the reproduction of the true orientation distribution function from pole figures. *Acta Met.*, 29, 167–185). It is based on the assumption that the true texture function $f(g)$ (equation 4.333), is the sum of a small number of Gaussian-shaped ideal orientations. The method works well if the assumption is fulfilled. However, it is not possible to be certain of this.

In Section 4.11 the role of the inversion centre as a symmetry element of second kind has been considered. However, there may also be other symmetry elements of second kind — e.g. mirror planes or inversion axes. In normal polycrystalline scattering experiments these symmetry elements cannot be distinguished. They can, however, be taken into account in texture analysis if anomalous scattering is used (H. J. BUNGE and C. ESLING, 1981. Determination of the odd part of the texture function by anomalous scattering. *J. Appl. Cryst.*, in press). It is then necessary to generalize the concept of crystal orientation from rotations g to orthogonal transformations u (C. ESLING, H. J. BUNGE and J. MULLER, 1980. Description de la texture par des fonctions de distribution sur l'espace des transformations orthogonales. Implication du centre d'inversion. *C. R. Acad. Sci., Paris*, B 291, 263–266).

This concept allows one to include all possible kinds of symmetry elements of second kind in the crystal symmetry as well as in the sample symmetry (H. J. BUNGE, C. ESLING and J. MULLER. The influence of crystal and sample symmetries on the orientation distribution function of the crystallites in polycrystalline materials. *Acta Cryst. A*, in press).

The orientation distribution $f(u)$ splits into a pair of functions $f^R(g)$ and $f^L(g)$ of pure rotations, as was considered in equations (4.279) and (4.280) for enantiomorphic crystals. In the generalized concept this description is, however, also applied to non-enantiomorphic crystals in order to take the symmetry elements of second kind fully into account.

The Inversion Formula

In this book the series expansion method has been used in order to calculate the orientation distribution function from experimentally determinable pole figures. There is an essentially different method which serves the same purpose. This is the biaxial pole figure method originally proposed by R. O. WILLIAMS. The same principle has later been developed in more detail by RUER and BARO and has been called the vector method.

Recently, a completely different, third method — the inversion formula — has been proposed by S. MATTHIES¹⁰⁴ and has since been developed in more detail (S. MATTHIES 1980/81. On the reproducibility of the orientation distribution function of texture samples from pole figures. *Kristall und Technik*, 15, 431, 601, 823, 1189, 1323; 16, 513). This method is an integral transformation, based on the ABEL transform, expressing the ODF in terms of pole figure values without recourse to series expansion:

$$f(g) = P^g(-1) + 2 \int_0^\pi d\Theta \cos \frac{\Theta}{2} \frac{d}{d\cos \Theta} P^g(\cos \Theta)$$

where $P^g(\cos \Theta)$ is related to the angular distribution function $W_{h\bar{y}}(\cos \Theta)$ (equation 4.121) by the integral

$$P^g(\cos \Theta) = \int W_{h,g,h}(\cos \Theta) dh$$

(see J. MULLER, C. ESLING and H. J. BUNGE, 1981. An inversion formula expressing the texture function in terms of angular distribution functions. *J. Phys.*, 42, 161–165). In its present form, however, this formula is not applicable to numerical calculations since it needs an integration over the crystal direction h — i.e. a continuous manifold of pole figures which is actually not available. However, the formula is of fundamental importance in theoretical considerations on the texture function.

5. Fibre Textures

The formulae derived for general textures are valid for every arbitrary crystal and sample symmetry. They were obtained by using generalized spherical harmonics which are invariant with respect to the existing sample and crystal symmetry. The highest possible sample symmetry is spherical symmetry, for which all orientations are equally probable. There exists only a single generalized spherical harmonic which satisfies this symmetry — namely the constant for $l = 0$. All orientation functions are then also constant. This case is trivial.

The case of rotational symmetry with respect to a sample direction is very important. When this symmetry occurs, all orientations which transform into one another by rotation about this direction thus occur with equal frequency. Prominent examples of the occurrence of textures of this kind are fibres and wires. Rotationally symmetric textures will therefore also frequently be denoted as fibre textures; however, textures of films also belong here, provided there is no distinction between directions in the film. The equally frequent occurrence of all orientations about an axis means that all distribution functions are independent of the angular coordinate concerned. The generally three-dimensional orientation distribution function will, in this case, be two-dimensional, and the usually two-dimensional pole figures will be one-dimensional. The reduction in turn of the problem by one coordinate naturally decreases considerably both the measurement and calculation requirements in comparison with the general case. A special simplification and peculiarity further results from the rotational symmetry, since, for example, the inverse pole figure of the fibre axis is synonymous with the complete three-dimensional orientation distribution function $f(g)$, which in this case actually depends on only two of its variables. On this basis it is appropriate to compile again the special formulae for rotationally symmetric textures, though naturally they are in principle already completely contained in the general formulae.

We fix the sample fixed coordinate system so that its Z-axis coincides with the axis of rotational symmetry (fibre axis). The generalized spherical harmonics of rotational symmetry, in terms of the coefficients given in Table 14.4, have the form of equation (14.126). The orientation distribution function

$$f(\varphi_1, \Phi, \varphi_2) = \sum_{l=0}^{\infty} \sum_{\mu=1}^{M(l)} \sum_{\nu=1}^{N(l)} C_l^{\mu\nu} \hat{T}_l^{\mu\nu}(\varphi_1, \Phi, \varphi_2) \quad (5.1)$$

thus transforms into

$$f(\varphi_1, \Phi, \varphi_2) = \sum_{l=0}^{\infty} \sum_{\mu=1}^{M(l)} \sqrt{\frac{4\pi}{2l+1}} C_l^{\mu 1} k_l^{\mu} \left(\Phi, \varphi_2 - \frac{\pi}{2} \right) \quad (5.2)$$

The $k_l^{\mu}(\Phi, \varphi_2 - \pi/2)$ are the spherical surface harmonics of the crystal symmetry. The function $f(\varphi_1, \Phi, \varphi_2)$ is, as it must be, independent of the angle φ_1 . We now employ the angle β in place of the angle φ_2 according to equation (2.126), and, in place of the function f , a new function $R(\Phi, \beta)$, with

$$R(\Phi, \beta) = f(\varphi_1, \Phi, \varphi_2) = \sum_{l=0}^{\infty} \sum_{\mu=1}^{M(l)} \sqrt{\frac{4\pi}{2l+1}} C_l^{*\mu 1} k_l^{\mu}(\Phi, \beta) \quad (5.3)$$

In place of the coefficients $C_l^{*\mu 1}$, we further introduce new fibre texture coefficients C_l^{μ} :

$$C_l^{\mu} = \sqrt{\frac{4\pi}{2l+1}} C_l^{*\mu 1} \quad (5.4)$$

From equation (4.15) we obtain for these the normalization

$$C_0^1 = \sqrt{4\pi} \quad (5.5)$$

With the abbreviated notation for the angles Φ and β introduced in equation (2.125), we finally obtain^{31–33}

$$R(\mathbf{h}) = \sum_{l=0}^{\infty} \sum_{\mu=1}^{M(l)} C_l^{\mu} k_l^{\mu}(\mathbf{h}) \quad (5.6)$$

As was illustrated in Section 2.5 on orientations in the case of rotational symmetry, \mathbf{h} is that crystal direction which coincides with the axis of rotational symmetry. The distribution function $R(\mathbf{h})$ thus describes the frequency with which the fibre axis lies in the different crystal directions. It is thus identical with the inverse pole figure of the fibre axis. On this basis we have already used the letter R for it. We shall return to this again. Since now — in contrast to the case of general textures — we have to consider only one kind of symmetry — namely crystal symmetry — we can omit the introduction of points on the spherical harmonics for distinction of the various symmetries. The $k_l^{\mu}(\mathbf{h})$ will then always denote the spherical surface harmonics of the crystal symmetry.

If we set

$$d\mathbf{h} = \sin \Phi d\Phi d\beta \quad (5.7)$$

we thus obtain the normalization condition for the function $R(\mathbf{h})$:

$$\oint R(\mathbf{h}) d\mathbf{h} = C_0^1 k_0^1 \oint d\mathbf{h} = 4\pi \quad (5.8)$$

For the case of random orientation distribution

$$R_r = 1 \quad (5.9)$$

In the defining equation for the orientation distribution function $f(g)$, dV denotes the volume of all crystals which have orientations g within the orientation

element dg . If for the function $f(\varphi_1, \Phi, \varphi_2)$ for rotational symmetry we substitute from equation (5.3) the function $R(\Phi, \beta)$, equation (3.3) assumes the form

$$\frac{dV(\varphi_1, \Phi, \varphi_2)}{V} = \frac{1}{8\pi^2} R(\Phi, \beta) \sin \Phi d\Phi d\varphi_1 d\varphi_2 \quad (5.10)$$

The volume of all those crystals which possess the orientation Φ, φ_2 or Φ, β results from $dV(\varphi_1, \Phi, \varphi_2)$ by integration with respect to φ_1 :

$$dV'(\Phi, \varphi_2) = dV'(\Phi, \beta) = \int_0^{2\pi} dV(\varphi_1, \Phi, \varphi_2) d\varphi_1 \quad (5.11)$$

Since the right-hand side of equation (5.10) is independent of φ_1 , we obtain

$$\frac{dV'(\Phi, \beta)}{V} = \frac{1}{4\pi} R(\Phi, \beta) \sin \Phi d\Phi d\varphi_2 \quad (5.12)$$

or

$$\frac{dV'}{V} = \frac{1}{4\pi} R(\mathbf{h}) d\mathbf{h} \quad (5.13)$$

dV' is the volume of crystals which have an orientation \mathbf{h} within the element of solid angle $d\mathbf{h}$, and V is the total volume of the sample.

5.1. Determination of the Coefficients C_l^{μ}

If one replaces l and μ in equation (5.6) by l' and μ' , multiplies by $k_l^{*\mu}(\mathbf{h})$ and integrates over all orientations, one obtains

$$C_l^{\mu} = \oint R(\mathbf{h}) k_l^{*\mu}(\mathbf{h}) d\mathbf{h} \quad (5.14)$$

The coefficients C_l^{μ} can be determined from this equation, if the orientation distribution function is known.

5.1.1. Individual Orientation Measurements

We first assume that there is only a single orientation $\mathbf{h} = \mathbf{h}_0$ present. The orientation distribution function $R(\mathbf{h})$ is then different from zero only at this point, and we obtain

$$C_l^{\mu} = k_l^{*\mu}(\mathbf{h}_0) \oint R(\mathbf{h}) d\mathbf{h} \quad (5.15)$$

This gives, with the normalization condition (5.8),

$$C_l^{\mu} = 4\pi k_l^{*\mu}(\mathbf{h}_0) \quad (5.16)$$

If more orientations \mathbf{h}_i with the volumes V_i are present, we thus obtain the coefficients as the weighted average value:

$$C_l^{\mu} = 4\pi \frac{\sum_i V_i k_l^{*\mu}(\mathbf{h}_i)}{\sum_i V_i} \quad (5.17)$$

If one inserts these coefficients in the series expansion (5.6) and truncates the series at a value $l = L$, which is sufficiently small for the function $R(\mathbf{h})$ not to have a maximum at each individual point \mathbf{h}_i , $R(\mathbf{h})$ thus represents the 'density distribution' of the orientations \mathbf{h}_i , as was indicated schematically in *Figure 4.1* for a one-dimensional case.

5.1.2. Interpolation of the Function $R(\mathbf{h})$

We assume that the orientation distribution function $R(\mathbf{h})$ is known at a few points \mathbf{h}_i and has there the values $R(\mathbf{h}_i)$. It will be approximated by a series (equation 5.6) with finite $l = L$. If, now, the number of coefficients to be determined is smaller than the number of points \mathbf{h}_i , the approximation expression assumes there not exactly the values $R(\mathbf{h}_i)$ but some different values $R'(\mathbf{h}_i)$:

$$R'(\mathbf{h}_i) = \sum_{l=0}^L \sum_{\mu=1}^{M(l)} C_l^\mu k_l^\mu(\mathbf{h}_i) \quad (5.18)$$

The coefficients C_l^μ will then be determined such that

$$\sum_i w_i [R(\mathbf{h}_i) - R'(\mathbf{h}_i)]^2 = \min. \quad (5.19)$$

If one substitutes equation (5.18) and differentiates with respect to C_l^μ , one obtains the condition

$$\sum_{l=0}^L \sum_{\mu=1}^{M(l)} C_l^\mu x_{il}^{\mu\mu'} = \gamma_l^{\mu'} \quad (5.20)$$

for determination of the coefficients C_l^μ , where the quantities $x_{il}^{\mu\mu'}$ and $\gamma_l^{\mu'}$ are defined by

$$x_{il}^{\mu\mu'} = \sum_i w_i k_l^\mu(\mathbf{h}_i) k_l^{\mu'}(\mathbf{h}_i) \quad (5.21)$$

$$\gamma_l^{\mu'} = \sum_i w_i R'(\mathbf{h}_i) k_l^{\mu'}(\mathbf{h}_i) \quad (5.22)$$

(See also Section 4.1.2.)

5.2. The General Axis Distribution Function $A(\mathbf{h}, \Phi)$

For the case of general textures we have derived the general axis distribution function $A(\mathbf{h}, \mathbf{y})$, which indicates how frequently the crystal direction \mathbf{h} coincides with the sample direction \mathbf{y} (equation 4.35). In this case of rotational symmetry, which we now consider, for each degree l only one linearly independent spherical surface harmonic $k_l^r(\mathbf{y})$ results. It is

$$k_l^1(\mathbf{y}) = k_l^1(\Phi, \gamma) = \frac{1}{\sqrt{2\pi}} \bar{P}_l(\Phi) \quad (5.23)$$

If we substitute these in equation (4.35) and replace the coefficients $C_l^{\mu 1}$ from equation (5.4) by the fibre texture coefficients C_l^μ , we obtain

$$A(\mathbf{h}, \mathbf{y}) = A(\mathbf{h}, \Phi) = \sum_{l=0}^{\infty} \sum_{\mu=1}^{M(l)} \sqrt{\frac{2}{2l+1}} C_l^\mu k_l^\mu(\mathbf{h}) \bar{P}_l(\Phi) \quad (5.24)$$

This function indicates how frequently the crystal direction \mathbf{h} falls into a sample direction which forms the angle Φ with the fibre axis; it is independent of the angle γ .

It is to be mentioned that the general axis distribution function $A(\mathbf{h}, \mathbf{y})$ and its specifications, the pole figures and inverse pole figures, cannot be determined unequivocally from polycrystal diffraction experiments. As has been shown in Section 4.11, only a superposition of $A(+\mathbf{h}, \mathbf{y})$ and $A(-\mathbf{h}, \mathbf{y})$ can be obtained experimentally. Because of equation (14.58a), this leads to a factor zero by which the terms of odd order are multiplied. Hence, the considerations of the following sections can, in general, only be applied to the even part of the series expansion. For the odd part see Section 5.10. The considerations concerning individual orientation measurements are to be applied to even and odd values of l .

5.2.1. Pole Figures $P_{\mathbf{h}}(\Phi)$

If we choose for \mathbf{h} a fixed low-index crystal direction

$$\mathbf{h} = \mathbf{h}_i = \{h_1, h_2, h_3\}; \quad (5.25)$$

function (5.24) is the pole figure belonging to the direction \mathbf{h}_i . It is represented in the form of a series of normalized LEGENDRE polynomials:

$$A(\mathbf{h}_i, \Phi) = P_{\mathbf{h}_i}(\Phi) = \sum_{l=0}^{\infty} F_l(\mathbf{h}_i) \bar{P}_l(\Phi) \quad (5.26)$$

with the coefficients

$$F_l(\mathbf{h}_i) = \sqrt{\frac{2}{2l+1}} \sum_{\mu=1}^{M(l)} C_l^\mu k_l^\mu(\mathbf{h}_i) \quad (5.27)$$

For $l = 0$ we obtain, according to equation (5.5),

$$F_0(\mathbf{h}_i) = \sqrt{2} \quad (5.28)$$

We obtain for normalization of the function $P_{\mathbf{h}_i}(\Phi)$

$$\int_0^\pi P_{\mathbf{h}_i}(\Phi) \sin \Phi d\Phi = F_0 \bar{P}_0 \int_0^\pi \sin \Phi d\Phi = 2 \quad (5.29)$$

and this naturally means, for the case of random distribution,

$$P_{\mathbf{h}_i}(\Phi)_r = 1 \quad (5.30)$$

With the orthonormalization condition we obtain for the coefficients

$$F_l(\mathbf{h}_i) = \int_0^\pi P_{\mathbf{h}_i}(\Phi) \bar{P}_l(\Phi) \sin \Phi d\Phi \quad (5.31)$$

If the pole figures are only known within an unknown factor, one thus obtains, by consideration of the normalization condition (5.29),

$$F_l(\mathbf{h}_i) = 2 \frac{\int_0^\pi \hat{P}_{\mathbf{h}_i}(\Phi) \bar{P}_l(\Phi) \sin \Phi d\Phi}{\int_0^\pi \hat{P}_{\mathbf{h}_i}(\Phi) \sin \Phi d\Phi} \quad (5.32)$$

If the pole figure is different from zero only at the point

$$\Phi = \Phi_0 \quad (5.33)$$

it follows from equation (5.31) with equation (5.29) that

$$F_l(\mathbf{h}_i) = 2 \bar{P}_l(\Phi_0) \quad (5.34)$$

If the pole figure is different from zero only at the points $\Phi = \Phi_j$ and has there the weights V_j , we obtain for the coefficients

$$F_l(\mathbf{h}_i) = 2 \frac{\sum_j V_j \bar{P}_l(\Phi_j)}{\sum_j V_j} \quad (5.35)$$

If one substitutes coefficients (5.35) in equation (5.26) and truncates the series (5.26) at a suitably small value $l = L$, $P_{\mathbf{h}_i}(\Phi)$ represents the 'density distribution' of the points Φ_j of the pole figure.

5.2.1.1. Determination of the Coefficients C_l^μ from Pole Figures

If one has determined the coefficients $F_l(\mathbf{h}_i)$ for a certain number, I_p , of different pole figures from equation (5.32) or equation (5.35), one can calculate the coefficients C_l^μ by solution of the linear system of equations (5.27). For this system of equations to be uniquely soluble, the number $M(l)$ of unknowns must not be greater than the number I_p of available equations. Since $M(l)$ increases with l (see Figure 4.4, p. 62), this is only the case up to a certain degree:

$$l = l_{\max}(I_p, \text{symmetry}) \quad (5.36)$$

This degree l_{\max} , which we have called the resolving power (Section 4.2.1.1) depends also on the crystal symmetry. For

$$l > l_{\max}(I_p, \text{symmetry}) \quad (5.37)$$

there exist, in general, several linearly independent solutions for the coefficients C_l^μ and, hence, several different functions $R(\mathbf{h})$. The first I_p pole figures corresponding to these functions are, however, exactly the same. If, for example, $R(\mathbf{h})$ and $R'(\mathbf{h})$ are two such functions, we can write

$$R'(\mathbf{h}) = R(\mathbf{h}) + R_0(\mathbf{h}) \quad (5.38)$$

where $R_0(\mathbf{h})$ is a non-vanishing function, the corresponding I_p pole figures of which are identically zero. The function $R_0(\mathbf{h})$ can be represented by a series which

only has terms with $l > l_{\max}$:

$$R_0(\mathbf{h}) = \sum_{l>l_{\max}}^{\infty} \sum_{\mu=1}^{M(l)} C_l^\mu k_l^\mu(\mathbf{h}) \quad (5.39)$$

Since the functions $k_l^\mu(\mathbf{h})$ will continuously 'decrease in wavelength' with increasing l — i.e. the distance between neighbouring maxima and minima will successively be shorter — $R_0(\mathbf{h})$ will always decrease in wavelength with increasing l_{\max} . The uncertainty in the determination of the function $R(\mathbf{h})$, which is expressed by the additive function $R_0(\mathbf{h})$, is thus concerned with ever-smaller angular distances with increasing l_{\max} . On this basis the quantity l_{\max} will also be denoted as 'resolving power'³⁸. Two maxima of the function $R(\mathbf{h})$, which have an angular separation of the order of the separation of maxima of the functions $k_{l_{\max}}^\mu(\mathbf{h})$ or smaller, are thus no longer clearly resolved, and this is true irrespective of whether the functions are represented by series or another representation is used (see, for example, Section 7.8).

5.2.1.2. Separation of Coincidences

As previously explained in Section 4.2.2.2, it can occur that the pole figures $P_{\mathbf{h}_i}(\Phi)$ belonging to different crystal directions \mathbf{h}_j can not be separately measured, since the associated reflection angles ϑ are equal or nearly equal. In this case, for the reflection angle ϑ we measure a linear combination of pole figures

$$P_\vartheta(\Phi) = q_1 P_{\mathbf{h}_1}(\Phi) + q_2 P_{\mathbf{h}_2}(\Phi) + \dots = \sum_{j=1}^{j_{\max}} q_j P_{\mathbf{h}_j}(\Phi) \quad (5.40)$$

If the pole figure $P_\vartheta(\Phi)$ is normalized in the same way as the pole figures $P_{\mathbf{h}_j}(\Phi)$, equation (4.96) is thus valid for the q_j . If the pole figure $P_\vartheta(\Phi)$ is also expressed in a series according to equation (5.26), an expression analogous to equation (5.40) is thus valid for the coefficients

$$F_l(\vartheta) = \sum_{j=1}^{j_{\max}} q_j F_l(\mathbf{h}_j) \quad (5.41)$$

If we substitute therein expression (5.27) for the $F_l(\mathbf{h}_j)$, we obtain

$$F_l(\vartheta) = \sqrt{\frac{2}{2l+1}} \sum_{\mu=1}^{M(l)} C_l^\mu \sum_{j=1}^{j_{\max}} q_j k_l^\mu(\mathbf{h}_j) \quad (5.42)$$

We suppose that there are a certain number of individually measurable pole figures. From these one can then determine the coefficients C_l^μ up to a certain degree $l = l'$ by solution of equation (5.27). If one substitutes these C_l^μ in equation (5.42), one obtains a system of linear equations from which the overlapping factors q_j can be determined for all those coinciding pole figures, for which the multiplicity j_{\max} is less than the number of equations. Since q_j is independent of l , in equation (5.42) the sums over j are thus also known for higher l . The equations of system (5.42) belonging to the ϑ -values concerned can therefore be combined with

system (5.27), which will thus be soluble up to a higher degree $l = l''$. The q_j can therefore now be calculated for coincidences of higher multiplicity j_{\max} , etc. In this way finally all equations (5.42) can be used for determination of the coefficients C_l^{μ} . This is important, since the number of measurable pole figures is frequently not great. (See Section 4.2.2.3 concerning the maximum resolving power obtainable from pole figure measurements.)

5.2.2. Inverse Pole Figures $R_{\Phi}(\mathbf{h})$

We now consider the second special case of the general axis distribution function $A(\mathbf{h}, \Phi)$, which occurs when the sample direction (i.e. the angle Φ) is held constant:

$$\Phi = \Phi_0 \quad (5.43)$$

and the crystal direction \mathbf{h} is allowed to vary continuously. We then obtain a distribution function $R_{\Phi_0}(\mathbf{h})$, which indicates the frequency with which the different crystal directions \mathbf{h} fall in a sample direction, which forms the angle Φ_0 with the fibre axis. This distribution function is the inverse pole figure belonging to the direction Φ_0 :

$$A(\mathbf{h}, \Phi_0) = R_{\Phi_0}(\mathbf{h}) = \sum_{l=0}^{\infty} \sum_{\mu=1}^{M(l)} H_l^{\mu}(\Phi_0) k_l^{\mu}(\mathbf{h}) \quad (5.44)$$

with the coefficients

$$H_l^{\mu}(\Phi_0) = \sqrt{\frac{2}{2l+1}} \bar{P}_l(\Phi_0) C_l^{\mu} \quad (5.45)$$

The coefficients $H_l^{\mu}(\Phi_0)$ of the inverse pole figure of the direction Φ_0 thus agree with those of the orientation distribution except for a known factor. By equation (14.53), for $\Phi_0 = 0$ equation (5.45) transforms into

$$H_l^{\mu}(0) = C_l^{\mu} \quad (5.46)$$

One thus obtains from equation (5.44)

$$A(\mathbf{h}, 0) = R_0(\mathbf{h}) = R(\mathbf{h}) = \sum_{l=0}^{\infty} \sum_{\mu=1}^{M(l)} C_l^{\mu} k_l^{\mu}(\mathbf{h}) \quad (5.47)$$

The orientation distribution function $R(\mathbf{h})$ is thus, as we have already seen, identical with the inverse pole figure of the direction $\Phi_0 = 0$ — i.e. the fibre axis. On this basis the inverse pole figure of the fibre axis will be denoted simply as the inverse pole figure, which, however, is not completely correct.

5.2.2.1. The Fundamental Equation for Fibre Textures

We have derived an integral relation between pole figures and inverse pole figures (equation 4.137). We apply this to the inverse pole figure of the fibre axis $R(\mathbf{h})$. The pole of the spherical angular coordinates Θ, ψ of the pole figure is also the fibre axis. The angles Θ and ψ are in this case identical with the angles Θ and γ , and, because of the rotational symmetry, the pole figures are independent of γ .

Considering this in equation (4.137), we immediately obtain

$$P_{\mathbf{h}_i}(\Phi) = \frac{1}{2\pi} \int_0^{2\pi} R(\Phi, \psi') d\psi' \quad (5.48)$$

This is the fundamental equation for fibre textures derived by JETTER, McHARGUE and WILLIAMS¹⁶⁷ in a somewhat different notation. The integration of the orientation distribution function $R(\mathbf{h})$ takes place around the direction \mathbf{h}_i , which is chosen as the pole of the spherical angular coordinate system Θ, ψ' (see Figure 5.1).

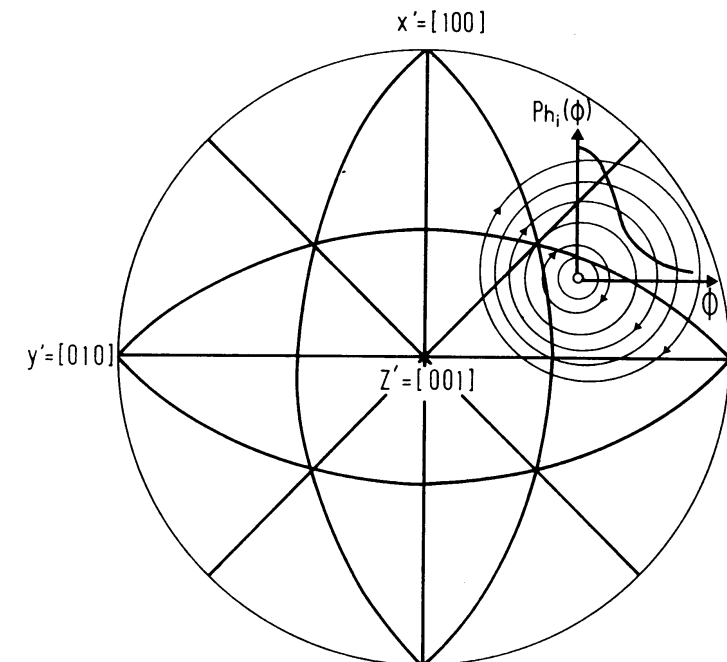


Figure 5.1 The average value of the inverse pole figure along the circle at the distance Φ from the direction \mathbf{h}_i gives the value of the \mathbf{h}_i pole figure at the point Φ (schematic)

5.2.2.2. The Method of Harris

If one sets $\Phi = 0$ in the fundamental equation (5.48), the function $R(\Phi = 0, \psi')$ is not dependent on ψ' . The average construction therefore gives the function value at the point itself. From equation (5.48) it therefore follows that

$$P_{\mathbf{h}_i}(0) = R(0, \psi') = R(\mathbf{h}_i) \quad (5.49)$$

The value of the \mathbf{h}_i pole figure at the point $\Phi = 0$ is thus equal to the value of the orientation distribution function or the inverse pole figure at the point \mathbf{h}_i (Figure 5.1). If, therefore, one has measured the value of the pole figures for $\Phi = 0$ for sufficiently many different \mathbf{h}_i , one thus knows the values of the function $R(\mathbf{h})$ at the corresponding points and can approximately construct the function

from them. However, in general, the number of function values measurable in this way suffices only to obtain a general view of the course of the function. Furthermore, the functions $P_{\mathbf{h}_i}(\Phi)$ are assumed to be so normalized that equation (5.29) is valid. In the case of X-ray diffraction measurements, however, one does not obtain these normalized functions. The measured functions thus differ from the latter by factors which depend on \mathbf{h}_i in a complicated way. In order to apply the method suggested by HARRIS¹⁴⁶ for determination of the function $R(\mathbf{h})$, one must make certain estimates of these factors. For a pole figure with arbitrary normalization, it follows from equation (5.49) that

$$\hat{P}_{\mathbf{h}_i}(0) \cdot N_i = R(\mathbf{h}_i) \quad (5.50)$$

For a comparable sample with random crystal distribution one obtains, correspondingly,

$$\hat{P}_{\mathbf{h}_i}(0)_r \cdot N_{ir} = R(\mathbf{h}_i)_r = 1 \quad (5.51)$$

The normalization factor N_{ir} can thus differ from N_i because of somewhat different conditions. It follows from equations (5.50) and (5.51) that

$$\frac{\hat{P}_{\mathbf{h}_i}(0)}{\hat{P}_{\mathbf{h}_i}(0)_r} = \frac{N_{ir}}{N_i} \cdot R(\mathbf{h}_i) \quad (5.52)$$

We now assume that the quotient N_{ir}/N_i no longer depends on i . It can then be determined from the normalization condition (5.8) of the function $R(\mathbf{h}_i)$. Since the function $R(\mathbf{h}_i)$ is, however, known only at a few points \mathbf{h}_i , equation (5.8) must be approximated by a sum,

$$\sum_i R(\mathbf{h}_i) \Delta O_i = 1 \quad (5.53)$$

ΔO_i is thus the element of surface of the pole sphere which adjoins the point \mathbf{h}_i . One can, for example, construct the regions ΔO_i , if one joins each point with its nearest neighbours, bisects these distances and there constructs great circles perpendicular to the first. In this way one obtains for each point \mathbf{h}_i a spherical polygon whose surface area is the fraction ΔO_i of the total surface of the sphere. With equation (5.53) it thus follows from equation (5.52) that

$$R(\mathbf{h}_i) = \frac{\hat{P}_{\mathbf{h}_i}(0)}{\hat{P}_{\mathbf{h}_i}(0)_r} \left| \sum_i \frac{\hat{P}_{\mathbf{h}_i}(0)}{\hat{P}_{\mathbf{h}_i}(0)_r} \Delta O_i \right. \quad (5.54)$$

According to another method derived by STURCKEN²⁷², one interpolates the function $(N_{ir}/N_i) R(\mathbf{h})$ known at the points \mathbf{h}_i by a series expansion corresponding to Section 5.1.2. The coefficients of this series are C_l^μ . They can be determined by solution of system (5.20). Because of equation (5.5) it is then true that

$$\hat{C}_0^1 = \frac{N_{ir}}{N_i} \sqrt{4\pi} \quad (5.55)$$

Table 5.1 WEIGHT FACTORS ΔO_i FOR TEN REFLECTIONS OF URANIUM (ACCORDING TO P. R. MORRIS²¹⁰)

hkl	ΔO_i	hkl	ΔO_i
020	0.053	112	0.106
110	0.077	131	0.222
021	0.095	023	0.098
002	0.044	200	0.043
111	0.145	113	0.117

The coefficients C_l^μ of the normalized function $R(\mathbf{h})$ follow:

$$C_l^\mu = \sqrt{4\pi} \frac{\hat{C}_l^\mu}{\hat{C}_0^1} \quad (5.56)$$

5.3. Determination of the Coefficients C_l^μ According to the Least Squares Method

For solution of system (5.27) for the desired coefficients C_l^μ of the inverse pole figure it is necessary that the number of equations, and thus of pole figures, is greater than or at least equal to the number of unknowns, which is given by $M(l)$ for each l . Because of unavoidable errors in measurement it is appropriate to employ at least one more equation than unknowns to be determined, and to solve the system of equations by the method of least squared errors⁸⁰. Since the coefficients $F_l(\mathbf{h}_i)$ calculated according to equation (5.31) from the measured pole figures now no longer exactly satisfy equations (5.27), we distinguish two kinds of coefficients, those measured according to equation (5.31), $F_l(\mathbf{h}_i)_{\text{obs.}}$, and those calculated, $F_l(\mathbf{h}_i)_{\text{cal.}}$, which satisfy equation (5.27). Between the two exists the relationship

$$F_l(\mathbf{h}_i)_{\text{obs.}} = F_l(\mathbf{h}_i)_{\text{cal.}} + \varepsilon_l(\mathbf{h}_i) \quad (5.57)$$

The coefficients C_l^μ will be so determined that the error quantities $\varepsilon_l(\mathbf{h}_i)$ satisfy the following condition:

$$\sum_i w_i [\varepsilon_l(\mathbf{h}_i)]^2 = \min. \quad (5.58)$$

The w_i are thereby weights so that we can consider individual pole figures in respect to their actual accuracy. Written completely, condition (5.58) reads

$$\sum_i w_i \left[F_l(\mathbf{h}_i)_{\text{obs.}} - \sqrt{\frac{2}{2l+1}} \sum_{\mu=1}^{M(l)} C_l^\mu k_l^\mu(\mathbf{h}_i) \right]^2 = \min. \quad (5.59)$$

If one sets the derivative with respect to C_l^μ equal to zero, one thus obtains

$$\sqrt{\frac{2}{2l+1}} \sum_i w_i k_l^\mu(\mathbf{h}_i) \left[F_l(\mathbf{h}_i)_{\text{obs.}} - \sqrt{\frac{2}{2l+1}} \sum_{\mu=1}^{M(l)} C_l^\mu k_l^\mu(\mathbf{h}_i) \right] = 0 \quad (5.60)$$

We use the abbreviations[†]

$$\sqrt{\frac{2}{2l+1}} \sum_i w_i k_l^\mu(\mathbf{h}_i) F_l(\mathbf{h}_i)_{\text{obs.}} = a_l^\mu \quad (5.61)$$

$$\frac{2}{2l+1} \sum_i w_i k_l^{\mu'}(\mathbf{h}_i) k_l^\mu(\mathbf{h}_i) = \alpha_l^{\mu'\mu} \quad (5.62)$$

(It should thereby be considered that the corresponding quantities $\alpha_l^{\mu'\mu}$ in the case of general textures were somewhat differently defined; see equation 4.144.) The following system of equations thereby results for determination of the coefficient C_l^μ :

$$\sum_{\mu=1}^{M(l)} \alpha_l^{\mu'\mu} C_l^\mu = a_l^{\mu'} \quad (5.63)$$

It contains just as many equations as unknowns, namely $M(l)$. The solution of this system of equations is

$$C_l^\mu = \sum_{\mu'=1}^{M(l)} \beta_l^{\mu\mu'} a_l^{\mu'} \quad (5.64)$$

(Here also the quantities $\beta_l^{\mu\mu'}$, the elements of the inverse of the matrix $\alpha_l^{\mu'\mu}$, have a somewhat different significance than in the case of general textures.)

5.4. Measures of Accuracy

As in the case of general textures, we can also estimate the experimental error for fibre textures from the difference between measured and calculated pole figures. The calculated pole figures result from the coefficients $F_l(\mathbf{h}_i)_{\text{cal.}}$:

$$P_{\mathbf{h}_i}(\Phi)_{\text{cal.}} = \sum_{l=0}^{\infty} F_l(\mathbf{h}_i)_{\text{cal.}} \bar{P}_l(\Phi) \quad (5.65)$$

We compare them with the measured $P_{\mathbf{h}_i}(\Phi)_{\text{obs.}}$, when we form the following measure of accuracy:

$$\Delta P = \sum_i w_i \int_0^\pi [P_{\mathbf{h}_i}(\Phi)_{\text{obs.}} - P_{\mathbf{h}_i}(\Phi)_{\text{cal.}}]^2 \sin \Phi d\Phi \quad (5.66)$$

By consideration of relations (5.57) and (5.65), this can be written

$$\Delta P = \sum_i w_i \int_0^\pi \left[\sum_{l=0}^{\infty} \varepsilon_l(\mathbf{h}_i) \bar{P}_l(\Phi) \right]^2 \sin \Phi d\Phi \quad (5.67)$$

If one removes the brackets and carries out the integration, only the squared terms remain because of the orthonormality of the $\bar{P}_l(\Phi)$:

$$\Delta P = \sum_i w_i \sum_{l=0}^{\infty} [\varepsilon_l(\mathbf{h}_i)]^2 \quad (5.68)$$

[†] The definition of the quantities a_l^μ and $\alpha_l^{\mu'\mu}$ has been changed with respect to I in order to be in better agreement with the definitions used in error analysis (see, e.g., reference 94)

From the minimum condition for the $\varepsilon_l(\mathbf{h}_i)$ (equation 5.58) it then follows immediately that the quantity ΔP is also minimal:

$$\Delta P = \sum_i w_i \int_0^\pi [P_{\mathbf{h}_i}(\Phi)_{\text{obs.}} - P_{\mathbf{h}_i}(\Phi)_{\text{cal.}}]^2 \sin \Phi d\Phi = \min. \quad (5.69)$$

In reference to the similar measure of accuracy used in crystal structure analysis, we call the quantity

$$R_{\mathbf{h}_i} = \frac{\sum_{l=0}^{\infty} |\varepsilon_l(\mathbf{h}_i)|}{\sum_{l=0}^{\infty} |F_l(\mathbf{h}_i)_{\text{obs.}}|} \quad (5.70)$$

the measure of accuracy (R -factor) of the pole figure \mathbf{h}_i and the quantity

$$R = \frac{\sum_i \sum_{l=0}^{\infty} |\varepsilon_l(\mathbf{h}_i)|}{\sum_i \sum_{l=0}^{\infty} |F_l(\mathbf{h}_i)_{\text{obs.}}|} \quad (5.71)$$

the measure of accuracy of the complete texture.

For the average error ΔF_l of the coefficients $F_l(\mathbf{h}_i)_{\text{obs.}}$, corresponding to unit weight, we obtain (see, for example, reference 94)

$$\Delta F_l = \sqrt{\frac{\sum_i w_i [\varepsilon_l(\mathbf{h}_i)]^2}{I_P - M(l)}} \quad (5.72)$$

I_P is thus the number of pole figures used. The average error of the coefficients C_l^μ results therefrom as

$$\Delta C_l^\mu = \sqrt{\beta_l^{\mu\mu}} \Delta F_l \quad (5.73)$$

The $\beta_l^{\mu\mu}$ are the quantities used in equation (5.64).

5.4.1. A Special Measure of Accuracy for Pole Figures of Materials with Cubic Symmetry

As for general textures, a special measure of accuracy also results for fibre textures of cubic materials, which does not emanate from the compatibility of different pole figures with one another, but is obtained for each pole figure.⁴⁵ It can therefore be used before carrying out extensive calculations. From the fact that no cubic spherical surface harmonics of second degree exist, it follows from equation (5.27) that

$$F_2(\mathbf{h}_i)_{\text{cal.}} = 0 \quad (5.74)$$

From equations (5.57) and (5.32) results

$$\epsilon_2(\mathbf{h}_i) = F_2(\mathbf{h}_i)_{\text{obs.}} = 2 \frac{\int_0^\pi \hat{P}_{\mathbf{h}_i}(\Phi) \bar{P}_2(\Phi) \sin \Phi d\Phi}{\int_0^\pi \hat{P}_{\mathbf{h}_i}(\Phi) \sin \Phi d\Phi} \approx 0 \quad (5.75)$$

For error-free measured pole figures expression (5.75) must vanish exactly. Its deviation from zero is therefore a measure of the accuracy of the pole figure. The vanishing of expression (5.75) is a necessary, but not sufficient, condition for freedom from error of the pole figure. Certainly error functions can exist which make expression (5.75) exactly equal to zero. If we explicitly express $\bar{P}_2(\Phi)$ in equation (5.75), we finally obtain as a measure of error of the pole figures of cubic materials:

$$F_2(\mathbf{h}_i)_{\text{obs.}} = \sqrt{\frac{5}{2}} \frac{\int_0^\pi \hat{P}_{\mathbf{h}_i}(\Phi) (3 \cos^2 \Phi - 1) \sin \Phi d\Phi}{\int_0^\pi \hat{P}_{\mathbf{h}_i}(\Phi) \sin \Phi d\Phi} \quad (5.76)$$

5.5. Truncation Error

If one truncates the series expansion of the pole figure at a finite value

$$l = L \quad (5.77)$$

a truncation error thus results. As in the case of general textures, we define as a measure of this error the quantity²⁴⁷

$$A_L(\mathbf{h}_i) = \frac{1}{2} \int_0^\pi \left[P_{\mathbf{h}_i}(\Phi) - \sum_{l=0}^L F_l(\mathbf{h}_i) \bar{P}_l(\Phi) \right]^2 \sin \Phi d\Phi \quad (5.78)$$

In complete analogy with the case of general textures, we obtain from this

$$A_L(\mathbf{h}_i) = \frac{1}{2} \int_0^\pi [P_{\mathbf{h}_i}(\Phi)]^2 \sin \Phi d\Phi - \frac{1}{2} \sum_{l=0}^L [F_l(\mathbf{h}_i)]^2 \quad (5.79)$$

or

$$A_L(\mathbf{h}_i) = \frac{1}{2} \sum_{l=L+1}^{\infty} [F_l(\mathbf{h}_i)]^2 \quad (5.80)$$

The truncation error can be calculated from the first of these two formulae, or estimated from the second by extrapolation of the quantity $F_l(\mathbf{h}_i)$ for $l \rightarrow \infty$.

In a similar manner we define the truncation error of the inverse pole figure:

$$A_L = \frac{1}{4\pi} \oint \left[R(\mathbf{h}) - \sum_{l=0}^L \sum_{\mu=1}^{M(l)} C_l^\mu k_l^\mu(\mathbf{h}) \right]^2 d\mathbf{h} \quad (5.81)$$

and by a transformation analogous to the general case we obtain

$$A_L = \frac{1}{4\pi} \oint [R(\mathbf{h})]^2 d\mathbf{h} - \frac{1}{4\pi} \sum_{l=0}^L \sum_{\mu=1}^{M(l)} [C_l^\mu]^2 \quad (5.82)$$

or

$$A_L = \frac{1}{4\pi} \sum_{l=L+1}^{\infty} \sum_{\mu=1}^{M(l)} [C_l^\mu]^2 \quad (5.83)$$

In the first of these two expressions, however, the integral is not known, in contrast to the corresponding formula for the truncation error of a pole figure, since the exact function $R(\mathbf{h})$ is not known, but only its approximate expression. The truncation error can therefore only be estimated from equation (5.83) when one plots the quantities

$$\frac{1}{4\pi} \sum_{\mu=1}^{M(l)} [C_l^\mu]^2 \quad (5.84)$$

against l and extrapolates to $l \rightarrow \infty$.

By use of the measure of sharpness (equation 5.109: texture index) of the function $R(\mathbf{h})$ and the analogously defined measure of sharpness of the approximation function of L th degree, we can also write

$$A_L = J - J_L \quad (5.85)$$

The truncation error is therefore given in an obvious way by the difference of the measures of sharpness of the actual texture and its approximation function.

5.5.1. Decrease of the Truncation Error by Smearing

If the series expansion is extended up to a suitably large $l = L$, the neglected terms with $l > L$ represent relatively 'short wavelength' variations about the actual course of the function. One can reduce these variations if one 'smears' the function $R(\mathbf{h})$ over a certain small region. The general features of the function will thereby not be greatly altered but the short-wave 'ripples' will be smoothed out. We obtain the value of the smeared function $\tilde{R}(\mathbf{h})$ at the point \mathbf{h} , if we average the function values of the function $R(\mathbf{h})$ at neighbouring points $\mathbf{h} + \Delta\mathbf{h}$ with the corresponding weight function $w(\Delta\mathbf{h})$ (Figure 5.2):

$$\tilde{R}(\mathbf{h}) = \oint R(\mathbf{h} + \Delta\mathbf{h}) w(\Delta\mathbf{h}) d\Delta\mathbf{h} \quad (5.86)$$

We now introduce a new system of coordinates Θ, ψ such that its pole falls in the direction \mathbf{h} . We imagine the distribution function $R(\mathbf{h} + \Delta\mathbf{h})$ expressed in these coordinates, and further assume that the smearing function $w(\Delta\mathbf{h})$ depends only on the angle Θ , so that the smearing also has rotational symmetry. Then equation (5.86) transforms into

$$\tilde{R}(\mathbf{h}) = \int_0^\pi \int_0^{2\pi} R(\Theta, \psi) w(\Theta) \sin \Theta d\Theta d\psi \quad (5.87)$$

We express $w(\Theta)$ as a series of LEGENDRE polynomials:

$$w(\Theta) = \sum_{\lambda=0}^{\infty} w_\lambda \bar{P}_\lambda(\Theta) \quad (5.88)$$

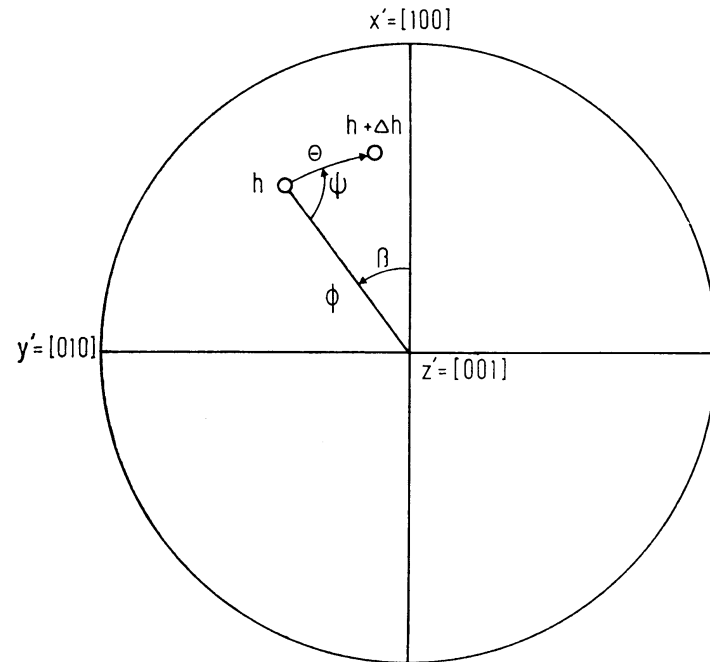


Figure 5.2 On the average of the inverse pole figure $R(\mathbf{h})$ over neighbouring points $\mathbf{h} + \Delta\mathbf{h}$

In the case of integration with respect to ψ , $w(\Theta)$ is thus constant. If we substitute the series expansion (5.6) for $R(\Theta, \psi)$, we obtain

$$\tilde{R}(\mathbf{h}) = \sum_{l=0}^{\infty} \sum_{\lambda=0}^{\infty} \sum_{\mu=1}^{M(l)} C_l^{\mu} w_{\lambda} \int_0^{\pi} \left[\int_0^{2\pi} k_l^{\mu}(\Theta, \psi) d\psi \right] \bar{P}_{\lambda}(\Theta) \sin \Theta d\Theta \quad (5.89)$$

If one substitutes the expression for the integral over ψ (equation 14.200), there results

$$\tilde{R}(\mathbf{h}) = \sum_{l=0}^{\infty} \sum_{\lambda=0}^{\infty} \sum_{\mu=1}^{M(l)} C_l^{\mu} w_{\lambda} 2\pi \sqrt{\frac{2}{2l+1}} k_l^{\mu}(\mathbf{h}) \int_0^{\pi} \bar{P}_l(\Theta) \bar{P}_{\lambda}(\Theta) \sin \Theta d\Theta \quad (5.90)$$

Because of the orthogonality of the LEGENDRE polynomials it follows that

$$\tilde{R}(\mathbf{h}) = \sum_{l=0}^{\infty} \sum_{\mu=1}^{M(l)} \tilde{C}_l^{\mu} k_l^{\mu}(\mathbf{h}) \quad (5.91)$$

with the coefficients

$$\tilde{C}_l^{\mu} = 2\pi \sqrt{\frac{2}{2l+1}} w_l C_l^{\mu} \quad (5.92)$$

The broader the smearing function $w(\Theta)$, the more quickly its coefficients w_l decrease with l . One can therefore ensure that the coefficients \tilde{C}_l^{μ} of the smeared

function will already be sufficiently small for $l < L$, so that the neglected terms of the series with $l > L$ are negligibly small. The course of the function $\tilde{R}(\mathbf{h})$ will thereby be ‘smoothed’. This function shows a smaller truncation error, but the accuracy will naturally not be improved, since the function $\tilde{R}(\mathbf{h})$ will agree only approximately with the desired function $R(\mathbf{h})$.

5.6. Determination of the Coefficients C_l^{μ} from Incompletely Measured Pole Figures

Some methods of measurement permit determination of pole figures of fibre textures only in limited intervals¹². We assume that the angle Φ is limited to the interval

$$\Phi_a \leq \Phi \leq \Phi_b \quad (5.93)$$

If the inverse pole figures are also to be calculated from such pole figures, the method must be somewhat modified, since now use can no longer be made of the orthogonality relations of the series terms⁷³. The measured and previously normalized pole figures are $P_{\mathbf{h}_i}(\Phi)_{\text{obs}}$. The pole figures calculated from the still to be determined coefficients C_l^{μ} are the $P_{\mathbf{h}_i}(\Phi)_{\text{cal}}$. We then require that the integral of the difference between the two be minimal:

$$\sum_i w_i \int_{\Phi_a}^{\Phi_b} [P_{\mathbf{h}_i}(\Phi)_{\text{obs}} - P_{\mathbf{h}_i}(\Phi)_{\text{cal}}]^2 \sin \Phi d\Phi = \min. \quad (5.94)$$

If we express the calculated pole figures by the coefficients C_l^{μ} and consider that the measured pole figures, in general, exist with an unknown normalization, we thus obtain

$$\sum_i w_i \int_{\Phi_a}^{\Phi_b} \left[N_i \hat{P}_{\mathbf{h}_i}(\Phi)_{\text{obs}} - \sum_{l=0}^L \sum_{\mu=1}^{M(l)} \sqrt{\frac{2}{2l+1}} C_l^{\mu} k_l^{\mu}(\mathbf{h}_i) \bar{P}_l(\Phi) \right]^2 \times \sin \Phi d\Phi = \min. \quad (5.95)$$

The coefficients C_l^{μ} and the normalization factors N_i therein are to be so selected that the expression will be minimal. By differentiation with respect to these two quantities one obtains

$$\sum_i w_i \int_{\Phi_a}^{\Phi_b} k_l^{\mu'}(\mathbf{h}_i) \bar{P}_{l'}(\Phi) \left[N_i \hat{P}_{\mathbf{h}_i}(\Phi)_{\text{obs}} - \sum_{l=0}^L \sum_{\mu=1}^{M(l)} \sqrt{\frac{2}{2l+1}} C_l^{\mu} k_l^{\mu}(\mathbf{h}_i) \bar{P}_l(\Phi) \right] \times \sin \Phi d\Phi = 0 \quad (5.96)$$

$$\int_{\Phi_a}^{\Phi_b} \hat{P}_{\mathbf{h}_i}(\Phi)_{\text{obs}} \left[N_i \hat{P}_{\mathbf{h}_i}(\Phi)_{\text{obs}} - \sum_{l=0}^L \sum_{\mu=1}^{M(l)} \sqrt{\frac{2}{2l+1}} C_l^{\mu} k_l^{\mu}(\mathbf{h}_i) \bar{P}_l(\Phi) \right] \times \sin \Phi d\Phi = 0 \quad (5.97)$$

For brevity we introduce the following quantities:

$$\int_{\Phi_a}^{\Phi_b} [\hat{P}_{\mathbf{h}_i}(\Phi)_{\text{obs.}}]^2 \sin \Phi d\Phi = P_i \quad (5.98)$$

$$k_l^\mu(\mathbf{h}_i) \int_{\Phi_a}^{\Phi_b} \hat{P}_{\mathbf{h}_i}(\Phi)_{\text{obs.}} \bar{P}_l(\Phi) \sin \Phi d\Phi = a_l^\mu(\mathbf{h}_i) \quad (5.99)$$

$$\int_{\Phi_a}^{\Phi_b} \bar{P}_l(\Phi) \bar{P}_{l'}(\Phi) \sin \Phi d\Phi = \zeta_{ll'} \quad (5.100)$$

$$\sum_i w_i \sqrt{\frac{2}{2l+1}} k_l^\mu(\mathbf{h}_i) k_{l'}^{\mu'}(\mathbf{h}_i) = \alpha_{ll'}^{\mu\mu'} \quad (5.101)$$

(The quantities $\alpha_{ll'}^{\mu\mu'}$ differ somewhat from the identically named quantities in the case of general textures; compare also the considerations in Section 5.8.) With these relations the two conditions (5.96) and (5.97) transform into

$$\sum_{l=0}^L \sum_{\mu=1}^{M(l)} C_l^\mu \alpha_{ll'}^{\mu\mu'} \zeta_{ll'} = \sum_i w_i N_i a_l^{\mu'}(\mathbf{h}_i) \quad (5.102)$$

$$\sum_{l=0}^L \sum_{\mu=1}^{M(l)} C_l^\mu \sqrt{\frac{2}{2l+1}} a_l^{\mu'}(\mathbf{h}_i) = N_i P_i \quad (5.103)$$

If one expresses the normalization factors N_i by equation (5.103) and substitutes them in equation (5.102), one obtains

$$\sum_{l=0}^L \sum_{\mu=1}^{M(l)} C_l^\mu \left[\alpha_{ll'}^{\mu\mu'} \zeta_{ll'} - \sqrt{\frac{2}{2l+1}} \sum_i w_i a_l^{\mu}(\mathbf{h}_i) a_{l'}^{\mu'}(\mathbf{h}_i) \right] = 0 \quad (5.104)$$

This is a system of linear equations with just as many unknowns C_l^μ as equations. If the C_l^μ have been calculated therefrom, the normalization factors thus result from equation (5.103). Since system (5.104) is homogeneous, the C_l^μ are only determined up to a common factor, which is then to be so determined that the normalization condition (5.5) is fulfilled. If the normalization factors N_i are experimentally known, the C_l^μ are thus to be determined by solution of the inhomogeneous system (5.102).

Because of the orthogonality of the LEGENDRE polynomials, for $\Phi_a = 0, \Phi_b = \pi$ equation (5.100) transforms into

$$\zeta_{ll'} = \delta_{ll'} \quad (5.105)$$

The system (5.102) thereby decomposes into partial systems for each value of l :

$$\sum_{\mu=1}^{M(l)} C_l^\mu \alpha_{ll'}^{\mu\mu'} = \sum_i w_i N_i a_{l'}^{\mu'}(\mathbf{h}_i) \quad (5.106)$$

In this case the normalization factors can be directly determined by application of equation (5.29). Equation (5.106) is then identical with equation (5.63), as it must be.

5.7. Texture Index

Just as in the case of general textures, we shall also define a sharpness measure for fibre textures. We set²⁷¹

$$J = \frac{1}{4\pi} \oint [R(\mathbf{h})]^2 d\mathbf{h} \quad (5.107)$$

If we express $R(\mathbf{h})$ by a series expansion of spherical surface harmonics, there results

$$J = \frac{1}{4\pi} \sum_{l,\mu} \sum_{l',\mu'} C_l^\mu C_{l'}^{*\mu'} \oint k_l^\mu(\mathbf{h}) k_{l'}^{*\mu'}(\mathbf{h}) d\mathbf{h} \quad (5.108)$$

and it follows, because of the orthogonality of the spherical surface harmonics, that

$$J = \frac{1}{4\pi} \sum_{l,\mu} [C_l^\mu]^2 \quad (5.109)$$

In the case of random orientation distribution, only the coefficient C_0^1 is different from zero. With equation (5.5) one therefore obtains

$$J_r = 1 \quad (5.110)$$

For an ideal single crystal, it is

$$J_{\text{ideal}} = 4\pi \sum_{l,\mu} [k_l^\mu(\mathbf{h}_0)]^2 \rightarrow \infty \quad (5.111)$$

As a measure of sharpness of the \mathbf{h}_i pole figure we define

$$J_{\mathbf{h}_i} = \frac{1}{2} \int_0^\pi [P_{\mathbf{h}_i}(\Phi)]^2 \sin \Phi d\Phi \quad (5.112)$$

If we express $P_{\mathbf{h}_i}(\Phi)$ by a series expansion (equation 5.26), we thus obtain

$$J_{\mathbf{h}_i} = \frac{1}{2} \sum_l [F_l(\mathbf{h}_i)]^2 \quad (5.113)$$

Finally it is also true here, as in the case of general textures, that

$$J_{\mathbf{h}_i} \leq J \quad (5.114)$$

One obtains the measure of sharpness of the inverse pole figure of the direction Φ_0 from equation (5.45) as

$$J_{\Phi_0} = \frac{1}{4\pi} \sum_{l,\mu} \left[\sqrt{\frac{2}{2l+1}} \bar{P}_l(\Phi_0) C_l^\mu \right]^2 \quad (5.115)$$

For $\Phi_0 = 0$ the factors standing with C_l^μ equal 1; for $\Phi_0 \neq 0$ they are smaller. It follows that

$$J_{\Phi_0} \leq J_0 = J \quad (5.116)$$

i.e. the inverse pole figure associated with the fibre axis $\Phi_0 = 0$ is the sharpest among the inverse pole figures of all directions.

5.8. The Approximation Condition for Fibre Textures

The pole figures of fibre textures are by definition rotationally symmetric. Thereby

$$P_{h_i}(\Phi_\gamma) = P_{h_i}(\Phi) \quad (5.117)$$

It is therefore sufficient to measure them along the section $\gamma = 0$ (Figure 5.3). If one approximates the measured pole figure by a theoretical function, perhaps

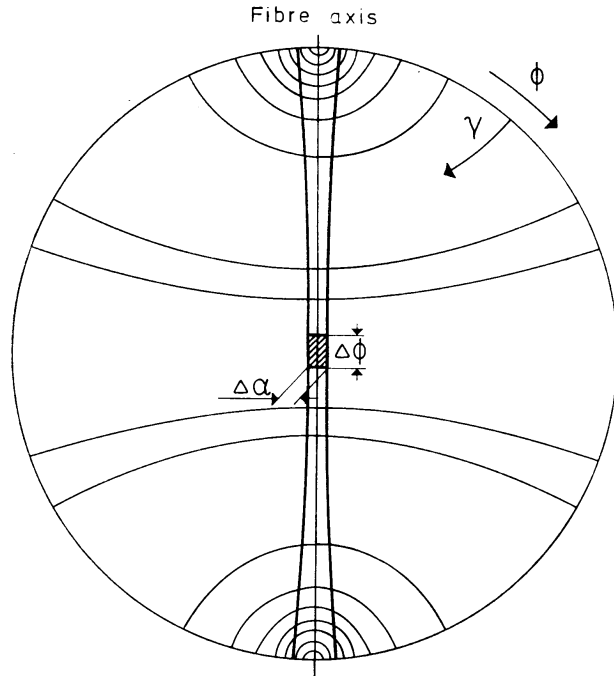


Figure 5.3 Measurement of a rotationally symmetric pole figure along a circle through its pole

a series expansion, in general, a least squares deviation is required as an approximation condition. If one starts from the definition of the pole figure as a two-dimensional function, which is defined on the whole pole sphere, one thus obtains as an approximation condition

$$\oint [P_{h_i}(\Phi_\gamma)_{\text{exp.}} - P_{h_i}(\Phi_\gamma)_{\text{cal.}}]^2 \sin \Phi d\Phi d\gamma = \min. \quad (5.118)$$

In this equation it is assumed that the experimental pole figure is approximated by the calculated one with equal weight over the whole pole sphere. With the condition of rotational symmetry this leads to

$$\int_0^\pi [P_{h_i}(\Phi)_{\text{exp.}} - P_{h_i}(\Phi)_{\text{cal.}}]^2 \sin \Phi d\Phi = \min. \quad (5.119)$$

Because of the rotational symmetry the pole figure, however, is not measured over the whole spherical surface, but only along the section $\gamma = 0$ (Figure 5.3); an approximation will thus be required, that equal angular intervals of the angle Φ will be given equal weight. This yields the approximation condition

$$\int_0^\pi [P_{h_i}(\Phi)_{\text{exp.}} - P_{h_i}(\Phi)_{\text{cal.}}]^2 d\Phi = \min. \quad (5.120)$$

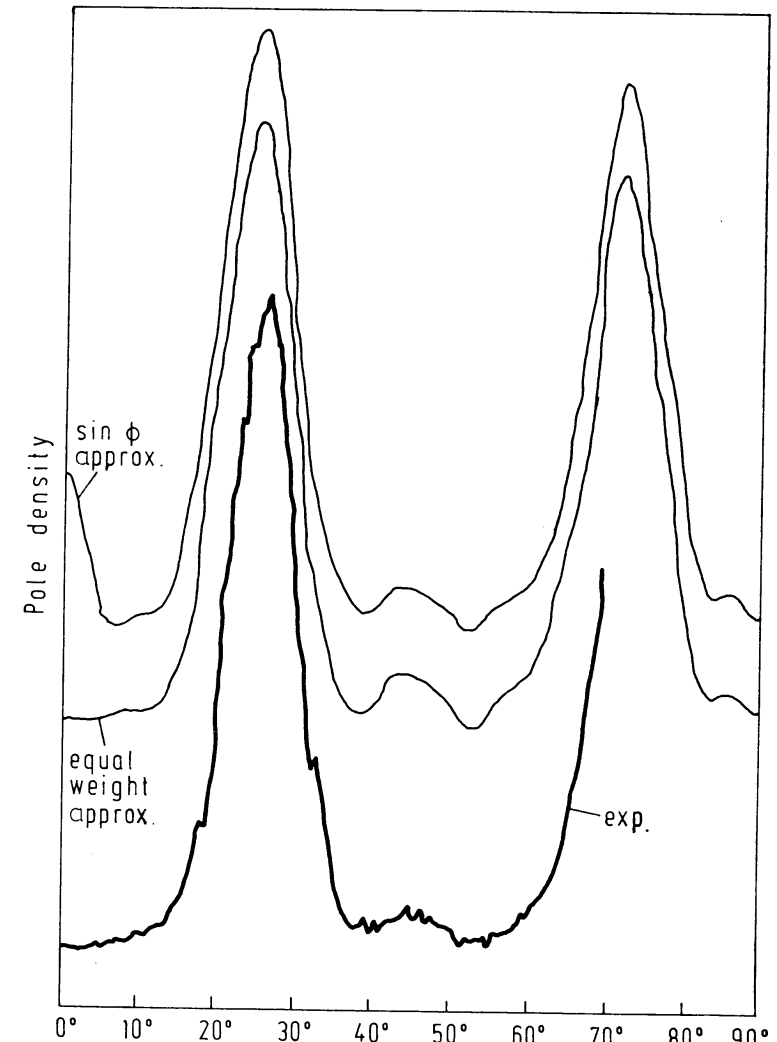


Figure 5.4 Experimental (311) pole figure of an electrolytically deposited nickel layer as well as the pole figures recalculated from the coefficients C_l^{μ} for the two approximation conditions (5.119) and (5.120)²⁸³

which deviates from the similar condition (5.119) by the missing factor $\sin \Phi$. If the theoretical function is a series expansion of LEGENDRE polynomials

$$P_{h_i}(\Phi)_{\text{cal.}} = \sum_{l=0}^L F_l(h_i) \bar{P}_l(\Phi) \quad (5.121)$$

the approximation condition (5.119) is recommended, since the orthogonality condition of the LEGENDRE polynomials (equation 14.49) leads to the simple expression (5.31) for the coefficients $F_l(h_i)$. If the pole figures are not measured in the entire region $0 \leq \Phi \leq \pi$, but only in a region $\Phi_a \leq \Phi \leq \Phi_b$, the orthogonality relations of the LEGENDRE polynomials are not valid over this region. In this case the more complicated method of Section 5.6 must be used. The use of the approximation condition (5.119) then yields no advantage in calculation with respect to condition (5.120). In the formulae in Section 5.6 condition (5.119) was assumed. If one used equation (5.120), the factor $\sin \Phi$ is omitted in each case in integrals (5.94)–(5.100). For example, the incompletely measured pole figures $0 \leq \Phi \leq 70^\circ$ as well as those calculated according to Section 5.6 are shown in Figure 5.4 for the two approximation conditions (5.119) and (5.120)²⁸³. As one sees, the small weight of the weight function $\sin \Phi$ in the neighbourhood of $\Phi = 0$ can lead to a non-existent maximum in the theoretical pole figure. It therefore seems more correct to use approximation condition (5.120), which associates the same weight with all measured values.

5.9. Calculation of the Function $R(\Phi, \beta)$ for Various Crystal Symmetries

If the coefficients C_l^m are known, the function $R(\Phi, \beta)$ can be calculated from equation (5.6). In general, the variables will traverse in certain steps the total region of variation. This can mean an important calculation expenditure. On this basis we will further put equation (5.6) in a form convenient for numerical calculation. If we are to express the symmetric spherical surface harmonics by means of the customary spherical surface harmonics, we have thus two cases to distinguish — the case of ‘lower’ symmetry and the case of ‘higher’ symmetry. The functions of the lower symmetry groups are contained among the customary spherical surface harmonics. These are distinguished from the latter only in that certain ‘selection rules’ must be fulfilled for the indices. For functions of higher symmetry this is not true. These can only be represented as linear combinations of the customary spherical surface harmonics.

5.9.1. Orthorhombic Symmetry

As an example of lower symmetry we consider orthorhombic symmetry²⁴⁷. The spherical surface harmonics of this symmetry can be written

$$k_l^{\mu}(\Phi, \beta) = N^m \bar{P}_l^m(\Phi) \cos m\beta \quad (5.122)$$

The ‘selection rule’ for m is thereby

$$m = 2(\mu - 1) \quad (5.123)$$

The normalization factor N^m is given by

$$N^m = \begin{cases} \sqrt{\frac{1}{2\pi}} & \text{for } m = 0 \\ \sqrt{\frac{1}{\pi}} & \text{for } m \neq 0 \end{cases} \quad (5.124)$$

We now further express $\bar{P}_l^m(\Phi)$ by a FOURIER series (see Section 14.3):

$$P_l^m(\Phi) = \sum_{s=0}^l a_l^{ms} \cos s\Phi \quad (5.125)$$

with

$$s = 2s' \quad (5.126)$$

If we substitute this in equation (5.6), we thus obtain

$$R(\Phi, \beta) = 1 + \sum_{l=2}^L \sum_{m=0}^l \sum_{s=0}^l C_l^m N^m a_l^{ms} \cos s\Phi \cos m\beta \quad (5.127)$$

For brevity we set

$$b(s, m) = \sum_{l=l_0}^L C_l^m N^m a_l^{ms} \quad (5.128)$$

where l_0 is the greatest of the numbers 2, s , m ; we thus obtain

$$R(\Phi, \beta) = 1 + \sum_{m=0}^L \sum_{s=0}^L b(s, m) \cos s\Phi \cos m\beta, \quad m = 2m', s = 2s' \quad (5.129)$$

5.9.2. Cubic Symmetry

As an example of ‘higher’ symmetry we consider the highest cubic symmetry, the group \mathfrak{O}_h ²⁸⁰. The functions of this symmetry can be represented in the form

$$k_l^{\mu}(\Phi, \beta) = \sum_{m=0}^l B_l^{m\mu} \bar{P}_l^m(\Phi) \cos m\beta \quad (5.130)$$

with

$$m = 4m' \quad (5.131)$$

If we substitute these as well as equation (5.125) in equation (5.6), we thus obtain

$$R(\Phi, \beta) = 1 + \sum_{l=4}^L \sum_{\mu=1}^{M(l)} \sum_{m=0}^l \sum_{s=0}^l C_l^{\mu} B_l^{m\mu} a_l^{ms} \cos s\Phi \cos m\beta \quad (5.132)$$

We introduce the abbreviation

$$b(s, m) = \sum_{l=l_0}^L \sum_{\mu=1}^{M(l)} C_l^{\mu} B_l^{m\mu} a_l^{ms}, \quad (5.133)$$

where l_0 is the greatest of the numbers 4, m , s , and obtain

$$R(\Phi, \beta) = 1 + \sum_{m=0}^L \sum_{s=0}^L b(s, m) \cos s\Phi \cos m\beta, \quad m = 4m', s = 2s' \quad (5.134)$$

In both cases the function $R(\Phi, \beta)$ is represented by a double FOURIER sum. The different symmetries are considered by the different definitions of the $b(s, m)$ (equation 5.128 or equation 5.133).

5.10. The Role of the Centre of Inversion

As has been considered in the case of general textures, the symmetries taken into account in equation (5.1) and the following are rotation axes only. Hence, the centre of inversion needs separate consideration.

5.10.1. Right- and Left-handed Crystals

We consider first crystals without a centre of inversion. They may be present in the sample in two forms, the right-handed and the left-handed, which may occur in different volume fractions and may each have a texture of its own.

The right-handed crystals are referred to by a right-handed coordinate system K_B^R (Figure 5.5) made up of the directions \mathbf{h}_1^R , \mathbf{h}_2^R , \mathbf{h}_3^R .

The orientation of this crystal is fully described by specifying the crystal direction \mathbf{h}^R which falls into the sample direction y_0 — i.e. the axis of axial symmetry. This direction may be described by the polar coordinates $\theta\beta$ as shown in Figure 5.5.

The left-handed crystals may be referred to by the coordinate system K_B^L made up of the directions \mathbf{h}_1^L , \mathbf{h}_2^L , \mathbf{h}_3^L , which are crystallographically equivalent to the directions \mathbf{h}_1^R , \mathbf{h}_2^R , \mathbf{h}_3^R of the right-handed crystals. This coordinate system is thus a left-handed one. The orientation of a crystal is then described by the crystal direction \mathbf{h}^L falling into the sample direction $-y_0$. (This definition of the orientation of a left-handed crystal allows one to describe the orientation of a centrosymmetric crystal either by the right-handed or by the left-handed coordinate system as being the same orientation.) We can choose also a right-handed coordinate system $K_B'^L$ in the left-handed crystals which is made up of the opposite directions $-\mathbf{h}_1^L$, $-\mathbf{h}_2^L$, $-\mathbf{h}_3^L$. The orientation of the crystal is then described by the crystal direction $-\mathbf{h}^L$ falling into the sample direction $+y_0$, as shown in Figure 5.5.

The right-handed crystals may be present with the volume fraction M^R and the left-handed ones with M^L , such that

$$M^R + M^L = 1 \quad (5.135)$$

The orientation distribution function of the right-handed crystals may be

$$R^R(\mathbf{h}^R) = \sum_{l=0}^{\infty} \sum_{\mu=1}^{M(l)} C_l^R k_l^\mu(\Phi\beta) \quad (5.136)$$

The distribution function of the left-handed crystals (referred to the coordinate system K_B^L) is

$$R^L(-\mathbf{h}^L) = \sum_{l=0}^{\infty} \sum_{\mu=1}^{M(l)} C_l^L k_l^\mu(\Phi\beta) \quad (5.137)$$

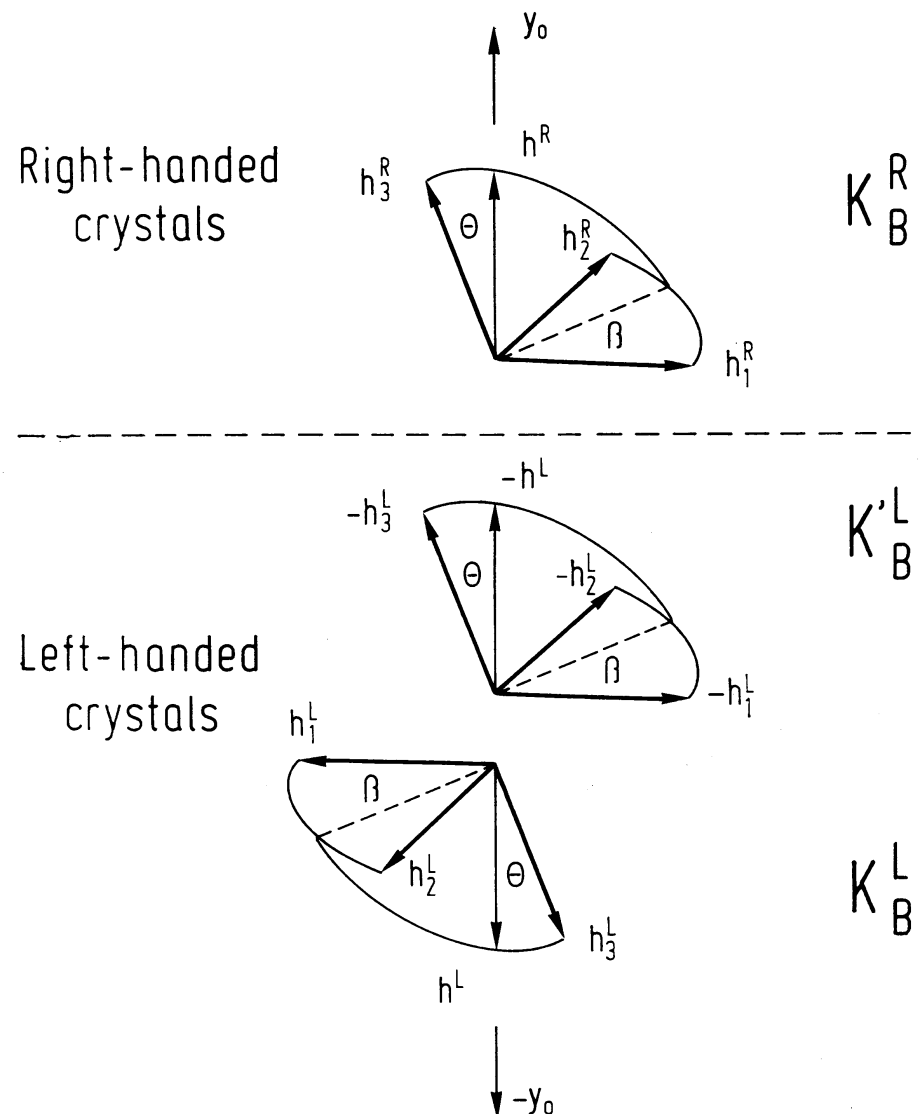


Figure 5.5 Coordinate systems in the right-handed and the left-handed crystals: K_B^R , right-handed system in right-handed crystals; K_B^L , left-handed system in left-handed crystals; $K_B'^L$, right-handed system in left-handed crystals

If we replace $-\mathbf{h}^L$ by $+\mathbf{h}^L$, we obtain

$$R^L(\mathbf{h}^L) = \sum_{l=0}^{\infty} \sum_{\mu=1}^{M(l)} C_l^L k_l^{\mu}(\pi - \Theta, \pi + \beta) \quad (5.138)$$

and, with equation (5.138a), this is

$$R^L(\mathbf{h}^L) = \sum_{l=0}^{\infty} \sum_{\mu=1}^{M(l)} C_l^L (-1)^l k_l^{\mu}(\Theta\beta) \quad (5.139)$$

In equations (5.136) and (5.139) crystallographically equivalent directions \mathbf{h}^R and \mathbf{h}^L are thus being considered.

According to equation (5.24), the general axis distribution functions of the right-handed and the left-handed crystals are considered:

$$A^R(\mathbf{h}^R, \Phi) = \sum_{l=0}^{\infty} \sum_{\mu=1}^{M(l)} \sqrt{\frac{2}{2l+1}} C_l^R k_l^{\mu}(\Theta\beta) \bar{P}_l(\Phi) \quad (5.140)$$

$$A^L(\mathbf{h}^L, \Phi) = \sum_{l=0}^{\infty} \sum_{\mu=1}^{M(l)} \sqrt{\frac{2}{2l+1}} (-1)^l C_l^L k_l^{\mu}(\Theta\beta) \bar{P}_l(\Phi) \quad (5.141)$$

If the crystal directions \mathbf{h}^R and \mathbf{h}^L are kept constant, the general axis distribution functions are the corresponding pole figures

$$A^R(\mathbf{h}^R, \Phi) = P_{\mathbf{h}^R}(\Phi) = \sum_{l=0}^{\infty} F_l^R(\mathbf{h}^R) \bar{P}_l(\Phi) \quad (5.142)$$

$$A^L(\mathbf{h}^L, \Phi) = P_{\mathbf{h}^L}(\Phi) = \sum_{l=0}^{\infty} F_l^L(\mathbf{h}^L) \bar{P}_l(\Phi) \quad (5.143)$$

with the coefficients

$$F_l^R(\mathbf{h}^R) = \sqrt{\frac{2}{2l+1}} C_l^R k_l^{\mu}(\Theta\beta) \quad (5.144)$$

$$F_l^L(\mathbf{h}^L) = \sqrt{\frac{2}{2l+1}} C_l^L (-1)^l k_l^{\mu}(\Theta\beta) \quad (5.145)$$

In a polycrystal diffraction experiment the two pole figures cannot be distinguished. Hence, the virtual pole figure is to be considered:

$$\tilde{P}_{\mathbf{h}}(\Phi) = M^R P_{\mathbf{h}^R}(\Phi) + M^L P_{\mathbf{h}^L}(\Phi) \quad (5.146)$$

It may be written

$$\tilde{P}_{\mathbf{h}}(\Phi) = \sum_{l=0}^{\infty} \tilde{F}_l(\mathbf{h}) \bar{P}_l(\Phi) \quad (5.147)$$

with the coefficients

$$\tilde{F}_l(\mathbf{h}) = \sqrt{\frac{2}{2l+1}} \sum_{\mu=1}^{M(l)} \tilde{C}_l^{\mu} k_l^{\mu}(\Theta\beta) \quad (5.148)$$

where the coefficients

$$\tilde{C}_l^{\mu} = M^R C_l^R \mu + (-1)^l M^L C_l^L \mu \quad (5.149)$$

may be regarded as belonging to a virtual texture

$$\tilde{R}(\Theta\beta) = \sum_{l=0}^{\infty} \sum_{\mu=1}^{M(l)} \tilde{C}_l^{\mu} k_l^{\mu}(\Theta\beta) \quad (5.150)$$

Because of the factor $(-1)^l$ it is convenient to split the orientation distribution functions into even and odd parts:

$$R^e(\Theta\beta) = \sum_{l=0(2)}^{\infty} \sum_{\mu=1}^{M(l)} C_l^{\mu} k_l^{\mu}(\Theta\beta) \quad (5.151)$$

$$R^o(\Theta\beta) = \sum_{l=1(2)}^{\infty} \sum_{\mu=1}^{M(l)} C_l^{\mu} k_l^{\mu}(\Theta\beta) \quad (5.152)$$

with

$$R(\Theta\beta) = R^e(\Theta\beta) + R^o(\Theta\beta) \quad (5.153)$$

Because of the orthogonality of the spherical harmonics we have

$$\int R^e(\Theta\beta) d\Omega = 1 \quad (5.154)$$

$$\int R^o(\Theta\beta) d\Omega = 0 \quad (5.155)$$

$$\int R^e(\Theta\beta) \cdot R^o(\Theta\beta) d\Omega = 0 \quad (5.156)$$

With these definitions the virtual texture equation (5.150), which is obtained from polycrystal diffraction experiments, is related to the true textures of the right-handed and the left-handed crystals by

$$\tilde{R}^e(\Theta\beta) = M^R R^{Re}(\Theta\beta) + M^L R^{Le}(\Theta\beta) \quad (5.157)$$

$$\tilde{R}^o(\Theta\beta) = M^R R^{Ro}(\Theta\beta) - M^L R^{Lo}(\Theta\beta) \quad (5.158)$$

5.10.2. Centrosymmetric Sample Symmetries

We consider centrosymmetric samples in which each right-handed crystal has its counterpart in a left-handed crystal in the same orientation. This requires

$$M^R = M^L = \frac{1}{2} \quad (5.159)$$

and

$$R^R(\Theta\beta) = R^L(\Theta\beta) \quad (5.160)$$

from which it follows that

$$C_l^R \mu = C_l^L \mu \quad (5.161)$$

For the virtual texture it follows in this case that

$$\tilde{R}^e(\Theta\beta) = R^{Re}(\Theta\beta) = R^{Le}(\Theta\beta) \quad (5.162)$$

$$\tilde{R}^o(\Theta\beta) = 0 \quad (5.163)$$

The even part of the virtual texture is thus identical with the even parts of the textures of the right-handed and the left-handed crystals, whereas the odd part is being ‘blotted out’.

5.10.3. Centrosymmetric Crystal Symmetries

If the crystals themselves are centrosymmetric, then they may be considered as right-handed and left-handed *at the same time*. It thus follows that

$$M^R = M^L = \frac{1}{2} \quad (5.164)$$

$$R^R(\Theta\beta) = R^L(\Theta\beta) = R(\Theta\beta) \quad (5.165)$$

$$C_l^{R\mu} = C_l^{L\mu} = C_l^\mu \quad (5.166)$$

This is formally equivalent with equations (5.159)–(5.161). Physically, however, the functions $R^R(\Theta\beta)$ and $R^L(\Theta\beta)$ are now not merely equal but identical, since they refer to one and the same group of crystals. The crystal directions \mathbf{h}^R and \mathbf{h}^L then correspond to the directions $+\mathbf{h}$ and $-\mathbf{h}$ of the centrosymmetric crystals. The virtual pole figure thus becomes

$$\tilde{P}_{\mathbf{h}}(\Phi) = \frac{1}{2} [P_{+\mathbf{h}}(\Phi) + P_{-\mathbf{h}}(\Phi)] \quad (5.167)$$

It corresponds to a virtual texture $\tilde{R}(\Theta\beta)$ with the coefficients

$$\tilde{C}_l^\mu = C_l^\mu \cdot \frac{1}{2} \cdot [1 + (-1)^l] = \begin{cases} C_l^\mu & \text{for } l \text{ even} \\ 0 & \text{for } l \text{ odd} \end{cases} \quad (5.168)$$

With the definition of the even and the odd parts of the texture function, this virtual texture may be written

$$\tilde{R}^e(\Theta\beta) = R^e(\Theta\beta) \quad (5.169)$$

$$\tilde{R}^o(\Theta\beta) = 0 \quad (5.170)$$

Hence, the even part of the experimentally determined texture function corresponds to the even part of the true texture function, whereas the odd part is being ‘blotted out’ because of the factor $[1 + (-1)^l]$.

5.10.4. Friedel’s Law

Because of Friedel’s law the crystal direction $+\mathbf{h}$ is indistinguishable from the direction $-\mathbf{h}$, even in non-centrosymmetric crystals. Hence, in polycrystal diffraction experiments of right-handed crystals we have to consider the symmetrical pole figure

$$\bar{P}_{\mathbf{h}^R}^R(\Phi) = \frac{1}{2} [P_{+\mathbf{h}^R}^R(\Phi) + P_{-\mathbf{h}^R}^R(\Phi)] \quad (5.171)$$

which may be written in the form of a series expansion

$$\bar{P}_{\mathbf{h}^R}^R(\Phi) = \sum_{l=0}^{\infty} \bar{F}_l(\mathbf{h}^R) \bar{P}_l(\Phi) \quad (5.172)$$

The coefficients $\bar{F}_l(\mathbf{h}^R)$ are given by

$$\bar{F}(\mathbf{h}^R) = \sqrt{\frac{2}{2l+1}} \sum_{\mu=1}^{M(l)} C_l^{R\mu} k_l^\mu(\Theta\beta) \cdot \frac{1}{2} [1 + (-1)^l] \quad (5.173)$$

They can thus be considered as belonging to a symmetrized texture with the coefficients $\bar{C}_l^{R\mu}$ such that

$$\bar{F}_l(\mathbf{h}^R) = \sqrt{\frac{2}{2l+1}} \sum_{\mu=1}^{M(l)} \bar{C}_l^{R\mu} k_l^\mu(\Theta\beta) \quad (5.174)$$

with

$$\bar{C}_l^{R\mu} = C_l^{R\mu} \cdot \frac{1}{2} \cdot [1 + (-1)^l] = \begin{cases} C_l^{R\mu} & \text{for } l \text{ even} \\ 0 & \text{for } l \text{ odd} \end{cases} \quad (5.175)$$

The symmetrized texture is expressed by the even and the odd parts of the true texture function:

$$\bar{R}^{Re}(\Theta\beta) = R^{Re}(\Theta\beta) \quad (5.176)$$

$$\bar{R}^{Ro}(\Theta\beta) = 0 \quad (5.177)$$

Correspondingly, for the left-handed crystals,

$$\bar{R}^{Le}(\Theta\beta) = R^{Le}(\Theta\beta) \quad (5.178)$$

$$\bar{R}^{Lo}(\Theta\beta) = 0 \quad (5.179)$$

Hence, Friedel’s law ‘blots out’ the odd part of the texture function and leaves the even part unchanged. Combining the symmetrization by Friedel’s law with that obtained by the indistinguishability of equivalent directions in right-handed and left-handed crystals, we obtain

$$\bar{R}^e(\Theta\beta) = M^R R^{Re}(\Theta\beta) + M^L R^{Le}(\Theta\beta) \quad (5.180)$$

$$\bar{R}^o(\Theta\beta) = 0 \quad (5.181)$$

This is what can be obtained from polycrystal diffraction experiments containing right-handed and left-handed crystals.

5.10.5. Black–White Sample Symmetries

In Section 4.11.5 the sample symmetries have been described by black–white symmetry groups (Figure 4.18). In the case of axially symmetric textures a rotation axis of infinite order has to be added to these symmetries. Thus, the five symmetry cases shown in Figure 5.6 result. Adding the condition of axial symmetry

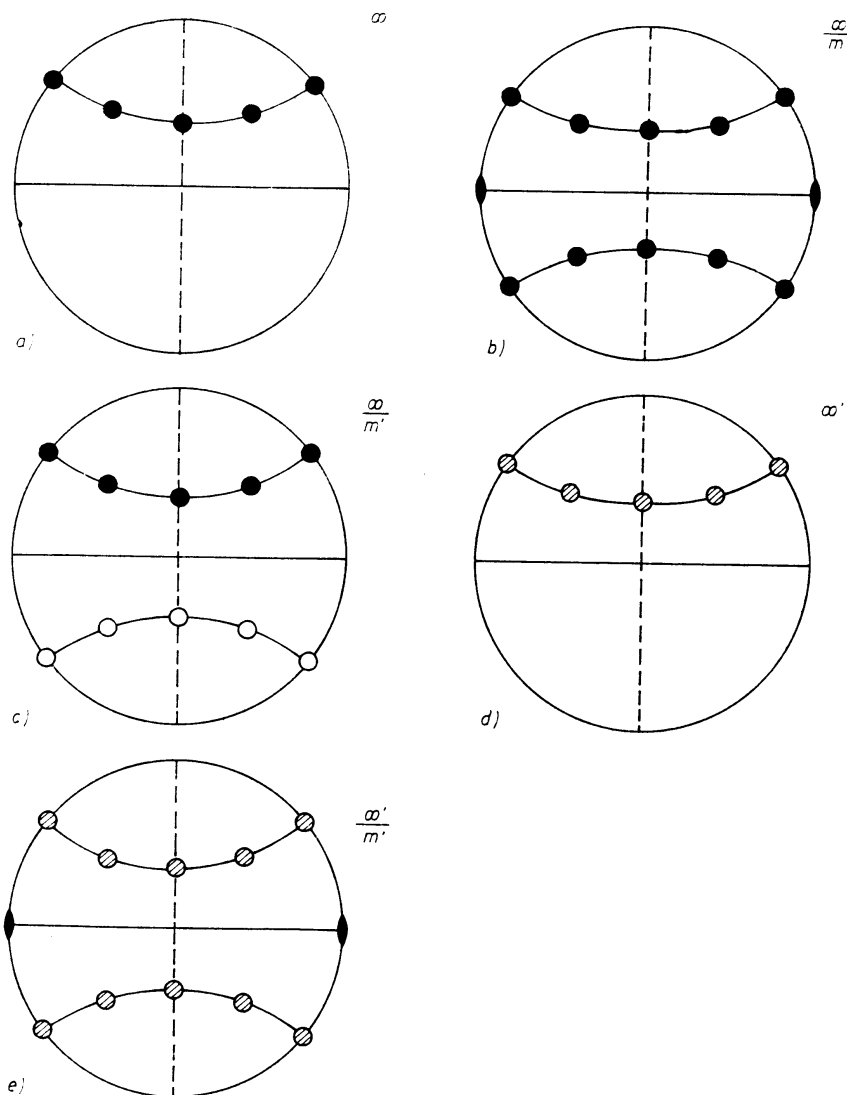


Figure 5.6 The five black–white symmetry groups obtained from Figure 4.18 by addition of an axis of infinite order

to the conditions of *Table 4.3* thus yields the conditions imposed by these five symmetry cases upon the coefficients of the textures $R^R(\mathbf{h})$ and $R^L(\mathbf{h})$ given in *Table 5.2*. Centrosymmetric crystals require a point of opposite colour in the centrosymmetrical position; they may thus belong to the two symmetry types shown in *Figure 5.6* (*c* or *e*).

Table 5.2 SYMMETRY CONDITIONS IN THE FIVE SAMPLE SYMMETRIES FOR CENTROSYMMETRIC AND NON-CENTROSYMMETRIC CRYSTALS

Sample symmetry					
	1	$\bar{1}$	$\bar{1}'$	1'	$(\bar{1}, 1')$
Crystal symmetry			$M^L = M^R$	$M^L = M^R$	$M^L = M^R$
	1		$C_l^{L\mu} = C_l^{R\mu}$	$C_l^{L\mu} = (-1)^l C_l^{R\mu}$	$C_l^{L\mu} = C_l^{R\mu}$
		$l = 2l'$			$l = 2l'$
$\bar{1}$	—	—		—	$l = 2l'$

Symmetries of pole figures

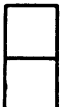
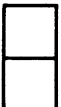
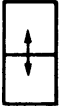
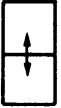
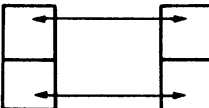
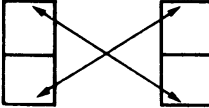
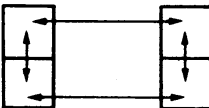
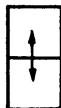
Left	Right	Centrosymmetr.	Conditions
		ϕ $\pi - \phi$	
			$l = 2l'$
			$C^L = (-1)^l C^R$
			$C^L = C^R$
			$l = 2l' \quad C^L = C^R$

Figure 5.7 Symmetries of axially symmetric pole figures in the five symmetry cases deduced from Figure 4.19

With equation (14.58a) it follows for the general axis distribution functions (equations 5.140 and 5.141) that

$$A(\mathbf{h}, \Phi) = A(-\mathbf{h}, \pi - \Phi) \quad (5.182)$$

The symmetries obtained by changing the sign of either \mathbf{h} or \mathbf{y} in the general axis distribution function in the five symmetry cases were considered in Figures 4.19 and 4.20 in the case of general texture. In the case of fibre textures the direction \mathbf{y} is replaced by the angle Φ and $-\mathbf{y}$ by $\pi - \Phi$. Thus, from Figure 4.19 the symmetries of the pole figures shown in Figure 5.7 result, whereas Figure 5.8 gives

Symmetries of inverse pole figures

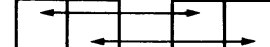
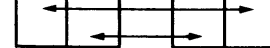
	Left	Right	Centrosymmetr.	Conditions
1	+ \mathbf{h} - \mathbf{h}	+ \mathbf{h} - \mathbf{h}	+ \mathbf{h} - \mathbf{h}	
$\bar{1}$				$l = 2l'$
l'				$C^L = (-1)^l C^R$
\bar{l}'				$C^L = C^R$
\bar{l}, l'				$l = 2l' \quad C^L = C^R$

Figure 5.8 Symmetries of inverse pole figures in the five symmetry cases according to Figure 4.20

the symmetries of the inverse pole figures. With $\Phi = 0$, the inverse pole figures are identical with the distribution functions (equations 5.136 and 5.139). Figure 5.8 thus shows the symmetries of these functions in the various cases.

Table 5.3 SYMMETRIES OF POLE FIGURES AND INVERSE POLE FIGURES OF CENTROSYMMETRIC CRYSTALS IN THE TWO POSSIBLE SAMPLE SYMMETRIES

Sample symmetry	$\bar{1}'$	$(\bar{1}, 1')$
Pole figure	$P(\pi - \Phi) = P(\Phi)$	$P(\pi - \Phi) = P(\Phi)$
Inverse pole figure	$R(-\mathbf{h}) + R(\mathbf{h})$	$R(-\mathbf{h}) = R(\mathbf{h})$

As has been considered in Section 4.11.5, the pole figures of centrosymmetric crystals are defined as the superpositions of the pole figures of the crystal $+\mathbf{h}$ - and $-\mathbf{h}$ -directions according to equation (5.167). Hence, the pole figures of centrosymmetric crystals are always centrosymmetric, whereas the inverse pole figures can be centrosymmetric or not, depending on whether the sample symmetry is $\bar{1}'$ or $(\bar{1}, 1')$. Thus, the conditions of Table 5.3 result.

The symmetry case shown in Figure 5.6 (c) corresponds to non-centrosymmetric inverse pole figures. According to equation (14.209a), the odd terms of equations

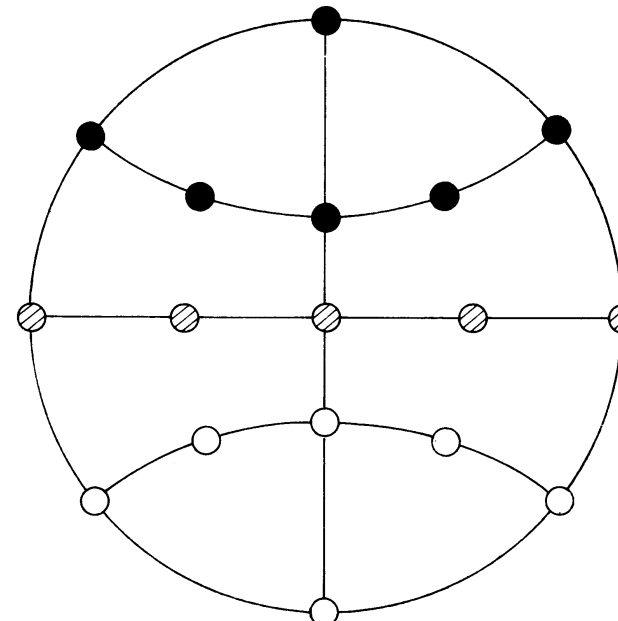


Figure 5.9 The black-white symmetry group $\frac{\infty}{m'}$. The grey points in the equatorial plane corresponding to centrosymmetric inverse pole figures

(5.140) and (5.141) must vanish for the sample direction $\Phi = \pi/2$ — i.e. for the equatorial directions. This is to be seen in *Figure 5.9*, which shows the equatorial points to be ‘grey’ points in the black—white symmetry group. Hence, in *Figure 5.6* black points and white points correspond to non-centrosymmetric inverse pole figures, whereas ‘grey’ points designate centrosymmetric inverse pole figures.

5.10.6. Determination of the Odd Part of the Texture Function

Although the odd part of the texture function is being ‘blotted out’ in the pole figures, it can, nevertheless, not be chosen arbitrarily, as has been shown in the case of general textures. Since the texture function describes the volume fraction of crystals having a certain orientation, it cannot be negative. Hence, it is required that

$$R(\mathbf{h}) = R^e(\mathbf{h}) + R^o(\mathbf{h}) \geq 0 \quad (5.183)$$

As will be shown in Section 7.6, there may be zero ranges z^0 in which the texture function is

$$R(\mathbf{h}) = 0 \quad \text{in } z^0 \quad (5.184)$$

Hence, it is

$$R^o(\mathbf{h}) = -R^e(\mathbf{h}) \quad \text{in } z^0 \quad (5.185)$$

Since $R^e(\mathbf{h})$ is known from pole figure measurements, $R^o(\mathbf{h})$ is thus also known in z^0 . It may be approximated there by a series containing odd terms only,

$$R_{L'}^o(\mathbf{h}) = \sum_{l=1(2)}^{L'} \sum_{\mu=1}^{M(l)} C_l^\mu k_l^\mu(\mathbf{h}) \quad (5.186)$$

such that the approximation condition

$$\int_{z^0} [-R^e(\mathbf{h}) - R_{L'}^o(\mathbf{h})]^2 d\mathbf{h} = \min. \quad (5.187)$$

is fulfilled. We put, for abbreviation,

$$\int_{z^0} R^e(\mathbf{h}) \cdot k_l^\mu(\mathbf{h}) d\mathbf{h} = -a_l^\mu \quad (5.188)$$

$$\int_{z^0} k_l^\mu(\mathbf{h}) \cdot k_{l'}^{\mu'}(\mathbf{h}) d\mathbf{h} = \alpha_{ll'}^{\mu\mu'} \quad (5.189)$$

and obtain the condition

$$\sum_{l=1(2)}^{L'} \sum_{\mu=1}^{M(l)} C_l^\mu \alpha_{ll'}^{\mu\mu'} = a_{l'}^{\mu'} \quad (5.190)$$

from which the coefficients C_l^μ may be obtained.

Instead of the approximation condition (5.187), another condition may be used by which only the coefficients C_l^μ of one degree l at a time are determined. We put

$$R_{l_0}(\mathbf{h}) = -R^e(\mathbf{h}) \quad (5.191)$$

The function $R_{L'}^o(\mathbf{h})$ (equation 5.186) may then be written

$$R_{L'}^o(\mathbf{h}) = \sum_{l=l_0}^{L'} \Delta R_l(\mathbf{h}) \quad (5.192)$$

where

$$\Delta R_l(\mathbf{h}) = \sum_{\mu=1}^{M(l)} C_l^\mu k_l^\mu(\mathbf{h}) \quad (5.193)$$

The approximation condition for the degree l will then be

$$\int_{z^0} [R_l(\mathbf{h}) - \Delta R_l(\mathbf{h})]^2 d\mathbf{h} = \min. \quad (5.194)$$

where

$$R_l(\mathbf{h}) = R_{l_0}(\mathbf{h}) - \sum_{\lambda=l_0}^{l-2} \Delta R_\lambda(\mathbf{h}) \quad (5.195)$$

We put, for abbreviation,

$$\int_{z^0} R_l(\mathbf{h}) k_l^\mu(\mathbf{h}) d\mathbf{h} = b_l^\mu \quad (5.196)$$

The approximation condition (5.194) then leads to

$$\sum_{\mu=1}^{M(l)} C_l^\mu \alpha_{ll'}^{\mu\mu'} = b_{l'}^{\mu'} \quad (5.197)$$

which can be solved for the coefficients C_l^μ . The quantities $\alpha_{ll'}^{\mu\mu'}$ are the same as those in equation (5.189). The quantities b_l^μ may be expressed in the form

$$b_l^\mu = \int_{z^0} \left[-R^e(\mathbf{h}) - \sum_{\lambda=l_0}^{l-2} \sum_{\mu'=1}^{M(\lambda)} C_\lambda^{\mu'} k_\lambda^{\mu'}(\mathbf{h}) \right] k_l^\mu(\mathbf{h}) d\mathbf{h} \quad (5.198)$$

With equations (5.188) and (5.189), this is

$$b_l^\mu = a_l^\mu - \sum_{\lambda=l_0}^{l-2} \sum_{\mu'=1}^{M(\lambda)} C_\lambda^{\mu'} \alpha_{l\lambda}^{\mu\mu'} \quad (5.199)$$

Equation (5.197) can thus be written

$$\sum_{\mu=1}^{M(l)} C_l^\mu \alpha_{ll'}^{\mu\mu'} = a_{l'}^{\mu'} - \sum_{\lambda=l_0}^{l-2} \sum_{\mu''=1}^{M(\lambda)} C_\lambda^{\mu''} \alpha_{l\lambda}^{\mu'\mu''} \quad (5.200)$$

This system of equations is to be solved for the coefficients C_l^μ . The coefficients $C_\lambda^{\mu''}$ at the right-hand side of this system of equations are already known by solving the same system for lower degrees of l .

In the case where z^0 is the complete orientation space (which is, of course, not possible) the two approximations (5.187) and (5.194) are identical.

The approximation to the odd part of the texture function thus obtained by the coefficients C_l^μ is defined in the whole orientation space (and not only in z^0) by equation (5.186).

6. Methods not Based on the Series Expansion

6.1. The Method of Perlwitz, Lücke and Pitsch

The simplest and most direct method for determination of the three-dimensional orientation distribution function is based on individual orientation measurements, such as can, for example, be obtained by optical measurements or by electron diffraction. For each crystal measured one thus obtains a point in the orientation space, as is represented in *Figure 6.1* for a marble sample according to WENK and

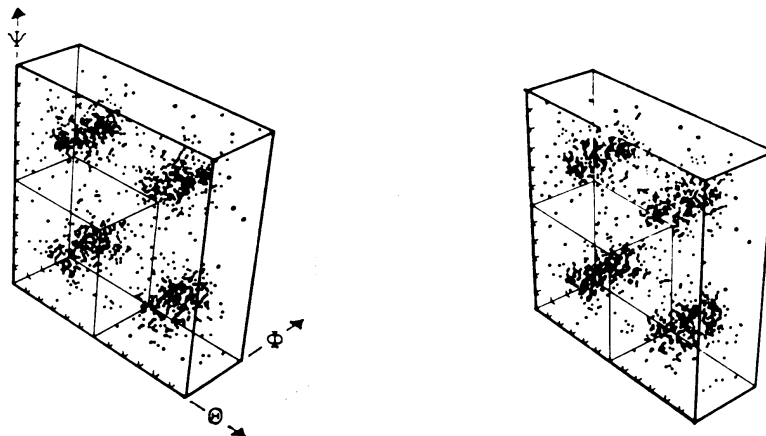


Figure 6.1 Orientations of individual crystallites in the orientation space of the EULER angles $\Psi\Theta\Phi$ (stereo pair) for a natural marble sample. After WENK and WILDE²⁹⁵

WILDE²⁹⁵. The measured orientations were thereby transformed into all symmetrically equivalent regions by the symmetry transformations. If one now divides the orientation space into regions of appropriate size and counts the points contained therein, one obtains a three-dimensional distribution function, which one can represent in contour lines in sections of constant value of one of the variables, as is represented in *Figure 6.2*. This method was first applied by PERLWITZ, LÜCKE and PITTSCH^{227,228,231} to electron diffraction measurements on copper and brass. The orientation coordinates described in Section 2.1.4 were used. The section for $\varrho_3 = 0$ for a cold-rolled copper sheet is reproduced in *Figure 6.3*. It has been constructed from curves of the number of points counted in each angular interval as they are shown in *Figure 6.4*.

This method has, however, a disadvantage. In order to obtain a sufficient statistical reliability, the regions must be chosen sufficiently large for one to obtain a sufficient number of orientation points in each region. The measured orientation coordinates of each point are thus replaced by those of the region in which it falls. This means that the existing experimental information is not completely exploited. This is all the more aggravating, as the number of measured points in the case of single orientation measurements is, in general, too small for a suffi-

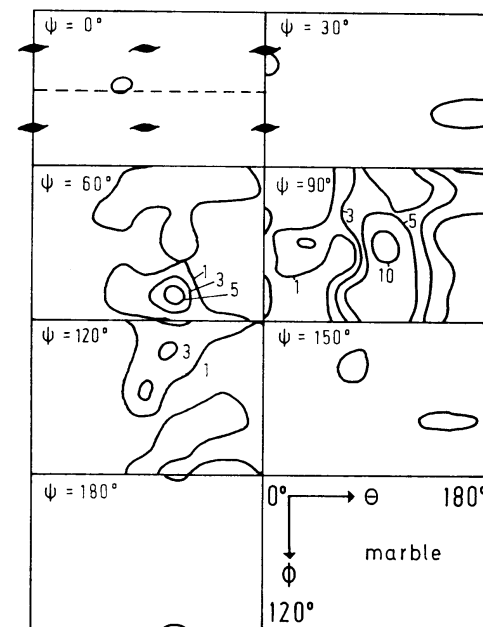


Figure 6.2 The orientation density distribution constructed from individual orientation measurements on marble crystallites²⁹⁵

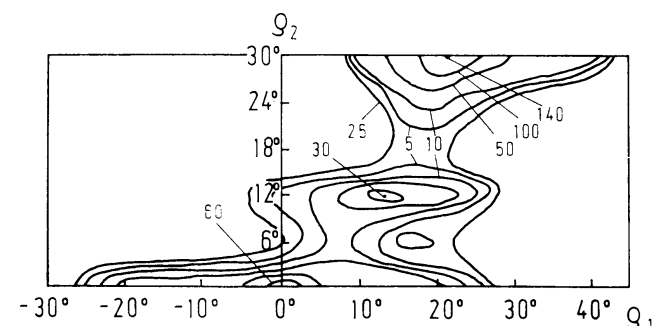


Figure 6.3 The $\varrho_3 = 0$ section of the orientation density distribution of a cold-rolled copper sheet, constructed from electron diffraction individual orientation measurements²⁰⁰

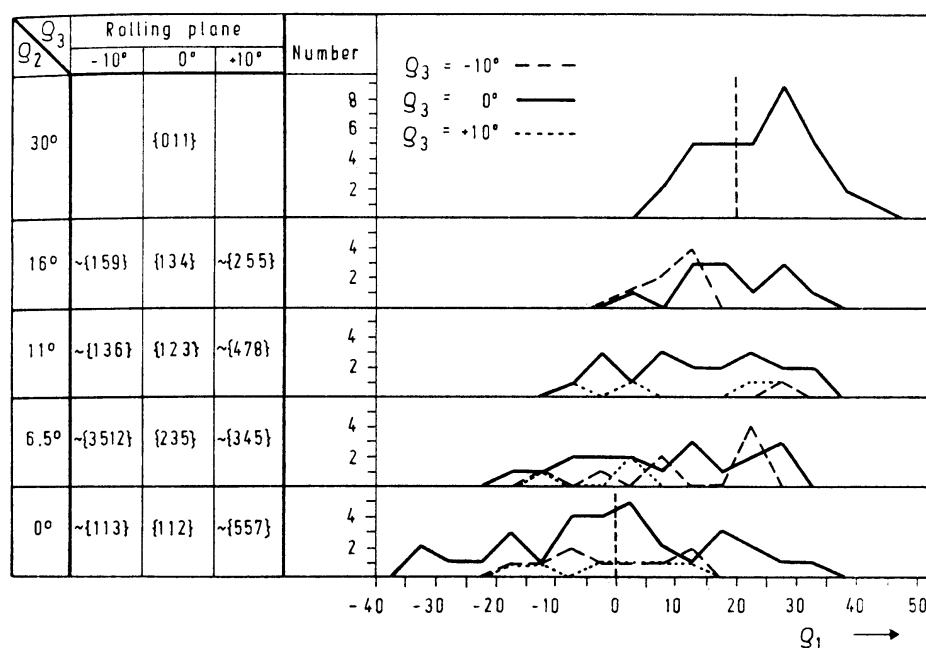


Figure 6.4 The number of orientation points counted in each orientation interval for cold-rolled copper sheet. After LÜCKE et al.²⁰²

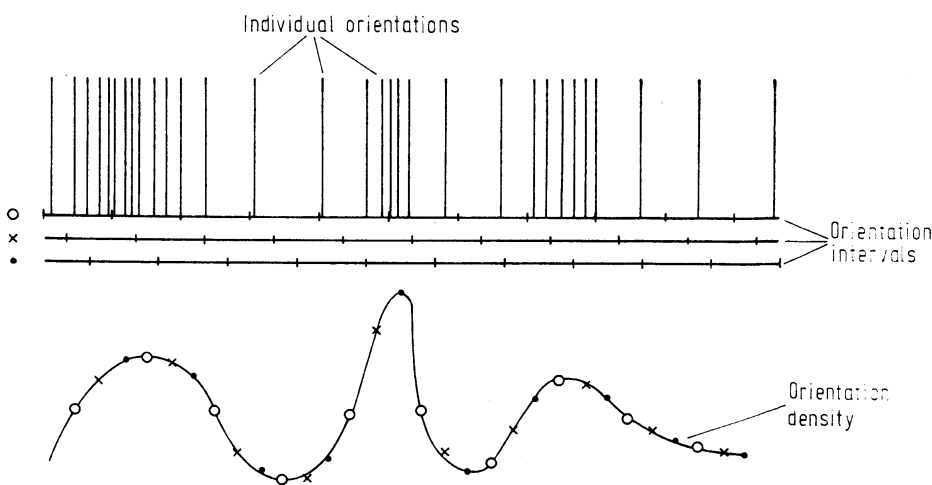


Figure 6.5 Construction of the density distribution from individual orientation measurements by use of several overlapping subregions (one-dimensional, schematic)¹³⁸

cient statistical reliability of the results. If, for example, one chooses a 10° division in the EULER space, in the cubic-orthorhombic case one thus requires about 120 orientation regions in the asymmetric unit of the space. If, further, one is to reach 80% statistical reliability, one must thus measure about 25 points per region — i.e. altogether about 3000 points. Measurements of this kind actually carried out, however, include only 500 or fewer points.

An improvement of this method can be obtained if one uses several different overlapping divisions of the orientation space, as is schematically represented in Figure 6.5. This method was suggested by HAESSNER¹³⁸. One then obtains a greater number of orientation density values, between which one can interpolate. By this variant of the method the experimental information is better exploited. Of course, the execution of the method will then also be correspondingly complicated. It then appears advantageous to construct an interpolation function according to the method described in Section 4.1.1., with the help of the series expansion.

6.2. The Method of Jetter, McHargue and Williams

A method for solution of the fundamental equation for fibre textures (equation 5.48), which does not depend on series expansion, was proposed by JETTER, McHARGUE and WILLIAMS¹⁶⁷. We consider the pole figures $P_{\mathbf{h}_p}(\Phi)$ only for discrete values of the angle Φ and number the Φ -values of all pole figures used with the index i from 1 up to i_{\max} . We will denote the value of the pole figure at the point i by P_i (for $1 \leq i \leq i_n$, the P_i thus represent the first pole figure; for $i_n + 1 \leq i \leq i_{n+1}$, the second; etc.). Equation (5.48) can then be written

$$P_i = \frac{1}{2\pi} \int_{W_i} R(\mathbf{h}) dW \quad (6.1)$$

W_i is thereby a certain path in the inverse pole figure. If i belongs to the \mathbf{h}_p pole figure, one thus obtains this path if one constructs a circle of radius Φ_i around \mathbf{h}_p and, by reflection in the region boundaries, brings all portions of this circle into a unit triangle (Figure 6.6). We now also consider the function $R(\mathbf{h})$ only at discrete points, which we shall call \mathbf{h}_j . We can then divide the total unit triangle into small regions B_j (Figure 6.6), in whose interiors we approximate the function $R(\mathbf{h})$ by a constant value R_j , which will be assumed exact at the points \mathbf{h}_j . If we designate by $2\pi \Delta W_{ij}$ the portion of the path W_i which falls in the region B_j , we can thus write equation (6.1) as

$$P_i = \sum_i \Delta W_{ij} R_j \quad (6.2)$$

If a path W_i does not cut a region B_j , the corresponding $\Delta W_{ij} = 0$. If we assume for the sake of simplicity that the number of j -values is equal to the number of i -values, we can then solve the system of linear equations (6.2) for the R_j and obtain

$$R_j = \sum_i \Delta W_{ij}^{-1} P_i \quad (6.3)$$

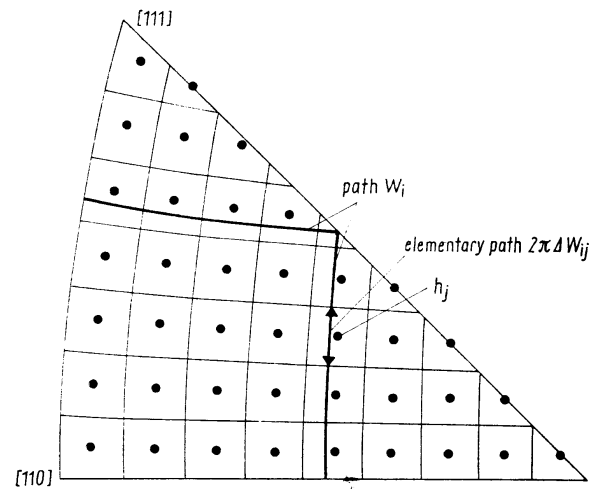


Figure 6.6 The path W_i in the inverse pole figure (method of JETTER et al.¹⁶⁷)

where ΔW_{ij}^{-1} denote the elements of the inverse of the matrix ΔW_{ij} . If the number of equations is greater than that of the unknowns R_j , equation (6.2) can thus be solved by the method of least squared errors. In this case the solution can also be written in the form of equation (6.3), but the ΔW_{ij}^{-1} have then a somewhat different meaning. We shall not, however, go into this here. The ΔW_{ij} depend only on the division of the region, the indices of the pole figures used and the choice of the angle Φ_i in the pole figures. By fixing these quantities the ΔW_{ij} and therefore also the ΔW_{ij}^{-1} can be calculated once and for all. The calculation of the function values R_j of the inverse pole figures requires then only substitution of the measured values P_i in equation (6.3), so that only minimal calculation is necessary. The method is thus particularly suited to routine investigation. However, it has disadvantages. First, the ΔW_{ij} depend on the somewhat arbitrary choice of the regions B_j , and their numerical calculation is then difficult. Furthermore, it is difficult initially to foresee how large the determinant of the matrix ΔW_{ij} will be, and thus how well the system of equations can be solved. It will, therefore, probably be relatively difficult to apply the concept of the ‘resolving power’ (which is associated with the number of linearly independent spherical surface harmonics and the number of pole figures) to this method. Last, but not least, in many important inquiries we are not interested in the values of the reciprocal pole figures themselves, but in integrals of these functions, which can be expressed in a very simple manner by a few coefficients of the series expansion. One then does not need to calculate the complete inverse pole figure, but only these coefficients (perhaps up to degree $l = 4$ or $l = 6$).

If one further ignores the definition of the quantities ΔW_{ij} and the inverse quantities ΔW_{ij}^{-1} given above, and considers only the linear dependence (6.2) between the quantities R_j and the experimental values P_i , one can thus in a round-

about way derive an expression for the coefficients ΔW_{ij}^{-1} in equation (6.3) by means of the series representation of the function $R(\mathbf{h})$. First, according to equation (5.6), $R_j = R(\mathbf{h}_j)$ depends linearly on the coefficients C_l^μ , which, according to equations (5.6) and (5.64), depend linearly on the coefficients $F_l(\mathbf{h}_p)$ of the pole figures; and, finally, these depend linearly on the values P_i of the pole figures. One thus obtains

$$R(\mathbf{h}_j) = \sum_{l=0}^L \sum_{\mu=1}^{M(l)} \sum_{\mu'=1}^{M(l)} \sum_p \sum_q k_l^\mu(\mathbf{h}_j) k_l^{\mu'}(\mathbf{h}_p) \beta_l^{\mu\mu'} w_p \bar{P}_l(\Phi_q) \sin \Phi_q \Delta \Phi_q P_{\mathbf{h}_p}(\Phi_q) \quad (6.4)$$

The $\beta_l^{\mu\mu'}$ are the quantities defined in equation (5.64), and the w_p are the weight factors, with which the various pole figures are considered. The $P_{\mathbf{h}_p}(\Phi_q)$ are the values of the \mathbf{h}_p pole figure at the points Φ_q , which are thus identical with the P_i (in other notation). If we choose the Φ_q equally distributed over the whole pole figure and the weights w_p identically 1, we thus finally obtain

$$\Delta W_{ij}^{-1} = \Delta \Phi \sum_{l=0}^L \sum_{\mu=1}^{M(l)} \sum_{\mu'=1}^{M(l)} k_l^\mu(\mathbf{h}_j) k_l^{\mu'}(\mathbf{h}_p) \beta_l^{\mu\mu'} \bar{P}_l(\Phi_q) \sin \Phi_q \quad (6.5)$$

The ΔW_{ij}^{-1} thus calculated assume no definite division of the region. Furthermore, the constancy of the function $R(\mathbf{h})$ within the regions was not assumed for this derivation. Only the pole figures are approximated by step functions, which are constant within the regions $\Delta \Phi_q$. The number of the Φ_q values for a pole figure must therefore be suitably large.

The method given by JETTER et al.¹⁶⁷ for solution of the integral equation (5.48) by a system of linear equations can also be applied to general, not rotationally symmetric, textures²⁹⁹. If, further, one denotes the values of the pole figures at specific points by P_i , equation (4.33) can be written

$$P_i = \frac{1}{2\pi} \int f(g) dW \quad (6.6)$$

where W_i is now a specified path in the orientation space g . If we assume the function $f(g)$ to be constant within specific regions B_j , with the values f_j , and that $2\pi \Delta W_{ij}$ is the portion of the path W_i in the region B_j , equation (6.6) thus transforms into a system of linear equations:

$$P_i = \sum_j \Delta W_{ij} f_j \quad (6.7)$$

The solution of this system of equations is

$$f_j = \sum_i \Delta W_{ij}^{-1} P_i \quad (6.8)$$

where ΔW_{ij}^{-1} are the elements of the inverse of the matrix ΔW_{ij} . The calculation of the ΔW_{ij} as elements of the path W_i is, of course, more complicated than in the case of fibre textures.

If, further, we consider only the linear dependence of the f_j on the measured values P_i of the pole figures (equation 6.8), we can thus, as in the case of fibre textures, derive an expression for the ΔW_{ij}^{-1} , if we express the f_j by the C_l^{μ} , these by the $F_l^v(\mathbf{h}_p)$, and, finally, these by the values of the pole figures P_i , which we shall write completely as $P_{\mathbf{h}_p}(\Phi_q, \gamma_q)$. The index p numerates the pole figures employed, and the index q , the points Φ, γ at which they are measured. One thus obtains

$$f_j = \sum_{l=0}^L \sum_{\mu=1}^{M(l)} \sum_{v=1}^{N(l)} \sum_{\mu'=1}^{M(l)} \sum_p \sum_q \bar{T}_l^{\mu v}(g_j) \beta_l^{\mu \mu'} w_p k_l^{*\mu'}(\mathbf{h}_p) \bar{P}_l^v(\Phi_q) N^v \cos m(v) \gamma_q \\ \times P_{\mathbf{h}_p}(\Phi_q \gamma_q) \quad (6.9)$$

This yields, corresponding to equation (6.8),

$$\Delta W_{ij}^{-1} = \sum_{l=0}^L \sum_{\mu=1}^{M(l)} \sum_{v=1}^{N(l)} \sum_{\mu'=1}^{M(l)} \bar{T}_l^{\mu v}(g_j) \beta_l^{\mu \mu'} w_p k_l^{*\mu'}(\mathbf{h}_p) \bar{P}_l^v(\Phi_q) N^v \cos m(v) \gamma_q \quad (6.10)$$

The $\beta_l^{\mu \mu'}$ are as defined in equation (4.146), and N^v is defined by equation (5.124). Each pair of values p, q corresponds to one value of the index i . The matrix ΔW_{ij}^{-1} is, of course, very large. For an angular increment of the points g_j of approximately 5° , WILLIAMS specified 1296 values of the index j , and as many or more points in the pole figures as values of the index i must be considered. One thus obtains in this case already more than 10^6 elements ΔW_{ij}^{-1} , many of which are, of course, zero.

Figure 6.7 shows the biaxial pole figure of cold-rolled copper obtained from the (111) and (200) pole figure by WILLIAMS²⁹⁹.

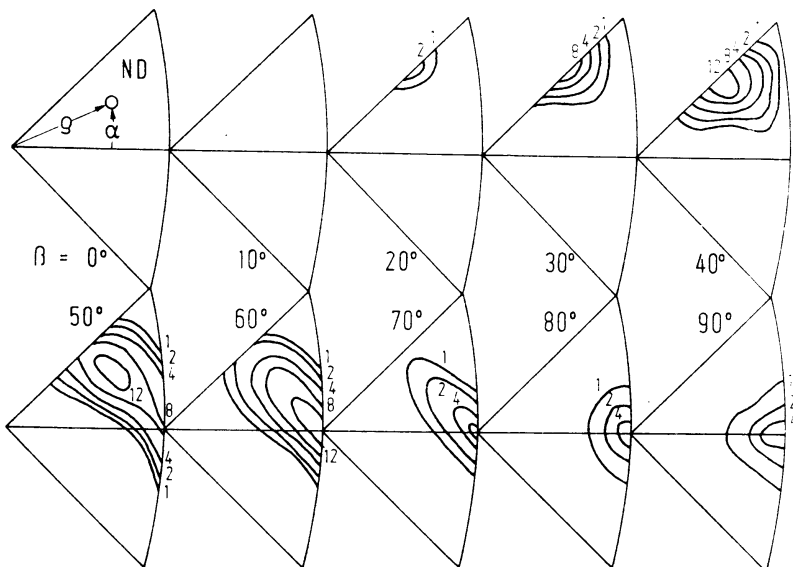


Figure 6.7 Biaxial pole figures for cold-rolled copper, calculated from two pole figures according to the method of WILLIAMS²⁹⁹

6.3. The Method of Ruer and Baro

The method suggested by WILLIAMS was considered by RUER and BARO^{250,251} and treated in mathematically rigorous fashion. The orientation was described by the coordinates ω, ψ, ζ indicated in Figure 2.15. A region division was used for ω and ψ as is represented in Figure 6.8. The angle ζ was divided in regions of 10° .

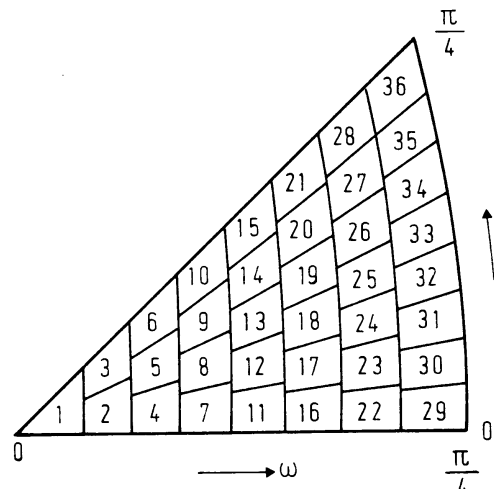


Figure 6.8 Subregions of the coordinates ω and ψ according to RUER²⁵⁰

One thus obtains an orientation space and a subdivision thereof, as is represented in Figure 6.9. The regions of this orientation space are enumerated from 1 to 2592. The orientation densities in these regions are assumed to be constant and denoted by f_j . Similarly, the pole figures are divided in regions of size $\Delta\Phi = 2^\circ$, $\Delta\gamma = 5^\circ$. These regions are numbered from 1 to 3240. The pole densities will be assumed constant within each and denoted by $P_i^{(hk)}$. One now calculates the orientation of the (hkl) pole in the (hk) pole figure for an arbitrary orientation $\omega\psi\zeta$ lying in the region j . If one lets $\omega\psi\zeta$ cover the entire region j , one thus obtains poles in different regions i of the pole figure. If one assumes a constant distribution of the orientation points in the region j with the density of the random distribution $f_j = 1$, one thus obtains a point distribution in the pole figure, as is schematically represented in Figure 6.10. Since the poles within a region i of the pole figure cannot be distinguished, one must consider the image points uniformly distributed within each region i . One thus obtains a density distribution in the pole figure, as is indicated in Figure 6.11, which we shall denote by $\Delta W_{ij}^{(hk)}$. This will be named the elementary pole figure. This is the pole figure which one would measure if one had a uniform density distribution corresponding to the random distribution in the orientation region j , but if in all other orientation regions the orientation density were zero. If, in the orientation region j , one has the density f_j , the ele-

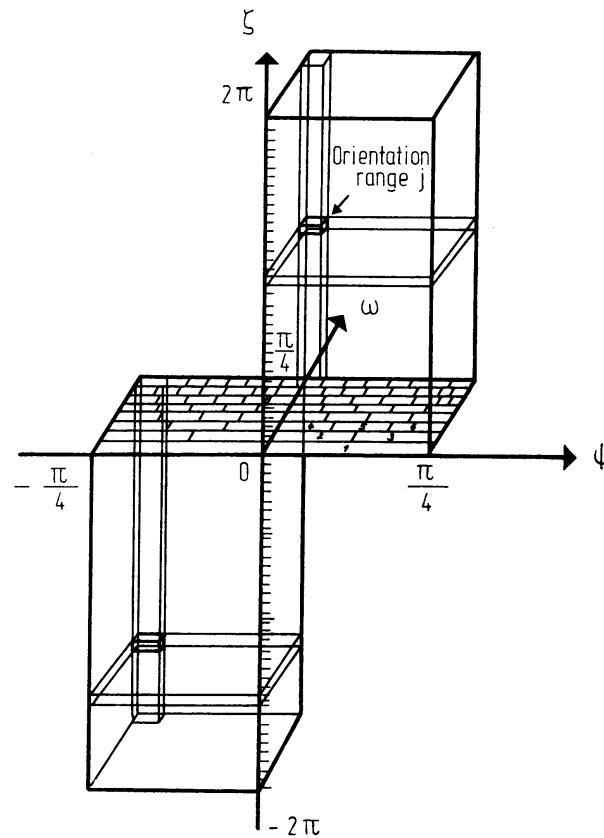


Figure 6.9 The orientation space $w\psi\zeta$ according to RUER²⁵⁰

mentary pole figure corresponding to j is multiplied by f_j and one obtains the complete pole figure, being the sum of all elementary pole figures multiplied by their corresponding factor f_j :

$$P_i^{(hkl)} = \sum_{j=1}^{2592} \Delta W_{ij}^{(hkl)} \cdot f_j, \quad 1 \leq i \leq 3240 \quad (6.11)$$

The matrices $\Delta W_{ij}^{(hkl)}$ were calculated by RUER on the basis of the relations between the coordinates $w\psi\zeta$ of the orientation g and $\Phi\gamma$ of the pole figure for $(hkl) = (111), (110), (100)$. They contain 8398080 elements, which, however, are for the most part zero. Since the system contains more equations than unknowns, equations can be omitted, in such a manner that only P_i -values of an incomplete (reflection) pole figure are used. The equations of several pole figures can also be combined. One thus obtains the final equation system (6.7). An iterative vector method described by DURAND¹²¹ will be used for its solution. If $f_j^{(n)}$ is the n th

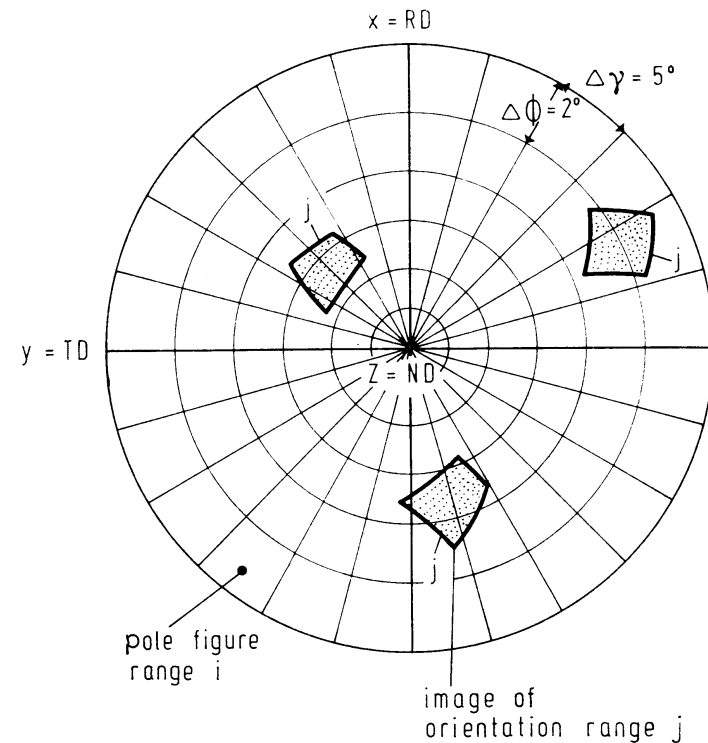


Figure 6.10 Distribution of the image points in the pole figure for random distribution of points in the orientation region j

approximation of the solution vector f_j , the difference

$$R_i^{(n)} = P_{i(\text{exp})} - \sum_j \Delta W_{ij} f_j^{(n)} \quad (6.12)$$

is then determined and a new approximation $f_j^{(n+1)}$ sought in such a way that the absolute value of the difference vector is reduced:

$$\| R_i^{(n+1)} \| < \| R_i^{(n)} \| \quad (6.13)$$

One obtains such an approximation vector $f_j^{(n+1)}$ in the form

$$f_j^{(n+1)} = f_j^{(n)} + u^{(n)} \cdot v_j^{(n)} \quad (6.14)$$

with

$$v_j^{(n)} = \sum_i \Delta W_{ij} \cdot R_i^{(n)} \quad (6.15)$$

and

$$u^{(n)} = \frac{\sum_j \left[\sum_i \Delta W_{ij} R_i^{(n)} \right]^2}{\sum_k \left[\sum_i \Delta W_{ij} \cdot \Delta W_{kj} \cdot R_k^{(n)} \right]^2} \quad (6.16)$$

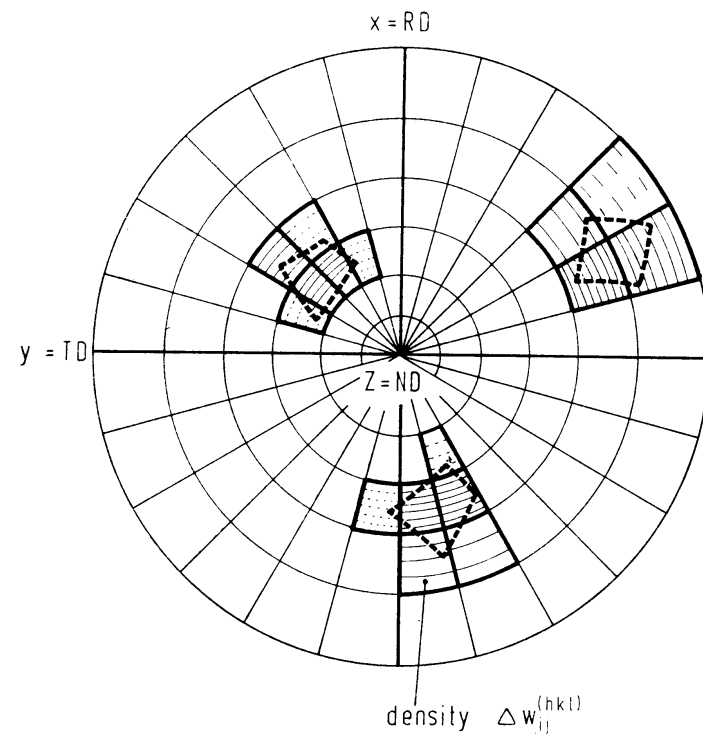


Figure 6.11 Homogeneous distribution of the image points falling in the region i of the pole figure over the total region i

If one chooses the normalization for f_i in multiples of the random distribution, it is then true that

$$\sum_{j=1}^N f_j = N, \quad N = 2592 \quad (6.17)$$

If the approximation vector $f_i^{(n)}$ contains negative values, which are physically meaningless, they will thus be replaced by zero and the vector will again be normalized according to equation (6.17). One thus obtains a non-negative approximation solution $f_i^{(n)}$. This method thus easily permits the condition of non-negativity of the orientation distribution function in the calculation, which is not so easily practicable in the case of the method of series expansion. This method is therefore of advantage for calculation of an approximate solution of the distribution function $f(g)$ from one single incomplete pole figure, i.e. with a minimum of experimental information. In RUER's method no symmetry of the pole figure (i.e. no sample symmetry) is assumed. Hence, also, cases with sample symmetry (sheet symmetry) are treated according to a sample symmetry $\bar{1}$. The crystal symmetry is, however, taken into account.

The orientation distribution of cold-rolled Fe-17% Cr alloy determined by this method is represented in $\zeta = \text{const.}$ sections in Figure 6.12. A three-dimensional illustration of the half-value surface of the density distribution of Figure 6.12 is shown in Figure 6.13.

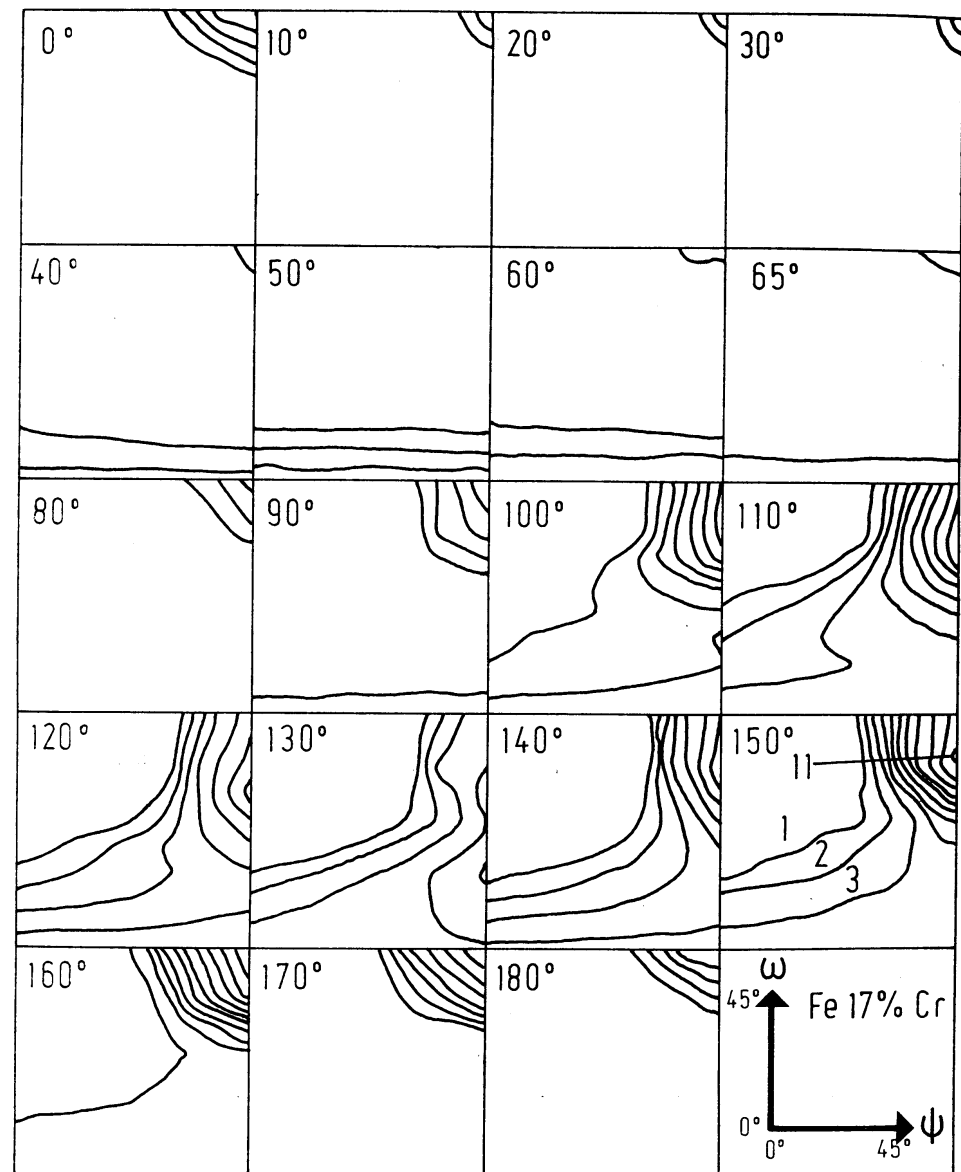


Figure 6.12 Orientation distribution function of an Fe-17% Cr alloy in multiples of the random distribution according to RUER

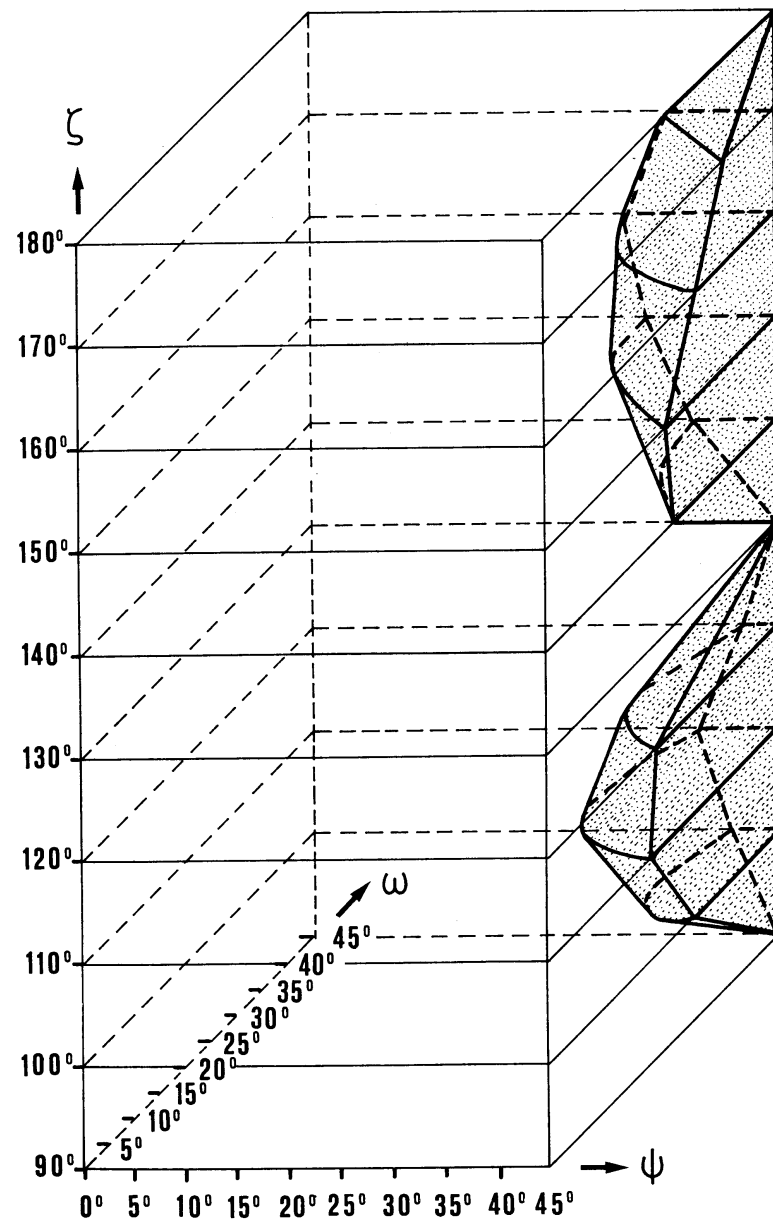


Figure 6.13 Spatial representation of the half-value surface of the texture of Figure 6.12 according to RUER

6.4. The Method of Imhof

If one considers an individual crystal orientation and its corresponding poles in the (hkl) pole figure (Figure 6.14), the pole density in all points p_1 to p_n resulting from this orientation must thus be equal. If this is not the only orientation present, pole densities associated with other orientations can contribute at each of the points p_i . The density at none of the points p_1 to p_n need then be equal to the assumed orientation density. IMHOFF¹⁶² now assumes that, of the points p_1 to p_n , that one which has the lowest pole density has the least superposition by other orientations and that this density therefore most closely approaches the true orientation density. The orientation of the points p_1 to p_n in the (hkl) pole figure is thus to be determined for each crystal orientation g and the associated pole densities P_1 to P_n are read off from the pole figure. The minimum among these n values is then taken as an approximation of the orientation density $f(g)$:

$$f(g) = \min (P_1, \dots, P_n) \quad (6.18)$$

This principle can naturally also be extended to several pole figures, if, in addition to the points p_1 to p_n , one also includes the corresponding points in other pole figures. Of course, pole figures must then be normalized so that their pole densities may be mutually comparable. This method is particularly applicable to textures

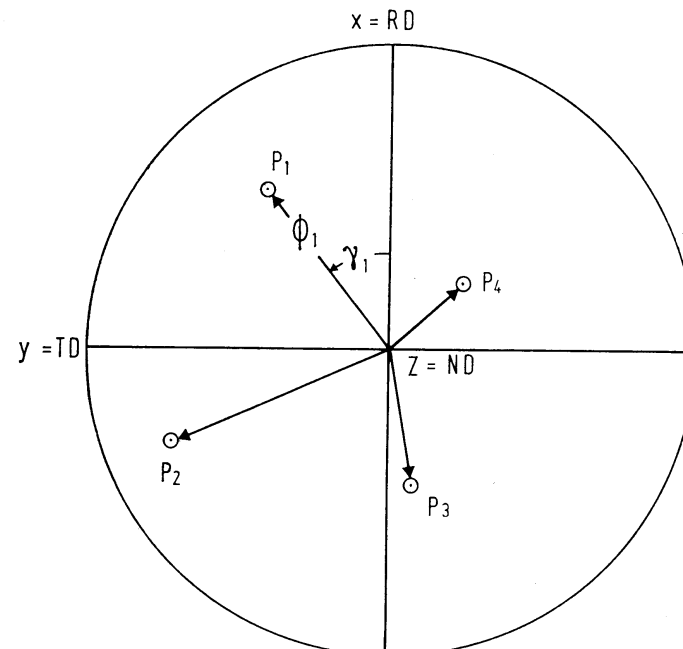


Figure 6.14 The (111) poles of a specific crystal orientation in the (111) pole figure according to IMHOFF¹⁶²

which are not too flat, in which case one can assume that at least one of the points considered has no superposition. For example, the orientation distribution of a cold-rolled aluminum sheet thus determined is reproduced in *Figure 6.15*. The orientation coordinates are here the EULER angles specified in the representation of *Figure 2.7*. *Figure 6.15* shows constant φ_2 sections, which are to be placed one upon another in the manner of *Figure 2.7* in order to obtain the three-dimensional representation.

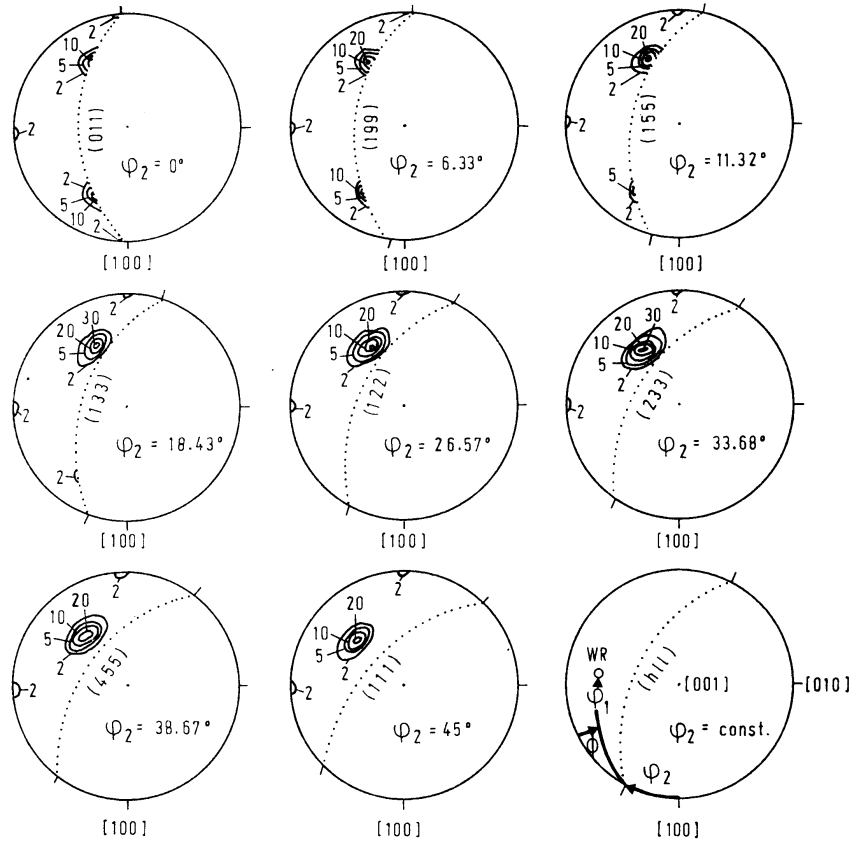


Figure 6.15 Orientation distribution function of an aluminium sheet, calculated according to the minimization method of IMHOFF from the (111) pole figure according to IMHOFF¹⁶²

7. Special Distribution Functions

Heretofore we have not made any assumptions about the course of the orientation distribution function considered. All derivations applied to completely arbitrary distribution functions. It is, however, frequently useful to approximate the essential features of an orientation distribution by a specialized and idealized distribution function. If one can show that under certain conditions distribution functions of a completely specified form always occur, the number of free parameters can thus be reduced. We shall, therefore, consider some special forms of the orientation distribution function in this section.

7.1. Ideal Orientations

By an ‘ideal’ texture we have up to now understood one which can be described by a single orientation g_0 (together with all its symmetric equivalents). For the coefficients of the series expansion of such a texture we have obtained

$$C_l^{\mu\nu} = (2l + 1) \hat{T}_l^{*\mu\nu}(g_0) \quad (7.1)$$

Such textures do not occur as actual textures (one can naturally form them from single crystals). In actuality a certain scatter of orientations always occurs about the orientation g_0 . We will therefore somewhat generalize the idea of ideal texture or ideal orientation, and by ideal orientation understand that which is different from zero only in the neighbourhood of the orientation g_0 , and depends there only on the orientation distance Δg . This means that all orientations g which result from g_0 by rotations with arbitrary rotation axes, but the same rotation angle ω , occur with equal frequency.

The orientation g_0 consists, in general, of a whole series of different but symmetrically equivalent orientations, which we have denoted by g_α . We can then decompose the texture function $f(g)$ into a sum of symmetrically equivalent partial functions, each of which is only different from zero in the neighbourhood of one of the points g . This is represented for the two-dimensional case in *Figure 7.1*:

$$f(g) = f_1(g) + f_2(g) + \dots + f_\alpha(g) + \dots + f_Z(g) \quad (7.2)$$

Z here denotes the ‘multiplicity’ of the orientation g_0 . The partial functions naturally no longer possess the symmetry of the function $f(g)$. For the coefficients $C_l^{\mu\nu}$

of the series expansion of the function $f(g)$ we then obtain

$$C_l^{\mu\nu} = (2l + 1) \sum_{\alpha=1}^z f_{\alpha}(g) \dot{T}_l^{*\mu\nu}(g) dg \quad (7.3)$$

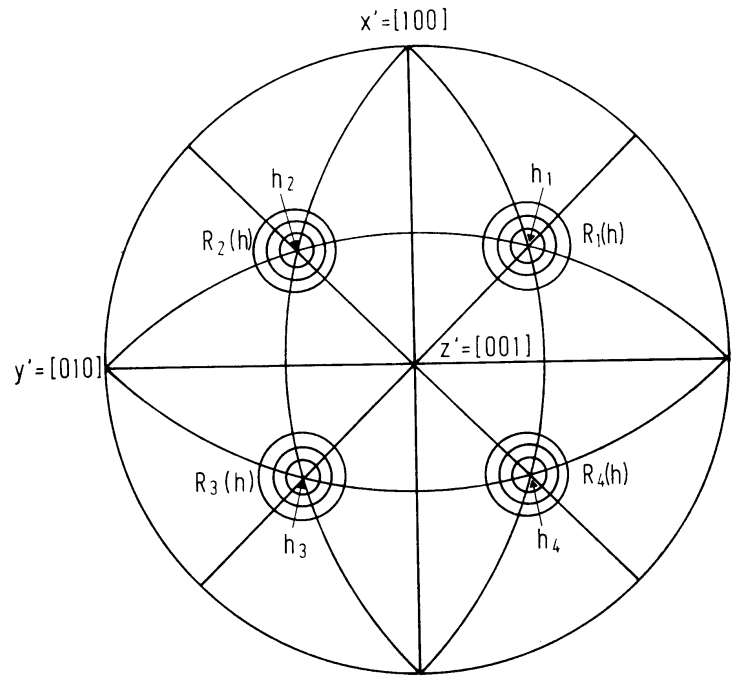


Figure 7.1 Decomposition of the inverse pole figure (or the orientation distribution function) into symmetrically equivalent portions (cubic symmetry)

Since the functions $f_{\alpha}(g)$ are assumed to be symmetrically equivalent, the integrals for different α are equal. We thus obtain

$$C_l^{\mu\nu} = (2l + 1) Z \oint f_{\alpha}(g) \dot{T}_l^{*\mu\nu}(g) dg \quad (7.4)$$

The partial function $f_{\alpha}(g)$ will now be different from zero only in the neighbourhood of the orientations g_{α} , and there only depend on the orientation distance. We therefore set

$$f_{\alpha}(g) = S(|\Delta g|) = S(\omega) \quad (7.5)$$

with

$$g = \Delta g \cdot g_{\alpha} \quad (7.6)$$

The spread about the ideal orientation g_0 will thus be described by the spread function $S(\omega)$. We thus obtain for the coefficients

$$C_l^{\mu\nu} = (2l + 1) Z \oint S(|\Delta g|) \sum_{s=-l}^{+l} \dot{T}_l^{*\mu s}(\Delta g) \cdot \dot{T}_l^{*\nu s}(g_{\alpha}) d\Delta g \quad (7.7)$$

A function depending only on the orientation interval $|\Delta g|$ can be expanded in a series of generalized spherical harmonics as follows:

$$S(|\Delta g|) = \sum_{\lambda=0}^{\infty} a_{\lambda} \left[\sum_{m=-\lambda}^{+\lambda} T_{\lambda}^{mm}(\Delta g) \right] = \sum_{\lambda=0}^{\infty} a_{\lambda} \chi_{\lambda}(|\Delta g|) \quad (7.8)$$

If one substitutes this in equation (7.7) and expresses the crystal symmetry by the coefficients \dot{A}_l^{nr} , one obtains

$$C_l^{\mu\nu} = (2l + 1) Z \sum_{\lambda} \sum_s \sum_m \dot{T}_e^{*sv}(g_{\alpha}) \dot{A}_e^{*nv} a_{\lambda} \oint T_{\lambda}^{mm}(\Delta g) T_l^{ns}(\Delta g) d\Delta g \quad (7.9)$$

With the orthonormal condition of the generalized spherical harmonics this yields

$$C_l^{\mu\nu} = Z \sum_m \dot{A}_l^{*m\mu} \dot{T}_l^{*\mu\nu}(g_{\alpha}) \quad (7.10)$$

It follows, according to the definition of the doubly symmetric generalized spherical harmonics, that

$$C_l^{\mu\nu} = Z a_l \dot{T}_l^{*\mu\nu}(g_0) \quad (7.11)$$

The following condition results for this, that the texture consists only of an ideal orientation g_0 in the above-mentioned sense:

$$C_l^{\mu\nu} : C_l^{\mu'\nu'} : C_l^{\mu''\nu''} : \dots = \ddot{T}_l^{*\mu\nu}(g_0) : \ddot{T}_l^{*\mu'\nu'}(g_0) : \ddot{T}_l^{*\mu''\nu''}(g_0) : \dots \quad (7.12)$$

The coefficients a_l of the spread function can be determined from equation (7.11) if the $C_l^{\mu\nu}$ and the orientation g_0 are known.

In general, however, a texture does not consist of a single ideal orientation g_0 (with all its symmetrically equivalent orientations). For interpretation of a texture more different orientations, which can occur with different spread functions, will frequently be specified. Thus we must, in general, write in place of equation (7.11)

$$C_l^{\mu\nu} = \sum_{i=1}^n Z_i a_l(i) \ddot{T}_l^{*\mu\nu}(g_i) \quad (7.13)$$

The g_i denote the different ideal orientations, Z_i their multiplicities and $a_l(i)$ the coefficients of the spread curve belonging to the orientation g_i . The proportion M_i belonging to the ideal orientation g_i is defined as follows:

$$M_i = \frac{Z_i \oint S_i(|\Delta g|) d\Delta g}{\oint f(g) dg} \quad (7.14)$$

If one substitutes equation (7.8) into equation (7.14),

$$M_i = Z_i a_0(i) \quad (7.15)$$

The proportions are thus essentially given by the constant terms of the series expansion of the spread functions of the different ideal orientations.

For fibre textures the distribution function depends only on the direction \mathbf{h} . An ideal orientation in the sense noted is then distinguished by rotationally symmetric distribution around the direction \mathbf{h}_0 (as well as all symmetric equivalents). If, further, we decompose the distribution function into Z portions, each of which is different from zero only in the neighbourhood of the equivalent points \mathbf{h}_α (Figure 7.1), we thus obtain for the coefficients

$$C_l^\mu = Z \phi R_\alpha(\mathbf{h}) k_l^{*\mu}(\mathbf{h}) d\mathbf{h} \quad (7.16)$$

If we fix a coordinate system Φ, β so that its pole $\Phi = 0$ coincides with the direction \mathbf{h}_α , the function $R_\alpha(\mathbf{h})$ thus depends only on the angle Φ :

$$R_\alpha(\mathbf{h}) = S(\Phi) = \sum_{\lambda=0}^{\infty} b_\lambda \bar{P}_\lambda(\Phi) \quad (7.17)$$

From this follows for the coefficients

$$C_l^\mu = Z \sum_{\lambda=0}^{\infty} b_\lambda \int_0^\pi \bar{P}_\lambda(\Phi) \left[\int_0^{2\pi} k_l^{*\mu}(\Phi, \beta) d\beta \right] \sin \Phi d\Phi \quad (7.18)$$

If we express the integral in the brackets according to equation (14.200), we thus obtain

$$C_l^\mu = Z \cdot 2\pi \sqrt{\frac{2}{2l+1}} k_l^{*\mu}(\mathbf{h}_0) \sum_{\lambda=0}^{\infty} b_\lambda \int_0^\pi \bar{P}_\lambda(\Phi) \bar{P}_l(\Phi) \sin \Phi d\Phi \quad (7.19)$$

It immediately follows that

$$C_l^\mu = Z \cdot 2\pi \sqrt{\frac{2}{2l+1}} b_l k_l^{*\mu}(\mathbf{h}_0) \quad (7.20)$$

As a condition for an ideal orientation or a rotationally symmetric distribution in the inverse pole figure one thereby obtains

$$C_l^\mu : C_l^{\mu'} : C_l^{\mu''} = k_l^{*\mu}(\mathbf{h}_0) : k_l^{*\mu'}(\mathbf{h}_0) : k_l^{*\mu''}(\mathbf{h}_0) \quad (7.21)$$

If we take cubic symmetry as an example and choose the cubic axes [100], [010], [001] for the direction \mathbf{h}_0 , the orientation distribution is thus to be written

$$R(\mathbf{h}) = R(\Phi, \beta) = S(\Phi_1) + S(\Phi_2) + S(\Phi_3) \quad (7.22)$$

where Φ_1, Φ_2, Φ_3 are the angles between the fibre axis and the three cubic axes. If we express $S(\Phi)$ according to equation (7.17) by a series of normalized LEGENDRE polynomials, we obtain

$$R(\Phi, \beta) = \sum_{l=0}^{\infty} b_l [\bar{P}_l(\Phi_1) + \bar{P}_l(\Phi_2) + \bar{P}_l(\Phi_3)] = \sum_{l=0}^{\infty} b_l k_l(\Phi, \beta) \quad (7.23)$$

The $k_l(\Phi, \beta)$ are the cubic spherical harmonics of l th degree. For every even degree $l \neq 2$ at least one such function results. For $l \leq 10$ only one linearly independent spherical harmonic of l th degree results. Therefore $k_l(\Phi, \beta)$ must agree with this

function within a factor:

$$k_l(\Phi, \beta) = \bar{P}_l(\Phi_1) + \bar{P}_l(\Phi_2) + \bar{P}_l(\Phi_3) = \text{const.} \cdot k_l^1(\Phi, \beta) \quad \text{for } l \leq 10 \quad (7.24)$$

However, for $l > 10$ more linearly independent cubic spherical harmonics result. Equation (7.23) therefore represents the general form of the series expansion of a cubic function $R(\Phi, \beta)$ only up to degree $l = 10$. If one considers terms with $l > 10$, it is thus — contrary to an occasionally expressed opinion¹⁴ — not possible to express a given orientation distribution function of a fibre texture by a series (7.23) in the general case. The function $R(\Phi, \beta)$ represents the sum of three portions which are rotationally symmetric with respect to the three cubic axes. The presence of this rotational symmetry is a special characteristic of this particular distribution function. This rotational symmetry must not be confused with the rotational symmetry about the fibre axis always assumed for fibre textures. If the texture consists not of a single ideal orientation, but of several not symmetrically equivalent orientations, it is generally true for the coefficients that

$$C_l^\mu = 2\pi \sqrt{\frac{2}{2l+1}} \sum_{i=1}^n Z_i b_l(i) k_l^{*\mu}(\mathbf{h}_i) \quad (7.25)$$

For the volume fraction Z_i of crystallites, which belong to a specific orientation \mathbf{h}_i , one obtains the expression

$$Z_i = \frac{Z_i \phi S_i(\Phi) \sin \Phi d\Phi d\beta}{\int \phi R(\mathbf{h}) d\mathbf{h}} \quad (7.26)$$

If we substitute equation (7.17) here, we thus obtain

$$Z_i = \frac{1}{\sqrt{2}} Z_i b_0(i) \quad (7.27)$$

7.2. Cone and Ring Fibre Textures

The condition for rotational symmetry with respect to the direction \mathbf{h}_0 in the inverse pole figure (equation 7.21), as well as the analogous condition for general textures (equation 7.12), are valid for arbitrary spread functions $S(\Phi)$. For consideration of ideal orientations (in the broader sense) we have tacitly assumed that the spread function has its greatest value at $\Phi = 0$ and falls more or less quickly to zero for larger Φ -values. Only then has the inverse pole figure the strongest value at the point \mathbf{h}_0 (as well as the symmetrically equivalent points) and decreases rapidly from there to zero, as it must, if one is to speak of an ‘ideal orientation’.

We now consider the case for which the spread function $S(\Phi)$ is only different from zero in the neighbourhood of the point $\Phi = \Phi_0$. The inverse pole figure then possesses a value different from zero only in a ring of diameter Φ_0 around the

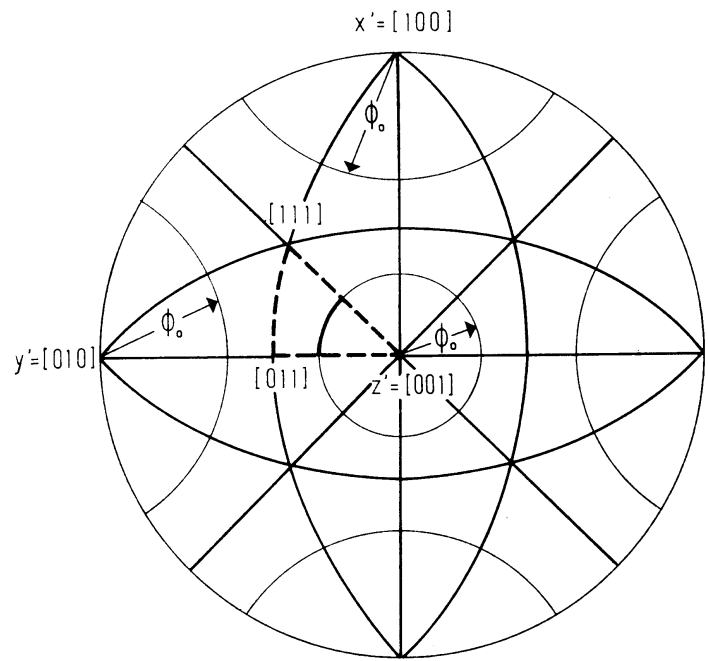


Figure 7.2 Inverse pole figure of an ideal [100] cone fibre texture for $\Phi_0 = 30^\circ$ for cubic symmetry

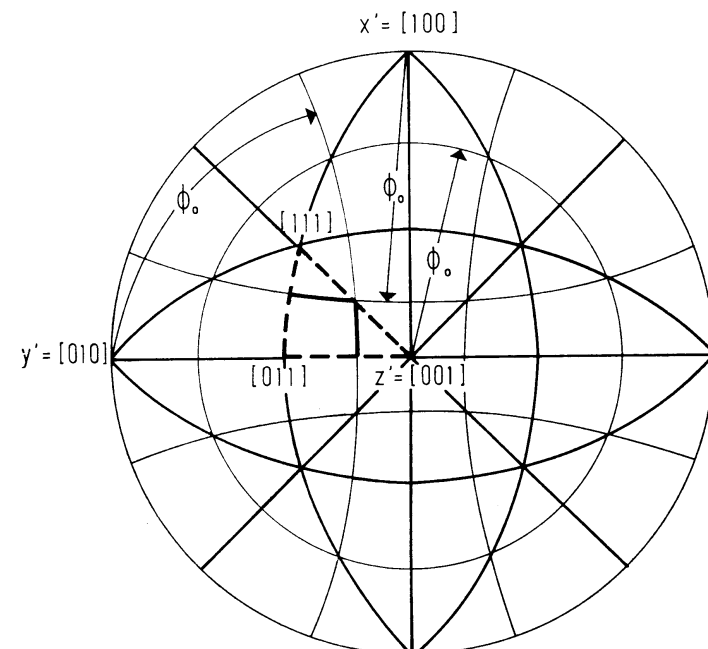


Figure 7.3 Inverse pole figure of an ideal [100] cone fibre texture with $\Phi_0 = 70^\circ$ for cubic symmetry

(symmetrically equivalent) points \mathbf{h}_0 . This is schematically represented in *Figure 7.2* for $\mathbf{h}_0 = [100]$ and $\Phi_0 = 30^\circ$. The rings can naturally overlap for greater Φ_0 values (*Figure 7.3*). For textures of this kind the fibre axis direction forms the angle Φ_0 with the direction \mathbf{h}_0 in all crystallites, and crystallites which differ only by a rotation about the direction \mathbf{h}_0 occur with equal frequency. We have thus two symmetry axes of infinite multiplicity (cylindrical symmetry, capable of free rotation) — namely one in the direction of the fibre axis (sample symmetry), which must be present for all fibre textures, and a second in the crystal direction \mathbf{h}_0 , which is present only for this special class of fibre textures. Such textures are known by the name Cone Fibre Textures⁶, since the directions \mathbf{h}_0 are situated in a cone with aperture angle $2\Phi_0$ about the fibre axis. If $\Phi_0 = 90^\circ$, the direction \mathbf{h}_0 thus always remains perpendicular to the fibre axis. Such textures will be called ring fibre textures. A [110] ring fibre texture is schematically represented in *Figure 7.4*.

If the spread function differs from zero only at the point $\Phi = \Phi_0$, one can thus speak of cone or ring fibre textures in the narrow sense. However, in actual cases a certain spread will be present about the angle Φ_0 . One can then speak of cone or ring fibre textures in the wider sense, just as in the case of ideal orientations. Thus the textures represented in *Figures 7.2* and *7.3* are cone fibre textures in the narrow sense; that represented in *Figure 7.4*, however, is a ring fibre texture in the wider

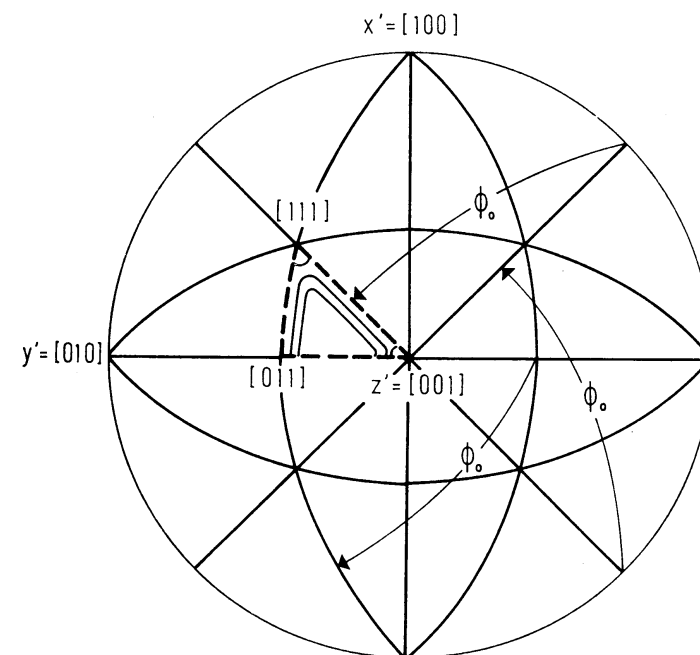


Figure 7.4 Inverse pole figure of a ring fibre texture (in the wider sense) for cubic symmetry

sense. Cone and ring fibre textures thus also fulfil the conditions (equation 7.23) established for ideal orientations for rotational symmetry with respect to a crystal direction \mathbf{h}_0 . For the ideal orientations in the narrow sense the axis of rotational symmetry in the direction \mathbf{h}_0 exactly coincides with the fibre axis. The two are thus indistinguishable. For ideal orientations in the wider sense the direction \mathbf{h}_0 coincides approximately with the fibre axis. The two axes of rotational symmetry are therefore difficult to distinguish, which frequently leads to confusion. On the other hand, for the ring and cone fibre textures the distinction between the two axes is obvious. It is therefore obviously convenient to deal with ideal orientations in the wider sense as cone fibre textures. In *Figure 7.1*, for example, each of the concentric circles about \mathbf{h}_1 can be interpreted as a cone fibre texture. The superposition of all these cone fibre textures then results in the ideal orientation in the wider sense.

7.3. 'Spherical' Textures

We consider the analogous situation in the case of general textures; thus we obtain a distribution function $f(g)$, which differs from zero only at such points g as result from the orientation g_0 by rotation through the angle Φ_0 for arbitrary orientation of the rotation axis. If we represent the orientation by a point in a three-dimensional space (*Figure 2.4*) the above-mentioned orientations g thus lie on a closed surface around the point g_0 and have the same orientation distance (defined according to Section 2.4) from g_0 . If we denote such a surface in the orientation space as an 'orientation sphere', we can thus describe such textures as 'spherical' textures. Naturally one must always consider that the designation 'spherical' refers not to actual space, but to orientation space. However, such textures appear not yet to have been considered, and it is doubtful that they really occur.

7.4. Fibre Axes

We have noted in the preceding section the form the coefficients $C_l^{\mu\nu}$ assume if the texture consists of one or more ideal orientations. An ideal orientation in the wider sense is distinguished in that all orientations which result from the orientation g by rotation about arbitrary rotation axes, but with equal rotation angles, occur with equal frequency. We now consider the inverse case: that all orientations which result from g by rotation about the same rotation axis, but with arbitrary rotation angle, occur with equal frequency. Textures for which this is the case are rotationally symmetric about this rotation axis; they are thus fibre textures. In Chapter 5 we have already very completely treated the case for which the fibre axis coincides with the Z -axis of the sample fixed coordinate system. We shall now consider the case in which the fibre axis possesses an arbitrary direction \mathbf{y}_0 in the sample fixed coordinate system, as well as the general case, in which the texture is composed of several fibre texture components with different fibre axes¹³⁶. In the latter case the complete texture naturally no longer has any axis of

rotational symmetry, unless we are concerned with the random distribution, for which every direction is an axis of rotational symmetry.

If, first of all, the orientation distribution

$$f(g) = \sum_{l=0}^L \sum_{\mu=1}^{M(l)} \sum_{\nu=1}^{N(l)} C_l^{\mu\nu} \dot{T}_l^{\mu\nu}(g) \quad (7.28)$$

is rotationally symmetric about the Z -axis of the sample coordinate system, equation (7.28) transforms into

$$f(g) = \sum_{l=0}^L \sum_{\mu=1}^{M(l)} C_l^{\mu 1} \dot{T}_l^{\mu 1}(g) \quad (7.29)$$

The circle used instead of a point signifies rotational symmetry, and since only one linearly independent spherical harmonic of this symmetry results, the summation over ν is dropped. We now introduce a new sample coordinate system

$$g = g' \cdot g_0 \quad (7.30)$$

which, with respect to the original system, is rotated through g_0 . With the addition theorem for the generalized spherical harmonics, we then obtain from equation (7.29), if we also imagine the function $f(g)$ to be expressed by the variable g' ,

$$f(g') = \sum_{l=0}^L \sum_{\mu=1}^{M(l)} \sum_{s=-1}^{+l} C_l^{\mu 1} \dot{T}_l^{\mu s}(g') \dot{T}_l^{s 1}(g_0) \quad (7.31)$$

The orientation distribution function is thus expressed in this coordinate system in the form

$$f(g') = \sum_{l=0}^L \sum_{\mu=1}^{M(l)} \sum_{s=-1}^{+l} C_l'^{\mu s} \dot{T}_l^{\mu s}(g') \quad (7.32)$$

with the coefficients

$$C_l'^{\mu s} = C_l^{\mu 1} \dot{T}_l^{s 1}(g_0) \quad (7.33)$$

If now we introduce the fibre texture coefficients C_l^{μ} from equation (5.4) for the coefficients $C_l^{\mu 1}$ and the spherical surface harmonics $k_l^s(\mathbf{y}_0)$ from equation (14.41) for the rotationally symmetric generalized spherical harmonics $\dot{T}_l^{s 1}(g_0)$, where \mathbf{y}_0 is the direction of the fibre axis in the rotated sample coordinate system, we obtain for the coefficients $C_l'^{\mu s}$

$$C_l'^{\mu s} = C_l^{\mu} k_l^s(\mathbf{y}_0) \quad (7.34)$$

The coefficients of an orientation distribution must fulfil this condition, if rotational symmetry with respect to an arbitrary sample direction \mathbf{y}_0 is to be present. Beyond that, however, which crystal direction \mathbf{h} falls in the direction \mathbf{y}_0 has not yet been asserted. If we now assume that we are dealing with an ideal fibre texture in the narrow sense, only a single crystal direction \mathbf{h}_0 (together with its

symmetric equivalents) falls in the sample direction \mathbf{y}_0 , and we obtain for the coefficients from equation (5.16)

$$C_l^{\mu s} = 4\pi k_l^{*\mu}(\mathbf{h}_0) k_l^s(\mathbf{y}_0) \quad (7.35)$$

If, now, we assume that the texture can be represented by several rotationally symmetric components with different rotation axes, we thus generally obtain for the coefficients the expression

$$C_l^{\mu s} = \sum_i M_i C_l^{\mu}(i) k_l^s(\mathbf{y}_i) \quad (7.36)$$

where M_i denotes the relative amount for the i th fibre axis. The coefficients $C_l^{\mu}(i)$ describe the frequency distribution of the various crystal directions \mathbf{h} which fall in the i th fibre axis. If we are concerned with an ideal fibre texture in the narrow sense, for which only individual crystal directions \mathbf{h}_j fall in the sample direction \mathbf{y}_i , and indeed with the relative amounts M_{ij} , it is true for the coefficients

$$C_l^{\mu s} = 4\pi \sum_i \sum_j M_{ij} k_l^{*\mu}(\mathbf{h}_j) k_l^s(\mathbf{y}_i) \quad (7.37)$$

As an example we shall consider the case for which the texture of a sheet is composed of two rotationally symmetric components with the rolling direction and the normal direction as axes. These two directions, \mathbf{y}_1 and \mathbf{y}_2 , have the spherical angular coordinates

$$\begin{aligned} \mathbf{y}_1 &= \{\Phi = 0^\circ, \gamma = 0^\circ\} \\ \mathbf{y}_2 &= \{\Phi = 90^\circ, \gamma = 0^\circ\} \end{aligned} \quad (7.38)$$

For the coefficients $C_l^{\mu s}$ one thus obtains from equation (7.36)

$$C_l^{\mu 0} = \frac{1}{\sqrt{2\pi}} [M_1 C_l^{\mu}(1) \bar{P}_l(0^\circ) + M_2 C_l^{\mu}(2) \bar{P}_l(90^\circ)] \quad (7.39)$$

$$C_l^{\mu s} = \frac{1}{\sqrt{\pi}} M_2 C_l^{\mu}(2) \bar{P}_l(90^\circ) \quad (7.40)$$

In the two fibre axis directions, the rolling direction and the normal direction, completely arbitrary distributions of the crystal direction \mathbf{h} can still occur.

7.5. Line and Surface Textures (Dimension of a Texture)

The fibre texture components described in the preceding section are so characterized that all orientations occurring result from one another by rotation about an arbitrary but fixed axis. In the representation of an orientation illustrated in *Figure 2.9*, all these orientations lie along a line parallel to the axis of the orientation space (for application of EULER angles as orientation parameters a straight line thus results only in exceptional cases). In contrast to the zero-dimensional ideal orientations, fibre texture components thus have one-dimension-

al orientation multiplicity. If we abandon the requirements of spatial constancy of a specified crystal direction, retaining, however, one-dimensional orientation multiplicity, we come to a generalization of the fibre texture components — namely to such textures as can be described by an arbitrary, not necessarily straight, line in the orientation space. In the real case a certain spread about this line will naturally be present. For this type of texture, however, we shall assume that the spread width is small by comparison with the longitudinal extension of the line. We then obtain a tubular form in orientation space (orientation tube). We can denote the line as the skeleton line of the texture. In general, the orientation density will not be constant along the length of the skeleton line. Some examples of this type of texture will be considered in Chapter 11.

By a further generalization we come to surface-confined distributions in orientation space — i.e. to textures which are characterized by a large extension into two dimensions, while an essentially smaller spread will be present in the third direction. In this case we shall also permit arbitrarily formed surfaces and notice the essential character of this type of texture in the two-dimensional extension.

7.6. Zero Regions

The value of the \mathbf{h} -pole figure at the point \mathbf{y} is given by an integral of the orientation distribution function along a specific path $W(\mathbf{h}, \mathbf{y})$:

$$P_{\mathbf{h}}(\mathbf{y}) = \int_{W(\mathbf{h}, \mathbf{y})} f(g) dW \quad (7.41)$$

If the \mathbf{h} -pole figure assumes the value zero at the point \mathbf{y}_0 ,

$$P_{\mathbf{h}}(\mathbf{y}_0) = 0 \quad (7.42)$$

it immediately follows from the condition

$$f(g) \geq 0 \quad (7.43)$$

that

$$f(g) = 0 \quad (7.44)$$

along the entire path $W(\mathbf{h}, \mathbf{y}_0)$. A pole figure frequently possesses zero values in extensive regions. Then the paths $W(\mathbf{h}, \mathbf{y})$ in the space of orientations g associated with the points of these regions describe certain regions in which the function $f(g)$ must be everywhere zero. Thus, from the zero regions of the different pole figures one obtains different zero regions of the function $f(g)$. The total region in which the function $f(g)$ vanishes, naturally, must include all these regions. In this way one can immediately construct a minimum zero region for the function $f(g)$.

These considerations are particularly obvious in the case of fibre textures. Namely every point of the inverse pole figure which contributes to the intensity of the \mathbf{h} -pole figure at the angle Φ lies on a circle of distance Φ around the point \mathbf{h} . If, therefore, the \mathbf{h} -pole figure vanishes in the interval from Φ_1 to Φ_2 , the inverse pole figure must thus be zero on a corresponding circular ring, as is schematically represented in *Figure 7.5*.

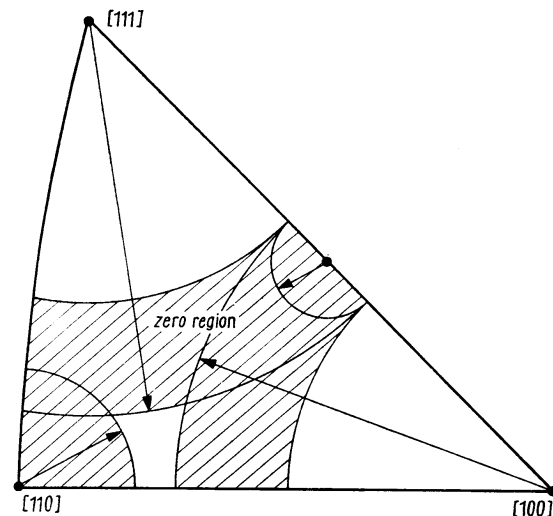


Figure 7.5 Determination of the zero region of the inverse pole figure (orientation distribution function) from zero regions of the pole figures

If the \mathbf{h} -pole figure assumes a value different from zero at the point y , the orientation distribution function or the inverse pole figure along the path in question must be different from zero at least one point. Such a path, therefore, can not lie completely within the zero region of the function $f(g)$. The zero region can be specified by these considerations without making use of the series expansion.

7.7. Gaussian Distributions

In many cases the spread of orientations around an ideal orientation appears to be given by a Gaussian distribution. Gaussian distributions were observed in pole figures of recrystallized Fe-Si alloys^{118,290,293}, rolled beryllium²⁶, pyrolytic graphite^{26,27} and recrystallized aluminium wires⁴⁹. In many cases the distributions in the pole figures may be interpreted by means of superimposed Gaussian distributions⁴¹. Orientation distributions which can not be interpreted in a simple way by Gaussian distributions have, however, also been observed⁴¹. All these observations refer to pole figures, and one can naturally not rigorously draw conclusions therefrom about the course of the spread function $S(\Delta g)$ in the inverse pole figure or in the three-dimensional orientation distribution function. In a further example given below the spread function $S(\Phi)$ in the inverse pole figure will be directly determined, from which a Gaussian distribution also results. In many cases, therefore, we may consider the spread of orientations around the ideal orientation to have Gaussian shape.

The spread function $S(\Phi)$ then has the form

$$S(\Phi) = S_0 e^{-\Phi^2/\Phi_0^2} \quad (7.45)$$

where S_0 is the value of the function for $\Phi = 0$ and Φ_0 is that angle for which the function value amounts to $1/e$ of its maximum value. If we develop $S(\Phi)$ in a FOURIER series

$$S(\Phi) = \sum_{n=-\infty}^{+\infty} c_n e^{in\Phi} \quad (7.46)$$

or

$$S(\Phi) = \sum_{n=0}^{\infty} c'_n \cos n\Phi \quad (7.47)$$

with

$$c'_0 = c_0, \quad c'_n = 2c_n \quad (7.48)$$

it is true for the coefficients (see, e.g., reference 245, p. 251)

$$c_n = \frac{S_0 \cdot \Phi_0}{\sqrt{4\pi}} e^{-n^2 \Phi_0^2/4} \quad (7.49)$$

In the case of general (not rotationally symmetric) textures we need the series expansion corresponding to equation (7.8) of the function $S(\Phi)$ in the functions $\chi_n(\Phi)$. If from equation (14.30) we express the $\cos n\Phi$ by the $\chi_n(\Phi)$, we obtain

$$S(\Phi) = c'_0 \chi_0 + \frac{1}{2} \sum_{n=1}^{\infty} c'_n [\chi_n(\Phi) - \chi_{n-1}(\Phi)] \quad (7.50)$$

This gives

$$S(\Phi) = \left[c'_0 - \frac{1}{2} c'_1 \right] \chi_0 + \sum_{n=1}^{\infty} \frac{1}{2} [c'_n - c'_{n+1}] \chi_n \quad (7.51)$$

In the case of general textures it is thus true for the coefficients a_l of the series expansion (equation 7.8) of the spread function $S(\Phi)$

$$a_l = \frac{1}{2} [c'_l - c'_{l+1}] \quad (7.52)$$

$$a_0 = c'_0 - \frac{1}{2} c'_1 \quad (7.53)$$

With equation (7.48) this gives, in general,

$$a_l = c_l - c_{l+1} \quad (7.54)$$

For the volume fraction of crystallites of the ideal orientation concerned we obtain with equations (7.15) and (7.49)

$$M = Z S_0 \Psi_1(\Phi_0) \quad (7.55)$$

with

$$\Psi_1(\Phi_0) = \frac{1}{\sqrt{4\pi}} \Phi_0 \left[1 - e^{-\Phi_0^2/4} \right] \quad (7.56)$$

In the case of rotationally symmetric textures (fibre textures) the spread function is expanded in a series of normalized LEGENDRE polynomials. We thus express the $\cos n\Phi$ in equation (7.47) by the $\bar{P}_l(\Phi)$ (see equations 11.107 and 11.108 in reference I) and obtain

$$S(\Phi) = \sum_{n=0}^{\infty} \sum_{l=0}^n c'_n M_l^n \bar{P}_l(\Phi) = \sum_{l=0}^{\infty} b_l \bar{P}_l(\Phi) \quad (7.57)$$

with

$$b_l = \sum_{n=-l}^{+l} c'_n M_l^n \quad (7.58)$$

Naturally, moreover,

$$b_l = \int_0^\pi S(\Phi) \bar{P}_l(\Phi) \sin \Phi d\Phi \quad (7.59)$$

If one substitutes equation (7.45) therein, one obtains

$$b_l = S_0 \int_0^\pi e^{-\Phi^2/\Phi_0^2} \bar{P}_l(\Phi) \sin \Phi d\Phi \quad (7.60)$$

For $l = 0$, there results, in particular,

$$b_0 = S_0 \frac{1}{\sqrt{2}} \int_0^\pi e^{-\Phi^2/\Phi_0^2} \sin \Phi d\Phi \quad (7.61)$$

and from this, by carrying out the integration (see, e.g., reference 245, p. 178)

$$b_0 = S_0 \Phi_0 \frac{\sqrt{2\pi}}{4} e^{-\Phi_0^2/4} F\left(\frac{\Phi_0}{2}\right) \quad (7.62)$$

$F(x)$ is thus the error integral

$$F(x) = \frac{2}{\sqrt{\pi}} \int_0^x e^{-t^2} dt \quad (7.63)$$

From equation (7.27) one therefore obtains for the volume fraction of crystallites associated with the ideal orientation \mathbf{h}_0

$$M = Z S_0 \Psi_2(\Phi_0) \quad (7.64)$$

with

$$\Psi_2(\Phi_0) = \frac{1}{4} \sqrt{\pi} \Phi_0 e^{-\Phi_0^2/4} F\left(\frac{\Phi_0}{2}\right) \quad (7.65)$$

The functions $\Psi_1(\Phi_0)$ and $\Psi_2(\Phi_0)$ are presented in Figure 7.6. The volume fraction of crystallites belonging to a specific ideal orientation can be directly specified from equations (7.55) and (7.64), if the values S_0 and Φ_0 of the spread are known.

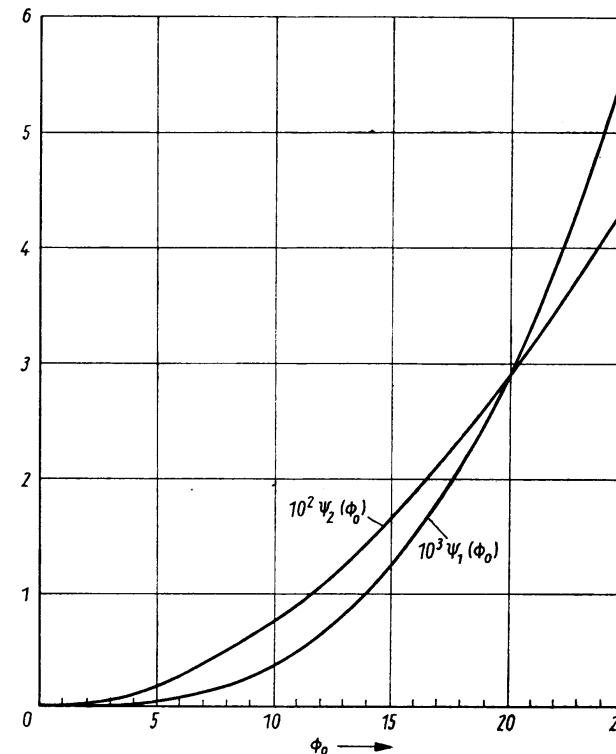


Figure 7.6 Volume fraction functions $\Psi_1(\Phi_0)$ and $\Psi_2(\Phi_0)$ for GAUSSIAN form ideal orientations of the $1/e$ -value width Φ_0

7.8. Polynomial Approximation (Angular Resolving Power)

In Section 7.1 we considered ideal orientations — i.e. textures which have values different from zero only at the point g_0 or in the neighbourhood of g_0 . The way in which the distribution density decreased from its maximum value near g_0 to zero thereby remained completely open. In Section 7.7 we then considered special ideal textures whose spread behaviour was described by GAUSSIAN curves. If one represents such distributions by series of generalized spherical harmonics, strictly speaking, one thus requires infinite series. Since in practice, however, one can always calculate only with finite series, we shall now consider ideal orientations with such spread behaviour as one obtains if one substitutes the coefficient expression (7.1) in the series expansion (4.7) and truncates the series for $l = L$. We thus obtain a spread function of the form

$$f_g^L(g) = \sum_{l=0}^L \sum_{\mu=1}^{M(l)} \sum_{\nu=1}^{N(l)} (2l+1) \hat{T}_l^{*\mu\nu}(g_0) \hat{T}_l^{\mu\nu}(g) \quad (7.66)$$

which is different from zero only in the neighbourhood of \mathbf{g}_0 . Because of series truncation effects, such a function naturally also assumes negative values. In the case of fibre textures we similarly obtain

$$R_{\mathbf{h}_0}^L(\mathbf{h}) = 4\pi \sum_{l=0}^L \sum_{\mu=1}^{M(l)} k_l^{*\mu}(\mathbf{h}_0) k_l^\mu(\mathbf{h}) \quad (7.67)$$

Figures 7.7 and 7.8 show two examples of such functions for the case of cubic crystal symmetry and $L = 30$, and indeed for $\mathbf{h}_0 = [111]$ and $\mathbf{h}_0 = [100]$. One notes that high values of the orientation density occur only in the neighbourhood of the corresponding points \mathbf{h}_0 . Figures 7.9 and 7.10 show the behaviour of the two functions along the sections [111]—[110] and [100]—[110]. One perceives that successive maxima are separated from one another by approximately 13 — 14° . The half-width of the principal maximum amounts to approximately 4° in both cases, so that two orientations which differ from each other by approximately 8° can indeed no longer be resolved. One can thus set the angular resolving power at about 12° . In Figure 7.11 the same section is represented as in Figure 7.9, except that the series expansion has been extended up to $L = 50$. In this case the interval between neighbouring maxima amounts to approximately 8° , while the principal maximum has a half-width of approximately 2.4° , so that we can set the angular resolving power at approximately 6° . For $L = 100$ the angular resolving power will amount to approximately 3° . Figure 7.12 shows the approximate behaviour of the angular resolving power with degree L of the series expansion as well as the number of pole figures required in the case of cubic symmetry.

In order to avoid relatively large truncation errors — i.e. relatively high negative values of functions (7.67) — one can thus introduce additional smearing factors (see equation 5.92) which might be chosen in the form, for example, of an

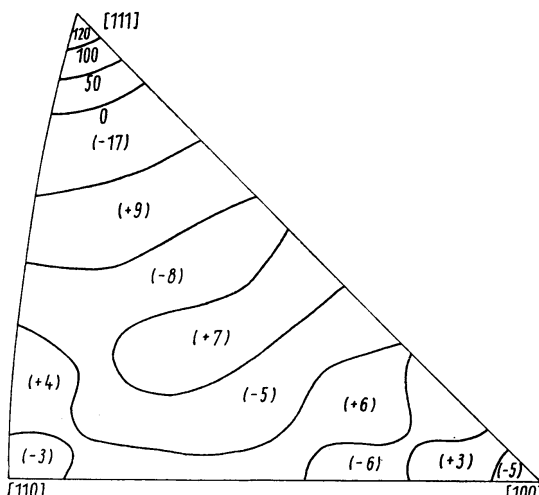


Figure 7.7 Approximation function $R_{\mathbf{h}_0}^L(\mathbf{h})$ of an ideal orientation for cubic symmetry with $\mathbf{h}_0 = [111]$, $L = 30$

exponential factor. We thus obtain distribution functions of the form

$$R_{\mathbf{h}_0}^{L,l_0}(\mathbf{h}) = 4\pi \sum_{l=0}^L \sum_{\mu=1}^{M(l)} e^{-(l/l_0)^2} k_l^{*\mu}(\mathbf{h}_0) k_l^\mu(\mathbf{h}) \quad (7.68)$$

Such functions have the advantages that, on the one hand, they are represented by a series with a finite number of terms, and that, on the other, they permit faithful reproduction of actual distributions. The section along [111]—[110] of function (7.68) for $\mathbf{h}_0 = [111]$, $L = 50$, $l_0 = 23$ is reproduced in Figure 7.13.

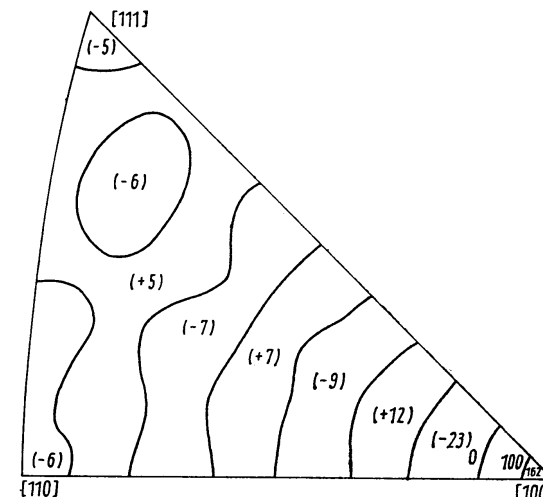


Figure 7.8 Approximation function $R_{\mathbf{h}_0}^L(\mathbf{h})$ of an ideal orientation for cubic symmetry with $\mathbf{h}_0 = [100]$, $L = 30$

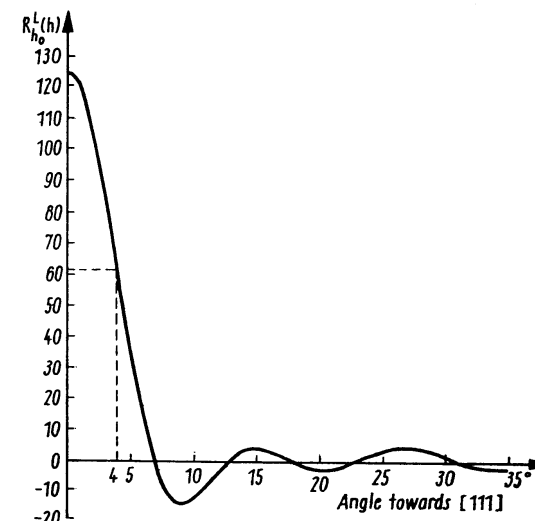


Figure 7.9 [111]—[110] section of the function represented in Figure 7.7

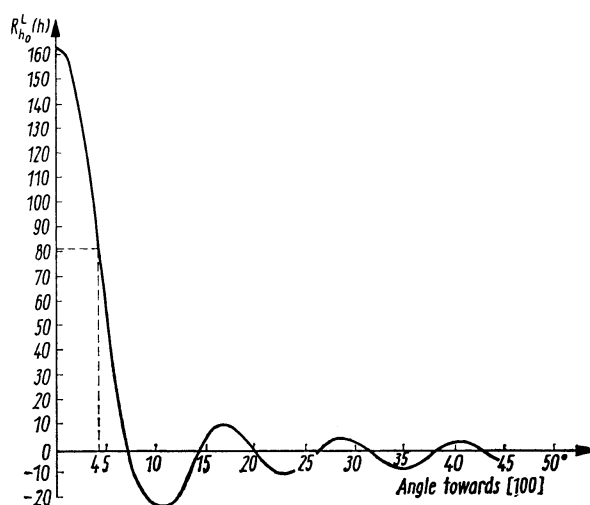


Figure 7.10 [100]—[110] section of the function represented in Figure 7.8

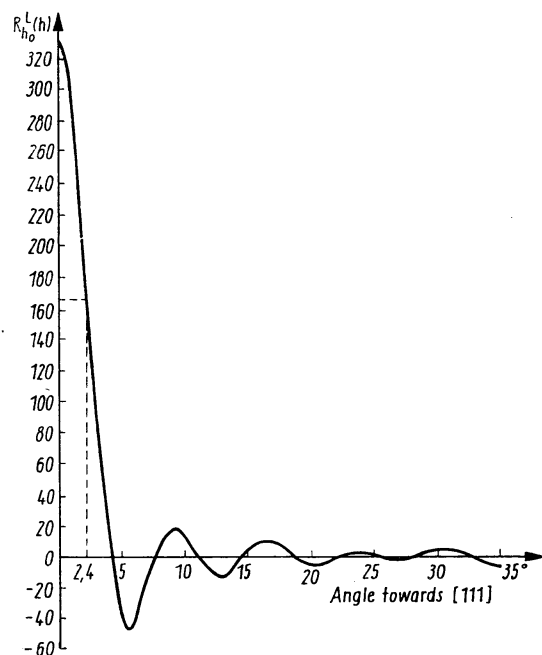


Figure 7.11 [111]—[100] section of the function $R_{h_0}^L(h)$ for $h_0 = [111]$, $L = 50$

One sees that now only a very small truncation error occurs. Beyond the neighbourhood of the ideal orientation [111] the variation of the function about the value zero now amounts to only about 2.5% of the maximum value.

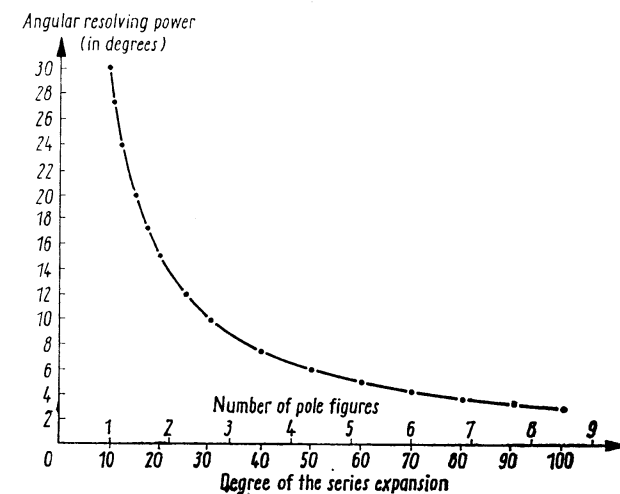


Figure 7.12 Angular resolving power depending on the degree L of the series expansion and number of pole figures used for cubic symmetry

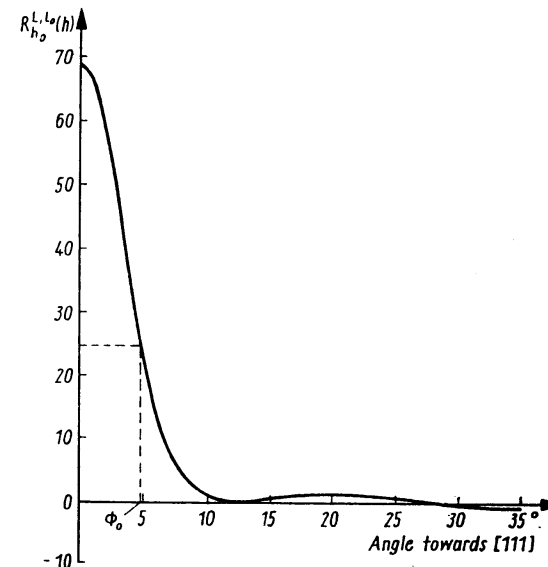


Figure 7.13 [111]—[110] section of the function $R_{h_0}^{L, l_0}(h)$ for $h_0 = [111]$, $L = 50$, $l_0 = 23$

8. Texture Transformation

New crystals can be formed from existing crystals by various processes such as phase transformation or recrystallization. The phase transformation frequently occurs with a completely specified orientation relation, which we can specify by a rotation Δg . One must assume from symmetry conditions that all rotations which are equivalent under the crystal symmetry of the vanishing crystals also must occur with equal statistical frequency. We shall call them Δg_i . The resulting crystals can have the same or a different symmetry. In any case we can add all possible symmetry rotations of the new crystals to each of the rotations Δg_i and thus obtain symmetrically equivalent rotations Δg_{ij} . Finally, we assume not only a rotation Δg and its symmetric equivalents Δg_{ij} , but also a completely continuous distribution of rotations, which can occur with the relative frequency $W(\Delta g)$, the orientation transformation function. If the crystal symmetry of the vanishing crystals is symbolized by (\cdot) and that of the resulting new crystals by $(:)$, the function

$W(\Delta g)$ must thus possess both these symmetries, $W(\Delta g)$. If a texture exists with the distribution $f_1(g')$ and each crystal orientation transforms according to the orientation relation described by $W(\Delta g)$, one thus obtains a transformed texture $f_2(g)$, which is related to the initial texture according to the relation

$$f_2(g) = \int f_1(g') W(\Delta g) d\Delta g \quad (8.1)$$

The orientation g is now given by

$$g = \Delta g \cdot g'$$

Equation (8.1) may thus be written

$$f_2(g) = \int f_1(\Delta g^{-1} \cdot g) W(\Delta g) d\Delta g \quad (8.2)$$

We expand the three distribution functions in series

$$f_1(g') = \sum_{l=0}^{\infty} \sum_{\mu=1}^{M(l)} \sum_{\nu=1}^{N(l)} C_l^{\mu\nu}(1) \dot{T}_l^{\mu\nu}(g') \quad (8.3)$$

$$f_2(g) = \sum_{l'=0}^{\infty} \sum_{\mu'=1}^{M'(l')} \sum_{\nu'=1}^{N(l')} C_l^{\mu'\nu'}(2) \dot{T}_l^{\mu'\nu'}(g) \quad (8.4)$$

$$W(\Delta g) = \sum_{l''=0}^{\infty} \sum_{\mu''=1}^{M''(l'')} \sum_{\nu''=1}^{N(l'')} w_l^{\mu''\nu''} \dot{T}_l^{\mu''\nu''}(\Delta g) \quad (8.5)$$

where (\cdot) symbolizes the sample symmetry. Introducing the series expansions (8.3)–(8.5) in equation (8.2), we thus obtain

$$f_2(g) = \sum_l^{\infty} \sum_{\mu}^M \sum_{\nu}^N \sum_{l''}^{\infty} \sum_{\mu''}^{M'} \sum_{\nu''}^{N'} C_l^{\mu\nu}(1) w_l^{\mu''\nu''} \int \dot{T}_l^{\mu\nu}(\Delta g^{-1} \cdot g) \dot{T}_{l''}^{\mu''\nu''}(\Delta g) d\Delta g \quad (8.6)$$

With the addition theorem equation (14.138) one obtains

$$\dot{T}_l^{\mu\nu}(\Delta g^{-1} \cdot g) = \sum_s \dot{T}_l^{\mu s}(\Delta g^{-1}) \dot{T}_l^{s\nu}(g) = \sum_s \dot{T}_l^{s\mu}(\Delta g) \dot{T}_l^{s\nu}(g) \quad (8.7)$$

For equation (8.6) it follows therefrom that

$$f_2(g) = \sum_l^{\infty} \sum_{\mu}^M \sum_{\nu}^N \sum_{l''}^{\infty} \sum_{\mu''}^{M'} \sum_{\nu''}^{N'} C_l^{\mu\nu}(1) w_l^{\mu''\nu''} \dot{T}_l^{s\nu}(g) \int \dot{T}_l^{s\mu}(\Delta g) \dot{T}_{l''}^{\mu''\nu''}(\Delta g) d\Delta g \quad (8.8)$$

This integral is then only different from zero when

$$l = l'', \nu'' = \mu, s = \mu'' \quad (8.9)$$

It thus follows that

$$f_2(g) = \sum_l^{\infty} \sum_{\mu}^M \sum_{\nu}^N \sum_{\mu''}^{M'} C_l^{\mu\nu}(1) w_l^{\mu''\mu} \dot{T}_l^{\mu''\nu}(g) \frac{1}{2l+1} \quad (8.10)$$

If one compares equations (8.10) and (8.4), for the coefficients of the new resulting texture one thus obtains (see equation 10.9 in reference I)

$$C_l^{\mu\nu}(2) = \frac{1}{2l+1} \sum_{\lambda=1}^{M(l)} w_l^{\mu\lambda} C_l^{\lambda\nu}(1) \quad \begin{cases} 1 \leq \mu \leq M' \text{ crystal sym. (2)} \\ 1 \leq \nu \leq N \text{ sample sym.} \\ 1 \leq \lambda \leq M \text{ crystal sym. (1)} \end{cases} \quad (8.11)$$

Similar results have recently been obtained also by SARGENT²⁵². One can thus calculate the coefficients of the resulting new texture according to equation (8.11), if one knows the initial texture and the distribution of the orientation relations:

$$(f_1(g), W(\Delta g)) \rightarrow f_2(g) \quad (8.12)$$

However, one will frequently also be interested in the inverse relationship — i.e. one desires to calculate the initial texture, if one has measured the final texture and knows the orientation relations

$$(f_2(g), W(\Delta g)) \rightarrow f_1(g) \quad (8.13)$$

For this purpose equation (8.11) is to be solved for the $C_l^{\mu\nu}(1)$. Finally, it may be that one has measured both textures and wants to calculate the orientation relations therefrom:

$$(f_1(g), f_2(g)) \rightarrow W(\Delta g) \quad (8.14)$$

Equation (8.11) is then to be solved for the $w_l^{\mu\lambda}$. The solution depends on the relative sizes of the matrices w and $C(2)$. If we assume that the system of equations

(8.11) can in principle be solved unequivocally if the number of equations is equal to or greater than the number of unknowns, then the condition of solubility represented in Figure 8.1 is dependent on the three symmetries of interest — the sample symmetry, the crystal symmetry (1) and the crystal symmetry (2). If a crystal of lower symmetry transforms into one of higher symmetry, the initial texture cannot be unequivocally deduced from the texture resulting from the transformation. Similarly, if a crystal with a symmetry lower than the sample symmetry transforms, one cannot unequivocally deduce the transformation rule from two texture measurements.

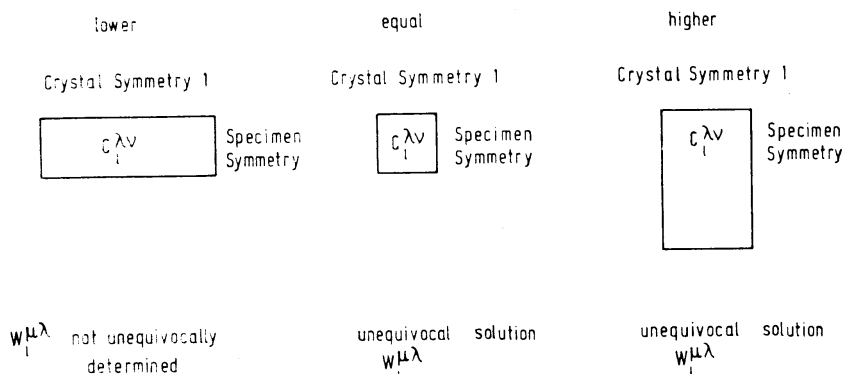


Figure 8.1 Solubility of the equation system (8.11) for various symmetry combinations

We consider the special case where there exists a specific orientation relation which is defined by a specific rotation Δg and its symmetric equivalents Δg_{ij} . The distribution function (8.5) then has the character of a δ -function, and from equation (4.19) we obtain for the coefficients $w_t^{\mu\lambda}$

$$w_t^{\mu\lambda} = (2l + 1) T_t^{*\mu\lambda}(\Delta g) \quad (8.15)$$

The relation between the coefficients of equation (8.11) will thus be

$$C_l^{\mu\nu}(2) = \sum_{i=1}^{M(l)} T_t^{*\mu\lambda}(\Delta g) \cdot C_l^{\lambda\nu}(1) \quad (8.16)$$

where Δg stands for one of the symmetrically equivalent rotations, since the functions $T_t^{*\mu\lambda}(\Delta g)$ satisfy the two crystal symmetries (1) and (2). Some important orientation relations for the transformation of f.c.c. crystals into b.c.c. crystals are

$[111]_{\text{f.c.c.}} \parallel [110]_{\text{b.c.c.}}, [211]_{\text{f.c.c.}} \parallel [110]_{\text{b.c.c.}}$ (NISHIYAMA—WASSERMANN)

$[111]_{\text{f.c.c.}} \parallel [110]_{\text{b.c.c.}}, [110]_{\text{f.c.c.}} \parallel [111]_{\text{b.c.c.}}$ (KURDJUMOV—SACHS)

$[100]_{\text{f.c.c.}} \parallel [100]_{\text{b.c.c.}}, [110]_{\text{f.c.c.}} \parallel [100]_{\text{b.c.c.}}$ (BAIN)

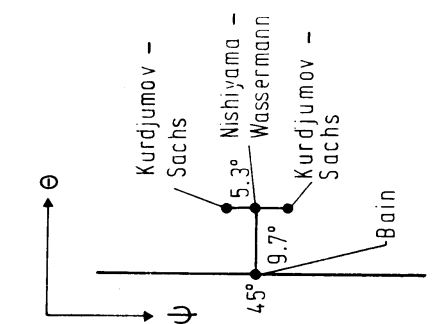


Figure 8.2 Illustration of the orientation relations according to BAIN, KURDJUMOV and SACHS and NISHIYAMA and WASSERMANN

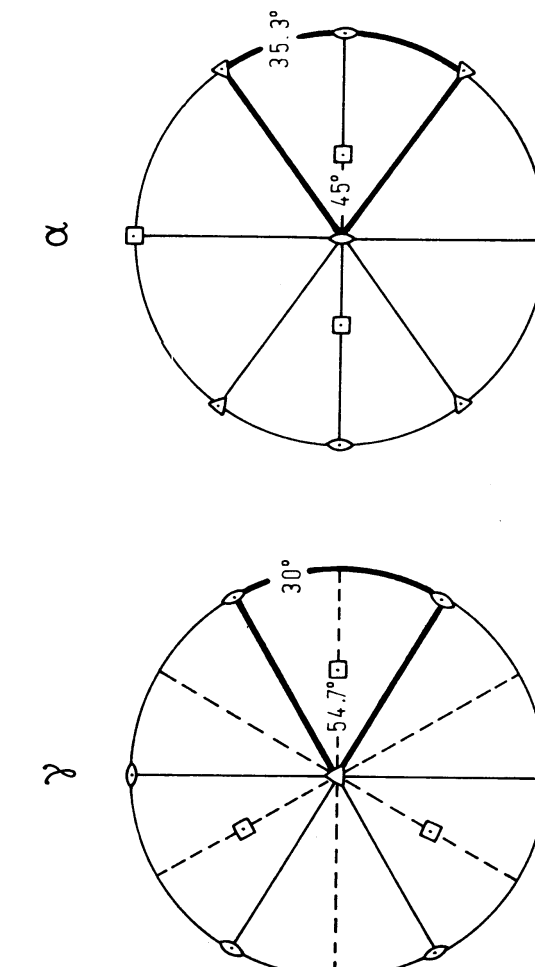


Table 8.1 EULER ANGLES OF THE ORIENTATION RELATIONS ACCORDING TO KURDJUMOV AND SACHS, NISHIYAMA AND WASSERMANN, AND BAIN

Orientation relation	EULER angles						Rotation
	First Definition		Second Definition		Axis [hkl]	Angle ω	
	φ_1	Φ	φ_2	Ψ	Θ	Φ	
BAIN (001) (001) [110] [100]	45°	0°	0°	45°	0°	0°	[001] 45°
KURDJUMOV— SACHS (111) (110) [110] [111]	84.23°	48.19°	84.23°	5.77°	48.19°	84.23°	[112] 90°
NISHIYAMA— WASSERMANN (111) (110) [211] [011]	80.26°	48.19°	45°	9.74°	48.19°	45°	[2.1 4.1 1.4] 95.26° ~[362]

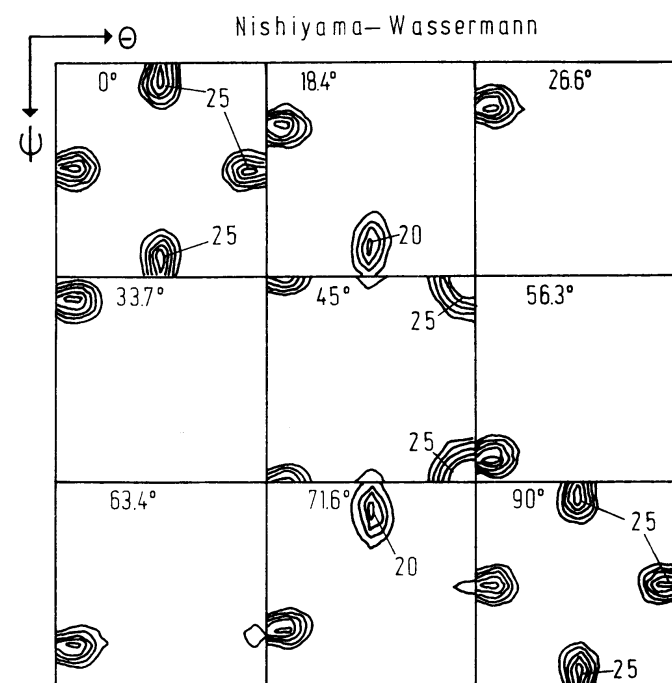


Figure 8.3 Orientation transformation function for the orientation relation according to NISHIYAMA and WASSERMANN in the $l = 20$ approximation according to KALLEND et al.¹⁷⁷

Although they appear very different in the representation by MILLER indices, they describe closely grouped rotations. This is illustrated in *Figure 8.2*. Their EULER angles are indicated in *Table 8.1*. In addition to these orientation relations, there occur in the theories of recrystallization rotations about the three symmetry axes of the cubic lattice — i.e. α -[111], α -[110], α -[100]. However, these are only some examples of a great number of orientation relations, which, e.g., appear in the martensitic transformation or also in epitaxial growth. For the above-mentioned orientation relations between two cubic lattices, the transformation coefficients in equation (8.15) are doubly cubic generalized spherical harmonics. Their values are given in Section 15.5.2. They were given by POSPIECH, JURA and MACIOSOWSKI²³⁹ for the KURDJUMOV-SACHS relation. *Figure 8.3* shows the function $W(\Delta g)$ for the KURDJUMOV-SACHS and *Figure 8.4* that for the NISHIYAMA-WASSERMANN relation in the approximation $l = 20$ ¹⁷⁷. One sees that these two orientation relations, which, according to *Figure 8.2*, only differ from each other by 5.3° , are practically indistinguishable in this approximation.

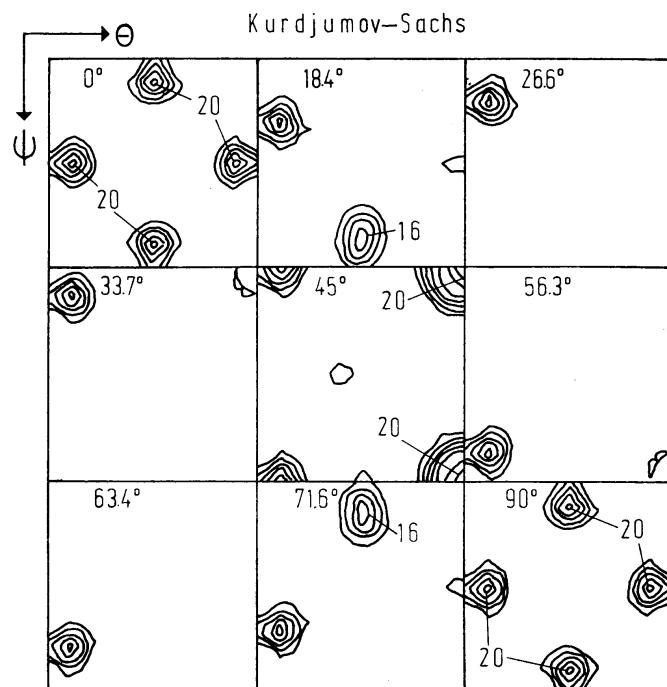


Figure 8.4 Orientation transformation function for the orientation relation according to KURDJUMOV and SACHS in the $l = 20$ approximation¹⁷⁷

9. A System of Programs for the Texture Analysis of Sheets of Cubic Materials

The practical application of mathematical methods described in the previous chapters requires a calculation expenditure which can only be accomplished with a computer⁵⁵. It is therefore necessary to have computer programs which carry out the necessary calculations. In detail, however, the kind of calculations carried out depends on very many influencing factors, so that it does not appear possible to prepare a single universally applicable system of programs. We therefore confine ourselves here to a system of programs for a standard case, namely the calculation of the orientation distribution function from complete pole figures, which are, in general, composed from a reflection and a transmission region and indeed for the case of cubic crystal symmetry and orthorhombic sample symmetry (sheet symmetry). The general structure of such a system of programs is represented in *Figure 9.1*. The same structure is naturally also valid for other symmetry combin-

ations, thus for other crystal and sample symmetries. The central quantities of the texture analysis are the coefficients $C_l^{\mu\nu}$. Not only the orientation distribution function $f(g)$, the pole figures $P(\Phi\gamma)$ and the inverse pole figures $R(\Phi\beta)$, but also average physical properties can be calculated from them. If one applies other experimental methods of texture determination than assumed here, e.g. incomplete pole figures¹⁷⁰ or individual orientation measurements⁷¹, that portion of the system of programs which applies to the determination of the coefficients $C_l^{\mu\nu}$ differs; from there on, however, the calculation remains the same, so that the scheme in *Figure 9.1* also has wider application.

The system of programs described in the following¹⁷¹ is written in FORTRAN 1900. It consists of a series of subroutines, which accomplish the various calculation steps (corresponding to the rectangular boxes in *Figure 9.1*) as well as organizing programs, which carry out data input and output as well as data transfer between subroutines. In each case there is a supervisory program (mainline program) which controls the complete path of the system of programs. In the individual subroutines certain mathematical constants are needed (coefficients, function values) which must be obtained from a permanent 'library' on magnetic tape or magnetic disc. An additional program²⁹² serves for creation of the library. Listings of these two programs are given in Appendix 2. Programs for low symmetries (crystal as well as sample symmetry) have been published by DURAND¹²³ and SPANGENBERG²⁶³.

9.1. The Subroutines

COREC

COREC calculates the complete unnormalized pole figure from measurements of the transmission and reflection regions with the aid of given correction factors. For blending the two measurements a matching factor $NC(h_i)$ will thereby be calculated from the overlapping region according to the method of least squared errors. The values of the reflection region (variant R) or of the transmission region (variant T) will be multiplied by this factor. It will be assumed that the background correction has previously been carried out. The measured values correspond to equidistant points of the pole figure (*Figure 9.2*), beginning with $\Phi = 0$ (normal direction) in steps of $\Delta\Phi$ up to the maximum Φ -value of the reflection region Φ_{GR} . For each Φ -value the γ -values will be varied from 0° in steps of $\Delta\gamma$ up to 90° . The transmission region then follows in the same way from Φ_{GT} to 90° . The values of Φ_{GR} , Φ_{GT} , $\Delta\Phi$, $\Delta\gamma$ are optional. The latter two must, however, be so chosen that 90° is integrally divisible by them, and also they must be $\geq 5^\circ$. If the storage capacity of the computer is large enough, this latter condition can easily be omitted. The subroutine COREC reads and prints the parameters and experimental values of the pole figure. It prints the correction factors and the values of the corrected complete (though unnormalized) pole figures. The latter are then available for subsequent calculations by means of the COMMON field. The subroutine

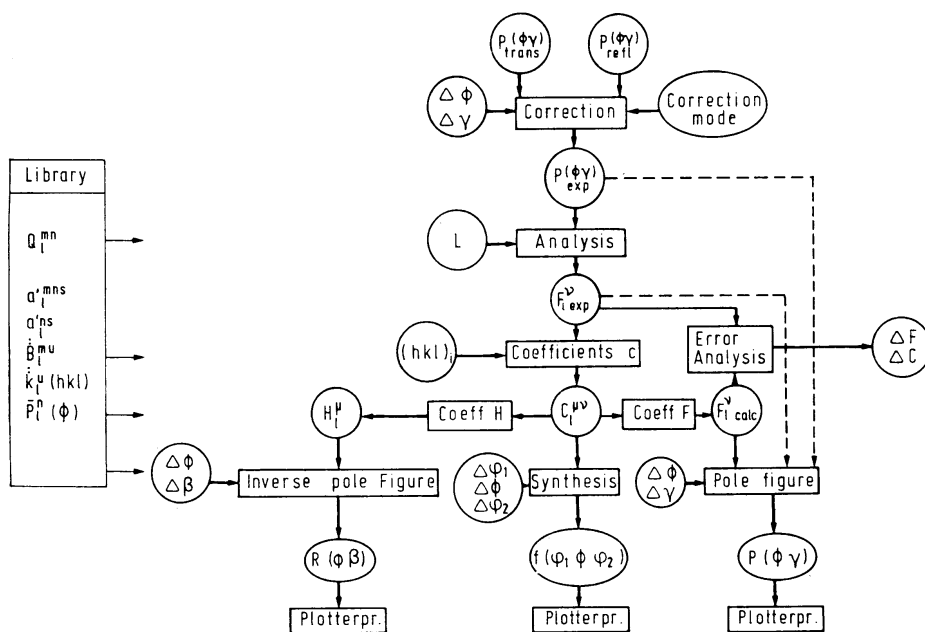


Figure 9.1 General structure of the program system for texture analysis

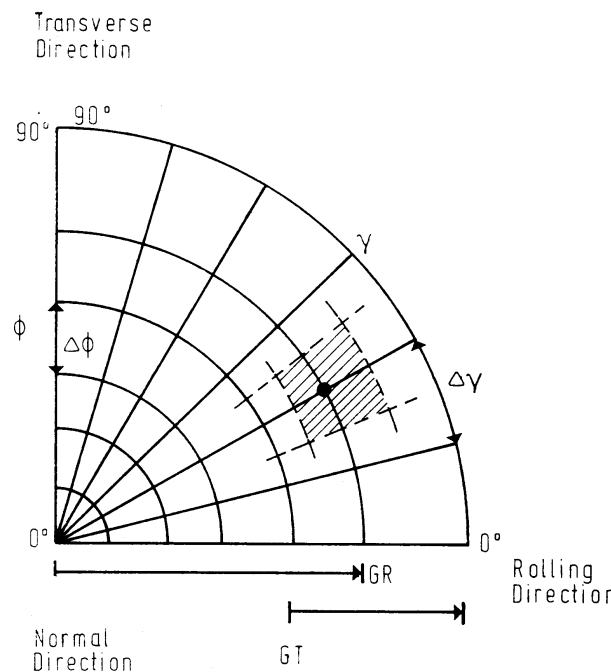


Figure 9.2 Division of the pole figure into equidistant points of interval $\Delta\Phi$ and $\gamma\Delta$ in the transmission and reflection regions

COREC is strongly dependent on the method of measurement. Thus, for example, measured values in the region $0 \leq \gamma \leq 180^\circ$ or $0 \leq \gamma \leq 360^\circ$ will frequently be used, from which one must form average values (since the sheet symmetry assumed here only permits independent measured values in the region $0 \leq \gamma \leq 90^\circ$). The correction for background can also be undertaken in different ways. In another experimental method the pole density is not measured at fixed angular positions $\Phi_i\gamma_i$ but is integrated over an angular range $\Delta\gamma$ during a continuous movement through γ . The density value obtained at the position γ_i must thus be associated with the point $(\gamma_i + \gamma_{i-1})/2$. The measurements will also frequently not be on concentric circles, but will be made with the help of a spiral movement. In many cases a complete pole figure will also be composed from back-reflection measurements on three mutually perpendicular surfaces. All these cases must be considered by other variants of the subroutine COREC. However, it seems appropriate to define the output values corresponding to an equidistant net in Φ and γ , so that the peculiarity of the measuring method plays no further role in all subsequent programs. (Further details relating to the input and output of the programs may be obtained from the program listing or a detailed description by POSPIECH *et al.*¹⁷¹.)

TWODIM

This subroutine calculates the normalization factor, the normalized pole figure and the coefficients F_l^v of the series expansion from the complete corrected pole figure. The degree L of the series expansion will thereby be given as a parameter. It can be a maximum of 34. The values of the pole figure are taken from the COMMON field of the program COREC, as are the values of $\Delta\Phi$ and $\Delta\gamma$.

COEF

This subroutine calculates the coefficients $C_l^{\mu\nu}$ of the three-dimensional orientation distribution from the F_l^v of several pole figures, as well as the recalculated F_l^v for the same pole figures. The error analysis is further carried out from the difference of the two kinds of quantities. The $\Delta C_l^{\mu\nu}$, the ΔF_l^v of the individual pole figures and the average values $|\overline{\Delta C_l^{\mu\nu}}|$, $|\overline{\Delta F_l^v}|$ are calculated. Moreover, the texture index J is calculated. The calculated values are printed. The coefficients $C_l^{\mu\nu}$, being the central quantities for all subsequent calculations, are also given on punched tape, cards, magnetic tape or magnetic disc, so that they are available for further applications (together with a heading which contains data on the sample characteristics).

POLO

This subroutine calculates values of the pole figures from the coefficients F_l^v , which are obtained from the subroutine COEF, and thus for those pole figures which also serve as input data (for calculation of other pole figures, see subroutine POLV). $\Delta\Phi = \Delta\gamma = 5^\circ$ will be assumed as increments. The degree of the series expansion is the same as in the two preceding subroutines.

POLV

This program calculates the F_l^v from the $C_l^{\mu\nu}$ as well as the values of the pole figures for arbitrary indices, which were not used as input data. The degree of series expansion is the same as in the previous subroutines. The increment is taken as 5° .

UNKC

This subroutine calculates the three-dimensional orientation distribution function $f(\varphi_1\Phi\varphi_2)$. Two variants are possible, namely for sections $\varphi_1 = \text{const.}$ or $\varphi_2 = \text{const.}$ The increment for all three variables is taken as 5° . Sections for $\varphi_{\min.} \leq \varphi_1(\varphi_2) \leq \varphi_{\max.}$ can be calculated. The function $f(\varphi_1\Phi\varphi_2)$ is normalized in multiples of the random distribution.

INVA

This subroutine calculates the coefficients H_l^v and the values of the inverse pole figures for the three principal directions — rolling direction, RD; transverse direction, TD; normal direction, ND — individually or collectively, or optionally

for an arbitrary sample direction which is specified by the angles Φ_{hkl}, γ_{hkl} in degrees. The calculation takes place in the angular region $0 \leq \Phi \leq 60^\circ$, $0 \leq \beta \leq 45^\circ$. The increment values are $\Delta\Phi = \Delta\beta = 2.5^\circ$. The degree of the series expansion is the same as in the previous subroutines. However, it is also possible to choose another region for the angle Φ , so that $45 \leq \Phi \leq 90$. This region is more convenient for a subsequent display subroutine.

SETS

This program (as well as those following) is an organizing program. It determines the input and output devices which are to be used for the various input and output data. It is assumed that (outside this program) the peripheral devices are designated by control card according to the following enumeration:

- 1, Magnetic tape MT2 for storage of the title heading and the coefficients $C_l^{\mu\nu}$.
- 2, Card reader CR.
- 3, Line printer LP.
- 4, Punched tape reader TR.
- 5, Tape punch TP or card punch CP.
- 6, Magnetic tape unit MT2 for reading the title heading and the coefficients $C_l^{\mu\nu}$.
- 7, Magnetic tape unit MT1 (or disc storage) with the tabulated library data.

CAPITE

This subroutine reads and prints the title heading with data about the sample investigated, and the following data cards are required:

- I. Title card (up to 80 alphanumeric characters).
- II. Sample card. It contains in columns:
 - 1–10, the number of data blocks,
 - 11–18, data on processing,
 - 21–28, sample material,
 - 31–38, data on experimenters,
 - 41–48, measuring laboratory,
 - 51–78, data on sample.
- III. Number of pole figures I_p and degree of series expansion L .
- IV. One card for each pole figure with the data $hkl, \Delta\Phi, \Delta\gamma$.
- V. One blank card.

The given values with the explanatory text will be printed as title heading for all output data, and will precede the coefficients $C_l^{\mu\nu}$ as heading for recording or punching, so that the data can later be clearly identified and can be used further. The date of the calculation will also be given.

XDATA

This subroutine reads the coefficients $C_l^{\mu\nu}$ for the subroutines UNKC, INVE, POLV, if these are not obtained from the immediately preceding calculation.

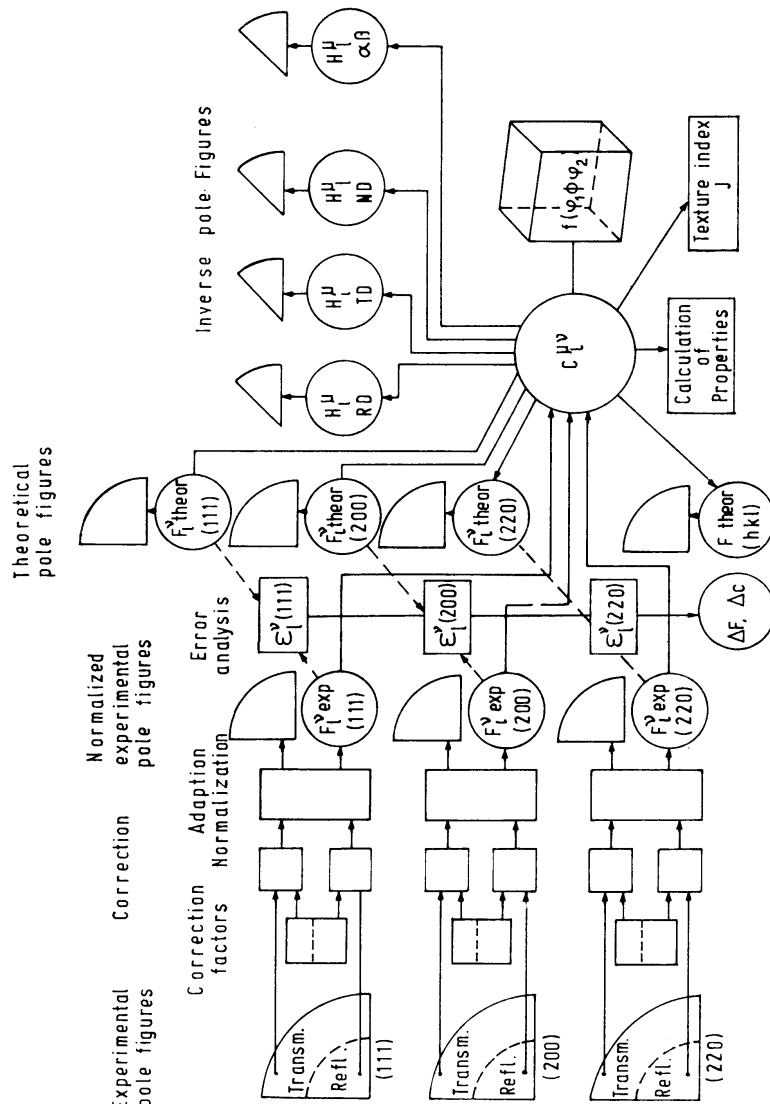


Figure 9.3 Structure of the texture analysis program system 171

9.2. The Mainline Programs

The mainline programs are relatively short supervisory programs, which simply regulate the order of the work and the coordination of the subroutines. Different variants of the program path can be realized with their help. It has been found appropriate to divide the total calculation in two parts — i.e. from the experimental data up to the coefficients $C_l^{\mu\nu}$. The error analysis will thus also be carried out. In the second calculation the orientation distribution will then be calculated from the $C_l^{\mu\nu}$. The total course of the calculation from the pole figure measurements through the coefficients $C_l^{\mu\nu}$ to the orientation distribution function, recalculated pole figures, and inverse pole figures is represented in *Figure 9.3*.

PING

This program realizes the course of the calculation scheme (*Figure 9.1*) up to the coefficients $C_l^{\mu\nu}$, including the error analysis and recalculation of the input pole figures. It uses the subroutines COREC, TWODIM, COEF, POLO, as well as the organizing programs SETS and CAPITE. The subroutines COREC and TWODIM are thus required as often as I_p , the number of pole figures. In addition, the $C_l^{\mu\nu}$ are stored on punched tape, cards or magnetic tape, according to the choice of the corresponding variables in the subroutine SETS.

POLF

This mainline program effects only the control of the subroutine POLV. It calls also the organizing programs SETS, CAPITE and XDATA. It thus calculates pole figures of arbitrary indices (hkl) from the coefficients $C_l^{\mu\nu}$. It can be automatically restarted with different sets of indices (hkl).

INVE

This program effects only the control of the subroutine INVA. It calls also the subroutines SETS, CAPITE and XDATA. This program calculates inverse pole figures from the coefficients $C_l^{\mu\nu}$.

FUNE

This program effects the control of the subroutine UNKC. It calls also the organizing programs SETS, CAPITE and XDATA. This program calculates the orientation distribution function from the coefficients $C_l^{\mu\nu}$.

9.3. The Library Program

The execution of numerical calculations of texture analysis, as was described, makes use of a large number of purely mathematically defined numerical values (coefficients, function values), which are independent of the experimental data

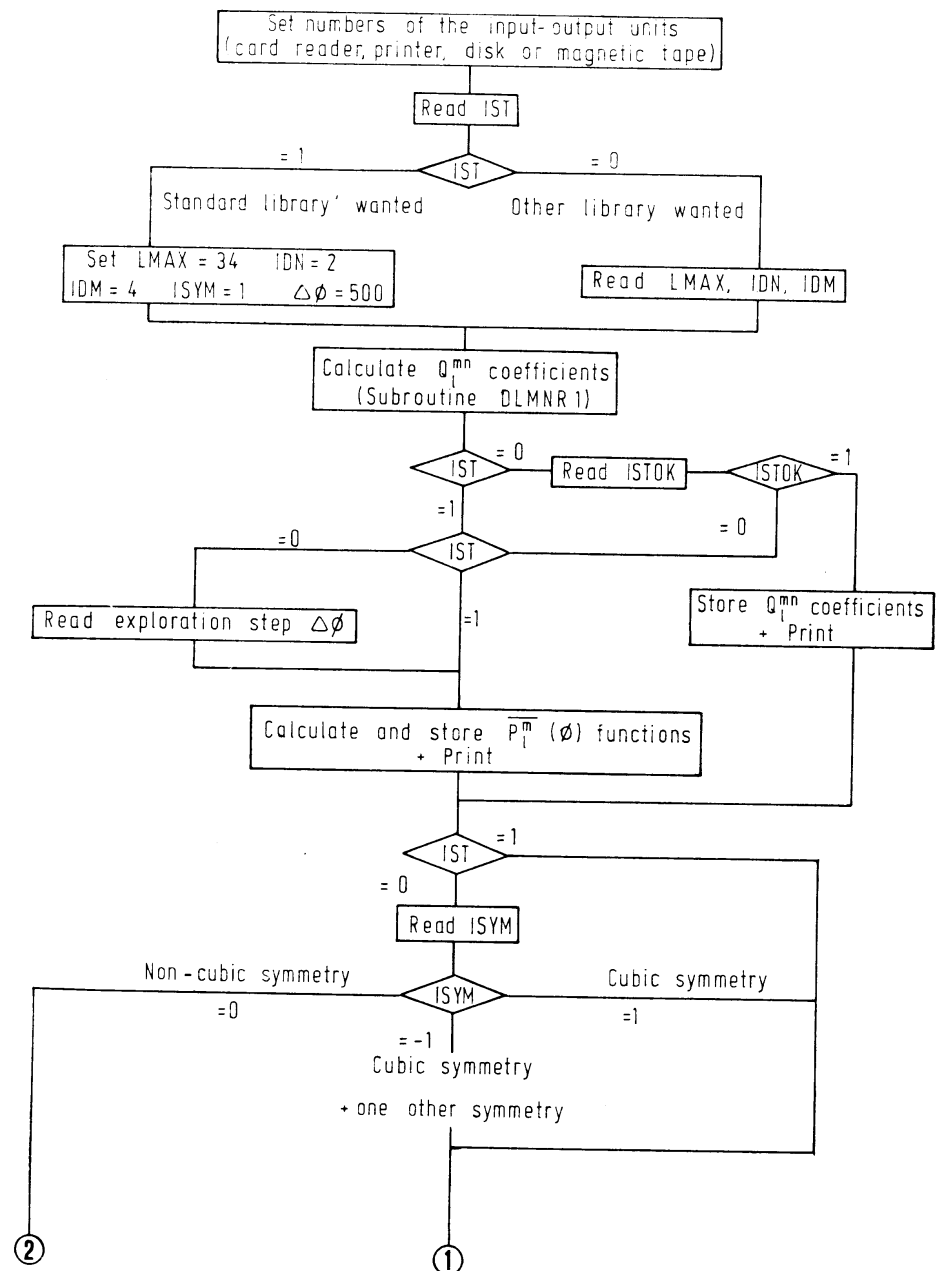


Figure 9.4 a

Figure 9.4 Flow chart of the program 'Library'²⁹²

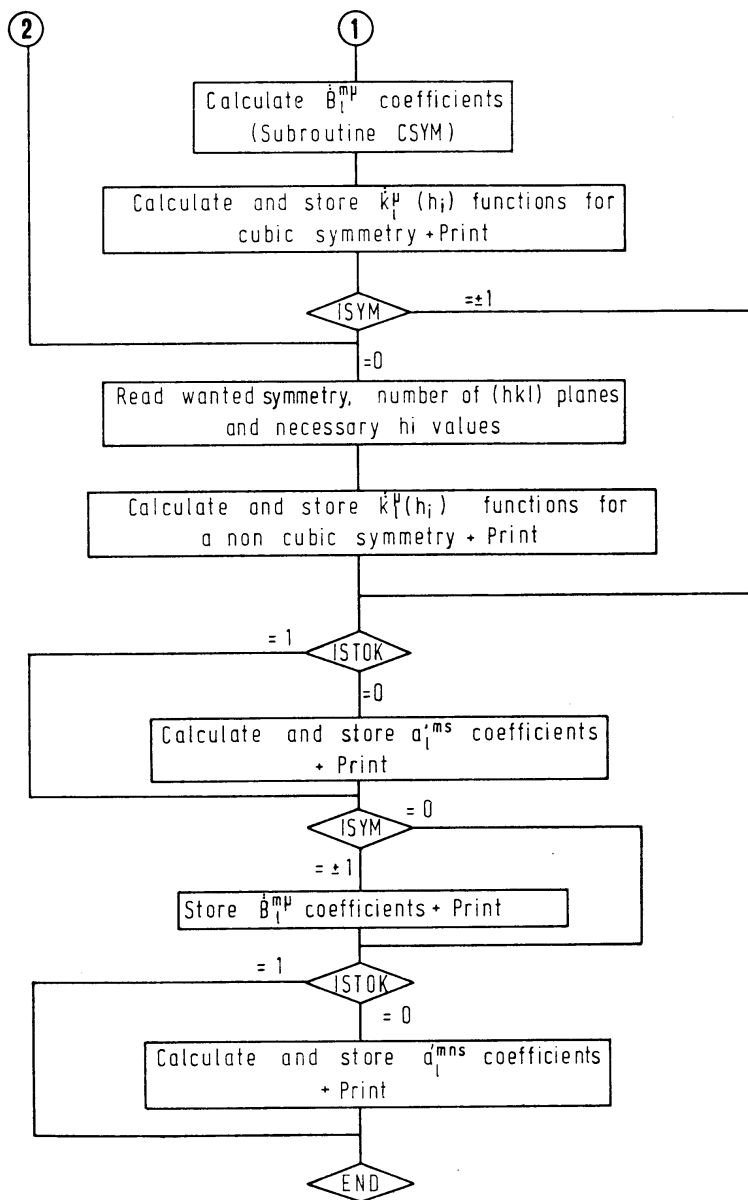


Figure 9.4b

and therefore remain the same in each calculation. It is therefore appropriate in many cases to calculate these quantities as tabular values, which are stored in the form of a 'library' in the computer, so that they can be called for each actual calculation. The generation of the library is carried out by a special calculation

program. We give in the following one such library program²⁹². With the corresponding selection of the parameters, it is compatible with the calculation program given for the case of cubic-orthorhombic symmetry. However, it is (for other choices of the parameter) in a position to produce libraries for other symmetry cases. Most of the numerical values given in the appendix were calculated with this program. The flow chart of the program is represented in Figure 9.4. There are two possibilities for the calculation:

(1) The coefficients Q_l^{mn} are calculated, the symmetry coefficients $\dot{B}_l^{m\mu}$, if cubic symmetry is required, and finally the function values of the symmetric spherical harmonics $\dot{k}_l^{\mu}(h_i)$.

(2) Function values of the associated LEGENDRE functions $\bar{P}_l^m(\Phi)$ are calculated as well as the coefficients a_l^{mns} , $a_l'^{mns}$, the function values of the symmetric spherical harmonics $\dot{k}_l^{\mu}(h_i)$ and, in the case of cubic symmetry, the coefficients $\dot{B}_l^{m\mu}$. Also, this variant is based on the calculation of the coefficients Q_l^{mn} , which, however, will not be stored in this case.

In both cases the degree of the series expansion L can be selected ($L_{\max} = 34$), as well as the increments of the indices m and n corresponding to the desired symmetry, and the increment of the angle Φ can be selected. In the case of cubic symmetry the symmetric spherical harmonics $\dot{k}_l^{\mu}(h_i)$ are calculated at the points $h_i = (100), (110), (111), (102), (112), (122), (103), (113)$. For other symmetries the orientation of the normal directions of these planes in the crystal coordinate system depends on the values of the lattice constants. In these cases the corresponding angles $\Phi_i \beta_i$ (spherical polar coordinates referred to the Z'-axis of the crystal coordinate system) are to be specified in radian measure.

(2a) In case (2) a special choice can be made by specifying only one parameter $IST = 1$. It corresponds to cubic crystal symmetry, $\Delta n = 2$, $\Delta m = 4$ — i.e. orthorhombic sample symmetry and an angular increment $\Delta\Phi = 5^\circ$. These assumptions meet the requirements of the standard calculation program described in this paragraph. The library so obtained is called the 'standard library'.

In other cases the following inputs are necessary:

- (1) Control parameter $IST = 0$.
- (2) L , Δ_n , Δ_m .
- (3) Control parameter $ISTOK = 0$ or 1 (according to whether variant 1 or 2 is desired).

(4*) $\Delta\Phi$ (in hundredths of a degree) (only for variant 2).

(5) Symmetry parameter $ISYM = -1, 0, +1$ (see flow chart), I_P = number of h_i (number of pole figures).

(6*) (in the case of non-cubic symmetry) I = order of the symmetry axes of highest symmetry; I_P = number of pole figures; $J = 1$ for monoclinic symmetry, otherwise $J = 0$.

(7*) Specification of the symmetry and indices hkl in format 15 (A4, 1X) — e.g. HEXAGONAL 10.0 11.0, etc.

(8) Values $\Phi_i \beta_i$ (in radian measure and in double precision) always 2 to a card in format 4 (D 20.13).

The inputs marked with * are only required with the corresponding choice of parameters. The calculations are carried out in double precision. The storage of the values follows in single precision. The algorithm used permits an accuracy of at least nine decimal places for $L = 34$. The accuracy obtained, therefore, depends entirely on the word length of the computer used. The error does not exceed one unit in the last decimal place. The program requires 25 K words (of 32 bits). The required storage can be reduced if one does not completely exhaust the possibilities of the program (e.g. $L < 34$). The calculation time for production of the standard library with an IBM 370/135 was 3 min. The results are stored sequentially on magnetic tape or disc in binary form without a format. Each write command generates a new record. The order of the data depends, therefore, on the choice of parameters. They must then further be recalled in the same form. (See reference 292.)

9.4. Calculation Times and Storage Requirements

A summary of the required calculation time in seconds and the storage requirements is given in *Table 9.1*. The values for the first four programs relate to the machine CONTROL DATA 6400 and a degree of series expansion of $l = 34$. Three pole figures and inverse pole figures were calculated. The values for the library program relate to the standard case (cubic crystal symmetry, orthorhombic sample symmetry, degree of series expansion $l = 34$) and to the machine IBM 370/135.

Table 9.1 CALCULATION TIME AND STORAGE REQUIREMENTS OF THE TEXTURE ANALYSIS PROGRAMS

	Execution time (s)	Peripheral time (s)	Memory space (words)
PING	11.3	125.2	24 847
INVE	5.0	16.0	26 300
POLF	4.4	27.1	20 677
FUNE	13.3	24.0	20 134
LIBRARY	180	—	25 000

9.5. Supplementary Programs

The program system described here naturally does not include all problems of texture analysis. In particular, the measurement of complete pole figures will frequently be waived. The coefficients C_l^{uv} are then calculated directly from the values of the incompletely measured pole figures. In place of the first three sub-

routines (*Figure 9.1*) others are then to be used. The correction program is different, since now an adaptation of the two regions is no longer required. The programs 'analysis' and 'coefficients C ' merge into one, since the intermediate stage of the calculation of the coefficients F disappears, and also the error analysis is different. A program for incomplete pole figures compatible with the program given here was produced by JURA and POSPIECH¹⁷⁰ and by MORRIS²¹⁷. Occasionally orientation distributions are calculated from individual orientation measurements. The coefficients C_l^{uv} are thereby adjusted according to a method of least squared errors at the measured orientations. Programs which do this were prepared at different times^{75,240}, but as yet have not been completely published. A further supplement considers calculation of the orientation distribution function in other orientation coordinates. One can then use the same calculation path as is represented in *Figure 9.1*. Only in place of the program section 'synthesis', which is realized in the subroutine FUNE, another program is to be used, which includes the coordinate transformation. One such program, which is compatible with the system given here, was developed by JURA and POSPIECH¹⁷⁰. The amount of data needed to represent an ODF in, e.g., 5° steps is very large, so that drawing contour maps of the function is a very time-consuming task. The same is already true for the drawing of pole figures and inverse pole figures by hand. Hence, the drawing of the calculated functions and often also of the experimental pole figures is carried out by means of appropriate plotter programs with the help of a computer-operated plotter. Several such programs have been developed^{22,123,151,249,287}. They allow one to draw contour mappings of ODF, inverse pole figures and normal pole figures whereby the values of the represented level lines can be chosen as necessary. Because of the length of these programs the program text will not be given here.

9.6. A Numerical Example (*Tables 9.2–9.14* appear in Appendix 1)

In the following we give a numerical example of a texture calculation with the specified program, beginning with complete pole figures, which were measured in the transmission and reflection regions. The example will serve as a check on the application of the computer programs. It therefore includes all input and output values which are required for testing the individual program sections. Numerical values for testing the library programs are contained in Chapter 15. The material used was cold-rolled silver. The calculations were carried out by JURA and POSPIECH. *Table 9.2* shows the heading of the computer output of the program. All the tables that follow, except *Tables 9.13* and *9.14*, are the original computer outputs. These tables appear in Appendix 1 at the end of the book.

Table 9.3 gives the measured pole figure values for the transmission and reflection regions. They were corrected with the appropriate factors (depending on the angle Φ). The accommodation factor NC was calculated and the reflection region was adjusted to the transmission region with it. *Table 9.4* contains the values so corrected of the complete pole figure. The normalization factor N_i was

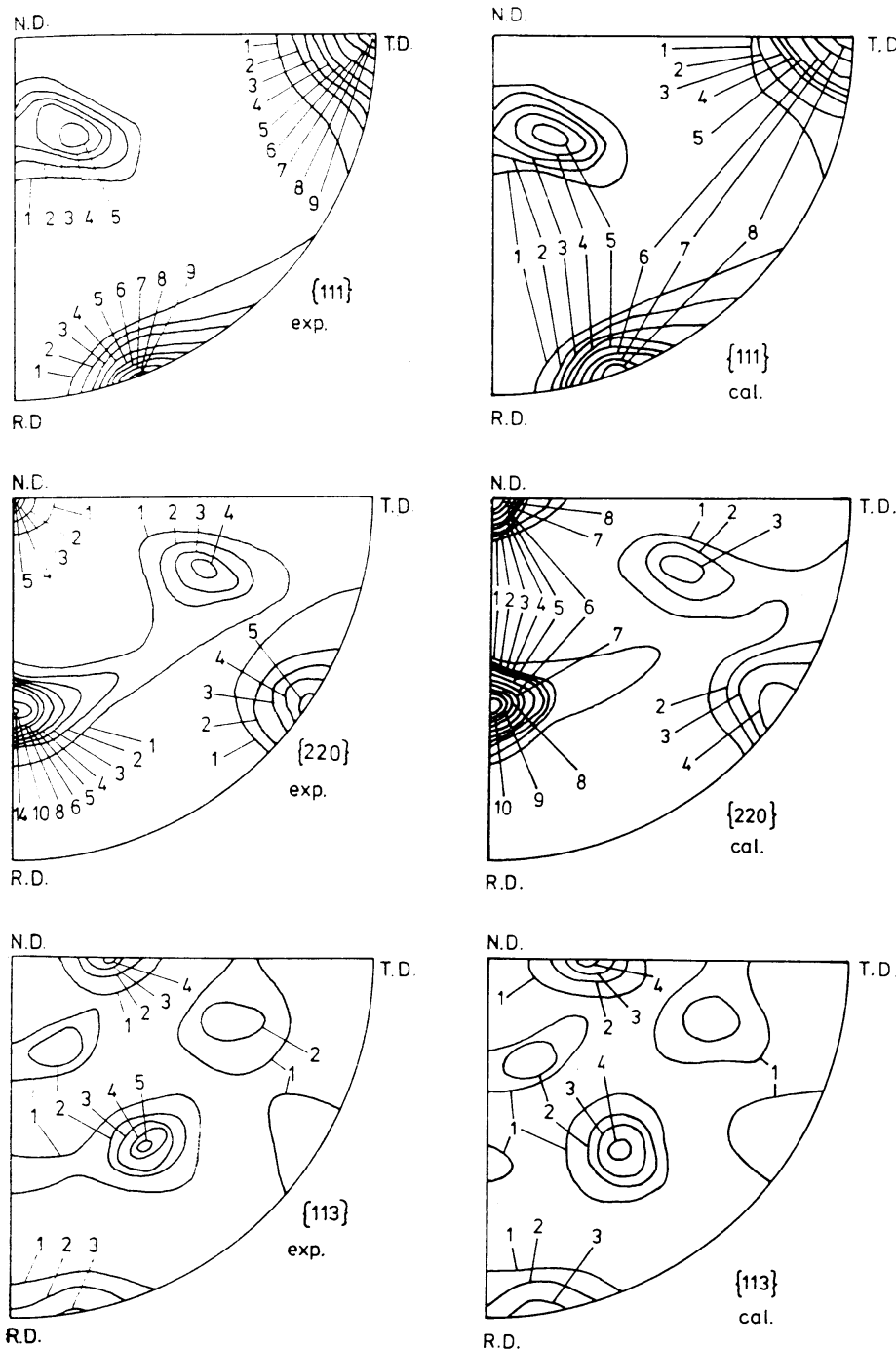


Figure 9.5 Experimental and calculated pole figures

then determined by integration over the complete pole figure (one quadrant) and the normalized pole figure, *Table 9.5*, calculated.

The normalized pole figures were then expanded in series and the coefficients $F_l^v_{\text{exp}}$ determined. They are given for the three pole figures (111), (220), (113) in *Table 9.7*. The coefficients $C_l^{\mu\nu}$ of the orientation distribution function (*Table 9.9*) were calculated from these coefficients.

New pole figure coefficients $F_l^v_{\text{cal}}$, which now are exactly compatible with one another, result from the coefficients $C_l^{\mu\nu}$ and the calculated pole figures follow from them (*Table 9.6*). The coefficients H_l^{μ} of the inverse pole figure (*Table 9.10*) also result from the coefficients $C_l^{\mu\nu}$, as well as the inverse pole figures themselves (*Table 9.11*). Finally, one obtains the three-dimensional orientation distribution itself $f(\varphi_1 \Phi \varphi_2)$ from the coefficients $C_l^{\mu\nu}$.

Since the numerical example only serves for testing the calculation programs, the table of the function $f(\varphi_1 \Phi \varphi_2)$ is not completely given. *Table 9.12* shows the four sections $\varphi_1 = 0^\circ$, $\varphi_1 = 35^\circ$, $\varphi_2 = 0^\circ$ and $\varphi_2 = 20^\circ$.

In the calculation of the coefficients $C_l^{\mu\nu}$ from the coefficients F_l^v , the error measures ΔF_l^v of the coefficients F_l^v were also calculated (*Table 9.13*). The error measures $\Delta C_l^{\mu\nu}$ of the coefficient $C_l^{\mu\nu}$ then follow from these error measures

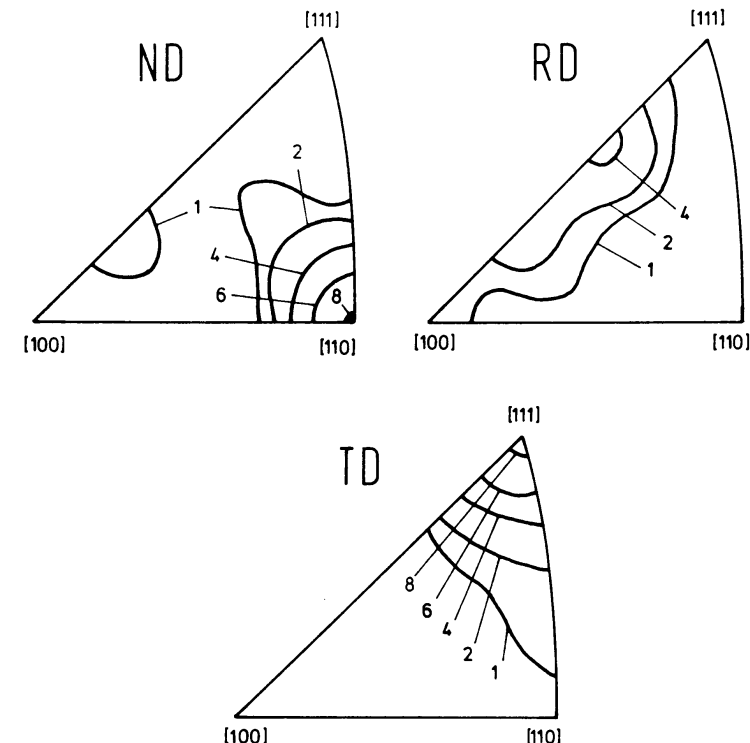
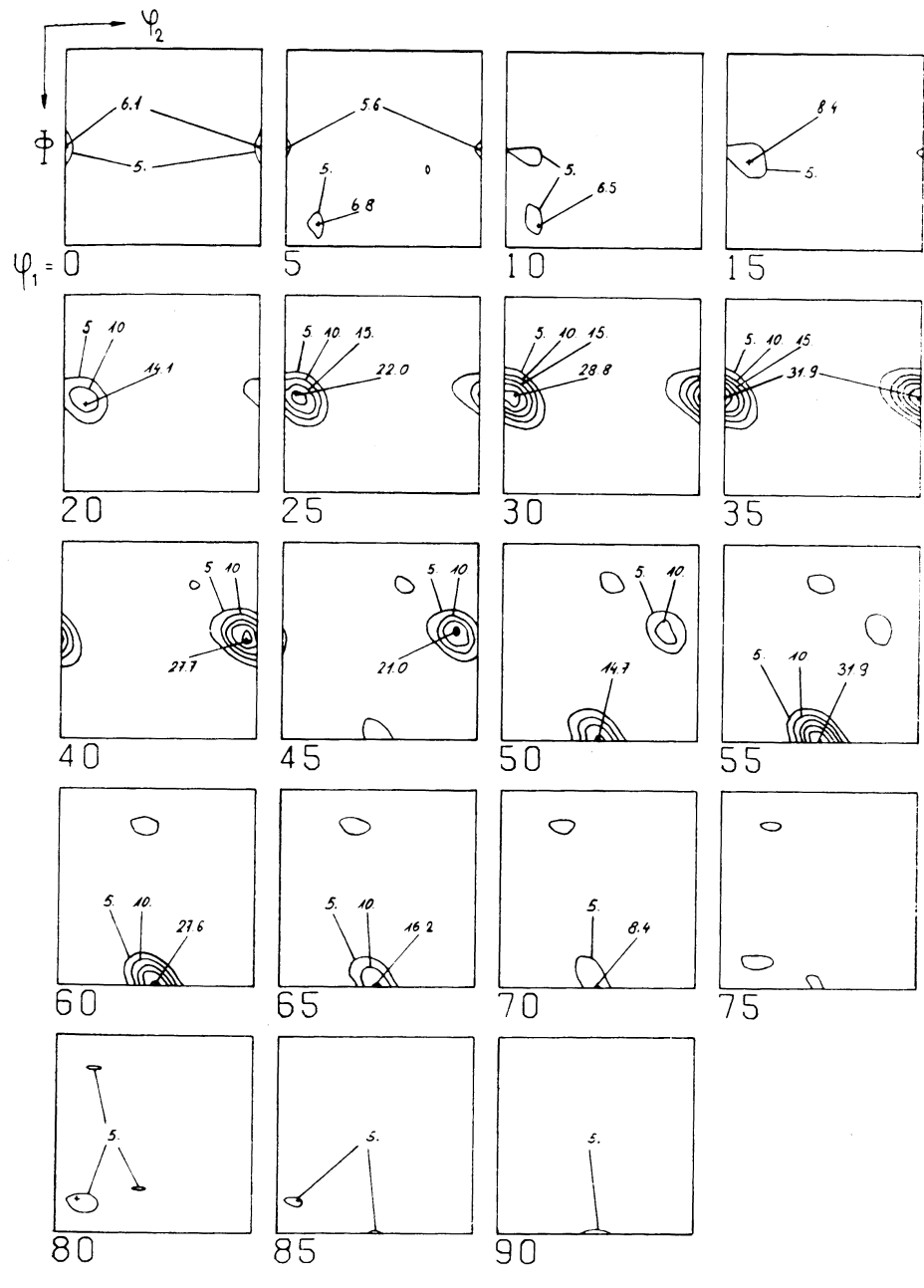


Figure 9.6 The inverse pole figures of the three principal directions



(a)

Figure 9.7a

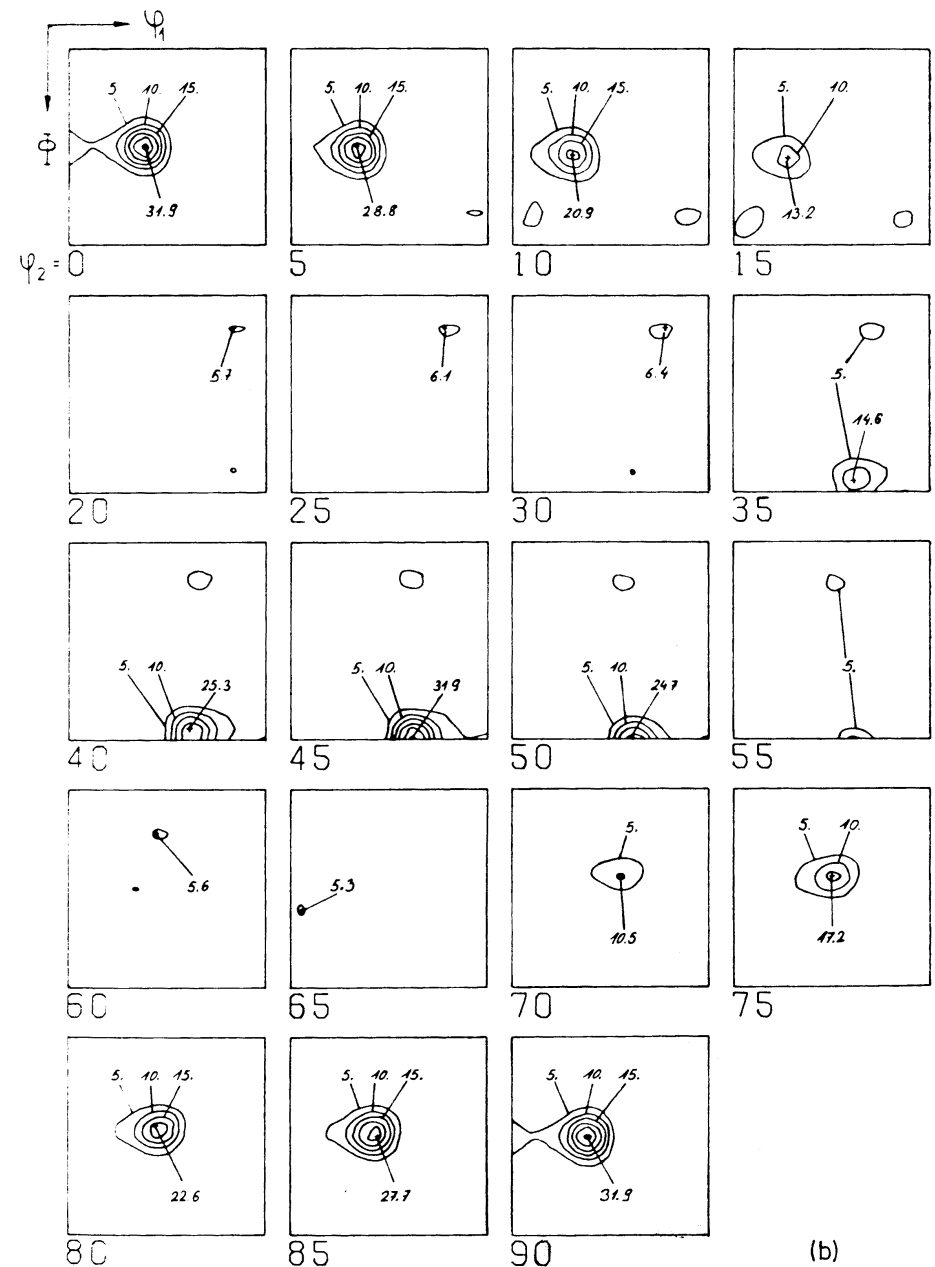
Figure 9.7 The orientation distribution function: (a) in φ_1 -sections; (b) in φ_2 -sections

Figure 9.7b

(b)

(Table 9.14). The average values ΔF_l and ΔC_l of the errors together with the average values C_l of the coefficients are given in Table 9.15. Finally, the texture index was also calculated as a measure of the texture severity. It amounts to $J = 11.526$. The experimental (normalized and corrected) pole figures according to Table 9.5 are graphically represented in Figure 9.5. They are directly comparable with the pole figures recalculated from the coefficients $C_l^{\mu\nu}$ according to Table 9.6. These are also given in Figure 9.5. The comparison of the two gives a direct measure of the quality of the measurements. The inverse pole figures of the three principal directions are reproduced in Figure 9.6. Finally, the calculated orientation distribution function, of which two sections were given in Table 9.12, is reproduced in Figure 9.7. For construction of the three-dimensional orientation space, the individual sections of Figure 9.7 were transferred to Plexiglas sheets and these then stacked one upon another, as is shown in Figure 9.8. Further analysis of the orientation distribution function then depends on the nature of the function itself. One tries, as far as possible, to completely comprehend the peculiarities of the respective distribution function by as few characteristic numbers as possible. For purely ideal orientations one will, e.g., give the EULER angles $\varphi_1 \Phi \varphi_2$ of the maximum orientation density, as well as the half-width of the spread. For tube-shaped distributions one can, as will be seen in Chapter 11, give the

skeleton line (line of maximum orientation density) transferred to the inverse pole figures and the intensity course along the skeleton line, as well as the half-width of the spread about this. One can also, if it appears reasonable, try to decompose a tube-shaped orientation distribution into a 'string' of ideal orientations. Because of the multiplicity of conceivable possibilities, it does not seem appropriate to further standardize evaluation of the orientation distribution function.

9.7. Listings of the ODF and Library Programs

See Appendix 2.

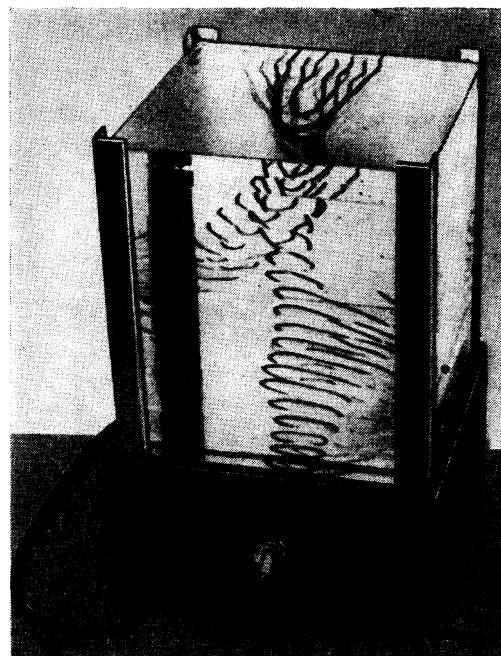


Figure 9.8 Plexiglas model showing a three-dimensional representation of an orientation distribution function

10. Estimation of the Errors

If one is to apply further the results of texture analysis calculations, in order to draw conclusions therefrom about the investigated material or the processes occurring in the material, it is necessary to be able to estimate the errors occurring. These can be caused by experimental errors, which propagate through all the calculation process to the end results. However, errors can also occur, which are caused by the mathematical process used. And, finally, one must consider further errors due to the representation of numbers by a limited number of decimal places in the computer.

One appropriately separates the experimental errors into systematic and statistical errors.

The statistical errors can further result from two principal causes. The first is the formation of the sample from individual crystallites. These errors thus concern the definition of the orientation distribution function itself. One must, moreover, consider statistically distributed inhomogeneities which result from an earlier stage of the sample preparation. Large crystallites, from the original cast structure of a material, for example, can lead to large regions with distinctive deformation texture, and, further, these can be distinctive after recrystallization. The statistical variations in the sample can therefore be larger than those corresponding to the actual grain size; they can correspond to the *largest* grain size having occurred during the previous history of the material. A second kind of statistical error is caused by the counting statistics of X-ray or neutron radiation. In the interest of as high an angular resolution capability as possible, one must work with measurements with as small angular apertures of the beam as possible. The available intensity is thus, however, reduced and the statistical error of measurement increased. If one is to reduce it, one must increase the time of measurement.

The errors caused by the mathematical process can be separated into two groups. In the series expansion process the truncation error, which is caused by the finite number of series terms, plays the largest role. It can be reduced by increasing the number of series terms. In addition, however, an error can occur which one can denote the 'indetermination' error. It results from the fact that a whole range of solution functions can be in exact agreement with the experimental data. Such an indetermination error of the orientation distribution functions results, e.g., from a finite number of pole figures and from the centrosymmetry of pole figures. Another error of this kind occurs if one works with incomplete pole

figures and chooses too small a region of measurement. These errors can even be increased by increasing the number of series terms.

Another error of this type is the integration error. It results from the fact that pole figures are being measured not as continuous functions but in certain discrete steps, and, consequently, the integration is to be replaced by a summation over finite terms.

Finally, the numerical representation in the computer is limited to a finite number of significant figures, and each calculation operation must be rounded off to this number of significant figures. If very many calculation operations are carried out one after another, these errors can accumulate: in general, however, it appears that this error in texture calculation can be neglected, by comparison with other errors.

The possible kinds of errors are listed in *Table 10.1*.

Table 10.1 ERRORS FOR THE TEXTURE ANALYSIS PROCESS

-
- 1. Experimental errors
 - 1.1. Systematic errors (e.g. absorption correction)
 - 1.2. Statistical errors
 - 1.2.1. Grain statistics
 - 1.2.2. Pulse statistics
 - 2. Mathematical errors
 - 2.1. Truncation error
 - 2.2. Ambiguity error
 - 2.3. Integration error
 - 3. Numerical errors
-

At present there is no completely developed theory for the errors of the texture analysis process. It is therefore important to be able empirically to estimate the probable size of the error present in the results. In the following we give some such error estimations.

10.1. A Reliability Criterion for Pole Figures of Materials with Cubic Symmetry

In Section 4.5.1 a reliability criterion for pole figures of materials with cubic symmetry was deduced. It depends on the fact that the coefficients of the series expansion of the pole figure of second order must theoretically be zero. Pole figures of cubic materials must thus satisfy an intrinsic condition, the fulfilment of which

one can easily check. The deviation from zero of the coefficients F_2^v for a series of pole figures taken from the literature is given in *Figure 10.1*, according to SCHLÄFER²⁵³. One sees that the combined transmission and reflection method generally yields poor results. This is probably due principally to the difficulties which occur in the measurement of the transmission region, as well as matching the two regions to each other, whereas neutron diffraction, particularly with use of a spherical sample, can yield the best results.

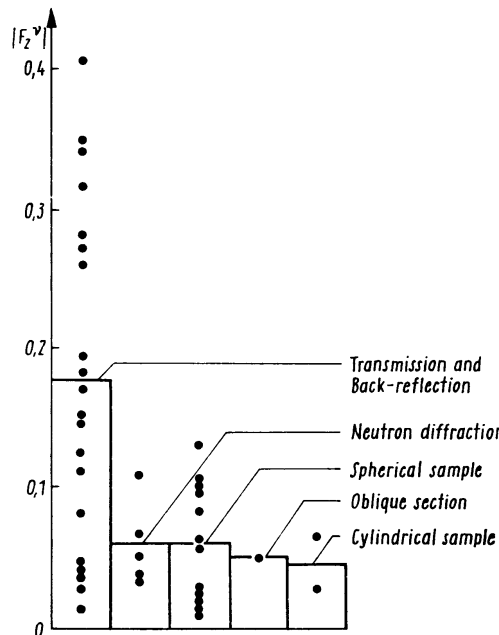


Figure 10.1 The reliability criterion for pole figures of cubic materials for 40 pole figures taken from the literature²⁵³

10.2. The Error Curve $|\overline{\Delta F_l^v}|$

Since the density distributions in the various pole figures are interpreted as ‘projections’ of the three-dimensional orientation distribution function, they are not independent of one another; they must satisfy mutual conditions, which can most easily be expressed by the coefficients $F_l^v(\mathbf{h}_i)$. The coefficients must satisfy the overdetermined equation system (4.61). In the case $M(l) = 2$ this is a system with two unknowns. The corresponding equations can thus be represented as straight lines in a plane which in the ideal error-free case will pass through one point. These straight lines for $l = 12$ for a fibre texture are represented in *Figure 10.2*.

Figure 10.2. Eight pole figures were measured, so that eight straight lines result. The eight equations thus have no exact solution, but only an optimal approximate solution. The accuracy can be estimated from the size of the ‘intersection region’.

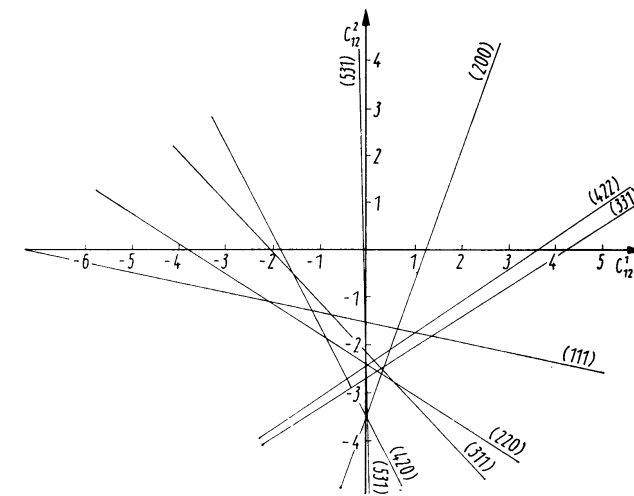


Figure 10.2 Graphic solution of the linear equation system (5.27) for $l = 12$

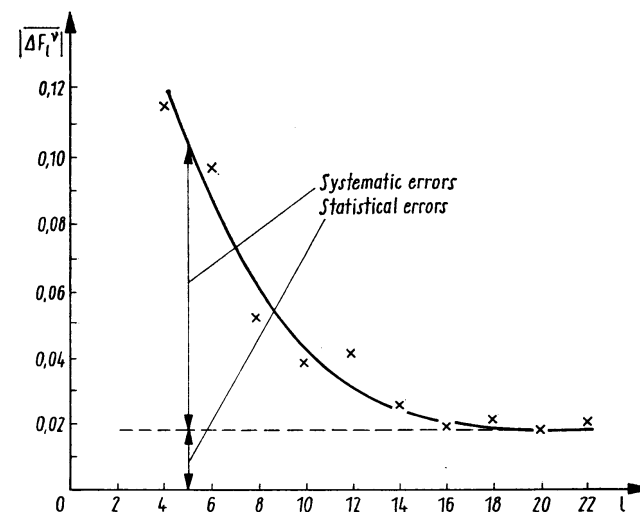


Figure 10.3 Average of the absolute values of the error $|\overline{\Delta F_l^v}|$ of the texture of a cold-rolled carbon steel

The error quantities ΔF_l^v and their average values $|\overline{\Delta F_l^v}|$ are defined from the difference between the coefficients $F_{l\text{exp}}^v$ and those of the approximate solution $F_{l\text{calc}}^v$. These quantities thus measure the mutual compatibility of the various pole figures. They are thus measures of the experimental error. The error curve for a steel texture is given in *Figure 10.3*. One sees that it approaches a constant value for high values of l . High l -values correspond to 'short-wave' components of the series expansion. These errors thus correspond to an error function rapidly varying from point to point in the pole figure. One may therefore regard them as statistical errors. The error size increases sharply for small l -values. This corresponds to an error distribution which varies slowly over the pole figure. Such errors result from, e.g., the effect of absorption or adjustment errors. We may generally attribute the increase of the error curve for small l -values to systematic errors. Truncation errors are, of course, not included in this definition; indetermination errors are likewise not considered. The error curves are, however, very well suited to estimate the experimental errors. *Figure 10.4* gives a comparison

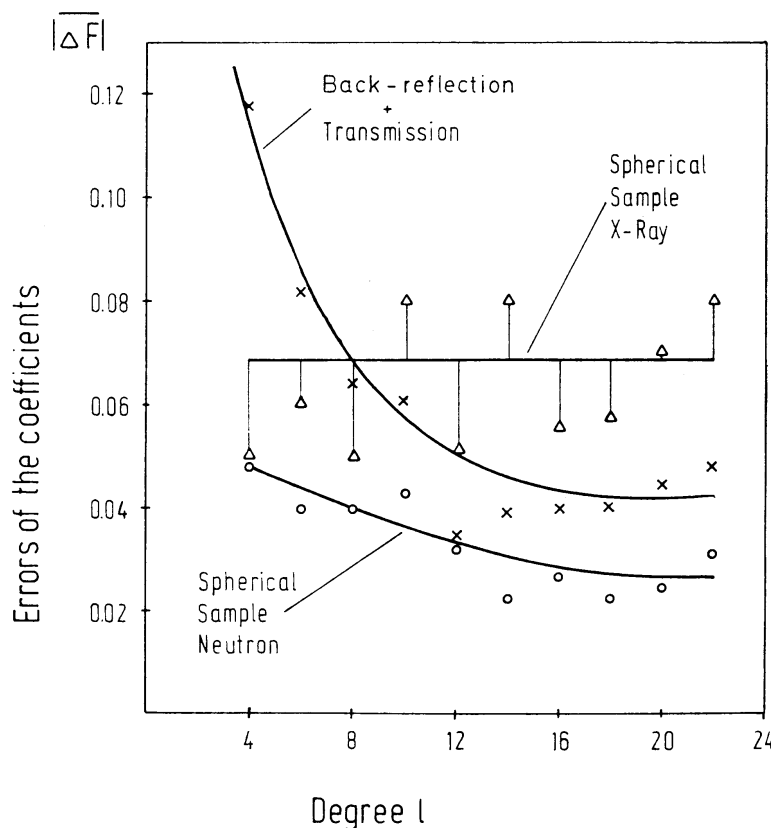


Figure 10.4 Error curves $|\overline{\Delta F_l^v}|$ for various methods

of the errors of X-ray diffraction and neutron diffraction measurements with transmission and reflection and the spherical sample methods. It is to be seen that neutron diffraction yields the best results, especially if the spherical sample method is used²⁸¹. This is to be expected because of several advantages of the neutron diffraction method mainly resulting from the lower absorption coefficient compared with X-rays¹⁷⁸. Hence, neutron diffraction has been used especially for high-precision texture determinations^{54,81–85,124,179,205,222,257,259,262,274,280,281}.

10.3. The Error Curve $|\overline{\Delta C_l^{\mu\nu}}|$

From the errors $\Delta C_l^{\mu\nu}$ of the pole figure coefficients those of the coefficients $C_l^{\mu\nu}$ can be determined according to Section 4.5 and one can obtain the average value $|\overline{\Delta C_l^{\mu\nu}}|$ for each degree l therefrom. They are compared with the average values of the coefficients themselves in *Figure 10.5*. One sees that they also approach a constant value for high l -values. For high values of l the curve of $|\overline{\Delta C_l^{\mu\nu}}|$ coincides with the corresponding curve of the absolute values of the coefficients $|C_l^{\mu\nu}|$. For these l -values, the errors of the coefficients $C_l^{\mu\nu}$ are of the same order as the coefficients themselves. The truncation error resulting from the omission of higher C -values is then only of the order of the experimental error. From these error curves one can thus estimate how far the series expansion must be extended in order

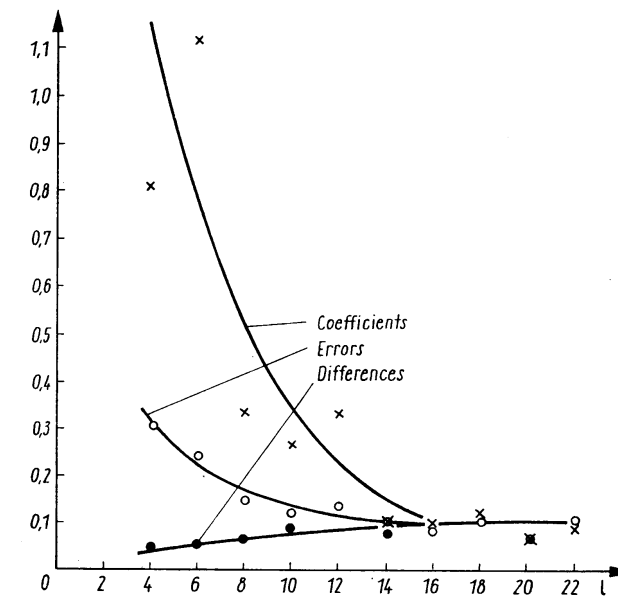


Figure 10.5 Average of the absolute values of the coefficients $|C_l^{\mu\nu}|$, as well as their errors $|\overline{\Delta C_l^{\mu\nu}}|$, of the texture of a cold-rolled carbon steel. The lower curve gives the differences between the coefficients $C_l^{\mu\nu}$ calculated from the different quadrants of the pole figures

that the truncation error not be greater than the experimental error. An additional curve is also introduced in *Figure 10.5*. In this case the pole figures were measured in all four quadrants, and the coefficients were determined from each quadrant separately. Because of the assumed orthorhombic sample symmetry (sheet symmetry), these values should coincide. The differences are thus also a measure of the accuracy of measurement. Since the absorption and adjustment errors in the four quadrants should be the same in each case, it is clear that they should not contribute to the difference curve. Accordingly, the difference curve does not show a sharp increase for small l -values.

10.4. Error Estimation According to the Harris Relation

A relation between normalized density values of pole figures and corresponding values of inverse pole figures was deduced in Section 4.3.1. The first are directly measurable, whereas the latter are calculated by means of a series expansion. The pole figures thus contain no truncation errors, in contrast to the values of the inverse pole figures. The comparison of corresponding values is thus a direct measure of the series truncation error. *Figure 10.6* shows an example. Values of the inverse pole figures for the rolling and transverse directions at the point $\langle 111 \rangle$ were compared with pole figure values of the (111) pole figure in the rolling and transverse directions⁸⁴. The series expansion amounted to $L = 22$. The measurement was carried out by neutron diffraction.

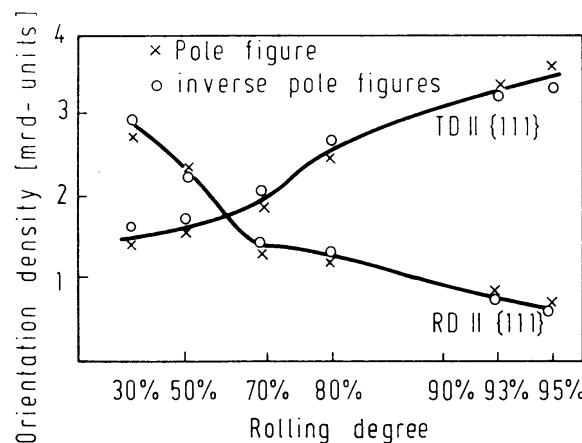


Figure 10.6 Measured values of the (111) pole figure in the rolling and transverse directions as well as values of the inverse pole figures of the rolling and transverse directions at the point $\langle 111 \rangle$ (HARRIS relation, equation 4.138)⁸⁴

10.5. Comparison of Experimental and Recalculated Pole Figures

One can carry out a similar comparison if one compares the measured pole figures with those recalculated from the coefficients $C_l^{\mu\nu}$. *Figure 10.7* shows this comparison

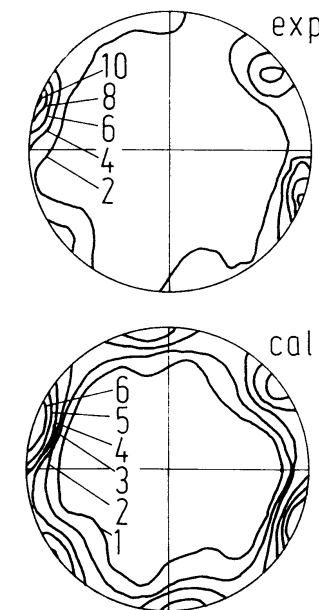


Figure 10.7 Measured ($20\bar{2}0$) pole figure and that calculated from the $C_l^{\mu\nu}$ coefficients for a natural quartz sample⁸⁶

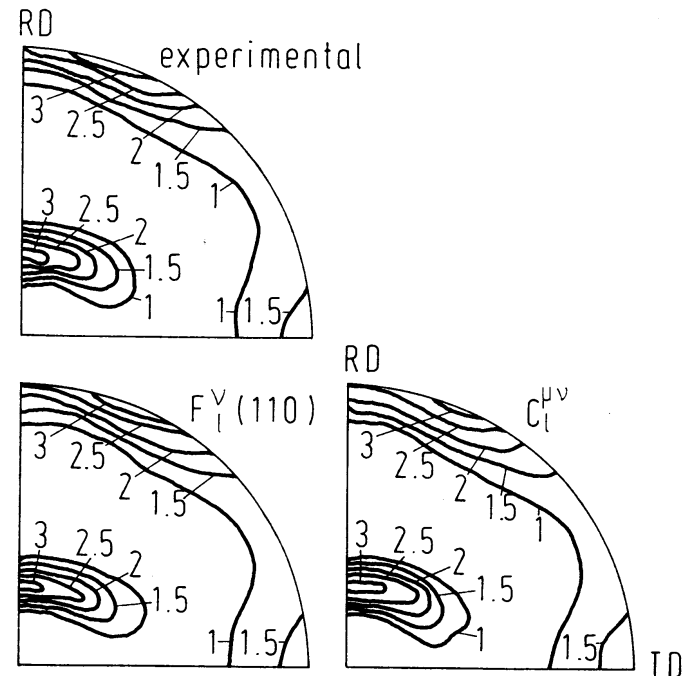


Figure 10.8 Measured (110) pole figure and those calculated from $F_l^v(110)_{\text{obs.}}$ and $C_l^{\mu\nu}$ (or $F_l^v(110)_{\text{cal.}}$) for a recrystallized steel sheet

for a texture determination on quartzite⁸⁶. The series expansion was here extended up to $L = 16$. The experimental accuracy for natural rock samples is, in general, lower than for metallic samples. Figure 10.8 thus shows the measured and calculated (110) pole figure of an 86% cold-rolled and recrystallized sheet of a low-carbon steel. The measurement was here carried out with neutron diffraction and the series expansion extended up to $L = 22$. The pole figure directly recalculated from the $F_{l\text{exp.}}$ values is also given in Figure 10.8. Thus, it does not contain the compat-

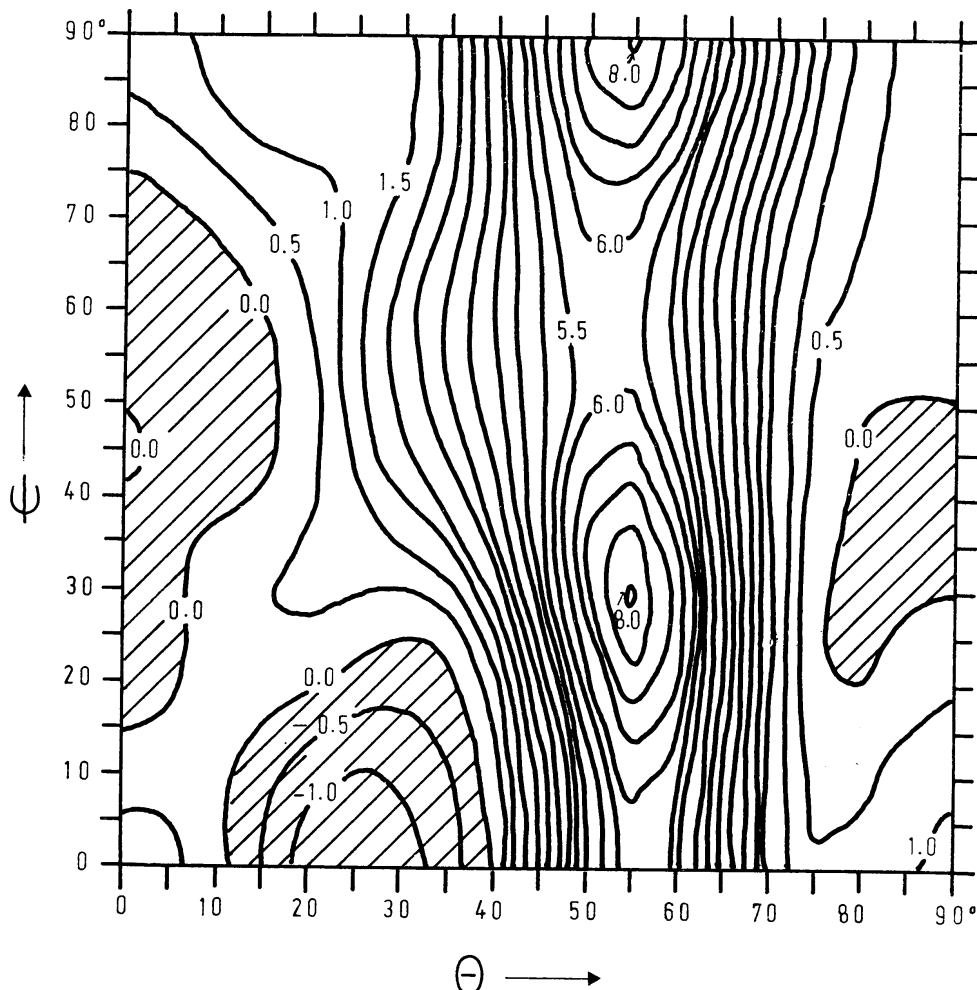


Figure 10.9 Regions of negative orientation density according to MORRIS and HECKLER²¹⁸

ibility errors of many pole figures with one another. The agreement of all three pole figures is here very good.

10.6. Negative Values

If one assumes that the error function

$$\Delta f(g) = \sum_{l=0}^{\infty} \sum_{\mu=1}^{M(l)} \sum_{\nu=1}^{N(l)} \Delta C_l^{\mu\nu} \dot{T}_l^{\mu\nu}(g) \quad (10.1)$$

can assume approximately equally as large positive as negative values, then one can directly estimate $|\Delta f(g)|$ at the points where $f(g) = 0$. The maximum occurring negative value of the calculated function $f(g)$ will thus be approximately equal to the absolute error of the calculation (Figure 10.9), assuming, naturally, that the texture is not so smooth that at no point does $f(g)$ assume the value zero. The error thus determined $|\Delta f(g)|$ has been found in the range of 5–20% of the maximum density value. It is, in general, customary to choose the contour lines for representation of the function $f(g)$ so that the lowest line is higher than $|\Delta f(g)|$, so that no negative values appear in the representation of the results. This error includes of course the indetermination error brought about by the centrosymmetry of pole figures (Section 4.11) and in fact a method of reducing this error is based on reducing the negative values.

10.7. Estimation of the Truncation Error by Extrapolation

The truncation error can be calculated according to equation (4.182) or for fibre textures according to equation (5.83) from the sum of the squares of the neglected series terms. These quantities are, of course, not known. One can, however, calculate the corresponding quantities for each value of l for $l \leq L$ and plot against l and extrapolate therefrom to $l \rightarrow \infty$, as is done in Figure 10.10. In the case represented one obtains an exponential dependence of the form

$$\sum_{\mu=1}^{M(l)} [C_l^{\mu}]^2 = B \cdot e^{-\alpha l} \quad (10.2)$$

Therefrom follows for the truncation error corresponding to the terms of even l

$$A_L = \frac{1}{4\pi} \cdot \frac{B}{2\alpha} \cdot e^{-\alpha(L+2)} \quad (10.3)$$

From Figure 10.10 there result $B = 12.5$, $\alpha = 0.109$, with which one obtains

$$A_{50} = 0.0155 \quad (10.4)$$

This estimation does not include the indetermination error due to terms of odd l .

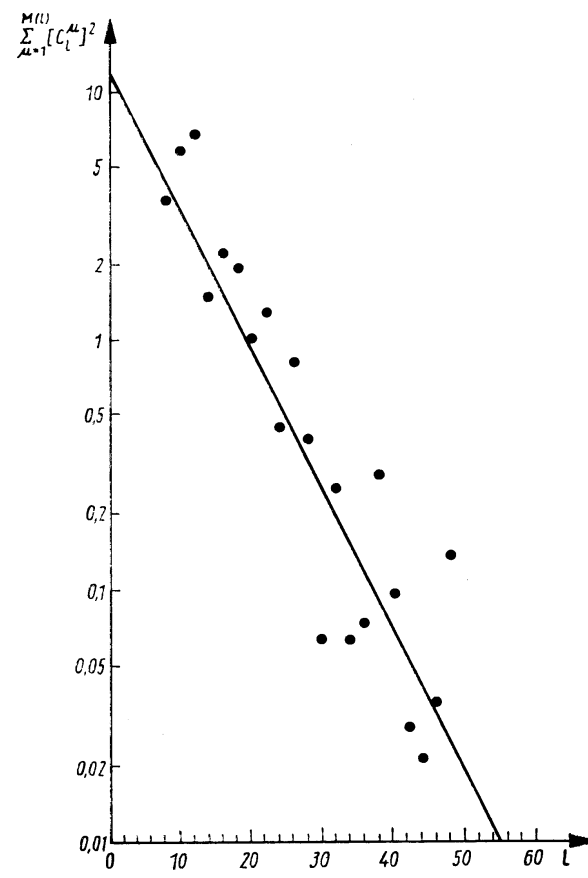


Figure 10.10 The quantities $\frac{M(l)}{\sum_{\mu=1}^{M(l)} [C_l^{\mu}]^2}$ of the recrystallization texture of an aluminium wire

10.8. The Integration Error

For calculation of the coefficients F_l^0 from the measured values of the pole figures according to equation (4.70) or equation (4.74) an integration over the complete pole figure is assumed. For the numerical calculation the integration will, however, be replaced by a summation, whereby the pole figure is approximated by a step function. This is usually already necessary, because the pole figure is only measured at certain intervals. Intervals of 5° are thus frequently used, as is represented in Figure 10.11. It is clear that, in particular, the higher 'short-wave' terms of the series expansion are thereby sharply reduced. This error was calculated by HUMBERT¹⁵⁷ and is given for various increments in Figure 10.12. One sees that, for the customary increment of 5° , a series expansion beyond $l = 22$ does not appear reasonable.

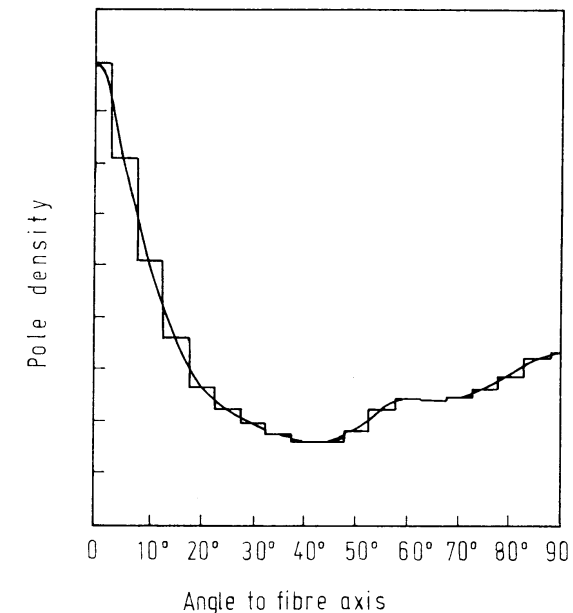


Figure 10.11 Approximation of a measured pole figure of a fibre texture by a 'step-function' with 5° intervals

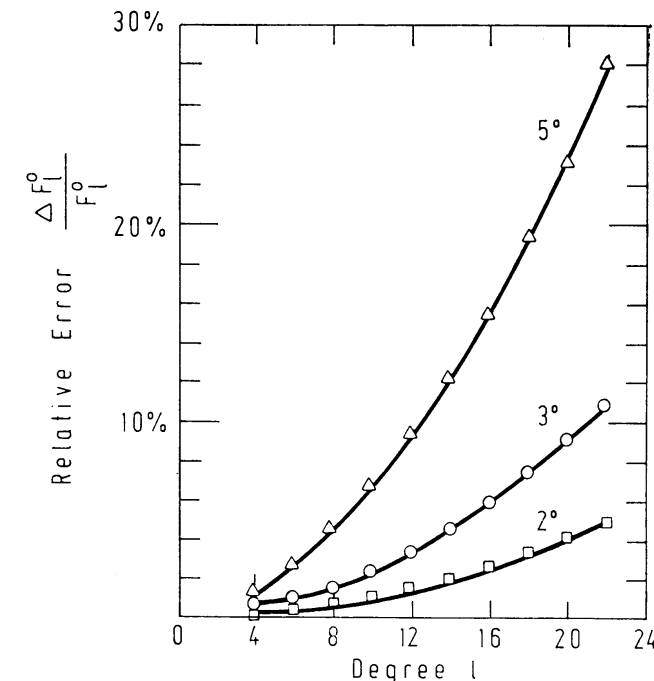


Figure 10.12 Relative error of the coefficients F_l^0 for different intervals of the integration. After HUMBERT¹⁵⁷

10.9. The Statistical Error

If, for measurement of a pole density value, N counts are measured, the probable error, which follows from the statistical nature of the counts, is given by \sqrt{N} . The relative error of a measurement is thus given by $1/\sqrt{N}$. If one assumes a statistical error of this size for each measured pole figure value, there results therefrom an error ΔF_l^v of the pole figure coefficients. It was calculated numerically by HUMBERT¹⁵⁷ for an actual pole figure with intervals $\Delta\Phi = \Delta\gamma = 5^\circ$ and a maximum of 1400 counts for the highest pole density value. The errors ΔF_l^v thus obtained

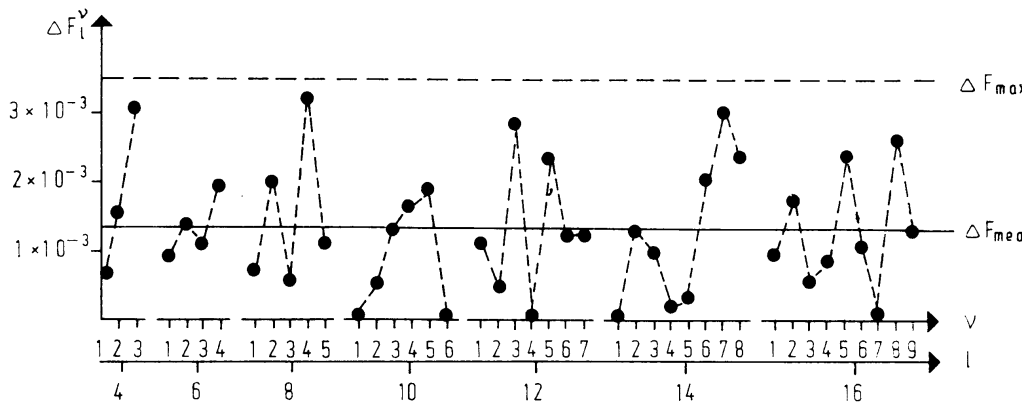


Figure 10.13 Errors of the coefficients F_l^v which result from the radiation statistics of the measured pole figure. After HUMBERT¹⁵⁷

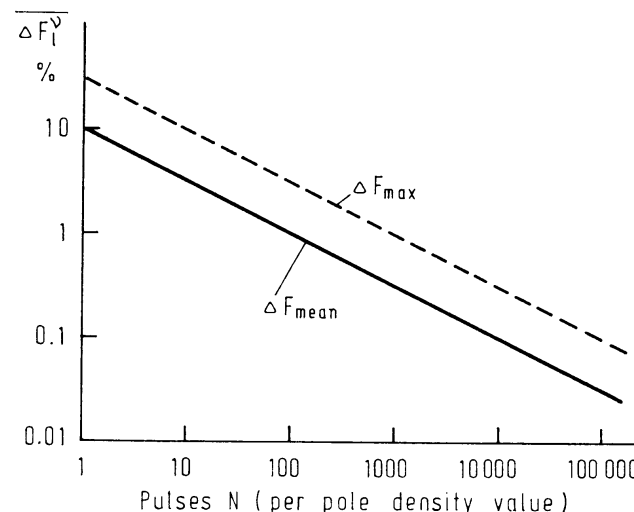


Figure 10.14 Average error of the coefficients F_l^v for different numbers of counts of the pole figure measurement

are represented in Figure 10.13. One obtains therefrom an average error of approximately

$$\Delta F_{\text{mean}} \sim \frac{0.1}{\sqrt{N}} \quad (10.5)$$

which is represented in Figure 10.14. The maximum error found is about three times as large. It is also given in Figure 10.14. Even for a relatively small number of counts, the statistical error may thus be neglected in comparison with other errors. If one compares this result with the integration error, it is thus appropriate, for the same total measuring time, to measure the pole figure in the smallest possible intervals.

10.10. The Indetermination Error for Incomplete Pole Figures

If one calculates the orientation distribution according to the method described in Section 4.7, the available experimental information will thus decrease as the region of measurement of the pole figures is reduced. It is to be expected that, for a specified limiting angle, the information no longer suffices unequivocally to solve the equation system for the orientation density values. It is difficult to estimate this limiting angle theoretically. The orientation distribution was therefore calculated by POSPIECH and JURA²³⁸ from pole figures which had been completely measured but were, however, used up to a certain value Φ_{max} . The mean square deviation of the distribution functions thus calculated with respect to the functions calculated from complete pole figures is given in Figure 10.15. One sees that the error increases sharply beyond a certain limiting angle. Beyond this limiting angle the solution is thus indeterminate.

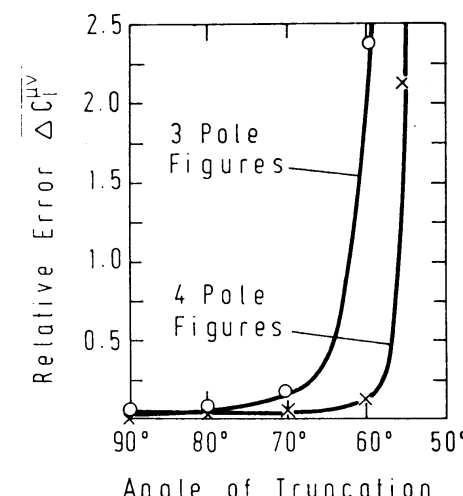


Figure 10.15 Mean square deviation of the orientation distribution function which was calculated from incomplete pole figures compared with the function calculated from complete pole figures. After POSPIECH and JURA²³⁸

11. Some Results of Texture Analysis

The execution of the texture analysis is associated with a considerable expenditure of numerical calculation. Therefore it could only be carried out in detail when sufficiently large computers had become readily accessible and when several systems of programs for carrying out the calculations and for graphic representation of the results had been developed. Since the calculations for the case of rotationally symmetric textures are at least a factor of 10 less complicated, fibre textures were considered first. Because of the higher symmetry, however, they give less information than the three-dimensional textures give about the processes occurring in the material, as, e.g., deformation mechanisms or orientation relations. Interest in fibre textures has therefore sharply declined in recent years and attention is now almost exclusively turned to three-dimensional textures.

11.1. Three-dimensional Orientation Distribution Functions (ODF)

Although some calculations of orientation distribution functions have been carried out with the method of biaxial pole figures, the large majority use the series expansion method in one of two variants — that developed by ROE or that developed by BUNGE. The two variants differ in the orientation coordinates used — namely the EULER angles $\Psi\Theta\Phi$ and $\varphi_1\Phi\varphi_2$. They differ, further, in the case of cubic sym-

Table 11.1 CARRIED-OUT TEXTURE ANALYSES FOR VARIOUS SYMMETRY COMBINATIONS AND MATERIALS

Crystal symmetry \ Specimen symmetry	Sheet symmetry			Axial symmetry
	$\bar{1}$	$2/m$	mmm	
Triclinic $\bar{1}$				Polyethylene-terephthalate
Monoclinic $2/m$				
Orthorhombic mmm	SiO_2	SiO_2	U, Polyethylene	U, Polyethylene SiO_2
Trigonal $\bar{3}m$		CaCO_3		
Hexagonal $6/mmm$			Ti, Mg	Ti, Mg, Zn
Tetragonal $4/mm$				
Cubic $m\bar{3}m$			Al, Cu, Ag, Ni, Fe, Mo, Cu-Zn , Fe-Si	Al, Cu, Ag, Ni, Fe

metry. The first variant here uses symmetry relations between the coefficients C_l^{mn} , while the other works with symmetry invariant functions $\dot{T}_l^{uvw}(g)$ and, consequently, uses independent coefficients C_l^{uv} . Further differences between the two variants exist in the normalization and in the notation of the quantities used (Section 4.10). Calculations of the orientation distribution functions according to these two variants of the series expansion method have by now been carried out in a great number of cases. The principally differing characteristics from the methodical standpoint are the crystal symmetry and the sample symmetry. Symmetry combinations treated to date, as well as the materials studied, are given in *Table 11.1* (see reference 68). Some examples will be given in the following paragraphs.

11.1.1. Determination of the Coefficients C_l^{uv} from Individual Orientation Measurements

The rolling texture of copper was studied with the help of electron microscopic selected-area diffraction by HAESSNER, JAKUBOWSKI and WILKENS¹³⁹⁻¹⁴¹ and by PERLWITZ, PITTSCH and LÜCKE^{227,228,231}. The orientations g_i of about 600 points of the material were determined. The points lay on a square grid, so that, to a first approximation, one could assume that the orientations were representative of volume elements of equal size. In equation (4.20), therefore, we can set $V_i = 1$. By inserting the orientation values g_i (expressed in terms of EULER angles) in equation (4.20) the C_l^{uv} for $l \leq 22$ were calculated and therefrom the orientation distribution function $f(\varphi_1\Phi\varphi_2)$ according to equation (4.7). It is represented in *Figure 11.1* in sections $\varphi_2 = n \cdot 5^\circ$ ⁷⁵. Although single orientation measurements do not suffer from the artificial symmetrization by a centre of inversion being introduced in the pole figures, thus 'blotting out' the odd terms of the series expansion, even terms only have been used. In this respect the results are immediately to be compared with the ones obtained from pole figure measurements. As was discussed in Section 6.1, the number of about 600 orientation values is not sufficient to determine a statistically reliable orientation distribution function with good angular resolution capability. The results, therefore, will not be discussed further here. It should merely be mentioned that the orientation distribution thus determined is, within the limits of error, in satisfactory agreement with the results of more exact determinations.

11.1.2. The Rolling Textures of Face-centred Cubic Metals and Alloys

Most of the calculations of orientation distribution functions carried out so far concern the rolling textures of face-centred cubic metals and alloys. Orthorhombic symmetry will thus be assumed for the sheet symmetry. Experimental input data were in most cases complete pole figures, which were measured in increments of approximately 5° in Φ and γ and either by X-ray diffraction on a thin foil from the mid-section of the sheet or with the aid of neutron diffraction, whereby usually the whole sheet was studied. For both methods of measurement the

orthorhombic symmetry is assured by the geometry of the problem. Orthorhombic symmetry was confirmed very well by neutron diffraction by measurement and comparison of several quadrants of the pole figure (TOBISCH). In the case of X-ray diffraction it is frequently not quantitatively so well fulfilled. The pole figures in this case are therefore usually averaged from four quadrants.

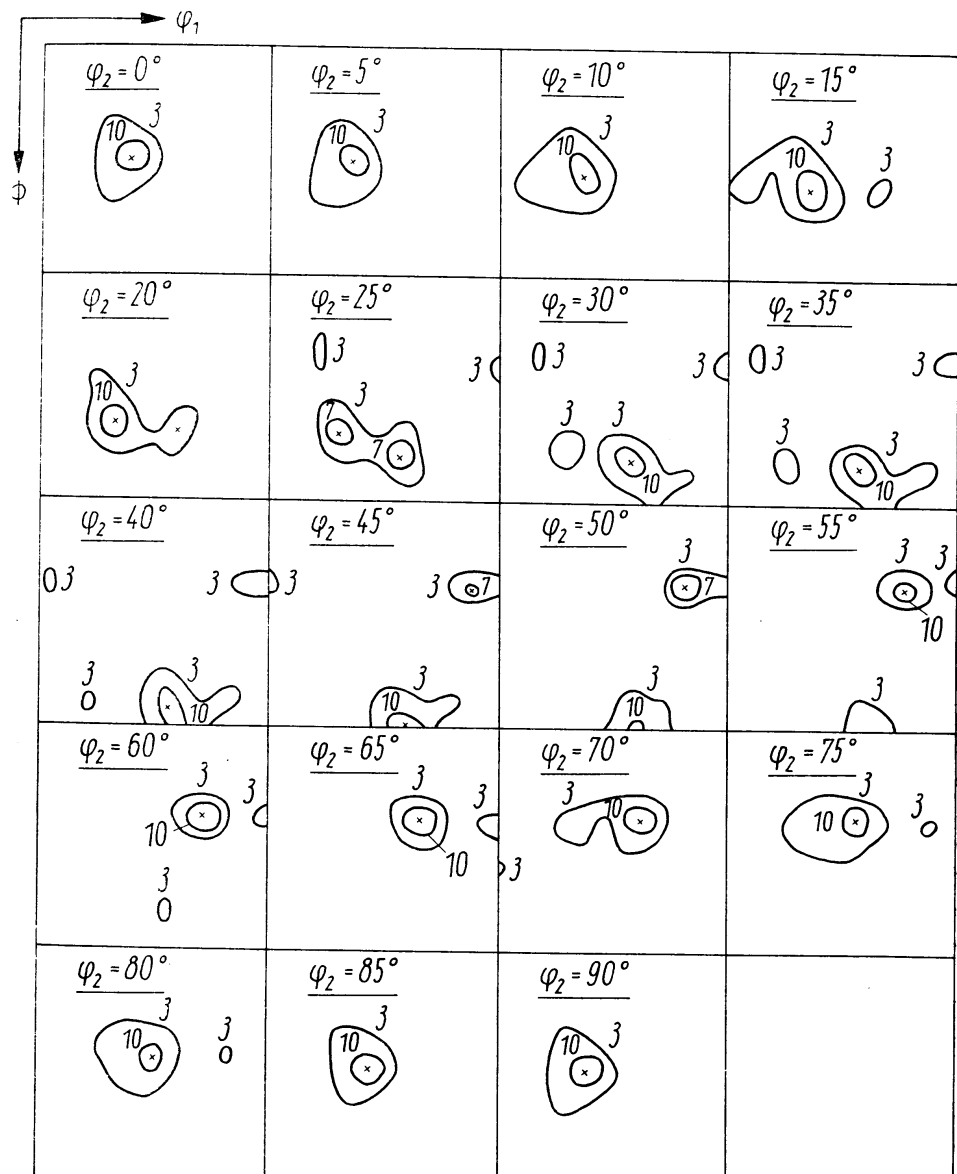


Figure 11.1 Orientation distribution for 95% cold-rolled copper, calculated from approximately 600 electron diffraction individual orientation measurements⁷⁵

With the help of neutron diffraction four pole figures, the (111), (200), (220) and (311) pole figures, were measured for 95% cold-rolled copper sheet by BUNGE and TOBISCH⁸². The coefficients $F_l^r(\mathbf{h}_i)$ were calculated therefrom according to equation (4.74) and, with the help of equation (4.145), the coefficients C_l^{uv} and finally the orientation distribution function $f(\varphi_1 \Phi \varphi_2)$ in sections of 5°. The result

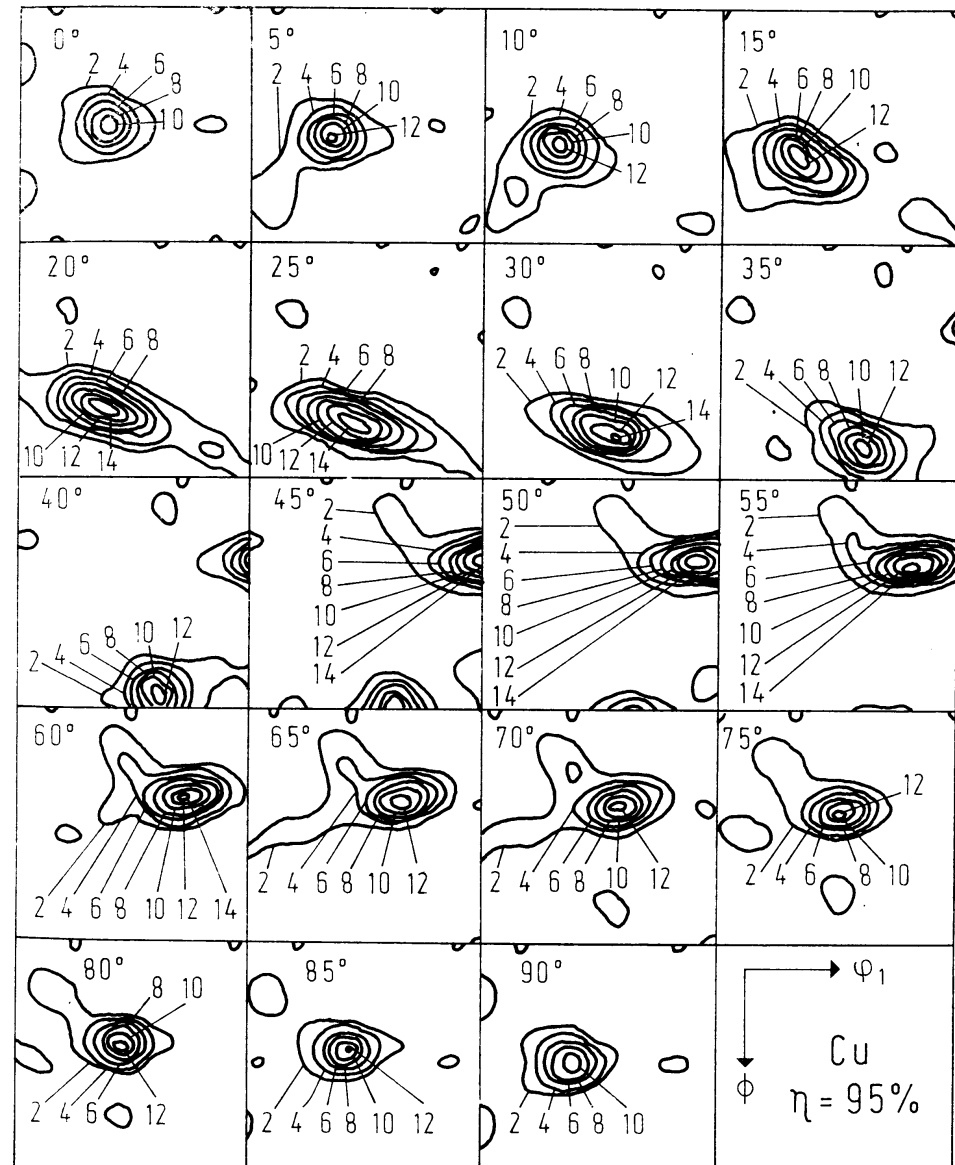


Figure 11.2 Orientation distribution for 95% cold-rolled copper, calculated from four pole figures measured by neutron diffraction⁸⁵

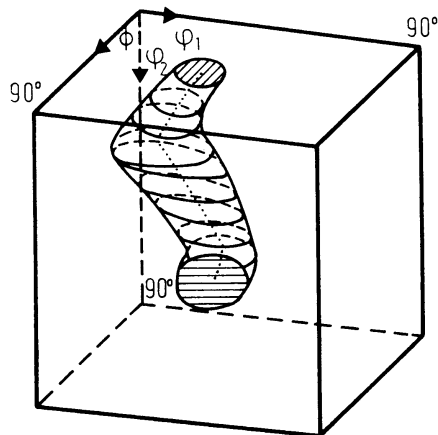


Figure 11.3 Spatial representation of the surface of half-maximum density of the orientation distribution of copper. The dotted line (skeleton line) is the line of maximum orientation density. (For the sake of Simplicity, one of the Symmetrically equivalent branches has been omitted)

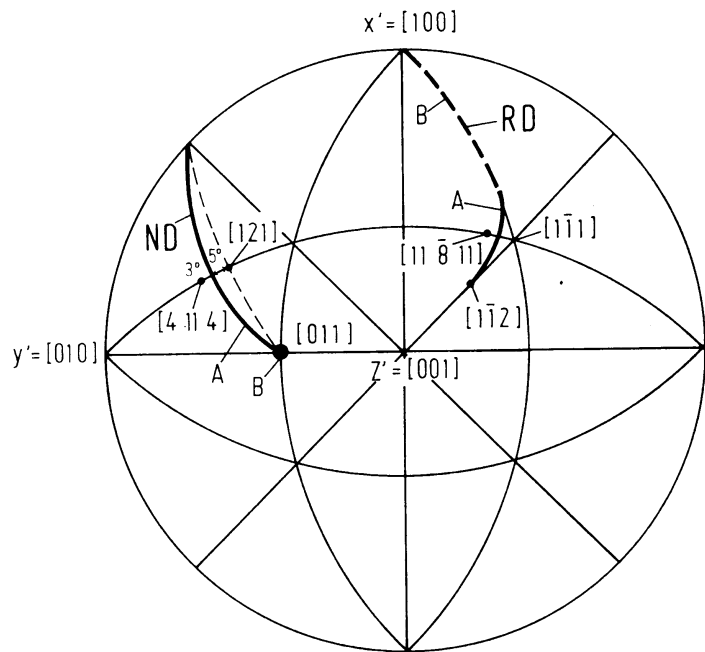


Figure 11.4 The line of maximum orientation density (skeleton line) for 95% cold-rolled copper, represented by the orientations of the rolling and normal directions relative to the crystal coordinate system

is given in *Figure 11.2*. If one imagines the sections superimposed on one another in the φ_2 direction, one thus recognizes that the texture is represented by a tube in orientation space. The contour of half-maximum density $f(g) = 6$ was selected; the constant-density surface thereby constructed is given in *Figure 11.3*. One clearly recognizes the tube-like character of the orientation density distribution. The rolling texture of copper is thus not described by two ideal orientations (which are points or spheres in orientation space), but by a continuous line of preferred orientations. This line is also indicated in *Figure 11.3*. We shall call this the skeleton line of the texture. According to *Figure 2.23*, the points of the skeleton line can be represented by the orientation of the normal direction and the rolling direction in stereographic projection. This representation corresponds to the ideal orientation representation, except that one now has a continuous line of 'ideal orientations', the skeleton line. This is reproduced in *Figure 11.4*. The skeleton line extends from the $\{110\} \langle 112 \rangle$ orientation to an orientation which differs by approximately 5° from $\{112\} \langle 111 \rangle$ (*Figure 11.4*, line A). This deviation was repeatedly confirmed, and is therefore to be considered as significant. It differs by

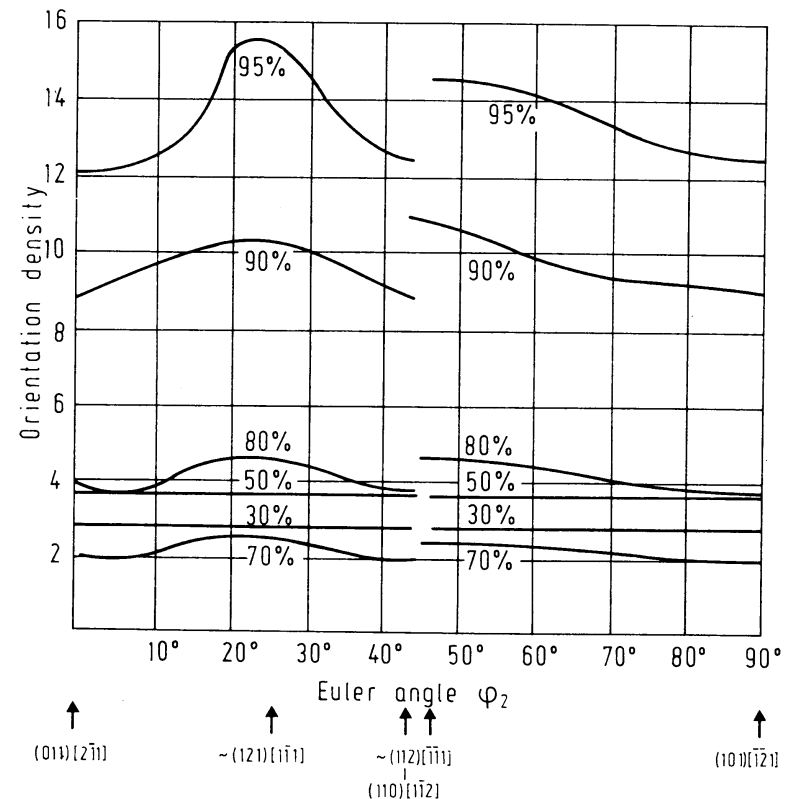


Figure 11.5 The orientation density along the skeleton line for cold-rolled copper for different reductions⁸⁵

approximately 3° from the theoretically calculated $\{4\ 4\ 11\} \langle 11\ 11\ 8\rangle$ orientation^{53,108}. Figure 11.5 shows the orientation density along the skeleton line. One sees that the density varies along the skeleton line and that a slight maximum exists at the orientation $\sim \{112\} \langle 111\rangle$.

The rolling textures for small rolling reduction are very similar⁸⁵. They also show tube-shaped distributions with the same skeleton line as in Figure 11.4, but, of course, with lower density along the skeleton line, as Figure 11.5 shows. The half-value width of the tube (see also Figure 11.3) is represented as a function of rolling reduction in Figure 11.6. The texture thus sharpens with increasing rolling reduction, while the relative density distribution along the skeleton line remains approximately the same. The orientations of the crystallites thus move towards the skeleton line with increasing rolling reductions. Results very similar to those for copper were obtained by BUNGE and KROL for nickel (see reference 58) and DAVIES, KALLEND and RUBERG¹⁰³ found very similar orientations for aluminium.

As is well known, silver and face-centred cubic alloys exhibit a rolling texture which is different from that of the other pure f.c.c. metals. The orientation distri-

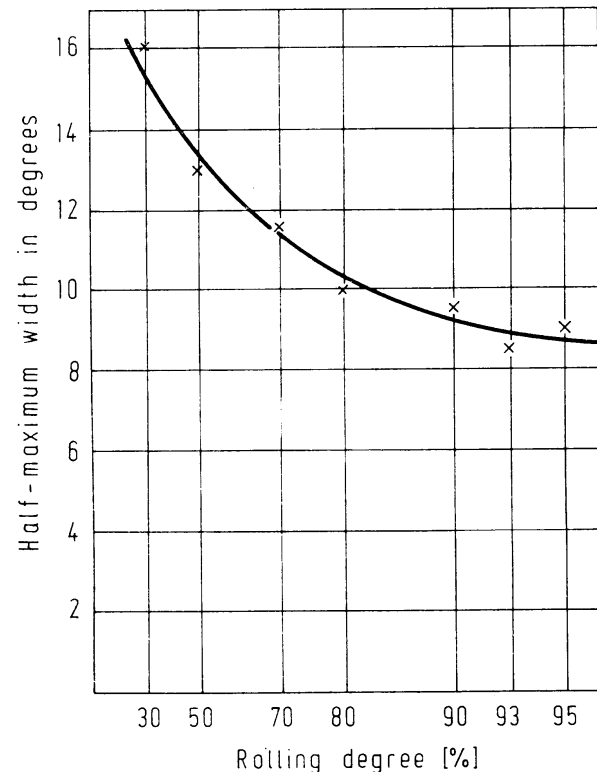


Figure 11.6 The half-value of the scatter about the skeleton line as a function of rolling reduction⁸⁵

bution function for 95% cold-rolled silver is represented in Figure 11.7. It was calculated by TRUSZKOWSKI *et al.*²⁴¹ from four pole figures measured by X-ray diffraction. As one sees from Figure 11.8, one can, to a good approximation, represent this texture by the ideal orientation $\{110\} \langle 112\rangle$. (One observes that a different section of the orientation space is represented in Figure 11.8 compared with

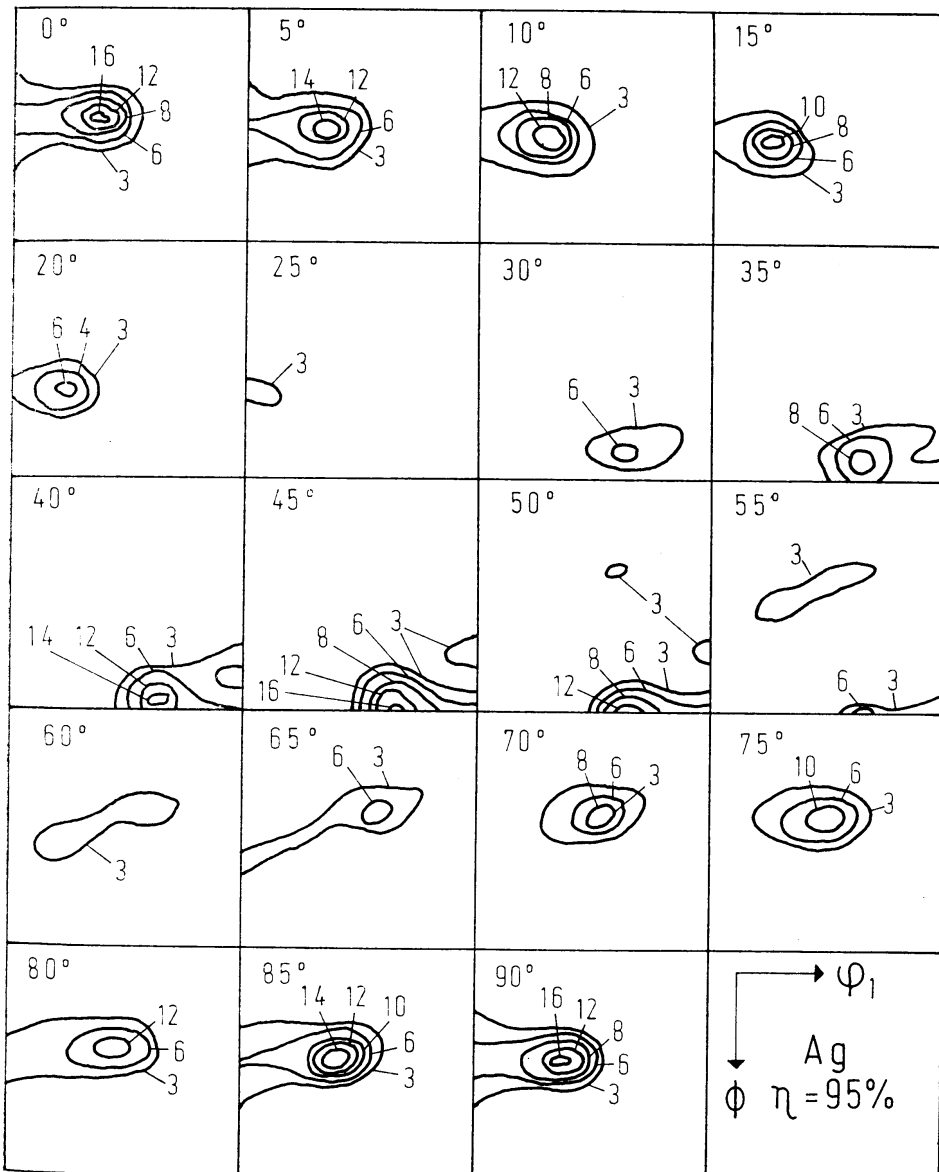


Figure 11.7 Orientation distribution function for 95% cold-rolled silver²⁴¹

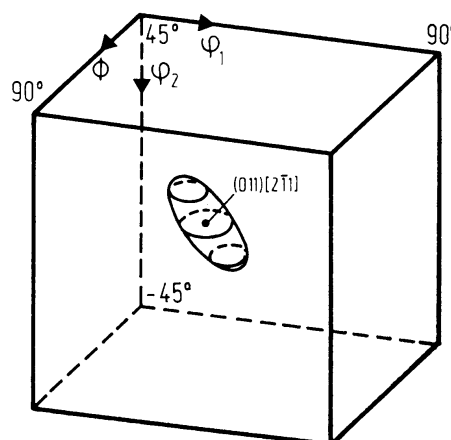


Figure 11.8 Spatial representation of the half-maximum density of the orientation distribution of silver¹³¹

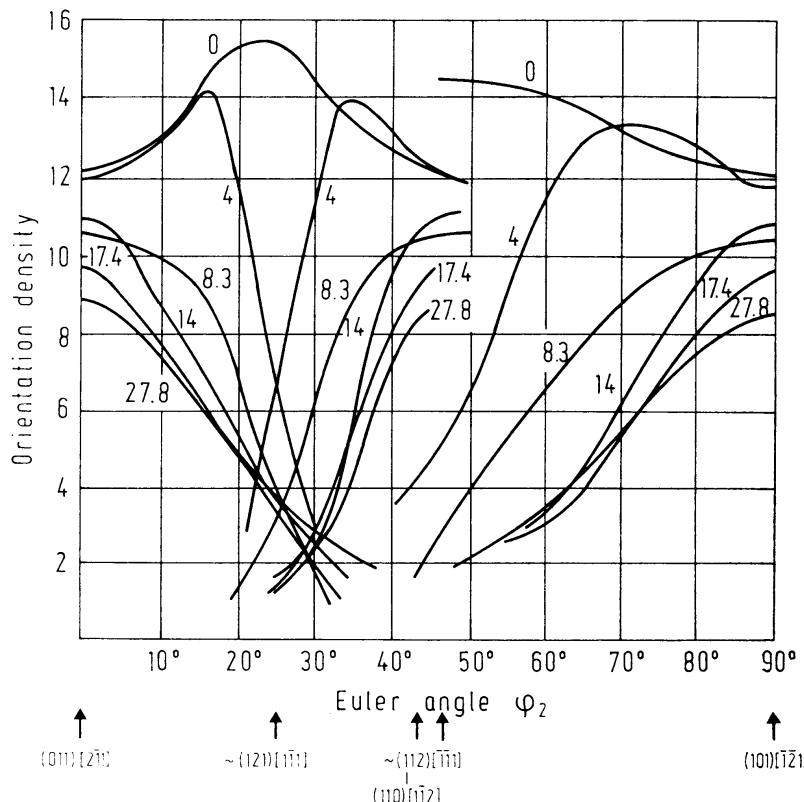


Figure 11.9 Orientation density along the skeleton line for 95% cold-rolled brass of different zinc concentrations⁸³

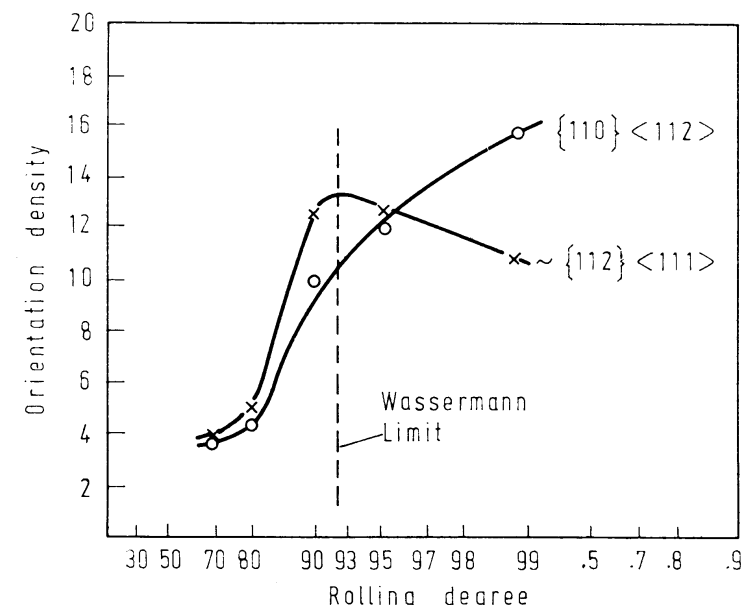


Figure 11.10 Orientation density in the orientations $\{110\} \langle 112 \rangle$ and $\sim \{112\} \langle 111 \rangle$ for copper with 1% zinc as a function of rolling reduction, constructed from measurements by KLEINSTÜCK et al.¹⁷⁹

Figure 11.3. This was done in order not to dissect the 'ideal orientation' by the region boundaries. Furthermore, one of the symmetrically equivalent orientations was omitted.)

The transition from copper to alloy or silver texture takes place continuously. The change of the orientation density along the skeleton line is represented in Figure 11.9, as one finds if one adds different proportions of zinc to copper⁸³. The rolling reduction is 95% in all cases. One sees that the orientation tube is, as it were, 'cut off' at the position $\sim \{112\} \langle 111 \rangle$ until, at higher zinc concentrations, only the ideal orientation $\{110\} \langle 112 \rangle$ is left, as in the case of silver. The beginning of the decomposition of the orientation $\sim \{112\} \langle 111 \rangle$ along with the simultaneous further formation of the orientation $\{110\} \langle 112 \rangle$ may be seen in Figure 11.10 for a copper alloy with 1% Zn¹⁷⁹. The ability to estimate such a course of the orientation density with relatively good accuracy depends on the calculation of the three-dimensional orientation distribution function together with accurate pole figure measurements with the help of neutron diffraction. Simultaneously with the decomposition of the 'copper tube' a region of relatively higher orientation density is being built up which extends up to the orientation $\{110\} \langle 001 \rangle$. This can clearly be recognized from the $\varphi_2 = 0$ section in Figure 11.7. The skeleton line of this tube is recorded in Figure 11.4 as the dashed line B. The $\{110\} \langle 001 \rangle$ orientation is nearly a twin orientation to the disappearing $\sim \{112\} \langle 111 \rangle$ orientation (see Figure 11.20). The results thus confirm the ideas of WASSER-

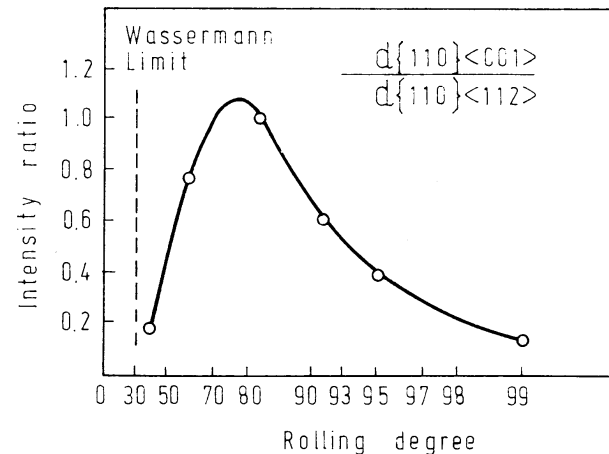


Figure 11.11 The intensity ratio of the orientations $\{110\} \langle 001 \rangle$ and $\{110\} \langle 112 \rangle$ for silver as a function of rolling reduction, constructed from measurements by TRUSZKOWSKI et al.²⁸⁵

MANN²⁹⁴ according to which the $\sim\{112\} \langle 111 \rangle$ orientation will be decomposed by twin formation for increasing alloy concentration — i.e. decreasing stacking-fault energy. The portion of the twin orientation can be deduced from Figure 11.11; the dependence of the intensity ratio of the orientations $\{110\} \langle 001 \rangle$ and $\{110\} \langle 112 \rangle$ on the rolling reduction for silver is plotted there (according to POSPIECH et al.²⁴¹). One sees that after exceeding the WASSERMANN limit (onset of twin formation), the twin orientation first increases, but then decreases. This is to be expected, since indeed the twin orientation $\{110\} \langle 001 \rangle$ is not stable and is transformed by slip into the stable orientation $\{110\} \langle 112 \rangle$, whereas it will be ‘supplemented’ still less from the disappearing orientation $\sim\{112\} \langle 111 \rangle$, because this orientation is already extensively decomposed. The texture with the highest portion of twin orientations is reproduced in Figure 11.12 (after reference 285). One sees here a strong scatter region of orientations between the twin orientation $\{110\} \langle 001 \rangle$ and the orientation tube A in the orientation $\{110\} \langle 112 \rangle$. It is indicated as the skeleton line B in Figure 11.4. In Figure 11.13 results from different investigations are summarized showing the rolling reduction for which the decomposition of the ‘copper tube’ at the orientation $\sim\{112\} \langle 111 \rangle$ just begins. The rolling degree is plotted against the relative stacking-fault energy $\gamma/G\mathbf{b}$ of the alloy where G is the shear modulus and \mathbf{b} the BURGERS vector. One thus obtains a straight line, which characterizes the beginning of twin formation (WASSERMANN limit). According to this, decomposition of the orientation tube and thus the onset of twin formation is strongly to be expected also for copper for still higher degrees of deformation. Certainly this has as yet not been explicitly observed. According to Figure 11.13, the WASSERMANN limit moves to a higher degree of deformation with increasing stacking-fault energy. The curve of Figure 11.11 will therefore likewise move towards a higher degree of deformation. If, therefore, one considers

the twinning fraction for a fixed degree of deformation (e.g. 95%), one also obtains a curve passing through a maximum as is shown in Figure 11.14 for Cu-Zn alloys^{83,179}.

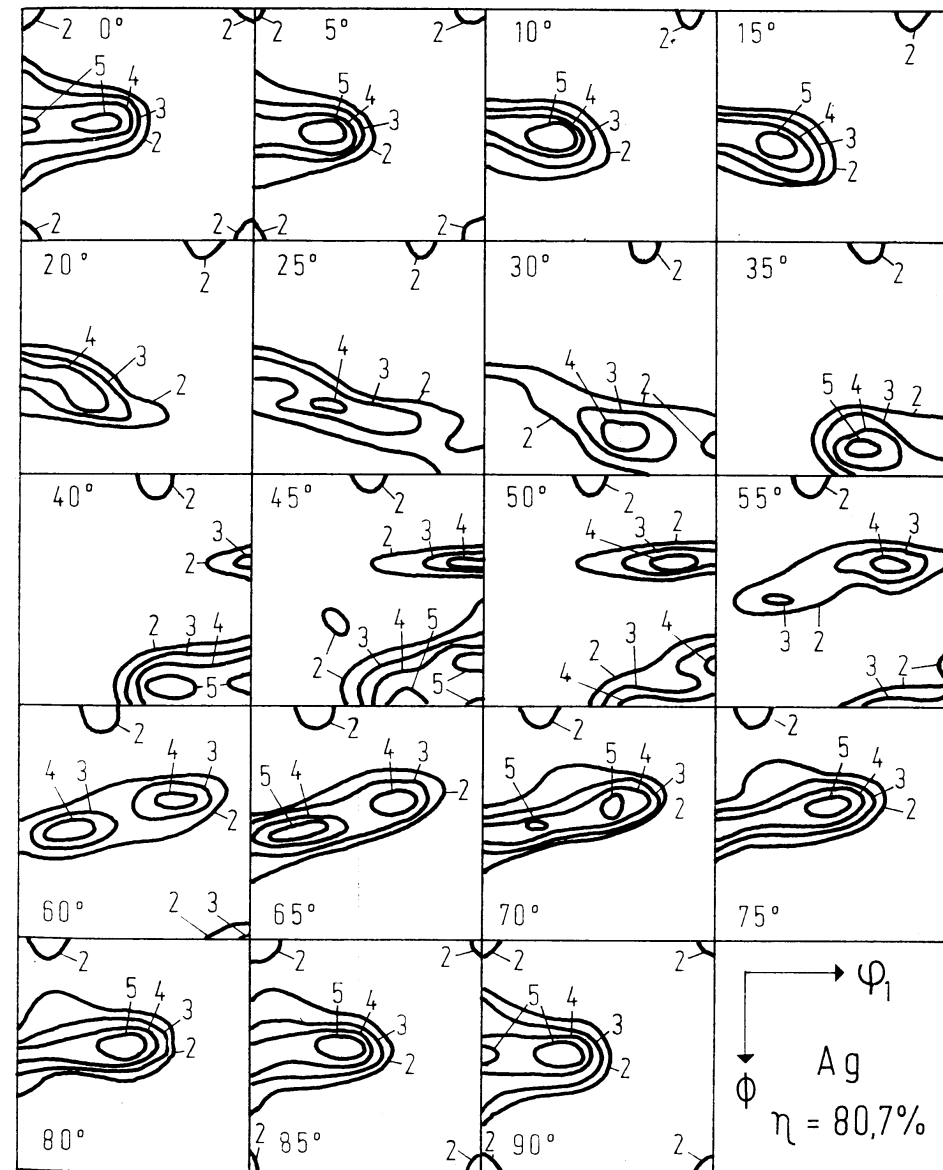


Figure 11.12 Orientation distribution function for 80.7% cold-rolled silver. After TRUSZKOWSKI et al.²⁸⁵

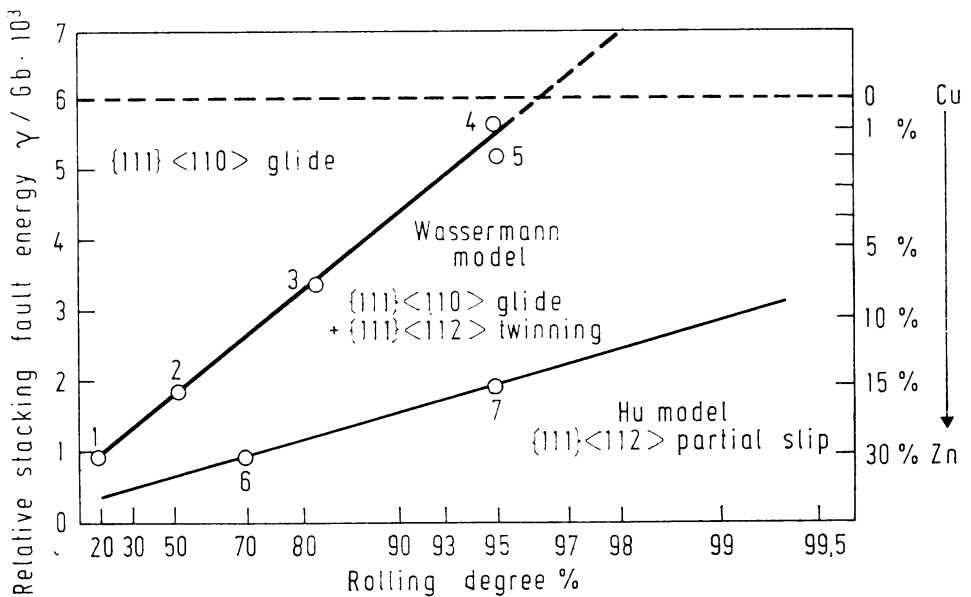


Figure 11.13 Three regions of texture development in face-centred cubic metals and alloys

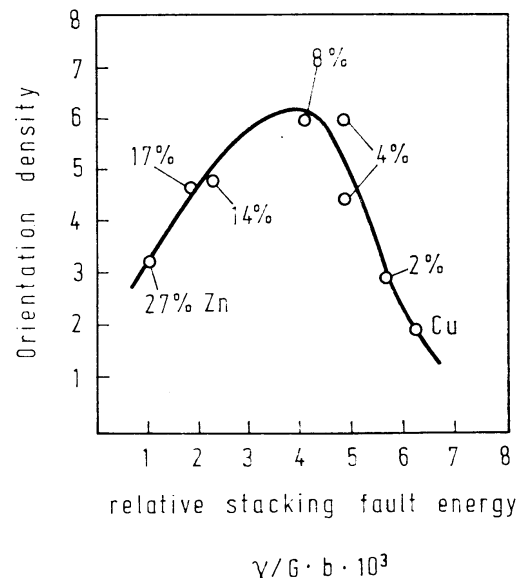


Figure 11.14 Orientation density of the {110}⟨001⟩ twin orientation for 95% rolled brass as a function of zinc concentration. After references 83 and 179

The line beyond which, in general, no orientation tube can be detected, only the ideal orientation $\{110\}\langle112\rangle$, is recorded in Figure 11.13. This texture is in better agreement with the model of Hu¹⁵⁶, which assumes slip of partial dislocations, and thus slip on the $\{111\}\langle112\rangle$ slip system.

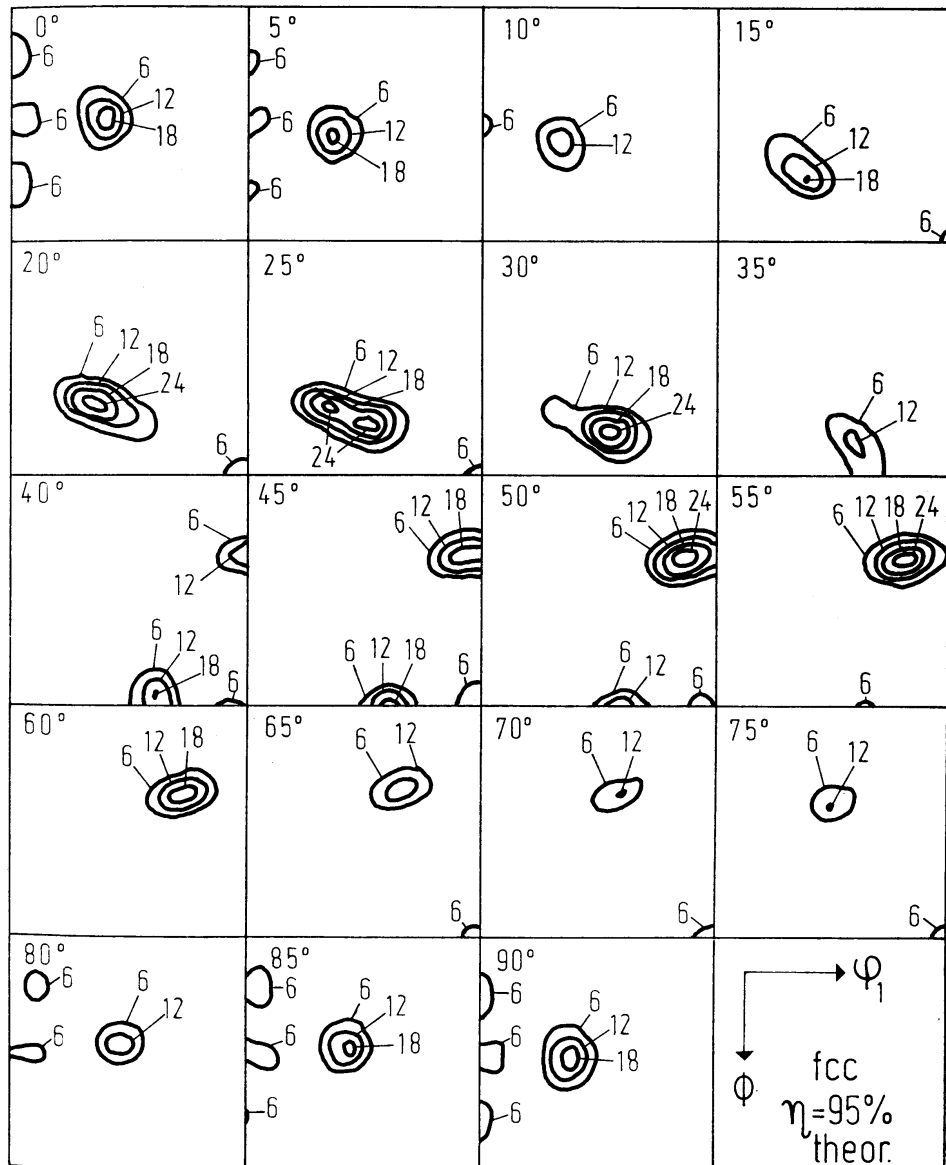


Figure 11.15 Theoretical orientation distribution function, calculated from 100 randomly distributed orientations after 95% deformation in the framework of the modified TAYLOR model⁷⁷

11.1.3. The Theoretical Rolling Texture for $\{111\} \langle 110 \rangle$ Slip

The orientation change of the crystallites of a polycrystalline material was calculated by LEFFERS¹⁹⁴. A modified TAYLOR model was used. Proceeding from 100 randomly distributed orientations, the orientation change was calculated for small deformation steps up to a total deformation of 95%. The resultant crystal orientations can be expressed by EULER angles. With the help of a method similar to that described for electron microscopic single-orientation measurements, a three-dimensional orientation distribution function can be calculated therefrom⁷⁷, which is reproduced in Figure 11.15. Only the even terms were used in the calculation. Hence, the results are directly comparable with the calculations from pole figures. The obtained function agrees very well with the experimental texture of copper (Figure 11.2). The statistical certainty is naturally not very high for only 100 single orientation values.

11.1.4. The Rolling Textures of Body-centred Cubic Metals

The development of the rolling texture of a carbon steel (0.06% C, 0.3% Mn, 0.014% P, 0.028% S) was studied by SCHLÄFER and BUNGE²⁵⁹ with the help of neutron diffraction. Four pole figures were measured — namely (110) (200) (211) and (310). The orientation distribution function was calculated therefrom in the approximation $L = 22$ in 5° sections. The result is represented in Figure 11.16 for a rolling reduction of 95%. Here one also finds an extended, tube-shaped density distribution. Certainly, it is more complex than in the case of copper. The half-value surface is spatially represented in Figure 11.17. One sees that the region of highest density here has approximately a triangular shape extended in two dimensions. If one combines the points of highest orientation density, one obtains two branches of the skeleton line, which are marked as lines A' and B' in Figure 11.17. (Additional symmetrically equivalent branches are omitted in Figure 11.17.) The skeleton line is represented in stereographic projection of the rolling and normal directions in Figure 11.18. One sees that the skeleton lines A' and B' correspond completely to those of the face-centred cubic metals A and B, if one simply interchanges rolling and normal directions. The component A' corresponds to the tube A of the copper texture, and component B' corresponds to the region B resulting through twin formation in silver and the alloy textures. The rolling texture of iron is in best agreement with that of silver for $\eta = 80.7\%$, which is represented in Figure 11.12. Tube A of the copper texture was derived from the TAYLOR theory with the assumption of $\{111\} \langle 110 \rangle$ slip. If in this theory one interchanges the roles of the slip direction and slip-plane normal, thus assuming $\{110\} \langle 111 \rangle$ slip, one obtains an interchange of the orientations of the rolling direction and sheet normals — i.e. just the tube A' of the body-centred cubic metals (Figure 11.18). Tube B of the face-centred cubic metals was explained by twin formation with the $\{111\} \langle 112 \rangle$ twinning system according to the WASSERMANN model. If, therefore, one assumes twin formation in body-centred cubic metals on the equivalent system $\{112\} \langle 111 \rangle$, one obtains the analogous

tube B' of the body-centred cubic metals, also by interchange of the rolling direction and sheet normal. The rolling texture of iron can thus also be understood according to the WASSERMANN model, if one assumes an appropriate threshold strain for the onset of twin formation (WASSERMANN limit). The WASSERMANN limit for iron can be deduced from Figure 11.19, where the course of the orient-

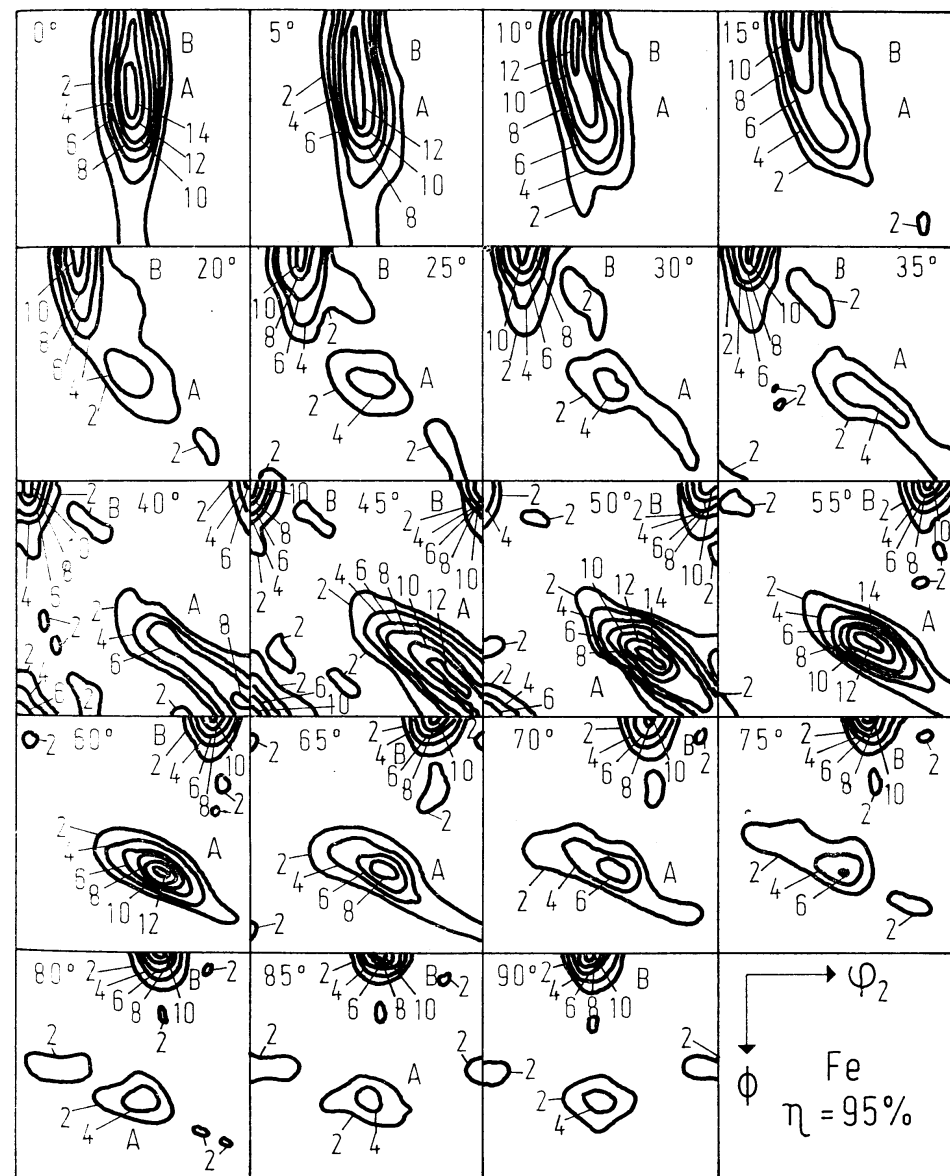


Figure 11.16 The orientation distribution of a 95% cold-rolled low-carbon steel²⁵⁹

ation density in the two orientations $\{112\}\langle 110\rangle$ and $\sim\{111\}\langle 112\rangle$ is plotted. *Figure 11.19* is largely analogous to *Figure 11.10* for Cu + 1% Zn, except that here the WASSERMANN limit lies at about 50%, while there it lies at about 92%.

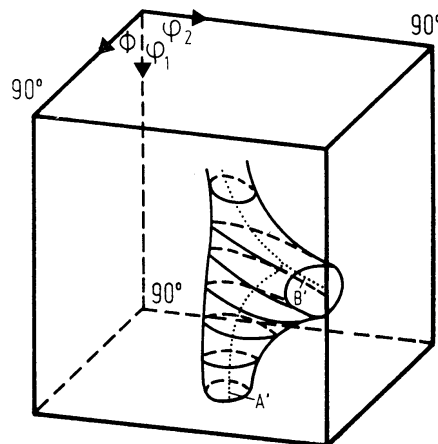


Figure 11.17 Spatial representation of the surface of half-maximum density of the texture of 95% rolled steel

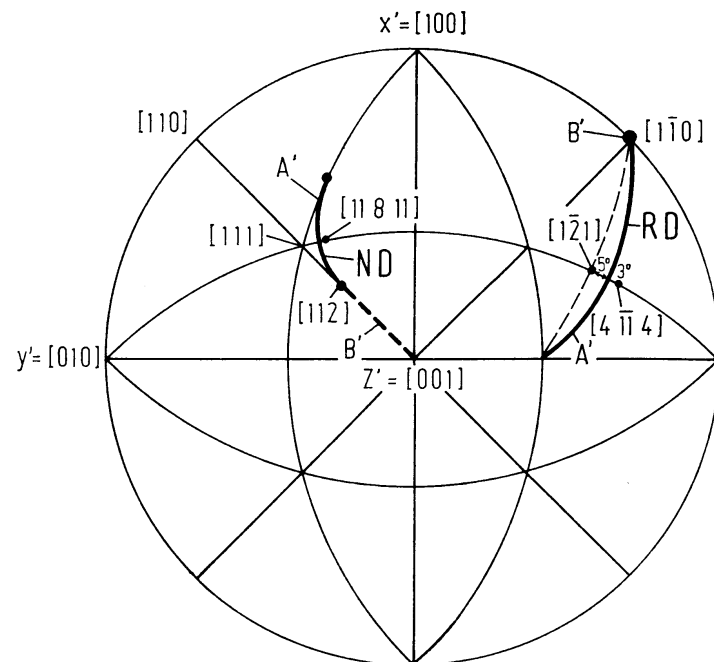


Figure 11.18 The line of maximum orientation density (skeleton line) of the steel texture, represented by the orientations of the rolling and normal directions relative to the crystal coordinate system²⁵⁹

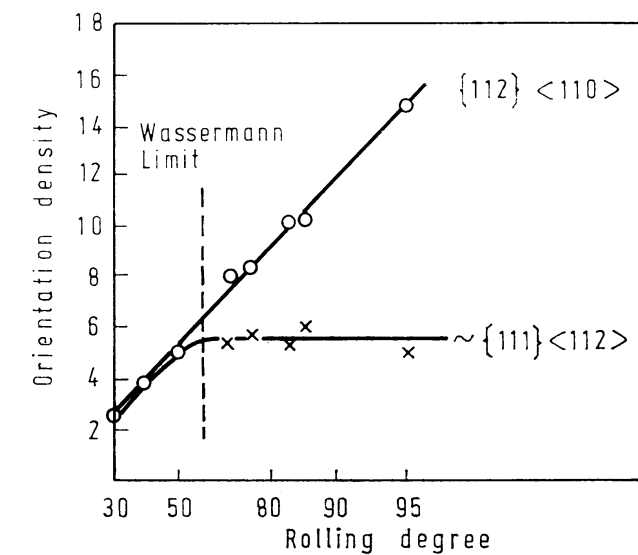


Figure 11.19 Orientation density of the orientations $\{112\} \langle 110 \rangle$ and $\sim\{111\} \langle 112 \rangle$ for cold-rolled iron as a function of cold-rolled reduction²⁵⁹

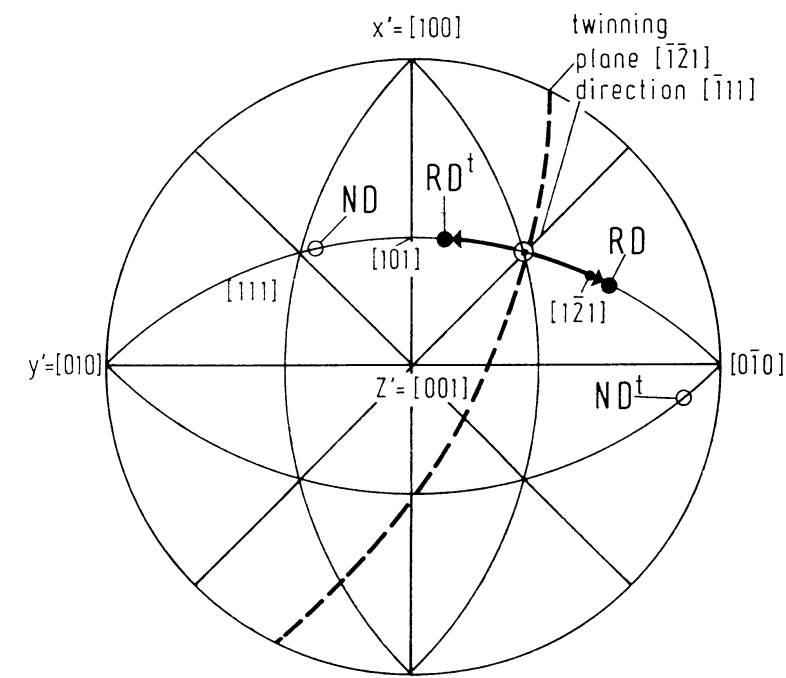


Figure 11.20 Twin formation of the orientation $\sim\{111\}\langle112\rangle$ leading to an orientation near to the $\{001\}\langle110\rangle$ orientation²⁵⁹

rolling reduction. The twin formation of the $\sim\{111\}\langle112\rangle$ orientation of iron is represented in *Figure 11.20*. It leads to an orientation which differs approximately 10° from the $\{001\}\langle110\rangle$ orientation. If one interchanges the twinning plane and direction and rolling plane and direction, *Figure 11.20* naturally explains also the twinning mechanism of the WASSERMANN model for face-centred cubic metals.

11.1.5. Textures of Tubes

If one cuts a tube parallel to its axis and uncoils it, one obtains a sheet-shaped sample which one can investigate with the methods of texture analysis for sheets (*Figure 11.21*), as was proposed by LINSSEN, MENGELEBERG and STÜWE¹⁹⁸. The sample symmetry is, however, no longer the orthorhombic symmetry. According

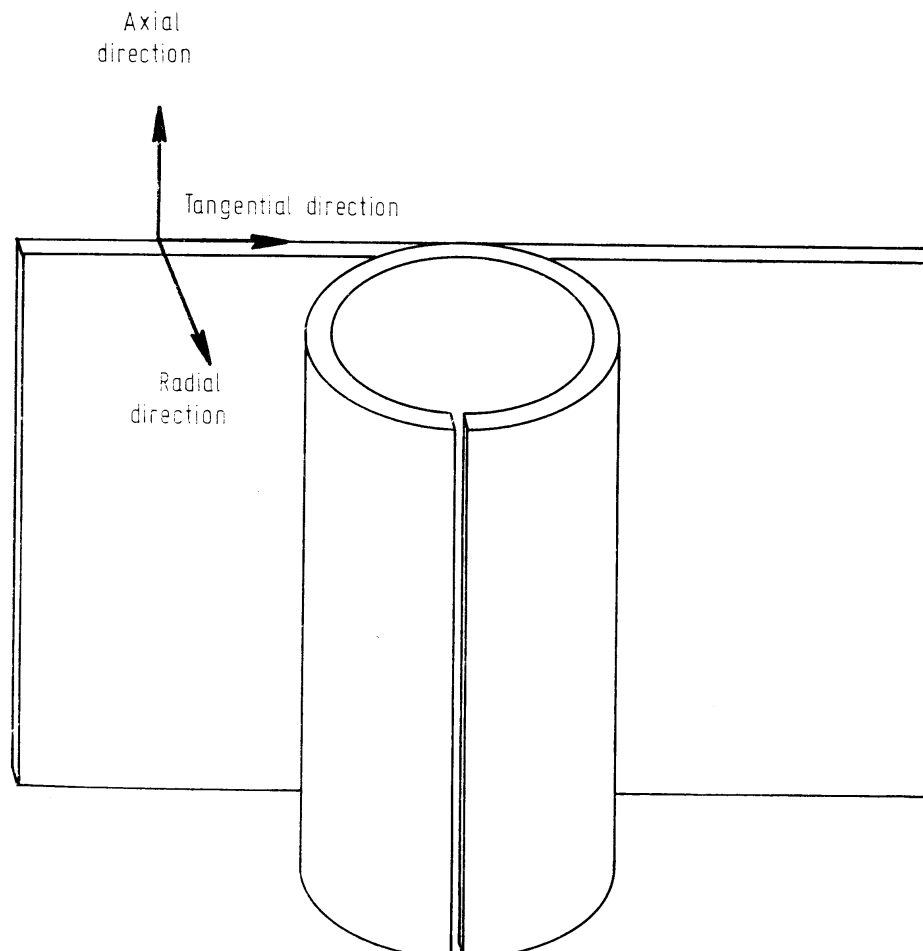


Figure 11.21 Unrolling a tube for texture measurement by sheet texture methods. After reference 198

to the geometry of the manufacturing process of tubes (tube drawing), one can only expect one mirror plane, which is defined by the tube axis and the radius. Together with the centre of symmetry this leads to monoclinic sample symmetry $2/m$. Texture investigations on tubes have as yet been much more rarely carried

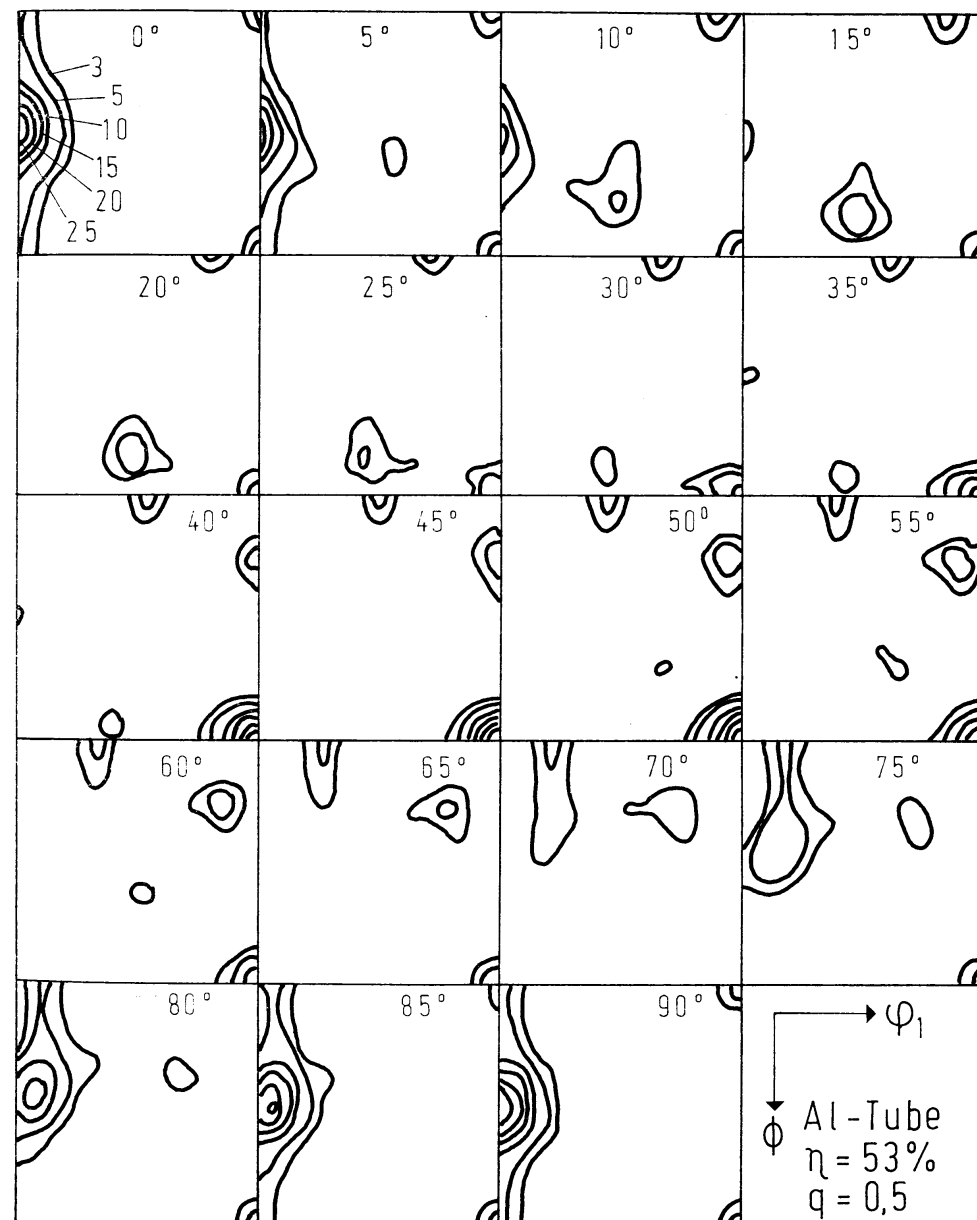


Figure 11.22 Orientation distribution of a 53% cold-drawn aluminium tube²⁵⁴

out than those on sheets. This is certainly due to the essentially greater technical significance of sheets. From a theoretical standpoint of texture formation, textures of tubes are, however, more interesting, since by variation of the ratio of wall thickness decrease to diameter decrease of the tube during the draw one can vary the axial ratio of the deformation tensor, while in rolling one is practically limited

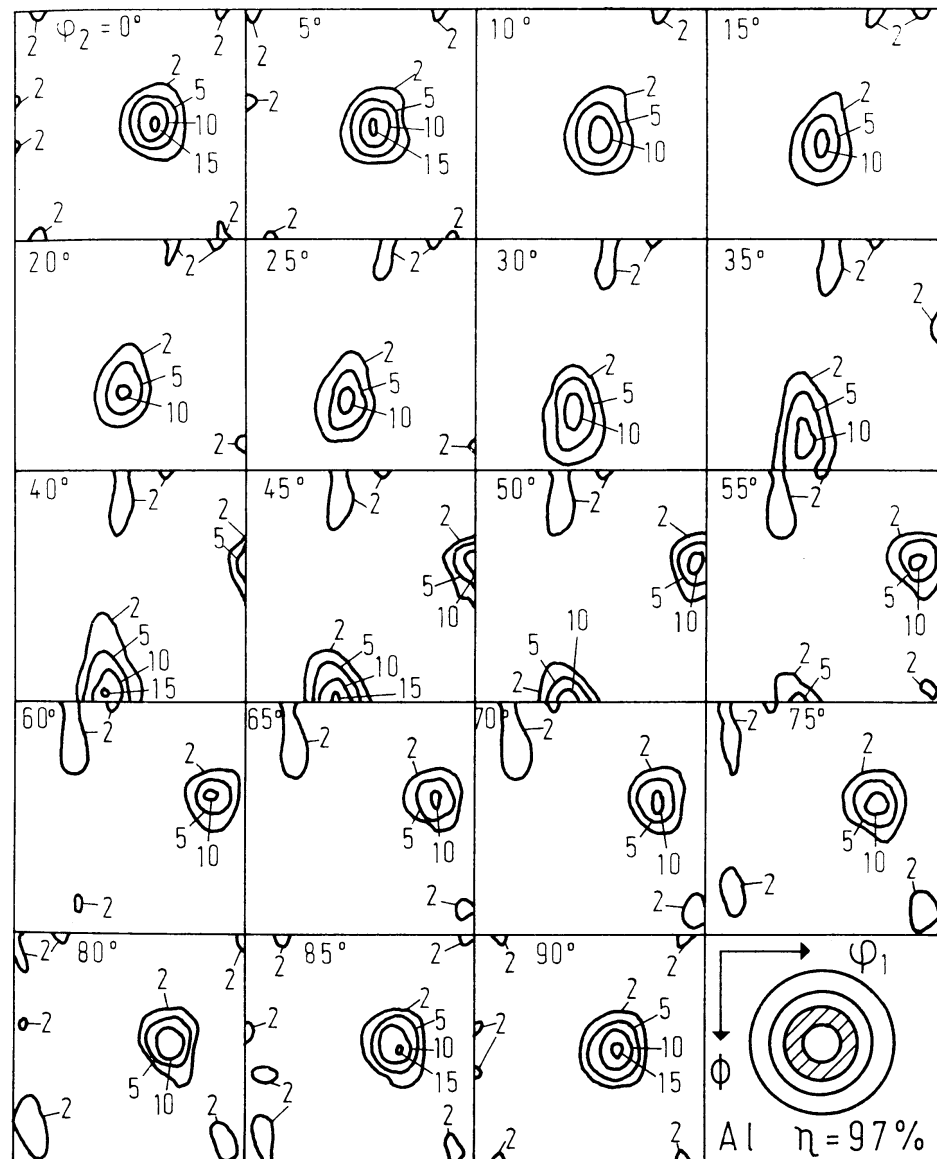


Figure 11.23 Orientation distribution of a cylindrical-shaped sample, which was prepared from a 97% cold-drawn aluminium rod²⁵⁷

to plane strain (no widening of the sheet). If one does not want to work with the sample symmetry $2/m$, but with orthorhombic symmetry $m\ m\ m$, this is naturally also possible. One then, however, carries out an additional symmetrization, which one must consider in the discussion of results. The texture of aluminium tubes was investigated in this way by SCHLÄFER²⁵⁴. Figure 11.22 shows the orientation distribution function of a tube, which was drawn with 53% reduction in cross-section, where the ratio of wall thickness reduction to diameter reduction was equal to 1. We see that we are dealing with three texture components — namely the $\{011\} \langle 100 \rangle$ orientation with an intensity of about 20, a fibre texture with the $\langle 100 \rangle$ direction in the axial direction with an intensity of about 5 and a limited fibre texture with the $\langle 111 \rangle$ direction in the axial direction, which has a maximum of about 5 for the orientation $\{112\} \langle 111 \rangle$.

The texture of cylinders which were prepared from aluminium ingots was studied by the same methods by SCHÄFER and BUNGE²⁵⁷. Figure 11.23 shows the texture of a 97% cold-rolled aluminium ingot in mid-section. It is essentially a $\langle 111 \rangle$ fibre texture with a slight preference for $\langle 110 \rangle$ and $\langle 112 \rangle$ directions parallel to the radial direction, as Figure 11.24 shows.

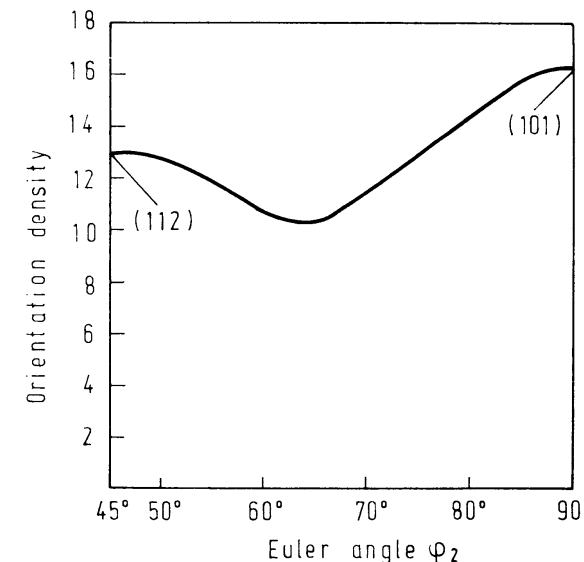


Figure 11.24 Orientation density along the skeleton line of the texture of the aluminium rod²⁵⁷

11.1.6. Orthorhombic Crystal Symmetry

11.1.6.1. The Rolling Texture of Uranium

In this symmetry the rolling texture of uranium was investigated^{211,214} for a reduction of 80%. The sample symmetry was orthorhombic symmetry. An asymmetric region in EULER space of $\pi/2, \pi/2, \pi$ thus results according to Table 14.9,

which is thus twice as large as that in the case of cubic-orthorhombic symmetry. (Since in the case of cubic-orthorhombic symmetry the asymmetric region of tetragonal-orthorhombic symmetry is essentially represented, this region includes three symmetrically equivalent points for each orientation. The region selected for the orthorhombic-orthorhombic case, on the other hand, is actually asymmetric. Each orientation occurs in it only once.)

The following 12 complete pole figures were measured: (020), (110), (021), (002), (111), (112), (131), (023), (200), (113), (042), (133). The orientation distribution function $f(\Psi, \Theta, \Phi)$ was calculated therefrom in the approximation $L = 16$. (According to Figure 4.4, $L = 16$ requires at least 9 pole figures, so that it was performed with an overdetermination of 3 pole figures.) The error analysis showed that $L = 16$ is a sufficient approximation for this not very sharp texture. The result of the

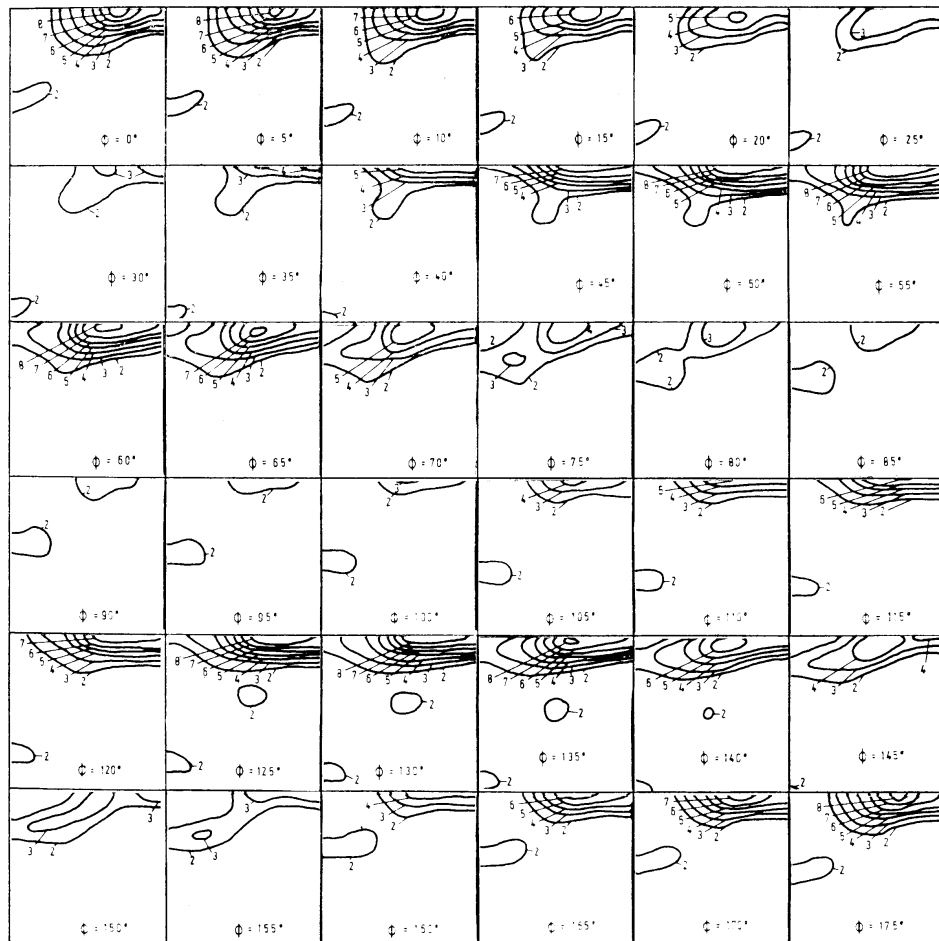


Figure 11.25 Orientation density for 80% cold-rolled uranium. After MORRIS²¹⁴

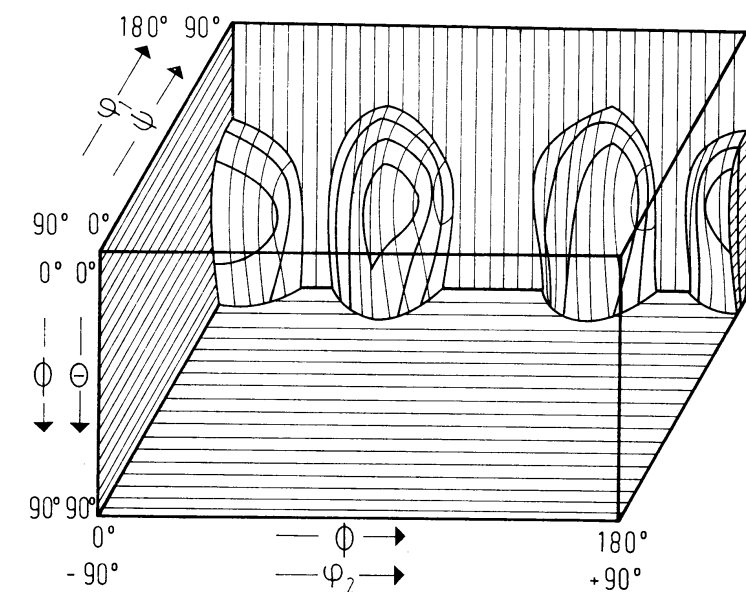


Figure 11.26 Spatial representation of the surface of half-maximum density of the texture of uranium²¹⁴

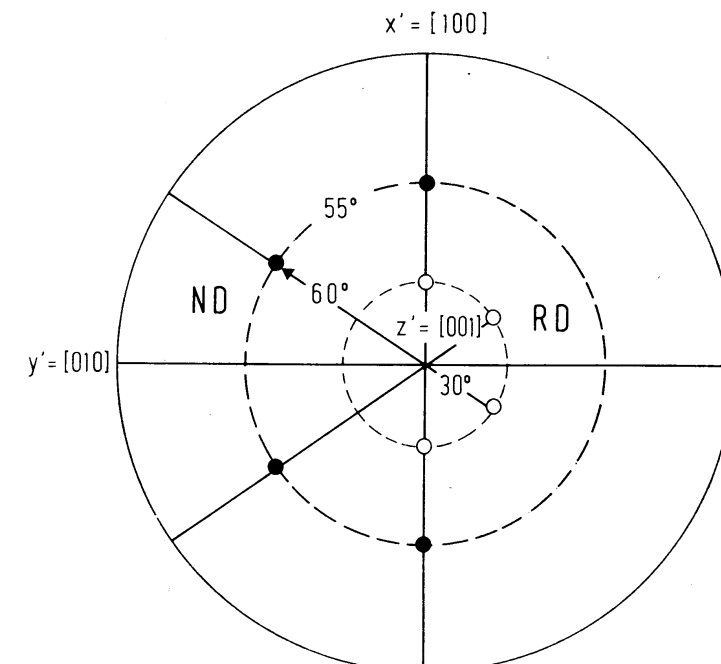


Figure 11.27 The orientations of maximum density (ideal orientations) for 80% cold-rolled uranium²¹⁴

calculation is reproduced in *Figure 11.25*. Since the maximum negative value is about -1 , contour lines for $f > 1$ are indicated. The maximum orientation density is 8. The half-value surface is represented in perspective in *Figure 11.26*. As one sees, the texture consists of two symmetrically non-equivalent orientations, which are represented in stereographic projection in *Figure 11.27*.

11.1.6.2. Biaxially Deformed Polyethylene (Separation of Partial Coincidences)

The texture of biaxially deformed polyethylene was studied by KRIGBAUM, ADACHI and DAWKINS¹⁸³. Multiple coincidences of different pole figures thereby occur (partial coincidences), whose overlapping factors q_i are not known. They must also be adjusted during the calculation of the coefficients C_l^{uv} . The measured

Table 11.2 CRYSTALLOGRAPHIC DATA OF POLE FIGURES FOR POLYETHYLENE

<i>i</i>	<i>hkl</i>	2θ	q_i
1	(110)	21.62°	1.000
2	(200)	24.02°	0.967
			0.033
3	(210)	30.15°	0.993
	(200)	24.02°	0.007
4	(020)	36.38°	1.000
5	(011)	39.79°	0.794
	(310)	40.85°	0.206
6	(310)	40.85°	0.510
	(011)	39.79°	0.387
	(110)	41.69°	0.103
7	(111)	41.69°	0.552
	(310)	40.85°	0.356
	(201)	43.07°	0.092
8	(201)	43.07°	0.801
	(220)	44.07°	0.199
	(111)	41.69°	0.000
9	(211)	47.01°	0.969
	(400)	49.18°	0.031
10	(311)	55.00°	0.884
	(121)	53.14°	0.116
11	(130)	57.32°	0.637
	(221)	57.61°	0.363
12	(401)	61.92°	0.549
	(230)	61.64°	0.287
	(420)	61.69°	0.164
13	(002)	74.42°	0.429
	(520)	74.74°	0.380
	(231)	73.12°	0.191

pole figures, their indices, crystallographic angles and the overlapping factors obtained are given in *Table 11.2*. The orientation distribution function is reproduced in some sections in *Figure 11.28*. Since in the original work a normalization of the distribution function was used, which differs from that used here by a factor of $8\pi^2$, in *Figure 11.28* new contour lines were constructed in multiples of the random distribution by interpolation.

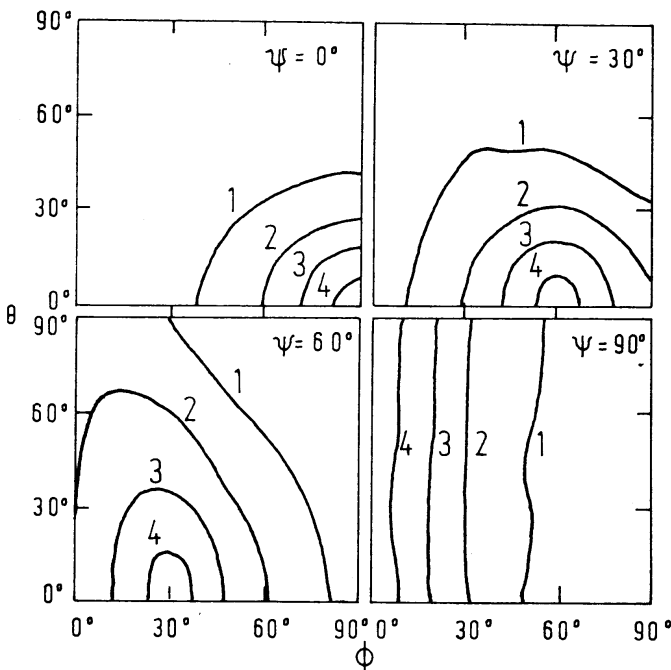


Figure 11.28 The orientation distribution function of a biaxially stretched polyethylene sample. After KRIGBAUM et al.¹⁸³

11.1.7. Hexagonal Crystal Symmetry

The calculation of the orientation distribution function in the case of hexagonal crystal symmetry and orthorhombic sheet symmetry was developed and carried out for the first time by MORRIS and HECKLER²¹⁹. They investigated a titanium sheet cold-rolled 65% and annealed 3 min at 1450°F. The following four pole figures were measured: (0110), (0111), (0112), (0002). The series was extended up to $l = 16$. The orientation distribution function in 5° steps so obtained is shown in *Figure 11.29*. It shows a maximum of the orientation density at $\Psi = 90^\circ$, $\Theta = 45^\circ$ which extends from $\Phi = 0^\circ$ to $\Phi = 60^\circ$ (according to the second definition of the EULER angles). The angles $\Psi = 90^\circ$, $\Theta = 45^\circ$ correspond to an orientation of the [0001] crystal direction in the plane ND-TD under 45° to the normal direction, whereas the angle Φ corresponds to a rotation about the

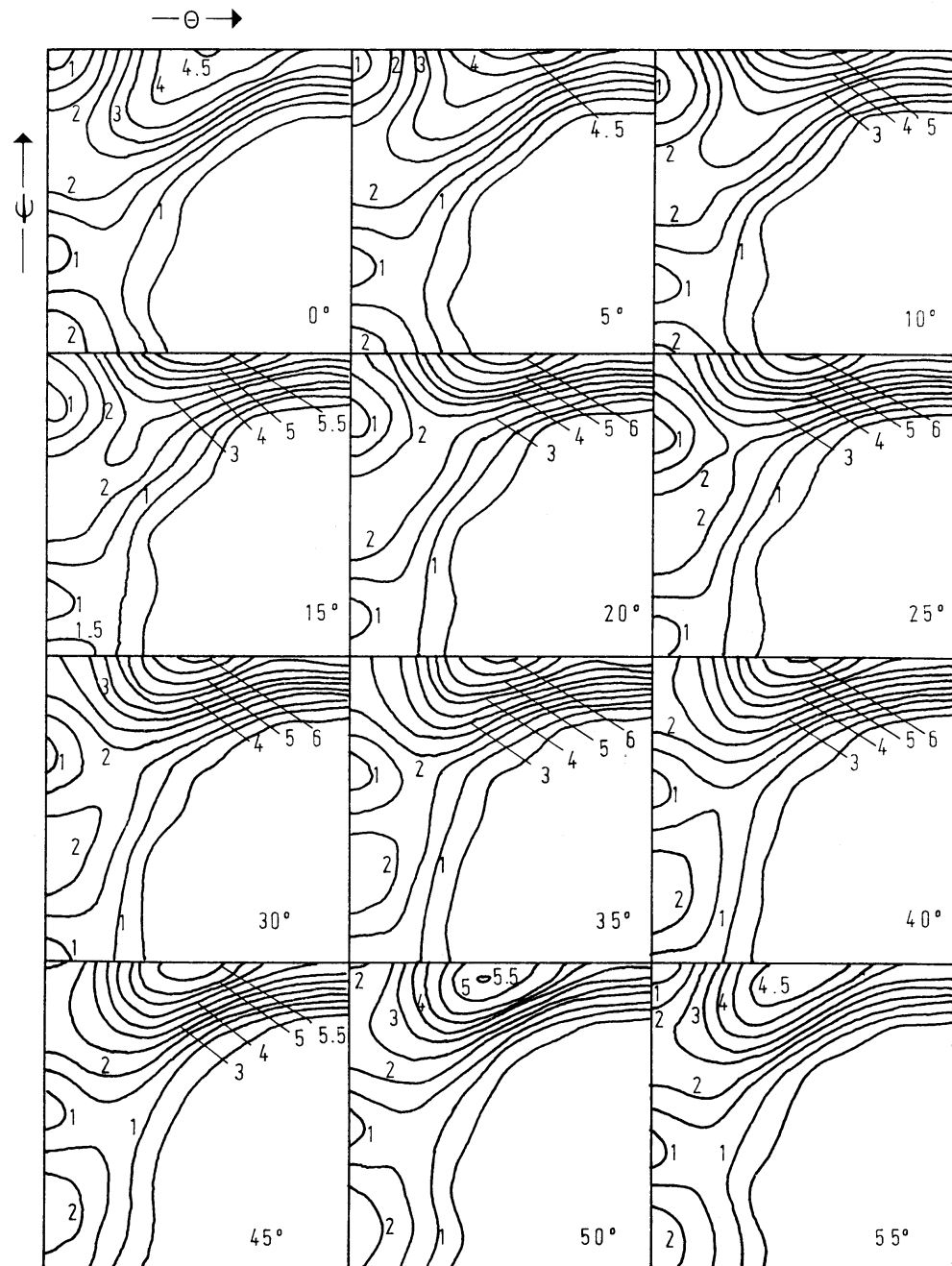


Figure 11.29 The orientation distribution of a titanium sheet cold-rolled 65% and annealed for 3 min at 1450°F. After MORRIS and HECKLER²¹⁹

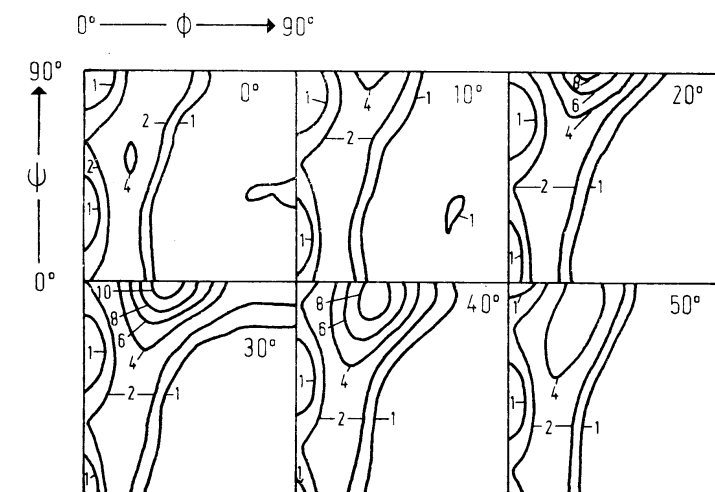


Figure 11.30 The orientation distribution function for a titanium sheet cold-rolled 95%. After DERVIN et al.¹⁰⁷

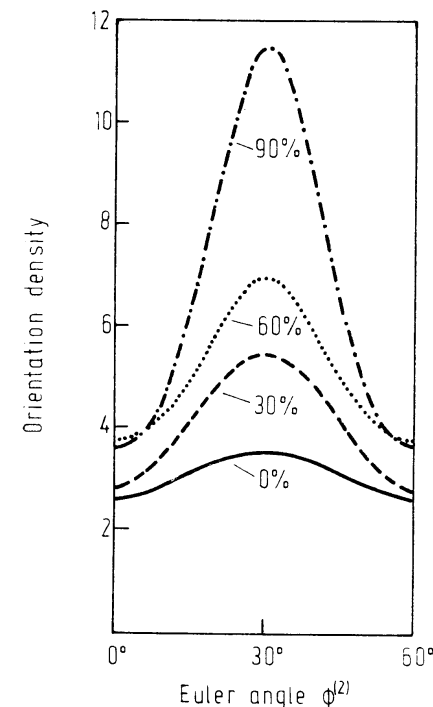


Figure 11.31 Orientation density along the line $\Psi = 90^\circ$, $\Theta = 35^\circ$ as a function of the Euler angle Φ for titanium sheet cold-rolled to different degrees of deformation¹⁰⁷

[0001] direction. Besides the pronounced preferred orientation of the [0001] direction, there is thus a moderate preference for the [0110] direction parallel to the rolling direction. Furthermore, a small amount of cube orientation is to be found. Similar results have been obtained by DERVIN *et al.*¹⁰⁷ in 90% cold-rolled titanium sheet. Figure 11.30 shows the ODF calculated in the same approximation but in 10° steps. The angle Θ (that is, the inclination of the [0001] direction with respect to the normal direction), however, is found to be 35° in this investigation. The development of the rolling texture with the degree of deformation is shown in Figure 11.31, which gives the orientation density along the line $\Psi = 90^\circ$, $\Theta = 35^\circ$ as a function of the third angle Φ — that is, for crystals having their [0001] direction in a fixed position but with various directions parallel to the rolling direction. The curve corresponding to a rolling degree of $\eta = 60\%$ is very similar to the corresponding values for $\eta = 65\%$ in Figure 11.29.

The texture of recrystallized magnesium was determined by DILLAMORE, HADDEN and STRATFORD¹¹⁰ by ODF methods.

11.1.8. Trigonal Crystal Symmetry (Separation of Real Coincidences)

The case of trigonal crystal symmetry was treated by BUNGE and WENK⁸⁶. They investigated natural quartz samples, which have no sample symmetry (I) (whereas BAKER and WENK¹⁷ studied monoclinic sample symmetry). According to Table 14.9,

Table 11.3 CRYSTALLOGRAPHIC DATA OF POLE FIGURES FOR QUARTZ

Diffraction peak $2\theta(\text{CuK}_\alpha)$	Indices $hkil$	Crystallographic angles θ	Relative intensity q_{hkil}	Difference $q_{hkil} - q_{khil}$
26.7°	1011	51.8	0.0	0.70
	0111	51.8	60.0	0.30
36.6°	1120	90.0	30.0	1
42.5°	2020	90.0	0.0	1
45.8°	2021	68.5	0.0	0.30
	0221	68.5	60.0	0.70
50.2°	1122	47.7	30.0	1
50.7° (6)	0003	0.0	0.0	1
60.0°	2131	73.4	19.1	0.54
60.0°	1231	73.4	40.9	0.46
	1123	36.2	30.0	1
73.5°	1014	17.7	0.0	0.22
	0114	17.7	60.0	0.78
mean value				0.36

this symmetry combination gives rise to the space group $P\bar{1}n\Theta$ with the asymmetric region $(\pi, \pi, 2\pi/3)$. Nine pole figures were measured, which are given in Table 11.3. Because of the overlap of the (0003) pole figure by the (1122) pole figure, however, the first was not used in the calculation. In the trigonal symmetry the $(hkil)$ and $(khil)$ reflections systematically have the same BRAGG angle, although they are symmetrically not equivalent. There thus occurs a case of systematic coincidences of the pole figures, as is discussed in Section 4.2.2.2. Since the BRAGG angles are here exactly equal, the relative intensities of the two overlapping reflections are proportional to the squares of the respective structure factors. The coefficients of the relative intensities of the overlapping pole figures are thus known; they are given in Table 11.3 as q_{hkil} . Thus we are concerned here with the simpler case of real coincidences with known superposition coefficients. The coefficients F_l^v were calculated from the pole figures, the C_l^{vv} from the F_l^v and, finally, the orientation distribution function $f(\varphi_1 \Phi \varphi_2)$ in the approximation $L = 14$. In the trigonal case according to Figure 4.4 this approximation requires at least five pole figures in order for a unique solution of equation (4.61) to be possible. Hence, the present calculations were carried out with an overdetermination of three pole figures. Since the essential character of the orientation distribution can already be recognized from the $\varphi_1 = 0$ section, only this section is represented in Figure 11.32. We are thus concerned with two preferred orientations

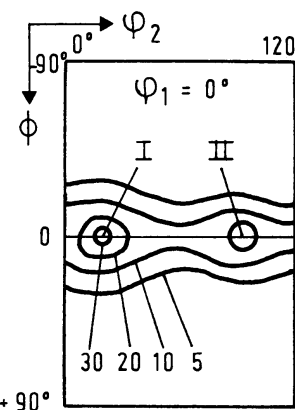


Figure 11.32 The $\varphi_1 = 0$ section of the orientation distribution function of a natural quartz sample⁸⁶

with the $Z' = [0001]$ crystal direction parallel to the sample direction Z , while the $X' = [10\bar{1}0]$ crystal direction forms 40° and 95° angles with the X sample direction. The two orientations occur with different intensities (Figure 11.33) and an extended scatter region is present between them. The comparison between measured pole figures and those recalculated from the C_l^{vv} coefficients is reproduced

in Section 10.5 in *Figure 10.7*. One sees that the recalculated pole figures do not reach as high maximum values as the measured ones. This may be associated with a certain series truncation error, which one can recognize with the aid of the error curves (*Figure 11.34*). The coefficients for $l = 14$ have still not completely decreased to the order of their errors. The error analysis is carried out in *Figure 11.34* separately for the C_l^{mn} with even and odd m and n indices. Coefficients with n

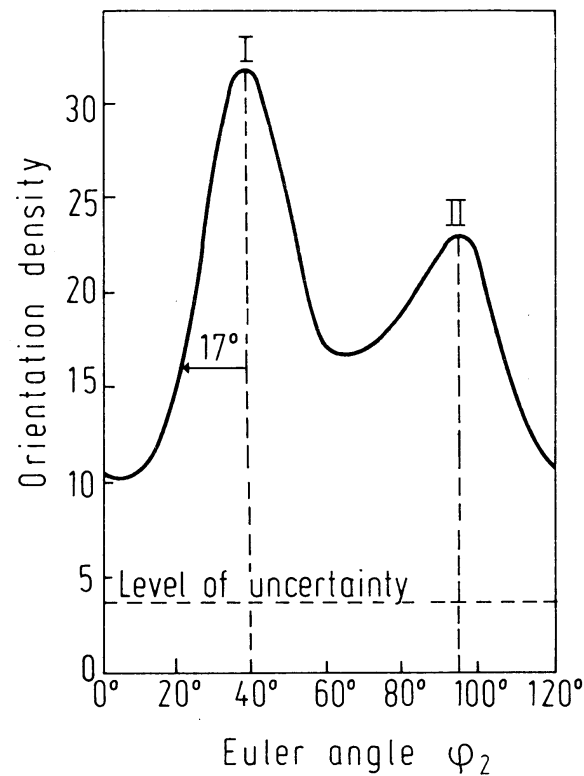


Figure 11.33 Orientation density along the intersection $\varphi_1 = \Phi = 0$ of the quartz texture⁸⁶

even correspond to a twofold axis of the sample symmetry parallel to the Z -direction, and with m even they correspond to a twofold axis of the crystal symmetry parallel to the Z' -direction. The two orientations denoted by I and II are rotated into each other by a 60° or, by consideration of the 120° crystal symmetry, a 180° rotation, whereby the rotation axis lies in the common Z - and Z' -direction of the crystal and sample coordinate systems. If they occurred with equal intensity, the orientation distribution would possess the twofold axes mentioned. Since

in *Figure 11.34* at least some of the coefficients are significantly larger than their errors, one must conclude that the deviation from the twofold axis is beyond the limit of error. Certainly, the deviation with respect to a function possessing this symmetry is comparatively small, as the error analysis for the coefficients with even m and n in *Figure 11.34* shows. One can thus carry out a symmetry analysis of the texture distribution with the help of the error analysis of *Figure 11.34*.

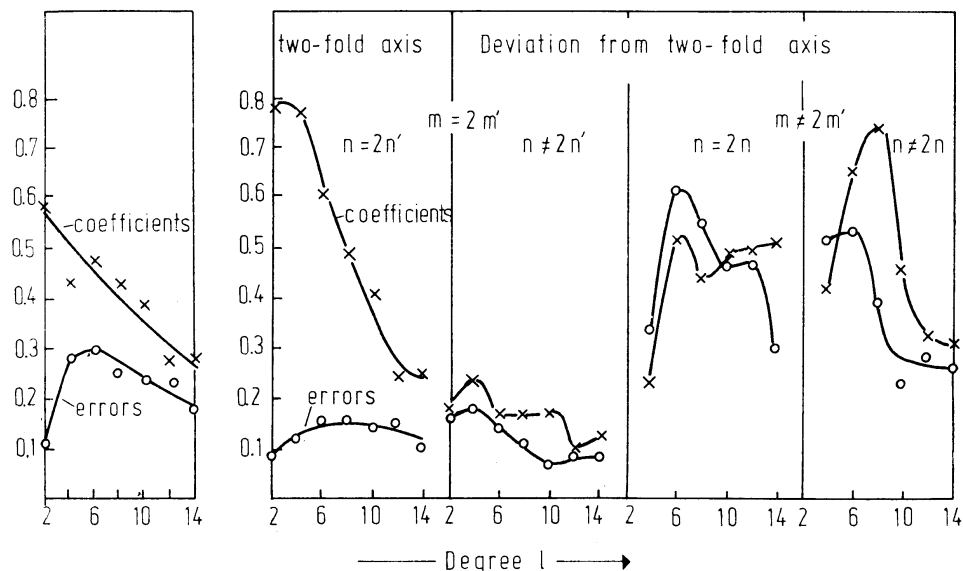


Figure 11.34 The average values of coefficients and their errors for the quartz texture. Left, for all coefficients; right, separated for even and uneven values of the indices m and n ⁸⁶

From the C_l^{mn} coefficients those of the pole figures, F_l^v , can be calculated and thus the pole figures themselves. Comparison of these recalculated pole figures with the experimental ones (*Figure 10.7*) will be used for the estimation of the accuracy of the process. In this way the $(hk\bar{l})$ and $(kh\bar{l})$ pole figures can naturally also be calculated, which, because of the same BRAGG angle, are not separately measurable. The differences between the weight factors, $q_{hk\bar{l}} - q_{kh\bar{l}}$, which enter into the calculation leading to separation of the pole figures, are small compared with their sums in *Table 11.3*, which enter into the overlapping pole figures. The average value of these differences amounts to about 0.36. That is, the separated pole figures — e.g. $(10\bar{1}1)$ and $(01\bar{1}1)$ (*Figure 11.35*) — are affected with about threefold higher uncertainty than their sum, $(10\bar{1}1) + (01\bar{1}1)$. One recognizes this qualitatively from the poor appearance of the separated pole figures compared with the overlapping ones.

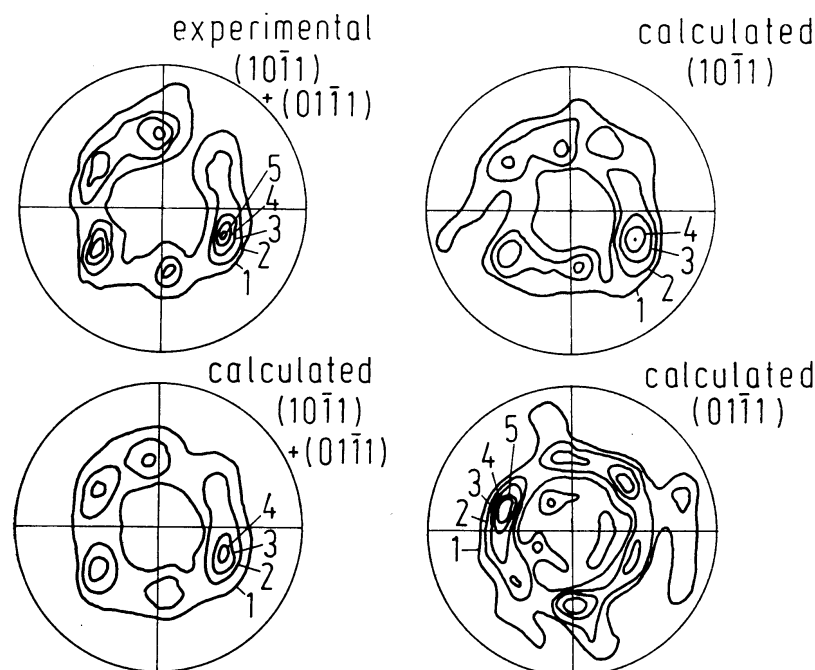


Figure 11.35 The pole figures $(10\bar{1}1)$ and $(01\bar{1}1)$ for the quartz texture: (1) experimentally measured overlap of the two pole figures; (2) recalculated overlapping pole figure; (3) calculated $(10\bar{1}1)$ pole figure; (4) calculated $(01\bar{1}1)$ pole figure

11.1.9. Transformation Textures

11.1.9.1. The Transformation Texture in Duplex $\alpha - \beta$ Brass

The transformation texture, which is formed by transformation of b.c.c. β -brass into f.c.c. α -brass, was investigated by DAVIES, KALLEND and MORRIS^{101,102} in a common commercial Cu—40.5% Zn alloy. Figure 11.36 shows the texture of b.c.c. β -brass, which was measured on a quenched sample. It can be regarded as the starting texture before the transformation. The texture of the transformed f.c.c. α -brass was studied on a slowly cooled sample (Figure 11.37). The expected transformation texture was calculated from the texture of β -brass, according to the method described in Chapter 8 with the KURDJUMOV—SACHS relation. This is represented in Figure 11.38. One sees that it is very similar to the measured texture of Figure 11.37.

11.1.9.2. Calculation of the Orientation Relation from Starting and Transformed Textures

One can also deduce the transformation relations from the experimentally determined textures of α - and β -brass, by solution of equation (8.11) for the $w_t^{\mu\lambda}$.

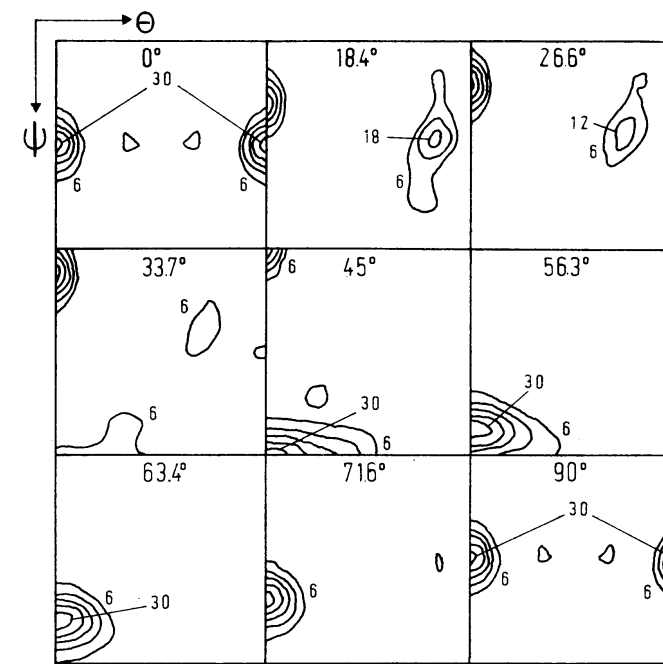


Figure 11.36 Orientation distribution of the quenched b.c.c. β -phase of a Cu—40.5% Zn alloy. After DAVIES et al.¹⁰¹

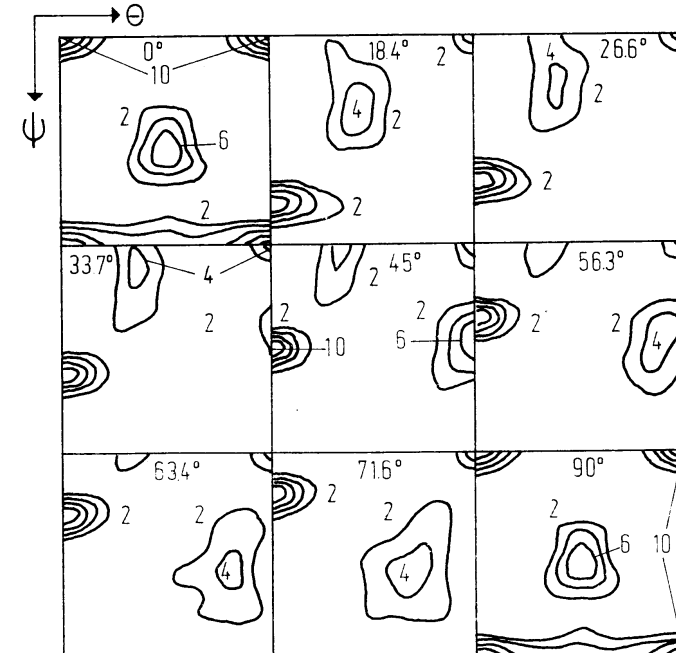


Figure 11.37 Orientation distribution of a slow-cooled f.c.c. α -phase of a Cu—40.5% Zn alloy. After DAVIES et al.¹⁰¹

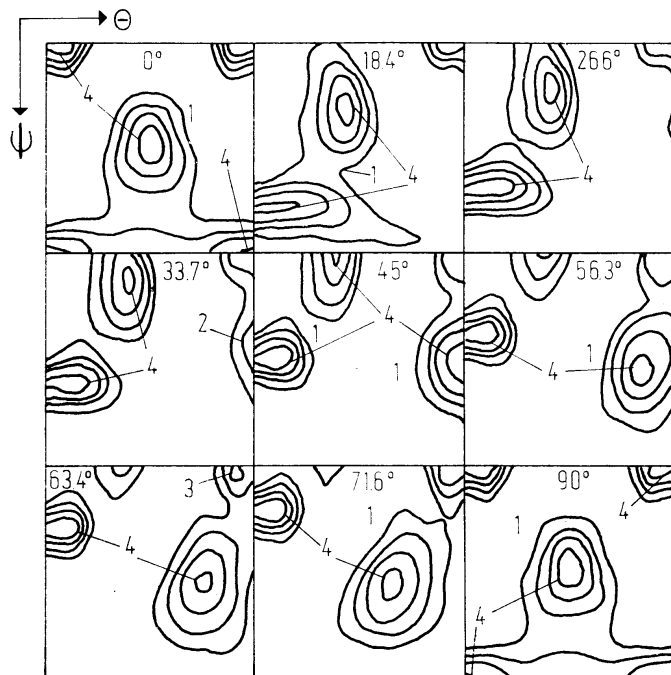


Figure 11.38 The orientation distribution of the α -phase calculated from the texture of the β -phase with the help of the KURDJUMOV—SACHS relation. After DAVIES *et al.*¹⁰¹

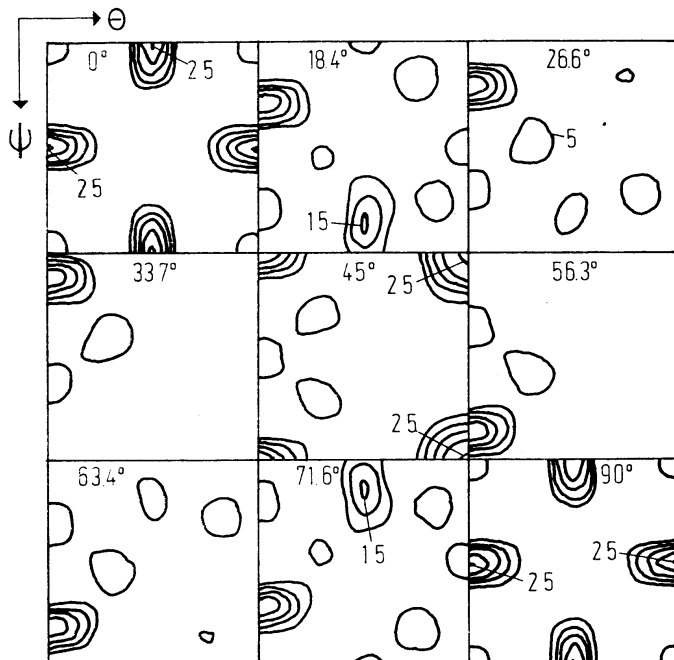


Figure 11.39 The orientation transformation function calculated from the textures of the α - and β -phases. After DAVIES *et al.*¹⁰¹

The corresponding transformation function according to reference 101 is represented in Figure 11.39. It agrees quite well with the distribution function for the KURDJUMOV—SACHS relation (Figure 8.4). The validity of this orientation relation for the α — β transformation can therefore be regarded as having been demonstrated. To be sure, as was shown in Chapter 8, the KURDJUMOV—SACHS relation is not distinguishable from the NISHIYAMA—WASSERMANN relation in this approximation. And in fact the agreement with the latter (Figure 8.3) must be regarded as even better.

11.1.9.3. Calculation of the Initial Texture of a Steel (Austenite) from the Transformation Texture (Ferrite)

The texture of the high-temperature phase can frequently not be measured. One would like to recalculate this texture from the texture of the low-temperature phase (i.e. after the transformation has occurred) and the transformation rule. Equation (8.11) is therefore to be solved for the coefficients $C_l^{xy}(1)$. The textures of a steel which was hot-rolled 80% at two different temperatures, 815°C and 1000°C, in the γ -phase and then quenched, were measured by DAVIES *et al.*¹⁰². The textures were thus measured for the b.c.c. α -iron. They are represented in Figures 11.40 and 11.41. The supposed starting textures recalculated therefrom

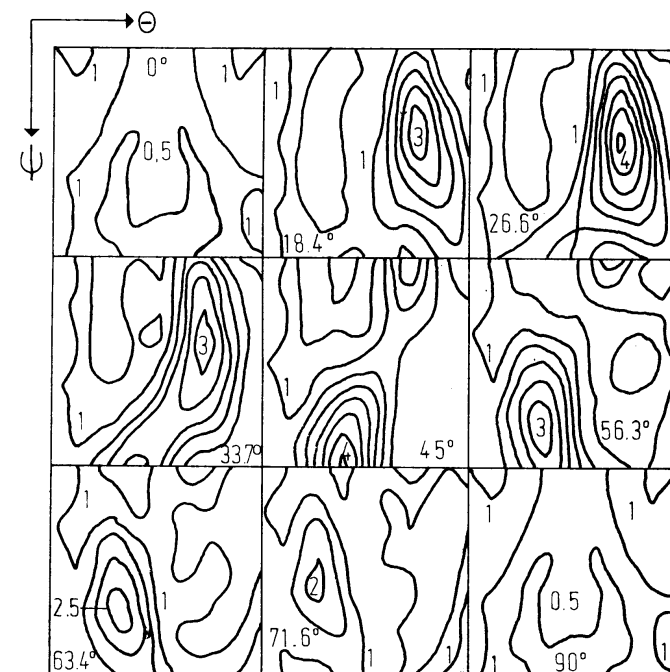


Figure 11.40 Orientation distribution of a carbon steel which was hot-rolled 80% at 815°C. After KALLEND *et al.*¹⁷⁷

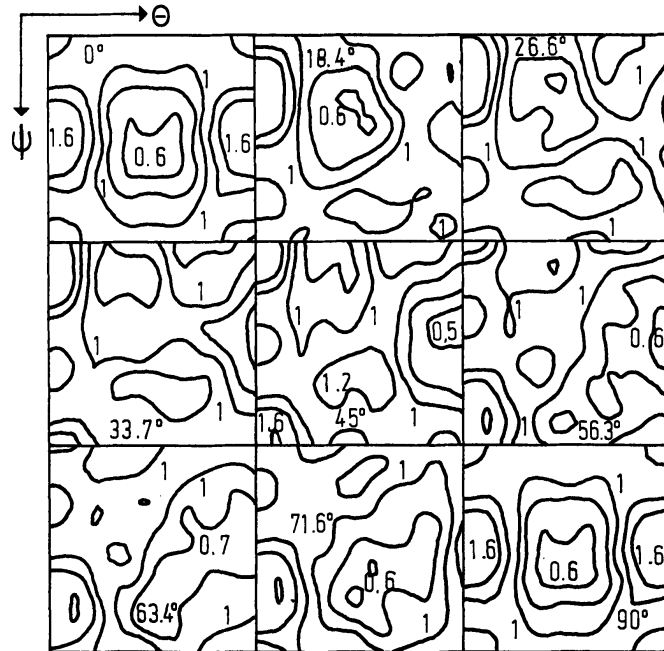


Figure 11.41 Orientation distribution of a carbon steel which was hot-rolled 80% at 1000°C. After KALLEND et al.¹⁷⁷

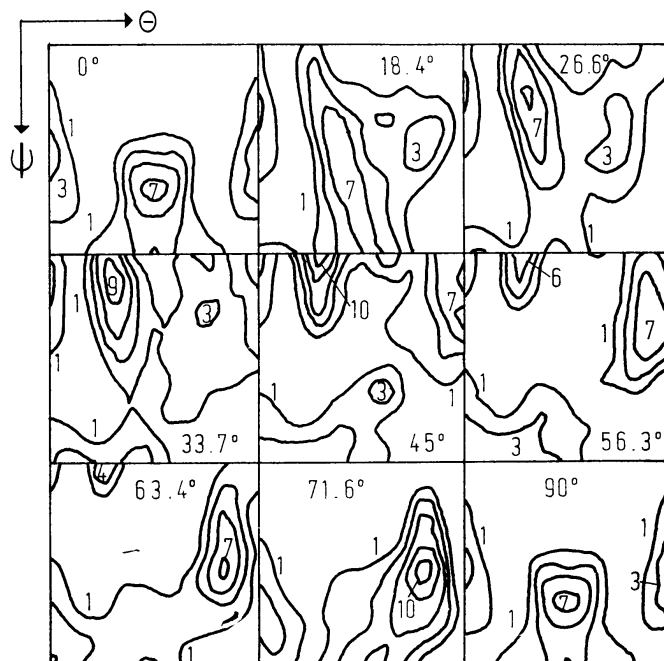


Figure 11.42 The orientation distribution of γ -iron hot-rolled at 815°C, calculated from the texture of α -iron with the help of the KURDJUMOV—SACHS relation. After KALLEND et al.¹⁷⁷

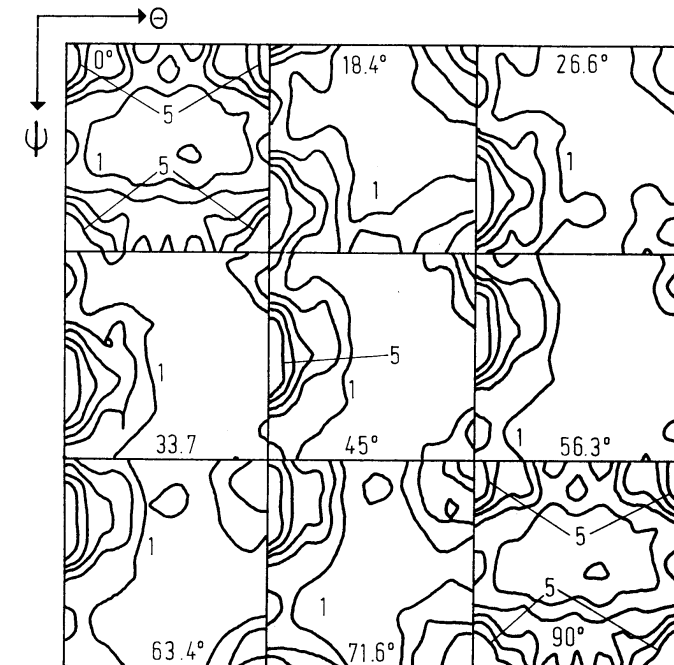


Figure 11.43 The orientation distribution of γ -iron hot-rolled at 1000°C, calculated from the texture of α -iron with the help of the KURDJUMOV—SACHS relation. After KALLEND et al.¹⁷⁷

with the help of the KURDJUMOV—SACHS relation are to be seen in Figures 11.42 and 11.43. One sees that the first is very similar to the rolling texture of f.c.c. metals, while the second essentially gives a cube texture. In the first case one may assume that the transformation of the rolling texture of the f.c.c. γ -phase into the b.c.c. α -phase occurs, while in the second case evidently transformation of the recrystallization texture of the γ -phase occurs.

11.1.10. Cubic-triclinic Symmetry

The case of triclinic (i.e. no) sample symmetry plays a role, particularly in the deformation of single crystals. Calculation programs for the cubic-triclinic case were given by CLÉMENT and DURAND⁹¹ as well as by POSPIECH and JURA^{168,236}. A calculation of an orientation distribution function was carried out by JURA¹⁶⁸. The (111) pole figure of an 80% cold-rolled aluminium crystal according to a measurement of LÜCKE, RIXEN and SENNA²⁰⁴ is represented in Figure 11.44(a). The orientation distribution function in the approximation $l = 22$ was calculated from this pole figure as well as the (100), (220) and (311) pole figures (Figure 11.45).

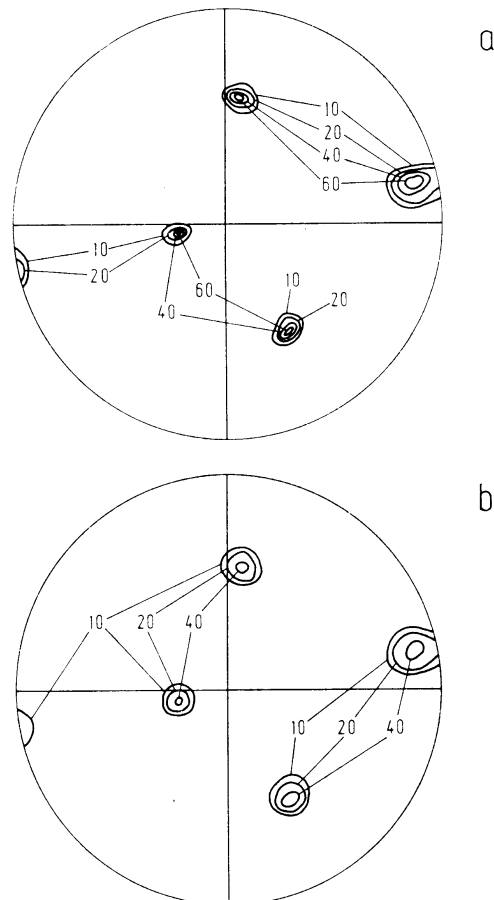


Figure 11.44 The (111) pole figure of an 80% cold-rolled aluminium single crystal according to LÜCKE et al.²⁰⁴ (a) as well as the pole figure recalculated from the coefficients $C_l^{\mu\nu}$ (b). The sample symmetry is triclinic

According to Table 14.9, the asymmetric unit for cubic-triclinic symmetry amounts to π , π , $\pi/2$, which is equivalent to 2π , $\pi/2$, $\pi/2$ used in Figure 11.45. The (111) pole figure recalculated from the $C_l^{\mu\nu}$ coefficients is represented in Figure 11.44(b).

11.1.11. Representation of the Orientation Distribution Function by Rotation Axis and Rotation Angle

The orientation distribution function $f(g)$ was represented in the coordinates $\vartheta\psi\omega$ of the rotation axis and the rotation angle by POSPIECH and JURA^{232,235,236}. The $C_l^{\mu\nu}$ coefficients were first calculated according to the process described in Chapter 4 and calculation of the orientation distribution function followed according to

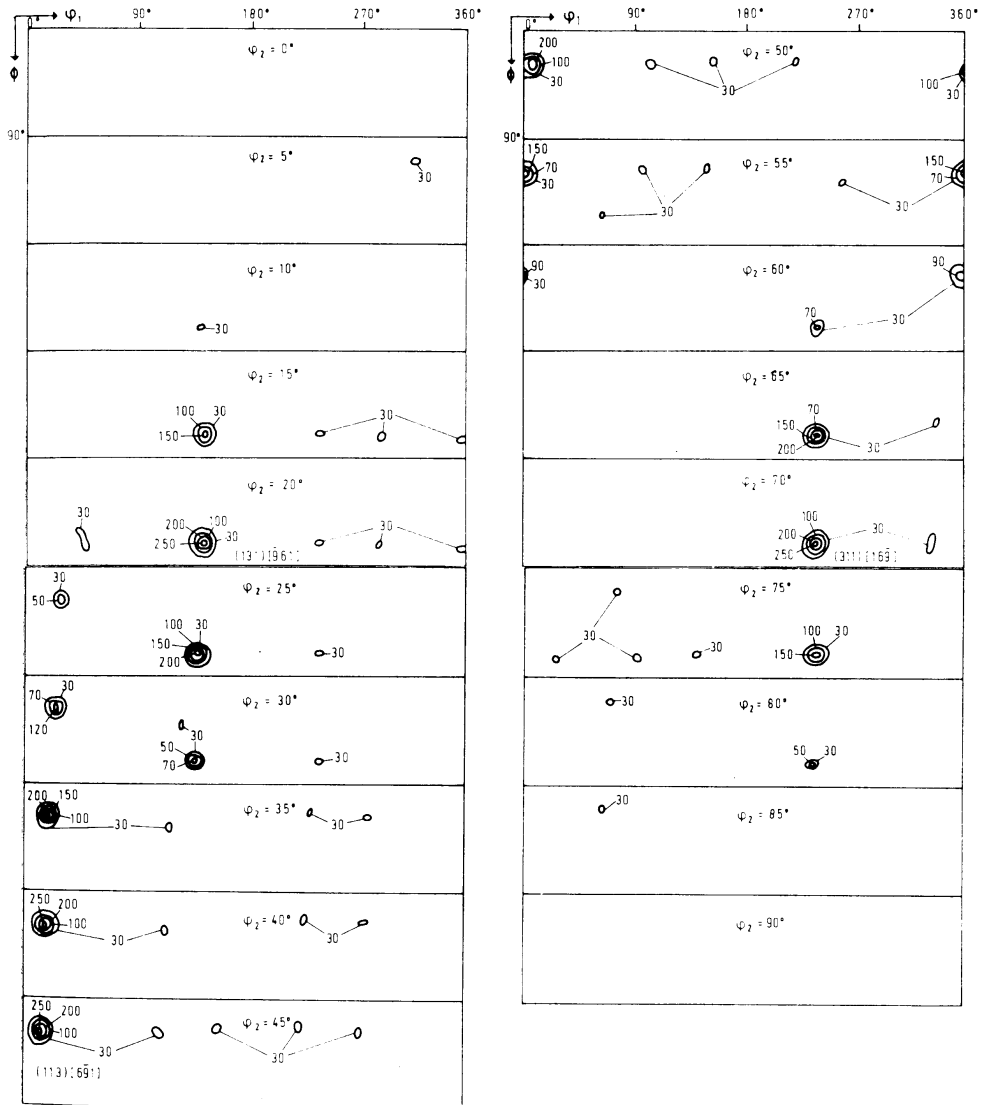


Figure 11.45 The orientation distribution function of an 80% cold-rolled aluminium crystal corresponding to the symmetry combination cubic-triclinic. After JURA¹⁶⁸

equation (4.7). The coordinate transformation

$$f(g) = f[\varphi_1(\vartheta\psi\omega), \Phi(\vartheta\psi\omega), \varphi_2(\vartheta\psi\omega)] = f(\vartheta\psi\omega) \quad (11.1)$$

was introduced and the function was calculated for points 'equidistant' in $\vartheta\psi\omega$. The orientation distribution function for an Fe–3% Si transformer steel is at first given in the representation by means of EULER angles in Figure 11.46. Fig-

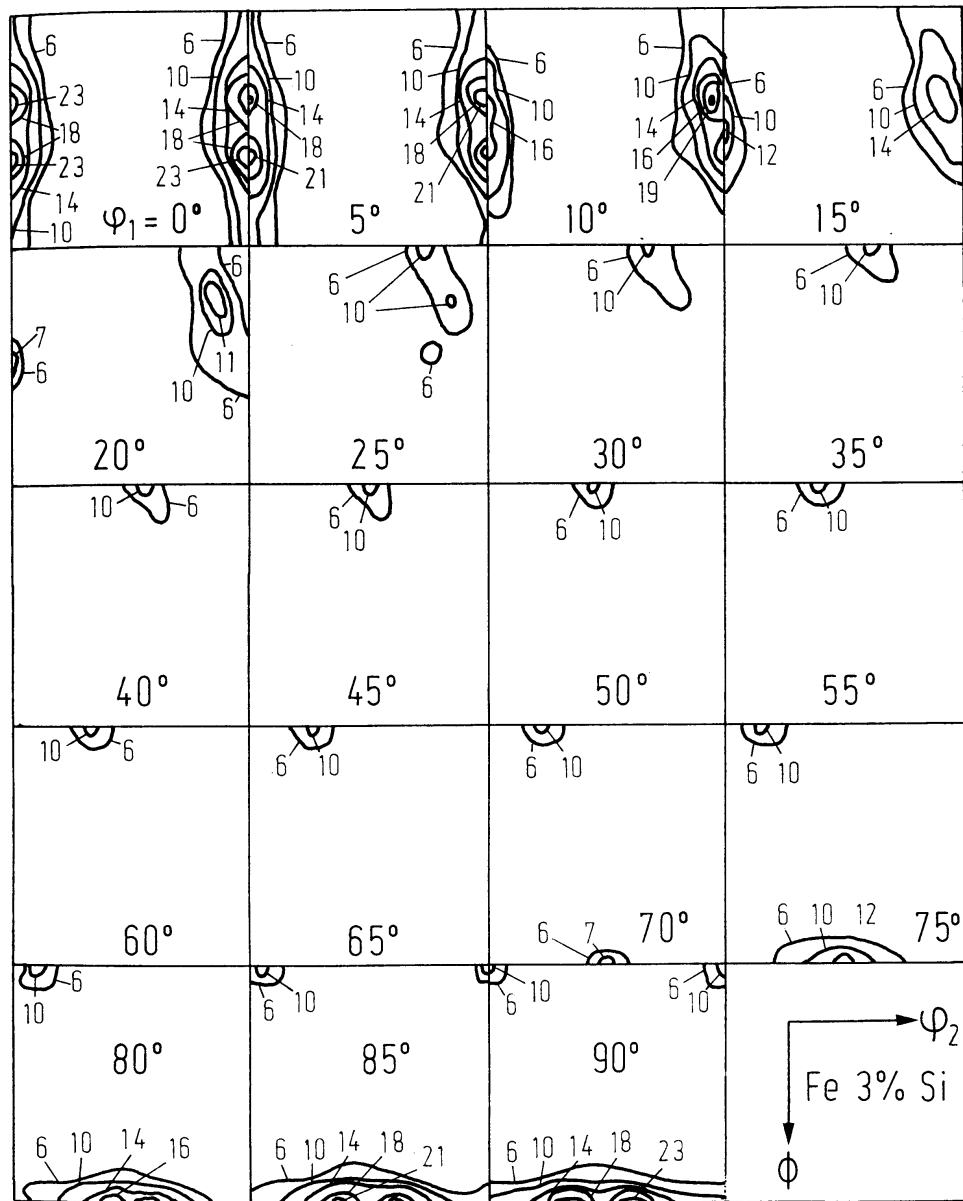


Figure 11.46 The orientation distribution function for an Fe-3% Si transformer steel in the coordinates $\phi_1\Phi\phi_2$. After POSPIECH and JURA²³⁵

Figure 11.47 shows the same distribution function in the representation by means of the rotation coordinates $\vartheta\psi\omega$, where these coordinates are plotted as Cartesian coordinates. Finally, the same function is given in Figure 11.48 in $\vartheta\psi\omega$ coordinates in the volume true representation (see Section 2.1.9).

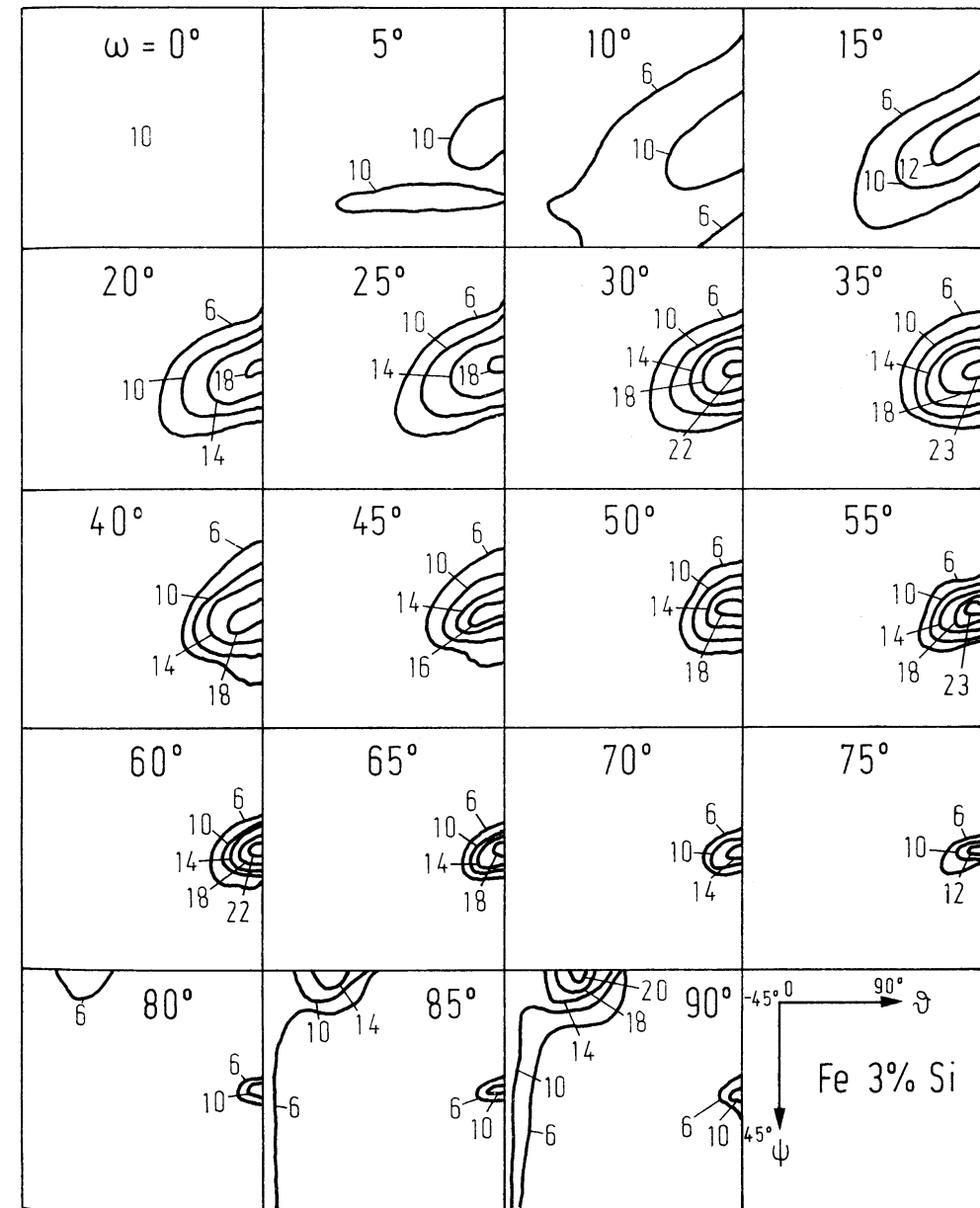


Figure 11.47 The same distribution function as Figure 11.46 in the coordinates $\vartheta\psi\omega$ in Cartesian representation. After POSPIECH and JURA²³⁵

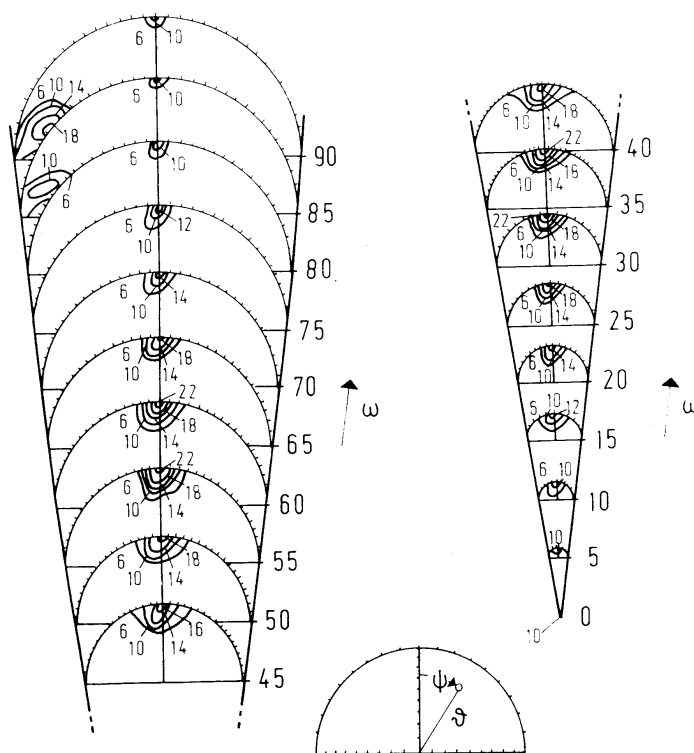


Figure 11.48 The same distribution as Figure 11.47 in the coordinates $\theta\psi\omega$ in volume-true representation. After POSPIECH²³²

11.2. Fibre Textures

Since the method for calculation of three-dimensional orientation functions was developed, interest in the investigation of fibre textures has sharply declined. This is principally because fibre textures, owing to the higher sample symmetry (rotational symmetry), can yield less information about processes in the material than three-dimensional textures.

11.2.1. The Drawing Texture of Aluminium Wires

The development of the deformation texture during drawing of aluminium wires was studied by BUNGE³⁹. Four pole figures — (111), (200), (220), (311) — were measured on commercially pure 99.6% aluminium and the inverse pole figure calculated in the $l = 22$ approximation. The starting texture was not a random one, but the recrystallization texture represented in Figure 11.49(a). The texture after 84% cold deformation is represented in Figure 11.49(b). It is essentially smoother than the starting texture. Only for high degrees of deformation does a sharp $\langle 111 \rangle$ texture form (Figure 11.49c). The course of the orientation densities in the principal orientations $\langle 111 \rangle$ and $\langle 100 \rangle$ is shown in Figure 11.50.

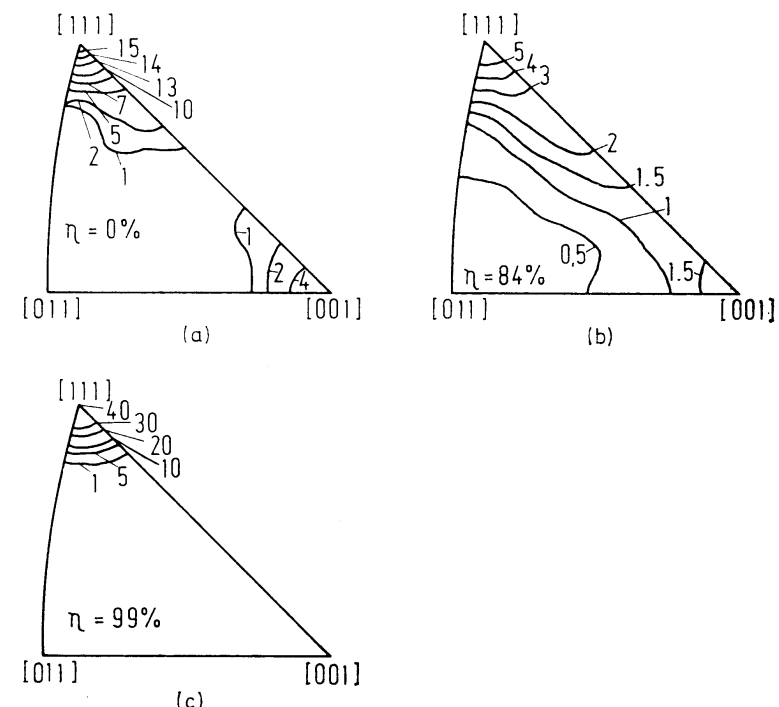


Figure 11.49 Inverse pole figures of aluminium wires calculated in the $l = 22$ approximation³⁹: (a) recrystallized; (b) 84% cold-drawn; (c) 99% cold-drawn

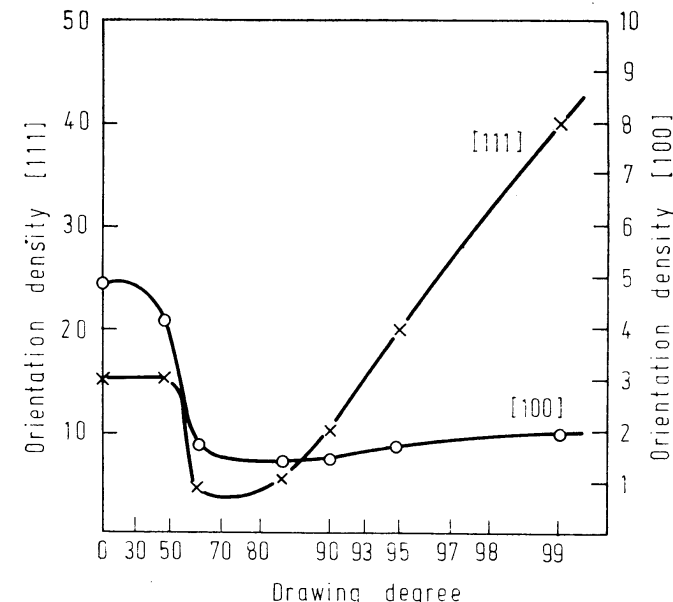


Figure 11.50 The orientation density in the orientations $\langle 111 \rangle$ and $\langle 100 \rangle$ of aluminium wires after various cold reductions³⁹

11.2.2. Transformation Texture in Au—Ge Taylor Wires

A process of producing very thin wires directly from the melt was described by TAYLOR²⁷⁹. The melt is contained in a glass tube which is drawn to a fine capillary. The melt in the glass tube therefore very quickly solidifies to a fine wire. In eutectic gold—germanium alloys a metastable h.c.p. phase thereby first forms, which transforms into the stable f.c.c. phase. Since this phase transformation can be assumed to occur in a crystallographically oriented manner, a certain texture of the h.c.p. phase should give rise to another texture in the resulting f.c.c. phase, related to the first one by a specific orientation relationship according to the considerations of Chapter 8. Fibre texture studies are thus well suited to the study of the mechanism of the phase transformation. *Figure 11.51* shows the texture

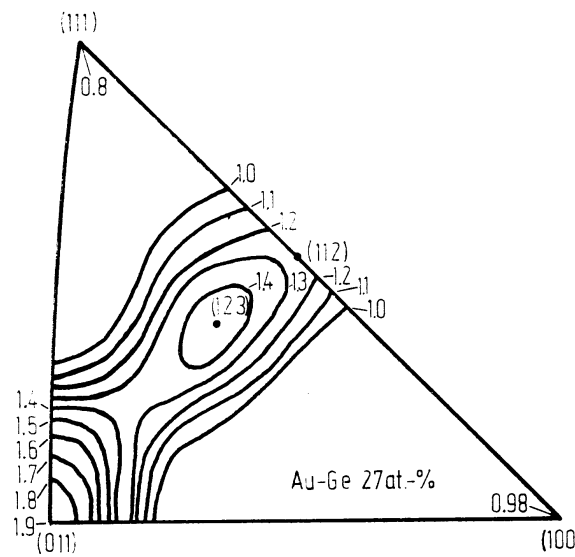


Figure 11.51 The inverse pole figure of the stable f.c.c. phase in a TAYLOR wire of the alloy Au—27% Ge⁷⁰

of the stable phase formed⁷⁰. It has a strong random component, as one recognizes from *Figure 11.52*, upon which is superimposed a sharp $\langle 111 \rangle$ ring fibre texture. In a ring fibre texture the preferred crystal direction is perpendicular to the fibre axis, so that in the direction of the fibre axis all crystal directions perpendicular to the preferred crystal direction occur with the same frequency, and thus all those on a great circle perpendicular to $\langle 111 \rangle$. This is the great circle which runs from $\langle 011 \rangle$ to $\langle 211 \rangle$. Two such circles intersect at the point $\langle 011 \rangle$, so that there the intensity assumes approximately the doubled value (about 1 compared with 0.5 for other points of the great circle). The random component has a density of about 0.9.

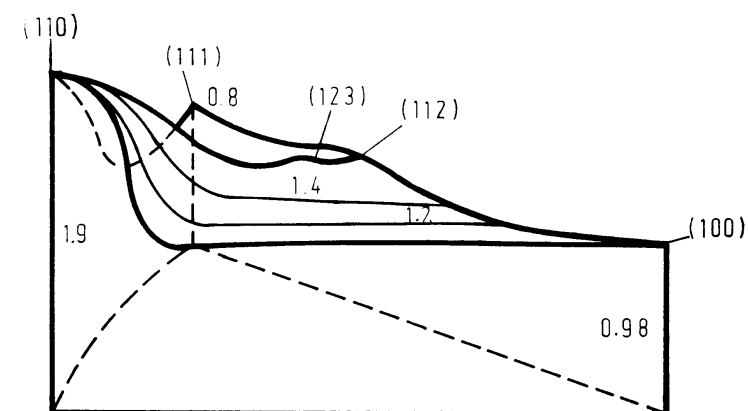


Figure 11.52 Spatial representation of the inverse pole figure of the Au—27% Ge TAYLOR wire

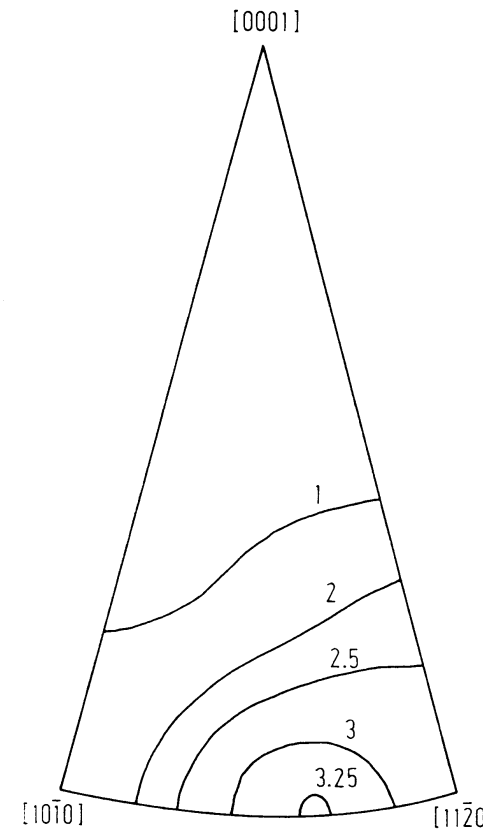


Figure 11.53 Inverse pole figure of an extruded Ti rod. After HAESSNER and SCHRÖDER¹⁴²

11.2.3. Hexagonal Crystal Symmetry (Titanium)

The drawing texture of a 99.8% commercially pure titanium bar is given in *Figure 11.53*. It was calculated from measured (0001), (1010), (1012), (1120) pole figures in the $L = 16$ approximation¹⁴². For the relatively smooth texture this approximation suffices for calculation of the inverse pole figure. No large truncation error will thus occur.

11.2.4. Orthorhombic Crystal Symmetry (Separation of Partial Coincidences)

A fibre texture of polyethylene, a material with orthorhombic crystal symmetry, was studied by KRIGBAUM and ROE¹⁸⁵. The problem was the separation of partial coincidences, as in the case of biaxially stretched polyethylene with three-dimensional texture. Twelve pole figures were measured (*Table 11.4*), of which some were threefold coincident. The series expansion was extended up to $l = 16$, which was sufficient for the not very sharp texture. The (020) measured pole figure, together with that calculated from the C_l^{μ} , is represented in *Figure 11.54*. The inverse pole figure is shown in *Figure 11.55*.

Table 11.4 BRAGG ANGLES AND MILLER INDICES OF A POLYETHYLENE SAMPLE.
AFTER KRIGBAUM AND ROE¹⁸⁵

	2θ	21.62°	24.02°	30.15°	36.38°	39.79°	40.85°	41.69°	43.07°	47.01°	55.00°	57.32°	61.92°
hkl	110	200	210	020	011	310	111	201	211	311	130	401	
					310	011	310	220		130	221	230	
					111	201	111				420		

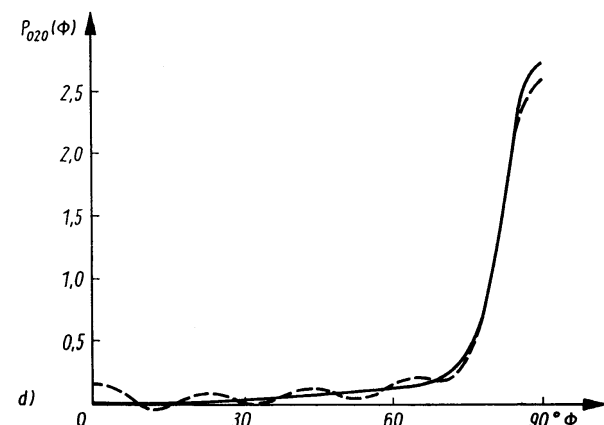


Figure 11.54 The (020) pole figure of a uniaxially stretched polyethylene sample together with the curve recalculated from the C_l^{μ} in the $l = 16$ approximation. After KRIGBAUM and ROE¹⁸⁵

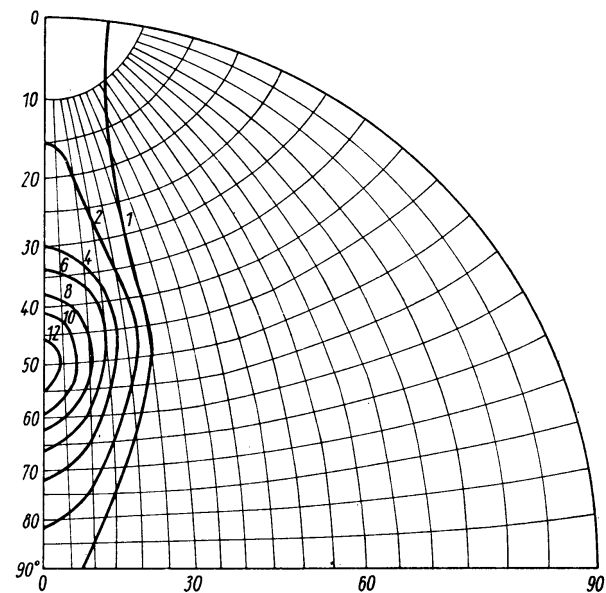


Figure 11.55 The inverse pole figure of a uniaxially stretched polyethylene sample calculated in the $l = 16$ approximation. After KRIGBAUM and ROE¹⁸⁵

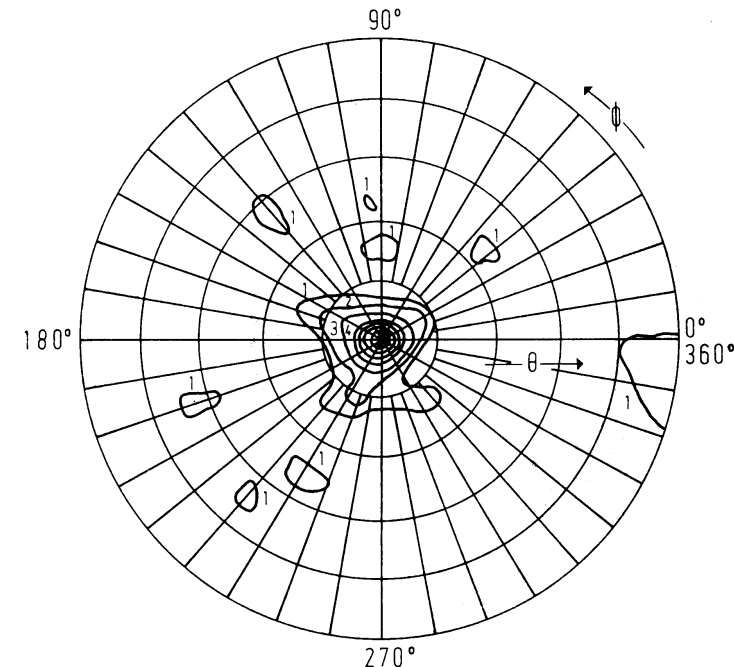


Figure 11.56 Orientation distribution (inverse pole figure) of the stretching direction of a stretched polyethylene terephthalate sample. It was calculated from measured pole figures in the $l = 16$ approximation with the help of KRIGBAUM's refinement procedure. After KRIGBAUM and VASEK¹⁸⁶

11.2.5. Triclinic Crystal Symmetry (Application of the Refinement Procedure)

The texture of stretched polyethylene terephthalate (triclinic crystal symmetry and rotational sample symmetry, i.e. fibre texture) was investigated by KRIGBAUM and BALTA¹⁸⁴ and KRIGBAUM and VASEK¹⁸⁶. The lattice constants are $a = 4.54 \text{ \AA}$, $b = 5.94 \text{ \AA}$, $c = 10.75 \text{ \AA}$, $\alpha = 98.5^\circ$, $\beta = 118.0^\circ$, $\gamma = 112.0^\circ$. The low crystal symmetry requires a very large number of pole figures; otherwise a very small value l_{\max} results, up to which one can solve the equation system (4.61). The refinement method developed by KRIGBAUM¹⁸², by which the coefficients beyond l_{\max} can be calculated (see Section 4.9.2), was therefore used. In this way the texture can be determined in the $l = 16$ approximation. This is represented in Figure 11.56. One sees that the c -axis of the crystal is oriented very nearly parallel to the fibre axis.

11.2.6. Orientation Distribution of the Number of Crystallites and the Mean Grain Size

The orientation distribution functions considered up till now were orientation distribution functions of the volume corresponding to definition (3.3). If the polycrystalline material consists of well-defined crystallites, within which the orientation is constant, one can thus describe all orientation distribution functions according to equation (3.4) as distribution functions of the number of the crystallites. A method with which one can measure pole figures of the numbers was described by GO^{133a} and later by BUNGE⁴⁶. A portion of the pole sphere was reproduced on the film with the help of a special high-resolution film texture goniometer. Each

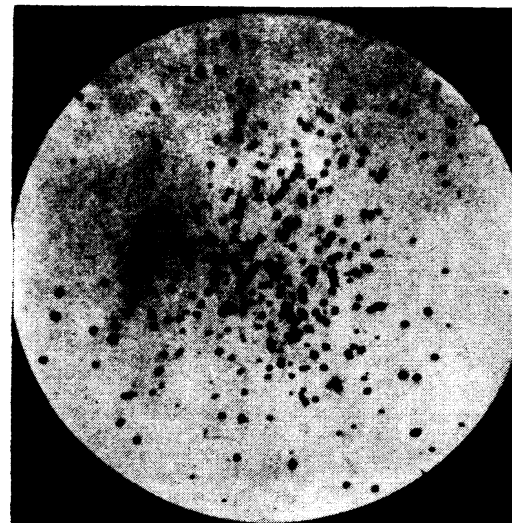


Figure 11.57 Part of a texture goniometer photograph for determination of pole figures of the number of crystals⁴⁶

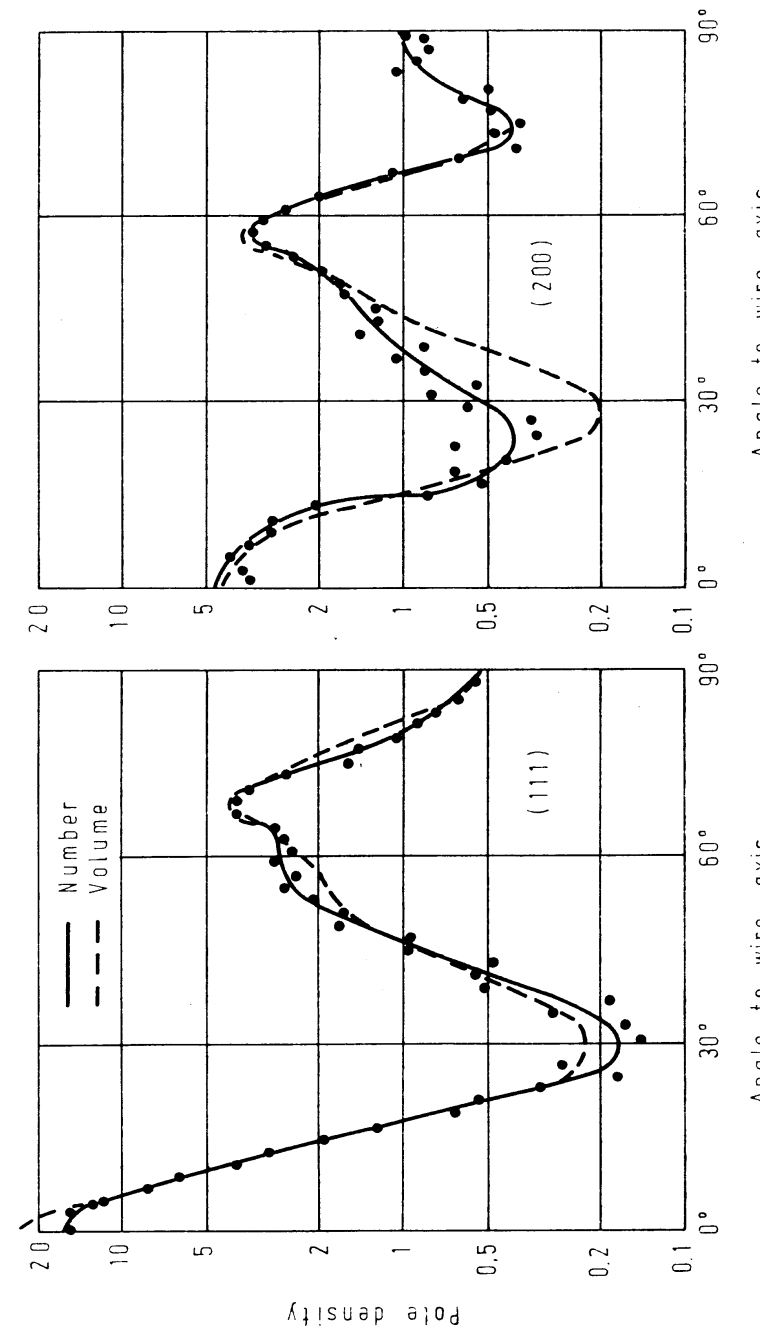


Figure 11.58 Pole figures of the number and the volume of a recrystallized aluminium wire⁴⁶

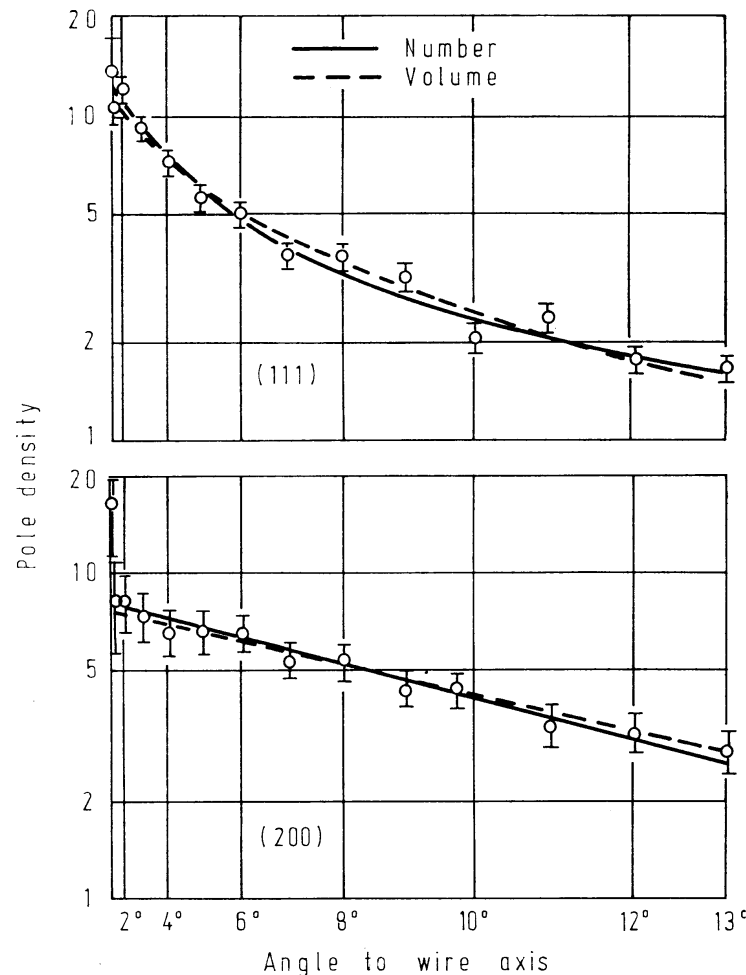


Figure 11.59 Course of the pole densities of the number and the volume in the neighbourhood of the two preferred orientations $\langle 111 \rangle$ and $\langle 100 \rangle$ ⁴⁶

crystallite causes a reflection on the film. One has then only to count the number of reflections in the various angular regions (Figure 11.57). In order to obtain sufficient statistics, in general, several exposures are evaluated to obtain a pole figure. Pole figures of recrystallized aluminium wires were determined by this method (Figure 11.58). They are in overall agreement with the corresponding volume pole figures, which were determined with a counter goniometer. The texture is the double $\langle 111 \rangle + \langle 100 \rangle$ fibre texture. One may conclude from Figure 11.58 that the average grain size is orientation independent. The two preferred orientations of the texture, $\langle 111 \rangle$ and $\langle 100 \rangle$, occur as a result of increased numbers of appropriate crystallites and not of particularly large crystallites. Two different theories were considered for the formation of the recrystallization textures: the theory

of oriented growth and the theory of oriented nucleation. According to the first, approximately equal numbers of crystallites should be present in all orientations; those in the vicinity of the preferred orientations, however, will grow more quickly to larger size. This theory is thus not in agreement with the experimental results of Figure 11.58. According to the theory of oriented nucleation, crystal nuclei will preferentially form in certain orientations; they will then, however, grow to approximately equal sized crystallites. This idea is compatible with the results of Figure 11.58. Table 11.5 shows the average grain size calculated from the sample volume studied and the number of crystallites. The distribution in the neighbourhood of the two preferred orientations is represented in more detail in Figure 11.59. The statistical errors which result from the number of crystallites are there given. One sees that the pole figures of the number and the volume agree within the error limits.

Table 11.5 AVERAGE GRAIN SIZE ACCORDING TO NUMBER AND VOLUME MEASUREMENTS

Pole figure	Sample volume, V (μm^3)	Number of crystallites, N	Mean grain size, $\frac{V}{N}$ (μm^3)
(111)	$6.2 \cdot 10^6$	5920	1050
(200)	$7.1 \cdot 10^6$	7245	980

11.2.7. Shape of the Spread about Preferred Orientations

The orientation distribution function or, in the case of fibre textures, the inverse pole figure can describe completely arbitrary distributions of the crystallites. Frequently, however, there results a simple distribution rule which permits good reproduction with fewer parameters. Some such special distribution functions were considered more precisely in Chapter 7. Among these, GAUSSIAN-type distributions about certain preferred orientations are particularly simple (see Section 7.7). The question is, however, in how far or in which cases GAUSSIAN distributions are good approximations of real distribution functions. Hence, the shape of the spread about the preferred orientations has been precisely investigated in some fibre textures^{26,27}. The pole densities of the (111) and (200) pole figures of a recrystallized aluminium wire were previously plotted in a form which translates a GAUSSIAN into a straight line (see Figure 11.59). One sees that the spread about the $\langle 100 \rangle$ preferred orientation can be well represented by a GAUSSIAN, while this is clearly not the case for the $\langle 111 \rangle$ orientation. Figure 11.60 shows the inverse pole figure of an aluminium wire cold-rolled 97% and recrystallized 30 min at 400°C. It was calculated from eight measured pole figures in the $l = 50$ approximation⁴⁹. One sees that the spread around the two preferred orientations is not rotationally symmetric, that, on the contrary, it reflects the symmetries of the two directions ($\langle 100 \rangle$ fourfold, $\langle 111 \rangle$ threefold). The course of the spread about the two preferred orientations in each of the two principal directions is represented in Figure 11.61.

One finds the spread about the $\langle 100 \rangle$ orientation to be described approximately by a Gaussian in both directions, although with slightly different half-value widths. In the neighbourhood of the $\langle 111 \rangle$ orientation one finds a Gaussian-shaped course only in the direction towards the $\langle 110 \rangle$ orientation, while the spread in the direction towards $\langle 100 \rangle$ can be represented as the sum of two Gaussians.

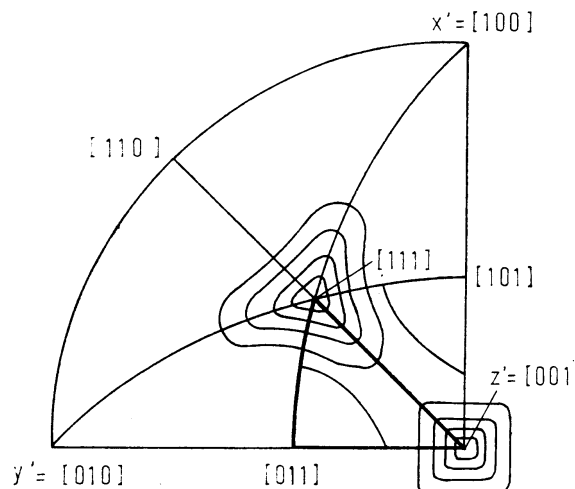


Figure 11.60 Inverse pole figure of an aluminium wire cold-drawn 97% and recrystallized at 400°C for 30 min⁴⁹

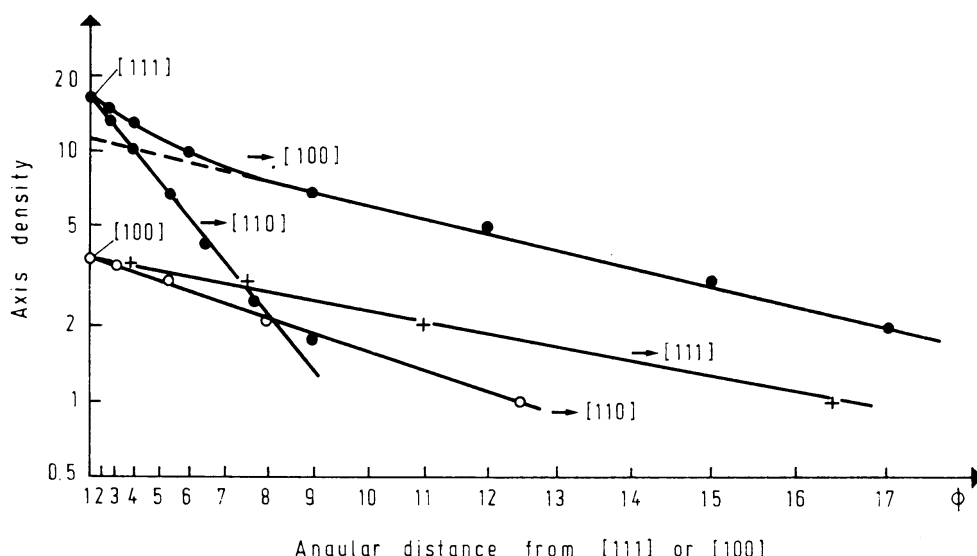


Figure 11.61 Course of the spread in the neighbourhood of the preferred orientations $\langle 111 \rangle$ and $\langle 100 \rangle$ of Figure 11.60

12. Orientation Distribution Functions of Other Structural Elements

The X-ray diffraction method of texture determination yields information concerning the orientation distribution function of either the volume $f(g)$ or the number $n(g)$ of crystallites. The different orientation correlation functions can not be determined in this way. Further, since the diffraction of X-rays is a volume effect, one obtains no information from it about the spatial and crystallographic distribution of grain boundaries and grain edges, and thus the two- and one-dimensional elements of the structure. It is therefore necessary to use other methods for determination of these quantities — first of all, the observation of crystallites, grain boundaries and grain edges on the outer surface of the sample, which can be either the natural surface or an artificially prepared cut surface. An arbitrary surface passing through the sample intersects the three-, two- and one-dimensional elements of the structure which are in each case reduced by one dimension, and thus into grain surfaces, grain boundary lines and corner points. The spatial distribution of the corresponding quantities must then be determined from the distribution of these elements. This problem has a certain similarity to that of the determination of the three-dimensional function $f(g)$ from different two-dimensional pole figures which was treated in the previous chapters.

12.1. Orientation Distribution Functions of the Grain Surfaces

We consider a certain choice among the crystallites of a structure — for instance, all those whose orientation g lies within the element of orientation dg , or those which have a certain orientation difference Δg with respect to their neighbours, or whose crystal directions \mathbf{h} point in a specific sample direction \mathbf{y} . We now make a planar cut through the structure perpendicular to the direction \mathbf{y} . It cuts the grains in a surface dO and the whole sample in the surface O . We imagine the cut surface to be displaced in the direction \mathbf{y} from y_1 to y_2 . The surface dO thus passes through the volume dV of the grains considered. It is

$$dV = \int_{y_1}^{y_2} dO(y) dy \quad (12.1)$$

For simplicity we assume that the sample has a uniform cross-section and that the grains considered are randomly distributed in the structure. Then, except for statistical fluctuations, dO is independent of \mathbf{y} , and it is true that

$$dV = (y_2 - y_1) dO \quad (12.2)$$

Under these conditions the total volume is given by

$$V = (y_2 - y_1) O \quad (12.3)$$

It follows directly therefrom that

$$\frac{dV}{V} = \frac{dO}{O} \quad (12.4)$$

All distribution functions defined as volume distributions can accordingly be determined directly from the surface distribution in an arbitrary cut surface. The orientation of the cut surface thus plays no role. This is the basis of the metallographic and electron microscopic methods of texture determination, as well as of some X-ray diffraction and electron diffraction methods. These methods permit measurement of the orientations g_i and the cut surface O_i of individual grains. By analogy with equation (4.20), one thus obtains the coefficients of the series expansion of the orientation distribution function:

$$C_l^{\mu\nu} = (2l + 1) \frac{\sum_i O_i T_l^{*\mu\nu}(g_i)}{\sum_i O_i} \quad (12.5)$$

12.1.1. Orientation Distribution of the Crystallographic Planes in the Outer Surface of an Arbitrary Section

We now consider all those grains for which the outer surface normal \mathbf{y}_0 of the cut surface coincides with the crystal directions in the region between \mathbf{h} and $\mathbf{h} + d\mathbf{h}$. The total size of their surface is dO , and O is the whole outer surface. The orientation distribution of the outer surface is then given by

$$\frac{dO}{O} = \frac{1}{4\pi} r_{y_0}(\mathbf{h}) d\mathbf{h} \quad (12.6)$$

The volume distribution of these crystallites, however, is none other than the inverse pole figure belonging to the sample direction \mathbf{y}_0 :

$$\frac{dV}{V} = \frac{1}{4\pi} R_{y_0}(\mathbf{h}) d\mathbf{h} = \frac{1}{4\pi} A(\mathbf{h}, \mathbf{y}_0) d\mathbf{h} \quad (12.7)$$

For the orientation distribution of the crystal surfaces in a section perpendicular to the direction \mathbf{y}_0 it is therefore true that

$$r_{y_0}(\mathbf{h}) = R_{y_0}(\mathbf{h}) = A(\mathbf{h}, \mathbf{y}_0) \quad (12.8)$$

If one has somehow measured the orientation distribution of the outer surface $r_{y_0}(\mathbf{h})$, one can thus determine the texture function $f(g)$ according to the method considered in Section 4.2.3. Conversely, equation (12.8) naturally also makes possible the calculation of the orientation distribution of the crystal surfaces in an arbitrary plane cut surface from X-ray diffraction texture measurements.

If the outer surface or cut surface is not plane, but curved in an arbitrary manner, we can thus consider it to be composed of small plane surface elements. We can describe the orientation distribution of these surface elements by the distribution function $O(\mathbf{y})$ of the normal directions. dO is the surface which has a normal direction between \mathbf{y} and $\mathbf{y} + d\mathbf{y}$, and O is the total surface. $O(\mathbf{y})$ is then defined by

$$\frac{dO}{O} = O(\mathbf{y}) d\mathbf{y} \quad (12.9)$$

For the distribution of crystal directions \mathbf{h} perpendicular to the outer surface of the curved section, one then obtains

$$r(\mathbf{h}) = \phi A(\mathbf{h}, \mathbf{y}) O(\mathbf{y}) d\mathbf{y} = \phi P_h(\mathbf{y}) O(\mathbf{y}) d\mathbf{y} \quad (12.10)$$

The frequency of occurrence of the crystal direction \mathbf{h} perpendicular to the outer surface is thus obtained by means of an integral over the pole figure $P_h(\mathbf{y})$ belonging to the direction \mathbf{h} . If the outer surface is a sphere or consists of many spheres (powder) or is completely random, the function $O(\mathbf{y})$ is independent of \mathbf{y} and it must be true that

$$O_r(\mathbf{y}) \equiv \frac{1}{4\pi} \quad (12.11)$$

Because of the normalization condition (4.66), in this case one obtains

$$r_r(\mathbf{h}) \equiv 1 \quad (12.12)$$

For arbitrary texture and spatially random arrangement of the crystal, the orientation distribution of the crystal surfaces in the outer surface is random if all normal directions occur with equal frequency in the cut surface (e.g. a powder).

12.2. Orientation Distribution Functions of the Grain Boundaries

The orientation of a grain boundary is defined by five parameters. Three parameters describe the orientation difference Δg of the two grains meeting in the grain boundary, and two others are necessary to fix the normal direction of the grain boundary surface with respect to one of the two crystal lattices. Since the orientation difference of the two lattices is fixed, the orientation of the normal direction is thus also determined in the other crystal lattice. The orientation distribution function of the grain boundaries is thus a function of five variables

$$F(\Delta g, \mathbf{h}) = F(\varphi_1 \Phi \varphi_2 \Theta \gamma) \quad (12.13)$$

where $\varphi_1 \Phi \varphi_2$ are the EULER angles of the orientation difference Δg and $\Theta \gamma$ are the polar coordinates of the direction \mathbf{h} , the normal direction of the boundary surface. The grain boundary energy is correspondingly also assumed to be a function of five variables

$$E_g = E(\varphi_1 \Phi \varphi_2 \Theta \gamma) \quad (12.14)$$

This five-dimensional function will frequently be considered too complicated. One can try then to separate the variables Δg and \mathbf{h} by splitting the five-dimensional function into a product of two functions

$$F(\Delta g, \mathbf{h}) = F_1(\Delta g) \cdot F_2(\mathbf{h}) \quad (12.15)$$

depending, respectively, on the orientation difference Δg and the orientation \mathbf{h} of the normal direction. Certainly, this is an approximation the validity of which must be proved. If, however, the approximation equation (12.15) seems acceptable, then the two functions $F_1(\Delta g)$ and $F_2(\mathbf{h})$ can be considered separately.

12.2.1. The Distribution Function $f(\Delta g)$ of the Orientation Differences

Let dF be the grain boundary surface between grains of orientation difference Δg to $\Delta g + d\Delta g$, and F the total grain boundary surface. One can then define the orientation distribution function of the orientation differences by

$$\frac{dF}{F} = f(\Delta g) d\Delta g \quad (12.16)$$

Δg is the rotation which transforms the axis system of one crystal, K_1 , into that of the other, K_2 . The function $f(\Delta g)$ must remain invariant if we carry out an operation of crystal symmetry in one of the two coordinate systems K_1 or K_2 . $f(\Delta g)$ can therefore be expanded in a series of generalized spherical harmonics, which satisfy the crystal symmetries on both sides:

$$f(\Delta g) = \sum_{l=0}^{\infty} \sum_{\mu=1}^{M(l)} \sum_{\mu'=1}^{M(l)} C_l^{\mu\mu'} \ddot{T}_l^{\mu\mu'} (\Delta g) \quad (12.17)$$

Since the function must also be invariant with respect to interchange of the two crystallites, it follows that

$$f(\Delta g^{-1}) = f(\Delta g) \quad (12.18)$$

Therefore it must be true that

$$C_l^{\mu\mu'} = C_l^{\mu'\mu} \quad (12.19)$$

For higher symmetry (e.g. cubic symmetry) the number of independent parameters of the function $f(\Delta g)$ is very small. For $l \leq 10$, for example, $M(l) = 1$. The function $f(\Delta g)$ in this approximation is therefore determined by five parameters:

$$f(\Delta g) = C_4^{11} \ddot{T}_4^{11}(\Delta g) + C_6^{11} \ddot{T}_6^{11}(\Delta g) + C_8^{11} \ddot{T}_8^{11}(\Delta g) + C_9^{11} \ddot{T}_9^{11}(\Delta g) + C_{10}^{11} \ddot{T}_{10}^{11}(\Delta g) \quad (12.20)$$

In the case of cubic crystal symmetry one can thus determine the orientation difference function with relatively high accuracy from relatively few measurements.

12.2.2. The Distribution Function $\varphi(\mathbf{y})$ of the Grain Boundaries in the Sample Fixed Coordinate System

Let dF be the grain boundary surface per unit volume whose normal lies parallel to the sample direction \mathbf{y} or deviates at most from it by $d\mathbf{y}$; F is the total grain boundary surface in the unit of volume. The orientation distribution of the grain boundary surfaces is then described by the function

$$\frac{dF}{F} = \frac{1}{4\pi} \varphi(\mathbf{y}) d\mathbf{y} \quad (12.21)$$

The function φ is expressed in multiples of the random distribution. We now consider a planar section of unit surface through the structure perpendicular to \mathbf{y}_0 (Figure 12.1). It cuts the surface elements of the normal orientation \mathbf{y} in a total length dz . If now we displace the plane in the direction of its normal \mathbf{y}_0 by unit length, the line of intersection with the grain boundary thus sweeps out the shaded surface in Figure 12.1:

$$dF = dz \frac{1}{\sin \langle \mathbf{y} \mathbf{y}_0 \rangle} \quad (12.22)$$

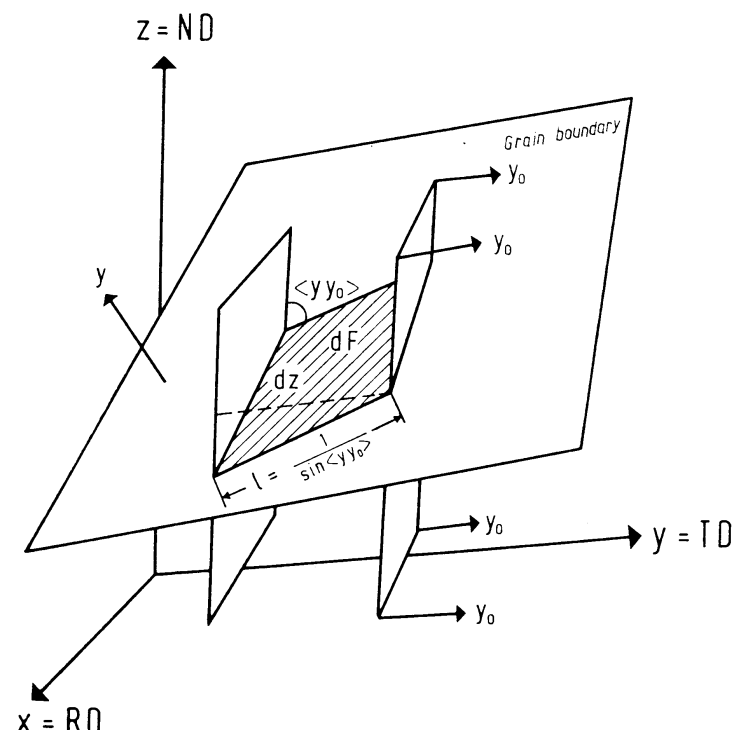


Figure 12.1 The surface swept out by the grain boundary line in the grain boundary by displacement of the cut surface in the direction \mathbf{y}_0

The length of intersection resulting from the surface elements of the normal orientation \mathbf{y} per unit of cutting surface is thus given by

$$dz = \frac{F}{4\pi} \varphi(\mathbf{y}) \sin \langle \mathbf{y} \mathbf{y}_0 \rangle d\mathbf{y} \quad (12.23)$$

The total length of grain boundary lines per unit surface is then given by¹⁵³

$$z(\mathbf{y}_0) = \frac{F}{4\pi} \oint \varphi(\mathbf{y}) \sin \langle \mathbf{y} \mathbf{y}_0 \rangle d\mathbf{y} \quad (12.24)$$

We develop $\varphi(\mathbf{y})$ in a series of spherical surface harmonics of the sample symmetry:

$$\varphi(\mathbf{y}) = \sum_{l=0}^{\infty} \sum_{r=1}^{N(l)} q_l^r k_l^r(\mathbf{y}) \quad (12.25)$$

We now introduce a spherical angular coordinate system Θ, ψ , whose pole coincides with the direction \mathbf{y}_0 . By use of equation (12.25), equation (12.24) then transforms into

$$z(\mathbf{y}_0) = \frac{F}{4\pi} \sum_{l=0}^{\infty} \sum_{r=1}^{N(l)} q_l^r \int_0^\pi \sin \Theta \left[\int_0^{2\pi} k_l^r(\Theta, \psi) d\psi \right] \sin \Theta d\Theta \quad (12.26)$$

If one substitutes for the integral in the brackets expression (14.200), one thus obtains

$$z(\mathbf{y}_0) = \frac{F}{2} \sum_{l=0}^{\infty} \sum_{r=1}^{N(l)} \sqrt{\frac{2}{2l+1}} q_l^r k_l^r(\mathbf{y}_0) \int_0^\pi \bar{P}_l(\Theta) \sin^2 \Theta d\Theta \quad (12.27)$$

If we set

$$\int_0^\pi \bar{P}_l(\Theta) \sin^2 \Theta d\Theta = A_l \quad (12.28)$$

we thus finally obtain

$$z(\mathbf{y}_0) = \frac{F}{2} \sum_{l=0}^{\infty} \sum_{r=1}^{N(l)} \sqrt{\frac{2}{2l+1}} q_l^r A_l k_l^r(\mathbf{y}_0) \quad (12.29)$$

Thus the total length of grain boundary lines per unit surface of a section of normal orientation \mathbf{y}_0 is here given by a series of spherical surface harmonics of the direction \mathbf{y}_0 with the coefficients

$$z_l^r = \frac{F}{2} \sqrt{\frac{2}{2l+1}} q_l^r A_l \quad (12.30)$$

Since the A_l are known quantities, the quantities Fq_l^r can be calculated from the z_l^r . Since the function $\varphi(\mathbf{y})$ was expressed in multiples of the random distribution,

the same normalization as equation (5.5) is valid for q_l^r . One thus obtains

$$z_l^1 = F \frac{\pi}{4} \sqrt{4\pi} \quad (12.31)$$

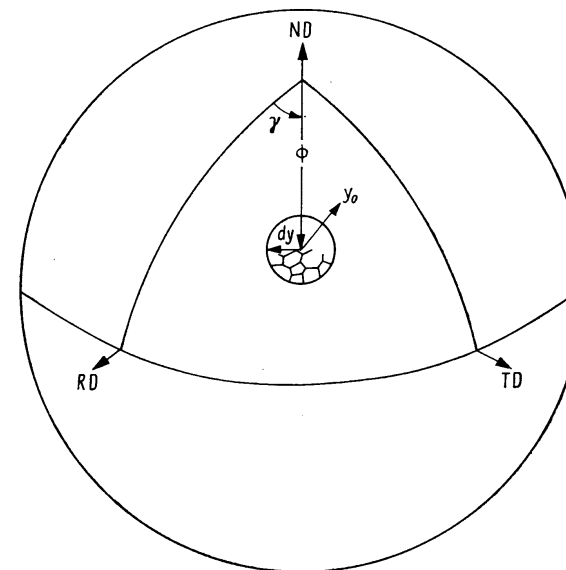


Figure 12.2 Surface element $d\mathbf{y}$ perpendicular to the direction \mathbf{y}_0 of a spherical sample

The coefficients z_l^r can be determined in different ways. We first assume that the function $z(\mathbf{y}_0)$ is known for very many directions \mathbf{y}_0 . This is the case, for example, for a spherical metallographic sample (Figure 12.2). It is then true that

$$z_l^r = \oint z(\mathbf{y}_0) k_l^{*r}(\mathbf{y}_0) d\mathbf{y}_0 \quad (12.32)$$

In particular, for $l = 0$ there results

$$z_0^1 = \frac{1}{\sqrt{4\pi}} \oint z(\mathbf{y}_0) d\mathbf{y}_0 \quad (12.33)$$

If we denote the average value of $z(\mathbf{y}_0)$ over all orientations \mathbf{y}_0 by $\overline{z(\mathbf{y}_0)}$,

$$\overline{z(\mathbf{y}_0)} = \frac{1}{4\pi} \oint z(\mathbf{y}_0) d\mathbf{y}_0 \quad (12.34)$$

We thus obtain from equation (12.31) the total grain boundary surface per element of volume:

$$F = \frac{4}{\pi} \overline{z(\mathbf{y}_0)} \quad (12.35)$$

$\bar{z}(\mathbf{y}_0)$ is the total length of grain boundary lines per unit surface of a spherical sample or the average value of this quantity over many differently oriented plane sections.

If the function $z(\mathbf{y}_0)$ is only known for certain directions \mathbf{y}_0 , the coefficients can be calculated up to a degree $l = L$ according to the interpolation method described by equations (4.81)–(4.87), where the function $z(\mathbf{y}_0)$ replaces the pole figure. Finally we consider the extreme case in which the function $z(\mathbf{y}_0)$ is known only for three mutually perpendicular directions, the rolling direction RD, the transverse direction TD and the normal direction ND. The sample symmetry will be the orthorhombic sheet symmetry. We can then determine an approximate expression of second degree for the function $\varphi(\mathbf{y})$. The three directions have the spherical angular coordinates

$$\text{RD} = \{90^\circ, 0^\circ\}; \quad \text{TD} = \{90^\circ, 90^\circ\}; \quad \text{ND} = \{0^\circ, 0^\circ\} \quad (12.36)$$

From equation (12.29), if one extends the sum to terms of second degree, therefore, results

$$z(\text{RD}) = \frac{F}{2} \left[\frac{\pi}{2} + \sqrt{\frac{2}{5}} \frac{1}{\sqrt{2\pi}} \bar{P}_2(90^\circ) A_2 \varphi_2^1 + \sqrt{\frac{2}{5}} \frac{1}{\sqrt{\pi}} \bar{P}_2^2(90^\circ) A_2 \varphi_2^2 \right] \quad (12.37)$$

$$z(\text{TD}) = \frac{F}{2} \left[\frac{\pi}{2} + \sqrt{\frac{2}{5}} \frac{1}{\sqrt{2\pi}} \bar{P}_2(90^\circ) A_2 \varphi_2^1 - \sqrt{\frac{2}{5}} \frac{1}{\sqrt{\pi}} \bar{P}_2^2(90^\circ) A_2 \varphi_2^2 \right] \quad (12.38)$$

$$z(\text{ND}) = \frac{F}{2} \left[\frac{\pi}{2} + \sqrt{\frac{2}{5}} \frac{1}{\sqrt{2\pi}} \bar{P}_2(0^\circ) A_2 \varphi_2^1 \right] \quad (12.39)$$

If one solves this system of equations for the unknowns $F, \varphi_2^1, \varphi_2^2$, one obtains

$$F = \frac{4}{3\pi} [z(\text{RD}) + z(\text{TD}) + z(\text{ND})] \quad (12.40)$$

$$\varphi_2^1 = \frac{3\pi}{8} \frac{\sqrt{5\pi}}{A_2 \bar{P}_2(90^\circ)} \frac{z(\text{RD}) + z(\text{TD}) - 2z(\text{ND})}{z(\text{RD}) + z(\text{TD}) + z(\text{ND})} \quad (12.41)$$

$$\varphi_2^2 = \frac{\frac{3}{4}\pi \sqrt{\frac{5}{2}\pi}}{A_2 \bar{P}_2^2(90^\circ)} \frac{z(\text{RD}) - z(\text{TD})}{z(\text{RD}) + z(\text{TD}) + z(\text{ND})} \quad (12.42)$$

If one inserts the numerical values $A_2 = -0.31045$, $\bar{P}_2(90^\circ) = -0.79057$ and $\bar{P}_2^2(90^\circ) = +0.96825$, one thus finally obtains

$$F = 0.425 [z(\text{RD}) + z(\text{TD}) + z(\text{ND})] \quad (12.43)$$

$$\varphi_2^1 = 19.0 \frac{z(\text{RD}) + z(\text{TD}) - 2z(\text{ND})}{z(\text{RD}) + z(\text{TD}) + z(\text{ND})} \quad (12.44)$$

$$\varphi_2^2 = -22.0 \frac{z(\text{RD}) - z(\text{TD})}{z(\text{RD}) + z(\text{TD}) + z(\text{ND})} \quad (12.45)$$

The total grain boundary surface as well as the two coefficients of an approximate expression (equation 12.25) of its orientation distribution can thus be determined from three planar sections.

If the sample symmetry is rotationally symmetric, only one linearly independent spherical surface harmonic thus results for each degree l :

$$k_l^1(\mathbf{y}) = k_l^1(\Phi, \gamma) = \frac{1}{\sqrt{2\pi}} \bar{P}_l(\Phi) \quad (12.46)$$

We introduce the fibre texture coefficients

$$\varphi_l = \frac{1}{\sqrt{2\pi}} \varphi_l^1 \quad (12.47)$$

Thus instead of equation (12.25) we obtain

$$\varphi(\mathbf{y}) = \varphi(\Phi) = \sum_{l=0}^{\infty} \varphi_l \bar{P}_l(\Phi) \quad (12.48)$$

If we also carry out the same specialization to rotational symmetry for the function $z(\mathbf{y}_0)$, the same relation between the coefficients z_l and φ_l (equation 12.30) is valid as between the z_l^r and the φ_l^r . Since the function $z(\mathbf{y}_0)$ in this case only

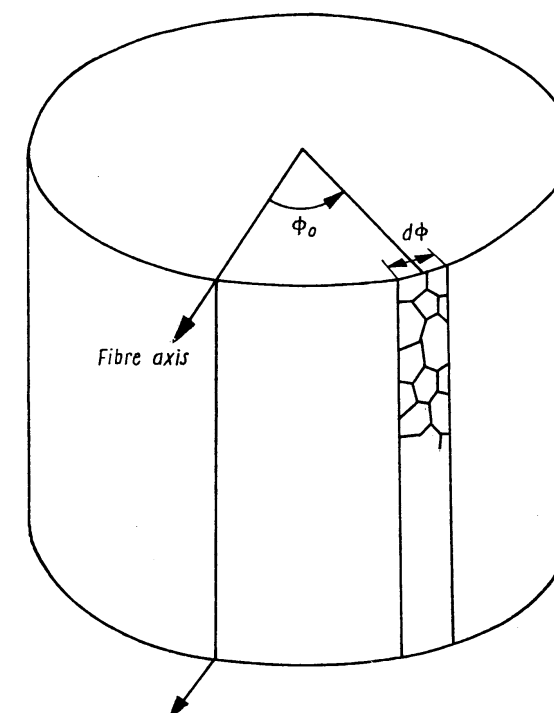


Figure 12.3 Surface element perpendicular to the direction Φ_0 of a polished cylinder

depends on the angle Φ_0 with respect to the fibre axis direction, it can be measured on a cylindrical sample, whose axis is perpendicular to the fibre axis (*Figure 12.3*). If no such sample is available, $z(y_0) = z(\Phi_0)$ can thus be approximately determined from many plane surfaces. One can already determine an approximate expression of second degree from two plane surfaces, perpendicular and parallel to the fibre axis direction, if one specializes formulae (12.43) and (12.44) to the case of rotational symmetry. The normal direction ND corresponds to the wire axis direction and directions RD and TD correspond to directions perpendicular to the wire axis. If we therefore set

$$z(ND) = z_{\perp}; \quad z(RD) = z(TD) = z_{\parallel} \quad (12.49)$$

taking equation (12.47) into consideration, we thus obtain from equations (12.43) — (12.45)

$$F = 0.425 [2z_{\parallel} + z_{\perp}] \quad (12.50)$$

$$\varphi_2 = 15.2 \frac{z_{\parallel} - z_{\perp}}{2z_{\parallel} + z_{\perp}} \quad (12.51)$$

z_{\perp} denotes the length of grain boundary lines per unit surface of a surface perpendicular to the wire axis and z_{\parallel} that of a surface which contains the wire axis.

12.2.3. The Distribution Function $\varphi'(\mathbf{h})$ of the Grain Boundaries in the Crystal Fixed Coordinate System

We now consider the orientation of grain boundaries in a crystal fixed coordinate system. dF is the grain boundary surface whose normal has a crystallographic orientation between \mathbf{h} and $\mathbf{h} + d\mathbf{h}$, and F is the total grain boundary surface. The orientation distribution function $\varphi'(\mathbf{h})$ is then defined by

$$\frac{dF}{F} = \frac{1}{4\pi} \varphi'(\mathbf{h}) d\mathbf{h} \quad (12.52)$$

In order to be able to use the results of the preceding sections, we ought to make a cut through the structure perpendicular to the crystal direction \mathbf{h}_0 and measure the total length of grain boundaries per unit surface. This is now not directly possible. However, we can take a plane cut perpendicular to the direction \mathbf{y} and on it consider only all those grain surfaces which by chance have the orientation \mathbf{h}_0 , and obtain the length of grain boundaries per unit surface of these \mathbf{h}_0 -grains. We thus, however, consider only a certain selection of grains. If we now form the average value over all surface directions \mathbf{y} (e.g. by use of a spherical sample, *Figure 12.4*), grains of all orientations corresponding to equation (12.12) will thus be cut with equal probability perpendicular to the crystal direction \mathbf{h}_0 . If, therefore, for a spherical sample we denote the total length of those grain boundary lines which are adjacent to grains having a surface orientation \mathbf{h}_0 to $\mathbf{h}_0 + d\mathbf{h}_0$ per unit

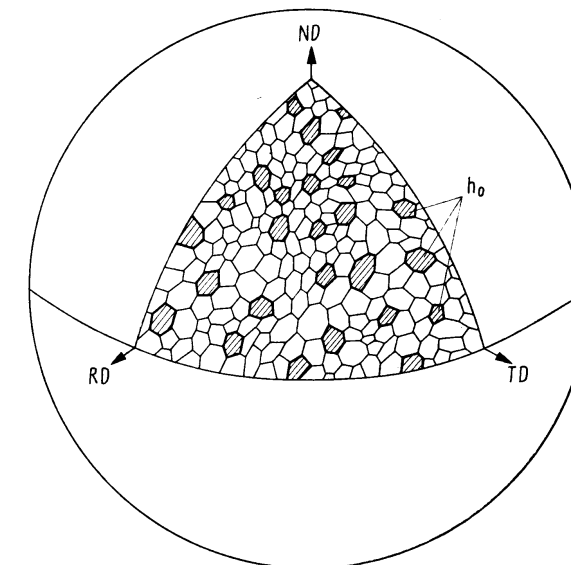


Figure 12.4 Grain boundary lines of the grains (shaded) which have the crystal direction \mathbf{h}_0 perpendicular to the surface of the spherical sample

surface of these grains by $z'(\mathbf{h}_0)$, this function is thus analogous to the function $z(y_0)$, which we have considered in the preceding section. The same relations therefore exist between $z'(\mathbf{h}_0)$ and $\varphi'(\mathbf{h})$ as between $z(y_0)$ and $\varphi(\mathbf{y})$. We expand $\varphi'(\mathbf{h})$ in a series of spherical surface harmonics of the crystal symmetry:

$$\varphi'(\mathbf{h}) = \sum_{l=0}^{\infty} \sum_{\mu=1}^{M(l)} \varphi_l^{\mu} k_l^{\mu}(\mathbf{h}) \quad (12.53)$$

Thus results, similarly to equation (12.29)

$$z'(\mathbf{h}_0) = \frac{F}{2} \sum_{l=0}^{\infty} \sum_{\mu=1}^{M(l)} \sqrt{\frac{2}{2l+1}} \varphi_l^{\mu} A_l k_l^{\mu}(\mathbf{h}) \quad (12.54)$$

This is also a series of spherical surface harmonics of the crystal symmetry with the coefficients

$$z_l^{\mu} = \frac{F}{2} \sqrt{\frac{2}{2l+1}} A_l \varphi_l^{\mu} \quad (12.55)$$

which can be calculated from the function $z'(\mathbf{h}_0)$ by means of the expression

$$z_l^{\mu} = \oint z'(\mathbf{h}_0) k_l^{*\mu}(\mathbf{h}_0) d\mathbf{h}_0 \quad (12.56)$$

The average value of the quantity $z'(\mathbf{h}_0)$ over all orientations \mathbf{h}_0 (which, indeed, according to equation 12.12, occur in the spherical sample with equal surface

portions) is the total length of the grain boundary lines per unit surface of the spherical sample. It is thus identical with the average value $\overline{z(\mathbf{y}_0)}$:

$$\overline{z'(\mathbf{h}_0)} = \frac{1}{4\pi} \oint z'(\mathbf{h}_0) d\mathbf{h}_0 = \overline{z(\mathbf{y}_0)} \quad (12.57)$$

12.3. Orientation Distribution Functions of the Grain Edges

After the orientation distribution functions of the grains and the grain boundaries we now consider the one-dimensional elements of the structure — the grain edges. In a two-dimensional section through the structure they are imaged as points of intersection of the grain boundary lines. We can again consider their orientation distribution in two different coordinate systems, in the sample fixed and in the crystal fixed coordinate systems.

12.3.1. The Distribution Function $\psi(\mathbf{y})$ of the Grain Edges in the Sample Fixed Coordinate System

dL is the length of all grain edges per unit volume whose direction lies between \mathbf{y} and $\mathbf{y} + dy$, and L is the total length of all grain edges per unit volume. The orientation distribution function $\psi(\mathbf{y})$ is then defined by

$$\frac{dL}{L} = \frac{1}{4\pi} \psi(\mathbf{y}) dy \quad (12.58)$$

It is expressed in multiples of the random distribution. We now further put a plane section of unit surface perpendicular to the direction \mathbf{y}_0 through the structure. This surface cuts the grain edges of the direction \mathbf{y} in points whose number per unit surface is given by dn . We now shift the section in the direction of the normal \mathbf{y}_0 through the structure by unit length; thus the point of intersection moves along the grain edge. It therefore sweeps out the length dL , which is

$$dL = dn \frac{1}{|\cos \langle \mathbf{y} \mathbf{y}_0 \rangle|} \quad (12.59)$$

It follows therefrom that

$$dn = \frac{L}{4\pi} \psi(\mathbf{y}) |\cos \langle \mathbf{y} \mathbf{y}_0 \rangle| dy \quad (12.60)$$

For the total number of the points of intersection per unit surface perpendicular to \mathbf{y}_0 one then obtains¹⁵³

$$n(\mathbf{y}_0) = \frac{L}{4\pi} \oint \psi(\mathbf{y}) |\cos \langle \mathbf{y} \mathbf{y}_0 \rangle| dy \quad (12.61)$$

We express $\psi(\mathbf{y})$ in a series of spherical surface harmonics of the sample symmetry:

$$\psi(\mathbf{y}) = \sum_{l=0}^{\infty} \sum_{r=1}^{N(l)} \psi_l^r k_l^r(\mathbf{y}) \quad (12.62)$$

and introduce a spherical angular coordinate system, whose pole is the direction \mathbf{y}_0 . Then results, similarly to equation (12.29),

$$n(\mathbf{y}_0) = \frac{L}{2} \sum_{l=0}^{\infty} \sum_{r=1}^{N(l)} \sqrt{\frac{2}{2l+1}} \psi_l^r B_l k_l^r(\mathbf{y}_0) \quad (12.63)$$

with

$$B_l = \int_0^\pi \bar{P}_l(\theta) |\cos \theta| \sin \theta d\theta \quad (12.64)$$

Here $n(\mathbf{y}_0)$ is represented by a series of spherical surface harmonics with the coefficients

$$n_l^r = \frac{L}{2} \sqrt{\frac{2}{2l+1}} B_l \psi_l^r \quad (12.65)$$

Expressions (12.63) and (12.65) are completely analogous to the corresponding expressions (12.29) and (12.30), except that now the coefficients B_l defined by equation (12.64) replace the coefficients A_l . In particular, for $l = 0$ there results from equation (12.65)

$$n_0^1 = \frac{L}{2} \sqrt{4\pi} \quad (12.66)$$

If the function $n(\mathbf{y}_0)$ is measured for very many directions \mathbf{y}_0 — e.g. on the spherical sample — the coefficients can thus be determined by integration:

$$n_l^r = \oint n(\mathbf{y}_0) k_l^{*r}(\mathbf{y}_0) d\mathbf{y}_0 \quad (12.67)$$

We set

$$\overline{n(\mathbf{y}_0)} = \frac{1}{4\pi} \oint n(\mathbf{y}_0) d\mathbf{y}_0 = \frac{1}{\sqrt{4\pi}} n_0^1 \quad (12.68)$$

Corresponding to equation (12.35), it is thus true that

$$L = \overline{2n(\mathbf{y}_0)} \quad (12.69)$$

If $n(\mathbf{y}_0)$ was measured for the three directions RD, TD and ND, one thus obtains, analogously with equations (12.43)–(12.45),

$$L = \frac{2}{3} [n(RD) + n(TD) + n(ND)] \quad (12.70)$$

$$\psi_2^1 = -14.9 \frac{n(RD) + n(TD) - 2n(ND)}{n(RD) + n(TD) + n(ND)} \quad (12.71)$$

$$\psi_2^2 = 17.35 \frac{n(RD) - n(TD)}{n(RD) + n(TD) + n(ND)} \quad (12.72)$$

For the case of fibre texture there result, with the same notation as in equations (12.46)–(12.48),

$$L = \frac{2}{3} [n_{\perp} + 2n_{\parallel}] \quad (12.73)$$

$$\psi_2 = -11.9 \frac{n_{\parallel} - n_{\perp}}{2n_{\parallel} + n_{\perp}} \quad (12.74)$$

12.3.2. The Distribution Function $\psi'(\mathbf{h})$ of the Grain Edges in the Crystal Fixed Coordinate System

We now consider the grain edges with respect to their crystallographic orientation in the neighbouring grains. If dL is now the length of those grain edges which have a crystallographic orientation between \mathbf{h} and $\mathbf{h} + d\mathbf{h}$, and L is the total length, both per unit volume, the distribution function is thus defined by

$$\frac{dL}{L} = \frac{1}{4\pi} \psi'(\mathbf{h}) d\mathbf{h} \quad (12.75)$$

The analogue to the number of points $n(\mathbf{y}_0)$ per unit surface of a section with the normal direction \mathbf{y}_0 is now the number of points per unit surface of those grain section surfaces of a spherical sample which have a crystallographic orientation between \mathbf{h}_0 and $\mathbf{h}_0 + d\mathbf{h}_0$ (Figure 12.5). We call it $n'(\mathbf{h}_0)$. The same relations again

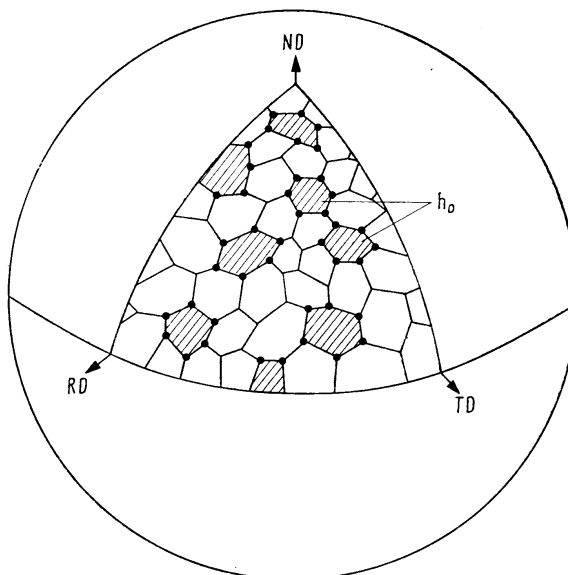


Figure 12.5 Grain corner points of the grains (shaded), which have the crystal direction \mathbf{h}_0 perpendicular to the surface of the spherical sample

exist between $n'(\mathbf{h}_0)$ and $\psi'(\mathbf{h})$ as between $n(\mathbf{y}_0)$ and $\psi(\mathbf{y})$. We expand $\psi'(\mathbf{h})$ in a series of spherical surface harmonics of the crystal symmetry:

$$\psi'(\mathbf{h}) = \sum_{l=0}^{\infty} \sum_{\mu=1}^{M(l)} \psi_l^{\mu} \dot{k}_l^{\mu}(\mathbf{h}) \quad (12.76)$$

It is thus true that

$$n'(\mathbf{h}_0) = \frac{L}{2} \sum_{l=0}^{\infty} \sum_{\mu=1}^{M(l)} \sqrt{\frac{2}{2l+1}} \psi_l^{\mu} B_l \dot{k}_l^{\mu}(\mathbf{h}_0) \quad (12.77)$$

This is thus a series of spherical surface harmonics of the crystal symmetry with the coefficients

$$n_l^{\mu} = \frac{L}{2} \sqrt{\frac{2}{2l+1}} B_l \psi_l^{\mu} \quad (12.78)$$

which can be calculated from the relation

$$n_l^{\mu} = \oint n'(\mathbf{h}_0) \dot{k}_l^{\mu}(\mathbf{h}_0) d\mathbf{h}_0 \quad (12.79)$$

The average value of the quantity $n'(\mathbf{h}_0)$ over all \mathbf{h}_0 can be directly observed as the number of corners per unit surface of the whole spherical sample. It is thus identical with the average value $\overline{n(\mathbf{y}_0)}$:

$$\overline{n'(\mathbf{h}_0)} = \frac{1}{4\pi} \oint n'(\mathbf{h}_0) d\mathbf{h}_0 = \overline{n(\mathbf{y}_0)} \quad (12.80)$$

13. Physical Properties of Polycrystalline Materials

One of the important objectives of many texture investigations is the calculation of the anisotropy of physical properties of polycrystalline materials from the corresponding properties of the individual crystallites and parameters characterizing the polycrystalline material. Questions of this kind possess not only theoretical, but also great practical interest. The directional dependence of magnetization energy of transformer sheet or the earing behaviour of deep-drawing sheet are suggested. In some cases, as with the magnetization energy, the property of the polycrystalline material is given by the average value of the properties of the individual crystallites. It therefore depends not only on the single crystal properties, but also on the orientation distribution function $f(g)$. In other cases (e.g. in the case of elastic and plastic properties) an additional interaction effect between crystallites, and thus a typical ‘polycrystal effect’, occurs. The properties of the polycrystalline materials can then also depend on the distribution of grain boundaries or in complete generality on the correlation of the orientations at different points of the material.

13.1. Physical Properties of Single Crystals

By a physical property of a material one understands with complete generality the relation between two (or more) measurable quantities of the material which depends on the material^{24,220,291}. Thus the relation between the volume and the mass of a material is characterized by its density, which is a property of the material. However, we are frequently concerned with essentially more complicated quantities, and therefore also essentially complicated properties of the material. Thus the diffracting power of a crystal depends in a complicated way on the directions of the incident and reflected beams. In this case we have thus to deal with a strongly directionally dependent property. We can thus with complete generality define a ‘property’ of a material by

$$Y = E(X) \quad (13.1)$$

where Y and X are some quantities, usually orientation dependent, which are specifically connected to each other by the property E of the material.

13.1.1. Representation by Tensors

A large class of directionally dependent physical quantities can be represented by tensors. By a tensor of n th order

$$E = \{E_{i_1 i_2 \dots i_n}\} \quad (13.2)$$

one understands a quantity with the components $E_{i_1 i_2 \dots i_n}$, which transforms to another coordinate system as the n -fold product of the coordinates. If we transform from one rectangular Cartesian coordinate system K , in which a point possesses the coordinates x_i , to another, K' , in which the point possesses the coordinates x'_i , the following relation holds for the coordinates of the transformation:

$$x'_i = a_{ij} x_j \quad (13.3)$$

The result is to be summed over the recurring indices according to the EINSTEIN convention. The components of the tensor in the coordinate system K' are then given in terms of those in the coordinate system K by the relation

$$E'_{i_1 i_2 \dots i_n} = a_{i_1 j_1} a_{i_2 j_2} \dots a_{i_n j_n} E_{j_1 j_2 \dots j_n} \quad (13.4)$$

(The summation signs of the n summations over the indices j_1 to j_n are omitted.) If, now, the quantity Y in equation (13.1) is a tensor of m th order and the quantity X one of n th order and the function E describes a continuous relation between two quantities, one can thus expand it in a series:

$$Y = E_0 + E_1 \cdot X + E_2 \cdot X^2 + \dots + E_r \cdot X^r \quad (13.5)$$

The powers X^r are tensors of $(r \cdot n)$ th order and the coefficients E_r tensors of $(r \cdot n + m)$ th order. The tensors E_r in this case describe the property concerned. Each term of this series thus has the general form

$$Y^{(m)} = E^{(m+n)} X^{(n)} \quad (13.6)$$

or, in component notation

$$Y_{i_1 i_2 \dots i_m} = E_{i_1 i_2 \dots i_m j_1 j_2 \dots j_n} X_{j_1 j_2 \dots j_n} \quad (13.7)$$

which is to be summed over all repeated indices. Equation (13.7) is a system of linear relations between the tensor components. Each component of the tensor Y is linearly dependent on each component of the tensor X . The scalar quantities, as, for example, the density, are naturally also included in this representation with $m = n = 0$.

13.1.2. Representation by Surfaces

In addition to the representation of a physical property by tensors, another representation plays an important role — namely the representation by surfaces or, which is the same thing, by scalar functions of a direction in space³⁰². For example, in a ferromagnetic crystal without the influence of an external magnetic field the

spontaneous magnetization lies in an easily magnetizable direction \mathbf{h}_0 . If one forces this by an external magnetic field into another direction \mathbf{h} , one must thus employ an energy (per unit volume) which depends on the direction \mathbf{h} :

$$E = E(\mathbf{h}) = E(\Phi, \beta) \quad (13.8)$$

This representation of a property by one (or more) functions of a direction in space has the advantage of being particularly intuitive. The function $E(\mathbf{h})$ must have the crystallographic symmetry — i.e. it must assume the same values for crystallographically equivalent directions \mathbf{h}_α . It can therefore be expanded in a series of spherical surface harmonics of the crystal symmetry (including the centre of inversion):

$$E(\mathbf{h}) = \sum_{l=0}^{\infty} \sum_{\mu=1}^{M(l)} e_l^\mu k_l^\mu(\mathbf{h}) \quad (13.9)$$

The coefficients e_l^μ here thus characterize the property concerned. Since the functions $k_l^\mu(\mathbf{h})$ will possess the complete crystal symmetry, symmetry conditions no longer exist between the coefficients e_l^μ in contrast to the components of a tensor (see, e.g., reference 24), which, in general, are not linearly independent. Both representations of a property, the surface and the tensor representation, can be transformed into each other. If in equation (13.8) we express the direction \mathbf{h} , not by spherical angular coordinates Φ and β , but by the components h_1, h_2, h_3 , we can thus write

$$E = E(\mathbf{h}) = E(h_1, h_2, h_3) \quad (13.10)$$

We can now expand E in a series of increasing powers of the h_i :

$$E(\mathbf{h}) = E^0 + E_1^1 h_1 + E_2^2 h_1 h_2 + E_{ijk}^3 h_1 h_2 h_3 + \dots \quad (13.11)$$

The quantities E_{ij}^n and the products of h_i therein are components of tensors. We have thus a special case of the general tensor representation (13.5).

Conversely, every tensor can be represented by a certain number of scalar functions of a direction — i.e. by surfaces. The component

$$E'_{33\dots 3} = a_{3j_1} a_{3j_2} \dots a_{3j_n} E_{i_1 i_2 \dots i_n} \quad (13.12)$$

of the tensor E in the coordinate system K' depends only on the orientation of the direction X'_3 of this coordinate system with respect to the crystal fixed coordinate system K , not on the orientation of the two other directions X'_1 and X'_2 . If Φ and β are the spherical angular coordinates of the direction X'_3 in the crystal fixed coordinate system K , the function

$$E'_{33\dots 3} = E'_{33\dots 3}(\Phi, \beta) \quad (13.13)$$

thus represents such a surface. Because of the commutability of the factors in the product $a_{3j_1} a_{3j_2} \dots a_{3j_n}$ in equation (13.12), the function $E'_{33\dots 3}(\Phi, \beta)$ depends only on the sum of all those components of the tensor E which are formed from $E_{i_1 i_2 \dots i_n}$ by permutation of the indices. If the tensor E is symmetric with respect

to all these permutations of indices, the function $E'_{33\dots 3}(\Phi, \beta)$ thus already completely describes the tensor E . If the tensor E is not symmetric with respect to all permutations of the indices, one must thus include further linear combinations of tensor components, which also depend only on the orientation of X'_3 in the coordinate system K . In this way, as was shown by WONDRTSCHER³⁰², every tensor can be expressed by a certain number of functions $E_i(\Phi, \beta)$ of the direction X'_3 . These functions must naturally satisfy the crystal symmetry. They can therefore be expressed in a series of symmetric spherical surface harmonics:

$$E_i(\Phi, \beta) = \sum_{l=0}^n \sum_{\mu=1}^{M(l)} e_l^\mu k_l^\mu(\Phi, \beta) \quad (13.14)$$

The coefficients e_l^μ then form a representation of the physical property, which is equivalent to the representation by the tensor components $E_{i_1 i_2 \dots i_n}$. Thus, e.g., the elastic properties of a crystal can be represented by the directional dependence of the two quantities

$$s'_{3333}(\Phi, \beta) \quad \text{and} \quad [s'_{1133}(\Phi, \beta) + s'_{2233}(\Phi, \beta)] \quad (13.15)$$

of YOUNG's modulus and the cross-modulus³⁰², instead of the components s_{ijkl} of the tensor of the elastic modulus, with respect to a crystal fixed coordinate system. As is known, a symmetric tensor of second order with components E_{ii} can be described by a surface of second order:

$$E(\Phi, \beta) = E_{ij} h_i h_j \quad (13.16)$$

13.1.3. Representation by Functions of the Orientation g

If we expose a ferromagnetic crystal to the influence of an inhomogeneous magnetic field, the magnetization in different portions of the crystal thus lies in different crystallographic directions. The magnetization energy in this case depends on the complete orientation of a coordinate system associated with the magnetic field relative to the crystal axes and not solely on the orientation of an individual direction, as in the case of a homogeneous magnetic field. If this orientation is given by the rotation g with the EULER angles $\varphi_1, \Phi, \varphi_2$, we thus have in this case to write for the magnetization energy

$$E = E(g) = E(\varphi_1, \Phi, \varphi_2) \quad (13.17)$$

Since the crystal symmetry (\vdash) must be realized in the crystal fixed coordinate system and also the distribution of magnetization directions of the inhomogeneous magnetic field can possess a certain symmetry (\vdash) (instrumental or external symmetry), we can expand the function $E(g)$ in a series of symmetric generalized spherical harmonics according to these two symmetries:

$$E(g) = \sum_{l=0}^{\infty} \sum_{\mu=1}^{M(l)} \sum_{\nu=1}^{N(l)} e_l^{\mu\nu} T_l^{\mu\nu}(g) \quad (13.18)$$

If the magnetic field is homogeneous, it thus possesses rotational symmetry with the field direction as symmetry axis. The generalized spherical harmonics of this symmetry are, however, identical with the spherical surface harmonics except for a factor, and equation (13.18) transforms, as it must, into equation (13.9).

Each component $E'_{i_1 i_2 \dots i_n}$ of the tensor \mathbf{E} in the coordinate system K' is a function of the orientation g of this coordinate system relative to the crystal fixed coordinate system K . Accordingly, the tensor \mathbf{E} is naturally represented trivially by a certain number of functions of the rotation g — namely the functions $E'_{i_1 i_2 \dots i_n}(g)$. These functions depend on the components $E_{j_1 j_2 \dots j_n}$ of the tensor \mathbf{E} in the crystal fixed coordinate system. If among the indices i_1, \dots, i_n some are equal to one another (and for $n > 3$ this must necessarily be the case), the $E_{i_1 i_2 \dots i_n}$ appear in equation (13.4) only as sums over all permutations of the indices j of the corresponding positions. If, now, the orientation dependence of a tensor component $E'_{i_1 i_2 \dots i_n}(g)$ is known, the corresponding sum of components $E_{i_1 i_2 \dots i_n}$ can thus be calculated therefrom. If the tensor \mathbf{E} is symmetric with respect to permutation of the indices concerned, it is thus completely described by the orientation dependence $E'_{i_1 i_2 \dots i_n}(g)$ of one of its components. The tensor of the elastic compliance, for example, has the symmetry

$$s_{ijkl} = s_{jikl} = s_{klij} \quad (13.19)$$

The component

$$s'_{1233}(g) = a_{1j_1} a_{2j_2} a_{3j_3} a_{3j_4} s_{j_1 j_2 j_3 j_4} \quad (13.20)$$

because of the commutability of the factors a_{ij} depends only on the sum of the tensor components

$$s_{j_1 j_2 j_3 j_4} + s_{j_1 j_3 j_2 j_4} \quad (13.21)$$

However, since because of the symmetry condition (13.19) these are equal, the function $s'_{1233}(g)$ completely describes this tensor, which is thus represented by a single function of g . If the tensor is not symmetric with respect to those indices which have the same values in the component $E'_{i_1 i_2 \dots i_n}$, one must use more of its components $E'_{i'_1 i'_2 \dots i'_n}$ for its characterization.

The transformation coefficients a_{ij} are the direction cosines of the coordinates X'_i in the system of axes X_j . They are thus functions of the rotation g which transforms the coordinate system K into the system K' . They form a representation of the group of rotations g , which is equivalent to the representation by $T_1^{mn}(g)$ (see, e.g., reference 199). The a_{ij} are therefore linearly expressible by generalized spherical harmonics of first degree (see equation 2.50 and Table 14.1):

$$a_{ij}(g) = \sum_{m=-1}^{+1} \sum_{n=-1}^{+1} \mu_{im} v_{jn} T_1^{mn}(g) \quad (13.22)$$

where the μ_{im} and v_{jn} are given by Table 13.1. Now it is true for the product of two generalized spherical harmonics (see Section 14.4) that

$$T_{l_1}^{m_1 n_1} T_{l_2}^{m_2 n_2} = \sum_{l=|l_2-l_1|}^{|l_1+l_2|} (l_1 l_2 m_1 m_2 | l, m_1 + m_2) (l_1 l_2 n_1 n_2 | l, n_1 + n_2) T_l^{m_1+m_2, n_1+n_2} \quad (13.23)$$

Table 13.1 THE COEFFICIENTS μ_{im} AND v_{jn} , BY WHICH THE TRANSFORMATION COEFFICIENTS a_{ij} CAN BE REPRESENTED BY THE GENERALIZED SPHERICAL HARMONICS OF FIRST DEGREE

μ_{im}			v_{jn}				
$i \backslash m$	-1	0	+1	$j \backslash n$	-1	0	+1
1	$-\frac{1}{\sqrt{2}}$	0	$+\frac{1}{\sqrt{2}}$	1	$-\frac{1}{\sqrt{2}}$	0	$+\frac{1}{\sqrt{2}}$
2	$+\frac{i}{\sqrt{2}}$	0	$+\frac{i}{\sqrt{2}}$	2	$-\frac{i}{\sqrt{2}}$	0	$-\frac{i}{\sqrt{2}}$
3	0	1	0	3	0	1	0

The symbols in parentheses are the CLEBSCH—GORDAN coefficients. By repeated application of formula (13.23) one can then express the product of the direction cosines as a series of generalized spherical harmonics:

$$a_{i_1 i_2} \cdot a_{i_2 i_3} \cdots a_{i_r i_r} = \sum_{l=0}^r \sum_{m=-l}^{+l} \sum_{n=-l}^{+l} a_l^{mn}(i_1 i_2 \dots i_r; j_1 j_2 \dots j_r) T_l^{mn}(g) \quad (13.24)$$

The function $s'_{1233}(g)$, which characterizes the tensor of the elastic compliances, for example, thereby assumes the form

$$s'_{1233}(g) = \sum_{l=0}^4 \sum_{m=-l}^{+l} \sum_{n=-l}^{+l} a_l^{mn}(1233; j_1 j_2 j_3 j_4) s_{j_1 j_2 j_3 j_4} T_l^{mn}(g) \quad (13.25)$$

13.2. The Problem of Averaging

We consider an arbitrary tensor property \mathbf{E} . Two quantities \mathbf{Y} and \mathbf{X} may be linked to each other by it:

$$\mathbf{Y} = \mathbf{E} \cdot \mathbf{X} \quad (13.26)$$

If, now, the material considered, which possesses the property \mathbf{E} , is polycrystalline, the property tensor \mathbf{E} is dependent on the orientation of the crystallites and, hence, on the position \mathbf{r} within the material. This is also true for the two quantities \mathbf{X} and \mathbf{Y} . We thus have to write

$$\mathbf{Y}(\mathbf{r}) = \mathbf{E}(\mathbf{r}) \cdot \mathbf{X}(\mathbf{r}) \quad (13.27)$$

The material may now be macroscopically homogeneous. We consider a volume V , which is large compared with the grain size. The average value of $\mathbf{E}(\mathbf{r})$ over this volume is then equal to the average value over the whole sample. We further assume that the quantities $\mathbf{X}(\mathbf{r})$ and $\mathbf{Y}(\mathbf{r})$ are macroscopically homogeneous. The average values over V are then likewise independent of the location of the region V within the whole sample. We denote this average value by a bar, so that, for example, for the average value of \mathbf{E} it is true that

$$\bar{\mathbf{E}} = \frac{1}{V} \int_V \mathbf{E}(\mathbf{r}) dV \quad (13.28)$$

The average values of \mathbf{Y} and \mathbf{X} are similarly defined. We now set

$$\mathbf{E}(\mathbf{r}) = \bar{\mathbf{E}} + \Delta\mathbf{E}(\mathbf{r}) \quad (13.29)$$

$$\mathbf{Y}(\mathbf{r}) = \bar{\mathbf{Y}} + \Delta\mathbf{Y}(\mathbf{r}) \quad (13.30)$$

$$\mathbf{X}(\mathbf{r}) = \bar{\mathbf{X}} + \Delta\mathbf{X}(\mathbf{r}) \quad (13.31)$$

With equation (13.28) it is then true that

$$\int_V \Delta\mathbf{E}(\mathbf{r}) dV = 0 \quad (13.32)$$

Corresponding relations are also valid for $\Delta\mathbf{Y}$ and $\Delta\mathbf{X}$. If one substitutes equations (13.29)–(13.31) in equation (13.27), one thus obtains

$$\bar{\mathbf{Y}} + \Delta\mathbf{Y}(\mathbf{r}) = \bar{\mathbf{E}} \cdot \bar{\mathbf{X}} + \bar{\mathbf{E}} \cdot \Delta\mathbf{X}(\mathbf{r}) + \Delta\mathbf{E}(\mathbf{r}) \cdot \bar{\mathbf{X}} + \Delta\mathbf{E}(\mathbf{r}) \cdot \Delta\mathbf{X}(\mathbf{r}) \quad (13.33)$$

If one forms the average value over V , one thus obtains with equation (13.32)

$$\bar{\mathbf{Y}} = \bar{\mathbf{E}} \cdot \bar{\mathbf{X}} + \frac{1}{V} \int_V \Delta\mathbf{E}(\mathbf{r}) \cdot \Delta\mathbf{X}(\mathbf{r}) dV \quad (13.34)$$

If we consider the averaged tensor $\bar{\mathbf{X}}$ as the independent variable, the components of the quantity $\Delta\mathbf{X}(\mathbf{r})$ must depend on those of $\bar{\mathbf{X}}$. For $\bar{\mathbf{X}} = 0$ it is also true that $\Delta\mathbf{X}(\mathbf{r}) = 0$. Because of the linear relation (13.27) a linear relation between $\bar{\mathbf{X}}$ and $\Delta\mathbf{X}(\mathbf{r})$ is generally valid:

$$\Delta\mathbf{X}(\mathbf{r}) = \mathbf{U}(\mathbf{r}) \cdot \bar{\mathbf{X}} \quad (13.35)$$

If $\bar{\mathbf{X}}$, and therefore also $\Delta\mathbf{X}(\mathbf{r})$, are n th-order tensors, $\mathbf{U}(\mathbf{r})$ is thus a tensor of order $2n$, which can depend on the values of $\mathbf{E}(\mathbf{r})$ at all positions \mathbf{r}' of the whole sample¹⁹⁶. If one substitutes equation (13.35) into equation (13.34), one thus obtains

$$\bar{\mathbf{Y}} = \left[\bar{\mathbf{E}} + \frac{1}{V} \int_V \Delta\mathbf{E}(\mathbf{r}) \mathbf{U}(\mathbf{r}) dV \right] \cdot \bar{\mathbf{X}} \quad (13.36)$$

The macroscopic quantities $\bar{\mathbf{Y}}$ and $\bar{\mathbf{X}}$ are related to each other in equation (13.36) in a similar way to the microscopic ones \mathbf{Y} and \mathbf{X} in equation (13.27). The quantity

in brackets,

$$\tilde{\mathbf{E}} = \bar{\mathbf{E}} + \frac{1}{V} \int_V \Delta\mathbf{E}(\mathbf{r}) \mathbf{U}(\mathbf{r}) dV \quad (13.37)$$

is thus the corresponding material property of the polycrystalline (macroscopically homogeneous) material. It is generally different from the simple arithmetic average value $\bar{\mathbf{E}}$.

The simple arithmetic average value $\bar{\mathbf{E}}$ is, in general, relatively easy to calculate, while the calculation of the additional quantity frequently leads to very great difficulties. For its calculation not only the orientation distribution function $f(g)$ is necessary, but also an orientation correlation function which describes simultaneously the orientation g at the point \mathbf{r} and the orientation g' at the point \mathbf{r}' . Moreover, the additional quantity in equation (13.37) is frequently relatively small in comparison with $\bar{\mathbf{E}}$. The approximation

$$\tilde{\mathbf{E}} \approx \bar{\mathbf{E}} \quad (13.38)$$

is therefore frequently employed.

One obtains a better approximation for the polycrystal property $\tilde{\mathbf{E}}$ than the average value $\bar{\mathbf{E}}$ in the following way. If one solves the system of linear equations (13.26) for the components of the tensor \mathbf{X} , one thus obtains

$$\mathbf{X} = \mathbf{E}^{-1} \cdot \mathbf{Y} \quad (13.39)$$

The tensor \mathbf{E}^{-1} is another representation of the same property as that described in equation (13.26) by the tensor \mathbf{E} . Examples of such tensor pairs \mathbf{E} and \mathbf{E}^{-1} are the tensors of the electrical conductivity and the electrical resistivity or the elastic stiffness and the elastic compliance. If, now, by analogy with equation (13.28), one forms the average value of the tensor \mathbf{E}^{-1} :

$$\bar{\mathbf{E}}^{-1} = \frac{1}{V} \int_V \mathbf{E}^{-1}(\mathbf{r}) dV \quad (13.40)$$

in general,

$$\bar{\mathbf{E}} \neq (\bar{\mathbf{E}}^{-1})^{-1} \quad (13.41)$$

The two averages (13.28) and (13.40) yield limiting values for the actual property of the polycrystalline material. Average (13.28) assumes

$$\mathbf{X} = \text{const.} \quad (13.42)$$

Thus, in general, the conditions for \mathbf{X} are invalid at the grain boundaries, and the average (13.40) requires

$$\mathbf{Y} = \text{const.} \quad (13.43)$$

This, in general, violates the boundary condition for the quantity \mathbf{Y} . The actual behaviour of the polycrystalline material will therefore lie between these two

extremes, so that one can frequently set

$$\tilde{\mathbf{E}} \approx \frac{1}{2} [\bar{\mathbf{E}} + (\bar{\mathbf{E}}^{-1})^{-1}] \quad (13.44)$$

In elasticity theory equations (13.28), (13.40) and (13.44) describe the well-known approximations of HILL¹⁵², REUSS²⁴⁴ and VOIGT²⁹¹. An essentially more general form of the average construction was given by ALEXANDROW and AISENBERG¹³, KRÖNER^{187,188}, KNEER^{180,181} and MORRIS²¹³.

13.3. The Calculation of the Simple Mean Values \bar{E}

We shall now discuss the calculation of the simple average value \bar{E} for the three forms noted for the representation of a physical property. This means that we must average either the tensor components $E_{i_1 i_2 \dots i_m j_1 j_2 \dots j_n}$ (equation 13.7) or the coefficients e_l^μ (equation 13.9) or the coefficients $e_l^{\mu\nu}$ (equation 13.18) over the volume V corresponding to equation (13.28). Since the property $E(\mathbf{r})$ will depend only on the orientation g of the crystallite present at the point \mathbf{r} , the integration over V can be carried out in two steps. We first integrate over all those volume elements dV which possess the orientation g , and then over all orientations g . We thereby obtain

$$\bar{E} = \frac{1}{V} \oint_g E(g) \int_{V(g)} dV \quad (13.45)$$

If here we substitute for dV from equation (3.3), we obtain

$$\bar{E} = \oint_g E(g) f(g) dg \quad (13.46)$$

The orientation distribution function $f(g)$ thus appears as a weight function for the calculation of the average values of orientation-dependent physical properties. Its great practical importance does not least depend thereon.

13.3.1. Tensor Representation

A property is described in a crystal fixed coordinate system K_B by the r th-order tensor \mathbf{E} with components $E_{j_1 j_2 \dots j_r}$. It has the components $E_{i_1 i_2 \dots i_r}$ in the sample fixed coordinate system K_A . The crystal coordinate system K_B is produced from the sample coordinate system K_A by the rotation g . K_B will then naturally be transformed into K_A by g^{-1} , and, according to equations (13.4) and (13.24), it is true for the components $E'_{i_1 i_2 \dots i_r}$ in the sample fixed system K_A that

$$E'_{i_1 i_2 \dots i_r} = \sum_{l=0}^r \sum_{m=-l}^{+l} \sum_{n=-l}^{+l} a_l^{mn}(i_1 i_2 \dots i_r; j_1 j_2 \dots j_r) T_l^{mn}(g^{-1}) E_{j_1 j_2 \dots j_r} \quad (13.47)$$

Setting

$$T_l^{mn}(g^{-1}) = T_l^{*mn}(g) \quad (13.48)$$

equation (13.47) transforms into

$$E'_{i_1 i_2 \dots i_r} = \sum_{l=0}^r \sum_{m=-l}^{+l} \sum_{n=-l}^{+l} a_l^{mn}(i_1 i_2 \dots i_r; j_1 j_2 \dots j_r) T_l^{*mn}(g) E_{j_1 j_2 \dots j_r} \quad (13.49)$$

If we expand the weight function of the average value (equation 13.46), and thus the orientation distribution function $f(g)$, in a series of symmetric generalized spherical harmonics and express the symmetry of these functions by the symmetry coefficients $\dot{A}_l^{m\mu}$ and $\dot{A}_l^{n\nu}$, we obtain

$$f(g) = \sum_{l=0}^{\infty} \sum_{\mu=1}^{M(l)} \sum_{\nu=1}^{N(l)} \sum_{m=-l}^{+l} \sum_{n=-l}^{+l} C_l^{\mu\nu} \dot{A}_l^{m\mu} \dot{A}_l^{n\nu} T_l^{mn}(g) \quad (13.50)$$

If, now, we average the components $E'_{i_1 i_2 \dots i_r}$ of the tensor \mathbf{E} over all orientations g in the sample fixed coordinate system according to equation (13.46), we obtain for the property tensor of the textured material

$$\bar{E}_{i_1 i_2 \dots i_r} = \bar{a}(i_1 i_2 \dots i_r; j_1 j_2 \dots j_r) E_{j_1 j_2 \dots j_r} \quad (13.51)$$

with

$$\bar{a}(i_1 i_2 \dots i_r; j_1 j_2 \dots j_r) = \sum_{l=0}^r \sum_{\mu=1}^{M(l)} \sum_{\nu=1}^{N(l)} \bar{a}_l^{\mu\nu}(i_1 i_2 \dots i_r; j_1 j_2 \dots j_r) C_l^{\mu\nu} \quad (13.52)$$

and

$$\bar{a}_l^{\mu\nu}(i_1 i_2 \dots i_r; j_1 j_2 \dots j_r) = \sum_{m=-l}^{+l} \sum_{n=-l}^{+l} \frac{1}{2l+1} a_l^{mn}(i_1 i_2 \dots i_r; j_1 j_2 \dots j_r) \dot{A}_l^{m\mu} \dot{A}_l^{n\nu} \quad (13.53)$$

Equation (13.51) expresses the components of the averaged property tensor $\bar{\mathbf{E}}$ of a textured material by those of the single crystal with respect to the crystal fixed coordinate system. The averaging coefficients $\bar{a}(i_1 \dots j_r)$ according to equation (13.52) depend on the coefficients $C_l^{\mu\nu}$ of the orientation distribution function. The quantities $\bar{a}_l^{\mu\nu}(i_1 \dots j_r)$ appearing in equation (13.52) are purely mathematical quantities. According to equation (13.53), they depend only on the crystal and sample symmetries, and according to equation (13.24), on the order of the tensor \mathbf{E} . They can thus generally be calculated. Further, an example of this is given below for the elastic properties (fourth-rank tensor properties).

13.3.2. Surface Representation

The calculation of the average value \bar{E} proceeds in a particularly simple way if one employs the surface representation $E(\Phi, \beta)$ of the property E ³⁵. The angles Φ and β are the spherical angular coordinates of the crystal direction \mathbf{h} . In a crystallite of orientation g the crystal direction \mathbf{h} may point in the sample direction \mathbf{y} . If we want to calculate the average value of the property E in the direction \mathbf{y} over all orientations g that occur,

$$\bar{E}(\mathbf{y}) = \oint_g E(\mathbf{h}) f(g) dg \quad (13.54)$$

we can carry out the average over g in two steps. First we average over all those orientations g for which the crystal direction \mathbf{h} falls in the sample direction \mathbf{y} . $E(\mathbf{h})$ is thus naturally constant, and the average of the function $f(g)$ over these orientations, according to equation (4.33), yields the general axis distribution function $A(\mathbf{h}, \mathbf{y})$ and, since the direction \mathbf{y} is constant during the integration, the inverse pole figure of the direction \mathbf{y} . By consideration of the normalization of this function, there results

$$\bar{E}(\mathbf{y}) = \frac{1}{4\pi} \oint E(\mathbf{h}) A(\mathbf{h}, \mathbf{y}) d\mathbf{h} = \frac{1}{4\pi} \oint E(\mathbf{h}) R_y(\mathbf{h}) d\mathbf{h} \quad (13.55)$$

For calculation of the average value $\bar{E}(\mathbf{y})$ in a sample direction \mathbf{y} one thus needs only the inverse pole figure of this direction and not the complete orientation distribution function $f(g)$. Herein lies the particular advantage of the surface representation of physical properties. If the average value $\bar{E}(\mathbf{y})$ for all sample directions \mathbf{y} is required, the general axis distribution function $A(\mathbf{h}, \mathbf{y})$ is needed as the weight function. This function will therefore incidentally be denoted as the generalized inverse pole figure. If one substitutes for $E(\mathbf{h})$ and $A(\mathbf{h}, \mathbf{y})$ the corresponding series expansions,

$$E(\mathbf{h}) = \sum_{l=0}^r \sum_{\mu=1}^{M(l)} e_l^\mu k_l^\mu(\mathbf{h}) \quad (13.56)$$

and

$$A(\mathbf{h}, \mathbf{y}) = 4\pi \sum_{l=0}^{\infty} \sum_{\mu=1}^{M(l)} \sum_{\nu=1}^{N(l)} \frac{C_l^{\mu\nu}}{2l+1} k_l^{*\mu}(\mathbf{h}) k_l^*(\mathbf{y}) \quad (13.57)$$

one obtains

$$\bar{E}(\mathbf{y}) = \sum_{l=0}^r \sum_{\nu=1}^{N(l)} \bar{e}_l^* k_l^*(\mathbf{y}) \quad (13.58)$$

with the averaged property coefficients

$$\bar{e}_l^* = \frac{1}{2l+1} \sum_{\mu=1}^{M(l)} C_l^{\mu*} e_l^\mu \quad (13.59)$$

If the orientation distribution of the crystallites is rotationally symmetric about the Z -axis of the sample coordinate system³⁴, equation (13.57) thus transforms into (see equation 5.24)

$$A(\mathbf{h}, \mathbf{y}) = A(\mathbf{h}, \Phi) = \sum_{l=0}^{\infty} \sum_{\mu=1}^{M(l)} \sqrt{\frac{2}{2l+1}} k_l^{*\mu}(\mathbf{h}) C_l^{\mu} \bar{P}_l(\Phi) \quad (13.60)$$

We obtain in this case for the property of the polycrystalline material, which is likewise rotationally symmetric about the Z -axis,

$$\bar{E}(\Phi) = \sum_{l=0}^r \bar{e}_l \bar{P}_l(\Phi) \quad (13.61)$$

with

$$\bar{e}_l = \frac{1}{4\pi} \sqrt{\frac{2}{2l+1}} \sum_{\mu=1}^{M(l)} C_l^{\mu} e_l^\mu \quad (13.62)$$

13.3.2.1. Rotationally Symmetric Properties

In many cases the property function $E(\mathbf{h})$ is rotationally symmetric with respect to a certain crystal direction \mathbf{h}_0 (though the crystal naturally does not possess such symmetry). Thus, e.g., in the case of hexagonal crystals the magnetization energy will be assumed as rotationally symmetric about the hexagonal axis. If, therefore, we establish for the crystal direction \mathbf{h} a new spherical angular coordinate system Θ, ψ' , such that its pole coincides with the direction \mathbf{h}_0 , the property $E(\mathbf{h})$ depends in this coordinate system only on the angle Θ . The integration in equation (13.55) can therefore be first carried out over the angle ψ' , where $E(\Theta)$ is constant:

$$\bar{E}(\mathbf{y}) = \frac{1}{4\pi} \int_0^\pi E(\Theta) \left[\int_0^{2\pi} R_y(\Theta, \psi') d\psi' \right] \sin \Theta d\Theta \quad (13.63)$$

The integral in the brackets can, according to equation (4.137), be replaced by an integral over the pole figure $P_{\mathbf{h}_0}(\Theta, \psi)$ belonging to the direction \mathbf{h}_0 :

$$\bar{E}(\mathbf{y}) = \frac{1}{4\pi} \int_0^\pi E(\Theta) \left[\int_0^{2\pi} P_{\mathbf{h}_0}(\Theta, \psi) d\psi \right] \sin \Theta d\Theta \quad (13.64)$$

The direction \mathbf{y} is the pole of the spherical angular coordinate system Θ, ψ . One sees that in the case of a rotationally symmetric property $E(\Theta)$ the average value $\bar{E}(\mathbf{y})$ depends only on the values of the \mathbf{h}_0 pole figure, where \mathbf{h}_0 is the axis of rotational symmetry of the property concerned. It is also obviously clear that, because of the rotational symmetry of the property of the single crystal, the polycrystal property will not be altered if one rotates each crystal arbitrarily about its symmetry axis. The polycrystal property, therefore, can depend only on the spatial distribution of the axes of rotational symmetry — i.e. the \mathbf{h}_0 pole figure. We represent the pole figure by its series expansion:

$$P_{\mathbf{h}_0}(\Theta, \psi) = \sum_{l=0}^{\infty} \sum_{\nu=1}^{N(l)} F_l^*(\mathbf{h}_0) k_l^*(\Theta, \psi) \quad (13.65)$$

and expand the property function $E(\Theta)$ in LEGENDRE polynomials:

$$E(\Theta) = \sum_{l=0}^{\infty} e_l \bar{P}_l(\Theta) \quad (13.66)$$

Taking equation (14.200) into account, there then results from equation (13.64)

$$\bar{E}(\mathbf{y}) = \sum_{l=0}^{\infty} \frac{e_l}{\sqrt{2(2l+1)}} \sum_{\nu=1}^{N(l)} F_l^*(\mathbf{h}_0) k_l^*(\mathbf{y}) \quad (13.67)$$

This can be written

$$\bar{E}(y) = \sum_{l=0}^{\infty} \sum_{\nu=1}^{N(l)} \bar{e}_l k_l(y) \quad (13.68)$$

with the averaged coefficients

$$\bar{e}_l = \frac{e_l}{\sqrt{2(2l+1)}} F_l(\mathbf{h}_0) \quad (13.69)$$

which, as they must, depend only on the coefficients $F_l(\mathbf{h}_0)$ of the \mathbf{h}_0 pole figure.

If, also, the orientation distribution is rotationally symmetric (i.e. we are concerned with a fibre texture), we express the pole figure according to equation (5.26) in a series of normalized LEGENDRE polynomials. The coefficients F_l thereby appearing differ from the coefficients F_l^1 by the normalization factor $1/\sqrt{2\pi}$ of the rotationally symmetric spherical surface harmonics. However, since we also expanded the rotationally symmetric property function of the polycrystalline material in a series of LEGENDRE polynomials with the coefficients \bar{e}_l (equation 13.61), it is also true for these coefficients that

$$\bar{e}_l = \frac{e_l}{\sqrt{2(2l+1)}} F_l(\mathbf{h}_0) \quad (13.70)$$

13.3.3. Representation by Orientation Functions

Finally, we have represented the property E by one or more functions of the rotation g' , which transforms the crystal fixed coordinate system K_B into the external coordinate system K' . In the previously mentioned example of the magnetization energy in an inhomogeneous magnetic field the coordinate system K' was considered to be fixed with respect to the magnetic field. The rotation g' thus describes the orientation of the magnetic field with respect to the crystal axes. If g is the rotation which transforms the sample fixed system K_A into K_B , the rotation

$$g'' = g' \cdot g \quad (13.71)$$

thus transforms the sample fixed coordinate system K_A into the external system K' (Figure 13.1). The property E (equation 13.18) is then represented as a function of this rotation as follows:

$$E(g') = E(g'' \cdot g^{-1}) = \sum_{l=0}^r \sum_{\mu=1}^{M(l)} \sum_{\nu=1}^{N(l)} \sum_{s=-l}^{+l} e_l^{\mu\nu} T_l^{\mu s}(g'') T_l^{*\nu s}(g) \quad (13.72)$$

In order to obtain from this the average value over all orientations g , we must, according to equation (13.46), multiply by

$$f(g) = \sum_{l=0}^{\infty} \sum_{\mu=1}^{M(l)} \sum_{\nu=1}^{N(l)} \sum_{n=-l}^{+l} C_l^{\mu\nu} A_l^{n\nu} T_l^{\mu n}(g) \quad (13.73)$$

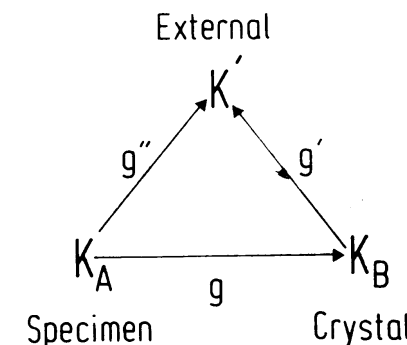


Figure 13.1 Specimen coordinate system K_A , crystal coordinate system K_B and external coordinate system K'

integrate over g , and obtain

$$\bar{E}(g'') = \sum_{l=0}^r \sum_{\mu=1}^{M(l)} \sum_{\nu=1}^{N(l)} \bar{e}_l^{\mu\nu} T_l^{\mu\nu}(g'') \quad (13.74)$$

with

$$\bar{e}_l^{\mu\nu} = \frac{1}{2l+1} \sum_{\lambda=1}^{M(l)} e_l^{\mu\lambda} C_l^{\lambda\nu} \quad (13.75)$$

Also, for this representation of the property E , the coefficients $\bar{e}_l^{\mu\nu}$ of the average value have thus been calculated from those of the individual crystallites and the texture coefficients $C_l^{\lambda\nu}$.

If the orientation distribution is rotationally symmetric about the Z-axis of the sample coordinate system, equation (13.73) thus transforms into

$$f(g) = R(\mathbf{h}) = \sum_{l=0}^{\infty} \sum_{\mu=1}^{M(l)} C_l^{\mu} \bar{k}_l^{\mu}(\mathbf{h}) \quad (13.76)$$

\mathbf{h} is that crystal direction which coincides with the axis of rotational symmetry. The average value $\bar{E}(g'')$ must in this case also be the same for all rotations g'' , which differ from each other only by a rotation about the axis of rotational symmetry. It can thus only depend on the orientation of the rotation axis — i.e. the Z-axis of the sample fixed coordinate system in the variable coordinate system K' . If we denote this by the vector \mathbf{z} , we thus obtain for the average value

$$\bar{E}(g'') = \bar{E}(\mathbf{z}) = \sum_{l=0}^r \sum_{\nu=1}^{N(l)} \bar{e}_l^{\nu} k_l^{\nu}(\mathbf{z}) \quad (13.77)$$

with

$$\bar{e}_l^{\nu} = \frac{1}{2l+1} \sum_{\mu=1}^{M(l)} C_l^{\mu} e_l^{\mu\nu} \quad (13.78)$$

We have thus derived completely general relations between the simple average value of a physical property of polycrystalline material and the corresponding

property of the single crystal. The relations are independent of which particular property is treated. They depend only on the form of the representation of the property. In many cases the simple average value \bar{E} is identical with the actual polycrystal property \tilde{E} . In many other cases equation (13.44) represents a sufficient, though only empirically based, approximation. Since, now, the calculation of the average value (\bar{E}^{-1}) from E^{-1} is formally identical with the calculation of \bar{E} from E , the calculation of the polycrystal quantity E essentially reduces to the simple average value in these cases.

13.4. Average Values of Special Properties

In the following the general formulae for the simple average values of physical properties will be applied to some special cases.

13.4.1. Magnetization Energy in a Homogeneous Magnetic Field

The magnetization energy of ferromagnetic crystals in a homogeneous magnetic field sufficient for saturation will, in general, be given as a function of the direction of magnetization — i.e. in the surface representation of a physical property. Since, further, the magnetization direction in each individual crystallite in this case agrees with the exterior magnetic field, the magnetization energy of a polycrystalline material is equal to the simple average value of the energies of the individual crystallites. In this case it is thus true that equation (13.28) is exact.

13.4.1.1. Magnetization Energy of Cubic Crystals

The magnetization energy of ferromagnetic cubic crystals can be described with sufficient accuracy by the expression

$$E(\mathbf{h}) = K_4(h_1^2 h_2^2 + h_1^2 h_3^2 + h_2^2 h_3^2) + K_6 h_1^2 h_2^2 h_3^2 \quad (13.79)$$

The functions

$$\varphi_4(\mathbf{h}) = h_1^2 h_2^2 + h_1^2 h_3^2 + h_2^2 h_3^2 \quad (13.80)$$

and

$$\varphi_6(\mathbf{h}) = h_1^2 h_2^2 h_3^2 \quad (13.81)$$

appearing here possess cubic symmetry. They are related to the cubic spherical harmonics in the manner described in Section 14.7.5. (See reference 193.)

It follows therefrom that

$$\varphi_4(\mathbf{h}) = \frac{1}{5} \frac{\dot{k}_4^1(\mathbf{h})}{n_4} + \frac{1}{5} \quad (13.82)$$

and

$$\varphi_6(\mathbf{h}) = \frac{1}{231} \frac{\dot{k}_6^1(\mathbf{h})}{n_6} + \frac{1}{55} \frac{\dot{k}_4^1(\mathbf{h})}{n_4} + \frac{1}{105} \quad (13.83)$$

Substituting in equation (13.79), by omission of the constant term, there results

$$E(\mathbf{h}) = \frac{\dot{k}_4^1(\mathbf{h})}{n_4} \left[\frac{K_4}{5} + \frac{K_6}{55} \right] + \frac{\dot{k}_6^1(\mathbf{h})}{n_6} \frac{K_6}{231} \quad (13.84)$$

The series expansion of the property function (13.9) thus has only two terms with the coefficients

$$e_4^1 = \frac{1}{n_4} \left[\frac{K_4}{5} + \frac{K_6}{55} \right]; \quad e_6^1 = \frac{1}{n_6} \frac{K_6}{231} \quad (13.85)$$

We now assume orthorhombic sample symmetry (sheet symmetry). The spherical surface harmonics of this symmetry are given by

$$\dot{k}_l^1(y) = \frac{1}{\sqrt{2\pi}} \bar{P}_l(\Phi); \quad \dot{k}_l^v(y) = \frac{1}{\sqrt{\pi}} \bar{P}_l^{2(v-1)}(\Phi) \cos 2(v-1)\gamma \quad (13.86)$$

By use of equations (13.85) and (13.86), we obtain from equation (13.58) with equation (13.59)

$$\bar{E}(\Phi, \gamma) = \frac{1}{9n_4\sqrt{\pi}} \left[\frac{K_4}{5} + \frac{K_6}{55} \right] F_4(\Phi, \gamma) + \frac{1}{13n_6\sqrt{\pi}} \frac{K_6}{231} F_6(\Phi, \gamma) \quad (13.87)$$

with

$$F_4(\Phi, \gamma) = \frac{1}{\sqrt{2}} C_4^{11} \bar{P}_4(\Phi) + C_4^{12} \bar{P}_4^2(\Phi) \cos 2\gamma + C_4^{13} \bar{P}_4^1(\Phi) \cos 4\gamma \quad (13.88)$$

and

$$F_6(\Phi, \gamma) = \frac{1}{\sqrt{2}} C_6^{11} \bar{P}_6(\Phi) + C_6^{12} \bar{P}_6^2(\Phi) \cos 2\gamma \\ + C_6^{13} \bar{P}_6^4(\Phi) \cos 4\gamma + C_6^{14} \bar{P}_6^6(\Phi) \cos 6\gamma \quad (13.89)$$

Φ and γ are the spherical angular coordinates of the direction of the magnetic field with respect to the coordinate system fixed in the sample. Since in the case of cubic symmetry only one linearly independent spherical surface harmonic of degree $l \leq 10$ exists, the texture coefficients C_l^{1v} in equations (13.88) and (13.89) can be determined by measurement of a single pole figure (see Section 4.2.2).

From the magnetization energy (equation 13.87) one obtains the torque exerted in the plane of the sheet $\Phi = 90^\circ$ on a sample with circular cross-section in a homogeneous magnetic field:

$$M = \frac{\partial \bar{E}(\Phi, \gamma)}{\partial \gamma} = \frac{1}{9n_4\sqrt{\pi}} \left[\frac{K_4}{5} + \frac{K_6}{55} \right] F'_4(\gamma) + \frac{1}{13n_6\sqrt{\pi}} \frac{K_6}{231} F'_6(\gamma) \quad (13.90)$$

with

$$F'_4(\gamma) = 2C_4^{12} \bar{P}_4^2(90^\circ) \sin 2\gamma + 4C_4^{13} \bar{P}_4^4(90^\circ) \sin 4\gamma \quad (13.91)$$

and

$$F'_6(\gamma) = 2C_6^{12} \bar{P}_6^2(90^\circ) \sin 2\gamma + 4C_6^{13} \bar{P}_6^4(90^\circ) \sin 4\gamma + 6C_6^{14} \bar{P}_6^6(90^\circ) \sin 6\gamma \quad (13.92)$$

The torque curves for different Fe–Si samples were calculated by this method by SZPUNAR and OJANEN²⁷⁴, from textures determined by neutron diffraction and the coefficients C_t^{uv} calculated therefrom. As Figure 13.2 shows, the agreement between measured values and those calculated from the texture was rather good. The calculation of the average values of a physical property can also be carried out by direct integration of equation (13.46), if the orientation distribution $f(g)$ is calculated — for example, not by methods based on series expansion, but, e.g., by the method of WILLIAMS. In this way the magnetic torque was calculated by HUTCHINSON and SWIFT^{158,159} from the texture (biaxial pole figures after WILLIAMS) for a rimmed steel cold-rolled 50% and annealed at 700°C (Figure 13.3) and compared with the experimental values. The agreement is similar to the calculation with the help of the coefficients from equations (13.90)–(13.92). This is also to be expected, since both methods are, of course, mathematically equivalent. The integration in equation (13.46) was carried out over 1296 orientation points.

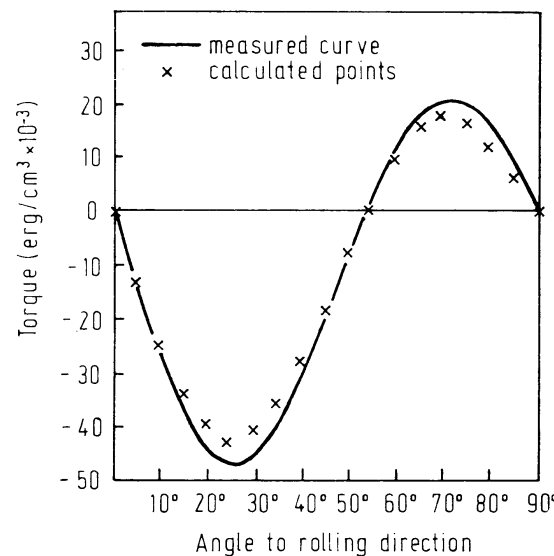


Figure 13.2 Torque curve of an Fe–Si sheet calculated according to equation (13.90) from neutron diffraction texture measurements. After SZPUNAR and OJANEN²⁷⁴

For rotationally symmetric textures (fibre, wire, rod) equation (13.87), in correspondence with equations (13.61) and (13.62), simplifies to

$$\bar{E}(\Phi) = \frac{1}{4\pi} \sqrt{\frac{2}{9}} \frac{1}{n_4} \left[\frac{K_1}{5} + \frac{K_6}{55} \right] C_4^1 \bar{P}_4(\Phi) + \frac{1}{4\pi} \sqrt{\frac{2}{13}} \frac{1}{n_6} \frac{K_6}{231} C_6^1 \bar{P}_6(\Phi) \quad (13.93)$$

where C_4^1 and C_6^1 are the fibre texture coefficients defined according to equation (5.4).

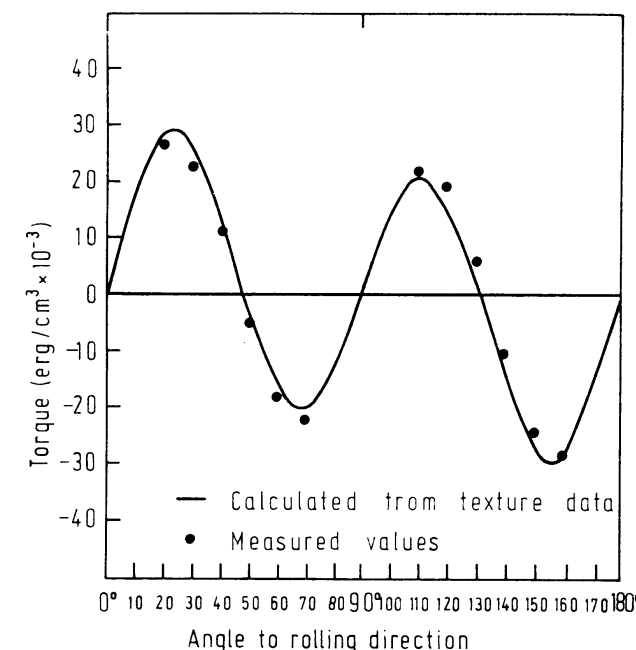


Figure 13.3 Torque curve of a rimmed steel, cold-rolled 50% and annealed at 700°C, calculated from biaxial pole figures and measured according to HUTCHINSON and SWIFT^{158,159}

The magnetic hysteresis (power loss) of a magnetic material can likewise be expressed by an expression of the form of equation (13.79), though with other coefficients. HUTCHINSON and SWIFT^{158,159} used as approximation for the power loss of a cubic crystal

$$P(\mathbf{h}) = A_0 + A_1(h_1^2 h_2^2 + h_2^2 h_3^2 + h_3^2 h_1^2) \quad (13.94)$$

This expression was averaged over all orientations with the help of the calculated biaxial pole figure according to equation (13.46). The result is represented in Figure 13.4. One sees that the direction dependence is well reproduced. The coefficients A_0 and A_1 were experimentally fitted.

13.4.1.2. Magnetization Energy of Hexagonal Crystals

For most cases the magnetization energy of hexagonal crystals can be described with sufficient accuracy by

$$E(\Phi) = K_2 \sin^2 \Phi + K_4 \sin^4 \Phi \quad (13.95)$$

Φ is the angle between the magnetization direction and the hexagonal axis. The energy is thus independent of the angle γ and can be expressed by two rotationally

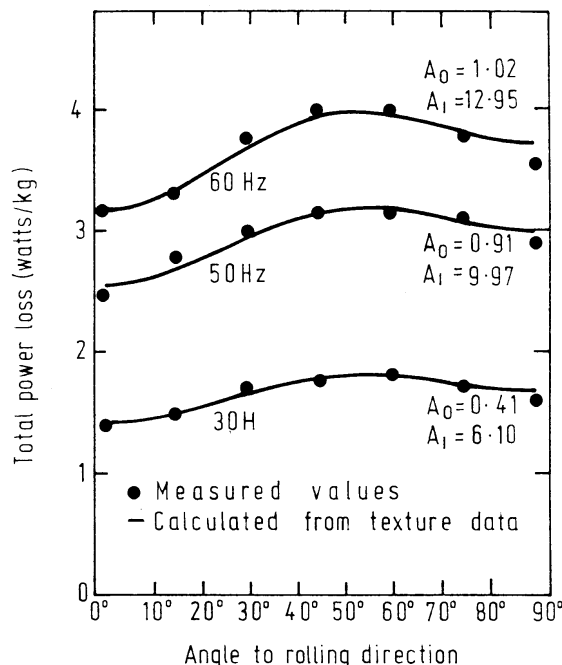


Figure 13.4 Power loss in Fe–Si according to HUTCHINSON and SWIFT^{158,159}. The curve was calculated from biaxial pole figures; the points were measured. The coefficients A_0 and A_1 were determined from the experiment

symmetric spherical surface harmonics of second and fourth order:

$$\dot{k}_2^1(\Phi) = \frac{1}{\sqrt{2\pi}} \sqrt{\frac{5}{2}} \left[\frac{3}{2} \cos^2 \Phi - \frac{1}{2} \right] \quad (13.96)$$

and

$$\dot{k}_4^1(\Phi) = \frac{1}{\sqrt{2\pi}} \sqrt{\frac{9}{2}} \left[\frac{35}{8} \cos^4 \Phi - \frac{15}{4} \cos^2 \Phi + \frac{3}{8} \right] \quad (13.97)$$

By a transformation one obtains therefrom

$$\sin^2 \Phi = \frac{2}{3} - \frac{2}{3} \sqrt{\frac{2}{5}} \sqrt{2\pi} \dot{k}_2^1(\Phi) \quad (13.98)$$

and

$$\sin^4 \Phi = \frac{8}{15} - \frac{16}{21} \sqrt{\frac{2}{5}} \sqrt{2\pi} \dot{k}_2^1(\Phi) + \frac{8}{35} \sqrt{\frac{2}{9}} \sqrt{2\pi} \dot{k}_4^1(\Phi) \quad (13.99)$$

By neglecting the constant terms there results

$$E(\Phi) = - \sqrt{\frac{2}{5}} \sqrt{2\pi} \left[\frac{2}{3} K_2 + \frac{16}{21} K_4 \right] \dot{k}_2^1(\Phi) + \sqrt{\frac{2}{9}} \sqrt{2\pi} \frac{8}{35} K_4 \dot{k}_4^1(\Phi) \quad (13.100)$$

The coefficients e_i^μ are thus given by

$$e_2^1 = - \sqrt{\frac{2}{5}} \sqrt{2\pi} \left[\frac{3}{2} K_2 + \frac{16}{21} K_4 \right]; \quad e_4^1 = \sqrt{\frac{2}{9}} \sqrt{2\pi} \frac{8}{35} K_4 \quad (13.101)$$

We now further assume orthorhombic sample symmetry and obtain for the averaged energy, according to equations (13.58) and (13.59),

$$\bar{E}(\Phi, \gamma) = - \frac{2}{5} \frac{1}{\sqrt{5}} \left[\frac{3}{2} K_2 + \frac{16}{21} K_4 \right] F_2(\Phi, \gamma) + \frac{2}{27} \cdot \frac{8}{35} K_4 F_4(\Phi, \gamma) \quad (13.102)$$

with

$$F_2(\Phi, \gamma) = \frac{1}{\sqrt{2}} C_2^{11} \bar{P}_2(\Phi) + C_2^{12} \bar{P}_2^2(\Phi) \cos 2\gamma \quad (13.103)$$

and

$$F_4(\Phi, \gamma) = \frac{1}{\sqrt{2}} C_4^{11} \bar{P}_4(\Phi) + C_4^{12} \bar{P}_4^2(\Phi) \cos 2\gamma + C_4^{13} \bar{P}_4^4(\Phi) \cos 4\gamma \quad (13.104)$$

Since only one linearly independent hexagonal spherical surface harmonic of second and fourth orders exists, the coefficients in equations (13.103) and (13.104) can also be determined from a single pole figure, as in the case of cubic symmetry.

13.4.2. The Remanence in Ferromagnetic Materials

In the previous section we have considered the energy which is necessary to bring about the spontaneous magnetization of a crystal in a specific crystallographic direction \mathbf{h} . We now consider those directions, \mathbf{h}_i , for which the energy assumes a minimum value. Several cases are to be differentiated. In the first case exactly one such direction \mathbf{h}_0 (as well as its opposite, $-\mathbf{h}_0$) results; in the second case there result several different directions \mathbf{h}_i for which the magnetization will be minimal. To the first group belong, e.g., many hexagonal materials; to the second, cubic materials. Finally, it can also occur that for a whole band of directions — e.g. all those perpendicular to a direction — a minimum energy will be assumed.

If one thinks of a crystal magnetized to saturation in the direction \mathbf{h} , the magnetization thus lies in the direction \mathbf{h} . If, now, one removes the magnetic field, the magnetization will rotate into the nearest direction \mathbf{h}_i of minimum energy. The component of magnetization in the direction of the original field then amounts to

$$I_R = I_S \cos \langle \mathbf{h} \mathbf{h}_i \rangle \quad (13.105)$$

The component I_R will be called the remanence; I_S is the saturation magnetization.

We now assume that only a single direction \mathbf{h}_0 of minimum energy exists, and choose a spherical angular coordinate system Θ, φ , such that its pole $\Theta = 0$ coincides with \mathbf{h}_0 . We then obtain for the relative remanence in the case of original

magnetization in the direction Θ, ψ

$$I_R(\Theta, \psi)/I_S = |\cos \Theta| \quad (13.106)$$

In this case the remanence is thus a property of the crystal independent of the angle ψ . With respect to this property the crystal thus has rotational symmetry. If we set

$$|\cos \Theta| = \sum_{l=0}^{\infty} e_l \bar{P}_l(\Theta) \quad (13.107)$$

we thus obtain a series expansion corresponding to equation (13.66) for $I_R(\Theta)/I_S$. The coefficients e_l are given in Table 13.2.

Table 13.2 COEFFICIENTS e_l OF THE SERIES EXPANSION OF THE REMANENCE IN HEXAGONAL FERROMAGNETIC CRYSTALS

l	e_l	l	e_l
0	0.707 107	16	-0.005 909
2	0.395 285	18	0.004 692
4	-0.088 388	20	-0.003 817
6	0.039 836	22	0.003 166
8	-0.022 777	24	-0.002 668
10	0.014 767	26	0.002 279
12	-0.010 358	28	-0.001 970
14	0.007 670	30	0.001 719

We now consider a polycrystalline material and assume that the magnetization is not influenced by interactions with neighbouring crystallites. The remanence of the polycrystal is then equal to the sum of the remanences of the individual crystallites. If Φ and γ are the spherical angular coordinates of an arbitrary sample direction \mathbf{y} , we thus obtain for the relative remanence in the case of magnetization in the direction Θ, ψ according to equations (13.68) and (13.69)

$$I_R(\Theta, \psi)/I_S = \sum_{l=0}^{\infty} \sum_{v=1}^{N(l)} \bar{e}_l \bar{k}_l^v(\Phi, \psi) \quad (13.108)$$

with

$$\bar{e}_l = \frac{e_l}{\sqrt{2(2l+1)}} F_l^v(\mathbf{h}_0) \quad (13.109)$$

The $\bar{k}_l^v(\Phi, \psi)$ are the normalized spherical surface harmonics of the sample symmetry (in the case of orthorhombic sheet symmetry see, e.g., equation 13.86), and the $F_l^v(\mathbf{h}_0)$ are the coefficients of the series expansion of the \mathbf{h}_0 pole figure, and thus the pole figure corresponding to the preferred direction of magnetization.

They can be directly determined from this pole figure according to equation (4.70) or, if this pole figure is not measurable, by means of the C_l^{uv} from other measurable pole figures.

In the case of rotationally symmetric textures equation (13.108) transforms into (see references 131, 264, 265)

$$I_R(\Phi) = \sum_{l=0}^{\infty} \bar{e}_l \bar{P}_l(\Phi) \quad (13.110)$$

with the coefficients

$$\bar{e}_l = \frac{e_l}{\sqrt{2(2l+1)}} F_l(\mathbf{h}_0) \quad (13.111)$$

The $F_l(\mathbf{h}_0)$ are the coefficients of pole figures for fibre textures defined by equation (5.26).

As one sees from Figure 13.5, the coefficients e_l decrease very rapidly with l . If, for example, one assumes a limit of 5%, one thus only needs to consider series terms up to sixth order⁶⁹. If, further, one also omits the sixth-order term and uses only the terms of second and fourth order, then, according to Figure 4.4, it is

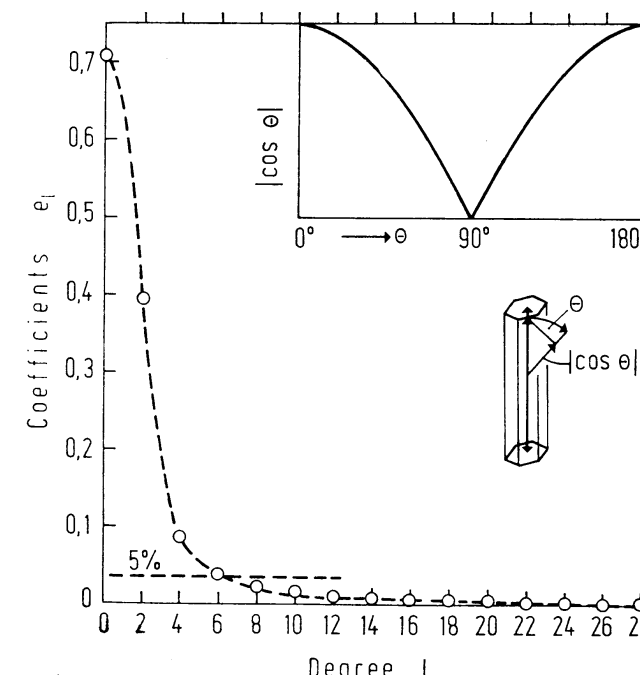


Figure 13.5 The relative remanence $|\cos \Theta|$ of an hexagonal single crystal and the coefficients e_l of the series expansion in LEGENDRE polynomials⁶⁹

$M(l=4) = 1$. The coefficients $F_l^v(\mathbf{h}_i)$, which are needed for calculation of the average values, can then be calculated from a single arbitrary pole figure.

We finally further consider the case of several different preferred directions, as occurs, e.g., in the case of cubic crystals. If we further assume that, on removing the magnetic field, the magnetization changes into the nearest preferred direction \mathbf{h}_i , it is thus true for the relative remanence of the single crystal in different angular regions that

$$I_R(\Phi, \beta)/I_S = \begin{cases} \cos \langle \mathbf{h}\mathbf{h}_1 \rangle & \text{in region } B_1 \\ \cos \langle \mathbf{h}\mathbf{h}_2 \rangle & \text{in region } B_2 \\ \dots & \dots \\ \cos \langle \mathbf{h}\mathbf{h}_i \rangle & \text{in region } B_i \end{cases} \quad (13.112)$$

The region B_i is so defined that within it the angle $\langle \mathbf{h}\mathbf{h}_i \rangle$ is the smallest among the angles $\langle \mathbf{h}\mathbf{h}_j \rangle$. If we expand $I_R(\Phi, \beta)/I_S$ in a series of spherical surface harmonics of the crystal symmetry

$$I_R(\Phi, \beta)/I_S = \sum_{l=0}^{\infty} \sum_{\mu=1}^{M(l)} e_l^{\mu} k_l^{\mu}(\Phi, \beta) \quad (13.113)$$

it is thus true for the coefficients that

$$e_l^{\mu} = \sum_i \int_{B_i} \cos \langle \mathbf{h}\mathbf{h}_i \rangle k_l^{*\mu}(\Phi, \beta) \sin \Phi d\Phi d\beta \quad (13.114)$$

If the directions \mathbf{h}_i are symmetrically equivalent, the integrals over the individual regions are equal. One thus obtains

$$e_l^{\mu} = n \int_{B_1} \cos \langle \mathbf{h}\mathbf{h}_1 \rangle k_l^{*\mu}(\Phi, \beta) \sin \Phi d\Phi d\beta \quad (13.115)$$

n is the number of symmetrically equivalent regions, and B_1 is an arbitrary one among them. The remanence of the polycrystalline material results therefrom according to equations (13.58) and (13.59). For cubic crystal symmetry and the preferred directions $\mathbf{h}_i = \langle 100 \rangle$, $\mathbf{h}_i = \langle 110 \rangle$ and $\mathbf{h}_i = \langle 111 \rangle$ the regions B_i are shown in Figure 13.6.

13.4.3. Tensor Properties of Second Order

A large number of physical properties can be described by tensors of second order – e.g. thermal expansion, optical refractive index and electrical conductivity. We will therefore calculate the orientation average value of such properties in general form (see references 34, 35, 271, 272). A symmetric tensor of second order can always be described by an ellipsoid, which we can relate to its principal axes:

$$E(\mathbf{h}) = E_{11} h_1^2 + E_{22} h_2^2 + E_{33} h_3^2 \quad (13.116)$$

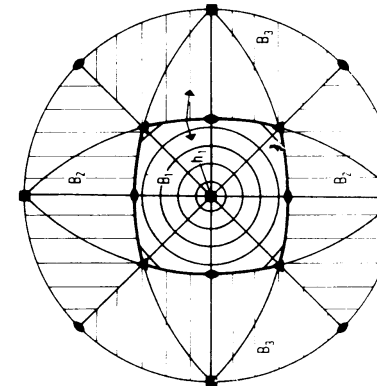
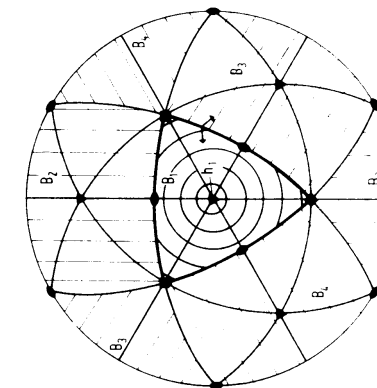
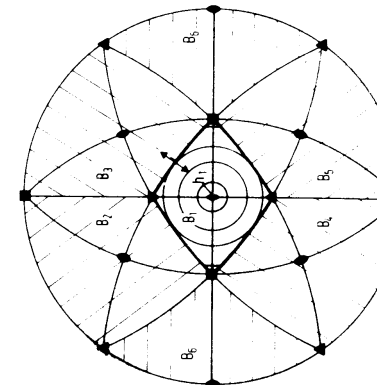


Figure 13.6 The regions B_i for cubic crystal symmetry, into which the magnetization transforms after removal of the field in the pertinent preferred direction \mathbf{h}_i and indeed for the three cases $\mathbf{h}_i = \langle 100 \rangle$, $\mathbf{h}_i = \langle 110 \rangle$ and $\mathbf{h}_i = \langle 111 \rangle$

With respect to such a property all crystals have at least orthorhombic symmetry. In the case of cubic symmetry all three coefficients are equal, and E is independent of the direction and thus the average value \bar{E} is independent of the texture. If one sets

$$h_1 = \sin \Phi \cos \beta \quad (13.117)$$

$$h_2 = \sin \Phi \sin \beta \quad (13.118)$$

$$h_3 = \cos \Phi \quad (13.119)$$

then

$$h_1^2 = \frac{1}{2} (1 - \cos^2 \Phi) (1 + \cos 2\beta) \quad (13.120)$$

$$h_2^2 = \frac{1}{2} (1 - \cos^2 \Phi) (1 - \cos 2\beta) \quad (13.121)$$

$$h_3^2 = \cos^2 \Phi \quad (13.122)$$

These can be expressed by means of the orthorhombic spherical surface harmonics of second order:

$$k_2^1(\Phi) = \frac{1}{\sqrt{2\pi}} \sqrt{\frac{5}{2}} \frac{1}{2} (3 \cos^2 \Phi - 1) \quad (13.123)$$

$$k_2^2(\Phi) = \frac{1}{\sqrt{\pi}} \sqrt{\frac{5}{3}} \frac{3}{4} (1 - \cos^2 \Phi) \cos 2\beta \quad (13.124)$$

One thereby obtains

$$h_1^2 = \frac{1}{3} - \frac{1}{3} \sqrt{2\pi} \sqrt{\frac{2}{5}} k_2^1(\Phi) + \frac{2}{3} \sqrt{\pi} \sqrt{\frac{3}{5}} k_2^2(\Phi, \beta) \quad (13.125)$$

$$h_2^2 = \frac{1}{3} - \frac{1}{3} \sqrt{2\pi} \sqrt{\frac{2}{5}} k_2^1(\Phi) - \frac{2}{3} \sqrt{\pi} \sqrt{\frac{3}{5}} k_2^2(\Phi, \beta) \quad (13.126)$$

$$h_3^2 = \frac{1}{3} + \frac{2}{3} \sqrt{2\pi} \sqrt{\frac{2}{5}} k_2^1(\Phi) \quad (13.127)$$

This yields

$$\begin{aligned} E(\Phi, \beta) &= \frac{1}{3} (E_{11} + E_{22} + E_{33}) \\ &+ \frac{1}{3} \sqrt{2\pi} \sqrt{\frac{2}{5}} k_2^1(\Phi) (2E_{33} - E_{11} - E_{22}) \\ &+ \frac{2}{3} \sqrt{\pi} \sqrt{\frac{3}{5}} k_2^2(\Phi, \beta) (E_{11} - E_{22}) \end{aligned} \quad (13.128)$$

One thus obtains for the coefficients of the series expansion of the property function

$$e_2^1 = \frac{1}{3} \sqrt{2\pi} \sqrt{\frac{2}{5}} (2E_{33} - E_{11} - E_{22}) \quad (13.129)$$

$$e_2^2 = \frac{2}{3} \sqrt{\pi} \sqrt{\frac{3}{5}} (E_{11} - E_{22}) \quad (13.130)$$

We further assume orthorhombic sample symmetry — i.e. sheet or foil. Then, according to equation (13.59), there result for the averaged coefficients

$$\bar{e}_2^1 = \frac{2}{15} \sqrt{\frac{\pi}{5}} [(2E_{33} - E_{11} - E_{22}) C_2^{11} + \sqrt{3} (E_{11} - E_{22}) C_2^{21}] \quad (13.131)$$

$$\bar{e}_2^2 = \frac{2}{15} \sqrt{\frac{\pi}{5}} [(2E_{33} - E_{11} - E_{22}) C_2^{12} + \sqrt{3} (E_{11} - E_{22}) C_2^{22}] \quad (13.132)$$

One thereby finally obtains for the averaged quantity $\bar{E}(\Phi, \gamma)$

$$\begin{aligned} \bar{E}(\Phi, \gamma) &= \frac{1}{3} (E_{11} + E_{22} + E_{33}) \\ &+ \frac{2}{15 \sqrt{10}} [(2E_{33} - E_{11} - E_{22}) C_2^{11} + 53(E_{11} - E_{22}) C_2^{21}] \bar{P}_2(\Phi) \\ &+ \frac{2}{15 \sqrt{5}} [(2E_{33} - E_{11} - E_{22}) C_2^{12} \\ &+ 53(E_{11} - E_{22}) C_2^{22}] \bar{P}_2(\Phi) \cos 2\gamma \end{aligned} \quad (13.133)$$

For fibre textures, according to equation (13.62), there results

$$\bar{e}_2 = \frac{1}{15} \frac{1}{\sqrt{2\pi}} [(2E_{33} - E_{11} - E_{22}) C_2^1 + \sqrt{3} (E_{11} - E_{22}) C_2^2] \quad (13.134)$$

It follows therefrom that

$$\begin{aligned} \bar{E}(\Phi) &= \frac{1}{3} (E_{11} + E_{22} + E_{33}) \\ &+ \frac{1}{15} \frac{1}{\sqrt{2\pi}} [(2E_{33} - E_{11} - E_{22}) C_2^1 + 53(E_{11} - E_{22}) C_2^2] \bar{P}_2(\Phi) \end{aligned} \quad (13.135)$$

13.4.3.1. Thermal Expansion of Uranium

We will consider thermal expansion as an example of a tensor property of second order. In addition, because of its strong thermal anisotropy and because of its great technical importance, uranium has been the object of many experimental

investigations. It has been shown that the thermal expansion of a polycrystalline uranium sample under certain conditions is given by the simple average value of the expansions of the individual crystallites¹¹⁵. In the case of the strongly anisotropic expansion of uranium this is by no means self-evident. Thus, e.g., the thermal expansion of a polycrystalline graphite sample differs noticeably from the simple average value²⁴².

If we set for the thermal expansion coefficients of uranium at 75°C in the axis directions²⁸,

$$E_{11} = +20.3 \cdot 10^{-6}; \quad E_{22} = -1.4 \cdot 10^{-6}; \quad E_{33} = +22.2 \cdot 10^{-6} \quad (13.136)$$

we thus obtain for the expansion of a polycrystalline sample with orthorhombic sample symmetry (sheet symmetry) in the direction Φ, γ according to equation (13.133)

$$\begin{aligned} \bar{E}(\Phi, \gamma) \cdot 10^6 &= 13.7 + [1.11C_2^{11} + 1.63C_2^{21}] \bar{P}_2(\Phi) \\ &\quad + [1.52C_2^{12} + 2.24C_2^{22}] \bar{P}_2^2(\Phi) \cos 2\gamma \end{aligned} \quad (13.137)$$

Thus results according to equation (13.135) for the expansion of a sample with rotationally symmetric texture

$$\bar{E}(\Phi) \cdot 10^6 = 13.7 + [0.68C_2^1 + 1.00C_2^2] \bar{P}_2(\Phi) \quad (13.138)$$

13.4.3.2. Growth of Uranium During Neutron Irradiation

As a second example of a tensor property of second order we consider the dimensional change of uranium during neutron irradiation. This property can be described with sufficient accuracy by a tensor of second order^{271,272}, and the dimensional change of a polycrystalline sample is given within the accuracy of measurement by the simple average value, in contrast to graphite. The experimentally determined dimensional changes in the axis directions are

$$E_{11} = -A; \quad E_{22} = +A; \quad E_{33} = 0 \quad (13.139)$$

According to equation (13.133) one thereby obtains for the length change in the direction Φ, γ of a polycrystalline sample with sheet symmetry

$$\bar{E}(\Phi, \gamma) = -A [0.150C_2^{21}\bar{P}_2(\Phi) + 0.206C_2^{22}\bar{P}_2^2(\Phi) \cos 2\gamma] \quad (13.140)$$

It follows directly therefrom that a sample with random orientation distribution shows no length change and that the length change of a textured sample is independent of the coefficients C_2^{11} and C_2^{12} . For a sample with rotationally symmetric texture the expansion in a direction which makes the angle Φ with the axis is given according to equation (13.135) by

$$\bar{E}(\Phi) = -A \cdot 0.092C_2^2\bar{P}_2(\Phi) \quad (13.141)$$

13.4.4. Elastic Properties

13.4.4.1. Cubic Crystal Symmetry

We denote the stress tensor by σ and the strain tensor by ε and limit ourselves to small deformations, so that a linear relation exists between the two tensors:

$$\varepsilon_{ij} = s_{ijkl}\sigma_{kl} \quad (13.142)$$

$$\sigma_{ij} = c_{ijkl}\varepsilon_{kl} \quad (13.143)$$

In the notation used in equation (13.39)

$$c_{ijkl} = (s_{ijkl})^{-1} \quad (13.144)$$

Correspondingly, for the polycrystalline material

$$\tilde{\varepsilon}_{ij} = \tilde{s}_{ijkl}\bar{\sigma}_{kl} \quad (13.145)$$

$$\bar{\sigma}_{ij} = \tilde{c}_{ijkl}\tilde{\varepsilon}_{kl} \quad (13.146)$$

Also in this case it is naturally true that

$$\tilde{c}_{ijkl} = (\tilde{s}_{ijkl})^{-1} \quad (13.147)$$

The polycrystal quantities \tilde{s}_{ijkl} and \tilde{c}_{ijkl} in equations (13.145) and (13.146) differ, in general, from the simple average values \bar{s}_{ijkl} and \bar{c}_{ijkl} . We set approximately

$$\tilde{c}_{ijkl} \approx \bar{c}_{ijkl} = c_{ijkl}^V \quad (13.148)$$

this thus corresponds to the approximation used by VOIGT²⁹¹ for random crystal orientation. Likewise

$$\tilde{s}_{ijkl} \approx \bar{s}_{ijkl} = s_{ijkl}^R \quad (13.149)$$

corresponds to the approximation of REUSS²⁴⁴.

If the stress tensor is a simple tensile stress and if the grain boundaries are perpendicular to the direction of σ (Figure 13.7a), then σ has the same value in all crystallites. After equation (13.42) this is the presumption for the exact validity of the approximation (13.149). If however, as is shown in Figure 13.7b, the grain boundaries are parallel to the directions of σ , then the strain ε is the same in all crystallites. After equation (13.43) this is the presumption for the exact validity of the approximation (13.148).

We further set

$$s_{ijkl}^V = (c_{ijkl}^V)^{-1} \quad (13.150)$$

whence, according to equation (13.44),

$$\tilde{s}_{ijkl} \approx \frac{1}{2} [s_{ijkl}^R + s_{ijkl}^V] = s_{ijkl}^H \quad (13.151)$$

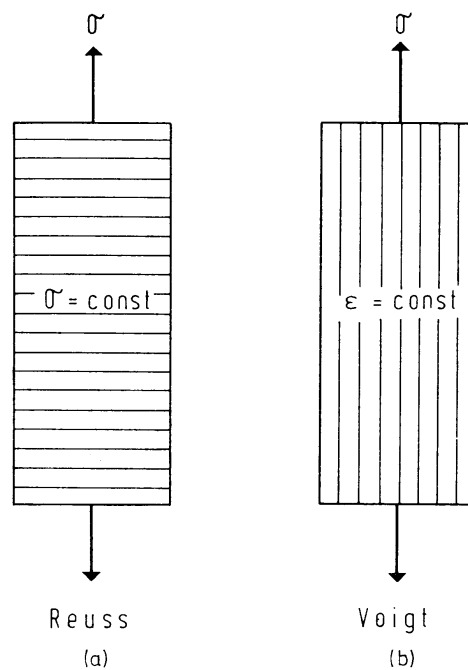


Figure 13.7 Validity of VOIGT's and REUSS' approximation for two extremes of grain shape

It is customary to call this approximation for the elastic properties of polycrystalline materials the VONGT-REUSS-HILL approximation. It is well fulfilled for weakly anisotropic crystals, and the deviations from it still are small for stronger anisotropy.^{88,89}

The quantities s_{ijkl} and c_{ijkl} obey the symmetry conditions

$$s_{ijkl} = s_{jikl} = s_{ijlk} = s_{klij} \quad (13.152)$$

One can therefore write them in matrix representation (Table 13.3). Because of the crystal symmetry a series of further relations exist between these quantities, which are illustrated for cubic symmetry by the scheme in Figure 13.8 (e.g. reference 220). The cubic axes were thus used as the coordinate system.

For isotropic materials the scheme in Figure 13.9 is valid. One sees that in the case of cubic symmetry only one more linearly independent constant results than in the isotropic case. We denote the components of the tensor s , with respect to the cubic axes, by s_{ijkl}^0 ; we can thus decompose the tensor s_{ijkl}^0 for cubic symmetry into an isotropic and an anisotropic part in the following manner:

$$s_{ijkl}^0 = s_{ijkl}^I + s_a t_{ijkl} \quad (13.153)$$

s_{ijkl}^I denotes the isotropic part according to Figure 13.9 and

$$s_a = s_{1111}^0 - s_{1122}^0 - 2s_{1212}^0 \quad (13.154)$$

Table 13.3 MATRIX REPRESENTATION OF THE ELASTICITY TENSOR

m	i, j	n	1	2	3	4	5	6
		kl	11	22	33	23	31	12
1	11							s_{1111}
2	22							s_{1122}
3	33							
4	23							
5	31							
6	12					s_{1211}		s_{1212}

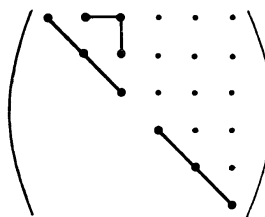


Fig. 13.8

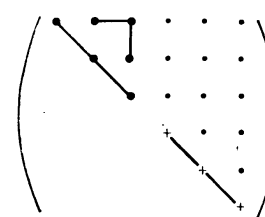


Fig. 13.9

Figure 13.8 Elasticity tensor for cubic symmetry. The heavy points represent components which can be different from zero; the components joined by a line are equal

Figure 13.9 Elasticity tensor for isotropic materials. The crosses denote $(1/2)$ ($s_{1111} - s_{1122}$)

is the amount of the anisotropy, and the tensor t_{ijkl} has the components

$$t_{1111} = t_{2222} = t_{3333} = 1 \quad (13.155)$$

All other components are zero. Since the isotropic part s_{ijkl}^I is orientation independent, one obtains for the average value

$$\bar{s}_{ijkl}^R = \bar{s}_{ijkl} = s_{ijkl}^I + s_a \bar{t}_{ijkl} = s_{ijkl}^0 + s_a (\bar{t}_{ijkl} - t_{ijkl}) \quad (13.156)$$

According to equation (13.51), the quantity \bar{t}_{ijkl} is given by

$$\bar{t}_{ijkl} = \bar{a}(ijkl; nnnn) = \bar{a}(ijkl) \quad (13.157)$$

(which is to be summed over n from $n = 1$ to $n = 3$). The $\bar{a}(ijkl, nnnn)$ are given by equation (13.52). Because $r = 4$, there appear therein in addition to $C_0^{11} = 1$ only the coefficients $C_4^{11}, C_4^{12}, C_4^{13}$. One thus obtains

$$\bar{t}_{ijkl} = \bar{a}_0^{11}(ijkl) + \bar{a}_4^{11}(ijkl) C_4^{11} + \bar{a}_4^{12}(ijkl) C_4^{12} + \bar{a}_4^{13}(ijkl) C_4^{13} \quad (13.158)$$

where the $\bar{a}_\lambda^{mn}(ijkl)$ result from the quantities defined in equation (13.53) by summation:

$$\bar{a}_\lambda^{mn}(ijkl) = \bar{a}_\lambda^{mn}(ijkl; nnnn) \quad (13.159)$$

For the components of the averaged tensor in REUSS' approximation, one thereby obtains

$$\begin{aligned}s_{ijkl}^R = \bar{s}_{ijkl} &= s_{ijkl}^0 + s_a[\bar{a}_0^{11}(ijkl) - t_{ijkl} + \bar{a}_4^{11}(ijkl) C_4^{11} \\ &\quad + \bar{a}_4^{12}(ijkl) C_4^{12} + \bar{a}_4^{13}(ijkl) C_4^{13}]\end{aligned}\quad (13.160)$$

In particular, for the case of random orientation distribution one obtains

$$s_{ijkl}^R = \bar{s}_{ijkl} = s_{ijkl}^0 + s_a[\bar{a}_0^{11}(ijkl) - t_{ijkl}] \quad (13.161)$$

$$s_{1111}^R = 0.6s_{1111}^0 + 0.4s_{1122}^0 + 0.8s_{1212}^0 \quad (13.162)$$

$$s_{1122}^R = 0.2s_{1111}^0 + 0.8s_{1122}^0 - 0.4s_{1212}^0 \quad (13.163)$$

$$s_{1212}^R = 0.2s_{1111}^0 - 0.2s_{1122}^0 + 0.6s_{1212}^0 \quad (13.164)$$

The three last quantities fulfil, as they must, the condition given in *Figure 13.9*.

The $\bar{a}_\lambda^{\mu\nu}(ijkl)$ are purely mathematical quantities; they depend neither on the elastic constants of the single crystals nor on the orientation distribution. They can therefore be calculated with complete generality in the manner described by equations (13.22)–(13.24). One thus obtains *Table 13.4* (see reference 50).

Table 13.4 THE AVERAGE COEFFICIENTS $\bar{a}_\lambda^{\mu\nu}(ijkl)$ FOR CUBIC CRYSTAL SYMMETRY AND ORTHORHOMBIC SAMPLE SYMMETRY

$ijkl$	$\bar{a}_0^{11}(ijkl) - t_{ijkl}$	$\bar{a}_4^{11}(ijkl)$	$\bar{a}_4^{12}(ijkl)$	$\bar{a}_4^{13}(ijkl)$
1111	-0.4	+0.021 818	-0.032 530	+0.043 032
2222	-0.4	+0.021 818	+0.032 530	+0.043 032
3333	-0.4	+0.058 182	0	0
1122	+0.2	+0.007 273	0	-0.043 032
1133	+0.2	-0.029 091	+0.032 530	0
2233	+0.2	-0.029 091	-0.032 530	0
1212	+0.2	+0.007 273	0	-0.043 032
1313	+0.2	-0.029 091	+0.032 530	0
2323	+0.2	-0.029 091	-0.032 530	0

In exactly the same manner there result for the constants c_{ijkl}^0 in the case of cubic symmetry

$$c_{ijkl}^0 = c_{ijkl}^I + c_a t_{ijkl} \quad (13.165)$$

with

$$c_a = c_{1111}^0 - c_{1122}^0 - 2c_{1212}^0 \quad (13.166)$$

It follows therefrom that

$$c_{ijkl}^V = \bar{c}_{ijkl} = c_{ijkl}^I + c_a \bar{t}_{ijkl} = c_{ijkl}^0 + c_a(\bar{t}_{ijkl} - t_{ijkl}) \quad (13.167)$$

$$\begin{aligned}c_{ijkl}^V = \bar{c}_{ijkl} &= c_{ijkl}^0 + c_a[\bar{a}_0^{11}(ijkl) - t_{ijkl} + \bar{a}_4^{11}(ijkl) C_4^{11} \\ &\quad + \bar{a}_4^{12}(ijkl) C_4^{12} + \bar{a}_4^{13}(ijkl) C_4^{13}]\end{aligned}\quad (13.168)$$

For random orientation distribution one further obtains

$$c_{ijkl}^V = c_{ijkl}^0 + c_a[\bar{a}_0^{11}(ijkl) - t_{ijkl}] \quad (13.169)$$

as well as the equations for c_{ijkl}^V analogous to equations (13.162)–(13.164). One then also obtains the constants s_{ijkl}^V according to equation (13.150). The elastic compliances \bar{s}_{ijkl} of the polycrystal are calculated according to the approximation given by equation (13.151).

One obtains YOUNG's modulus $\tilde{E}(y)$ in an arbitrary sample direction y from the elastic compliances \bar{s}_{ijkl} (see, e.g., reference 220):

$$\begin{aligned}\frac{1}{\tilde{E}(y)} &= y_1^4 \bar{s}_{1111} + y_2^4 \bar{s}_{2222} + y_3^4 \bar{s}_{3333} + 2y_1^2 y_2^2 (\bar{s}_{1122} + 2\bar{s}_{1212}) \\ &\quad + 2y_1^2 y_3^2 (\bar{s}_{1133} + 2\bar{s}_{1313}) + 2y_2^2 y_3^2 (\bar{s}_{2233} + 2\bar{s}_{2323})\end{aligned}\quad (13.170)$$

YOUNG's modulus $\tilde{E}(y)$ was calculated in this way for a Cu–Si sample deformed by shear spinning by DURAND¹²³. It is represented in *Figure 13.10*. If one sets

$$y_3 = 0; \quad y_1 = \cos \gamma; \quad y_2 = \sin \gamma \quad (13.171)$$

the YOUNG's modulus in the plane of the sheet is

$$\frac{1}{\tilde{E}(y)} = \bar{s}_{1111} \cos^4 \gamma + \bar{s}_{2222} \sin^4 \gamma + \left(\bar{s}_{1212} + \frac{1}{2} \bar{s}_{1122} \right) \sin^2 2\gamma \quad (13.172)$$

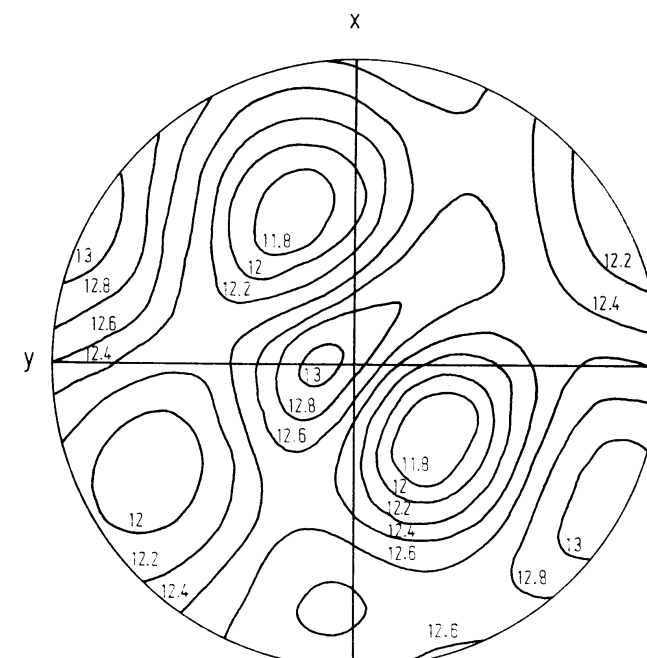


Figure 13.10 Elasticity modulus $\tilde{E}(y)$ as a function of the sample direction y , after DURAND¹²³. The material studied is Cu–Si deformed by shear spinning

The coefficients

$$C_4^{11} = -1.02 \pm 0.15; \quad C_4^{12} = -0.48 \pm 0.15; \quad C_4^{13} = -1.60 \pm 0.08 \quad (13.173)$$

were determined for a 90% cold-rolled copper sheet from the first four pole figures (111), (200), (220), (311)⁸². One obtains therefrom the values given in Table 13.5 for the quantities t_{ijkl} as well as the s_{ijkl} in the three approximations V—R—H.

Table 13.5 THE COMPONENTS OF THE TEXTURE TENSOR \bar{t}_{ijkl} AND THE ELASTIC COMPLIANCES OF A 90% COLD-ROLLED COPPER SHEET IN THREE APPROXIMATIONS (IN $10^{-12} \text{ cm}^2 \text{ dyn}^{-1}$)

$ijkl$	s_{ijkl}^0	$\bar{t}_{ijkl} - t_{ijkl}$	s_{ijkl}^R	s_{ijkl}^V	s_{ijkl}^H
1111	+1.49	-0.4753	+0.7960	+0.6293	+0.7126
2222	+1.49	-0.5067	+0.7503	+0.6074	+0.6788
3333	+1.49	-0.4596	+0.8190	+0.6403	+0.7297
1122	-0.63	+0.2612	-0.2486	-0.1832	-0.2159
1133	-0.63	+0.2141	-0.3174	-0.2161	-0.2667
2233	-0.63	+0.2455	-0.2716	-0.1942	-0.2329
1212	+0.33	+0.2612	+0.7139	+0.5182	+0.6160
1313	+0.33	+0.2141	+0.6451	+0.4708	+0.5580
2323	+0.33	+0.2455	+0.6909	+0.5013	+0.5961

If one inserts the last three columns into equation (13.172), one thus obtains the behaviour of the E -modulus in the plane of the sheet represented in Figure 13.11. One sees that the curve E^H agrees well with the measurements of WEERTS.

The case of rotational symmetry is naturally obtained as a special case of orthorhombic symmetry. It results from the general case when one sets

$$C_4^{11} = \sqrt{\frac{2l+1}{4\pi}} C_4^1; \quad C_4^{12} = C_4^{13} = 0 \quad (13.174)$$

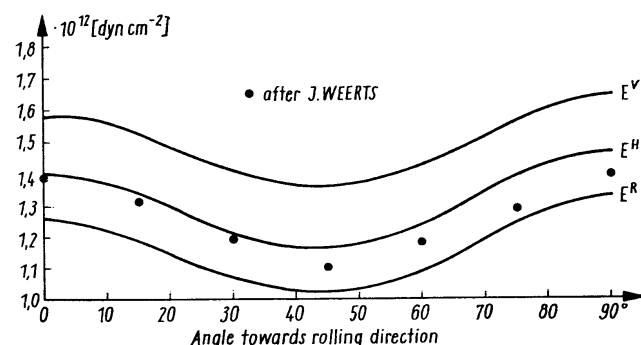


Figure 13.11 Elasticity modulus of a cold-rolled copper sheet as a function of angle from the rolling direction

One then obtains in place of equation (13.158)

$$\bar{t}_{ijkl} = \bar{a}_0^1(ijkl) + \bar{a}_4^1(ijkl) C_4^1 \quad (13.175)$$

The coefficients $\bar{a}_4^1(ijkl)$ are given in Table 13.6 (see reference 243).

Table 13.6 THE AVERAGE COEFFICIENTS $\bar{a}_4^1(ijkl)$ FOR FIBRE TEXTURES IN THE CASE OF CUBIC CRYSTAL SYMMETRY

$ijkl$	$\bar{a}_0^1(ijkl) - t_{ijkl}$	$\bar{a}_4^1(ijkl)$
1111	-0.4	+0.018 465
3333	-0.4	+0.049 240
1122	+0.2	+0.006 155
1133	+0.2	-0.024 620
1212	+0.2	+0.006 155

The VOIGHT—REUSS—HILL approximation is the mean value of two unrealistic assumptions (see, e.g., Figure 13.7) without good theoretical basis. Practically, however, it agrees with the measured polycrystal values within a few per cent^{88,89}. Better-based approximations must, however, make explicit or implicit assumptions about the shape and arrangement (orientation correlation) of the crystallites (see, e.g., references 29, 65, 66, 188). KRÖNER's theory¹⁸⁷ assumes statistically random orientation correlation. It was originally carried out for random orientation distribution. It was extended by KNEER^{180,181} to rotationally symmetric textures and by MORRIS^{213,215} to textures of cubic crystal and orthorhombic sample symmetry. To be sure, the calculation according to this theory requires a considerable calculation expenditure. Since the results also agree within about 2% with those of the V—R—H approximation, which is essentially simpler to calculate, this approximation is used for nearly all practical calculations.

13.4.4.2. Orthorhombic Crystal Symmetry

The averaging of elastic properties for orthorhombic (or higher) crystal symmetry was carried out by MORRIS²¹². Since the elastic anisotropy in this case can not be described by a single quantity s_a or c_a , one must begin with the general averaging formula (13.51). If we use the two-index notation for the components of the elastic tensor according to Table 13.3, equation (13.51) can thus be written

$$\bar{s}_{mn} = \bar{a}(mnpq) s_{pq} \quad (13.176)$$

with

$$\bar{a}(mnpq) = \sum_{l=0}^4 \sum_{\mu=0(2)}^l \sum_{\nu=0(2)}^l \bar{a}_l^{\mu\nu}(mnpq) C_l^{\mu\nu} \quad (13.177)$$

(we have here used a different enumeration for μ and ν). The coefficients $\bar{a}_l^{\mu\nu}$ were given by MORRIS²¹², for a different normalization of the coefficients $C_l^{\mu\nu}$. They are converted to the normalization used here in Table 13.7.

Table 13.7 AVERAGE COEFFICIENTS FOR TENSOR COMPONENTS OF FOURTH ORDER ACCORDING TO MORRIS

l	0	2	4				$\bar{a}_l^{mn}(mnpq)$							
μ	0	0	2	2	0	2	0	4	4	4				
ν	0	0	2	0	2	0	2	4	2	4				
(mnpq)	$B_0 \times$	$B_1 \times$	$B_2 \times$	$B_3 \times$	$B_4 \times$	$B_5 \times$	$B_6 \times$	$B_7 \times$	$B_8 \times$	$B_9 \times$				
1111	6	6	-6	-6	6	9	-3	1	3	-1	1	0	0.047 14	
1122	6	6	-6	-6	6	9	-3	-1	3	-1	1	1	0.375 97	
1133	6	-12	12	-4	-4	24	-8	-6	8	2	-2	2	0.920 98	
1112	4	4	-2	-2	2	6	-2	-8	2	2	-2	3	2.255 91	
1113	4	-2	-2	2	2	-24	6	8	-2	2	-2	4	0.031 34	
1123	4	-2	2	2	-2	-24	-6	8	2	-8	-2	5	0.198 16	
2211	6	6	-6	6	-6	9	-3	3	-1	3	-1	1	6	1.253 29
2222	6	6	6	6	6	9	3	3	1	3	1	1	7	0.262 14
2233	6	-12	-12	4	4	24	8	6	-6	8	-2	9	1.657 94	
2212	4	4	-2	-2	-2	-24	6	-8	2	-6	-2	-2	2.193 24	
2213	4	-2	2	-2	2	-24	-6	-8	-2	-8	2	-2		
2223	4	-2	2	-2	2	-24	-6	-8	-2	-8	-2			
3311	6	-12	12	-12	-12	24	-8	8	8	8				
3322	6	6	-12	-12	-12	24	8	8	8	8				
3333	6	24	24	24	24	64	16	-16	-16	-16				
3312	4	-8	-8	-8	-8	16	16	16	16	16				
3313	4	4	4	4	4	-64	-64	-64	-64	-64				
3323	4	4	4	4	4	-64	-64	-64	-64	-64				

l	2	2	2	2	2	3	-1	1	-3	1	-1	-1
1211	2	2	2	2	2	3	1	1	-3	1	-1	-1
1222	2	2	2	2	2	8	-8	-8	-8	-8		
1233	2	2	-4	-4	-4	2	-2	-2	-2	-2	2	
1212	8	8	20	20	20	-8	2	-8	-8	-8		
1213	8	-10	-10	-10	-10	-8	2	-2	-2	-2		
1223	8	-10	-10	-10	-10	-8	-2	-2	-2	-2		
4412	-2	4	-4	-4	-4	-8	-2	-2	8	8	2	
4413	-2	-2	-2	-2	-2	32	-8	8	-2	-2		
4423	-2	-2	-2	-2	-2	32	8	8	2	2		
5512	-2	4	4	4	4	-8	2	2	8	8	-2	
5513	-2	-2	-2	-2	-2	32	-8	-8	2	2		
5523	-2	-2	-2	-2	-2	32	8	-8	-2	-2		
6612	-2	-8	-8	-8	-8	2	-2	-2	-2	-2	2	
6613	-2	4	4	4	4	-8	2	2	8	8	-2	
6623	-2	4	-4	-4	-4	-8	-2	-2	-2	-2	2	
1311	2	-1	1	-1	1	-12	4	3	-1	-4	1	
1322	2	-1	-1	-1	-1	-12	-4	3	1	-4	1	
1333	2	2	2	2	2	-32	8	8	8	8		
1312	8	-10	-10	-10	-10	-8	-8	2	2	2		
1313	8	5	5	5	5	32	-8	-8	2	2		
1323	8	5	-5	-5	-5	32	8	-8	-2	-2		
2311	2	-1	1	1	-1	-12	4	-3	1	-4	-1	
2322	2	-1	-1	1	1	-12	-4	-3	-1	-4	-1	
2333	2	2	2	-2	-2	-32	8	-8	-8	-8		
2312	8	-10	-10	10	10	-8	-2	-2	8	8	2	
2313	8	5	5	-5	-5	32	-8	8	-2	-2		
2323	8	5	-5	-5	5	32	8	8	8	8	2	

13.4.5. Plastic Anisotropy

We consider a volume element of a plastically deformed material with coordinates $x_1x_2x_3$. During the plastic deformation the material undergoes a displacement with components $u_1u_2u_3$. If the deformation is homogeneous (*Figure 13.12*),

$$u_i = e_{ij}x_j \quad (13.178)$$

The deformation tensor e_{ij} can be decomposed into a symmetric and an antisymmetric portion, the latter simply describing a rigid rotation. The symmetric portion of the deformation tensor is the strain tensor:

$$\varepsilon_{ij} = \frac{1}{2}(e_{ij} + e_{ji}) \quad (13.179)$$

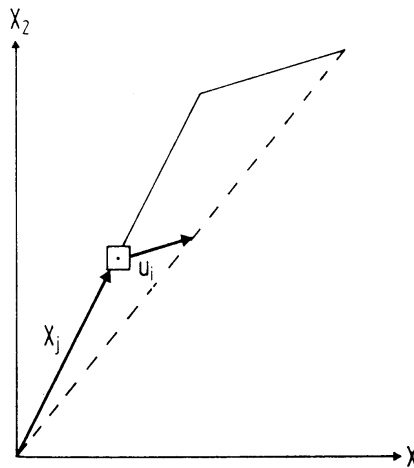


Figure 13.12 Definition of a homogeneous displacement

By suitable choice of the coordinate system it can be written in principal axis form. If one further assumes that the volume remains constant during the deformation, the sum of the diagonal terms must be equal to zero. One can thus bring the strain tensor into the form

$$\varepsilon_{ij} = \eta \begin{bmatrix} 1 & 0 & 0 \\ 0 & -q & 0 \\ 0 & 0 & -(1-q) \end{bmatrix} \quad (13.180)$$

η can thus be considered as the absolute amount of the deformation, while q characterizes the axial ratio of the deformation. This deformation is represented in *Figure 13.13*. The material offers a resistance to deformation, which may be described by the stress tensor σ_{ij} . The required deformation work dA is then given by

$$dA = \sigma_{ij} \cdot d\varepsilon_{ij} \quad (13.181)$$

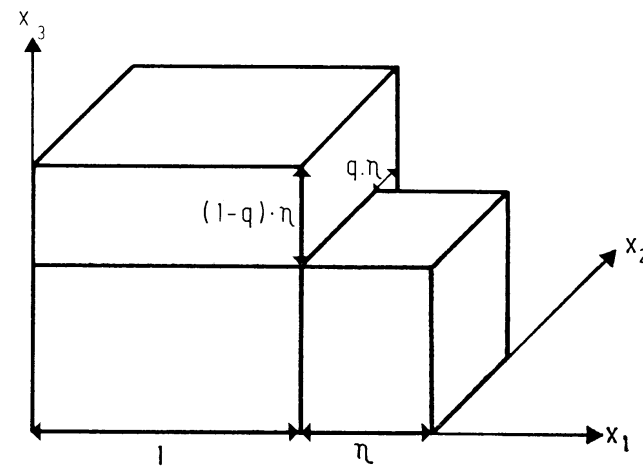


Figure 13.13 General deformation in the principal axis representation corresponding to the deformation tensor (13.180)

In the principal axis representation one thus obtains

$$dA = d\eta [\sigma_{11} - \sigma_{33} - q(\sigma_{22} - \sigma_{33})] = M'(q) \cdot d\eta \quad (13.182)$$

The factor M' is a measure of the deformation resistance of the material. If the material is crystalline, M' will thus also depend on the orientation of the principal axes with respect to the crystal axes. It may be described by the rotation g' which transforms the principal axis system of the strain tensor into the crystal coordinate system. The deformation resistance is thus generally given by

$$dA = M'(q, g') d\eta = M(q, g') \tau_0 d\eta \quad (13.183)$$

The function $M'(q, g')$ can be experimentally determined. It can, with certain assumptions (e.g. in the framework of the TAYLOR theory²⁷⁸), also be calculated^{53,60}. Then τ_0 is the critical resolved shear stress in the crystallographically equivalent glide systems and $M(q, g)$ is the Taylor factor. $M(0, g')$ is, for example, given in *Figure 13.14* for cubic crystal symmetry and $\{111\}\langle 110 \rangle$ slip in the framework of the TAYLOR theory. The case $q = 0$ represents the so-called plane-strain deformation, which, in general, can also be assumed as an idealized deformation for rolling. Since the strain tensor has orthorhombic symmetry, the deformation resistance can be developed in a series of cubic orthorhombic generalized spherical harmonics:

$$M(q, g') = \sum_{l=0}^L \sum_{\mu=1}^{M(l)} \sum_{\nu=1}^{N(l)} m_l^{\mu\nu}(q) T_l^{\mu\nu}(g') \quad (13.184)$$

If $M(q, g')$ is numerically known, the coefficients $m_l^{\mu\nu}(q)$ can be calculated in the manner described in Section 4.1.2. They are given in *Table 13.8* for $l \leq 10$ for different values of q in the framework of the TAYLOR theory. *Figure 13.15* shows the rapid decrease of these coefficients with the degree l for $q = 0$.

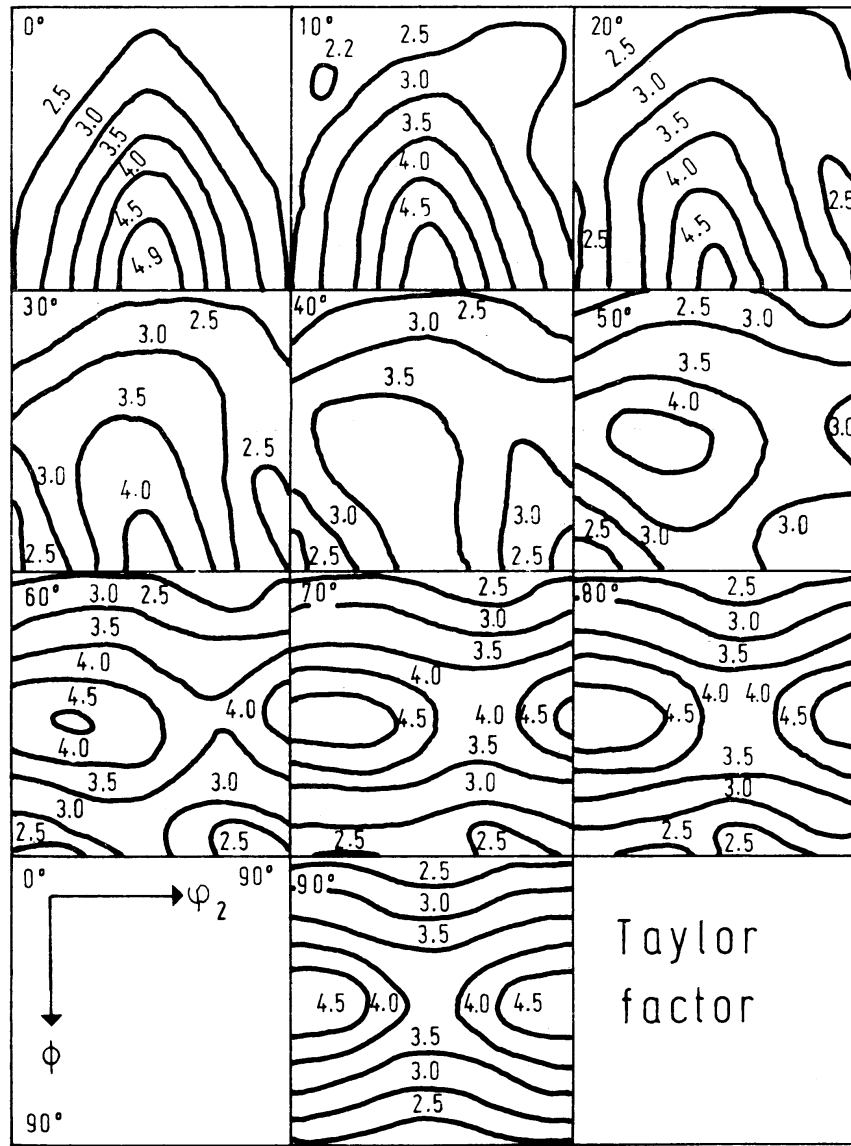
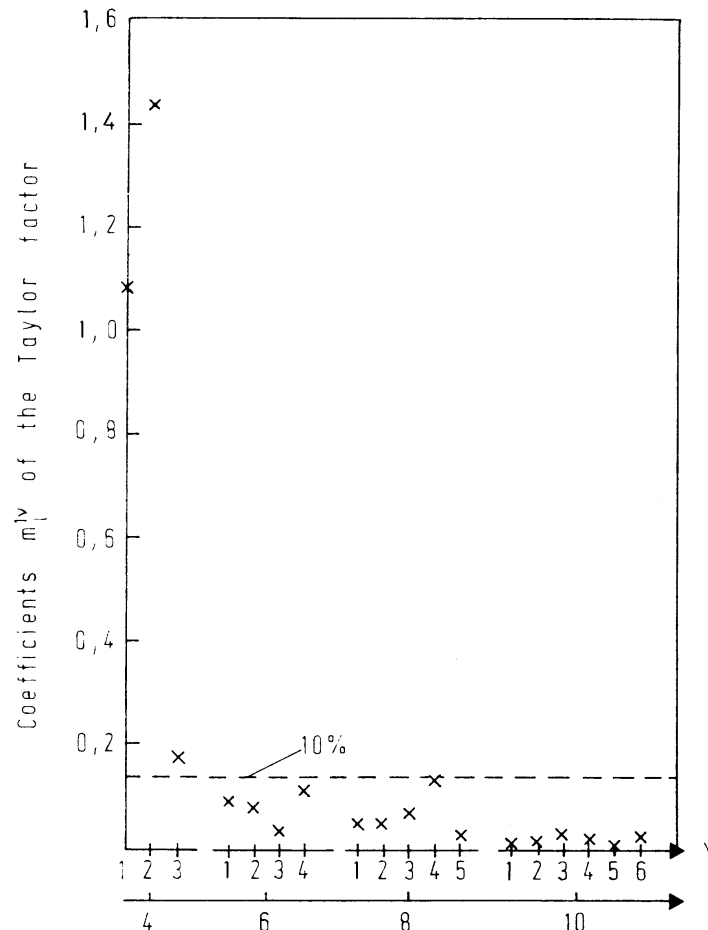


Figure 13.14 The TAYLOR factor $M(0, g)$ for 'plane strain' deformation $q = 0$ as a function of the crystal orientation relative to the principal axes of deformation^{53,60}

We shall now calculate the average value $\bar{M}(q, g'')$ of the deformation resistance $M(q, g')$ for a polycrystalline material. We thereby permit the principal axes of the strain tensor not to coincide with the sample coordinate system. If the principal axes of the strain tensor form the coordinate system K' , the relations be-

Table 13.8 COEFFICIENTS $m_l^{\mu\nu}$ OF THE TAYLOR FACTOR FOR VARIOUS CONTRACTION RATIOS q

Plane strain				Axial symmetry						
l	μ	v	$q = 0$	$q = 0.1$	$q = 0.2$	$q = 0.3$	$q = 0.35$	$q = 0.4$	$q = 0.45$	$q = 0.5$
0	1	1	3.3198	3.2079	3.1415	3.1016	3.0873	3.0766	3.0690	3.0766
4	1	1	-1.0861	-1.0026	-0.8899	-0.7461	-0.6694	-0.5913	-0.5105	-0.4189
4	1	2	1.4435	1.3083	1.1282	0.9511	0.8617	0.7726	0.6873	0.6244
4	1	3	0.1771	0.0394	-0.1563	-0.3701	-0.4843	-0.5979	-0.7099	-0.8257
6	1	1	-0.0874	-0.0037	0.0431	0.0703	0.0825	0.0911	0.0933	0.0938
6	1	2	-0.0767	-0.1112	-0.1234	-0.1350	-0.1404	-0.1404	-0.1528	-0.1359
6	1	3	-0.0265	0.0321	0.0963	0.1325	0.1497	0.1641	0.1766	0.1492
6	1	4	-0.1112	-0.1602	-0.2026	-0.2224	-0.2280	-0.2327	-0.2349	-0.2018
8	1	1	0.0475	0.0042	0.0191	0.0566	0.0767	0.0946	0.1085	0.1014
8	1	2	0.0465	0.0049	-0.0186	-0.0627	-0.0879	-0.1115	-0.1293	-0.1492
8	1	3	-0.0737	-0.0108	0.0487	0.0950	0.1141	0.1301	0.1438	0.1565
8	1	4	-0.1413	-0.1528	-0.1587	-0.1729	-0.1729	-0.1683	-0.1661	-0.1742
8	1	5	0.0269	0.2146	0.3182	0.3243	0.3160	0.3018	0.2814	0.2383
10	1	1	0.0130	-0.0029	0.0255	0.0421	0.0421	0.0419	0.0382	0.0348
10	1	2	0.0147	-0.0132	-0.0328	-0.0436	-0.0424	-0.0407	-0.0426	-0.0497
10	1	3	0.0304	0.4083	0.0642	0.0703	0.0659	0.0637	0.0622	0.0512
10	1	4	0.0181	0.0105	0.0100	-0.0108	-0.0167	-0.0211	-0.0243	-0.0544
10	1	5	0.0091	-0.0311	-0.0443	-0.0171	-0.0017	0.0093	0.0147	0.0610
10	1	6	0.0316	0.1019	0.0801	0.0171	-0.0152	-0.0407	-0.0585	-0.0840

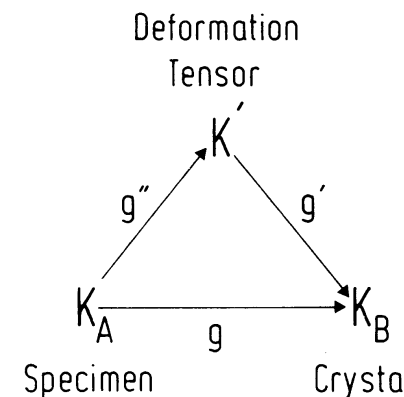
Figure 13.15 The coefficients $m_l^{\mu\nu}$ of the TAYLOR factors for $l \leq 10^{53}$

tween g , g' and g'' are thus demonstrated in Figure 13.16. In contrast to the general case treated in Section 13.3.3, we have here used g' as rotation, which transforms the principal axis system into the crystal system, while there the opposite rotation was assumed. In place of equation (13.184) we must thus average the function

$$M(q, g'^{-1}) = \sum_{l=0}^L \sum_{\mu=1}^{M(l)} \sum_{\nu=1}^{N(l)} m_l^{\mu\nu}(q) \ddot{T}_l^{\mu\nu}(g'^{-1}) \quad (13.185)$$

which corresponds to equation (13.18) and thus to the assumptions in Section 13.3.3. The usual assumption will be made that the functions $\ddot{T}_l^{\mu\nu}$ are real in the cubic-orthorhombic case. According to equation (13.74), for the average deformation resistance $\bar{M}(q, g'')$ one then obtains

$$\bar{M}(q, g'') = \sum_{l=0}^L \sum_{\mu=1}^{M(l)} \sum_{\nu=1}^{N(l)} \bar{m}_l^{\mu\nu}(q) \ddot{T}_l^{\mu\nu}(g'') \quad (13.186)$$

Figure 13.16 Relations between the crystal coordinate system K_B , sample coordinate system K_A and principal axes system K' of the deformation tensor

with

$$\bar{m}_l^{\mu\nu}(q) = \frac{1}{2l+1} \sum_{\lambda=1}^{M(l)} m_l^{\lambda\mu}(q) C_l^{\lambda\nu} \quad (13.187)$$

The symmetry of the deformation tensor is the same as that of the sample — namely the orthorhombic symmetry. The functions $\ddot{T}_l^{\mu\nu}(g'')$ thus are orthorhombic in both coordinate systems.

We consider, in particular, the case in which the X_3 -direction of the strain tensor coincides with the Z -direction of the sample coordinate system. The rotation g'' then has the form

$$g'' = \{\alpha, 0, 0\} \quad (13.188)$$

The functions $\ddot{T}_l^{\mu\nu}(g'')$ can then be written

$$\ddot{T}_l^{\mu\nu} = \delta_{\mu\nu} \cos 2(\nu - 1) \alpha \quad (13.189)$$

For the average deformation resistance one thereby obtains

$$\bar{M}(q, \alpha) = \sum_{\nu=1}^{N(L)} a^{\nu}(q) \cos 2(\nu - 1) \alpha \quad (13.190)$$

with the coefficients

$$a^{\nu}(q) = \sum_{l=0}^L \frac{1}{2l+1} \sum_{\lambda=1}^{M(l)} m_l^{\lambda\nu} C_l^{\lambda\nu} \quad (13.191)$$

$\bar{M}(q, \alpha)$ is plotted as a function of q for $\alpha = 0$ and 45° in Figure 13.17 for a steel sheet⁷⁹ whose texture coefficients $C_l^{\mu\nu}$ are contained in Table 13.9. A deformation tensor with the principal axes described by equation (13.188) corresponds to a

sample which is rotated through the angle α from the rolling direction and is extended in that direction, where the relative width and thickness decreases are given by q and $(1 - q)$, respectively (Figure 13.18). As one sees from Figure 13.17, the deformation resistance has a minimum for a certain width decrease q . If the sample (Figure 13.18) is elongated in its long direction by $d\eta$, without any restriction to the shape change in the two directions perpendicular thereto (free tension), the width contraction will be so selected that $\bar{M}(q)$ is a minimum. The values of q for the minima read from Figure 13.17 are plotted in Figure 13.19 as a function of the angle α and compared with experimental values, while Figure 13.20 shows

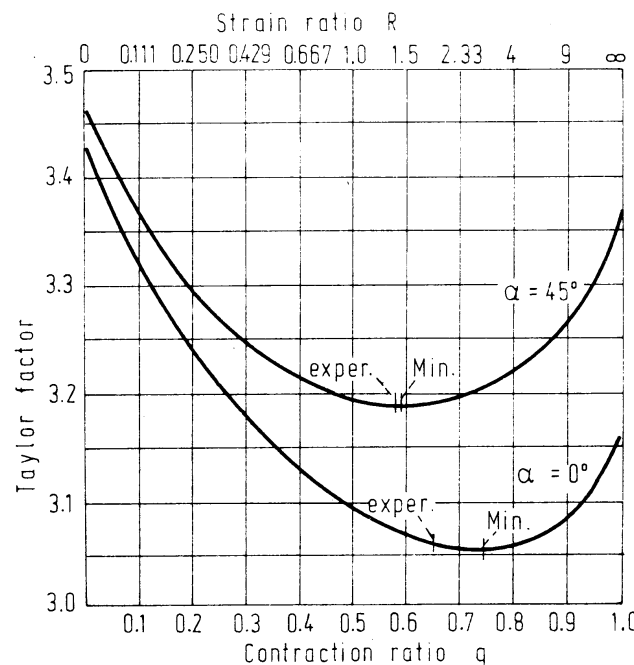


Figure 13.17 The average TAYLOR factor $\bar{M}(q, \alpha)$ as a function of the axial ratio q of the deformation⁵³

Table 13.9 COEFFICIENTS $C_l^{l,v}$ OF THE STEEL TEXTURE

v	$l = 4$	$l = 6$	$l = 8$	$l = 10$
1	-1.4689	2.6861	-0.0707	-1.0248
2	-0.4590	-1.2023	0.2859	0.1910
3	0.4973	0.4641	-0.6541	0.0920
4		-0.1406	-0.4697	-0.2714
5			-0.2219	-0.0488
6				0.0202

the corresponding \bar{M} -values. The quantity

$$R = \frac{q}{1 - q} \quad (13.192)$$

which is frequently used as a measure of plastic anisotropy, is also given in Figures 13.19 and 13.20.

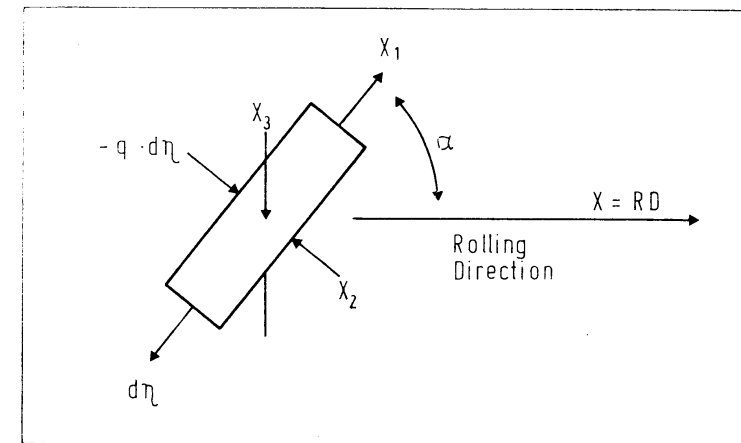


Figure 13.18 Orientation of a tensile specimen relative to the sample coordinate system K_A

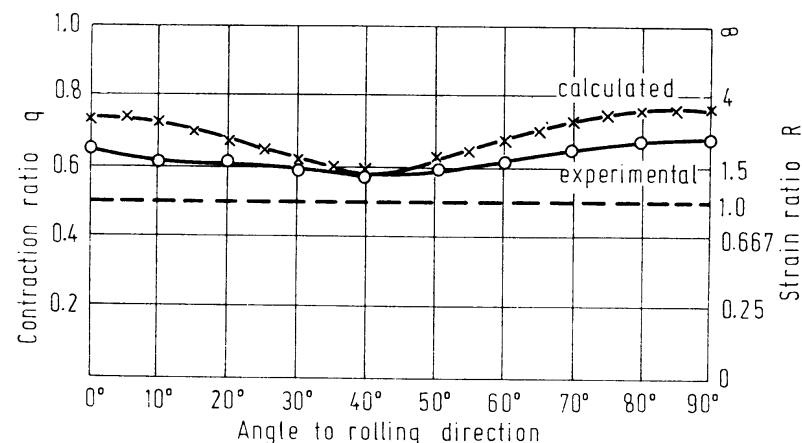


Figure 13.19 The transverse contraction ratio q determined from Figure 13.17 and measured, as well as the associated R -value of the plastic anisotropy for a 95% cold-rolled steel sheet as a function of the sample angle⁷⁹

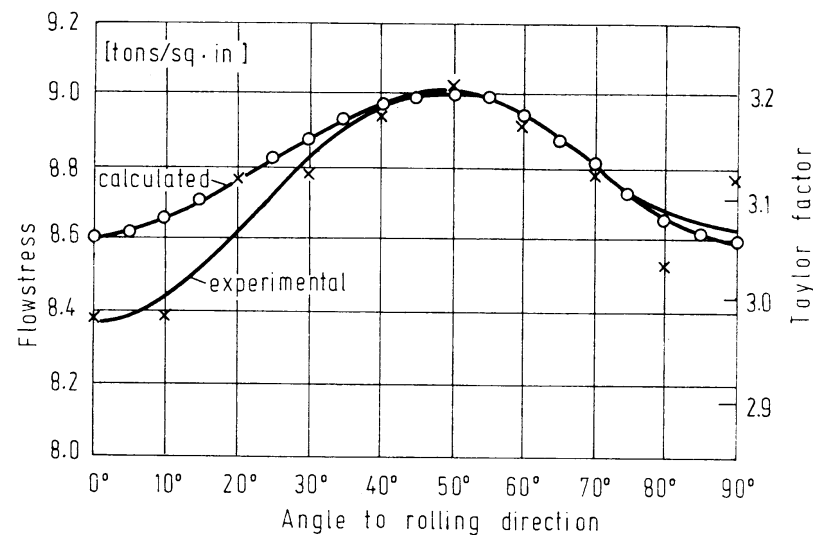


Figure 13.20 The measured and calculated average TAYLOR factor $\bar{M}(q_{\min.}, \alpha)$ for a 95% cold-rolled steel sheet⁷⁹

13.4.6. The Reflectivity of Crystallites for X-rays

It is also of interest to specify the diffracting power of crystals for X-ray beams, which, in general, is described with the help of the reciprocal lattice, in the representation by functions of a direction. If an X-ray beam of wavelength λ falls on a crystal, it can thus be reflected by a lattice plane (hkl). The BRAGG relation

$$\lambda = 2d_{hkl} \sin \vartheta_{hkl} \quad (13.193)$$

is true for the reflection angle $2\vartheta_{hkl}$. The reflection can thus only occur for certain angles $2\vartheta_{hkl}$. The usual reflection condition, which says that the normal to the reflecting lattice plane (hkl) must fall in the direction of the bisector of the angle between the incident beam and the reflected beam, is added thereto. If we consider the reflection for a specific angle $2\vartheta_{hkl}$ in the case of fixed incident and reflecting directions, and bring the crystal into all possible orientations, we thus see that reflections only occur when the normal to the (hkl) plane, or a symmetrically equivalent plane, falls in the direction of the angle bisector. We can thus specify the diffracting power for the reflection angle $2\vartheta_{hkl}$ by a function of those crystal directions \mathbf{h} which fall in the direction of the angle bisector. It is clear that this function has the character of a δ -function — i.e. is different from zero only in the direction of the normals of the symmetrically equivalent (hkl) planes. We denote it by $E_{hkl}(\mathbf{h})$ and set^{38,39}

$$E_{hkl}(\mathbf{h}) = S(hkl) E'_{hkl}(\mathbf{h}) \quad (13.194)$$

$S(hkl)$ is a factor depending on hkl , and the function $E'_{hkl}(\mathbf{h})$ describes the orientation dependence. We so normalize it that

$$\oint E'_{hkl}(\mathbf{h}) d\mathbf{h} = 1 \quad (13.195)$$

We expand it in a series of spherical surface harmonics of the crystal symmetry:

$$E'_{hkl}(\mathbf{h}) = \sum_{\lambda=0}^{\infty} \sum_{\mu=1}^{M(\lambda)} e_{\lambda}^{\mu}(hkl) k_{\lambda}^{\mu}(\mathbf{h}) \quad (13.196)$$

We obtain the coefficients $e_{\lambda}^{\mu}(hkl)$ in the following manner. We multiply by $k_{\lambda}^{*\mu}(\mathbf{h})$ and integrate over all \mathbf{h} . This yields

$$\oint E'_{hkl}(\mathbf{h}) k_{\lambda}^{*\mu}(\mathbf{h}) d\mathbf{h} = e_{\lambda}^{\mu}(hkl) \quad (13.197)$$

Since the function E' is different from zero only in the immediate vicinity of the points $\mathbf{h} = [hkl]$, the functions $k_{\lambda}^{\mu}(\mathbf{h})$ can, however, be regarded as constant within these small regions, so that we obtain with equation (13.195)

$$e_{\lambda}^{\mu}(hkl) = k_{\lambda}^{*\mu}(hkl) \oint E'_{hkl}(\mathbf{h}) d\mathbf{h} = k_{\lambda}^{*\mu}(hkl) \quad (13.198)$$

$k_{\lambda}^{\mu}(hkl)$ denotes the value of the spherical surface harmonics $k_{\lambda}^{\mu}(\mathbf{h})$ for the directions of the normals of the lattice plane (hkl) and its symmetric equivalents. We thus obtain the representation of the diffracting power for the reflecting angle $2\vartheta_{hkl}$:

$$E_{hkl}(\mathbf{h}) = S(hkl) \sum_{\lambda=0}^{\infty} \sum_{\mu=0}^{M(\lambda)} k_{\lambda}^{*\mu}(hkl) k_{\lambda}^{\mu}(\mathbf{h}) \quad (13.199)$$

The complete reflection behaviour of the crystal can thus be described by as many functions $E_{hkl}(\mathbf{h})$ as different reflecting planes (hkl) occur (which are, strictly speaking, naturally infinitely many). If one thinks of the functions $E_{hkl}(\mathbf{h})$ as distributions on spheres of radii $1/d_{hkl}$, one thus obtains a point distribution in space, the so-called reciprocal lattice. For the representation used here, however, the association with spheres of radius $1/d_{hkl}$ is not necessary.

According to equation (13.58), one obtains for the diffracting power of a polycrystalline material with the sample direction \mathbf{y} as the angle bisector

$$\bar{E}_{hkl}(\mathbf{y}) = \sum_{\lambda=0}^{\infty} \sum_{\nu=1}^{N(\lambda)} \bar{e}_{\lambda}^{\nu}(hkl) k_{\lambda}^{\nu}(\mathbf{y}) \quad (13.200)$$

with the coefficients

$$\bar{e}_{\lambda}^{\nu}(hkl) = \frac{S(hkl)}{2\lambda + 1} \sum_{\mu=1}^{M(\lambda)} C_{\lambda}^{\mu\nu} k_{\lambda}^{*\mu}(hkl) \quad (13.201)$$

This yields

$$\bar{E}_{hkl}(\mathbf{y}) = S(hkl) \sum_{\lambda=0}^{\infty} \sum_{\mu=1}^{M(\lambda)} \sum_{\nu=1}^{N(\lambda)} \frac{C_{\lambda}^{\mu\nu}}{2\lambda + 1} k_{\lambda}^{*\mu}(hkl) k_{\lambda}^{\nu}(\mathbf{y}) \quad (13.202)$$

The averaged function $\bar{E}_{hkl}(\mathbf{y})$ is naturally essentially the (hkl) pole figure (see equation 4.35).

Because of the δ -character of the function $\bar{E}_{hkl}(\mathbf{h})$, its series expansion (equation 13.199) includes infinitely many terms, in contrast to the series expansions of most other physical properties, which frequently contain only terms of very small order. This is the reason that texture determination from X-ray diffraction measurements considerably exceeds that from other physical properties as far as accuracy is concerned.

13.5. Determination of the Texture Coefficients from Anisotropic Polycrystal Properties

We have derived relations between physical properties of polycrystals and those of the individual crystals together with the orientation distribution function. The relation is particularly simple when the property of the polycrystal is given exactly or to sufficient approximation by the simple average value. If we use the representation of a property by functions of the orientation g (or, as a special case thereof, the representation by surfaces), for the relation between the coefficients $e_l^{\mu\lambda}$ of the single crystal and $\bar{e}_l^{\mu\nu}$ of the polycrystal (see equation 13.75) it is thus true that

$$\bar{e}_l^{\mu\nu} = \frac{1}{2l+1} \sum_{\lambda=1}^{M(l)} e_l^{\mu\lambda} C_l^{\lambda\nu}, \quad (13.203)$$

$1 \leq \lambda \leq M(l)$ (crystal symmetry)
 $1 \leq \mu \leq N'(l)$ (instrumental symmetry)
 $1 \leq \nu \leq N(l)$ (sample symmetry)
 $0 \leq l \leq r$ (order of property)

We have thereby first regarded the single crystal coefficients $e_l^{\mu\lambda}$ and the texture coefficients $C_l^{\lambda\nu}$ as given and calculated the polycrystal coefficients $\bar{e}_l^{\mu\nu}$ therefrom.

We shall now regard the single-crystal and polycrystal coefficients as given and calculate the texture coefficients $C_l^{\lambda\nu}$ from equation (13.203). (If, for example, we assume the diffracting power for X-ray beams as the crystal property, we thus obtain the method of texture determination from pole figures measurable by X-ray diffraction described in previous sections.) A very important theorem first results. Many of the property functions lead to a very small value of r . Thus for tensor properties of second order $r = 2$, in the case of elastic properties $r = 4$, and for the magnetization energy of cubic crystals we have $r = 6$. For $l > r$ all coefficients $e_l^{\mu\lambda}$ and consequently also all $\bar{e}_l^{\mu\nu}$ thus vanish. Equation (13.203) is therefore identically satisfied for arbitrary values of the texture coefficients $C_l^{\mu\lambda}$ with $l > r$. From the measurement of the anisotropy of a physical property one can thus in principle determine the texture coefficients at most up to a degree $l = r$, which is equal to the order of the property function considered. One can therefore regard a property which is represented by a function of lower order as 'long wavelength'. If one uses this to 'look into' the texture, there thus results a correspondingly poor 'resolving power'. One can no longer detect details of the texture which are finer than the resolving power. This is completely analogous to the dependence of the resolving power of optical instruments on the wavelength

of the radiation used. In particular, magnetic measurements thus allow determination of the texture to at most $l = 6$.

For each pair of values l and ν relation (13.203) represents a linear system of equations with $M(l)$ unknowns $C_l^{\lambda\nu}$. For each value of μ one equation results, so that the number of these is $N'(l)$. In order for the system of equations to have a unique solution, the number of equations must be at least equal to the number of unknowns:

$$N'(l) \geq M(l) \quad (13.204)$$

$M(l)$ denotes the number of linearly independent spherical surface harmonics of the crystal symmetry and $N'(l)$ that of the symmetry in the coordinate system K' . In the previously considered example this was the symmetry of the distribution of magnetization directions in an inhomogeneous magnetic field. Since the property was investigated with the help of the variable coordinate system K' , we shall refer to this symmetry as 'instrumental' symmetry. Now, the higher the symmetry is, the smaller the number of linearly independent spherical surface harmonics is. Equation (13.204) means therefore in somewhat simplified form

$$\text{instrumental symmetry} \leq \text{crystal symmetry} \quad (13.205)$$

The solubility of the system of equations (13.203) for the $C_l^{\lambda\nu}$ can thus be limited in two ways: firstly, that beyond a certain order $l = r$ all coefficients are zero; secondly, that too few equations are available.

In many cases the 'instrumental' symmetry is the symmetry of rotation — i.e. the property depends not on all three orientation parameters of the crystal, but only on the orientation with respect to a direction (e.g. the direction of a homogeneous magnetic field). It is independent with respect to a rotation about this direction. In this important case the number of spherical surface harmonics of the instrumental symmetry is

$$N'(l) = 1 \quad (13.206)$$

For each pair of values l and ν we then have only one equation. Thus we must have

$$M(l) \leq 1 \quad (13.207)$$

The allowable values of l_{\max} according to this condition are given for different crystal symmetries in Table 13.10. Only in the case of rotationally symmetric crystal symmetry is the resolving power not limited by equation (13.207) (orientations of fibres or ellipsoids of rotation). For cubic and hexagonal symmetries

Table 13.10 HIGHEST DEGREE $l = l_{\max}$ FOR WHICH THE RELATION $M(l) \leq 1$ IS FULFILLED

Crystal symmetry:	tri-clinic	mono-clinic	ortho-rhombic	tetragonal	hexagonal	cubic	rotational
l_{\max}	0	0	0	2	4	10	∞

the resolving power is not more severely limited by equation (13.207) than it is with magnetic measurements anyway because of $l \leq 6$. For crystals of lower symmetry equation (13.207) indicates the impossibility of texture determination from a single physical property. If one is to avoid the solution limit established by equation (13.207), one must thus measure more property functions. One then obtains one equation from each property for each pair of values l, ν . If I_E is the number of different measured properties, in place of equation (13.207) there results the condition

$$M(l) \leq I_E \quad (13.208)$$

By measurement of several properties one can thus obtain as good a resolving power as by measurement of several pole figures, if one has suitably 'short wavelength' properties — i.e. those whose series expansions contain terms with sufficiently high values of l . Now nearly all property functions are in this sense very 'long wavelength' with the exception of the diffraction effects of the crystal lattice, which are very strongly angularly dependent and therefore contain terms of higher order in their series expansions. A quantitative texture determination with suitably good resolving power is, in general, therefore not possible from the average values of several physical properties.

The reflection of light by etch pits is one of the few properties of medium 'wavelength' which can be used for texture determination. If one can so etch the crystallites that completely plane crystal surfaces result which are suitably large in comparison with the wavelength of light, the reflected light beam will not be broadened compared with the incident beam. The reflection curve will be very sharp and its series expansion will contain terms of higher order. In actuality, however, the etched crystal surfaces are not completely plane and also not always large in comparison with the wavelength of light. The reflection curve will be broadened, and its series expansion will no longer contain as many terms as in the ideal case, but still many more than, for example, the magnetic properties. If one therefore successively etches different crystal surfaces and measures the angular dependence of the reflection curve of the polycrystal, one can calculate the texture coefficients therefrom, as from X-ray diffraction measurements. Unfortunately, the exact form of the reflection curve depends on many factors which are very difficult to control, so that the 'property function' of the single crystal can only be inexactly determined. The coefficients $e_l^{\mu\lambda}$ are thus inexactly known and also the $C_l^{\mu\nu}$ can not be exactly calculated. Therefore to the best of our knowledge no quantitative texture determination has been made by this method.

13.6. Determination of Single Crystal Properties from Polycrystal Measurements

If one knows the texture coefficients $C_l^{\mu\nu}$ and one has measured the orientation dependence of the polycrystal properties, one can thus use equation (13.203) to calculate the single crystal coefficients $e_l^{\mu\lambda}$. For each pair of values l, μ one obtains

$N(l)$ equations with $M(l)$ unknowns. For a unique solution we must thus have

$$N(l) \geq M(l) \quad (13.209)$$

This means, in general

$$\text{sample symmetry} \leq \text{crystal symmetry} \quad (13.210)$$

The sample symmetry must be lower than the crystal symmetry, since otherwise an additional symmetrization of the property will be produced by the orientation distribution. In the extreme case of spherical symmetry (thus random orientation distribution) one can not make any assertions about the orientation-dependent terms of the single crystal properties, since the polycrystal properties are quasi-isotropic.

In the case of rotationally symmetric textures (fibre textures) $N(l) = 1$. In order for a solution to be possible it is thus necessary that

$$M(l) \leq 1 \quad (13.211)$$

From *Figure 4.4*, as well as *Table 13.10* in the preceding section, one thus recognizes that in principle most properties of cubic and hexagonal crystals can already be calculated from measurements on fibre-textured samples.

13.7. Textures with Equal Physical Properties

From equation (13.203), which gives the relation between single crystal and polycrystal coefficients, one recognizes that texture coefficients $C_l^{\mu\nu}$ with $l > r$ have no influence on the polycrystal properties. r is the highest order occurring in the series expansion. We have further seen by some examples that in most cases r is very small. For tensor properties of second order $r = 2$; in the case of elastic properties $r = 4$; and in the case of magnetic properties of ferromagnetic cubic crystals $r = 6$.

All textures which differ in their series expansions only in the coefficients with $l > r$ therefore yield the same average value of the physical property considered. They are — for the properties estimated — equivalent. We therefore ask of the totality of all different textures, which are equivalent with respect to a specific physical property. We obtain them if we allow the coefficients $C_l^{\mu\nu}$ with $l > r$ to traverse all possible value combinations, under the condition that for no choice of coefficients is the orientation distribution function $f(g)$ allowed to assume negative values, since orientation distributions with negative frequencies are naturally physically meaningless. We must thus have

$$f(g) = \sum_{l=0}^{\infty} \sum_{\mu=1}^{M(l)} \sum_{\nu=1}^{N(l)} C_l^{\mu\nu} \dot{T}_l^{\mu\nu}(g) \geq 0 \quad (13.212)$$

Thus, if the orientation distribution consists of only a single orientation g , according to equation (4.19), one obtains for the coefficients

$$C_l^{\mu\nu} = (2l + 1) \dot{T}_l^{\mu\nu}(g) \quad (13.213)$$

If one allows g to traverse all possible orientations, one thus obtains value combinations of the coefficients $C_l^{\mu\nu}$, which are all ‘allowable’ — i.e. the texture function $f(g)$ is nowhere allowed to be negative. If one regards the $C_l^{\mu\nu}$ as coordinates of a multidimensional space, then the point corresponding to g traverses a certain region of this space. Each point of this region corresponds to an allowable value combination of the coefficients and thus to an allowable ‘texture’; however, all these ‘textures’ correspond exactly to single orientations. We shall call the region in the coefficient space so obtained the ‘single crystal region’. If the texture consists of two orientations g_1 and g_2 which are present with relative frequencies V_1 and V_2 , one thus obtains for the coefficients

$$C_l^{\mu\nu} = (2l + 1) [V_1 \dot{T}_l^{*\mu\nu}(g_1) + V_2 \dot{T}_l^{*\mu\nu}(g_2)] \quad (13.214)$$

The point represented in the coefficient space thus lies on the straight line through the points 1 and 2. Since V_1 and V_2 can not be negative, it moreover lies between these two points. Every point so obtained also again corresponds to an allowable texture. We can also form many-fold combinations with positive weights. In this way, however, we obtain also all points of the coefficient space, because each texture is defined by its component orientations and the associated weights. We thus obtain an essentially greater ‘texture region’ which includes the ‘single crystal region’. In addition to the points of the ‘single crystal region’ themselves, it also contains all straight lines between each two points of this region. Each point of this ‘texture region’ corresponds to an allowable value combination of the indices and thus to an allowable, non-negative orientation distribution function.

If now we require that the material possess certain values of a physical property — for example, certain magnetic properties — a certain number of the coefficients $C_l^{\mu\nu}$ with $l \leq r$ are thereby fixed. With the allowable ‘texture region’ in the coefficient space at hand, one can then directly recognize in which region the remaining parameters may still vary without the representing point leaving the ‘texture region’. In this way one obtains the totality of all textures which are equivalent with respect to a specific physical property.

13.7.1. Fibre Textures of Ferromagnetic Cubic Materials

We shall illustrate the above with a simple example. We consider fibre textures of ferromagnetic cubic materials. If the texture consists only of a single component with the crystal direction \mathbf{h} parallel to the fibre axis, the coefficients $C_l^{\mu\nu}$ are thus given by

$$C_l^{\mu\nu} = 4\pi k_l^{\mu\nu}(\mathbf{h}) \quad (13.215)$$

If we take the values of the first two cubic spherical harmonics $k_4^1(\mathbf{h})$ and $k_6^1(\mathbf{h})$ for different values of \mathbf{h} from a table and introduce C_4^1 and C_6^1 as coordinates of a point in a rectangular coordinate system, the point thus sweeps out the ‘single crystal region’ (Figure 13.21).

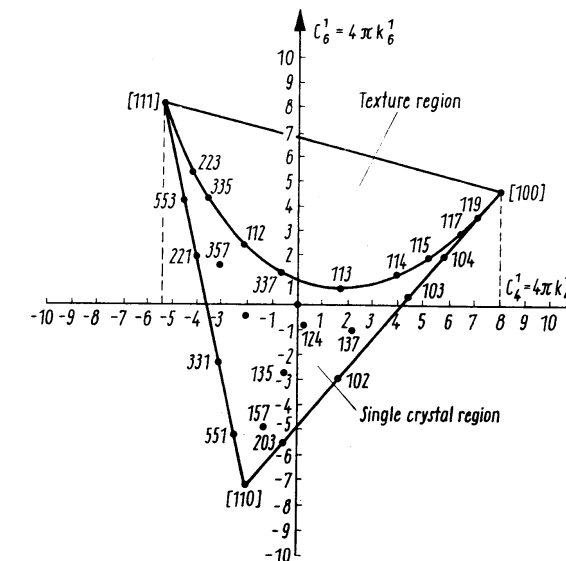


Figure 13.21 Coefficient diagram for the magnetization energy of cubic materials with fibre texture

The convex envelope of this region is the total ‘texture region’ (or its projection in two dimensions). Value combinations of the coefficients C_4^1 and C_6^1 which correspond to a point in the ‘single crystal region’ can be realized by a single orientation (which in the case of fibre textures is naturally not a single crystal, but contains all orientations which transform into one another by rotations about the fibre axis). It can, however, also be realized by real textures. Points which lie in the ‘texture region’ but outside the ‘single crystal region’ can only be realized by two (or more) orientations. Since each point of the diagram corresponds to a value combination of the coefficients C_4^1 and C_6^1 and since the magnetization energy depends only on these two values, a completely determined magnetic anisotropy is associated with each point. Different textures which correspond to the same point have the same anisotropy. The zero point $C_4^1 = 0, C_6^1 = 0$ naturally corresponds to random orientation distribution. Since the zero point lies in the ‘single crystal region’, quasi-isotropic behaviour can, however, also be generated by a single orientation, which, as one sees, lies in the neighbourhood of the orientation [124]. One can infer its exact orientation from the graphic representation of the two functions $k_4^1(\Phi, \beta)$ and $k_6^1(\Phi, \beta)$. One obtains the values

$$\Phi_0 = 74.5^\circ; \quad \beta_0 = 26^\circ \quad (13.216)$$

One thus sees that a sharply developed texture can also yield quasi-isotropic behaviour with respect to a specific property. From Figure 13.21 one also recognizes that in the general case (K_4 and $K_6 \neq 0$) it is not possible to realize isotropic behaviour by a double fibre texture [111] + [100] in certain relative proportions.

However, this is possible by a threefold fibre texture $[111] + [100] + [110]$. One can then even generate any arbitrarily obtainable anisotropy behaviour by such a threefold fibre texture. If the second ferromagnetic anisotropy constant is zero,

$$K_6 = 0 \quad (13.217)$$

the anisotropy of the polycrystal will thus be independent of C_6^1 . All points on a straight line parallel to the C_6^1 axis of the diagram then yield the same anisotropy. One can therefore directly read off in which interval C_6^1 may move, in order to get the texture of the anisotropy behaviour concerned. If $K_6 \neq 0$ and one seeks from all textures those which contain no component of sixth order in their anisotropy, the representing point must thus lie on the C_4^1 axis. The coefficient C_4^1 can then vary on the interval

$$-3.58 \leq C_4^1 \leq +4.40 \quad (13.218)$$

All these textures yield an anisotropy without sixth-order components.

13.7.2. Magnetic Anisotropy of an Fe–Si Sheet

An example of a general (not rotationally symmetric) texture was (of course without use of the coefficient diagram) considered by DUNN and WALTER¹²⁰. The texture of an Fe–Si alloy was determined by X-ray diffraction measurements. Among others it possessed the components $(305)[5, 21, 3]$, $(017)[27\bar{1}]$, $(110)[1\bar{1}5]$. The orientation $(110)[001]$ only amounted to 0.4%. The magnetic torque curve calculated from these orientations was in good general agreement with the measured curve. The torque curve could, however, be equally well explained by a texture with the components

$$28\% (110)[001] + 72\% \text{ random} \quad (13.219)$$

By application of the coefficient diagram, however, one can construct arbitrarily many additional textures which will also all yield the same torque curve.

13.7.3. Tensor Properties of Second Rank for Fibre Textures

We further consider tensor properties of second rank in the case of fibre textures of orthorhombic crystals. The anisotropy of the polycrystal quantities then depends on the two texture coefficients C_2^1 and C_2^2 . For single orientations it is now true that

$$C_2^1 = 4\pi k_2^1(\Phi) = 2\sqrt{2\pi} \bar{P}_2(\Phi) \quad (13.220)$$

$$C_2^2 = 4\pi k_2^2(\Phi, \beta) = 4\sqrt{\pi} \bar{P}_2^2(\Phi) \cos 2\beta \quad (13.221)$$

If one now allows Φ and β to vary, the factor $\cos 2\beta$ thus assumes all values between -1 and $+1$ for each value of Φ . If one therefore plots $\pm 4\sqrt{\pi} \bar{P}_2^2(\Phi)$ versus $2\sqrt{2\pi} \bar{P}_2(\Phi)$, one thus obtains the limits of the single crystal region (*Figure 13.22*).

Since it is linearly confined, in these cases it coincides with the total texture region. Every anisotropy behaviour obtainable by a texture can in these cases thus be produced by a single ideal orientation — in particular, naturally also the isotropic behaviour. This results for an ideal orientation with the spherical angular coordinates

$$\Phi_0 = 55^\circ; \quad \beta_0 = 45^\circ \quad (13.222)$$

Which $\{h_1 h_2 h_3\}$ indices these coordinates correspond to naturally depends on the axis ratio of the orthorhombic unit cell. One recognizes from equation (13.135) that for given values E_{11}, E_{22}, E_{33} the anisotropy depends only on a linear combination of the coefficients C_2^1 and C_2^2 . There are therefore a multiplicity of coefficients C_2^1 and C_2^2 which yield the same anisotropy behaviour. The corresponding points lie on a straight line whose slope is determined by the constants E_{11}, E_{22}, E_{33} . Thus follows, e.g., according to equation (13.138), a slope of -1.47 for the thermal expansion of uranium. The straight line through the zero point for this case is shown in *Figure 13.22*. All textures whose points are contained on this straight line thus yield isotropic behaviour. The anisotropy of a material with arbitrary texture is determined by the distance of the points from this straight line.

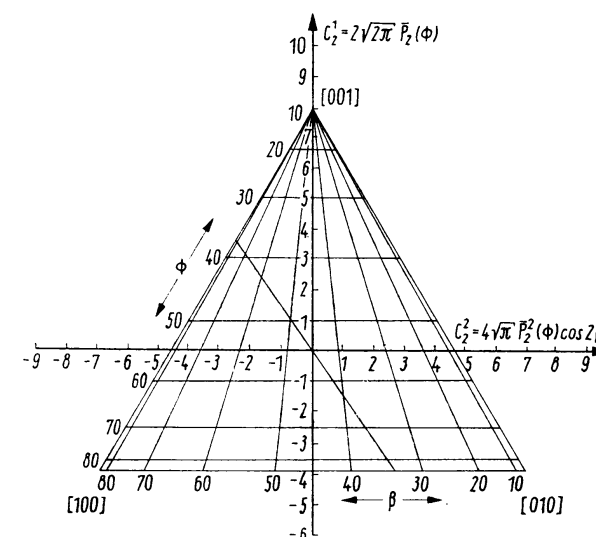


Figure 13.22 Coefficient diagram for tensor properties of second rank of orthorhombic materials with fibre texture

According to equation (13.141), the irradiation growth of uranium depends only on the texture coefficient C_2^2 . The lines of equal anisotropy are here thus parallel to the C_2^1 axis.

The coefficient diagram thus permits a survey of the anisotropic behaviour of polycrystals in a very simple way. Of course, we have only considered two very

simple cases which allow two-dimensional representation. If more texture coefficients enter into the anisotropy expression for the polycrystal, one is confronted with correspondingly multidimensional representations. One can, however, eventually use several two-dimensional projections which are also simply representable.

13.8. Physical Meaning of the Coefficients $C_l^{\mu\nu}$

The series expansion of the orientation distribution function $f(g)$ (equation 4.7) can be understood as the function $f(g)$ being composed of 'elementary portions' of the form $\tilde{T}_l^{\mu\nu}(g)$. This decomposition of the actual distribution function into elementary terms is purely mathematical. The elementary terms $T_l^{\mu\nu}(g)$, in general, have no physical meaning, and the coefficients $C_l^{\mu\nu}$ which characterize the individual amounts of such elementary distribution functions thereby also have no physical meaning. However, one can associate a certain physical sense with the coefficients $C_l^{\mu\nu}$ with small l -values. We consider the elastic anisotropy of a sheet. The E -modulus in the direction γ is then given by expression (13.172), which we can write as a FOURIER series:

$$\frac{1}{E(\gamma)} = E_1 + E_2 \cos 2\gamma + E_3 \cos 4\gamma \quad (13.223)$$

The coefficients E_i are then given by

$$E_1 = \frac{1}{4} \left[\frac{1}{E(90^\circ)} + \frac{1}{E(0^\circ)} + \frac{2}{E(45^\circ)} \right] \quad (13.224)$$

$$E_2 = \frac{1}{2} \left[\frac{1}{E(90^\circ)} - \frac{1}{E(0^\circ)} \right] \quad (13.225)$$

$$E_3 = \frac{1}{4} \left[\frac{1}{E(90^\circ)} + \frac{1}{E(0^\circ)} - \frac{2}{E(45^\circ)} \right] \quad (13.226)$$

The coefficients E_i thus characterize the average value, the 'second-order' term and the 'fourth-order' term, respectively, of the curve of the elastic modulus (Figure 13.11). If for \tilde{s}_{ijkl} in equation (13.172) we substitute the expression $\tilde{s}_{ijkl} = \tilde{s}_{ijkl}^R$, the REUSS approximation according to equation (13.160) with the values of Table 13.4, we thus obtain

$$E_1 = s_{1111}^r + s_a \bar{a}_4^{11}(1111) C_4^{11} \quad (13.227)$$

$$E_2 = -s_a \bar{a}_4^{12}(1111) C_4^{12} \quad (13.228)$$

$$E_3 = s_a \bar{a}_4^{13}(1111) C_4^{13} \quad (13.229)$$

s_{1111}^r is thereby the expression (13.161) for a material with random orientation distribution. If, as in Figure 13.11, the anisotropy is not too great, a linear relation also

exists between the coefficients C_4^{1v} and the quantities

$$E^1 = \frac{1}{4} [\tilde{E}(90^\circ) + \tilde{E}(0^\circ) + 2\tilde{E}(45^\circ)] \approx E^r + a^1 C_4^{11} \quad (13.230)$$

$$E^2 = \frac{1}{2} [\tilde{E}(90^\circ) - \tilde{E}(0^\circ)] \approx a^2 C_4^{12} \quad (13.231)$$

$$E^3 = \frac{1}{4} [\tilde{E}(90^\circ) + \tilde{E}(0^\circ) - 2\tilde{E}(45^\circ)] \approx a^3 C_4^{13} \quad (13.232)$$

\tilde{E} are the polycrystal values calculated according to HILL's approximation. The coefficients a^i are, however, no longer as simple expressions as in equations (13.227)–(13.229). They can, however, be easily calculated numerically according to the algorithm of the HILL's approximation. The dependence of the quantity E^1 on C_4^{11} and E^3 on C_4^{13} is represented in Figure 13.23 for differently textured copper sheets^{72,78}. The coefficients C_4^{1v} thus describe the texture dependence of 'zero-order', 'second-order' and 'fourth-order' terms of the anisotropy of the elastic modulus. They have a physical meaning of their own in these cases. One obtains a similar linear relation for all properties whose directional dependence in a single crystal can be described in satisfactory approximation by a function of fourth order: for example, the magnetic properties, if one restricts them to the term of fourth order. Also, one can for many purposes describe the plastic anisotropy by a fourth-order function as a satisfactory approximation. The zero-, second- and fourth-order terms of the anisotropy of these properties can then likewise be described by expressions of the type of equations (13.230)–(13.232). Thereby

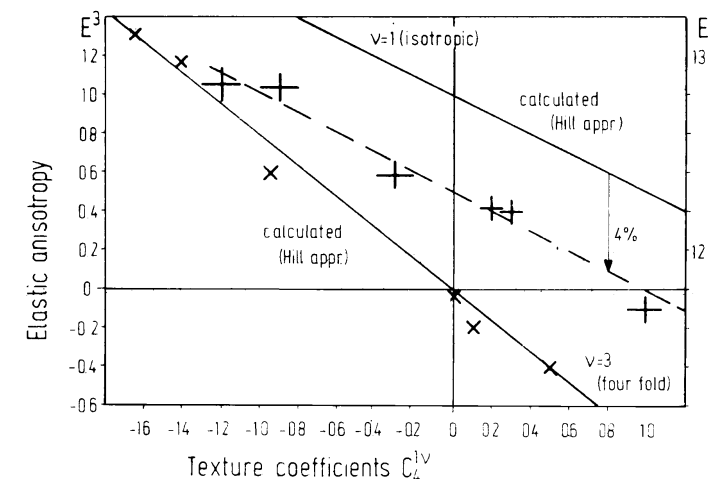


Figure 13.23 The isotropic part E^1 and the constituents of fourfold symmetry E^3 of elastic anisotropy of copper sheets with different textures as a function of texture coefficients C_4^{1v} . The crosses correspond to measured values; the solid lines were calculated according to HILL's approximation according to references 72 and 78

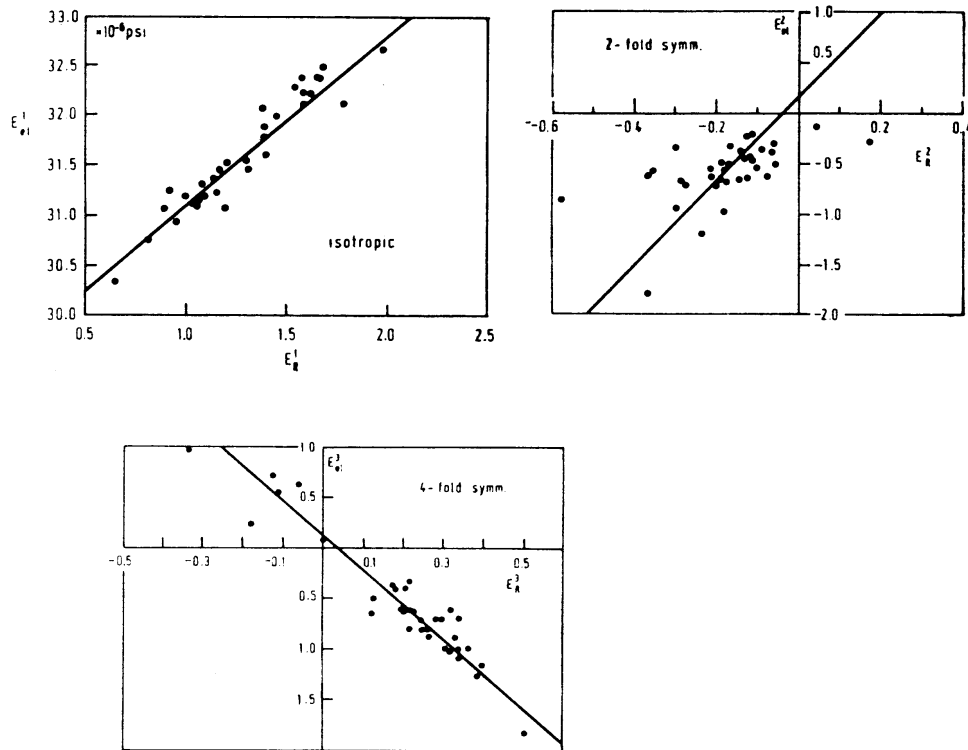


Figure 13.24 Relations between the isotropic parts and the constituents of twofold and fourfold symmetry of the anisotropy of the elastic modulus and the r -values of the plastic anisotropy for 35 samples of rolled and annealed carbon steels according to STICKELS and MOULD²⁶⁹

one immediately obtains a linear relation between the corresponding anisotropy quantities of different properties — e.g. the elastic, magnetic and plastic:

$$(E_{\text{el.}}^1 - E_{\text{el.}}^{\text{r}}) \sim (E_{\text{mag.}}^1 - E_{\text{mag.}}^{\text{r}}) \sim (E_{\text{plast.}}^1 - E_{\text{plast.}}^{\text{r}}) \sim C_4^{11} \quad (13.233)$$

$$E_{\text{el.}}^2 \sim E_{\text{mag.}}^2 \sim E_{\text{plast.}}^2 \sim C_4^{12} \quad (13.234)$$

$$E_{\text{el.}}^3 \sim E_{\text{mag.}}^3 \sim E_{\text{plast.}}^3 \sim C_4^{13} \quad (13.235)$$

These relations were, for example, confirmed by STICKELS and MOULD²⁶⁹ on a large number of low-carbon steels. They compared the quantities $E_{\text{el.}}^i$ and $E_{\text{plast.}}^i$, where the r -value was used as a measure of plastic anisotropy. The relation given by equations (13.233)–(13.235) for the three terms of the elastic and plastic anisotropy is reproduced in Figure 13.24.

14. Mathematical Aids

In this chapter some mathematical aids which are necessary for the representation of textures will be compiled. In addition to the properties of the spherical harmonics and generalized spherical harmonics, some properties of the symmetric functions of different symmetries are particularly important. That is not to say that a complete representation of these functions will be given. We shall simply compile in unified notation the important definitions and relations which are frequently employed for calculations with orientation distributions. The derivations and proofs will be largely omitted. In some tables in Chapter 15 we have given a series of numerical values which are necessary for carrying out texture analyses.

14.1. Generalized Spherical Harmonics

The generalized spherical harmonics are the matrix elements of the irreducible representation of the three-dimensional rotation group. They are defined by

$$T_l^{mn}(g) = T_l^{mn}(\varphi_1, \Phi, \varphi_2) = e^{im\varphi_1} P_l^{mn}(\cos \Phi) e^{in\varphi_2} \quad (14.1)$$

with

$$P_l^{mn}(\cos \Phi) = P_l^{mn}(x) = \frac{(-1)^{l-m} i^{n-m}}{2^l (l-m)!} \left[\frac{(l-m)! (l+n)!}{(l+m)! (l-n)!} \right]^{1/2} \times (1-x)^{-\frac{n-m}{2}} (1+x)^{-\frac{n+m}{2}} \frac{d^{l-n}}{dx^{l-n}} [(1-x)^{l-m} (1+x)^{l+m}] \quad (14.2)$$

One finds detailed representations of these functions and their properties in references 132, 297 and 298. The functions $P_l^{mn}(x)$ for $-1 \leq x \leq +1$ are either real or purely imaginary, according to whether $m+n$ is even or odd. Hence, we can introduce the real functions

$$Q_l^{mn}(x) = i^{m+n} P_l^{mn}(x) \quad (14.3)$$

In particular, it is true for $l=0$ that

$$T_0^{00}(g) = P_0^{00}(\cos \Phi) = 1 \quad (14.4)$$

For $l=1$ and $l=2$ the $P_l^{mn}(\Phi)$ have the form given in Tables 14.1 and 14.2.

If two rotations g' and g are carried out successively, the corresponding matrices of their representation are to be multiplied:

$$\mathfrak{T}_{gg'} = \mathfrak{T}_g \cdot \mathfrak{T}_{g'} \quad (14.5)$$

Table 14.1 THE FUNCTIONS $P_1^{mn}(\Phi)$

m	$P_1^{mn}(\Phi)$		
	$n = -1$	$n = 0$	$n = +1$
-1	$\frac{1}{2}(1 + \cos \Phi)$	$-\frac{i}{\sqrt{2}} \sin \Phi$	$\frac{1}{2}(\cos \Phi - 1)$
0	$-\frac{i}{\sqrt{2}} \sin \Phi$	$\cos \Phi$	$-\frac{i}{\sqrt{2}} \sin \Phi$
+1	$\frac{1}{2}(\cos \Phi - 1)$	$-\frac{i}{\sqrt{2}} \sin \Phi$	$\frac{1}{2}(1 + \cos \Phi)$

The following formula, called the addition theorem, results for the matrix elements:

$$T_l^{mn}(g \cdot g') = \sum_{s=-l}^{+l} T_l^{ms}(g) T_l^{sn}(g') \quad (14.6)$$

In particular, if one sets

$$g = \{0, \Phi, 0\} \text{ and } g' = \{0, \Phi', 0\} \quad (14.7)$$

one thus obtains

$$P_l^{mn}(\Phi + \Phi') = \sum_{s=-l}^{+l} P_l^{ms}(\Phi) P_l^{sn}(\Phi') \quad (14.8)$$

For the sake of brevity, and since confusion is scarcely to be feared, we have written $P_l^{mn}(\Phi)$ instead of $P_l^{mn}(\cos \Phi)$.

The functions $T_l^{mn}(g)$ form a complete system of orthonormal functions. It is true that

$$\oint T_l^{mn}(g) T_l^{*m'n'}(g) dg = \frac{1}{2l+1} \delta_{ll'} \delta_{mm'} \delta_{nn'} \quad (14.9)$$

We have set

$$dg = \frac{1}{8\pi^2} \sin \Phi d\Phi d\varphi_1 d\varphi_2 \quad (14.10)$$

The orthonormalization condition for the $P_l^{mn}(\Phi)$ follows therefrom:

$$\int_0^\pi P_l^{mn}(\Phi) P_l^{*mn}(\Phi) \sin \Phi d\Phi = \frac{2}{2l+1} \delta_{ll'} \quad (14.11)$$

(The asterisk denotes the complex conjugate quantity.)

Besides the normalization condition (equation 14.11) another condition is being used which defines the so-called augmented JACOBI polynomials²¹⁶:

$$\int_0^\pi Z_{lmn}(\Phi) \cdot Z_{l'mn}^*(\Phi) \sin \Phi d\Phi = \delta_{ll'} \quad (14.12)$$

Table 14.2 THE FUNCTIONS $P_2^{mn}(\Phi)$

m	$P_2^{mn}(\Phi)$		
	$n = -2$	$n = -1$	$n = 0$
-2	$\frac{1}{4}(\cos \Phi + 1)^2$	$-\frac{i}{2} \sin \Phi (\cos \Phi + 1)$	$-\frac{1}{2} \sqrt{\frac{3}{2}} (1 - \cos^2 \Phi)$
-1	$-\frac{i}{2} \sin \Phi (\cos \Phi + 1)$	$\frac{1}{2} (2 \cos^2 \Phi + \cos \Phi - 1)$	$-\sqrt{\frac{3}{2}} i \sin \Phi \cos \Phi$
0	$-\frac{1}{2} \sqrt{\frac{3}{2}} (1 - \cos^2 \Phi)$	$-\frac{1}{2} i \sin \Phi \cos \Phi$	$-\sqrt{\frac{3}{2}} i \sin \Phi \cos \Phi$
+1	$-\frac{i}{2} \sin \Phi (\cos \Phi - 1)$	$\frac{1}{2} (2 \cos^2 \Phi - \cos \Phi - 1)$	$\frac{1}{2} (2 \cos^2 \Phi + \cos \Phi - 1)$
+2	$\frac{1}{4}(\cos \Phi - 1)^2$	$-\frac{i}{2} \sin \Phi (\cos \Phi - 1)$	$-\frac{1}{2} \sqrt{\frac{3}{2}} (1 - \cos^2 \Phi)$

These functions are related to the $P_l^{mn}(\Phi)$ by

$$Z_{lmn}(\Phi) = i^{n-m} \sqrt{\frac{2l+1}{2}} P_l^{mn}(\Phi) \quad (14.13)$$

The identity element $e = \{0, 0, 0\}$ of the rotation group is to be associated with the identity matrix \mathfrak{E} :

$$\mathfrak{T}_e = \mathfrak{E} \quad (14.14)$$

This means in component notation:

$$T_l^{mn}(e) = \delta_{mn} \quad (14.15)$$

and

$$P_l^{mn}(\Phi = 0) = \delta_{mn} \quad (14.16)$$

The following relations are true with respect to interchange of indices:

$$P_l^{nm}(\Phi) = P_l^{mn}(\Phi) = P_l^{-m-n}(\Phi) \quad (14.17)$$

It also results that

$$P_l^{mn}(\pi - \Phi) = (-1)^{l+m+n} P_l^{-mn}(\Phi) \quad (14.18)$$

In particular, it follows therefrom that

$$P_l^{mn}\left(\frac{\pi}{2}\right) = (-1)^{l+m+n} P_l^{-mn}\left(\frac{\pi}{2}\right) \quad (14.19)$$

Finally

$$P_l^{mn}(\pi) = (-1)^l \delta_{m-n} \quad (14.20)$$

Since the $T_l^{mn}(g)$ are the elements of a unitary matrix, the following relation is valid:

$$T_l^{mn}(g^{-1}) = T_l^{*nm}(g) \quad (14.21)$$

The following recursion relations exist between functions with the same l index:

$$\alpha_l^{n+1} P_l^{m,n+1}(\Phi) - \alpha_l^n P_l^{m,n-1}(\Phi) = 2i \frac{m-n \cos \Phi}{\sin \Phi} P_l^{mn}(\Phi) \quad (14.22)$$

$$\alpha_l^{m+1} P_l^{m+1,n}(\Phi) - \alpha_l^m P_l^{m-1,n}(\Phi) = 2i \frac{n-m \cos \Phi}{\sin \Phi} P_l^{mn}(\Phi) \quad (14.23)$$

with

$$\alpha_l^n = \sqrt{(l+n)(l-n+1)} \quad (14.24)$$

A certain number of recursion relations also exist between functions with different l indices (see, e.g., reference 132, p. 95).

If g and g' are two arbitrary rotations, the rotation

$$g'^{-1} \cdot g \cdot g' = \tilde{g} \quad (14.25)$$

has the same rotation angle as g . According to the definition (equation 2.120), these rotations thus all have the same absolute value $|g|$. If g' traverses all elements of the rotation group, the rotation axis of \tilde{g} traverses all possible orientations. The rotations \tilde{g} form a class of conjugate elements. A function $f(|g|)$, which depends only on the class of the elements g , can be expanded in a series of characters of the irreducible representations

$$f(|g|) = \sum_{l=0}^{\infty} a_l \chi_l(g) \quad (14.26)$$

$\chi_l(g)$ is thereby the trace of the representation matrix:

$$\chi_l(g) = \sum_{m=-l}^{+l} T_l^{mn}(g) \quad (14.27)$$

Since $\chi_l(g)$ depends only on the rotation angle ω , for g it is sufficient to insert one element of this angle.

With

$$g = \{\omega, 0, 0\} \quad (14.28)$$

one obtains

$$\chi_l(\omega) = \sum_{m=-l}^{+l} e^{im\omega} = 1 + 2 \sum_{m=1}^l \cos m\omega \quad (14.29)$$

Conversely, for $n \geq 2$ it follows that

$$\cos n\omega = \frac{1}{2} [\chi_n(\omega) - \chi_{n-1}(\omega)] \quad (14.30)$$

If one sets

$$g = \{0, \omega, 0\} \quad (14.31)$$

there thus results

$$\chi_l(\omega) = \sum_{m=-l}^{+l} P_l^{mn}(\omega) \quad (14.32)$$

According to the definition of the functions $T_l^{mn}(g)$,

$$\begin{aligned} T_l^{mn}(\varphi_1, \Phi, \varphi_2) &= P_l^{mn}(\Phi) [(\cos m\varphi_2 \cos n\varphi_1 - \sin m\varphi_2 \sin n\varphi_1) \\ &\quad + i(\cos m\varphi_2 \sin n\varphi_1 + \sin m\varphi_2 \cos n\varphi_1)] \end{aligned} \quad (14.33)$$

Therefrom follow

$$\frac{1}{2} [T_l^{mn} + T_l^{-m-n}] = P_l^{mn}(\Phi) [\cos m\varphi_2 \cos n\varphi_1 - \sin m\varphi_2 \sin n\varphi_1] \quad (14.34)$$

$$\frac{i}{2} [T_l^{-m-n} - T_l^{mn}] = P_l^{mn}(\Phi) [\cos m\varphi_2 \sin n\varphi_1 + \sin m\varphi_2 \cos n\varphi_1] \quad (14.35)$$

Now, according to equation (14.2), $P_l^{mn}(\Phi)$ is either real or purely imaginary, depending on whether $m + n$ is even or odd. The functions

$$T_l'^{mn} = \frac{1}{\sqrt{2}} i^{m-n} [T_l^{mn} + T_l^{-m-n}] \quad (14.36)$$

$$T_l''^{mn} = \frac{1}{\sqrt{2}} i^{1+m-n} [T_l^{mn} - T_l^{-m-n}] \quad (14.37)$$

together with T_l^{00} therefore form a purely real and normalized basis of the generalized spherical harmonics.

14.2. Spherical Surface Harmonics

The normalized spherical surface harmonics are defined by

$$k_l^m(\Phi, \beta) = \frac{1}{\sqrt{2\pi}} e^{im\beta} \bar{P}_l^m(\cos \Phi) \quad (14.38)$$

(see, e.g., reference 195). The normalized associated LEGENDRE functions $\bar{P}_l^m(\cos \Phi)$ are defined by the following expression †:

$$\begin{aligned} \bar{P}_l^m(\cos \Phi) &= \bar{P}_l^m(x) \\ &= \sqrt{\frac{(l+m)!}{(l-m)!}} \sqrt{\frac{2l+1}{2}} \frac{(-1)^{l-m}}{2l!} (1-x^2)^{-m/2} \frac{d^{l-m}}{dx^{l-m}} (1-x^2)^l \end{aligned} \quad (14.39)$$

They are thus real functions for $-1 \leq x \leq +1$. In the following for the sake of simplicity we have also written $\bar{P}_l^m(\Phi)$ for $\bar{P}_l^m(\cos \Phi)$. The following relation with the functions $P_l^{0m}(\Phi)$ and $P_l^{m0}(\Phi)$ results from the definitions given in equations (14.2) and (14.39). It is

$$P_l^{0m}(\Phi) = P_l^{m0}(\Phi) = i^{-m} \sqrt{\frac{2}{2l+1}} \bar{P}_l^m(\Phi) \quad (14.40)$$

† It should be mentioned that several different definitions of these functions are being used in the literature. They deviate from one another by ‘phase factors’

$$p = i^{(\alpha l + \beta m)}$$

where α and β are integers. The definition assumed in equation (14.39) deviates from the definition used in the first edition of this book (equation 11.36) (I) by the factor $(-1)^m$ because it seems more suitable for a unified representation of the symmetric harmonics. The present definition is the same as that one used by HOFSSOMMER and POTTERS¹⁵⁴ in their tables of the FOURIER coefficients of the functions $\bar{P}_l^m(\Phi)$.

It follows therefrom, with equations (2.126) and (2.129), that

$$T_l^{m0}(\Phi, \varphi_2) = \sqrt{\frac{4\pi}{2l+1}} k_l^m \left(\Phi, \varphi_2 - \frac{\pi}{2} \right) = \sqrt{\frac{4\pi}{2l+1}} k_l^{*m}(\Phi, \beta) \quad (14.41)$$

and

$$T_l^{0n}(\varphi_1, \Phi) = \sqrt{\frac{4\pi}{2l+1}} k_l^n \left(\Phi, \varphi_1 - \frac{\pi}{2} \right) = \sqrt{\frac{4\pi}{2l+1}} k_l^n(\Phi, \gamma) \quad (14.42)$$

With equation (14.55) it follows that

$$T_l^{-m0}(\Phi, \varphi_2) = \sqrt{\frac{4\pi}{2l+1}} k_l^m(\Phi, \beta + \pi) \quad (14.43)$$

$$T_l^{0-n}(\varphi_1, \Phi) = \sqrt{\frac{4\pi}{2l+1}} k_l^{*n}(\Phi, \gamma + \pi) \quad (14.44)$$

The functions $T_l^{m0}(g)$ are thus independent of φ_1 and the functions $T_l^{0n}(g)$ are independent of φ_2 . They thus possess rotational symmetry with respect to the Z-axes of the sample fixed and crystal fixed coordinate systems, respectively.

If in the addition theorem for generalized spherical harmonics (equation 14.6) one sets $m = 0$, one thus obtains the addition theorem for spherical surface harmonics:

$$k_l^n(\Phi', \gamma') = \sum_{s=-l}^{+l} k_l^s(\Phi, \gamma) T_l^{sn}(g) \quad (14.45)$$

Φ', γ' denote the coordinates of the direction Φ, γ in the coordinate system rotated through g^{-1} . In particular, it follows from equation (14.8) with equation (14.40) that

$$\bar{P}_l^n(\Phi + \Phi') = \sum_{s=-l}^{+l} i^{n-s} \bar{P}_l^s(\Phi) P_l^{sn}(\Phi') \quad (14.46)$$

and

$$\bar{P}_l(\Phi + \Phi') = \sqrt{\frac{2}{2l+1}} \sum_{s=-l}^{+l} (-1)^s \bar{P}_l^s(\Phi) \bar{P}_l^s(\Phi') \quad (14.47)$$

The spherical harmonics fulfil the orthonormalization condition

$$\oint k_l^m(\Phi, \beta) k_l^{*m'}(\Phi, \beta) \sin \Phi d\Phi d\beta = \delta_{ll'} \delta_{mm'} \quad (14.48)$$

For the normalized associated LEGENDRE functions it is true that

$$\int_0^\pi \bar{P}_l^m(\Phi) \bar{P}_l^m(\Phi) \sin \Phi d\Phi = \delta_{ll'} \quad (14.49)$$

In particular, it follows therefrom that

$$\bar{P}_0(\Phi) = \frac{1}{\sqrt{2}} \quad (14.50)$$

In addition to the functions $\bar{P}_l^m(\Phi)$, a different normalization will sometimes be employed:

$$P_l^m(\Phi) = \sqrt{\frac{2}{2l+1}} \sqrt{\frac{(l-m)!}{(l+m)!}} \bar{P}_l^m(\Phi) \quad (14.51)$$

The orthonormalization condition in this case reads

$$\int_0^\pi P_l^m(\Phi) P_{l'}^m(\Phi) \sin \Phi d\Phi = \frac{2}{2l+1} \frac{(l-m)!}{(l+m)!} \delta_{ll'} \quad (14.52)$$

With $n = 0$, it follows from equation (14.16) with equation (14.40) that

$$\bar{P}_l^m(\Phi = 0) = \sqrt{\frac{2l+1}{2}} \delta_{m0} \quad (14.53)$$

We further obtain therefrom with equation (14.38)

$$k_l^m(0, 0) = k_l^m(0, \beta) = \sqrt{\frac{2l+1}{4\pi}} \delta_{m0} \quad (14.54)$$

With $n = 0$, if one considers equation (14.40), there results from equation (14.17)

$$\bar{P}_l^{-m}(\Phi) = (-1)^m \bar{P}_l^m(\Phi) \quad (14.55)$$

From equation (14.20) there results

$$\bar{P}_l^m(\pi) = (-1)^l \sqrt{\frac{2l+1}{2}} \delta_{m0} \quad (14.56)$$

Correspondingly, one obtains from equation (14.18)

$$\bar{P}_l^m(\pi - \Phi) = (-1)^{l+m} \bar{P}_l^m(\Phi) \quad (14.57)$$

In particular, there follows therefrom

$$\bar{P}_l^m\left(\frac{\pi}{2}\right) = 0 \quad \text{for } l+m \text{ odd} \quad (14.58)$$

With equation (14.38) it follows from equation (14.57)

$$k_l^m(-\mathbf{h}) = k_l^m(\pi - \Phi, \beta + \pi) = (-1)^l k_l^m(\Phi, \beta) = (-1)^l k_l^m(\mathbf{h}) \quad (14.58a)$$

The recursion formula results from equation (14.23):

$$\alpha_l^{m+1} \bar{P}_l^{m+1}(\Phi) + \alpha_l^m \bar{P}_l^{m-1}(\Phi) = + \frac{2m}{\tan \Phi} \bar{P}_l^m(\Phi) \quad (14.59)$$

According to equation (14.38),

$$k_l^m(\Phi, \beta) = \frac{1}{\sqrt{2\pi}} \bar{P}_l^m(\Phi) [\cos m\beta + i \sin m\beta] \quad (14.60)$$

According to equation (14.39), the $\bar{P}_l^m(\Phi)$ are real. The functions

$$k_l^0(\Phi, \beta) = \frac{1}{\sqrt{2\pi}} \bar{P}_l^0(\Phi) \quad (14.61)$$

$$k_l'^m(\Phi, \beta) = \frac{1}{\sqrt{2}} [k_l^m(\Phi, \beta) + (-1)^m k_l^{-m}(\Phi, \beta)] = \frac{1}{\sqrt{\pi}} \bar{P}_l^m(\Phi) \cos m\beta \quad (14.62)$$

$$k_l''^m(\Phi, \beta) = \frac{-i}{\sqrt{2}} [k_l^m(\Phi, \beta) - (-1)^m k_l^{-m}(\Phi, \beta)] = \frac{1}{\sqrt{\pi}} \bar{P}_l^m(\Phi) \sin m\beta \quad (14.63)$$

therefore form a real basis for the spherical harmonics.

The functions $\cos m\beta$ are symmetric and the functions $\sin m\beta$ are antisymmetric with respect to a mirror plane at $\beta = 0$. Hence, the real representation of the spherical harmonics allows one to take a mirror plane at $\beta = 0$ into account by the ‘selection rule’:

$$k'''^m(\Phi, \beta) = 0 \quad (14.64)$$

14.3. Fourier Expansion of the $P_l^{mn}(\Phi)$

The rotation with EULER’s angles $\left\{\frac{\pi}{2}, \frac{\pi}{2}, \frac{\pi}{2}\right\}$ interchanges the positive X -axis with the positive Z -axis. For every Φ it is therefore true that

$$\{0, \Phi, 0\} = \left\{\frac{\pi}{2}, \frac{\pi}{2}, \frac{\pi}{2}\right\} \cdot \{\Phi, 0, 0\} \cdot \left\{\frac{\pi}{2}, \frac{\pi}{2}, \frac{\pi}{2}\right\} \quad (14.65)$$

The addition theorem then yields

$$P_l^{mn}(\Phi) = \sum_{s=-l}^{+l} \sum_{\sigma=-l}^{+l} e^{im\pi/2} P_l^{ms}\left(\frac{\pi}{2}\right) e^{is\pi/2} P_l^{s\sigma}(0) e^{i\sigma\Phi} e^{i\sigma\pi/2} P_l^{\sigma n}\left(\frac{\pi}{2}\right) e^{in\pi/2} \quad (14.66)$$

If, according to equation (14.16), we substitute $\delta_{s\sigma}$ for $P_l^{s\sigma}(0)$, we thus obtain⁴⁷

$$P_l^{mn}(\Phi) = e^{i\frac{\pi}{2}(m+n)} \sum_{s=-l}^{+l} e^{is\pi} P_l^{ms}\left(\frac{\pi}{2}\right) P_l^{sn}\left(\frac{\pi}{2}\right) e^{is\Phi} \quad (14.67)$$

$P_l^{mn}(\Phi)$ is thus represented as a FOURIER series:

$$P_l^{mn}(\Phi) = \sum_{s=-l}^{+l} a_l^{mn s} e^{is\Phi} \quad (14.68)$$

with the coefficients

$$a_l^{mn s} = i^{m+n+2s} P_l^{ms}\left(\frac{\pi}{2}\right) P_l^{sn}\left(\frac{\pi}{2}\right) \quad (14.69)$$

With the real functions $Q_l^{mn}(x)$ defined in equation (14.3) we thus obtain

$$a_l^{mns} = Q_l^{ms} \left(\frac{\pi}{2} \right) \cdot Q_l^{ns} \left(\frac{\pi}{2} \right) \quad (14.70)$$

If we set

$$Q_l^{ms} \left(\frac{\pi}{2} \right) = Q_l^{ms} \quad (14.71)$$

equation (14.70) can be written in the form

$$a_l^{mns} = Q_l^{ms} \cdot Q_l^{ns} \quad (14.72)$$

The coefficients Q_l^{ms} have been tabulated by BUNGE⁶⁷ for $0 \leq l \leq 31$ (see also Section 15.1.1). With the definition of the quantities Q_l^{mn} (equation 14.3) it follows from equation (14.19) that

$$Q_l^{-mn} = (-1)^{l+n} Q_l^{mn} \quad (14.73)$$

The addition theorem (equation 14.8), putting $\Phi = \Phi' = \frac{\pi}{2}$ and taking equation (14.73) into account, leads to

$$\sum_{s=-l}^{+l} Q_l^{ms} Q_l^{ns} = \delta_{mn} \quad (14.74)$$

Under the considerations of equation (14.73), for a_l^{mn-s} we obtain

$$a_l^{mn-s} = (-1)^{m+n} a_l^{mns} \quad (14.75)$$

Correspondingly, for a_l^{-mns} we obtain

$$a_l^{-mns} = (-1)^{l+s} a_l^{mns} \quad (14.76)$$

According to equation (14.17), it must also be true that

$$a_l^{nms} = a_l^{mns} = a_l^{-m-n}s \quad (14.77)$$

By consideration of equation (14.75) we can write

$$P_l^{mn}(\Phi) = a_l^{mn0} + \sum_{s=1}^l a_l^{mns} [e^{is\Phi} + (-1)^{m+n} e^{-is\Phi}] \quad (14.78)$$

For $m+n$ even this gives

$$P_l^{mn}(\Phi) = a_l^{mn0} + 2 \sum_{s=1}^l a_l^{mns} \cos s\Phi \quad (14.79)$$

and for $m+n$ odd

$$P_l^{mn}(\Phi) = 2i \sum_{s=1}^l a_l^{mns} \sin s\Phi \quad (14.80)$$

If we set

$$a_l'^{mn0} = a_l^{mn0} \quad (14.81)$$

$$a_l'^{mns} = 2a_l^{mns} \quad (14.82)$$

$$a_l'^{mn0} = 0 \quad (14.83)$$

$$a_l'^{mns} = 2ia_l^{mns} \quad (14.84)$$

there thus result

$$P_l^{mn}(\Phi) = \sum_{s=0}^l a_l'^{mns} \cos s\Phi \quad \text{for } m+n \text{ even} \quad (14.85)$$

$$P_l^{mn}(\Phi) = \sum_{s=1}^l a_l'^{mns} \sin s\Phi \quad \text{for } m+n \text{ odd} \quad (14.86)$$

Similarly to equation (14.68), for the associated LEGENDRE functions we set

$$\bar{P}_l^m(\Phi) = \sum_{s=-l}^{+l} a_l^{ms} e^{is\Phi} \quad (14.87)$$

Because of equation (14.40), it is then true that

$$a_l^{m0s} = a_l^{0ms} = i^{-m} \sqrt{\frac{2}{2l+1}} a_l^{ms} \quad (14.88)$$

Because of equation (14.76), it follows therefrom that

$$a_l^{ms} = 0 \quad \text{for } l+s \text{ odd} \quad (14.89)$$

Analogously to equations (14.81)–(14.84), we set

$$a_l'^{m0} = a_l^{m0} \quad (14.90)$$

$$a_l'^{ms} = 2a_l^{ms} \quad (14.91)$$

$$a_l'^{m0} = 0 \quad (14.92)$$

$$a_l'^{ms} = 2ia_l^{ms} \quad (14.93)$$

Equation (14.88) is then also true for the coefficients $a_l'^{ms}$. With these coefficients, equation (14.87) transforms into

$$\bar{P}_l^m(\Phi) = \sum_{s=0}^l a_l'^{ms} \cos s\Phi \quad \text{for } m \text{ even} \quad (14.94)$$

$$\bar{P}_l^m(\Phi) = \sum_{s=1}^l a_l'^{ms} \sin s\Phi \quad \text{for } m \text{ odd} \quad (14.95)$$

Because of equation (14.89), we are required to sum either only over even or only over odd s . The coefficients $a_l'^{ms}$ have been tabulated (references 125, 154).

14.4. Clebsch—Gordan Coefficients

The product of two generalized spherical harmonics can be expressed as a sum in the following manner:

$$T_{l_1}^{m_1}(g) \cdot T_{l_2}^{m_2}(g) = \sum_{l=|l_1-l_2|}^{|l_1+l_2|} (l_1 l_2 m_1 m_2 | lm) (l_1 l_2 n_1 n_2 | ln) T_l^{mn}(g) \quad (14.96)$$

Thereby

$$m = m_1 + m_2; \quad n = n_1 + n_2 \quad (14.97)$$

The CLEBSCH—GORDAN coefficients appearing therein are defined in the following manner:

$$\begin{aligned} (l_1 l_2 m_1 m_2 | lm) &= \\ &= \left[\frac{2l+1}{(l_1 + l_2 + l + 1)!} (l_2 + l - l_1)! (l + l_1 - l_2)! (l_1 + l_2 - l)! \right. \\ &\quad \times (l_1 + m_1)! (l_1 - m_1)! (l_2 + m_2)! (l_2 - m_2)! (l + m)! (l - m)! \left. \right]^{1/2} \\ &\quad \times \sum_z \frac{(-1)^z}{z! (l_1 + l_2 - l - z)! (l + z - l_1 - m_2)! (l_2 + m_2 - z)!} \\ &\quad \times \frac{1}{(z + l - l_2 + m_1)! (l_1 - m_1 - z)!} \end{aligned} \quad (14.98)$$

In the sum z traverses positive integers greater than $m_2 + l_1 - l$ and $l_2 - l - m_1$ and smaller than $l_1 + l_2 - l$, $l_2 + m_2$ and $l_1 - m_1$.

The case where one of the two indices l_1 or l_2 is equal to 1 is particularly important. In this case one obtains the expressions given in Table 14.3¹¹.

Table 14.3 CLEBSCH—GORDAN COEFFICIENTS FOR $l_1 = 1$

m_1	$l = l_2 + 1$	$l = l_2$	$l = l_2 - 1$
-1	$\sqrt{\frac{(l_2 - m + 1)(l_2 - m)}{(2l_2 + 2)(2l_2 + 1)}}$	$-\sqrt{\frac{(l_2 + m + 1)(l_2 - m)}{2l_2(l_2 + 1)}}$	$\sqrt{\frac{(l_2 + m + 1)(l_2 + m)}{2l_2(2l_2 + 1)}}$
0	$\sqrt{\frac{(l_2 + m + 1)(l_2 - m + 1)}{(l_2 + 1)(2l_2 + 1)}}$	$-\frac{m}{\sqrt{l_2(l_2 + 1)}}$	$-\sqrt{\frac{(l_2 + m)(l_2 - m)}{l_2(2l_2 + 1)}}$
+1	$\sqrt{\frac{(l_2 + m + 1)(l_2 + m)}{(2l_2 + 2)(2l_2 + 1)}}$	$\sqrt{\frac{(l_2 - m + 1)(l_2 + m)}{2l_2(l_2 + 1)}}$	$\sqrt{\frac{(l_2 - m + 1)(l_2 - m)}{2l_2(2l_2 + 1)}}$

The CLEBSCH—GORDAN coefficients possess the following interchange properties:

$$(l_1 l_2 m_1 m_2 | lm) = (-1)^{l_1 + l_2 - l} (l_1 l_2 m_1 m_2 | lm) \quad (14.99)$$

$$(l_1 l_2 - m_1 - m_2 | l_1 - m_1) = (-1)^{l_1 + m_1} \sqrt{\frac{2l_1 + 1}{2l + 1}} (l_1 l_2 m_1 m_2 | lm) \quad (14.100)$$

$$(l_1 l_2 - m_1 - m_2 | l - m) = (-1)^{l_1 + l_2 - l} (l_1 l_2 m_1 m_2 | lm) \quad (14.101)$$

Also, the following relation is valid:

$$\sum_{m_1=-l_1}^{+l_1} (l_1 l_2 m_1 m_2 | lm) (l_1 l_2 m_1 m_2 | l'm) = \delta_{ll'} \quad (14.102)$$

If in equation (14.96) we set $n_1 = n_2 = n = 0$ and consider equation (14.41), we obtain

$$k_{l_1}^{m_1}(\mathbf{h}) k_{l_2}^{m_2}(\mathbf{h}) = \sum_{l=|l_1-l_2|}^{|l_1+l_2|} ((l_1 l_2 m_1 m_2 | lm)) k_l^m(\mathbf{h}) \quad (14.103)$$

with

$$((l_1 l_2 m_1 m_2 | lm)) = \frac{1}{\sqrt{4\pi}} \sqrt{\frac{(2l_1 + 1)(2l_2 + 1)}{2l + 1}} (l_1 l_2 m_1 m_2 | lm) (l_1 l_2 00 | l0) \quad (14.104)$$

If, in addition, we set $m_1 = m_2 = m = 0$, we obtain

$$\bar{P}_{l_1}(\Phi) \bar{P}_{l_2}(\Phi) = \sum_{l=|l_1-l_2|}^{|l_1+l_2|} (l_1 l_2 | l) \bar{P}_l(\Phi) \quad (14.105)$$

with

$$(l_1 l_2 | l) = \sqrt{\frac{(2l_1 + 1)(2l_2 + 1)}{2(2l + 1)}} (l_1 l_2 00 | l0)^2 \quad (14.106)$$

14.5. Symmetric Generalized Spherical Harmonics

We assume that in the coordinate system K_A a symmetry corresponding to the point group symmetry of the first kind G_A exists, which only contains pure rotations g_A . Correspondingly, the symmetry G_B with the elements g_B exists in the second coordinate system. The presence of these symmetries requires for every function of g

$$f(g \cdot g_A) = f(g) \quad (14.107)$$

$$f(g_B \cdot g) = f(g) \quad (14.108)$$

We shall therefore also denote the symmetries G_A and G_B as right-handed and left-handed symmetries. (In the case of texture representation we have called them the sample and crystal symmetries.)

Equation (14.107) is not generally fulfilled by the generalized spherical harmonics $T_l^{mn}(g)$. We therefore introduce new functions⁴⁴:

$$T_l^{mn}(g) = \sum_{n=-l}^{+l} \dot{A}_l^{mn} T_l^{mn}(g) \quad (14.109)$$

and determine the coefficients \dot{A}_l^{mn} so that the $T_l^{mn}(g)$ fulfil equation (14.107). It must thus be true that

$$\dot{T}_l^{mn}(g \cdot g_A) = T_l^{mn}(g) \quad (14.110)$$

With the addition theorem for generalized spherical harmonics we obtain

$$\dot{T}_l^{mv}(g \cdot g_A) = \sum_{n=-l}^{+l} \dot{A}_l^{mnv} \sum_{s=-l}^{+l} T_l^{ms}(g) T_l^{sn}(g_A) = \dot{T}_l^{mv}(g) \quad (14.111)$$

Moreover, according to equation (14.109),

$$\dot{T}_l^{mv}(g) = \sum_{s=-l}^{+l} \dot{A}_l^{msv} T_l^{ms}(g) \quad (14.112)$$

Since equation (14.107) is true for all g and since the functions $T_l^{ms}(g)$ are orthogonal for different s , the coefficients of $T_l^{ms}(g)$ in equations (14.111) and (14.112) must agree. It must thus be true that

$$\sum_{n=-l}^{+l} \dot{A}_l^{mnv} T_l^{sn}(g_A) = \dot{A}_l^{msv} \quad (14.113)$$

It follows therefrom that

$$\sum_{n=-l}^{+l} \dot{A}_l^{mnv} [T_l^{sn}(g_A) - \delta_{sn}] = 0 \quad (14.114)$$

Herein s can assume values from $-l$ to $+l$, and g_A traverse all elements of the group G_A . Equation (14.114) thus represents a system of linear homogeneous equations with the unknowns \dot{A}_l^{mnv} . The coefficients of this system of equations are independent of the index m . The solutions must also be independent of m in the sense that each solution for a specific m is also a solution for every other m . We can thus omit the index m in the quantities \dot{A}_l^{mnv} and obtain as a definition of the right-handed symmetric functions

$$\dot{T}_l^{mv}(g) = \sum_{n=-l}^{+l} \dot{A}_l^{nv} T_l^{mn}(g) \quad (14.115)$$

where the \dot{A}_l^{nv} must be so determined that the conditions

$$\sum_{n=-l}^{+l} \dot{A}_l^{nv} [T_l^{sn}(g_A) - \delta_{sn}] = 0; \quad g_A \in G_A; \quad -l \leq s \leq +l \quad (14.116)$$

are fulfilled. The index v will thereby enumerate in some sequence the linearly independent orthogonal solutions of this system of equations. In general, we will begin the enumeration with $v = 1$:

$$1 \leq v \leq M_A(l) \quad (14.117)$$

$M_A(l)$ naturally depends on the symmetry G_A . The values $M_A(l)$ for even l and the various symmetry groups have been given in Figure 4.4. The corresponding values for the odd orders are contained in Figure 14.1.

However, how one chooses the linearly independent solutions from the set of all solutions is arbitrary. In most cases it is immaterial which linearly independent basis we choose for the solutions; it must only be the same within a calculation.

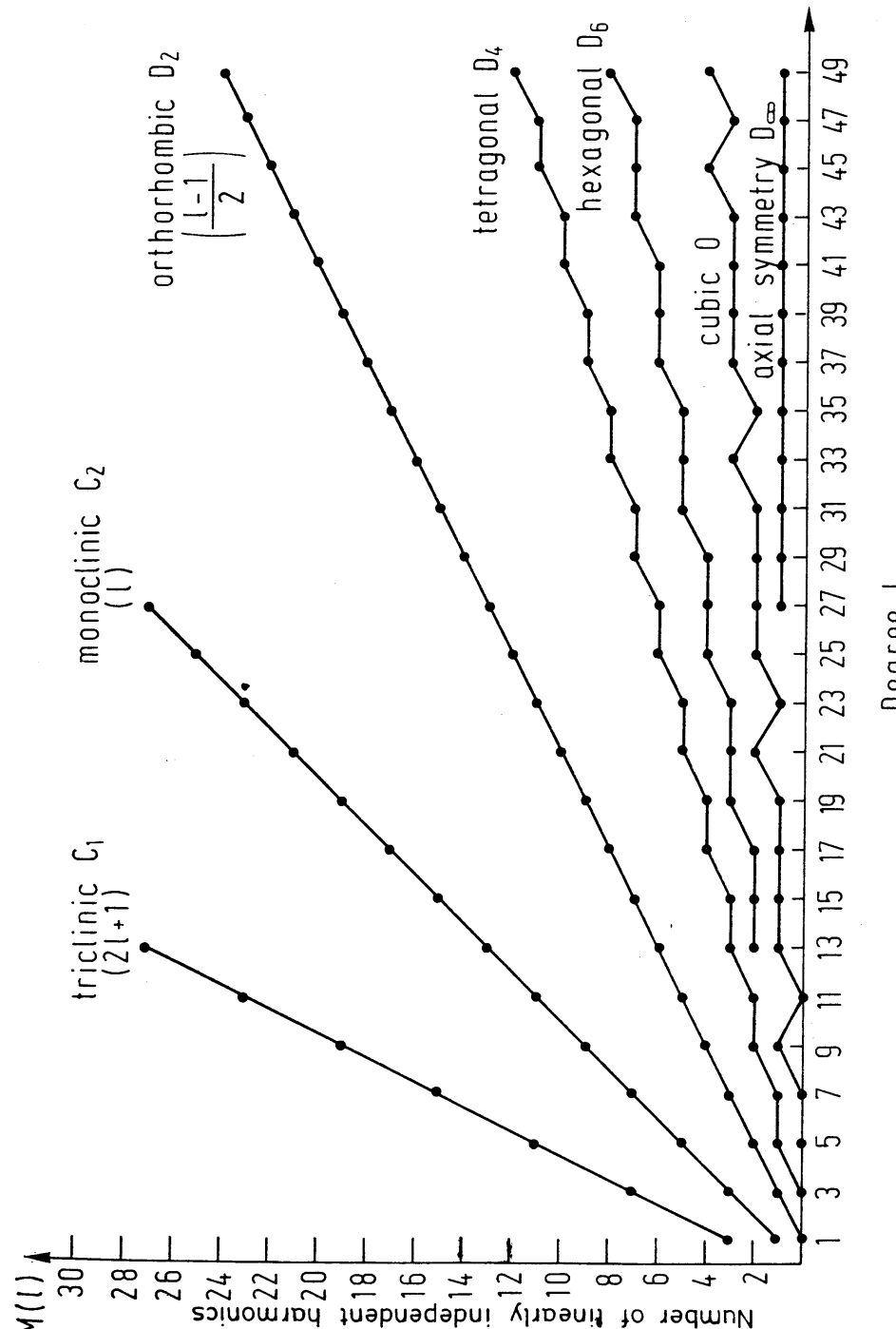


Figure 14.1 Number of linearly independent spherical harmonics of odd order for the various symmetry groups

The point on the right side of the function symbol $T_l^{mn}(g)$ will, as has been said, signify right-handed symmetry; further, if different symmetry groups are to be considered simultaneously, these will be distinguished by different numbers of points.

For $m = 0$, equation (14.115) transforms into

$$\dot{T}_l^{0r}(g) = \sum_{n=-l}^{+l} \dot{A}_l^{nr} T_l^{0n}(g) = \sum_{n=-l}^{+l} \dot{A}_l^{nr} T_l^{0n}(g_A, \Phi) \quad (14.118)$$

$$\dot{T}_l^{0r}(g) = \sqrt{\frac{4\pi}{2l+1}} \sum_{n=-l}^{+l} \dot{A}_l^{nr} k_l^n(\Phi, \gamma) \quad (14.119)$$

If we set

$$\dot{k}_l^r(\Phi, \gamma) = \sum_{n=-l}^{+l} \dot{A}_l^{nr} k_l^n(\Phi, \gamma) \quad (14.120)$$

the functions $\dot{k}_l^r(\Phi, \gamma)$ are the symmetric spherical surface harmonics, which are invariant with respect to the rotations g_A . We thus have for symmetric functions, similarly to equation (14.42),

$$\dot{T}_l^{0r}(g) = \sqrt{\frac{4\pi}{2l+1}} \dot{k}_l^r \left(\Phi, \varphi_1 - \frac{\pi}{2} \right) = \sqrt{\frac{4\pi}{2l+1}} \dot{k}_l^r(\Phi, \gamma) \quad (14.121)$$

The symmetry group G_A was assumed to be a pure rotation group for which every element g_A further transforms a right-handed coordinate system into such a system. Every arbitrary symmetry group can now be generated from a pure rotation group and an element $g_{A'}$, which transforms a right-handed coordinate system into a left-handed coordinate system. If the symmetry group $G_{A'}$ is not a pure rotation group, we must thus require that the spherical surface harmonics $\dot{k}_l^r(\Phi, \gamma)$ are also invariant with respect to the symmetry operation $g_{A'}$. This can yield a further symmetry condition for the \dot{A}_l^{nr} in equation (14.120) in addition to those in equation (14.116).

Analogously to the right-handed symmetric functions $T_l^{mn}(g)$, we introduce the left-handed symmetric functions:

$$\dot{T}_l^{mn}(g) = \sum_{m=-l}^{+l} \dot{A}_l^{m\mu} T_l^{mn}(g) \quad (14.122)$$

It is true for these that

$$\dot{T}_l^{mn}(g_B \cdot g) = \dot{T}_l^{mn}(g) \quad (14.123)$$

The coefficient $\dot{A}_l^{m\mu}$ must fulfil the condition

$$\sum_{m=-l}^{+l} \dot{A}_l^{m\mu} [T_l^{ms}(g_B) - \delta_{ms}] = 0; \quad g_B \in G_B; \quad -l \leq s \leq +l \quad (14.124)$$

The index μ again enumerates the linearly independent solutions:

$$1 \leq \mu \leq M_B(l) \quad (14.125)$$

For $n = 0$ there results

$$\dot{T}_l^{00}(g) = \dot{T}_l^{00}(\Phi, \varphi_2) = \sqrt{\frac{4\pi}{2l+1}} \dot{k}_l^0 \left(\Phi, \varphi_2 - \frac{\pi}{2} \right) = \sqrt{\frac{4\pi}{2l+1}} \dot{k}_l^{*\mu}(\Phi\beta) \quad (14.126)$$

with

$$\dot{k}_l^{\mu}(\Phi\beta) = \sum_{m=-l}^{+l} \dot{A}_l^{*m\mu} k_l^m(\Phi\beta) \quad (14.127)$$

where $\dot{k}_l^{\mu}(\Phi\beta)$ are symmetric spherical harmonics corresponding to the symmetry group G_B . If we assume the group G_B to be the same as G_A , then equation (14.127) defines a set of symmetrical harmonics of symmetry G_A , which however, may be different from the one defined in equation (14.120) because of the complex conjugate coefficients $\dot{A}_l^{*m\mu}$. According to equation (14.116), these coefficients were defined as the solutions of a homogeneous system of linear equations, where the index μ defines a certain basis within the vector space of all solutions. Because of the completeness of the solution, the symmetric harmonics defined in equation (14.127) can only represent another basis within the vector space of functions defined according to equation (14.120). We can thus change the basis so that the functions equations (14.120) and (14.127) are the same. This requires

$$\dot{A}_l^{*m\mu} = \dot{A}_l^{m\mu} \quad (14.128)$$

The coefficients $\dot{A}_l^{m\mu}$ can thus be chosen real. This can also be concluded from equation (14.124), the left-sided symmetry condition. If we assume the symmetry group G_B to be the same as G_A , then equation (14.124) reads

$$\sum_{n=-l}^{+l} \dot{A}_l^{nr} [T_l^{ns}(g_A) - \delta_{ns}] = 0 \quad (14.129)$$

Now, along with the symmetry operation g_A , the inverse operation g_A^{-1} also belongs to the group G_A . Equation (14.129) must therefore also be fulfilled for this element. If, now, one considers equation (14.21), one obtains

$$\sum_{n=-l}^{+l} \dot{A}_l^{nr} [T_l^{*sn}(g_A) - \delta_{ns}] = 0 \quad (14.130)$$

The quantities \dot{A}_l^{nr} fulfil both equation (14.116) and the corresponding equation with complex conjugate coefficients. The solutions can therefore always be chosen as real.

Finally, we set

$$\dot{T}_l^{uv}(g) = \sum_{m=-l}^{+l} \sum_{n=-l}^{+l} \dot{A}_l^{m\mu} \dot{A}_l^{nv} T_l^{mn}(g) \quad (14.131)$$

This can be written

$$\ddot{T}_l^{\mu\nu}(g) = \sum_{m=-l}^{+l} \dot{A}_l^{m\mu} \dot{T}_l^{mn}(g) = \sum_{n=-l}^{+l} \dot{A}_l^{n\nu} \dot{T}_l^{mn}(g) \quad (14.132)$$

The functions $\dot{T}_l^{\mu\nu}(g)$ therefore have right-handed and left-handed symmetry.

The functions belonging to different values n and n' are orthogonal. This requires

$$\oint T_l^{mn}(g) \dot{T}_l^{*mn'}(g) dg = \frac{1}{2l+1} \delta_{nn'} \quad (14.133)$$

With equations (14.115) and (14.128) one obtains the orthonormal condition for the coefficients:

$$\sum_{n=-l}^{+l} \dot{A}_l^{n\nu} \dot{A}_l^{n\nu'} = \delta_{\nu\nu'} \quad (14.134)$$

If the corresponding condition is also true for the $\dot{A}_l^{m\mu}$, the two-handed symmetric functions thus fulfil the orthonormal condition

$$\oint \dot{T}_l^{\mu\nu}(g) \dot{T}_l^{*\mu'\nu'}(g) dg = \frac{1}{2l+1} \delta_{\mu'\mu} \delta_{\nu'\nu} \quad (14.135)$$

From the addition theorem (equation 14.6) it follows by multiplication with $\dot{A}_l^{n\nu}$ and summation over all n that

$$\dot{T}_l^{mn}(g \cdot g') = \sum_{s=-l}^{+l} \dot{T}_l^{ms}(g) \dot{T}_l^{sn}(g') \quad (14.136)$$

By multiplication with $\dot{A}_l^{m\mu}$ and summation over m there results

$$\dot{T}_l^{\mu n}(g \cdot g') = \sum_{s=-l}^{+l} \dot{T}_l^{\mu s}(g) \dot{T}_l^{sn}(g') \quad (14.137)$$

If one carries out both at the same time, one thus obtains

$$\dot{T}_l^{\mu\nu}(g \cdot g') = \sum_{s=-l}^{+l} \dot{T}_l^{\mu s}(g) \dot{T}_l^{sn}(g') \quad (14.138)$$

These formulae are extensions of the addition theorem to symmetric functions.

If one sets $g = e$ (e is the identity rotation with the EULER angles 0, 0, 0) in equation (14.115), one thus obtains

$$\dot{T}_l^{mn}(g_A) = \dot{T}_l^{mn}(e) = \sum_{n=-l}^{+l} \dot{A}_l^{n\nu} \dot{T}_l^{mn}(e) \quad (14.139)$$

With equation (14.15) it follows therefrom that

$$\dot{T}_l^{mn}(g_A) = \dot{T}_l^{mn}(e) = \dot{A}_l^{m\mu} \quad (14.140)$$

Similarly one obtains

$$\dot{T}_l^{\mu n}(g_B) = \dot{T}_l^{\mu n}(e) = \dot{A}_l^{\mu\nu} \quad (14.141)$$

Finally, it follows from equation (14.131) that

$$\dot{T}_l^{\mu\nu}(g_B \cdot g_A) = \dot{T}_l^{\mu\nu}(e) = \sum_{m=-l}^{+l} \dot{A}_l^{m\mu} \dot{A}_l^{m\nu} \quad (14.142)$$

If both symmetries are equal, it is thus true, because of equation (14.134), that

$$\dot{T}_l^{\mu\nu}(g_A) = \dot{T}_l^{\mu\nu}(e) = \delta_{\mu\nu} \quad (14.143)$$

From equation (14.21), it further follows that

$$\dot{T}_l^{\mu\nu}(g^{-1}) = \dot{T}_l^{*\nu\mu}(g) \quad (14.144)$$

Finally, it follows from equation (14.4) that

$$\dot{T}_0^{01}(g) = \dot{T}_0^{10}(g) = \dot{T}_0^{11}(g) = T_0^{00}(g) = 1 \quad (14.145)$$

(The different enumeration of the indices m and n on the one hand and μ and ν on the other is thereby to be considered; in other words, for $l = 0$ m and n can only assume the value zero; on the other hand, μ and ν can only assume the value 1.)

14.5.1. Transformation of the Coefficients $\dot{A}_l^{n\nu}$

The left-side symmetric functions $\dot{T}_l^{\mu n}(g)$ were chosen so that symmetry condition (14.123) is true. The rotation g_B is thus an element of the symmetry group of the left-side symmetry (crystal symmetry). A certain orientation of the symmetry elements relative to the crystal coordinate system is thereby assumed. One can require, for example, that the axis of highest multiplicity fall in the Z -direction of the crystal coordinate system. We now consider a different arrangement of the crystal symmetry group, for which the symmetry elements g'_B show an orientation rotated about g_1^{-1} relative to the crystal coordinate system. These are the rotations

$$g'_B = g_1 g_B \cdot g_1^{-1} \quad (14.146)$$

They form the same symmetry group as the rotations g_B . In the case of cubic symmetry the g_B can, for example, be chosen so that the Z' -axis of the crystal coordinate system is a fourfold axis, while the g'_B can be chosen so that the Z' -axis is a threefold axis (Figure 14.2). In place of the functions $\dot{T}_l^{\mu n}(g)$ we then naturally obtain other functions $\dot{T}'_l^{\mu n}(g)$, which are defined similarly to equation (14.122):

$$\dot{T}'_l^{\mu n}(g) = \sum_{m=-l}^{+l} \dot{A}'_l^{m\mu} \dot{T}_l^{mn}(g) \quad (14.147)$$

with other coefficients $\dot{A}'_l^{m\mu}$. We seek the relation of the coefficients $\dot{A}'_l^{m\mu}$ of the rotated symmetry with the coefficients $\dot{A}_l^{m\mu}$ of the original symmetry. According

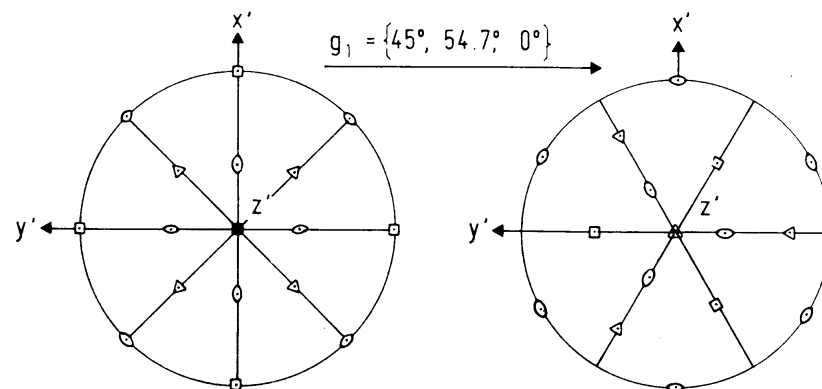


Figure 14.2 The rotation g_1 , which transforms the Z' -axis of the crystal coordinate system from a fourfold axis into a threefold axis

to equation (14.124), the coefficients $\dot{A}_l^{m\mu}$ fulfil the condition

$$\sum_{m=-l}^{+l} \dot{A}_l^{m\mu} T_l^{ms}(g_1^{-1} \cdot g_B \cdot g_1) = \dot{A}_l^{s\mu} \quad (14.148)$$

By two applications of the addition theorem (equation 14.6) we obtain therefrom

$$\sum_{m=-l}^{+l} \dot{A}_l^{m\mu} \sum_{p=-l}^{+l} \sum_{q=-l}^{+l} T_l^{mp}(g_1^{-1}) T_l^{pq}(g_B) T_l^{qs}(g_1) = \dot{A}_l^{s\mu} \quad (14.149)$$

By multiplication with $T_l^{sr}(g_1^{-1})$ and summation over s there results

$$\begin{aligned} & \sum_{m=-l}^{+l} \dot{A}_l^{m\mu} \sum_{p=-l}^{+l} \sum_{q=-l}^{+l} T_l^{mp}(g_1^{-1}) T_l^{pq}(g_B) \sum_{s=-l}^{+l} T_l^{qs}(g_1) T_l^{sr}(g_1^{-1}) \\ &= \sum_{s=-l}^{+l} \dot{A}_l^{s\mu} T_l^{sr}(g_1^{-1}) \end{aligned} \quad (14.150)$$

With the addition theorem the summation over s on the left side is equal to $T_l^{qr}(e) = \delta_{qr}$. One thereby obtains

$$\sum_{m=-l}^{+l} \dot{A}_l^{m\mu} \sum_{p=-l}^{+l} T_l^{mp}(g_1^{-1}) T_l^{pr}(g_B) = \sum_{p=-l}^{+l} \dot{A}_l^{p\mu} T_l^{pr}(g_1^{-1}) \quad (14.151)$$

Moreover, according to equation (14.124), the coefficients $\dot{A}_l^{m\mu}$ satisfy the condition

$$\sum_{m=-l}^{+l} \dot{A}_l^{m\mu} T_l^{ms}(g_B) = \dot{A}_l^{s\mu} \quad (14.152)$$

For the coefficients $\dot{A}_l^{s\mu}$, there follows directly by comparing equation (14.151) with equation (14.152)

$$\dot{A}_l^{s\mu} = \sum_{p=-l}^{+l} \dot{A}_l^{p\mu} T_l^{ps}(g_1^{-1}) \quad (14.153)$$

By multiplication with $T_l^{sr}(g_1)$ and summation over s one obtains the solution of equation (14.153) for the $\dot{A}_l^{r\mu}$

$$\dot{A}_l^{r\mu} = \sum_{s=-l}^{+l} \dot{A}_l^{s\mu} T_l^{sr}(g_1) \quad (14.154)$$

Equation (14.154) is the transformation formula for an arbitrary rotation g_1 of the symmetry relative to the selected coordinate system. If, for example, one selects

$$g_1 = \{45, 54.7^\circ, 0\} \quad (14.155)$$

one thus obtains an arrangement of cubic symmetry, for which a threefold axis [111] falls in the Z' -direction and a twofold [110] in the X' -direction, if in the original arrangement Z' was parallel to [001] and X' parallel to [100].

14.5.2. The Fundamental Integral

We introduce in addition to the coordinate systems K_A and K_B an additional system K , so that its Z'' -direction has the polar coordinates $\Phi_A \gamma_A$ in system K_A and the coordinates $\Phi_B \beta_B$ in system K_B (Figure 14.3). The vectors y and h

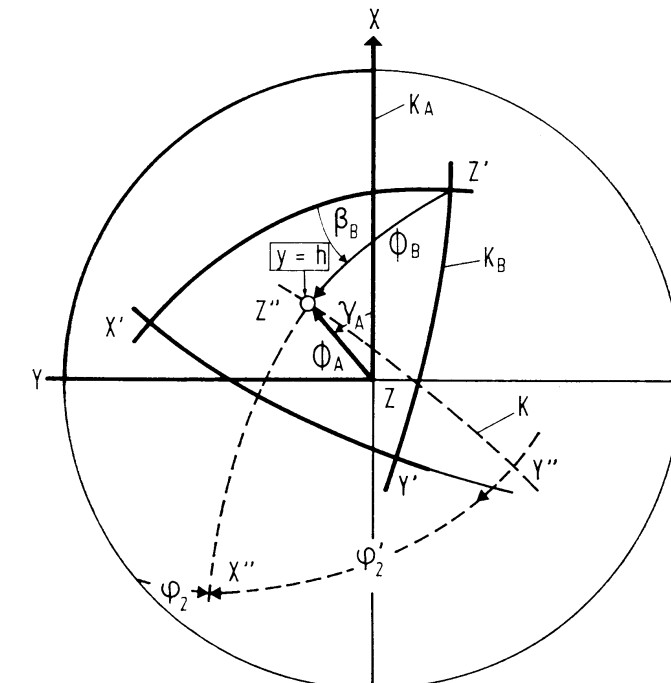


Figure 14.3 Relation between the sample coordinate system K_B , the crystal coordinate system K_A and the variable coordinate system K

will also be used in place of these coordinates. The rotation $g_1 = \left\{ \gamma_A + \frac{\pi}{2}, \Phi_A, \varphi_2 \right\}$ transforms K_A into K . The angle φ_2 is arbitrary. The rotation $g_2 = \left\{ \varphi'_2, \Phi_B, \frac{\pi}{2} - \beta_B \right\}$ transforms K into K_B . K_A is then transformed into K_B by $g = g_2 \cdot g_1$. With the addition theorem (equation 14.6) we obtain

$$T_l^{mn}(g) = \sum_{s=-l}^{+l} T_l^{ms}(g_2) \cdot T_l^{sn}(g_1) \quad (14.156)$$

With definition (14.1) it follows that

$$T_l^{mn}(g) = \sum_{s=-l}^{+l} e^{im(\frac{\pi}{2} - \beta_B)} P_l^{ms}(\Phi_B) e^{is\varphi'_2} \cdot e^{is\varphi_1} P_l^{sn}(\Phi_A) e^{in(\gamma_A + \frac{\pi}{2})} \quad (14.157)$$

We integrate with respect to φ_2 :

$$\int_0^{2\pi} T_l^{mn}(g) d\varphi_2 = 2\pi e^{im(\frac{\pi}{2} - \beta_B)} P_l^{m0}(\Phi_B) P_l^{n0}(\Phi_A) e^{in(\gamma_A + \frac{\pi}{2})} \quad (14.158)$$

$$\int_0^{2\pi} T_l^{mn}(g) d\varphi_2 = 2\pi T_l^{m0}(g_2) T_l^{n0}(g_1) \quad (14.159)$$

With relations (14.41) and (14.42) it follows that

$$\int_{[y\hbar]} T_l^{mn}(g) d\varphi_2 = \frac{8\pi^2}{2l+1} k_l^{*m}(\Phi_B \beta_B) k_l^n(\Phi_A \gamma_A) \quad (14.160)$$

With the definitions of the symmetric functions (equations 14.131, 14.120 and 14.127) it follows that

$$\int_{[y\hbar]} \dot{T}_l^{mn}(g) d\varphi_2 = \frac{8\pi^2}{2l+1} k_l^{*m}(\Phi_B \beta_B) k_l^n(\Phi_A \gamma_A) \quad (14.161)$$

The index $[y\hbar]$ on the integral implies that the integration is over all those orientations g for which the direction y of the first coordinate system K_A coincides with the direction \hbar of the second coordinate system K_B and thus the crystal direction \hbar with the sample direction y . For the completely real functions, equations (14.36) and (14.37), one obtains

$$\begin{aligned} \int_{[y\hbar]} T_l'^{mn}(g) d\varphi_2 &= \frac{8\pi^2}{2l+1} \cdot i^{m-n} \cdot \frac{1}{\sqrt{2}} \\ &\times [k_l^{*m}(\Phi_B \beta_B) k_l^n(\Phi_A \gamma_A) + k_l^{*-m}(\Phi_B \beta_B) k_l^{-n}(\Phi_A \gamma_A)] \end{aligned} \quad (14.162)$$

If one also expresses k by the real functions k' and k'' (equations 14.62 and 14.63) one thus obtains

$$k_l^m = \frac{1}{\sqrt{2}} [k_l'^m + ik_l''^m] \quad (14.163)$$

$$k_l^{-m} = \frac{1}{\sqrt{2}} (-1)^m [k_l'^m - ik_l''^m] \quad (14.164)$$

It thus follows from equation (14.162), for $m+n$ even,

$$\begin{aligned} \int_{[y\hbar]} T_l'^{mn}(g) d\varphi_2 &= \frac{8\pi^2}{2l+1} (-1)^{\frac{m-n}{2}} \\ &\times [k_l'^m(\Phi_B \beta_B) k_l^n(\Phi_A \gamma_A) + k_l''^m(\Phi_B \beta_B) k_l''^n(\Phi_A \gamma_A)] \end{aligned} \quad (14.165)$$

and for $m+n$ odd,

$$\begin{aligned} \int_{[y\hbar]} T_l'^{mn}(g) d\varphi_2 &= \frac{8\pi^2}{2l+1} (-1)^{\frac{m-n+1}{2}} \\ &\times [k_l''^m(\Phi_B \beta_B) k_l^n(\Phi_A \gamma_A) - k_l'^m(\Phi_B \beta_B) k_l''^n(\Phi_A \gamma_A)] \end{aligned} \quad (14.166)$$

Correspondingly, there results, for $m+n$ even,

$$\begin{aligned} \int_{[y\hbar]} T_l''^{mn}(g) d\varphi_2 &= \frac{8\pi^2}{2l+1} (-1)^{\frac{m-n}{2}+1} \\ &\times [k_l'^m(\Phi_B \beta_B) k_l^n(\Phi_A \gamma_A) - k_l''^m(\Phi_B \beta_B) k_l''^n(\Phi_A \gamma_A)] \end{aligned} \quad (14.167)$$

and for $m+n$ odd,

$$\begin{aligned} \int_{[y\hbar]} T_l''^{mn}(g) d\varphi_2 &= \frac{8\pi^2}{2l+1} (-1)^{\frac{m-n+1}{2}} \\ &\times [k_l''^m(\Phi_B \beta_B) \cdot k_l^n(\Phi_A \gamma_A) + k_l'^m(\Phi_B \beta_B) k_l''^n(\Phi_A \gamma_A)] \end{aligned} \quad (14.168)$$

14.5.3. Convolution Integrals

Let $f(g)$ and $w(g)$ be two functions of arbitrary symmetries

$$\hat{f}(g) = \sum_{l,\mu,\nu} C_l^{\mu\nu} \dot{T}_l^{\mu\nu}(g) \quad (14.169)$$

$$\hat{w}(g) = \sum_{\lambda,\alpha,\beta} w_\lambda^{\alpha\beta} \dot{T}_\lambda^{\alpha\beta}(g) \quad (14.170)$$

We calculate the integral

$$F(g', g'') = \oint f(g' \cdot g \cdot g'') \dot{w}^*(g) dg \quad (14.171)$$

If we insert the series expansions (14.169) and (14.170), we thus obtain

$$F(g', g'') = \sum_{l,\mu,\nu} \sum_{\lambda,\alpha,\beta} C_l^{\mu\nu} w_\lambda^{*\alpha\beta} \oint \dot{T}_l^{\mu\nu}(g' \cdot g \cdot g'') \dot{T}_\lambda^{*\alpha\beta}(g) dg \quad (14.172)$$

With the addition theorem it follows therefrom that

$$F(g', g'') = \sum_{l,\mu,\nu,\lambda,\alpha,\beta,s,\sigma} C_l^{\mu\nu} w_\lambda^{*\alpha\beta} \dot{T}_l^{\mu s}(g') \dot{T}_l^{\sigma\nu}(g'') \oint T_l^{s\sigma}(g) T_\lambda^{*\alpha\beta}(g) dg \quad (14.173)$$

We express the symmetry of the second factor under the integral by the corresponding symmetry coefficients:

$$F(g', g'') = \sum_{\substack{l,\mu,\nu,\lambda,\alpha,\beta \\ s,\sigma,m,n}} C_l^{\mu\nu} w_\lambda^{*\alpha\beta} \dot{T}_l^{\mu s}(g') \dot{T}_l^{\sigma\nu}(g'') A_\lambda^{m\alpha} A_\lambda^{n\beta} \oint T_l^{s\sigma}(g) T_\lambda^{*mn}(g) dg \quad (14.174)$$

Because of the orthogonality of the generalized spherical harmonics, only the terms with

$$\lambda = l; \quad s = m; \quad \sigma = n \quad (14.175)$$

are different from zero. One thus obtains

$$F(g', g'') = \sum_{l,\mu,\nu,\alpha,\beta,m,n} C_l^{\mu\nu} w_l^{*\alpha\beta} \dot{T}_l^{\mu m}(g') \dot{T}_l^{\nu n}(g'') A_l^{m\alpha} A_l^{n\beta} \frac{1}{2l+1} \quad (14.176)$$

If we carry out the summation over m and n , for the desired integral we thus obtain the expression

$$F(g', g'') = \sum_{l,\mu,\nu,\alpha,\beta} C_l^{\mu\nu} w_l^{*\alpha\beta} \dot{T}_l^{\mu\alpha}(g') \dot{T}_l^{\nu\beta}(g'') \frac{1}{2l+1} \quad (14.177)$$

We shall consider this integral for some special cases. We first set

$$g'' = e \quad (14.178)$$

thus considering the integral

$$\dot{F}(g') = \oint f(g' \cdot g) \dot{w}^*(g) dg \quad (14.179)$$

With equation (14.142) it follows in this case from equation (14.177) that

$$\dot{F}(g') = \sum_{l,\mu,\alpha} \bar{C}_l^{\mu\alpha} \dot{T}_l^{\mu\alpha}(g') \quad (14.180)$$

with the coefficients

$$\bar{C}_l^{\mu\alpha} = \frac{1}{2l+1} \sum_{\nu,\beta} C_l^{\mu\nu} w_l^{*\alpha\beta} \sum_m \dot{A}_l^{m\beta} \dot{A}_l^{m\nu} \quad (14.181)$$

In particular, if the two symmetries (\cdot) and $(\ddot{\cdot})$ are equal, equation (14.179) thus transforms into the following frequently used convolution integral:

$$\dot{F}(g') = \oint f(g' \cdot g) \dot{w}^*(g) dg \quad (14.182)$$

With equation (14.134) it follows in this case from equation (14.181) that

$$\bar{C}_l^{\mu\alpha} = \frac{1}{2l+1} \sum_{\nu} C_l^{\mu\nu} w_l^{*\alpha\nu} \quad (14.183)$$

We return again to the integral of equation (14.171) and consider the special case in which the function $w(g)$ is only different from zero at the symmetrically equivalent points

$$g = g_i \quad (14.184)$$

We assume that the function $w(g)$ is normalized in the customary fashion:

$$\oint \dot{w}(g) dg = 1 \quad (14.185)$$

The integral of equation (14.171) then transforms into a sum which naturally, also depends, in addition to g' and g'' , on g_0 (one of the equivalent points g_i):

$$F(g', g_0, g'') = \frac{1}{Z} \sum_{i=1}^Z (g' \cdot g_i \cdot g'') \quad (14.186)$$

According to equation (4.19), in this case there result for the coefficients $w_l^{*\alpha\beta}$

$$w_l^{*\alpha\beta} = (2l+1) \dot{T}_l^{\alpha\beta}(g_0) \quad (14.187)$$

If we insert this expression in equation (14.177), we thus obtain

$$\frac{1}{Z} \sum_{i=1}^Z f(g' \cdot g_i \cdot g'') = \sum_{l,\mu,\nu,\alpha,\beta} C_l^{\mu\nu} \dot{T}_l^{\mu\alpha}(g') \dot{T}_l^{\nu\beta}(g_0) \dot{T}_l^{\beta\nu}(g'') \quad (14.188)$$

In particular, therefore,

$$\frac{1}{Z} \sum_{i=1}^Z \dot{T}_l^{\mu\nu}(g' \cdot g_i \cdot g'') = \sum_{\alpha,\beta} \dot{T}_l^{\mu\alpha}(g') \dot{T}_l^{\nu\beta}(g_0) \dot{T}_l^{\beta\nu}(g'') \quad (14.189)$$

If the two symmetries (\cdot) and $(\ddot{\cdot})$ are equal, because of equations (14.142) and (14.134) there results

$$\frac{1}{Z} \sum_{i=1}^Z \dot{T}_l^{\mu\nu}(g' \cdot g_i \cdot g'') = \sum_{\alpha} \dot{T}_l^{\mu\alpha}(g') \dot{T}_l^{\nu\alpha}(g'') \quad (14.190)$$

14.6. Symmetric Spherical Surface Harmonics

The symmetric spherical surface harmonics

$$\dot{k}_l^v(\Phi, \beta) = \sum_{n=-l}^{+l} \dot{A}_l^{nv} k_l^n(\Phi, \beta) \quad (14.191)$$

defined by equations (14.118)–(14.121) satisfy the orthonormal condition

$$\oint \dot{k}_l^v(\Phi, \beta) \dot{k}_l^{*v'}(\Phi, \beta) \sin \Phi d\Phi d\beta = \delta_{vv'} \delta_{rr'} \quad (14.192)$$

The orthonormal condition (equation 14.134) is valid for the coefficients \dot{A}_l^{nv} . It follows from the addition theorem (equation 14.136) with $m = 0$ that

$$\dot{k}_l^v(\Phi', \beta') = \sum_{s=-l}^{+l} k_l^s(\Phi, \beta) \dot{T}_l^{sv}(g) \quad (14.193)$$

Φ', β' denote the spherical angular coordinates of the direction Φ, β in the coordinate system rotated through g^{-1} . One obtains the same result from the addition theorem of the usual spherical surface harmonics (equation 14.45) by multiplication by \dot{A}_l^{rv} and summation over all n .

From equation (14.191) it follows with equation (14.54) that

$$\dot{k}_l^v(\Phi = 0, \beta) = \sqrt{\frac{2l+1}{4\pi}} \dot{A}_l^{0v} \quad (14.194)$$

Correspondingly, there results

$$\dot{k}_l^v(\Phi = \pi, \beta) = (-1)^l \sqrt{\frac{2l+1}{4\pi}} \dot{A}_l^{0v} \quad (14.195)$$

If we introduce a new coordinate system Θ, ψ (see Figure 5.2), such that its pole $\Theta = 0$ has the coordinates $\mathbf{r}_1 = \{\Phi_1, \beta_1\}$ in the original system Φ, β , we can thus write the function $\dot{k}_l^v(\Phi, \beta)$ in this system:

$$\dot{k}_l^v(\Phi, \beta) = \sum_{n=-l}^{+l} \dot{A}_l^{nv} k_l^n(\Theta, \psi) \quad (14.196)$$

If we form the integral

$$\oint \dot{k}_l^v(\Phi, \beta) d\psi = \sum_{n=-l}^{+l} \dot{A}_l^{nv} \oint k_l^n(\Theta, \psi) d\psi \quad (14.197)$$

we thus obtain from equation (14.38)

$$\oint \dot{k}_l^v(\Phi, \beta) d\psi = \sqrt{2\pi} \dot{A}_l^{0v} \bar{P}_l^0(\Theta) \quad (14.198)$$

If we express \dot{A}_l^{0v} according to equation (14.194), we thus obtain

$$\oint \dot{k}_l^v(\Phi, \beta) d\psi = 2\pi \sqrt{\frac{2}{2l+1}} \dot{k}_l^v(\Theta = 0, \psi) \bar{P}_l^0(\Theta) \quad (14.199)$$

Finally it follows that

$$\int_{[r_1]} \dot{k}_l^v(\Phi, \beta) d\psi = 2\pi \sqrt{\frac{2}{2l+1}} \dot{k}_l^v(r_1) \bar{P}_l^0(\Theta) \quad (14.200)$$

If we express the spherical harmonics $k_l^n(\Phi, \beta)$ in equation (14.191) according to equation (14.60), we thus obtain

$$\begin{aligned} \dot{k}_l^v(\Phi, \beta) &= \frac{1}{\sqrt{2\pi}} \\ &\times \left[\dot{A}_l^{0v} \bar{P}_l^0(\Phi) + \sum_{n=1}^l \dot{A}_l^{nv} \bar{P}_l^n(\Phi) \cos n\beta + i \sum_{n=1}^l \dot{A}_l'^{nv} \bar{P}_l^n(\Phi) \sin n\beta \right] \end{aligned} \quad (14.201)$$

with real coefficients

$$\dot{A}_l^{nv} = [\dot{A}_l^{nv} + (-1)^n \dot{A}_l^{-nv}] \quad (14.202)$$

$$\dot{A}_l'^{nv} = [\dot{A}_l'^{nv} - (-1)^n \dot{A}_l^{-nv}] \quad (14.203)$$

If the symmetry group contains a mirror plane in the plane $\beta = 0$, then the sin terms in equation (14.201) must vanish; thus we have from equation (14.203)

$$\dot{A}_l^{-nv} = (-1)^n \dot{A}_l^{+nv} \quad (14.204)$$

Thus in this case

$$\dot{A}_l'^{nv} = 0 \quad (14.205)$$

and equation (14.201) transforms into

$$\dot{k}_l^v(\Phi, \beta) = \dot{A}_l^{0v} \frac{1}{\sqrt{2\pi}} \bar{P}_l^0(\Phi) + \frac{2}{\sqrt{2\pi}} \sum_{n=1}^l \dot{A}_l^{nv} \bar{P}_l^n(\Phi) \cos n\beta \quad (14.206)$$

We now set

$$\dot{A}_l^{0v} \cdot \frac{1}{\sqrt{2\pi}} = \dot{B}_l^{0v} \quad (14.207)$$

$$\dot{A}_l^{nv} \cdot \frac{2}{\sqrt{2\pi}} = \dot{B}_l^{nv} \quad (14.208)$$

Equation (14.206) then transforms into

$$\dot{k}_l^v(\Phi, \beta) = \sum_{n=0}^l \dot{B}_l^{nv} \bar{P}_l^n(\Phi) \cos n\beta \quad (14.209)$$

From equation (14.58a) it follows that harmonics of odd order must vanish for all those directions \mathbf{h} which are symmetrically equivalent with their opposite direction

$$\dot{k}_{2l+1}^v(\mathbf{h}) = 0 \quad \text{for } \mathbf{h} \text{ equiv. } -\mathbf{h} \quad (14.209a)$$

This equivalence holds for all directions \mathbf{h} when a centre of inversion is present in the symmetry group. In fact, this is the definition of the centre of inversion.

Hence, harmonics of odd order must be zero everywhere, thus leading to the selection rule equation (14.226). The equivalence assumed in equation (14.209a) holds also for all directions perpendicular to a twofold axis (*Figure 14.4*). Hence, all planes perpendicular to twofold axes must be zero planes to odd harmonics of all orders. In *Figure 14.5* these zero planes are shown for the various symmetry groups in stereographic projection.

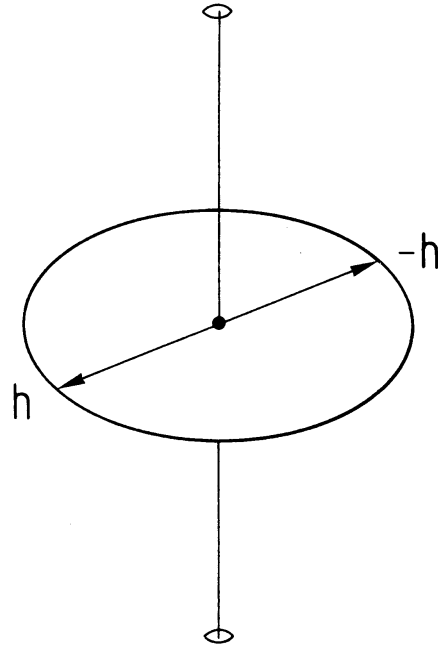


Figure 14.4 A direction \mathbf{h} perpendicular to a twofold axis is symmetrically equivalent with its opposite direction $-\mathbf{h}$

14.7. The Symmetric Functions of the Various Symmetry Groups

The symmetry properties of the symmetric generalized spherical harmonics are, as we have said, completely determined by those of the symmetric spherical surface harmonics of the non-centrosymmetric groups. The latter ones can be relatively easily surveyed²⁰⁴. We first consider individual symmetry elements in particular positions.

(1) An n th-order rotation axis in the direction $\Phi = 0$. If the function

$$k_l^m(\Phi, \beta) = \frac{1}{\sqrt{2\pi}} e^{im\beta} \bar{P}_l^m(\Phi) \quad (14.210)$$

is invariant with respect to a rotation $\beta = 2\pi/n$, it must thus be true that

$$m = n\mu$$

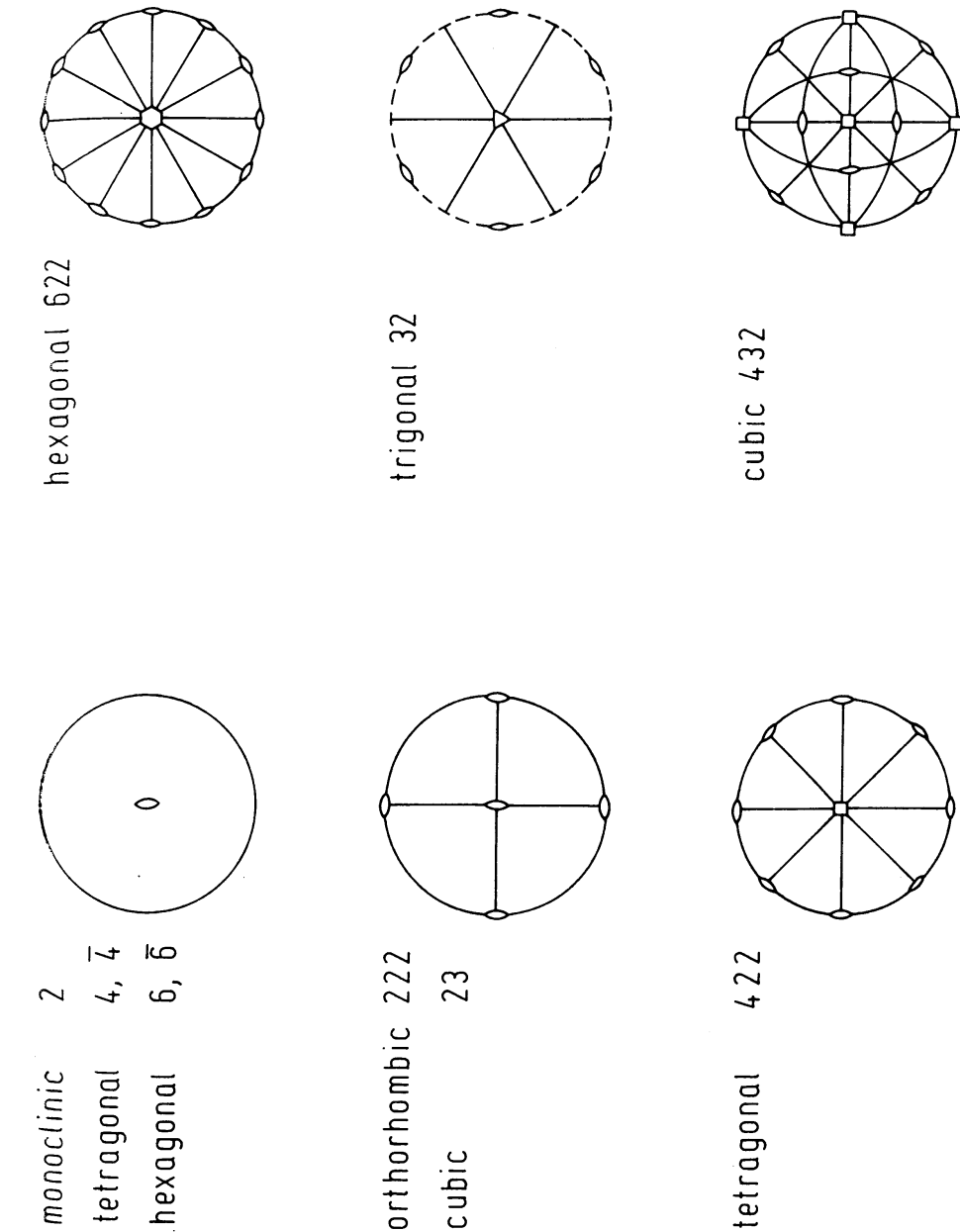


Figure 14.5 The planes perpendicular to twofold axes in the various non-centrosymmetric symmetry groups are zero planes of the odd harmonics of the corresponding symmetry

where μ is a positive or negative integer. Equation (14.211) represents a ‘selection rule’ for the indices m . The linearly independent functions of this symmetry are contained among the customary functions. They are distinguished from the latter only in that the ‘selection rule’ for the indices must be followed. If we represent the linearly independent functions in the previously used form

$$\dot{k}_l^{\mu}(\Phi, \beta) = \sum_{m=-l}^{+l} \dot{A}_l^{m\mu} k_l^m(\Phi, \beta) \quad (14.212)$$

the coefficients in this case thus assume the form

$$\dot{A}_l^{m\mu} = \delta_{m,n\mu} \quad (14.213)$$

If the rotation axis is of infinite order, $k_l^m(\Phi, \beta)$ thus transforms into itself for every rotation β , so that we must have

$$m = 0 \quad (14.214)$$

The rotationally symmetric functions thus have the form

$$k_l^0(\Phi, \beta) = \frac{1}{\sqrt{2\pi}} \bar{P}_l(\Phi) \quad (14.215)$$

(2) A mirror plane perpendicular to the direction $\Phi = 0$. In this symmetry the function must be unchanged if Φ is replaced by $\pi - \Phi$. According to equation (14.57), this is the case for $l + m$ even. The selection rule is thus

$$l + m = 2l' \quad (14.216)$$

(3) A mirror plane in the plane $\beta = 0$. If in the expression (equation 14.191) for the symmetric functions we group the terms with $+m$ and $-m$, we thus obtain

$$\begin{aligned} \dot{k}_l^{\mu}(\Phi, \beta) &= \frac{1}{\sqrt{2\pi}} \dot{A}_l^{\mu} \bar{P}_l(\Phi) \\ &+ \frac{1}{\sqrt{2\pi}} \sum_{m=1}^l \bar{P}_l^m(\Phi) [\dot{A}_l^{m\mu} e^{im\beta} + (-1)^m \dot{A}_l^{-m\mu} e^{-im\beta}] \end{aligned} \quad (14.217)$$

The symmetry requires that this expression transforms into itself if we replace $+\beta$ by $-\beta$. It must thus be true that

$$\dot{A}_l^{-m\mu} = (-1)^m \dot{A}_l^{+m\mu} \quad (14.218)$$

We can so choose the linearly independent functions that in each case only one coefficient is different from zero

$$\dot{A}_l^{+m\mu} = \frac{1}{\sqrt{2}} \delta_{m\mu}; \quad \dot{A}_l^{-m\mu} = (-1)^m \frac{1}{\sqrt{2}} \delta_{m\mu} \quad (14.219)$$

$$\dot{A}_l^{m0} = \delta^{m0} \quad (14.220)$$

We thus have the linearly independent functions

$$\dot{k}_l^{\mu}(\Phi, \beta) = \frac{1}{\sqrt{4\pi}} \bar{P}_l^{\mu}(\Phi) [e^{i\mu\beta} + e^{-i\mu\beta}] = \frac{1}{\sqrt{\pi}} \bar{P}_l^{\mu}(\Phi) \cos \mu\beta \quad (14.221)$$

$$\dot{k}_l^0(\Phi, \beta) = \frac{1}{\sqrt{2\pi}} \bar{P}_l(\Phi) \quad (14.222)$$

(Note that here another enumeration of the linearly independent functions has been used.) Thus (in contrast to the definition of equation 14.125)

$$0 \leq \mu \leq l \quad (14.223)$$

(4) A 2n-fold rotation reflection axis in $\Phi = 0$. The point Φ, β will be transformed into $\pi - \Phi, \pi/n + \beta$ by this symmetry operation. If we insert this in equation (14.38), we thus obtain with equation (14.57)

$$k_l^m\left(\pi - \Phi, \frac{\pi}{n} + \beta\right) = (-1)^{l+m+m/n} k_l^m(\Phi, \beta) \quad (14.224)$$

We thus obtain the selection rule

$$m = m'n; \quad l + m'(n + 1) = 2l' \quad (14.225)$$

For a twofold rotation reflection axis, i.e. a centre of symmetry, $n = 1$. There thus results from equation (14.225)

$$l = 2l' \quad (14.226)$$

(5) A twofold rotation axis in the direction $\Phi = 90^\circ, \beta = 0^\circ$. This transforms the point Φ, β into the point $\pi - \Phi, -\beta$. One sees that the condition

$$\dot{A}_l^{-m\mu} = (-1)^l \dot{A}_l^{+m\mu} \quad (14.227)$$

must then be fulfilled. This yields the linearly independent functions

$$\dot{k}_l^{\mu}(\Phi, \beta) = \frac{1}{\sqrt{4\pi}} \bar{P}_l^{\mu}(\Phi) [e^{i\mu\beta} + (-1)^{l+\mu} e^{-i\mu\beta}] \quad (14.228)$$

$$\dot{k}_l^0(\Phi, \beta) = \frac{1}{\sqrt{2\pi}} \bar{P}_l^0(\Phi); \quad l = 2l' \quad (14.229)$$

We thus see that, in addition to ‘pure’ selection rules (equations 14.213, 14.216 and 14.225), we also obtain conditions such that two coefficients with equal but opposite m are different from zero (14.218) and (14.227). The linearly independent functions in this case thus have the form of either equation (14.62) or equation (14.63). In the case of a real basis for the spherical harmonics, conditions such as, e.g., equation (14.227) thus lead to ‘pure’ selection rules. We shall therefore group them with the selection rules in the general sense.

14.7.1. 'Lower' Symmetry Groups (Non-cubic)

Each of the symmetry elements mentioned above by itself indeed represents a symmetry group — i.e. a simply cyclic group. Additional symmetry groups may be generated by combination of the symmetry elements. Combination of the symmetry elements leads to combination of the corresponding selection rules. All symmetry groups thus generated can be satisfied with the normal spherical surface harmonics by satisfying appropriate selection rules for the indices. We shall call these 'lower' symmetry groups. If only these groups existed, we would not need to introduce special symmetric functions. We would simply have to specify the 'selection rules' belonging to each group. The following belong to the lower symmetry groups:

- (1) The groups \mathfrak{C}_n having an n -fold rotation axis, which we place in the direction $\Phi = 0$. They require the selection rule (equation 14.211)

$$m = n \cdot \mu \quad (14.230)$$

In particular, cylindrical symmetry \mathfrak{C}_∞ , which in this sense is thus a lower symmetry, belongs hereto.

- (2) The group \mathfrak{D}_n results from \mathfrak{C}_n , if one further adds a twofold axis in the direction $\Phi = 90^\circ, \beta = 0^\circ$. The conditions of equations (14.211) and (14.227) are thus to be simultaneously fulfilled.

$$m = n \cdot \mu; \quad A_l^{-m\mu} = (-1)^l A_l^{+m\mu} \quad (14.231)$$

- (3) The groups \mathfrak{S}_{2n} have $2n$ -fold rotation-reflection axes. They require fulfilment of condition (14.225).

$$m = m' \cdot n; \quad l + m'(n + 1) = 2l' \quad (14.232)$$

- (4) The groups \mathfrak{C}_{nh} contain, in addition to n -fold rotation axes in the direction $\Phi = 0$, a mirror plane perpendicular thereto. Equations (14.211) and (14.216) must be fulfilled.

$$m = n \cdot \mu; \quad l + m = 2l' \quad (14.233)$$

- (5) The groups \mathfrak{D}_{nh} result from \mathfrak{D}_n by addition of a mirror plane perpendicular to $\Phi = 0$. They thus require conditions (14.211), (14.216) and (14.227).

$$m = n \cdot \mu; \quad l + m = 2l'; \quad A_l^{-m\mu} = (-1)^l A_l^{+m\mu} \quad (14.234)$$

- (6) The groups \mathfrak{D}_{nd} result from \mathfrak{S}_{2n} by addition of a mirror plane in $\beta = 0$ and a twofold rotation axis in $\Phi = 90^\circ, \beta = 0$. Accordingly, they require conditions (14.218) and (14.225), which leads to

$$m = n' \cdot m; \quad l + m'(n + 1) = 2l'; \quad A_l^{-m\mu} = (-1)^m A_l^{+m\mu} \quad (14.235)$$

All lower symmetry groups are thereby exhausted. One thus obtains *Table 14.4* for the coefficients $A_l^{m\mu}$ for some frequently used lower symmetry groups. In the

Table 14.4 SYMMETRY COEFFICIENTS $A_l^{m\mu}$ FOR SOME LOW SYMMETRY GROUPS

		Orthorhombic symmetry \mathfrak{D}_{2h}						Tetragonal symmetry \mathfrak{D}_{4h}						Hexagonal symmetry \mathfrak{D}_{6h}						Cylindrical symmetry \mathfrak{C}_∞					
m	μ	0	± 2	± 4	± 6	± 8	± 10	± 12	± 14	± 16	± 18	± 20	± 22	± 24	± 26	± 28	± 30	± 32	± 34	± 36	± 38	± 40	± 42	± 44	± 46
1	1	1	0	0	0	1	1	0	0	0	1	1	0	0	0	1	1	0	0	0	0	0	0	0	0
2	0	$\frac{1}{\sqrt{2}}$	0	0	2	0	$\frac{1}{\sqrt{2}}$	0	0	2	0	$\frac{1}{\sqrt{2}}$	0	0	2	0	0	0	0	0	0	0	0	0	0
3	0	0	$\frac{1}{\sqrt{2}}$	0	3	0	0	$\frac{1}{\sqrt{2}}$	0	3	0	0	$\frac{1}{\sqrt{2}}$	0	3	0	0	$\frac{1}{\sqrt{2}}$	0	3	0	0	0	0	0
4	0	0	0	$\frac{1}{\sqrt{2}}$	4	0	0	0	$\frac{1}{\sqrt{2}}$	4	0	0	$\frac{1}{\sqrt{2}}$	0	4	0	0	$\frac{1}{\sqrt{2}}$	0	4	0	0	$\frac{1}{\sqrt{2}}$	0	\dots
																									$M(l)$

particularly important case of cylindrical symmetry only one linearly independent function thus results for each order l :

$$\dot{k}_l^1(\Phi, \beta) = \frac{1}{\sqrt{2\pi}} \bar{P}_l(\Phi) \quad (14.236)$$

This is naturally — except for the different designation of the index μ of the symmetric functions, compared with the index m of the customary functions — identical with equation (14.215).

14.7.2. 'Higher' Symmetry Groups (Cubic)

Groups of higher symmetry cannot be satisfied by selection rules of the indices alone. The linearly independent functions of these symmetries can only be represented by linear combinations with coefficients different from zero^{23,191}. The symmetry groups of the tetrahedron, the octahedron and the icosahedron belong to these groups. The icosahedral groups can not occur as crystal symmetries. Instead of higher and lower symmetries, one can thus also divide the symmetry groups into cubic and non-cubic. The diagonal threefold rotation axis, which can not be satisfied by a simple selection rule for the indices, is characteristic of the cubic symmetry groups. If one arranges the cubic symmetries so that the threefold axis falls in the direction $\Phi = 0$, other twofold and fourfold axes will lie diagonally, so that one cannot fulfil all symmetry elements of this group by selection rules in any arrangement. We must therefore write the linearly independent functions of cubic symmetry in the form⁷⁴

$$\dot{k}_l^\mu(\Phi, \beta) = \sum_{m=-l}^{+l} \dot{A}_l^{m\mu} \frac{1}{\sqrt{2\pi}} e^{im\beta} \bar{P}_l^m(\Phi) \quad (14.237)$$

and choose the $\dot{A}_l^{m\mu}$ so that the symmetry in question is fulfilled. We express the $\bar{P}_l^m(\Phi)$ according to equation (14.87) by a FOURIER series and obtain

$$\dot{k}_l^\mu(\Phi, \beta) = \frac{1}{\sqrt{2\pi}} \sum_{m=-l}^{+l} \sum_{s=-l}^{+l} \dot{A}_l^{m\mu} a_l^{ms} e^{im\beta} e^{is\Phi} \quad (14.238)$$

The threefold axis now requires

$$\dot{k}_l^\mu(\Phi = \alpha, \beta = 0) = \dot{k}_l^\mu(\Phi = 90^\circ, \beta = \alpha) \quad (14.239)$$

By correspondingly renaming the indices, this yields the condition

$$\sum_{m=-l}^{+l} \sum_{s=-l}^{+l} \dot{A}_l^{m\mu} a_l^{ms} e^{is\alpha} = \sum_{n=-l}^{+l} \sum_{s=-l}^{+l} \dot{A}_l^{s\mu} a_l^{sn} e^{in\pi/2} e^{is\alpha} \quad (14.240)$$

This must be true for all α , so that coefficients of $e^{is\alpha}$ must agree:

$$\sum_{m=-l}^{+l} \dot{A}_l^{m\mu} a_l^{ms} = \dot{A}_l^{s\mu} \sum_{n=-l}^{+l} a_l^{sn} e^{in\pi/2} \quad (14.241)$$

If we set

$$b_l^s = \sum_{n=-l}^{+l} a_l^{sn} e^{in\pi/2} \quad (14.242)$$

we thus obtain the following equation for determination of the coefficients $\dot{A}_l^{m\mu}$:

$$\sum_{m=-l}^{+l} \dot{A}_l^{m\mu} [a_l^{ms} - \delta_{ms} b_l^s] = 0 \quad (14.243)$$

Different selection rules are now to be added to this basic condition for the different cubic groups. Another straight forward calculation of the coefficients $A_l^{m\mu}$ has been proposed by ESLING and BUNGE¹²⁸.

14.7.2.1. Tetrahedral Groups

If one adds a twofold axis in the direction $\Phi = 0$, one obtains the tetrahedral group \mathfrak{T} . This is the pure rotation group of the tetrahedron. The twofold axis requires selection rule (1) for m with $n = 2$. If one further considers equation (14.89), for even l one thus obtains

$$\sum_{m=-l}^{+l} \dot{A}_l^{m\mu} [a_l^{ms} - \delta_{ms} b_l^s] = 0 \quad \begin{cases} l = 2l' \\ m = 2m' \\ s = 2s' \end{cases} \quad (14.244)$$

and for odd l

$$\sum_{m=-l}^{+l} \dot{A}_l^{m\mu} a_l^{ms} = 0 \quad \begin{cases} m = 2m' \\ l = 2l' + 1 \\ s = 2s' + 1 \end{cases} \quad (14.245)$$

The group \mathfrak{T}_d results from \mathfrak{T} , if one now adds a mirror plane in $\beta = 45^\circ$. In addition to equations (14.244) and (14.245), it must also be true that

$$\dot{A}_l^{-m\mu} = i^m \dot{A}_l^{m\mu} = (-1)^{m/2} \dot{A}_l^{m\mu} \quad (14.246)$$

The group \mathfrak{T}_h results from \mathfrak{T} by addition of a centre of inversion, i.e. a twofold rotation-reflection axis. This yields selection rule 4, with $n = 1$. We must thus have $l = 2l'$.

14.7.2.2. Octahedral Groups

One obtains the octahedral group \mathfrak{O} , if one adds to the threefold axis a fourfold axis in $\Phi = 0$. Because of selection rule (1), m must therefore be a multiple of 4. Now the octahedral group can also be generated by a fourfold axis in $\Phi = 0$ and an additional fourfold axis in $\Phi = 90^\circ, \beta = 90^\circ$. This fourfold axis requires that the function must be 'fourfold' along $\beta = 0$. The coefficients on the left side

of equation (14.240) must vanish for non-fourfold s . We thus obtain the condition

$$\sum_{m=-l}^{+l} \dot{A}_l^{m\mu} a_l^{ms} = 0; \quad m = 4m' \quad (14.247)$$

Thereby either

$$l = 2l'; \quad s = 4s' + 2 \quad (14.248)$$

or

$$l = 2l' + 1; \quad s = 2s' + 1 \quad (14.249)$$

Finally we turn to the highest cubic symmetry \mathfrak{Q}_h , so that we must add a centre of symmetry to the group \mathfrak{Q} . We thus obtain the additional condition

$$l = 2l' \quad (14.250)$$

We have thus exhausted all cubic symmetry groups. There remain now only the two icosahedral groups \mathfrak{Y} and \mathfrak{Y}_h , which, however, cannot occur as crystal symmetries and are therefore not of interest here.

14.7.3. Subgroups

One turns from a symmetry group to one of its subgroups, when one omits certain symmetry elements, so that the symmetric spherical harmonics of the subgroup have fewer symmetry conditions to fulfil, and the number of linearly independent functions is thus increased. New functions occur, which indeed satisfy the lower symmetry of the subgroup — not, however, the higher symmetry. It is then frequently appropriate to choose the functions occurring so that they are orthogonal to those of the higher symmetry.

In the case of lower symmetry groups this is easy to attain. By omission of a selection rule there occur either functions of the form of equation (14.38) or of the form of equations (14.62) and (14.63), which are orthogonal to each other at the outset.

If both the group and its subgroups belong to cubic symmetry, they can thus be distinguished only by symmetry elements, which lead to selection rules. The orthogonality of the functions of the subgroups to those of the higher symmetry is thus given in the same way as in the case of functions of the lower symmetry groups.

It is a somewhat different matter if we are concerned with a higher symmetry group, while the subgroup is of lower symmetry. The linearly independent functions of the higher symmetry can then only be represented as linear combinations of functions of lower symmetry, which can then naturally not be orthogonal to all functions of lower symmetry, since otherwise all coefficients of the linear combination must vanish. We therefore introduce a new orthonormal basis for the functions of lower symmetry:

$$\dot{k}_l^\mu(\Phi, \beta) = \sum_{m=-l}^{+l} \dot{A}_l^{m\mu} k_l^m(\Phi, \beta) \quad (14.251)$$

The $k_l^m(\Phi, \beta)$ are functions of lower symmetry, represented by customary spherical surface harmonics and selection rules, and the $\dot{k}_l^\mu(\Phi, \beta)$ functions of the same symmetry but in general representation. The coefficients $\dot{A}_l^{m\mu}$ must fulfil the orthonormalization condition

$$\sum_{m=-l}^{+l} \dot{A}_l^{m\mu} \dot{A}_l^{m\mu} = \delta_{\mu\mu} \quad (14.252)$$

Equation (14.251) represents an orthogonal transformation in the function space of the subgroup. There are naturally very many such transformations. We now choose one, for which the first M functions agree with those of the higher symmetry. It must then be true that

$$\dot{A}_l^{m\mu} = \dot{A}_l^{m\mu} \quad \text{for } 1 \leq \mu \leq M \quad (14.253)$$

where M denotes the number of the linearly independent functions of the higher symmetry. The coefficients $\dot{A}_l^{m\mu}$ for $M < \mu \leq M'$ must then also be determined so that the orthonormalization condition of equation (14.252) is fulfilled. These functions, which then have only the symmetry of the subgroup, are, however, orthogonal to those of the higher symmetry. Thus, for example, the functions of the highest cubic symmetry \mathfrak{Q}_h are most simply expressed by tetragonal functions with $m = 4m'$. It is thus frequently convenient to introduce such a basis among the tetragonal spherical harmonics which is orthogonal to the cubic functions.

14.7.4. Explicit Representation of Symmetric Generalized Spherical Harmonics

We consider right- and left-handed symmetries which are at least orthorhombic (or higher). This requires twofold rotation axes in the directions $\Phi = 0$ and $\Phi = 90^\circ, \gamma = 0^\circ$ in both coordinate systems. According to the first selection rule, equation (14.211), m and n must thus be even, and equation (14.227) requires

$$\dot{A}_l^{-m\mu} = (-1)^l \dot{A}_l^{+m\mu}, \quad \dot{A}_l^{-n\nu} = (-1)^l \dot{A}_l^{+n\nu} \quad (14.254)$$

The symmetric generalized spherical harmonics then depend only on the quantities

$$S_l^{mn} = \frac{1}{4} [T_l^{mn} + T_l^{-m-n} + (-1)^l T_l^{m-n} + (-1)^l T_l^{-mn}] \quad (14.255)$$

According to equation (14.34), it follows that

$$\begin{aligned} S_l^{mn} = & \frac{1}{2} P_l^{mn}(\Phi) [\cos m\varphi_2 \cos n\varphi_1 - \sin m\varphi_2 \sin n\varphi_1] \\ & + (-1)^l \frac{1}{2} P_l^{m-n}(\Phi) [\cos m\varphi_2 \cos n\varphi_1 + \sin m\varphi_2 \sin n\varphi_1] \end{aligned} \quad (14.256)$$

If we express the $P_l^{mn}(\Phi)$ according to equation (14.85) by its FOURIER coefficients $a_l'^{mns}$ and consider equations (14.76) and (14.77), we thus obtain

$$\begin{aligned} S_l^{mn} &= \sum_{s=0,2,\dots}^t a_l'^{mns} \cos s\Phi \cos m\varphi_2 \cos n\varphi_1 \\ &\quad - \sum_{s=1,3,\dots}^l a_l'^{mns} \cos s\Phi \sin m\varphi_2 \sin n\varphi_1 \end{aligned} \quad (14.257)$$

If both symmetries are lower symmetries, the symmetric generalized spherical harmonics are thus given by

$$\ddot{T}_l^{\mu\nu} = \varepsilon_m \varepsilon_n S_l^{mn} \quad (14.258)$$

ε_m and ε_n are normalization factors, which are defined in the following manner:

$$\varepsilon_m = \begin{cases} 1 & \text{for } m = 0 \\ \sqrt{2} & \text{for } m \neq 0 \end{cases} \quad (14.259)$$

The relations given in Table 14.4,

$$|m| = Z(\mu - 1); \quad |n| = Z(\nu - 1) \quad (14.260)$$

exist between m and μ and between n and ν , where Z is the multiplicity of the rotation axis in the direction $\Phi = 0$.

If the left-hand symmetry is 'high' and the right-hand symmetry 'low', one thus obtains

$$\ddot{T}_l^{\mu\nu} = \varepsilon_n \sqrt{2\pi} \sum_{m=0}^{l/4} \dot{B}_l^{4m,\mu} S_l^{4m,n} \quad (14.261)$$

The $\dot{B}_l^{4m,\mu}$ are related to the $\dot{A}_l^{4m,\mu}$ of cubic symmetry according to equations (14.207) and (14.208). The $\dot{B}_l^{4m,\mu}$ are given in Table 15.2.1

With equation (14.257) and the index n instead of ν according to equation (14.260) the cubic orthorhombic functions may be written

$$\ddot{T}_l^{\mu n}(\varphi_1 \Phi \varphi_2) = p_l^{\mu n}(\Phi \varphi_2) \cos n\varphi_1 + q_l^{\mu n}(\Phi \varphi_2) \sin n\varphi_1 \quad (14.262)$$

with

$$p_l^{\mu n}(\Phi \varphi_2) = \varepsilon_n \sqrt{2\pi} \sum_{m=0}^{l/4} \dot{B}_l^{4m,\mu} \sum_{s=0,2}^l a_l'^{4m,n,s} \cos s\Phi \cos 4m\varphi_2 \quad (14.263)$$

$$q_l^{\mu n}(\Phi \varphi_2) = -\varepsilon_n \sqrt{2\pi} \sum_{m=0}^{l/4} \dot{B}_l^{4m,\mu} \sum_{s=1,3,\dots}^l a_l'^{4m,n,s} \cos s\Phi \sin 4m\varphi_2 \quad (14.264)$$

Hence, the functions $\ddot{T}_l^{\mu n}(\varphi_1 \Phi \varphi_2)$ are essentially determined by the functions

$$p_l^{\mu n}(\Phi \varphi_2) = \ddot{T}_l^{\mu n}(0 \Phi \varphi_2) \quad (14.265)$$

$$q_l^{\mu n}(\Phi \varphi_2) = \ddot{T}_l^{\mu n} \left(\frac{\pi}{2n} \Phi \varphi_2 \right) \quad (14.266)$$

Table 14.5 CUBIC-ORTORHOMBIC GENERALIZED SPHERICAL HARMONICS FOR $l \leq 6$

	$\cdot \cos \Phi$	$\cdot \cos 2\Phi$	$\cdot \cos 3\Phi$	$\cdot \cos 4\Phi$	$\cdot \cos 5\Phi$	$\cdot \cos 6\Phi$
$\ddot{T}_4^{11} =$	+0.10741	+0.23868	+0.41768	+0.05966	+0.41768	$\cdot \cos 4\varphi_2$
	+0.11390	-0.23868	-0.05966			$\cdot \cos 2\varphi_1$
$\ddot{T}_4^{12} =$	-0.16010	-0.21349	-0.37359	+0.05337	+0.37359	$\cdot \cos 2\varphi_1 \cos 4\varphi_2$
	-0.20686	+0.21349	+0.05337			$\cdot \sin 2\varphi_1 \sin 4\varphi_2$
$\ddot{T}_4^{13} =$	+0.21184	-0.28242	-0.21349	+0.07061	+0.07061	$\cdot \cos 4\varphi_1$
	+0.35301	+0.28242	-0.05337	+0.01008	+0.01008	$\cdot \cos 4\varphi_1 \cos 4\varphi_2$
		-0.56484	-0.08069			$\cdot \sin 4\varphi_1 \sin 4\varphi_2$
$\ddot{T}_6^{11} =$	+0.03452	+0.07252	+0.08701	+0.08701	+0.15952	$\cdot \cos 4\varphi_2$
	-0.19013	-0.07252	+0.37702	-0.15952	-0.15952	
$\ddot{T}_6^{12} =$	-0.05003	-0.08505	-0.03003	+0.16511	+0.16511	$\cdot \cos 2\varphi_1$
	+0.21013	+0.08505	-0.13007	-0.16511	-0.16511	$\cdot \cos 2\varphi_1 \cos 4\varphi_2$
$\ddot{T}_6^{13} =$	+0.05482	+0.02740	-0.14250	+0.06028	+0.06028	$\cdot \sin 2\varphi_1 \sin 4\varphi_2$
	-0.23021	-0.02740	-0.61751	-0.06028	-0.06028	
$\ddot{T}_6^{14} =$	-0.07422	+0.117539	+0.43846	+0.32155	+0.00742	$\cdot \cos 6\varphi_1$
	+0.31167	+0.11132	-0.19296	-0.04452	-0.00742	$\cdot \cos 6\varphi_1 \cos 4\varphi_2$
		-0.35622	+0.29683	+0.05936	+0.05936	$\cdot \sin 6\varphi_1 \sin 4\varphi_2$

From equation (14.257) one deduces the symmetry relation

$$\ddot{T}_l^{\mu n}(\varphi_1, \Phi, 45 + \alpha) = (-1)^{\frac{n}{2}} \ddot{T}_l^{\mu n}(90^\circ - \varphi_1, \Phi, 45 - \alpha) \quad (14.267)$$

from which it follows that it is sufficient to represent the functions in the angular range

$$0 \leq \varphi_1 \leq 90^\circ; \quad 0 \leq \Phi \leq 90^\circ; \quad 0 \leq \varphi_2 \leq 45^\circ \quad (14.268)$$

or

$$0 \leq \varphi_1 \leq 45^\circ; \quad 0 \leq \Phi \leq 90^\circ; \quad 0 \leq \varphi_2 \leq 90^\circ \quad (14.269)$$

Finally, the cubic-cubic functions have the form

$$\ddot{T}_l^{\mu\nu} = 2\pi \sum_{m=0}^{l/4} \sum_{n=0}^{l/4} \dot{B}_l^{4m,\mu} \dot{B}_l^{4n,\nu} S_l^{4m,4n} \quad (14.270)$$

Hence, they are linear combinations of the cubic-orthorhombic ones

$$\ddot{T}_l^{\mu\nu} = \frac{\sqrt{2\pi}}{\varepsilon_{4n}} \sum_{n=0}^{l/4} B_l^{4n,\nu} \ddot{T}_l^{\mu,4n} \quad (14.271)$$

Hence, with n being a multiple of 4, it follows from equation (14.267) that

$$\ddot{T}_l^{\mu\nu}(\varphi_1 \Phi, 45 + \alpha) = \ddot{T}_l^{\mu\nu}(90^\circ - \varphi_1, \Phi, 45^\circ - \alpha) \quad (14.272)$$

They can thus be restricted to the same angular ranges given in equations (14.268) and (14.269). Furthermore the cubic-cubic functions are symmetric with respect to φ_1 and φ_2 , leading to the symmetry relation

$$\ddot{T}_l^{\mu\nu}(\varphi_1 \Phi \varphi_2) = \ddot{T}_l^{\mu\nu}(\varphi_2 \Phi \varphi_1) \quad (14.273)$$

The functions with both sides of lower symmetry are thus given essentially by expression (14.257), whose coefficients are known, e.g., according to *Table 15.1.2*. For the cubic-orthorhombic functions — i.e. the functions necessary for the representation of sheet textures of cubic metals — one obtains, according to equation (14.261), the explicit representation given in *Tables 14.5* and *15.5.1* and *Figure 16.3.1*. Since the orthorhombic symmetry contains the cylindrical symmetry as a special case, the cylindrically symmetric functions \ddot{T}_4^{11} and \ddot{T}_6^{11} , which are independent of φ_1 , according to equation (14.41), are identical with the cubic spherical harmonics $k_l^1(\Phi, \beta)$ except for the factor $\sqrt{4\pi/(2l+1)}$. For the two-handed cubic functions, according to equation (14.270), one obtains the representation given in *Tables 14.6* and *15.5.2* and *Figure 16.3.2*.

14.7.5. Representation of the Cubic Spherical Harmonics by Products of Powers of Cubic Polynomials

In order to obtain the cubic spherical harmonics, we started with the functions $\overline{P}_l^m(\Phi) \cos m\beta$, which are spherical harmonics but do not possess the cubic symmetry. We then formed linear combinations of these functions and selected the

Table 14.6 CUBIC-CUBIC GENERALIZED SPHERICAL HARMONICS FOR $l \leq 6$

	• cos Φ	• cos 2Φ	• cos 3Φ	• cos 4Φ	• cos 5Φ	• cos 6Φ
$\ddot{T}_4^{11} =$	+0.08203 +0.13672 +0.22787	+0.18229 -0.18229 +0.18229	+0.31900 +0.04557 +0.00651	-0.05208	+0.03076 +0.13330 +0.57762	+0.05640 -0.05640 +0.05640
$\ddot{T}_6^{11} =$	+0.01221 -0.05127 +0.21534	+0.02564 -0.02564 +0.02564	-0.41015 -0.16406	-0.30077	-0.30077	
						cos $4\varphi_1 + \cos 4\varphi_2$ cos $4\varphi_1 \cdot \cos 4\varphi_2$ sin $4\varphi_1 \cdot \sin 4\varphi_2$

coefficients so that cubic symmetry is fulfilled. Conversely, one can now proceed from polynomials, which indeed possess cubic symmetry but are not spherical harmonics, and then represent the cubic spherical harmonics as linear combinations of these functions.

Let x_1, x_2, x_3 be the rectangular coordinates of a point on the unit sphere. It is then true that

$$\varphi_2 = x_1^2 + x_2^2 + x_3^2 = 1 \quad (14.274)$$

We further set

$$\varphi_4 = x_1^2 x_2^2 + x_2^2 x_3^2 + x_3^2 x_1^2 \quad (14.275)$$

$$\varphi_6 = x_1^2 x_2^2 x_3^2 \quad (14.276)$$

The functions φ_4 and φ_6 are homogeneous polynomials of fourth and sixth degree, respectively, in the x_i . The cubic spherical harmonics of even order can now be represented as products of powers of φ_4 and φ_6 (see reference 193):

$$k_l^\mu = \sum_{\alpha, \beta} B_{l\mu}^{\alpha\beta} \varphi_4^\alpha \varphi_6^\beta \quad (14.277)$$

Here the indices α and β assume all positive integers subject to the condition

$$4\alpha + 6\beta \leq l \quad (14.278)$$

For $l \leq 10$ there result explicitly

$$k_4 = n_4[5\varphi_4 - 1] \quad (14.279)$$

$$k_6 = n_6[231\varphi_6 - 21\varphi_4 + 2] \quad (14.280)$$

$$k_8 = n_8[52\varphi_6 - 65\varphi_4^2 + 18\varphi_4 - 1] \quad (14.281)$$

$$k_{10} = n_{10}[3553\varphi_4\varphi_6 - 979\varphi_6 - 187\varphi_4^2 + 55\varphi_4 - 2] \quad (14.282)$$

Since for the direction [100] it is true that

$$\varphi_4(100) = \varphi_6(100) = 0 \quad (14.283)$$

one obtains for the normalization factors n_4 to n_{10}

$$n_4 = -k_4(100) = +0.646360 \quad (14.284)$$

$$n_6 = +\frac{1}{2}k_6(100) = +0.359601 \quad (14.285)$$

$$n_8 = -k_8(100) = +0.835193 \quad (14.286)$$

$$n_{10} = -\frac{1}{2}k_{10}(100) = +0.531858 \quad (14.287)$$

Similar expressions also exist for the odd harmonics (see reference 193).

14.7.6. Space Groups in the Euler Space

In Section 2.1.1 it was shown that the EULER space (i.e. the representation of the EULER angles in Cartesian coordinates) is three-dimensionally periodic with period 2π in all three directions. Furthermore, there is an m glide plane perpendi-

cular to Φ at $\Phi = \pi$ with glide components π in both directions φ_1 and φ_2 . The elementary cell is thereby subdivided into two equivalent asymmetric units, and the space group is Pn . Every arbitrary orientation distribution function must thus be three-dimensionally periodic and have the space group Pn . If now there exists in the sample coordinate system the symmetry corresponding to group G_A and in the crystal coordinate system the symmetry corresponding to group G_B , a series of symmetrically equivalent orientations g_α will be generated for each orientation g . In many cases (except for cubic symmetry) the transformations of the orientation space which transform the symmetrically equivalent points g_α into one another are linear transformations, which can be represented by symmetry elements in EULER space. There thus result additional symmetry elements in the EULER space whereby the elementary cell or at least the asymmetric unit is reduced. The symmetry can moreover correspond to another space group. Every combination of two points symmetry groups $\{G_A, G_B\}$ of the sample and crystal symmetries thus gives rise to a space group G_E in EULER space:

$$\{G_A, G_B\} \rightarrow G_E \quad (14.288)$$

For its derivation, according to BAKER,^{15,16} one must first of all consider the symmetries induced in EULER space by individual symmetry elements of G_A and G_B (i.e. simple cyclic groups). The symmetry elements induced in the EULER space by different rotation axes of the sample and crystal symmetries are compiled in

**Table 14.7 SYMMETRIES IN EULER SPACE, GENERATED BY ROTATIONS OF THE CRYSTAL AND SAMPLE SYMMETRIES.
ACCORDING TO BAKER^{15,16}**

Symmetry element	Equivalent orientation	Symmetry element in ODF
EULER angle identity	$\varphi_1 + \pi, -\Phi, \varphi_2 + \pi$	Glide plane $\perp \Phi$ axis at $\Phi = 0, \pi, 2\pi$. Translation components: $\Delta\varphi_1 = \pi, \Delta\varphi_2 = \pi$
U -fold rotation axis parallel crystal z' -axis	$\varphi_1, \Phi, \varphi_2 \pm \frac{2\pi}{U}$	Unit cell of ODF reduced to $\frac{2\pi}{U}$ in φ_2 direction
Diad axis parallel crystal x' -axis	$\varphi_1, \Phi + \pi, -\varphi_2$	Glide plane $\perp \varphi_2$ axis at $\varphi_2 = 0$. Translation $\Delta\Phi = \pi$
V -fold rotation axis parallel specimen z -axis	$\varphi_1 \frac{2\pi}{V}, \Phi, \varphi_2$	Unit cell of ODF reduced to $\frac{2\pi}{V}$ in φ_1 direction
Diad axis parallel specimen x -axis	$-\varphi_1, \Phi + \pi, \varphi_2$	Glide plane $\perp \varphi_1$ axis at $\varphi_1 = 0$. Translation component $\Delta\Phi = \pi$

Table 14.7, while the symmetry elements generated by mirror planes are given in Table 14.8. Mirror planes must always occur simultaneously in the crystal and sample systems, since they transform a right-handed coordinate system into a left-handed coordinate system. This must thus always happen simultaneously for both coordinate systems (sample and crystal systems). If one combines the symmetry elements from Tables 14.7 and 14.8 for symmetry groups G_A and G_B ,

Table 14.8 SYMMETRIES IN EULER SPACE, GENERATED BY MIRROR PLANES OF THE CRYSTAL AND SAMPLE SYMMETRIES. ACCORDING TO BAKER^{15, 16}

Mirror plane \perp crystal axis				
	X'	Y'	Z'	
X	$-\varphi_1, \Phi, -\varphi_2$ Diad parallel Φ axis at $0, \bullet, 0$	$-\varphi_1, \Phi, \pi - \varphi_2$ Diad parallel Φ axis at $0, \bullet, \frac{\pi}{2}$	$\pi - \varphi_1, \pi - \Phi, \varphi_2$ Diad parallel φ_2 axis at $\frac{\pi}{2}, \frac{\pi}{2}, \bullet$	
Mirror plane \perp specimen axis	$\pi - \varphi_1, \Phi, -\varphi_2$ Diad parallel Φ axis at $\frac{\pi}{2}, \bullet, 0$	$-\varphi_1, -\Phi, -\varphi_2$ Inversion centre at $0, 0, 0$	$-\varphi_1, \pi - \Phi, \varphi_2$ Diad parallel φ_2 axis at $0, \frac{\pi}{2}, \bullet$	
Z	$\varphi_1, \pi - \Phi, \pi - \varphi_2$ Diad parallel φ_1 axis at $\bullet, \frac{\pi}{2}, \frac{\pi}{2}$	$\varphi_1, \pi - \Phi, -\varphi_2$ Diad parallel φ_1 axis at $\bullet, \frac{\pi}{2}, 0$	$\varphi_1, -\Phi, \varphi_2$ Mirror plane $\perp \Phi$ axis at $\Phi = 0$	

one thus obtains Table 14.9 (due to BAKER) of the space groups and asymmetric units in EULER space. A graphical representation of these groups¹⁶⁶ is given in Figure 14.6. A complete group-theoretical derivation was given by POSPIECH, GNATEK and FICHTNER²³⁴. Figure 14.7 shows the space group $P \frac{2_1}{\Phi} \frac{2}{n} \frac{2_1}{\Phi}$ which is induced in EULER space by trigonal crystal symmetry $\bar{3}m$ and monoclinic sample symmetry $\frac{2}{m}$ for the second definition of the EULER angles ($\psi\Theta\Phi$). This

symmetry case was used on natural quartz samples. Figure 14.8 shows the symmetry for cubic crystal and orthorhombic sample symmetries (sheet symmetry). This is the most frequently treated symmetry to date. For the cubic symmetry the threefold axis will not be considered, so that for this symmetry actually only the tetragonal subsymmetry will be considered.

Table 14.9 SYMMETRIES IN EULER SPACE, GENERATED BY VARIOUS SYMMETRIES OF CRYSTAL AND SAMPLE SYMMETRY. ACCORDING TO BAKER^{15, 16}

Crystal symmetry	$\bar{1}$	Specimen symmetry		
		$2/m$	mmm	
		$P n$ $2\pi, \pi, 2\pi$	$P \Phi n 2_1$ $2\pi, \pi, \pi$	$P \Phi \varphi_2 2_1$ π, π, π
		$P_{2_1} n \Phi$ $\pi, \pi, 2\pi$	$P \frac{2_1}{\Phi} \frac{2}{n} \frac{2_1}{\Phi}$ π, π, π	$P \frac{2}{\Phi} \frac{2}{\varphi_2} \frac{2_1}{\Phi}$ $\pi, \pi/2, \pi$
		$P_{2_1} \varphi_1 \Phi$ π, π, π	$P \frac{2_1}{\Phi} \frac{2}{\varphi_1} \frac{2}{\Phi}$ $\pi, \pi/2, \pi$	$P \frac{2}{\Phi} \frac{2}{m} \frac{2}{\Phi}$ $\pi/2, \pi/2, \pi$
		$P_{2_1} n \Phi$ $\pi, \pi, 2\pi/3$	$P \frac{2_1}{\Phi} \frac{2}{n} \frac{2_1}{\Phi}$ $\pi, \pi/2, 2\pi/3$	$P \frac{2}{\Phi} \frac{2}{\varphi_2} \frac{2}{\Phi}$ $\pi/2, \pi/2, 2\pi/3$
		$P_{2_1} \varphi_1 \Phi$ $\pi, \pi, \pi/2$	$P \frac{2_1}{\Phi} \frac{2}{\varphi_1} \frac{2}{\Phi}$ $\pi, \pi/2, \pi/2$	$P \frac{2}{\Phi} \frac{2}{m} \frac{2}{\Phi}$ $\pi/2, \pi/2, \pi/2$
		$P_{2_1} \varphi_1 \Phi$ $\pi, \pi, \pi/3$	$P \frac{2_1}{\Phi} \frac{2}{\varphi_1} \frac{2}{\Phi}$ $\pi, \pi/2, \pi/3$	$P \frac{2}{\Phi} \frac{2}{m} \frac{2}{\Phi}$ $\pi/2, \pi/2, \pi/3$
		$P_{2_1} \varphi_1 \Phi$ $\pi, \pi, \pi/2$	$P \frac{2_1}{\Phi} \frac{2}{\varphi_1} \frac{2}{\Phi}$ $\pi, \pi/2, \pi/2$	$P \frac{2}{\Phi} \frac{2}{m} \frac{2}{\Phi}$ $\pi/2, \pi/2, \pi/2$

14.7.7. Cubic Symmetry

If one considers the full cubic symmetry, one must include the threefold axis in the consideration. Since it is inclined to the selected axes of the crystal coordinate system $X' = [100]$, $Y' = [010]$, $Z' = [001]$, its application gives rise to compli-

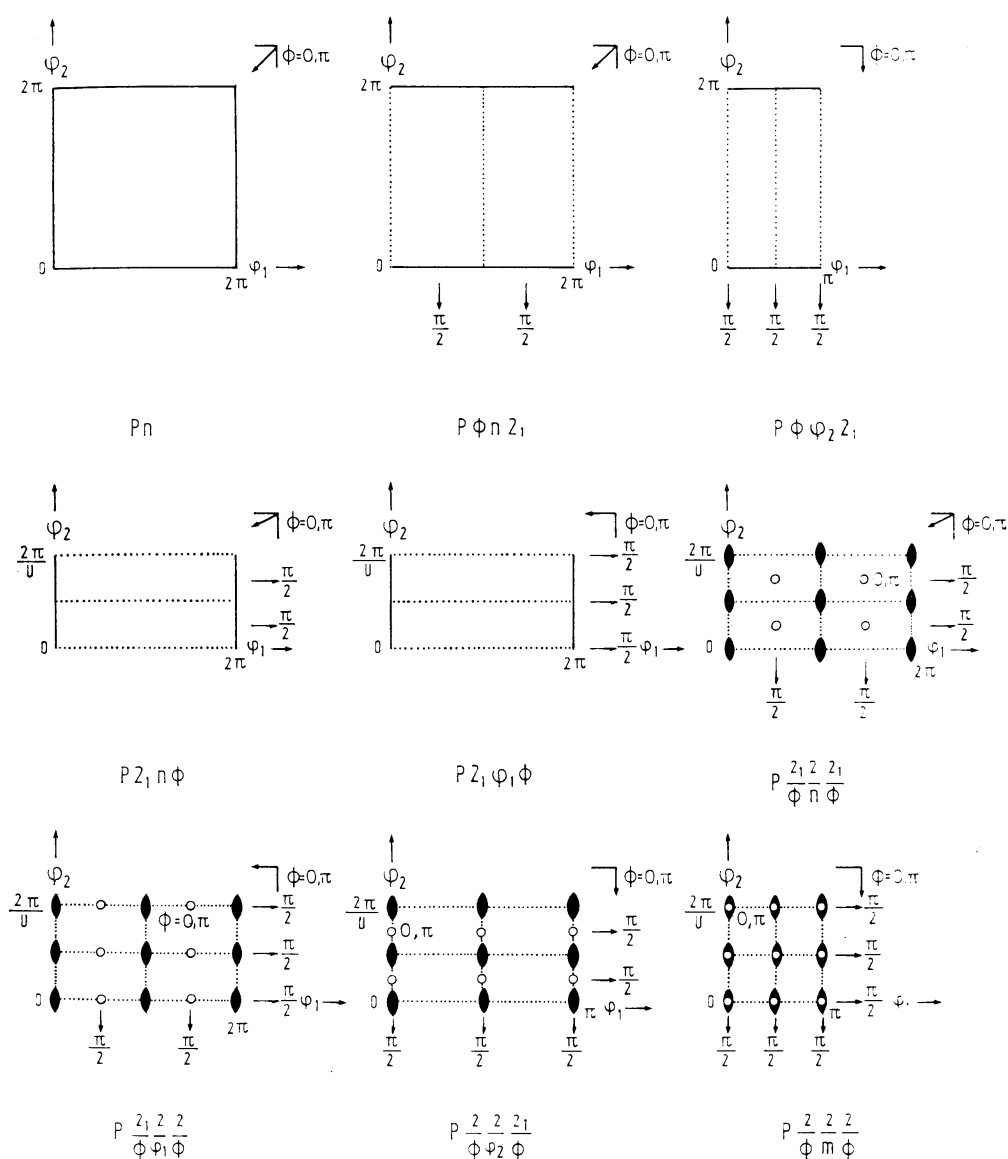


Figure 14.6 Possible space groups in the Euler space in the representation according to the International Tables¹⁶⁶ as given by BAKER¹⁶

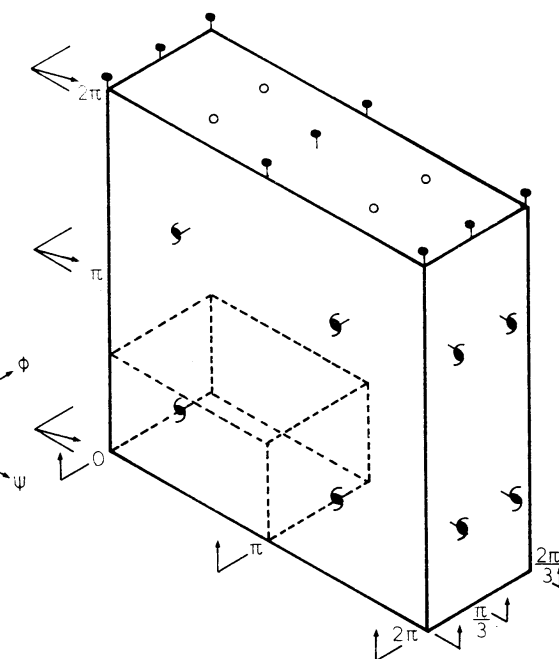


Figure 14.7 Symmetry $P \frac{\bar{2}_1}{\Theta} \frac{\bar{2}}{n} \frac{\bar{2}_1}{\Theta}$ for trigonal crystal and monoclinic sample symmetry^{15,16}

cated non-linear relations between the EULER angles of equivalent points. If we consider the threefold axis in Figure 14.9, we recognize that it forms the straight line $A-A'''$ in the orientation space (Figure 14.10) — i.e. orientations for which the $Z = ND$ direction lies in the [111] direction are represented by points on this line (see reference 232). This line will therefore be transformed into itself by the threefold rotation axis. One further sees that, in general, orientations with the same coordinates $\Phi\varphi_2$ must have equal coordinates $\Phi'\varphi'_2$ after application of the threefold axis — i.e. a line parallel to φ_1 transforms into a similar line, but in another fundamental region defined by the points A—F, so that the axis $A-A'''$ is a pseudo-screw axis (screw axis with distortion of the space). In particular, the boundary lines of the region AB up to AG for $\varphi_1 = 0$ transform into the lines A'B' up to A'G', A''B'' up to A''G'' and finally A'''B''' up to A'''G''', which all have the same projections, namely A'''B''' up to A'''G'''. The cylindrical surfaces defined by the lines AB and A'''B''' up to AG and A'''G''' thus define regions in the orientation space, which in each case are transformed completely into themselves. Since three equivalent points must lie in each of the four cubic regions of the orientation space of Figure 14.10, one can thus select the boundaries of

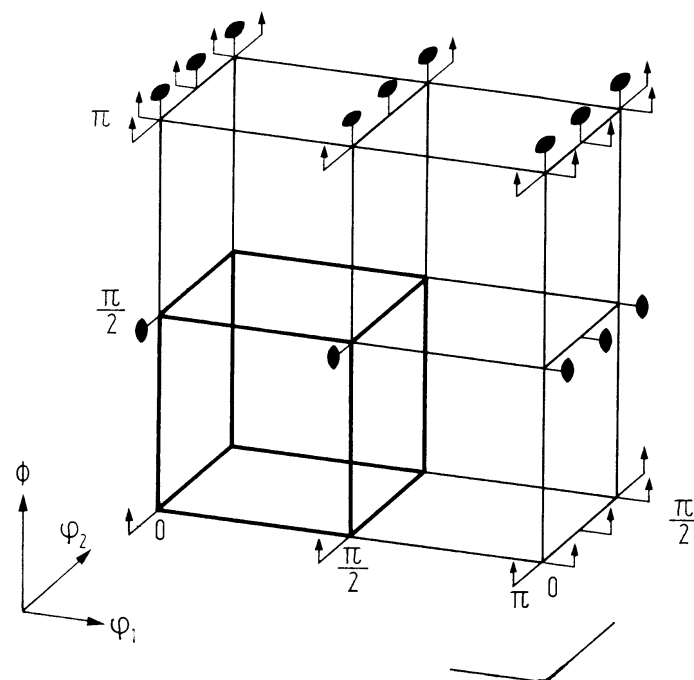


Figure 14.8 Symmetry $P \frac{2}{\Phi} \frac{2}{m} \frac{2}{\Phi}$ for cubic (tetragonal) crystal and orthorhombic sample symmetry

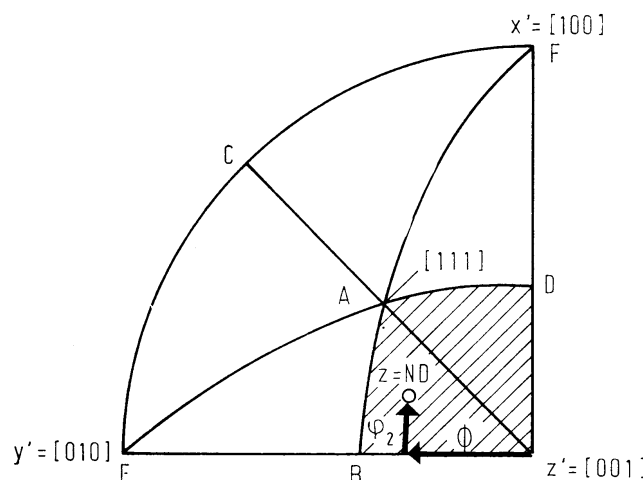


Figure 14.9 The threefold axis of cubic crystal symmetry

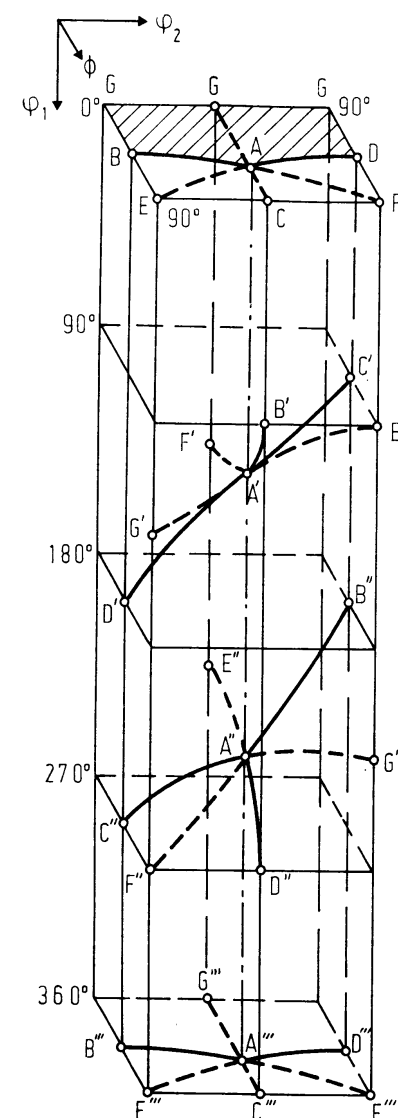


Figure 14.10 The orientation space and the symmetrically equivalent regions for cubic orthorhombic symmetry. After POSPIECH²³²

asymmetric regions, as is represented by shading in Figure 14.11. This region, however, contains a singular plane $\Phi = 0$, on which each orientation is represented by a line. One can therefore also choose either of the two other elementary regions of Figure 14.11 as asymmetric units. The course of the boundary lines in the $\Phi - \varphi_2$ plane is shown in Figure 14.12.

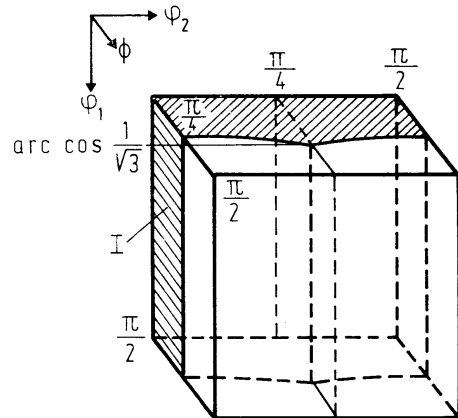


Figure 14.11 The elementary region of cubic-orthorhombic symmetry

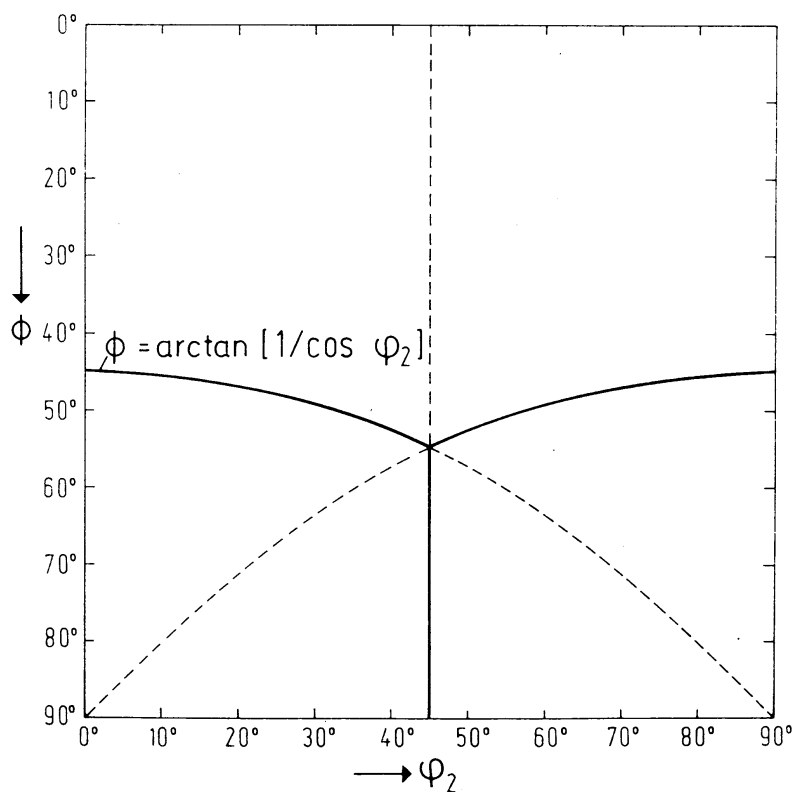


Figure 14.12 The course of the boundary lines of the elementary regions for cubic-orthorhombic symmetry in the $\varphi_1 = 0$ section

14.8. CLEBSCH—GORDAN Coefficients for Symmetric Functions

The product of two symmetric generalized spherical harmonics can be expressed as a sum of generalized spherical harmonics of the same symmetry. We therefore set

$$\dot{T}_{l_1}^{\mu_1 \nu_1} \dot{T}_{l_2}^{\mu_2 \nu_2} = \sum_{l=|l_2-l_1|}^{|l_2+l_1|} \sum_{\mu=1}^{M(l)} \sum_{\nu=1}^{N(l)} \{l_1 l_2 \mu_1 \mu_2 | l \mu\} \{l_1 l_2 \nu_1 \nu_2 | l \nu\} \dot{T}_l^{\mu \nu} \quad (14.289)$$

We express the symmetric functions by their symmetry coefficients:

$$\begin{aligned} & \sum_{m_1, m_2, n_1, n_2} \dot{A}_{l_1}^{m_1 \mu_1} \dot{A}_{l_1}^{n_1 \nu_1} \dot{A}_{l_2}^{m_2 \mu_2} \dot{A}_{l_2}^{n_2 \nu_2} T_{l_1}^{m_1 n_1} T_{l_2}^{m_2 n_2} \\ &= \sum_{l=|l_2-l_1|}^{|l_2+l_1|} \sum_{\mu, \nu} \sum_{m, n} \{l_1 l_2 \mu_1 \mu_2 | l \mu\} \{l_1 l_2 \nu_1 \nu_2 | l \nu\} \dot{A}_l^{m \mu} \dot{A}_l^{n \nu} T_l^{mn} \end{aligned} \quad (14.290)$$

If now we transform the left side with the help of equation (14.96) and equate the coefficients of the functions T_l^{mn} on both sides, we obtain

$$\begin{aligned} & \sum_{\mu, \nu} \{l_1 l_2 \mu_1 \mu_2 | l \mu\} \{l_1 l_2 \nu_1 \nu_2 | l \nu\} \dot{A}_l^{m \mu} \dot{A}_l^{n \nu} \\ &= \sum_{m_1, m_2, n_1, n_2} (l_1 l_2 m_1 m_2 | lm) (l_1 l_2 n_1 n_2 | ln) \dot{A}_{l_1}^{m_1 \mu_1} \dot{A}_{l_1}^{n_1 \nu_1} \dot{A}_{l_2}^{m_2 \mu_2} \dot{A}_{l_2}^{n_2 \nu_2} \end{aligned} \quad (14.291)$$

This equation is fulfilled if we set

$$\sum_{\mu} \{l_1 l_2 \mu_1 \mu_2 | l \mu\} \dot{A}_l^{m \mu} = \sum_{m_1, m_2} (l_1 l_2 m_1 m_2 | lm) \dot{A}_{l_1}^{m_1 \mu_1} \dot{A}_{l_2}^{m_2 \mu_2} \quad (14.292)$$

$$\sum_{\nu} \{l_1 l_2 \nu_1 \nu_2 | l \nu\} \dot{A}_l^{n \nu} = \sum_{n_1, n_2} (l_1 l_2 n_1 n_2 | ln) \dot{A}_{l_1}^{n_1 \nu_1} \dot{A}_{l_2}^{n_2 \nu_2} \quad (14.293)$$

where

$$m = m_1 + m_2; \quad n = n_1 + n_2 \quad (14.294)$$

If we multiply the first of these equations by $\dot{A}_l^{m \mu}$ and sum over all m , because of equation (14.134) we obtain

$$\{l_1 l_2 \mu_1 \mu_2 | l \mu\} = \sum_{m_1=-l_1}^{+l_1} \sum_{m_2=-l_2}^{+l_2} (l_1 l_2 m_1 m_2 | lm) \dot{A}_{l_1}^{m_1 \mu_1} \dot{A}_{l_2}^{m_2 \mu_2} \dot{A}_l^{m \mu} \quad (14.295)$$

The quantities $\{l_1 l_2 \mu_1 \mu_2 | l \mu\}$ (which are analogous to the CLEBSCH—GORDAN coefficients) for the symmetric functions are expressed by CLEBSCH—GORDAN coefficients themselves and the symmetry coefficients $\dot{A}_l^{m \mu}$. In the case of lower symmetry the latter have the form of the selection rule:

$$\dot{A}_l^{m \mu} = \delta_{m \mu} \quad (14.296)$$

so that it is naturally true, as it must be, that

$$\{l_1 l_2 m_1 m_2 | lm\} = (l_1 l_2 m_1 m_2 | lm) \quad (14.297)$$

It therefore follows from the interchange relation for the CLEBSCH—GORDAN coefficients (equation 14.99) that

$$\{l_2 l_1 \mu_2 \mu_1 | l \mu\} = (-1)^{l_1 + l_2 - l} \{l_1 l_2 \mu_1 \mu_2 | l \mu\} \quad (14.298)$$

One further finds that

$$\begin{aligned} \{l_2 \mu_2 \mu_2 | l_1 \mu_1\} &= \sum_{m=-l}^{+l} \sum_{m_2=-l_2}^{+l_2} (l_2 m m_2 | l_1 m + m_2) \dot{A}_l^{m\mu} \dot{A}_{l_2}^{m_2\mu_2} \dot{A}_{l_1}^{m+m_2\mu_1} \\ &= \sum_{m=-l}^{+l} \sum_{m_2=-l_2}^{+l_2} (-1)^{l_1 + m_2} \\ &\times \sqrt{\frac{2l_1 + 1}{2l + 1}} (l_1 l_2 - (m + m_2) m_2 | l - m) \dot{A}_l^{m\mu} \dot{A}_{l_2}^{m_2\mu_2} \dot{A}_{l_1}^{m+m_2\mu_1} \end{aligned} \quad (14.299)$$

If we assume it is true that

$$\dot{A}_l^{-m\mu} = \dot{A}_l^{+m\mu} \quad (14.300)$$

when we replace m_2 by $-m_2$, we thus obtain

$$\begin{aligned} \{l_2 \mu_2 \mu_2 | l_1 \mu_1\} &= (-1)^{l_1} \sqrt{\frac{2l_1 + 1}{2l + 1}} \sum_{m=-l}^{+l} \sum_{m_2=-l_2}^{+l_2} (-1)^{m_2} \\ &\times (l_1 l_2 - (m - m_2) - m_2 | l - m) \dot{A}_l^{m\mu} \dot{A}_{l_2}^{m_2\mu_2} \dot{A}_{l_1}^{m-m_2\mu_1} \end{aligned} \quad (14.301)$$

With equations (14.97) and (14.101), equation (14.301) transforms into

$$\begin{aligned} \{l_2 \mu_2 \mu_2 | l_1 \mu_1\} &= (-1)^{l_1 - l} \sqrt{\frac{2l_1 + 1}{2l + 1}} \sum_{m_1=-l_1}^{+l_1} \sum_{m_2=-l_2}^{+l_2} (-1)^{m_2} \\ &\times (l_1 l_2 m_1 m_2 | lm) \dot{A}_{l_1}^{m_1\mu_1} \dot{A}_{l_2}^{m_2\mu_2} \dot{A}_l^{m\mu} \end{aligned} \quad (14.302)$$

It follows finally for even m_2 that

$$\{l_2 \mu_2 \mu_2 | l_1 \mu_1\} = (-1)^{l_1 - l} \sqrt{\frac{2l_1 + 1}{2l + 1}} \{l_1 l_2 \mu_1 \mu_2 | l \mu\} \quad (14.303)$$

For $l_1 \leq 6$, $l_2 \leq 6$ one obtains the values given in Table 14.10 for the coefficients of the symmetry \mathfrak{D}_h . If in equation (14.289) we change to one-sided symmetric functions, we obtain with equation (14.297)

$$\dot{T}_{l_1}^{\mu_1 n_1} \dot{T}_{l_2}^{\mu_2 n_2} = \sum_{l=|l_2-l_1|}^{|l_2+l_1|} \sum_{\mu=1}^{M(l)} \{l_1 l_2 \mu_1 \mu_2 | l \mu\} (l_1 l_2 n_1 n_2 | ln) \dot{T}_l^{\mu n} \quad (14.304)$$

If now we set $n_1 = n_2 = n = 0$ and change to the symmetric spherical harmonics, we obtain

$$\dot{k}_{l_1}^{\mu_1} \dot{k}_{l_2}^{\mu_2} = \sum_{l=|l_2-l_1|}^{|l_2+l_1|} \sum_{\mu=1}^{M(l)} \{\{l_1 l_2 \mu_1 \mu_2 | l \mu\}\} k_l^{\mu} \quad (14.305)$$

with the coefficients

$$\{\{l_1 l_2 \mu_1 \mu_2 | l \mu\}\} = \frac{1}{\sqrt{4\pi}} \sqrt{\frac{(2l_1 + 1)(2l_2 + 1)}{(2l + 1)}} \{l_1 l_2 \mu_1 \mu_2 | l \mu\} (l_1 l_2 00 | l 0) \quad (14.306)$$

For $l_1 \leq 6$, $l_2 \leq 6$ one obtains the values given in Table 14.11 for the cubic symmetry \mathfrak{D}_h .

Table 14.10 THE COEFFICIENTS $\{l_1 l_2 11 | l \mu\}$ FOR CUBIC SYMMETRY FOR $l_{1,2} \leq 6$

l_1	l_2	$l = 0$	$l = 4$	$l = 6$	$l = 8$	$l = 9$	$l = 10$	$l = 12$	
								$\mu = 1$	$\mu = 2$
4	4	+0.33333	+0.47795	-0.63563	+0.50637				
4	6		-0.52888	-0.44330	-0.29693	-0.55282	+0.36059		
6	6	+0.27735	-0.36885	+0.04740	+0.61853	0.00000	+0.44482	0.00000	-0.45200

Table 14.11 THE COEFFICIENTS $\{l_1 l_2 11 | l \mu\}$ FOR CUBIC SYMMETRY FOR $l_{1,2} \leq 6$

l_1	l_2	$l = 0$	$l = 4$	$l = 6$	$l = 8$	$l = 9$	$l = 10$	$l = 12$	
								$\mu = 1$	$\mu = 2$
4	4	+0.28218	+0.16272	+0.20117	+0.19239				
4	6		+0.20117	-0.14517	+0.09464	0.00000	+0.14204		
6	6	+0.28218	-0.14517	-0.01618	+0.19745	0.00000	-0.14433	0.00000	-0.18628

15. Numerical Tables

In the course of numerical calculations of orientation distribution functions a large number of mathematical quantities are used — e.g. functional values of spherical harmonics and generalized harmonics, coefficients of their FOURIER representation, symmetry invariant functions and their symmetry coefficients. The selection of numerical tables of these quantities relating to this section appear in Appendix 3. In the case of lower symmetries all these quantities can easily be deduced from the coefficients Q_l^{mn} . In the case of cubic symmetry a second fundamental table, the symmetry coefficients $B_l^{m\mu}$, is needed in addition. Tables of these quantities are therefore given up to $l = 34$, which is assumed, at present, to be a reasonable upper limit for the series expansion in most texture calculations. All other tables based on the two fundamental ones are only intended for checking purposes. Therefore they are given only up to lower degrees of l .

The FOURIER coefficients Q_l^{mn} and the symmetry coefficients $B_l^{m\mu}$ have been given in earlier publications (references 67, 74 and in the first edition). The algorithms for their numerical calculations have, however, been essentially improved by C. ESLING^{127,128}. Thus it was decided to recalculate these tables and to present the original computer outputs. The calculations were made with an accuracy better than the number of decimals given in the tables, so that the maximum error can be assumed not to exceed half a unit in the last decimal.

In Table 15.2 (the symmetry coefficients $B_l^{m\mu}$) the choice of a basis among these coefficients is arbitrary. The basis chosen here corresponds to the algorithm proposed by ESLING¹²⁷. It deviates in some places from the basis used in Table 12.3.1 in the first edition. The present basis is consistent with that used in the Library program²⁹² (the choice of one or the other basis does not matter in the final results unless different choices are being mixed up in one and the same calculation).

Table 15.2.2 (the symmetry coefficients $B_l^{m\mu}$ in the second setting, with the crystal Z'-axis parallel to the [111] direction) has not previously been published. Table 15.2.4, the symmetry coefficients in Roe's notation, has been extended from $l = 22$ in Roe's paper to $l = 34$, which is now frequently used for the series expansion. Furthermore Tables 15.5.1.2, 15.5.2.2 and 15.5.2.3 containing the symmetrical generalized spherical harmonics for specific low index orientations and orientation relationships have been extended. On the other hand, some tables given in the first edition of this book have been reduced or omitted because they are regarded as of minor value for texture analysis. All the tables given in this section have been prepared by C. ESLING and E. BECHLER. They have been computed on the machine PDP 11/70 in the computer centre of IRSID in Maizières-les-Metz.

References

- I H. J. BUNGE (1969). *Mathematische Methoden der Texturanalyse*, Akademie-Verlag, Berlin

Proceedings of Texture Conferences

1. *Textures in Research and Practice: Proceedings of the International Symposium, Clausthal-Zellerfeld, 1968* (ed. J. GREWEN and G. WASSERMANN), Springer-Verlag, Berlin/Heidelberg/New York (1969)
2. *Quantitative Analysis of Textures: Proceedings of the International Seminar, Cracow, 1971* (ed. J. KARP, S. GÓRCZYCA, H. J. BUNGE, J. POSPIECH and W. DĄBROWSKI), The Society of Polish Metallurgical Engineers
3. *3^e Colloque Européen sur les Textures de Déformation et de Recristallisation des Métaux et leur Applications Industrielles: Proceedings of the Conference at Pont-à-Mousson 1973* (ed. R. PENELLE), Société Francaise de Métallurgie
4. *Texture and the Properties of Materials: Proceedings of the 4th International Conference on Texture, Cambridge, 1975* (ed. G. J. DAVIES, I. L. DILLAMORE, R. C. HUDD and J. S. KALLEND), The Metals Society
- 4a. *Textures of Materials: Proceedings of the 5th International Conference on Textures of Materials* (ed. G. GOTTSSTEIN and K. LÜCKE), Springer-Verlag, Berlin/Heidelberg/New York (1978)

Surveys on Textures

5. F. A. UNDERWOOD (1961). *Textures in Metal Sheets*, Macdonald, London
6. G. WASSERMANN and J. GREWEN (1962). *Texturen metallischer Werkstoffe*, Springer-Verlag, Berlin/Göttingen/Heidelberg
7. I. P. KUDRIAWZEW (1965). *Textures in Metals and Alloys* (Russ.), Izdatel'stvo Metallurgii, Moscow
8. I. L. DILLAMORE and W. T. ROBERTS (1965). Preferred orientation in wrought and annealed metals. *Metallurg. Rev.* **10**, 271–380
9. P. COULOMB (1972). *Les Textures dans les Métaux de Réseau Cubique*, Dunod, Paris

Individual References

10. M. ABRAMOWITZ and J. A. STEGUN (1970). *Handbook of Mathematical Functions*, Dover, New York
11. Academia Sinica (1965). *Tables of the Clebsch-Gordan Coefficients*, Science Press, Peking
12. H. AELBORN and G. WASSERMANN (1962). Über die doppelte Fasertextur in gezogenen Drähten kubisch-flächenzentrierter Metalle. *Z. Metallkde.*, **53**, 422–427

13. K. S. ALEXANDROW and L. A. AISENBERG (1966). A method for the calculation of physical constants of polycrystalline materials (Russ). *Dokl. Akad. Nauk SSSR*, **167**, 1028–1031
14. M. A. ATOJI (1958). Spherical Fourier method. *Acta Cryst.*, **11**, 827–829
15. D. W. BAKER (1970). On the symmetry of orientation distribution in crystal aggregates. *Adv. X-ray Analysis*, **13**, 435–454
16. D. W. BAKER (1971). Symmetry of the orientation distribution in crystal aggregates and mechanical twinning. In reference 2, pp. 125–147
17. D. W. BAKER and H. R. WENK (1972). Preferred orientation in a low-symmetry quartz-mylonite. *J. Geol.*, **80**, 81–105
18. D. W. BAKER, H. R. WENK and J. M. CHRISTIE (1969). X-Ray analysis of preferred orientation in fine-grained quartz aggregates. *J. Geol.*, **77**, 144–172
19. C. S. BARRETT (1943). *Structure of Metals*, McGraw-Hill, New York
20. R. E. BAUER, H. MECKING and K. LÜCKE (1977). Textures of copper single crystals after rolling at room temperature. *Mat. Sci. Eng.*, **27**, 163–180
21. S. L. BELOUSOV (1962). *Tables of Normalized Associated Legendre Polynomials*, Pergamon Press, Oxford
22. H. W. BERGMANN, R. KERN and W. BRUNN (1976). A new computer program for contour maps of texture functions. *J. Appl. Cryst.*, **9**, 254–256
23. D. D. BETTS, A. B. BHATIA and M. WYMAN (1956). Houston's method and its application to the calculation of characteristic temperatures of cubic crystals. *Phys. Rev.*, **104**, 37–42
24. S. BHAGAVANTAM (1966). *Crystal Symmetry and Physical Properties*, Academic Press, London/New York
25. J. BORDAS, A. M. GLAZER, C. J. HOWARD and A. J. BOURDILLON (1977). Energy-dispersive diffraction from polycrystalline material using synchrotron radiation. *Phil. Mag.*, **35**, 311–323
26. R. H. BRAGG and C. M. PACKER (1962). Orientation dependence of structure in pyrolytic graphite. *Nature, Lond.*, **195**, 1080–1082
27. R. H. BRAGG and C. M. PACKER (1964). Quantitative determination of preferred orientation. *J. Appl. Phys.*, **35**, 1322–1328
28. J. R. BRIDGE, C. M. SCHWARTZ and D. A. VAUGHAM (1956). X-Ray diffraction determination of the coefficients of thermal expansion of alpha uranium. *J. Metals, Trans AIME*, **S**, 1282–1285
29. D. A. G. BRUGGEMANN (1930). Elastizitätskonstanten von Kristallaggregaten. Thesis, Utrecht
30. D. A. G. BRUGGEMANN (1935). Berechnung der elastischen Moduln für die verschiedenen Texturen der regulären Metalle. *Z. Phys.*, **92**, 561–588
31. H. J. BUNGE (1959). Zur Darstellung von Fasertexturen. *Mber. Dt. Akad. Wiss.*, **1**, 27–81
32. H. J. BUNGE (1959). Zur Darstellung von Fasertexturen II. *Mber. Dt. Akad. Wiss.*, **1**, 400–404
33. H. J. BUNGE (1960). Zur Darstellung von Fasertexturen in reziproker Polfigur. *Z. Metallkde.*, **51**, 535–536
34. H. J. BUNGE (1960). Zur Berechnung einiger physikalischer Eigenschaften von Materialien mit Fasertextur. *Mber. Dt. Akad. Wiss.*, **2**, 479–489
35. H. J. BUNGE (1961). Zur Berechnung einiger physikalischer Eigenschaften von Materialien mit allgemeiner Textur. *Mber. Dt. Akad. Wiss.*, **3**, 97–106
36. H. J. BUNGE (1961). Zur Bestimmung der Betragsquadrate der Strukturfaktoren aus Texturaufnahmen. *Mber. Dt. Akad. Wiss.*, **3**, 285–295
37. H. J. BUNGE (1962). Zur Bestimmung der Betragsquadrate von Strukturfaktoren aus Texturaufnahmen. *Acta Cryst.*, **15**, 612–613
38. H. J. BUNGE (1962). Zur Frage des Auflösungsvermögens verschiedener Texturuntersuchungsmethoden. *Fiz. Metallov Metalloved.*, **13**, 512–516
39. H. J. BUNGE (1963). Zur Frage der Entstehung der Ziehtextur von Aluminiumdrähten. *Mber. Dt. Akad. Wiss.*, **5**, 293–299
40. H. J. BUNGE (1964). *Zur Darstellung von Fasertexturen*, Habilitationsschrift, Berlin
41. H. J. BUNGE (1965). Einige Untersuchungen zur Entstehung der Verformungs- und Rekristallisationstexturen von Aluminiumdrähten. *Z. Metallkde.*, **56**, 38–39
42. H. J. BUNGE (1965). Einige Bemerkungen zur Darstellung von Blechtexturen durch drei inverse Polfiguren. *Z. Metallkde.*, **56**, 378–379
43. H. J. BUNGE (1965). Zur Darstellung allgemeiner Texturen. *Z. Metallkde.*, **56**, 872–874
44. H. J. BUNGE (1965). Einige Bemerkungen zur Symmetrie verallgemeinerter Kugelfunktionen. *Mber. Dt. Akad. Wiss.*, **7**, 351–360
45. H. J. BUNGE (1966). Ein Zuverlässigkeitsskriterium für Polfiguren von Texturen kubischer Metalle. *Kristall Techn.*, **1**, 171–173
46. H. J. BUNGE (1967). Eine röntgenographische Methode zur Messung der Orientierungsabhängigkeit der Korngroße. *Z. Metallkde.*, **58**, 649–657
47. H. J. BUNGE (1967). Über eine FOURIER-Entwicklung verallgemeinerter Kugelfunktionen. *Mber. Dt. Akad. Wiss.*, **9**, 652–658
48. H. J. BUNGE (1968). The orientation distribution function of the crystallites in cold rolled and annealed low-carbon steel sheets. *Phys. Stat. Sol.*, **26**, 167–172
49. H. J. BUNGE (1968). Über die Rekristallisationstextur von Aluminiumdrähten. *Kristall Techn.*, **3**, 295–312
50. H. J. BUNGE (1968). Über die elastischen Konstanten kubischer Materialien mit beliebiger Textur. *Kristall Techn.*, **3**, 431–438
51. H. J. BUNGE (1968). Die dreidimensionale Orientierungsverteilungsfunktion und Methoden zu ihrer Bestimmung. *Kristall Techn.*, **3**, 439–454
52. H. J. BUNGE (1968). Texturbeschreibung durch dreidimensionale Polfiguren. In reference 1, pp. 24–35
53. H. J. BUNGE (1970). Some applications of the Taylor theory of polycrystal plasticity. *Kristall Techn.*, **5**, 145–175
54. H. J. BUNGE (1971). Zum augenblicklichen Stand und den Entwicklungstendenzen auf dem Texturgebiet. *Kristall Techn.*, **6**, 325–334
55. H. J. BUNGE (1971). Automatische Texturanalyse mit Hilfe der elektronischen Datenverarbeitung. *Kristall Techn.*, **6**, 429–438
56. H. J. BUNGE (1971). Charakterization of the polycrystalline state by distribution functions. In reference 2, pp. 7–17
57. H. J. BUNGE (1971). The calculation of the three-dimensional orientation distribution function from experimental data. In reference 2, pp. 19–31
58. H. J. BUNGE (1971). Some results obtained by the three-dimensional texture analysis. In reference 2, pp. 33–58
59. H. J. BUNGE (1971). Some methodical details of texture analysis. In reference 2, pp. 59–72
60. H. J. BUNGE (1971). Some applications of Taylor's analysis on polycrystal plasticity. In reference 2, pp. 279–296

61. H. J. BUNGE (1971). Entstehung von Verformungstexturen in metallischen Werkstoffen. *Kristall Techn.*, **6**, 677–728
62. H. J. BUNGE (1973). Dreidimensionale Texturanalyse. *Neue Hütte*, **18**, 742–746
63. H. J. BUNGE (1973). Moderni metody a racionalni zpusoby vydohodnocovani texturni analýzy. *Hutnické Listy*, **28**, 138–140
64. H. J. BUNGE (1973). Three-dimensional representation of textures and its applications. In reference 3, pp. 97–116
65. H. J. BUNGE (1974). Mittelungsverfahren bei dreidimensionalen Texturen. In *Mechanische Anisotropie* (ed. H. P. STÜWE), Springer-Verlag, Wien, pp. 177–199
66. H. J. BUNGE (1974). The effective elastic constants of textured polycrystals in second order approximation. *Kristall Techn.*, **9**, 413–423
67. H. J. BUNGE (1974). Calculation of the Fourier coefficients of the generalized spherical functions. *Kristall Techn.*, **9**, 939–963
68. H. J. BUNGE (1977). Texture analysis by orientation distribution functions. *Z. Metallkde.*, **68**, 571–581
69. H. J. BUNGE (1977). Textur und Anisotropie magnetischer Werkstoffe. *J. Magnetism Magnetic Mat.*, **4**, 305–320
70. H. J. BUNGE (1977). Textures and metastable phases in Taylor wires. *Z. Metallkde.*, **67**, 720–728
71. H. J. BUNGE (1977). Determination of the orientation distribution function from isolated axis-density values. *Texture*, **2**, 169–174
72. H. J. BUNGE, R. EBERT and F. GÜNTHER (1969). On the angular variation and texture dependence of Young's modulus in cold-rolled copper sheet. *Phys. Stat. Sol.*, **31**, 565–569
73. H. J. BUNGE and J. EHLLERT (1968). Zur Bestimmung der reziproken Polfigur von Drähten aus unvollständig gemessenen Polfiguren. *Kristall Techn.*, **3**, 313–321
- 73a. H. J. BUNGE and C. ESLING (1979). Determination of the odd part of the texture function. *J. Phys. Lett.*, **40**, 627–628
- 73b. H. J. BUNGE and C. ESLING (1979). Non-random orientation distribution functions with random pole figures. *Texture*, **3**, 169–190
74. H. J. BUNGE and J. EHLLERT (1966). Über die verallgemeinerten Kugelfunktionen kubischer Symmetrie. *Mber. Dt. Akad. Wiss.*, **8**, 241–259
75. H. J. BUNGE and F. HAESSNER (1968). Three-dimensional orientation distribution function of crystallites in cold-rolled copper. *J. Appl. Phys.*, **39**, 5503–5514
76. H. J. BUNGE and K. KÜTTNER (1974). Generalized spherical functions of cubic symmetry. *Kristall Techn.*, **9**, 1051–1071
77. H. J. BUNGE and T. LIEFFERS (1971). The three-dimensional orientation distribution obtained by computer simulation of the plastic deformation in face-centered cubic polycrystals. *Scripta Met.*, **5**, 143–149
78. H. J. BUNGE, K. ÖHME and F. GÜNTHER (1970). On the influence of the grain form or the orientation correlation on the Young's modulus of copper sheet. *Phys. Stat. Sol (a)*, **1**, K 135–137
79. H. J. BUNGE and W. T. ROBERTS (1969). Orientation distribution, elastic and plastic anisotropy in stabilized steel sheet. *J. Appl. Cryst.*, **2**, 116–128
80. H. J. BUNGE and H. SANDMANN (1963). Zur Berechnung der reziproken Polfigur von Fasertexturen mit Hilfe des Rechenautomaten URAL I. *Mber. Dt. Akad. Wiss.*, **5**, 344–350
81. H. J. BUNGE, D. SCHLEUSENER and D. SCHLÄFER (1974). Neutron-diffraction studies of the recrystallization textures in cold-rolled low-carbon steel. *Metal Sci.*, **8**, 413–423

82. H. J. BUNGE and J. TOBISCH (1968). Bestimmung der Walztextur des Kupfers mit Hilfe der Neutronenbeugung. *Z. Metallkde.*, **59**, 471–475
83. H. J. BUNGE and J. TOBISCH (1972). The texture transition in α -brasses determined by neutron diffraction. *J. Appl. Cryst.*, **5**, 27–40
84. H. J. BUNGE, J. TOBISCH and A. MÜCKLICH (1974). The development of rolling texture in α -brass determined by neutron diffraction. *Texture*, **1**, 211–231
85. H. J. BUNGE, J. TOBISCH and W. SONNTAG (1971). On the development of the rolling texture in copper measured by neutron diffraction. *J. Appl. Cryst.*, **4**, 303–310
86. H. J. BUNGE and H. R. WENK (1977). Three-dimensional texture analysis of three quartzes (trigonal crystal and triclinic specimen symmetry). *Tectonophysics*, **40**, 257–285
87. B. BURAS, J. STAUN-OLSEN, L. GERWARD, B. SELSMARK and A. LINDEGAARD-ANDERSEN (1975). Energy-dispersive spectroscopic methods applied to X-ray diffraction in single crystals. *Acta Cryst.*, **A 31**, 327–333
88. D. H. CHUNG and W. R. BUESSEM (1967). The elastic anisotropy of crystals. *J. Appl. Phys.*, **38**, 2010–2012
89. D. H. CHUNG and W. R. BUESSEM (1967). The Voigt-Reuss-Hill approximation and elastic moduli of polycrystalline MgO, CaF₂, β -ZnS, ZnSe and CdTe. *J. Appl. Phys.*, **38**, 2535–2540
90. A. CLEMENT and P. COULOMB (1976). Representation de la Fonction de Répartition de la Texture par une Serie de Projections Stereographiques ou par une Serie de Coefficients. *Mem. Sci. Rev. Métall.*, **73**, 63–69
91. A. CLEMENT and G. DURAND (1975). Programme Fortran pour l'Analyse Tridimensionnelle des Textures sans Hypothèse Restrictive sur les Symétries de l'Echantillon. *J. Appl. Cryst.*, **8**, 589–597
92. R. COURANT and D. HILBERT (1968). *Methoden der mathematischen Physik*, 3rd edn, Springer-Verlag, Berlin/Heidelberg/New York
93. C. P. CUTLER, J. W. EDINGTON, J. S. KALLEND and K. M. MELTON (1974). Quantitative texture studies of the superplastically deformed Al–Cu eutectic alloy. *Acta Met.*, **22**, 665–671
94. E. CZUBER (1941). *Wahrscheinlichkeitsrechnung und ihre Anwendung auf Fehlerausgleichung, Statistik und Lebensversicherung*, Verlag Teubner, Leipzig
95. G. J. DAVIES, D. J. GOODWILL and J. S. KALLEND (1971). Charts for analysing crystallite distribution function plots for cubic materials. *J. Appl. Cryst.*, **4**, 67–70
96. G. J. DAVIES, D. J. GOODWILL and J. S. KALLEND (1973). A study of annealing texture development in an aluminium killed steel using an interrupted heating technique. In reference 3, pp. 383–395
97. G. J. DAVIES, D. J. GOODWILL and J. S. KALLEND (1974). Earing in deep-drawing steels. *Texture*, **1**, 173–182
98. G. J. DAVIES, D. J. GOODWILL and J. S. KALLEND (1971). Charts for analysing crystallite orientation distribution function plots for hexagonal materials. *J. Appl. Cryst.*, **4**, 193–196
99. G. J. DAVIES, D. J. GOODWILL and J. S. KALLEND (1972). Elastic and plastic anisotropy in sheets of cubic metals. *Metall. Trans.*, **3**, 1627–1631
100. G. J. DAVIES, and J. S. KALLEND (1971). The texture transition in FCC metals. In reference 2, pp. 345–353
101. G. J. DAVIES, J. S. KALLEND and P. P. MORRIS (1973). Texture development in a duplex α – β -brass. In reference 3, pp. 137–148
102. G. J. DAVIES, J. S. KALLEND and P. P. MORRIS (1976). The quantitative prediction of transformation textures. *Acta Met.*, **24**, 159–172

103. G. J. DAVIES, J. S. KALLEND and T. RUBERG (1973). A comparative study of texture development in aluminium and aluminium alloys. In reference 3, pp. 299–315
104. G. J. DAVIES, J. S. KALLEND and T. RUBERG (1975). Quantitative textural measurements on cube-texture copper. *Metal Sci.*, **9**, 421–424
105. M. DEGUEN, P. PARNIÈRE and G. SANZ (1977). Effet des Trajectoires de Déformation sur les Courbes Limite l'Emboutissage. Etude de l'Influence de la Microstructure sur cet Effet. IRSID Rep. 488
106. P. DELAYEN and P. PARNIÈRE (1974). Modification de Texture Cristallographique Associées aux Déformations par Traction des Toles Mincees d'Acier Extra-Doux. *Mem. Sci. Rev. Metall.*, **71**, 67–71
107. P. DERVIN, J. P. MARDON, M. PERNOT, R. PENELLE and P. LACOMBE (1977). Application de la Représentation Tridimensionnelle des Textures à l'Etude de l'Evolution des Textures de Laminage et de Recristallisation de Titane. *J. Less Common Met.*, **55**, 25–43
108. I. L. DILLAMORE, E. BUTLER and D. GREEN (1968). Crystal rotations under conditions of imposed strain and the influence of twinning and cross-slip. *Met. Sci. J.*, **2**, 161–167
109. I. L. DILLAMORE and M. HATHERLY (1973). An analysis of the development of textures in deformed and annealed cubic metals. In reference 3, pp. 174–194
110. I. L. DILLAMORE, P. HADDEN and D. J. STRATFORD (1972). Texture control and the yield anisotropy of plane strain magnesium extrusions. *Texture*, **1**, 17–29
111. I. L. DILLAMORE and H. KATOH (1971). Polycrystalline plasticity and texture development in cubic metals. In reference 2, pp. 315–344
112. I. L. DILLAMORE and H. KATOH (1974). A comparison of the observed and predicted deformation textures in cubic metals. *Metal Sci.*, **8**, 21–27
113. I. L. DILLAMORE and H. KATOH (1974). The mechanism of recrystallization in cubic metals with particular reference to their orientation dependence. *Metal Sci.*, **8**, 73–83
114. I. L. DILLAMORE, H. KATOH and K. HASLAM (1974). The nucleation of crystallization and the development of textures in heavily compressed iron-carbon alloys. *Texture*, **1**, 151–156
115. W. R. McDONELL (1957, 1960). USAEC Rep. TID 7526, 230; USAEC Rep. DP 400.
116. W. DREYER (1975). Material behaviour of anisotropic solids-thermal and electrical properties. In *Applied Mineralogy*, Vol. 7 (ed. H. KIRSCH, L. B. SOEND and F. TROJER), Springer Verlag Wien/New York
117. C. G. DUNN (1944). Probability method applied to the analysis of recrystallization data. *Phys. Rev.*, **66**, 215–220
118. C. G. DUNN (1954). The analysis of quantitative pole-figure data. *J. Appl. Phys.*, **25**, 233–236
119. C. G. DUNN (1959). On the determination of preferred orientations. *J. Appl. Phys.*, **30**, 850–857
120. C. G. DUNN and J. L. WALTER (1959). Synthesis of a (110) [001] type torque curve in silicon iron. *J. Appl. Phys.*, **30**, 1067–1072
121. E. DURAND (1961). *Solutions Numériques des Équations Algébriques*, Masson, Paris
122. G. DURAND (1976). Harmoniques Sphériques Generalisées, Coefficients de Fourier des Polynomes de Legendre Associés Generalisés: Exemple d'un Programme Fortran. *J. Appl. Cryst.*, **9**, 441–443
123. G. DURAND (1977). Elements de Calcul Numerique des Fonctions de Répartition Relatives à la Représentation Tridimensionnelle des Textures et au Tracé Automatique des Figures de Poles Correspondantes. Thesis, Université de Toulouse
124. O. J. EDER and R. KLEMENCIC (1975). Textures of cold-rolled pure aluminium measured by neutron and X-ray diffraction. *J. Appl. Cryst.*, **8**, 628–635
125. J. EHLERT (1964). Berechnung von Koeffizienten einer Fourier-Entwicklung normierter zugeordneter Legendre-Funktionen. *Mber. Dt. Akad. Wiss.*, **6**, 321–324
126. J. A. ELIAS and A. J. HECKLER (1967). Complete pole figure determination by composite sampling techniques. *Trans. Met. Soc. AIME*, **239**, 1237–1241
127. C. ESLING. An effective algorithm for the calculation of the matrix elements of the representation of the rotation group. To be published
128. C. ESLING and H. J. BUNGE. Calculation of the symmetry coefficients of the cubic spherical harmonics by the projector method. To be published
129. C. ESLING and C. TAVARD (1972). Sur la Texture des Matériaux Polycristallins et la Description de ses Symétries. *C. R. Acad. Sci. Paris*, **274**, 125–127
130. P. P. EWALD (1972). The 'poststift'—a model for the theory of pole figures. *J. Less Common Met.*, **28**, 1–5
131. E. H. FREI, S. SHTRIKMAN and D. TREVES (1959). Method of measuring the distribution of the easy axes of uniaxial ferromagnetics. *J. Appl. Phys.*, **30**, 443
132. I. M. GELFAND, R. A. MINLOS and Z. YA. SHAPIRO (1963). *Representations of the Rotation and Lorentz Groups and their Applications*. Pergamon Press, Oxford/London/New York/Paris
133. L. GERWARD, S. LEHN and G. CHRISTIANSEN (1976). Quantitative determination of preferred orientation by energy-dispersive X-ray diffraction. *Texture*, **2**, 95–111
- 133a. Y. GO (1940). Über die Bestimmung der Verteilung der Kristallite in Fasern auf direktem und indirektem Wege. *Bull. Chem. Soc. Japan*, **15**, 239
134. J. GREWEN, H. J. BUNGE and H. W. BERGMANN. Unpublished
135. J. GREWEN, D. SAUER and H. P. WAHL (1970). Automatisierte quantitative Texturbestimmung an Blechen ohne regellose Vergleichsprüfung. *Z. Metallkde.*, **61**, 430–433
136. J. GREWEN and G. WASSERMANN (1955). Über die idealen Orientierungen einer Walztextur. *Acta Met.*, **3**, 354–360
137. M. GRUMBACH, P. PARNIÈRE, L. ROESCH and C. SAUZAY (1975). Etude des Relations Quantitatives Entre le Coefficient d'Anisotropie, les Cornes d'Emboutissage et la Texture des Toles Mincees d'Acier Extra-Doux. *Mem. Sci. Rev. Mét.*, **72**, 241–253
138. F. HAESSNER. Private Communication
139. F. HAESSNER, U. JAKUBOWSKI and M. WILKENS (1964). Anwendung elektronenmikroskopischer Feinbereichsbeugung zur Ermittlung der Walztextur von Kupfer. *Phys. Stat. Sol.*, **7**, 701–710
140. F. HAESSNER, U. JAKUBOWSKI and M. WILKENS (1966). Topographische Anordnung von Kristallorientierungen in gewalztem, hochreinen Kupfer, bestimmt mittels elektronenmikroskopischer Feinbereichsbeugung. *Acta Met.*, **14**, 454–456
141. F. HAESSNER, U. JAKUBOWSKI and M. WILKENS (1966). Determination of the rolling texture of copper using three different methods. *Trans. Met. Soc. AIME*, **236**, 228–230
142. F. HAESSNER and G. SCHRÖDER (1977). Anisotropie der Plastizität bei stranggepreßten Stäben aus Magnesium, Titan und Zink. *Z. Metallkde.*, **68**, 624–635
143. G. A. J. HANSEN (1975). Berechnung von Walztexturen kubisch-flächenzentrierter Metalle nach dem Taylor-Prinzip und Vergleich mit Experimenten. Thesis, Aachen
144. J. HANSEN, J. POSPIECH and K. LÜCKE (1978). *Tables for Texture Analysis of Cubic Crystals*, Springer Verlag, Berlin/Heidelberg/New York
145. C. J. MCARGUE and L. K. JETTER (1960). Use of axis distribution charts to represent sheet textures. *Trans. Met. Soc. AIME*, **218**, 550–553

146. G. B. HARRIS (1952). Quantitative measurement of preferred orientation in rolled uranium bars. *Phil. Mag. (VII)*, **43**, 113–123
147. Z. HASHIN and S. SHTRIKMAN (1962). A variational approach to the theory of the elastic behaviour of polycrystals. *J. Mech. Phys. Sol.*, **10**, 343–352
148. Z. HASHIN and S. SHTRIKMAN (1962). On some variational principles in anisotropic and homogeneous elasticity. *J. Mech. Phys. Sol.*, **10**, 335–342
149. K. HASLAM, T. COLEMAN, D. DULIEN and I. L. DILLAMORE (1973). Texture formation in the rolling of steel plate. In reference 3, pp. 369–395
150. A. J. HECKLER and W. G. GRANZOW (1970). Crystallite orientation distribution analysis of the cold rolled and recrystallization textures in low-carbon steels. *Met. Trans.*, **1**, 2089–2094
151. A. J. HECKLER, J. A. ELIAS and A. P. WOODS (1967). Automatic computer plotting of pole-figures and axis density figures. *Trans. Met. Soc. AIME*, **239**, 1241–1244
152. R. HILL (1952). The elastic behaviour of a crystalline aggregate. *Proc. Phys. Soc., A* **65**, 349–354
153. J. E. HILLIARD (1962). Specification and measurement of microstructural anisotropy. *Trans. Met. Soc. AIME*, **224**, 1201–1211
154. D. HOF SOMMER and M. L. POTTERS (1960). Table of Fourier coefficients of associated Legendre functions. *Indag. Math.*, **22**, 460–480
155. R. E. HOCK, A. J. HECKLER and J. A. ELIAS (1975). Texture in deep drawing columbium (Nb)-treated interstitialfree steels. *Met. Trans.*, **6A**, 1683–1692
- 155a. P. VAN HOUTTE. ODF analysis from incomplete pole figures normalized by an iterative method. To be published
156. H. HU, R. S. CLINE and S. R. GOODMAN (1966). Deformation textures in metals. In *Recrystallization Grain Growth and Texture*, ASM, Metals Park, Ohio
157. M. HUMBERT (1976). Evaluation de Certaines Erreurs Relatives à la Méthode Tridimensionnelle d'Analyse des Textures. Thesis, Université de Metz
158. W. B. HUTCHINSON and J. G. SWIFT (1971). Textures and magnetic properties in steel. In reference 2, pp. 263–268
159. W. B. HUTCHINSON and J. G. SWIFT (1973). Anisotropy in some soft magnetic materials. *Texture*, **1**, 117–123
160. G. IBE (1965). Orientierungszusammenhänge bei der Rekristallisation von Einkristallen aus 3%igem Siliziumeisen und anderen Metallen. Thesis, Aachen
161. G. IBE and K. LÜCKE (1972). Description of orientation distributions of cubic crystals by means of 3-D rotation coordinates. *Texture*, **1**, 87–89
162. J. IMHOF (1977). Die Bestimmung einer Näherung für die Funktion der Orientierungsverteilung aus einer Polfigur. *Z. Metallkde.*, **68**, 38–43
163. H. INAGAKI (1977). Transformation textures in control-rolled high tensile strength steels. *Trans. ISIJ*, **17**, 166–173
164. H. INAGAKI, K. KURIHARA and I. KOZASU (1977). Influence of crystallographic texture on the strength and toughness of control-rolled high tensile strength steel. *Trans. ISIJ*, **17**, 75–81
165. H. INAGAKI and T. SUDA (1972). The development of rolling textures in low-carbon steels. *Texture*, **1**, 129–140
166. International Union of Crystallography (1952). *International Tables for X-ray Crystallography*, Kynoch Press, Birmingham
167. L. K. JETTER, C. J. MC HARGUE and R. O. WILLIAMS (1956). Method of representing preferred orientation data. *J. Appl. Phys.*, **27**, 368–374
168. J. JURA (1976). Three-dimensional texture analysis based on incomplete and non-symmetrical pole figures of metals crystallizing in cubic system. Thesis, Cracow
169. J. JURA and J. POSPIECH (1976). Data processing in three-dimensional texture analysis. *Texture*, **2**, 81–93
170. J. JURA and J. POSPIECH (1978). The determination of orientation distribution function from incomplete pole figures. An example of a computer program. *Texture*, **3**, 1–25
171. J. JURA, J. POSPIECH and H. J. BUNGE (1976). A standard system of FORTRAN programs for three-dimensional texture analysis: Proceedings of Metallurgical-Casting Commission, Polish Academy of Sciences, Cracow. *Metallurgia*, **24**, 111–176
172. J. JURA, J. POSPIECH and H. J. BUNGE (1974). A system of FORTRAN for three-dimensional texture analysis. *Texture*, **1**, 201–203
173. J. S. KALLEND and G. J. DAVIES (1970). The prediction of plastic anisotropy in annealed sheets of copper and α -brass. *J. Inst. Met.*, **98**, 242–244
174. J. S. KALLEND and G. J. DAVIES (1971). Prediction of rolling textures in FCC-metals. In reference 2, pp. 297–313
175. J. S. KALLEND and G. J. DAVIES (1971). The elastic and plastic anisotropy of cold rolled sheets of copper, gilding metal and α -brass. *J. Inst. Met.*, **5**, 257–260
176. J. S. KALLEND and G. J. DAVIES (1972). The development of texture in copper and copper-zinc alloys. *Texture*, **1**, 51–69
177. J. S. KALLEND, P. P. MORRIS and G. J. DAVIES (1976). Texture transformation — the misorientation distribution function. *Acta Met.*, **24**, 361–370
- 177a. R. KERN and H. BERGMANN (1979). A simple way for calculation of ODF from incomplete pole figures. In reference 4a, p. 139
178. K. KLEINSTÜCK and J. TOBISCH (1968). Die Methode der Texturuntersuchung mittels Neutronenbeugung und ihre besonderen Anwendungsvorteile. *Kristall Techn.*, **3**, 455–466
179. K. KLEINSTÜCK, J. TOBISCH, M. BETZL, A. MÜCKLICH, D. SCHLÄFER and U. SCHLÄFER (1976). Texturuntersuchungen von Metallen mittels Neutronenbeugung. *Kristall Techn.*, **11**, 409–429
180. G. KNEER (1964). Zur Elastizität vielkristalliner Aggregate mit und ohne Textur. Thesis, Clausthal
181. G. KNEER (1965). Über die Berechnung der Elastizitätsmoduln vielkristalliner Aggregate mit Textur. *Phys. Stat. Sol.*, **9**, 825–838
182. W. R. KRIGBAUM (1970). A refinement procedure for determining the crystallite orientation distribution function. *J. Phys. Chem.*, **74**, 1108–1113
183. W. R. KRIGBAUM, T. ADACHI and J. V. DAWKINS (1968). Crystallite orientation distribution in biaxially oriented polyethylene. *J. Chem. Phys.*, **49**, 1532–1542
184. W. R. KRIGBAUM and Y. I. BALTA (1967). Pole-figure inversion for the triclinic crystal class polyethylene terephthalate. *J. Phys. Chem.*, **71**, 1770–1779
185. W. R. KRIGBAUM and R. J. ROE (1964). Crystallite orientation in materials having fiber texture II: A study of strained samples of crosslinked polyethylene. *J. Chem. Phys.*, **41**, 737–748
186. W. R. KRIGBAUM and A. M. H. VASEK (1972). A test of the refinement procedure for determining the crystallite orientation distribution: polyethylene terephthalate. *Texture*, **1**, 9–16
187. E. KRÖNER (1958). Berechnung der elastischen Konstanten des Vielkristalles aus den Konstanten des Einkristalls. *Z. Phys.*, **151**, 504–518

188. E. KRÖNER (1974). Elastizität und Plastizität der Vielkristalle. In *Mechanische Anisotropie* (ed. H. P. STÜWE), Springer-Verlag, Wien/New York
189. A. KUMAR and W. B. HUTCHINSON (1973). Elastic and plastic anisotropy in molybdenum TZM alloy. In reference 3, pp. 527–541
190. J. KUSNIERZ and Z. JASIENSKI (1973). Influence de la Texture sur la Rupture des Bandes Minces du Laiton Application à l'Essai d'expansion sur Poinçon. In reference 3, pp. 469–494
191. F. C. VON DER LAGE and H. A. BETHE (1947). A method for obtaining electronic eigenfunctions and eigenvalues in solids with an application to sodium. *Phys. Rev.*, **71**, 612–622
192. E. LAINE, J. KIVILÄ and I. LÄHTEENMÄKI (1977). A study of preferred orientation by energy dispersive X-ray diffraction. *Texture*, **2**, 243–251
193. O. LAPORTE (1948). Polyhedral harmonics. *Z. Naturforsch.*, **3a**, 447–456
194. T. LEFFERS (1968). Computer simulation of the plastic deformation in face-centered cubic polycrystals and the rolling texture derived. *Phys. Stat. Sol.*, **25**, 337–344
195. J. LENSE (1954). *Kugelfunktionen*, Akadem. Verlagsgesellschaft Geest & Portig K.-G., Leipzig
196. J. M. LIFSHITZ and L. N. ROSENZWEIG (1946). *J. Exp. Teor. Fiz.*, **11**, 967
197. F. LIHL and W. PEXA (1967). Kristallographische Zusammenhänge zwischen der Walz- und der Rekrystallisationstextur des Aluminiums. *Z. Metallkde.*, **58**, 465–470
198. G. LINSSEN, H. D. MENGELEBERG and H. P. STÜWE (1964). Zyklische Texturen in Drähten kubisch-flächenzentrierter Metalle. *Z. Metallkde.*, **55**, 600–604
199. G. J. LJUBARSKI (1962). *Anwendungen der Gruppentheorie in der Physik*, VEB Deutscher Verlag der Wissenschaften, Berlin
200. K. LÜCKE (1968). Beispiele für die Anwendung eines dreidimensionalen Orientierungsraumes zur Ermittlung und Darstellung von Orientierungsverteilungen. In reference 1, pp. 36–50
201. K. LÜCKE, H. PERLWITZ and W. PITTSCH (1964). Elektronenmikroskopische Bestimmung der Orientierungsverteilung der Kristallite in gewalztem Kupfer. *Phys. Stat. Sol.*, **7**, 733–746
202. K. LÜCKE and H. PERLWITZ (1970). Neuere Gesichtspunkte zur Ermittlung und Beschreibung der Orientierungsverteilungen vielkristalliner Werkstoffe. In *Neuere metallkundliche Untersuchungsverfahren*, Verlag Stahleisen, Düsseldorf
203. K. LÜCKE, R. RIXEN and M. SENNA (1976). Formation of recrystallization textures in rolled aluminium single crystals. *Acta Met.*, **24**, 103–110
204. S. MATTHIES (1979). On the reproducibility of the orientation distribution function of texture samples from pole figures (ghost phenomena). *Phys. Stat. Sol. (b)*, **92**, K 135–138
205. J. P. MARDON, M. PERNOT, P. DERVIN and R. PENELLE (1977). Contribution de la Diffraction Neutronique à l'Etude de la Fonction de Texture du Titane Recristallisé, Comparaison avec la Diffraction des Rayons X. *J. Appl. Cryst.*, **10**, 372–375
206. H. MARGENAU and G. M. MURPHY (1943). *The Mathematics of Physics and Chemistry*, Van Nostrand, New York
207. M. MATSUO, S. HAYAMI and S. NAGASHIMA (1971). A study of recrystallization texture formation in cold rolled iron sheets with X-ray diffraction technique. *Adv. X-Ray Anal.*, **14**, 214–230
208. K. N. MELTON, J. W. EDINGTON, J. S. KALLEND and C. P. CUTLER (1974). Textures in superplastic Zn–40wt.% Al. *Acta Met.*, **22**, 165–170
209. B. MEYER (1954). On the symmetries of spherical harmonics. *Can. J. Math.*, **6**, 135–157
210. P. R. MORRIS (1959). Reducing the effects of nonuniform pole distribution in inverse pole figure studies. *J. Appl. Phys.*, **30**, 595–596
211. P. R. MORRIS (1966). Inversion of pole figures for materials having orthorhombic symmetry. *J. Appl. Phys.*, **37**, 359–364
212. P. R. MORRIS (1969). Averaging fourth-rank tensors with weight functions. *J. Appl. Phys.*, **40**, 447–448
213. P. R. MORRIS (1970). Elastic constants of polycrystals. *Int. Eng. Sci.*, **8**, 49–61
214. P. R. MORRIS (1971). Crystallite orientation analysis for materials with tetragonal hexagonal and orthorhombic crystal symmetries. In reference 2, pp. 87–123
215. P. R. MORRIS (1971). Iterative scheme for calculating polycrystal elastic constants. *Int. J. Eng. Sci.*, **9**, 917–920
216. P. R. MORRIS (1976). Program for calculation of augmented Jacobi polynomials. *Texture*, **2**, 57–66
217. P. R. MORRIS (1975). Crystallite orientation analysis from incomplete pole figures. *Adv. X-Ray Anal.*, **18**, 514–534
218. P. R. MORRIS and A. J. HECKLER (1968). Crystallite orientation analysis for rolled cubic materials. *Adv. X-Ray Anal.*, **11**, 454–472
219. P. R. MORRIS and A. J. HECKLER (1969). Crystallite orientation analysis for rolled hexagonal materials. *Trans. Met. Soc. AIME*, **245**, 1877–1881
- 219a. A. NIGGLI and H. WONDRTSCHECK (1960). Eine Verallgemeinerung der Punktgruppen. *Z. Krist.*, **114**, 215
220. J. F. NYE (1957). *Physical Properties of Crystals*, Clarendon Press, Oxford
221. P. PARNIÈRE (1977). Modifications de Texture Cristallographique Associées aux Déformations en Expansion Biaxiale des Toles Minces d'Acier Extra Doux. *Mem. Sci. Rev. Mét.*, **74**, 129–132
222. P. PARNIÈRE (1978). Etude de la Formation des Textures de Toles Minces d'Acier Extra Doux au Vue d'Améliorer leurs Propriétés d'Emploi. Thesis, Paris
223. P. PARNIÈRE and G. DOMEY (1973). Relations Entre la Texture et l'Emboutissabilité des Toles Minces. In reference 3, pp. 495–525
224. P. PARNIÈRE and L. ROESCH (1973). Analyse Quantitative des Relations Entre Coefficient d'Anisotropie et la Texture des Toles Minces d'Acier Extra Doux. In reference 3, pp. 585 to 617
225. P. PARNIÈRE and L. ROESCH (1975). Calcul du Facteur de Taylor pour des Métaux de Structure Cubique Centrée se Déformant par Glissement non Cristallographique ('Pencil Glide'). *Mem. Sci. Rev. Mét.*, **72**, 221–240
226. R. PENELLE (1973). Les Figures de Poles Directes et Inverse leurs Limitations-Introduction et Interet de la Representation Tridimensionnelle des Textures. In reference 3, pp. 13–28
227. H. PERLWITZ, K. LÜCKE and W. PITTSCH (1969). Determination of the orientation distribution of the crystallites in rolled copper and brass by electron microscopy. *Acta Met.*, **17**, 1183–1195
228. H. PERLWITZ, W. PITTSCH and K. LÜCKE. Determination of the true distribution of crystal orientations in cold rolled metals by electron diffraction. In *Recrystallisation, Grain Growth and Textures*, pp. 367–374

229. M. PERNOT, P. PARNIÈRE, R. PENELLE and P. LACOMBE (1973). Relations Entre les Textures et l'Anisotropie Magnetocrystalline de Tôles d'Aciers Extra-Doux. In reference 3, pp. 439–452
230. M. PERNOT, R. PENELLE and P. LACOMBE (1974). The influence of the crystallite orientation distribution function (ODF) on the magnetocrystalline anisotropy of a rimmed steel thin sheet. *IEEE Trans. Magnetics*, **10**, 120–122
231. W. PITSCHE, H. PERLWITZ and K. LÜCKE (1964). Elektronenmikroskopische Bestimmung der Orientierungsverteilung der Kristallite in vielkristallinen Metallen. *Phys. Stat. Sol.*, **7**, K 105–108
232. J. POSPIECH (1972). Die Parameter der Drehung und die Orientierungsverteilungsfunktion (OVF). *Kristall Techn.*, **7**, 1057–1072
233. J. POSPIECH (1976). The analysis of texture on the basis of its three-dimensional representation. *Scientific Bulletin of the Stanislaw Staszic University of Mining and Metallurgy*, No. 586 (in Polish)
234. J. POSPIECH, A. GNATEK and K. FICHTNER (1974). Symmetry in the space of Euler angles. *Kristall Techn.*, **9**, 729–742
235. J. POSPIECH and J. JURA (1971). The orientation distribution function in space of rotation. In reference 2, pp. 73–85
236. J. POSPIECH and J. JURA (1972). Analiza tekstury przy użyciu parametrow osi i kata obrotu. *Hutnik*, **39**, 539–545
237. J. POSPIECH and J. JURA (1975). FOURIER coefficients of the generalized spherical functions and an exemplary computer program. *Kristall Techn.*, **10**, 783–787
238. J. POSPIECH and J. JURA (1974). Determination of the orientation distribution function from incomplete pole figures. *Z. Metallkde.*, **65**, 324–330
239. J. POSPIECH, J. JURA and A. MACIOSOWSKI (1973). Transformation of texture on the example of the bainitic transformation. In reference 3, pp. 117–135
240. J. POSPIECH and K. LÜCKE (1975). The rolling textures of copper and α -brasses discussed in terms of the orientation distribution function. *Acta Met.*, **23**, 997–1007
241. J. POSPIECH, W. TRUSZKOWSKI, J. JURA and J. KROL (1975). The development of rolling texture in polycrystalline silver within a wide range of deformation. In reference 4 pp. 23–32
242. R. J. PRICE and J. C. BOKROS (1965). Relationship between preferred orientation, thermal expansion and radiation induced length changes in graphite. *J. Appl. Phys.*, **36**, 1897–1906
243. H. PURSEY and H. L. COX (1954). The correction of elasticity measurements on slightly anisotropic materials. *Phil. Mag.*, **45**, 295–302
244. A. REUSS (1929). Berechnung der Fließgrenze von Mischkristallen auf Grund der Plastizitätsbedingung für Einkristalle. *Z. Angew. Math. Mech.*, **9**, 49–58
245. I. M. RHYSIK and I. S. GRADSTEIN (1957). *Summen-, Produkt- und Integral-Tafeln*, VEB Deutscher Verlag der Wissenschaften, Berlin
246. R. J. ROE (1965). Description of crystallite orientation in polycrystalline materials. III. General solution to pole figure inversion. *J. Appl. Phys.*, **36**, 2024–2031
247. R. J. ROE and W. R. KRIGBAUM (1964). Description of crystallite orientation in polycrystalline materials having fibre texture. *J. Chem. Phys.*, **40**, 2608–2615
248. R. J. ROE (1966). Inversion of pole-figures for materials having cubic crystal symmetry. *J. Appl. Phys.*, **37**, 2069–2072
249. M. A. ROTHWELL (1971). A computer program for the construction of pole figures. *J. Appl. Cryst.*, **4**, 494–497
250. D. RUER (1976). Méthode Vectorielle d'Analyse de la Texture. Thesis, University of Metz
251. D. RUER and R. BARO (1977). A new method for the determination of the texture of materials of cubic structure from incomplete reflection pole figures. *Adv. X-Ray Anal.*, **20**, 187
252. C. M. SARGENT (1974). Texture transformation. *Scripta Met.*, **8**, 821–824
253. D. SCHLÄFER (1968). Die Anwendung des Zuverlässigkeitsskriteriums für Polfiguren kubischer Metalle. *Kristall Techn.*, **3**, 473–476
254. U. SCHLÄFER (1976). Texturuntersuchungen an Aluminiumrohren. *Neue Hütte*, **21**, 287–291
255. D. SCHLÄFER and H. J. BUNGE (1971). Rolling and recrystallization textures of iron. In reference 2, pp. 155–161
256. U. SCHLÄFER and H. J. BUNGE (1971). Cyclic textures in aluminium wires. In reference 2, pp. 149–154
257. U. SCHLÄFER and H. J. BUNGE (1971). Cyclic textures in aluminium wires. *Texture*, **1**, 31–49
258. D. SCHLÄFER and H. J. BUNGE (1973). Anwendung der dreidimensionalen Orientierungsverteilungsfunktion zur Beurteilung der Walztextur des Eisens. *Neue Hütte*, **18**, 299–303
259. D. SCHLÄFER and H. J. BUNGE (1974). The development of the rolling texture of iron determined by neutron-diffraction. *Texture*, **1**, 157–171
260. U. SCHMIDT (1975). Rekristallisationstexturen von Cu–Zn, Cu–Ge und Cu–P sowie Silber nach Walzen bei verschiedenen Temperaturen. Thesis, Aachen
261. K. SCHMIDT, K. LÜCKE and J. POSPIECH (1975). Recrystallization textures in rolled high purity copper and copper alloys. In reference 4, pp. 147–158
262. D. F. SCOTT and W. B. HUTCHINSON (1973). Application of neutron diffraction to the study of texture and magnetic properties in grain oriented silicon iron. In reference 3, pp. 427–438
263. H. J. SPANGENBERG (1977). Rechenprogramm zur Berechnung der Orientierungsverteilungsfunktion verschiedener Symmetrien. Thesis, Aachen
264. H. STÄBLEIN (1966). Quantitative Beziehungen zwischen Textur und Remanenz in hexagonalen Ferriten. *Techn. Mitt. Krupp. Forsch. Ber.*, **24**, 103–112
265. H. STÄBLEIN and J. WILLBRAND (1966). Quantitative Texturbestimmung von vorzugsgerichtetem Bariumferrit. *Z. Angew. Phys.*, **21**, 47–51
266. H. STADELMAIER and B. F. BROWN (1956). Einfluß elastischer Spannungen auf Rekristallisationstexturen. *Z. Metallkde.*, **47**, 1–8
267. R. S. STEIN and T. HOTTA (1964). Light scattering from oriented polymer films. *J. Appl. Phys.*, **35**, 2237–2242
268. R. S. STEIN and S. N. STIDHAM (1964). A theory of orientation correlations in crystalline polymeric solids. *J. Appl. Phys.*, **35**, 42–46
269. C. A. STICKELS and P. R. MOULD (1970). The use of Young's modulus for predicting the plastic-strain ratio of low-carbon steel sheets. *Met. Trans.*, **1**, 1303–1312
270. D. E. STOTT, R. PENELLE, M. PERNOT and W. B. HUTCHINSON (1975). A comparison of the series expansion and iterative least squares method in the determination of orientation distribution. In reference 4, pp. 1–11
271. E. F. STURCKEN and J. W. CROACH (1963). Predicting physical properties in oriented metals. *Trans. Met. Soc. AIME*, **227**, 934–940
272. E. F. STURCKEN and W. R. McDONELL (1962). An X-ray method for predicting anisotropic irradiation growth in uranium. *J. Nucl. Mat.*, **7**, 85–91

273. J. SZPUNAR (1973). About the correlation of the torque curve measurements with texture in Fe—Si steel sheets. In reference 3, pp. 673—677
274. J. SZPUNAR and M. OJANEN (1975). Texture and magnetic properties in Fe—Si steels. *Met. Trans. AIME*, **6A**, 561—567
275. J. SZPUNAR, M. OJANEN and E. LAINE (1974). Application of the energy dispersive X-ray diffraction method to texture measurements. *Z. Metallkde.*, **65**, 221—226
276. I. P. TALASCHKEWITZ, N. F. KOSTIN and K. S. ALEXANDROW (1964). Elastic properties of fibre textures of cubic metals. *Fiz. Metallov Metalloved.*, **17**, 237—242 (in Russian)
277. C. TAVARD and F. ROYER (1977). Indices de Texture partiels des Solides Polycristallines et Interprétation de l'Approximation de Williams. *C. R. Acad. Sci., Paris*, **284**, 247
278. G. I. TAYLOR (1938). Plastic strain in metals. *J. Inst. Met.*, **62**, 307—324
279. G. F. TAYLOR (1924). A method of drawing metallic filaments and a discussion of their properties and uses. *Phys. Rev.*, **23**, 655—660
280. J. TOBISCH, M. BETZL and P. REICHEL (1971). Texture investigations by neutron diffraction using a fully automatic, programmable goniometer. In reference 2, pp. 269—277
281. J. TOBISCH and H. J. BUNGE (1972). The spherical sample method in neutron diffraction texture determination. *Texture*, **1**, 125—127
282. I. TOMOV and H. J. BUNGE (1979). An analytical method for the quantitative determination of the volume fractions in fibre textures. *Texture*, **3**, 73—83
283. I. TOMOV, K. KÜTTNER and H. J. BUNGE. An analytical method for the quantitative determination of the volume fractions in fibre textures. *Texture* (private communication)
284. I. TOMOV, D. SCHLÄFER and K. KÜTTNER (1977). Bestimmung der Mengenanteile von Fasertexturen. *Kristall Techn.*, **12**, 709—715
285. W. TRUSZKOWSKI, J. POSPIECH, J. JURA and B. MAJOR (1973). A quantitative approach to texture in silver submitted to cold rolling. In reference 3, pp. 235—257
286. G. E. G. TUCKER and P. C. MURPHY (1952/53). A method of determining orientations in aluminium single crystals and polycrystalline aggregates. *J. Inst. Met.*, **8**, 235—244
287. A. VADON and R. BARO. Automatic drawing of isointensity curves. *Texture* (to be published)
288. C. A. VERBRAAK (1958). The formation of cube recrystallization textures by <112>-slip. *Acta Met.*, **6**, 580—597
289. A. S. VIGLIN (1960/61). A quantitative measure of the texture of a polycrystalline material. Texture function. *Soviet Phys., Solid State*, **2**, 2195—2207
290. A. S. VIGLIN and I. P. KUDRYAVTSEV (1959/60). Determination of the degree of perfection of the texture of polycrystalline ferromagnetic. *Soviet Phys., Solid State*, **1**, 229—233
291. W. VOIGT (1928). *Lehrbuch der Kristallphysik*, B. G. Teubner Verlag, Leipzig
292. F. WAGNER, C. ESLING and R. BARO (1977). A new library program for texture calculations. *Texture*, **2**, 235—241
293. J. L. WALTER and C. G. DUNN (1960). Growth of (100) [001]-oriented grains in high-purity silicon iron — a unique form of secondary recrystallization. *Trans. Met. Soc. AIME*, **218**, 1033—1038
294. G. WASSERMANN (1963). Der Einfluß mechanischer Zwillingsbildung auf die Entstehung der Walztextur kubisch flächenzentrierter Metalle. *Z. Metallkde.*, **54**, 61—65
295. H. R. WENK and W. R. WILDE (1972). Orientation distribution for three yule marble fabrics. In *Flow and Fracture of Rocks* (ed. H. C. HEARD, I. Y. BORG, N. L. CARTER and C. B. RAYLEIGH), Geophysical Monograph Series, Vol. 16, Washington
296. K. WEISSENBERG, (1922). Statistische Anisotropie in kristallinen Medien und ihre röntgenographische Bestimmung. *Ann. Phys.*, **69**, 409—435
297. E. WIGNER (1931). *Gruppentheorie und ihre Anwendung auf die Quantenmechanik der Atomspektren*, Friedrich Vieweg, Braunschweig
298. N. J. WILENKEN (1965). *Special Functions and the Representation Theory of Groups* (in Russian), Izdatelstvo Nauka, Moscow
299. R. O. WILLIAMS (1968). The representation of the textures of rolled copper, brass and aluminium by biaxial pole figures. *Trans. Met. Soc. AIME*, **242**, 104—115
300. D. J. WILLIS and M. HATHERLY (1975). Texture development in niobium-stabilized steel sheet. In reference 4, pp. 48—52
301. S. D. WOLKOV and N. A. KLINSKICH (1965). Zur Theorie der elastischen Eigenschaften von Polykristallen. *Fiz. Metallov Metalloved.*, **19**, 25—32
302. H. WONDRTSCHEK (1958). Über die Möglichkeit der Beschreibung kristallographischer Eigenschaften durch Flächen. *Z. Kristallog.*, **110**, 127—135

Appendix 1

Table 9.2—Table 9.14

Table 9.2 The heading of the computer output of the ODF program

```

THREE DIMENSIONAL ANALYSIS OF TEXTURES
*****  

PING PROGRAM — VERSION FEBRUARY 1975
*****  

DATA BLOCK NO. 1.  

*****  

*****  

THE INVESTIGATION OF ROLLING TEXTURE IN SILVER      20/05/75  

*****  

*****  

MATERIAL SILVER MEASURED B.MAJUR LABORATORY ZPM-PAN  

*****  

SPECIMEN DATA SAMPLE / SERIES Z R = 98.  

*****  

NUMBER OF MEASURED POLE FIGURES S. MAXIMAL L VALUE Z.  

*****  

KIND OF POLE FIGURES ANGULAR STEPS  

*****  

HKL D-ALF D-BEI  

113. 5. >  

111. 5. >  

110. 5. >  

*****  

PROGRAMMER J.JURA
*****
```

Table 9.3 Transmission and reflection region of the pole figure, and the correction factors and the calculated accommodation factor

EVIDENCE FOR RULE FIGURE HKL# 113.

TYPE OF CORRECTION	COR R	GR#	GT#
ANGULAR LIMITS		35.0	35.0
ANGULAR INTERVALS RAD#	5.0	HOR#	5.0

CORRECTIONS FOR MATRIX R

1.000	1.000	1.000	1.000	1.000	1.091	1.500	1.866
-------	-------	-------	-------	-------	-------	-------	-------

CORRECTIONS FOR MATRIX T

1.111 1.000	1.111 1.000	1.000 1.000	1.000 1.000	1.000 1.000	1.000 1.000	1.000 1.000	1.000 1.000
----------------	----------------	----------------	----------------	----------------	----------------	----------------	----------------

MATRIX R

44.000 44.000 44.000	44.000 44.000 44.000	44.000 44.000 44.000	44.000 44.000 44.000	44.000 44.000 44.000	44.000 44.000 44.000	44.000 44.000 44.000	44.000 44.000 44.000
20.000 24.000 41.000	19.000 20.000 41.000	18.000 28.000 40.000	16.000 31.000 40.000	16.000 34.000 37.000	17.000 37.000 38.000	19.000 38.000 40.000	22.000 40.000 40.000
9.000 18.000 57.000	9.000 19.000 58.000	9.000 22.000 58.000	10.000 25.000 28.000	11.000 31.000 34.000	11.000 34.000 36.000	12.000 38.000 34.000	12.000 42.000 24.000
7.000 16.000 50.000	8.000 17.000 55.000	9.000 22.000 54.000	10.000 28.000 32.000	11.000 37.000 37.000	12.000 42.000 47.000	13.000 45.000 47.000	13.000 46.000 47.000
12.000 19.000 90.000	14.000 20.000 105.000	15.000 22.000 108.000	16.000 27.000 55.000	17.000 35.000 46.000	17.000 39.000 59.000	17.000 42.000 71.000	18.000 44.000 71.000
58.000 50.000 132.000	43.000 44.000 163.000	47.000 40.000 179.000	52.000 59.000 32.000	58.000 42.000 58.000	61.000 51.000 67.000	62.000 68.000 57.000	57.000 90.000 57.000
81.000 97.000 100.000	85.000 74.000 155.000	93.000 61.000 180.000	106.000 51.000 155.000	116.000 46.000 180.000	121.000 47.000 178.000	118.000 54.000 109.000	109.000 64.000 109.000
42.000 36.000 60.000	42.000 35.000 90.000	42.000 31.000 110.000	42.000 31.000 32.000	43.000 32.000 33.000	44.000 37.000 37.000	44.000 45.000 42.000	42.000 12.000 42.000

MATRIX T

56.000 37.000 34.000	57.000 26.000 43.000	58.000 16.000 55.000	40.000 12.000 11.000	45.000 10.000 10.000	47.000 11.000 11.000	50.000 12.000 12.000	48.000 19.000 19.000
15.000 17.000 28.000	15.000 12.000 37.000	12.000 9.000 44.000	12.000 8.000 8.000	12.000 8.000 8.000	14.000 10.000 10.000	17.000 12.000 12.000	19.000 18.000 18.000
Φ 3.000 8.000 19.000	3.000 0.000 23.000	3.000 4.000 26.000	2.000 4.000 6.000	2.000 6.000 9.000	4.000 8.000 12.000	6.000 12.000 18.000	8.000 12.000 12.000
8.000 10.000 17.000	7.000 9.000 16.000	6.000 7.000 15.000	5.000 8.000 12.000	6.000 12.000 14.000	9.000 12.000 14.000	11.000 18.000 18.000	12.000 18.000 18.000
25.000 17.000 21.000	20.000 11.000 15.000	15.000 9.000 12.000	13.000 10.000 17.000	14.000 17.000 21.000	17.000 20.000 27.000	21.000 30.000 36.000	27.000 30.000 30.000
48.000 56.000 56.000	40.000 57.000 27.000	38.000 79.000 24.000	25.000 16.000 22.000	30.000 22.000 40.000	45.000 40.000 56.000	55.000 56.000 55.000	60.000 60.000 60.000
41.000 115.000 48.000	58.000 60.000 58.000	50.000 54.000 55.000	24.000 24.000 24.000	29.000 24.000 38.000	51.000 58.000 59.000	98.000 59.000 59.000	135.000 68.000 68.000
10.000 70.000 42.000	11.000 38.000 34.000	12.000 20.000 24.000	13.000 17.000 17.000	18.000 19.000 25.000	25.000 28.000 45.000	49.000 45.000 56.000	80.000 80.000 56.000
6.000 28.000 28.000	4.000 17.000 20.000	7.000 10.000 17.000	9.000 12.000 17.000	9.000 12.000 17.000	11.000 22.000 22.000	18.000 27.000 32.000	29.000 32.000 32.000
11.000 15.000 15.000	15.000 15.000 16.000	19.000 16.000 17.000	17.000 20.000 24.000	17.000 20.000 24.000	12.000 24.000 29.000	9.000 25.000 25.000	11.000 19.000 16.000
34.000 8.000 5.000	43.000 11.000 8.000	32.000 23.000 12.000	32.000 32.000 12.000	38.000 32.000 19.000	51.000 38.000 19.000	11.000 19.000 8.000	7.000 8.000 4.000
55.000 9.000 2.000	74.000 13.000 5.000	85.000 25.000 5.000	64.000 41.000 46.000	56.000 46.000 25.000	56.000 46.000 25.000	20.000 25.000 7.000	15.000 10.000 7.000
NORMALISATION FROM *CORRECTION* PROGRAM NC# 0.475453							

Table 9.4 The corrected complete pole figure

CORRECTED MATRIX P FOR FIGURE HKL= 113.								
γ								
18.6/V	18.6/V	18.6/V	18.6/V	18.6/V	18.6/V	18.6/V	18.6/V	18.6/V
18.6/V	18.6/V	18.6/V	18.6/V	18.6/V	18.6/V	18.6/V	18.6/V	18.6/V
18.6/V	18.6/V	18.6/V	18.6/V	18.6/V	18.6/V	18.6/V	18.6/V	18.6/V
8.309	7.893	7.478	6.647	6.647	7.064	7.893	9.140	10.617
9.970	10.001	11.032	12.878	14.125	15.371	15.780	16.617	17.000
17.033	17.053	16.617						
3.739	3.739	3.739	3.739	4.124	4.570	5.401	6.251	
7.478	7.893	9.140	10.380	11.032	12.878	14.125	15.371	16.950
15.371	15.780	15.780						
3.739	3.739	3.739	3.739	4.124	4.570	5.401	6.251	
7.478	7.893	9.140	10.380	11.032	12.878	14.125	15.371	16.950
2.908	3.323	3.739	4.124	4.124	4.570	4.985	5.810	
6.657	7.893	9.140	11.032	13.494	15.371	17.448	19.323	
20.772	22.078	22.433						
4.985	5.016	6.451	6.647	7.002	7.064	7.064	7.478	
7.893	8.309	9.140	11.217	14.360	19.110	24.371	29.490	
57.389	42.390	44.867						
17.463	19.489	21.304	23.308	26.688	27.647	28.701	29.555	
26.606	19.462	18.169	17.076	19.030	23.115	30.820	40.791	
39.847	73.878	81.149						
45.763	45.905	50.220	57.247	62.047	65.368	65.747	68.867	
52.380	39.965	32.946	27.543	24.843	25.383	29.163	34.564	
54.000	82.710	97.211						
44.572	45.569	44.720	47.080	50.011	52.319	58.850	60.496	
45.549	26.448	18.836	14.124	12.947	11.770	14.947	23.240	
46.018	56.903	62.381						
14.443	14.443	15.334	15.334	15.334	15.256	18.887	21.109	
18.887	13.332	9.999	8.888	8.888	11.110	14.443	19.998	
31.108	41.107	48.884						
5.000	5.000	5.000	5.000	5.000	6.000	6.000	8.000	
8.000	6.000	4.000	4.000	6.000	9.000	12.000	15.000	
19.000	25.000	26.000						
8.000	7.000	6.000	5.000	6.000	7.000	11.000	12.000	
10.000	9.000	7.000	8.000	12.000	18.000	19.000	19.000	
17.000	16.000	15.000						
23.000	24.000	15.000	15.000	14.000	21.000	27.000	29.000	
17.000	11.000	9.000	10.000	17.000	20.000	36.000	50.000	
21.000	15.000	12.000						
48.000	40.000	30.000	25.000	30.000	45.000	75.000	80.000	
56.000	51.000	19.000	16.000	22.000	40.000	56.000	55.000	
58.000	27.000	24.000						
61.000	56.000	50.000	44.000	29.000	51.000	98.000	135.000	
113.000	68.000	56.000	44.000	24.000	38.000	59.000	68.000	
66.000	58.000	55.000						
10.000	11.000	12.000	15.000	18.000	23.000	49.000	80.000	
70.000	58.000	20.000	17.000	19.000	28.000	45.000	56.000	
42.000	34.000	24.000						
6.000	6.000	7.000	9.000	9.000	11.000	18.000	29.000	
28.000	17.000	10.000	12.000	17.000	22.000	27.000	32.000	
26.000	20.000	17.000						
11.000	15.000	19.000	17.000	12.000	9.000	9.000	11.000	
13.000	15.000	14.000	20.000	29.000	29.000	19.000	16.000	
15.000	16.000	17.000						
34.000	43.000	52.000	58.000	60.000	11.000	7.000	8.000	
8.000	11.000	25.000	32.000	38.000	19.000	8.000	4.000	
5.000	6.000	12.000						
22.000	16.000	85.000	64.000	36.000	60.000	15.000	10.000	
9.000	15.000	25.000	41.000	46.000	25.000	7.000	2.000	
6.000	5.000	7.000						

Table 9.5 The normalized pole figure

NORMALIZED PULSE FIGURE NKL = 715.																		
0.0	5.0	10.0	15.0	20.0	25.0	30.0	35.0	40.0	45.0	50.0	55.0	60.0	65.0	70.0	75.0	80.0	85.0	90.0
0.0	0.7	0.7	0.7	0.7	0.7	0.7	0.7	0.7	0.7	0.7	0.7	0.7	0.7	0.7	0.7	0.7	0.7	0.7
5.0	0.3	0.3	0.3	0.3	0.3	0.3	0.3	0.3	0.3	0.3	0.3	0.3	0.3	0.3	0.3	0.3	0.3	0.3
10.0	0.7	0.7	0.7	0.7	0.7	0.7	0.7	0.7	0.7	0.7	0.7	0.7	0.7	0.7	0.7	0.7	0.7	0.7
15.0	0.7	0.7	0.7	0.7	0.7	0.7	0.7	0.7	0.7	0.7	0.7	0.7	0.7	0.7	0.7	0.7	0.7	0.7
20.0	0.2	0.2	0.2	0.2	0.2	0.2	0.2	0.2	0.2	0.2	0.2	0.2	0.2	0.2	0.2	0.2	0.2	0.2
25.0	0.7	0.7	0.7	0.7	0.7	0.7	0.7	0.7	0.7	0.7	0.7	0.7	0.7	0.7	0.7	0.7	0.7	0.7
30.0	7.7	1.0	2.0	2.5	2.5	2.0	2.5	2.5	2.7	2.0	2.5	2.5	2.5	2.5	2.5	2.5	2.5	2.5
35.0	7.7	7.7	1.0	1.0	1.0	2.0	2.2	2.5	2.6	7.7	1.1	1.1	0.7	0.6	0.5	0.5	0.5	0.5
40.0	0.0	0.0	0.0	0.0	0.0	0.0	0.0	0.0	0.0	0.0	0.0	0.0	0.0	0.0	0.0	0.0	0.0	0.0
45.0	0.7	0.1	0.7	0.7	0.7	0.2	0.2	0.2	0.3	0.3	0.2	0.2	0.2	0.2	0.2	0.2	0.2	0.2
50.0	0.3	0.3	0.2	0.2	0.2	0.2	0.4	0.4	0.5	0.4	0.4	0.3	0.3	0.3	0.3	0.3	0.3	0.3
55.0	0.9	0.8	0.0	0.5	0.6	0.8	1.1	1.1	0.7	0.4	0.4	0.6	0.6	0.7	1.0	1.4	0.8	0.0
60.0	1.9	1.0	1.2	2.0	1.4	1.8	3.0	3.2	2.6	1.4	0.7	0.6	0.9	1.0	2.4	2.4	1.4	0.9
65.0	1.0	1.4	1.6	0.9	1.7	2.0	3.9	3.3	4.5	2.4	1.5	0.9	0.9	1.0	2.3	2.7	1.9	1.5
70.0	0.4	0.4	0.2	0.6	0.7	1.0	1.9	3.2	2.8	1.5	0.8	0.7	0.7	1.1	1.8	2.2	1.7	1.3
75.0	0.7	0.2	0.3	0.4	0.4	0.4	0.7	1.1	1.1	0.7	0.4	0.3	0.7	0.9	1.7	1.5	1.7	0.0
80.0	0.4	0.0	0.7	0.7	0.5	0.4	0.4	0.4	0.5	0.5	0.6	0.8	1.1	1.0	0.7	0.6	0.0	0.0
85.0	1.3	1.7	2.7	1.5	0.8	0.4	0.5	0.3	0.3	0.4	0.9	1.3	1.2	0.7	0.3	0.2	0.6	0.3
90.0	2.4	2.9	3.4	2.5	1.4	0.8	0.5	0.6	0.6	0.5	1.0	1.6	1.8	1.0	0.3	0.1	0.7	0.3

Table 9.6 The pole figure recalculated from the coefficients $C_{hkl}^{\mu\nu}$

CALCULATED	PULSE	FIGURE	HELI# 115.	
0.0	0.0	0.0	10.0	15.0
0.0	0.0	0.0	20.0	25.0
0.0	0.0	0.0	30.0	35.0
0.0	0.0	0.0	40.0	45.0
0.0	0.0	0.0	50.0	55.0
0.0	0.0	0.0	60.0	65.0
0.0	0.0	0.0	70.0	75.0
0.0	0.0	0.0	80.0	85.0
0.0	0.0	0.0	90.0	95.0
0.0	0.0	0.0	100.0	115.0
0.0	0.0	0.0	120.0	135.0
0.0	0.0	0.0	140.0	155.0
0.0	0.0	0.0	160.0	175.0
0.0	0.0	0.0	180.0	195.0
0.0	0.0	0.0	200.0	215.0
0.0	0.0	0.0	220.0	235.0
0.0	0.0	0.0	240.0	255.0
0.0	0.0	0.0	260.0	275.0
0.0	0.0	0.0	280.0	295.0
0.0	0.0	0.0	300.0	315.0
0.0	0.0	0.0	320.0	335.0
0.0	0.0	0.0	340.0	355.0
0.0	0.0	0.0	360.0	375.0
0.0	0.0	0.0	380.0	395.0
0.0	0.0	0.0	400.0	415.0
0.0	0.0	0.0	420.0	435.0
0.0	0.0	0.0	440.0	455.0
0.0	0.0	0.0	460.0	475.0
0.0	0.0	0.0	480.0	495.0
0.0	0.0	0.0	500.0	515.0
0.0	0.0	0.0	520.0	535.0
0.0	0.0	0.0	540.0	555.0
0.0	0.0	0.0	560.0	575.0
0.0	0.0	0.0	580.0	595.0
0.0	0.0	0.0	600.0	615.0
0.0	0.0	0.0	620.0	635.0
0.0	0.0	0.0	640.0	655.0
0.0	0.0	0.0	660.0	675.0
0.0	0.0	0.0	680.0	695.0
0.0	0.0	0.0	700.0	715.0
0.0	0.0	0.0	720.0	735.0
0.0	0.0	0.0	740.0	755.0
0.0	0.0	0.0	760.0	775.0
0.0	0.0	0.0	780.0	795.0
0.0	0.0	0.0	800.0	815.0
0.0	0.0	0.0	820.0	835.0
0.0	0.0	0.0	840.0	855.0
0.0	0.0	0.0	860.0	875.0
0.0	0.0	0.0	880.0	895.0
0.0	0.0	0.0	900.0	915.0
0.0	0.0	0.0	920.0	935.0
0.0	0.0	0.0	940.0	955.0
0.0	0.0	0.0	960.0	975.0
0.0	0.0	0.0	980.0	995.0
0.0	0.0	0.0	1000.0	1015.0

Table 9.7 The coefficients $F_{i,\text{exp}}^v$

MATRIX F EXPERIMENTAL 110										
1	$\bar{V} = 1$	2	3	4	5	6	7	8	9	10
11	12									
2	-0.0303	0.0689								
4	-0.0381	0.0724	0.2568							
6	2.1572	-1.4378	1.3084	1.7054						
8	0.3303	0.7043	-0.9951	1.4022	-0.0201					
10	-0.9018	0.5124	-0.0578	-0.0262	-0.0127	0.0573				
12	1.5508	-0.9450	0.5863	-0.9791	-0.1203	1.5169	0.7732			
14	-0.2401	0.0879	-0.7933	0.6600	-0.2032	0.1678	0.0473	0.2402		
16	-0.2478	0.0890	-0.2939	-0.1050	0.1924	-0.5131	0.3329	0.0399	-0.1498	
18	0.3412	-0.0213	0.4447	-0.1610	0.1213	-0.0870	-0.3167	0.2727	0.4770	-0.0530
20	-0.0703 0.2109	0.0719	-0.0919	0.1109	-0.2107	0.2488	-0.0401	-0.0501	0.2232	-0.0773
22	-0.2673 0.0914	0.1583	-0.0753	0.0885	0.0600	-0.1410	0.1409	-0.1014	0.0771	-0.0053

MATRIX F EXPERIMENTAL 111										
1	$\bar{V} = 1$	2	3	4	5	6	7	8	9	10
11	12									
2	0.2652	-0.0916								
4	0.8667	1.7571	0.5868							
6	-2.3977	1.0668	-1.2821	-1.6011						
8	0.6018	0.4889	-0.3678	0.3712	0.0746					
10	-0.4206	-0.0786	0.0971	-1.4603	0.7666	-1.0464				
12	0.9401	-0.6759	0.5972	-0.2767	-0.0778	0.0864	0.1921			
14	-0.6722	0.2849	0.1727	-0.8502	0.2410	-0.2644	-0.0492	-0.3361		
16	0.3338	-0.1386	-0.1716	0.1065	-0.4230	0.4905	-0.0454	0.1227	0.4007	
18	-0.3204	0.2374	-0.0855	-0.2548	-0.0057	-0.0136	0.0073	-0.0704	-0.1904	0.0336
20	0.4458 0.2770	-0.3371	-0.0151	0.0958	-0.3702	0.2506	-0.0577	-0.0311	0.1149	-0.0388
22	-0.2583 -0.1424	0.1700	0.0642	-0.3002	0.0922	-0.1376	0.1410	-0.0365	-0.0614	0.0743

MATRIX F EXPERIMENTAL 113										
1	$\bar{V} = 1$	2	3	4	5	6	7	8	9	10
11	12									
2	-0.7654	0.0303								
4	-0.2913	-0.2944	-0.1559							
6	0.1605	0.7227	-0.1059	-0.0358						
8	-1.6350	-0.3408	0.0672	-0.8590	-0.0099					
10	-0.0379	0.0688	-0.0378	0.3370	-0.0759	0.2745				
12	1.2265	-0.6246	0.1797	-0.6571	0.0000	1.1087	0.0294			
14	-0.3070	0.2503	0.2698	-0.4677	0.1390	-0.1708	-0.0155	-0.2361		
16	0.1501	0.0938	-0.0975	-0.0271	0.2241	-0.2914	0.1461	-0.0754	-0.2386	
18	-0.1650	-0.7589	0.0214	-0.0600	-0.0614	0.1591	-0.0603	-0.0218	-0.1978	-0.0078
20	-0.2706 -0.0176	-0.0490	0.0850	-0.0492	0.0578	0.0506	0.0101	0.0520	-0.0770	0.0360
22	0.1795 0.1867	-0.1209	-0.1971	0.1891	0.0992	-0.1872	0.1463	-0.0899	0.1402	-0.0954

Table 9.8 The coefficients F_{calc}^{ν}

TABLE 9.8 FUR CALCULATED POLE FIGURE 115.

$\nu = 1$	11	12	3	4	5	6	7	8	9	10
4	-0.1664	-0.3983	-0.1881							
6	-0.1841	0.1212	0.1002	-0.1278						
8	-0.0106	-0.3796	0.8660	-1.1365	-0.0129					
10	0.1043	0.0217	0.0206	0.3879	-0.0445	0.4715				
12	1.1438	-0.3948	0.2477	-0.7080	-0.0293	1.1231	0.0399			
14	-0.2203	0.7657	0.1584	-0.5142	0.1505	-0.1582	-0.0292	-0.2092		
16	-0.1483	0.1927	-0.0755	-0.0840	0.2243	-0.2970	0.1569	-0.0289	-0.2077	
18	-0.1897	0.7453	-0.0170	-0.1478	-0.0193	0.0456	0.0156	-0.0311	-0.1105	0.0734
20	-0.0531 -0.0758	-0.0907	0.0743	-0.0616	0.0806	-0.1058	0.0169	0.0447	-0.1257	0.0439
22	0.0554 0.1901 -0.0885	-0.0469	-0.1913	0.6119	0.0929	-0.1859	0.1561	-0.1075	0.1465	-0.0863

Table 9.9 The coefficients C_l^{ν}

MATRIX	C	COEFFICIENTS											
		1	2	3	4	5	6	7	8	9	10	11	12
1	μ												
4	1	-0.8578	-3.0851	-0.9700									
6	1	-6.0043	4.6378	-2.1791	-2.7798								
8	1	2.2018	1.6518	-2.5254	3.1993	0.0365							
10	1	0.7978	0.1660	0.1572	2.9206	-0.3404	2.0760						
12	1	-3.5000	7.0469	0.2732	3.2101	-0.2208	-0.2410	0.5779					
12	2	-2.5353	4.0543	-1.5954	0.3950	0.5836	-1.5157	-0.8143					
14	1	-1.2317	0.7020	0.7730	-2.8723	0.8406	-0.8858	-0.1629	-1.1685				
16	1	-0.7117	1.8421	-1.6729	-0.5513	0.7500	-1.5658	1.6663	0.2886	-0.6049			
16	2	0.6671	-0.3902	-0.5394	0.4139	-1.1735	1.3847	-0.2070	0.5511	1.1347			
18	1	0.7700	0.0058	-1.0876	4.2813	-0.1062	-0.5699	0.7590	-0.4088	-0.0191	-0.0097		
18	2	1.6654	-4.2240	2.0783	-1.4377	0.4666	-0.1616	-1.4328	1.1352	1.7132	-0.1889		
20	1	0.2146	-1.2887	0.5949	-0.5507	0.0385	-0.6490	0.0438	0.5240	-0.8256	0.2655	-0.1555	
20	2	-1.2428	1.0169	0.0261	-0.2879	1.1602	-0.7867	0.1174	0.0820	-0.5516	0.1764	-0.8688	
22	1	-0.1808	0.1618	0.8043	-0.8521	-0.4160	0.8251	-0.6978	0.4697	-0.6105	0.5574	-0.8141	0.3767
22	2	-1.1692	0.7996	0.1135	-0.9525	0.5060	-0.8153	0.8311	-0.3507	-0.0546	0.2280	-0.3269	0.0579

Table 9.10 The coefficients H^i of the normal-direction inverse pole figure

TABLE N FOR INVERSE FIGURE OF THE NORMAL DIRECTION		
1	$\mu = 1$	
4	-1.0156	
6	-3.9369	
8	1.9618	
10	0.6171	
12	-2.5264	-1.6357
14	0.8508	
16	-0.4392	0.4117
18	0.4487	0.9389
20	0.1188	-0.6879
22	-0.0955	-0.4179

Table 9.11 The normal-direction inverse pole figure

Table 9.12 Four sections of the orientation distribution functions $f(\phi_1 \Phi \phi_2)$

(b)

section $\phi_1 = 35^\circ$

$\Phi_1 \approx 35.0$	0.0	5.0	10.0	15.0	20.0	25.0	30.0	35.0	40.0	45.0	50.0	55.0	60.0	65.0	70.0	75.0	80.0	85.0	90.0
0.0	-0.7	-0.9	-1.5	-0.9	-0.7	-1.6	-1.6	-0.7	-0.7	-1.6	-2.1	-2.0	-2.1	-1.6	-0.7	-0.7	-1.6	-1.4	-0.7
5.0	-0.2	-0.0	-1.5	-1.1	-0.8	-1.1	-1.0	-0.3	-0.5	-1.3	-1.7	-1.5	-1.5	-1.3	-1.0	-1.2	-1.6	-0.9	-0.2
10.0	1.1	0.4	-1.1	-1.3	-0.6	-0.1	0.2	0.5	0.2	-0.6	-0.6	-0.0	0.6	0.3	-0.7	-1.6	-1.1	0.5	1.1
15.0	2.3	1.1	-0.4	-0.9	-0.1	0.9	1.1	0.6	0.4	0.6	0.5	1.4	2.9	5.2	1.6	-0.2	0.5	1.8	2.5
20.0	2.8	1.8	0.2	-0.8	-0.6	0.4	0.7	0.2	0.3	0.8	0.8	1.2	5.1	4.6	3.8	2.0	1.8	2.7	2.8
25.0	1.9	1.4	0.4	-1.0	-1.8	-1.3	-0.5	-0.6	-0.5	0.5	0.5	0.4	1.8	4.0	4.5	2.9	1.9	2.0	1.9
30.0	2.8	1.4	0.4	-0.4	-1.6	-1.7	-0.9	-0.9	-1.6	-0.9	0.6	1.3	2.0	3.5	4.0	3.6	3.1	3.4	2.8
35.0	11.0	5.9	1.9	0.7	0.3	0.5	1.0	0.5	-1.6	-1.7	1.1	3.5	3.7	5.6	4.3	5.8	9.0	12.1	17.0
40.0	24.7	15.8	5.9	1.7	1.6	2.6	3.6	3.1	-0.0	-1.5	-1.4	4.8	4.9	5.8	4.6	8.4	16.1	24.5	24.7
45.0	31.9	23.9	10.9	3.1	1.4	2.5	4.0	4.2	1.2	-1.1	1.1	4.2	4.9	5.7	5.8	7.2	15.8	27.5	31.9
50.0	24.7	22.5	12.8	4.6	1.0	0.6	2.0	3.0	1.2	-1.1	-0.0	2.7	5.5	2.8	2.5	3.5	8.0	17.4	24.7
55.0	11.0	12.0	9.7	5.0	1.2	-0.9	-0.6	0.9	1.0	-0.2	-0.4	0.5	0.8	0.8	1.2	1.1	1.7	5.5	11.0
60.0	2.8	4.3	4.7	5.9	1.7	-1.0	-2.1	-0.9	1.0	1.9	1.4	0.1	-1.2	-1.6	0.1	1.1	1.0	1.2	2.8
65.0	7.9	1.0	1.9	2.0	2.4	0.7	-1.6	-2.1	0.1	2.9	3.6	1.6	-0.7	-1.6	-0.2	1.0	2.1	1.9	
70.0	2.6	2.6	1.0	1.7	2.5	2.7	0.9	-1.5	1.8	3.7	2.6	0.2	-0.2	0.4	0.8	1.4	2.4	2.8	
75.0	2.3	2.7	2.1	1.0	1.1	2.4	2.5	0.2	-1.5	0.1	2.5	1.6	-0.4	-0.5	0.9	1.5	2.3	2.5	
80.0	1.1	2.0	1.9	0.4	-1.0	-0.5	1.1	0.6	-1.5	-0.9	1.0	0.7	-1.0	-0.0	1.2	0.4	1.1	1.1	
85.0	-0.2	0.4	0.0	-0.4	-1.4	-3.0	-1.4	-0.5	-1.6	-1.8	-0.1	0.4	-2.1	-3.2	-1.5	-0.1	-0.6	-0.2	
90.0	-0.7	-0.6	-0.0	-0.8	-1.5	-2.4	-0.6	-1.5	-2.5	-1.5	-0.6	-2.4	-3.7	-2.5	-0.8	-0.7	-0.7	-0.7	

(c)

section $\phi_2 = 0^\circ$

$\Phi_2 \approx 0.0$	0.0	5.0	10.0	15.0	20.0	25.0	30.0	35.0	40.0	45.0	50.0	55.0	60.0	65.0	70.0	75.0	80.0	85.0	90.0
0.0	-2.0	-2.1	-1.0	-0.7	-0.7	-1.6	-0.7	-0.7	-1.3	-0.9	-0.9	-0.7	-1.4	-1.6	-0.7	-0.7	-1.6	-2.1	-2.0
5.0	1.7	-1.0	-1.0	-1.1	-1.2	-1.5	-0.9	-0.2	-0.5	-1.2	-1.0	-0.7	-1.1	-1.1	-0.4	-0.9	-1.3	-1.3	-1.3
10.0	-1.0	-1.3	-1.7	-2.0	-2.0	-1.3	0.2	1.1	0.4	-0.7	-1.0	-0.6	0.0	0.6	0.5	0.6	0.9	1.4	1.5
15.0	-0.1	-0.5	-1.3	-2.4	-2.2	-0.5	1.6	2.3	1.3	-0.3	-1.4	-0.8	0.8	1.6	1.0	0.8	2.2	3.8	4.4
20.0	1.3	0.7	-0.6	-1.5	-1.0	0.9	2.6	2.8	1.7	-0.3	-2.5	-2.5	-0.5	0.9	0.5	-0.3	0.8	2.1	2.6
25.0	2.9	2.1	0.7	-0.0	0.2	1.2	2.0	1.9	1.1	-0.5	-2.6	-3.7	-2.6	-1.0	-0.9	-1.7	-2.3	-2.4	-2.6
30.0	4.0	3.1	1.0	0.8	0.5	0.9	2.1	2.8	1.8	0.2	-1.2	-2.4	-2.5	-1.7	-1.0	-1.5	-2.7	-3.9	-4.4
35.0	4.8	3.9	2.0	1.9	2.1	4.4	8.8	11.0	7.8	2.7	0.1	-0.6	-1.0	-0.7	0.5	0.7	-0.3	-1.2	-1.4
40.0	5.7	5.0	4.2	4.3	6.1	11.9	21.0	24.7	17.4	5.9	-0.5	-1.3	-0.9	0.1	2.2	3.1	2.4	1.8	1.7
45.0	6.1	5.0	3.1	5.7	8.4	16.2	27.6	31.9	22.4	7.4	-1.0	-2.3	-1.4	0.3	2.9	4.1	3.6	2.7	2.6
50.0	5.7	5.0	4.2	4.3	6.1	11.9	21.0	24.7	17.4	5.9	-0.5	-1.3	-0.9	0.1	2.2	3.1	2.4	1.8	1.7
55.0	4.8	3.9	2.0	1.9	2.1	4.4	8.8	11.0	7.8	2.7	0.1	-0.6	-1.0	-0.7	0.5	0.7	-0.3	-1.2	-1.4
60.0	4.0	3.1	1.0	0.8	0.5	0.9	2.1	2.8	1.8	0.2	-1.2	-2.4	-2.5	-1.7	-1.0	-1.5	-2.7	-3.9	-4.4
65.0	2.9	2.1	0.7	-0.0	0.2	1.2	2.0	1.9	1.1	-0.5	-2.6	-3.7	-2.6	-1.0	-0.9	-1.7	-2.3	-2.4	-2.6
70.0	1.3	0.7	-0.0	-1.5	-1.0	0.9	2.6	2.8	1.7	-0.3	-2.5	-2.5	-0.5	0.9	0.5	-0.3	0.8	2.1	2.6
75.0	-0.1	-0.5	-1.3	-2.4	-2.2	-0.5	1.6	2.5	1.5	-0.3	-1.4	-0.8	0.8	1.6	1.0	0.8	2.2	3.8	4.4
80.0	-1.0	-1.3	-1.7	-2.0	-2.0	-1.5	0.2	1.1	0.4	-0.7	-1.0	-0.6	0.0	0.4	0.5	0.6	0.9	1.4	1.5
85.0	-1.7	-1.0	-1.0	-1.1	-1.2	-1.5	-0.9	-0.2	-0.5	-1.2	-1.0	-0.7	-1.1	-1.1	-0.4	-0.5	-0.3	-0.9	-1.5
90.0	-2.0	-2.1	-1.0	-0.7	-0.7	-1.6	-1.4	-0.7	-0.9	-1.5	-0.9	-0.7	-1.4	-1.6	-0.7	-0.7	-1.6	-2.1	-2.0

(d) section $\phi_2 = 20^\circ$

	Φ ₂ =0.3	3.0	5.0	10.0	15.0	20.0	25.0	30.0	35.0	40.0	45.0	50.0	55.0	60.0	65.0	70.0	75.0	80.0	85.0	90.0
0.0	-0.7	-1.0	-1.4	-0.7	-0.9	-1.5	-0.9	-0.7	-1.5	-1.6	-0.7	-0.7	-1.6	-0.7	-1.6	-0.7	-1.6	-0.7	-0.7	
5.0	-0.6	-1.3	-1.0	-0.4	-0.9	-1.5	-1.2	-0.8	-1.1	-1.0	-0.2	-0.6	-1.1	-1.5	-1.3	-1.6	-0.9	-0.4	-0.6	
10.0	-1.5	-0.9	-0.0	0.5	-0.5	-1.5	-1.5	-0.6	-0.1	0.2	0.4	0.3	0.1	0.5	1.4	2.2	2.1	1.4	0.7	
15.0	-2.2	-0.9	0.0	1.1	0.2	-0.7	-0.8	-0.1	0.7	0.9	0.5	0.1	0.9	2.5	4.4	5.7	3.1	3.1	2.6	
20.0	-2.9	-0.7	1.4	1.8	1.1	0.5	-0.4	-0.6	-0.1	0.1	-0.4	-0.7	0.2	7.6	5.0	4.2	3.5	1.3	0.3	
25.0	-4.6	-0.9	1.4	2.1	1.9	1.1	-0.4	-1.8	-2.1	-1.5	-1.4	-1.8	-2.2	-2.5	-2.7	-0.9	-0.5	-1.3	-1.6	
30.0	-7.4	-0.0	0.9	1.8	2.1	1.6	0.1	-1.6	-2.2	-1.5	-1.1	-1.9	-3.4	-4.6	-4.2	-2.5	-0.8	0.0	0.5	
35.0	-0.5	0.4	0.0	1.2	1.6	1.5	0.9	0.5	0.2	0.6	0.5	-0.4	-1.7	-2.0	-1.5	-0.7	0.9	2.2	3.2	
40.0	2.0	2.4	1.0	1.5	1.7	1.7	1.4	1.6	1.9	1.7	1.0	0.2	-0.0	0.6	0.7	0.0	-0.3	0.6	1.3	
45.0	3.7	3.3	2.7	2.0	3.2	3.1	2.2	1.4	0.8	-0.5	-1.5	-1.7	-1.7	-0.8	-1.4	-2.3	-2.7	-1.8	-1.4	
50.0	5.8	3.7	3.0	3.5	4.5	4.4	2.9	1.0	-0.6	-2.4	-3.5	-2.7	-1.4	-1.6	-2.7	-2.8	-1.6	-0.7	-0.9	
55.0	4.0	5.0	3.7	2.8	3.5	3.6	2.6	1.2	-0.1	-1.4	-1.8	-0.5	1.5	1.1	-0.3	-0.6	-0.0	-0.5	-1.1	
60.0	4.0	4.2	3.4	2.7	1.5	1.5	1.5	1.7	1.9	1.5	1.0	2.2	5.5	5.0	1.7	0.5	-0.4	-2.7	-3.6	
65.0	2.4	3.4	3.7	1.3	0.7	0.2	1.0	2.4	3.5	3.1	2.1	1.8	1.7	1.2	0.8	0.1	-1.7	-3.5	-6.1	
70.0	0.2	1.0	1.9	0.2	-0.9	-0.5	1.0	2.5	3.6	3.5	1.9	0.6	-0.5	-0.9	0.5	1.4	0.4	-1.6	-1.5	
75.0	-0.0	1.7	1.5	-0.5	-1.3	-0.4	0.4	1.1	1.9	2.2	1.6	0.7	-0.2	-0.0	2.2	4.2	3.2	0.9	0.6	
80.0	1.5	2.8	4.0	-0.1	-0.7	0.0	-0.2	-1.0	-0.6	0.6	1.4	1.6	1.4	1.8	3.7	3.5	4.0	1.5	0.7	
85.0	2.5	3.0	1.8	0.2	0.3	0.9	-0.4	-2.4	-2.5	-0.4	1.4	2.4	2.4	2.0	2.2	2.7	2.3	1.3	0.6	
90.0	2.6	2.1	0.8	-0.3	0.3	0.9	-0.5	-2.5	-2.5	-0.3	1.7	2.8	2.6	0.9	-2.0	-2.5	-0.8	0.7	3.3	

Table 9.13 The error measures, ΔF_i^v , of the coefficients F_i^v

ℓ	v	$\{113\}$	$\{111\}$	$\{110\}$	$F_\ell^V(h)_{\text{exp}}$	ΔF_ℓ^V	ΔF_ℓ	ℓ	v	$\{113\}$	$\{111\}$	$\{110\}$	$F_\ell^V(h)_{\text{exp}}$	ΔF_ℓ^V	ΔF_ℓ		
2	1	-0.1254	0.5252	-0.8363				16	1	0.1501	0.3338	-0.2918	0.3400				
	2	0.0303	-0.0812	0.0689					2	0.0938	-0.1384	0.4090	0.1126				
4	1	-0.2913	0.8627	-0.8381	0.7746				3	-0.0975	-0.1712	-0.2939	0.0251				
	2	-0.2944	1.9517	0.7024	0.2253				4	-0.0271	0.1665	-0.1050	0.0648				
3	-0.1339	0.5686	0.2568	0.0469	0.3489				5	0.2241	-0.4230	0.1924	0.0002				
6	1	0.1865	-2.5977	2.1572	0.2859				6	-0.2914	0.4905	-0.3131	0.0064				
	2	0.1227	1.6648	-1.4518	0.0365				7	0.1461	-0.0434	0.3329	0.0100				
3	-0.1059	-1.2827	1.3004	0.0669					8	-0.0754	0.1221	0.0599	0.0529				
	4	-0.0358	-1.6011	1.7054	0.1420	0.1328			9	0.2386	0.4007	-0.1498	0.0352	0.0711			
8	1	-1.2336	0.4618	0.3363	0.4410			18	1	-0.1650	-0.3204	0.5412	0.0306				
	2	-0.3466	0.4589	0.7045	0.2340				2	0.1589	0.2374	-0.6215	0.0169				
3	0.6672	-0.3818	-0.9931	0.1754				3	0.0214	-0.0855	0.4447	0.0476					
	4	-0.8590	0.5712	1.4022	0.2846				4	-0.0606	-0.2648	-0.1610	0.1078				
5	-0.0099	0.0746	-0.0201	0.0534	0.2377				5	0.0614	-0.0051	0.1213	0.0521				
10	1	-0.0619	-0.4268	-0.9018	0.6431				6	0.1591	-0.0136	-0.0870	0.1405				
	2	0.0648	-0.0786	0.3154	0.2263				7	-0.0205	0.0675	-0.3167	0.0420				
3	-0.0518	-0.0971	-0.0378	0.0586					8	-0.0218	-0.0704	0.2727	0.0115				
	4	0.3376	-1.4805	-0.0262	0.0324					9	-0.1078	-0.1904	0.4770	0.0033			
5	-0.0759	0.1646	-0.0727	0.0584					10	-0.0018	0.0336	-0.0530	0.0188	0.0471			
	6	0.2745	-1.0444	0.0373	0.0410	0.1767		20	1	-0.2768	0.4458	-0.0103	0.2826				
12	1	1.2265	0.9461	1.5568	0.1327				2	-0.0496	-0.3317	0.0779	0.0525				
	2	-0.6248	-0.6759	-0.9456	0.0481				3	0.0836	-0.0151	-0.0919	0.0119				
3	0.1797	0.3972	0.5865	0.1089					4	-0.0492	0.0958	0.1109	0.0159				
	4	-0.6571	-0.2761	-0.9191	0.0817				5	0.0518	-0.3782	-0.2107	0.0367				
5	0.0000	-0.0778	-0.1205	0.0470					6	-0.0304	0.2506	0.2488	0.0935				
	6	1.1087	0.6864	1.5169	0.0231				7	0.0101	-0.0577	-0.0401	0.0087				
7	0.0294	0.1921	0.1752	0.0169	0.0655				8	0.0526	-0.0311	-0.0587	0.0098				
14	1	-0.3670	-0.6122	-0.2401	0.3973				9	-0.0770	0.1149	0.2232	0.0586				
	2	0.2565	0.2849	0.0819	1.1897				10	0.0346	-0.0588	-0.0773	0.0119				
3	0.2038	0.1727	-0.1933	0.0696					11	-0.0116	0.2770	0.2109	0.0818	0.0601			
	4	-0.4677	-0.8502	0.6600	0.0689			22	1	0.1795	-0.2385	-0.2673	0.2656				
5	0.1390	0.2410	-0.2032	0.0276					2	-0.1209	0.1706	0.1585	0.1583				
	6	-0.1788	-0.2644	0.1678	0.0187				3	-0.1971	0.0842	-0.0733	0.0120				
7	-0.0135	-0.0492	0.0475	0.0152					4	0.1891	-0.3002	0.0885	0.0487				
	8	-0.2321	-0.3361	0.2462	0.0231	0.1010			5	0.0982	0.0822	0.0600	0.0134				
									6	-0.1812	-0.1316	-0.1410	0.0100				
									7	0.1443	0.1416	0.1409	0.0251				

Table 9.14 The error measures $\Delta C_l^{\mu\nu}$ of the coefficients $C_l^{\mu\nu}$

ℓ	μ	ν	$C_l^{\mu\nu}$	$\Delta C_l^{\mu\nu}$	C_ℓ	δC_ℓ	ℓ	μ	ν	$C_l^{\mu\nu}$	$\Delta C_l^{\mu\nu}$	C_ℓ	δC_ℓ	
4	1	1	-0.8678	1.1541			18	1	1	0.7700	0.3446			
2	-3.0651	0.3356			2	0.0058	0.1351							
3	-0.9700	0.0698	1.6376	0.5198	3	-1.0876	0.3808							
6	1	1	-4.0043	0.3410			4	2.2613	0.8633					
2	2.6378	0.0436			5	-0.1062	0.4189							
3	-2.1791	0.0797			6	-0.3299	1.1246							
4	-2.7798	0.1694	2.9003	0.1584	7	0.7590	0.3361							
8	1	1	2.2818	0.8331			8	-0.4068	0.0922					
2	1.6318	0.4420			9	-0.0191	0.0263							
3	-2.3264	0.3314			10	-0.0097	0.1505							
4	3.1993	0.5376			2	1	1.6454	0.1715						
5	0.0363	0.1008	1.8949	0.4490	3	-2.2240	0.0948							
10	1	1	0.7978	1.2374			3	2.0183	0.2870					
2	0.1660	0.4354			4	-1.4577	0.6064							
3	0.1572	0.1128			5	0.4666	0.2924							
4	2.9206	0.0624			6	-0.1616	0.7887							
5	-0.3404	0.1123			7	-1.4328	0.2387							
6	2.0760	0.0789	1.0763	0.3399	8	1.1352	0.0647							
12	1	1	-3.5606	0.9662			9	1.7153	0.0184					
2	1.0469	0.3502			10	-0.1889	0.1065	0.9102	0.3207					
3	0.2732	0.7933			20	1	1	0.2146	1.6012					
4	3.2101	0.5946			2	-1.2687	0.2973							
5	-0.2208	0.3425			3	0.5949	0.0875							
6	-4.2410	0.1683			4	-0.3807	0.0898							
7	0.5779	0.1231			5	0.0385	0.2061							
2	-2.3353	0.5814			6	-0.4290	0.5299							
2	2.0543	0.2143			7	0.0438	0.0491							
3	-1.5954	0.4855			8	0.3240	0.0556							
4	0.3956	0.3639			9	-0.8256	0.3374							
5	0.3854	0.2096			10	0.2655	0.0676							
6	-1.5157	0.1030			11	-0.1553	0.4633							
7	-0.8143	0.0753	1.5876	0.3844	2	1	-1.2428	0.8877						
14	1	1	-1.2317	0.9757			2	1.0169	0.1611					
2	0.7020	0.4660			3	0.0261	0.0366							
3	0.7730	0.1708			4	-0.2879	0.0487							
4	-2.8723	0.1692			5	1.1602	0.1128							
5	0.8406	0.0677			6	-0.7866	0.2873							
6	-0.8838	0.0409			7	0.1774	0.0266							
7	-0.1629	0.0372			8	0.0820	0.0301							
8	-1.1885	0.0566	1.0794	0.2480	9	-0.3514	0.1829							
16	1	1	-0.7117	1.6711			10	0.1764	0.0366					
2	1.8421	0.5534			11	-0.8688	0.2511	0.4867	0.2640					
3	-1.6729	0.1232			22	1	1	-0.1808	1.0026					
4	-0.3313	0.3184			2	0.1618	0.5976							
5	0.7500	0.0009			3	0.8043	0.0481							
6	-1.3258	0.0314			4	-0.8521	0.1839							
7	1.6883	0.0493			5	-0.4160	0.0507							
8	0.2886	0.2601			6	0.8231	0.0379							
9	-0.6049	0.1732			7	-0.6978	0.0949							
2	0.6871	0.8510			8	0.4697	0.1423							
2	-0.3902	0.2818			9	-0.6165	0.0503							
3	-0.3394	0.0628			10	0.3374	0.0898							
4	0.4139	0.1621			11	-0.8141	0.0766							
5	-1.1753	0.0004			12	0.3727	0.1724							
6	1.3847	0.0160			2	1	-1.1692	1.1155						
7	-0.2076	0.0251			3	0.1135	0.0502							
8	0.3511	0.1325			4	-0.9525	0.2046							
9	1.1347	0.0882	0.8588	0.2667	5	0.5040	0.0564							
					6	-0.8153	0.0482							
					7	0.8311	0.1056							
					8	-0.3307	0.1583							
					9	-0.0546	0.0560							
					10	0.2280	0.0999							
					11	-0.3269	0.0653							
					12	0.0319	0.1919	0.5293	0.2239					

Listings of the ODF and Library Programs

Appendix 2

ODF Program

CORE

TWO DIM

```

SUBROUTINE TWDIM
  DIMENSION X(511,19)
  COMMON FEX(1:7,4:6),P(2:3),A(4:5)
  COMMON /FTD/ L1,L2,L3,L4,L5,L6,L7,L8,L9
  COMMON /FTD/ L10,L11,L12,L13,L14,L15,L16
  COMMON /FTD/ L17,L18,L19,L20,L21,L22,A(CT1:19)
  COMMON /FTD/ LM1,LM2,LM3,LM4,LM5,LM6,LM7,LM8
  COMMON /FTD/ LM9,LM10,LM11,LM12,LM13,LM14,LM15,LM16
  COMMON /FTD/ LM17,LM18,LM19,LM20,L21,A(CT1:19)
  DATA NDR/1.2,3.4,5.6,7.8,9.10,11.12,13.14,15.16,17.18/
  X#/.0743323/
  NF=HF*AD(LN0K-1)
  NF=HF*AD(LN0K)
  JP=I+J
  IP1=I
  NO=75; JX=1+.101
  DECRF=LNF-LNFAT(JX-1)
  DO A=1,19; PI=A;
  YSIN=FLOAT(IW-1)*PI*A;
  DO S=1,19; PI=S;
  L1=IP1; L2=5*P(JP);
  L3=L-1
  DO 14 H=.1,PI;
  X=-5*PI;
  XN=FN*FDAT(N-1)*DF4*X#*2.
  NO 11 JN=2,JP1
  X#*+COS(FLOAT(IJM-1)*YNN)*P(JM)
  N#*IN#)=X
  CONTINUE
  DO 12 Ne=1,LP1
  DFNU(TP1)=5*DN(N,IP1)
  YDNU(TP1)=1
  NO 201 L22=1,J
  Q(L22,L20)=R(L22,L20)**4
  K#*X
  WRITE(LUO,1004) Y
  WRITE(LUO,2201) HEN1(L0K)
  WRITE(LUO,3000) (HESCP1(JX),JX=1,JP1)
  DO 26 L22=1,1
  XY=DFF(DAT(L20-1))
  WRITE(LUO,2320) XY,Z,(P(L22,L20)+L22=1,11)
  LN1=L1
  LN2=L2
  LN3=L3
  LN4=L4
  LN5=L5
  LN6=L6
  LN7=L7
  LN8=L8
  LN9=L9
  LN10=L10
  LN11=L11
  LN12=L12
  LN13=L13
  LN14=L14
  LN15=L15
  LN16=L16
  LN17=L17
  LN18=L18
  LN19=L19
  LN20=L20
  LN21=L21
  ISNE=2
  IF(ER.EQ.5.) ISG01=1
  IF(ER.EQ.11) GO TO 710
  READ(L1B)
  CONTINUE

```

```

SUBROUTINE COFF
DIMENSION X(16,3,9),R(3,12),F1(1,8,4),NFA(18),NC(1,8,3),S(1,8,3)

```

8-8

```

SUBROUTINE POLO
REAL NO
DIMENSION OCS(3707),A(4,40),N(149),E(161),NO(149),M(177),HDF(119),
X XP(12,20)
COMMON /SET1/ INP,OUT,LTP,LMA
COMMON /DATA1/ D122,ACT101
COMMON /PAR1/ HAKLIM
COMMON /ORG1/ L01,J1,I
DATA P142 56627/
DATA NO 389842.17/544.98/
DATA N0P/12.3456.7.8.9,10.11.12.13.14.15.16.17.18/
DATA VBA/1464523/
TF1FLT1,N1 GO TO 50
DO 14 I1=1,92
    C0S(I1)=COS(YR*FLOAT(I1-1))
    JDR=5
    TIR=5
    NP1,I1=0,
    DO 8 I2=2,25
        X1=5.*FLOAT(I2-2)
        XNP1,I1=XX
        XNP1,I1=XX
        CONTINUE
    DO 21 I3=1,98
        LPM1,NAK1=0
        SPFL1,TI1=0

```

SUPORTING POLYTRIUM, SOIANI

三

INVA

CAPITE

SUBROUTINE CAPITE(NAME)

COMMON /SET/,INP,LIB,IOUT,LTP,LMAX

COMMON/PAR/LMAX,LTPMAX

CALL RATE(XDATE),ACT(10)

IFINP=.NE.0D GO TO 666

READ(INP,10) ACT,HEAD

LMAX=1F(X(HEAD(19)))

LMAX=INT(HEAD(10)+.0001)/2

J1=10*3*FMAX

READ(INP,6006) (WF0,D(J)),J=11,19

6007 READ(INP,6007)

CONTINUE

WRITE(100,6011) NAME

WRITE(100,6002) NAME

WRITE(100,6003) HEAD(1)

WRITE(100,6004) ACT(J),J=1,10),XNATE

WRITE(100,6005) HEAD(J),J=3,J1)

RETURN

6000 FORMAT(1F0.0,7'0A0A,2K1)/2F10.0)

6001 FORMAT(1H1//1M-37X,

X 6M+1H,PF DIMENSIONAL ANALYSIS OF TEXTURES/

X 1H + 36+,*4.(1M*) 1H ,

6002 FORMAT(1H1//1M-39+,*4.(1M*) 1H ,PROGRAM --- VERSION FEBRUARY 1973

X 1H + 36+,*4.(1M*) 1H)

6003 FORMAT(1H1//1M-39+,*4.(1M*) 1H ,NO.,F0.1H *4X,24(1H //1H)

6004 FORMAT(1H1//1M-10+,*4.(1M*) 1H ,DATA BLOCK NO.,0.01X.12HEAUSUPN *4,

X 10+,*4.(1M*) 1H ,8X,1M*,10+,*4.(1M*) 1H ,AX.10+,*1M*) 1H)

6005 FORMAT(1H1//1M-10+,*4.(1M*) 1H ,*4.*0.01X.12HEAUSUPN *4,

X 1M + 35+,*4.(1M*) 1H ,22X,1M*,1H) 22X,1. ((1M*) 1H)/

X 1H + 25+,*8H NUMBER OF MEASURED POLE FIGURES *4.0,

X 4X,1M+1H,PF DIMENSIONAL L VALUE *4.0 1H .27X,1M*) 1H ,X,

X 27X,1M+1H,PF X,23H,1M+1H ,X,23H,1M+1H ,X,23H,1M+1H ,X,

X 15H,1GULAF STIPS14 ,2,X ,311M*) 1L,X 2911M*) 1H ,

X 39X,5H HKL 21X,5HNO-ALF,15X,5HNO-RET/4*1H *24X,F20.0,6X,PF20.1

6006 FORMAT(1H1//1M-12M,1H,PFATPL *

X 1M + 35+,*4.(1M*) 1H ,*4.*0.01X.12HEAUSUPN *4,

X 1H + 25+,*8H NUMBER OF MEASURED POLE FIGURES *4.0,

X 4X,1M+1H,PF DIMENSIONAL L VALUE *4.0 1H .27X,1M*) 1H ,X,

X 27X,1M+1H,PF X,23H,1M+1H ,X,23H,1M+1H ,X,23H,1M+1H ,X,

X 15H,1GULAF STIPS14 ,2,X ,311M*) 1L,X 2911M*) 1H ,

X 39X,5H HKL 21X,5HNO-ALF,15X,5HNO-RET/4*1H *24X,F20.0,6X,PF20.1

6007 FORMAT(1F1.0)

6008 FORMAT(1H1//1M-10+,*4.(1M*) 1H ,10W,PROGR&HMPR,*4,X,1M+1H *

X,10+,*4.(1M*) 1H ,10+,*4.(1M*) 1H ,

6009 FORMAT(1H1//1M-10+,*4.(1M*) 1H ,

X 1M + 35+,*4.(1M*) 1H ,22X,1M*,1H) 22X,1. ((1M*) 1H)/

X 1H + 25+,*8H NUMBER OF MEASURED POLE FIGURES *4.0,

X 4X,1M+1H,PF DIMENSIONAL L VALUE *4.0 1H .27X,1M*) 1H ,X,

X 27X,1M+1H,PF X,23H,1M+1H ,X,23H,1M+1H ,X,23H,1M+1H ,X,

X 15H,1GULAF STIPS14 ,2,X ,311M*) 1L,X 2911M*) 1H ,

X 39X,5H HKL 21X,5HNO-ALF,15X,5HNO-RET/4*1H *24X,F20.0,6X,PF20.1

6010 FORMAT(1H1//1M-12M,1H,PFATPL *

X 1M + 35+,*4.(1M*) 1H ,*4.*0.01X.12HEAUSUPN *4,

X 1H + 25+,*8H NUMBER OF MEASURED POLE FIGURES *4.0,

X 4X,1M+1H,PF DIMENSIONAL L VALUE *4.0 1H .27X,1M*) 1H ,X,

X 27X,1M+1H,PF X,23H,1M+1H ,X,23H,1M+1H ,X,23H,1M+1H ,X,

X 15H,1GULAF STIPS14 ,2,X ,311M*) 1L,X 2911M*) 1H ,

X 39X,5H HKL 21X,5HNO-ALF,15X,5HNO-RET/4*1H *24X,F20.0,6X,PF20.1

6011 FORMAT(1H1//1M-12M,1H,PFATPL *

X 1M + 35+,*4.(1M*) 1H ,*4.*0.01X.12HEAUSUPN *4,

X 1H + 25+,*8H NUMBER OF MEASURED POLE FIGURES *4.0,

X 4X,1M+1H,PF DIMENSIONAL L VALUE *4.0 1H .27X,1M*) 1H ,X,

X 27X,1M+1H,PF X,23H,1M+1H ,X,23H,1M+1H ,X,23H,1M+1H ,X,

X 15H,1GULAF STIPS14 ,2,X ,311M*) 1L,X 2911M*) 1H ,

X 39X,5H HKL 21X,5HNO-ALF,15X,5HNO-RET/4*1H *24X,F20.0,6X,PF20.1

6012 FORMAT(1H1//1M-12M,1H,PFATPL *

X 1M + 35+,*4.(1M*) 1H ,*4.*0.01X.12HEAUSUPN *4,

X 1H + 25+,*8H NUMBER OF MEASURED POLE FIGURES *4.0,

X 4X,1M+1H,PF DIMENSIONAL L VALUE *4.0 1H .27X,1M*) 1H ,X,

X 27X,1M+1H,PF X,23H,1M+1H ,X,23H,1M+1H ,X,23H,1M+1H ,X,

X 15H,1GULAF STIPS14 ,2,X ,311M*) 1L,X 2911M*) 1H ,

X 39X,5H HKL 21X,5HNO-ALF,15X,5HNO-RET/4*1H *24X,F20.0,6X,PF20.1

6013 FORMAT(1H1//1M-12M,1H,PFATPL *

X 1M + 35+,*4.(1M*) 1H ,*4.*0.01X.12HEAUSUPN *4,

X 1H + 25+,*8H NUMBER OF MEASURED POLE FIGURES *4.0,

X 4X,1M+1H,PF DIMENSIONAL L VALUE *4.0 1H .27X,1M*) 1H ,X,

X 27X,1M+1H,PF X,23H,1M+1H ,X,23H,1M+1H ,X,23H,1M+1H ,X,

X 15H,1GULAF STIPS14 ,2,X ,311M*) 1L,X 2911M*) 1H ,

X 39X,5H HKL 21X,5HNO-ALF,15X,5HNO-RET/4*1H *24X,F20.0,6X,PF20.1

6014 FORMAT(1H1//1M-12M,1H,PFATPL *

X 1M + 35+,*4.(1M*) 1H ,*4.*0.01X.12HEAUSUPN *4,

X 1H + 25+,*8H NUMBER OF MEASURED POLE FIGURES *4.0,

X 4X,1M+1H,PF DIMENSIONAL L VALUE *4.0 1H .27X,1M*) 1H ,X,

X 27X,1M+1H,PF X,23H,1M+1H ,X,23H,1M+1H ,X,23H,1M+1H ,X,

X 15H,1GULAF STIPS14 ,2,X ,311M*) 1L,X 2911M*) 1H ,

X 39X,5H HKL 21X,5HNO-ALF,15X,5HNO-RET/4*1H *24X,F20.0,6X,PF20.1

6015 FORMAT(1H1//1M-12M,1H,PFATPL *

X 1M + 35+,*4.(1M*) 1H ,*4.*0.01X.12HEAUSUPN *4,

X 1H + 25+,*8H NUMBER OF MEASURED POLE FIGURES *4.0,

X 4X,1M+1H,PF DIMENSIONAL L VALUE *4.0 1H .27X,1M*) 1H ,X,

X 27X,1M+1H,PF X,23H,1M+1H ,X,23H,1M+1H ,X,23H,1M+1H ,X,

X 15H,1GULAF STIPS14 ,2,X ,311M*) 1L,X 2911M*) 1H ,

X 39X,5H HKL 21X,5HNO-ALF,15X,5HNO-RET/4*1H *24X,F20.0,6X,PF20.1

6016 FORMAT(1H1//1M-12M,1H,PFATPL *

X 1M + 35+,*4.(1M*) 1H ,*4.*0.01X.12HEAUSUPN *4,

X 1H + 25+,*8H NUMBER OF MEASURED POLE FIGURES *4.0,

X 4X,1M+1H,PF DIMENSIONAL L VALUE *4.0 1H .27X,1M*) 1H ,X,

X 27X,1M+1H,PF X,23H,1M+1H ,X,23H,1M+1H ,X,23H,1M+1H ,X,

X 15H,1GULAF STIPS14 ,2,X ,311M*) 1L,X 2911M*) 1H ,

X 39X,5H HKL 21X,5HNO-ALF,15X,5HNO-RET/4*1H *24X,F20.0,6X,PF20.1

6017 FORMAT(1H1//1M-12M,1H,PFATPL *

X 1M + 35+,*4.(1M*) 1H ,*4.*0.01X.12HEAUSUPN *4,

X 1H + 25+,*8H NUMBER OF MEASURED POLE FIGURES *4.0,

X 4X,1M+1H,PF DIMENSIONAL L VALUE *4.0 1H .27X,1M*) 1H ,X,

X 27X,1M+1H,PF X,23H,1M+1H ,X,23H,1M+1H ,X,23H,1M+1H ,X,

X 15H,1GULAF STIPS14 ,2,X ,311M*) 1L,X 2911M*) 1H ,

X 39X,5H HKL 21X,5HNO-ALF,15X,5HNO-RET/4*1H *24X,F20.0,6X,PF20.1

6018 FORMAT(1H1//1M-12M,1H,PFATPL *

X 1M + 35+,*4.(1M*) 1H ,*4.*0.01X.12HEAUSUPN *4,

X 1H + 25+,*8H NUMBER OF MEASURED POLE FIGURES *4.0,

X 4X,1M+1H,PF DIMENSIONAL L VALUE *4.0 1H .27X,1M*) 1H ,X,

X 27X,1M+1H,PF X,23H,1M+1H ,X,23H,1M+1H ,X,23H,1M+1H ,X,

X 15H,1GULAF STIPS14 ,2,X ,311M*) 1L,X 2911M*) 1H ,

X 39X,5H HKL 21X,5HNO-ALF,15X,5HNO-RET/4*1H *24X,F20.0,6X,PF20.1

6019 FORMAT(1H1//1M-12M,1H,PFATPL *

X 1M + 35+,*4.(1M*) 1H ,*4.*0.01X.12HEAUSUPN *4,

X 1H + 25+,*8H NUMBER OF MEASURED POLE FIGURES *4.0,

X 4X,1M+1H,PF DIMENSIONAL L VALUE *4.0 1H .27X,1M*) 1H ,X,

X 27X,1M+1H,PF X,23H,1M+1H ,X,23H,1M+1H ,X,23H,1M+1H ,X,

X 15H,1GULAF STIPS14 ,2,X ,311M*) 1L,X 2911M*) 1H ,

X 39X,5H HKL 21X,5HNO-ALF,15X,5HNO-RET/4*1H *24X,F20.0,6X,PF20.1

6020 FORMAT(1H1//1M-12M,1H,PFATPL *

X 1M + 35+,*4.(1M*) 1H ,*4.*0.01X.12HEAUSUPN *4,

X 1H + 25+,*8H NUMBER OF MEASURED POLE FIGURES *4.0,

X 4X,1M+1H,PF DIMENSIONAL L VALUE *4.0 1H .27X,1M*) 1H ,X,

X 27X,1M+1H,PF X,23H,1M+1H ,X,23H,1M+1H ,X,23H,1M+1H ,X,

X 15H,1GULAF STIPS14 ,2,X ,311M*) 1L,X 2911M*) 1H ,

X 39X,5H HKL 21X,5HNO-ALF,15X,5HNO-RET/4*1H *24X,F20.0,6X,PF20.1

6021 FORMAT(1H1//1M-12M,1H,PFATPL *

X 1M + 35+,*4.(1M*) 1H ,*4.*0.01X.12HEAUSUPN *4,

X 1H + 25+,*8H NUMBER OF MEASURED POLE FIGURES *4.0,

X 4X,1M+1H,PF DIMENSIONAL L VALUE *4.0 1H .27X,1M*) 1H ,X,

X 27X,1M+1H,PF X,23H,1M+1H ,X,23H,1M+1H ,X,23H,1M+1H ,X,

X 15H,1GULAF STIPS14 ,2,X ,311M*) 1L,X 2911M*) 1H ,

X 39X,5H HKL 21X,5HNO-ALF,15X,5HNO-RET/4*1H *24X,F20.0,6X,PF20.1

6022 FORMAT(1H1//1M-12M,1H,PFATPL *

X 1M + 35+,*4.(1M*) 1H ,*4.*0.01X.12HEAUSUPN *4,

X 1H + 25+,*8H NUMBER OF MEASURED POLE FIGURES *4.0,

X 4X,1M+1H,PF DIMENSIONAL L VALUE *4.0 1H .27X,1M*) 1H ,X,

X 27X,1M+1H,PF X,23H,1M+1H ,X,23H,1M+1H ,X,23H,1M+1H ,X,

X 15H,1GULAF STIPS14 ,2,X ,311M*) 1L,X 2911M*) 1H ,

X 39X,5H HKL 21X,5HNO-ALF,15X,5HNO-RET/4*1H *24X,F20.0,6X,PF20.1

6023 FORMAT(1H1//1M-12M,1H,PFATPL *

X 1M + 35+,*4.(1M*) 1H ,*4.*0.01X.12HEAUSUPN *4,

X 1H + 25+,*8H NUMBER OF MEASURED POLE FIGURES *4.0,

X 4X,1M+1H,PF DIMENSIONAL L VALUE *4.0 1H .27X,1M*) 1H ,X,

X 27X,1M+1H,PF X,23H,1M+1H ,X,23H,1M+1H ,X,23H,1M+1H ,X,

X 15H,1GULAF STIPS14 ,2,X ,311M*) 1L,X 2911M*) 1H ,

X 39X,5H HKL 21X,5HNO-ALF,15X,5HNO-RET/4*1H *24X,F20.0,6X,PF20.1

6024 FORMAT(1H1//1M-12M,1H,PFATPL *

X 1M + 35+,*4.(1M*) 1H ,*4.*0.01X.12HEAUSUPN *4,

X 1H + 25+,*8H NUMBER OF MEASURED POLE FIGURES *4.0,

X 4X,1M+1H,PF DIMENSIONAL L VALUE *4.0 1H .27X,1M*) 1H ,X,

X 27X,1M+1H,PF X,23H,1M+1H ,X,23H,1M+1H ,X,23H,1M+1H ,X,

X 15H,1GULAF STIPS14 ,2,X ,311M*) 1L,X 2911M*) 1H ,

X 39X,5H HKL 21X,5HNO-ALF,15X,5HNO-RET/4*1H *24X,F20.0,6X,PF20.1

6025 FORMAT(1H1//1M-12M,1H,PFATPL *

X 1M + 35+,*4.(1M*) 1H ,*4.*0.01X.12HEAUSUPN *4,

X 1H + 25+,*8H NUMBER OF MEASURED POLE FIGURES *4.0,

X 4X,1M+1H,PF DIMENSIONAL L VALUE *4.0 1H .27X,1M*) 1H ,X,

X 27X,1M+1H,PF X,23H,1M+1H ,X,23H,1M+1H ,X,23H,1M+1H ,X,

X 15H,1GULAF STIPS14 ,2,X ,311M*) 1L,X 2911M*) 1H ,

Library Program

```

C
C ****LIBRARY PROGRAM****
C
0001 DOUBLE PRECISION DOLMN(7766),DANG(2,12),DRB(35,3,9),PI,PI2,ST,CX,
*CT,CP,CF,C
0002 DIMENSION RR(31,3,9),RES(73),XK(31,3,R),YK(35,12,12),NOMB(35),
*HKL(15)
0003 COMMON/PREM/DOLMN,PT,LMAX,LMIN,LP
0004 COMMON/DEHS/DBB
0005 DATA HKL/' CU', 'R1Q1', 'E ', '100','110','111','102','112',
*'122','103','113','4*0'/
0006 DATA NOMB/1,0,0,0,1,0,1,0,1,1,0,2,1,1,1,2,1,2,2,2,1,3,2,2,2,
*3,2,3,2,3,3,3/
0007 DATA LEC,IMP,LIR/5,6,9/
0008 DATA DANG/0,157079632679490D01,0,D0,0,157079632679490D01,
*0,785398163397448D0,0,955316618124509D0,0,785398163397448D0,
*0,463647609000806D0,0,D0,0,615479708670387D0,0,785398163397448D0,
*0,84106567056793D0,0,110714871779409D01,0,32175055439664200,
*D0,0,0,440510663004699D0,0,785398163397448D0,8*D0,D0/
0009 PI = 3.14159265389793 D0
0010 PI2=1.570796326794897D0
0011 READ(LEC,10) IST
0012 LMN=2
0013 LMAX = 34
0014 LP=2
0015 IDN = 2
0016 IDM = 4
0017 IPAS=500
0018 JV = 40
0019 ISYM = 1
0020 IF(IST) 100,100,101
0021 100 READ (LEC,10) LMAX, IDN, IDM, LMN, LP
0022 101 CALL DLMR1
0023 102 IF(IST) 102,102,103
0024 102 READ (LEC,10) ISTOK
0025 102 IF (ISTOK) 103, 103, 104
C
C ***STORAGE OF COEFFICIENTS Q(L,M,N) ***
C
0026 104 WRITE(IMP,11)LMIN,LMAX,LP, IDN, IDN
0027   JI=1
0028   DO 170 L = LMIN, LMAX, LP
0029     WRTTE (IMP,12)L
0030     TI=L+1
0031     DO 106 IM=1,II, IDN
0032       M= IM-1
0033       J2=M*(M+1)/2
0034       JT= JI+J2
0035       I=M/IDN+1
0036       DO 105 N=1,IM, IDN
0037         J=(N-1)/IDN+1
0038         JIN1=JT+N-1
0039 105  PFS(J)=DOLMN(JIN1)
0040       WRITE(LIB) (RES(J),J=1,I)
0041 106  WRITE(IMP,13)M,(RES(J),J=1,I)
0042       JI = JI+(L**2+3*L+2)/2
0043 170  CONTINUE
0044 103  IF(IST)118,118,119
0045 118  IF(ISTOK)107, 107, 125
C
C ***CALCULATION AND STORAGE OF FUNCTIONS P(L,M,PHI) ***
C
0046 107 READ (LEC,10) IPAS
0047 119 CP=DFLOAT(IPAS)*PI/18.D03
0048   JF = 9000/IPAS + 1
0049   IF((IPAS>=250).LT.0) JV = JF
0050   RES(1) = DFLOAT(IPAS)/100.
0051   WRITE(IMP,14) LMIN,LMAX,LP, IDN,RES(1)
0052   JI=1
0053   DO 171 L=LMIN,LMAX,LP
0054     WRITE(IMP,12)L

```

```

0055   CT=DSORT(DFLOAT(4*L+2))
0056   IL = L+1
0057   DO 120 IM = 1,IL, IDN
0058     M = IM-1
0059     CX=0,D0
0060     SI=1,D0
0061     IF(M/2*2=M)109,110,110
0062     109 CX=PI2
0063     IF((M-1)/4*4=M+1)111,112,112
0064     110 IF(M/4*4=M)111,112,112
0065     111 SI=-1,D0
0066     112 J2=JI+(M+1)*M/2
0067     DO 123 JE=1,JF
0068       CF = 0.
0069       ISMIN = 1
0070       JF(L/2*2-L)184,185,185
0071     185 ISMIN = 2
0072       CF=DOLMN(J1)*DOLMN(J2)*SI*CT/2,D0
0073     184 DO 124 IS = ISMIN,L,2
0074       J=(IS+1)*IS/2
0075       IF(M-IS)113,114,114
0076     114 JI=J2+IS
0077       GO TO 175
0078     113 JI=JI+I+M
0079     175 J1PI=JI+1
0080     124 CF=CF+DOLMN(J1)*DOLMN(J1PI)+SI*CT*DCOS(CP*DFLOAT((J-1)*IS)-CX)
0081     123 RES(J)=CF
0082       WRITE(IMP,13)M,(RES(I),I=1,JF)
0083       WRITE(LIB) (RES(J), J = 1,JV)
0084 120  CONTINUE
0085     JI = JI+(L**2+3*L+2)/2
0086 171  CONTINUE
0087     JV = 40
0088 125  JF= 8
0089     IF(IST) 126,126,127
0090 126  READ(LEC,10) ISYM,JF
0091 127  IF(ISYM) 128,129,128
C
C ***CALCULATION OF CUBIC SYMMETRY'S COEFFICIENTS R(L,M,MU) ***
C
0092 128 CALL CSYM
C
C ***CALCULATION AND STORAGE OF FUNCTIONS K(L,MU,PHI)-CUBIC SYMMETRY
C
0093   LM1=4
0094   ITAS=3
0095   IF(LP=2)190,191,191
0096   191 IF(LMIN/2*2,E0,LMTN) GO TO 192
0097   LM1=9
0098   GO TO 190
0099   192 ITAS=1
0100   190 WRITE(IMP,17)(HKL(J),J=1,3),LM1,LMAX,LP
0101   DO 130 I=1,JF
0102     WRITE(IMP,18) HKL(J+3)
0103   JI=1
0104   IF(LM1,LP,LMTN) GO TO 194
0105   LM11=LM1-LP
0106   DO 193 I=LMTN,LM11,LP
0107   193 JI=JI+(I**2+3*L+2)/2
0108   194 DO 130 L=LM1,LMAX,LP
0109   L2=L+1
0110   TI=L/LP-ITAS
0111   I = NOMB(L2)
0112   JJ=L/4+1
0113   CT=DSORT(DFLOAT(4*I+2))
0114   DO 131 MU=1,I
0115   C=0,D0
0116   DO 132 IM= 1,JI
0117   M = 4*(IM-1)
0118   J2=JI+(M+1)*M/2
0119   CF=DOLMN(J1)*DOLMN(J2)*CT/2,D0
0120   DO 133 IS = 2,L,2
0121   IN=(IS+1)*IS/2
0122   IF(M-IS)115,116,116
0123   115 N=JN+M+JI
0124   GO TO 174
0125   116 N=J2+IS

```

```

0126      174 J1PIN=J1+IN
0127      133 CF=CF*DQLMN(N)*DOLMN(J1PIN)*CT*DOS(DFLOAT(TS)*DANG(1,J))
0128      132 C=C+DOS(DFLOAT(M)*DANG(2,J1)*CF*DDB(L2,MU,IM)
0129      131 XK(IL,MU,J)=C
0130      WRITE(IMP,19)I,(XK(IL,MU,J),MU=1,I)
0131      WRITE(XK)
0132      J1=J1+(L**2+3*I+2)/2
0133      130 CONTINUE
0134      DO 158 J=1,JV
0135      158 RES(J)=0.
0136      DO 159 J=1,17
0137      159 WRITE(LIB)RES
0138      129 IF(ISYM) 134, 134, 135
C      ***CALCULATION AND STORAGE OF FUNCTIONS K(I,MU,PHT)-NON CUBIC SYMMETRY***
C
0139      134 READ(LEC,10)I,JF,J
0140      IF(J.EQ.1)T=1
0141      JF=JF+3
0142      READ(LEC,20) (HKL(J), J=1,JF)
0143      READ(LEC,21) DANG
0144      C=1.0/DQSRT(P1)
0145      WRITE(IMP,25) (HKL(J),J=1,3),L,MIN,L,MAX,LP,I
0146      JF=JF-3
0147      DO 136 J=1,JF
0148      WRITE(IMP,26)HKL(J+3),DANG(1,J),DANG(2,J)
0149      J1=1
0150      DO 136 L=L,MIN,L,MAX,LP
0151      JI=L/I+1
0152      I2=(L-L,MIN)/LP+1
0153      CT=DQSRT(DFLOAT(4*I+2))
0154      CM=0.0
0155      IF(L/2*2.NE.L) CM=PI2
0156      DO 137 MU = 1,JI
0157      M = (MU-1)*I
0158      CX=C
0159      IF(M)121,121,122
0160      121 CX=C/DQSRT(2.00)
0161      122 CP=0.00
0162      ST=1.00
0163      J2=J1+(M+1)*M/2
0164      IF(M/2*2-M)117,138,138
0165      117 CX=-C
0166      CP = PT2
0167      IF((M-1)/4*4-M+1)139,108,108
0168      138 IF(M/4*4-M)139,108,108
0169      139 ST=-1.00
0170      108 IF(L/2*2.E0,L) GO TO 211
0171      ISMIN=1
0172      CF=0.00
0173      GO TO 210
0174      211 ISMIN=2
0175      CF=DQLMN(J1)*DQLMN(J2)*CT*ST/2.00
0176      DO 140 IS=ISMIN,L,2
0177      IM=(IS+1)*IS/2
0178      IF(M-IS)160,161,161
0179      160 N=J1+M*IM
0180      GO TO 176
0181      161 N=J2+IS
0182      176 J1PTM=J1+IM
0183      CF=CF+DQLMN(N)*DOLMN(J1PTM)*CT*SI* DCOS(DFLOAT(TS)*DANG(1,J)-CP)
0184      137 YK(L,MU,J)=CF*CX*DOS(DFLOAT(M)*DANG(2,J)-CM)
0185      J1 = J1+(L**2+3*I+2)/2
0186      136 WRITE(IMP,19)L,(YK(L,MU,J),MU=1,JI)
0187      WRITE(LIB)YK
0188      135 IF(IST,EQ.1) TSTOK=0
0189      IF(ISTOK)142,142,141
C      ***CALCULATION AND STORAGE OF COEFFICIENTS APRTM(L,M,S)**
C
0190      142 WRITE(IMP,23) L,MIN,L,MAX,LP,TDN
0191      JI=1
0192      DO 172 L=L,MIN,L,MAX,LP
0193      WRITE(IMP,12)L
0194      CT=DQSRT(DFLOAT(4*L+2))
0195      IL = L + 1
0196      JF=L/2+1

```

```

0197      0198      DO 143 IM = 1,IL,1DN
0198      M = TM - 1
0199      J2=J1+(M+1)*M/2
0200      SI=1.00
0201      IF(M/2*2-M)162,163,163
0202      163 IF(M/4*4-M)164,165,165
0203      162 IF((M-1)/4*4-M+1)164,165,165
0204      164 SI=-1.00
0205      165 ISMIN = 2
0206      IF(L/2*2-L)168,178,178
0207      168 ISMIN=1
0208      RES(1)=0.
0209      GO TO 183
0210      178 RES(1) = DQLMN(J1)*DQLMN(J2)*CT*SI/2.00
0211      183 DO 144 IS=ISMIN,L,2
0212      I=(IS+1)*IS/2
0213      IF(M-IS)167,166,166
0214      166 JI=J2+IS
0215      GO TO 177
0216      167 JI=J1+I+M
0217      177 J1PT=J1+1
0218      ISS2P1=IS/2+1
0219      144 RES(ISS2P1)=DQLMN(J1)*DQLMN(J1PT)*CT*SI
0220      WRITE(IMP,13) M, (RES(J), J = 1,JF)
0221      143 WRITE(LIB) (RES(J), J = 1,JV)
0222      J1 = J1+(L**2+3*I+2)/2
0223      172 CONTINUE
0224      141 IF(ISYM) 145, 146, 145
C      ***STORAGE OF CUBIC SYMMETRY'S COEFFICIENTS R(L,M,MU)**
C
0225      145 LM1 = 4
0226      ITAS=3
0227      IF(ILP-2)186,187,187
0228      187 IF(L,MIN/2*2.E0,L,MTN) GO TO 182
0229      LM1=9
0230      GO TO 186
0231      182 ITAS=1
0232      186 WRITE(IMP,15)LM1,L,MAX,LP
0233      DO 147 L=LM1,L,MAX,LP
0234      WRITE(IMP,12)L
0235      I2 = L+1
0236      IL=L/LP+ITAS
0237      , JI = L/4+1
0238      JF = NORM(L,2)
0239      DO 147 MU = 1, JF
0240      DO 148 IM=1,JI
0241      148 RR(IL,MU,IM)=DRB(I2,MU,TM)
0242      147 WRITE(IMP,16)MU, (RR(IL,MU,TM),TM=1,JI)
0243      WRITE(LIB) RR
0244      146 IF(ISTOK)149,149,157
C      ***CALCULATION AND STORAGE OF COEFFICIENTS APRIM(L,M,N,S)**
C
0245      149 LM1=L,MIN
0246      IF(IST,EQ.1) LM1=4
0247      JI=1
0248      TF(ILM1,LF,LMTN) GO TO 200
0249      LM1=LM1+LP
0250      DO 201 L=L,MIN,L,MIN,LP
0251      JI=J1+(L**2+3*I+2)/2
0252      200 WRITE(IMP,22)L,LM1,L,MAX,LP,TDM,TDN
0253      DO 173 L=L,MIN,L,MAX,LP
0254      WRITE(IMP,12)L
0255      TI = L+1
0256      DO 150 IM = 1,IL,1DN
0257      M = TI-1
0258      JI=(M+1)*N/2+J1
0259      DO 150 IN=1,TL,1DN
0260      N = IN-1
0261      JF=(N+1)*N/2+J1
0262      RES(1)=DQLMN(JT)*DQLMN(JF)
0263      DO 151 IS=1,L
0264      TF (M-IS) 152, 153, 153
0265      152 J=(IS+1)*IS/2+M+J1
0266      GO TO 154
0267      153 T=JI+IS

```

```

0268 154 IF (N-TS) 155, 156, 156
0269 155 J=(IS+1)*TS/2+N+11
0270      GO TO 151
0271 156 J=JF+1S
0272 151 RES(TS+1)=DQLMN(I)*DQLMN(J)*2.D0
0273      WRITE(LIB),RES(T),I = 1,JV
0274 150 WRITE(IMP,24)M,N,(RES(J),J=1,IL)
0275      .J1 = J1+(I,*2+3*L+2)/2
0276 173 CONTINUE
0277 157REWIND LTR
0278      STOP
0279 10 FORMAT(5T3)
0280 11 FORMAT(1H1,54X,21HCoefficients Q(I,M,N),10X,2HL=,J1,1H,,I2,1H,C,I2,
0281      *1H)/54X,23(1H*),9X,7HM=0, L,(I2,1H)/96X,7HN=0, M,(I2,1H)///
0282 12 FORMAT(1X,64X,2HL=,I2/63X,6(1H*)/)
0283 13 FORMAT(1X/2X,2HM=,I2,4X,10F12.8/7(10X,10F12.8/))
0284 14 FORMAT(1H1,49X,32HFONCTIONS DE LEGENDRE P(I,M,PHT),10X,2HL=,I2,1H,
0285      *,I2,1H,(I2,1H)/49X,34(1H*),9X,7HM=0, L,(I2,1H)/90X,9HPHI=0,90C,F5,
0286      *2,1H)///
0287 15 FORMAT(1H1,43X,44HCoefficients DE SYMETRIE (CUBIQUE) R(I,M,MII),10X
0288      *,2HL=,I2,1H,,I2,1H,(I2,1H)/43X,46(1H*),9X,9HM=0, L(4)/97X,9HMII=1,M
0289      *(I,)//)
0290 16 FORMAT(1X/1X,3HMII=,I2,4X,10F12.8/2(10X,10F12.8/))
0291 17 FORMAT(1H1,36X,34HFONCTIONS HARMONIQUES SYMETRISEES(,3A4,11H)K(I,M
0292      *II,HI),10X,2HL=,I2,1H,,I2,1H,(I2,1H)/36X,59(1H*),8X,9HMII=1,M(L)/103
0293      *X,18HHI=ANGLES POUR HKI//)
0294 18 FORMAT(1X///61X,5HHKL=(,A4,1H)/60X,12(1H=)//)
0295 19 FORMAT(1X/2X,2HL=,I2,4X,10F12.8/2(10X,10F12.8/))
0296 20 FORMAT(16(A4,1X))
0297 21 FORMAT(4D20.13)
0298 22 FORMAT(1H1,52X,27HCoefficients APRTM(L,M,N,S),10X,2HL=,I2,1H,,I2,
0299      *1H,(I2,1H)/52X,29(1H*),9X,7HM=0, L,(I2,1H)/90X,7HN=0, L,(I2,1H)/90
0300      *X,10HS=0, L( 1)//)
0301 23 FORMAT(1H1, 52X ,25HCoefficients APRTM(L,M,S),10X,2HL=,I2,1H,,I2,1
0302      *H,(I2,1H)/52X,27(1H*),9X,7HM=0, L,(I2,1H)/88X,10HS=0, L( 2)//)
0303 24 FORMAT(1X/1X,2HM=,I2,3H N=,I2,10F12.8/(10X,10F12.8))
0304 25 FORMAT(1H1,36X,34HFONCTIONS HARMONIQUES SYMETRISEES(,3A4,11H)K(I,M
0305      *II,HI),10X,2HL=,I2,1H,,I2,1H,(I2,1H)/36X,59(1H*),8X,9HMII=1,M(L)/103
0306      *X,18HHI=ANGLES POUR HKI//49X,33HI,AXE Z DE KB EST UN AXE D'ORDRE ,
0307      *I2//)
0308 26 FORMAT(1X///61X,5HHKL=(,A4,1H)/60X,12(1H=)//33X,4HPHI=D20.13,
0309      *4HRAD.,10X,5HRETA=D20.13,4HRAD,//)
0310      END

```

Appendix 3

Tables for Chapter 15

Table 15.1 FOURIER coefficients

Table 15.1.1 FOURIER coefficients Q_l^{ms} of the generalized spherical functions $P_l^{mn}(\Phi)$ for $l = 0(1)34$, $m = 0(1)l$, $s = 0(1)m$. The coefficients are defined according to equations (14.3) and (14.71) (see also reference 67)

M S $l=0$

$$(0, 0) 1.00000000$$

M S $l=1$

$$(0, 0) 0.00000000 \\ (1, 0) 0.70710677 \quad (1, 1)-0.50000000$$

M S $l=2$

$$(0, 0)-0.50000000 \\ (1, 0) 0.00000000 \quad (1, 1) 0.50000000 \\ (2, 0) 0.61237246 \quad (2, 1)-0.50000000 \quad (2, 2) 0.25000000$$

M S $l=3$

$$(0, 0) 0.00000000 \\ (1, 0)-0.43301269 \quad (1, 1) 0.12500000 \\ (2, 0) 0.00000000 \quad (2, 1) 0.39528471 \quad (2, 2)-0.50000000 \\ (3, 0) 0.55901700 \quad (3, 1)-0.48412293 \quad (3, 2) 0.30618623 \quad (3, 3)-0.12500000$$

M S $l=4$

$$(0, 0) 0.37500000 \\ (1, 0) 0.00000000 \quad (1, 1)-0.37500000 \\ (2, 0)-0.39528471 \quad (2, 1) 0.17677669 \quad (2, 2) 0.25000000 \\ (3, 0) 0.00000000 \quad (3, 1) 0.33071890 \quad (3, 2)-0.46770719 \quad (3, 3) 0.37500000 \\ (4, 0) 0.52291250 \quad (4, 1)-0.46770719 \quad (4, 2) 0.33071890 \quad (4, 3)-0.17677669 \\ (4, 4) 0.06250000$$

M S $l=5$

$$(0, 0) 0.00000000 \\ (1, 0) 0.34232661 \quad (1, 1)-0.06250000 \\ (2, 0) 0.00000000 \quad (2, 1)-0.33071890 \quad (2, 2) 0.25000000$$

$$(3, 0)-0.36975500 \quad (3, 1) 0.20252314 \quad (3, 2) 0.15309311 \quad (3, 3)-0.40625000 \\ (4, 0) 0.00000000 \quad (4, 1) 0.28641099 \quad (4, 2)-0.43301269 \quad (4, 3) 0.39774758 \\ (4, 4)-0.25000000 \\ (5, 0) 0.49607837 \quad (5, 1)-0.45285553 \quad (5, 2) 0.34232661 \quad (5, 3)-0.20963137 \\ (5, 4) 0.09882118 \quad (5, 5)-0.03125000$$

M S $l=6$

$$(0, 0)-0.31250000 \\ (1, 0) 0.00000000 \quad (1, 1) 0.31250000 \\ (2, 0) 0.32021722 \quad (2, 1)-0.0982118 \\ (3, 0) 0.00000000 \quad (3, 1)-0.29646352 \quad (3, 2) 0.28125000 \quad (3, 3) 0.03125000 \\ (4, 0)-0.35078037 \quad (4, 1) 0.21650635 \quad (4, 2) 0.08558165 \quad (4, 3)-0.34232661 \\ (4, 4) 0.40625000 \\ (5, 0) 0.00000000 \quad (5, 1) 0.25387621 \quad (5, 2)-0.40141353 \quad (5, 3) 0.40141353 \\ (5, 4)-0.29315099 \quad (5, 5) 0.15625000 \\ (6, 0) 0.47495887 \quad (6, 1)-0.43972647 \quad (6, 2) 0.34763432 \quad (6, 3)-0.23175620 \\ (6, 4) 0.12693810 \quad (6, 5)-0.05412659 \quad (6, 6) 0.01562500$$

M S $l=7$

$$(0, 0) 0.00000000 \\ (1, 0)-0.29231697 \quad (1, 1) 0.03906250 \\ (2, 0) 0.00000000 \quad (2, 1) 0.28704959 \quad (2, 2)-0.15625000 \\ (3, 0) 0.30378473 \quad (3, 1)-0.12178482 \quad (3, 2)-0.20992233 \quad (3, 3) 0.30468750 \\ (4, 0) 0.00000000 \quad (4, 1)-0.26927638 \quad (4, 2) 0.29315099 \quad (4, 3)-0.05182226 \\ (4, 4) 0.25000000 \\ (5, 0)-0.33584663 \quad (5, 1) 0.22439697 \quad (5, 2) 0.03664387 \quad (5, 3)-0.28502244 \\ (5, 4) 0.39062500 \quad (5, 5)-0.33593750 \\ (6, 0) 0.00000000 \quad (6, 1) 0.22884092 \quad (6, 2)-0.37369564 \quad (6, 3) 0.39636409 \\ (6, 4)-0.31868872 \quad (6, 5) 0.19918045 \quad (6, 6)-0.09375000 \\ (7, 0) 0.45768183 \quad (7, 1)-0.42812216 \quad (7, 2) 0.34956026 \quad (7, 3)-0.24717644 \\ (7, 4) 0.14905301 \quad (7, 5)-0.07452650 \quad (7, 6) 0.02923170 \quad (7, 7)-0.00781250$$

M S $l=8$

$$(0, 0) 0.27343750 \\ (1, 0) 0.00000000 \quad (1, 1)-0.27343750 \\ (2, 0)-0.27731624 \quad (2, 1) 0.06536406 \quad (2, 2) 0.25000000 \\ (3, 0) 0.00000000 \quad (3, 1) 0.26551008 \quad (3, 2)-0.19040716 \quad (3, 3) 0.13281250 \\ (4, 0) 0.29085171 \quad (4, 1)-0.13710882 \quad (4, 2)-0.16387638 \quad (4, 3) 0.30257681 \\ (4, 4)-0.14062500 \\ (5, 0) 0.00000000 \quad (5, 1)-0.24717644 \quad (5, 2) 0.29543236 \quad (5, 3)-0.10909563 \\ (5, 4)-0.16901022 \quad (5, 5) 0.35156250 \\ (6, 0) 0.32362992 \quad (6, 1) 0.22884092 \quad (6, 2) 0.00000000 \quad (6, 3)-0.23567349 \\ (6, 4) 0.36510378 \quad (6, 5)-0.35441551 \quad (6, 6) 0.25000000 \\ (7, 0) 0.00000000 \quad (7, 1) 0.20890222 \quad (7, 2)-0.34956026 \quad (7, 3) 0.38725105 \\ (7, 4)-0.33329263 \quad (7, 5) 0.23109686 \quad (7, 6)-0.12837248 \quad (7, 7) 0.05468750 \\ (8, 0) 0.44314852 \quad (8, 1)-0.41780445 \quad (8, 2) 0.34956026 \quad (8, 3)-0.25816736 \\ (8, 4) 0.16664632 \quad (8, 5)-0.09243875 \quad (8, 6) 0.04279083 \quad (8, 7)-0.01562500 \\ (8, 8) 0.00390625$$

M S $l=9$

$$(0, 0) 0.00000000 \\ (1, 0) 0.25940558 \quad (1, 1)-0.02734375 \\ (2, 0) 0.00000000 \quad (2, 1)-0.25650710 \quad (2, 2) 0.10937500 \\ (3, 0)-0.26551008 \quad (3, 1) 0.08396166 \quad (3, 2) 0.21480824 \quad (3, 3)-0.22656250 \\ (4, 0) 0.00000000 \quad (4, 1) 0.24717644 \quad (4, 2)-0.21079278 \quad (4, 3)-0.06899813 \\ (4, 4) 0.28125000 \\ (5, 0) 0.28027174 \quad (5, 1)-0.14771618 \quad (5, 2)-0.12597278 \quad (5, 3) 0.28863990 \\ (5, 4)-0.19609219 \quad (5, 5)-0.07031250$$

(6, 0) 0.00000000 (6, 1)-0.22884092 (6, 2) 0.29273430 (6, 3)-0.14905301
 (6, 4)-0.10126157 (6, 5) 0.30257681 (6, 6)-0.35937500
 (7, 0)-0.31335333 (7, 1) 0.23121239 (7, 2)-0.02816837 (7, 3)-0.19362552
 (7, 4) 0.33616453 (7, 5)-0.35812026 (7, 6) 0.28416458 (7, 7)-0.17382812
 (8, 0) 0.00000000 (8, 1) 0.19259833 (8, 2)-0.32849681 (8, 3) 0.37634039
 (8, 4)-0.34089726 (8, 5) 0.25465634 (8, 6)-0.15780476 (8, 7) 0.07972004
 (8, 8)-0.03125000 (9, 0) 0.43066296 (9, 1)-0.40856275 (9, 2) 0.34842348 (9, 3)-0.26611283
 (9, 4) 0.18078807 (9, 5)-0.10804154 (9, 6) 0.05579241 (9, 7)-0.02415882
 (9, 8)-0.00828641 (9, 9)-0.00195312

M S L=10

(0, 0)-0.24609375 (1, 0) 0.24609375
 (2, 0) 0.24836195 (2, 1)-0.04736076 (2, 2)-0.23242187
 (3, 0) 0.00000000 (3, 1)-0.24149346 (3, 2) 0.13942632 (3, 3) 0.16406250
 (4, 0)-0.25585192 (4, 1) 0.09757809 (4, 2) 0.16309440 (4, 3)-0.24306795
 (4, 4) 0.00781250 (5, 0) 0.00000000 (5, 1) 0.23142678 (5, 2)-0.22269051 (5, 3)-0.01746928
 (5, 4) 0.24705294 (5, 5)-0.24218750 (6, 0) 0.27137193 (6, 1)-0.15524580 (6, 2)-0.09461071 (6, 3) 0.26953125
 (6, 4)-0.22925272 (6, 5) 0.00873464 (6, 6) 0.23144531 (7, 0) 0.00000000 (7, 1)-0.21336494 (7, 2) 0.28743470 (7, 3)-0.17716469
 (7, 4)-0.04555431 (7, 5) 0.25209692 (7, 6)-0.34627646 (7, 7) 0.31445312
 (8, 0)-0.304552469 (8, 1) 0.23228233 (8, 2)-0.05029060 (8, 3)-0.15780476
 (8, 4) 0.30685824 (8, 5)-0.35286218 (8, 6) 0.30574673 (8, 7)-0.21050303
 (9, 0) 0.00000000 (9, 1) 0.17898555 (9, 2)-0.31001207 (9, 3) 0.36479020
 (9, 4)-0.34392750 (9, 5) 0.27189857 (9, 6)-0.18239510 (9, 7) 0.10322040
 (9, 8)-0.04815948 (9, 9) 0.01757812
 (10, 0) 0.41975832 (10, 1)-0.40022385 (10, 2) 0.34660402 (10, 3)-0.27189857
 (10, 4) 0.19226132 (10, 5)-0.12159674 (10, 6) 0.06797464 (10, 7)-0.03297254
 (10, 8) 0.01346099 (10, 9)-0.00436732 (10, 10) 0.00097656

M S L=11

(0, 0) 0.00000000 (1, 1) 0.02050781
 (2, 0) 0.00000000 (2, 1) 0.23382504 (2, 2)-0.08203125
 (3, 0) 0.23932755 (3, 1)-0.06249237 (3, 2)-0.20827585 (3, 3) 0.17480469
 (4, 0) 0.00000000 (4, 1)-0.22818987 (4, 2) 0.16010861 (4, 3) 0.11767477
 (4, 4)-0.25000000 (5, 0)-0.24772756 (5, 1) 0.10780958 (5, 2) 0.15507062 (5, 3)-0.24765536
 (5, 4) 0.06711728 (5, 5) 0.19287109 (6, 0) 0.00000000 (6, 1) 0.21776468 (6, 2)-0.22919071 (6, 3) 0.02382092
 (6, 4) 0.20875607 (6, 5)-0.26136413 (6, 6) 0.09179687 (7, 0) 0.26372612 (7, 1)-0.16068089 (7, 2)-0.06845000 (7, 3) 0.24858360
 (7, 4)-0.24755426 (7, 5) 0.07017504 (7, 6) 0.16212849 (7, 7)-0.31396484
 (8, 0) 0.00000000 (8, 1)-0.20011193 (8, 2) 0.28081563 (8, 3)-0.19700924
 (8, 4) 0.00000000 (8, 5) 0.20392393 (8, 6)-0.32306364 (8, 7) 0.32776877
 (8, 8)-0.25000000 (9, 0)-0.29681396 (9, 1) 0.23250905 (9, 2)-0.06797464 (9, 3)-0.12716891
 (9, 4) 0.27861312 (9, 5)-0.34223406 (9, 6) 0.31801844 (9, 7)-0.23905095
 (9, 8) 0.1475621 (9, 9)-0.07373047 (10, 0) 0.00000000 (10, 1) 0.16742565 (10, 2)-0.29368404 (10, 3) 0.35320660
 (10, 4)-0.34392750 (10, 5) 0.28435832 (10, 6)-0.20272082 (10, 7) 0.12465046
 (10, 8)-0.06536406 (10, 9) 0.02847982 (10, 10)-0.00976562 (11, 0) 0.41010743 (11, 1) -0.39264795 (11, 2) 0.34437504 (11, 3) -0.27611431
 (11, 4) 0.20164537 (11, 5)-0.13337588 (11, 6) 0.07923708 (11, 7)-0.04176161 (11, 8) 0.01910154 (11, 9)-0.00742123 (11, 10) 0.00229024 (11, 11)-0.00048828

M S L=12

(0, 0) 0.00000000 (1, 1)-0.22558594 (2, 0)-0.22704606 (2, 1) 0.03635646 (2, 2) 0.21679687
 (3, 0) 0.00000000 (3, 1) 0.22263697 (3, 2)-0.10764359 (3, 3)-0.17285156
 (4, 0) 0.03125000 (4, 1) 0.25465634 (4, 2)-0.15780476 (4, 3) 0.07972004
 (4, 4)-0.34089726 (4, 5) 0.25465634 (4, 6)-0.15780476 (4, 7) 0.07972004
 (4, 8)-0.03125000 (4, 9) 0.0195312 (4, 10)-0.00195312 (4, 11) 0.02312500 (4, 12) 0.017435127 (5, 3) 0.07687290
 (5, 4)-0.24200729 (5, 5) 0.12841797 (5, 6)-0.24074791 (5, 7) 0.111565156 (5, 8) 0.12841797 (5, 9) 0.12841797
 (5, 10)-0.24074791 (5, 11) 0.111565156 (5, 12) 0.13047256 (5, 13) 0.24501990
 (5, 14)-0.111565156 (5, 15) 0.13047256 (5, 16) 0.26269531 (5, 17) 0.23217760 (5, 18) 0.05687167
 (5, 19)-0.20580345 (5, 20) 0.26334208 (5, 21) 0.15118910 (5, 22) 0.07861328 (5, 23) 0.22748667
 (5, 24)-0.25592250 (5, 25) 0.11704092 (5, 26) 0.09905493 (5, 27) 0.27148437 (5, 28) 0.32892510
 (5, 29)-0.210862198 (5, 30) 0.27359265 (5, 31) 0.21097706 (5, 32) 0.29465416 (5, 33) 0.32892510
 (5, 34)-0.27746063 (5, 35) 0.15962765 (5, 36) 0.29465416 (5, 37) 0.32892510 (5, 38)-0.28998974 (5, 39) 0.23217760 (5, 40) 0.10082269
 (5, 41)-0.25205672 (5, 42) 0.32852802 (5, 43) 0.3248403 (5, 44) 0.26055467 (5, 45)-0.17572291 (5, 46) 0.09917039 (5, 47) 0.04589844
 (5, 48)-0.00000000 (5, 49) 0.15747051 (5, 50) 0.27916539 (5, 51) 0.34190637 (5, 52)-0.34190637 (5, 53) 0.21939754 (5, 54) 0.14383924
 (5, 55)-0.08219385 (5, 56) 0.04035638 (5, 57) 0.01655842 (5, 58) 0.00537109 (5, 59)-0.40147260 (5, 60) 0.38572240 (5, 61) 0.34190637 (5, 62) 0.27916539
 (5, 63)-0.20937404 (5, 64) 0.14362940 (5, 65) 0.08956867 (5, 66) 0.05033325 (5, 67)-0.02516662 (5, 68) 0.01098362 (5, 69) 0.00405597 (5, 70) 0.00119604
 (5, 71)-0.00244414 (5, 72) 0.000405597 (5, 73) 0.00119604 (5, 74) 0.000244414

M S L=13

(0, 0) 0.00000000 (1, 1) 0.21738005 (1, 2) 0.00000000 (1, 3)-0.21618235 (1, 4) 0.00000000 (1, 5)-0.21983640 (1, 6) 0.048868608 (1, 7) 0.19919182 (1, 8) 0.13952637
 (1, 9)-0.00000000 (1, 10) 0.21246548 (1, 11) 0.12668993 (1, 12) 0.13846938 (1, 13)-0.21386719 (1, 14) 0.21386719 (1, 15)-0.21386719
 (1, 16)-0.22519904 (1, 17) 0.08346432 (1, 18) 0.16423607 (1, 19) 0.20820504 (1, 20)-0.22519904 (1, 21) 0.0742324 (1, 22) 0.21911621 (1, 23) 0.00000000 (1, 24)-0.20580345 (1, 25) 0.18407620 (1, 26) 0.04162580
 (1, 27)-0.22560707 (1, 28) 0.17006318 (1, 29) 0.06738281 (1, 30)-0.23465204 (1, 31) 0.12175497 (1, 32) 0.10890095 (1, 33) 0.23805282 (1, 34)-0.14480339 (1, 35) 0.08458424 (1, 36) 0.24554043 (1, 37) 0.20239258 (1, 38)-0.00000000 (1, 39) 0.19524230 (1, 40) 0.23284003 (1, 41) 0.08336714 (1, 42)-0.13460985 (1, 43) 0.25461596 (1, 44) 0.19146603 (1, 45) 0.00639443 (1, 46)-0.21093750 (1, 47) 0.16754061 (1, 48) 0.02775053 (1, 49) 0.20708573 (1, 50)-0.25113848 (1, 51) 0.15223974 (1, 52) 0.04372503 (1, 53) 0.22514810 (1, 54)-0.31494993 (1, 55) 0.29956055 (1, 56)-0.00000000 (1, 57) 0.17855477 (1, 58) 0.26617375 (1, 59) 0.22069961 (1, 60)-0.06770755 (1, 61) 0.11969117 (1, 62) 0.26406401 (1, 63) 0.32163432 (1, 64)-0.29472134 (1, 65) 0.21777946 (1, 66) 0.13183594 (1, 67)-0.28388402 (1, 68) 0.23147170 (1, 69) 0.09410663 (1, 70) 0.07802910 (1, 71)-0.22741322 (1, 72) 0.31314743 (1, 73) 0.32401666 (1, 74) 0.27616477 (1, 75)-0.19971614 (1, 76) 0.12336025 (1, 77) 0.06456493 (1, 78) 0.02795410 (1, 79)-0.00000000 (1, 80) 0.14879565 (1, 81) 0.26617375 (1, 82) 0.33104941 (1, 83)-0.33853775 (1, 84) 0.2992792 (1, 85) 0.23299766 (1, 86) 0.16081716 (1, 87)-0.09824044 (1, 88) 0.05268858 (1, 89) 0.02441406 (1, 90) 0.00949484 (1, 91)-0.00292969

(13, 0) 0.39367628 (13, 1)-0.37935597 (13, 2) 0.33930629 (13, 3)-0.28133792
 (13, 4) 0.21577632 (13, 5)-0.15257691 (13, 6) 0.09900497 (13, 7)-0.05857213
 (13, 8) 0.03130812 (13, 9)-0.01492556 (13, 10) 0.00622439 (13, 11)-0.00220065
 (13, 12) 0.00062244 (13, 13)-0.00012207

M S L=14

(0, 0)-0.20947266 (1, 1) 0.20947266 (2, 2)-0.02904863 (3, 3) 0.20343018
 (2, 0) 0.21047732 (2, 1)-0.020744872 (3, 2) 0.08630388 (3, 3) 0.17321777
 (3, 0) 0.00000000 (3, 1)-0.20744872 (3, 2) 0.08630388 (3, 3) 0.17321777
 (4, 0)-0.21364258 (4, 1) 0.05897095 (4, 2) 0.18195605 (4, 3)-0.16146207
 (4, 4)-0.09289551 (5, 0) 0.00000000 (5, 1) 0.20321463 (5, 2)-0.14090399 (5, 3)-0.10654473
 (5, 4) 0.21874101 (5, 5)-0.04992676 (6, 0) 0.21949688 (6, 1)-0.09088034 (6, 2)-0.14493261 (6, 3) 0.21353476
 (6, 4)-0.03499088 (6, 5)-0.18752182 (6, 6) 0.20367432 (7, 0) 0.00000000 (7, 1)-0.19632398 (7, 2) 0.19057666 (7, 3) 0.01143689
 (7, 4)-0.20482162 (7, 5) 0.19635533 (7, 6) 0.00553774 (7, 7)-0.20922852 (8, 0)-0.22925702 (8, 1) 0.12656190 (8, 2) 0.08994876 (8, 3)-0.22855943
 (8, 4) 0.16858675 (8, 5) 0.03763252 (8, 6)-0.21808581 (8, 7) 0.23025762 (8, 8)-0.06909180 (9, 0) 0.00000000 (9, 1) 0.18584570 (9, 2)-0.23194946 (9, 3) 0.10465591
 (9, 4) 0.10156132 (9, 5)-0.23946108 (9, 6) 0.21692640 (9, 7)-0.05338647 (9, 8)-0.14913616 (9, 9) 0.28491211 (10, 0) 0.24585076 (10, 1)-0.16965315 (10, 2)-0.01176333 (10, 3) 0.18778029
 (10, 4)-0.25495905 (10, 5) 0.17824067 (10, 6)-0.00375998 (10, 7)-0.17869484 (10, 8)-0.29192001 (10, 9)-0.30822766 (10, 10) 0.24969482 (11, 0) 0.00000000 (11, 1)-0.16965315 (11, 2) 0.25879323 (11, 3)-0.22731298
 (11, 4) 0.09271238 (11, 5) 0.08407579 (11, 6)-0.23311898 (11, 7) 0.30865473 (11, 8)-0.30370152 (11, 9) 0.24270421 (11, 10)-0.16174316 (11, 11) 0.08996582 (12, 0)-0.27837119 (12, 1) 0.23051323 (12, 2)-0.10389091 (12, 3)-0.05819055
 (12, 4) 0.20470339 (12, 5)-0.29701489 (12, 6) 0.32100368 (12, 7)-0.28694367 (12, 8) 0.21966450 (12, 9)-0.14565602 (12, 10) 0.08355243 (12, 11)-0.04096764 (12, 12) 0.01672363 (13, 0) 0.00000000 (13, 1) 0.14115995 (13, 2)-0.25447971 (13, 3) 0.32070860
 (13, 4)-0.33427924 (13, 5) 0.30313957 (13, 6)-0.24402265 (13, 7) 0.17571639 (13, 8)-0.11327704 (13, 9) 0.06508878 (13, 10)-0.03300981 (13, 11) 0.01452432 (13, 12)-0.00538218 (13, 13) 0.00158691 (14, 0) 0.38658243 (14, 1) 0.37347412 (14, 2) 0.33664501 (14, 3)-0.28283837
 (14, 4) 0.22110493 (14, 5)-0.16040638 (14, 6) 0.10760387 (14, 7)-0.06641455 (14, 8) 0.03746286 (14, 9)-0.019113430 (14, 10) 0.00873357 (14, 11)-0.00349343 (14, 12) 0.00118666 (14, 13)-0.00032297 (14, 14) 0.00006104

M S L=15

(0, 0) 0.00000000 (1, 1) 0.01309204 (2, 0) 0.00000000 (2, 1) 0.20197417 (2, 2)-0.05236816 (3, 0) 0.20454720 (3, 1)-0.03961039 (3, 2)-0.18999498 (3, 3) 0.11447144 (4, 0) 0.00000000 (4, 1) 0.19936794 (4, 2) 0.10338484 (4, 3) 0.14699690 (4, 4)-0.18261719 (5, 0)-0.20823303 (5, 1) 0.06720692 (5, 2) 0.16554235 (5, 3)-0.17599732 (5, 4)-0.05114932 (5, 5) 0.21365356 (6, 0) 0.00000000 (6, 1) 0.19478416 (6, 2)-0.15151179 (6, 3)-0.07758631 (6, 4) 0.21515176 (6, 5)-0.09508197 (6, 6)-0.14147949 (7, 0) 0.21445030 (7, 1)-0.09689895 (7, 2)-0.12741511 (7, 3) 0.21433504 (7, 4)-0.06964486 (7, 5)-0.15246087 (7, 6) 0.21857497 (7, 7)-0.06045532 (8, 0) 0.00000000 (8, 1)-0.18777162 (8, 2) 0.19474283 (8, 3)-0.01432208 (8, 4)-0.18211254 (8, 5) 0.21102856 (8, 6)-0.04659953 (8, 7)-0.16434234 (8, 8) 0.24218750 (9, 0)-0.22443001 (9, 1) 0.13038206 (9, 2) 0.07324558 (9, 3)-0.21767956

(9, 4) 0.18528818 (9, 5)-0.00325624 (9, 6)-0.18560386 (9, 7) 0.24077871 (9, 8)-0.12697253 (9, 9)-0.07565308 (10, 0) 0.00000000 (10, 1) 0.17742750 (10, 2)-0.23001833 (10, 3) 0.12179783 (10, 4) 0.07170007 (10, 5)-0.22067292 (10, 6) 0.23117021 (10, 7)-0.10130940 (10, 8)-0.09043095 (10, 9) 0.24556194 (10, 10)-0.30529785 (11, 0) 0.24107650 (11, 1)-0.17117564 (11, 2) 0.00201739 (11, 3) 0.16973110 (11, 4)-0.24933952 (11, 5) 0.19740472 (11, 6)-0.04392910 (11, 7)-0.13424191 (11, 8) 0.26329148 (11, 9)-0.30640531 (11, 10) 0.27175203 (11, 11)-0.19522095 (12, 0) 0.00000000 (12, 1)-0.16171904 (12, 2) 0.25158453 (12, 3)-0.23162287 (12, 4) 0.11327704 (12, 5) 0.05250531 (12, 6)-0.20289981 (12, 7) 0.20199409 (12, 8)-0.30614883 (12, 9) 0.26129511 (12, 10)-0.18803425 (12, 11) 0.11512472 (12, 12)-0.05957031

(13, 0)-0.27335507 (13, 1) 0.22938491 (13, 2)-0.11208799 (13, 3)-0.04082420 (13, 4) 0.18384813 (13, 5)-0.28071117 (13, 6) 0.31546912 (13, 7)-0.29381233 (13, 8) 0.23591276 (13, 9)-0.16574244 (13, 10) 0.10218655 (13, 11)-0.05498525 (13, 12) 0.02545254 (13, 13)-0.00985718 (14, 0) 0.00000000 (14, 1) 0.13438027 (14, 2)-0.24389622 (14, 3) 0.31090787 (14, 4)-0.32944605 (14, 5) 0.30540466 (14, 6)-0.25299908 (14, 7) 0.18871392 (14, 8)-0.12719703 (14, 9) 0.07728103 (14, 10)-0.04206646 (14, 11) 0.02029210 (14, 12)-0.00852047 (14, 13) 0.00302139 (14, 14)-0.00085449 (15, 0) 0.38080478 (15, 1)-0.36801553 (15, 2) 0.33396864 (15, 3)-0.28381878 (15, 4) 0.22555628 (15, 5)-0.16727702 (15, 6) 0.11543211 (15, 7)-0.07383063 (15, 8) 0.04354293 (15, 9)-0.02351587 (15, 10) 0.01152038 (15, 11)-0.00505202 (15, 12) 0.00194452 (15, 13)-0.00063649 (15, 14) 0.00016715 (15, 15)-0.00003052

M S L=16

(0, 0) 0.19638062 (0, 1) 0.00000000 (1, 1)-0.19638062 (1, 2) 0.19201660 (1, 3) 0.17019653 (1, 4) 0.09271238 (1, 5) 0.08407579 (1, 6)-0.23311898 (1, 7) 0.30865473 (1, 8)-0.19710661 (1, 9) 0.2390269 (1, 10) 0.19492051 (1, 11) 0.07117491 (1, 12) 0.04835383 (1, 13) 0.17656322 (1, 14) 0.13532232 (1, 15) 0.11145020 (1, 16) 0.00000000 (1, 17) 0.19189832 (1, 18) 0.11678559 (1, 19) 0.12172993 (1, 20) 0.19361913 (1, 21) 0.00167847 (1, 22) 0.20344542 (1, 23) 0.15014525 (1, 24) 0.18504050 (1, 25) 0.02351213 (1, 26) 0.19865799 (1, 27) 0.13879395 (1, 28) 0.00000000 (1, 29) 0.18708001 (1, 30) 0.15939458 (1, 31) 0.05165786 (1, 32) 0.20607483 (1, 33) 0.12926951 (1, 34) 0.09395286 (1, 35) 0.21932983 (1, 36) 0.20993505 (1, 37) 0.10183346 (1, 38) 0.11155297 (1, 39) 0.21203229 (1, 40) 0.09756217 (1, 41) 0.11703815 (1, 42) 0.21993348 (1, 43) 0.010504150 (1, 44) 0.00000000 (1, 45) 0.18001783 (1, 46) 0.19719964 (1, 47) 0.03627326 (1, 48) 0.15869675 (1, 49) 0.21709928 (1, 50) 0.08898106 (1, 51) 0.11708046 (1, 52) 0.23521313 (1, 53) 0.17770386 (1, 54) 0.22007173 (1, 55) 0.13343810 (1, 56) 0.05846964 (1, 57) 0.20613772 (1, 58) 0.19654192 (1, 59) 0.03823537 (1, 60) 0.15140435 (1, 61) 0.23888627 (1, 62) 0.16884910 (1, 63) 0.00946921 (1, 64) 0.19104004 (1, 65) 0.00000000 (1, 66) 0.16983896 (1, 67) 0.22739354 (1, 68) 0.13562146 (1, 69) 0.04496286 (1, 70) 0.2007002 (1, 71) 0.23705930 (1, 72) 0.13866411 (1, 73) 0.03705342 (1, 74) 0.20174557 (1, 75) 0.29015374 (1, 76) 0.12768921 (1, 77) 0.021724814 (1, 78) 0.01397692 (1, 79) 0.15297090 (1, 80) 0.24192172 (1, 81) 0.21022004 (1, 82) 0.07755549 (1, 83) 0.09290174 (1, 84) 0.23173732 (1, 85) 0.29672495 (1, 86) 0.28494647 (1, 87) 0.22279182 (1, 88) 0.14538574 (1, 89) 0.00000000 (1, 90) 0.15459745 (1, 91) 0.24462101 (1, 92) 0.23421010 (1, 93) 0.13022499 (1, 94) 0.02461021 (1, 95) 0.17402045 (1, 96) 0.27309474 (1, 97) 0.30355385 (1, 98) 0.27426860 (1, 99) 0.21037276 (1, 100) 0.13903339 (1, 101) 0.07921293 (1, 102) 0.03848267 (1, 103) 0.26876053 (1, 104) 0.22814402 (1, 105) 0.11900917 (1, 106) 0.02553922 (1, 107) 0.16472302 (1, 108) 0.26460266 (1, 109) 0.30816856 (1, 110) 0.29754335 (1, 111) 0.24886855 (1, 112) 0.18351850 (1, 113) 0.12000716 (1, 114) 0.06948508

(14,12) 0.035333930 (14,13)-0.01553731 (14,14) 0.00573730
 (15, 0) 0.00000000 (15, 1) 0.12831484 (15, 2)-0.23426977 (15, 3) 0.30164403
 (15, 4)-0.32425758 (15, 5) 0.30639464 (15, 6)-0.25998446 (15, 7) 0.20000012
 (15, 8)-0.13997093 (15, 9) 0.08907695 (15,10)-0.05135529 (15,11) 0.02663003
 (15,12)-0.01227626 (15,13) 0.00493923 (15,14)-0.00168207 (15,15) 0.00045776
 (16, 0) 0.37409884 (16, 1)-0.36292917 (16, 2) 0.33130750 (16, 3)-0.28439271
 (16, 4) 0.22928473 (16, 5)-0.17332298 (16, 6) 0.12255785 (16, 7)-0.08081225
 (16, 8) 0.04948720 (16, 9)-0.02799419 (16,10) 0.01452547 (16,11)-0.00684737
 (16,12) 0.00289354 (16,13)-0.00107463 (16,14) 0.00033983 (16,15)-0.00008632

M S I=17

(0, 0) 0.00000000 (1, 0) 0.19084765 (1, 1)-0.01091003 (2, 0) 0.00000000 (2, 1)-0.19022295 (2, 2) 0.04364014
 (3, 0)-0.19211575 (3, 1) 0.03294758 (3, 2) 0.18140864 (3, 3)-0.09600830 (4, 0) 0.00000000 (4, 1) 0.18831111
 (4, 2)-0.08640306 (4, 3)-0.14965449 (4, 4) 0.15710449 (5, 0) 0.19478416 (5, 1)-0.05567535 (5, 2)-0.16349185
 (5, 3) 0.15043736 (5, 4) 0.07741486 (5, 5)-0.19830322 (5, 6) 0.00000000 (6, 1)-0.18498966 (6, 2) 0.12731862
 (6, 3) 0.09800992 (6, 4)-0.19720387 (6, 5) 0.04055969 (6, 6) 0.17144775 (7, 0)-0.19916187 (7, 1) 0.07969729
 (7, 2) 0.13582261 (7, 3) -0.19001095 (7, 4) 0.01794174 (7, 5) 0.17779727 (7, 6)-0.16809382
 (7, 7)-0.03695679 (8, 0) 0.00000000 (8, 1) 0.18001783 (8, 2)-0.16519569 (8, 3)-0.02861273
 (8, 4) 0.19357249 (8, 5)-0.15412876 (8, 6)-0.04860867 (8, 7) 0.20545927 (8, 8)-0.15795898
 (9, 0) 0.20585826 (9, 1) 0.10591320 (9, 2)-0.09719262 (9, 3) 0.20762248 (9, 4)-0.11977883
 (9, 5)-0.08301819 (9, 6) 0.21187738 (9, 7)-0.14983872 (9, 8)-0.04714975 (9, 9) 0.21035767
 (10, 0) 0.00000000 (10, 1) 0.17295553 (10, 2) 0.19839360 (10, 3)-0.05498045 (10, 4)-0.13627730
 (10, 5) 0.21690902 (10, 6)-0.12240364 (10, 7)-0.07111552 (10, 8) 0.21573907 (10, 9)-0.20855945
 (11, 0) 0.21610615 (11, 1) 0.13589363 (11, 2) 0.04534711 (11, 3)-0.19439515 (11, 4) 0.20361432
 (11, 5)-0.06778407 (11, 6)-0.11750749 (11, 7) 0.22841340 (11, 8)-0.19706202 (11, 9) 0.04731833
 (11,10) 0.13427734 (11,11) 0.26068115 (12, 0) 0.00000000 (12, 1) 0.16296001 (12, 2)-0.22431354
 (12, 3) 0.14677514 (12, 4) 0.021114848 (12, 5)-0.17882666 (12, 6) 0.23681019 (12, 7)-0.16694610
 (12, 8) 0.01005581 (12, 9) 0.15678245 (12,10)-0.206649109 (12,11) 0.29225457 (12,12) -0.24890137
 (13, 0) 0.23275346 (13, 1)-0.17297317 (13, 2) 0.02442016 (13, 3) 0.13746515 (13, 4)-0.23311347
 (13, 5) 0.21901703 (13, 6)-0.10546621 (13, 7)-0.05517347 (13, 8) 0.19910543 (13, 9)-0.28138560
 (13,10) 0.29055700 (13,11)-0.24421249 (13,12) 0.17297727 (13,13)-0.10418701 (14, 0) 0.00000000
 (14, 1) 0.14816521 (14, 2) 0.23794001 (14, 3)-0.23549955 (14, 4) 0.14421342 (14, 5) 0.00000000
 (14, 6)-0.14680275 (14, 7) 0.25298238 (14, 8) 0.29714304 (14, 9) 0.28240740 (14,10)-0.22875464
 (14,11) 0.16104327 (14,12) -0.09905662 (14,13) 0.05301338 (14,14)-0.02435303 (14,15) 0.26452783
 (14,16) 0.00188446 (15, 0) 0.22683074 (15, 1)-0.12489250 (15, 2)-0.01201779 (15, 3)-0.01201779
 (15, 4) 0.14718722 (15, 5)-0.24891616 (15, 6) 0.29965985 (15, 7)-0.29877317 (15, 8) 0.25894621
 (15, 9)-0.19901654 (15,10) 0.13672104 (15,11)-0.08404982 (15,12) 0.04604688 (15,13)-0.02226693
 (15,14) 0.00934406 (15,15)-0.00330353 (16, 0) 0.00000000 (16, 1) 0.12285211 (16, 2)-0.22547364
 (16, 3) 0.29289886 (16, 4)-0.31886789 (16, 5) 0.30639464 (16, 6)-0.26557615 (16, 7) 0.20976190
 (16, 8)-0.15161723 (16, 9) 0.10035422 (16,10)-0.06069547 (16,11) 0.03338251 (16,12) 0.01656472
 (16,13) 0.00732606 (16,14)-0.00283403 (16,15) 0.00092972 (17, 0) 0.36855632 (17, 1)-0.35817236
 (17, 2) 0.32868150 (17, 3)-0.28464654 (17, 4) 0.23241292 (17, 5)-0.17865723 (17, 6) 0.12904681
 (17, 7)-0.08736511 (17, 8) 0.05525455 (17, 9)-0.03250892 (17,10) 0.01769562 (17,11)-0.00884781
 (17,12) 0.00402450 (17,13)-0.00164300 (17,14) 0.00059018 (17,15)-0.00018071

(17,16) 0.00004449 (17,17)-0.00000763 M S L=18
 (0, 0)-0.18547058 (1, 0) 0.00000000 (1, 1) 0.18547058 (2, 0) 0.18601528 (2, 1)-0.02011711
 (2, 2)-0.18219757 (3, 0) 0.00000000 (3, 1) 0.18437634 (3, 2) 0.05999527 (3, 3) 0.16583252
 (4, 0)-0.18769871 (4, 1) 0.04059834 (4, 2) 0.17063592 (4, 3)-0.11531090 (5, 0) 0.00000000
 (5, 1) 0.18212777 (5, 2)-0.09877265 (5, 3) 0.12932377 (5, 4) 0.17085692 (5, 5) 0.03570557
 (6, 0) 0.19068298 (6, 1)-0.06186573 (6, 2)-0.15098131 (6, 3) 0.16107336 (6, 4) 0.04594613
 (6, 5) 0.19378772 (6, 6) 0.08497620 (6, 7) 0.00000000 (6, 8) 0.17859097 (6, 9) 0.13559638
 (6, 10)-0.19546217 (6, 11) 0.07547072 (6, 12) 0.13875224 (6, 13) 0.07608743 (6, 14) 0.04540611
 (6, 15) 0.15384734 (6, 16) 0.18548629 (6, 17) 0.01445077 (7, 0) 0.00000000 (7, 1) 0.17352353
 (7, 2) 0.16939142 (7, 3) 0.00821428 (7, 4) 0.17906366 (7, 5) 0.17130321 (7, 6) 0.00734422
 (7, 7) 0.18654126 (7, 8) 0.01669312 (7, 9) 0.20214880 (7, 10) 0.10930955 (7, 11) 0.08417962
 (7, 12) 0.20180579 (7, 13) 0.13723940 (7, 14) 0.05133624 (7, 15) 0.19754826 (7, 16) 0.17575617
 (7, 17) 0.00000000 (7, 18) 0.00552802 (7, 19) 0.17416033 (7, 20) 0.22514343 (7, 21) 0.00000000
 (7, 22) 0.16649534 (7, 23) 0.19864851 (7, 24) 0.11454073 (7, 25) 0.21223825 (7, 26) 0.14798191
 (7, 27) 0.22321312 (7, 28) 0.13787125 (7, 29) 0.03364703 (7, 30) 0.18274379 (7, 31) 0.02847913
 (7, 32) 0.022288983 (8, 0) 0.00000000 (8, 1) 0.17352353 (8, 2) 0.16939142 (8, 3) 0.00821428
 (8, 4) 0.17906366 (8, 5) 0.17130321 (8, 6) 0.00734422 (8, 7) 0.18232803 (8, 8) 0.00000000
 (8, 9) 0.17859097 (8, 10) 0.13559638 (8, 11) 0.07608743 (8, 12) 0.19546217 (8, 13) 0.04540611
 (8, 14) 0.15384734 (8, 15) 0.18548629 (8, 16) 0.01445077 (8, 17) 0.17352353 (8, 18) 0.00000000
 (8, 19) 0.16649534 (8, 20) 0.19864851 (8, 21) 0.11454073 (8, 22) 0.21223825 (8, 23) 0.14798191
 (8, 24) 0.22321312 (8, 25) 0.13787125 (8, 26) 0.03364703 (8, 27) 0.18274379 (8, 28) 0.02847913
 (8, 29) 0.022288983 (8, 30) 0.16649534 (8, 31) 0.19864851 (8, 32) 0.11454073 (8, 33) 0.21223825
 (8, 34) 0.17352353 (8, 35) 0.16939142 (8, 36) 0.00734422 (8, 37) 0.18232803 (8, 38) 0.00000000
 (8, 39) 0.17859097 (8, 40) 0.13559638 (8, 41) 0.07608743 (8, 42) 0.19546217 (8, 43) 0.04540611
 (8, 44) 0.15384734 (8, 45) 0.18548629 (8, 46) 0.01445077 (8, 47) 0.17352353 (8, 48) 0.00000000
 (8, 49) 0.16649534 (8, 50) 0.19864851 (8, 51) 0.11454073 (8, 52) 0.21223825 (8, 53) 0.14798191
 (8, 54) 0.22321312 (8, 55) 0.13787125 (8, 56) 0.03364703 (8, 57) 0.18274379 (8, 58) 0.02847913
 (8, 59) 0.022288983 (8, 60) 0.16649534 (8, 61) 0.19864851 (8, 62) 0.11454073 (8, 63) 0.21223825
 (8, 64) 0.17352353 (8, 65) 0.16939142 (8, 66) 0.00734422 (8, 67) 0.18232803 (8, 68) 0.00000000
 (8, 69) 0.17859097 (8, 70) 0.13559638 (8, 71) 0.07608743 (8, 72) 0.19546217 (8, 73) 0.04540611
 (8, 74) 0.15384734 (8, 75) 0.18548629 (8, 76) 0.01445077 (8, 77) 0.17352353 (8, 78) 0.00000000
 (8, 79) 0.16649534 (8, 80) 0.19864851 (8, 81) 0.11454073 (8, 82) 0.21223825 (8, 83) 0.14798191
 (8, 84) 0.22321312 (8, 85) 0.13787125 (8, 86) 0.03364703 (8, 87) 0.18274379 (8, 88) 0.02847913
 (8, 89) 0.022288983 (8, 90) 0.16649534 (8, 91) 0.19864851 (8, 92) 0.11454073 (8, 93) 0.21223825
 (8, 94) 0.17352353 (8, 95) 0.16939142 (8, 96) 0.00734422 (8, 97) 0.18232803 (8, 98) 0.00000000
 (8, 99) 0.17859097 (8, 100) 0.13559638 (8, 101) 0.07608743 (8, 102) 0.19546217 (8, 103) 0.04540611
 (8, 104) 0.15384734 (8, 105) 0.18548629 (8, 106) 0.01445077 (8, 107) 0.17352353 (8, 108) 0.00000000
 (8, 109) 0.16649534 (8, 110) 0.19864851 (8, 111) 0.11454073 (8, 112) 0.21223825 (8, 113) 0.14798191
 (8, 114) 0.22321312 (8, 115) 0.13787125 (8, 116) 0.03364703 (8, 117) 0.18274379 (8, 118) 0.02847913
 (8, 119) 0.022288983 (8, 120) 0.16649534 (8, 121) 0.19864851 (8, 122) 0.11454073 (8, 123) 0.21223825
 (8, 124) 0.17352353 (8, 125) 0.16939142 (8, 126) 0.00734422 (8, 127) 0.18232803 (8, 128) 0.00000000
 (8, 129) 0.17859097 (8, 130) 0.13559638 (8, 131) 0.07608743 (8, 132) 0.19546217 (8, 133) 0.04540611
 (8, 134) 0.15384734 (8, 135) 0.18548629 (8, 136) 0.01445077 (8, 137) 0.17352353 (8, 138) 0.00000000
 (8, 139) 0.16649534 (8, 140) 0.19864851 (8, 141) 0.11454073 (8, 142) 0.21223825 (8, 143) 0.14798191
 (8, 144) 0.22321312 (8, 145) 0.13787125 (8, 146) 0.03364703 (8, 147) 0.18274379 (8, 148) 0.02847913
 (8, 149) 0.022288983 (8, 150) 0.16649534 (8, 151) 0.19864851 (8, 152) 0.11454073 (8, 153) 0.21223825
 (8, 154) 0.17352353 (8, 155) 0.16939142 (8, 156) 0.00734422 (8, 157) 0.18232803 (8, 158) 0.00000000
 (8, 159) 0.17859097 (8, 160) 0.13559638 (8, 161) 0.07608743 (8, 162) 0.19546217 (8, 163) 0.04540611
 (8, 164) 0.15384734 (8, 165) 0.18548629 (8, 166) 0.01445077 (8, 167) 0.17352353 (8, 168) 0.00000000
 (8, 169) 0.16649534 (8, 170) 0.19864851 (8, 171) 0.11454073 (8, 172) 0.21223825 (8, 173) 0.14798191
 (8, 174) 0.22321312 (8, 175) 0.13787125 (8, 176) 0.03364703 (8, 177) 0.18274379 (8, 178) 0.02847913
 (8, 179) 0.022288983 (8, 180) 0.16649534 (8, 181) 0.19864851 (8, 182) 0.11454073 (8, 183) 0.21223825
 (8, 184) 0.17352353 (8, 185) 0.16939142 (8, 186) 0.00734422 (8, 187) 0.18232803 (8, 188) 0.00000000
 (8, 189) 0.17859097 (8, 190) 0.13559638 (8, 191) 0.07608743 (8, 192) 0.19546217 (8, 193) 0.04540611
 (8, 194) 0.15384734 (8, 195) 0.18548629 (8, 196) 0.01445077 (8, 197) 0.17352353 (8, 198) 0.00000000
 (8, 199) 0.16649534 (8, 200) 0.19864851 (8, 201) 0.11454073 (8, 202) 0.21223825 (8, 203) 0.14798191
 (8, 204) 0.22321312 (8, 205) 0.13787125 (8, 206) 0.03364703 (8, 207) 0.18274379 (8, 208) 0.02847913
 (8, 209) 0.022288983 (8, 210) 0.16649534 (8, 211) 0.19864851 (8, 212) 0.11454073 (8, 213) 0.21223825
 (8, 214) 0.17352353 (8, 215) 0.16939142 (8, 216) 0.00734422 (8, 217) 0.18232803 (8, 218) 0.00000000
 (8, 219) 0.17859097 (8, 220) 0.13559638 (8, 221) 0.07608743 (8, 222) 0.19546217 (8, 223) 0.04540611
 (8, 224) 0.15384734 (8, 225) 0.18548629 (8, 226) 0.01445077 (8, 227) 0.17352353 (8, 228) 0.00000000
 (8, 229) 0.16649534 (8, 230) 0.19864851 (8, 231) 0.11454073 (8, 232) 0.21223825 (8, 233) 0.14798191
 (8, 234) 0.22321312 (8, 235) 0.13787125 (8, 236) 0.03364703 (8, 237) 0.18274379 (8, 238) 0.02847913
 (8, 239) 0.022288983 (8, 240) 0.16649534 (8, 241) 0.19864851 (8, 242) 0.11454073 (8, 243) 0.21223825
 (8, 244) 0.17352353 (8, 245) 0.16939142 (8, 246) 0.00734422 (8, 247) 0.18232803 (8, 248) 0.00000000
 (8, 249) 0.17859097 (8, 250) 0.13559638 (8, 251) 0.07608743 (8, 252) 0.19546217 (8, 253) 0.04540611
 (8, 254) 0.15384734 (8, 255) 0.18548629 (8, 256) 0.01445077 (8, 257) 0.17352353 (8, 258) 0.00000000
 (8, 259) 0.16649534 (8, 260) 0.19864851 (8, 261) 0.11454073 (8, 262) 0.21223825 (8, 263) 0.14798191
 (8, 264) 0.22321312 (8, 265) 0.13787125 (8, 266) 0.03364703 (8, 267) 0.18274379 (8, 268) 0.02847913
 (8, 269) 0.022288983 (8, 270) 0.16649534 (8, 271) 0.19864851 (8, 272) 0.11454073 (8, 273) 0.21223825
 (8, 274) 0.17352353 (8, 275) 0.16939142 (8, 276) 0.00734422 (8, 277) 0.18232803 (8, 278) 0.00000000
 (8, 279) 0.17859097 (8, 280) 0.13559638 (8, 281) 0.07608743 (8, 282) 0.19546217 (8, 283) 0.04540611
 (8, 284) 0.15384734 (8, 285) 0.18548629 (8, 286) 0.01445077 (8, 287) 0.17352353 (8, 288) 0.00000000
 (8, 289) 0.16649534 (8, 290) 0.19864851 (8, 2

M	S	L=19
(0, 0) 0.00000000		
(1, 0)-0.18077436	(1, 1) 0.00927353	
(2, 0) 0.00000000	(2, 1) 0.18029802	(2, 2)-0.03709412
(3, 0) 0.18173850	(3, 1)-0.02796897	(3, 2)-0.17358725
(4, 0) 0.00000000	(4, 1)-0.17884593	(4, 2) 0.07359073
(4, 4)-0.13647461		(4, 3) 0.14935748
(5, 0)-0.18374673	(5, 1) 0.04713004	(5, 2) 0.15999110
(5, 4)-0.09346515	(5, 5) 0.18080902	(5, 3)-0.13011083
(6, 0) 0.00000000	(6, 1) 0.17634445	(6, 2)-0.10884216
(6, 4) 0.17837790	(6, 5)-0.00185553	(6, 3)-0.10974783
(7, 0) 0.18698005	(7, 1)-0.06714312	(7, 2)-0.13912548
(7, 4) 0.01748999	(7, 5)-0.18298139	(7, 3) 0.16821732
(8, 0) 0.00000000	(8, 1)-0.17265373	(8, 2) 0.14208560
(8, 4)-0.18996431	(8, 5) 0.10355151	(8, 3) 0.05602142
(8, 8) 0.06787109		(8, 6) 0.10409799
(9, 0)-0.19177519	(9, 1) 0.08854073	(9, 2) 0.11030906
(9, 4) 0.06865525	(9, 5) 0.12867002	(9, 3)-0.19168398
(9, 8) 0.13911726	(9, 9)-0.20262909	(9, 6)-0.19342776
(10, 0) 0.00000000	(10, 1) 0.16753271	(10, 2)-0.17233905
(10, 4) 0.16351841	(10, 5)-0.18227445	(10, 3) 0.00980258
(10, 8)-0.20065367	(10, 9) 0.07080853	(10, 10) 0.12362671
(11, 0) 0.19875109	(11, 1)-0.11215287	(11, 2)-0.07236873
(11, 4)-0.15076391	(11, 5)-0.02242176	(11, 3) 0.19507718
(11, 8) 0.05120459	(11, 9) 0.13242395	(11, 6) 0.17926937
(12, 0) 0.00000000	(12, 1)-0.16056229	(12, 2) 0.19820240
(12, 4)-0.09402901	(12, 5) 0.20442526	(12, 3)-0.08455262
(12, 8) 0.15734063	(12, 9)-0.22525352	(12, 10) 0.15530612
(12, 12)-0.17211914		(12, 11) 0.00660813
(13, 0)-0.20912760	(13, 1) 0.13946426	(13, 2) 0.02317517
(13, 4) 0.20889570	(13, 5)-0.11299501	(13, 6)-0.05482314
(13, 8)-0.22208212	(13, 9) 0.13155983	(13, 10) 0.02800864
(13, 12) 0.26905152	(13, 13)-0.27729984	(13, 11)-0.18066370
(14, 0) 0.00000000	(14, 1) 0.15095662	(14, 2)-0.21740238
(14, 4)-0.01875230	(14, 5)-0.13713120	(14, 6) 0.22425750
(14, 8) 0.08517049	(14, 9) 0.07129497	(14, 10)-0.20499830
(14, 12)-0.27582437	(14, 13) 0.22620614	(14, 14)-0.15674591
(15, 0) 0.22569375	(15, 1)-0.17366765	(15, 2) 0.04168500
(15, 4)-0.21393758	(15, 5) 0.22712079	(15, 6)-0.14723121
(15, 8) 0.13515799	(15, 9)-0.24040674	(15, 10) 0.28422567
(15, 12) 0.21734980	(15, 13)-0.15181339	(15, 14) 0.09248701
(16, 0) 0.00000000	(16, 1)-0.13699090	(16, 2) 0.22547364
(16, 4) 0.16531223	(16, 5)-0.04084087	(16, 6)-0.09780003
(16, 8)-0.27662027	(16, 9) 0.28716215	(16, 10)-0.25453198
(16, 12)-0.13692220	(16, 13) 0.08432787	(16, 14)-0.04613862
(16, 16)-0.00927734		(16, 15) 0.02222953
(17, 0)-0.25696361	(17, 1) 0.22409324	(17, 2)-0.13424531
(17, 4) 0.11632123	(17, 5)-0.21928924	(17, 6) 0.28055987
(17, 8) 0.27200061	(17, 9)-0.22366434	(17, 10) 0.16624182
(17, 12) 0.06874463	(17, 13)-0.03812863	(17, 14) 0.01901026
(17, 16) 0.00325737	(17, 17)-0.00106621	(17, 15)-0.00842368
(18, 0) 0.00000000	(18, 1) 0.11339547	(18, 2)-0.20996761
(18, 4)-0.30788711	(18, 5) 0.30425766	(18, 6)-0.27322268
(18, 8)-0.17173122	(18, 9) 0.12109301	(18, 10)-0.07900918
(18, 12)-0.02638054	(18, 13) 0.01336656	(18, 14)-0.00613795
(18, 16)-0.00090940	(18, 17) 0.00027893	(18, 18)-0.00006866
(19, 0) 0.35858795	(19, 1) -0.34950832	(19, 2) 0.32358181
(19, 4) 0.23724294	(19, 5)-0.18755701	(19, 6) 0.14035481
(19, 8) 0.06616390	(19, 9)-0.04147042	(19, 10) 0.02435227
(19, 12) 0.00677586	(19, 13)-0.00316912	(19, 14) 0.00135132
(19, 16) 0.00017519		(19, 15)-0.00051821

M	S	L=20
(0, 0) 0.17619705		
(1, 0) 0.00000000	(1, 1)-0.17619705	
(2, 0)-0.17661807	(2, 1) 0.01723616	(2, 2) 0.17366791
(3, 0) 0.00000000	(3, 1) 0.17535198	(3, 2)-0.05146047
(4, 0) 0.17791200	(4, 1)-0.03472487	(4, 2)-0.16474952
(4, 4) 0.12648201		(4, 3) 0.09966820
(5, 0) 0.00000000	(5, 1)-0.17362434	(5, 2) 0.08492243
(5, 4)-0.15125275	(5, 5)-0.05841827	(5, 3) 0.13272397
(6, 0)-0.18017848	(6, 1) 0.05275086	(6, 2) 0.14964747
(6, 4)-0.06682146	(6, 5) 0.18276085	(6, 3)-0.04338074
(7, 0) 0.00000000	(7, 1) 0.17093232	(7, 2) -0.11704802
(7, 4) 0.18113023	(7, 5)-0.03466374	(7, 6) 0.15886398
(8, 0) 0.18361077	(8, 1)-0.07167430	(8, 2) 0.12795822
(8, 4)-0.00785606	(8, 5)-0.16807359	(8, 3) 0.17264058
(8, 8)-0.19057465		(8, 7) 0.05211033
(9, 0) 0.00000000	(9, 1) 0.16713335	(9, 2) 0.14714566
(9, 4)-0.18187831	(9, 5) 0.12554856	(9, 6) 0.06976217
(9, 8) 0.11015917	(9, 9) 0.09018707	
(10, 0)-0.18855184	(10, 1) 0.09200388	(10, 2) 0.09900125
(10, 4) 0.08816405	(10, 5) 0.10348435	(10, 6)-0.19408987
(10, 8) 0.09867813	(10, 9)-0.2048705	(10, 10) 0.12159729
(11, 0) 0.00000000	(11, 1) 0.16198954	(11, 2) -0.17430969
(11, 4) 0.14759462	(11, 5)-0.18831037	(11, 6) 0.06030538
(11, 8)-0.20332982	(11, 9) 0.11395799	(11, 10) 0.07079157
(12, 0) 0.19562095	(12, 1) -0.11454391	(12, 2) 0.06162778
(12, 4) 0.16104624	(12, 5) 0.03598800	(12, 6) 0.15872428
(12, 8) 0.08932345	(12, 9) 0.08920792	(12, 10) 0.20958483
(12, 12)-0.05641460		(12, 11) 0.19364622
(13, 0) 0.00000000	(13, 1) -0.15509318	(13, 2) 0.19723225
(13, 4) -0.07486387	(13, 5) 0.19446886	(13, 6) 0.18021257
(13, 8) 0.12441140	(13, 9) -0.21785186	(13, 10) 0.18404171
(13, 12)-0.11892699	(13, 13) 0.23940086	
(14, 0)-0.20602925	(14, 1) 0.14074478	(14, 2) 0.01376810
(14, 4) 0.20843655	(14, 5) -0.12984572	(14, 6) 0.02699208
(14, 8)-0.22310632	(14, 9) 0.16022794	(14, 10) -0.01785696
(14, 12) 0.24442963	(14, 13) -0.27821472	(14, 14) 0.24751663
(15, 0) 0.00000000	(15, 1) 0.14568467	(15, 2) -0.21377011
(15, 4)-0.03536923	(15, 5) -0.11742585	(15, 6) 0.21420249
(15, 8) 0.11388674	(15, 9) 0.03289900	(15, 10) -0.17128241
(15, 12)-0.27820647	(15, 13) 0.24430294	(15, 14) 0.18206538
(15, 16) 0.22253703	(15, 17) 0.17373912	(15, 18) 0.04886268
(16, 0)-0.20404707	(16, 1) 0.22777347	(16, 2) 0.16243376
(16, 4) 0.10516452	(16, 5) 0.21720460	(16, 6) 0.27462047
(16, 8) 0.23365669	(16, 9)-0.17293468	(16, 10) 0.27501494
(16, 12) 0.03240776		(16, 14) 0.11262136
(17, 0) 0.00000000	(17, 1) 0.13210171	(17, 2) 0.21968442
(17, 4) 0.17318650	(17, 5) -0.05772883	(17, 6) 0.07600354
(17, 8)-0.26390833	(17, 9) 0.28509220	(17, 10) 0.26257926
(17, 12)-0.15414289	(17, 13) 0.10017107	(17, 14) -0.05842203
(17, 16)-0.01401515	(17, 17) 0.00560951	
(18, 0)-0.25355998	(18, 1) 0.22270428	(18, 2) -0.13797575
(18, 4) 0.10272921	(18, 5) -0.20545842	(18, 6) 0.27049857
(18, 8) 0.27565140	(18, 9) -0.23313978	(18, 10) 0.17895189
(18, 12) 0.08025350	(18, 13) -0.04688612	(18, 14) 0.02488684
(18, 16) 0.00507887	(18, 17) -0.00189394	(18, 18) 0.00059891
(19, 0) 0.00000000	(19, 1) 0.10927061	(19, 2) -0.20309481
(19, 4) 0.30242661	(19, 5) 0.30242661	(19, 6) 0.27565140
(19, 8)-0.18033238	(19, 9) 0.13050221	(19, 10) -0.08780335

(19,12)-0.03173640 (19,13) 0.01692809 (19,14)-0.000827184 (19,15) 0.00366950
 (19,16)-0.00145871 (19,17) 0.00050960 (19,18)-0.00015161 (19,19) 0.00003624
 (20, 0) 0.35407722 (20, 1)-0.34554401 (20, 2) 0.32112107 (20, 3)-0.28408033
 (20, 4) 0.23908922 (20, 5)-0.19127138 (20, 6) 0.14528103 (20, 7)-0.10461430
 (20, 8) 0.07128263 (20, 9)-0.04585380 (20,10) 0.02776586 (20,11)-0.01576995
 (20,12) 0.00836328 (20,13)-0.00411779 (20,14) 0.00186842 (20,15)-0.00077360
 (20,16) 0.00028830 (20,17)-0.00009479 (20,18) 0.00002663 (20,19)-0.00000603
 (20,20) 0.00000095

M S L=21

(0, 0) 0.00000000 (1, 1)-0.000800896 (2, 0) 0.00000000 (2, 1)-0.17177299 (2, 2) 0.03203583
 (3, 0)-0.17289938 (3, 1) 0.02413202 (3, 2) 0.16652387 (3, 3)-0.07102680
 (4, 0) 0.00000000 (4, 1) 0.17063916 (4, 2)-0.06364874 (4, 3)-0.14754094
 (4, 4) 0.11971283 (5, 0) 0.17445706 (5, 1)-0.04058238 (5, 2)-0.15591428 (5, 3) 0.11377354
 (5, 4) 0.10331690 (5, 5)-0.16394138 (6, 0) 0.00000000 (6, 1)-0.16869780 (6, 2) 0.09438691 (6, 3) 0.11639524
 (6, 4)-0.16085716 (6, 5)-0.02562952 (6, 6) 0.17750549 (7, 0)-0.17693175 (7, 1) 0.05762127 (7, 2) 0.13970350 (7, 3)-0.14946446
 (7, 4)-0.04199025 (7, 5) 0.17877284 (7, 6)-0.07794350 (7, 7)-0.12806320
 (8, 0) 0.00000000 (8, 1) 0.16586235 (8, 2)-0.12373395 (8, 3)-0.07387826
 (8, 4) 0.18027858 (8, 5)-0.06265581 (8, 6)-0.13412075 (8, 7) 0.16825534
 (8, 8) 0.00280762 (9, 0) 0.18052465 (9, 1)-0.07558890 (9, 2)-0.11747836 (9, 3) 0.17494541
 (9, 4)-0.03018715 (9, 5)-0.15067612 (9, 6) 0.16102389 (9, 7) 0.01138457
 (9, 8)-0.17394675 (9, 9) 0.14693069 (10, 0) 0.00000000 (10, 1)-0.16198954 (10, 2) 0.15105604 (10, 3) 0.02122154
 (10, 4)-0.17206760 (10, 5) 0.14227569 (10, 6) 0.03714288 (10, 7)-0.18054162
 (10, 8) 0.14142476 (10, 9) 0.04098140 (10,10)-0.18730164 (11, 0)-0.18558234 (11, 1) 0.09497479 (11, 2) 0.08856445 (11, 3)-0.18663347
 (11, 4) 0.10440277 (11, 5) 0.07906435 (11, 6)-0.18929189 (11, 7) 0.12301708 (11, 8) 0.05821271 (11, 9)-0.19036488 (11,10) 0.15753466 (11,11) 0.01097250
 (12, 0) 0.00000000 (12, 1) 0.15684570 (12, 2)-0.17551124 (12, 3) 0.03042549 (12, 4) 0.13173318 (12, 5)-0.19046520 (12, 6) 0.08668111 (12, 7) 0.09165644
 (12, 8)-0.19733493 (12, 9) 0.14630094 (12,10) 0.02000435 (12,11)-0.17598945 (12,12) 0.21184921
 (13, 0) 0.19272271 (13, 1)-0.11656154 (13, 2)-0.05183877 (13, 3) 0.18018855 (13, 4)-0.16866519 (13, 5) 0.02677531 (13, 6) 0.13711224 (13, 7)-0.20110533
 (13, 8) 0.12004172 (13, 9) 0.04714683 (13,10)-0.18646733 (13,11) 0.20993957 (13,12)-0.10789399 (13,13)-0.05765200
 (14, 0) 0.00000000 (14, 1)-0.15003443 (14, 2) 0.19587095 (14, 3)-0.10613891 (14, 4)-0.05707623 (14, 5) 0.18311064 (14, 6)-0.18894455 (14, 7) 0.07243932
 (14, 8) 0.09151172 (14, 9)-0.20365885 (14,10) 0.20195858 (14,11)-0.09203932 (14,12)-0.06671719 (14,13) 0.20237167 (14,14)-0.26888657
 (15, 0)-0.20314758 (15, 1) 0.14176922 (15, 2) 0.00528802 (15, 3)-0.14981867 (15, 4) 0.20655245 (15, 5)-0.14357251 (15, 6)-0.00170034 (15, 7) 0.14809816
 (15, 8)-0.21877022 (15, 9) 0.18123031 (15,10)-0.05789007 (15,11)-0.09374122 (15,12) 0.21459715 (15,13)-0.27068311 (15,14) 0.26095286 (15,15)-0.20782948
 (16, 0) 0.00000000 (16, 1) 0.14082091 (16, 2)-0.21010588 (16, 3) 0.17341430 (16, 4)-0.05009257 (16, 5)-0.09873149 (16, 6) 0.20267610 (16, 7)-0.21633458
 (16, 8) 0.13742727 (16, 9)-0.00195719 (16,10)-0.13746563 (16,11) 0.23647419 (16,12)-0.27458531 (16,13) 0.25673130 (16,14)-0.20391317 (16,15) 0.14043178
 (16,16)-0.08435059 (17, 0) 0.21958938 (17, 1)-0.17367578 (17, 2) 0.05525472 (17, 3) 0.08645951 (17, 4)-0.19419704 (17, 5) 0.22681995 (17, 6)-0.17460607 (17, 7) 0.05963933
 (17, 8) 0.07695611 (17, 9)-0.19334242 (17,10) 0.26203153 (17,11)-0.27609590 (17,12) 0.24612668 (17,13)-0.19166546 (17,14) 0.13214251 (17,15)-0.08098953
 (17,16) 0.04402426 (17,17)-0.02104664 (18, 0) 0.00000000 (18, 1)-0.12760058 (18, 2) 0.21417868 (18, 3)-0.23291506

(18, 4) 0.17966817 (18, 5)-0.07264052 (18, 6)-0.05591870 (18, 7) 0.17189884
 (18, 8)-0.25024843 (18, 9) 0.28079605 (18,10)-0.26787817 (18,11) 0.22534338 (18,12)-0.16990741 (18,13) 0.11565299 (18,14)-0.07119630 (18,15) 0.03954906
 (18,16)-0.01970246 (18,17) 0.00870723 (18,18)-0.00335312 (19, 0)-0.25037041 (19, 1) 0.22131743 (19, 2)-0.14120707 (19, 3) 0.02899383
 (19, 4) 0.09020761 (19, 5)-0.19230311 (19, 6) 0.26033741 (19, 7)-0.28768933 (19, 8) 0.27776775 (19, 9)-0.24095072 (19,10) 0.19031452 (19,11)-0.13776298
 (19,12) 0.09162089 (19,13)-0.05596601 (19,14) 0.03131482 (19,15)-0.01596729 (19,16) 0.00735919 (19,17)-0.00302829 (19,18) 0.00109171 (19,19)-0.00033426
 (20, 0) 0.00000000 (20, 1) 0.10547972 (20, 2)-0.19672067 (20, 3) 0.26255026 (20, 4)-0.29704171 (20, 5) 0.30023772 (20, 6)-0.27734771 (20, 7) 0.23683070
 (20, 8)-0.18805936 (20, 9) 0.13927031 (20,10)-0.09627772 (20,11) 0.06209260 (20,12)-0.03728820 (20,13) 0.02078334 (20,14)-0.01070067 (20,15) 0.00505559
 (20,16)-0.00217158 (20,17) 0.00083695 (20,18)-0.00028380 (20,19) 0.00008204 (20,20)-0.00001907 (21, 0) 0.34983665 (21, 1)-0.34179333 (21, 2) 0.31872392 (21, 3)-0.28358671
 (21, 4) 0.24063130 (21, 5)-0.19457628 (21, 6) 0.14978489 (21, 7)-0.10963131 (21, 8) 0.076171275 (21, 9)-0.05014304 (21,10) 0.03119755 (21,11)-0.01829118
 (21,12) 0.01006897 (21,13)-0.00518044 (21,14) 0.00247672 (21,15)-0.00109213 (21,16) 0.00043979 (21,17)-0.00015953 (21,18) 0.00005109 (21,19)-0.00001399
 (21,20) 0.00000309 (21,21)-0.00000048

M S L=22

(0, 0)-0.16818810 (1, 0) 0.00000000 (1, 1) 0.16818810 (2, 0) 0.16852146 (2, 1)-0.01498339 (2, 2)-0.16618586
 (3, 0) 0.00000000 (3, 1)-0.16751935 (3, 2) 0.04477143 (3, 3) 0.15617466 (4, 0)-0.16954179 (4, 1) 0.03014821 (4, 2) 0.15913458 (4, 3)-0.08720228
 (4, 4)-0.12871075 (5, 0) 0.00000000 (5, 1) 0.16615738 (5, 2)-0.07401238 (5, 3)-0.13372135 (5, 4) 0.13462457 (5, 5) 0.07375050
 (6, 0) 0.17131343 (6, 1)-0.04569487 (6, 2)-0.14722808 (6, 3) 0.12488816 (6, 4) 0.08069167 (6, 5)-0.16983482 (6, 6) 0.01187754
 (7, 0) 0.00000000 (7, 1)-0.16404960 (7, 2) 0.10230289 (7, 3) 0.10065274 (7, 4)-0.16632243 (7, 5) 0.00414576 (7, 6) 0.16540015 (7, 7)-0.11169815
 (8, 0)-0.17395790 (8, 1) 0.06186698 (8, 2) 0.13021033 (8, 3)-0.15528488 (8, 4)-0.01921314 (8, 5) 0.17050214 (8, 6)-0.10562533 (8, 7)-0.09423631
 (8, 8) 0.17833328 (9, 0) 0.00000000 (9, 1) 0.16110677 (9, 2)-0.12917277 (9, 3)-0.05776782 (9, 4) 0.17673860 (9, 5)-0.08606514 (9, 6)-0.10757926 (9, 7) 0.17706729
 (9, 8)-0.04100668 (9, 9)-0.14487076 (10, 0) 0.04100668 (10, 1) 0.17768157 (10, 2)-0.07898909 (10, 3) 0.17560263 (10, 4) 0.13462457 (10, 5) 0.07375050
 (10, 6) 0.17131343 (10, 7)-0.04569487 (10, 8)-0.14722808 (10, 9) 0.12488816 (10, 10)-0.16404960 (10, 11) 0.10230289 (10, 12)-0.16632243 (10, 13)-0.14487076
 (11, 0) 0.00000000 (11, 1)-0.15718630 (11, 2) 0.15403596 (11, 3) 0.00626245 (11, 4)-0.16116732 (11, 5) 0.15452157 (11, 6) 0.00703679 (11, 7)-0.16369379
 (11, 8) 0.16261977 (11, 9)-0.00504809 (11, 10)-0.16065566 (11, 11) 0.18278551 (12, 0)-0.18283282 (12, 1) 0.09753492 (12, 2) 0.07892600 (12, 3)-0.18263565
 (12, 4) 0.11780911 (12, 5) 0.05587929 (12, 6)-0.18050952 (12, 7) 0.14452142 (12, 8) 0.01978864 (12, 9)-0.16995853 (12,10) 0.17977743 (12,11)-0.04262220
 (13, 0) 0.00000000 (13, 1) 0.15205927 (13, 2)-0.17610472 (13, 3) 0.05210041 (13, 4) 0.11622415 (13, 5)-0.18960036 (13, 6) 0.10850963 (13, 7) 0.06106318
 (13, 8)-0.18502682 (13, 9) 0.16874228 (13,10)-0.02611763 (13,11) 0.13882700 (13,12) 0.21351771 (13,13)-0.15323019 (14, 0) 0.19002716 (14, 1)-0.11826833 (14, 2)-0.04289730 (14, 3) 0.17245638
 (14, 4)-0.17410000 (14, 5) 0.04725543 (14, 6) 0.11527269 (14, 7)-0.19770180 (14, 8) 0.14390098 (14, 9) 0.00790399 (14, 10)-0.15783195 (14, 11) 0.21397679
 (14, 12)-0.14739759 (14, 13)-0.0058699 (14, 14) 0.15411067 (15, 0) 0.00000000 (15, 1)-0.14534037 (15, 2) 0.19421925 (15, 3)-0.11465188
 (15, 4)-0.04064219 (15, 5) 0.17089868 (15, 6)-0.19392696 (15, 7) 0.09699053

(15, 8) 0.05975519	(15, 9)-0.18481241	(15, 10) 0.21080093	(15, 11)-0.12837246	(10, 4) 0.17122459	(10, 5)-0.10527331	(10, 6)-0.08070315	(10, 7) 0.17797653
(15, 12)-0.01777291	(15, 13) 0.16120090	(15, 14)-0.25019589	(15, 15) 0.26761723	(10, 8)-0.07799345	(10, 9)-0.10972053	(10, 10) 0.18159151	
(16, 0)-0.2045675	(16, 1) 0.14258224	(16, 2)-0.00238167	(16, 3)-0.13974306	(11, 0) 0.17504910	(11, 1)-0.08195642	(11, 2)-0.09848513	(11, 3) 0.17498113
(16, 4) 0.20359090	(16, 5)-0.15463375	(16, 6) 0.02108569	(16, 7) 0.12529644	(11, 4)-0.06662899	(11, 5)-0.11273973	(11, 6) 0.17582282	(11, 7)-0.05722407
(16, 8)-0.21042016	(16, 9) 0.19563057	(16, 10)-0.09200616	(16, 11)-0.05255840	(11, 8)-0.12175933	(11, 9) 0.18043558	(11, 10)-0.06057312	(11, 11)-0.12108696
(16, 12) 0.18164092	(16, 13)-0.25636119	(16, 14) 0.26696485	(16, 15)-0.22833209	(12, 0) 0.00000000	(12, 1)-0.15269154	(12, 2) 0.15625894	(12, 3)-0.00724454
(16, 16) 0.16638088				(12, 4)-0.14964253	(12, 5) 0.16300663	(12, 6)-0.02016147	(12, 7)-0.14348684
(17, 0) 0.00000000	(17, 1) 0.13631806	(17, 2)-0.20645101	(17, 3) 0.17705195	(12, 8) 0.17507002	(12, 9)-0.04592091	(12, 10)-0.12717347	(12, 11) 0.19212495
(17, 4)-0.06314110	(17, 5)-0.08112251	(17, 6) 0.19022119	(17, 7)-0.21808229	(12, 12)-0.09453201			
(17, 8) 0.15637942	(17, 9)-0.03315350	(17, 10)-0.10446034	(17, 11) 0.21245760	(13, 0)-0.18027559	(13, 1) 0.09974951	(13, 2) 0.07001641	(13, 3)-0.17802128
(17, 12)-0.26603252	(17, 13) 0.26386014	(17, 14)-0.22190176	(17, 15) 0.16246639	(13, 4) 0.12877691	(13, 5) 0.03419193	(13, 6)-0.16891460	(13, 7) 0.15987942
(17, 16) 0.10460864	(17, 17) 0.05928898			(13, 8)-0.01536686	(13, 9)-0.14428589	(13, 10) 0.19019581	(13, 11)-0.08769984
(18, 0) 0.21682714	(18, 1) 0.17350456	(18, 2) 0.06096933	(18, 3) 0.07603846	(13, 12)-0.08385139	(13, 13) 0.19987428		
(18, 4)-0.18449922	(18, 5) 0.22462425	(18, 6)-0.18421569	(18, 7) 0.08036164	(14, 0) 0.00000000	(14, 1) 0.14759384	(14, 2)-0.17621584	(14, 3) 0.06302407
(18, 8) 0.05068110	(18, 9) 0.16940929	(18, 10) 0.24724911	(18, 11)-0.27365586	(14, 4) 0.10125263	(14, 5) 0.18641220	(14, 6) 0.12623525	(14, 7) 0.03207840
(18, 12) 0.25499743	(18, 13)-0.20780392	(18, 14) 0.15057643	(18, 15)-0.09766435	(14, 8)-0.16833454	(14, 9) 0.18256214	(14, 10)-0.06619032	(14, 11)-0.09845614
(18, 16) 0.05673389	(18, 17)-0.02938883	(18, 18) 0.01344466		(14, 12) 0.20241845	(14, 13)-0.18341769	(14, 14) 0.05758238	
(19, 0) 0.00000000	(19, 1) 0.12344125	(19, 2) 0.20894338	(19, 3)-0.23114680	(15, 0) 0.18751013	(15, 1)-0.11971442	(15, 2)-0.03471155	(15, 3) 0.16471764
(19, 4) 0.18498343	(19, 5)-0.08581724	(19, 6)-0.03744622	(19, 7) 0.15297896	(15, 4)-0.17774571	(15, 5) 0.06523611	(15, 6) 0.09378097	(15, 7)-0.19057986
(19, 8)-0.23601264	(19, 9) 0.27472749	(19, 10)-0.27078110	(19, 11) 0.23549634	(15, 8) 0.16162337	(15, 9)-0.02758176	(15, 10)-0.12624520	(15, 11) 0.20834504
(19, 12) 0.18410315	(19, 13) 0.13051099	(19, 14)-0.08417573	(19, 15) 0.04937501	(15, 12)-0.17547649	(15, 13) 0.04997509	(15, 14) 0.10359477	(15, 15)-0.22003353
(19, 16)-0.02624460	(19, 17) 0.01255226	(19, 18)-0.00534013	(19, 19) 0.00198412	(16, 0) 0.00000000	(16, 1)-0.14097188	(16, 2) 0.19235396	(16, 3)-0.12193634
(20, 0)-0.24737185	(20, 1) 0.21994041	(20, 2) -0.14401479	(20, 3) 0.03680307	(16, 4)-0.02550589	(16, 5) 0.15823600	(16, 6)-0.19587660	(16, 7) 0.11746720
(20, 4) 0.07865280	(20, 5)-0.17981528	(20, 6) 0.25019810	(20, 7)-0.28248057	(16, 8) 0.02983989	(16, 9)-0.16299289	(16, 10) 0.21224406	(16, 11)-0.15641375
(20, 8) 0.27859020	(20, 9)-0.24726987	(20, 10) 0.20038253	(20, 11)-0.14934689	(16, 12) 0.02649841	(16, 13) 0.11847215	(16, 14)-0.22450441	(16, 15) 0.26524737
(20, 12) 0.10270983	(20, 13)-0.06522040	(20, 14) 0.03818283	(20, 15)-0.02053782	(16, 16)-0.24548340			
(20, 16) 0.01009169	(20, 17)-0.00449144	(20, 18) 0.00017879	(20, 19)-0.00062446	(17, 0)-0.19793519	(17, 1) 0.14321958	(17, 2)-0.00933997	(17, 3)-0.13015297
(20, 20) 0.00018549				(17, 4) 0.19982204	(17, 5)-0.16342716	(17, 6) 0.04147545	(17, 7) 0.10289548
(21, 0) 0.00000000	(21, 1) 0.10198217	(21, 2)-0.19079117	(21, 3) 0.25597322	(17, 8)-0.19914159	(17, 9) 0.20444763	(17, 10)-0.12041607	(17, 11)-0.01428326
(21, 4)-0.29175842	(21, 5) 0.29777470	(21, 6)-0.27842900	(21, 7) 0.24128051	(17, 12)-0.14722595	(17, 13)-0.23683527	(17, 14) 0.26631337	(17, 15)-0.24328005
(21, 8)-0.19498411	(21, 9) 0.14741270	(21, 10)-0.10439725	(21, 11) 0.06924930	(17, 16) 0.18945964	(17, 17)-0.12815511		
(21, 12)-0.04296955	(21, 13) 0.02488221	(21, 14)-0.01339811	(21, 15) 0.00667500	(18, 0) 0.00000000	(18, 1) 0.13213596	(18, 2)-0.20283467	(18, 3) 0.17987971
(21, 16)-0.00305588	(21, 17) 0.00127353	(21, 18)-0.00047675	(21, 19) 0.00015718	(18, 4)-0.07471004	(18, 5)-0.06461987	(18, 6) 0.17724231	(18, 7)-0.21716750
(21, 20)-0.00000442	(21, 21) 0.000001001			(18, 8) 0.17131358	(18, 9)-0.06073967	(18, 10)-0.07288783	(18, 11) 0.18690781
(22, 0) 0.34583837	(22, 1) -0.33823660	(22, 2) 0.31639138	(22, 3)-0.28298905	(18, 12)-0.25355360	(18, 13) 0.26620734	(18, 14)-0.23590957	(18, 15) 0.18234466
(22, 4) 0.24191330	(22, 5)-0.19752139	(22, 6) 0.15390742	(22, 7)-0.11431956	(18, 16)-0.12464532	(18, 17) 0.07568084	(18, 18)-0.04072809	
(22, 8) 0.08083614	(22, 9)-0.05432362	(22, 10) 0.03462465	(22, 11)-0.02087945	(19, 0) 0.21423031	(19, 1)-0.17324671	(19, 2) 0.06609657	(19, 3) 0.06639060
(22, 12) 0.01187616	(22, 13)-0.00634807	(22, 14) 0.00317404	(22, 15)-0.00147590	(19, 4)-0.17502864	(19, 5) 0.22147332	(19, 6)-0.19166051	(19, 7) 0.09843732
(22, 16) 0.000633345	(22, 17)-0.00024846	(22, 18) 0.000008784	(22, 19)-0.00002744	(19, 8) 0.02638786	(19, 9)-0.14583305	(19, 10) 0.23092416	(19, 11)-0.26829386
(22, 20) 0.00000733	(22, 21)-0.00000158	(22, 22) 0.0000024		(19, 12) 0.26057824	(19, 13)-0.22128846	(19, 14) 0.16758282	(19, 15)-0.11418111
M S	L=23			(19, 16) 0.07018602	(19, 17)-0.03885858	(19, 18) 0.01926688	(19, 19)-0.00846493
(0, 0) 0.00000000				(20, 0) 0.00000000	(20, 1)-0.11958469	(20, 2) 0.20396434	(20, 3)-0.22913279
(1, 0)-0.16464689	(1, 1) 0.00700784			(20, 4) 0.18931787	(20, 5)-0.09746964	(20, 6)-0.02047743	(20, 7) 0.13497790
(2, 0) 0.00000000	(2, 1) 0.16434835	(2, 2) -0.02803135		(20, 8)-0.22148706	(20, 9) 0.26726872	(20, 10)-0.27161813	(20, 11) 0.24353364
(3, 0) 0.16524890	(3, 1)-0.02110038	(3, 2) 0.16015074	(3, 3) 0.06230044	(20, 12)-0.19668786	(20, 13) 0.14455257	(20, 14)-0.0971602	(20, 15) 0.05970379
(4, 0) 0.00000000	(4, 1)-0.16344285	(4, 2) 0.05575381	(4, 3) 0.14495210	(20, 16)-0.03352455	(20, 17) 0.01711584	(20, 18)-0.00788430	(20, 19) 0.00323783
(4, 4)-0.10596466				(20, 20)-0.00116348			
(5, 0)-0.16648674	(5, 1) 0.03543073	(5, 2) 0.15168145	(5, 3)-0.10047394	(21, 0) 0.24454466	(21, 1) 0.21857874	(21, 2)-0.14646074	(21, 3) 0.04387559
(5, 4)-0.10928469	(5, 5) 0.14860749			(21, 4) 0.06797177	(21, 5) 0.16797614	(21, 6) 0.24016912	(21, 7) 0.27672359
(6, 0) 0.00000000	(6, 1) 0.16189945	(6, 2)-0.0828099	(6, 3) 0.11994819	(21, 8) 0.27832574	(21, 9)-0.25226066	(21, 10) 0.20922570	(21, 11)-0.16007301
(6, 4) 0.14524092	(6, 5) 0.04528278	(6, 6)-0.170404920		(21, 12) 0.11341656	(21, 13)-0.07452229	(21, 14) 0.04538383	(21, 15)-0.02555831
(7, 0) 0.16843401	(7, 1)-0.05018320	(7, 2)-0.13878252	(7, 3) 0.13351749	(21, 16) 0.01325641	(21, 17)-0.00629403	(21, 18) 0.00271144	(21, 19) 0.00104630
(7, 4) 0.05911191	(7, 5)-0.17039721	(7, 6) 0.04473773	(7, 7) 0.14465594	(21, 20) 0.00035473	(21, 21)-0.00010240		
(8, 0) 0.00000000	(8, 1) 0.15966183	(8, 2) 0.10892805	(8, 3) 0.08565856	(22, 0) 0.00000000	(22, 1) 0.09874381	(22, 2)-0.18525982	(22, 3) 0.24974422
(8, 4)-0.16851005	(8, 5) 0.03059319	(8, 6) 0.14869204	(8, 7)-0.13629812	(22, 4) 0.28659415	(22, 5) 0.29510400	(22, 6)-0.27899319	(22, 7) 0.24502152
(8, 8)-0.05285645				(22, 8)-0.20117562	(22, 9) 0.15495247	(22, 10)-0.11214064	(22, 11) 0.07627600
(9, 0)-0.17121823	(9, 1) 0.06558779	(9, 2) 0.12118915	(9, 3)-0.15918310	(22, 12)-0.04872290	(22, 13) 0.02917698	(22, 14)-0.01633519	(22, 15) 0.00851759
(9, 4) 0.00144214	(9, 5) 0.15925007	(9, 6)-0.12691922	(9, 7)-0.05995129	(22, 16)-0.00411489	(22, 17) 0.00182897	(22, 18)-0.00074082	(22, 19) 0.00026981
(9, 8) 0.17715202	(9, 9)-0.08460295			(22, 20)-0.00008662	(22, 21) 0.00002375	(22, 22)-0.00000525	
(10, 0) 0.00000000	(10, 1) 0.15663956	(10, 2)-0.13358267	(10, 3)-0.04287608	(23, 0) 0.34205860	(23, 1)-0.33485657	(23, 2) 0.31412330	(23, 3) 0.28230795
				(23, 4) 0.24297200	(23, 5) -0.20014928	(23, 6) 0.15768532	(23, 7) -0.11870120
				(23, 8) 0.08527746	(23, 9)-0.05838548	(23, 10) 0.03802874	(23, 11)-0.02351496

(23,12)	0.01376895	(23,13)-0.00761107	(23,14) 0.000395681	(23,15)-0.00192564
(23,16)	0.00087214	(23,17)-0.00036484	(23,18) 0.00013957	(23,19)-0.00004816
(23,20)	0.00001469	(23,21)-0.000000384	(23,22) 0.00000081	(23,23)-0.00000012
M S	L=24			
(0, 0)	0.16118026	(1, 1)-0.16118026		
(1, 0)	0.00000000	(2, 1) 0.01318230	(2, 2) 0.15956306	
(2, 0)	-0.16144957	(3, 1) 0.16064028	(3, 2)-0.03941442	(3, 3)-0.15147710
(3, 0)	0.00000000	(4, 1)-0.02649878	(4, 2)-0.15387340	(4, 3) 0.07709587
(4, 4)	0.12922144			
(5, 0)	0.00000000	(5, 1)-0.15954375	(5, 2) 0.06524229	(5, 3) 0.13331079
(5, 4)	-0.12055077	(5, 5)-0.08417106		
(6, 0)	-0.16368844	(6, 1) 0.04009531	(6, 2) 0.14428650	(6, 3)-0.11127185
(6, 4)	-0.08959551	(6, 5) 0.15685901	(6, 6) 0.01189995	
(7, 0)	0.00000000	(7, 1) 0.15785542	(7, 2)-0.09037263	(7, 3)-0.10647355
(7, 4)	0.15230508	(7, 5) 0.01866760	(7, 6)-0.16458187	(7, 7) 0.07867503
(8, 0)	0.16578135	(8, 1)-0.05414396	(8, 2)-0.13063256	(8, 3) 0.14008465
(8, 4)	0.03886546	(8, 5)-0.16686825	(8, 6) 0.07262457	(8, 7) 0.11946190
(8, 8)	-0.15550333			
(9, 0)	0.00000000	(9, 1)-0.15551668	(9, 2) 0.11447190	(9, 3) 0.07149633
(9, 4)	-0.16812672	(9, 5) 0.05367176	(9, 6) 0.12912998	(9, 7)-0.15264295
(9, 8)	-0.01297980	(9, 9) 0.16510618		
(10, 0)	-0.16868153	(10, 1) 0.06886394	(10, 2) 0.11264224	(10, 3)-0.16153076
(10, 4)	0.02001284	(10, 5) 0.14602120	(10, 6)-0.14251073	(10, 7)-0.02692376
(10, 8)	0.16741979	(10, 9)-0.11839157	(10, 10)-0.06549931	
(11, 0)	0.00000000	(11, 1) 0.15233684	(11, 2)-0.13713934	(11, 3)-0.02915755
(11, 4)	0.16429086	(11, 5)-0.12072180	(11, 6)-0.05448319	(11, 7) 0.17275503
(11, 8)	-0.10777004	(11, 9)-0.07217105	(11, 10) 0.17996271	(11, 11)-0.10522830
(12, 0)	0.17260073	(12, 1)-0.08455674	(12, 2)-0.08990235	(12, 3) 0.17337067
(12, 4)	-0.08123261	(12, 5)-0.09361023	(12, 6) 0.17604370	(12, 7)-0.08424914
(12, 8)	-0.09160294	(12, 9) 0.18119226	(12, 10)-0.09935444	(12, 11)-0.07713206
(12, 12)	0.18723321			
(13, 0)	0.00000000	(13, 1)-0.14847676	(13, 2) 0.15786333	(13, 3)-0.01943163
(13, 4)	-0.13783169	(13, 5) 0.16836707	(13, 6)-0.04431965	(13, 7)-0.12138662
(13, 8)	0.18020095	(13, 9)-0.08068613	(13, 10)-0.09045949	(13, 11) 0.18856645
(13, 12)	-0.13406740			
(14, 0)	-0.17788772	(14, 1) 0.10167131	(14, 2) 0.06177078	(14, 3)-0.17297867
(14, 4)	0.13765341	(14, 5) 0.01412662	(14, 6)-0.15542322	(14, 7) 0.16959080
(14, 8)	-0.04661380	(14, 9)-0.11570565	(14, 10) 0.19088817	(14, 11)-0.12341318
(14, 12)	-0.03558959	(14, 13) 0.17399698	(14, 14)-0.20161343	
(15, 0)	0.00000000	(15, 1) 0.14341767	(15, 2)-0.17594354	(15, 3) 0.07267178
(15, 4)	0.08693092	(15, 5)-0.18145955	(15, 6) 0.14032497	(15, 7) 0.00518746
(15, 8)	-0.14879148	(15, 9) 0.18899405	(15, 10)-0.09966949	(15, 11)-0.05773425
(15, 12)	0.18204825	(15, 13)-0.19991471	(15, 14) 0.10571983	(15, 15) 0.04636681
(16, 0)	0.18515141	(16, 1)-0.12094040	(16, 2)-0.02720091	(16, 3) 0.15706107
(16, 4)	-0.17992751	(16, 5) 0.08093413	(16, 6) 0.07302032	(16, 7)-0.18071805
(16, 8)	0.17398918	(16, 9)-0.05986525	(16, 10)-0.09362184	(16, 11) 0.19539548
(16, 12)	-0.19323201	(16, 13) 0.09284540	(16, 14) 0.05383203	(16, 15)-0.18334904
(16, 16)	0.25319684			
(17, 0)	0.00000000	(17, 1)-0.13689524	(17, 2) 0.19033413	(17, 3)-0.12816773
(17, 4)	-0.01159411	(17, 5) 0.14541687	(17, 6)-0.19539328	(17, 7) 0.13426417
(17, 8)	0.00216959	(17, 9)-0.13949354	(17, 10) 0.20780630	(17, 11)-0.17687100
(17, 12)	0.06534486	(17, 13) 0.07614997	(17, 14)-0.19398344	(17, 15) 0.25513676
(17, 16)	-0.25528982	(17, 17) 0.21197188		
(18, 0)	-0.19556463	(18, 1) 0.14371006	(18, 2)-0.01567131	(18, 3)-0.12104506
(18, 4)	0.19545637	(18, 5)-0.17029484	(18, 6) 0.05961972	(18, 7) 0.08125568
(18, 8)	-0.18579912	(18, 9) 0.20861363	(18, 10)-0.14350292	(18, 11) 0.02055236
(18, 12)	0.11263593	(18, 13)-0.21353725	(18, 14) 0.25991401	(18, 15)-0.25273544
(18, 16)	0.20900470	(18, 17)-0.15067562	(18, 18) 0.09559345	
(19, 0)	0.00000000	(19, 1) 0.12824030	(19, 2)-0.19927716	(19, 3) 0.18203339

(19, 4)	-0.08497207	(19, 5)-0.04921012	(19, 6) 0.16403924	(19, 7)-0.21414827
(19, 8)	0.18276155	(19, 9)-0.08487096	(19, 10)-0.04314912	(19, 11) 0.16065829
(19, 12)	-0.23805274	(19, 13) 0.26436111	(19, 14)-0.24600771	(19, 15) 0.19968270
(19, 16)	-0.14386675	(19, 17) 0.09266440	(19, 18)-0.05340526	(19, 19) 0.02742660
(20, 0)	0.21178189	(20, 1)-0.17291918	(20, 2) 0.07071191	(20, 3) 0.05744663
(20, 4)	-0.16583414	(20, 5) 0.21759406	(20, 6)-0.19727798	(20, 7) 0.11413638
(20, 8)	0.00405807	(20, 9)-0.12291701	(20, 10) 0.21358521	(20, 11)-0.26055142
(20, 12)	0.26321203	(20, 13)-0.23215890	(20, 14) 0.18293597	(20, 15)-0.13018455
(20, 16)	0.080404733	(20, 17)-0.04924225	(20, 18) 0.02610038	(20, 19)-0.01243193
(20, 20)	0.05261666			
(21, 0)	0.00000000	(21, 1)-0.11599772	(21, 2) 0.19922698	(21, 3)-0.22693640
(21, 4)	0.192842453	(21, 5)-0.10778119	(21, 6)-0.00490141	(21, 7) 0.11764868
(21, 8)	-0.20699003	(21, 9) 0.25873885	(21, 10)-0.27069089	(21, 11) 0.24963342
(21, 12)	-0.20767075	(21, 13) 0.15764447	(21, 14)-0.10981502	(21, 15) 0.07034396
(21, 16)	-0.04141390	(21, 17) 0.02234588	(21, 18)-0.01099293	(21, 19) 0.00489036
(21, 20)	0.00194322	(21, 21) 0.00067675		
(22, 0)	-0.24187195	(22, 1) 0.21723638	(22, 2)-0.14859600	(22, 3) 0.05029998
(22, 4)	0.05080142	(22, 5) 0.15676048	(22, 6) 0.23031417	(22, 7)-0.27056181
(22, 8)	0.27715173	(22, 9) 0.25607452	(22, 10) 0.21692327	(22, 11)-0.16993387
(22, 12)	0.12366529	(22, 13)-0.08376513	(22, 14) 0.05281850	(22, 15)-0.03096104
(22, 16)	0.01682352	(22, 17) 0.00843645	(22, 18) 0.00387935	(22, 19)-0.00162096
(22, 20)	0.00060749	(22, 21)-0.00020026	(22, 22) 0.00005627	
(23, 0)	0.00000000	(23, 1) 0.09573568	(23, 2)-0.18008646	(23, 3) 0.24383822
(23, 4)	-0.28156012	(23, 5) 0.29227871	(23, 6)-0.27912232	(23, 7) 0.24813999
(23, 8)	-0.20699891	(23, 9) 0.16191748	(23, 10)-0.11949711	(23, 11) 0.08313427
(23, 12)	-0.05449907	(23, 13) 0.03362335	(23, 14)-0.01948185	(23, 15) 0.01056966
(23, 16)	-0.00534787	(23, 17) 0.00250994	(23, 18)-0.00104895	(23, 19) 0.00042779
(23, 20)	0.000015180	(23, 21) 0.00004752	(23, 22)-0.00001271	(23, 23) 0.00000274
(24, 0)	0.33847675	(24, 1) 0.33163813	(24, 2) 0.31191888	(24, 3)-0.28156012
(24, 4)	0.24383822	(24, 5) 0.20249662	(24, 6) 0.16115135	(24, 7)-0.12279745
(24, 8)	0.08950325	(24, 9) 0.06232207	(24, 10) 0.04139501	(24, 11)-0.02618050
(24, 12)	0.01573252	(24, 13)-0.00895959	(24, 14) 0.00482051	(24, 15)-0.00244096
(24, 16)	0.00115785	(24, 17)-0.000051145	(24, 18) 0.00020880	(24, 19)-0.00007800
(24, 20)	0.00002629	(24, 21)-0.00000784	(24, 22) 0.00000200	(24, 23)-0.0000041
(24, 24)	0.00000006			
M S	L=25			
(0, 0)	0.00000000			
(1, 0)	0.15805024	(1, 1)-0.00619924		
(2, 0)	0.00000000	(2, 1)-0.15780690	(2, 2) 0.02479696	
(3, 0)	-0.15854032	(3, 1) 0.01865539	(3, 2) 0.15438768	(3, 3)-0.05521560
(4, 0)	0.00000000	(4, 1) 0.15707006	(4, 2)-0.04936236	(4, 3)-0.14199591
(5, 0)	0.15954375	(5, 1)-0.03128910	(5, 2)-0.14749825	(5, 3) 0.08950858
(6, 0)	0.00000000	(6, 1)-0.15581849	(6, 2) 0.07345354	(6, 3) 0.12156794
(6, 4)	-0.13155317	(6, 5)-0.05944292	(6, 6) 0.16125277	
(7, 0)	-0.16111051	(7, 1) 0.04423492	(7, 2) 0.13703097	(7, 3)-0.11996896
(7, 4)	-0.07117919	(7, 5) 0.16043012	(7, 6)-0.01845148	(7, 7) 0.15152928
(8, 0)	0.00000000	(8, 1) 0.15401408	(8, 2)-0.09680391	(8, 3)-0.09345791
(8, 4)	0.15645857	(8, 5)-0.00568593	(8, 6)-0.15406166	(8, 7) 0.10571016
(9, 0)	0.16332519	(9, 1)-0.05765527	(9, 2)-0.12280861	(9, 3) 0.14494212
(9, 4)	0.02009509	(9, 5)-0.16027041	(9, 6) 0.09560256	(9, 7) 0.09205477
(9, 8)	-0.16470958	(9, 9) 0.02999809		
(10, 0)	0.00000000	(10, 1)-0.15159696	(10, 2) 0.11910582	(10, 3) 0.05819849
(10, 4)	-0.16574658	(10, 5) 0.07350320	(10, 6) 0.10803872	(10, 7) 0.16185598
(10, 8)	0.02351614	(10, 9) 0.14451806	(10, 10)-0.14603114	
(11, 0)	-0.16632223	(11, 1) 0.07176064	(11, 2) 0.10456017	(11, 3)-0.16262861
(11, 4)	0.03659694	(11, 5) 0.13158067	(11, 6)-0.15314785	(11, 7) 0.00376842
(11, 8)	0.15154046	(11, 9)-0.14249177	(11, 10)-0.02148639	(11, 11) 0.16544831

(12, 0) 0.00000000 (12, 1) 0.14847676 (12, 2)-0.13998523 (12, 3)-0.01654857
 (12, 4) 0.15636589 (12, 5)-0.13286106 (12, 6)-0.02956196 (12, 7) 0.16293928
 (12, 8)-0.13054322 (12, 9)-0.03486194 (12,10) 0.16798110 (12,11)-0.13798846
 (12,12)-0.02600241 (13, 1)-0.08684371 (13, 2)-0.08187704 (13, 3) 0.17099959
 (13, 4)-0.09375726 (13, 5)-0.07496203 (13, 6) 0.17278458 (13, 7)-0.10649267
 (13, 8)-0.06120327 (13, 9) 0.17414530 (13,10)-0.12915440 (13,11)-0.03283495
 (13,12) 0.16937836 (13,13)-0.16451490 (14, 1)-0.14451668 (14, 2) 0.15896024
 (14, 3)-0.03042471 (14, 4)-0.12597923 (14, 5) 0.17115298 (14, 6)-0.06547161
 (14, 7)-0.09848745 (14, 8) 0.17938636 (14, 9)-0.1098040 (14,10)-0.05318088
 (14,11) 0.17516118 (14,12)-0.16193948 (14,13) 0.02370259 (14,14) 0.13493228
 (15, 0)-0.17565006 (15, 1) 0.10334343 (15, 2) 0.05412951 (15, 3)-0.16765392
 (15, 4) 0.14474103 (15, 5)-0.00428358 (15, 6)-0.14074264 (15, 7) 0.17556168
 (15, 8)-0.07370993 (15, 9)-0.08599715 (15,10) 0.18390647 (15,11)-0.14984702
 (15,12) 0.00974579 (15,13) 0.14028935 (15,14)-0.20455916 (15,15) 0.14787501
 (16, 0) 0.00000000 (16, 1) 0.13950300 (16, 2)-0.17536625 (16, 3) 0.08119718
 (16, 4) 0.07332086 (16, 5)-0.17518863 (16, 6) 0.15123403 (16, 7)-0.01935819
 (16, 8)-0.12758905 (16, 9) 0.18944843 (16,10)-0.12655768 (16,11)-0.01864723
 (16,12) 0.15543525 (16,13)-0.20469277 (16,14) 0.14308712 (16,15)-0.00717986
 (16,16)-0.13688278 (17, 0) 0.18293396 (17, 1)-0.12197942 (17, 2)-0.02029470
 (17, 3) 0.14954825 (17, 4)-0.18091293 (17, 5) 0.09456852 (17, 6) 0.05323532
 (17, 7)-0.16890243 (17, 8)-0.18176611 (17, 9)-0.08583187 (17,10)-0.06134425
 (17,11) 0.17716134 (17,12)-0.20202337 (17,13) 0.12762786 (17,14) 0.06697288
 (17,15)-0.14292836 (17,16) 0.23277329 (17,17)-0.25821191 (18, 0) 0.00000000
 (18, 1)-0.13308124 (18, 2) 0.18820530 (18, 3)-0.13349390 (18, 4) 0.00117446
 (18, 5) 0.13265431 (18, 6)-0.19297481 (18, 7) 0.14778483 (18, 8)-0.02305697
 (18, 9)-0.11529075 (18,10) 0.19881386 (18,11)-0.19059473 (18,12) 0.09848120
 (18,13) 0.03565802 (18,14)-0.16051835 (18,15) 0.23871174 (18,16)-0.25812146
 (18,17) 0.22933378 (18,18)-0.17456460 (19, 0)-0.19332953 (19, 1) 0.14407715
 (19, 2)-0.02144798 (19, 3)-0.11240748 (19, 4) 0.19065829 (19, 5)-0.17552938
 (19, 6) 0.07568861 (19, 7) 0.06060912 (19, 8)-0.17107463 (19, 9) 0.20895684
 (19,10)-0.16173916 (19,11) 0.05169428 (19,12) 0.07882804 (19,13)-0.18770748
 (19,14) 0.24872957 (19,15)-0.25700539 (19,16) 0.22464965 (19,17)-0.17141686
 (19,18) 0.11517276 (19,19)-0.06938922 (20, 0) 0.00000000 (20, 1) 0.12460154
 (20, 2)-0.2019579242 (20, 3) 0.18362419 (20, 4)-0.09407914 (20, 5)-0.03485828
 (20, 6) 0.15083250 (20, 7)-0.20948203 (20, 8) 0.19120643 (20, 9)-0.10576392
 (20,10)-0.01548143 (20,11) 0.13435329 (20,12)-0.22031902 (20,13) 0.25892663
 (20,14)-0.25239924 (20,15) 0.21426830 (20,16)-0.16180792 (20,17) 0.10974646
 (20,18)-0.06706943 (20,19) 0.03688240 (20,20)-0.01814985 (20,21)-0.00323331
 (21, 0) 0.20946726 (21, 1)-0.17253561 (21, 2) 0.07487898 (21, 3) 0.04914351
 (21, 4)-0.15694588 (21, 5) 0.21316615 (21, 6)-0.20135374 (21, 7) 0.12771137
 (21, 8)-0.01636978 (21, 9)-0.10086942 (21,10) 0.19565625 (21,11)-0.25090721
 (21,12) 0.26324973 (21,13)-0.24052510 (21,14) 0.19650424 (21,15)-0.14539468
 (21,16) 0.09801581 (21,17)-0.06031440 (21,18) 0.03383576 (21,19)-0.01723292
 (22, 0) 0.00000000 (22, 1)-0.11265187 (22, 2) 0.19471687 (22, 3)-0.22460727
 (22, 4) 0.19563033 (22, 5)-0.11691148 (22, 6) 0.00939056 (22, 7) 0.10130273
 (22, 8)-0.19238663 (22, 9) 0.24940281 (22,10)-0.26627034 (22,11) 0.25397938
 (22,12)-0.21709743 (22,13) 0.16970195 (22,14)-0.12211050 (22,15) 0.08112287
 (22,16)-0.04978132 (22,17) 0.02817399 (22,18)-0.01465426 (22,19) 0.00696516
 (22,20)-0.00299943 (22,21) 0.00115560 (22,22)-0.00039077 (23, 0)-0.23933920
 (23, 1) 0.21591608 (23, 2)-0.15046303 (23, 3) 0.05615182 (23, 4) 0.04890758
 (23, 5)-0.14613935 (23, 6) 0.22067806 (23, 7)-0.26411068 (23, 8) 0.27521977
 (23, 9)-0.25884989 (23,10) 0.22355862 (23,11)-0.17894003 (23,12) 0.13340333
 (23,13)-0.09286138 (23,14) 0.06039697 (23,15)-0.03667789 (23,16) 0.02075642
 (23,17)-0.01091052 (23,18) 0.00530175 (23,19)-0.00236585 (23,20) 0.00096056
 (23,21)-0.00035019 (23,22) 0.00011241 (23,23)-0.00003079 (24, 0) 0.00000000
 (24, 1) 0.09293305 (24, 2)-0.17523624 (24, 3) 0.23823199 (24, 4)-0.27666306
 (24, 5) 0.28934115 (24, 6)-0.27888528 (24, 7) 0.25071147

(24, 8)-0.21161450 (24, 9) 0.16833830 (24,10)-0.12646385 (24,11) 0.08979527
 (24,12)-0.06025668 (24,13) 0.03818099 (24,14)-0.02280816 (24,15) 0.01281503
 (24,16)-0.00675082 (24,17) 0.00332034 (24,18)-0.00151641 (24,19) 0.00063844
 (24,20)-0.00024540 (24,21) 0.00008495 (24,22)-0.00002596 (24,23) 0.00000679
 (24,24)-0.00000143 (25, 0) 0.33507487 (25, 1)-0.32856795 (25, 2) 0.30977684
 (25, 3)-0.28075910 (25, 4) 0.24453790 (25, 5)-0.20459509 (25, 6) 0.16433473
 (25, 7)-0.12662841 (25, 8) 0.09352128 (25, 9)-0.06612953 (25,10) 0.04471172
 (25,11)-0.02886129 (25,12) 0.01775329 (25,13)-0.01038386 (25,14) 0.00575993
 (25,15)-0.00302053 (25,16) 0.00149173 (25,17)-0.00069054 (25,18) 0.00029785
 (25,19)-0.00011880 (25,20) 0.00004338 (25,21)-0.00001430 (25,22) 0.00000417
 (25,23)-0.00000104 (25,24) 0.00000021 (25,25)-0.00000003

M

S

L=26

(0, 0)-0.15498102 (1, 0) 0.00000000 (1, 1) 0.15498102 (2, 0) 0.15520225
 (2, 1)-0.01171546 (2, 2)-0.15365261 (3, 0) 0.00000000 (3, 1)-0.15453757
 (3, 2) 0.03504583 (3, 3) 0.14701056 (4, 0)-0.15587559 (4, 1) 0.02353258
 (4, 2) 0.14898252 (4, 3)-0.06877745 (5, 0) 0.00000000 (5, 1) 0.15363909
 (5, 2)-0.05807012 (5, 3) 0.13206853 (5, 4) 0.10859969 (5, 5) 0.09125590
 (5, 6) 0.01570311 (5, 7)-0.03556054 (5, 8) 0.09612171 (5, 9)-0.14460747
 (5, 10) 0.00000000 (5, 11)-0.15226114 (5, 12) 0.08056902 (5, 13) 0.10994259
 (5, 14)-0.13951476 (5, 15)-0.03579339 (5, 16) 0.15987962 (5, 17)-0.0510897
 (5, 18) 0.04792508 (5, 19) 0.12996778 (5, 20) 0.12688525 (5, 21)-0.04526836
 (5, 22) 0.13350590 (5, 23)-0.12979975 (5, 24) 0.12979975 (5, 25)-0.14025471
 (5, 26) 0.12611867 (6, 0) 0.00000000 (6, 1) 0.15036373 (6, 2)-0.10229786
 (6, 3) 0.08099856 (6, 4) 0.15824580 (6, 5)-0.02759957 (6, 6) 0.12611867
 (6, 7) 0.05244904 (6, 8) 0.15532329 (6, 9) 0.06078093 (6, 10) 0.11532463
 (6, 11)-0.06070803 (6, 12) 0.11396277 (6, 13) 0.06408235 (6, 14) 0.02028482
 (6, 15)-0.15143180 (6, 16) 0.06707560 (6, 17) 0.11380725 (6, 18) 0.01951500
 (6, 19)-0.00000000 (6, 20) 0.12297077 (6, 21) 0.12297077 (6, 22) 0.12297077
 (6, 23)-0.16169751 (6, 24) 0.16169751 (6, 25) 0.09029999 (6, 26) 0.08639810
 (6, 27) 0.05558128 (6, 28) 0.11847049 (6, 29)-0.16174820 (6, 30) 0.16510412
 (6, 31) 0.07433136 (6, 32) 0.09692641 (6, 33) 0.15956704 (6, 34) 0.03150898
 (6, 35)-0.15767708 (6, 36) 0.15767708 (6, 37) 0.01951500 (6, 38) 0.14106894
 (6, 39)-0.16169751 (6, 40) 0.16169751 (6, 41) 0.03174131 (6, 42) 0.16124178
 (6, 43)-0.15029405 (6, 44) 0.03174131 (6, 45) 0.14259489 (6, 46)-0.18008043
 (6, 47) 0.00000000 (6, 48) 0.14078876 (6, 49) 0.15963946 (6, 50) 0.00000000
 (6, 51) 0.11425962 (6, 52) 0.17183350 (6, 53) 0.08375202 (6, 54) 0.07558730
 (6, 55) 0.13127682 (6, 56) 0.01721487 (6, 57) 0.15470171 (6, 58)-0.17684831
 (6, 59) 0.06898709 (6, 60) 0.09045707 (6, 61) 0.16683888 (6, 62) 0.12426481
 (6, 63)-0.03174131 (6, 64) 0.16124178 (6, 65)-0.15029405 (6, 66) 0.00901449
 (6, 67)-0.14777970 (6, 68) 0.14777970 (6, 69) 0.00000000 (6, 70) 0.14212237
 (6, 71) 0.00000000 (6, 72) 0.14212237 (6, 73)-0.00633047 (6, 74) 0.14981532
 (6, 75)-0.00000000 (6, 76) 0.14981532 (6, 77)-0.15917589 (6, 78) 0.14981532
 (6, 79)-0.02194433 (6, 80) 0.13821924 (6, 81)-0.00000000 (6, 82) 0.16817212
 (6, 83)-0.08886147 (6, 84) 0.07437006 (6, 85) 0.16808147 (6, 86)-0.05705629
 (6, 87) 0.16683888 (6, 88) 0.16683888 (6, 89)-0.03174131 (6, 90) 0.16124178
 (6, 91)-0.15029405 (6, 92) 0.16124178 (6, 93)-0.14078876 (6, 94) 0.15963946
 (6, 95)-0.00000000 (6, 96) 0.15963946 (6, 97)-0.07558730 (6, 98) 0.17746888
 (6, 99)-0.09667318 (6, 100) 0.17111515 (6, 101) 0.16764481 (6, 102)-0.16215754
 (6, 103) 0.10238643 (6, 104)-0.19523433 (6, 105) 0.17639944 (6, 106)-0.04146694

(17, 8)-0.10563466 (17, 9) 0.18508211 (17, 10)-0.14719418 (17, 11) 0.01750535
 (17, 12) 0.12507845 (17, 13)-0.19988330 (17, 14) 0.16985846 (17, 15)-0.05487323
 (17, 16)-0.08848687 (17, 17) 0.20196372
 (18, 0) 0.18084322 (18, 1) 0.12285877 (18, 2)-0.01393087 (18, 3) 0.14222105
 (18, 4)-0.18092215 (18, 5) 0.10635046 (18, 6) 0.03457124 (18, 7)-0.15575753
 (18, 8) 0.18567130 (18, 9)-0.10858057 (18, 10)-0.03037404 (18, 11) 0.15534061
 (18, 12)-0.20327942 (18, 13) 0.11446605 (18, 14)-0.03555682 (18, 15)-0.10109171
 (18, 16) 0.20600873 (18, 17)-0.25286067 (18, 18) 0.24277171
 (19, 0) 0.00000000 (19, 1) -0.12950452 (19, 2) 0.18600281 (19, 3)-0.13803977
 (19, 4) 0.01288343 (19, 5) 0.12010040 (19, 6)-0.18903193 (19, 7) 0.15841889
 (19, 8) -0.04578122 (19, 9) -0.09110718 (19, 10) 0.18639560 (19, 11)-0.19847749
 (19, 12) 0.12594701 (19, 13)-0.00202860 (19, 14)-0.12567681 (19, 15) 0.21739155
 (19, 16)-0.25463784 (19, 17) 0.24129419 (19, 18)-0.19542444 (19, 19) 0.13831985
 (20, 0)-0.19121657 (20, 1) 0.14434008 (20, 2)-0.02673216 (20, 3)-0.10422307
 (20, 4) 0.18555631 (20, 5)-0.17938018 (20, 6) 0.08985777 (20, 7) 0.04109519
 (20, 8)-0.1555099 (20, 9) 0.20619856 (20, 10)-0.17563209 (20, 11) 0.07908468
 (20, 12) 0.04648969 (20, 13)-0.16038711 (20, 14) 0.23369984 (20, 15)-0.25655231
 (20, 16) 0.23626754 (20, 17)-0.19892616 (20, 18) 0.13536344 (20, 19)-0.08627984
 (20, 20) 0.04919946
 (21, 0) 0.00000000 (21, 1) 0.12119412 (21, 2)-0.19238970 (21, 3) 0.18474364
 (21, 4)-0.10216460 (21, 5)-0.02151647 (21, 6) 0.13778260 (21, 7)-0.20354240
 (21, 8) 0.19707967 (21, 9)-0.12366652 (21, 10) 0.00999785 (21, 11) 0.10847995
 (21, 12)-0.20102543 (21, 13) 0.25049144 (21, 14)-0.25537086 (21, 15) 0.22602570
 (21, 16)-0.17812629 (21, 17) 0.12649547 (21, 18)-0.08136305 (21, 19) 0.04743523
 (21, 20)-0.02499528 (21, 21) 0.01182687
 (22, 0) 0.20727383 (22, 1)-0.17210703 (22, 2) 0.07865177 (22, 3) 0.04142421
 (22, 4)-0.14838068 (22, 5) 0.20833229 (22, 6)-0.20412946 (22, 7) 0.13939434
 (22, 8)-0.03498396 (22, 9) -0.07982639 (22, 10) 0.17747349 (22, 11)-0.23977748
 (22, 12) 0.26103362 (22, 13)-0.24654251 (22, 14) 0.20823072 (22, 15)-0.15960081
 (22, 16) 0.11182816 (22, 17)-0.07185175 (22, 18) 0.04234017 (22, 19)-0.02282025
 (22, 20) 0.01120659 (22, 21)-0.00496946 (22, 22) 0.00196655
 (23, 0) 0.00000000 (23, 1) -0.10952265 (23, 2) 0.19042009 (23, 3)-0.22218439
 (23, 4) 0.19784090 (23, 5)-0.12499937 (23, 6) 0.02250246 (23, 7) 0.08583889
 (23, 8)-0.17810014 (23, 9) 0.23947918 (23, 10)-0.26459685 (23, 11) 0.25675288
 (23, 12)-0.22503817 (23, 13) 0.18067917 (23, 14)-0.13387655 (23, 15) 0.09188925
 (23, 16)-0.05849861 (23, 17) 0.03452142 (23, 18)-0.01884107 (23, 19) 0.00947216
 (23, 20)-0.00435988 (23, 21) 0.00182116 (23, 22)-0.00068155 (23, 23) 0.00022414
 (24, 0)-0.23693372 (24, 1) 0.21461968 (24, 2)-0.15209740 (24, 3) 0.06149586
 (24, 4) 0.04038411 (24, 5)-0.13608208 (24, 6) 0.21129158 (24, 7)-0.25746304
 (24, 8) 0.27265903 (24, 9)-0.26071191 (24, 10) 0.22921573 (24, 11)-0.18711476
 (24, 12) 0.14259668 (24, 13)-0.10174064 (24, 14) 0.06803974 (24, 15)-0.04264284
 (24, 16) 0.02501429 (24, 17)-0.01370114 (24, 18) 0.00698237 (24, 19)-0.00329428
 (24, 20) 0.00142910 (24, 21)-0.00056471 (24, 22) 0.00020057 (24, 23)-0.00006278
 (24, 24) 0.00001678
 (25, 0) 0.00000000 (25, 1) 0.09031469 (25, 2)-0.17067872 (25, 3) 0.23290417
 (25, 4)-0.27190632 (25, 5) 0.28632534 (25, 6)-0.27834004 (25, 7) 0.25280201
 (25, 8)-0.21597815 (25, 9) 0.17424670 (25, 10)-0.13304399 (25, 11) 0.09623811
 (25, 12)-0.06596134 (25, 13) 0.04281375 (25, 14)-0.02628510 (25, 15) 0.01523602
 (25, 16)-0.00831710 (25, 17) 0.00426154 (25, 18)-0.00204073 (25, 19) 0.00090825
 (25, 20)-0.00037295 (25, 21) 0.00013992 (25, 22)-0.00004731 (25, 23) 0.00001413
 (25, 24)-0.00000361 (25, 25) 0.00000075
 (26, 0) 0.33183736 (26, 1)-0.32563424 (26, 2) 0.30769545 (26, 3)-0.27991599
 (26, 4) 0.24509303 (26, 5)-0.20647214 (26, 6) 0.16726156 (26, 7)-0.13021295
 (26, 8) 0.09734003 (26, 9)-0.06980616 (26, 10) 0.04796969 (26, 11)-0.03154467
 (26, 12) 0.01981892 (26, 13)-0.01187440 (26, 14) 0.00676945 (26, 15)-0.00366228
 (26, 16) 0.00187423 (26, 17)-0.00090384 (26, 18) 0.00040878 (26, 19)-0.00017235
 (26, 20) 0.00006723 (26, 21)-0.00002402 (26, 22) 0.00000775 (26, 23)-0.00000222
 (26, 24) 0.00000054 (26, 25)-0.00000011 (26, 26) 0.00000001

M S L=27

(0, 0) 0.00000000 (1, 1) 0.00553504
 (1, 0)-0.15218833 (2, 1) 0.15198690 (2, 2)-0.02214015
 (2, 0) 0.00000000 (3, 1)-0.01664933 (3, 2)-0.14915788 (3, 3) 0.04937252
 (3, 0) 0.15259363 (4, 1)-0.015137772 (4, 2) 0.04410281 (4, 3) 0.13889761
 (4, 0)-0.08501816 (5, 1)-0.15342070 (5, 2) 0.02789929 (5, 3)-0.14346373 (5, 4)-0.08035913
 (5, 0) 0.11457996 (5, 1) 0.12302942 (5, 2)-0.06570327 (5, 3)-0.12195649
 (5, 3) 0.00000000 (6, 1) 0.15034583 (6, 2)-0.06570327 (6, 3)-0.12195649
 (6, 0) 0.00000000 (6, 1) 0.15111078 (6, 2)-0.06838397 (6, 3)-0.11235984
 (6, 4) 0.11962137 (6, 5) 0.06970588 (6, 6)-0.15148672 (6, 7) 0.07972506 (6, 8)-0.13482875 (6, 9) 0.10841624
 (6, 10) 0.00000000 (6, 11) 0.15014574 (6, 12)-0.00225822 (6, 13) 0.15258539
 (6, 14) 0.14491825 (6, 15) 0.01364973 (6, 16) 0.15401833 (6, 17)-0.07845990 (6, 18) 0.12313004 (6, 19)-0.13229355
 (6, 20) 0.04648969 (6, 21) 0.23369984 (6, 22)-0.25655231 (6, 23) 0.01288397 (6, 24)-0.11235984
 (6, 25) 0.154550687 (6, 26) 0.01352169 (6, 27) 0.00000000 (6, 28) 0.12313004 (6, 29)-0.13229355
 (6, 30) 0.00000000 (6, 31) 0.15711078 (6, 32)-0.06838397 (6, 33) 0.11235984
 (6, 34) 0.14550687 (6, 35) 0.01352169 (6, 36) 0.00000000 (6, 37) 0.12313004 (6, 38)-0.13229355
 (6, 39) 0.00000000 (6, 40) 0.15812358 (6, 41)-0.04704624 (6, 42) 0.12428788 (6, 43) 0.14046708
 (6, 44) 0.01934148 (6, 45) 0.09738106 (6, 46) 0.07904879 (6, 47) 0.10198715 (6, 48)-0.06357360 (6, 49) 0.10699037 (6, 50)-0.06914923
 (6, 51) 0.15890773 (6, 52) 0.14101420 (6, 53) 0.12811497 (6, 54) 0.03671345 (6, 55) 0.15989127 (6, 56) 0.10198715 (6, 57) 0.14046708
 (6, 58) 0.00000000 (6, 59) 0.15890773 (6, 60) 0.06357360 (6, 61) 0.1018363 (6, 62) 0.15064967 (6, 63) 0.12811497 (6, 64) 0.03671345
 (6, 65) 0.01288899 (6, 66) 0.14101420 (6, 67) 0.12811497 (6, 68) 0.03671345 (6, 69) 0.15991782 (6, 70) 0.09738106 (6, 71) 0.07904879 (6, 72) 0.10198715 (6, 73) 0.14046708
 (6, 74) 0.00000000 (6, 75) 0.14436981 (6, 76) 0.12618333 (6, 77) 0.03417276 (6, 78) 0.15675913 (6, 79) 0.10431925 (6, 80) 0.06491543 (6, 81) 0.16349781
 (6, 82) 0.08274990 (6, 83) 0.08946250 (6, 84) 0.016705911 (6, 85) 0.06691167 (6, 86) 0.10569191 (6, 87) 0.07662035 (6, 88) 0.08972044 (6, 89) 0.16200371
 (6, 90) 0.16205472 (6, 91) 0.07662035 (6, 92) 0.08972044 (6, 93) 0.16200371 (6, 94) 0.06434146 (6, 95) 0.10121869 (6, 96) 0.16245408 (6, 97) 0.05600626
 (6, 98) 0.10903281 (6, 99) 0.16505083 (6, 100) 0.05578893 (6, 101) 0.11051668
 (6, 102) 0.17179328 (6, 103) 0.06964387 (6, 104) 0.00000000 (6, 105) 0.14120716 (6, 106) 0.14398892 (6, 107) 0.00563328 (6, 108) 0.13443252
 (6, 109) 0.15741834 (6, 110) 0.03253738 (6, 111) 0.12422908 (6, 112) 0.16989359 (6, 113) 0.01884107 (6, 114) 0.1006212 (6, 115) 0.18240970
 (6, 116) 0.06403319 (6, 117) 0.1006212 (6, 118) 0.18240970 (6, 119) 0.16615802 (6, 120) 0.09064663 (6, 121) 0.06734357 (6, 122) 0.11348642 (6, 123) 0.04005674
 (6, 124) 0.14416550 (6, 125) 0.16353181 (6, 126) 0.04664204 (6, 127) 0.11037434 (6, 128) 0.18274614 (6, 129) 0.11598387 (6, 130) 0.03846382
 (6, 131) 0.151387652 (6, 132) 0.14890358 (6, 133) 0.06964387 (6, 134) 0.18274614 (6, 135) 0.11598387 (6, 136) 0.03456487 (6, 137) 0.14398892 (6, 138) 0.00563328
 (6, 139) 0.15741834 (6, 140) 0.12422908 (6, 141) 0.16989359 (6, 142) 0.01884107 (6, 143) 0.1006212 (6, 144) 0.18240970 (6, 145) 0.16465922 (6, 146) 0.13796890
 (6, 147) 0.11348642 (6, 148) 0.04005674 (6, 149) 0.15886469 (6, 150) 0.16353181 (6, 151) 0.04664204 (6, 152) 0.11037434 (6, 153) 0.18274614 (6, 154) 0.11598387 (6, 155) 0.03846382
 (6, 156) 0.00000000 (6, 157) 0.13727304 (6, 158) 0.15997405 (6, 159) 0.04928704 (6, 160) 0.17080502 (6, 161) 0.09935246 (6, 162) 0.05325285 (6, 163) 0.16465922 (6, 164) 0.13796890
 (6, 165) 0.16474967 (6, 166) 0.14770746 (6, 167) 0.01619236 (6, 168) 0.12958997 (6, 169) 0.18248335 (6, 170) 0.10623889 (6, 171) 0.04467206 (6, 172) 0.17010611
 (6, 173) 0.19367981 (6, 174) 0.17156294 (6, 175) 0.10607462 (6, 176) 0.04044799 (6, 177) 0.15653746 (6, 178) 0.01619236 (6, 179) 0.17634504 (6, 180) 0.03627891 (6, 181) 0.10984011
 (6, 182) 0.11156842 (6, 183) 0.02800348 (6, 184) 0.15413098 (6, 185) 0.17774922 (6, 186) 0.06313559 (6, 187) 0.17661203 (6, 188) 0.19224788 (6, 189) 0.00000000 (6, 190) 0.13236368
 (6, 191) 0.04832055 (6, 192) 0.16003813 (6, 193) 0.16517238 (6, 194) 0.08360568 (6, 195) 0.17694765 (6, 196) 0.16210902 (6, 197) 0.04994547 (6, 198) 0.09296287 (6, 199) 0.18756154
 (6, 200) 0.04084738 (6, 201) 0.16541073 (6, 202) 0.23834890 (6, 203) 0.17886673 (6, 204) 0.12360108 (6, 205) 0.00805493 (6, 206) 0.01710287 (6, 207) 0.14177479 (6, 208) 0.18013661
 (6, 209) 0.18635312 (6, 210) 0.12734140 (6, 211) 0.00134919 (6, 212) 0.013131328 (6, 213) 0.17384841 (6, 214) 0.07291154 (6, 215) 0.05967795

(19,16) 0.17483377 (19,17)-0.24036641 (19,18) 0.24925894 (19,19)-0.21491621
 (20, 0) 0.00000000 (20, 1)-0.12614283 (20, 2) 0.18375404 (20, 3)-0.14191119
 (20, 4) 0.02361517 (20, 5) 0.10786170 (20, 6)-0.18390217 (20, 7) 0.16653031
 (20, 8)-0.06603807 (20, 9)-0.06746562 (20,10) 0.17194911 (20,11)-0.20139182
 (20,12) 0.14799392 (20,13)-0.03629292 (20,14)-0.09071510 (20,15) 0.19250180
 (20,16)-0.24566184 (20,17) 0.24789424 (20,18)-0.21266045 (20,19) 0.15962002
 (20,20)-0.10612297
 (21, 0)-0.18921424 (21, 1) 0.14451477 (21, 2)-0.03157751 (21, 3)-0.09647164
 (21, 4) 0.18025109 (21, 5)-0.18205950 (21, 6) 0.10229995 (21, 7) 0.02278690
 (21, 8)-0.13949098 (21, 9) 0.20095809 (21,10)-0.18568924 (21,11) 0.10280031
 (21,12) 0.01609139 (21,13)-0.13242716 (21,14) 0.21569911 (21,15)-0.25192466
 (21,16) 0.24391447 (21,17)-0.20553543 (21,18) 0.15397814 (21,19)-0.10355425
 (21,20) 0.06272519 (21,21)-0.03417657
 (22, 0) 0.00000000 (22, 1) 0.11799581 (22, 2)-0.18907478 (22, 3) 0.18546748
 (22, 4)-0.10934533 (22, 5)-0.00912974 (22, 6) 0.12500463 (22, 7)-0.19663382
 (22, 8) 0.20076214 (22, 9)-0.13883828 (22,10) 0.03325740 (22,11) 0.08339731
 (22,12)-0.18073542 (22,13) 0.23960479 (22,14)-0.25525665 (22,15) 0.23498327
 (22,16)-0.19258863 (22,17) 0.14255027 (22,18)-0.09594318 (22,19) 0.05885646
 (22,20)-0.03287808 (22,21) 0.01665909 (22,22)-0.00760129
 (23, 0) 0.20519061 (23, 1)-0.17164235 (23, 2) 0.08207632 (23, 3) 0.03423729
 (23, 4)-0.14014581 (23, 5) 0.20320591 (23, 6)-0.20580953 (23, 7) 0.14939608
 (23, 8)-0.05188805 (23, 9)-0.05986980 (23,10) 0.15930031 (23,11)-0.22751950
 (23,12) 0.25688702 (23,13)-0.25039366 (23,14) 0.21811600 (23,15)-0.17265339
 (23,16) 0.12526251 (23,17)-0.08364293 (23,18) 0.05146791 (23,19)-0.02915368
 (23,20) 0.01515427 (23,21)-0.00718950 (23,22) 0.00308720 (23,23)-0.00118502
 (24, 0) 0.00000000 (24, 1)-0.10658883 (24, 2) 0.18632333 (24, 3)-0.21969849
 (24, 4) 0.19954467 (24, 5)-0.13216580 (24, 6) 0.03453214 (24, 7) 0.07123984
 (24, 8)-0.16412117 (24, 9) 0.22914758 (24,10)-0.25988162 (24,11) 0.25812775
 (24,12)-0.23157904 (24,13) 0.19056071 (24,14)-0.14501904 (24,15) 0.10251381
 (24,16)-0.06744497 (24,17) 0.04130419 (24,18)-0.02351421 (24,19) 0.01240911
 (24,20)-0.00604381 (24,21) 0.00269942 (24,22)-0.00109569 (24,23) 0.00039895
 (24,24)-0.00012779
 (25, 0) 0.23464444 (25, 1) 0.21334840 (25, 2)-0.15352909 (25, 3) 0.06638790
 (25, 4) 0.03245198 (25, 5)-0.12655753 (25, 6) 0.20217480 (25, 7)-0.25069350
 (25, 8) 0.26597962 (25, 9)-0.26177308 (25,10) 0.23397675 (25,11)-0.19449021
 (25,12) 0.15122636 (25,13)-0.11034763 (25,14) 0.07567763 (25,15)-0.04879351
 (25,16) 0.02955424 (25,17)-0.01678803 (25,18) 0.00891936 (25,19)-0.00441539
 (25,20) 0.00026069 (25,21)-0.00085580 (25,22) 0.00032959 (25,23)-0.00011419
 (25,24) 0.00003490 (25,25)-0.00000911
 (26, 0) 0.00000000 (26, 1) 0.08786225 (26, 2)-0.16638723 (26, 3) 0.22783510
 (26, 4)-0.26729089 (26, 5) 0.28325859 (26, 6)-0.27753559 (26, 7) 0.25446945
 (26, 8)-0.21984096 (26, 9) 0.17967460 (26,10)-0.13924497 (26,11) 0.10244834
 (26,12)-0.07158486 (26,13) 0.04748964 (26,14)-0.02988517 (26,15) 0.01781418
 (26,16)-0.01003809 (26,17) 0.00533273 (26,18)-0.00266175 (26,19) 0.00124277
 (26,20)-0.00053971 (26,21) 0.00021641 (26,22)-0.00007933 (26,23) 0.00002623
 (26,24)-0.00000766 (26,25) 0.00000192 (26,26)-0.00000039
 (27, 0) 0.32875043 (27, 1)-0.32282650 (27, 2) 0.30567285 (27, 3)-0.27903986
 (27, 4) 0.24552235 (27, 5)-0.20815170 (27, 6) 0.16955155 (27, 7)-0.13356864
 (27, 8) 0.10096841 (27, 9)-0.07335185 (27,10) 0.05116187 (27,11)-0.03421993
 (27,12) 0.02191829 (27,13)-0.01342216 (27,14) 0.00784322 (27,15)-0.00436357
 (27,16) 0.000230514 (27,17)-0.00115257 (27,18) 0.00054333 (27,19)-0.000024033
 (27,20) 0.00009915 (27,21)-0.00003786 (27,22) 0.00001325 (27,23)-0.00000419
 (27,24) 0.00000117 (27,25)-0.00000028 (27,26) 0.00000005 (27,27)-0.00000001
 M S L=28

(0, 0) 0.14944598 (1, 0) 0.00000000 (1, 1)-0.14944598 (2, 0) 0.01050199 (2, 2) 0.14833897
 (2, 1) 0.01050199 (3, 0) 0.00000000 (3, 1) 0.14907652 (3, 2)-0.03142809 (3, 3)-0.14280394
 (4, 0) 0.15019043 (4, 1)-0.02108260 (4, 2)-0.14444961 (4, 3) 0.06183901
 (4, 4) 0.12749957

(5, 0) 0.00000000 (5, 1)-0.14832927 (5, 2) 0.05211759 (5, 3) 0.13033924
 (5, 4)-0.09839454 (5, 5)-0.09603288 (6, 0)-0.15114768 (6, 1) 0.03182546 (6, 2) 0.13791537 (6, 3)-0.09019868
 (6, 4)-0.10016353 (6, 5) 0.13336296 (6, 6) 0.04357333 (7, 0) 0.00000000 (7, 1) 0.14718679 (7, 2)-0.07240263 (7, 3)-0.11184773
 (7, 4) 0.12803544 (7, 5) 0.04871762 (7, 6)-0.15324143 (7, 7) 0.02821835 (8, 0) 0.15254077 (8, 1)-0.04282505 (8, 2)-0.12865348 (8, 3) 0.11543719
 (8, 4) 0.06383388 (8, 5)-0.15231057 (8, 6) 0.02290510 (8, 7) 0.14028573
 (8, 8)-0.10475049 (8, 9) 0.00000000 (9, 1)-0.14562093 (9, 2) 0.09209877 (9, 3) 0.08758909
 (9, 4)-0.14818485 (9, 5) 0.00674899 (9, 6) 0.14478512 (9, 7)-0.10071987 (10, 0) 0.15443055 (10, 1) 0.05419450 (10, 2) 0.11653707 (10, 3)-0.13642567
 (10, 4)-0.02050575 (10, 5) 0.15168576 (10, 6)-0.08784899 (10, 7)-0.08954600 (10, 8) 0.15379381 (10, 9)-0.02256257 (10, 10)-0.13890527
 (11, 0) 0.00000000 (11, 1) 0.14358985 (11, 2)-0.11099513 (11, 3)-0.05793371 (11, 4) 0.15647243 (11, 5)-0.06409456 (11, 6)-0.10704535 (11, 7) 0.14946030
 (11, 8)-0.08018295 (11, 9) 0.15485942 (11, 10) 0.12773454 (11, 11) 0.03766365 (12, 0) 0.15690881 (12, 1)-0.06607703 (12, 2)-0.10138135 (12, 3) 0.15194494
 (12, 4)-0.02716873 (12, 5) 0.12954083 (12, 6) 0.13851880 (12, 7) 0.01074144 (12, 8)-0.14917138 (12, 9) 0.12075064 (12, 10) 0.04316646 (12, 11)-0.16155976
 (13, 0) 0.00000000 (13, 1)-0.14103316 (13, 2) 0.12884040 (13, 3) 0.02338923 (13, 4)-0.15082294 (13, 5) 0.11583369 (13, 6) 0.04408690 (13, 7)-0.15804112
 (13, 8) 0.10495216 (13, 9) 0.05942947 (13, 10)-0.16375750 (13, 11) 0.10042625
 (13, 12) 0.06625500 (13, 13)-0.16950421 (14, 0)-0.16011387 (14, 1) 0.07866453 (14, 2) 0.08291970 (14, 3)-0.16063970
 (14, 4) 0.07579512 (14, 5) 0.08603763 (14, 6)-0.16242579 (14, 7) 0.07719027 (14, 8) 0.08531610 (14, 9)-0.16583620 (14, 10) 0.08643691 (14, 11) 0.07683612
 (14, 12)-0.17032689 (14, 13) 0.10797510 (14, 14) 0.05335477 (15, 0) 0.00000000 (15, 1) 0.13786346 (15, 2)-0.14532085 (15, 3) 0.01535613
 (15, 4) 0.12957716 (15, 5)-0.15356320 (15, 6) 0.03433924 (15, 7) 0.11763016 (15, 8)-0.16300076 (15, 9) 0.06086578 (15, 10) 0.09706443 (15, 11)-0.17163055
 (15, 12) 0.09882984 (15, 13) 0.05898221 (15, 14) 0.17134580 (15, 15) 0.14916770 (16, 0) 0.16425900 (16, 1)-0.09222978 (16, 2)-0.06076170 (16, 3) 0.16094601
 (16, 4)-0.12110050 (16, 5)-0.02405703 (16, 6) 0.14940122 (16, 7)-0.14804572 (16, 8) 0.02152165 (16, 9) 0.12432081 (16, 10)-0.16984400 (16, 11) 0.07905183
 (16, 12) 0.07556163 (16, 13)-0.17489086 (16, 14) 0.14586513 (16, 15)-0.01132873
 (16, 16)-0.13448368 (17, 0) 0.00000000 (17, 1) 0.13391565 (17, 2) 0.16002376 (17, 3)-0.05736066
 (17, 4)-0.09167054 (17, 5) 0.16840023 (17, 6)-0.11249252 (17, 7)-0.03187311 (17, 8) 0.15294260 (17, 9)-0.15894175 (17, 10) 0.04627942 (17, 11) 0.10180203
 (17, 12)-0.17975570 (17, 13) 0.13497403 (17, 14) 0.00059265 (17, 15)-0.13889855 (17, 16)-0.19685176 (17, 17)-0.14506431 (18, 0) 0.0-0.16968787 (18, 1) 0.10718779 (18, 2) 0.03431422 (18, 3)-0.15096544
 (18, 4) 0.15770498 (18, 5)-0.05001091 (18, 6) 0.09432820 (18, 7) 0.17277579 (18, 8)-0.13101900 (18, 9) 0.00124489 (18, 10) 0.13431004 (18, 11)-0.18122889
 (18, 12) 0.11372779 (18, 13) 0.02466260 (18, 14)-0.15142377 (18, 15) 0.19694696 (18, 16)-0.14110765 (18, 17) 0.01590459 (18, 18) 0.12031773 (18, 19) 0.24883230
 (18, 20) 0.17699373 (18, 21)-0.12422524 (18, 22)-0.00261890 (18, 23) 0.1282299 (18, 24) 0.12557425 (18, 25) 0.21629681 (18, 26) 0.24883230
 (18, 27) 0.12513267 (18, 28) 0.12513267 (18, 29) 0.00085556 (18, 30) 0.17373725 (18, 31) 0.18438500 (18, 32) 0.14241858 (18, 33) 0.02534156 (18, 34) 0.10617487
 (18, 35) 0.18861306 (18, 36) 0.18646444 (18, 37) 0.10469114 (18, 38) 0.02007586 (18, 39) 0.14097801 (18, 40) 0.22200695 (18, 41) 0.24913910 (18, 42) 0.22932470
 (18, 43) 0.18146990 (18, 44) 0.03344867 (18, 45) 0.09601071 (18, 46) 0.17786197 (18, 47) 0.17245147

(21, 8)-0.08392268 (21, 9)-0.04473336 (21, 10) 0.15488410 (21, 11)-0.20015429
 (21, 12) 0.16500416 (21, 13)-0.06679510 (21, 14)-0.05660500 (21, 15) 0.16522682
 (21, 16)-0.12320857 (21, 17) 0.24941801 (21, 18)-0.22593895 (21, 19) 0.17892106
 (21, 20)-0.12588377 (21, 21) 0.07921182 (22, 1) 0.14461440 (22, 2)-0.03603055 (22, 3)-0.08913143
 (22, 4)-0.17482138 (22, 5)-0.18374786 (22, 6) 0.11318003 (22, 7) 0.00571022
 (22, 8)-0.12336104 (22, 9) 0.19376144 (22, 10)-0.19239706 (22, 11) 0.12300641
 (22, 12)-0.01206695 (22, 13)-0.10450636 (22, 14) 0.19551329 (22, 15)-0.24370606
 (22, 16) 0.24777907 (22, 17)-0.21833633 (22, 18) 0.17110597 (22, 19)-0.12072741
 (22, 20) 0.07710114 (22, 21)-0.04460724 (22, 22) 0.02331553
 (23, 0) 0.00000000 (23, 1) 0.11498722 (23, 2)-0.18585099 (23, 3) 0.18585862
 (23, 4)-0.11572372 (23, 5) 0.00235997 (23, 6) 0.11257925 (23, 7)-0.18900371
 (23, 8) 0.20258707 (23, 9)-0.15153737 (23, 10) 0.05432646 (23, 11) 0.05936154
 (23, 12)-0.15991320 (23, 13) 0.22676614 (23, 14)-0.25241101 (23, 15) 0.24124540
 (23, 16)-0.20505534 (23, 17) 0.15762159 (23, 18)-0.11049563 (23, 19) 0.07090523
 (23, 20)-0.04167278 (23, 21) 0.02238551 (23, 22)-0.01093924 (23, 23) 0.00482542
 (24, 0) 0.20320806 (24, 1)-0.171114891 (24, 2) 0.08519210 (24, 3) 0.02753642
 (24, 4)-0.132224183 (24, 5) 0.19787727 (24, 6)-0.20656700 (24, 7) 0.15790638
 (24, 8)-0.06719310 (24, 9)-0.04104112 (24, 10) 0.14134036 (24, 11)-0.21443667
 (24, 12) 0.25110844 (24, 13)-0.25227454 (24, 14) 0.22620356 (24, 15)-0.18445498
 (24, 16) 0.13813794 (24, 17)-0.09549484 (24, 18) 0.06106916 (24, 19)-0.03612708
 (24, 20) 0.01973344 (24, 21)-0.00991555 (24, 22) 0.0045649 (24, 23)-0.00189840
 (25, 0) 0.00000000 (25, 1)-0.10383191 (25, 2) 0.18241407 (25, 3)-0.21717384
 (25, 4) 0.20081589 (25, 5)-0.13851617 (25, 6) 0.04557062 (25, 7) 0.05747879
 (25, 8)-0.15051481 (25, 9) 0.21855485 (25, 10)-0.25430900 (25, 11) 0.25826743
 (25, 12)-0.23681509 (25, 13) 0.19935443 (25, 14)-0.15547116 (25, 15) 0.11288869
 (25, 16)-0.07650957 (25, 17) 0.04843697 (25, 18)-0.02862604 (25, 19) 0.01576325
 (25, 20)-0.00806197 (25, 21) 0.00381158 (25, 22)-0.00165489 (25, 23) 0.00065377
 (25, 24)-0.00023193 (25, 25) 0.00007246
 (26, 1) 0.23246166 (26, 2)-0.11753488 (26, 3) 0.07087620
 (26, 4) 0.02505852 (26, 5)-0.11753397 (26, 6) 0.19333978 (26, 7)-0.24386187
 (26, 8) 0.26607510 (26, 9)-0.26213390 (26, 10) 0.23792048 (26, 11)-0.20110418
 (26, 12) 0.15928510 (26, 13)-0.11864012 (26, 14) 0.08329513 (26, 15)-0.05507229
 (26, 16) 0.03433297 (26, 17)-0.02014712 (26, 18) 0.01110605 (26, 19)-0.00573427
 (26, 20) 0.00276208 (26, 21)-0.00123459 (26, 22) 0.00050846 (26, 23)-0.00019110
 (26, 24) 0.00006467 (26, 25)-0.00001931 (26, 26) 0.00000493
 (27, 0) 0.00000000 (27, 1) 0.08555978 (27, 2)-0.16233827 (27, 3) 0.22300674
 (27, 4)-0.26281598 (27, 5) 0.28016278 (27, 6)-0.27651337 (27, 7) 0.25576448
 (27, 8)-0.22324954 (27, 9) 0.18465337 (27, 10)-0.14507739 (27, 11) 0.10841674
 (27, 12)-0.07710444 (27, 13) 0.05218066 (27, 14)-0.03358267 (27, 15) 0.02053091
 (27, 16)-0.01190371 (27, 17) 0.00653124 (27, 18)-0.00338171 (27, 19) 0.00164653
 (27, 20)-0.00075049 (27, 21) 0.00031841 (27, 22)-0.00012481 (27, 23) 0.000004476
 (27, 24)-0.00001448 (27, 25) 0.00000414 (27, 26)-0.00000102 (27, 27) 0.00000020
 (28, 0) 0.32580194 (28, 1)-0.32013538 (28, 2) 0.30370709 (28, 3)-0.27813828
 (28, 4) 0.24584183 (28, 5)-0.20965461 (28, 6) 0.17243637 (28, 7)-0.13671187
 (28, 8) 0.10441541 (28, 9)-0.07676774 (28, 10) 0.05428299 (28, 11)-0.03687803
 (28, 12) 0.02404153 (28, 13)-0.01501863 (28, 14) 0.00897535 (28, 15)-0.00512131
 (28, 16) 0.00278373 (28, 17)-0.00143751 (28, 18) 0.00070296 (28, 19)-0.00032425
 (28, 20) 0.00014040 (28, 21)-0.00005673 (28, 22) 0.00002123 (28, 23)-0.00000728
 (28, 24) 0.00000226 (28, 25)-0.00000062 (28, 26) 0.00000015 (28, 27)-0.00000003
 M S L=29
 (0, 0) 0.00000000 (1, 1)-0.00498153 (2, 2) 0.01992613
 (2, 0) 0.00000000 (2, 1)-0.14676511 (3, 2) 0.14439286 (3, 3)-0.04448786
 (3, 0)-0.14727384 (3, 1) 0.01497915 (3, 2) 0.14439286 (3, 3)-0.04448786
 (4, 0) 0.00000000 (4, 1) 0.14625463 (4, 2)-0.03971364 (4, 3)-0.13578410
 (5, 0) 0.14796527 (5, 1)-0.02508246 (5, 2)-0.13962209 (5, 3) 0.07264086

(5, 4) 0.11531025 (5, 5)-0.11253299
 (6, 0) 0.00000000 (6, 1)-0.14539176 (6, 2) 0.05921901 (6, 3) 0.12155186
 (6, 4)-0.10922226 (6, 5)-0.07716703 (6, 6) 0.14182065
 (7, 0)-0.14903362 (7, 1) 0.03536899 (7, 2) 0.13239820 (7, 3)-0.09851066
 (7, 4)-0.08577694 (7, 5) 0.14016290 (7, 6) 0.01858089 (7, 7)-0.15021515
 (8, 0) 0.00000000 (8, 1) 0.14415736 (8, 2)-0.07828832 (8, 3)-0.10187592
 (8, 4) 0.13420936 (8, 5) 0.02870072 (8, 6)-0.15085016 (8, 7) 0.05497054
 (8, 8) 0.12131441 (9, 0) 0.15052028 (9, 1)-0.04592804 (9, 2)-0.12263341 (9, 3) 0.12113155
 (9, 4) 0.04862491 (9, 5) 0.15172102 (9, 6) 0.04531421 (9, 7) 0.12447049
 (9, 8)-0.12423062 (9, 9) 0.04655323
 (10, 0) 0.00000000 (10, 1)-0.14252226 (10, 2) 0.09675041 (10, 3) 0.07702147
 (10, 4)-0.14967750 (10, 5) 0.02529484 (10, 6) 0.13311070 (10, 7)-0.11799581
 (10, 8) 0.05153549 (10, 9) 0.15565959 (10, 10)-0.05934341
 (11, 0)-0.15248795 (11, 1) 0.05686808 (11, 2) 0.11019850 (11, 3)-0.13947821
 (11, 4)-0.005082557 (11, 5) 0.14452899 (11, 6)-0.10384777 (11, 7)-0.06617541
 (11, 8) 0.15576483 (11, 9)-0.05447281 (11, 10)-0.11464220 (11, 11) 0.14667211
 (12, 0) 0.00000000 (12, 1) 0.14044428 (12, 2)-0.11440776 (12, 3)-0.04735547
 (12, 4) 0.15360762 (12, 5)-0.07887095 (12, 6)-0.08920790 (12, 7) 0.15384495
 (12, 8) 0.03944254 (12, 9)-0.12186959 (12, 10) 0.14462219 (12, 11)-0.00244124
 (12, 12)-0.14460526
 (13, 0) 0.15502959 (13, 1)-0.06832794 (13, 2)-0.09490886 (13, 3) 0.15243641
 (13, 4) 0.04006629 (13, 5)-0.11742125 (13, 6) 0.14564095 (13, 7)-0.01332663
 (13, 8)-0.13474350 (13, 9) 0.13747613 (13, 10) 0.00830605 (13, 11)-0.14710689
 (13, 12) 0.13236311 (13, 13) 0.02076614
 (14, 0) 0.00000000 (14, 1)-0.13786346 (14, 2) 0.13102295 (14, 3) 0.01337247
 (14, 4)-0.14426307 (14, 5) 0.12511386 (14, 6) 0.02424777 (14, 7)-0.14961194
 (14, 8) 0.12237367 (14, 9) 0.02980889 (14, 10)-0.15366285 (14, 11) 0.12587167
 (14, 12) 0.02620118 (14, 13)-0.15542521 (14, 14) 0.13922319
 (15, 0)-0.15828393 (15, 1) 0.08049492 (15, 2) 0.07650091 (15, 3)-0.15875946
 (15, 4) 0.08583082 (15, 5) 0.07118563 (15, 6)-0.16002433 (15, 7) 0.09513729
 (15, 8) 0.06135779 (15, 9)-0.16124758 (15, 10) 0.11114596 (15, 11) 0.04240485
 (15, 12)-0.15961877 (15, 13) 0.13609582 (15, 14) 0.00694872 (15, 15)-0.14706707
 (16, 0) 0.00000000 (16, 1) 0.13469377 (16, 2)-0.14629774 (16, 3) 0.02426361
 (16, 4) 0.12030131 (16, 5)-0.15641914 (16, 6) 0.05168788 (16, 7) 0.10006765
 (16, 8)-0.16436629 (16, 9) 0.08512626 (16, 10) 0.06871572 (16, 11)-0.16600166
 (16, 12) 0.12580697 (16, 13) 0.01810591 (16, 14)-0.15025109 (16, 15) 0.16866653
 (16, 16)-0.06124783
 (17, 0) 0.00000000 (17, 1)-0.16246377 (17, 2)-0.05459085 (17, 3) 0.15699857
 (17, 4)-0.12745327 (17, 5)-0.00910089 (17, 6) 0.13888603 (17, 7)-0.15493858
 (17, 8) 0.04456493 (17, 9) 0.10284638 (17, 10)-0.17028090 (17, 11) 0.10581824
 (17, 12) 0.04036273 (17, 13)-0.15894027 (17, 14) 0.16490607 (17, 15)-0.05596792
 (17, 16)-0.09297302 (17, 17) 0.18671215
 (18, 0) 0.00000000 (18, 1)-0.13080865 (18, 2) 0.15983765 (18, 3)-0.06464925
 (18, 4)-0.08049043 (18, 5) 0.16489708 (18, 6)-0.12340093 (18, 7)-0.01170246
 (18, 8) 0.13922375 (18, 9)-0.16560562 (18, 10) 0.07264576 (18, 11) 0.07290550
 (18, 12)-0.17033340 (18, 13) 0.15536374 (18, 14)-0.03971267 (18, 15)-0.10297581
 (18, 16) 0.18834278 (18, 17)-0.17157361 (18, 18) 0.06614718
 (19, 0) 0.00000000 (19, 1) 0.10816160 (19, 2) 0.02859706 (19, 3) 0.14538157
 (19, 4) 0.15990643 (19, 5)-0.06235621 (19, 6)-0.07909868 (19, 7) 0.16726346
 (19, 8)-0.14300211 (19, 9) 0.02343238 (19, 10) 0.11276020 (19, 11)-0.17916791
 (19, 12) 0.13619138 (19, 13)-0.01152546 (19, 14)-0.12204354 (19, 15) 0.19228786
 (19, 16)-0.16619986 (19, 17) 0.06089823 (19, 18) 0.07369356 (19, 19)-0.18480989
 (20, 0) 0.00000000 (20, 1) 0.12601364 (20, 2)-0.17108725 (20, 3) 0.10651527
 (20, 4) 0.02822956 (20, 5)-0.14300202 (20, 6) 0.17097630 (20, 7)-0.09363895
 (20, 8)-0.04115860 (20, 9) 0.15285297 (20, 10)-0.17728978 (20, 11) 0.10238791
 (20, 12) 0.02915486 (20, 13)-0.14773822 (20, 14) 0.19559804 (20, 15)-0.15370621
 (20, 16) 0.04475111 (20, 17) 0.08456480 (20, 18)-0.18851307 (20, 19) 0.24075897
 (20, 20)-0.23936899
 (21, 0) 0.17521484 (21, 1) 0.12474713 (21, 2) 0.00241954 (21, 3) 0.12157836
 (21, 4)-0.17675389 (21, 5) 0.13248040 (21, 6)-0.01417945 (21, 7)-0.11274061
 (21, 8) 0.18026623 (21, 9)-0.15415169 (21, 10) 0.04948532 (21, 11) 0.08077595

(21,12)-0.17510045 (21,13) 0.19310242 (21,14)-0.13082398 (21,15) 0.01672133
 (21,16) 0.10592248 (21,17)-0.19908558 (21,18) 0.24301817 (21,19)-0.23843166
 (21,20) 0.20012690 (21,21)-0.14742798 (22, 1)-0.11998898 (22, 2) 0.17919841 (22, 3)-0.14797756
 (22, 4) 0.04245842 (22, 5) 0.08459458 (22, 6)-0.17113717 (22, 7) 0.17648146 (22, 8)-0.0956696 (22, 9)-0.02315810 (22,10) 0.13719374 (22,11)-0.19550693
 (22,12) 0.17743160 (22,13)-0.09340367 (22,14)-0.02406995 (22,15) 0.13658893 (22,16)-0.21480429 (22,17) 0.24630016 (22,18)-0.23514460 (22,19) 0.19570932 (22,20)-0.14492258 (22,21) 0.09637316 (22,22)-0.0773287 (23, 0)-0.18550272 (23, 1) 0.14465003 (23, 2)-0.04013180 (23, 3)-0.08218014 (23, 4) 0.16932873 (23, 5)-0.18459870 (23, 6) 0.12265231 (23, 7)-0.01014172 (23, 8)-0.10735108 (23, 9) 0.18505149 (23,10)-0.19620901 (23,11) 0.13992287 (23,12)-0.03781702 (23,13)-0.07715282 (23,14) 0.17383045 (23,15)-0.23247930 (23,16) 0.24813992 (23,17)-0.22815259 (23,18) 0.18641016 (23,19)-0.13737093 (23,20) 0.09196279 (23,21)-0.05607137 (23,22) 0.03111329 (23,23)-0.01565221 (24, 0) 0.00000000 (24, 1) 0.11215128 (24, 2)-0.18271980 (24, 3) 0.18596959 (24, 4)-0.12138950 (24, 5) 0.01301133 (24, 6) 0.10056110 (24, 7)-0.18085280 (24, 8) 0.20284440 (24, 9)-0.16201259 (24,10) 0.07327556 (24,11) 0.03654728 (24,12)-0.13983527 (24,13) 0.21242060 (24,14) -0.24718998 (24,15) 0.244496929 (24,16)-0.21546397 (24,17) 0.17148864 (24,18)-0.12474336 (24,19) 0.08334193 (24,20)-0.05123018 (24,21) 0.02895350 (24,22)-0.01500131 (24,23) 0.00708804 (24,24)-0.00302923 (25, 0) 0.20131770 (25, 1)-0.17063273 (25, 2) 0.08803312 (25, 3) 0.02127989 (25, 4)-0.12466456 (25, 5) 0.19241816 (25, 6)-0.20654845 (25, 7) 0.16505927 (25, 8)-0.08101220 (25, 9)-0.02335209 (25,10) 0.12374958 (25,11)-0.20078428 (25,12) 0.24396905 (25,13)-0.25238469 (25,14) 0.23256762 (25,15)-0.19495143 (25,16) 0.15031199 (25,17)-0.10723618 (25,18) 0.07099650 (25,19)-0.04365463 (25,20) 0.02490773 (25,21)-0.01315454 (25,22) 0.00640400 (25,23)-0.00285612 (26, 0) 0.00000000 (26, 1)-0.10123570 (26, 2) 0.17868051 (26, 3)-0.21462961 (26, 4)-0.20117120 (26, 5)-0.14414255 (26, 6) 0.05570197 (26, 7) 0.04452288 (26, 8)-0.13732630 (26, 9) 0.20782050 (26,10)-0.24803893 (26,11) 0.25732329 (26,12)-0.24084562 (26,13) 0.20708556 (26,14)-0.16518901 (26,15) 0.12292597 (26,16)-0.08559301 (26,17) 0.05583616 (26,18)-0.03412338 (26,19) 0.01951325 (26,20)-0.01041715 (26,21) 0.00517356 (26,22)-0.00237853 (26,23) 0.00100545 (26,24)-0.00038714 (26,25) 0.00013399 (26,26)-0.00004087 (27, 0)-0.23037677 (27, 1) 0.21088360 (27, 2)-0.15588219 (27, 3) 0.07500269 (27, 4) 0.01815662 (27, 5)-0.10898422 (27, 6) 0.18479253 (27, 7)-0.23701602 (27, 8) 0.26222512 (27, 9)-0.26188377 (27,10) 0.24112140 (27,11)-0.20699796 (27,12) 0.16677484 (27,13)-0.12658699 (27,14) 0.09071163 (27,15)-0.06142678 (27,16) 0.03930796 (27,17)-0.02375191 (27,18) 0.01353189 (27,19)-0.00725232 (27,20) 0.00364502 (27,21)-0.00171092 (27,22) 0.00074595 (27,23)-0.00029992 (27,24) 0.00011013 (27,25)-0.00003644 (27,26) 0.00001065 (27,27)-0.00000266 (28, 0) 0.00000000 (28, 1) 0.08339336 (28, 2)-0.15851109 (28, 3) 0.21840259 (28, 4)-0.25847957 (28, 5) 0.27705550 (28, 6)-0.27530852 (28, 7) 0.25673145 (28, 8)-0.22624631 (28, 9) 0.18921340 (28,10)-0.15055393 (28,11) 0.11413834 (28,12)-0.08250199 (28,13) 0.05686256 (28,14)-0.03735397 (28,15) 0.02336788 (28,16)-0.01390291 (28,17) 0.00785285 (28,18)-0.00420139 (28,19) 0.00212300 (28,20)-0.0010955 (28,21) 0.00044973 (28,22)-0.00018660 (28,23) 0.00007158 (28,24)-0.00002513 (28,25) 0.00000797 (28,26)-0.00000223 (28,27) 0.00000054

M S L=30
 (29, 0) 0.31755245 (29, 2) 0.30179611 (29, 3)-0.27721742 (29, 4)-0.2298109 (29, 5)-0.21099919 (29, 6) 0.17472392 (29, 7)-0.13965775 (29, 8) 0.10769004 (29, 9)-0.08005591 (29,10) 0.05732923 (29,11)-0.03951144 (29,12) 0.02617985 (29,13)-0.01665586 (29,14) 0.01015998 (29,15)-0.00593215 (29,16) 0.00330879 (29,17)-0.00175899 (29,18) 0.00088880 (29,19)-0.00042548 (29,20) 0.00019221 (29,21)-0.00008155 (29,22) 0.00003230 (29,23)-0.00001185 (29,24) 0.00000399 (29,25)-0.00000121 (29,26) 0.00000033 (29,27)-0.00000008 (29,28) 0.00000001 (29,29) 0.00000000 (0, 0)-0.14446445 (1, 0) 0.00000000 (1, 1) 0.14446445 (2, 0) 0.14462003 (2, 1)-0.00948456 (2, 2)-0.14353041 (3, 0) 0.00000000 (3, 1)-0.14415276 (3, 2) 0.02839228 (3, 3) 0.13886023 (4, 0)-0.14509188 (4, 1) 0.01903100 (4, 2) 0.14025036 (4, 3)-0.05598333 (5, 0) 0.00000000 (5, 1) 0.14352328 (5, 2)-0.04711382 (5, 3)-0.12833428 (5, 4) 0.08962417 (5, 5) 0.09918704 (6, 0) 0.14589572 (6, 1)-0.02870465 (6, 2)-0.13474554 (6, 3) 0.08196035 (6, 4) 0.10272402 (6, 5)-0.12318305 (6, 6)-0.05401992 (7, 0) 0.00000000 (7, 1)-0.14256324 (7, 2) 0.06551815 (7, 3) 0.11269604 (7, 4)-0.11780524 (7, 5)-0.05851744 (7, 6) 0.14576605 (7, 7)-0.00957073 (8, 0)-0.14705957 (8, 1) 0.03857819 (8, 2) 0.12695570 (8, 3)-0.10548618 (8, 4) 0.07166491 (8, 5) 0.14395954 (8, 6)-0.00471647 (8, 7)-0.14239658 (9, 0) 0.00000000 (9, 1) 0.14125229 (9, 2)-0.08346301 (9, 3)-0.09213454 (9, 4) 0.13847138 (9, 5) 0.00991357 (9, 6)-0.14518669 (9, 7) 0.07771830 (9, 8) 0.09902539 (9, 9)-0.13929169 (10, 0) 0.14862686 (10, 1)-0.04873667 (10, 2)-0.11678975 (10, 3) 0.12568405 (10, 4) 0.03420695 (10, 5)-0.14891429 (10, 6) 0.06487973 (10, 7) 0.10637267 (10, 8)-0.13735949 (10, 9)-0.01357240 (10,10) 0.14818923 (11, 0) 0.00000000 (11, 1)-0.13956058 (11, 2) 0.10078862 (11, 3) 0.06691689 (11, 4)-0.14970635 (11, 5) 0.04196939 (11, 6) 0.11975820 (11, 7)-0.13066611 (11, 8)-0.02347692 (11, 9) 0.14951158 (11,10)-0.08976293 (11,11)-0.08236143 (12, 0)-0.15066168 (12, 1) 0.05928469 (12, 2) 0.10411717 (12, 3)-0.14161776 (12, 4) 0.00772111 (12, 5) 0.13609605 (12, 6)-0.11664072 (12, 7)-0.04307157 (12, 8) 0.15253723 (12, 9)-0.08150952 (12,10)-0.08666659 (12,11) 0.15513425 (12,12)-0.04394750 (13, 0) 0.00000000 (13, 1) 0.13744591 (13, 2)-0.11730896 (13, 3)-0.03740437 (13, 4) 0.14978942 (13, 5)-0.09153382 (13, 6)-0.07128998 (13, 7) 0.15435094 (13, 8)-0.06388727 (13, 9)-0.09907550 (13,10) 0.15344732 (13,11)-0.03904747 (13,12)-0.11960921 (13,13) 0.15142912 (14, 0) 0.15325776 (14, 1)-0.07035728 (14, 2)-0.08875428 (14, 3) 0.15226385 (14, 4)-0.05166891 (14, 5)-0.10497306 (14, 6) 0.14993002 (14, 7)-0.03519706 (14, 8)-0.11779043 (14, 9) 0.14812009 (14,10)-0.02405182 (14,11)-0.12639762 (14,12) 0.14966507 (14,13)-0.02228649 (14,14)-0.12942749 (15, 0) 0.00000000 (15, 1)-0.13484885 (15, 2) 0.13279891 (15, 3) 0.00407751 (15, 4)-0.13726953 (15, 5) 0.13241783 (15, 6) 0.00561221 (15, 7)-0.13895954 (15, 8) 0.13535431 (15, 9) 0.00162161 (15,10)-0.13847537 (15,11) 0.14343183 (15,12)-0.01195175 (15,13)-0.13275070 (15,14) 0.15777308 (15,15)-0.04108832 (16, 0)-0.15655401 (16, 1) 0.08213773 (16, 2) 0.07044092 (16, 3)-0.15647008 (16, 4) 0.09458629 (16, 5) 0.05682020 (16, 6)-0.15571852 (16, 7) 0.11001546 (16, 8) 0.03787823 (16, 9)-0.15241703 (16,10) 0.13000248 (16,11) 0.00898832 (16,12)-0.14196417 (16,13) 0.15416288 (16,14)-0.03596572 (16,15)-0.11424027 (16,16) 0.17590985 (17, 0) 0.00000000 (17, 1) 0.13168481 (17, 2)-0.14697403 (17, 3) 0.03242355 (17, 4) 0.11106890 (17, 5)-0.15775031 (17, 6) 0.06709942 (17, 7) 0.08225449 (17, 8)-0.16223289 (17, 9) 0.10529245 (17,10) 0.04044211 (17,11)-0.15458696 (17,12) 0.14506306 (17,13)-0.02031690 (17,14)-0.12230545 (17,15) 0.17568205 (17,16)-0.10245947 (17,17)-0.04409752 (18, 0) 0.16072653 (18, 1)-0.09488900 (18, 2)-0.04879985 (18, 3) 0.15288846 (18, 4)-0.13269950 (18, 5) 0.00480301 (18, 6) 0.12767108 (18, 7)-0.15907234 (18, 8) 0.06501573 (18, 9) 0.08064307 (18,10)-0.16587684 (18,11) 0.12691554 (18,12) 0.00640840 (18,13)-0.13716063 (18,14) 0.17402439 (18,15)-0.09367601 (18,16)-0.04938462 (18,17) 0.16523448 (18,18)-0.18741603 (19, 0) 0.00000000 (19, 1)-0.12782978 (19, 2) 0.15945628 (19, 3)-0.07123145 (19, 4)-0.07063899 (19, 5) 0.16052693 (19, 6)-0.13230377 (19, 7) 0.00710537 (19, 8) 0.12422618 (19, 9)-0.16832976 (19,10) 0.09515117 (19,11) 0.04410292 (19,12)-0.15578046 (19,13) 0.16799624 (19,14)-0.07495217 (19,15)-0.06508618

(19, 16) 0.17072019 (19, 17)-0.18625388 (19, 18) 0.10802311 (19, 19) 0.02258850
 (20, 0)-0.16622339 (20, 1) 0.10901360 (20, 2) 0.02326055 (20, 3)-0.13985795
 (20, 4) 0.16130356 (20, 5)-0.07341507 (20, 6)-0.06431045 (20, 7) 0.16023415
 (20, 8)-0.15197657 (20, 9) 0.04581450 (20, 10) 0.09036624 (20, 11)-0.17259888
 (20, 12) 0.15279396 (20, 13)-0.04442820 (20, 14)-0.09044854 (20, 15) 0.18011656
 (20, 16)-0.18188293 (20, 17) 0.09917708 (20, 18) 0.02796192 (20, 19)-0.14829323
 (20, 20) 0.22401802 (21, 0) 0.00000000 (21, 1) 0.12309369 (21, 2)-0.16971143 (21, 3) 0.11113019
 (21, 4) 0.01621573 (21, 5)-0.13419455 (21, 6) 0.17156680 (21, 7)-0.10671278
 (21, 8)-0.02133168 (21, 9) 0.13828973 (21, 10)-0.17884184 (21, 11) 0.12234195
 (21, 12)-0.00060571 (21, 13)-0.12330982 (21, 14) 0.18997960 (21, 15)-0.17168047
 (21, 16) 0.08043642 (21, 17) 0.04410450 (21, 18)-0.15675364 (21, 19) 0.22607070
 (22, 0) 0.17352191 (22, 1) -0.12518017 (22, 2) 0.00709778 (22, 3) 0.11517683
 (22, 4)-0.17438263 (22, 5) 0.13867003 (22, 6)-0.02803396 (22, 7)-0.09821048
 (22, 8) 0.17442644 (22, 9)-0.16289014 (22, 10) 0.07100532 (22, 11) 0.05576164
 (22, 12)-0.1583082 (22, 13) 0.19457890 (22, 14)-0.15147074 (22, 15) 0.05005287
 (22, 16) 0.07088742 (22, 17)-0.17284860 (22, 18) 0.23166417 (22, 19)-0.24230017
 (22, 20) 0.21506195 (22, 21)-0.16739376 (22, 22) 0.11595742 (23, 0) 0.00000000
 (23, 1) -0.11716443 (23, 2) 0.17692110 (23, 3)-0.15031497
 (23, 4) 0.05071381 (23, 5) 0.07364152 (23, 6)-0.16391177 (23, 7) 0.17888644
 (23, 8)-0.11312316 (23, 9)-0.00289647 (23, 10) 0.11892590 (23, 11)-0.18810976
 (23, 12) 0.18576053 (23, 13)-0.11613919 (23, 14) 0.00637618 (23, 15) 0.10744511
 (23, 16)-0.19467013 (23, 17) 0.23906872 (23, 18)-0.24033546 (23, 19) 0.20963988
 (23, 20)-0.16269812 (23, 21) 0.11369624 (23, 22)-0.07191624 (23, 23) 0.04120783
 (24, 0)-0.18377708 (24, 1) 0.14463091 (24, 2)-0.04391662 (24, 3) -0.07559559
 (24, 4) 0.16382118 (24, 5)-0.18474256 (24, 6) 0.13085930 (24, 7)-0.02479822
 (24, 8)-0.09164023 (24, 9) 0.17519857 (24, 10)-0.19753951 (24, 11) 0.15379992
 (24, 12)-0.06109003 (24, 13)-0.05076611 (24, 14) 0.15123993 (24, 15)-0.21880241
 (24, 16) 0.24533115 (24, 17)-0.23501253 (24, 18) 0.19965926 (24, 19)-0.15312290
 (24, 20) 0.10695939 (24, 21)-0.06832519 (24, 22) 0.03994425 (24, 23)-0.02133060
 (24, 24) 0.01035718 (25, 0) 0.00000000 (25, 1) 0.10947295 (25, 2)-0.17968129 (25, 3) 0.18584438
 (25, 4)-0.12642138 (25, 5) 0.02288192 (25, 6) 0.08898525 (25, 7)-0.17234348
 (25, 8) 0.20178515 (25, 9)-0.17049858 (25, 10) 0.09020232 (25, 11) 0.01506522
 (25, 12)-0.1118102421 (25, 13) 0.19695817 (25, 14)-0.23993772 (25, 15) 0.24634618
 (25, 16)-0.22381367 (25, 17) 0.18399300 (25, 18)-0.13845047 (25, 19) 0.09593828
 (25, 20)-0.06138768 (25, 21) 0.03628505 (25, 22)-0.01978077 (25, 23) 0.00991065
 (25, 24)-0.00453763 (25, 25) 0.00188245 (26, 0) 0.19951212 (26, 1) -0.17009877
 (26, 4)-0.11740661 (26, 5) 0.18688570 (26, 6)-0.20587815 (26, 7) 0.17111436
 (26, 8)-0.09345701 (26, 9)-0.00679283 (26, 10) 0.10664052 (26, 11)-0.18677534
 (26, 12) 0.23571183 (26, 13)-0.25092033 (26, 14) 0.23730347 (26, 15)-0.20412366
 (26, 16) 0.16167711 (26, 17)-0.11871893 (26, 18) 0.08110979 (26, 19)-0.05163620
 (26, 20) 0.03062734 (26, 21)-0.01689953 (26, 22) 0.00864930 (26, 23)-0.00408770
 (26, 24) 0.00177245 (26, 25)-0.00069874 (26, 26) 0.00024720 (27, 0) 0.00000000
 (27, 1) -0.09878597 (27, 2) 0.17511164 (27, 3)-0.21208096
 (27, 4) 0.020230161 (27, 5)-0.14912544 (27, 6) 0.06500340 (27, 7) 0.03233562
 (27, 8)-0.12458546 (27, 9) 0.19704126 (27, 10)-0.24120951 (27, 11) 0.25543395
 (27, 12)-0.24377042 (27, 13) 0.21379198 (27, 14)-0.17414759 (27, 15) 0.13255589
 (27, 16)-0.09460795 (27, 17) 0.06342203 (27, 18)-0.03995009 (27, 19) 0.02363107
 (27, 20)-0.01310500 (27, 21) 0.00679587 (27, 22)-0.00328309 (27, 23) 0.00147004
 (27, 24)-0.00060586 (27, 25) 0.00022767 (27, 26)-0.00007696 (27, 27) 0.00002295
 (28, 0) -0.22838213 (28, 1) 0.20969045 (28, 2)-0.15684378 (28, 3) 0.07880394
 (28, 4) 0.01170413 (28, 5)-0.10087691 (28, 6) 0.17653458 (28, 7)-0.23019409
 (28, 8) 0.25809729 (28, 9)-0.26110211 (28, 10) 0.24364920 (28, 11)-0.21221448
 (28, 12) 0.17370448 (28, 13)-0.13416648 (28, 14) 0.09801669 (28, 15)-0.06781011
 (28, 16) 0.04443846 (28, 17)-0.02757449 (28, 18) 0.01618328 (28, 19)-0.00896761
 (28, 20) 0.00468029 (28, 21)-0.00229317 (28, 22) 0.00105031 (28, 23)-0.00044722
 (28, 24) 0.00017574 (28, 25)-0.00006311 (28, 26) 0.00002044 (28, 27)-0.00000585
 (29, 0) 0.00000143 (29, 1) 0.08135077 (29, 2)-0.15488724 (29, 3) 0.21400747

(29, 4)-0.25427878 (29, 5) 0.27395093 (29, 6)-0.27395093 (29, 7) 0.25740933
 (29, 8)-0.22886974 (29, 9) 0.19338374 (29, 10)-0.15568870 (29, 11) 0.11961147
 (29, 12)-0.08776342 (29, 13) 0.06151453 (29, 14)-0.04117755 (29, 15) 0.02630737
 (29, 16)-0.01602407 (29, 17) 0.00929216 (29, 18)-0.00512025 (29, 19) 0.00267464
 (29, 20)-0.00132054 (29, 21) 0.00061398 (29, 22)-0.00026760 (29, 23) 0.00010869
 (29, 24)-0.00004083 (29, 25) 0.00001405 (29, 26)-0.00000437 (29, 27) 0.00000120
 (29, 28)-0.00000028 (29, 29) 0.00000005 (30, 1) -0.31507015 (30, 2) 0.29993784 (30, 3)-0.27628246
 (30, 4) 0.24620436 (30, 5)-0.21220148 (30, 6) 0.17683455 (30, 7)-0.14242031
 (30, 8) 0.11080109 (30, 9)-0.08321911 (30, 10) 0.06029797 (30, 11)-0.04211393
 (30, 12) 0.02832552 (30, 13)-0.01832652 (30, 14) 0.01139143 (30, 15)-0.00679253
 (30, 16) 0.00387881 (30, 17)-0.00211696 (30, 18) 0.00110170 (30, 19)-0.00054520
 (30, 20) 0.00025572 (30, 21)-0.00011324 (30, 22) 0.00004711 (30, 23)-0.00001830
 (30, 24) 0.00000659 (30, 25)-0.00000218 (30, 26) 0.00000065 (30, 27)-0.00000017
 M S I=31
 (0, 0) 0.00000000 (1, 1) 0.00451451
 (2, 0) 0.00000000 (2, 1) 0.14204587 (2, 2)-0.01805806
 (3, 0) 0.14247739 (3, 1)-0.01357099 (3, 2)-0.14003336 (3, 3) 0.04035591
 (4, 0) 0.00000000 (4, 1)-0.14161302 (4, 2) 0.03600606 (4, 3) 0.13272664
 (4, 4)-0.07003449 (5, 0) 0.00000000 (5, 1) 0.02271120 (5, 2) 0.13598886 (5, 3)-0.06606489
 (5, 4)-0.14218928 (5, 5) 0.10331898 (5, 6) 0.11008267 (5, 7)-0.05373054 (5, 8)-0.12063460
 (6, 0) 0.00000000 (6, 1) 0.14088267 (6, 2)-0.05373054 (6, 3)-0.12063460
 (6, 4) 0.10013714 (6, 5) 0.08258722 (6, 6) 0.13260889 (6, 7)-0.12987205 (6, 8)-0.08996426
 (7, 0) 0.014396325 (7, 1) 0.03195886 (7, 2)-0.12987205 (7, 3) 0.08996426
 (7, 4) 0.09003577 (7, 5)-0.13076431 (7, 6) 0.03147838 (7, 7) 0.14585871 (7, 8)-0.12870347
 (8, 0) 0.00000000 (8, 1) 0.13984074 (8, 2) 0.07111089 (8, 3) 0.10388999 (8, 4)-0.12870347
 (8, 5)-0.04046091 (8, 6) 0.14594378 (8, 7)-0.03504501 (8, 8)-0.12870347
 (9, 0)-0.14520970 (9, 1) 0.04149371 (9, 2) 0.12161868 (9, 3)-0.11129410
 (9, 4)-0.05799754 (9, 5) 0.14523606 (9, 6)-0.02598856 (9, 7)-0.13097320
 (9, 8) 0.10324008 (9, 9) 0.07084016 (9, 10) 0.13846597 (9, 11) 0.08801475 (9, 12)-0.08268734
 (10, 0) 0.00000000 (10, 1) 0.13846597 (10, 2)-0.08801475 (10, 3)-0.08268734
 (10, 4) 0.14111078 (10, 5)-0.00749569 (10, 6)-0.13700889 (10, 7) 0.09644599
 (10, 8) 0.07498101 (10, 9) 0.14672205 (10, 10) 0.02198073 (10, 11) 0.01528631 (10, 12) 0.11113541
 (11, 0) 0.14684685 (11, 1)-0.05128631 (11, 2) 0.11113541 (11, 3) 0.12925422 (11, 4)-0.02063985
 (11, 5)-0.14434956 (11, 6) 0.08164152 (11, 7) 0.08698477 (11, 8)-0.14479992 (11, 9) 0.01728816
 (11, 10) 0.13357365 (11, 11)-0.11643156 (12, 0) 0.00000000 (12, 1)-0.13672817 (12, 2) 0.10429215 (12, 3) 0.05729309
 (12, 4)-0.14853479 (12, 5) 0.05681375 (12, 6) 0.10534284 (12, 7)-0.13919799 (12, 8) 0.00306816 (12, 9) 0.13797548
 (12, 10)-0.11335658 (12, 11)-0.04792513 (13, 0)-0.14893977 (13, 1) 0.06147495 (13, 2) 0.09829129 (13, 3)-0.14298555
 (13, 4) 0.02016344 (13, 5) 0.12675746 (13, 6)-0.12652542 (13, 7)-0.02082483 (13, 8) 0.14516585
 (13, 9)-0.10343024 (13, 10)-0.05706702 (13, 11) 0.15455656 (13, 12)-0.07923637 (13, 13)-0.08550775
 (14, 0) 0.00000000 (14, 1) 0.13458522 (14, 2)-0.11976717 (14, 3)-0.02806135 (14, 4) 0.00000000
 (14, 5)-0.14523208 (14, 6) 0.05367237 (14, 7) 0.15165833 (14, 8)-0.08472674 (14, 9)-0.07475740 (14, 10) 0.15526412 (14, 11)-0.07078418
 (14, 12)-0.15401892 (14, 13) 0.06147495 (14, 14) 0.09829129 (14, 15) 0.12652542 (14, 16) 0.05706702
 (14, 17)-0.07923637 (14, 18) 0.08550775 (14, 19) 0.15455656 (14, 20)-0.02082483 (14, 21) 0.15455656
 (14, 22)-0.08965334 (14, 23) 0.15861335 (14, 24) 0.06496609 (14, 25) 0.15158276 (14, 26) 0.07219137
 (14, 27)-0.08290403 (14, 28) 0.15454372 (14, 29)-0.05473169 (14, 30) 0.15158276 (14, 31) 0.06206916
 (14, 32)-0.09244000 (14, 33) 0.15180250 (14, 34)-0.05473169 (14, 35) 0.15158276 (14, 36)-0.09244000
 (14, 37) 0.09926471 (14, 38) 0.15338539 (14, 39)-0.05296498 (14, 40) 0.15338539 (14, 41)-0.10161199
 (14, 42) 0.15758637 (14, 43) 0.06044693 (14, 44) 0.09637889 (14, 45) 0.16491465 (14, 46)-0.00000000
 (14, 47) 0.13197842 (14, 48) 0.13422558 (14, 49) 0.00000000 (14, 50) 0.13422558 (14, 51) 0.00454178
 (14, 52)-0.12999323 (14, 53) 0.13798554 (14, 54) 0.01169551 (14, 55) 0.12671182 (14, 56)-0.00000000
 (14, 57) 0.14431722 (14, 58) 0.02444703 (14, 59) 0.11970218 (14, 60) 0.15370128 (14, 61)-0.00000000
 (14, 62)-0.04649385 (14, 63) 0.10443515 (14, 64) 0.16465743 (14, 65) 0.08213201

(16, 16)-0.07206821
 (17, 0)-0.15491465
 (17, 4) 0.10218997
 (17, 8) 0.01539245
 (17, 12)-0.11946485
 (17, 16) 0.16988368
 (18, 0) 0.00000000
 (18, 4) 0.10196263
 (18, 8)-0.15725332
 (18, 12) 0.05170065
 (18, 16)-0.13372549
 (19, 0) 0.15914679
 (19, 4)-0.13697614
 (19, 8) 0.08287477
 (19, 12)-0.02515933
 (19, 16)-0.00668011
 (20, 0) 0.00000000
 (20, 4)-0.06078501
 (20, 8) 0.10846163
 (20, 12)-0.13749637
 (20, 16) 0.14645547
 (20, 20)-0.10432683
 (21, 0)-0.16461734
 (21, 4) 0.16201699
 (21, 8)-0.15828367
 (21, 12) 0.16400405
 (21, 16)-0.18904580
 (21, 20) 0.20046341
 (22, 0) 0.00000000
 (22, 4) 0.00684701
 (22, 8)-0.00267079
 (22, 12)-0.02812891
 (22, 16) 0.11062421
 (22, 20)-0.23992124
 (23, 0) 0.17910772
 (23, 4)-0.17167690
 (23, 8) 0.16723195
 (23, 12)-0.14064063
 (23, 16) 0.03684153
 (23, 20) 0.22598064
 (24, 0) 0.00000000
 (24, 4) 0.05827897
 (24, 8)-0.12475259
 (24, 12) 0.19047743
 (24, 16)-0.17246635
 (24, 20)-0.17877728
 (24, 24)-0.02887309
 (25, 0)-0.18212882
 (25, 4) 0.15833603
 (25, 8)-0.07635973
 (25, 12)-0.08189083
 (25, 16) 0.23971571
 (25, 20)-0.12176790
 (25, 24) 0.01439987
 (26, 0) 0.00000000
 (26, 4)-0.13088851
 (26, 8) 0.19962594
 (26, 12)-0.09765086
 (26, 16)-0.23015127
 (26, 20)-0.07197800
 (26, 24)-0.00646376
 (27, 0) 0.19778472

(17, 1) 0.08361527
 (17, 5) 0.04304772
 (17, 9)-0.14035733
 (17, 13) 0.16296937
 (17, 17)-0.13686110
 (18, 1) 0.12882458
 (18, 5) 0.15779936
 (18, 9) 0.12150516
 (18, 13)-0.05478529
 (18, 17) 0.00362023
 (19, 1) -0.09600540
 (19, 5) 0.01767026
 (19, 9) 0.05840694
 (19, 13)-0.11155130
 (19, 17) 0.13577212
 (20, 1) -0.12500222
 (20, 5) 0.15548180
 (20, 9)-0.16771786
 (20, 13) 0.17369957
 (20, 17)-0.19033186
 (21, 1) 0.10975872
 (21, 5)-0.08328786
 (21, 9) 0.06581281
 (21, 13)-0.07344555
 (21, 17) 0.13013877
 (21, 21)-0.23932683
 (22, 1) 0.12032550
 (22, 5)-0.12534703
 (22, 9) 0.12277953
 (22, 13)-0.09750376
 (22, 17) 0.00553208
 (22, 21)-0.22836421
 (23, 1) -0.12553574
 (23, 5) 0.14383499
 (23, 9)-0.16897652
 (23, 13) 0.19169259
 (23, 17)-0.14443417
 (23, 21)-0.18514423
 (24, 1) -0.11448956
 (24, 5) 0.06316578
 (24, 9) 0.01596347
 (24, 13)-0.13512936
 (24, 17) 0.22829731
 (24, 21) 0.13070424
 (25, 1) 0.14456490
 (25, 5) -0.18429051
 (25, 9) 0.16451035
 (25, 13)-0.02563841
 (25, 17)-0.23902391
 (25, 21)-0.08111322
 (25, 25)-0.00676478
 (26, 1) 0.10693894
 (26, 5) 0.03202719
 (26, 9)-0.17721322
 (26, 13) 0.18071592
 (26, 17) 0.19503106
 (26, 21) 0.04428338
 (26, 25) 0.00287327
 (27, 1) -0.16955112

(17, 2) 0.06471715
 (17, 6)-0.14909881
 (17, 10) 0.14334992
 (17, 14)-0.07332239
 (17, 18)-0.13686110
 (18, 2)-0.14739530
 (18, 6) 0.08066438
 (18, 10) 0.01317018
 (18, 14)-0.09030358
 (18, 18) 0.13202336
 (19, 2)-0.04335989
 (19, 6) 0.11603718
 (19, 10)-0.15759766
 (19, 14) 0.17450143
 (19, 18)-0.19014089
 (20, 2) 0.15891327
 (20, 6)-0.13941726
 (20, 10) 0.11383725
 (20, 14)-0.10444157
 (20, 18) 0.14063524
 (21, 2) 0.01827237
 (21, 6)-0.05007393
 (21, 10) 0.06781946
 (21, 14)-0.05822599
 (21, 18)-0.01501233
 (22, 2)-0.16826460
 (22, 6) 0.17093690
 (22, 10)-0.17717959
 (22, 14) 0.179331785
 (22, 18)-0.12262597
 (22, 22)-0.18721201
 (23, 2) -0.01144896
 (23, 6) -0.04075472
 (23, 10) 0.08991761
 (23, 14)-0.16694799
 (23, 18) 0.21592455
 (23, 22) 0.13517506
 (24, 2) -0.15633531
 (24, 6) 0.1047799
 (24, 10) 0.17854039
 (24, 14) 0.03439182
 (24, 18)-0.24170011
 (24, 22)-0.08679072
 (25, 2) -0.04741601
 (25, 6) 0.13793138
 (25, 10)-0.19676192
 (25, 14) 0.12823683
 (25, 18) 0.21071440
 (25, 22) 0.04966595
 (26, 2) -0.17673463
 (26, 6) 0.07787195
 (26, 10) 0.10522092
 (26, 14)-0.23097922
 (26, 18) 0.15142292
 (26, 22) -0.02524887
 (26, 26) -0.00115902
 (27, 2) 0.09300477

(17, 3)-0.15385918
 (17, 7) 0.12204652
 (17, 11)-0.02217289
 (17, 15)-0.07671320
 (17, 19)-0.13686110
 (18, 3) 0.03989919
 (18, 7) 0.06457733
 (18, 11)-0.13883971
 (18, 15) 0.17201045
 (19, 3) 0.14867263
 (19, 7) -0.16084176
 (19, 11) 0.14258495
 (19, 15)-0.12359521
 (19, 19) 0.14392039
 (20, 3) -0.07711764
 (20, 7) 0.02447101
 (20, 11) 0.01628478
 (20, 15)-0.02738902
 (20, 19)-0.02511515
 (21, 3) -0.13442138
 (21, 7) 0.15204599
 (21, 11)-0.16246602
 (21, 15) 0.16219947
 (21, 19)-0.10896310
 (22, 3) 0.11521068
 (22, 7)-0.11788452
 (22, 11) 0.13833788
 (22, 15)-0.18291129
 (22, 19) 0.20594738
 (23, 3) 0.10901810
 (23, 7)-0.08391672
 (23, 11) 0.03160818
 (23, 15) 0.07952797
 (23, 19)-0.24120587
 (23, 23)-0.08871292
 (24, 3) -0.15226679
 (24, 7) 0.17990153
 (24, 11)-0.17854039
 (24, 15) 0.07849453
 (24, 19) 0.22051920
 (24, 23) 0.05247883
 (25, 3) -0.06935617
 (25, 7)-0.03830344
 (25, 11) 0.16490082
 (25, 15)-0.20319362
 (25, 19) 0.16769111
 (25, 23) -0.02793921
 (26, 3) 0.18551996
 (26, 7) -0.16360681
 (26, 11)-0.00502339
 (26, 15) 0.24558680
 (26, 19) 0.10848422
 (26, 23) 0.01331167
 (27, 3) 0.00995343

(27, 4)-0.11045837
 (27, 8)-0.10463537
 (27, 12) 0.22655235
 (27, 16) 0.17215651
 (27, 20) 0.03683259
 (27, 24) 0.00258144
 (27, 28) 0.00000000
 (28, 0) 0.00000000
 (28, 4) 0.20261417
 (28, 8)-0.11231016
 (28, 12)-0.24568745
 (28, 16)-0.10347895
 (28, 20)-0.01611496
 (28, 24)-0.00090059
 (28, 28)-0.00001283
 (28, 29) 0.00000000
 (29, 0) 0.22647093
 (29, 4) 0.00566324
 (29, 8) 0.25374910
 (29, 12) 0.18008810
 (29, 16) 0.04968600
 (29, 20) 0.00587082
 (29, 24) 0.00026621
 (29, 28) 0.00000320
 (30, 0) 0.00000000
 (30, 4) -0.25021005
 (30, 8)-0.23115470
 (30, 12)-0.09287804
 (30, 16)-0.01825530
 (30, 20) -0.00168648
 (30, 24) -0.00006295
 (30, 28) -0.00000064
 (30, 32) 0.00000015
 (30, 36) -0.00000003
 (31, 0) 0.31768489
 (31, 4) 0.24626948
 (31, 8) 0.11375711
 (31, 12) 0.03047177
 (31, 16) 0.00449195
 (31, 20) 0.00033198
 (31, 24) 0.00001033
 (31, 28) 0.00000009
 M S L=32
 (0, 0) 0.13994993
 (1, 0) 0.00000000
 (2, 0) -0.14008266
 (3, 0) 0.00000000
 (4, 0) 0.14048462
 (4, 4) 0.12412319
 (5, 0) 0.00000000
 (5, 4) -0.08203689
 (6, 0)-0.141616757
 (6, 4) -0.10423739
 (7, 0) 0.00000000
 (7, 4) 0.10870842
 (7, 8) 0.14215231
 (7, 12) 0.03499548
 (7, 16) 0.14215231
 (7, 20) 0.06597321
 (7, 24) 0.13833179
 (7, 28) 0.13833179
 (8, 0) 0.14215231
 (8, 4) 0.07746322
 (8, 8) 0.06147973
 (8, 12) 0.02606479
 (8, 16) 0.11402498
 (8, 20) 0.06202647
 (8, 24) 0.01729246
 (8, 28) 0.13568294
 (9, 0) 0.00000000
 (9, 4) -0.12934417
 (9, 8) 0.11132810
 (9, 12) 0.12181290
 (9, 16) 0.14304018
 (9, 20) 0.14347060
 (9, 24) 0.04415002
 (9, 28) 0.11936064
 (10, 0) 0.04415002
 (10, 4) 0.04488895
 (10, 8) 0.04181374
 (10, 12) 0.14737427
 (10, 16) 0.20466161
 (10, 20) 0.09009999
 (10, 24) 0.17609854
 (10, 28) 0.17258616
 (10, 32) 0.21190836
 (10, 36) 0.05996973
 (10, 40) 0.00561676
 (10, 44) 0.00014460
 (10, 48) 0.20953982
 (10, 52) 0.02087866
 (10, 56) 0.25272536
 (10, 60) 0.14172482
 (10, 64) 0.02808371
 (10, 68) 0.00206230
 (10, 72) 0.00004397
 (10, 76) 0.00000000
 (10, 80) 0.20980750
 (10, 84) 0.25783238
 (10, 88) 0.12483712
 (10, 92) 0.02933250
 (10, 96) 0.00330294
 (10, 100) 0.00001581
 (10, 104) 0.00000023
 (10, 108) 0.27533767
 (10, 112) 0.14501244
 (10, 116) 0.04468038
 (10, 120) 0.06313866
 (10, 124) 0.01266421
 (10, 128) 0.00769881
 (10, 132) 0.00134223
 (10, 136) 0.00068440
 (10, 140) 0.00006632
 (10, 144) 0.00000035
 (10, 148) 0.00000000
 (10, 152) 0.00000000
 (10, 156) 0.13516986
 (10, 160) 0.05098984
 (10, 164) 0.12618569
 (10, 168) 0.07487447
 (10, 172) 0.11282213
 (10, 176) 0.05965265
 (10, 180) 0.112807203
 (10, 184) 0.00565879
 (10, 188) 0.12504019
 (10, 192) 0.09680326
 (10, 196) 0.14154044
 (10, 200) 0.01064499
 (10, 204) 0.14154044
 (10, 208) 0.05746540
 (10, 212) 0.09521984
 (10, 216) 0.14304018
 (10, 220) 0.11608288
 (10, 224) 0.11696818

(11, 0) 0.00000000	(11, 1) 0.13579273	(11, 2)-0.09201930	(11, 3)-0.07357604	(23, 20)-0.23134880	(23, 21) 0.23475005	(23, 22)-0.20367980	(23, 23) 0.15554763
(11, 4) 0.14238001	(11, 5)-0.02345812	(11, 6)-0.12696046	(11, 7) 0.11131117	(24, 0) 0.17036591	(24, 1)-0.12582357	(24, 2) 0.01550250	(24, 3) 0.10309897
(11, 8) 0.05040678	(11, 9)-0.14756450	(11, 10) 0.05357758	(11, 11) 0.11079316	(24, 4)-0.16870695	(24, 5) 0.14809430	(24, 6)-0.05239771	(24, 7)-0.06998485
(12, 0) 0.14516854	(12, 1)-0.05360704	(12, 2)-0.10567724	(12, 3) 0.13197954	(24, 8) 0.15899275	(24, 9)-0.17273664	(24, 10) 0.10630289	(24, 11) 0.00865522
(12, 4) 0.00794854	(12, 5)-0.13841490	(12, 6) 0.09572277	(12, 7) 0.06708630	(24, 12)-0.12122828	(24, 13) 0.18519537	(24, 14)-0.17766947	(24, 15) 0.10496818
(12, 8)-0.14730543	(12, 9) 0.04507269	(12, 10) 0.11386694	(12, 11)-0.13439786	(24, 16) 0.00452415	(24, 17)-0.11484466	(24, 18) 0.19666407	(24, 19)-0.23557414
(12, 12)-0.00910177				(24, 20) 0.23279008	(24, 21)-0.20020573	(24, 22) 0.15341845	(24, 23)-0.10594578
(13, 0) 0.00000000	(13, 1)-0.13401759	(13, 2) 0.10732844	(13, 3) 0.04815469	(24, 24) 0.06625476			
(13, 4)-0.14638552	(13, 5) 0.06990714	(13, 6) 0.09035301	(13, 7)-0.14409250	(25, 0) 0.00000000	(25, 1)-0.11195233	(25, 2) 0.17241810	(25, 3)-0.15388153
(13, 8) 0.02748484	(13, 9) 0.12247548	(13, 10)-0.13019854	(13, 11)-0.01370225	(25, 4) 0.06521285	(25, 5) 0.05317130	(25, 6)-0.14852902	(25, 7) 0.17973316
(13, 12) 0.14354945	(13, 13)-0.11044778			(25, 8)-0.13461795	(25, 9) 0.03338468	(25, 10) 0.08215965	(25, 11)-0.16729777
(14, 0)-0.14731197	(14, 1) 0.06346498	(14, 2) 0.09271582	(14, 3)-0.14370137	(25, 12) 0.19205263	(25, 13)-0.15057400	(25, 14) 0.05977375	(25, 15) 0.05029228
(14, 4) 0.03154662	(14, 5) 0.11681218	(14, 6) 0.13381097	(14, 7) 0.00015918	(25, 16)-0.14889172	(25, 17) 0.21456969	(25, 18)-0.23951966	(25, 19) 0.22827742
(14, 8) 0.13460344	(14, 9) -0.12030850	(14, 10)-0.02746757	(14, 11) 0.14657895	(25, 20)-0.19283533	(25, 21) 0.14697443	(25, 22)-0.10198539	(25, 23) 0.06469326
(14, 12)-0.10722597	(14, 13)-0.04844290	(14, 14) 0.15469013		(25, 24)-0.03754547	(25, 25) 0.01989839		
(15, 0) 0.00000000	(15, 1) 0.13185337	(15, 2)-0.12184065	(15, 3)-0.01930176	(26, 0) 0.18055192	(26, 1) 0.14445864	(26, 2)-0.05065724	(26, 3)-0.06344108
(15, 4) 0.14011151	(15, 5)-0.112121543	(15, 6)-0.03662986	(15, 7) 0.14638098	(26, 4) 0.15290210	(26, 5)-0.18333718	(26, 6) 0.14398697	(26, 7)-0.05071092
(15, 8)-0.10198382	(15, 9)-0.05003251	(15, 10) 0.15122269	(15, 11)-0.09694158	(26, 8)-0.06160314	(26, 9) 0.15324102	(26, 10)-0.19420893	(26, 11) 0.17348997
(15, 12)-0.05733805	(15, 13) 0.15555368	(15, 14)-0.09967594	(15, 15)-0.05530918	(26, 12)-0.10027750	(26, 13)-0.00197361	(26, 14) 0.10522955	(26, 15)-0.18612304
(16, 0) 0.14999546	(16, 1) -0.07385267	(16, 2)-0.07734367	(16, 3) 0.15037328	(26, 16) 0.23166525	(26, 17)-0.24035199	(26, 18) 0.21951538	(26, 19)-0.18085137
(16, 4)-0.07136036	(16, 5)-0.08000689	(16, 6) 0.15163614	(16, 7)-0.07190311	(26, 20) 0.13610192	(26, 21)-0.09418136	(26, 22) 0.06011260	(26, 23)-0.03541077
(16, 8)-0.07993307	(16, 9) 0.15402688	(16, 10)-0.07790912	(16, 11)-0.07458895	(26, 24) 0.01922474	(26, 25)-0.00958675	(26, 26) 0.00436652	
(16, 12) 0.15735283	(16, 13)-0.09226590	(16, 14)-0.05980607	(16, 15) 0.15957794	(27, 0) 0.00000000	(27, 1) 0.10453742	(27, 2)-0.17387824	(27, 3) 0.18502760
(16, 16)-0.11786752				(27, 4)-0.13485168	(27, 5) 0.04049983	(27, 6) 0.06723043	(27, 7)-0.15474819
(17, 0) 0.00000000	(17, 1)-0.12924217	(17, 2) 0.13535142	(17, 3)-0.01253111	(27, 8) 0.19655322	(27, 9)-0.18235672	(27, 10) 0.11845447	(27, 11)-0.02369521
(17, 4)-0.12255365	(17, 5) 0.14203632	(17, 6)-0.02761699	(17, 7)-0.11338692	(27, 12)-0.07776254	(27, 13) 0.16398163	(27, 14)-0.22061440	(27, 15) 0.24291030
(17, 8) 0.14972036	(17, 9)-0.04797391	(17, 10)-0.09862863	(17, 11) 0.15750594	(27, 16)-0.23445910	(27, 17) 0.20445492	(27, 18) 0.16350703	(27, 19) 0.12079211
(17, 12)-0.07637735	(17, 13)-0.07303121	(17, 14) 0.16149586	(17, 15)-0.11454971	(27, 20)-0.08283611	(27, 21) 0.05283924	(27, 22)-0.03135845	(27, 23) 0.01729280
(17, 16)-0.02809632	(17, 17) 0.15098104			(27, 24)-0.00883702	(27, 25) 0.00416671	(27, 26)-0.00180129	(27, 27) 0.00070758
(18, 0)-0.15335768	(18, 1) 0.08494662	(18, 2) 0.05930802	(18, 3)-0.15099853	(28, 0) 0.19612959	(28, 1) 0.16899319	(28, 2) 0.09518331	(28, 3) 0.00481921
(18, 4) 0.10876014	(18, 5) 0.02993594	(18, 6)-0.14293398	(18, 7) 0.13147911	(28, 4)-0.10380887	(28, 5) 0.17577256	(28, 6)-0.20298851	(28, 7) 0.18016763
(18, 8)-0.00574742	(18, 9) -0.12594779	(18, 10) 0.15168364	(18, 11)-0.05026760	(28, 8)-0.114644995	(28, 9) 0.02304829	(28, 10) 0.07418546	(28, 11)-0.15836139
(18, 12)-0.09394622	(18, 13) 0.16366889	(18, 14)-0.10396922	(18, 15)-0.03767202	(28, 12) 0.21668017	(28, 13)-0.24401069	(28, 14) 0.24233244	(28, 15)-0.21855159
(18, 16) 0.15333942	(18, 17)-0.15871753	(18, 18) 0.05186302		(28, 16) 0.18169995	(28, 17)-0.14043269	(28, 18) 0.10138825	(28, 19)-0.06855468
(19, 0) 0.00000000	(19, 1) 0.12610221	(19, 2)-0.14759988	(19, 3) 0.04674900	(28, 20) 0.04345728	(28, 21)-0.02582120	(28, 22) 0.01436216	(28, 23)-0.00746048
(19, 4) 0.09304328	(19, 5)-0.15677628	(19, 6) 0.09249469	(19, 7) 0.04732351	(28, 24) 0.00360644	(28, 25)-0.00161437	(28, 26) 0.00066463	(28, 27)-0.00024931
(19, 8)-0.15000694	(19, 9) 0.13401106	(19, 10)-0.01244787	(19, 11)-0.12004107				
(19, 12) 0.16265953	(19, 13)-0.08440430	(19, 14)-0.05657052	(19, 15) 0.15969720	(29, 0) 0.00000000	(29, 1)-0.09427707	(29, 2) 0.16842780	(29, 3)-0.20701560
(19, 16)-0.15483876	(19, 17) 0.04721456	(19, 18) 0.09279632	(19, 19)-0.18035717	(29, 4) 0.20269330	(29, 5)-0.15743436	(29, 6) 0.08139284	(29, 7) 0.01011302
(20, 0) 0.15760911	(20, 1)-0.09701669	(20, 2)-0.03824450	(20, 3) 0.14439632	(29, 8)-0.10050911	(29, 9) 0.17564367	(29, 10)-0.22633085	(29, 11) 0.24931107
(20, 4)-0.14040391	(20, 5) 0.02953273	(20, 6) 0.10420657	(20, 7) -0.16060591	(29, 12)-0.24669106	(29, 13) 0.22432271	(29, 14)-0.18976057	(29, 15) 0.15039328
(20, 8) 0.09821871	(20, 9) 0.03666246	(20, 10)-0.14631337	(20, 11) 0.15323435	(29, 16)-0.11214210	(29, 17) 0.07886252	(29, 18)-0.05236401	(29, 19) 0.03283487
(20, 12)-0.05359663	(20, 13)-0.08380184	(20, 14) 0.16777359	(20, 15)-0.14554964	(29, 20)-0.01943136	(29, 21) 0.01083754	(29, 22)-0.00568425	(29, 23) 0.00279518
(20, 16) 0.03298044	(20, 17) 0.10137542	(20, 18)-0.18178798	(20, 19) 0.16823010	(29, 24)-0.00128342	(29, 25) 0.00054728	(29, 26)-0.00021520	(29, 27) 0.00007727
(20, 20)-0.07198799				(29, 28)-0.00000250	(29, 29) 0.00000714		
(21, 0) 0.00000000	(21, 1)-0.12231448	(21, 2) 0.15823658	(21, 3)-0.08255080	(30, 0) 0.22463714	(30, 1) 0.20738190	(30, 2)-0.15841717	(30, 3) 0.08555505
(21, 4) 0.05138554	(21, 5) 0.14992070	(21, 6)-0.14494368	(21, 7) 0.04036916	(30, 4) 0.00000000	(30, 5)-0.08588473	(30, 6) 0.16087686	(30, 7)-0.21673641
(21, 8) 0.09232380	(21, 9) -0.16432868	(21, 10) 0.12886740	(21, 11)-0.00991662	(30, 8) 0.24922936	(30, 9) -0.25821710	(30, 10) 0.246493929	(30, 11)-0.22078894
(21, 12)-0.11669073	(21, 13) 0.17341501	(21, 14)-0.12795201	(21, 15) 0.00849999	(30, 12) 0.18594363	(30, 13)-0.14817382	(30, 14) 0.11203416	(30, 15)-0.08050291
(21, 16) 0.11778535	(21, 17) -0.18534975	(21, 18) 0.16383110	(21, 19)-0.06754648	(30, 16) 0.05501490	(30, 17)-0.03575969	(30, 18) 0.02209746	(30, 19)-0.01296850
(21, 20)-0.05925933	(21, 21) 0.16832916			(30, 20) 0.00721725	(30, 21)-0.00380086	(30, 22) 0.00188903	(30, 23)-0.00088294
(22, 0)-0.16308598	(22, 1) 0.11040973	(22, 2)-0.01360339	(22, 3)-0.12909146	(30, 24) 0.00038639	(30, 25)-0.00015742	(30, 26) 0.00005927	(30, 27)-0.0002042
(22, 4) 0.16214992	(22, 5)-0.09207220	(22, 6)-0.03646238	(22, 7) 0.14299779	(30, 28) 0.00000635	(30, 29)-0.00000175	(30, 30) 0.00000041	
(22, 8)-0.16225070	(22, 9) 0.08342831	(22, 10) 0.04564786	(22, 11)-0.14960776	(31, 0) 0.00000000	(31, 1) 0.07759520	(31, 2)-0.14818569	(31, 3) 0.20578992
(22, 12) 0.17036819	(22, 13)-0.09828395	(22, 14)-0.02660551	(22, 15) 0.14014469	(31, 4)-0.24626948	(31, 5) 0.26779273	(31, 6) -0.27087572	(31, 7) 0.25803062
(22, 16)-0.18877582	(22, 17) 0.15367155	(22, 18)-0.05388951	(22, 19)-0.06876036	(31, 8)-0.23313271	(31, 9) 0.20066398	(31, 10)-0.16499326	(31, 11) 0.12981832
(22, 20) 0.17174713	(22, 21)-0.228785987	(22, 22) 0.23527446		(31, 12)-0.09783807	(31, 13) 0.07066082	(31, 14)-0.04890590	(31, 15) 0.03242738
(23, 0) 0.00000000	(23, 1) 0.11769717	(23, 2)-0.16676447	(23, 3) 0.11881617	(31, 16)-0.02058469	(31, 17) 0.01249785	(31, 18)-0.00724802	(31, 19) 0.00400848
(23, 4)-0.00191135	(23, 5) 0.11654244	(23, 6) 0.16928704	(23, 7) -0.12731710	(31, 20)-0.00210973	(31, 21) 0.00105407	(31, 22)-0.00049839	(31, 23) 0.00022217
(23, 8) 0.01473362	(23, 9) 0.10674227	(23, 10) -0.17285156	(23, 11) 0.15065017	(31, 24)-0.00009294	(31, 25) 0.00003627	(31, 26)-0.00001310	(31, 27) 0.00000434
(23, 12)-0.05308001	(23, 13)-0.07125627	(23, 14) 0.16473658	(23, 15)-0.18810713	(31, 28)-0.00000130	(31, 29) 0.00000034	(31, 30)-0.00000008	(31, 31) 0.00000001
(23, 16) 0.13517559	(23, 17)-0.03016650	(23, 18)-0.0853546	(23, 19) 0.18161052	(32, 0) 0.31519321	(32, 1) -0.31038082	(32, 2) 0.29637137	(32, 3) -0.27438658

(32, 4) 0.24626948 (32, 5)-0.21423417 (32, 6) 0.18058382 (32, 7)-0.14744607
 (32, 8) 0.11656635 (32, 9)-0.08918399 (32, 10) 0.06599730 (32, 11)-0.04720666
 (32, 12) 0.03261269 (32, 13)-0.02174179 (32, 14) 0.01397312 (32, 15)-0.00864730
 (32, 16) 0.00514617 (32, 17)-0.00294067 (32, 18) 0.00161067 (32, 19)-0.00084389
 (32, 20) 0.00042195 (32, 21)-0.00020077 (32, 22) 0.00009062 (32, 23)-0.00003864
 (32, 24) 0.00001549 (32, 25)-0.00000580 (32, 26) 0.00000202 (32, 27)-0.00000064
 (32, 28) 0.00000019 (32, 29)-0.00000005 (32, 30) 0.00000001 (32, 31) 0.00000000

M S 1=33

(0, 0) 0.00000000 (1, 1)-0.00411618 (2, 0) 0.13787648 (2, 1)-0.13775355 (2, 2) 0.01646470
 (3, 0)-0.13812336 (3, 1) 0.01237063 (3, 2) 0.13602877 (3, 3)-0.03682427
 (4, 0) 0.00000000 (4, 1) 0.13738275 (4, 2)-0.03284076 (4, 3)-0.12976423
 (5, 0) 0.13862380 (5, 1)-0.02069242 (5, 2)-0.13256447 (5, 3) 0.06041161
 (5, 4) 0.11478972 (5, 5)-0.04520948 (6, 0) 0.00000000 (6, 1)-0.13675798 (6, 2) 0.04903712 (6, 3) 0.11938820
 (6, 4)-0.09217073 (6, 5)-0.08650242 (6, 6) 0.12400398 (7, 0)-0.13939181 (7, 1) 0.02912989 (7, 2) 0.12733030 (7, 3)-0.08254351
 (7, 4)-0.09298836 (7, 5) 0.12205881 (7, 6) 0.04170181 (7, 7) 0.14050028 (8, 0) 0.00000000 (8, 1) 0.13586870 (8, 2)-0.06495766 (8, 3)-0.10500067
 (8, 4) 0.11558583 (8, 5) 0.04968419 (8, 6)-0.14014263 (8, 7) 0.01827102 (8, 8) 0.13710616
 (9, 0) 0.14044942 (9, 1)-0.03773699 (9, 2)-0.12027822 (9, 3) 0.10261238 (9, 4) 0.06516445 (9, 5)-0.13831814 (9, 6) 0.00988041 (9, 7) 0.13367273
 (9, 8)-0.08363985 (9, 9)-0.08822260 (10, 0) 0.00000000 (10, 1)-0.13469908 (10, 2) 0.08049810 (10, 3) 0.08674731 (10, 4)-0.13278979 (10, 5)-0.00705905 (10, 6) 0.13766876 (10, 7)-0.07668438
 (10, 8)-0.09159574 (10, 9) 0.13380055 (10, 10) 0.00909050 (11, 0)-0.14183088 (11, 1) 0.04657652 (11, 2) 0.11133918 (11, 3)-0.11998264 (11, 4)-0.03241152 (11, 5) 0.14189722 (11, 6)-0.06190852 (11, 7)-0.10123940
 (11, 8) 0.13053089 (11, 9) 0.01338588 (11, 10)-0.14083137 (11, 11) 0.08387642 (12, 0) 0.00000000 (12, 1) 0.13322692 (12, 2)-0.09554197 (12, 3)-0.06482608 (12, 4) 0.14249797 (12, 5)-0.03796085 (12, 6)-0.11557902 (12, 7) 0.12257814 (12, 8) 0.02623118 (12, 9)-0.14293681 (12, 10) 0.08032734 (12, 11) 0.08374068 (12, 12)-0.14508985
 (13, 0) 0.14358194 (13, 1)-0.05572458 (13, 2)-0.10041774 (13, 3) 0.13397844 (13, 4)-0.00386670 (13, 5)-0.13143541 (13, 6) 0.10729718 (13, 7) 0.04727490 (13, 8)-0.14564604 (13, 9) 0.06922936 (13, 10) 0.09088030 (13, 11)-0.14418684 (13, 12) 0.02726199 (13, 13) 0.12316135
 (14, 0) 0.00000000 (14, 1)-0.13142177 (14, 2) 0.10995535 (14, 3) 0.03949713 (14, 4)-0.14344631 (14, 5) 0.08135176 (14, 6) 0.07517077 (14, 7)-0.14584893 (14, 8) 0.04941572 (14, 9) 0.10425588 (14, 10)-0.14071444 (14, 11) 0.01857194 (14, 12) 0.12574221 (14, 13)-0.13208053 (14, 14)-0.00684557 (15, 0)-0.14576939 (15, 1) 0.06527715 (15, 2) 0.08738365 (15, 3)-0.14386687 (15, 4) 0.04192546 (15, 5) 0.10649955 (15, 6)-0.13880168 (15, 7) 0.01961844 (15, 8) 0.12168384 (15, 9)-0.13242468 (15, 10) 0.00092557 (15, 11) 0.13285397 (15, 12)-0.12760709 (15, 13)-0.01132348 (15, 14) 0.14043978 (15, 15)-0.12801677 (16, 0) 0.00000000 (16, 1) 0.12924217 (16, 2)-0.12357914 (16, 3)-0.01109773 (16, 4) 0.13457185 (16, 5)-0.11858398 (16, 6)-0.02035451 (16, 7) 0.13906038 (16, 8)-0.11580603 (16, 9)-0.02575264 (16, 10) 0.14246422 (16, 11)-0.11730052 (16, 12)-0.02474070 (16, 13) 0.14422134 (16, 14)-0.12544687 (16, 15)-0.01349176

(18, 4)-0.11504496 (18, 5) 0.14476813 (18, 6)-0.04214127 (18, 7)-0.09940673 (18, 8) 0.15202445 (18, 9)-0.06873549 (18, 10)-0.07631738 (18, 11) 0.15577596 (18, 12)-0.10107116 (18, 13)-0.04063038 (18, 14) 0.15016723 (18, 15)-0.13776185 (18, 16) 0.01429283 (18, 17) 0.12268241 (18, 18)-0.16919832 (18, 19) 0.015187593 (18, 20) 0.08614818 (18, 21) 0.05419304 (18, 22) 0.12350783 (18, 23) 0.14762008 (18, 24) 0.05302670 (18, 25) 0.08435464 (18, 26) 0.15486199 (18, 27) 0.10271348 (18, 28) 0.03070109 (18, 29) 0.16259640 (18, 30)-0.10874796 (18, 31)-0.02295106 (18, 32) 0.14080413 (18, 33)-0.09268441 (18, 34) 0.16630675 (18, 35)-0.08474091 (18, 36) 0.05107512 (18, 37)-0.15982571 (18, 38) 0.18232881 (18, 39) 0.15614294 (18, 40)-0.09789155 (18, 41) 0.03342937 (18, 42) 0.14308903 (18, 43) 0.04043288 (18, 44) 0.09235340 (18, 45) 0.15868632 (18, 46) 0.11117370 (18, 47) 0.01579321 (18, 48)-0.13278712 (18, 49) 0.15528915 (18, 50) 0.15592123 (18, 51) 0.15984121 (18, 52) 0.06813944 (18, 53) 0.06466132 (18, 54) 0.16461568 (18, 55) 0.18141916 (18, 56)-0.11097617 (18, 57) 0.11975617 (18, 58)-0.15744960 (18, 59) 0.14397494 (18, 60) 0.14906946 (18, 61) 0.05481311 (18, 62) 0.07847337 (18, 63) 0.05528915 (18, 64) 0.15592123 (18, 65) 0.15984121 (18, 66) 0.06813944 (18, 67) 0.06466132 (18, 68) 0.16461568 (18, 69) 0.18141916 (18, 70)-0.11097617 (18, 71) 0.11975617 (18, 72)-0.15744960 (18, 73) 0.14397494 (18, 74) 0.14906946 (18, 75) 0.05481311 (18, 76) 0.03407717 (18, 77) 0.07616767 (18, 78) 0.14048201 (18, 79) 0.03407717 (18, 80) 0.09438043 (18, 81) 0.16811107 (18, 82) 0.14585163 (18, 83) 0.17297153 (18, 84) 0.17800047 (18, 85) 0.21000086 (18, 86) 0.01529766 (18, 87) 0.13182580 (18, 88) 0.21000086 (18, 89) 0.16162330 (18, 90) 0.11097761 (18, 91) 0.09922738 (18, 92) 0.12388218 (18, 93) 0.16179067 (18, 94) 0.09986117 (18, 95) 0.02352070 (18, 96) 0.13333718 (18, 97) 0.16418369 (18, 98) 0.09872442 (18, 99) 0.02424411 (18, 100) 0.12424411 (18, 101) 0.02424411 (18, 102) 0.17249236 (18, 103)-0.11887733 (18, 104) 0.0349653 (18, 105) 0.11536244 (18, 106) 0.18224046 (18, 107) 0.17022771 (18, 108) 0.087719294 (18, 109) 0.21206012 (18, 110) 0.23583905 (18, 111)-0.21759933 (18, 112) 0.13949467 (18, 113) 0.17022771 (18, 114) 0.21206012 (18, 115) 0.23583905 (18, 116) 0.01000000 (18, 117) 0.11519801 (18, 118) 0.16525554 (18, 119) 0.12199880 (18, 120) 0.01009468 (18, 121) 0.10784452 (18, 122) 0.16678993 (18, 123) 0.13517028 (18, 124) 0.03083944 (18, 125) 0.09051342 (18, 126) 0.16635008 (18, 127) 0.07528295 (18, 128) 0.04530205 (18, 129) 0.14724131 (18, 130) 0.180833884 (18, 131) 0.05266290 (18, 132) 0.15424648 (18, 133) 0.21708060 (18, 134) 0.23601140 (18, 135) 0.21633111 (18, 136) 0.17408396 (18, 137) 0.12510470 (18, 138) 0.16889085 (18, 139) 0.12605199 (18, 140) 0.01928460 (18, 141) 0.09741422 (18, 142) 0.16553110 (18, 143) 0.15155379 (18, 144) 0.06302403 (18, 145) 0.05650543 (18, 146) 0.14996949 (18, 147) 0.17447363 (18, 148) 0.01286651 (18, 149) 0.12028464 (18, 150) 0.01286651 (18, 151) 0.17102271 (18, 152) 0.010116756 (18, 153) 0.17577600 (18, 154) 0.18410192 (18, 155) 0.12635726 (18, 156) 0.02552679 (18, 157) 0.08493569 (18, 158) 0.17472038 (18, 159) 0.22592600 (18, 160) 0.23556174 (18, 161) 0.21226177 (18, 162) 0.217017262 (18, 163) 0.12311070 (18, 164) 0.08092098 (18, 165) 0.04844425 (18, 166) 0.00000000 (18, 167) 0.10954201 (18, 168) 0.17020607 (18, 169) 0.15520109 (18, 170) 0.07156939 (18, 171) 0.04365458 (18, 172) 0.14287826 (18, 173) 0.04936749 (18, 174) 0.06420828 (18, 175) 0.15480816 (18, 176) 0.19092879 (18, 177) 0.16271828 (18, 178) 0.08242754 (18, 179) 0.02326594 (18, 180) 0.12455471 (18, 181) 0.19845410 (18, 182) 0.23413560 (18, 183) 0.23295461 (18, 184) 0.20464958 (18, 185) 0.16214848 (18, 186) 0.11714356 (18, 187) 0.07759250 (18, 188) 0.04722089 (18, 189) 0.02639218 (18, 190) 0.01351048 (18, 191) 0.17904100 (18, 192) 0.14431778 (18, 193) 0.05366440 (18, 194) 0.05783047 (18, 195) 0.14754149 (18, 196) 0.18196325 (18, 197) 0.14913325 (18, 198) 0.06207957 (18, 199) 0.14159933 (18, 200) 0.19017446 (18, 201) 0.17982480 (18, 202) 0.11634529 (18, 203) 0.02009587 (18, 204) 0.08254877 (18, 205) 0.16226177 (18, 206) 0.22154564 (18, 207) 0.23920110 (18, 208) 0.22606644 (18, 209) 0.19244292 (18, 210) 0.14971636 (18, 211) 0.10728704 (18, 212) 0.07110510 (18, 213) 0.04365229 (18, 214) 0.02481464 (18, 215) 0.01303464 (18, 216) 0.00630236 (18, 217) 0.00278828 (18, 218) 0.10225784 (18, 219) 0.17111009 (18, 220) 0.18439367

(28, 4)-0.13836446	(28, 5) 0.04834947	(28, 6) 0.05706174	(28, 7)-0.14585201	(28, 0) 0.00000000	(28, 1) -0.13444281	(28, 2) 0.05460814	(28, 3) 0.11245149
(28, 8) 0.19272707	(28, 9)-0.18611139	(28, 10) 0.13002951	(28, 11)-0.04095537	(28, 4)-0.10061617	(28, 5)-0.07165371	(28, 6) 0.13050249	(28, 7) 0.01810400
(28, 12)-0.05857412	(28, 13) 0.14698912	(28, 14)-0.20911615	(28, 15) 0.23853594	(28, 8)-0.03772239	(28, 9) 0.03193898	(28, 10) 0.12301196	(28, 11)-0.08919229
(28, 16)-0.23714486	(28, 17) 0.21251956	(28, 18)-0.17458670	(28, 19) 0.13269903	(28, 4)-0.08174576	(28, 5) 0.12773445	(28, 6) 0.02209077	(28, 7)-0.13883214
(28, 20)-0.09380452	(28, 21) 0.06183644	(28, 22)-0.03804772	(28, 23) 0.02184044	(28, 8) 0.04373675			
(28, 24)-0.01167535	(28, 25) 0.00579438	(28, 26)-0.0265746	(28, 27) 0.00111896	(28, 9, 0) 0.00000000	(28, 10, 1) 0.13349099	(28, 11, 2) -0.06971340	(28, 12, 3)-0.09724821
(28, 28)-0.00042862				(28, 9, 4) 0.12089204	(28, 10, 5) 0.03396252	(28, 11, 6)-0.13936114	(28, 12, 7) 0.03989649
(29, 0) 0.19454147	(29, 1)-0.16842780	(29, 2) 0.09718400	(29, 3) 0.00000000	(29, 9, 8) 0.11889318	(29, 10, 9) -0.10418517		
(29, 4)-0.09744631	(29, 5) 0.17025606	(29, 6)-0.20093513	(29, 7) 0.18342784	(29, 10, 0) 0.13884464	(29, 11, 1)-0.04024905	(29, 12, 2)-0.11560659	(29, 13, 3) 0.10751195
(29, 8)-0.12359740	(29, 9) 0.03640921	(29, 10) 0.05893520	(29, 11)-0.14421874	(29, 11, 4) 0.05325164	(29, 12, 5) 0.13901541	(29, 13, 6) 0.02815197	(29, 14, 7) 0.12312249
(29, 12) 0.20626076	(29, 13)-0.23890792	(29, 14) 0.24286054	(29, 15)-0.22388351	(29, 12, 8)-0.10144937	(29, 13, 9) 0.06331858	(29, 14, 10) 0.14044585	
(29, 16) 0.19027960	(29, 17)-0.15048027	(29, 18) 0.11133274	(29, 19)-0.07729468	(29, 13, 0) 0.00000000	(29, 14, 1) -0.13227187	(29, 15, 2) 0.08442712	(29, 16, 3) 0.07851563
(29, 20) 0.05043149	(29, 21)-0.03093169	(29, 22) 0.01782146	(29, 23)-0.00962939	(29, 14, 4) 0.13496944	(29, 15, 5) 0.00802549	(29, 16, 6) 0.13036595	(29, 17, 7)-0.09271517
(29, 24) 0.00486656	(29, 25)-0.00229183	(29, 26) 0.00100057	(29, 27)-0.00040217	(29, 14, 8) 0.07050969	(29, 15, 9) 0.13982643	(29, 16, 10) 0.02157820	(29, 17, 11) 0.12666991
(29, 28) 0.00014741	(29, 29)-0.00004862			(29, 15, 0) 0.14028077	(29, 16, 1) 0.04879844	(29, 17, 2) 0.10641994	(29, 18, 3) 0.12310719
(30, 0) 0.00000000	(30, 1) -0.09219684	(30, 2) 0.16529445	(30, 3)-0.20451568	(29, 16, 4) 0.02060669	(29, 17, 5) 0.13798596	(29, 18, 6) 0.07653846	(29, 19, 7) 0.0449020
(30, 4) 0.20257182	(30, 5)-0.16087686	(30, 6) 0.08860406	(30, 7) 0.00000000	(29, 17, 8) 0.13722534	(29, 18, 9) 0.01340475	(29, 19, 10) 0.12864351	(29, 20, 11) 0.10747623
(30, 8)-0.08918399	(30, 9) 0.16513667	(30, 10)-0.21847039	(30, 11) 0.24529301	(29, 18, 12) 0.05067273			
(30, 12)-0.24687092	(30, 13) 0.22825506	(30, 14)-0.19642974	(30, 15) 0.15853384	(29, 19, 13) 0.00000000	(30, 1, 1) 0.13076302	(30, 2, 2) -0.09863932	(30, 3, 3)-0.05645089
(30, 16)-0.12054428	(30, 17) 0.08658764	(30, 18)-0.05884043	(30, 19) 0.03784624	(29, 19, 4) 0.14165354	(30, 1, 5) -0.05102969	(30, 2, 6) 0.10330743	(30, 3, 7) 0.13057029
(30, 20)-0.02303445	(30, 21) 0.01325320	(30, 22)-0.00719675	(30, 23) 0.00367956	(29, 19, 8) 0.00313142	(30, 1, 9) -0.13393626	(30, 2, 10) 0.10183964	(30, 3, 11) 0.05459979
(30, 24)-0.00176568	(30, 25) 0.00079188	(30, 26)-0.00033011	(30, 27) 0.00012699	(29, 19, 12) 0.14653671	(30, 1, 13) 0.06325414		
(30, 28)-0.00004464	(30, 29) 0.00001415	(30, 30)-0.00000396		(29, 19, 14) 0.14207843	(30, 1, 14) -0.05766107	(30, 2, 15) 0.09535629	(30, 3, 16) 0.13535300
(31, 1) -0.22287525	(31, 2) 0.20626575	(31, 3)-0.15905465	(31, 4) 0.08855788	(29, 19, 15) 0.01482258	(30, 1, 15) 0.12368137	(30, 2, 16) 0.11656582	(30, 3, 17) 0.02799684
(31, 4)-0.00531613	(31, 5) -0.07894995	(31, 6) 0.15346673	(31, 7)-0.21014298	(29, 19, 16) 0.14056194	(30, 1, 16) 0.08951125	(30, 2, 17) 0.06613909	(30, 3, 18) 0.14668761
(31, 8) 0.24457940	(31, 9)-0.25623080	(31, 10) 0.24781610	(31, 11)-0.22423165	(29, 19, 17) 0.05944925	(30, 1, 17) 0.09661426	(30, 2, 18) 0.14541686	
(31, 12) 0.19129159	(31, 13)-0.15459174	(31, 14) 0.11869897	(31, 15)-0.08674506	(29, 19, 18) 0.00000000	(30, 1, 18) 0.12893407	(30, 2, 19) 0.11222271	(30, 3, 20) 0.03130950
(31, 16) 0.06039242	(31, 17)-0.04006663	(31, 18) 0.02532424	(31, 19)-0.01523788	(29, 19, 19) 0.13987498	(30, 1, 19) 0.09126212	(30, 2, 20) 0.0609016	(30, 3, 21) 0.14494301
(31, 20) 0.00871820	(31, 21)-0.00473493	(31, 22) 0.00243572	(31, 23)-0.00118343	(29, 19, 20) 0.06866555	(30, 1, 20) 0.08436818	(30, 2, 21) 0.14553897	(30, 3, 22) 0.0471251
(31, 24) 0.00054114	(31, 25)-0.00023183	(31, 26) 0.00000252	(31, 27)-0.00003414	(29, 19, 21) 0.10303847	(30, 1, 21) 0.14439337	(30, 2, 22) 0.03208004	(30, 3, 23) 0.11569884
(31, 28) 0.00001153	(31, 29)-0.00000352	(31, 30) 0.00000095	(31, 31)-0.00000022	(29, 19, 22) 0.14430434	(30, 1, 22) 0.06693078	(30, 2, 23) 0.08286267	(30, 3, 24) 0.14356843
(32, 0) 0.00000000	(32, 1) 0.07586423	(32, 2)-0.14508016	(32, 3) 0.20194305	(29, 19, 23) 0.05135995	(30, 1, 23) 0.09600972	(30, 2, 24) 0.14178701	(30, 3, 25) 0.03740055
(32, 4) -0.24245292	(32, 5) 0.26475528	(32, 6)-0.26919848	(32, 7) 0.25803062	(29, 19, 24) 0.10711922	(30, 1, 24) 0.14018437	(30, 2, 25) 0.02726287	(30, 3, 26) 0.11492977
(32, 8)-0.23483236	(32, 9) 0.20382424	(32, 10)-0.16919391	(32, 11) 0.13455969	(29, 19, 25) 0.14061286	(30, 1, 25) 0.02367533	(30, 2, 26) 0.11855228	(30, 3, 27) 0.14519560
(32, 12)-0.10263810	(32, 13) 0.07512794	(32, 14)-0.05277791	(32, 15) 0.03557719	(29, 19, 26) 0.03033495			
(32, 16)-0.02300507	(32, 17) 0.01424974	(32, 18)-0.00845095	(32, 19) 0.00479105	(29, 19, 27) 0.00000000	(30, 1, 27) 0.12674396	(30, 2, 28) 0.12502530	(30, 3, 29) 0.00341974
(32, 20)-0.00259199	(32, 21) 0.00133536	(32, 22)-0.00065345	(32, 23) 0.00003077	(29, 19, 28) 0.12873097	(30, 1, 28) 0.12452704	(30, 2, 29) 0.13047249	(30, 3, 30) 0.13016598
(32, 24)-0.00013233	(32, 25) 0.00005430	(32, 26)-0.00002079	(32, 27) 0.00000738	(29, 19, 29) 0.00254413	(30, 1, 29) 0.13005769	(30, 2, 30) 0.13198842	
(32, 28)-0.00000240	(32, 29) 0.00000071	(32, 30)-0.00000018	(32, 31) 0.00000004	(29, 19, 30) 0.00656301	(30, 1, 30) 0.12657201	(30, 2, 31) 0.14219300	(30, 3, 32) 0.02606697
(32, 32)-0.00000001				(29, 19, 31) 0.11566608	(30, 1, 31) 0.15631409		
(33, 0) 0.31279626	(33, 1)-0.30816197	(33, 2) 0.29465923	(33, 3)-0.27343220	(29, 19, 32) 0.14705324	(30, 1, 32) 0.07673149	(30, 2, 33) 0.06703354	(30, 3, 34) 0.14699341
(33, 4) 0.24621210	(33, 5)-0.21508820	(33, 6) 0.18224822	(33, 7)-0.14973219	(29, 19, 33) 0.08697585	(30, 1, 33) 0.05595566	(30, 2, 34) 0.14649487	(30, 3, 35) 0.0940439
(33, 8) 0.11923670	(33, 9) -0.09199311	(33, 10) 0.06872689	(33, 11) 0.04968946	(29, 19, 34) 0.04112862	(30, 1, 34) 0.14439501	(30, 2, 35) 0.11526848	(30, 3, 36) 0.01945558
(33, 12) 0.03474316	(33, 13)-0.02347470	(33, 14) 0.01531321	(33, 15)-0.00963435	(29, 19, 35) 0.13799372	(30, 1, 35) 0.13481034	(30, 2, 36) 0.01309849	(30, 3, 37) 0.12165967
(33, 16) 0.00583930	(33, 17)-0.00340487	(33, 18) 0.00190711	(33, 19)-0.00102428	(29, 19, 36) 0.15540150	(30, 1, 36) 0.06080256	(30, 2, 37) 0.08464452	
(33, 20) 0.00005264	(33, 21)-0.00002580	(33, 22) 0.000012056	(33, 23)-0.000005347	(29, 19, 37) 0.00000000	(30, 1, 37) 0.12413637	(30, 2, 38) 0.13685933	(30, 3, 39) 0.02679507
(33, 24) 0.00000240	(33, 25)-0.00000882	(33, 26) 0.00000325	(33, 27)-0.00000111	(29, 19, 38) 0.10754046	(30, 1, 38) 0.14635809	(30, 2, 39) 0.05529092	(30, 3, 40) 0.08511037
(33, 28) 0.00000035	(33, 29)-0.00000010	(33, 30) 0.00000002	(33, 31)-0.00000001	(29, 19, 39) 0.15167280	(30, 1, 39) 0.08665624	(30, 2, 40) 0.05362293	(30, 3, 41) 0.14945930
(33, 32) 0.00000000	(33, 33) 0.00000000			(29, 19, 40) 0.12043025	(30, 1, 40) 0.08866169	(30, 2, 41) 0.13258536	(30, 3, 42) 0.15194884
M S	L=34			(29, 19, 41) 0.050267256	(30, 1, 41) 0.088615326	(30, 2, 42) 0.16680281	(30, 3, 43) 0.12729266
(0, 0)-0.13583376				(29, 19, 42) 0.04318551	(30, 1, 42) 0.09293702	(30, 2, 43) 0.15562367	(30, 3, 44) 0.09562550
(1, 0) 0.00000000	(1, 1) 0.13583376			(29, 19, 43) 0.13963781	(30, 1, 43) 0.14603601	(30, 2, 44) 0.14384231	(30, 3, 45) 0.03568742
(2, 0) 0.13594805	(2, 1)-0.00788187	(2, 2)-0.13514774		(29, 19, 44) 0.09978174	(30, 1, 44) 0.16803563	(30, 2, 45) 0.14071151	
(3, 0) 0.00000000	(3, 1)-0.13560489	(3, 2) 0.02360578	(3, 3)-0.13171758	(29, 19, 45) 0.12826766			
(4, 0)-0.13629383	(4, 1) 0.01580384	(4, 2) 0.13274038	(4, 3)-0.04669203	(29, 19, 46) 0.00000000	(29, 1, 46) 0.12103247	(29, 2, 47) 0.14748333	(29, 3, 48) 0.05878145
(4, 4)-0.12219471				(29, 19, 47) 0.07592732	(29, 1, 47) 0.15221180	(29, 2, 48) 0.11144799	(29, 3, 49) 0.01485536
(5, 0) 0.00000000	(5, 1) 0.13514365	(5, 2)-0.03920915	(5, 3)-0.12397681	(29, 19, 48) 0.13799372	(29, 1, 48) 0.14916448	(29, 2, 49) 0.05716766	(29, 3, 50) 0.07747792
(5, 4) 0.07543054	(5, 5) 0.10234762			(29, 19, 49) 0.13780145	(29, 1, 49) 0.12773852	(29, 2, 50) 0.06915854	(29, 3, 51) 0.11726303
(6, 0) 0.13688004	(6, 1)-0.02380772	(6, 2)-0.12870643	(6, 3) 0.06873336	(29, 19, 50) 0.16909166	(29, 1, 50) 0.11510664	(29, 2, 51) 0.00971161	(29, 3, 52) 0.13153148
(6, 4) 0.10500254	(6, 5)-0.10580528	(6, 6)-0.06817557		(29, 19, 51) 0.18416807	(29, 1, 51) 0.14384757		

(22, 0) 0.15474252	(22, 1)-0.09868675	(22, 2)-0.02889222	(22, 3) 0.13579850	(30, 24) 0.00637670	(30, 25)-0.00314023	(30, 26) 0.00144265	(30, 27)-0.00061505
(22, 4)-0.14512476	(22, 5) 0.05041952	(22, 6) 0.08061276	(22, 7)-0.15536761	(30, 28) 0.00024162	(30, 29)-0.00008664	(30, 30) 0.00002797	
(22, 8) 0.12189610	(22, 9)-0.00393095	(22, 10)-0.11767440	(22, 11) 0.16151877	(31, 0) 0.00000000	(31, 1)-0.09022059	(31, 2) 0.16228902	(31, 3)-0.20204572
(22, 12)-0.09959908	(22, 13)-0.02709761	(22, 14) 0.13842916	(22, 15)-0.16708414	(31, 4) 0.20227791	(31, 5)-0.16391091	(31, 6) 0.09523267	(31, 7)-0.00949824
(22, 16) 0.09792282	(22, 17) 0.02776622	(22, 18)-0.14078786	(22, 19) 0.18451372	(31, 8)-0.07833119	(31, 9) 0.15481243	(31, 10)-0.21043226	(31, 11) 0.24076219
(22, 20)-0.14111310	(22, 21) 0.03451038	(22, 22) 0.08884885		(31, 12)-0.24631131	(31, 13) 0.23137456	(31, 14)-0.20236433	(31, 15) 0.16612944
(23, 0) 0.00000000	(23, 1)-0.11731789	(23, 2) 0.15657191	(23, 3)-0.09179693	(31, 16)-0.12864222	(31, 17) 0.09424106	(31, 18)-0.06542677	(31, 19) 0.04307873
(23, 4)-0.03393949	(23, 5) 0.13775282	(23, 6)-0.15196438	(23, 7) 0.06784309	(31, 20)-0.02690132	(31, 21) 0.01592280	(31, 22)-0.00892213	(31, 23) 0.00472411
(23, 8) 0.06022577	(23, 9)-0.15118192	(23, 10) 0.14896558	(23, 11)-0.05593706	(31, 24)-0.00235763	(31, 25) 0.00110534	(31, 26)-0.00048474	(31, 27) 0.00019775
(23, 12)-0.07139945	(23, 13) 0.15872170	(23, 14)-0.15765172	(23, 15) 0.07068279	(31, 28)-0.00007449	(31, 29) 0.00002566	(31, 30)-0.00000797	(31, 31) 0.00000219
(23, 16) 0.05463200	(23, 17)-0.15484792	(23, 18) 0.18389985	(23, 19)-0.13239613	(32, 0)-0.22118035	(32, 1) 0.20517434	(32, 2)-0.15960708	(32, 3) 0.09134250
(23, 20) 0.02582449	(23, 21) 0.09298156	(23, 22)-0.18508078	(23, 23) 0.22960447	(32, 4)-0.01031269	(32, 5) 0.07235862	(32, 6) 0.14632647	(32, 7)-0.20366029
(24, 0)-0.16022393	(24, 1) 0.11147183	(24, 2) 0.00512070	(24, 3)-0.11880320	(32, 8) 0.23983440	(32, 9)-0.25394872	(32, 10) 0.24824917	(32, 11)-0.22716554
(24, 4) 0.16101490	(24, 5)-0.10674237	(24, 6)-0.01127236	(24, 7) 0.12326809	(32, 12) 0.19615430	(32, 13)-0.16062017	(32, 14) 0.12511188	(32, 15)-0.09288077
(24, 8)-0.16436377	(24, 9) 0.11180650	(24, 10) 0.00389067	(24, 11)-0.11851967	(32, 16) 0.06578884	(32, 17)-0.04448098	(32, 18) 0.02870560	(32, 19)-0.01767294
(24, 12) 0.17096871	(24, 13)-0.13532269	(24, 14) 0.03142905	(24, 15) 0.08905197	(32, 20) 0.01037046	(32, 21)-0.00579225	(32, 22) 0.00307380	(32, 23)-0.00154626
(24, 16)-0.17060436	(24, 17) 0.17968680	(24, 18)-0.11623476	(24, 19) 0.00813160	(32, 24) 0.00073520	(32, 25)-0.00032921	(32, 26) 0.00013820	(32, 27)-0.00005407
(24, 20) 0.10521568	(24, 21)-0.19034220	(24, 22) 0.23041028	(24, 23)-0.22650903	(32, 28) 0.000001957	(32, 29)-0.00000649	(32, 30) 0.00000194	(32, 31)-0.00000052
(24, 24) 0.19187172				(32, 32) 0.00000012			
(25, 0) 0.00000000	(25, 1) 0.11281840	(25, 2)-0.16365968	(25, 3) 0.12480434	(33, 0) 0.00000000	(33, 1) 0.07422077	(33, 2)-0.14212196	(33, 3) 0.19825611
(25, 4)-0.01773794	(25, 5)-0.09930162	(25, 6) 0.16359404	(25, 7)-0.14159699	(33, 4)-0.23875603	(33, 5) 0.26175362	(33, 6)-0.26745021	(33, 7) 0.25785574
(25, 8) 0.04564027	(25, 9) 0.07435745	(25, 10)-0.15811025	(25, 11) 0.16551429	(33, 8)-0.23627947	(33, 9) 0.20669548	(33, 10)-0.17311397	(33, 11) 0.13906702
(25, 12)-0.09468103	(25, 13)-0.02020213	(25, 14) 0.12770972	(25, 15)-0.18348816	(33, 12)-0.10727481	(33, 13) 0.07951009	(33, 14)-0.05663644	(33, 15) 0.03876825
(25, 16) 0.16794658	(25, 17)-0.09049435	(25, 18) 0.01896313	(25, 19) 0.12495509	(33, 16)-0.02549157	(33, 17) 0.01609077	(33, 18)-0.00974144	(33, 19) 0.00564971
(25, 20)-0.20012087	(25, 21) 0.23243318	(25, 22)-0.22491471	(25, 23) 0.19019884	(33, 20)-0.00313438	(33, 21) 0.00166044	(33, 22)-0.00083R12	(33, 23) 0.00040203
(25, 24)-0.143362040	(25, 25) 0.09785344			(33, 24)-0.000018270	(33, 25) 0.000007835	(33, 26)-0.00003156	(33, 27) 0.00001187
(26, 0) 0.16747752	(26, 1)-0.12622820	(26, 2) 0.02281864	(26, 3) 0.09195726	(33, 28)-0.00000414	(33, 29) 0.000000132	(33, 30)-0.000000038	(33, 31) 0.000000010
(26, 4)-0.16219774	(26, 5) 0.15430738	(26, 6)-0.07269692	(26, 7)-0.04354153	(33, 32)-0.00000002	(33, 33) 0.000000000		
(26, 8) 0.14038007	(26, 9)-0.17446518	(26, 10) 0.13201283	(26, 11)-0.03281198	(34, 0) 0.31048778	(34, 1)-0.30602008	(34, 2) 0.29299194	(34, 3)-0.27247694
(26, 12)-0.08092257	(26, 13) 0.16405235	(26, 14)-0.18673292	(26, 15) 0.14379869	(34, 4) 0.24610409	(34, 5)-0.21584757	(34, 6) 0.18378758	(34, 7)-0.15188093
(26, 16)-0.05294477	(26, 17)-0.05541677	(26, 18) 0.15087444	(26, 19)-0.21283375	(34, 8) 0.12177566	(34, 9)-0.09469192	(34, 10) 0.07137672	(34, 11)-0.05212619
(26, 20) 0.23449428	(26, 21)-0.22113866	(26, 22) 0.18502536	(26, 23)-0.13973989	(34, 12) 0.03685878	(34, 13)-0.02521758	(34, 14) 0.01667986	(34, 15)-0.01065637
(26, 24) 0.09610298	(26, 25)-0.06042477	(26, 26) 0.03476023		(34, 16) 0.00656903	(34, 17)-0.00390258	(34, 18) 0.00223139	(34, 19)-0.00122602
(27, 0) 0.00000000	(27, 1)-0.10724892	(27, 2) 0.16802678	(27, 3)-0.15626173	(34, 20) 0.0064617	(34, 21)-0.00032601	(34, 22) 0.00015707	(34, 23)-0.00007207
(27, 4) 0.07739785	(27, 5) 0.03460672	(27, 6)-0.13259950	(27, 7) 0.17654462	(34, 24) 0.000003139	(34, 25)-0.00001292	(34, 26) 0.00000500	(34, 27)-0.00000181
(27, 7) 0.14968570	(27, 8) 0.06393916	(27, 9) 0.04680216	(27, 11)-0.14143227	(34, 28) 0.00000061	(34, 29)-0.00000019	(34, 30) 0.000000005	(34, 31)-0.000000001
(27, 12) 0.18751447	(27, 13)-0.17183259	(27, 14) 0.10234234	(27, 15)-0.00226709	(34, 32) 0.00000000	(34, 33) 0.000000000	(34, 34) 0.000000000	
(27, 16)-0.09997380	(27, 17) 0.18048613	(27, 18)-0.22592366	(27, 19) 0.23466812				
(27, 20)-0.21408910	(27, 21) 0.17593649	(27, 22)-0.13193642	(27, 23) 0.09090754				
(27, 24)-0.05773947	(27, 25) 0.03383003	(27, 26)-0.01826047	(27, 27) 0.00905024				
(28, 0)-0.17759125	(28, 1) 0.14414717	(28, 2)-0.05645880	(28, 3)-0.05250562				
(28, 4) 0.14227091	(28, 5)-0.18023755	(28, 6) 0.15346673	(28, 7)-0.07247084				
(28, 8)-0.03389513	(28, 9) 0.12975569	(28, 10)-0.18491641	(28, 11) 0.18415071				
(28, 12)-0.13021421	(28, 13) 0.04049470	(28, 14) 0.06045695	(28, 15)-0.14921778				
(28, 16) 0.20970669	(28, 17)-0.23579948	(28, 18) 0.23042302	(28, 19)-0.20236188				
(28, 20) 0.16240916	(28, 21)-0.12020642	(28, 22) 0.08245984	(28, 23)-0.05255168				
(28, 24) 0.03112949	(28, 25)-0.01712094	(28, 26) 0.00872024	(28, 27)-0.00409579				
(28, 28)-0.00066926	(28, 29) 0.00025777						
(29, 0) 0.00000000	(29, 1) 0.10009076	(29, 2)-0.16842780	(29, 3) 0.18364064				
(29, 4)-0.14147410	(29, 5) 0.05562251	(29, 6) 0.04736086	(29, 7)-0.13698554				
(29, 8) 0.18828477	(29, 9)-0.18864231	(29, 10) 0.14007218	(29, 11)-0.05683014				
(29, 12)-0.04018498	(29, 13) 0.12996812	(29, 14)-0.19672950	(29, 15) 0.23267727				
(29, 16)-0.23803316	(29, 17) 0.21896544	(29, 18)-0.18457955	(29, 19) 0.14406732				
(29, 20)-0.10473698	(29, 21) 0.07115664	(29, 22)-0.04524409	(29, 23) 0.02692752				
(29, 24)-0.01498534	(29, 25) 0.00778087	(29, 26)-0.00375669	(29, 27) 0.00167840				
(29, 28)-0.00066926	(29, 29) 0.00025777						
(30, 0) 0.19301564	(30, 1)-0.16785730	(30, 2) 0.09902404	(30, 3)-0.00452904				
(30, 4)-0.09135845	(30, 5) 0.16479783	(30, 6)-0.19856645	(30, 7) 0.18597332				
(30, 8)-0.13156798	(30, 9) 0.04879227	(30, 10) 0.04437155	(30, 11)-0.13025297				
(30, 12) 0.19543755	(30, 13)-0.23291320	(30, 14) 0.24222253	(30, 15)-0.22803381				
(30, 16) 0.19788624	(30, 17)-0.15989895	(30, 18) 0.12102318	(30, 19)-0.08609942				
(30, 20) 0.05768407	(30, 21)-0.03641991	(30, 22) 0.02166400	(30, 23)-0.01212757				

Table 15.1.2 FOURIER coefficients a_l^{mn} of the generalized spherical functions $p_l^{mn}(\Phi)$ for $l = 0(1)6$, $m = 0(1)l$, $n = 0(1)m$, $s = 0(1)l$. The coefficients are defined according to equations (14.85), (14.86), (14.72) and (14.81)–(14.84)

N S	L= 0	M= 0
(0, 0) 1.00000000		
N S	L= 1	M= 0
(0, 0) 0.00000000	(0, 1) 1.00000000	
N S	L= 1	M= 1
(0, 0) 0.00000000	(0, 1) -0.70710678	
(1, 0) 0.50000000	(1, 1) 0.50000000	
N S	L= 2	M= 0
(0, 0) 0.25000000	(0, 1) 0.00000000	(0, 2) 0.75000000
N S	L= 2	M= 1
(0, 0) 0.00000000	(0, 1) 0.00000000	(0, 2) -0.61237244
(1, 0) 0.00000000	(1, 1) 0.50000000	(1, 2) 0.50000000
N S	L= 2	M= 2
(0, 0) -0.30618622	(0, 1) 0.00000000	(0, 2) 0.30618622
(1, 0) 0.00000000	(1, 1) -0.50000000	(1, 2) -0.25000000
(2, 0) 0.37500000	(2, 1) 0.50000000	(2, 2) 0.12500000
N S	L= 3	M= 0
(0, 0) 0.00000000	(0, 1) 0.37500000	(0, 2) 0.00000000
(0, 0) 0.00000000	(0, 1) -0.10825318	(0, 2) 0.00000000
(1, 0) 0.18750000	(1, 1) 0.03125000	(1, 2) 0.31250000
N S	L= 3	M= 1
(0, 0) 0.00000000	(0, 1) -0.10825318	(0, 2) 0.00000000
(1, 0) 0.18750000	(1, 1) 0.03125000	(1, 2) 0.31250000
N S	L= 3	M= 2
(0, 0) 0.00000000	(0, 1) -0.34232660	(0, 2) 0.00000000
(1, 0) 0.00000000	(1, 1) 0.09882118	(1, 2) -0.39528471
(2, 0) 0.00000000	(2, 1) 0.31250000	(2, 2) 0.50000000
N S	L= 3	M= 3
(0, 0) 0.00000000	(0, 1) 0.41926275	(0, 2) 0.00000000
(1, 0) -0.24206146	(1, 1) -0.12103073	(1, 2) 0.24206146
(2, 0) 0.00000000	(2, 1) -0.38273277	(2, 2) -0.30618622
(3, 0) 0.31250000	(3, 1) 0.46875000	(3, 2) 0.18750000

N S	L= 4	M= 0
(0, 0) 0.14062500	(0, 1) 0.00000000	(0, 2) 0.31250000
(0, 4) 0.54687500		(0, 3) 0.00000000
N S	L= 4	M= 1
(0, 0) 0.00000000	(0, 1) 0.00000000	(0, 2) -0.13975425
(0, 4) 0.48913987		(0, 3) 0.00000000
(1, 0) 0.00000000	(1, 1) 0.28125000	(1, 2) 0.06250000
(1, 4) 0.43750000		(1, 3) 0.21875000
N S	L= 4	M= 2
(0, 0) -0.14823177	(0, 1) 0.00000000	(0, 2) -0.19764235
(0, 4) 0.34587412		(0, 3) 0.00000000
(1, 0) 0.00000000	(1, 1) -0.13258252	(1, 2) 0.08838835
(1, 4) -0.30935922		(1, 3) -0.30935922
(2, 0) 0.15625000	(2, 1) 0.06250000	(2, 2) 0.12500000
(2, 4) 0.21875000		(2, 3) 0.43750000
N S	L= 4	M= 3
(0, 0) 0.00000000	(0, 1) 0.00000000	(0, 2) 0.36975499
(0, 4) -0.18487749		(0, 3) 0.00000000
(1, 0) 0.00000000	(1, 1) -0.24803919	(1, 2) -0.16535946
(1, 4) 0.16535946		(1, 3) 0.24803919
(2, 0) 0.00000000	(2, 1) 0.11692679	(2, 2) -0.23385359
(2, 4) -0.11692679		(2, 3) -0.35078038
(3, 0) 0.00000000	(3, 1) 0.21875000	(3, 2) 0.43750000
(3, 4) 0.06250000		(3, 3) 0.28125000
N S	L= 4	M= 4
(0, 0) 0.19609219	(0, 1) 0.00000000	(0, 2) -0.26145626
(0, 4) 0.06536406		(0, 3) 0.00000000
(1, 0) 0.00000000	(1, 1) 0.35078038	(1, 2) 0.11692679
(1, 4) -0.05846340		(1, 3) -0.11692679
(2, 0) -0.20669932	(2, 1) -0.16535946	(2, 2) 0.16535946
(2, 4) 0.04133986		(2, 3) 0.16535946
(3, 0) 0.00000000	(3, 1) -0.30935922	(3, 2) -0.30935922
(3, 4) -0.02209709		(3, 3) -0.13258252
(4, 0) 0.27343750	(4, 1) 0.43750000	(4, 2) 0.21875000
(4, 4) 0.00781250		(4, 3) 0.06250000
N S	L= 5	M= 0
(0, 0) 0.00000000	(0, 1) 0.23437500	(0, 2) 0.00000000
(0, 4) 0.00000000	(0, 5) 0.49218750	
N S	L= 5	M= 1
(0, 0) 0.00000000	(0, 1) -0.04279082	(0, 2) 0.00000000
(0, 4) 0.00000000	(0, 5) -0.44930366	
(1, 0) 0.11718750	(1, 1) 0.00781250	(1, 2) 0.21875000
(1, 4) 0.16406250	(1, 5) 0.41015625	(1, 3) 0.08203125
N S	L= 5	M= 2
(0, 0) 0.00000000	(0, 1) -0.22642776	(0, 2) 0.00000000
(0, 4) 0.00000000	(0, 5) 0.33964164	
(1, 0) 0.00000000	(1, 1) 0.04133986	(1, 2) -0.16535946
		(1, 3) 0.06200980

(1, 4)-0.24803919 (1, 5)-0.31004898
 (2, 0) 0.00000000 (2, 1) 0.21875000 (2, 2) 0.12500000 (2, 3) 0.04687500
 (2, 4) 0.37500000 (2, 5) 0.23437500

N S L= 5 M= 3

(0, 0) 0.00000000 (0, 1) 0.13865812 (0, 2) 0.00000000 (0, 3) 0.30042593
 (0, 4) 0.00000000 (0, 5)-0.26798718 (1, 1)-0.02531539 (1, 2)-0.10126157 (1, 3)-0.16455006
 (1, 4) 0.22783854 (1, 5) 0.18986545 (2, 0) 0.00000000 (2, 1)-0.13395647 (2, 2) 0.07654655 (2, 3)-0.12438815
 (2, 4)-0.34445950 (2, 5)-0.14352479 (3, 0) 0.13671875 (3, 1) 0.08203125 (3, 2) 0.04687500 (3, 3) 0.33007813
 (3, 4) 0.31640625 (3, 5) 0.08789062

N S L= 5 M= 4

(0, 0) 0.00000000 (0, 1) 0.19609210 (0, 2) 0.00000000 (0, 3)-0.29413829
 (0, 4) 0.00000000 (0, 5) 0.09804610 (1, 0) 0.00000000 (1, 1)-0.03580137 (1, 2) 0.28641098 (1, 3) 0.16110618
 (1, 4)-0.14320549 (1, 5)-0.08950343 (2, 0) 0.00000000 (2, 1)-0.18944306 (2, 2)-0.21650635 (2, 3) 0.12178482
 (2, 4) 0.21650635 (2, 5) 0.06765823 (3, 0) 0.00000000 (3, 1) 0.11600971 (3, 2)-0.13258252 (3, 3)-0.32316990
 (3, 4)-0.19887378 (3, 5)-0.04143204 (4, 0) 0.00000000 (4, 1) 0.16406250 (4, 2) 0.37500000 (4, 3) 0.31640625
 (4, 4) 0.12500000 (4, 5) 0.01953125

N S L= 5 M= 5

(0, 0) 0.00000000 (0, 1)-0.31004898 (0, 2) 0.00000000 (0, 3) 0.15502449
 (0, 4) 0.00000000 (0, 5)-0.03100490 (1, 0) 0.16982082 (1, 1) 0.05660694 (1, 2)-0.22642776 (1, 3)-0.08491041
 (1, 4) 0.05660694 (1, 5) 0.02830347 (2, 0) 0.00000000 (2, 1) 0.29953577 (2, 2) 0.17116330 (2, 3)-0.06418624
 (2, 4)-0.08558165 (2, 5)-0.02139541 (3, 0)-0.18342745 (3, 1)-0.18342745 (3, 2) 0.10481569 (3, 3) 0.17032549
 (3, 4) 0.07861176 (3, 5) 0.01310196 (4, 0) 0.00000000 (4, 1)-0.25940559 (4, 2)-0.29646353 (4, 3)-0.16676074
 (4, 4)-0.04941059 (4, 5)-0.00617632 (5, 0) 0.24609375 (5, 1) 0.41015625 (5, 2) 0.23437500 (5, 3) 0.08789062
 (5, 4) 0.01953125 (5, 5) 0.00195312

N S L= 6 M= 0

(0, 0) 0.09765625 (0, 1) 0.00000000 (0, 2) 0.20507813 (0, 3) 0.00000000
 (0, 4) 0.24609375 (0, 5) 0.00000000 (0, 6) 0.45117187

N S L= 6 M= 1

(0, 0) 0.00000000 (0, 1) 0.00000000 (0, 2)-0.06328848 (0, 3) 0.00000000
 (0, 4)-0.15189236 (0, 5) 0.00000000 (0, 6)-0.41770399 (1, 0) 0.00000000 (1, 1) 0.19531250 (1, 2) 0.01953125 (1, 3) 0.17578125
 (1, 4) 0.09375000 (1, 5) 0.12890625 (1, 6) 0.38671875

N S L= 6 M= 2

(0, 0)-0.10006788 (0, 1) 0.00000000 (0, 2)-0.17011539 (0, 3) 0.00000000
 (0, 4)-0.06004073 (0, 5) 0.00000000 (0, 6) 0.33022400 (1, 0) 0.00000000 (1, 1)-0.06176324 (1, 2) 0.05249875 (1, 3)-0.16676074
 (1, 4) 0.03705794 (1, 5)-0.20381868 (1, 6)-0.30572802 (2, 0) 0.10253906 (2, 1) 0.01953125 (2, 2) 0.14111328 (2, 3) 0.15820312
 (2, 4) 0.01464844 (2, 5) 0.32226563 (2, 6) 0.24169922

N S L= 6 M= 3

(0, 0) 0.00000000 (0, 1) 0.00000000 (0, 2) 0.18012218 (0, 3) 0.00000000
 (0, 4) 0.24016291 (0, 5) 0.00000000 (0, 6)-0.22014933 (1, 0) 0.00000000 (1, 1)-0.18528971 (1, 2)-0.05558691 (1, 3)-0.01852897
 (1, 4)-0.14823177 (1, 5) 0.20381868 (1, 6) 0.20381868 (2, 0) 0.00000000 (2, 1) 0.05859375 (2, 2)-0.14941406 (2, 3) 0.01757813
 (2, 4)-0.05859375 (2, 5) 0.32226563 (2, 6)-0.16113281 (3, 0) 0.00000000 (3, 1) 0.17578125 (3, 2) 0.15820312 (3, 3) 0.00195313
 (3, 4) 0.23437500 (3, 5) 0.32226563 (3, 6) 0.10742188

N S L= 6 M= 4

(0, 0) 0.10961887 (0, 1) 0.00000000 (0, 2) 0.05480943 (0, 3) 0.00000000
 (0, 4)-0.28500906 (0, 5) 0.00000000 (0, 6) 0.12058076 (1, 0) 0.00000000 (1, 1) 0.13531647 (1, 2)-0.01691456 (1, 3) 0.20297470
 (1, 4) 0.17591141 (1, 5)-0.14884812 (1, 6)-0.11163609 (2, 0)-0.11237592 (2, 1)-0.04279082 (2, 2)-0.04546525 (2, 3)-0.19255871
 (2, 4) 0.06953509 (2, 5) 0.23534954 (2, 6) 0.08825608 (3, 0) 0.00000000 (3, 1)-0.12837247 (3, 2) 0.04813968 (3, 3)-0.02139541
 (3, 4)-0.27814036 (3, 5) 0.23534954 (3, 6)-0.05883738 (4, 0) 0.12304688 (4, 1) 0.09375000 (4, 2) 0.01464844 (4, 3) 0.23437500
 (4, 4) 0.33007813 (4, 5) 0.17187500 (4, 6) 0.03222656

N S L= 6 M= 5

(0, 0) 0.00000000 (0, 1) 0.00000000 (0, 2)-0.25707903 (0, 3) 0.00000000
 (0, 4) 0.20566323 (0, 5) 0.00000000 (0, 6) 0.05141581 (1, 0) 0.00000000 (1, 1) 0.15867263 (1, 2) 0.07933631 (1, 3)-0.23800894
 (1, 4)-0.12693810 (1, 5) 0.07933631 (1, 6) 0.04760179 (2, 0) 0.00000000 (2, 1)-0.05017669 (2, 2) 0.21325093 (2, 3) 0.22579510
 (2, 4)-0.05017669 (2, 5) 0.12544172 (2, 6) 0.03763252 (3, 0) 0.00000000 (3, 1)-0.15053007 (3, 2)-0.22579510 (3, 3) 0.02508834
 (3, 4) 0.20070676 (3, 5) 0.12544172 (3, 6) 0.02508834 (4, 0) 0.00000000 (4, 1) 0.10993162 (4, 2)-0.06870726 (4, 3)-0.27482905
 (4, 4)-0.23818518 (4, 5) 0.09160968 (4, 6) 0.01374145 (5, 0) 0.00000000 (5, 1) 0.12890625 (5, 2) 0.32226563 (5, 3) 0.32226563
 (5, 4) 0.17187500 (5, 5) 0.04882813 (5, 6) 0.00585938

N S L= 6 M= 6

(0, 0)-0.14842465 (0, 1) 0.00000000 (0, 2) 0.22263697 (0, 3) 0.00000000
 (0, 4)-0.08905479 (0, 5) 0.00000000 (0, 6) 0.01484246 (1, 0) 0.00000000 (1, 1)-0.27482905 (1, 2)-0.06870726 (1, 3) 0.13741452
 (1, 4) 0.05496581 (1, 5)-0.02748290 (1, 6)-0.01374145 (2, 0) 0.15209001 (2, 1) 0.08690858 (2, 2)-0.18468072 (2, 3)-0.13036286
 (2, 4) 0.02172714 (2, 5) 0.04345429 (2, 6) 0.01086357 (3, 0) 0.00000000 (3, 1) 0.26072573 (3, 2) 0.19554430 (3, 3)-0.01448476
 (3, 4)-0.08690858 (3, 5) 0.04345429 (3, 6)-0.00724238 (4, 0)-0.16660626 (4, 1)-0.19040715 (4, 2) 0.05950223 (4, 3) 0.15867263
 (4, 4) 0.10313721 (4, 5) 0.03173453 (4, 6) 0.00396682 (5, 0) 0.00000000 (5, 1)-0.22327217 (5, 2)-0.27909022 (5, 3)-0.18606015
 (5, 4)-0.07442406 (5, 5) 0.01691456 (5, 6) 0.00169146 (6, 0) 0.22558594 (6, 1) 0.38671875 (6, 2) 0.24169922 (6, 3) 0.10742188
 (6, 4) 0.03222656 (6, 5) 0.00585938 (6, 6) 0.00048828

Table 15.1.3 FOURIER coefficients a_l^{ms} of the associated LEGENDRE functions $p_l^m(\Phi)$ for $l = 0(1)9, m = 0(1)l, s = 0(1)l$. The coefficients are defined according to equations (14.94), (14.95) (see also reference 154)

M	S	L= 0
(0, 0)	0.70710678	
M	S	L= 1
(0, 0)	0.00000000	(0, 1) 1.22474487
(1, 0)	0.00000000	(1, 1) 0.86602540
M	S	L= 2
(0, 0)	0.39528471	(0, 1) 0.00000000 (0, 2) 1.18585412
(1, 0)	0.00000000	(1, 1) 0.00000000 (1, 2) 0.96824584
(2, 0)	0.48412292	(2, 1) 0.00000000 (2, 2)-0.48412292
M	S	L= 3
(0, 0)	0.00000000	(0, 1) 0.70156076 (0, 2) 0.00000000 (0, 3) 1.16926793
(1, 0)	0.00000000	(1, 1) 0.20252315 (1, 2) 0.00000000 (1, 3) 1.01261573
(2, 0)	0.00000000	(2, 1) 0.64043442 (2, 2) 0.00000000 (2, 3)-0.64043442
(3, 0)	0.00000000	(3, 1) 0.78436877 (3, 2) 0.00000000 (3, 3)-0.26145626
M	S	L= 4
(0, 0)	0.29831067	(0, 1) 0.00000000 (0, 2) 0.66291261 (0, 3) 0.00000000
(0, 4)	1.16009706	
(1, 0)	0.00000000	(1, 1) 0.00000000 (1, 2) 0.29646353 (1, 3) 0.00000000
(1, 4)	1.03762236	
(2, 0)	0.31444706	(2, 1) 0.00000000 (2, 2) 0.41926275 (2, 3) 0.00000000
(2, 4)	-0.73370981	
(3, 0)	0.00000000	(3, 1) 0.00000000 (3, 2) 0.78436877 (3, 3) 0.00000000
(3, 4)	-0.39218439	
(4, 0)	0.41597436	(4, 1) 0.00000000 (4, 2)-0.55463248 (4, 3) 0.00000000
(4, 4)	0.13R65812	
M	S	L= 5
(0, 0)	0.00000000	(0, 1) 0.54965810 (0, 2) 0.00000000 (0, 3) 0.64126778
(0, 4)	0.00000000	(0, 5) 1.15428200
(1, 0)	0.00000000	(1, 1) 0.10035338 (1, 2) 0.00000000 (1, 3) 0.35123683
(1, 4)	0.00000000	(1, 5) 1.05371048
(2, 0)	0.00000000	(2, 1) 0.53102017 (2, 2) 0.00000000 (2, 3) 0.26551009
(2, 4)	0.00000000	(2, 5)-0.79653026
(3, 0)	0.00000000	(3, 1) 0.32518212 (3, 2) 0.00000000 (3, 3) 0.70456125
(3, 4)	0.00000000	(3, 5)-0.48777317
(4, 0)	0.00000000	(4, 1) 0.45987696 (4, 2) 0.00000000 (4, 3)-0.68981544
(4, 4)	0.00000000	(4, 5) 0.22993848
(5, 0)	0.00000000	(5, 1) 0.72712932 (5, 2) 0.00000000 (5, 3)-0.36356466

M	S	L= 6
(0, 0)	0.24897556	(0, 1) 0.00000000 (0, 2) 0.52284868 (0, 3) 0.00000000
(0, 4)	0.62741842	(0, 5) 0.00000000 (0, 6) 1.15026710
(1, 0)	0.00000000	(1, 1) 0.00000000 (1, 2) 0.16135461 (1, 3) 0.00000000
(1, 4)	0.38725105	(1, 5) 0.00000000 (1, 6) 1.06494040
(2, 0)	0.25512403	(2, 1) 0.00000000 (2, 2) 0.43371086 (2, 3) 0.00000000
(2, 4)	0.15307442	(2, 5) 0.00000000 (2, 6)-0.84190931
(3, 0)	0.00000000	(3, 1) 0.00000000 (3, 2) 0.45922326 (3, 3) 0.00000000
(3, 4)	0.61229768	(3, 5) 0.00000000 (3, 6)-0.56127287
(4, 0)	0.27947438	(4, 1) 0.00000000 (4, 2) 0.13973719 (4, 3) 0.00000000
(4, 4)	-0.72663338	(4, 5) 0.00000000 (4, 6) 0.30742181
(5, 0)	0.00000000	(5, 1) 0.00000000 (5, 2) 0.65542551 (5, 3) 0.00000000
(5, 4)	-0.52434041	(5, 5) 0.00000000 (5, 6) 0.13108510
(6, 0)	0.37841009	(6, 1) 0.00000000 (6, 2)-0.56761514 (6, 3) 0.00000000
(6, 4)	0.22704606	(6, 5) 0.00000000 (6, 6)-0.03784101
M	S	L= 7
(0, 0)	0.00000000	(0, 1) 0.46802465 (0, 2) 0.00000000 (0, 3) 0.50546662
(0, 4)	0.00000000	(0, 5) 0.61779253 (0, 6) 0.00000000 (0, 7) 1.14732899
(1, 0)	0.00000000	(1, 1) 0.06254242 (1, 2) 0.00000000 (1, 3) 0.20263745
(1, 4)	0.00000000	(1, 5) 0.41278000 (1, 6) 0.00000000 (1, 7) 1.07322800
(2, 0)	0.00000000	(2, 1) 0.45959108 (2, 2) 0.00000000 (2, 3) 0.34928922
(2, 4)	0.00000000	(2, 5) 0.06740669 (2, 6) 0.00000000 (2, 7) -0.87628699
(3, 0)	0.00000000	(3, 1) 0.19498798 (3, 2) 0.00000000 (3, 3) 0.50696875
(3, 4)	0.00000000	(3, 5) 0.52430102 (3, 6) 0.00000000 (3, 7)-0.61962847
(4, 0)	0.00000000	(4, 1) 0.43113465 (4, 2) 0.00000000 (4, 3)-0.08622693
(4, 4)	0.00000000	(4, 5)-0.71855775 (4, 6) 0.00000000 (4, 7) 0.37365003
(5, 0)	0.00000000	(5, 1) 0.35927887 (5, 2) 0.00000000 (5, 3) 0.47424811
(5, 4)	0.00000000	(5, 5)-0.61795966 (5, 6) 0.00000000 (5, 7) 0.18682501
(6, 0)	0.00000000	(6, 1) 0.36639400 (6, 2) 0.00000000 (6, 3) 0.65950919
(6, 4)	0.00000000	(6, 5) 0.36639400 (6, 6) 0.00000000 (6, 7)-0.07327880
(7, 0)	0.00000000	(7, 1) 0.68546040 (7, 2) 0.00000000 (7, 3) 0.41127624
(7, 4)	0.00000000	(7, 5) 0.13709208 (7, 6) 0.00000000 (7, 7)-0.01958458
M	S	L= 8
(0, 0)	0.21798450	(0, 1) 0.00000000 (0, 2) 0.44842526 (0, 3) 0.00000000
(0, 4)	0.49326778	(0, 5) 0.00000000 (0, 6) 0.61071249 (0, 7) 0.00000000
(0, 8)	1.14505892	
(1, 0)	0.00000000	(1, 1) 0.00000000 (1, 2) 0.10569485 (1, 3) 0.00000000
(1, 4)	0.23252866	(1, 5) 0.00000000 (1, 6) 0.43183894 (1, 7) 0.00000000
(1, 8)	1.07959736	
(2, 0)	0.22107663	(2, 1) 0.00000000 (2, 2) 0.40425441 (2, 3) 0.00000000
(2, 4)	0.27792491	(2, 5) 0.00000000 (2, 6) 0.00000000 (2, 7) 0.00000000
(2, 8)	-0.90325596	
(3, 0)	0.00000000	(3, 1) 0.00000000 (3, 2) 0.30789172 (3, 3) 0.00000000
(3, 4)	0.51315287	(3, 5) 0.00000000 (3, 6) 0.44473249 (3, 7) 0.00000000
(3, 8)	-0.66709873	
(4, 0)	0.23186713	(4, 1) 0.00000000 (4, 2) 0.26499100 (4, 3) 0.00000000
(4, 4)	-0.23849190	(4, 5) 0.00000000 (4, 6)-0.68897661 (4, 7) 0.00000000
(4, 8)	0.43061038	
(5, 0)	0.00000000	(5, 1) 0.00000000 (5, 2) 0.47771933 (5, 3) 0.00000000
(5, 4)	0.28663160	(5, 5) 0.00000000 (5, 6)-0.66880706 (5, 7) 0.00000000
(5, 8)	0.23885966	
(6, 0)	0.25799792	(6, 1) 0.00000000 (6, 2) 0.00000000 (6, 3) 0.00000000
(6, 4)	-0.61919502	(6, 5) 0.00000000 (6, 6) 0.47176763 (6, 7) 0.00000000
(6, 8)	-0.11057054	
(7, 0)	0.00000000	(7, 1) 0.00000000 (7, 2) 0.56524513 (7, 3) 0.00000000
(7, 4)	-0.56524513	(7, 5) 0.00000000 (7, 6) 0.24224791 (7, 7) 0.00000000

(7, 8)-0.04037465
 (8, 0) 0.35327821 (8, 1) 0.00000000 (8, 2)-0.56524513 (8, 3) 0.00000000
 (8, 4) 0.28262256 (8, 5) 0.00000000 (8, 6)-0.08074930 (8, 7) 0.00000000
 (8, 8) 0.01009366

M S $\ell=9$

(0, 0) 0.00000000	(0, 1) 0.41481118	(0, 2) 0.00000000	(0, 3) 0.43456410
(0, 4) 0.00000000	(0, 5) 0.48422857	(0, 6) 0.00000000	(0, 7) 0.60528571
(0, 8) 0.00000000	(0, 9) 1.14331745		
(1, 0) 0.00000000	(1, 1) 0.04372494	(1, 2) 0.00000000	(1, 3) 0.13742123
(1, 4) 0.00000000	(1, 5) 0.25521086	(1, 6) 0.00000000	(1, 7) 0.44661901
(1, 8) 0.00000000	(1, 9) 1.08464617		
(2, 0) 0.00000000	(2, 1) 0.41017628	(2, 2) 0.00000000	(2, 3) 0.35157967
(2, 4) 0.00000000	(2, 5) 0.21764455	(2, 6) 0.00000000	(2, 7)-0.05441114
(2, 8) 0.00000000	(2, 9)-0.92498936		
(3, 0) 0.00000000	(3, 1) 0.13426170	(3, 2) 0.00000000	(3, 3) 0.37081804
(3, 4) 0.00000000	(3, 5) 0.49868632	(3, 6) 0.00000000	(3, 7) 0.37401474
(3, 8) 0.00000000	(3, 9)-0.70647229		
(4, 0) 0.00000000	(4, 1) 0.39525575	(4, 2) 0.00000000	(4, 3) 0.11293021
(4, 4) 0.00000000	(4, 5)-0.33879064	(4, 6) 0.00000000	(4, 7)-0.64934873
(4, 8) 0.00000000	(4, 9) 0.47995341		
(5, 0) 0.00000000	(5, 1) 0.23621049	(5, 2) 0.00000000	(5, 3) 0.47242098
(5, 4) 0.00000000	(5, 5) 0.12147968	(5, 6) 0.00000000	(5, 7)-0.69175929
(5, 8) 0.00000000	(5, 9) 0.28682702		
(6, 0) 0.00000000	(6, 1) 0.36593572	(6, 2) 0.00000000	(6, 3)-0.24395715
(6, 4) 0.00000000	(6, 5)-0.52276531	(6, 6) 0.00000000	(6, 7) 0.54890358
(6, 8) 0.00000000	(6, 9)-0.14811684		
(7, 0) 0.00000000	(7, 1) 0.36972790	(7, 2) 0.00000000	(7, 3) 0.31690963
(7, 4) 0.00000000	(7, 5)-0.61872832	(7, 6) 0.00000000	(7, 7) 0.33577330
(7, 8) 0.00000000	(7, 9)-0.06413647		
(8, 0) 0.00000000	(8, 1) 0.30798080	(8, 2) 0.00000000	(8, 3)-0.61596160
(8, 4) 0.00000000	(8, 5) 0.43997257	(8, 6) 0.00000000	(8, 7)-0.15399040
(8, 8) 0.00000000	(8, 9) 0.02199863		
(9, 0) 0.00000000	(9, 1) 0.65332594	(9, 2) 0.00000000	(9, 3)-0.43555062
(9, 4) 0.00000000	(9, 5) 0.18666455	(9, 6) 0.00000000	(9, 7)-0.04666614
(9, 8) 0.00000000	(9, 9) 0.00518513		

Table 15.2

Table 15.2.1

Symmetry coefficients $B_l^{m\mu}$

Symmetry coefficients $B_l^{m\mu}$ for cubic symmetry, [001] parallel to the Z-axis for $l = 4$ (1) 34, $\mu = l(1)$ M (1), $m = 0$ (4) l . The coefficients are defined by equation (14.209) (see also reference 74)

MU M	L= 4
(1, 0) 0.30469720	(1, 4) 0.36418281
MU M	L= 6
(1, 0)-0.14104740	(1, 4) 0.52775103
MU M	L= 8
(1, 0) 0.28646862	(1, 4) 0.21545346 (1, 8) 0.32826995
MU M	L= 9
(1, 0) 0.00000000	(1, 4)-0.47483629 (1, 8) 0.30469720
MU M	L=10
(1, 0)-0.16413497	(1, 4) 0.33078546 (1, 8) 0.39371345
MU M	L=12
(1, 0) 0.26141975	(1, 4) 0.27266871 (1, 8) 0.03277460 (1,12) 0.32589402
(2, 0) 0.09298802	(2, 4)-0.23773812 (2, 8) 0.49446631 (2,12) 0.00000000
MU M	L=13
(1, 0) 0.00000000	(1, 4)-0.44370187 (1, 8)-0.12875807 (1,12) 0.32382078
MU M	L=14
(1, 0)-0.17557309	(1, 4) 0.25821932 (1, 8) 0.27709173 (1,12) 0.33645360
MU M	L=15
(1, 0) 0.00000000	(1, 4) 0.16910989 (1, 8)-0.45704580 (1,12) 0.28429012
MU M	L=16
(1, 0) 0.24370673	(1, 4) 0.29873515 (1, 8) 0.06447688 (1,12) 0.00377000
(1,16) 0.32574495	
(2, 0) 0.12039646	(2, 4)-0.25330128 (2, 8) 0.23950998 (2,12) 0.40962508
(2,16) 0.00000000	
MU M	L=17
(1, 0) 0.00000000	(1, 4)-0.41566875 (1, 8)-0.19764468 (1,12)-0.02159338
(1,16) 0.32557592	

MU	M	L=18	MU	M	L=27
(1, 0)-0.16914245	(1, 4) 0.17017340	(1, 8) 0.34598142	(1,12) 0.07433932	(1, 0) 0.00000000	(1, 4) 0.26006122
(1,16) 0.32696037	(1,20) 0.00000000	(2, 4) 0.16006562	(2, 8)-0.24743528	(1,16)-0.08789922	(1, 8)-0.21389471
(2, 0)-0.06901768	(2, 4) 0.16006562	(2, 8)-0.24743528	(2,12) 0.47110273	(1,20)-0.00787673	(1,24) 0.32565174
(2,16) 0.00000000	(2,20) 0.00000000	(2,24) 0.00000000	(2, 0) 0.00000000	(2, 4) 0.04887363	(2, 8)-0.12030002
MU	M	L=19	MU	M	L=28
(1, 0) 0.00000000	(1, 4) 0.21950324	(1, 8)-0.36729917	(1,12)-0.18180666	(1, 0) 0.21225019	(1, 4) 0.32031716
(1,16) 0.31963396	(1,20) 0.00000000	(2, 4) 0.31151832	(2, 8) 0.09287682	(1,16) 0.00362703	(1,20) 0.00018294
MU	M	L=20	MU	M	L=29
(1, 0) 0.23067026	(1, 4) 0.31151832	(1, 8) 0.09287682	(1,12) 0.01089683	(2, 0) 0.13219496	(2, 4)-0.17206256
(1,16) 0.00037564	(1,20) 0.32573563	(2, 4)-0.25048007	(2, 8) 0.12882081	(2,16) 0.17973107	(2,20) 0.02567515
(2, 0) 0.13615420	(2, 4)-0.25048007	(2, 8) 0.12882081	(2,12) 0.28642879	(3, 0) 0.07989184	(3, 4)-0.16735346
(2,16) 0.34620433	(2,20) 0.00000000	(2,24) 0.00000000	(3,16) 0.12926808	(3,20) 0.42715602	(3,24) 0.00000000
MU	M	L=21	MU	M	L=30
(1, 0) 0.00000000	(1, 4)-0.38704231	(1, 8)-0.24503942	(1,12)-0.04858614	(1, 0) 0.00000000	(1, 4)-0.33678345
(1,16)-0.00282954	(1,20) 0.32572258	(2, 4)-0.08431638	(2, 8) 0.21737195	(1,16)-0.01811467	(1,20)-0.00131538
(2, 0) 0.00000000	(2, 4)-0.08431638	(2, 8) 0.21737195	(2,12)-0.44006168	(2, 0) 0.00000000	(2, 4)-0.15916432
(2,16) 0.26513353	(2,20) 0.00000000	(2,24) 0.00000000	(2,16)-0.28245490	(2,20)-0.06715810	(2,24) 0.32375554
MU	M	L=22	MU	M	L=31
(1, 0)-0.16109560	(1, 4) 0.10244188	(1, 8) 0.36285175	(1,12) 0.13377513	(1, 0)-0.14878368	(1, 4) 0.01524973
(1,16) 0.01314399	(1,20) 0.32585583	(2, 4) 0.20244115	(2, 8)-0.22389483	(1,16) 0.05790047	(1,20) 0.00609812
(2, 0)-0.09620055	(2, 4) 0.20244115	(2, 8)-0.22389483	(2,12) 0.17928946	(2, 0)-0.11721726	(2, 4) 0.20915005
(2,16) 0.42017231	(2,20) 0.00000000	(2,24) 0.00000000	(2,16) 0.31318947	(2,20) 0.13655742	(2,24) 0.33241385
MU	M	L=23	MU	M	L=32
(1, 0) 0.00000000	(1, 4) 0.24724582	(1, 8)-0.28925823	(1,12)-0.25687091	(1, 0) 0.00000000	(1, 4) 0.26400089
(1,16)-0.04378248	(1,20) 0.32497615	(2, 4) 0.31770654	(2, 8) 0.11661736	(1,16)-0.13483032	(1,20)-0.02099736
MU	M	L=24	MU	M	L=33
(1, 0) 0.22050742	(1, 4) 0.31770654	(1, 8) 0.11661736	(1,12) 0.02049853	(1, 0) 0.20533892	(1, 4) 0.32087437
(1,16) 0.00150861	(1,20) 0.00003426	(1,24) 0.32573505	(1,24) 0.000522051	(1,16) 0.00670516	(1,20) 0.00054977
(2, 0) 0.13651722	(2, 4)-0.21386648	(2, 8) 0.00522051	(2,12) 0.33939435	(1,32) 0.32573501	(1,24) 0.00002018
(2,16) 0.10837396	(2,20) 0.32914497	(2,24) 0.00000000	(2, 0) 0.12775091	(2, 4)-0.13523423	(2, 8)-0.14935701
(3, 0) 0.05378596	(3, 4)-0.11945819	(3, 8) 0.16272298	(3,12)-0.26449730	(2,16) 0.23670434	(2,20) 0.05661270
(3,16) 0.44923956	(3,20) 0.00000000	(3,24) 0.00000000	(2,32) 0.00000000	(2, 0) 0.09703829	(3, 4)-0.19373733
MU	M	L=25	MU	M	L=34
(1, 0) 0.00000000	(1, 4)-0.36047640	(1, 8)-0.27572179	(1,12)-0.07851106	(1, 8) 0.15187897	(1,12) 0.04249238
(1,16)-0.00879594	(1,20)-0.00031974	(1,24) 0.32573408	(1,24) 0.00000000	(1,16) 0.00670516	(1,20) 0.00054977
(2, 0) 0.00000000	(2, 4)-0.12765450	(2, 8) 0.25841719	(2,12)-0.29816697	(1,32) 0.32573501	(1,24) 0.00002018
(2,16)-0.21893166	(2,20) 0.31368799	(2,24) 0.00000000	(2, 0) 0.12775091	(2, 4)-0.13523423	(2, 8)-0.14935701
MU	M	L=26	MU	M	L=35
(1, 0)-0.15435003	(1, 4) 0.05261630	(1, 8) 0.35524646	(1,12) 0.18578869	(1, 0) 0.00000000	(1, 4)-0.31590161
(1,16) 0.03259103	(1,20) 0.00186197	(1,24) 0.32574594	(1,24) 0.05439948	(1,16)-0.02996836	(1,20)-0.00337720
(2, 0)-0.11306511	(2, 4) 0.22072681	(2, 8)-0.18706142	(2,12) 0.00000000	(1,32) 0.32573500	(1,24) 0.00017242
(2,16) 0.28122966	(2,20) 0.35634355	(2,24) 0.00000000	(2, 0) 0.00000000	(2, 4)-0.18043837	(2, 8) 0.25132442

M	M	L=34
(1, 0)-0.14409234	(1, 4)-0.01343681	(1, 8) 0.31248977
(1,16) 0.08571889	(1,20) 0.01351208	(1,24) 0.00095792
(1,32) 0.32573508		(1,28) 0.00002550
(2, 0)-0.11527834	(2, 4) 0.18472133	(2, 8)-0.04403280
(2,16) 0.27227021	(2,20) 0.21086614	(2,24) 0.04041752
(2,32) 0.00000000		(2,28) 0.32688152
(3, 0)-0.06773139	(3, 4) 0.14120811	(3, 8)-0.15835721
(3,16)-0.19364673	(3,20) 0.08377174	(3,24) 0.43116318
(3,32) 0.00000000		(3,28) 0.00000000

Table 15.2.2 Symmetry coefficients $B_l^{m\mu}$ for cubic symmetry, [111] parallel to the Z-axis for $l = 4(1)34$, $\mu = l(1)M(l)$, $m = 0(3)l$. The coefficients are defined by equation (14.209)

MU	M	L= 4
(1, 0)-0.20313147	(1, 3) 0.48557708	
MU	M	L= 6
(1, 0) 0.25075093	(1, 3) 0.30281051	(1, 6) 0.31759034
MU	M	L= 8
(1, 0) 0.08487959	(1, 3)-0.34965546	(1, 6) 0.42619462
MU	M	L= 9
(1, 0) 0.00000000	(1, 3)-0.43931136	(1, 6)-0.22794747
MU	M	L=10
(1, 0)-0.25937379	(1, 3) 0.06534034	(1, 6) 0.25411428
MU	M	L=12
(1, 0) 0.16568843	(1, 3) 0.28513523	(1, 6) 0.30034179
(1,12) 0.28533825		(1, 9) 0.10236877
(2, 0)-0.00161153	(2, 3) 0.23036435	(2, 6)-0.34672080
(2,12) 0.00000000		(2, 9) 0.38081708
MU	M	L=13
(1, 0) 0.00000000	(1, 3) 0.32321810	(1, 6)-0.26139229
(1,12) 0.25585839		(1, 9)-0.28293197
MU	M	L=14
(1, 0) 0.18496588	(1, 3)-0.28023908	(1, 6)-0.06987197
(1,12) 0.35445318		(1, 9) 0.20206940
MU	M	L=15
(1, 0) 0.00000000	(1, 3)-0.31703256	(1, 6)-0.31911148
(1,12)-0.04367694	(1,15) 0.28112679	(1, 9)-0.18715811
MU	M	L=16
(1, 0)-0.23899398	(1, 3)-0.12445599	(1, 6) 0.05749891
(1,12) 0.14778990	(1,15) 0.29128665	(1, 9) 0.28033631

(2, 0)-0.03930324 (2, 3)-0.10668277 (2, 6) 0.26207154 (2, 9)-0.34681261
 (2,12) 0.33893761 (2,15) 0.00000000
 MU M L=17
 (1, 0) 0.00000000 (1, 3)-0.18961894 (1, 6) 0.33432651 (1, 9)-0.12993605
 (1,12)-0.31089734 (1,15) 0.23883006

MU M L=18
 (1, 0) 0.10643633 (1, 3) 0.20632992 (1, 6) 0.32116853 (1, 9) 0.24481833
 (1,12) 0.09982070 (1,15) 0.01708930 (1,18) 0.28238096
 (2, 0)-0.07523620 (2, 3) 0.34083654 (2, 6)-0.13378468 (2, 9)-0.13237092
 (2,12) 0.14851500 (2,15) 0.36516059 (2,18) 0.00000000

MU M L=19
 (1, 0) 0.00000000 (1, 3) 0.34853069 (1, 6) 0.01520079 (1, 9)-0.23818997
 (1,12)-0.23675600 (1,15)-0.07825879 (1,18) 0.27873441

MU M L=20
 (1, 0) 0.23361028 (1, 3)-0.10867608 (1, 6)-0.14641450 (1, 9)-0.06404273
 (1,12) 0.22687358 (1,15) 0.17550654 (1,18) 0.29923072
 (2, 0) 0.04450170 (2, 3) 0.01127287 (2, 6)-0.16273476 (2, 9) 0.28409229
 (2,12) -0.34265639 (2,15) 0.29936195 (2,18) 0.00000000

MU M L=21
 (1, 0) 0.00000000 (1, 3)-0.22178330 (1, 6)-0.28991056 (1, 9)-0.27940781
 (1,12)-0.15834496 (1,15)-0.04859136 (1,18)-0.00642917 (1,21) 0.28200994
 (2, 0) 0.00000000 (2, 3) 0.08331514 (2, 6)-0.27301474 (2, 9) 0.28577676
 (2,12) -0.03037483 (2,15) -0.32486178 (2,18) 0.22069269 (2,21) 0.00000000

MU M L=22
 (1, 0)-0.18711795 (1, 3)-0.17962513 (1, 6)-0.14004928 (1, 9) 0.15404494
 (1,12) 0.26143521 (1,15) 0.151113570 (1,18) 0.03539543 (1,21) 0.28325182
 (2, 0)-0.02351127 (2, 3)-0.27089137 (2, 6) 0.26386751 (2, 9)-0.03427166
 (2,12) -0.16267047 (2,15) 0.09372954 (2,18) 0.37118011 (2,21) 0.00000000

MU M L=23
 (1, 0) 0.00000000 (1, 3)-0.28181120 (1, 6) 0.21147791 (1, 9) 0.15517782
 (1,12) -0.13697694 (1,15) -0.25159832 (1,18)-0.11208741 (1,21) 0.27470219

MU M L=24
 (1, 0) 0.06969092 (1, 3) 0.14347345 (1, 6) 0.26959056 (1, 9) 0.28978448
 (1,12) 0.20736325 (1,15) 0.09097447 (1,18) 0.02201142 (1,21) 0.00233730
 (1,24) 0.28211993 (2, 3) 0.28668209 (2, 6) 0.05225268 (2, 9)-0.09356429
 (2,12) -0.15817985 (2,15) 0.16630335 (2,18) 0.18968148 (2,21) 0.30844740
 (2,24) 0.00000000 (3, 0)-0.02949549 (3, 3) 0.03968586 (3, 6) 0.07147654 (3, 9)-0.20125500
 (3,12) 0.29906256 (3,15)-0.33330175 (3,18) 0.26240047 (3,21) 0.00000000
 (3,24) 0.00000000

MU M L=25
 (1, 0) 0.00000000 (1, 3) 0.31262288 (1, 6) 0.16173771 (1, 9)-0.05522601
 (1,12) -0.24330783 (1,15) 0.21257343 (1,18)-0.08597819 (1,21)-0.01530073

(1,24) 0.28170072 (2, 0) 0.00000000 (2, 3)-0.01605486 (2, 6) 0.17240728 (2, 9)-0.29486498
 (2,12) 0.22300639 (2,15) 0.04761538 (2,18)-0.32943140 (2,21) 0.20213458
 (2,24) 0.00000000

MU M L=26
 (1, 0) 0.22539264 (1, 3) 0.03176320 (1, 6)-0.03339589 (1, 9)-0.21060225
 (1,12) 0.01088433 (1,15) 0.22749618 (1,18) 0.18434185 (1,21) 0.05634643
 (1,24) 0.28495418 (2, 0) 0.08011906 (2, 3) 0.13021183 (2, 6)-0.28755380 (2, 9) 0.18531696
 (2,12) 0.03849990 (2,15)-0.17281904 (2,18) 0.03868635 (2,21) 0.37238932
 (2,24) 0.00000000

MU M L=27
 (1, 0) 0.00000000 (1, 3)-0.15322602 (1, 6)-0.23096896 (1, 9)-0.28698696
 (1,12)-0.24201899 (1,15)-0.13631652 (1,18)-0.04800635 (1,21)-0.00946264
 (1,24)-0.00082943 (1,27) 0.28208734 (2, 0) 0.00000000 (2, 3) 0.17558002 (2, 6)-0.30166978 (2, 9) 0.05231725
 (2,12) 0.19424684 (2,15)-0.04608901 (2,18)-0.24636042 (2,21)-0.14439805
 (2,24) 0.26896004 (2,27) 0.00000000

MU M L=28
 (1, 0)-0.14017844 (1, 3)-0.17377334 (1, 6)-0.22721267 (1, 9)-0.02382481
 (1,12) 0.18877852 (1,15) 0.24220401 (1,18) 0.14379234 (1,21) 0.04418551
 (1,24) 0.00625240 (1,27) 0.28222634 (2, 0) 0.04793726 (2, 3) 0.34042159 (2, 6) 0.11275785 (2, 9) 0.10449185
 (2,12)-0.03307996 (2,15) 0.15328924 (2,18) 0.10618837 (2,21) 0.19251062
 (2,24) 0.31822319 (2,27) 0.00000000 (3, 0) 0.00982807 (3, 3) 0.05030523 (3, 6)-0.00657254 (3, 9) 0.11666441
 (3,12)-0.23001351 (3,15) 0.30784353 (3,18)-0.31945606 (3,21) 0.22848694
 (3,24) 0.00000000 (3,27) 0.00000000

MU M L=29
 (1, 0) 0.00000000 (1, 3)-0.31572313 (1, 6) 0.05025337 (1, 9) 0.18560773
 (1,12) 0.09675717 (1,15) 0.15878411 (1,18)-0.23008659 (1,21)-0.12009795
 (1,24)-0.02746392 (1,27) 0.28100034 (2, 0) 0.00000000 (2, 3) 0.01569794 (2, 6)-0.07993477 (2, 9) 0.22985366
 (2,12)-0.28491129 (2,15) 0.15807308 (2,18) 0.10939229 (2,21)-0.32706230
 (2,24) 0.18369330 (2,27) 0.00000000

MU M L=30
 (1, 0) ..0.04631830 (1, 3) 0.09888524 (1, 6) 0.20778568 (1, 9) 0.27179037
 (1,12) 0.26223401 (1,15) 0.17781509 (1,18) 0.08157581 (1,21) 0.02371501
 (1,24) 0.00390344 (1,27) 0.00028865 (1,30) 0.28209700 (2, 0)-0.20145631 (2, 3) 0.15540189 (2, 6) 0.08631011 (2, 9)-0.09549185
 (2,12) -0.17235922 (2,15) -0.08285892 (2,18) 0.17355679 (2,21) 0.20208922
 (2,24) 0.07836748 (2,27) 0.28765595 (2,30) 0.00000000 (3, 0)-0.08665229 (3, 3) 0.01081374 (3, 6) 0.21897451 (3, 9)-0.26399804
 (3,12) 0.11202157 (3,15) 0.09252568 (3,18) -0.16791419 (3,21)-0.01517491
 (3,24) 0.36877585 (3,27) 0.00000000 (3,30) 0.00000000

MU M L=31
 (1, 0) 0.00000000 (1, 3) 0.25750317 (1, 6) 0.21429253 (1, 9) 0.09832050
 (1,12)-0.11980483 (1,15)-0.23889823 (1,18)-0.19356991 (1,21)-0.08665331
 (1,24)-0.02123806 (1,27)-0.00246723 (1,30) 0.28205139 (2, 0) 0.00000000 (2, 3)-0.07325887 (2, 6) 0.27736020 (2, 9)-0.21727134

(2,12)-0.06146535 (2,15) 0.18303788 (2,18) 0.02912427 (2,21)-0.22772233
 (2,24)-0.17440184 (2,27) 0.26154344 (2,30) 0.00000000

MU M L=32

(1, 0) 0.19464375 (1, 3) 0.10483820 (1, 6) 0.09322154 (1, 9)-0.16505372
 (1,12)-0.15950384 (1,15) 0.06022017 (1,18) 0.22281791 (1,21) 0.17954986
 (1,24) 0.06856710 (1,27) 0.01236127 (1,30) 0.28249833
 (2, 0) 0.05244054 (2, 3) 0.26544562 (2, 6)-0.24669487 (2, 9)-0.00168106
 (2,12) 0.10650339 (2,15) 0.02062624 (2,18)-0.15914019 (2,21) 0.04959041
 (2,24) 0.18557927 (2,27) 0.32786342 (2,30) 0.00000000
 (3, 0) 0.00455165 (3, 3) 0.03633675 (3, 6)-0.02637537 (3, 9)-0.04711071
 (3,12) 0.15273322 (3,15)-0.25176543 (3,18) 0.31113759 (3,21)-0.30225684
 (3,24) 0.19787355 (3,27) 0.00000000 (3,30) 0.00000000

MU M L=33

(1, 0) 0.00000000 (1, 3)-0.10545031 (1, 6)-0.17394605 (1, 9)-0.25277749
 (1,12)-0.26942878 (1,15)-0.21137872 (1,18)-0.11834337 (1,21)-0.04533521
 (1,24)-0.01111871 (1,27)-0.00155811 (1,30)-0.00009890 (1,33) 0.24209414
 (2, 0) 0.00000000 (2, 3) 0.24953368 (2, 6)-0.22242720 (2, 9)-0.11308771
 (2,12) 0.09795717 (2,15) 0.16415351 (2,18)-0.07013891 (2,21)-0.22336715
 (2,24)-0.14951692 (2,27)-0.04264183 (2,30) 0.27973589 (2,33) 0.00000000
 (3, 0) 0.00000000 (3, 3) 0.02272292 (3, 6) 0.01627993 (3, 9)-0.14210989
 (3,12) 0.25970623 (3,15)-0.25749720 (3,18) 0.09532202 (3,21) 0.15802287
 (3,24)-0.31943690 (3,27) 0.16578214 (3,30) 0.00000000 (3,33) 0.00000000

MU M L=34

(1, 0)-0.10343216 (1, 3)-0.14818922 (1, 6)-0.24219804 (1, 9)-0.14445174
 (1,12) 0.04583066 (1,15) 0.20794781 (1,18) 0.22387209 (1,21) 0.13414498
 (1,24) 0.04786493 (1,27) 0.00966889 (1,30) 0.00094442 (1,33) 0.28210896
 (2, 0) 0.12131229 (2, 3)-0.29315416 (2, 6)-0.01408581 (2, 9) 0.02471749
 (2,12) 0.15242781 (2,15)-0.10256102 (2,18)-0.13469868 (2,21) 0.11331942
 (2,24) 0.20614277 (2,27) 0.09981502 (2,30) 0.29143061 (2,33) 0.00000000
 (3, 0) 0.05689657 (3, 3)-0.10028641 (3, 6)-0.10369633 (3, 9) 0.25534901
 (3,12)-0.22215002 (3,15) 0.04548671 (3,18) 0.13111462 (3,21)-0.15108023
 (3,24)-0.06624676 (3,27) 0.36055159 (3,30) 0.00000000 (3,33) 0.00000000

Table 15.2.3 Symmetry coefficients $B_l^{m\mu}$ for tetragonal functions which are orthogonal to the cubic functions according to *Table 15.2.1* for $l = (4)(1) 34$, $\mu = 1(1) M'(1)$, $m = 0(4) l$

MU M L= 4

(1, 0)-0.25751613 (1, 4) 0.43090691

MU M L= 5

(1, 0) 0.00000000 (1, 4) 0.56418958

(2, 0) 0.39894228 (2, 4) 0.00000000

MU M L= 6

(1, 0) 0.37317633 (1, 4) 0.19947114

MU M L= 7

(1, 0) 0.00000000 (1, 4) 0.56418958

(2, 0) 0.39894228 (2, 4) 0.00000000

MU M L= 8

(1, 0)-0.20494242 (1, 4)-0.15413749 (1, 8) 0.45885589

(2, 0)-0.18732132 (2, 4) 0.49812782 (2, 8) 0.00000000

MU M L= 9

(1, 0) 0.00000000 (1, 4) 0.30469720 (1, 8) 0.47483629

(2, 0) 0.39894228 (2, 4) 0.00000000 (2, 8) 0.00000000

MU M L=10

(1, 0) 0.15991486 (1, 4)-0.32228056 (1, 8) 0.40410346

(2, 0) 0.32656070 (2, 4) 0.32407731 (2, 8) 0.00000000

MU M L=11

(1, 0) 0.00000000 (1, 4) 0.00000000 (1, 8) 0.56418958

(2, 0) 0.00000000 (2, 4) 0.56418958 (2, 8) 0.00000000

(3, 0) 0.39894228 (3, 4) 0.00000000 (3, 8) 0.00000000

MU M L=12

(1, 0)-0.18498709 (1, 4)-0.19294713 (1, 8)-0.02319212 (1,12) 0.46054639

(2, 0)-0.21896955 (2, 4) 0.38757406 (2, 8) 0.26870227 (2,12) 0.00000000

MU	M	L=13	MU	M	L=20
(1, 0) 0.00000000	(1, 4) 0.31099106	(1, 8) 0.09024665	(1,12) 0.46200648	(1, 0)-0.16310897	(1, 4)-0.22027734
(2, 0) 0.00000000	(2, 4)-0.15723580	(2, 8) 0.54183650	(2,12) 0.00000000	(1,16)-0.00026562	(1,20) 0.46065843
(3, 0) 0.39894228	(3, 4) 0.00000000	(3, 8) 0.00000000	(3,12) 0.00000000	(2, 0)-0.10610391	(2, 4) 0.19426640
MU	M	L=14	(2,16) 0.44547979	(2,20) 0.00000000	(2, 8)-0.10023048
(1, 0) 0.13043403	(1, 4)-0.19183229	(1, 8)-0.20585268	(3, 0)-0.15371477	(3, 4) 0.25445658	(2,12)-0.22261173
(2, 0) 0.16918112	(2, 4)-0.24881851	(2, 8) 0.44626756	(3,16) 0.00000000	(3, 8)-0.14060917	(3,12) 0.41189621
(3, 0) 0.28756521	(3, 4) 0.39105293	(3, 8) 0.00000000	(4, 0)-0.16098882	(4, 4) 0.08669640	(4,12) 0.00000000
MU	M	L=15	(4,16) 0.00000000	(4,20) 0.00000000	(4, 8) 0.50887997
(1, 0) 0.00000000	(1, 4)-0.09865270	(1, 8) 0.26662429	(1,12) 0.48732845	MU	M
(2, 0) 0.00000000	(2, 4) 0.52913077	(2, 8) 0.19578179	(2,16) 0.00000000	L=21	
(3, 0) 0.39894228	(3, 4) 0.00000000	(3, 8) 0.00000000	(3,12) 0.00000000	(1, 0) 0.00000000	(1, 4) 0.27366458
MU	M	L=16	(2, 0)-0.00200068	(1,20) 0.46066765	(1, 8) 0.17325912
(1, 0)-0.17233457	(1, 4)-0.21124732	(1, 8)-0.04559413	(2, 4) 0.04159139	(1,12) 0.03435363	
(1,16) 0.46065184		(1,12)-0.00266591	(2,16) 0.49799808	(2, 8)-0.11781688	
(2, 0)-0.13067969	(2, 4) 0.26310691	(2, 8)-0.25383936	(2,20) 0.00000000	(2,12) 0.23387419	
(2,16) 0.00000000		(2,12) 0.38793796	(3, 0) 0.00000000	(3, 4)-0.29116446	
(3, 0)-0.19618940	(3, 4) 0.22595349	(3, 8) 0.43620448	(3,16) 0.00000000	(3, 8) 0.40879758	
(3,16) 0.00000000		(3,12) 0.00000000	(4, 0) 0.39894228	(4, 4) 0.00000000	
MU	M	L=17	(4,16) 0.00000000	(4,20) 0.00000000	(4, 8) 0.00000000
(1, 0) 0.00000000	(1, 4) 0.29370695	(1, 8) 0.13965355	(1,12) 0.01525765	MU	M
(1,16) 0.46077132		(1,16)-0.00929938	L=22		
(2, 0) 0.00000000	(2, 4)-0.02387810	(2, 8)-0.01135370	(1,20) 0.46057341	(1, 0) 0.11397518	(1, 4)-0.07247766
(2,16) 0.00000000		(2,12) 0.56356971	(2, 0) 0.11589929	(1,16)-0.25671772	(1,12)-0.09464595
(3, 0) 0.00000000	(3, 4)-0.24227142	(3, 8) 0.50952374	(2,16) 0.37617266	(2, 8) 0.23105819	(2,12)-0.20727437
(3,16) 0.00000000		(3,12) 0.00000000	(3, 0) 0.15825268	(3, 4)-0.22540135	
(4, 0) 0.39894228	(4, 4) 0.00000000	(4, 8) 0.00000000	(3,16) 0.00000000	(3, 8) 0.03267148	
(4,16) 0.00000000		(4,12) 0.00000000	(4,20) 0.00000000	(3,12) 0.46513317	
MU	M	L=18	(4, 0) 0.26922427	(4, 4) 0.39646712	(4, 8) 0.12712313
(1, 0) 0.12027857	(1, 4)-0.12101169	(1, 8)-0.24603020	(4,16) 0.00000000	(4, 2) 0.00000000	(4,12) 0.00000000
(1,16) 0.45978995		(1,12)-0.05286330	(1,12) 0.00000000	(1, 0) 0.17421932	(1, 8) 0.20382294
(2, 0) 0.17337624	(2, 4)-0.31831510	(2, 8) 0.26232709	(1,16)-0.03085089	(1,12) 0.18100154	
(2,16) 0.00000000		(2,12) 0.29673429	(1,20) 0.46119452		
(3, 0) 0.28505452	(3, 4) 0.38439766	(3, 8) 0.08964464	(2, 0) 0.00000000	(2, 4) 0.02884376	
(3,16) 0.00000000		(3,12) 0.00000000	(2,16) 0.56164153	(2, 8)-0.03374494	
MU	M	L=19	(3, 0) 0.00000000	(2,20) 0.00000000	
(1, 0) 0.00000000	(1, 4)-0.15091147	(1, 8) 0.25252318	(3, 4) 0.20509976	(3, 12) 0.46761915	
(1,16) 0.46491291		(1,12) 0.12499456	(3,16) 0.00000000	(3, 8)-0.23995064	
(2, 0) 0.00000000	(2, 4) 0.11318046	(2, 8)-0.18938713	(3,20) 0.00000000	(3,12) 0.00000000	
(2,16) 0.00000000		(2,12) 0.51926158	(4, 0) 0.00000000	(4, 4) 0.42886961	
(3, 0) 0.00000000	(3, 4) 0.48429756	(3, 8) 0.28942315	(4,16) 0.00000000	(4, 8) 0.36657979	
(3,16) 0.00000000		(3,12) 0.00000000	(4,20) 0.00000000	(4,12) 0.00000000	
(4, 0) 0.39894228	(4, 4) 0.00000000	(4, 8) 0.00000000	(5, 0) 0.39894228	(5, 4) 0.00000000	
(4,16) 0.00000000		(4,12) 0.00000000	(5,16) 0.00000000	(5, 8) 0.00000000	
MU	M	L=20	(5,20) 0.00000000	(5, 0) 0.00000000	(5,12) 0.00000000
(1, 0) 0.00000000	(1, 4)-0.15592232	(1, 8)-0.22465249	(1, 0)-0.08246094	(1,12) 0.01449466	
(1,16) 0.00106675		(1,12)-0.00024222	(1,24) 0.46065884		
(2, 0) 0.09808486		(2, 4) 0.15358436	(2, 8)-0.00376296	(2,12) 0.24378878	
(2,16) 0.07784503		(2,12) 0.45822862	(2,24) 0.00000000		
(3, 0) 0.14990679		(3, 4) 0.28038146	(3, 8)-0.23627552	(3,12) 0.20060005	
(3,16) 0.31414253		(3,12) 0.00000000	(3,24) 0.00000000		
(4, 0) 0.18054662		(4, 4) 0.06850291	(4, 8) 0.46428888	(4,12) 0.18127025	
(4,16) 0.00000000		(4,12) 0.00000000	(4,20) 0.00000000	(4,24) 0.00000000	
MU	M	L=21	(4, 0) 0.00000000	(4, 4) 0.25489421	(4, 8) 0.19496391
(1, 16) 0.00621964		(4,12) 0.00000000	(4,20) 0.00022609	(4,24) 0.46065952	(4,12) 0.05551547

(2, 0) 0.00000000 (2, 4) 0.08502230 (2, 8) -0.17314307 (2,12) 0.19937031
 (2,16) 0.14643932 (2,20) 0.46894517 (2,24) 0.00000000
 (3, 0) 0.00000000 (3, 4) -0.09052279 (3, 8) 0.15695703 (3,12) -0.19147248
 (3,16) 0.49881689 (3,20) 0.00000000 (3,24) 0.00000000
 (4, 0) 0.00000000 (4, 4) -0.30278170 (4, 8) 0.28789403 (4,12) 0.37914398
 (4,16) 0.00000000 (4,20) 0.00000000 (4,24) 0.00000000
 (5, 0) 0.39894228 (5, 4) 0.00000000 (5, 8) 0.00000000 (5,12) 0.00000000
 (5,16) 0.00000000 (5,20) 0.00000000 (5,24) 0.00000000

MU M L=26

(1, 0) 0.10914745 (1, 4) -0.03720722 (1, 8) -0.25120983 (1,12) -0.13137906
 (1,16) -0.02304650 (1,20) -0.00131668 (1,24) 0.46065114
 (2, 0) 0.09309688 (2, 4) -0.18015653 (2, 8) 0.15012578 (2,12) -0.04550423
 (2,16) -0.22931880 (2,20) 0.43740594 (2,24) 0.00000000
 (3, 0) 0.14109108 (3, 4) -0.24632701 (3, 8) 0.16195417 (3,12) -0.08093833
 (3,16) 0.43016199 (3,20) 0.00000000 (3,24) 0.00000000
 (4, 0) 0.12838068 (4, 4) -0.10854320 (4, 8) -0.13643322 (4,12) 0.50492677
 (4,16) 0.00000000 (4,20) 0.00000000 (4,24) 0.00000000
 (5, 0) 0.25608359 (5, 4) 0.40065161 (5, 8) 0.16318872 (5,12) 0.00000000
 (5,16) 0.00000000 (5,20) 0.00000000 (5,24) 0.00000000

MU M L=27

(1, 0) 0.00000000 (1, 4) -0.18382056 (1, 8) 0.15118842 (1,12) 0.21333061
 (1,16) 0.06213030 (1,20) 0.00556755 (1,24) 0.46071773
 (2, 0) 0.00000000 (2, 4) -0.01774407 (2, 8) 0.05360330 (2,12) -0.12618851
 (2,16) 0.20489655 (2,20) 0.50716425 (2,24) 0.00000000
 (3, 0) 0.00000000 (3, 4) 0.20228306 (3, 8) -0.31125637 (3,12) 0.31039872
 (3,16) 0.29010955 (3,20) 0.00000000 (3,24) 0.00000000
 (4, 0) 0.00000000 (4, 4) 0.41625248 (4, 8) 0.36806937 (4,12) 0.09781969
 (4,16) 0.00000000 (4,20) 0.00000000 (4,24) 0.00000000
 (5, 0) 0.39894228 (5, 4) 0.00000000 (5, 8) 0.00000000 (5,12) 0.00000000
 (5,16) 0.00000000 (5,20) 0.00000000 (5,24) 0.00000000

MU M L=28

(1, 0) -0.15008355 (1, 4) -0.22649844 (1, 8) -0.09619977 (1,12) -0.02214989
 (1,16) -0.00256470 (1,20) -0.00012936 (1,24) -0.00000208 (1,28) 0.46065886
 (2, 0) -0.09367662 (2, 4) 0.12192208 (2, 8) 0.06194964 (2,12) -0.23151475
 (2,16) -0.12735916 (2,20) -0.01819365 (2,24) 0.46033257 (2,28) 0.00000000
 (3, 0) -0.10697123 (3, 4) 0.21249417 (3, 8) -0.21006162 (3,12) 0.20650559
 (3,16) -0.16924136 (3,20) 0.36722292 (3,24) 0.00000000 (3,28) 0.00000000
 (4, 0) -0.13779417 (4, 4) 0.21596250 (4, 8) -0.07819345 (4,12) -0.05628265
 (4,16) 0.47372320 (4,20) 0.00000000 (4,24) 0.00000000 (4,28) 0.00000000
 (5, 0) -0.16886718 (5, 4) 0.01157541 (5, 8) 0.43969515 (5,12) 0.26040703
 (5,16) 0.00000000 (5,20) 0.00000000 (5,24) 0.00000000 (5,28) 0.00000000

MU M L=29

(1, 0) 0.00000000 (1, 4) 0.23814179 (1, 8) 0.20844472 (1,12) 0.07601054
 (1,16) 0.01280900 (1,20) 0.00093012 (1,24) 0.00002315 (1,28) 0.46065891
 (2, 0) 0.00000000 (2, 4) 0.11148911 (2, 8) -0.18633103 (2,12) 0.12761372
 (2,16) 0.19791151 (2,20) 0.04705690 (2,24) 0.46205220 (2,28) 0.00000000
 (3, 0) 0.00000000 (3, 4) -0.02973867 (3, 8) 0.04665482 (3,12) -0.03305203
 (3,16) -0.05073125 (3,20) 0.55819596 (3,24) 0.00000000 (3,28) 0.00000000
 (4, 0) 0.00000000 (4, 4) -0.17533300 (4, 8) 0.24000203 (4,12) -0.18350197
 (4,16) 0.44305110 (4,20) 0.00000000 (4,24) 0.00000000 (4,28) 0.00000000
 (5, 0) 0.00000000 (5, 4) -0.28068867 (5, 8) 0.15090744 (5,12) 0.46556493
 (5,16) 0.00000000 (5,20) 0.00000000 (5,24) 0.00000000 (5,28) 0.00000000
 (6, 0) 0.39894228 (6, 4) 0.00000000 (6, 8) 0.00000000 (6,12) 0.00000000
 (6,16) 0.00000000 (6,20) 0.00000000 (6,24) 0.00000000 (6,28) 0.00000000

MU M L=30

(1, 0) 0.10520640 (1, 4) -0.01078324 (1, 8) -0.23778996 (1,12) -0.16003724
 (1,16) -0.04094199 (1,20) -0.00431204 (1,24) -0.00016191 (1,28) 0.46065821
 (2, 0) 0.08558660 (2, 4) -0.15252313 (2, 8) 0.08523360 (2,12) 0.05681864
 (2,16) -0.22842052 (2,20) -0.09958189 (2,24) 0.45586275 (2,28) 0.00000000
 (3, 0) 0.13515365 (3, 4) -0.25562812 (3, 8) 0.21979754 (3,12) -0.18289094
 (3,16) 0.16575836 (3,20) 0.32740684 (3,24) 0.00000000 (3,28) 0.00000000
 (4, 0) 0.14624538 (4, 4) -0.13939631 (4, 8) 0.18040592 (4,12) 0.40906765
 (4,16) 0.23710861 (4,20) 0.00000000 (4,24) 0.00000000 (4,28) 0.00000000
 (5, 0) 0.25176135 (5, 4) 0.39685597 (5, 8) 0.18114883 (5,12) 0.03511085
 (5,16) 0.00000000 (5,20) 0.00000000 (5,24) 0.00000000 (5,28) 0.00000000

MU M L=31

(1, 0) 0.00000000 (1, 4) 0.18666964 (1, 8) 0.10347201 (1,12) 0.22635330
 (1,16) 0.09533576 (1,20) 0.01484681 (1,24) 0.00082972 (1,28) 0.46066478
 (2, 0) 0.00000000 (2, 4) -0.05188038 (2, 8) 0.11157430 (2,12) -0.17102937
 (2,16) 0.15433135 (2,20) 0.16012575 (2,24) 0.47377212 (2,28) 0.00000000
 (3, 0) 0.00000000 (3, 4) 0.07678940 (3, 8) 0.13625618 (3,12) 0.17154356
 (3,16) -0.18383891 (3,20) 0.48023285 (3,24) 0.00000000 (3,28) 0.00000000
 (4, 0) 0.00000000 (4, 4) 0.22660617 (4, 8) -0.27019821 (4,12) 0.13365249
 (4,16) 0.41963016 (4,20) 0.00000000 (4,24) 0.00000000 (4,28) 0.00000000
 (5, 0) 0.00000000 (5, 4) 0.38359621 (5, 8) 0.39000249 (5,12) 0.13806480
 (5,16) 0.00000000 (5,20) 0.00000000 (5,24) 0.00000000 (5,28) 0.00000000
 (6, 0) 0.39894228 (6, 4) 0.00000000 (6, 8) 0.00000000 (6,12) 0.00000000
 (6,16) 0.00000000 (6,20) 0.00000000 (6,24) 0.00000000 (6,28) 0.00000000

MU M L=32

(1, 0) -0.14519654 (1, 4) -0.22689244 (1, 8) -0.10739465 (1,12) -0.03004665
 (1,16) -0.00474126 (1,20) -0.00038875 (1,24) -0.00001427 (1,28) -0.00000017
 (1,32) 0.46065887 (1,36) 0.09035648 (2, 4) 0.09564891 (2, 8) 0.10563788 (2,12) -0.19964809
 (2,16) -0.16741747 (2,20) -0.04004133 (2,24) -0.00332296 (2,28) 0.46062013
 (2,32) 0.00000000 (3, 0) -0.08496879 (3, 4) 0.16762049 (3, 8) -0.15646319 (3,12) 0.11837337
 (3,16) -0.00577218 (3,20) -0.23058927 (3,24) 0.42904097 (3,28) 0.00000000
 (3,32) 0.00000000 (4, 0) -0.13080426 (4, 4) 0.23521479 (4, 8) -0.16969725 (4,12) 0.09695489
 (4,16) -0.05081927 (4,20) 0.43357164 (4,24) 0.00000000 (4,28) 0.00000000
 (4,32) 0.00000000 (5, 0) -0.11384510 (5, 4) 0.12083013 (5, 8) 0.08639465 (5,12) -0.19687661
 (5,16) 0.48121109 (5,20) 0.00000000 (5,24) 0.00000000 (5,28) 0.00000000
 (5,32) 0.00000000 (6, 0) -0.15721850 (6, 4) -0.02959109 (6, 8) 0.39352827 (6,12) 0.33635463
 (6,16) 0.00000000 (6,20) 0.00000000 (6,24) 0.00000000 (6,28) 0.00000000
 (6,32) 0.00000000

MU M L=33

(1, 0) 0.00000000 (1, 4) 0.22337617 (1, 8) 0.21635522 (1,12) 0.09456231
 (1,16) 0.02119083 (1,20) 0.00238804 (1,24) 0.00012192 (1,28) 0.00000221
 (1,32) 0.46065887 (1,36) 0.00000000 (2, 4) 0.12742195 (2, 8) -0.17748785 (2,12) 0.05394180
 (2,16) 0.21839208 (2,20) 0.08638673 (2,24) 0.01075210 (2,28) 0.46085627
 (2,32) 0.00000000 (3, 0) 0.00000000 (3, 4) 0.00560628 (3, 8) -0.02176210 (3,12) 0.06089671
 (3,16) -0.13164428 (3,20) 0.17770536 (3,24) 0.51496315 (3,28) 0.00000000
 (3,32) 0.00000000 (4, 0) 0.00000000 (4, 4) -0.15619390 (4, 8) 0.25373353 (4,12) -0.27373695

(4,16) 0.24253752	(4,20) 0.30947742	(4,24) 0.00000000	(4,28) 0.00000000
(4,32) 0.00000000			
(5, 0) 0.00000000	(5, 4)-0.30731970	(5, 8) 0.11389989	(5,12) 0.42812680
(5,16) 0.16612869	(5,20) 0.00000000	(5,24) 0.00000000	(5,28) 0.00000000
(5,32) 0.00000000			
(6, 0) 0.39894228	(6, 4) 0.00000000	(6, 8) 0.00000000	(6,12) 0.00000000
(6,16) 0.00000000	(6,20) 0.00000000	(6,24) 0.00000000	(6,28) 0.00000000
(6,32) 0.00000000			

MU M L=34

(1, 0) 0.10188870	(1, 4) 0.00950127	(1, 8)-0.22096371	(1,12)-0.18072045
(1,16)-0.06061243	(1,20)-0.00955449	(1,24)-0.00067735	(1,28)-0.00001803
(1,32) 0.46065881			
(2, 0) 0.08195759	(2, 4)-0.13130803	(2, 8) 0.03127472	(2,12) 0.12017364
(2,16)-0.19355040	(2,20)-0.14989531	(2,24)-0.02873087	(2,28) 0.45984602
(2,32) 0.00000000			
(3, 0) 0.10104313	(3, 4)-0.20001793	(3, 8) 0.19559061	(3,12)-0.19205107
(3,16) 0.18532043	(3,20)-0.13584012	(3,24) 0.36048271	(3,28) 0.00000000
(3,32) 0.00000000			
(4, 0) 0.12402637	(4, 4)-0.20496769	(4, 8) 0.09994418	(4,12) 0.01478153
(4,16)-0.09845339	(4,20) 0.47500805	(4,24) 0.00000000	(4,28) 0.00000000
(4,32) 0.00000000			
(5, 0) 0.13657833	(5, 4)-0.08804735	(5, 8)-0.23443509	(5,12) 0.32269301
(5,16) 0.33787525	(5,20) 0.00000000	(5,24) 0.00000000	(5,28) 0.00000000
(5,32) 0.00000000			
(6, 0) 0.24325183	(6, 4) 0.39618721	(6, 8) 0.20158554	(6,12) 0.04864097
(6,16) 0.00000000	(6,20) 0.00000000	(6,24) 0.00000000	(6,28) 0.00000000
(6,32) 0.00000000			

Table 15.2.4 Symmetry coefficients R_l^{ny} for cubic symmetry, [001] parallel to the Z-axis for $l = 4$ (1) 34. The coefficients are defined by equation (4.257) (see also reference 248)

M L= 4

$$W(4) = 0.5976143 W(0)$$

M L= 6

$$W(4) = -1.8708287 W(0)$$

M L= 8

$$W(4) = 0.3760507 W(0)$$

$$W(8) = 0.5729597 W(0)$$

M L= 9

$$W(8) = -0.6416889 W(4)$$

M L=10

$$W(4) = -1.0076629 W(0)$$

$$W(8) = -1.1993588 W(0)$$

M L=12

$$W(8) = 0.8149151 W(0) -1.4423922 W(4)$$

$$W(12) = 0.4427061 W(0) 0.3463169 W(4)$$

M L=13

$$W(8) = 0.2901905 W(4)$$

$$W(12) = -0.7298161 W(4)$$

M L=14

$$W(4) = -0.7353613 W(0)$$

$$W(8) = -0.7891065 W(0)$$

$$W(12) = -0.9581582 W(0)$$

M L=15

$$W(8) = -2.7026557 W(4)$$

$$W(12) = 1.6810970 W(4)$$

M L=16
 $w(8) = 0.4497647 w(0) -0.5179990 w(4)$
 $w(12) = 0.6311516 w(0) -1.0171612 w(4)$
 $w(16) = 0.4222794 w(0) 0.4014267 w(4)$

M L=17
 $w(8) = 0.4754860 w(4)$
 $w(12) = 0.0519485 w(4)$
 $w(16) = -0.7832581 w(4)$

M L=18
 $w(8) = -3.1798277 w(0) -4.2880159 w(4)$
 $w(12) = 2.2268365 w(0) 4.8635359 w(4)$
 $w(16) = -1.7070715 w(0) -1.4721226 w(4)$

M L=19
 $w(8) = -1.6733201 w(4)$
 $w(12) = -0.8282642 w(4)$
 $w(16) = 1.4561697 w(4)$

M L=20
 $w(8) = 0.3163591 w(0) -0.1703671 w(4)$
 $w(12) = 0.4589014 w(0) -0.6446265 w(4)$
 $w(16) = 0.5386767 w(0) -0.7965430 w(4)$
 $w(20) = 0.4071663 w(0) 0.4426492 w(4)$

M L=21
 $w(12) = 1.1297868 w(4) -1.5862311 w(8)$
 $w(16) = -0.6140975 w(4) 0.9815206 w(8)$
 $w(20) = -0.6756460 w(4) -0.2620762 w(8)$

M L=22
 $w(8) = -2.1178228 w(0) -3.1187645 w(4)$
 $w(12) = -0.1914726 w(0) 0.7036609 w(4)$
 $w(16) = 0.8872353 w(0) 2.9187611 w(4)$
 $w(20) = -1.4493438 w(0) -1.3774637 w(4)$

M L=23
 $w(8) = -1.1699216 w(4)$
 $w(12) = -1.0389292 w(4)$
 $w(16) = -0.1770808 w(4)$
 $w(20) = 1.3143848 w(4)$

M L=24
 $w(12) = 0.9960080 w(0) -0.3779049 w(4) -2.5613076 w(8)$
 $w(16) = -0.1588211 w(0) -0.6512131 w(4) 2.3876867 w(8)$
 $w(20) = 0.7169718 w(0) -0.6468540 w(4) -0.9488398 w(8)$
 $w(24) = 0.3694861 w(0) 0.4742437 w(4) 0.1038941 w(8)$

M L=25
 $w(12) = 0.7985929 w(4) -0.7593264 w(8)$
 $w(16) = 0.4880175 w(4) -0.6061285 w(8)$
 $w(20) = -0.6732194 w(4) 0.8813211 w(8)$
 $w(24) = -0.6558240 w(4) -0.3239679 w(8)$

M L=26
 $w(8) = -1.5692481 w(0) -2.4551428 w(4)$
 $w(12) = -0.6782731 w(0) -0.4484211 w(4)$
 $w(16) = 0.1351977 w(0) 1.4126147 w(4)$
 $w(20) = 0.3260742 w(0) 1.9484665 w(4)$
 $w(24) = -1.2784593 w(0) -1.3097560 w(4)$

M L=27
 $w(12) = -4.2553035 w(4) -3.7627328 w(8)$
 $w(16) = 3.8556389 w(4) 5.0987767 w(8)$
 $w(20) = -2.5814782 w(4) -3.1018328 w(8)$
 $w(24) = 1.8806039 w(4) 0.7640226 w(8)$

M L=28
 $w(12) = 0.6484740 w(0) -0.0444512 w(4) -1.6884919 w(8)$
 $w(16) = 0.3679195 w(0) -0.4611645 w(4) -0.3555468 w(8)$
 $w(20) = 0.0961931 w(0) -0.7661776 w(4) 1.5051323 w(8)$
 $w(24) = 0.6352276 w(0) -0.4450832 w(4) -0.9341155 w(8)$
 $w(28) = 0.3590608 w(0) 0.4867616 w(4) 0.1278635 w(8)$

M L=29
 $w(12) = 0.6028991 w(4) -0.3241383 w(8)$
 $w(16) = 0.6454474 w(4) -0.6759538 w(8)$
 $w(20) = 0.1476364 w(4) -0.1642080 w(8)$
 $w(24) = -0.6993064 w(4) 0.7990475 w(8)$
 $w(28) = -0.6346499 w(4) -0.3799216 w(8)$

M L=30
 $w(12) = -7.1704715 w(0) -11.3029439 w(4) -5.1593406 w(8)$
 $w(16) = 11.7539490 w(0) 20.0881146 w(4) 9.6619234 w(8)$
 $w(20) = -10.3690054 w(0) -15.7032484 w(4) -8.4449635 w(8)$
 $w(24) = 4.3304872 w(0) 8.3786610 w(4) 3.4526384 w(8)$
 $w(28) = -1.7703564 w(0) -2.2620192 w(4) -0.4953223 w(8)$

M L=31
 $w(12) = -2.7783781 w(4) -2.8247786 w(8)$
 $w(16) = 0.3449013 w(4) 1.5435899 w(8)$
 $w(20) = 0.9645940 w(4) 1.8836709 w(8)$
 $w(24) = -1.3318413 w(4) -2.3947018 w(8)$
 $w(28) = 1.6703408 w(4) 0.7875294 w(8)$

M L=32
 $w(12) = 0.4674189 w(0) 0.0879759 w(4) -1.1699803 w(8)$
 $w(16) = 0.4278142 w(0) -0.2151026 w(4) -0.6582068 w(8)$
 $w(20) = 0.2473107 w(0) -0.5873904 w(4) 0.5758748 w(8)$
 $w(24) = 0.2077551 w(0) -0.7335477 w(4) 0.9881316 w(8)$
 $w(28) = 0.5772487 w(0) -0.3040555 w(4) -0.9184905 w(8)$

$W(32) = -0.3502993 W(0) \quad 0.4955448 W(4) \quad 0.1505621 W(8)$
 M L=33
 $W(16) = 1.8498894 W(4) \quad -0.6856124 W(8) \quad -2.5770792 W(12)$
 $W(20) = -0.9450566 W(4) \quad -0.2825628 W(8) \quad 2.9041710 W(12)$
 $W(24) = 0.7881393 W(4) \quad -0.0355014 W(8) \quad -1.7792364 W(12)$
 $W(28) = -0.9943598 W(4) \quad 0.7638207 W(8) \quad 0.6013167 W(12)$
 $W(32) = -0.5653075 W(4) \quad -0.4366552 W(8) \quad -0.1013148 W(12)$

M L=34
 $W(12) = -5.0009656 W(0) \quad -8.1451332 W(4) \quad -4.1443567 W(8)$
 $W(16) = 4.3720229 W(0) \quad 8.0397275 W(4) \quad 4.6519834 W(8)$
 $W(20) = 0.8006938 W(0) \quad 2.3513361 W(4) \quad 0.882624 W(8)$
 $W(24) = -4.8905058 W(0) \quad -7.0316372 W(4) \quad -4.8094173 W(8)$
 $W(28) = 2.9243380 W(0) \quad 6.1252243 W(4) \quad 2.9603478 W(8)$
 $W(32) = -1.5983113 W(0) \quad -2.1195137 W(4) \quad -0.5227475 W(8)$

Table 15.3

Generalized LEGENDRE functions $P_l^{mn}(\Phi)$ for $l = 2, 4, m = 0 (1) l, n = 0 (1) m; \Phi = 0^\circ (5^\circ) 180^\circ$. The functions are defined by equation (14.2) or equations (14.85), (14.86) (see also Figures A.4.1.1-A.4.1.4)

PHI				L= 1	M= 0	N= 0
(0) 1.00000000	(5) 0.99619470	(10) 0.98480775	(15) 0.96592583			
(20) 0.93969262	(25) 0.90630779	(30) 0.86602540	(35) 0.81915204			
(40) 0.76604444	(45) 0.70710678	(50) 0.64278761	(55) 0.57357644			
(60) 0.50000000	(65) 0.42261826	(70) 0.34202014	(75) 0.25881905			
(80) 0.17364818	(85) 0.08715574	(90) 0.00000000	(95) -0.08715574			
(100) -0.17364818	(105) -0.25881905	(110) -0.34202014	(115) -0.42261826			
(120) -0.50000000	(125) -0.57357644	(130) -0.64278761	(135) -0.70710678			
(140) -0.76604444	(145) -0.81915204	(150) -0.86602540	(155) -0.90630779			
(160) -0.93969262	(165) -0.96592583	(170) -0.98480775	(175) -0.99619470			
(180) -1.00000000						
PHI				L= 1	M= 1	N= 0
(0) 0.00000000	(5) -0.06162842	(10) -0.12278780	(15) -0.18301270			
(20) -0.24184476	(25) -0.29883624	(30) -0.35355339	(35) -0.40557979			
(40) -0.45451948	(45) -0.50000000	(50) -0.54167522	(55) -0.57922797			
(60) -0.61237244	(65) -0.64085638	(70) -0.66446302	(75) -0.68301270			
(80) -0.69636424	(85) -0.70441603	(90) -0.70710678	(95) -0.70441603			
(100) -0.69636424	(105) -0.68301270	(110) -0.66446302	(115) -0.64085638			
(120) -0.61237244	(125) -0.57922797	(130) -0.54167522	(135) -0.50000000			
(140) -0.45451948	(145) -0.40557979	(150) -0.35355339	(155) -0.29883624			
(160) -0.24184476	(165) -0.18301270	(170) -0.12278780	(175) -0.06162842			
(180) 0.00000000						
PHI				L= 1	M= 1	N= 1
(0) 1.00000000	(5) 0.99809735	(10) 0.99240388	(15) 0.98296291			
(20) 0.96984631	(25) 0.95315389	(30) 0.93301270	(35) 0.90957602			
(40) 0.88302222	(45) 0.85355339	(50) 0.82139380	(55) 0.78678822			
(60) 0.75000000	(65) 0.71130913	(70) 0.67101007	(75) 0.62940952			
(80) 0.58682409	(85) 0.54357787	(90) 0.50000000	(95) 0.45642213			
(100) 0.41317591	(105) 0.37059048	(110) 0.32898993	(115) 0.28869087			
(120) 0.25000000	(125) 0.21321178	(130) 0.17860620	(135) 0.14644661			
(140) 0.11697778	(145) 0.09042398	(150) 0.06698730	(155) 0.04684611			
(160) 0.03015369	(165) 0.01703709	(170) 0.00759612	(175) 0.00190265			
(180) 0.00000000						
PHI				L= 2	M= 0	N= 0
(0) 1.00000000	(5) 0.98860581	(10) 0.95476947	(15) 0.89951905			
(20) 0.82453333	(25) 0.73209071	(30) 0.62500000	(35) 0.50651511			
(40) 0.38023613	(45) 0.25000000	(50) 0.11976387	(55) 0.00651511			
(60) -0.12500000	(65) -0.23209071	(70) -0.32453333	(75) -0.39951905			
(80) -0.45476947	(85) -0.48860581	(90) -0.50000000	(95) -0.48860581			

(100)-0.45476947 (105)-0.39951905 (110)-0.32453333 (115)-0.23209071
 (120)-0.12500000 (125)-0.00651511 (130) 0.11976387 (135) 0.25000000
 (140) 0.38023613 (145) 0.50651511 (150) 0.62500000 (155) 0.73209071
 (160) 0.82453333 (165) 0.89951905 (170) 0.95476947 (175) 0.98860581

PHI L= 2 M= 1 N= 0

(0) 0.00000000 (5)-0.10633736 (10)-0.20944371 (15)-0.30618622
 (20)-0.39362541 (25)-0.46910450 (30)-0.53033009 (35)-0.57544186
 (40)-0.60306912 (45)-0.61237244 (50)-0.60306912 (55)-0.57544186
 (60)-0.53033009 (65)-0.46910450 (70)-0.39362541 (75)-0.30618622
 (80)-0.20944371 (85)-0.10633736 (90) 0.00000000 (95) 0.10633736
 (100) 0.20944371 (105) 0.30618622 (110) 0.39362541 (115) 0.46910450
 (120) 0.53033009 (125) 0.57544186 (130) 0.60306912 (135) 0.61237244
 (140) 0.60306912 (145) 0.57544186 (150) 0.53033009 (155) 0.46910450
 (180) 0.00000000 (165) 0.30618622 (170) 0.20944371 (175) 0.10633736

PHI L= 2 M= 1 N= 1

(0) 1.00000000 (5) 0.99050123 (10) 0.96225019 (15) 0.91597562
 (20) 0.85286853 (25) 0.77454770 (30) 0.68301270 (35) 0.58058609
 (40) 0.46984631 (45) 0.35355339 (50) 0.23456972 (55) 0.11577815
 (60) 0.00000000 (65)-0.11008467 (70)-0.21201215 (75)-0.30360318
 (80)-0.38302222 (85)-0.44882604 (90)-0.50000000 (95)-0.53598175
 (100)-0.55667040 (105)-0.56242222 (110)-0.55403229 (115)-0.53270294
 (120)-0.50000000 (125)-0.45779829 (130)-0.40821789 (135)-0.35355339
 (140)-0.29619813 (145)-0.23856595 (150)-0.18301270 (155)-0.13176009
 (160)-0.08682409 (165)-0.04995021 (170)-0.02255757 (175)-0.00569347

PHI L= 2 M= 2 N= 0

(0) 0.00000000 (5)-0.00465166 (10)-0.01846529 (15)-0.04102117
 (20)-0.07163397 (25)-0.10937351 (30)-0.15309311 (35)-0.20146436
 (40)-0.25301754 (45)-0.30618622 (50)-0.35935490 (55)-0.41090807
 (60)-0.45927933 (65)-0.50299892 (70)-0.54073847 (75)-0.57135126
 (80)-0.59390715 (85)-0.60772078 (90)-0.61237244 (95)-0.60772078
 (100)-0.59390715 (105)-0.57135126 (110)-0.54073847 (115)-0.50299892
 (120)-0.45927933 (125)-0.41090807 (130)-0.35935490 (135)-0.30618622
 (140)-0.25301754 (145)-0.20146436 (150)-0.15309311 (155)-0.10937351
 (160)-0.07163397 (165)-0.04102117 (170)-0.01846529 (175)-0.00465166

PHI L= 2 M= 2 N= 1

(0) 0.00000000 (5)-0.08698992 (10)-0.17232912 (15)-0.25440952
 (20)-0.33170697 (25)-0.40282024 (30)-0.46650635 (35)-0.52171137
 (40)-0.56759574 (45)-0.60355339 (50)-0.62922416 (55)-0.64449918
 (60)-0.64951905 (65)-0.64466500 (70)-0.63054321 (75)-0.60796291
 (80)-0.57790891 (85)-0.54150939 (90)-0.50000000 (95)-0.45468530
 (100)-0.40689884 (105)-0.35796291 (110)-0.30914941 (115)-0.26164278
 (120)-0.21650635 (125)-0.17465287 (130)-0.13682028 (135)-0.10355339
 (140)-0.07519187 (145)-0.05186506 (150)-0.03349365 (155)-0.01979802
 (180) 0.00000000 (165)-0.00440952 (170)-0.00131905 (175)-0.00016583

PHI L= 2 M= 2 N= 2

(0) 1.00000000 (5) 0.99619832 (10) 0.98406545 (15) 0.96621609
 (20) 0.94060187 (25) 0.90850234 (30) 0.87051270 (35) 0.82732854

(40) 0.77972824 (45) 0.72855339 (50) 0.67468778 (55) 0.61903570
 (60) 0.56250000 (65) 0.50596068 (70) 0.45025452 (75) 0.39615635
 (80) 0.34436251 (85) 0.29547690 (90) 0.25000000 (95) 0.20832116
 (100) 0.17071433 (105) 0.13733730 (110) 0.10823437 (115) 0.08334242
 (120) 0.06250000 (125) 0.04545926 (130) 0.03190017 (135) 0.02144661
 (140) 0.01368380 (145) 0.00817650 (150) 0.00448730 (155) 0.00219456
 (160) 0.00090924 (165) 0.00029026 (170) 0.00005770 (175) 0.00000362

PHI L= 3 M= 0 N= 0

(0) 1.00000000 (5) 0.97727665 (10) 0.91056878 (15) 0.80416392
 (20) 0.66488473 (25) 0.50162732 (30) 0.32475953 (35) 0.14542011
 (40)-0.02523333 (45)-0.17677670 (50)-0.30022052 (55)-0.38861248
 (60)-0.43750000 (65)-0.44522179 (70)-0.41300832 (75)-0.34488460
 (80)-0.24738193 (85)-0.12907850 (90) 0.00000000 (95) 0.12907850
 (100) 0.24738193 (105) 0.34488460 (110) 0.41300832 (115) 0.44522179
 (120) 0.43750000 (125) 0.38861248 (130) 0.30022052 (135) 0.17677670
 (140) 0.02523333 (145)-0.14542011 (150)-0.32475953 (155)-0.50162732
 (160)-0.66488473 (165)-0.80416392 (170)-0.91056878 (175)-0.97727665

PHI L= 3 M= 1 N= 0

(0) 0.00000000 (5)-0.14952480 (10)-0.28943091 (15)-0.41075076
 (20)-0.50577477 (25)-0.56857246 (30)-0.59539247 (35)-0.58491416
 (40)-0.53833380 (45)-0.45927933 (50)-0.35355968 (55)-0.22876573
 (60)-0.09375000 (65) 0.04197922 (70) 0.16890823 (75) 0.27816823
 (80) 0.36214143 (85) 0.41498145 (90) 0.43301270 (95) 0.41498145
 (100) 0.36214143 (105) 0.27816823 (110) 0.16890823 (115) 0.04197922
 (120)-0.09375000 (125)-0.22876573 (130)-0.35355968 (135)-0.45927933
 (140)-0.53833380 (145)-0.58491416 (150)-0.59539247 (155)-0.56857246
 (160)-0.50577477 (165)-0.41075076 (170)-0.28943091 (175)-0.14952480

PHI L= 3 M= 1 N= 1

(0) 0.00000000 (5)-0.97916124 (10) 0.91787859 (15) 0.81977442
 (20) 0.69062928 (25) 0.53801467 (30) 0.37081329 (35) 0.19865837
 (40) 0.03132894 (45)-0.12185922 (50)-0.25262735 (55)-0.35423476
 (60)-0.42187500 (65)-0.45294204 (70)-0.44715017 (75)-0.40650115
 (80)-0.33510244 (85)-0.23885023 (90)-0.12500000 (95)-0.00165461
 (100) 0.12279455 (105) 0.24023527 (110) 0.34337239 (115) 0.42619978
 (120) 0.48437500 (125) 0.51547217 (130) 0.51909724 (135) 0.49685922
 (140) 0.45220117 (145) 0.39010422 (150) 0.31668671 (155) 0.23872758
 (160) 0.16314849 (165) 0.09649145 (170) 0.04442929 (175) 0.01134361

PHI L= 3 M= 2 N= 0

(0) 0.00000000 (5)-0.01036184 (10)-0.04066236 (15)-0.08860064
 (20)-0.15051848 (25)-0.22165262 (30)-0.29646353 (35)-0.36901818
 (40)-0.43340069 (45)-0.48412292 (50)-0.51650683 (55)-0.52701257
 (60)-0.51348990 (65)-0.47533557 (70)-0.41354612 (75)-0.33066210
 (80)-0.23060769 (85)-0.11843637 (90) 0.00000000 (95) 0.11843637
 (100) 0.23060769 (105) 0.33066210 (110) 0.41354612 (115) 0.47533557
 (120) 0.51348990 (125) 0.52701257 (130) 0.51650683 (135) 0.48412292
 (140) 0.43340069 (145) 0.36901818 (150) 0.29646353 (155) 0.22165262
 (160) 0.15051848 (165) 0.08860064 (170) 0.04066236 (175) 0.01036184

PHI	L= 3	M= 2	N= 1		(140)=0.01077258	(145)=0.00574386	(150)=0.00274790	(155)=0.00113590
(0) 0.00000000	(5)-0.13675804	(10)-0.26626698	(15)-0.38169692		(160)=0.00038087	(165)=0.00009201	(170)=0.00001227	(175)=0.00000039
(20)-0.47703023	(25)-0.54740380	(30)-0.58937954	(35)-0.60112641		(180) 0.00000000			
(40)-0.58250337	(45)-0.53503896	(50)-0.46180980	(55)-0.36722696		PHI	L= 3	M= 3	N= 3
(60)-0.25674495	(65)-0.13651284	(70)-0.01299082	(75) 0.10744295		(0) 1.00000000	(5) 0.99430290	(10) 0.97738429	(15) 0.94975458
(80) 0.21886948	(85) 0.31616644	(90) 0.39528471	(95) 0.45344738		(20) 0.91223925	(25) 0.86954255	(30) 0.81219941	(35) 0.75251820
(100) 0.48926014	(105) 0.50272765	(110) 0.49517741	(115) 0.46909846		(40) 0.68851737	(45) 0.62185922	(50) 0.55418436	(55) 0.48705000
(120) 0.42790825	(125) 0.37566528	(130) 0.31674909	(135) 0.25553046		(60) 0.42187500	(65) 0.35989445	(70) 0.30212532	(75) 0.24934458
(140) 0.19605552	(145) 0.14176584	(150) 0.09527366	(155) 0.05820751		(80) 0.20208022	(85) 0.16061471	(90) 0.12500000	(95) 0.09508239
(160) 0.03113800	(165) 0.01358778	(170) 0.00412368	(175) 0.00052289		(100) 0.07053505	(105) 0.05089590	(110) 0.03568082	(115) 0.02406020
(180) 0.00000000					(120) 0.01562500	(125) 0.00969245	(130) 0.00569757	(135) 0.00314078
PHI	L= 3	M= 2	N= 2		(140) 0.00160070	(145) 0.00073935	(150) 0.00030059	(155) 0.00010281
(0) 1.00000000	(5) 0.98482581	(10) 0.93997850	(15) 0.86744704		(160) 0.000002742	(165) 0.00000495	(170) 0.00000044	(175) 0.00000001
(20) 0.77042617	(25) 0.65314356	(30) 0.52063294	(35) 0.37846651		(180) 0.00000000			
(40) 0.23246298	(45) 0.08838835	(50) -0.04833272	(55)-0.17287853		PHI	L= 4	M= 0	N= 0
(60)-0.28125000	(65)-0.37043669	(70)-0.43852069	(75)-0.48471427		(0) 1.00000000	(5) 0.96227182	(10) 0.85320950	(15) 0.68469544
(80)-0.50933125	(85)-0.51369628	(90)-0.50000000	(95)-0.47111148		(20) 0.47497774	(25) 0.24653228	(30) 0.02343750	(35) 0.17142426
(100) 0.43036137	(105) 0.38131113	(110) 0.32752375	(115) 0.27235092		(40) 0.31900435	(45) 0.40625000	(50) 0.42753446	(55) 0.38518685
(120)-0.21875000	(125)-0.16914162	(130)-0.12531545	(135)-0.08838835		(60) 0.28906250	(65) 0.15520998	(70) 0.00380004	(75) 0.14342956
(140)-0.05881480	(145)-0.03644637	(150)-0.02063294	(155)-0.01035595		(80) 0.26590161	(85) 0.34676698	(90) 0.37500000	(95) 0.34676698
(160) 0.00438172	(165)-0.00142164	(170)-0.00028588	(175)-0.00001806		(100) 0.26590161	(105) 0.14342956	(110)-0.00380004	(115)-0.15520998
(180) 0.00000000					(120) 0.28906250	(125)-0.38518685	(130)-0.42753446	(135)-0.40625000
PHI	L= 3	M= 3	N= 0		(140)-0.31900435	(145)-0.17142426	(150) 0.02343750	(155) 0.24653228
(0) 0.00000000	(5) 0.00037009	(10) 0.00292709	(15) 0.00969201		(160) 0.47497774	(165) 0.68469544	(170) 0.85320950	(175) 0.96227182
(20) 0.02236557	(25) 0.04219585	(30) 0.06987712	(35) 0.10548699		(180) 1.00000000			
(40) 0.14946617	(45) 0.19764235	(50) 0.25129677	(55) 0.30726887		PHI	L= 4	M= 1	N= 0
(60) 0.36309219	(65) 0.41615215	(70) 0.46385523	(75) 0.50379789		(0) 0.00000000	(5) -0.19156376	(10) -0.36221182	(15) -0.49348468
(80) 0.53392393	(85) 0.55265956	(90) 0.55901699	(95) 0.55265956		(20) -0.57154104	(25) -0.58876670	(30) -0.54463828	(35) -0.44573908
(100) 0.53392393	(105) 0.50379789	(110) 0.46385523	(115) 0.41615215		(40) -0.30492676	(45) -0.13975425	(50) 0.02966462	(55) 0.18308701
(120) 0.36309219	(125) 0.30726887	(130) 0.25129677	(135) 0.19764235		(60) 0.30257682	(65) 0.37465077	(70) 0.39187644	(75) 0.35373043
(140) 0.14846617	(145) 0.10548699	(150) 0.06987712	(155) 0.04219585		(80) 0.26661428	(85) 0.14302762	(90) 0.00000000	(95) -0.14302762
(160) 0.02236557	(165) 0.00969201	(170) 0.00292709	(175) 0.00037009		(100) 0.26661428	(105) -0.35373043	(110) -0.39187644	(115) -0.37465077
(180) 0.00000000					(120) -0.30257682	(125) -0.18308701	(130) -0.02966462	(135) 0.13975425
PHI	L= 3	M= 3	N= 1		(140) 0.30492676	(145) 0.44573908	(150) 0.54463828	(155) 0.58876670
(0) 0.00000000	(5)-0.00734092	(10)-0.02897441	(15)-0.06375514		(160) 0.57154104	(165) 0.49348468	(170) 0.36221182	(175) 0.19156376
(20)-0.10984794	(25)-0.16483339	(30)-0.22584642	(35)-0.28973919		(180) 0.00000000			
(40)-0.35325821	(45)-0.41322476	(50)-0.46670773	(55)-0.51117844		PHI	L= 4	M= 1	N= 1
(60)-0.54463828	(65)-0.56571207	(70)-0.57370193	(75)-0.56859954		(0) 1.00000000	(5) 0.96414204	(10) 0.86029547	(15) 0.69922283
(80)-0.55105696	(85)-0.52231904	(90)-0.48412292	(95)-0.43857188		(20) 0.49751241	(25) 0.27571888	(30) 0.05606964	(35) -0.13999834
(100)-0.3799270	(105)-0.33478612	(110)-0.28128066	(115)-0.22959906		(40) -0.29418751	(45) -0.39330583	(50) -0.43062757	(55) -0.40649860
(120)-0.18154609	(125)-0.13852427	(130)-0.10148225	(135)-0.07089816		(60) 0.32812500	(65) 0.20858019	(70) -0.06515659	(75) 0.08273666
(140)-0.04679765	(145)-0.02880394	(150)-0.01621504	(155)-0.00810132		(80) 0.21587721	(85) 0.31746092	(90) 0.37500000	(95) 0.38166915
(160)-0.00341530	(165)-0.00110503	(170)-0.00022178	(175)-0.00001399		(100) 0.33695011	(105) 0.24651016	(110) 0.12134319	(115) -0.02371041
(180) 0.00000000					(120)-0.17187500	(125)-0.30654280	(130)-0.41330949	(135)-0.48169417
PHI	L= 3	M= 3	N= 2		(140)-0.50633751	(145)-0.48753803	(150)-0.43106964	(155)-0.34731258
(0) 0.00000000	(5)-0.10633774	(10)-0.20945598	(15)-0.30627823		(160)-0.24981469	(165)-0.15346966	(170)-0.07254500	(175)-0.01881003
(20)-0.39400629	(25)-0.47024040	(30)-0.53307798	(35)-0.58118572		(180) 0.00000000			
(40)-0.61384171	(45)-0.63094574	(50)-0.63299815	(55)-0.62104897		PHI	L= 4	M= 2	N= 0
(60)-0.59662135	(65)-0.56161424	(70)-0.51819059	(75)-0.46865799		(0) 0.00000000	(5) -0.01785613	(10) -0.06899988	(15) -0.14645801
(80)-0.41534879	(85)-0.36050674	(90)-0.30618622	(95)-0.25416939		(20) 0.23957418	(25) 0.33533423	(30) -0.41999000	(35) -0.48078438
(100)-0.20590509	(105)-0.16247177	(110)-0.12456518	(115)-0.09250974		(40) 0.50756736	(45) 0.49410588	(50) -0.43892689	(55) -0.34558905
(120)-0.06629126	(125)-0.04560711	(130)-0.02992903	(135)-0.01857331		(180) 0.00000000			

(80) 0.30244624	(85) 0.37142331	(90) 0.3952P471	(95) 0.37142331	PHI	L= 4	M= 3	N= 2
(100) 0.30244624	(105) 0.19586859	(110) 0.06323147	(115)-0.08125012	(0) 0.00000000	(5)-0.16119737	(10) -0.31022780	(15) -0.43596467
(120)-0.22234765	(125)-0.34558905	(130)-0.43892689	(135)-0.49410588	(20)-0.52926200	(25)-0.58370508	(30) -0.59610170	(35) -0.56667096
(140)-0.50756736	(145)-0.48078438	(150)-0.41999000	(155)-0.33533423	(40)-0.49891777	(45)-0.39921304	(50) -0.27612858	(55) -0.13959922
(160)-0.23957418	(165)-0.14645801	(170)-0.06899988	(175)-0.01785613	(60) 0.00000000	(65) 0.13276848	(70) 0.25009766	(75) 0.34531657
(180) 0.00000000				(80) 0.41411159	(85) 0.45469275	(90) 0.46770717	(95) 0.45592661
PHI	L= 4	M= 2	N= 1	(100) 0.42375868	(105) 0.37664701	(110) 0.32043321	(115) 0.26075213
(0) 0.00000000	(5)-0.18208199	(10) -0.34632400	(15) -0.47678365	(120) 0.20252315	(125) 0.14958357	(130) 0.10449044	(135) 0.06849413
(20)-0.56110325	(25)-0.59179980	(30) -0.56701686	(35) -0.49065866	(140) 0.04166652	(145) 0.02314821	(150) 0.01146774	(155) 0.00488022
(40)-0.37189690	(45)-0.22411165	(50) -0.06339110	(55) 0.09323685	(160) 0.00167520	(165) 0.00041206	(170) 0.00005567	(175) 0.00000177
(60) 0.22963966	(65) 0.33227624	(70) 0.39156708	(75) 0.40279223	(180) 0.00000000			
(80) 0.36642751	(85) 0.28789561	(90) 0.17677670	(95) 0.04558449	PHI	L= 4	M= 3	N= 3
(100)-0.09173822	(105)-0.22142200	(110)-0.33138150	(115)-0.41246127	(0) 1.00000000	(5) 0.97916841	(10) 0.91798964	(15) 0.82030617
(120)-0.45927933	(125)-0.47058345	(130)-0.44909633	(135)-0.40088835	(20) 0.69218022	(25) 0.54141425	(30) 0.37694306	(35) 0.20815269
(140)-0.33437379	(145)-0.25906987	(150) 0.18428409	(155)-0.11789990	(40) 0.04418751	(45) -0.10669417	(50) -0.23766172	(55) -0.34370838
(160)-0.06541441	(165)-0.02934611	(170)-0.00908065	(175)-0.00116478	(60) 0.42187500	(65) -0.47129148	(70) 0.49304417	(75) -0.48893232
(180) 0.00000000				(80) -0.46587721	(85) -0.42585014	(90) -0.37500000	(95) -0.31839507
PHI	L= 4	M= 2	N= 2	(100) -0.26059828	(105) -0.20537900	(110) -0.15553869	(115) -0.11285370
(0) 1.00000000	(5) 0.96976345	(10) 0.88172040	(15) 0.74360776	(120) -0.07812500	(125) -0.05131480	(130) -0.03174201	(135) -0.01830583
(20) 0.56747188	(25) 0.36849048	(30) 0.16350159	(35) -0.03060603	(140) -0.00970693	(145) -0.00464062	(150) -0.00194306	(155) -0.00068112
(40) -0.19847396	(45) -0.32766504	(50) -0.40972567	(55) -0.44081876	(160) -0.00018531	(165) -0.00003394	(170) -0.00000304	(175) -0.00000005
(60) -0.42187500	(65) -0.35826290	(70) -0.25902987	(75) -0.13581120	(180) 0.00000000			
(80) 0.00153634	(85) 0.13092069	(90) 0.25000000	(95) 0.34649289	PHI	L= 4	M= 4	N= 0
(100) 0.41425763	(105) 0.45055485	(110) 0.45598984	(115) 0.43409492	(0) 0.00000000	(5) 0.00003017	(10) 0.00047546	(15) 0.00234646
(120) 0.39062500	(125) 0.33266928	(130) 0.26769811	(135) 0.20266504	(20) 0.00715543	(25) 0.01668100	(30) 0.03268203	(35) 0.05659711
(140) 0.14327048	(145) 0.09346663	(150) 0.05524841	(155) 0.02873534	(40) 0.08926866	(45) 0.13072813	(50) 0.18007147	(55) 0.23544372
(160) 0.01251031	(165) 0.00414859	(170) 0.00084720	(175) 0.00005401	(60) 0.29413829	(65) 0.35280269	(70) 0.40772966	(75) 0.45520199
(180) 0.00000000				(80) 0.49185249	(85) 0.51499847	(90) 0.52291252	(95) 0.51499847
PHI	L= 4	M= 3	N= 0	(100) 0.49185249	(105) 0.45520199	(110) 0.40772966	(115) 0.35280269
(0) 0.00000000	(5)-0.00097545	(10) -0.00762669	(15) -0.02476889	(120) 0.29413829	(125) 0.23544372	(130) 0.18007147	(135) 0.13072813
(20) -0.05560514	(25) 0.10117996	(30) 0.16010861	(35) 0.22861907	(140) 0.08926866	(145) 0.05659711	(150) 0.03268203	(155) 0.01668100
(40) 0.30090575	(45) 0.36975499	(50) 0.42736940	(55) 0.46629299	(160) 0.00715543	(165) 0.00234646	(170) 0.00047546	(175) 0.00003017
(60) 0.48032582	(65) 0.46531754	(70) 0.41974271	(75) 0.34498610	(180) 0.00000000			
(80) 0.24530062	(85) 0.12743911	(90) 0.00000000	(95) -0.12743911	PHI	L= 4	M= 4	N= 1
(100) -0.24530062	(105) -0.34498610	(110) -0.41974271	(115) -0.46531754	(0) 0.00000000	(5) 0.00061811	(10) 0.00486075	(15) 0.01594152
(120) -0.48032582	(125) -0.46629299	(130) -0.42736940	(135) -0.36975499	(20) 0.03629627	(25) 0.06729950	(30) 0.10909418	(35) 0.16055245
(140) -0.30090575	(145) -0.22861907	(150) -0.16010861	(155) -0.10117996	(40) 0.21937046	(45) 0.28228625	(50) 0.34539604	(55) 0.40453438
(160) -0.05560514	(165) -0.02476889	(170) -0.00762669	(175) -0.00097545	(60) 0.45567708	(65) 0.49532420	(70) 0.52082343	(75) 0.53060174
(180) 0.00000000				(80) 0.52428368	(85) 0.50268795	(90) 0.46770717	(95) 0.42204838
PHI	L= 4	M= 3	N= 1	(100) 0.36914195	(105) 0.31241337	(110) 0.25535483	(115) 0.20103154
(0) 0.00000000	(5)-0.01496808	(10) -0.05817705	(15) -0.12472303	(120) 0.15189236	(125) 0.10962479	(130) 0.07510389	(135) 0.04843266
(20) -0.20701932	(25) -0.29560796	(30) -0.38016769	(35) -0.45060803	(140) 0.02906096	(145) 0.01596105	(150) 0.00783261	(155) 0.00330767
(40) -0.49813006	(45) -0.51613984	(50) -0.50091744	(55) -0.45197332	(160) 0.00112849	(165) 0.00027630	(170) 0.00003721	(175) 0.00000118
(60) -0.37205878	(65) -0.26683670	(70) -0.14422557	(75) -0.01370224	(180) 0.00000000			
(80) 0.11496861	(85) 0.23241903	(90) 0.33071891	(95) 0.40404964	PHI	L= 4	M= 4	N= 2
(100) 0.44915090	(105) 0.46547267	(110) 0.45502969	(115) 0.42198999	(0) 0.00000000	(5)-0.01001052	(10) -0.03928587	(15) -0.08562208
(120) 0.37205878	(125) 0.31174046	(130) 0.24757206	(135) 0.18542092	(20) -0.14555537	(25) -0.21465529	(30) -0.28789502	(35) -0.36006394
(140) 0.12992720	(145) 0.08415011	(150) 0.04944878	(155) 0.02559720	(40) -0.42618414	(45) -0.48189277	(50) -0.52375696	(55) -0.54949502
(160) 0.01110267	(165) 0.00367150	(170) 0.00074831	(175) 0.00004765	(60) -0.55808817	(65) -0.54977782	(70) -0.52595518	(75) -0.48895985
(180) 0.00000000				(80) -0.44181231	(85) -0.38791003	(90) -0.33071891	(95) -0.27348963
PHI	L= 4	M= 3	N= 1	(100) -0.21902411	(105) -0.16950991	(110) -0.12643167	(115) -0.09056003
(0) 0.00000000	(5)-0.05817705	(10) -0.12472303	(15) -0.45060803	(120) -0.06200980	(125) -0.04035250	(130) -0.02476395	(135) -0.01418560

(140)-0.00747930	(145)-0.00355852	(150)-0.00148403	(155)-0.00051852
(160)-0.00014070	(165)-0.00002572	(170)-0.00000230	(175)-0.00000074
(180) 0.00000000			

PHI L= 4 M= 4 N= 3

(0) 0.00000000	(5)-0.12255463	(10)-0.24002174	(15)-0.34763430
(20)-0.44124057	(25)-0.51755003	(30)-0.57431171	(35)-0.61041235
(40)-0.62588911	(45)-0.62185922	(50)-0.60037588	(55)-0.56422596
(60)-0.51668924	(65)-0.46128131	(70)-0.40150220	(75)-0.34061103
(80)-0.28144287	(85)-0.22627915	(90)-0.17677670	(95)-0.13395511
(100)-0.09823617	(105)-0.06952509	(110)-0.04732042	(115)-0.03083826
(120)-0.01913664	(125)-0.01122828	(130)-0.00617246	(135)-0.00314078
(140)-0.00145510	(145)-0.00059973	(150)-0.00021255	(155)-0.00006144
(160)-0.00001326	(165)-0.00000181	(170)-0.00000011	(175) 0.00000000
(180) 0.00000000			

PHI L= 4 M= 4 N= 4

(0) 1.00000000	(5) 0.99241109	(10) 0.96995996	(15) 0.93357353
(20) 0.88473187	(25) 0.82537651	(30) 0.75779236	(35) 0.68447251
(40) 0.60797613	(45) 0.53079004	(50) 0.45520360	(55) 0.38320520
(60) 0.31640625	(65) 0.25599621	(70) 0.20272913	(75) 0.15693985
(80) 0.11858554	(85) 0.08730660	(90) 0.06250000	(95) 0.04339771
(100) 0.02914338	(105) 0.01886153	(110) 0.01171468	(115) 0.00694596
(120) 0.00390625	(125) 0.00206654	(130) 0.00101762	(135) 0.00004596
(140) 0.00018725	(145) 0.00006686	(150) 0.00002014	(155) 0.00000482
(160) 0.00000083	(165) 0.00000008	(170) 0.00000000	(175) 0.00000000
(180) 0.00000000			

Table 15.4

Cubic spherical harmonics \hat{k}_l^{μ} . The functions are defined by equation (14.209) with the coefficients of Table 15.2.1

Table 15.4.1

Cubic spherical harmonics $\hat{k}_l^{\mu}(\Phi\beta)$ for $l = 4, 6, 8, 9, \mu = 1, \Phi = 52.5^\circ (2.5^\circ) 90^\circ, \beta = 0^\circ (2.5^\circ) 45^\circ$ (for values for $l = 0 (2) 32$ see reference I, p. 291)

L=4 MU=1								
52.5	55.0	57.5	60.0	62.5	65.0	67.5	70.0	
0.0 -0.107468	-0.067078	-0.017285	0.040398	0.104217	0.172236	0.242385	0.312535	
2.5 -0.109899	-0.069841	-0.020390	0.036945	0.100418	0.168095	0.237914	0.307749	
5.0 -0.117119	-0.078047	-0.029612	0.026694	0.089136	0.155798	0.224636	0.293538	
7.5 -0.128909	-0.091447	-0.044669	0.009954	0.070714	0.135720	0.202954	0.270334	
10.0 -0.144909	-0.109632	-0.065105	-0.012766	0.045711	0.108469	0.173528	0.238841	
12.5 -0.164635	-0.132052	-0.090298	-0.040774	0.014888	0.074875	0.137251	0.200016	
15.0 -0.187486	-0.158024	-0.119483	-0.073221	-0.020820	0.035957	0.095226	0.155039	
17.5 -0.212769	-0.186759	-0.151173	-0.109119	-0.060327	-0.007102	0.044730	0.105277	
20.0 -0.239715	-0.217384	-0.186188	-0.147379	-0.102433	-0.052993	-0.000825	0.052241	
22.5 -0.267505	-0.248970	-0.221681	-0.186839	-0.145858	-0.100322	-0.051932	-0.002456	
25.0 -0.295295	-0.280555	-0.257174	-0.226298	-0.189283	-0.147651	-0.103040	-0.051754	
27.5 -0.322241	-0.311180	-0.291588	-0.264558	-0.231388	-0.193542	-0.152595	-0.110189	
30.0 -0.347524	-0.339915	-0.323879	-0.300457	-0.270895	-0.236600	-0.199091	-0.159952	
32.5 -0.370375	-0.365887	-0.353064	-0.332903	-0.306603	-0.275518	-0.241116	-0.204928	
35.0 -0.390101	-0.388307	-0.378257	-0.360911	-0.337426	-0.309112	-0.277393	-0.243753	
37.5 -0.406101	-0.406492	-0.398692	-0.383631	-0.362429	-0.336363	-0.306819	-0.275246	
40.0 -0.417891	-0.419892	-0.413750	-0.400371	-0.380851	-0.356442	-0.328500	-0.298451	
42.5 -0.425111	-0.428098	-0.422971	-0.410622	-0.392134	-0.368738	-0.341779	-0.312662	
45.0 -0.427542	-0.430861	-0.426076	-0.414075	-0.395933	-0.372879	-0.346250	-0.317447	

L=4 MU=1

L=4 MU=1								
72.5	75.0	77.5	80.0	82.5	85.0	87.5	90.0	
0.0 0.380553	0.444373	0.502055	0.551848	0.592238	0.621998	0.640223	0.646360	
2.5 0.375475	0.439030	0.496480	0.546075	0.586308	0.615953	0.634109	0.640223	
5.0 0.360397	0.423165	0.479922	0.528933	0.568698	0.598004	0.615953	0.621998	
7.5 0.335776	0.397259	0.452885	0.500940	0.539944	0.568694	0.586306	0.592238	
10.0 0.302360	0.362099	0.416191	0.462950	0.500919	0.528916	0.546070	0.551848	
12.5 0.261165	0.318753	0.370954	0.416115	0.452808	0.479877	0.496467	0.502055	
15.0 0.213443	0.268540	0.318549	0.361858	0.397074	0.423067	0.439003	0.444373	
17.5 0.160643	0.212984	0.260569	0.301829	0.335410	0.360213	0.375426	0.380553	
20.0 0.104369	0.153773	0.198774	0.237851	0.269690	0.293224	0.307667	0.312535	
22.5 0.046333	0.092707	0.135043	0.171868	0.201911	0.224136	0.237784	0.242385	
25.0 -0.011704	0.031641	0.071312	0.105885	0.134131	0.155049	0.167901	0.172236	
27.5 -0.067977	-0.027570	0.009517	0.041907	0.068411	0.088060	0.100141	0.104217	
30.0 -0.120778	-0.083126	-0.048463	-0.018122	0.006747	0.025206	0.036564	0.040398	
32.5 -0.168500	-0.133339	-0.100868	-0.072378	-0.048987	-0.031604	-0.020899	-0.017285	
35.0 -0.209695	-0.176684	-0.146105	-0.119213	-0.097098	-0.080643	-0.070503	-0.067078	
37.5 -0.243111	-0.211844	-0.182799	-0.157204	-0.136123	-0.120422	-0.110739	-0.107468	
40.0 -0.267732	-0.237750	-0.209836	-0.185196	-0.164877	-0.149731	-0.140386	-0.137227	
42.5 -0.282810	-0.253616	-0.226394	-0.202339	-0.182487	-0.167680	-0.158542	-0.155453	
45.0 -0.287888	-0.258958	-0.231969	-0.208112	-0.188417	-0.173725	-0.164656	-0.161590	

	L=6 MU=1								
	→ φ	52.5	55.0	57.5	60.0	62.5	65.0	67.5	70.0
0.0	0.521120	0.473931	0.415757	0.348364	0.273801	0.194334	0.112376	0.030418	
2.5	0.512381	0.465476	0.407864	0.341306	0.267830	0.189667	0.109184	0.028814	
5.0	0.486429	0.440368	0.384425	0.320345	0.250096	0.175808	0.099707	0.024053	
7.5	0.444053	0.399369	0.346152	0.286119	0.221140	0.153178	0.084232	0.016279	
10.0	0.386541	0.343725	0.294208	0.239668	0.181841	0.122466	0.063229	0.005728	
12.5	0.315639	0.275128	0.230171	0.182402	0.133393	0.084603	0.037336	-0.007279	
15.0	0.233503	0.195661	0.155988	0.116063	0.077268	0.040740	0.007341	-0.022347	
17.5	0.142628	0.107739	0.073912	0.042665	0.015172	-0.007789	-0.025846	-0.039019	
20.0	0.045775	0.014033	-0.013564	-0.035561	-0.051010	-0.059510	-0.061215	-0.056787	
22.5	-0.054113	-0.082609	-0.103781	-0.116238	-0.119265	-0.112853	-0.097693	-0.075113	
25.0	-0.154002	-0.179251	-0.193997	-0.196916	-0.187520	-0.166195	-0.134171	-0.093438	
27.5	-0.250855	-0.272957	-0.281473	-0.275142	-0.253701	-0.217917	-0.169541	-0.111206	
30.0	-0.341730	-0.360879	-0.363549	-0.348540	-0.315798	-0.266446	-0.202728	-0.127878	
32.5	-0.423866	-0.440346	-0.437733	-0.414879	-0.371923	-0.310308	-0.232723	-0.142946	
35.0	-0.494768	-0.508943	-0.501769	-0.472145	-0.420371	-0.348171	-0.258615	-0.155953	
37.5	-0.552280	-0.564586	-0.553713	-0.518596	-0.459670	-0.378884	-0.279618	-0.166504	
40.0	-0.594656	-0.605585	-0.591986	-0.552822	-0.488626	-0.401513	-0.295093	-0.174278	
42.5	-0.620607	-0.630694	-0.615425	-0.573783	-0.506359	-0.415372	-0.304571	-0.179039	
45.0	-0.629347	-0.639149	-0.623318	-0.580841	-0.512331	-0.420039	-0.307762	-0.180643	

	L=8 MU=1								
	→ φ	52.5	55.0	57.5	60.0	62.5	65.0	67.5	70.0
0.0	0.282212	0.162066	0.037289	-0.075037	-0.159009	-0.201896	-0.195748	-0.138445	
2.5	0.277877	0.157528	0.032270	-0.080885	-0.166081	-0.210598	-0.206466	-0.151503	
5.0	0.265367	0.144522	0.017957	-0.097523	-0.186197	-0.235391	-0.237069	-0.188875	
7.5	0.246104	0.124789	-0.003515	-0.122342	-0.216200	-0.272495	-0.283100	-0.234387	
10.0	0.222272	0.100993	-0.028886	-0.151367	-0.251277	-0.316149	-0.337756	-0.313132	
12.5	0.196554	0.076389	-0.054189	-0.179763	-0.285576	-0.359342	-0.392748	-0.382457	
15.0	0.171818	0.054419	-0.075252	-0.202464	-0.312962	-0.394710	-0.439349	-0.443176	
17.5	0.150776	0.038283	-0.088239	-0.214828	-0.327816	-0.415495	-0.469516	-0.485852	
20.0	0.135665	0.030534	-0.090148	-0.213257	-0.325787	-0.416431	-0.476928	-0.502998	
22.5	0.127986	0.032755	-0.079220	-0.195697	-0.304388	-0.394463	-0.457831	-0.490052	
25.0	0.128336	0.045347	-0.055197	-0.161951	-0.263387	-0.349209	-0.411582	-0.446005	
27.5	0.136341	0.067459	-0.019398	-0.113775	-0.204913	-0.283095	-0.340810	-0.373598	
30.0	0.150715	0.097072	0.025386	-0.054736	-0.133290	-0.201154	-0.251194	-0.279072	
32.5	0.169424	0.131222	0.075189	0.010153	-0.054594	-0.110511	-0.150859	-0.171488	
35.0	0.189940	0.166341	0.125300	0.074967	0.023996	-0.019604	-0.049485	-0.061709	
37.5	0.209552	0.198666	0.170795	0.133531	0.095000	0.062753	0.042795	0.038850	
40.0	0.225706	0.224683	0.207094	0.180116	0.151475	0.128375	0.116548	0.119541	
42.5	0.236312	0.241537	0.230488	0.210083	0.187803	0.170632	0.164128	0.171720	
45.0	0.240006	0.247371	0.238565	0.220421	0.200334	0.185216	0.180563	0.189764	

	L=6 MU=1								
	72.5	75.0	77.5	80.0	82.5	85.0	87.5	90.0	
0.0	-0.049050	-0.123613	-0.191006	-0.249180	-0.296369	-0.331138	-0.352431	-0.359602	
2.5	-0.049019	-0.121971	-0.187848	-0.244673	-0.290739	-0.324666	-0.345438	-0.352431	
5.0	-0.048925	-0.117093	-0.178472	-0.231287	-0.274021	-0.305447	-0.324669	-0.331138	
7.5	-0.048771	-0.101929	-0.163161	-0.209431	-0.246722	-0.274066	-0.290757	-0.296369	
10.0	-0.048563	-0.098319	-0.142382	-0.179767	-0.209672	-0.231474	-0.244732	-0.249180	
12.5	-0.048306	-0.084993	-0.116765	-0.143198	-0.163997	-0.178968	-0.187991	-0.191006	
15.0	-0.048008	-0.069556	-0.087089	-0.100834	-0.111085	-0.118141	-0.122260	-0.123613	
17.5	-0.047679	-0.052476	-0.054256	-0.053963	-0.052542	-0.050843	-0.049535	-0.049050	
20.0	-0.047328	-0.034273	-0.019263	-0.004009	0.009851	0.020883	0.027973	0.030418	
22.5	-0.046966	-0.015499	0.016827	0.047511	0.074199	0.094856	0.107911	0.112376	
25.0	-0.046605	0.003275	0.052917	0.099031	0.138548	0.168829	0.187849	0.194334	
27.5	-0.046254	0.021478	0.087910	0.148985	0.200941	0.240554	0.265357	0.273801	
30.0	-0.045925	0.038558	0.120743	0.195857	0.259483	0.307853	0.338082	0.348364	
32.5	-0.045627	0.053996	0.150419	0.238220	0.312396	0.368679	0.403813	0.415757	
35.0	-0.045370	0.067321	0.176036	0.274790	0.358071	0.421186	0.460554	0.473931	
37.5	-0.045162	0.078131	0.196815	0.304453	0.395121	0.463777	0.506579	0.521120	
40.0	-0.045008	0.086095	0.212126	0.326309	0.422419	0.495159	0.540491	0.555889	
42.5	-0.044914	0.090973	0.221502	0.339695	0.439137	0.514378	0.561260	0.577182	
45.0	-0.044883	0.092615	0.224660	0.344202	0.444767	0.520850	0.568253	0.584353	

	L=8 MU=1								
	72.5	75.0	77.5	80.0	82.5	85.0	87.5	90.0	
0.0	-0.034036	0.107662	0.272161	0.441976	0.598655	0.724949	0.806839	0.835192	
2.5	-0.049661	0.089366	0.251240	0.418628	0.573232	0.697936	0.778827	0.806839	
5.0	-0.094483	0.036785	0.191017	0.351337	0.499890	0.619955	0.697931	0.724949	
7.5	-0.162590	-0.043448	0.098807	0.248025	0.387061	0.499823	0.573205	0.598655	
10.0	-0.244944	-0.141181	-0.014185	0.120841	0.247678	0.351064	0.418541	0.441976	
12.5	-0.330495	-0.243979	-0.134218	-0.015304	0.097636	0.190312	0.251035	0.272161	
15.0	-0.407547	-0.338648	-0.246675	-0.144512	-0.046098	0.035342	0.088964	0.107662	
17.5	-0.465209	-0.412847	-0.337830	-0.251810	-0.167499	-0.097022	-0.050352	-0.034036	
20.0	-0.494762	-0.456607	-0.396511	-0.324928	-0.253371	-0.192883	-0.152577	-0.138445	
22.5	-0.490758	-0.463562	-0.415451	-0.355767	-0.294903	-0.242884	-0.208009	-0.195748	
25.0	-0.451740	-0.431752	-0.392168	-0.341347	-0.288678	-0.243266	-0.212674	-0.201896	
27.5	-0.380473	-0.363892	-0.329275	-0.284148	-0.237040	-0.196256	-0.168721	-0.159009	
30.0	-0.283670	-0.267080	-0.234167	-0.191788	-0.147760	-0.109729	-0.084079	-0.075037	
32.5	-0.171243	-0.151973	-0.118139	-0.076080	-0.033058	0.003811	0.028575	0.037289	
35.0	-0.055154	-0.031533	0.004977	0.048410	0.091923	0.128801	0.153424	0.162066	
37.5	0.051971	0.080511	0.120470	0.166141	0.210597	0.248552	0.273485	0.282212	
40.0	0.138329	0.171289	0.214523	0.262487	0.308828	0.347310	0.372716	0.381588	
42.5	0.194327	0.230327	0.275874	0.325513	0.372997	0.412201	0.437998	0.446994	
45.0	0.213717	0.250797	0.297176	0.347424	0.395331	0.434806	0.460753	0.469796	

L=9 MU=1									
$\rightarrow \phi$									
52.5	55.0	57.5	60.0	62.5	65.0	67.5	70.0		
0.0	0.000000	0.000000	0.000000	0.000000	0.000000	0.000000	0.000000	0.000000	
2.5	0.109415	0.137488	0.156883	0.166176	0.165053	0.154325	0.135806	0.112050	
5.0	0.210447	0.264641	0.301715	0.318926	0.315721	0.293773	0.256729	0.209683	
7.5	0.295576	0.372180	0.423690	0.446240	0.439185	0.405149	0.349635	0.280251	
10.0	0.358914	0.452819	0.514349	0.538783	0.525580	0.478419	0.404682	0.314421	
β	12.5	0.396778	0.501970	0.568407	0.590832	0.569024	0.507820	0.416461	0.307331
15.0	0.408019	0.518137	0.584221	0.600807	0.568199	0.492458	0.384613	0.259197	
17.5	0.394052	0.502970	0.563840	0.571314	0.526384	0.436337	0.313843	0.175306	
20.0	0.358604	0.460948	0.512639	0.508716	0.450964	0.347812	0.213322	0.065392	
22.5	0.307200	0.398762	0.438577	0.422284	0.352472	0.238532	0.095562	-0.057519	
25.0	0.246462	0.324460	0.351190	0.323021	0.243271	0.122004	-0.025101	-0.178683	
27.5	0.183295	0.246457	0.260415	0.222321	0.136048	0.011956	-0.134245	-0.283406	
30.0	0.124067	0.172539	0.175417	0.130610	0.042301	-0.079309	-0.219095	-0.358823	
32.5	0.073880	0.108969	0.103533	0.056144	-0.029005	-0.142369	-0.270051	-0.395456	
35.0	0.036015	0.059819	0.049475	0.004095	-0.072450	-0.171769	-0.281830	-0.388366	
37.5	0.011624	0.026582	0.014887	-0.023956	-0.086713	-0.166617	-0.254073	-0.337770	
40.0	-0.000310	0.008128	-0.001710	-0.030067	-0.074615	-0.130608	-0.191360	-0.249029	
42.5	-0.002726	0.001001	-0.004566	-0.019519	-0.042641	-0.071484	-0.102617	-0.132026	
45.0	0.000000	0.000000	0.000000	0.000000	0.000000	0.000000	0.000000	0.000000	
L=9 MU=1									
72.5	75.0	77.5	80.0	82.5	85.0	87.5	90.0		
0.0	0.000000	0.000000	0.000000	0.000000	0.000000	0.000000	0.000000	0.000000	
2.5	0.085991	0.060539	0.038185	0.020674	0.008792	0.002296	0.000001	0.000000	
5.0	0.158469	0.108852	0.065749	0.032584	0.010863	0.000045	-0.002291	0.000000	
7.5	0.205648	0.134338	0.073537	0.028214	0.000477	-0.010620	-0.008821	0.000000	
10.0	0.218980	0.129444	0.055136	0.002386	-0.026263	-0.032298	-0.020888	0.000000	
12.5	0.194275	0.090711	0.007820	-0.046939	-0.070785	-0.065885	-0.038920	0.000000	
15.0	0.132283	0.019316	-0.066972	-0.118264	-0.131737	-0.110360	-0.062371	0.000000	
17.5	0.038673	-0.078965	-0.163683	-0.206595	-0.205025	-0.162817	-0.089730	0.000000	
20.0	-0.076596	-0.194366	-0.273201	-0.303939	-0.284211	-0.218741	-0.118672	0.000000	
22.5	-0.200438	-0.314247	-0.383877	-0.400184	-0.361215	-0.272495	-0.146300	0.000000	
25.0	-0.318189	-0.424580	-0.482889	-0.484269	-0.427243	-0.317969	-0.169483	0.000000	
27.5	-0.415372	-0.511626	-0.557769	-0.545505	-0.473836	-0.349305	-0.185224	0.000000	
30.0	-0.479451	-0.563607	-0.597922	-0.574875	-0.493905	-0.361615	-0.191028	0.000000	
32.5	-0.501363	-0.572165	-0.595954	-0.566178	-0.482628	-0.351601	-0.185224	0.000000	
35.0	-0.476658	-0.533432	-0.548638	-0.516853	-0.438106	-0.318014	-0.167192	0.000000	
37.5	-0.406086	-0.448585	-0.457413	-0.428398	-0.361692	-0.261875	-0.137479	0.000000	
40.0	-0.295576	-0.323809	-0.328336	-0.306326	-0.257948	-0.186443	-0.097784	0.000000	
42.5	-0.155602	-0.169676	-0.171504	-0.159656	-0.134240	-0.096932	-0.050810	0.000000	
45.0	0.000000	0.000000	0.000000	0.000000	0.000000	0.000000	0.000000	0.000000	

Table 15.4.2

Cubic spherical harmonics $\dot{k}_l^m(hkl)$ for $l = 4$ (1) 34, $\mu = 1$ (1) M (1). The functions $\dot{k}_l^\mu(hkl)$ ($\Phi_{hkl}\beta_{hkl}$) are the same as in Table 15.4.1. The angles $\Phi_{hkl}\beta_{hkl}$ correspond to some low-index crystal directions (for values for some other crystal directions and for $l = 4$ (2) 50 see reference I, p. 312)

L	MU	(100)	(110)	(111)	(102)	(112)	(122)	(103)	(113)
4	1	0.646360	-0.161590	-0.430907	0.129272	-0.161590	-0.311211	0.355498	0.138887
6	1	-0.359602	0.584353	-0.639292	0.244529	-0.184795	-0.152424	-0.019778	-0.047551
8	1	0.835192	0.469796	0.247464	-0.180402	-0.334464	0.193618	-0.078090	-0.490545
10	1	-0.531858	0.016621	0.840467	0.535262	-0.430288	-0.133566	0.381688	-0.218541
12	1	0.924258	-0.447688	-0.121713	0.468784	0.232194	-0.207514	-0.102015	-0.392450
2	2	0.328762	0.718311	0.573042	-0.250210	0.334182	0.633504	-0.359284	0.376019
14	1	-0.668562	0.464860	-0.704329	0.134568	0.581660	-0.167142	0.553458	-0.413152
16	1	0.989941	0.498838	0.057939	0.291908	0.097226	0.196703	0.421933	0.194874
2	2	0.488903	0.111517	-0.982131	0.277547	-0.076524	0.591730	-0.429904	0.376734
18	1	-0.727509	-0.316864	0.454180	0.212698	0.346318	0.450110	0.237967	0.312476
2	2	-0.296856	0.822660	-0.328664	-0.407857	-0.440364	0.366529	0.167465	-0.193169
20	1	1.044404	-0.521182	-0.027167	0.460124	-0.166746	-0.163702	0.698276	0.398031
2	2	0.616464	0.512617	1.076393	0.412836	0.130870	-0.005070	-0.081807	-0.213344
22	1	-0.764144	-0.397370	-0.265028	0.689465	-0.752474	-0.482799	0.061950	0.847189
2	2	-0.456319	0.180268	0.854396	-0.318991	-0.171229	0.132098	-0.176246	-0.038790
24	1	1.091456	0.545995	0.012618	0.109312	0.016109	0.132908	0.225940	0.045762
2	2	0.675726	-0.250692	-0.867288	0.072348	-0.603878	-0.156775	0.222075	-0.349110
3	3	0.266227	0.910061	0.031153	-0.039056	0.263734	0.518666	0.247155	0.235923
26	1	-0.794565	-0.392530	0.146976	0.198893	0.087972	0.453062	0.407761	0.121142
2	2	-0.582038	0.565644	-1.222427	0.217060	0.481273	-0.206809	-0.506445	-0.298222
28	1	1.133106	-0.566484	-0.005822	0.543205	0.080735	-0.108643	-0.388678	-0.272963
2	2	0.705728	0.385769	0.600748	0.499076	0.107769	0.116292	0.058063	-0.017930
3	3	0.426506	0.234526	-0.517047	-0.509653	0.183369	-0.886890	0.474069	0.482342
30	1	-0.821685	0.412272	-0.078811	-0.180697	0.517154	-0.433742	0.836381	-0.637477
2	2	-0.647353	-0.191508	1.216307	0.074335	-0.032335	-0.311422	-0.365178	-0.071246
3	3	-0.237348	0.985114	0.216018	0.355957	-0.547894	-0.445061	-0.243919	-0.329376
32	1	1.170612	0.585324	0.002673	-0.363091	-0.040768	0.088846	-0.268408	-0.164034
2	2	0.728292	-0.352578	-0.384193	0.778992	0.843205	-0.192653	-0.199003	-0.086997
3	3	0.553203	0.618642	1.083392	-0.287269	-0.075231	0.246915	0.282996	0.075815
34	1	-0.846351	-0.422756	0.041233	0.420174	-0.299662	0.412962	0.719441	-0.603763
2	2	-0.677107	0.394670	-0.989719	-0.021957	0.068783	0.501131	-0.058936	0.639328
3	3	-0.397832	0.278842	0.085164	-0.047049	0.062944	0.143858	-0.029169	-0.081981

L	MU	(123)	(135)	(137)	(157)	(124)	(357)
4	1	-0.161590	-0.036935	0.183083	-0.099970	0.030779	-0.240755
6	1	0.039446	0.220751	0.092476	0.391758	0.072573	-0.124001
8	1	-0.099986	-0.144461	-0.297544	0.132521	-0.358841	-0.038384
9	1	0.550098	0.570020	0.380593	0.387829	0.532330	0.409650
10	1	-0.299994	0.019644	0.274712	0.071366	-0.105592	-0.283071
12	1	0.166647	0.324683	0.038278	0.164428	0.132036	0.102714
2	-0.209780	-0.075657	-0.144095	0.088967	0.080942	-0.261486	
13	1	-0.399473	0.075692	0.627553	-0.116960	0.319073	-0.520949
14	1	-0.073226	-0.304412	-0.074799	-0.116664	-0.327335	0.192896
15	1	-0.146067	0.407866	-0.106879	0.705063	-0.134460	-0.484420
16	1	-0.259345	-0.325469	0.338730	-0.402855	0.076347	-0.146163
2	-0.369308	-0.269878	0.010168	-0.041817	-0.204201	0.040507	
17	1	-0.104013	-0.277863	0.168436	0.195975	-0.557868	0.200864
18	1	-0.207070	-0.269660	-0.396965	0.053846	-0.201480	-0.166812
2	0.288232	0.259065	0.089417	-0.088786	0.426317	0.208037	
19	1	-0.328477	0.232872	0.342456	0.047591	-0.082338	0.136884
20	1	0.190094	-0.091219	-0.201481	0.442024	-0.305154	0.160053
2	0.486475	-0.267359	-0.078258	-0.265738	-0.302465	0.511129	
21	1	0.324377	0.361470	-0.288245	0.065858	-0.246867	0.108483
2	-0.442111	-0.177003	-0.292678	0.593096	0.019571	-0.157159	
22	1	0.408097	-0.148228	-0.366180	-0.225169	-0.181117	0.407483
2	-0.050741	-0.175173	0.291952	-0.262431	0.265006	0.225885	
23	1	0.069880	-0.553805	0.480954	-0.003892	-0.402281	0.281628
24	1	0.006896	0.354802	-0.497912	-0.320307	0.079737	-0.100791
2	0.172375	-0.245743	-0.204219	-0.299037	0.417601	-0.137076	
3	-0.148419	0.477617	-0.189405	0.126449	-0.103072	-0.471466	
25	1	-0.391465	-0.238542	0.064728	-0.285110	0.416528	-0.245524
2	-0.158762	-0.159733	-0.321432	0.180713	-0.153108	0.406018	
26	1	0.023352	0.121360	-0.314781	0.026377	0.293755	-0.382901
2	0.344575	-0.220387	0.238471	-0.271570	-0.263461	-0.353451	
27	1	0.045616	-0.137700	-0.225975	0.247308	-0.256556	-0.325748
2	0.326046	0.015622	0.129959	0.124898	0.376916	0.417713	
28	1	-0.150711	-0.310177	0.111694	0.040060	0.286429	0.011264
2	0.035171	-0.273594	-0.205380	-0.144108	0.365166	-0.316540	
3	0.006725	0.199400	0.079810	-0.327197	0.000642	0.226775	
29	1	0.291204	-0.290690	0.296456	0.408433	-0.140003	0.271318
2	0.776078	-0.488542	0.056795	-0.313468	-0.320820	0.071020	
30	1	-0.394045	-0.091422	-0.218231	-0.024095	0.526569	0.054409
2	0.056783	0.313691	-0.026402	0.517445	0.070177	-0.179239	
3	-0.528537	0.015310	-0.261218	0.505537	0.074817	0.030633	
31	1	0.215169	0.015514	-0.683609	-0.432818	0.204836	0.342632
2	0.126380	-0.282849	0.050788	0.055322	0.438052	-0.035634	
32	1	0.176994	0.010428	0.404705	0.255594	-0.172355	0.052279
2	-0.101277	0.517330	-0.362078	-0.096846	0.063680	0.082750	
3	0.028500	-0.229875	0.444306	-0.187470	-0.293948	-0.315894	
33	1	0.004095	0.509929	-0.310950	-0.379310	-0.295335	-0.208143
2	-0.113349	-0.298222	0.054928	0.137348	0.341329	-0.437367	
3	-0.100774	0.505079	-0.025002	-0.193225	-0.263706	-0.413331	
34	1	0.466483	0.062594	-0.006810	-0.022070	-0.270940	0.253146
2	-0.253829	0.056369	0.156517	-0.201310	0.296971	0.103743	
3	-0.009993	0.095504	-0.473521	-0.130682	-0.001212	0.186023	

Table 15.5 Cubic generalized spherical harmonics

Table 15.5.1 Cubic-orthorhombic generalized harmonics $T_l^{\mu n}$. The functions are defined by equation (14.262) with the coefficients of *Table 15.2.1*.

Table 15.5.1.1 The cubic-orthorhombic functions $T_l^{\mu n}(\varphi_1 \Phi \varphi_2)$ in sections $\varphi_2 = \text{const.}$ for $l = 4, 8, \mu = 1, n = 2, 4, 8, 9, \varphi_1 = 0^\circ (10^\circ) 90^\circ, \Phi = 0^\circ (10^\circ) 90^\circ, \varphi_2 = 0^\circ (10^\circ) 80^\circ$ (see also *Figure A.4.3.1 (a)-(n)* and reference 76)

L=4 MU=1 N=2		SECTION	PHI2= 0
0	10	20	30
0	0.0000	0.0000	0.0000
10	-0.0999	-0.0939	-0.0765
20	-0.3528	-0.3315	-0.2703
30	-0.6404	-0.6018	-0.4906
40	-0.8282	-0.7782	-0.6344
50	-0.8282	-0.7782	-0.6344
60	-0.6404	-0.6018	-0.4906
70	-0.3528	-0.3315	-0.2703
80	-0.0999	-0.0939	-0.0765
90	0.0000	0.0000	0.0000
L=4 MU=1 N=2		SECTION	PHI2=10
0	10	20	30
0	0.0000	0.0000	0.0000
10	-0.0940	-0.0827	-0.0615
20	-0.3308	-0.2902	-0.2146
30	-0.5967	-0.5201	-0.3807
40	-0.7627	-0.6573	-0.4726
50	-0.7453	-0.6296	-0.4379
60	-0.5468	-0.4434	-0.2866
70	-0.2543	-0.1823	-0.0882
80	-0.0001	0.0315	0.0593
90	0.0999	0.0939	0.0765
L=4 MU=1 N=2		SECTION	PHI2=20
0	10	20	30
0	0.0000	0.0000	0.0000
10	-0.0789	-0.0656	-0.0444
20	-0.2751	-0.2269	-0.1513
30	-0.4861	-0.3945	-0.2553
40	-0.5968	-0.4698	-0.2861
50	-0.5356	-0.3948	-0.2064
60	-0.3097	-0.1831	-0.0345
70	-0.0048	0.0823	0.1596
80	0.2526	0.2858	0.2845
90	0.3528	0.3315	0.2703

SECTION PHI2=30									
$\rightarrow \varphi_1$									
0	10	20	30	40	50	60	70	80	90
0	0.0000	0.0000	0.0000	0.0000	0.0000	0.0000	0.0000	0.0000	0.0000
10	-0.0618	-0.0506	-0.0333	-0.0119	0.0109	0.0324	0.0499	0.0615	0.0656
20	-0.2117	-0.1712	-0.1100	-0.0355	0.0433	0.1168	0.1763	0.2145	0.2268
30	-0.3602	-0.2838	-0.1730	-0.0415	0.0951	0.2202	0.3188	0.3789	0.3933
40	-0.4083	-0.3036	-0.1623	-0.0014	0.1596	0.3014	0.4068	0.4632	0.4637
50	-0.2971	-0.1837	-0.0483	0.0930	0.2231	0.3263	0.3901	0.4069	0.3746
60	-0.0400	0.0572	0.1476	0.2201	0.2662	0.2801	0.2602	0.2089	0.1325
70	0.2789	0.3384	0.3572	0.3328	0.2684	0.1715	0.0540	-0.0701	-0.1857
80	0.5400	0.5500	0.4937	0.3778	0.2164	0.0289	-0.1621	-0.3336	-0.4648
90	0.6404	0.6018	0.4906	0.3202	0.1112	-0.1112	-0.3202	-0.4906	-0.6018

L=4 MU=1 N=2 SECTION PHI2=40

0	10	20	30	40	50	60	70	80	90
0	0.0000	0.0000	0.0000	0.0000	0.0000	0.0000	0.0000	0.0000	0.0000
10	-0.0507	-0.0447	-0.0333	-0.0178	-0.0003	0.0173	0.0329	0.0444	0.0506
20	-0.1704	-0.1491	-0.1099	-0.0574	0.0202	0.0612	0.1130	0.1512	0.1711
30	-0.2781	-0.2397	-0.1724	-0.0843	0.0140	0.1106	0.1938	0.2537	0.2830
40	-0.2852	-0.2364	-0.1590	-0.0625	0.0415	0.1406	0.2226	0.2779	0.2996
50	-0.1414	-0.0952	-0.0375	0.0247	0.0839	0.1330	0.1661	0.1791	0.1705
60	0.1360	0.1652	0.1746	0.1628	0.1315	0.0842	0.0269	-0.0338	-0.0903
70	0.4640	0.4662	0.4122	0.3084	0.1674	0.0063	-0.1556	-0.2988	-0.4059
80	0.7275	0.7005	0.5889	0.4064	0.1748	-0.0779	-0.3212	-0.5257	-0.6668
90	0.8282	0.7782	0.6344	0.4141	0.1438	-0.1438	-0.4141	-0.6344	-0.7782

L=4 MU=1 N=2 SECTION PHI2=50

0	10	20	30	40	50	60	70	80	90
0	0.0000	0.0000	0.0000	0.0000	0.0000	0.0000	0.0000	0.0000	0.0000
10	-0.0507	-0.0506	-0.0444	-0.0329	-0.0173	0.0003	0.0178	0.0333	0.0447
20	-0.1704	-0.1711	-0.1512	-0.1130	-0.0612	-0.0020	0.0574	0.1099	0.1491
30	-0.2781	-0.2830	-0.2537	-0.1938	-0.1106	-0.0140	0.0843	0.1724	0.2397
40	-0.2852	-0.2996	-0.2779	-0.2226	-0.1406	-0.0415	0.0625	0.1590	0.2364
50	-0.1414	-0.1705	-0.1791	-0.1661	-0.1330	-0.0839	0.0247	0.0375	0.0952
60	0.1360	0.0903	0.0338	-0.0269	-0.0842	-0.1315	-0.1628	-0.1746	-0.1652
70	0.4640	0.4059	0.2988	0.1556	-0.0063	-0.1674	-0.3084	-0.4122	-0.4662
80	0.7275	0.6668	0.5257	0.3212	0.0779	-0.1748	-0.4064	-0.5889	-0.7005
90	0.8282	0.7782	0.6344	0.4111	0.1438	-0.1438	-0.4141	-0.6344	-0.7782

L=4 MU=1 N=2 SECTION PHI2=60

0	10	20	30	40	50	60	70	80	90
0	0.0000	0.0000	0.0000	0.0000	0.0000	0.0000	0.0000	0.0000	0.0000
10	-0.0618	-0.0656	-0.0615	-0.0499	-0.0324	-0.0109	0.0119	0.0333	0.0506
20	-0.2117	-0.2268	-0.2145	-0.1763	-0.1168	-0.0433	0.0355	0.1100	0.1712
30	-0.3602	-0.3933	-0.3789	-0.3188	-0.2202	-0.0951	0.0415	0.1730	0.2838
40	-0.4083	-0.4637	-0.4632	-0.4068	-0.3014	-0.1596	0.0014	0.1623	0.3036
50	-0.2971	-0.3746	-0.4069	-0.3901	-0.3263	-0.2231	-0.0930	0.0483	0.1837
60	-0.0400	-0.1325	-0.2089	-0.2602	-0.2801	-0.2662	-0.2201	-0.1476	-0.0572
70	0.2789	0.1857	0.0701	-0.0540	-0.1715	-0.2684	-0.3328	-0.3572	-0.3384
80	0.5400	0.4648	0.3336	0.1621	-0.0289	-0.2164	-0.3778	-0.4937	-0.5500
90	0.6404	0.6018	0.4906	0.3202	0.1112	-0.1112	-0.3202	-0.4906	-0.6018

L=4 MU=1 N=4 SECTION PHI2=60

SECTION PHI2=70									
$\rightarrow \varphi_1$									
0	10	20	30	40	50	60	70	80	90
0	0.0000	0.0000	0.0000	0.0000	0.0000	0.0000	0.0000	0.0000	0.0000
10	-0.0789	-0.0827	-0.0765	-0.0611	-0.0383	-0.0109	0.0178	0.0444	0.0656
20	-0.2751	-0.2901	-0.2702	-0.2176	-0.1388	-0.0433	0.0575	0.1513	0.2269
30	-0.4861	-0.5190	-0.4894	-0.4007	-0.2637	-0.0949	0.0854	0.2553	0.3945
40	-0.5968	-0.6519	-0.6283	-0.5289	-0.3658	-0.1585	0.0679	0.2861	0.4698
50	-0.5356	-0.6118	-0.6142	-0.5425	-0.4054	-0.2194	-0.0069	0.2064	0.3948
60	-0.3097	-0.3989	-0.4399	-0.4279	-0.3643	-0.2568	-0.1183	0.0345	0.1831
70	-0.0048	-0.0914	-0.1669	-0.2224	-0.2510	-0.2493	-0.2175	-0.1596	-0.0823
80	0.2526	0.1889	0.1025	0.0037	-0.0956	-0.1833	-0.2490	-0.2858	-0.2526
90	0.3528	0.3315	0.2703	0.1764	0.0613	-0.0613	-0.1764	-0.2703	-0.3315

L=4 MU=1 N=2 SECTION PHI2=80

SECTION PHI2=80									
$\rightarrow \varphi_1$									
0	10	20	30	40	50	60	70	80	90
0	0.0000	0.0000	0.0000	0.0000	0.0000	0.0000	0.0000	0.0000	0.0000
10	-0.0940	-0.0939	-0.0825	-0.0611	-0.0324	0.0003	0.0329	0.0615	0.0827
20	-0.3308	-0.3315	-0.2922	-0.2177	-0.1169	-0.0020	0.1132	0.2146	0.2902
30	-0.5967	-0.6014	-0.5335	-0.4013	-0.2207	-0.0134	0.1955	0.3807	0.5201
40	-0.7627	-0.7761	-0.6959	-0.5318	-0.3035	-0.0387	0.2309	0.4726	0.6573
50	-0.7453	-0.7712	-0.7040	-0.5520	-0.3333	-0.0745	0.1934	0.4379	0.6296
60	-0.5468	-0.5842	-0.5512	-0.4516	-0.2977	-0.1078	0.0951	0.2866	0.4434
70	-0.2543	-0.2957	-0.3014	-0.2707	-0.2074	-0.1191	-0.0164	0.0882	0.1823
80	-0.0001	-0.0317	-0.0595	-0.0801	-0.0911	-0.0910	-0.0800	-0.0593	-0.0315
90	0.0999	0.0939	0.0765	0.0499	0.0173	-0.0499	-0.0765	-0.0939	-0.0999

L=4 MU=1 N=4 SECTION PHI2=10

SECTION PHI2=10									
$\rightarrow \varphi_1$									
0	10	20	30	40	50	60	70	80	90
0	0.4945	0.1121	-0.3227	-0.6066	-0.6066	-0.3227	0.1121	0.4945	0.6455
10	0.4801	0.1091	-0.3130	-0.5886	-0.5886	-0.3135	0.1085	0.4797	0.6265
20	0.4452	0.1051	-0.2842	-0.5405	-0.5439	-0.2928	0.0953	0.4388	0.5770
30	0.4100	0.1120	-0.2384	-0.4773	-0.4928	-0.2778	0.0673	0.3808	0.5162
40	0.3971	0.1421	-0.1794	-0.4170	-0.4594	-0.2869	0.0198	0.3173	0.4663
50	0.4201	0.2007							

L=4 MU=1 N=4			SECTION PHI2=20								
$\rightarrow \Phi_1$											
0	10	20	30	40	50	60	70	80	90		
0	0.1121	-0.3227	-0.6066	-0.6066	-0.3227	0.1121	0.4945	0.6455	0.4945	0.1121	
10	-0.1092	-0.3127	-0.5883	-0.5886	-0.3135	0.1082	0.4794	0.6262	0.4800	0.1092	
20	-0.1069	-0.2796	-0.5353	-0.5405	-0.2928	0.0919	0.4336	0.5724	0.4434	0.1069	
30	0.1202	-0.2175	-0.4535	-0.4773	-0.2777	0.0518	0.3571	0.4953	0.4017	0.1202	
40	0.1646	-0.1223	-0.3519	-0.4169	-0.2868	-0.0225	0.2523	0.4091	0.3744	0.1646	
ϕ	0.2456	0.0026	-0.2417	-0.3729	-0.3296	-0.1321	0.1272	0.3270	0.3738	0.2456	
50	0.3536	0.1432	-0.1342	-0.3488	-0.4002	-0.2643	-0.0048	0.2570	0.3986	0.3536	
60	0.4644	0.2777	-0.0389	-0.3374	-0.4780	-0.3949	-0.1271	0.2002	0.4338	0.4644	
70	0.5478	0.3831	0.0391	-0.3232	-0.5342	-0.4953	-0.2247	0.1511	0.4562	0.5478	
80	0.5788	0.4434	0.1005	-0.2894	-0.5439	-0.5439	-0.2894	0.1005	0.4434	0.5788	

L=4 MU=1 N=4			SECTION PHI2=30								
$\rightarrow \Phi_1$											
0	10	20	30	40	50	60	70	80	90		
0	-0.3227	-0.6066	-0.6066	-0.3227	0.1121	0.4945	0.6455	0.4945	0.1121	-0.3227	
10	-0.3125	-0.5880	-0.5883	-0.3133	0.1082	0.4791	0.6258	0.4791	0.1082	-0.3135	
20	-0.2778	-0.5307	-0.5353	-0.2894	0.0919	0.4302	0.5672	0.4302	0.0919	-0.2928	
30	-0.2093	-0.4326	-0.4535	-0.2622	0.0518	0.3415	0.4715	0.3415	0.0518	-0.4540	
40	-0.0999	-0.2949	-0.3519	-0.2443	-0.0224	0.2100	0.3442	0.3173	0.1419	-0.0999	
50	0.0473	-0.1270	-0.2418	-0.2435	-0.1312	0.0424	0.1963	0.2582	0.1994	0.0473	
60	0.2143	0.0519	0.1348	-0.2585	-0.2611	-0.1417	0.0441	0.2093	0.2765	0.2143	
70	0.3712	0.2157	-0.0407	-0.2781	-0.3853	-0.3123	-0.0931	0.1696	0.3530	0.3712	
80	0.4836	0.3383	0.0347	-0.2851	-0.4715	-0.4373	-0.1985	0.1332	0.4026	0.4836	
90	0.5245	0.4018	0.0911	-0.2622	-0.4928	-0.4928	-0.2622	0.0911	0.4018	0.5245	

L=4 MU=1 N=4			SECTION PHI2=40								
$\rightarrow \Phi_1$											
0	10	20	30	40	50	60	70	80	90		
0	-0.6066	-0.6066	-0.3227	0.1121	0.4945	0.6455	0.4945	0.1121	-0.3227	-0.6066	
10	-0.5878	-0.5880	-0.3130	0.1085	0.4791	0.6256	0.4794	0.1088	-0.3127	-0.5880	
20	-0.5289	-0.5307	-0.2842	0.0953	0.4302	0.5638	0.4336	0.1005	-0.2796	-0.5289	
30	-0.4244	-0.4326	-0.2384	0.0673	0.3416	0.4560	0.3571	0.0911	-0.2175	-0.4244	
40	-0.2725	-0.2950	-0.1795	0.0200	0.2101	0.3019	0.2524	0.0848	-0.1225	-0.2725	
50	-0.0822	-0.1274	-0.1130	-0.0457	0.0430	0.1116	0.1280	0.0845	0.0015	-0.0822	
60	0.1234	0.0502	-0.0465	-0.1215	-0.1396	-0.0924	-0.0020	0.0894	0.1389	0.1234	
70	0.3103	0.2106	0.0124	-0.1917	-0.3060	-0.2772	-0.1186	0.0954	0.2648	0.3103	
80	0.4417	0.3256	0.0572	-0.2379	-0.4218	-0.4083	-0.2037	0.0961	0.3510	0.4417	
90	0.4890	0.3746	0.0849	-0.2445	-0.4595	-0.4595	-0.2445	0.0849	0.3746	0.4890	

L=4 MU=1 N=4			SECTION PHI2=50								
$\rightarrow \Phi_1$											
0	10	20	30	40	50	60	70	80	90		
0	-0.6066	-0.3227	0.1121	0.4945	0.6455	0.4945	0.1121	-0.3227	-0.6066		
10	-0.5878	-0.3127	0.1088	0.4794	0.6256	0.4791	0.1085	-0.3120	-0.5880		
20	-0.5289	-0.2796	0.1005	0.4336	0.5638	0.4302	0.0953	-0.2842	-0.5307		
30	-0.4244	-0.2175	0.0911	0.3571	0.4560	0.3416	0.0673	-0.2384	-0.4326		
40	-0.2725	-0.1225	0.0848	0.2524	0.3019	0.2101	0.0200	-0.1795	-0.2950		
50	-0.0822	0.0015	0.0845	0.1280	0.1116	0.0430	-0.0457	-0.1130	-0.1274	-0.0822	
60	0.1234	0.1389	0.0894	-0.0202	-0.0924	-0.1396	-0.1215	-0.0465	0.0502	0.1234	
70	0.3103	0.2648	0.0954	-0.1186	-0.2772	-0.3060	-0.1917	0.0124	0.2106	0.3103	
80	0.4417	0.3510	0.0961	-0.2037	-0.4083	-0.4218	-0.2379	0.0572	0.3256	0.4417	
90	0.4890	0.3746	0.0849	-0.2445	-0.4595	-0.4595	-0.2445	0.0849	0.3746	0.4890	

L=4 MU=1 N=4			SECTION PHI2=60									
$\rightarrow \Phi_1$												
0	10	20	30	40	50	60	70	80	90			
0	-0.3227	0.1121	0.4945	0.6455	0.4945	0.1121	-0.3227	-0.6066	-0.6066	-0.3227		
10	-0.3125	0.1091	0.4797	0.6258	0.4791	0.1082	-0.3133	-0.5883	-0.5880	-0.3125		
20	-0.2778	0.1051	0.4388	0.5672	0.4302	0.0919	-0.2894	-0.5353	-0.5307	-0.2778		
30	-0.2093	0.1120	0.3808	0.4715	0.3415	0.2100	-0.2622	-0.4535	-0.4326	-0.2093		
40	-0.0999	0.1419	0.3173	0.3442	0.2100	0.1120	-0.2093	-0.2443	-0.2418	-0.1270		
ϕ	0.0473	0.1994	0.2582	0.1963	0.2582	0.1994	0.0473	0.1417	0.2611	0.2585	0.1348	
60	0.2143	0.2765	0.2093	0.0441	0.2093	0.2765	0.2143	0.1417	0.2611	0.2585	0.1348	
70	0.3712	0.3530	0.1696	-0.0931	-0.3123	-0.3853	-0.2781	-0.0407	0.2157	0.3712	0.1348	
80	0.4836	0.4026	0.1332	-0.1985	-0.4373	-0.4715	-0.2851	0.0347	0.3383	0.4836	0.1348	
90	0.5245	0.4018	0.0911	-0.2622	-0.4928	-0.4928	-0.2622	0.0911	0.4018	0.5245	0.1348	

L=4 MU=1 N=4			SECTION PHI2=70								
$\rightarrow \Phi_1$											
0	10	20	30	40	50	60	70	80	90		
0	0.1121	0.4945	0.6455	0.4945	0.1121	-0.3227	-0.6066	-0.6066	-0.3227	0.1121	
10	0.1092	0.4800	0.6262	0.4794	0.1082	-0.3135	-0.5886	-0.5883	-0.3127	0.1092	
20	0.1069	0.4434	0.5724	0.4336	0.0919	-0.2928	-0.5405	-0.5353	-0.2796	0.1069	
30	0.1202	0.4017	0.4953	0.3571	0.0518	-0.2777	-0.4773	-0.4535	-0.2175	0.1202	
40	0.1646	0.3744	0.4091	0.2523	-0.0225	-0.2868	-0.4169	-0.3519	-0.1223	0.1646	
50	0.2456	0.3738	0.3270	0.1272	-0.1321	-0.3296	-0.3729	-0.2417	0.0026	0.2456	
60	0.3536	0.3986	0.2570	-0.0048	-0.2643	-0.4002	-0.3488	-0.1342	0.1432	0.3536	
70	0.4644	0.4338	0.2002	-0.1271	-0.3949	-0.4780	-0.3374	-0.0389	0.2777	0.4644	
80	0.5478	0.4562	0.1511	-0.2247	-0.4953	-0.5342	-0.3232	0.0391	0.3831	0.5478	
90	0.5788	0.4434	0.1005	-0.2894	-0.5439	-0.5439	-0.2894	0.1005	0.4434	0.5788	

L=4 MU=1 N=4			SECTION PHI2=80								

<tbl_r cells="2" ix="1" maxcspan="9" maxrspan="1"

L=9	MU=1	N=2	SECTION PHI2=10								
→ Φ ₁											
0	0.0000	0.0000	0.0000	0.0000	0.0000	0.0000	0.0000	0.0000	0.0000	0.0000	0.0000
10	0.1611	0.1050	0.0363	-0.0368	-0.1054	-0.1614	-0.1979	-0.2105	-0.1977	-0.1611	
20	0.3047	0.1934	0.0589	-0.0828	-0.2144	-0.3202	-0.3874	-0.4079	-0.3791	-0.3047	
30	0.0164	-0.0255	-0.0643	-0.0954	-0.1149	-0.1206	-0.1118	-0.0894	-0.0563	-0.0164	
40	-0.4089	-0.3532	-0.2550	-0.1260	0.0181	0.1601	0.2828	0.3714	0.4152	0.4089	
50	-0.3657	-0.3098	-0.2165	-0.0971	0.0340	0.1610	0.2686	0.3438	0.3775	0.3657	
60	0.0887	0.1212	0.1392	0.1403	0.1245	0.0938	0.0516	0.0033	-0.0454	-0.0887	
70	0.2933	0.3768	0.4148	0.4027	0.3421	0.2403	0.1094	-0.0346	-0.1745	-0.2933	
80	0.0155	0.1290	0.2270	0.2975	0.3322	0.3268	0.2820	0.2032	0.0999	-0.0155	
90	-0.2102	-0.1975	-0.1610	-0.1051	-0.0365	0.0365	0.1051	0.1610	0.1975	0.2102	

L=9	MU=1	N=2	SECTION PHI2=20								
→ Φ ₁											
0	0.0000	0.0000	0.0000	0.0000	0.0000	0.0000	0.0000	0.0000	0.0000	0.0000	0.0000
10	0.0366	-0.0366	-0.1054	-0.1615	-0.1981	-0.2108	-0.1981	-0.1615	-0.1054	-0.0366	
20	0.0724	-0.0756	-0.2144	-0.3274	-0.4010	-0.4261	-0.3999	-0.3254	-0.2117	-0.0724	
30	0.0309	-0.0449	-0.1153	-0.1717	-0.2075	-0.2182	-0.2026	-0.1626	-0.1029	-0.0309	
40	-0.0022	0.0061	0.0136	0.0194	0.0229	0.0237	0.0216	0.0169	0.0101	0.0022	
50	0.0789	0.0459	0.0073	-0.0322	-0.0678	-0.0952	-0.1112	-0.1137	-0.1025	-0.0789	
60	0.1667	0.1064	0.0333	-0.0438	-0.1156	-0.1735	-0.2104	-0.2220	-0.2068	-0.1667	
70	0.0511	0.1021	0.1407	0.1624	0.1645	0.1467	0.1112	0.0624	0.0060	-0.0511	
80	-0.2369	-0.1064	0.0369	0.1758	0.2935	0.3758	0.4128	0.3999	0.3389	0.2369	
90	-0.3950	-0.3712	-0.3026	-0.1975	-0.0686	0.0686	0.1975	0.3026	0.3712	0.3950	

L=9	MU=1	N=2	SECTION PHI2=30								
→ Φ ₁											
0	0.0000	0.0000	0.0000	0.0000	0.0000	0.0000	0.0000	0.0000	0.0000	0.0000	0.0000
10	-0.1051	-0.1612	-0.1979	-0.2107	-0.1981	-0.1616	-0.1056	-0.0369	0.0363	0.1051	
20	-0.1975	-0.3133	-0.3913	-0.4220	-0.4019	-0.3333	-0.2245	-0.0886	0.0579	0.1975	
30	0.0000	-0.0763	-0.1433	-0.1931	-0.2196	-0.1931	-0.1433	-0.0763	0.0000		
40	0.3026	0.2522	0.1713	0.0698	-0.0402	-0.1453	-0.2329	-0.2923	-0.3166	-0.3026	
50	0.3026	0.1793	0.0343	-0.1147	-0.2500	-0.3551	-0.4174	-0.4293	-0.3894	-0.3026	
60	0.0000	-0.1524	-0.2864	-0.3859	-0.4388	-0.3859	-0.2864	-0.1524	0.0000		
70	-0.1975	-0.2390	-0.2517	-0.2340	-0.1880	-0.1195	-0.0364	0.0510	0.1322	0.1975	
80	-0.1051	-0.0557	0.0005	0.0565	0.1058	0.1423	0.1616	0.1615	0.1418	0.1051	
90	0.0000	0.0000	0.0000	0.0000	0.0000	0.0000	0.0000	0.0000	0.0000	0.0000	

L=9	MU=1	N=2	SECTION PHI2=40								
→ Φ ₁											
0	0.0000	0.0000	0.0000	0.0000	0.0000	0.0000	0.0000	0.0000	0.0000	0.0000	0.0000
10	-0.1976	-0.2104	-0.1978	-0.1613	-0.1054	-0.0367	0.0363	0.1050	0.1610	0.1976	
20	-0.3771	-0.4051	-0.3843	-0.3171	-0.2117	-0.0807	0.0600	0.1934	0.3036	0.3771	
30	-0.0473	-0.0775	-0.0983	-0.1073	-0.1033	-0.0869	-0.0600	-0.0258	0.0114	0.0473	
40	0.4110	0.3634	0.2719	0.1476	0.0056	-0.1372	-0.2634	-0.3578	-0.4091	-0.4110	
50	0.2868	0.2073	0.1028	-0.0140	-0.1292	-0.2288	-0.3008	-0.3365	-0.3316	-0.2868	
60	-0.2553	-0.3280	-0.3612	-0.3507	-0.2980	-0.2093	-0.0954	0.0300	0.1518	0.2553	
70	-0.3445	-0.3708	-0.3524	-0.2915	-0.1954	-0.0758	0.0530	0.1754	0.2766	0.3445	
80	0.2214	0.2098	0.1729	0.1152	0.0436	-0.0333	-0.1062	-0.1663	-0.2063	-0.2214	
90	0.6052	0.5687	0.4636	0.3026	0.1051	-0.1051	-0.3026	-0.4636	-0.5687	-0.6052	

L=9	MU=1	N=2	SECTION PHI2=50								
→ Φ ₁											
0	0.0000	0.0000	0.0000	0.0000	0.0000	0.0000	0.0000	0.0000	0.0000	0.0000	0.0000
10	-0.1976	-0.1610	-0.1050	-0.0363	0.0367	0.1050	0.1610	0.1976	0.2107	0.2771	0.3771
20	-0.3771	-0.3036	-0.1934	-0.0600	0.0807	0.2117	0.3171	0.3843	0.4051	0.3771	
30	-0.0473	-0.0114	0.0258	0.0600	0.0869	0.1033	0.1073	0.0983	0.0775	0.0473	
40	0.4110	0.4091	0.3578	0.2634	0.1372	-0.0056	-0.1476	-0.2719	-0.3634	-0.4110	
50	0.2868	0.3316	0.3365	0.3008	0.2288	0.1292	0.0140	-0.1028	-0.2073	-0.2868	
60	-0.2553	-0.1518	-0.0300	0.0954	0.2093	0.2980	0.3507	0.3612	0.3280	0.2553	
70	-0.3445	-0.2766	-0.1754	-0.0530	0.0758	0.1954	0.2914	0.3708	0.3445	-0.2098	
80	0.2214	0.2063	0.1663	0.1062	0.0333	-0.0436	-0.1152	-0.1729	-0.2098	-0.2214	
90	0.6052	0.5687	0.4636	0.3026	0.1051	-0.1051	-0.3026	-0.4636	-0.5687	-0.6052	

L=9	MU=1	N=2	SECTION PHI2=60								
→ Φ ₁											
0	0.0000	0.0000	0.0000	0.0000	0.0000	0.0000	0.0000	0.0000	0.0000	0.0000	0.0000
10	-0.1051	-0.1051	-0.0363	0.0369	0.1056	0.1616	0.1981	0.2107	0.1612	0.1051	
20	-0.1975	-0.0579	0.0886	0.2245	0.3333	0.4019	0.4220	0.3913	0.3133	0.1975	
30	0.0000	0.0309	0.1029	0.126	0.2026	0.2182	0.2075	0.1717	0.1153	0.0449	-0.0309
40	0.3026	0.3166	0.2923	0.2329	0.1453	0.0402	-0.0698	-0.1713	-0.2522	-0.3026	
50	0.3026	0.3894	0.4293	0.4174	0.3551	0.2500	0.1147	-0.0343	-0.1793	-0.3026	
60	0.0000	0.1524	0.2864	0.3859	0.4388	0.4388	0.3859	0.2864	0.1524	0.0000	
70	-0.1975	-0.1322	-0.0510	0.0364	0.1112	0.1467	0.1645	-0.1624	-0.1407	-0.1021	-0.0511
80	-0.2369	-0.3389	-0.3999	-0.4128	-0.3758	-0.2935	-0.1758	-0.0369	0.1064	0.2369	
90	0.6050	-0.3712	-0.3026	-0.1975	-0.0686	0.0686	0.1975	0.3026	0.3712	0.3950	

L=9	MU=1	N=2	SECTION PHI2=70								
→ Φ ₁											
0	0.0000	0.									

L=9 MU=1 N=8

SECTION PHI2=0

$\rightarrow \psi_1$										
0	10	20	30	40	50	60	70	80	90	
0	0.5401	0.0938	-0.5075	-0.2700	0.4137	0.4137	-0.2700	-0.5075	0.0938	0.5401
10	0.4337	0.0753	-0.4076	-0.2169	0.3322	0.3322	-0.2169	-0.4076	0.0753	0.4337
20	0.1314	0.0228	-0.1234	-0.0657	0.1006	0.1006	-0.0657	-0.1234	0.0228	0.1314
30	-0.2700	-0.0469	0.2537	0.1350	-0.2069	-0.2069	0.1350	0.2537	-0.0469	-0.2700
40	-0.5651	-0.0981	0.5310	0.2825	-0.4329	-0.4329	0.2825	0.5310	-0.0981	-0.5651
50	-0.5651	-0.0981	0.5310	0.2825	-0.4329	-0.4329	0.2825	0.5310	-0.0981	-0.5651
60	-0.2700	-0.0469	0.2537	0.1350	-0.2069	-0.2069	0.1350	0.2537	-0.0469	-0.2700
70	0.1314	0.0228	-0.1234	-0.0657	0.1006	0.1006	-0.0657	-0.1234	0.0228	0.1314
80	0.4337	0.0753	-0.4076	-0.2169	0.3322	0.3322	-0.2169	-0.4076	0.0753	0.4337
90	0.5401	0.0938	-0.5075	-0.2700	0.4137	0.4137	-0.2700	-0.5075	0.0938	0.5401

L=9 MU=1 N=8

SECTION PHI2=40

$\rightarrow \psi_1$										
0	10	20	30	40	50	60	70	80	90	
0	0.4137	0.4137	-0.2700	-0.5075	0.0938	0.5401	0.0938	-0.5075	-0.2700	0.4137
10	0.3406	0.3385	-0.2231	-0.4159	0.0786	0.4433	0.0753	-0.4171	-0.2202	0.3406
20	0.2063	0.1790	-0.1441	-0.2291	0.0645	0.2515	0.0228	-0.2436	-0.1074	0.2063
30	0.1449	0.0542	-0.1261	-0.0980	0.0920	0.1300	-0.0469	-0.1463	-0.0039	0.1449
40	0.1545	0.0034	-0.1533	-0.0566	0.1337	0.1031	-0.0979	-0.1371	0.0503	0.1545
50	0.1082	-0.0286	-0.1181	-0.0124	0.1138	0.0519	-0.0958	-0.0852	0.0662	0.1082
60	-0.0692	-0.0901	0.0379	0.1033	-0.0020	-0.1040	-0.0341	0.0922	0.0661	-0.0692
70	-0.3112	-0.1540	0.2577	0.2435	-0.1731	-0.3036	0.0677	0.3271	0.0459	-0.3112
80	-0.4984	-0.1609	0.4426	0.3146	-0.3333	-0.4303	0.1839	0.4942	-0.0122	-0.4984
90	-0.5651	-0.0981	0.5310	0.2825	-0.4329	-0.2825	0.5310	-0.0981	-0.5651	

L=9 MU=1 N=8

SECTION PHI2=10

0	10	20	30	40	50	60	70	80	90	
0	0.0938	-0.5075	-0.2700	0.4137	0.4137	-0.2700	-0.5075	0.0938	0.5401	0.0938
10	0.0724	-0.4097	-0.2147	0.3352	0.3311	-0.2202	-0.4076	0.0786	0.4349	0.0724
20	-0.0139	-0.1507	-0.0385	0.1373	0.0861	-0.1074	-0.1234	0.0645	0.1458	-0.0139
30	-0.1691	0.1631	0.2257	-0.0847	-0.2551	-0.0039	0.2538	0.0920	-0.2218	-0.1691
40	-0.3021	0.3801	0.4341	-0.2293	-0.5138	0.0509	0.5314	0.1337	-0.4850	-0.3021
50	-0.2860	0.3965	0.4237	-0.2493	-0.5103	0.0721	0.5354	0.1138	-0.4958	-0.2860
60	-0.0947	0.2452	0.1799	-0.1827	0.2433	0.0982	0.2774	-0.0019	-0.2781	-0.0947
70	0.1658	0.0751	-0.1398	-0.1236	0.0968	0.1572	-0.0422	-0.1719	-0.0175	0.1658
80	0.3638	0.0196	-0.3570	-0.1436	0.3071	0.2503	-0.2202	0.3267	0.1067	0.3638
90	0.4337	0.0753	-0.4076	-0.2169	0.3322	0.3322	-0.2169	0.4076	0.0753	0.4337

L=9 MU=1 N=8

SECTION PHI2=50

0	10	20	30	40	50	60	70	80	90	
0	0.4137	-0.2700	-0.5075	0.0938	0.5401	0.0938	-0.5075	-0.2700	0.4137	0.4137
10	0.3406	-0.2202	-0.4171	0.753	0.4433	0.0786	-0.4159	-0.2231	0.3385	0.3406
20	0.2063	-0.104	-0.2436	0.0228	0.2515	0.0645	-0.2291	-0.1441	0.1790	0.2063
30	0.1449	-0.0039	-0.1463	-0.0469	0.1300	0.0920	-0.0980	-0.1261	0.0542	0.1449
40	0.1545	0.0503	-0.1371	-0.0979	0.1031	0.1337	-0.0566	-0.1533	0.0034	0.1545
50	0.1082	0.0662	-0.0852	-0.0958	0.0519	0.1138	-0.0124	-0.1181	0.0286	0.1082
60	-0.0692	0.0661	0.0922	-0.0341	-0.1040	-0.0020	0.1033	0.0379	-0.0901	-0.0692
70	-0.3112	0.0459	0.3271	0.0677	-0.3036	-0.1731	0.2435	0.2577	-0.1540	-0.3112
80	-0.4984	-0.0122	0.4942	0.1839	-0.4303	-0.3333	0.3146	0.4426	-0.1609	-0.4984
90	-0.5651	-0.0981	0.5310	0.2825	-0.4329	-0.2825	0.5310	-0.0981	-0.5651	

L=9 MU=1 N=8

SECTION PHI2=20

0	10	20	30	40	50	60	70	80	90	
0	-0.5075	-0.2700	0.4137	0.4137	-0.2700	-0.5075	0.0938	0.5401	0.0938	-0.5075
10	-0.4130	-0.2147	0.3385	0.3322	-0.2231	-0.4097	0.0808	0.4378	0.0712	-0.4130
20	-0.1924	-0.0385	0.1790	0.1006	-0.1441	-0.1507	0.0918	0.1825	-0.0284	-0.1924
30	0.0242	0.2257	0.0542	-0.2069	-0.1261	-0.1631	0.1827	-0.0996	-0.2173	0.0242
40	0.1476	0.4347	0.0034	-0.4335	-0.1539	-0.3801	0.2859	-0.3835	0.1476	
50	0.1778	0.4296	-0.0286	-0.4396	-0.1240	-0.3965	0.2617	-0.3679	0.1778	
60	0.1639	0.2120	-0.0903	-0.2434	0.0058	0.2454	0.0794	-0.2178	-0.1551	0.1639
70	0.1454	-0.0285	-0.1552	-0.0254	0.1464	0.0763	-0.1199	0.1179	0.0789	0.1454
80	0.1346	-0.0945	-0.1674	0.0363	0.1801	0.0262	-0.1710	0.0856	0.1412	0.1346
90	0.1314	0.0228	-0.1234	-0.0657	0.1006	0.1006	-0.0657	0.1234	0.0228	0.1314

L=9 MU=1 N=8

SECTION PHI2=60

0	10	20	30	40	50	60	70	80	90	
0	-0.5075	0.0938	0.5401	0.0938	-0.5075	-0.2700	0.4137	0.4137	-0.2700	-0.5075
10	-0.4130	0.0712	0.4378	0.0808	-0.4097	-0.2231	0.3322	0.3385	-0.2147	-0.4130
20	-0.1924	-0.0284	0.1825	0.0918	-0.1507	-0.1441	0.1006	0.1790	-0.0385	-0.1924
30	0.0242	-0.2173	-0.0996	0.1827	0.1261	-0.1261	-0.2069	0.0542	0.2257	0.0242
40	0.1476	-0.3835	-0.2808	0.2859	0.3801	-0.1539	-0.4335	0.0034	0.4347	0.1476
50	0.1778	-0.3679	-0.3056	0.2617	0.3965	-0.1240	-0.4136	-0.026	0.4296	0.1778
60	0.1639	-0.1551	-0.2178	0.0794	0.2454	0.0058	-0.2434	0.0903	0.2120	0.1639
70	0.1454	0.0789	-0.1179	-0.1199	0.0763	0.1464	-0.0254	0.1552	-0.0285	0.1454
80	0.1346	0.1412	-0.0856	-0.1710	0.0262	0.1801	0.0363	-0.1674	-0.0945	0.1346
90	0.1314	0.0228	-0.1234	-0.0469	0.1006	0.1006	-0.0657	0.1234	0.0228	0.1314

L=9 MU=1 N=8

SECTION PHI2=30

0	10	20	30	40	50	60	70	80	90	
0	-0.2700	0.4137	0.4137	-0.2700	-0.5075	0.0938	0.5401	0.0938	-0.5075	-0.2700
10	-0.2169	0.3406	0.3352	-0.2242	-0.4130	0.0808	0.4411	0.0724	-0.4159	-0.2169
20	-0.0657	0.2063	0.1373	-0.1586	-0.1924	0.0918	0.2243	-0.0139	-0.2291	-0.0657
30	0.1350	0.1449	-0.0847	-0.1743	0.0241	0.1827	0.0393	-0.1691	-0.0980	0.1350
40	0.2825	0.1552	-0.2286	-0.2346	0.1472	0.2857	-0.0479	-0.3024	0.0571	0.2825
50	0.28									

I=9	MU=1	N=8	SECTION	PHI2=80
$\rightarrow \Phi_1$				
0	0.0938	0.5401	0.0938	-0.5075
10	0.0724	0.4349	0.0786	-0.4076
20	-0.0139	0.1458	0.0645	-0.1234
30	-0.1691	-0.2218	0.0920	0.2538
40	-0.3021	-0.4850	0.1337	0.5314
50	-0.2860	-0.4958	0.1138	0.5354
60	-0.0947	-0.2781	-0.0019	0.2774
70	0.1658	-0.0175	-0.1719	-0.0422
80	0.3638	0.1067	-0.3267	-0.2202
90	0.4337	0.0753	-0.4076	-0.2169
	0	10	20	30
	40	50	60	70
	80	90		

Table 15.5.1.2 Cubic-orthorhombic functions $\dot{T}_l^{\mu n}(g_i)$ for $l = 4(1)22$, $\mu = 1(1)M(1)$, $n = 0(2)l$. The functions $\dot{T}_l^{\mu n}(g_i) = \dot{T}(\Phi_1^i \Phi^i \Phi_2^i)$ correspond to certain low-index orientations according to equations (2.57)–(2.59)

L	MU	N	(100)[001]	(100)[011]	(100)[012]	(110)[001]	(110)[\bar{1}\bar{0}]	(110)[\bar{1}\bar{1}]	(110)[\bar{1}\bar{2}]	
4	1	0	0.7638	0.7638	0.7638	-0.1909	-0.1909	-0.1909	-0.1909	
	2	0	0.0000	0.0000	0.0000	-0.8539	0.8539	0.2846	-0.2846	
	4	0	0.6455	-0.6455	-0.1807	0.4841	0.4841	-0.3765	-0.3765	
	6	1	-0.3536	-0.3536	-0.3536	0.5745	0.5745	0.5745	0.5745	
6	2	0	0.0000	0.0000	0.0000	-0.3202	0.3202	0.1067	-0.1067	
	4	0	0.9354	-0.9354	-0.2619	-0.5846	0.5846	0.4547	0.4547	
	6	0	0.0000	0.0000	0.0000	-0.4750	0.4750	-0.4046	0.4046	
	8	1	0	0.7181	0.7181	0.7181	0.4039	0.4039	0.4039	0.4039
8	2	0	0.0000	0.0000	0.0000	0.2503	-0.2503	-0.0834	0.0834	
	4	0	0.3819	-0.3819	-0.1069	0.5967	0.5967	-0.4641	-0.4641	
	6	0	0.0000	0.0000	0.0000	-0.5577	0.5577	-0.4751	0.4751	
	8	0	0.5818	0.5818	-0.4906	0.3273	0.3273	0.0687	0.0687	
9	1	0	0.0000	0.0000	0.0000	0.0000	0.0000	0.0000	0.0000	
	2	0	0.0000	0.0000	0.0000	-0.7096	0.7096	0.2365	-0.2365	
	4	0	-0.8416	0.8416	0.2357	0.1052	0.1052	-0.0818	-0.0818	
	6	0	0.0000	0.0000	0.0000	-0.3409	0.3409	-0.2904	0.2904	
10	8	0	0.5401	0.5401	-0.4554	-0.6076	-0.6076	-0.1275	-0.1275	
	10	1	0	-0.4114	-0.4114	-0.4114	0.0129	0.0129	0.0129	0.0129
	2	0	0.0000	0.0000	0.0000	-0.4294	0.4294	0.1431	-0.1431	
	4	0	0.5863	-0.5863	-0.1642	0.5680	0.5680	-0.4418	-0.4418	
12	6	0	0.0000	0.0000	0.0000	0.5377	-0.5377	-0.4580	0.4580	
	8	0	0.6978	0.6978	-0.5884	-0.0218	-0.0218	-0.0046	0.0046	
	10	0	0.0000	0.0000	0.0000	-0.4509	0.4509	0.4472	-0.4472	
	12	1	0	0.6553	0.6553	-0.6553	-0.3174	-0.3174	-0.3174	0.3174
12	2	0	0.0000	0.0000	0.0000	-0.4316	0.4316	0.1439	-0.1439	
	4	0	0.4833	-0.4833	-0.1353	-0.1133	-0.1133	0.0881	0.0881	
	6	0	0.0000	0.0000	0.0000	-0.4232	0.4232	-0.3605	0.3605	
	8	0	0.0581	0.0581	-0.0490	0.4947	0.4947	0.1038	-0.1038	
13	10	0	0.0000	0.0000	0.0000	-0.4966	0.4966	0.4926	-0.4926	
	12	0	0.5776	-0.5776	0.4345	0.1723	0.1723	0.0778	-0.0778	
	2	0	0.2331	0.2331	0.2331	0.5093	0.5093	0.5093	-0.5093	
	4	0	0.0000	0.0000	0.0000	-0.3125	0.3125	0.1042	-0.1042	
13	6	0	-0.4214	0.4214	0.1180	-0.3230	-0.3230	0.2512	0.2512	
	8	0	0.0000	0.0000	0.0000	0.1885	-0.1885	0.1606	-0.1606	
	10	0	0.8764	0.8764	-0.7390	0.4451	0.4451	0.0934	0.0934	
	12	0	0.0000	0.0000	0.0000	0.4248	-0.4248	-0.4213	0.4213	
13	1	0	0.0000	0.0000	0.0000	0.3529	0.3529	0.1593	-0.1593	
	2	0	0.0000	0.0000	0.0000	0.0000	0.0000	0.0000	0.0000	
	4	0	0.0000	0.0000	0.0000	0.2126	-0.2126	-0.0709	0.0709	
	4	4	-0.7864	0.7864	0.2202	0.6636	0.6636	-0.5161	-0.5161	
12	6	0	0.0000	0.0000	0.0000	-0.1748	0.1748	-0.1489	0.1489	
	8	0	-0.2282	-0.2282	0.1924	0.4208	0.4208	0.0883	-0.0883	
	10	0	0.0000	0.0000	0.0000	0.2690	-0.2690	-0.2668	0.2668	
	12	0	0.5740	-0.5740	0.4317	-0.4843	-0.4843	-0.2186	0.2186	

L	M	N	(100)[001]	(100)[011]	(100)[012]	(110)[001]	(110)[$\bar{1}\bar{1}0$]	(110)[$\bar{1}\bar{1}1$]	(110)[$\bar{1}\bar{1}2$]
14	1	0	-0.4401	-0.4401	-0.4401	0.3060	0.3060	0.3060	0.3060
	2	0,0000	0,0000	0,0000	-0,0853	0,0853	0,0284	-0,0284	
	4	0,4577	-0,4577	-0,1282	0,1394	0,1394	-0,1085	-0,1085	
	6	0,0000	0,0000	0,0000	-0,7017	0,7017	-0,5977	0,5977	
	8	0,4911	0,4911	-0,4141	-0,3415	-0,3415	-0,0717	-0,0717	
	10	0,0000	0,0000	0,0000	0,2675	-0,2675	-0,2653	0,2653	
	12	0,5963	-0,5963	0,4486	0,1817	0,1817	0,0820	0,0820	
	14	0,0000	0,0000	0,0000	-0,4076	0,4076	-0,2816	0,2816	
15	1	/	0,0000	0,0000	0,0000	0,0000	0,0000	0,0000	0,0000
	2	0,0000	0,0000	0,0000	-0,6310	0,6310	0,2103	-0,2103	
	4	0,2997	-0,2997	-0,0839	0,2904	0,2904	-0,2258	-0,2258	
	6	0,0000	0,0000	0,0000	0,1510	-0,1510	0,1286	-0,1286	
	8	-0,8101	-0,8101	0,6831	0,0253	0,0253	0,0053	0,0053	
	10	0,0000	0,0000	0,0000	0,2930	-0,2930	-0,2906	0,2906	
	12	0,5039	-0,5039	0,3790	0,4881	0,4881	0,2203	0,2203	
	14	0,0000	0,0000	0,0000	0,4122	-0,4122	0,2848	-0,2848	
16	1	0	0,6109	0,6109	0,6109	0,3078	0,3078	0,3078	0,3078
	2	0,0000	0,0000	0,0000	0,3736	-0,3736	-0,1245	0,1245	
	4	0,5295	-0,5295	-0,1483	0,2999	0,2999	-0,2333	-0,2333	
	6	0,0000	0,0000	0,0000	0,0321	-0,0321	0,0273	-0,0273	
	8	0,1143	0,1143	-0,0964	0,3147	0,3147	0,0661	0,0661	
	10	0,0000	0,0000	0,0000	-0,4239	0,4239	0,4204	-0,4204	
	12	0,0067	-0,0067	0,0050	0,5150	0,5150	0,2324	0,2324	
	14	0,0000	0,0000	0,0000	-0,3498	0,3498	-0,2417	0,2417	
	16	0,5774	0,5774	0,2436	0,0917	0,0917	-0,0836	0,0836	
2	0	0,3018	0,3018	0,3018	0,0688	0,0688	0,0688	0,0688	
	2	0,0000	0,0000	0,0000	-0,3577	0,3577	0,1192	-0,1192	
	4	-0,4490	0,4490	0,1257	0,4535	0,4535	-0,3527	0,3527	
	6	0,0000	0,0000	0,0000	0,1998	-0,1998	0,1702	-0,1702	
	8	0,4245	0,4245	-0,3580	-0,4237	0,4237	-0,0889	-0,0889	
	10	0,0000	0,0000	0,0000	-0,4746	0,4746	0,4707	-0,4707	
	12	0,7260	-0,7260	0,5461	-0,1305	0,1305	-0,0589	0,0589	
	14	0,0000	0,0000	0,0000	0,1932	-0,1932	0,1335	-0,1335	
	16	0,0000	0,0000	0,0000	0,4034	0,4034	-0,3678	0,3678	
17	1	0	0,0000	0,0000	0,0000	0,0000	0,0000	0,0000	0,0000
	2	0,0000	0,0000	0,0000	-0,2890	0,2890	0,0963	-0,0963	
	4	-0,7368	0,7368	0,2063	-0,2705	0,2705	0,2104	0,2104	
	6	0,0000	0,0000	0,0000	-0,5449	0,5449	-0,4642	0,4642	
	8	-0,3503	-0,3503	0,2954	0,2217	0,2217	0,0465	0,0465	
	10	0,0000	0,0000	0,0000	-0,4424	0,4424	0,4388	-0,4388	
	12	-0,0383	0,0383	-0,0288	-0,0141	0,0141	-0,0063	0,0063	
	14	0,0000	0,0000	0,0000	0,4098	-0,4098	0,2832	-0,2832	
	16	0,5771	0,5771	0,2435	-0,3652	0,3652	0,3330	0,3330	
18	1	0	-0,4240	-0,4240	-0,4240	-0,1847	-0,1847	-0,1847	-0,1847
	2	0,0000	0,0000	0,0000	-0,2236	0,2236	0,0745	-0,0745	
	4	0,3016	-0,3016	-0,0845	0,3387	0,3387	-0,2635	0,2635	
	6	0,0000	0,0000	0,0000	-0,0106	0,0106	-0,0090	0,0090	
	8	0,6132	0,6132	-0,5171	0,6713	0,6713	0,1409	0,1409	
	10	0,0000	0,0000	0,0000	0,1239	-0,1239	0,1228	0,1228	
	12	0,1318	-0,1318	0,0991	-0,2693	0,2693	-0,1215	0,1215	
	14	0,0000	0,0000	0,0000	0,1660	-0,1660	0,1147	-0,1147	
	16	0,5795	0,5795	0,2445	0,3912	0,3912	-0,3567	0,3567	
	18	0,0000	0,0000	0,0000	-0,2864	0,2864	0,0238	-0,0238	
2	0	-0,1730	-0,1730	-0,1730	0,4794	0,4794	0,4794	0,4794	
	2	0,0000	0,0000	0,0000	-0,3060	0,3060	0,1020	-0,1020	
	4	0,2837	-0,2837	-0,0794	-0,2715	0,2715	0,2112	0,2112	
	6	0,0000	0,0000	0,0000	0,2321	-0,2321	0,1977	-0,1977	
	8	-0,4386	0,4386	0,3698	0,2249	0,2249	0,0472	0,0472	
	10	0,0000	0,0000	0,0000	-0,1086	0,1086	0,1077	-0,1077	

L	M	N	(100)[001]	(100)[011]	(100)[012]	(110)[$\bar{1}\bar{1}1$]	(110)[$\bar{1}\bar{1}0$]	(110)[$\bar{1}\bar{1}1$]	(110)[$\bar{1}\bar{1}2$]
18	2	12	0,8350	-0,8350	0,6281	-0,3555	-0,3555	-0,1605	-0,1605
	14	0,0000	0,0000	0,0000	-0,4044	0,4044	-0,2794	0,2794	
	16	0,0000	0,0000	0,0000	-0,3401	0,3401	0,3101	0,3101	
	18	0,0000	0,0000	0,0000	-0,2845	0,2845	0,0236	-0,0236	
19	1	0	0,0000	0,0000	0,0000	0,0000	0,0000	0,0000	0,0000
	2	0,0000	0,0000	0,0000	0,1410	-0,1410	-0,0470	0,0470	
	4	0,3891	-0,3891	-0,1089	0,4802	0,4802	-0,3735	-0,3735	
	6	0,0000	0,0000	0,0000	-0,4927	0,4927	-0,4197	0,4197	
	8	-0,6510	0,6510	0,5489	-0,1526	-0,1526	-0,0320	-0,0320	
	10	0,0000	0,0000	0,0000	-0,0543	0,0543	0,0538	-0,0538	
	12	-0,3222	0,3222	-0,2424	0,3978	-0,3978	-0,1795	0,1795	
	14	0,0000	0,0000	0,0000	-0,3263	0,3263	-0,2255	0,2255	
	16	0,5665	0,5665	0,2391	0,1328	0,1328	-0,1211	0,1211	
	18	0,0000	0,0000	0,0000	0,4451	-0,4451	-0,0369	0,0369	
20	1	0	0,5782	0,5782	0,5782	-0,2885	-0,2885	-0,2885	-0,2885
	2	0,0000	0,0000	0,0000	-0,3730	0,3730	0,1243	-0,1243	
	4	0,5522	-0,5522	-0,1546	0,2669	-0,2669	0,2076	-0,2076	
	6	0,0000	0,0000	0,0000	-0,2002	0,2002	-0,1705	0,1705	
	8	0,1646	0,1646	-0,1388	0,0104	0,0104	0,0022	0,0022	
	10	0,0000	0,0000	0,0000	-0,2427	0,2427	0,2407	-0,2407	
	12	0,0193	-0,0193	0,0145	0,3600	0,3600	0,1625	-0,1625	
	14	0,0000	0,0000	0,0000	-0,4836	0,4836	-0,3341	0,3341	
	16	0,0007	0,0007	0,0003	0,4326	0,4326	-0,395	0,3945	
	18	0,0000	0,0000	0,0000	-0,2332	0,2332	0,0193	-0,0193	
	20	0,5774	-0,5774	-0,5707	0,0486	0,0486	0,0471	-0,0471	
2	0	0,3413	0,3413	0,3413	0,2838	0,2838	0,2838	-0,2838	
	2	0,0000	0,0000	0,0000	-0,1674	0,1674	-0,0558	0,0558	
	4	-0,4440	0,4440	0,1243	0,1077	0,1077	-0,0838	0,0838	
	6	0,0000	0,0000	0,0000	-0,4410	0,4410	-0,3757	0,3757	
	8	0,2283	-0,2283	-0,1925	0,0330	0,0330	0,0069	-0,0069	
	10	0,0000	0,0000	0,0000	0,5822	-0,5822	0,5774	-0,5774	
	12	0,5077	-0,5077	0,3819	0,3362	0,3362	0,1518	-0,1518	
	14	0,0000	0,0000	0,0000	-0,1262	0,1262	-0,0872	0,0872	
	16	0,6136	-0,6136	0,2589	-0,2232	0,2232	0,2036	-0,2036	
	18	0,0000	0,0000	0,0000	0,0195	-0,0195	-0,0016	0,0016	
21	1	0	0,0000	0,0000	0,0000	0,4076	0,4076	0,3942	-0,3942
	2	0,0000	0,0000	0,0000	0,2192	-0,2192	-0,0731	0,0731	
	4	-0,6860	0,6860	0,1921	0,3738	0,3738	-0,2908	0,2908	
	6	0,0000	0,0000	0,0000	0,2289	-0,2289	0,1950	-0,1950	
	8	-0,4343	0,4343	0,3662	0,4267	0,4267	0,0896	-0,0896	
	10	0,0000	0,0000	0,0000	-0,2429	0,2429	0,2409	-0,2409	
	12	-0,0861	0,0861	-0,0648	0,4345	0,4345	0,1961	-0,1961	
	14	0,0000	0,0000	0,0000	-0,1549	0,1549	-0,1070	0,1070	
	16	-0,0050	0,0050	-0,0021	0,2320	0,2320	0,2116	-0,2116	
	18	0,0000	0,0000	0,0000	0,4351	-0,4351	-0,0361	0,0361	
	20	0,5773	-0,5773	-0,5707	0,2506	-0,2506	-0,2424	0,2424	

L	MU	N	(100)[001]	(100)[011]	(100)[012]	(110)[001]	(110)[110]	(110)[111]	(110)[112]
22	1	4	0.1816	-0.1816	-0.0508	-0.0184	-0.0184	0.0143	0.0143
	6	0.0000	0.0000	0.0000	-0.4654	0.4654	-0.3965	0.3965	
	8	0.6431	0.6431	-0.5423	-0.0053	-0.0053	-0.0011	-0.0011	
	10	0.0000	0.0000	0.0000	-0.5973	0.5973	0.5924	-0.5924	
	12	0.2371	-0.2371	0.1784	0.0395	0.0395	0.0178	0.0178	
	14	0.0000	0.0000	0.0000	0.1780	-0.1780	0.1230	-0.1230	
	16	0.0233	0.0233	0.0098	-0.3202	-0.3202	0.2920	0.2920	
	18	0.0000	0.0000	0.0000	-0.1120	0.1120	0.0093	-0.0093	
	20	0.5776	-0.5776	-0.5709	0.4226	0.4226	0.4087	0.4087	
	22	0.0000	0.0000	0.0000	-0.1870	0.1870	0.1051	-0.1051	
2	0	-0.2411	-0.2411	-0.2411	0.0953	0.0953	0.0953	0.0953	
	2	0.0000	0.0000	0.0000	-0.3287	0.3287	0.1096	-0.1096	
	4	0.3588	-0.3588	-0.1005	0.3938	0.3938	-0.3063	-0.3063	
	6	0.0000	0.0000	0.0000	0.1136	-0.1136	0.0968	-0.0968	
	8	-0.3968	-0.3968	0.3346	-0.3944	-0.3944	-0.0828	-0.0828	
	10	0.0000	0.0000	0.0000	-0.1572	0.1572	0.1559	-0.1559	
	12	0.3178	-0.3178	0.2390	0.3166	0.3166	0.1429	0.1429	
	14	0.0000	0.0000	0.0000	0.4372	-0.4372	0.3021	-0.3021	
	16	0.7447	0.7447	0.3143	0.2216	0.2216	-0.2021	-0.2021	
	18	0.0000	0.0000	0.0000	-0.0593	0.0593	0.0049	-0.0049	
	20	0.0000	0.0000	0.0000	-0.2434	0.2434	-0.2355	-0.2355	
	22	0.0000	0.0000	0.0000	-0.3623	0.3623	0.2036	-0.2036	

L	MU	N	(111)[110]	(111)[112]	(112)[110]	(112)[111]	(112)[112]	(441)[111]	(441)[112]
12	2	2	0.0000	0.0000	0.3129	-0.3129	-0.1422	0.0967	-0.1604
	4	0.0000	0.0000	0.4302	0.4302	-0.2524	0.5176	0.4476	
	6	-0.3999	0.3999	-0.2597	0.2597	-0.2565	0.1093	0.2248	
	8	0.0000	0.0000	0.2519	0.2519	-0.0784	-0.0982	-0.0716	
	10	0.0000	0.0000	0.0962	-0.0962	-0.0678	0.3630	0.1921	
	12	0.4957	0.4957	0.3026	0.3026	0.2881	0.1588	0.4718	
13	1	0	0.0000	0.0000	-0.4120	0.4120	0.1873	-0.5075	-0.3416
	2	0.0000	0.0000	-0.0980	-0.0980	0.0575	-0.0132	0.1978	
	4	0.0000	0.0000	-0.2738	0.2738	-0.2705	-0.2204	-0.0949	
	6	0.4633	-0.4633	-0.2738	0.2738	-0.2705	-0.2204	-0.0949	
	8	0.0000	0.0000	-0.2665	-0.2665	0.0830	0.1627	0.1615	
	10	0.0000	0.0000	0.2225	-0.2225	-0.1569	-0.1616	-0.2121	
	12	0.4535	0.4535	0.2132	-0.2132	0.2030	0.0687	0.3573	
14	1	0	-0.4636	-0.4636	0.3829	0.3829	-0.2085	-0.1871	
	2	0.0000	0.0000	-0.0434	0.0434	0.0197	0.3393	-0.5228	
	4	0.0000	0.0000	-0.1258	0.1258	0.0738	-0.1694	0.3076	
	6	-0.1238	0.1238	-0.4968	0.4968	-0.4908	-0.2839	0.1285	
	8	0.0000	0.0000	-0.1797	0.1797	0.0560	-0.4098	0.2396	
	10	0.0000	0.0000	-0.2671	0.2671	0.1883	-0.3069	-0.3180	
	12	-0.6283	-0.6283	0.2410	0.2410	0.2295	0.4274	-0.4577	
	14	0.0000	0.0000	-0.2283	0.2283	0.0367	-0.2793	-0.0566	
15	1	0	0.0000	0.0000	0.0000	0.0000	0.0000	0.0000	0.0000
	2	0.0000	0.0000	-0.1324	0.1324	0.0602	-0.0673	-0.2883	
	4	0.0000	0.0000	0.2609	-0.2609	-0.1531	-0.2562	0.5240	
	6	-0.5656	0.5656	-0.1915	0.1915	-0.1892	0.2412	0.1665	
	8	0.0000	0.0000	-0.1001	0.1001	0.0312	-0.4543	0.0044	
	10	0.0000	0.0000	0.2324	-0.2324	-0.1638	0.1001	0.2250	
	12	0.0774	-0.0774	-0.2387	0.2387	-0.2273	-0.1942	0.0792	
	14	0.0000	0.0000	-0.2874	0.2874	0.0462	-0.3106	0.1906	
16	1	0	0.0358	-0.0358	0.0600	0.0600	0.0600	0.1926	0.0380
	2	0.0000	0.0000	0.1341	-0.1341	-0.0610	-0.1814	0.1188	
	4	0.0000	0.0000	-0.2577	0.2577	0.1512	-0.2733	0.1062	
	6	-0.4307	0.4307	-0.2118	0.2118	-0.2092	0.3790	0.1337	
	8	0.0000	0.0000	0.4449	-0.4449	-0.1385	0.1449	0.5833	
	10	0.0000	0.0000	0.1596	-0.1596	-0.1125	-0.1460	-0.2455	
	12	0.5284	-0.5284	0.0988	-0.0988	0.0941	0.1384	0.1810	
	14	0.0000	0.0000	0.2892	-0.2892	-0.0465	0.3207	0.1642	
	16	0.0000	0.0000	0.1275	-0.1275	-0.1028	0.2320	-0.0395	
2	0	-0.6061	-0.6061	-0.0472	0.0472	-0.0472	0.1389	0.0388	
	2	0.0000	0.0000	0.2403	-0.2403	-0.1092	0.1604	-0.2043	
	4	0.0000	0.0000	-0.3641	0.3641	0.2137	0.1518	-0.1108	
	6	-0.2017	0.2017	0.0583	-0.0583	0.0576	-0.2807	-0.0663	
	8	0.0000	0.0000	0.0885	-0.0885	-0.0276	-0.0038	-0.1198	
	10	0.0000	0.0000	0.3485	-0.3485	-0.2457	0.1812	0.3214	
	12	0.3878	-0.3878	-0.1214	0.1214	-0.1156	0.2447	0.1917	
	14	0.0000	0.0000	0.3820	-0.3820	-0.0614	-0.0141	-0.1554	
	16	0.0000	0.0000	-0.2690	0.2690	0.2168	-0.1834	0.1869	
17	1	0	0.0000	0.0000	0.0000	0.0000	0.0000	0.0000	0.0000
	2	0.0000	0.0000	0.3981	-0.3981	-0.1810	-0.3832	0.2042	
	4	0.0000	0.0000	-0.2570	0.2570	0.1508	-0.0443	0.0796	
	6	-0.5926	0.5926	-0.0578	0.0578	-0.0571	-0.0537	0.0021	
	8	0.0000	0.0000	-0.0687	0.0687	0.0214	-0.1129	0.3466	
	10	0.0000	0.0000	0.1486	-0.1486	-0.1048	0.4536	-0.2894	
	12	-0.5511	0.5511	0.5550	-0.5550	0.5284	0.2647	-0.2466	
	14	0.0000	0.0000	-0.0648	0.0648	0.0104	0.1120	-0.3765	
	16	0.0000	0.0000	-0.2965	0.2965	0.2390	-0.2037	0.1994	
18	1	0	0.2647	-0.2647	0.2018	0.2018	0.2018	0.3557	0.1269
	2	0.0000	0.0000	0.0389	-0.0389	-0.0177	0.0831	0.4305	
	4	0.0000	0.0000	-0.0364	0.0364	0.0213	-0.0679	-0.0123	
	6	-0.4084	0.4084	0.2171	-0.2171	0.2145	-0.2851	-0.1799	

L	MU	N	(111)[110]	(111)[112]	(112)[111]	(112)[110]	(112)[311]	(4411)[111]8	(111)8[4411]
18	1	8	0.0000	0.0000	-0.1228	-0.1228	0.0382	0.0409	-0.0359
	10	0.0000	0.0000	0.2134	-0.2134	-0.1504	-0.0871	0.1556	
	12	-0.1919	-0.1919	-0.2571	-0.2571	-0.2448	0.1734	0.0668	
	14	0.0000	0.0000	-0.0945	0.0945	0.0152	0.2596	0.2878	
	16	0.0000	0.0000	0.1176	0.1176	-0.0948	-0.2237	-0.3145	
	18	-0.1617	0.1617	0.2442	-0.2442	0.2182	0.2950	0.1317	
2	0	-0.1915	-0.1915	-0.2566	-0.2566	-0.0789	0.1941		
	2	0.0000	0.0000	-0.2368	0.2368	0.1076	-0.3410	0.1115	
	4	0.0000	0.0000	-0.3191	0.3191	0.1872	-0.1357	-0.4849	
	6	0.4621	-0.4621	-0.2151	0.2151	-0.2125	-0.3648	-0.0436	
	8	0.0000	0.0000	0.2748	0.2748	-0.0856	-0.1706	-0.0408	
	10	0.0000	0.0000	-0.2972	0.2972	0.2095	0.2293	-0.3053	
	12	-0.2525	-0.2525	-0.0132	-0.0132	-0.0126	-0.3327	-0.0893	
	14	0.0000	0.0000	-0.0438	0.0438	0.0070	0.0741	0.0510	
	16	0.0000	0.0000	-0.2268	0.2268	0.1828	-0.3773	-0.1884	
	18	0.4737	-0.4737	-0.2259	0.2259	-0.2018	-0.0859	-0.4398	
19	1	0	0.0000	0.0000	0.0000	0.0000	0.0000	0.0000	
	2	0.0000	0.0000	0.3797	-0.3797	-0.1726	-0.0391	0.2493	
	4	0.0000	0.0000	0.2157	0.2157	-0.1266	0.4369	-0.2969	
	6	0.0269	-0.0269	0.1396	-0.1396	0.1379	0.0943	-0.2423	
	8	0.0000	0.0000	0.2961	0.2961	-0.0922	0.1209	-0.2161	
	10	0.0000	0.0000	0.2068	-0.2068	-0.1458	0.0507	0.3879	
	12	0.4196	-0.4196	-0.1094	0.1094	-0.1042	0.2298	0.1148	
	14	0.0000	0.0000	-0.2375	0.2375	0.0382	-0.4823	0.0694	
	16	0.0000	0.0000	-0.1087	-0.1087	0.0877	-0.0535	-0.0021	
	18	0.4940	-0.4940	-0.0074	0.0074	-0.0066	0.2166	-0.3598	
20	1	0	-0.0150	-0.0150	-0.0923	0.0923	0.0923	0.1475	-0.0239
	2	0.0000	0.0000	0.0505	-0.0505	-0.0230	0.0853	-0.0616	
	4	0.0000	0.0000	0.2221	-0.2221	-0.1303	-0.3282	-0.1018	
	6	0.2269	-0.2269	-0.2527	0.2527	-0.2497	-0.1328	-0.0784	
	8	0.0000	0.0000	-0.2525	-0.2525	0.0786	0.3893	-0.3963	
	10	0.0000	0.0000	0.3364	-0.3364	-0.2371	0.0284	-0.0716	
	12	-0.6787	-0.6787	-0.0176	0.0176	-0.0168	-0.1982	0.0123	
	14	0.0000	0.0000	-0.3208	0.3208	0.0516	-0.0629	-0.5270	
	16	0.0000	0.0000	-0.2493	0.2493	0.2010	-0.1689	0.2083	
	18	0.1124	-0.1124	-0.2264	0.2264	-0.2023	-0.3040	-0.0279	
	20	0.0000	0.0000	-0.0848	0.0848	0.0005	-0.1851	-0.0135	
2	0	0.5959	0.5959	0.0725	0.0725	0.0725	-0.1594	-0.0588	
	2	0.0000	0.0000	-0.4187	0.4187	0.1903	0.2568	0.4510	
	4	0.0000	0.0000	0.2134	0.2134	-0.1252	-0.2710	-0.1267	
	6	0.3147	-0.3147	0.2398	-0.2398	0.2398	0.1606	0.0113	
	8	0.0000	0.0000	0.3970	-0.3970	-0.1236	0.2613	-0.1321	
	10	0.0000	0.0000	0.0380	-0.0380	-0.0268	0.4362	0.0798	
	12	0.2643	0.2643	0.1183	-0.1183	0.1183	0.1127	0.0977	-0.0570
	14	0.0000	0.0000	-0.0016	0.0016	0.0003	0.0477	-0.1227	
	16	0.0000	0.0000	0.4186	0.4186	-0.3374	0.0639	0.3867	
	18	-0.5183	0.5183	-0.3409	0.3409	-0.3046	-0.1785	0.3362	
	20	0.0000	0.0000	0.2114	-0.2114	-0.0013	0.1874	0.0655	
21	1	0	0.0000	0.0000	0.0000	0.0000	0.0000	0.0000	
	2	0.0000	0.0000	0.0951	-0.0951	-0.0432	0.3143	-0.1099	
	4	0.0000	0.0000	0.2742	-0.2742	-0.1609	-0.2240	-0.1714	
	6	0.4415	-0.4415	-0.2059	0.2059	-0.2034	-0.0614	0.0014	
	8	0.0000	0.0000	-0.0648	0.0648	0.0202	-0.1608	-0.4364	
	10	0.0000	0.0000	-0.2434	0.2434	0.1716	-0.0452	0.1881	
	12	-0.0314	-0.0314	-0.2226	0.2226	-0.2120	0.2994	0.2375	
	14	0.0000	0.0000	0.1154	-0.1154	-0.0185	-0.1687	0.3245	
	16	0.0000	0.0000	-0.1772	0.1772	0.1428	-0.3410	-0.2011	
	18	-0.3908	0.3908	0.0574	-0.0574	0.0513	-0.1109	0.1020	
	20	0.0000	0.0000	0.2470	-0.2470	-0.0015	0.2484	0.0955	
2	0	0.0000	0.0000	0.0000	0.0000	0.0000	0.0000	0.0000	

L	MU	N	(111)[110]	(111)[112]	(112)[111]	(112)[110]	(112)[311]	(4411)[111]8	(111)8[4411]	
21	2	2	0.0000	0.0000	0.0042	-0.0042	-0.0019	0.0961	0.0435	
	4	0.0000	0.0000	0.1094	0.1094	-0.0642	0.0575	-0.3841		
	6	0.5507	-0.5507	-0.5507	-0.2470	0.2470	-0.2440	0.2708	0.1337	
	8	0.0000	0.0000	0.2499	0.2499	-0.0778	-0.2124	-0.1157		
	10	0.0000	0.0000	-0.0628	0.0628	0.0443	0.3158	-0.3868		
	12	-0.2841	-0.2841	-0.2841	-0.2225	-0.2225	-0.2119	-0.0165	-0.0739	
	14	0.0000	0.0000	0.2432	-0.2432	-0.0391	-0.0830	-0.0589		
	16	0.0000	0.0000	-0.0680	0.0680	0.0548	0.2298	-0.0852		
	18	-0.0197	0.0197	0.1580	-0.1580	0.1412	0.1679	-0.0242		
	20	0.0000	0.0000	0.3266	-0.3266	-0.0020	0.2620	-0.2012		
22	1	0	-0.1401	-0.1401	-0.3976	0.3976	0.3976	0.3602	-0.1123	
	2	0.0000	0.0000	0.1240	-0.1240	-0.0564	-0.0820	-0.2780		
	4	0.0000	0.0000	0.2668	-0.2668	0.1565	-0.0802	-0.2064		
	6	0.5285	-0.5285	0.0008	-0.0008	0.0008	0.1549	0.1955		
	8	0.0000	0.0000	0.1060	-0.1060	-0.0330	-0.2451	-0.2549		
	10	0.0000	0.0000	-0.3364	0.3364	0.2371	-0.0339	0.2164		
	12	0.4540	-0.4540	-0.4540	-0.1853	0.1853	-0.1764	-0.3433	-0.0113	
	14	0.0000	0.0000	-0.4659	0.4659	0.0749	-0.1469	0.2055		
	16	0.0000	0.0000	0.1173	-0.1173	0.0945	0.0374	-0.2017		
	18	0.5732	-0.5732	0.3679	-0.3679	0.3287	0.0444	-0.1820		
	20	0.0000	0.0000	-0.1242	0.1242	0.0008	0.1380	-0.2684		
	22	0.0000	0.0000	-0.2205	0.2205	0.1958	-0.2960	0.0822		
2	0	0.4515	-0.4515	-0.4515	-0.0905	0.0905	-0.0905	-0.0914	-0.3712	
	2	0.0000	0.0000	0.0100	-0.0100	-0.0045	-0.2205	0.1505		
	4	0.0000	0.0000	-0.0530	0.0530	0.0311	-0.0219	0.2641		
	6	-0.0329	0.0329	0.3407	-0.3407	0.3366	-0.1547	0.2246		
	8	0.0000	0.0000	-0.1633	0.1633	0.0509	0.3417	0.0883		
	10	0.0000	0.0000	-0.1468	0.1468	0.1035	-0.0321	-0.2180		
	12	-0.3029	0.3029	-0.2163	0.2163	-0.2060	-0.1315	0.0475		
	14	0.0000	0.0000	0.1192	-0.1192	0.0192	-0.2617	0.0015		
	16	0.0000	0.0000	-0.2740	0.2740	0.2208	0.1292	-0.3106		
	18	0.3289	-0.3289	-0.0370	0.0370	0.0370	-0.0331	-0.3876	-0.1119	
	20	0.0000	0.0000	-0.2049	0.2049	0.0013	0.2055	0.1464		
22	0.0000	0.0000	0.2237	-0.2237	-0.1986	0.1105	-0.1941			

Table 15.5.2 Cubic-cubic generalized harmonics $T_l^{\mu\mu'}$. The functions are defined by equation (14.270) with the coefficients of *Table 15.2.1*

Table 15.5.2.1 The cubic-cubic functions $T_l^{\mu\mu'}(\varphi_1 \Phi \varphi_2)$ in sections $\varphi_2 = \text{const.}$ for $l = 4$, $\mu = \mu' = 1$, $\varphi_1 = 0^\circ (10^\circ) 90^\circ$, $\Phi = 0^\circ (10^\circ) 90^\circ$, $\varphi_2 = 0^\circ (10^\circ) 80^\circ$ (see also *Figure A.4.3.2(a)-(c)* and reference 72)

L=4 MU=1 NU=1										SECTION PHI2=0									
→ φ_1										SECTION PHI2=0									
0	10	20	30	40	50	60	70	80	90	0	10	20	30	40	50	60	70	80	90
0	1.0000	0.9025	0.6557	0.3750	0.1918	0.1918	0.3750	0.6557	0.9025	1.0000	0.9025	0.6557	0.3750	0.1918	0.1918	0.3750	0.6557	0.9025	1.0000
10	0.9025	0.8079	0.5683	0.2958	0.1179	0.1179	0.2958	0.5683	0.8079	0.9025	0.8079	0.5683	0.2958	0.1179	0.1179	0.2958	0.5683	0.8079	0.9025
20	0.6557	0.5683	0.3469	0.0952	-0.0690	-0.0690	0.0952	0.3469	0.5683	0.6557	0.6557	0.5683	0.3469	0.0952	-0.0690	-0.0690	0.0952	0.3469	0.5683
30	0.3750	0.2958	0.0952	-0.1328	-0.2817	-0.2817	-0.1328	0.0952	0.2958	0.3750	0.3750	0.2958	0.0952	-0.1328	-0.2817	-0.2817	-0.1328	0.0952	0.2958
40	0.1918	0.1179	-0.0690	-0.2817	-0.4205	-0.4205	-0.2817	-0.0690	0.1179	0.1918	0.1918	0.1179	-0.0690	-0.2817	-0.4205	-0.4205	-0.2817	-0.0690	0.1179
50	0.0918	0.1179	-0.0690	-0.2817	-0.4205	-0.4205	-0.2817	-0.0690	0.1179	0.1918	0.1918	0.1179	-0.0690	-0.2817	-0.4205	-0.4205	-0.2817	-0.0690	0.1179
60	0.0952	0.2958	0.0952	-0.1328	-0.2817	-0.2817	-0.1328	0.0952	0.2958	0.3750	0.3750	0.2958	0.0952	-0.1328	-0.2817	-0.2817	-0.1328	0.0952	0.2958
70	0.6557	0.5683	0.3469	0.0952	-0.0690	-0.0690	0.0952	0.3469	0.5683	0.6557	0.6557	0.5683	0.3469	0.0952	-0.0690	-0.0690	0.0952	0.3469	0.5683
80	0.9025	0.8079	0.5683	0.2958	0.1179	0.1179	0.2958	0.5683	0.8079	0.9025	0.9025	0.8079	0.5683	0.2958	0.1179	0.1179	0.2958	0.5683	0.8079
90	1.0000	0.9025	0.6557	0.3750	0.1918	0.1918	0.3750	0.6557	0.9025	1.0000	0.9025	0.6557	0.3750	0.1918	0.1918	0.3750	0.6557	0.9025	1.0000
L=4 MU=1 NU=1										SECTION PHI2=10									
→ φ_1										SECTION PHI2=10									
0	10	20	30	40	50	60	70	80	90	0	10	20	30	40	50	60	70	80	90
0	0.9025	0.6557	0.3750	0.1918	0.1918	0.3750	0.6557	0.9025	1.0000	0.9025	0.8079	0.5683	0.3469	0.1179	0.0918	0.0710	0.0502	0.0306	0.0102
10	0.8079	0.5684	0.2959	0.1180	0.1179	0.2956	0.5680	0.8076	0.9024	0.9025	0.9025	0.8079	0.5683	0.3469	0.1179	0.0918	0.0710	0.0502	0.0306
20	0.5683	0.3487	0.0974	-0.0680	-0.0702	-0.0919	0.3424	0.5642	0.6534	0.6534	0.5683	0.3469	0.1179	0.0918	0.0710	0.0502	0.0306	0.0102	0.0000
30	0.2958	0.1034	-0.1228	-0.2770	-0.2870	-0.1482	0.0746	0.2770	0.3643	0.2958	0.2958	0.1179	0.0918	0.0710	0.0502	0.0306	0.0102	0.0000	
40	0.1179	-0.0467	-0.2542	-0.4076	-0.4350	-0.3236	-0.1256	0.0664	0.1626	0.1179	0.1179	0.0918	0.0710	0.0502	0.0306	0.0102	0.0000	0.0000	
50	0.1179	-0.0237	-0.2259	-0.3941	-0.4496	-0.3664	-0.1835	0.0137	0.1327	0.1179	0.1179	0.0918	0.0710	0.0502	0.0306	0.0102	0.0000	0.0000	
60	0.2958	0.1701	-0.0406	-0.2377	-0.3289	-0.2717	-0.0927	0.1243	0.2777	0.2958	0.2958	0.1701	0.1179	0.0918	0.0710	0.0502	0.0306	0.0102	
70	0.5683	0.4529	0.2264	-0.0051	-0.1334	-0.0984	0.0835	0.3272	0.5186	0.5683	0.5683	0.4529	0.2264	0.1179	0.0918	0.0710	0.0502	0.0306	
80	0.9025	0.7012	0.4620	0.2020	0.0431	0.0594	0.2435	0.5091	0.7320	0.8079	0.8079	0.7012	0.4620	0.2020	0.0431	0.0594	0.0306	0.0102	
90	0.9025	0.8079	0.5683	0.2958	0.1179	0.1179	0.2958	0.5683	0.8079	0.9025	0.9025	0.8079	0.5683	0.2958	0.1179	0.1179	0.2958	0.5683	0.8079
L=4 MU=1 NU=1										SECTION PHI2=20									
→ φ_1										SECTION PHI2=20									
0	10	20	30	40	50	60	70	80	90	0	10	20	30	40	50	60	70	80	90
0	0.6557	0.3750	0.1918	0.1918	0.3750	0.6557	0.9025	1.0000	0.9025	0.6557	0.5683	0.3469	0.1179	0.0918	0.0710	0.0502	0.0306	0.0102	0.0000
10	0.5683	0.2959	0.1180	0.1178	0.2954	0.5676	0.8072	0.9020	0.8076	0.5683	0.4620	0.2264	0.1179	0.0918	0.0710	0.0502	0.0306	0.0102	0.0000
20	0.3469	0.0974	-0.0676	-0.0710	-0.0889	0.3373	0.5578	0.6474	0.5642	0.3469	0.2264	0.1179	0.0918	0.0710	0.0502	0.0306	0.0102	0.0000	
30	0.0952	-0.1228	-0.2751	-0.2905	-0.1617	0.0510	0.2481	0.3373	0.2770	0.0952	0.0952	0.1228	0.2751	0.2905	0.1617	0.0510	0.0306	0.0102	0.0000
40	-0.0690	-0.2542	-0.4024	-0.4444	-0.3604	-0.1898	-0.0124	0.0888	0.0664	-0.0690	0.0690	0.2542	0.4024	0.4444	0.3604	0.1898	0.0664	-0.0690	0.0000
50	-0.0690	-0.2259	-0.3836	-0.4683	-0.4403	-0.3128	-0.1455	-0.0165	0.0137	-0.0690	0.0690	0.2259	0.3836	0.4683	0.4403	0.3128	0.1455	-0.0165	0.0000
60	0.0952	-0.0406	-0.2197	-0.3582	-0.3914	-0.3036	-0.1361	0.0329	0.1243	0.0952	0.0952	0.2197	0.3582	0.3914	0.3036	0.1361	0.0329	0.0952	0.0000
70	0.3469	0.2264	0.0220	-0.1706	-0.2614	-0.2078	-0.0349	0.1764	0.3272	0.3469	0.3469	0.2264	0.0220	-0.1706	-0.2614	-0.2078	-0.0349	0.1764	0.3272
80	0.5683	0.4620	0.2399	0.0061	-0.1302	-0.1051	0.0696	0.3122	0.5091	0.5683	0.5683	0.4620	0.2399	0.0061	-0.1302	-0.1051	0.0696	0.3122	0.5091
90	0.6557	0.5683	0.3469	0.0952	-0.0690	0.0952	0.3469	0.5683	0.6557	0.6557	0.5683	0.3469	0.0952	-0.0690	0.0952	0.3469	0.5683	0.6557	0.6557

I=4 MU=1 NU=1										SECTION PHI2=30									
→ φ_1										SECTION PHI2=30									
0	10	20	30	40	50	60	70	80	90	0	10	20	30	40	50	60	70	80	90
0	0.3750	0.1918	0.1918	0.3750	0.6557	0.9025	1.0000	0.9025	0.6557	0	10	20	30	40	50	60	70	80	90
10	0.2958	0.1180	0.1178	0.2954	0.5676	0.8068	0.9015	0.8068	0.5676	0	10	20	30	40	50	60	70	80	90
20	0.0952	-0.0680	-0.0710	-0.0878	0.3339	0.5523	0.6407	0.5523	0.3339	0	10	20	30	40	50	60	70	80	90
30	-0.1328	-0.2770	-0.2905	-0.1670	0.0357	0.2227	0.3066	0.2227	0.0357	0	10	20	30	40	50	60	70	80	90
40	-0.2817	-0.4076	-0.4444	-0.3749	-0.2316	-0.0816	0.0050	-0.0497	-0.1089	0	10	20	30	40	50	60	70	80	90
50	-0.2817	-0.3941	-0.4683	-0.4683	-0.3969	-0.2848	-0.1455	-0.1455	-0.2848	0	10	20	30	40	50	60	70	80	90
60	0.0952	0.2958	0.0952	-0.1328	-0.2377	-0.3289	-0.2717	-0.0927	0.1243	0	10	20	30	40	50	60	70	80	9

L=4 MU=1 NU=1 SECTION PHI2=70

$\rightarrow \Phi_1$									
0	10	20	30	40	50	60	70	80	90
0 0.6557 0.9025 1.0000 0.9025 0.6557 0.3750 0.1918 0.1918 0.3750 0.6557	10 0.5683 0.8076 0.9020 0.8072 0.5676 0.2954 0.1178 0.1180 0.2959 0.5683	20 0.3469 0.5642 0.6474 0.5578 0.3373 0.0889 -0.0710 -0.0676 0.0974 0.3469	30 0.0952 0.2770 0.3373 0.2481 0.0510 -0.1617 -0.2905 -0.2751 -0.1228 0.0952	40 -0.0690 0.0137 -0.0165 -0.1455 -0.3128 -0.4403 -0.4683 -0.3836 -0.2259 -0.0690	50 -0.0690 0.0137 -0.0165 -0.1455 -0.3128 -0.4403 -0.4683 -0.3836 -0.2259 -0.0690	60 0.0952 0.1243 0.0329 -0.1361 -0.3036 -0.3914 -0.3582 -0.2197 -0.0406 0.0952	70 0.3469 0.3272 0.1764 -0.0349 -0.2078 -0.2614 -0.1706 0.0220 0.2264 0.3469	80 0.5683 0.5091 0.3122 0.0696 -0.1051 -0.1302 0.0061 0.2399 0.4620 0.5683	90 0.6557 0.5683 0.3469 0.0952 -0.0690 -0.0690 0.0952 0.3469 0.5683 0.6557

L=4 MU=1 NU=1 SECTION PHI2=80

0	10	20	30	40	50	60	70	80	90
0 0.9025 1.0000 0.9025 0.6557 0.3750 0.1918 0.1918 0.3750 0.6557 0.9025	10 0.8079 0.9024 0.8076 0.5680 0.2956 0.1179 0.1180 0.2959 0.5684 0.8079	20 0.5683 0.6534 0.5642 0.3424 0.0919 -0.0702 -0.0680 0.0974 0.3487 0.5683	30 0.2958 0.3643 0.2770 0.0746 -0.1482 -0.2870 -0.2770 -0.1228 0.1034 0.2958	40 0.1179 0.1626 0.0664 -0.1256 -0.3236 -0.4350 -0.4076 -0.2542 -0.0467 0.1179	50 0.1179 0.1327 0.0137 -0.1835 -0.3664 -0.4496 -0.3941 -0.2259 -0.0237 0.1179	60 0.2958 0.2777 0.1243 -0.0927 -0.2717 -0.3289 -0.2377 -0.0406 0.1701 0.2958	70 0.5683 0.5186 0.3272 0.0835 -0.0984 -0.1334 -0.0051 0.2264 0.4529 0.5683	80 0.8079 0.7320 0.5091 0.2435 0.0594 0.0431 0.2020 0.4620 0.7012 0.8079	90 0.9025 0.8079 0.5683 0.2958 0.1179 0.1179 0.2958 0.5683 0.8079 0.9025

L=9 MU=1 NU=1 SECTION PHI2= 0

0	10	20	30	40	50	60	70	80	90
0 1.0000 0.5933 -0.1511 -0.5000 -0.4422 -0.4422 -0.5000 -0.1511 0.5933 1.0000	10 0.5933 0.3157 -0.1578 -0.2966 -0.1580 -0.1580 -0.2966 -0.1578 0.3157 0.5933	20 -0.1511 -0.1578 -0.1052 0.0755 0.2630 0.2630 0.0755 -0.1052 -0.1578 -0.1511	30 -0.5000 -0.2966 0.0755 0.2500 0.2211 0.2211 0.2500 0.0755 -0.2966 -0.5000	40 -0.4422 -0.1580 0.2630 0.2211 -0.1050 -0.1050 0.2211 0.2630 -0.1580 -0.4422	50 -0.4422 -0.1580 0.2630 0.2211 -0.1050 -0.1050 0.2211 0.2630 -0.1580 -0.4422	60 -0.5000 -0.2966 0.0755 0.2500 0.2211 0.2211 0.2500 0.0755 -0.2966 -0.5000	70 -0.1511 -0.1578 -0.1052 0.0755 0.2630 0.2630 0.0755 -0.1052 -0.1578 -0.1511	80 0.5933 0.3157 -0.1578 -0.2966 -0.1580 -0.1580 -0.2966 -0.1578 0.3157 0.5933	90 1.0000 0.5933 -0.1511 -0.5000 -0.4422 -0.4422 -0.5000 -0.1511 0.5933 1.0000

L=9 MU=1 NU=1 SECTION PHI2=10

0	10	20	30	40	50	60	70	80	90
0 0.5933 -0.1511 -0.5000 -0.4422 -0.4422 -0.5000 -0.1511 0.5933 1.0000 0.5933	10 0.3157 -0.1571 -0.2943 -0.1564 -0.1597 -0.3002 -0.1593 0.3169 0.5945 0.3157	20 -0.1578 -0.0979 0.1042 0.2821 0.2402 0.0307 -0.1244 -0.1423 -0.1349 -0.1578	30 -0.2966 0.0929 0.3346 0.2753 0.1414 0.1046 0.0213 -0.2343 -0.4392 -0.2966	40 -0.1580 0.2563 0.3075 -0.0630 -0.2573 -0.0025 0.2210 0.0010 -0.3050 -0.1580	50 -0.1580 0.1666 0.1594 -0.1934 -0.2962 0.0661 0.3514 0.1297 -0.2255 -0.1580	60 -0.2966 -0.0940 -0.0042 -0.0276 0.0789 0.3041 0.3242 0.0152 -0.2999 -0.2966	70 -0.1578 -0.1597 -0.1349 0.0424 0.2790 0.3230 0.1153 -0.1193 -0.1882 -0.1578	80 0.3157 0.0970 -0.1796 -0.1438 0.0512 0.0257 -0.1719 -0.1483 0.1539 0.3157	90 0.5933 0.3157 -0.1578 -0.2966 -0.1580 -0.1580 -0.2966 -0.1578 0.3157 0.5933

L=9 MU=1 NU=1 SECTION PHI2=70

$\rightarrow \Phi_1$									
0	10	20	30	40	50	60	70	80	90
0 -0.1511 -0.5000 -0.4422 -0.4422 -0.5000 -0.1511 0.5933 1.0000 0.5933 -0.1511	10 -0.1578 -0.2943 -0.1558 -0.1609 -0.3034 -0.1611 0.3187 0.5977 0.3169 -0.1578	20 -0.1052 0.1042 0.2895 0.2247 -0.0095 -0.1472 -0.1195 -0.0947 -0.1423 -0.1052	30 0.0755 0.3346 0.2927 0.0791 -0.0391 -0.0584 -0.1547 -0.2955 -0.2343 0.0755	40 0.2630 0.3075 -0.0701 -0.4170 -0.2914 0.0691 0.1540 -0.0161 0.0010 0.2630	50 0.2630 0.1594 -0.2936 -0.5909 -0.3305 0.1639 0.3280 0.1711 0.1297 0.2630	60 0.0755 -0.0042 -0.2177 -0.2715 -0.0426 0.2026 0.1960 0.0468 0.0151 0.0755	70 -0.1052 -0.1349 -0.0832 0.1067 0.2630 0.2025 -0.0015 -0.1281 -0.1193 -0.1052	80 -0.1578 -0.1796 -0.0569 0.1995 0.3393 0.2052 -0.0417 -0.1598 -0.1483 -0.1578	90 -0.1511 -0.1578 -0.1052 0.0755 0.2630 0.0755 0.2630 0.0755 -0.1052 -0.1578 -0.1511

I=9 MU=1 NU=1 SECTION PHI2=30

0	10	20	30	40	50	60	70	80	90
0 -0.5000 -0.4422 -0.4422 -0.5000 -0.1511 0.5933 1.0000 0.5933 -0.1511 -0.5000	10 -0.2966 -0.1564 -0.1609 -0.3046 -0.1623 0.3202 0.6012 0.3187 -0.1593 -0.2966	20 0.0755 0.2821 0.2247 -0.0257 -0.1626 -0.1004 -0.0499 -0.1195 -0.1244 0.0755	30 0.2500 0.2753 0.0791 -0.0999 -0.1207 -0.1004 -0.1501 -0.1547 0.0213 0.2500	40 0.2211 -0.0630 -0.4170 -0.4295 -0.0910 0.1960 0.2084 0.1540 0.2210 0.2211	50 0.2211 -0.1934 -0.5909 -0.5567 -0.1346 0.2396 0.3356 0.3280 0.3514 0.2211	60 0.2500 -0.0276 -0.2715 -0.2948 -0.1684 -0.0527 0.0448 0.1960 0.3242 0.2500	70 0.0755 0.0424 0.1067 0.1198 -0.0409 -0.2220 -0.1953 -0.0015 0.1153 0.0755	80 -0.2966 -0.1438 0.1995 0.3534 0.1855 -0.0276 -0.0568 -0.0417 -0.1719 -0.2966	90 -0.5000 -0.2966 0.0755 0.2500 0.2211 0.2211 0.2500 0.0755 -0.2966 -0.5000

L=9 MU=1 NU=1 SECTION PHI2=40

0	10	20	30	40	50	60	70	80	90
0 -0.4422 -0.4422 -0.5000 -0.1511 0.5933 1.0000 0.5933 -0.1511 -0.5000 -0.4422	10 -0.1580 -0.1597 -0.3034 -0.1623 0.3209 0.6036 0.3202 -0.1611 -0.3002 -0.1580	20 0.2630 0.2402 -0.0095 -0.1626 -0.0930 -0.0212 -0.1004 -0.1472 0.0307 0.2630	30 0.2211 0.1414 -0.0391 -0.1207 -0.0831 -0.0655 -0.1004 -0.0584 0.1046 0.2211	40 -0.1050 -0.2573 -0.2914 -0.0910 0.1882 0.2938 0.1960 0.0691 -0.0205 -0.1050	50 -0.1050 -0.2962 -0.3305 -0.1346 0.1323 0.2644 0.2396 0.1639 0.0661 -0.1050	60 0.2211 0.0789 -0.0426 -0.1684 -0.2815 -0.2616 -0.0527 0.2026 0.3041 0.2211	70 0.2630 0.2790 0.2630 -0.0409 -0.4815 -0.5860 -0.2220 0.2025 0.3230 0.2630	80 -0.1580 0.0512 0.3393 0.1855 -0.2564 -0.3651 -0.0276 0.2052 0.0257 -0.1580	90 -0.4422 -0.1580 0.2630 0.2211 -0.1050 0.2211 0.2630 -0.1580 -0.4422

L=9 MU=1 NU=1 SECTION PHI2=50

0	10	20	30	40	50	60	70	80	90
0 -0.4422 -0.5000 -0.1511 0.5933 1.0000 0.5933 -0.1511 -0.5000 -0.4422 -0.4422	10 -0.1580 -0.3002 -0.1611 0.3202 0.6036 0.3209 -0.1623 -0.3034 -0.1597 -0.1580	20 0.2630 0.0307 -0.1472 -0.1004 -0.0212 -0.0930 -0.1626 -0.0095 0.2402 0.2630	30 0.2211 0.1046 -0.0584 -0.1004 -0.0655 -0.0831 -0.1207 0.0391 0.1414 0.2211	40 -0.1050 -0.0025 0.0691 0.1960 0.2938 0.1882 -0.0910 -0.2914 -0.2573 -0.1050	50 -0.1050 0.0661 0.1639 0.2396 0.2644 0.1323 -0.1346 -0.3305 -0.2962 -0.1050	60 0.2211 0.3041 0.2026 -0.0527 -0.2616 -0.2815 -0.1684 0.0426 0.0789 0.2211	70 0.2630 0.3230 0.2025 -0.2220 -0.5860 -0.4815 -0.0409 0.2630 0.2790 0.2630	80 -0.1580 0.0257 0.2052 -0.0276 -0.3651 -0.2564 0.1855 0.3393 0.0512 -0.1580	90 -0.4422 -0.1580 0.2630 0.2211 -0.1050 0.2211 0.2630 -0.1580 -0.4422

L=9 MU=1 NU=1			SECTION PHI2=60								
			$\rightarrow \psi_1$								
0	0	10	20	30	40	50	60	70	80	90	
0	-0.5000	-0.1511	0.5933	1.0000	0.5933	-0.1511	-0.5000	-0.4422	-0.4422	-0.5000	
10	-0.2966	-0.1593	0.3187	0.6012	0.3202	-0.1623	-0.3046	-0.1609	-0.1564	-0.2966	
20	0.0755	-0.1244	-0.1195	-0.0499	-0.1004	-0.1626	-0.0257	0.2247	0.2821	0.0755	
30	0.2500	0.0213	-0.1547	-0.1501	-0.1004	-0.1207	-0.0999	0.0791	0.2753	0.2500	
40	0.2211	0.2210	0.1540	0.2084	0.1960	-0.0910	-0.4295	-0.4170	-0.0630	0.2211	
50	0.2211	0.3514	0.3280	0.3356	0.2396	-0.1346	-0.5567	-0.5909	-0.1934	0.2211	
60	0.2500	0.3242	0.1960	0.0448	-0.0527	-0.1684	-0.2948	-0.2715	-0.0276	0.2500	
70	0.0755	0.1153	-0.0015	-0.1953	-0.2220	-0.0409	0.1198	0.1067	0.0424	0.0755	
80	-0.2966	-0.1719	-0.0417	-0.0568	-0.0276	0.1855	0.3534	0.1995	-0.1438	-0.2966	
90	-0.5000	-0.2966	0.0755	0.2500	0.2211	0.2211	0.2500	0.0755	-0.2966	-0.5000	
L=9 MU=1 NU=1			SECTION PHI2=70								
0	0	10	20	30	40	50	60	70	80	90	
0	-0.1511	0.5933	1.0000	0.5933	-0.1511	-0.5000	-0.4422	-0.4422	-0.5000	-0.1511	
10	-0.1578	0.3169	0.5977	0.3187	-0.1611	-0.3034	-0.1609	-0.1558	-0.2943	-0.1578	
20	-0.1052	-0.1423	-0.0947	-0.1195	-0.1472	-0.0095	0.2247	0.2895	0.1042	-0.1052	
30	0.0755	-0.2343	-0.2955	-0.1547	-0.0584	-0.0391	0.0791	0.2927	0.3346	0.0755	
40	0.2630	0.0010	-0.0161	0.1540	0.0691	-0.2914	-0.4170	-0.0701	0.3075	0.2630	
50	0.2630	0.1297	0.1711	0.3280	0.1639	-0.3305	-0.5909	-0.2936	0.1594	0.2630	
60	0.0755	0.0151	0.0468	0.1960	0.2026	-0.0426	-0.2715	-0.2177	-0.0042	0.0755	
70	-0.1052	-0.1193	-0.1281	-0.0015	0.2025	0.2630	0.1067	-0.0832	-0.1349	-0.1052	
80	-0.1578	-0.1483	-0.1598	-0.0417	0.2052	0.3393	0.1995	-0.0569	-0.1796	-0.1578	
90	-0.1511	-0.1578	-0.1052	0.0755	0.2630	0.2630	0.0755	-0.1052	-0.1578	-0.1511	
L=9 MU=1 NU=1			SECTION PHI2=80								
0	0	10	20	30	40	50	60	70	80	90	
0	0.5933	1.0000	0.5933	-0.1511	-0.5000	-0.4422	-0.4422	-0.5000	-0.1511	0.5933	
10	0.3157	0.5945	0.3169	-0.1593	-0.3002	-0.1597	-0.1564	-0.2943	-0.1571	0.3157	
20	-0.1578	-0.1349	-0.1423	-0.1244	0.0307	0.2402	0.2821	0.1042	-0.0979	-0.1578	
30	-0.2966	-0.4392	-0.2343	0.0213	0.1046	0.1414	0.2753	0.3346	0.0929	-0.2966	
40	-0.1580	-0.3050	0.0010	0.2210	-0.0025	-0.2573	-0.0630	0.3075	0.2563	-0.1580	
50	-0.1580	-0.2255	0.1297	0.3514	0.0661	-0.2962	-0.1934	0.1594	0.1666	-0.1580	
60	-0.2966	-0.2999	0.0151	0.3242	0.3041	0.0789	-0.0276	-0.0042	-0.0940	-0.2966	
70	-0.1578	-0.1882	-0.1193	0.1153	0.3230	0.2790	0.0424	-0.1349	-0.1597	-0.1578	
80	0.3157	0.1539	-0.1483	-0.1719	0.0257	0.0512	-0.1438	-0.1796	0.0970	0.3157	
90	0.5933	0.3157	-0.1578	-0.2966	-0.1580	-0.1580	-0.2966	-0.1578	0.3157	0.5933	

Table 15.5.2.2 The cubic-cubic functions $T_l^{\mu\mu'}(g_i)$ for $l = 4(1)34$, $\mu = 1(1)M(1)$, $\mu' = 1(1)M(1)$. The functions $T_l^{\mu\mu'}(g_i) = T_l^{\mu\mu'}(\phi_1^i \Phi_1^i \phi_2^i)$ are those of the Kurdjumov-Sachs and the Nishiyama-Wassermann orientation relationships according to Table 8.1. $\gamma \rightarrow \alpha$ transformation

Kurdjumov-Sachs				Nishiyama-Wassermann			
L	MU	MU'=1	2	3	MU'=1	2	3
4	1	0.097222			0.097222		
6	1	-0.588863			-0.628472		
8	1	0.444820			0.507234		
9	1	-0.117327			-0.137731		
10	1	0.214646			0.250522		
12	1	-0.235595	0.053776		-0.289455	0.125718	
	2	0.053776	0.221620		0.054134	0.306437	
13	1	-0.168096			-0.300596		
14	1	-0.119370			-0.169132		
15	1	-0.055699			-0.047617		
16	1	0.122038	-0.101953		0.269288	0.006653	
	2	-0.101953	-0.098859		-0.152524	-0.132585	
17	1	0.278559			0.330645		
18	1	-0.025714	0.073143		0.053447	-0.037174	
	2	0.073143	0.051222		0.146380	-0.029574	
19	1	-0.104885			0.039725		
20	1	-0.142473	-0.192692		-0.311665	-0.018931	
	2	-0.192692	0.091835		-0.330377	0.109118	
21	1	0.094070	0.052415		-0.082611	-0.005917	
	2	0.052415	0.086229		0.243422	0.115757	
22	1	-0.225503	0.105502		-0.321610	0.061316	
	2	0.105502	-0.001838		0.156431	-0.076146	
23	1	-0.073460			-0.008025		
24	1	0.019152	-0.143785	-0.057593	0.269851	0.012473	0.071297
	2	-0.143785	0.148194	-0.130679	-0.306561	0.142611	0.035129
	3	-0.057593	-0.130679	-0.181931	-0.277424	-0.326622	-0.130749
25	1	0.122335	0.100079		0.245529	-0.050585	
	2	0.100079	0.236605		0.384552	0.036787	
26	1	-0.137039	0.152749		-0.059489	-0.021174	
	2	0.152749	-0.121035		0.128663	-0.012328	
27	1	-0.037334	0.026328		0.142828	0.042060	
	2	0.026328	-0.045768		-0.343067	-0.108845	
28	1	0.017770	-0.08380	-0.025003	-0.274541	0.082457	0.198985
	2	-0.08380	0.195642	-0.077062	-0.205850	0.033186	-0.093850
29	1	-0.025003	-0.077062	-0.010392	-0.370972	-0.042114	0.222353
	2	0.050234	0.002137		-0.140759	-0.111592	
	2	0.002137	0.007595		0.319415	-0.176795	
30	1	-0.049241	0.088208	-0.041172	-0.120649	0.070868	-0.158145
	2	0.088208	-0.130945	0.149172	-0.119443	-0.185323	-0.122572
	3	-0.041172	0.149172	0.218490	0.282531	0.428415	0.162340
31	1	-0.062960	-0.118100		0.081230	0.132931	
	2	0.118100	-0.332564		-0.292812	-0.052926	
32	1	-0.083256	0.006981	0.037627	0.265100	0.077449	0.337841
	2	0.006981	0.182799	-0.201605	-0.070591	0.044028	0.060297
	3	0.037627	-0.201605	0.214862	-0.314138	-0.046490	-0.083164
33	1	-0.038531	-0.015696	-0.069291	0.134442	-0.217615	-0.180022
	2	-0.015696	-0.031751	-0.124617	0.212610	0.045686	-0.125026
	3	-0.069291	-0.124617	-0.001958	0.168734	0.321140	0.060513
34	1	0.026670	0.186943	-0.029933	0.052227	0.092222	-0.214600
	2	0.186943	-0.242423	0.057702	-0.107216	0.137340	0.143302
	3	-0.029933	0.057702	0.057896	0.203538	-0.124452	-0.231442

Table 15.5.2.3 The functions $\tilde{T}_l^{\mu\mu'}(hkl, \omega)$ for $l = 4(1) 22$, $\mu = 1(1) M(1)$, $\mu' = 1(1) M(1)$, $[hkl] = [100], [110], [111]$, $\omega = 0^\circ (5^\circ) \omega_{M_{hkl}}$. The functions are the same as in *Table 15.5.2.1* but with the rotation g expressed by the rotation axis $[hkl]$ and the rotation angle ω according to equations (2.7) and (2.70)–(2.72) (see also reference I, p. 319, and reference 223)

[100]

L	MU	MU'	5	10	15	20	25	30	35	40	45
4	1	1	0.9749	0.9025	0.7917	0.6557	0.5110	0.3750	0.2641	0.1918	0.1667
6	1	1	0.9472	0.7953	0.5625	0.2769	-0.0269	-0.3125	-0.5453	-0.6972	-0.7500
8	1	1	0.9120	0.6861	0.4193	0.2228	0.1722	0.2734	0.4627	0.6379	0.7083
9	1	1	0.8890	0.5933	0.2083	-0.1511	-0.3971	-0.5000	-0.4920	-0.4422	-0.4167
10	1	1	0.8653	0.5172	0.0977	-0.2286	-0.3480	-0.2461	-0.0095	0.2193	0.3125
12	1	1	0.8183	0.4421	0.2108	0.3000	0.5525	0.6446	0.4179	0.0457	-0.1345
12	2	0	0.0004	0.0056	0.0255	0.0695	0.1403	0.2291	0.3176	0.3831	0.4073
12	2	1	0.0004	0.0056	0.0255	0.0695	0.1403	0.2291	0.3176	0.3831	0.4073
12	2	2	0.8096	0.3237	-0.2409	-0.6366	-0.6983	-0.4185	0.0517	0.4759	0.6449
13	1	1	0.7858	0.3181	-0.0462	-0.1063	0.0084	-0.0059	-0.3000	-0.7060	-0.8958
14	1	1	0.7531	0.2182	-0.1778	-0.1744	0.1085	0.3240	0.2529	0.0038	-0.1302
15	1	1	0.7141	0.0558	-0.5371	-0.7280	-0.5053	-0.1191	0.1721	0.2913	0.3125
16	1	1	0.7045	0.2769	0.3401	0.6649	0.5676	0.0598	-0.1526	0.1776	0.4392
16	1	2	0.0006	0.0082	0.0364	0.0951	0.1825	0.2838	0.3773	0.4425	0.4657
16	2	1	0.0006	0.0082	0.0364	0.0951	0.1825	0.2838	0.3773	0.4425	0.4657
16	2	2	0.6821	0.0132	-0.4254	-0.3068	0.1503	0.4273	0.2315	-0.2239	-0.4574
17	1	1	0.6626	0.1235	0.0421	0.2333	0.0463	-0.4978	-0.7067	-0.3590	-0.0885
18	1	1	0.6203	-0.0095	-0.1481	0.0908	0.0765	-0.2043	-0.1315	0.4320	0.7833
18	1	2	0.0027	0.0372	0.1406	0.2859	0.3662	0.2751	0.0161	-0.2681	-0.3912
18	2	1	0.0027	0.0372	0.1406	0.2859	0.3662	0.2751	0.0161	-0.2681	-0.3912
18	2	2	0.6015	-0.2236	-0.7232	-0.4855	0.1838	0.5908	0.3503	-0.2470	-0.5555
19	1	1	0.5746	-0.1640	-0.4006	-0.1780	-0.1268	-0.3442	-0.2920	0.1862	0.4896
20	1	1	0.5839	0.2592	0.6395	0.6170	0.0008	0.0020	0.4189	0.1263	-0.2772
20	1	2	0.0007	0.0108	0.0460	0.1149	0.2098	0.3107	0.3962	0.4516	0.4707
20	2	1	0.0007	0.0108	0.0460	0.1149	0.2098	0.3107	0.3962	0.4516	0.4707
20	2	2	0.5359	-0.2062	-0.2570	0.2613	0.4506	0.0613	-0.2504	-0.0923	0.0903
21	1	1	0.5326	0.0763	0.3002	0.1561	-0.5106	-0.4889	-0.0109	-0.2436	-0.6227
21	1	2	0.0013	0.0181	0.0689	0.1397	0.1712	0.1008	-0.0718	-0.2585	-0.3394
21	2	1	0.0013	0.0181	0.0689	0.1397	0.1712	0.1008	-0.0718	-0.2585	-0.3394
21	2	2	0.4772	-0.4688	-0.7819	-0.2706	0.3300	0.4126	0.1053	-0.1731	-0.2614
22	1	1	0.4812	-0.0819	0.0830	0.0079	-0.4584	-0.1711	0.5507	0.4788	0.1545
22	1	2	0.0038	0.0490	0.1735	0.3241	0.3769	0.2591	0.0245	-0.1940	-0.2810
22	2	1	0.0038	0.0490	0.1735	0.3241	0.3769	0.2591	0.0245	-0.1940	-0.2810
22	2	2	0.4466	-0.3876	-0.3345	0.3069	0.3632	-0.2613	-0.4838	0.1036	0.5405

[110]

L	MU	MU'	5	10	15	20	25	30	35	40	45
4	1	1	0.9748	0.9012	0.7851	0.6357	0.4645	0.2839	0.1063	-0.0572	-0.1979
6	1	1	0.9476	0.8011	0.5898	0.3552	0.1413	-0.0151	-0.0920	-0.0861	-0.0117
8	1	1	0.9108	0.6689	0.3419	0.0168	-0.2284	-0.3481	-0.3389	-0.2340	-0.0858
9	1	1	0.8898	0.6039	0.2571	-0.0173	-0.1257	-0.0545	0.1272	0.3017	0.3581
10	1	1	0.8663	0.5299	0.1448	-0.1386	-0.2577	-0.2566	-0.2339	-0.2594	-0.3220
12	1	1	0.8122	0.3600	-0.0972	-0.3205	-0.2363	0.0390	0.2998	0.3931	0.3029
12	1	2	-0.0001	-0.0023	-0.0147	-0.0511	-0.1165	-0.1875	-0.2136	-0.1561	-0.0389
12	2	1	-0.0001	-0.0023	-0.0147	-0.0511	-0.1165	-0.1875	-0.2136	-0.1561	-0.0389
12	2	2	0.8144	0.3896	0.0162	-0.0835	0.0876	0.3362	0.4564	0.3882	0.2285
13	1	1	0.7841	0.2959	-0.1265	-0.2559	-0.1477	-0.0459	-0.1290	-0.3474	-0.4978
14	1	1	0.7541	0.2256	-0.1875	-0.3080	-0.2853	-0.3112	-0.3447	-0.1980	0.1578
15	1	1	0.7241	0.1861	-0.0731	-0.1374	0.4780	0.5000	0.1465	-0.2340	-0.3220
16	1	1	0.6849	0.0471	-0.3199	-0.1501	0.2730	0.4810	0.3129	0.0013	-0.1529
16	1	2	-0.0002	-0.0045	-0.0269	-0.0743	-0.1092	-0.0722	0.0158	0.0224	-0.1440
16	2	1	-0.0002	-0.0045	-0.0269	-0.0743	-0.1092	-0.0722	0.0158	0.0224	-0.1440
16	2	2	0.6903	0.1045	-0.1971	-0.1392	-0.0591	-0.0969	0.0590	0.1085	0.1243
17	1	1	0.6523	0.0035	-0.2975	-0.1707	-0.0616	-0.2010	-0.3165	-0.1499	0.1091
18	1	1	0.6186	-0.0385	-0.2767	-0.1778	-0.2018	-0.2882	-0.0687	0.3383	0.4505
18	1	2	-0.0009	-0.0203	-0.1102	-0.2600	-0.2838	-0.0409	0.2364	0.1899	-0.0744
18	2	1	-0.0009	-0.0203	-0.1102	-0.2600	-0.2838	-0.0409	0.2364	0.1899	-0.0744
18	2	2	0.6235	0.0299	-0.0136	0.3636	0.4919	0.2360	0.0286	0.0818	0.1959
19	1	1	0.5849	-0.0552	-0.1409	0.0603	-0.0629	-0.3538	-0.3791	-0.2925	-0.3479
20	1	1	0.5367	-0.1980	-0.2362	0.3020	0.5420	0.2039	-0.1596	-0.1317	0.0673
20	1	2	-0.0003	-0.0071	-0.0357	-0.0640	-0.0337	-0.0009	-0.1233	-0.3319	-0.2903
20	2	1	-0.0003	-0.0071	-0.0357	-0.0640	-0.0337	-0.0009	-0.1233	-0.3319	-0.2903
20	2	2	0.5479	-0.1177	-0.2522	-0.2007	-0.2057	0.0759	0.4024	0.2041	-0.1593
21	1	1	0.5024	-0.2119	-0.2357	-0.0032	-0.1189	-0.2067	0.0411	0.1282	-0.1554
21	1	2	-0.0005	-0.0122	-0.0578	-0.0949	-0.0470	-0.0352	-0.2278	-0.3727	-0.1363
21	2	1	-0.0005	-0.0122	-0.0578	-0.0949	-0.0470	-0.0352	-0.2278	-0.3727	-0.1363
21	2	2	0.5169	-0.0440	0.2475	0.6384	0.2857	-0.1988	-0.1087	0.1207	-0.0103
22	1	1	0.4678	-0.2188	-0.2079	-0.1453	-0.3133	-0.1024	0.2889	0.2103	-0.0339
22	1	2	-0.0015	-0.0330	-0.1437	-0.1883	0.0436	0.2646	0.1180	-0.0480	0.0487
22	2	1	-0.0015	-0.0330	-0.1437	-0.1883	0.0436	0.2646	0.1180	-0.0480	0.0487
22	2	2	0.4763	-0.1439	-0.0660	0.0353	-0.0129	0.1110	-0.0115	-0.3170	-0.1008

[110]

L	MU	MU'	50	55	60	65	70	75	80	85	90
4	1	1	-0.3104	-0.3925	-0.4453	-0.4729	-0.4814	-0.4778	-0.4692	-0.4614	-0.4583
6	1	1	0.1039	0.2285	0.3335	0.4002	0.4237	0.4122	0.3828	0.3549	0.3437
8	1	1	0.0553	0.1569	0.2113	0.2298	0.2318	0.2333	0.2401	0.2487	0.2526
9	1	1	0.2430	-0.0160	-0.3257	-0.5719	-0.6726	-0.6152	-0.4587	-0.3034	-0.2396
10	1	1	-0.3458	-0.2598	-0.0661	0.1451	0.2501	0.1776	-0.0351	-0.2589	-0.3535
12	1	1	0.1296	-0.0033	-0.0357	0.0031	0.0368	0.0074	-0.0835	-0.1820	-0.2240
12	1	2	0.0405	-0.0285	-0.2709	-0.5724	-0.7341	-0.6138	-0.2493	0.1437	0.3118
12	2	1	0.0405	-0.0285	-0.2709	-0.5724	-0.7341	-0.6138	-0.2493	0.1437	0.3118
12	2	2	0.1133	0.0957	0.1292	0.1471	0.1417	0.1597	0.2332	0.3285	0.3726
13	1	1	-0.4434	-0.2496	-0.1024	-0.1034	-0.1585	-0.0793	0.2056	0.5492	0.7038
14	1	1	0.4944	0.5757	0.4285	0.2797	0.2499	0.2116	-0.0010	-0.3186	-0.4746
15	1	1	-0.1618	-0.0372	-0.1084	-0.2703	-0.3476	-0.3198	-0.2950	-0.3263	-0.3535
16	1	1	-0.0914	0.0226	0.0415	-0.0228	-0.0677	-0.0385	0.0337	0.0935	0.1147
16	1	2	-0.3600	-0.3648	-0.0594	0.3444	0.5384	0.4360	0.2066	0.0395	-0.0127
16	2	1	-0.3600	-0.3648	-0.0594	0.3444	0.5384	0.4360	0.2066	0.0395	-0.0127
16	2	2	-0.1710	-0.4730	-0.4075	-0.0739	0.1150	0.0360	-0.0404	0.0542	0.1392
17	1	1	0.1338	-0.0289	-0.0543	0.1484	0.3078	0.1878	-0.1251	-0.3930	-0.4882
18	1	1	0.1853	-0.0975	-0.2169	-0.3097	-0.3991	-0.2890	0.0790	0.4813	0.6499
18	1	2	-0.1048	0.1256	0.1293	-0.2530	-0.5322	-0.3683	-0.0910	-0.0682	-0.1337
18	2	1	-0.1048	0.1256	0.1293	-0.2530	-0.5322	-0.3683	-0.0910	-0.0682	-0.1337
18	2	2	0.2306	0.2448	0.2366	0.1507	0.0775	0.1280	0.2166	0.2187	0.1923
19	1	1	-0.2573	0.1589	0.3987	0.1243	-0.1551	0.0142	0.2252	0.0486	-0.1405
20	1	1	0.1006	-0.0007	-0.0390	0.0123	0.0497	0.0298	-0.0121	-0.0423	-0.0525
20	1	2	0.0749	0.3436	0.1844	-0.1780	-0.3490	-0.2829	-0.1774	-0.1363	-0.1319
20	2	1	0.0749	0.3436	0.1844	-0.1780	-0.3490	-0.2829	-0.1774	-0.1363	-0.1319
20	2	2	-0.1012	0.0730	0.0827	0.2956	0.5815	0.3139	-0.2220	-0.2907	-0.1555
21	1	1	-0.2601	0.0136	0.1458	-0.0968	-0.3005	-0.1751	0.0813	0.2248	0.2544
21	1	2	0.1351	-0.0420	-0.2423	0.1199	0.5150	0.2466	-0.1178	0.1449	0.4501
21	2	1	0.1351	-0.0420	-0.2423	0.1199	0.5150	0.2466	-0.1178	0.1449	0.4501
21	2	2	-0.2176	-0.2185	-0.1840	-0.2171	-0.2314	-0.2421	-0.2711	-0.2534	-0.2247
22	1	1	-0.0266	-0.0567	-0.0878	0.2864	0.6627	0.3694	-0.2223	-0.4038	-0.3458
22	1	2	0.0319	-0.1136	-0.0206	0.0564	-0.0570	0.1174	0.3768	0.0547	-0.2929
22	2	1	0.0319	-0.1136	-0.0206	0.0564	-0.0570	0.1174	0.3768	0.0547	-0.2929
22	2	2	0.2195	-0.0347	-0.3114	-0.2305	-0.1899	-0.1066	0.1497	0.1684	0.0567

[111]

L	MU	MU'	5	10	15	20	25	30	35	40	45	50	55	60
4	1	1	0.9748	0.9008	0.7830	0.6296	0.4510	0.2593	0.0675	-0.1111	-0.2645	-0.3822	-0.4562	-0.4815
6	1	1	0.9477	0.8030	0.5988	0.3807	0.1952	0.0782	0.0461	0.0926	0.1914	0.3040	0.3912	0.4239
8	1	1	0.9105	0.6632	0.3169	-0.0480	-0.3495	-0.5254	-0.5483	-0.4321	-0.2263	-0.0020	0.1685	0.2318
9	1	1	0.8900	0.6067	0.2658	-0.0089	-0.1474	-0.1632	-0.1353	-0.1543	-0.2658	-0.4435	-0.6072	-0.6735
10	1	1	0.8666	0.5357	0.1769	-0.0330	-0.0448	0.2198	0.4988	0.6756	0.6685	0.5125	0.3301	0.2511
12	1	1	0.8101	0.3309	0.2157	-0.5945	-0.6750	-0.4836	-0.1680	0.0983	0.2105	0.1750	0.0827	0.0372
12	1	2	-0.0002	-0.0020	-0.0010	0.0228	0.0922	0.1984	0.2784	0.2399	0.0302	-0.3015	-0.6100	-0.7357
12	2	1	-0.0002	-0.0020	-0.0010	0.0228	0.0922	0.1984	0.2784	0.2399	0.0302	-0.3015	-0.6100	-0.7357
12	2	2	0.8159	0.4098	0.0855	0.0312	0.1667	0.2508	0.1321	-0.1067	-0.2468	-0.1655	0.0370	0.1415
13	1	1	0.7836	0.2887	-0.1514	-0.2975	-0.1759	-0.0090	0.0098	-0.1228	-0.2599	-0.2779	-0.2061	-0.1594
14	1	1	0.7546	0.2389	-0.0960	0.0050	0.3722	0.5943	0.4259	0.0149	-0.2635	-0.1884	0.0966	0.2500
15	1	1	0.7271	0.2154	-0.0361	0.0090	-0.0303	-0.3139	-0.5178	-0.3349	0.0241	0.0985	-0.1670	-0.3482
16	1	1	0.6781	-0.0407	-0.6294	-0.7180	-0.3580	0.0950	0.3184	0.2559	0.0736	-0.0504	-0.0751	-0.0681
16	1	2	-0.0003	-0.0009	0.0138	0.0690	0.1345	0.0964	-0.1234	-0.4041	-0.4669	-0.1605	0.3123	0.5401
16	2	1	-0.0003	-0.0009	0.0138	0.0690	0.1345	0.0964	-0.1234	-0.4041	-0.4669	-0.1605	0.3123	0.5401
16	2	2	0.6934	0.1499	-0.0021	0.3095	0.5830	0.4770	0.2315	0.2341	0.4360	0.4750	0.2620	0.1167
17	1	1	0.6489	-0.0336	-0.3880	-0.2344	0.0125	-0.0475	-0.3171	-0.4204	-0.2193	0.0811	0.2029	0.3096
18	1	1	0.6184	-0.0276	-0.1710	0.1477	0.2554	-0.0860	-0.3673	-0.1588	0.2374	0.2453	-0.1526	-0.4004
18	1	2	-0.0014	-0.0042	0.0588	0.2585	0.4247	0.2631	-0.1508	-0.3729	-0.2572	-0.1811	-0.3783	-0.5351
18	2	1	-0.0014	-0.0042	0.0588	0.2585	0.4247	0.2631	-0.1508	-0.3729	-0.2572	-0.1811	-0.3783	-0.5351
18	2	2	0.6304	0.0920	0.0609	0.1851	-0.0652	-0.3374	-0.1675	0.0597	-0.1150	-0.3176	-0.1235	0.0766
19	1	1	0.5883	-0.0179	-0.0459	0.1779	0.0787	-0.0687	0.0961	0.1335	-0.3063	-0.6456	-0.4110	-0.1582
20	1	1	0.5201	-0.3913	-0.7912	-0.4054	0.1965	0.3968	0.1755	-0.0811	-0.1298	-0.0427	0.0302	0.0501
20	1	2	-0.0003	0.0018	0.0309	0.0777	0.0202	-0.2015	-0.3413	-0.1041	0.3100	0.3476	-0.0733	-0.3504
20	2	1	-0.0003	0.0018	0.0309	0.0777	0.0202	-0.2015	-0.3413	-0.1041	0.3100	0.3476	-0.0733	-0.3504
20	2	2	0.5534	-0.0190	0.1866	0.6429	0.4805	0.0573	0.1280	0.4357	0.3839	0.2219	0.3982	0.5854
21	1	1	0.4924	-0.3081	-0.4143	-0.0639	-0.0604	-0.3467	-0.2763	0.1735	0.4123	0.1966	-0.1537	-0.3026
21	1	2	-0.0006	0.0032	0.0509	0.1220	0.0421	-0.2420	-0.4548	-0.3586	-0.0687	0.2157	0.4306	0.5195
21	2	1	-0.0006	0.0032	0.0509	0.1220	0.0421	-0.2420	-0.4548	-0.3586	-0.0687	0.2157	0.4306	0.5195
21	2	2	0.5281	0.0660	0.0394	-0.1921	-0.5533	-0.2230	0.1088	-0.1910	-0.2008	0.2158	0.0778	-0.2313
22	1	1	0.4641	-0.2301	-0.1111	0.1464	-0.1549	-0.3822	-0.0835	0.0647	-0.2618	-0.3147	0.2649	0.6672
22	1	2	-0.0016	0.0087	0.1304	0.2739	0.0521	-0.3719	-0.2860	0.1316	0.0182	-0.3921	-0.2925	-0.0592
22	2	1	-0.0016	0.0087	0.1304	0.2739	0.0521	-0.3719	-0.2860	0.1316	0.0182	-0.3921	-0.2925	-0.0592
22	2	2	0.4875	-0.0088	0.3241	0.4882	0.1676	0.1864	0.3300	0.0430	-0.0999	0.1096	0.0139	-0.1903

Appendix 4

Graphic Representations

- A.4.1 Generalized LEGENDRE Functions $P_l^{mn}(\Phi)$ for $l = 1 \text{ (1) } 4$, $m = 0 \text{ (1) } l$, $n = 0 \text{ (1) } m$ (see also *Table 15.3*)
- A.4.2 Cubic Spherical Harmonics $\dot{k}_l^{\mu}(\Phi\beta)$ for $l = 4 \text{ (1) } 17$, $\mu = 1 \text{ (1) } M(l)$ (see also *Table 15.4*)
- A.4.3 Cubic Generalized Spherical Harmonics
- A.4.3.1 Cubic-orthorhombic Generalized Spherical Harmonics $\dot{T}_l^{\mu n}(\varphi_1\Phi\varphi_2)$ for $l = 4, 6, 9$ (see also *Table 15.5.1* and reference 76)
Sections $\varphi_1 = \text{constant}$. The level lines correspond to 0 (heavy line), ± 0.2 , ± 0.4 , ± 0.6 , ± 0.8
Sections $\varphi_2 = \text{constant}$. The level lines correspond to 0 (heavy line), ± 0.2 , ± 0.4 , ± 0.6 , ± 0.8
- A.4.3.2 Cubic-cubic Generalized Spherical Harmonics $\dot{T}_l^{\mu\mu'}(\varphi_1\Phi\varphi_2)$ for $l = 4, 6, 9$ (see also *Table 15.5.2* and reference 76)
The level lines correspond to 0 (heavy line) ± 0.2 , ± 0.4 , ± 0.6 , ± 0.8

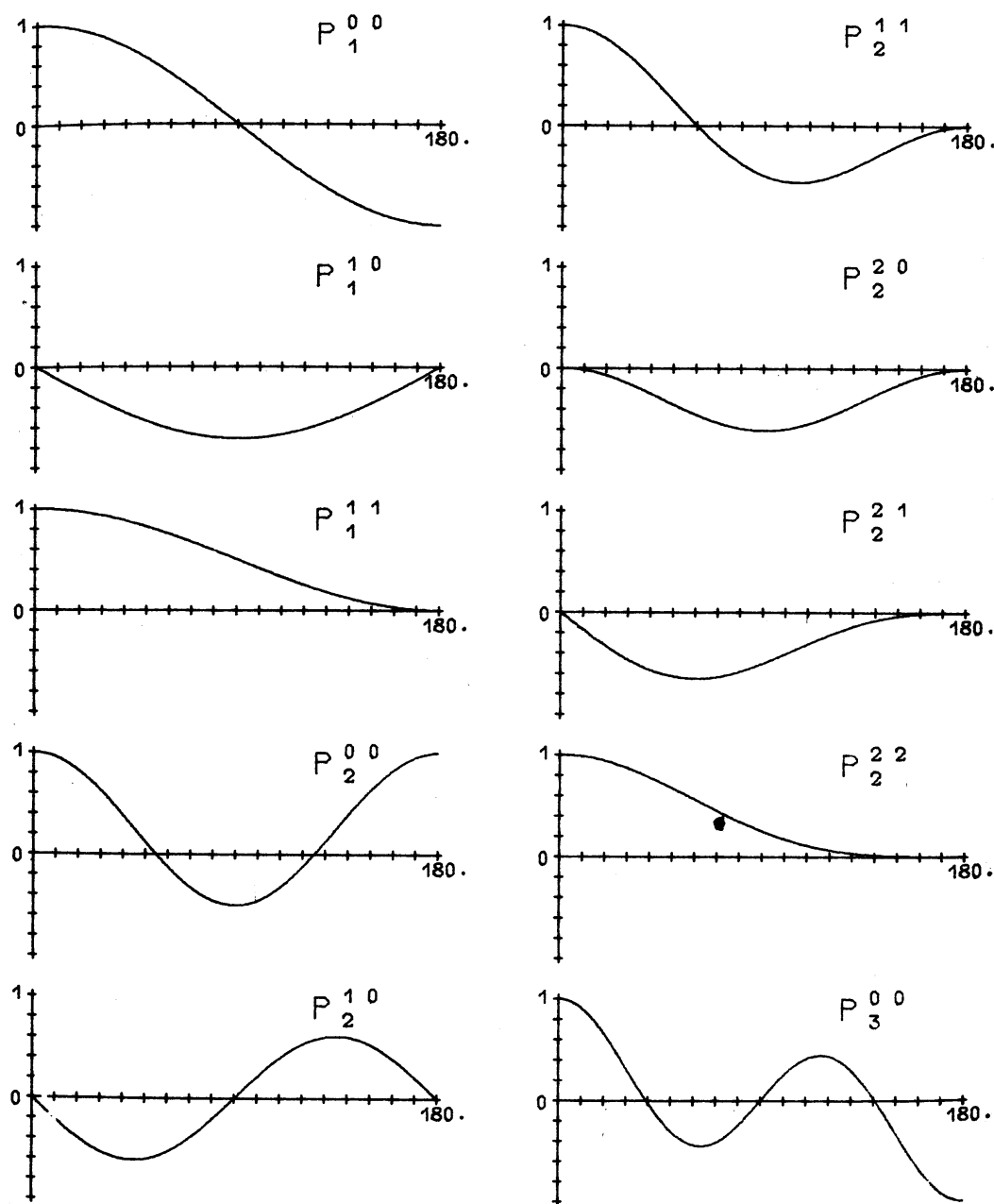


Figure A.4.1.1

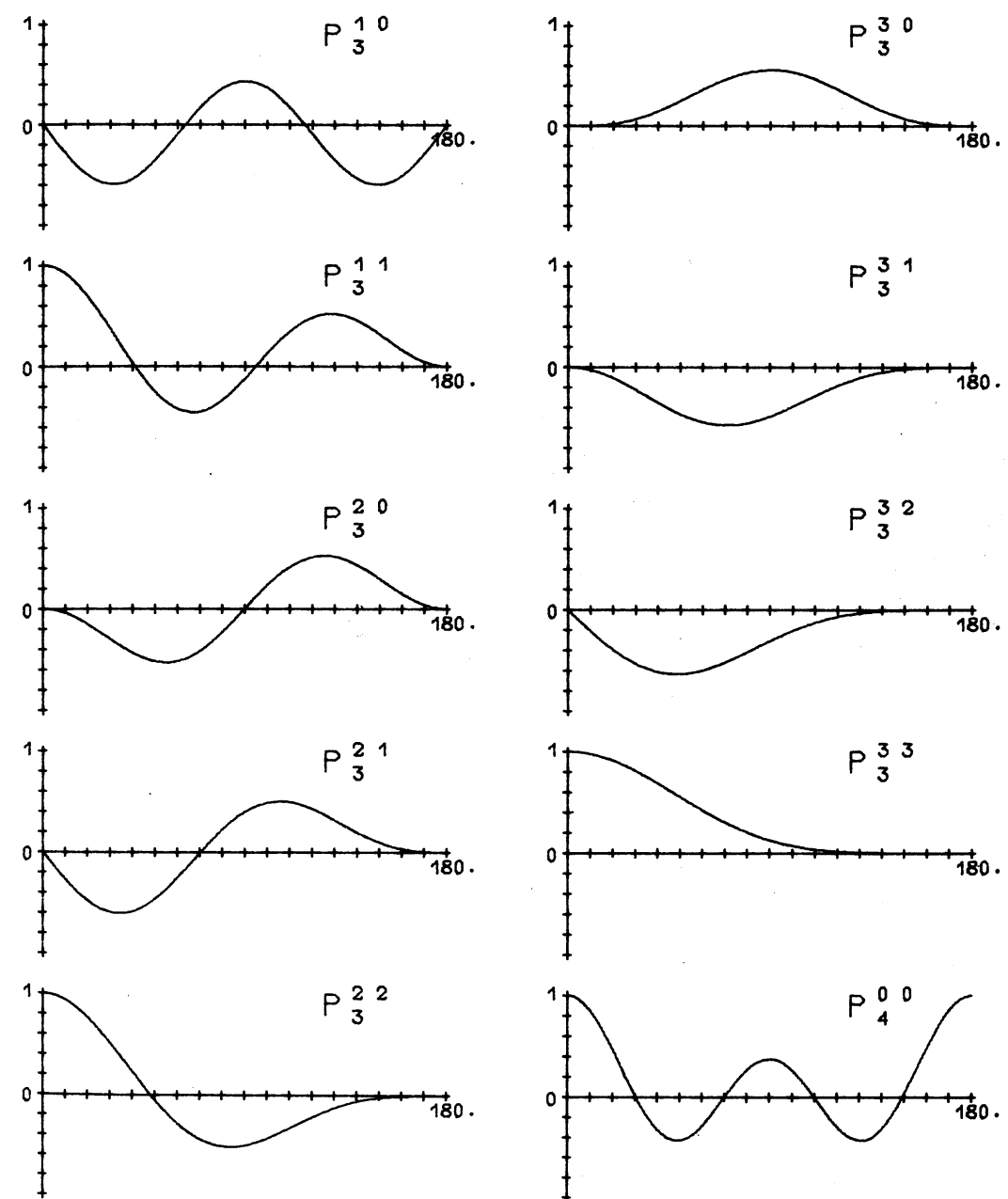


Figure A.4.1.2

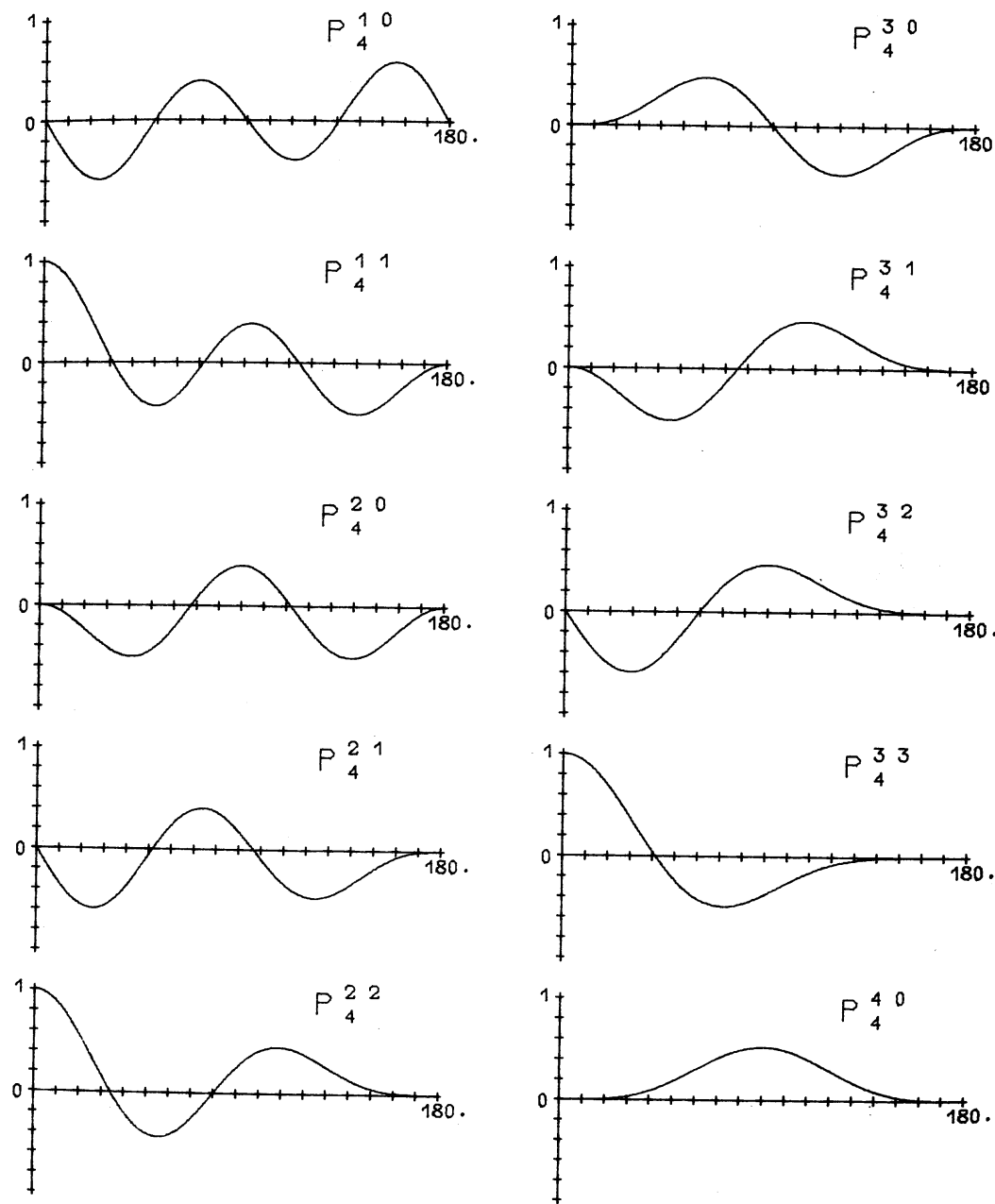


Figure A.4.1.3

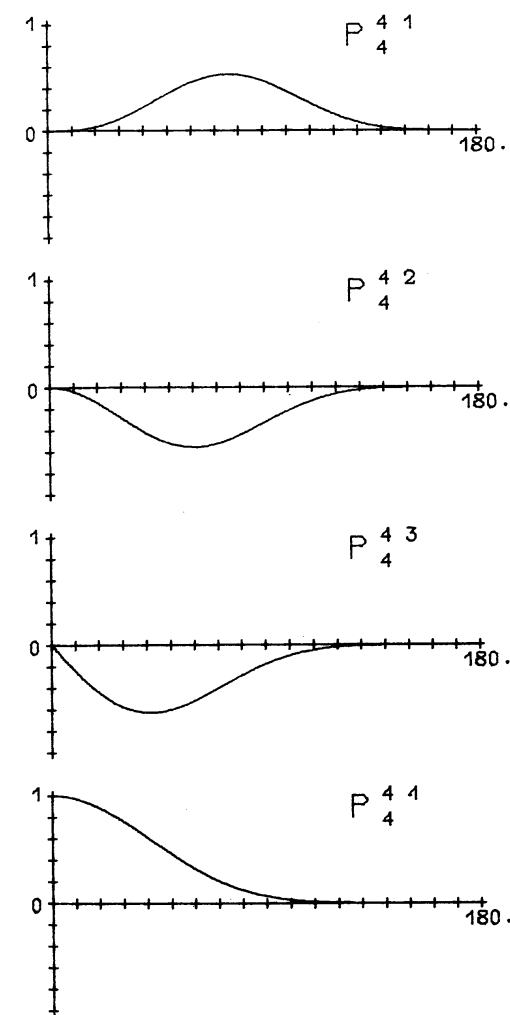


Figure A.4.1.4

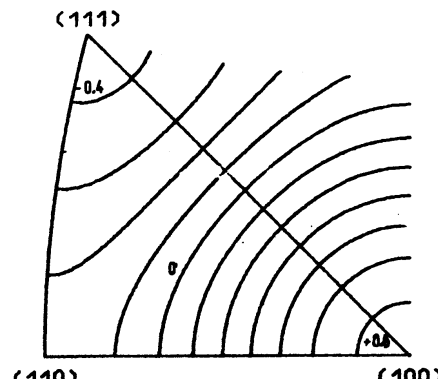
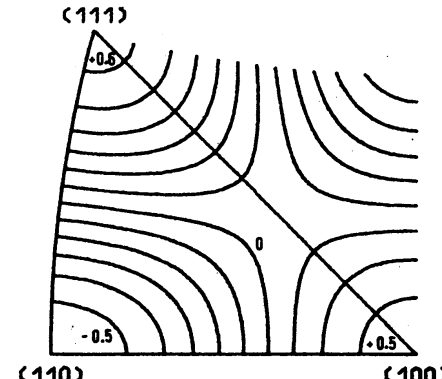
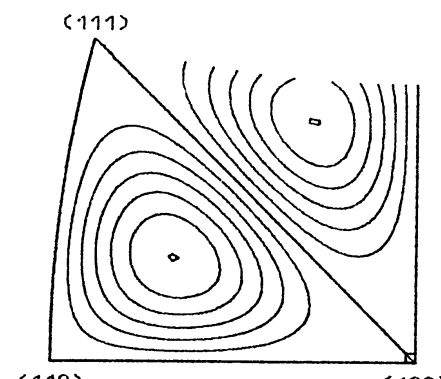
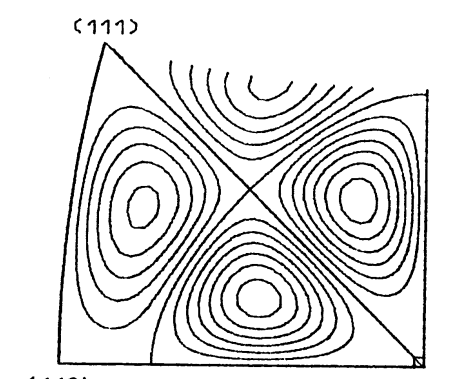
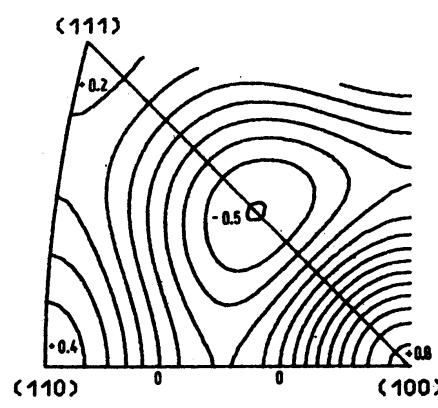
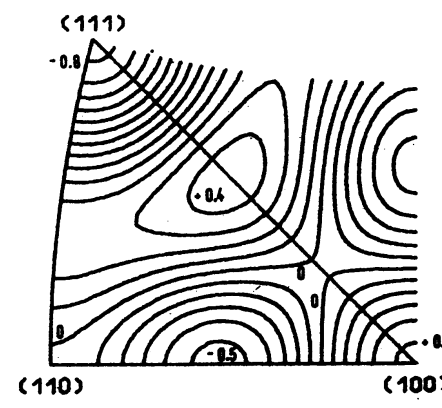
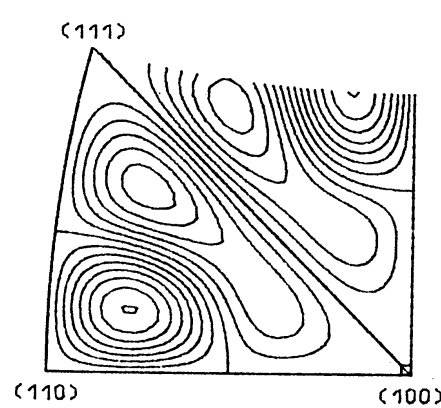
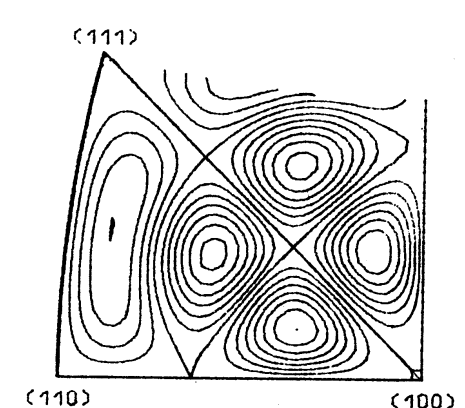
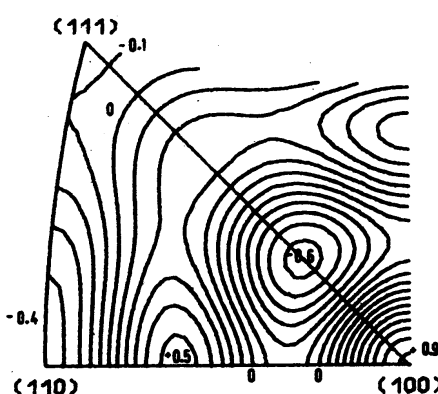
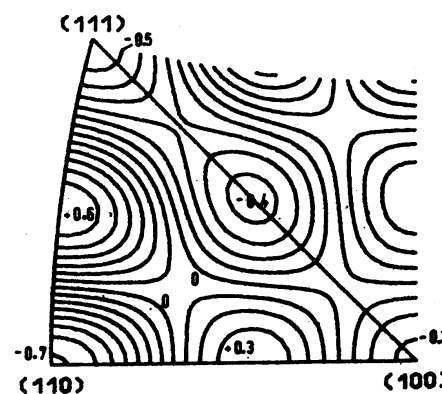
 K_4^1  K_6^1  K_9^1  K_{13}^1  K_8^1  K_{10}^1  K_{15}^1  K_{17}^1  K_{12}^1  K_{12}^2

Figure A.4.2

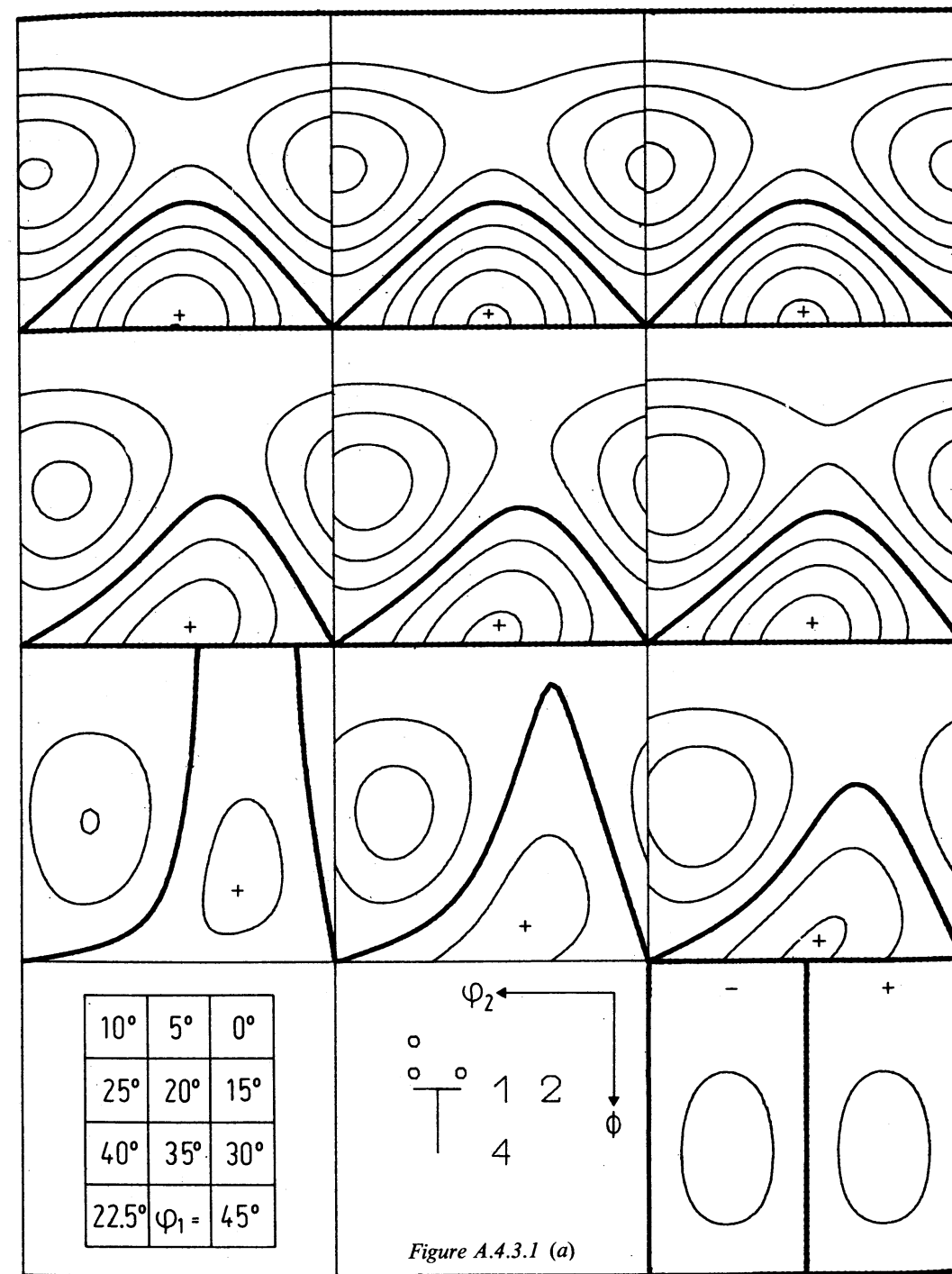


Figure A.4.3.1 (a)

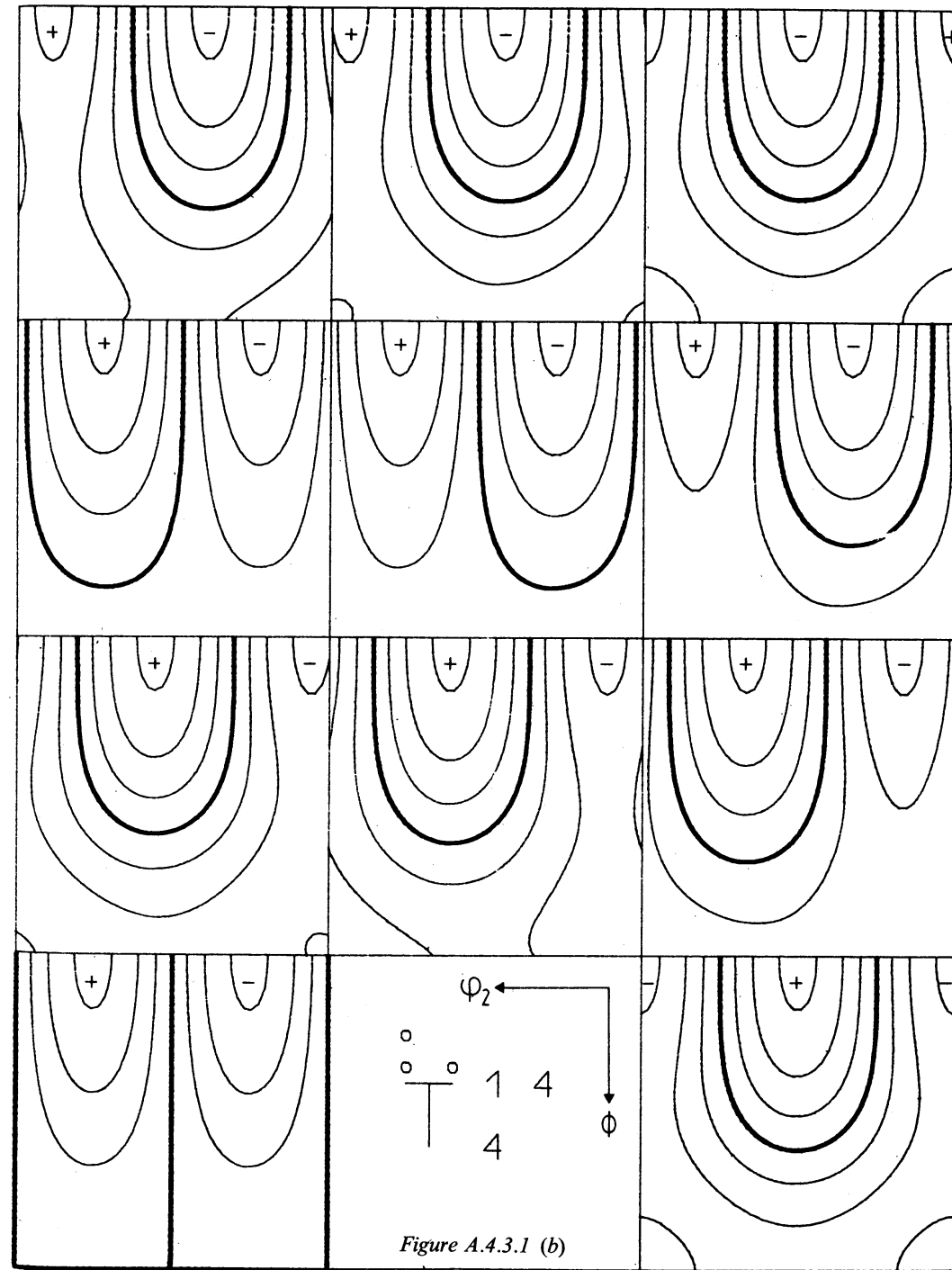


Figure A.4.3.1 (b)

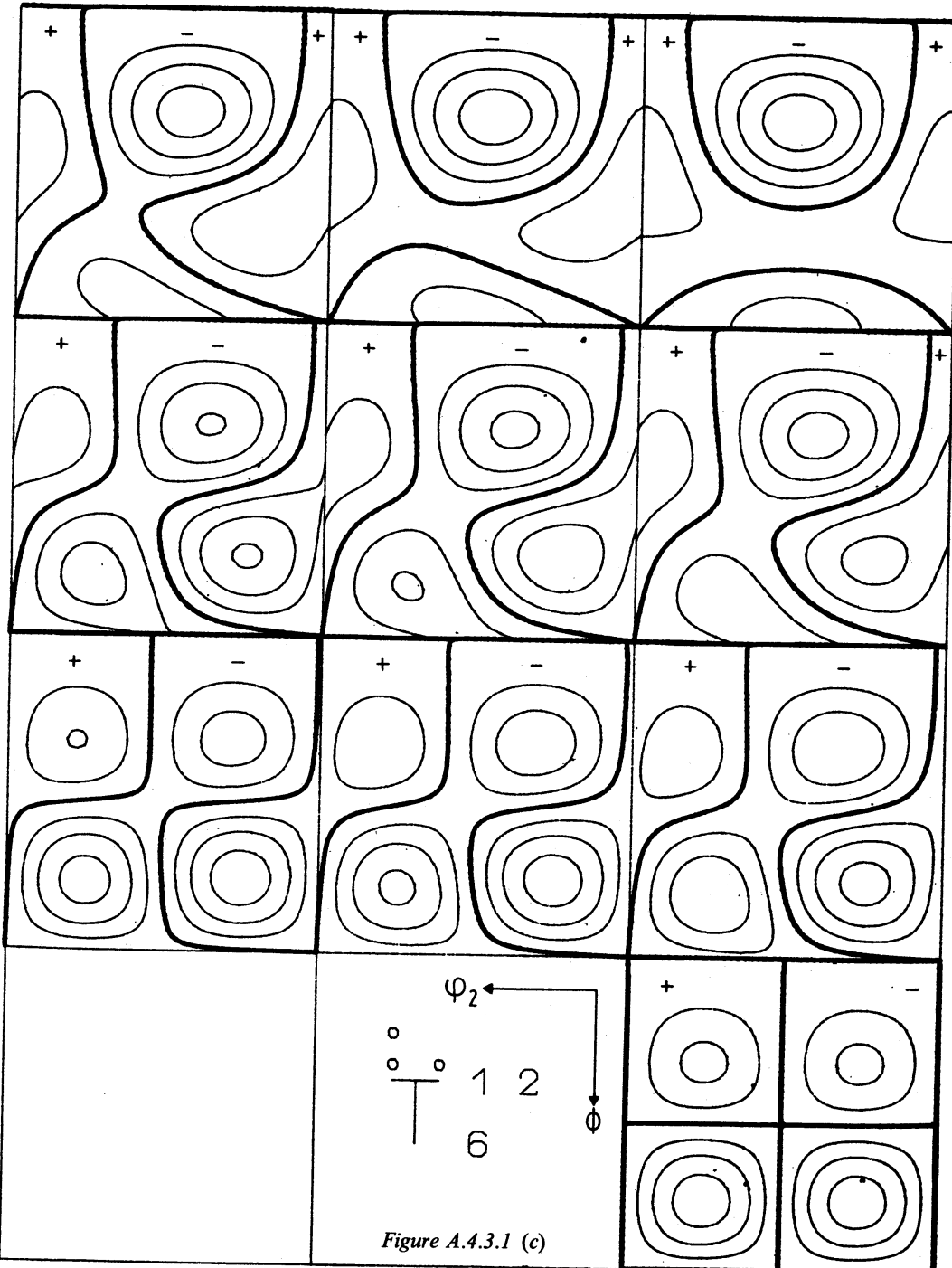


Figure A.4.3.1 (c)

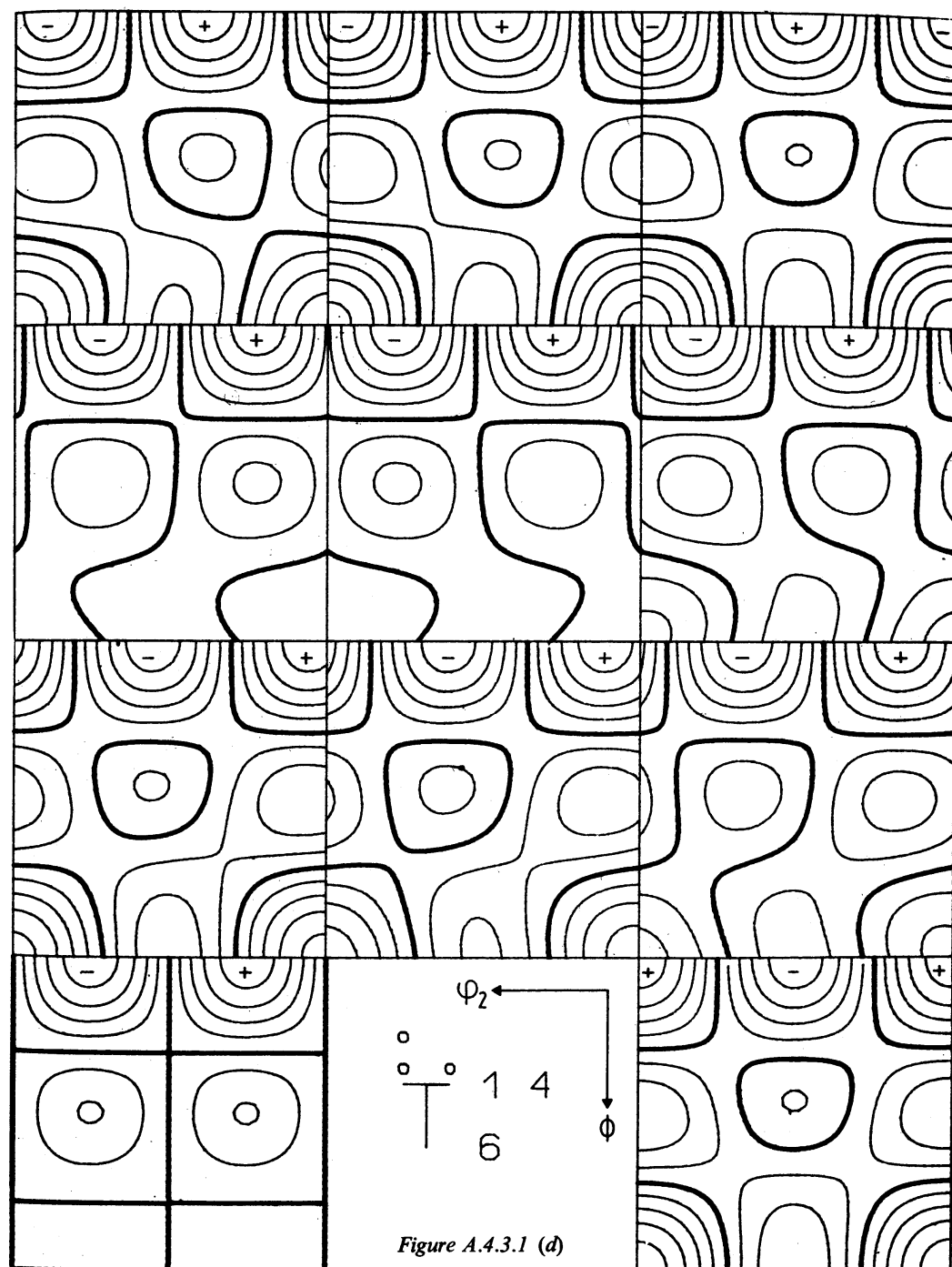


Figure A.4.3.1 (d)

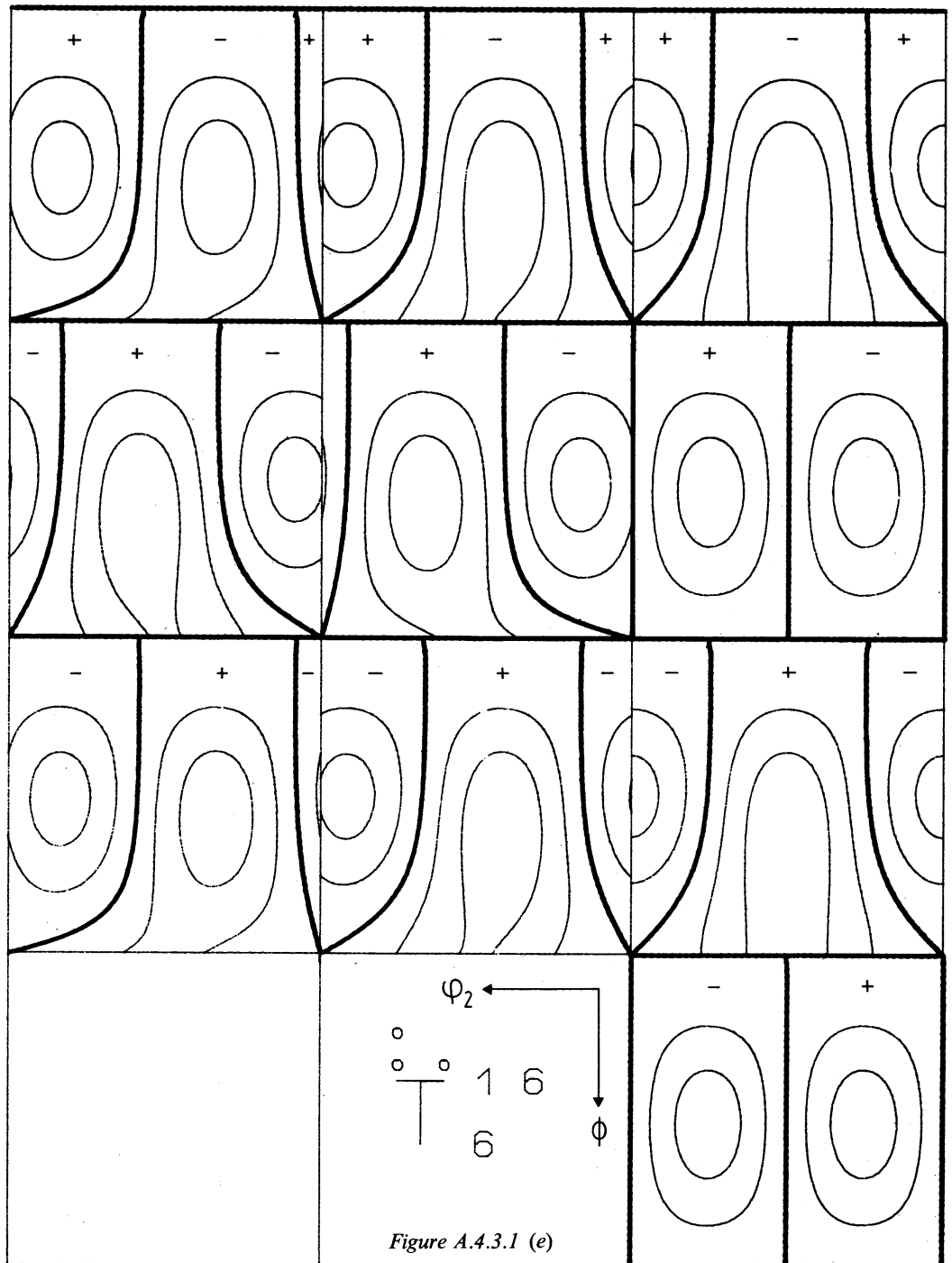


Figure A.4.3.1 (e)

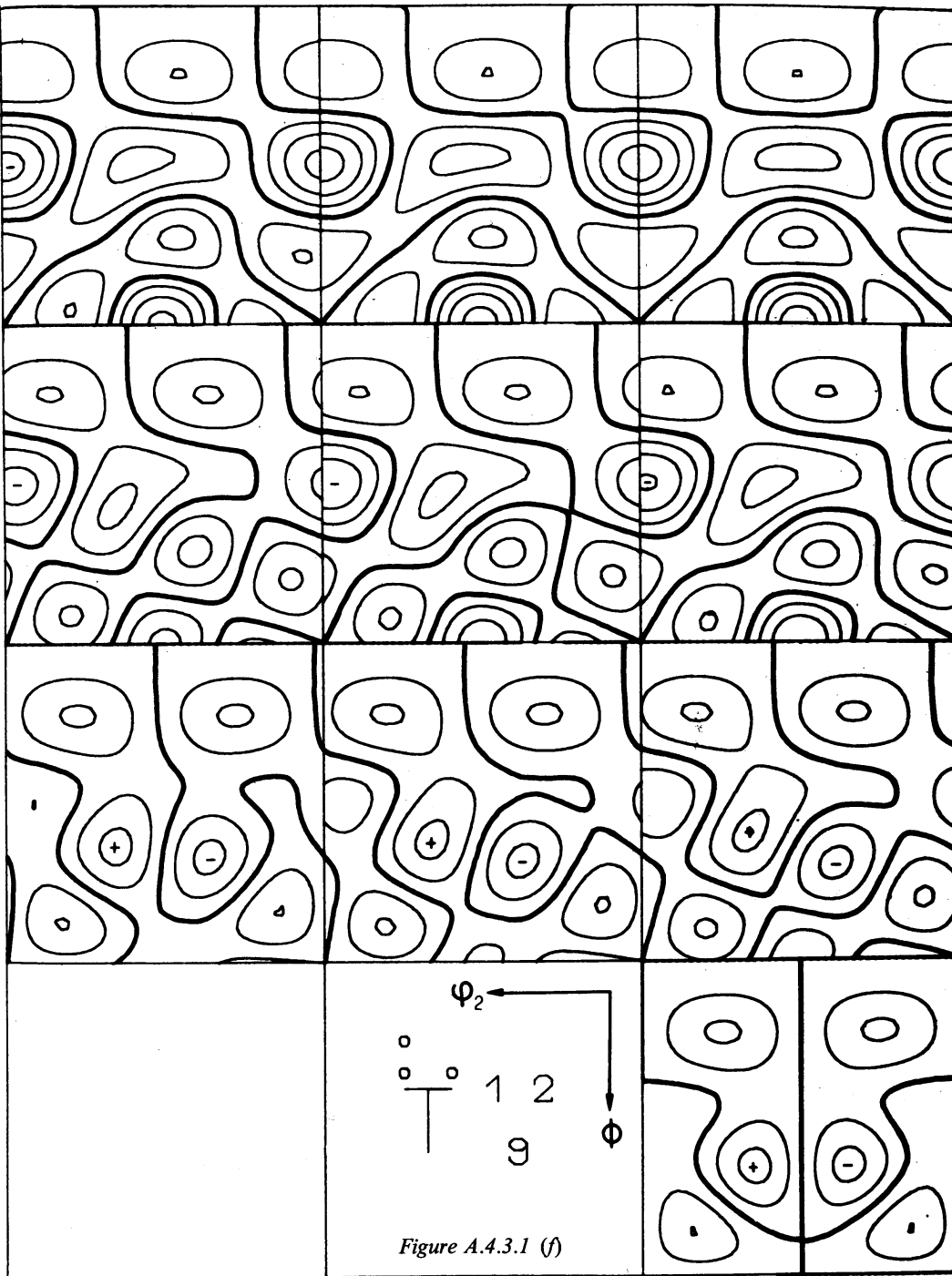
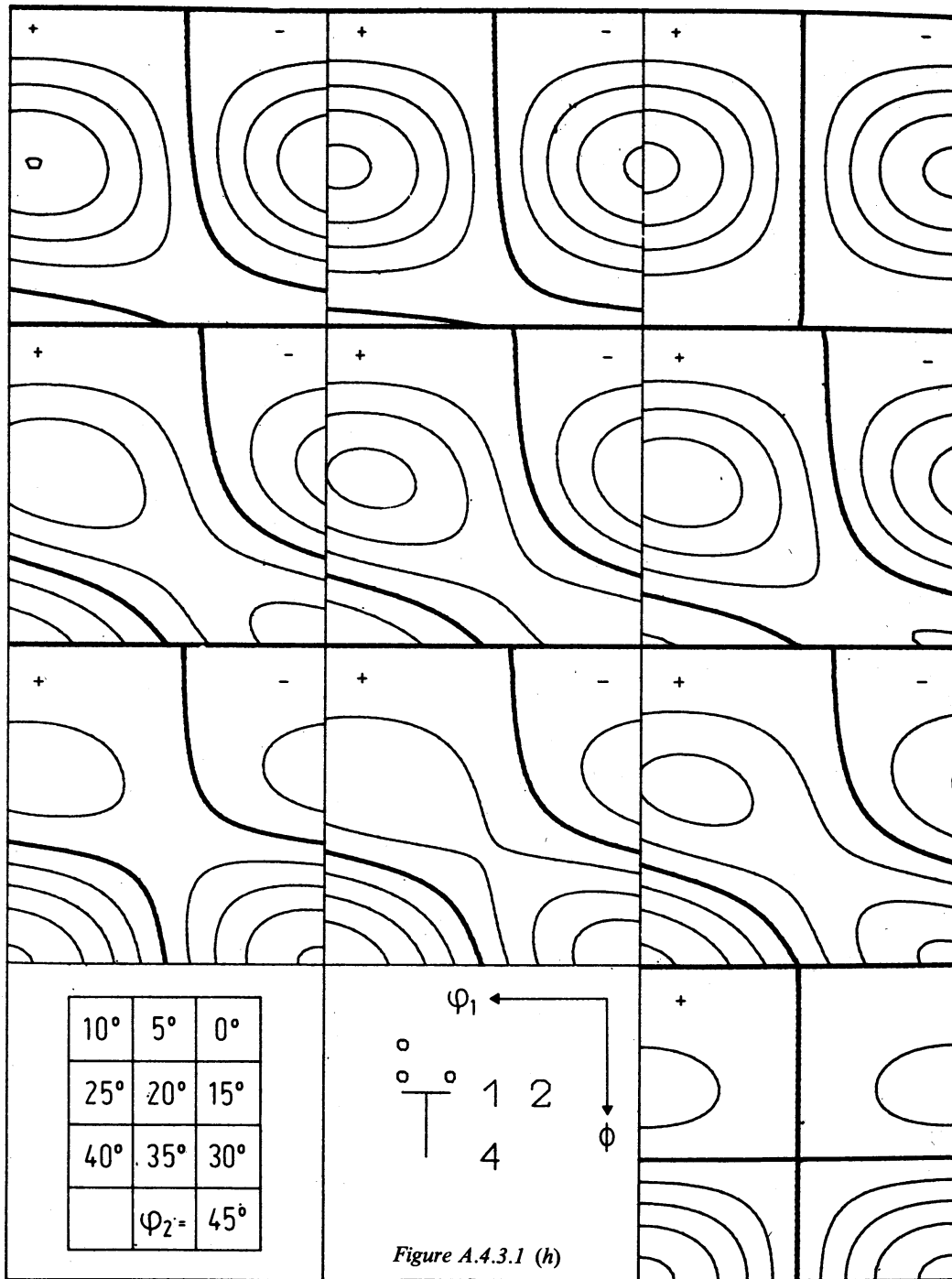
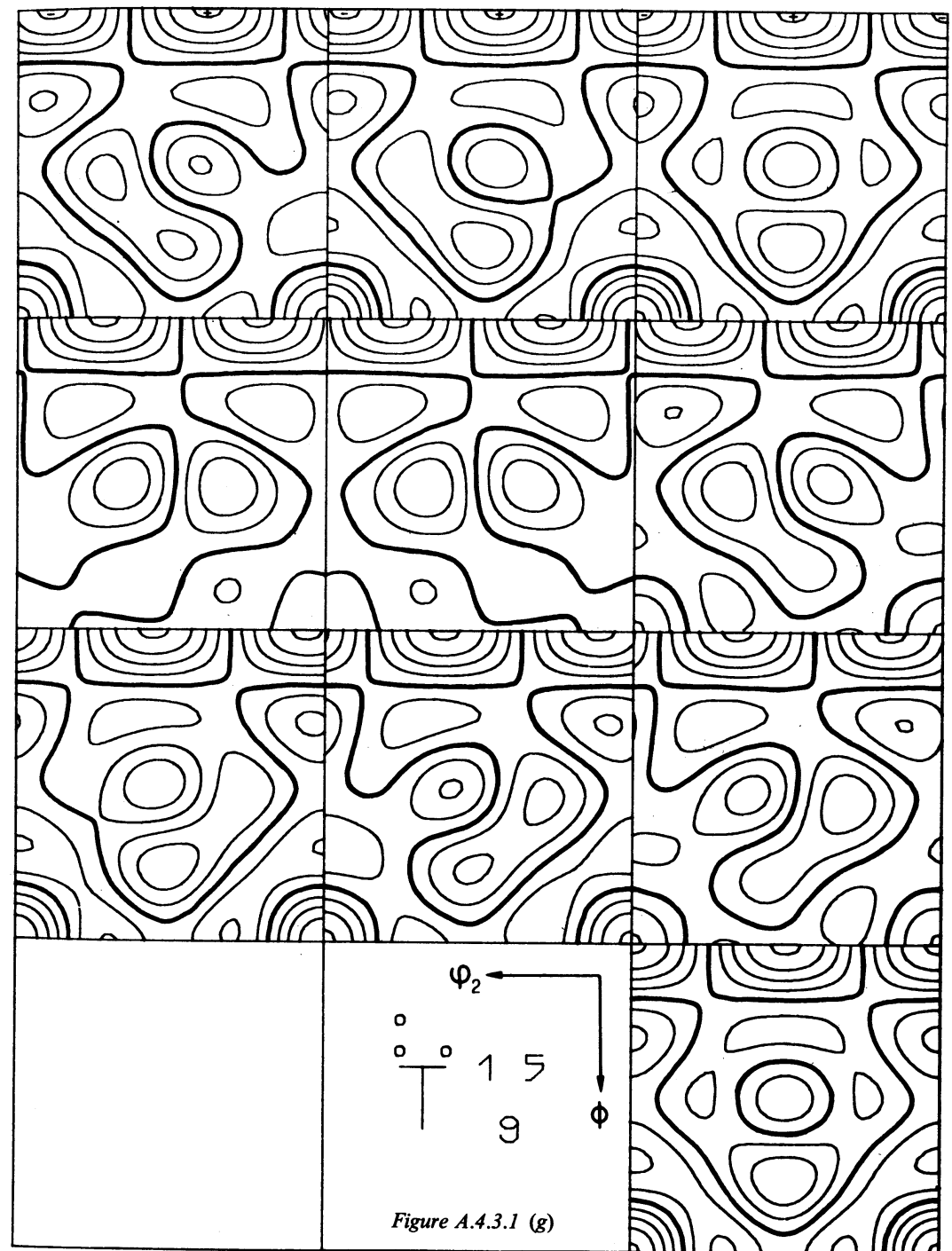


Figure A.4.3.1 (f)



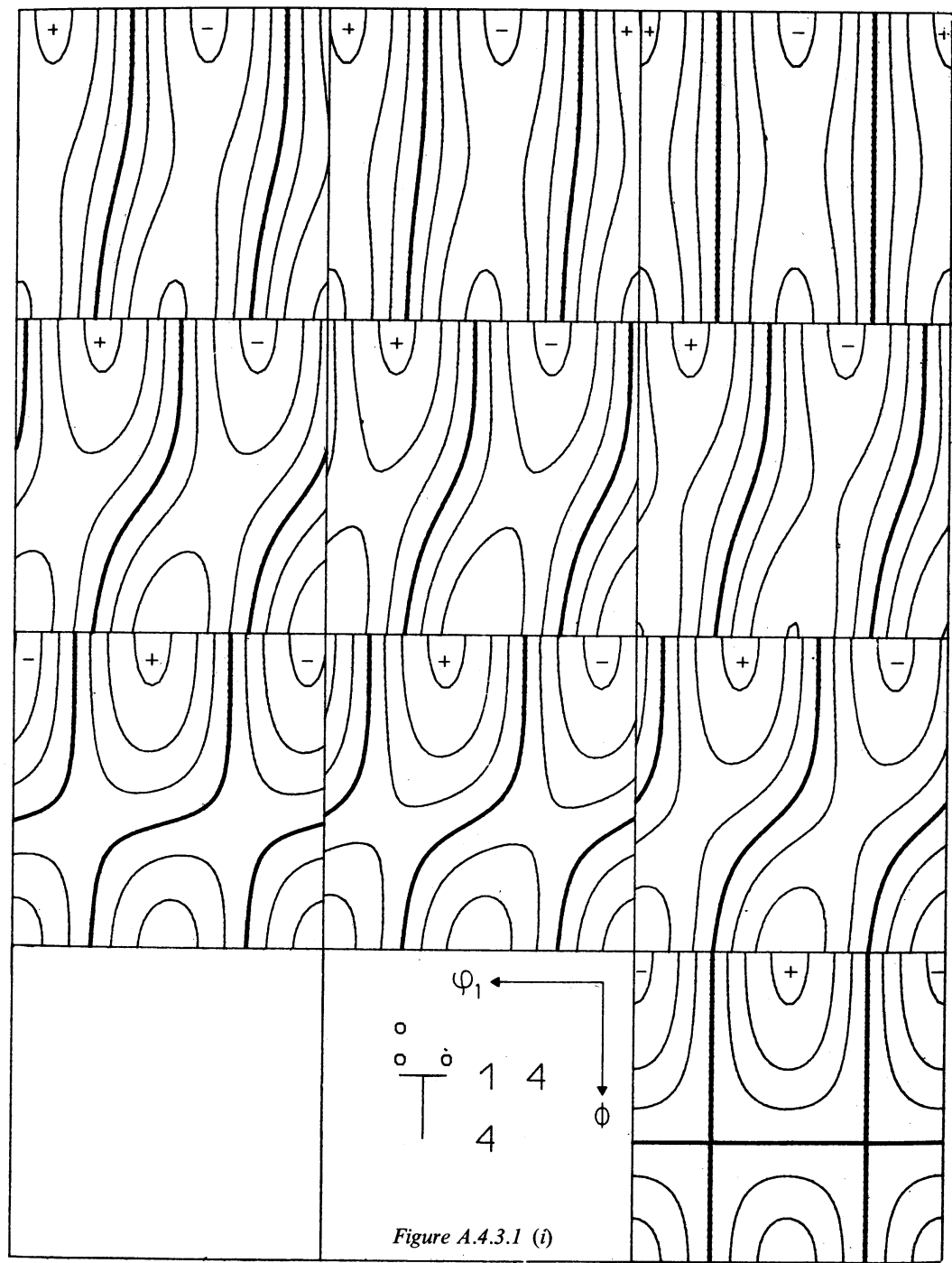


Figure A.4.3.1 (i)

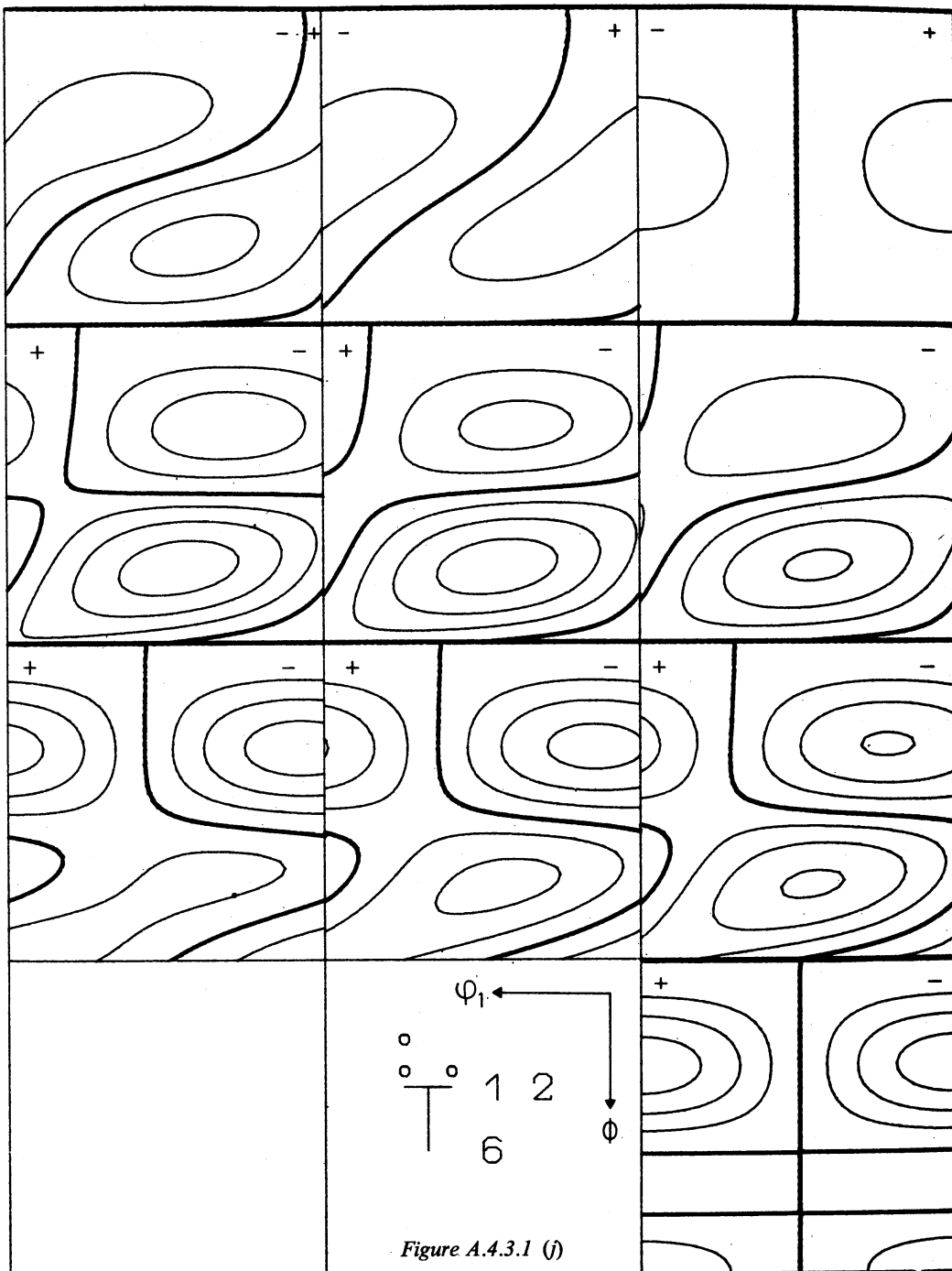


Figure A.4.3.1 (j)

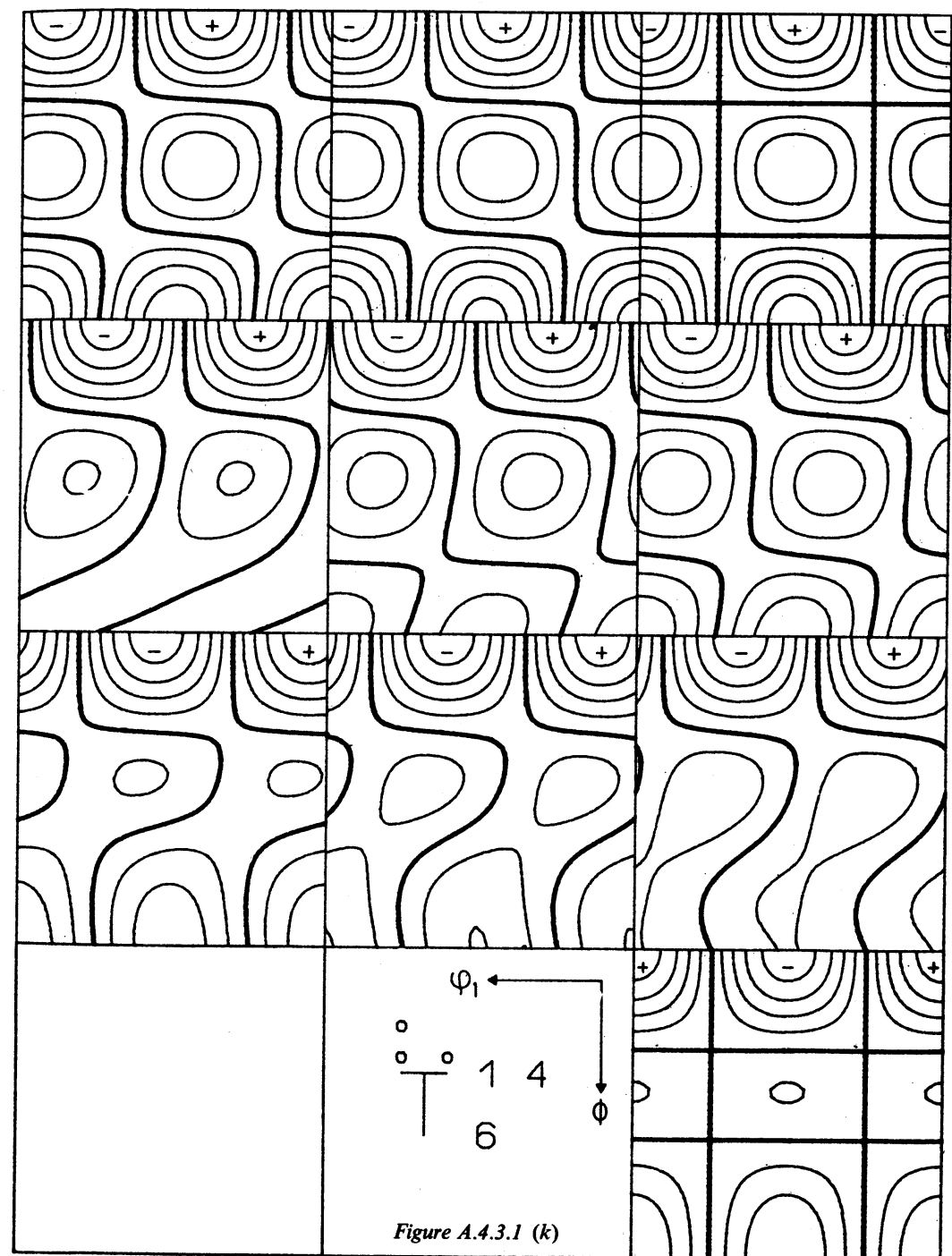


Figure A.4.3.1 (k)

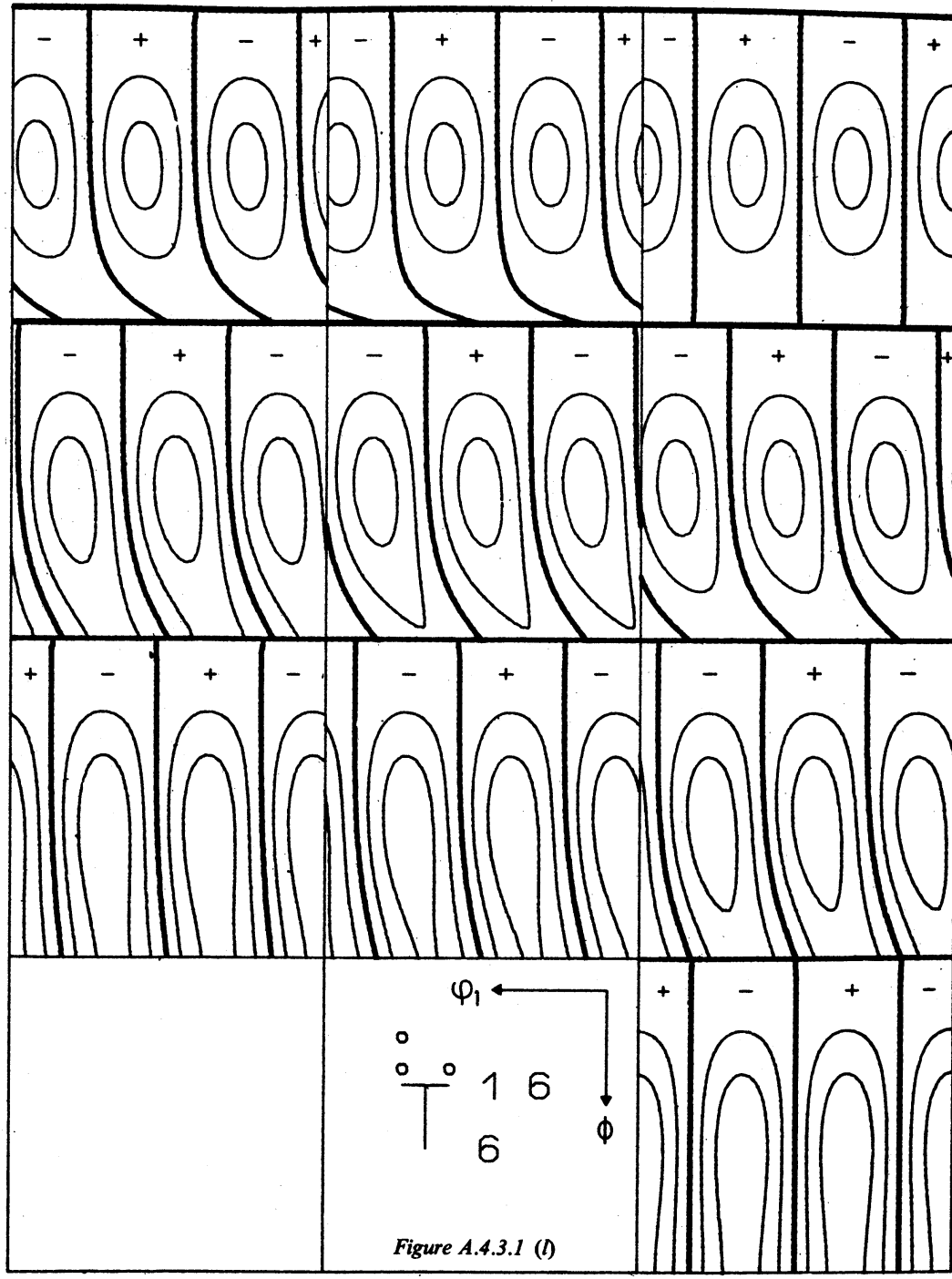


Figure A.4.3.1 (l)

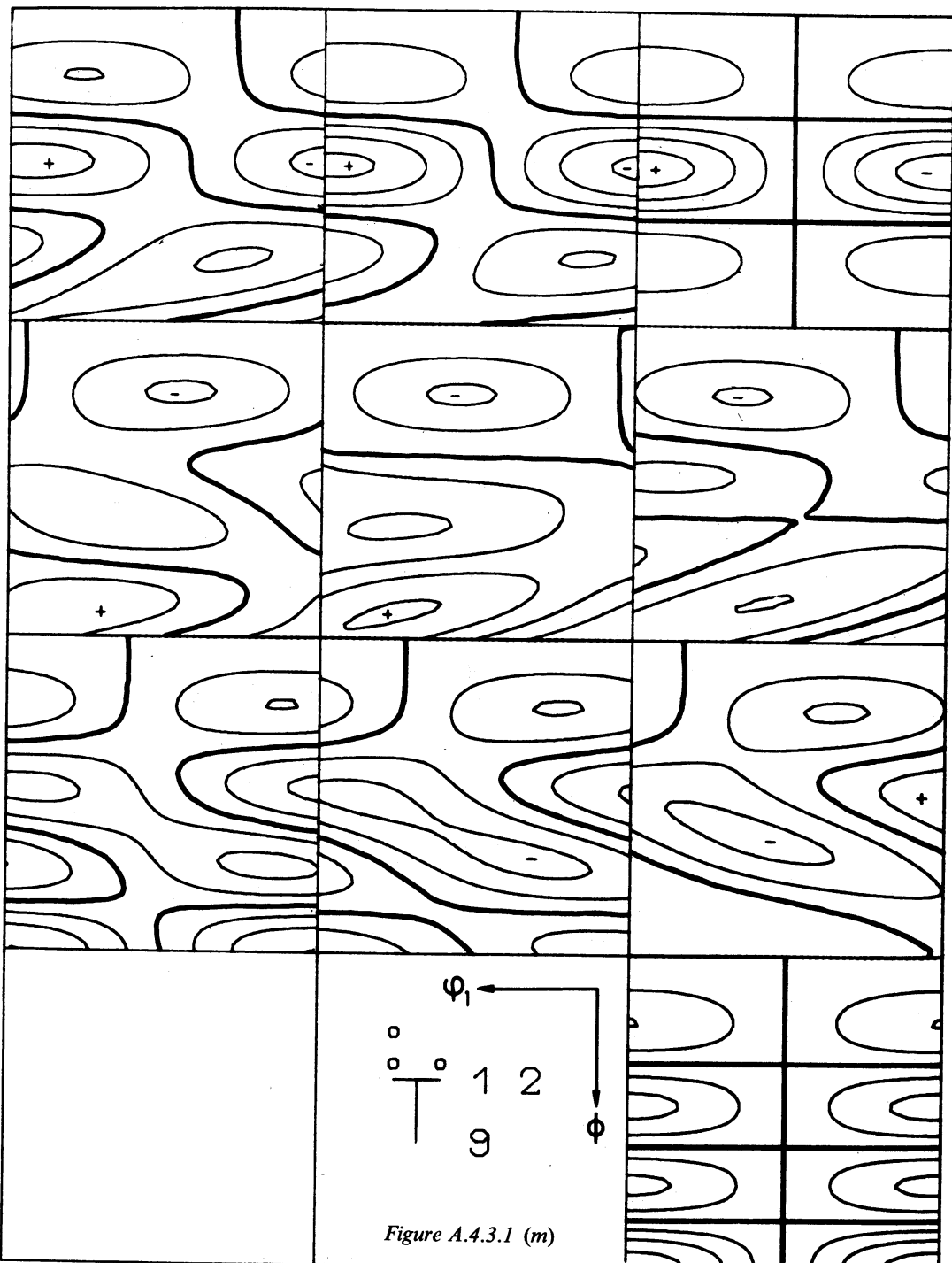


Figure A.4.3.1 (m)

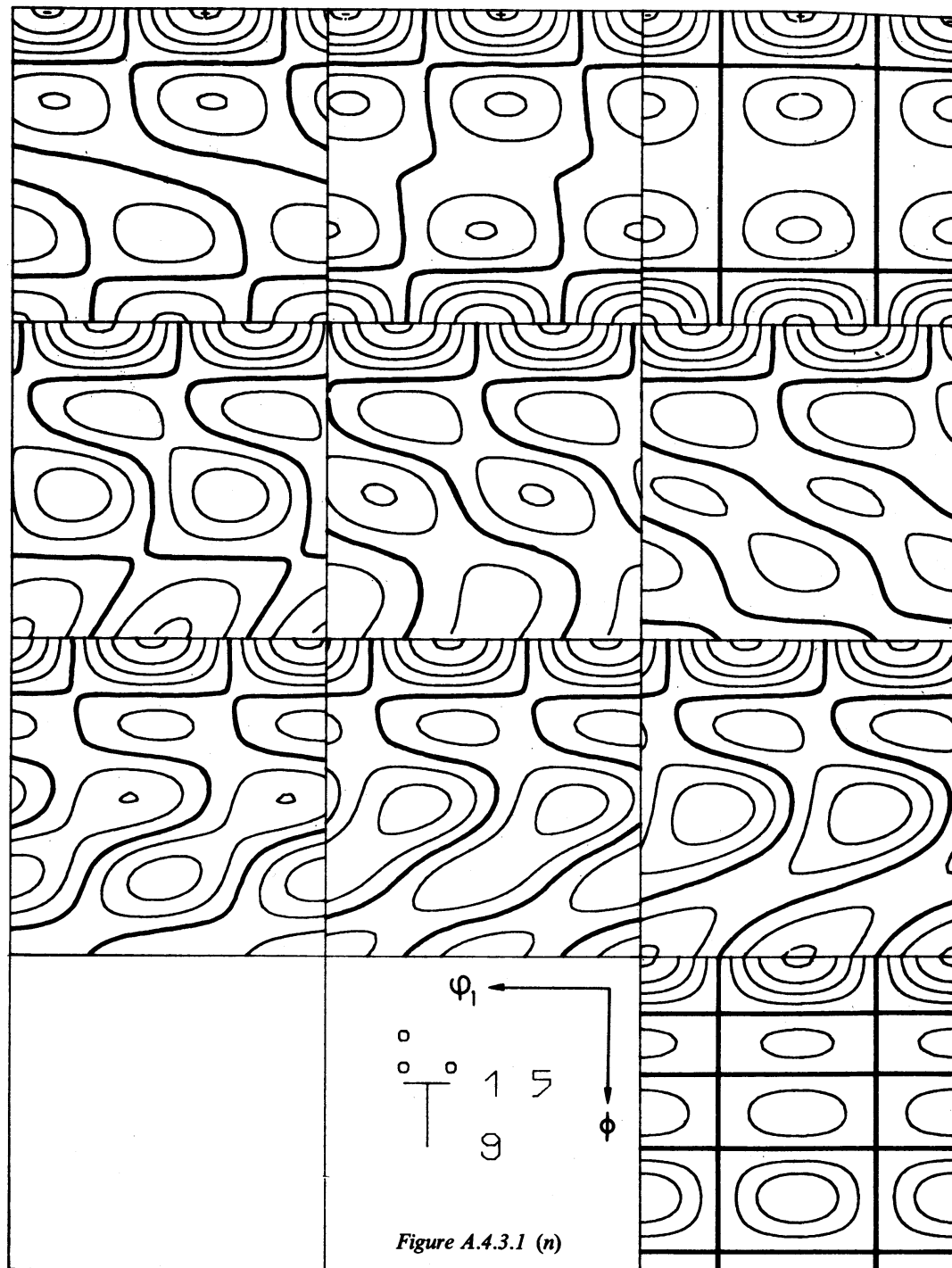


Figure A.4.3.1 (n)

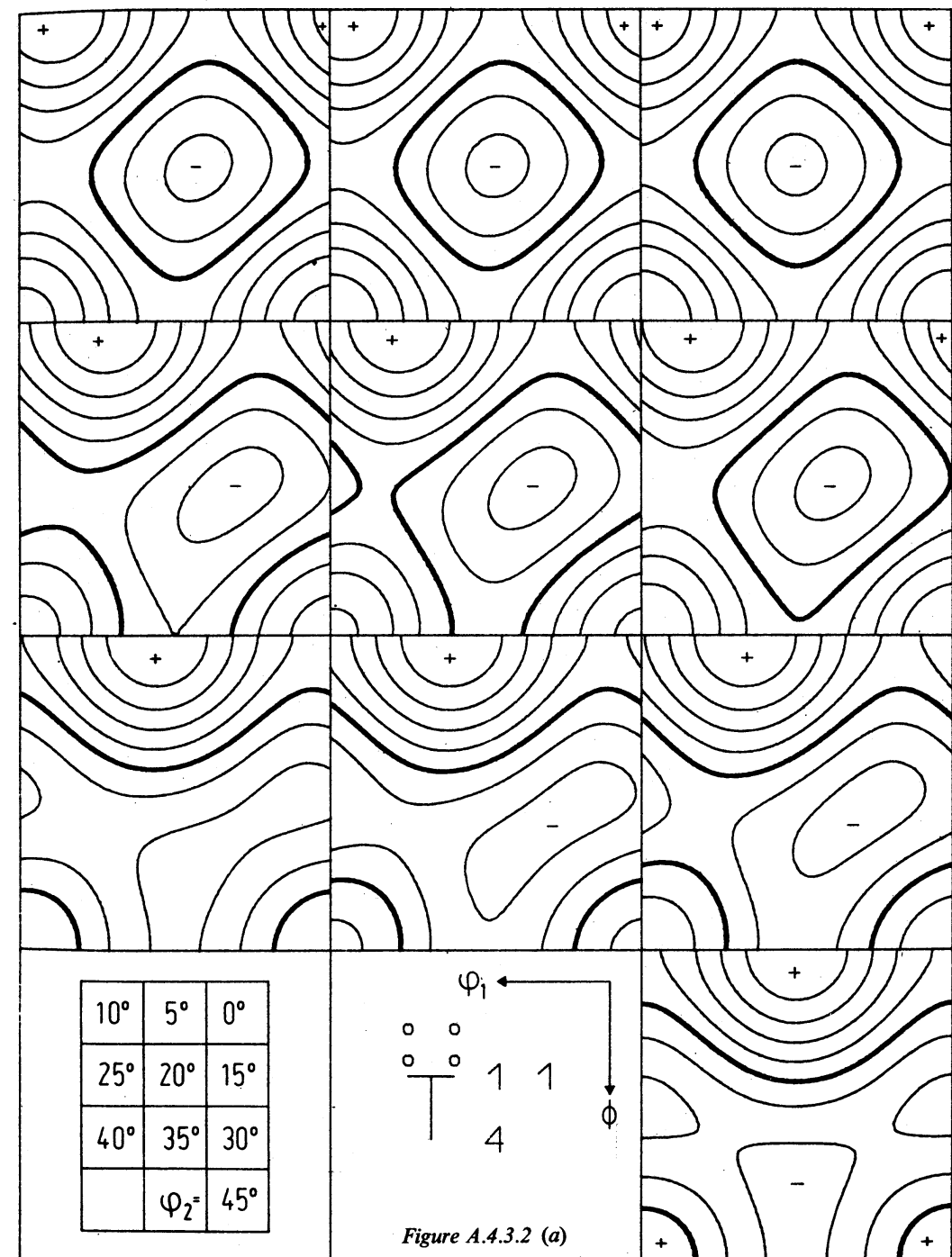


Figure A.4.3.2 (a)

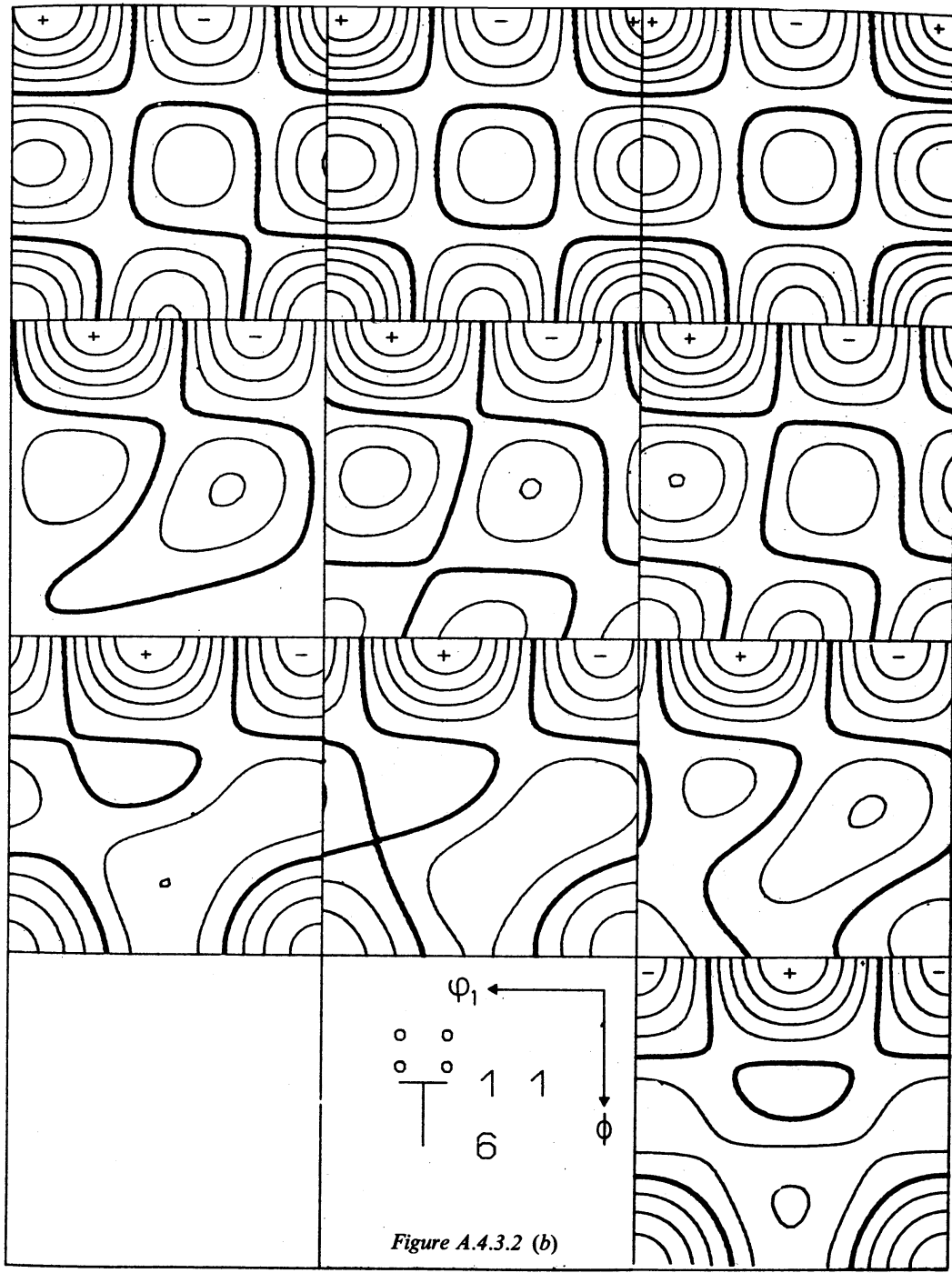
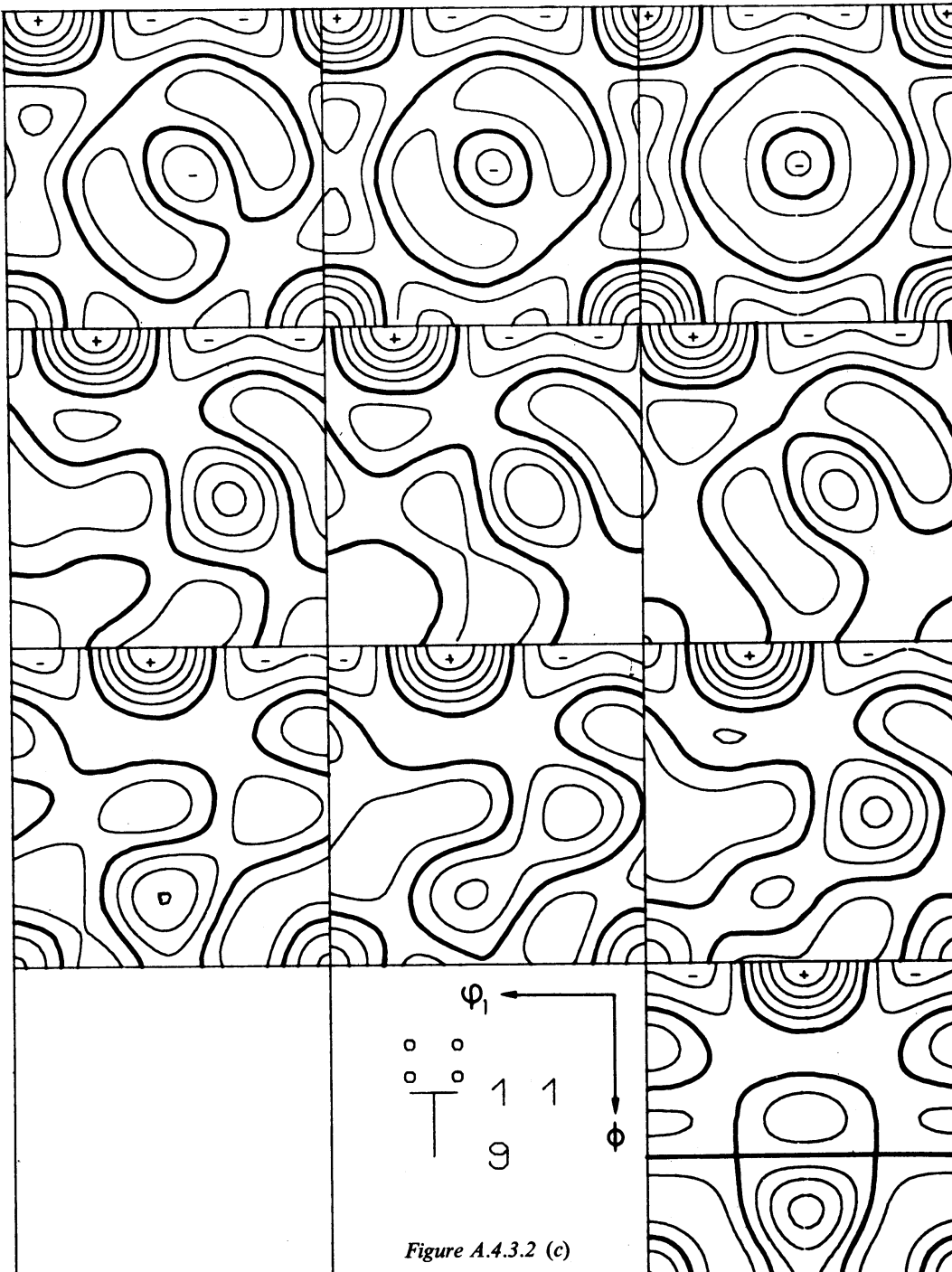


Figure A.4.3.2 (b)



INDEX

- Absolute value, *see* Amount of rotation
- Absorption correction, 194, 213, 426
- Accommodation factor, *see* Adaption factor
- Accuracy measure, 79, 130, 212, 257, 437
special, 80, 131
- Adaption, 82
- Adaption factor, 82, 424
- Addition theorem, 352, 357, 368
- Alloy, 227 (*see also* Brass; Iron-silicon alloy)
- Aluminium, 222, 245, 264, 268, 274
- Ambiguity of a rotation, 36
- Ambiguity of the solution, 90
- Amount of rotation, 36
- Analysis, 194 (*see also* TWODIM program)
- Angle, *see* BRAGG angle; EULER angles;
Reflection angle; Rotation angle
- Angular coordinates, *see* Coordinates
- Angular resolving power, 66, 183
- Anisotropy, 1, 294, 310, 315, 325, 326,
330, 337, 340, 344, 349
elastic, 327
magnetic, 308, 313, 344, 346, 350
plastic, 330
- Anisotropy constant, 308, 311, 320, 323
- Approximation condition, 138
HILL, 302, 326
REUSS, 302, 322
VOIGT, 322
- Approximation, polynomial, 183
- Austenite, 261
- Average coefficients, 303, 324, 328
- Average value, 308 (*see also* Mean value)
- Averaging, 229
- Axis distribution function, 52, 122
principal, 330
twofold, 378
- Axis of rotation, *see* Symmetry element
(*see also* Rotation axis)
- Back-reflection region, 86, 196, 424
- Back-rotation, *see* Inverse rotation
- BAIN relation, 190
- Basis, real, 356, 359
- Black-white symmetry, 107, 147
- Biaxial pole figure, 157
- Blending (of transmission and back-
reflection regions), *see* Adaption
- Body-centred cubic lattice, 67, 69, 240
- BRAGG angle, 63, 338
- BRAGG equation, 63, 338
- Brass, 284, 259
- Calculation time, 204
- CAPITE program, 198, 448
- Cartesian coordinate system, 3
- Character of representation, 355
- Central symmetry, *see* Centrosymmetry
- Centre of inversion, 100, 142 (*see also*
Symmetry centre)
- CLEBSCH-GORDAN coefficients, 299, 362
symmetric, 401
- Coefficient diagram, 345, 347
- Coefficients, *see* Average coefficients;
CLEBSCH-GORDAN coefficients;
FOURIER coefficients; LEGENDRE func-
tion; Multiplication coefficients; Sym-
metry coefficients; Transformation
coefficients (*see also* Angular distribu-
tion function; Inverse pole figure;
Orientation distribution function; Pole
figure)
- Coefficient space, 344
- COEF program, 197, 442
- Coincidence, 63
real, 64, 254
partial, 64, 250
- multiphase, 65

Computer program, 194, 439

Cone fibre texture, 173

Conferences (on textures, proceedings), 305

Conjugate complex quantity, 49, 352

Conjugate rotation, 36, 354

Contraction ratio, 330

Convex envelope, 344

Convolution integral, 373

Coordinates

Cartesian (rectangular), 3

spherical polar (angular), 16, 19

Coordinate system

crystal, 3, 100, 142, 288, 292

external, 307

intermediate, 53, 371

left-handed, 100, 142

right-handed, 1, 100, 142

sample, 1, 3, 283, 290

variable, 371

Corner, *see* Grain corner

Copper, 228, 325, 349

COREC program, 195, 440

Correction, 194, 440

Correlation, *see* Orientation correlation

Criterion, *see* Reliability criterion

Crystal, *see* Crystallite; Polycrystal;

Single crystal

left-handed, 102, 143

right-handed, 102, 143

Crystal coordinate system, 3, 100, 142, 288, 292

Crystal direction, 10, 39, 101, 142

Crystal energy, *see* Magnetization energy

Crystallite, 3, 42, 50, 227, 274, 279

Crystal number, 154, 212, 227, 274

Crystal orientation, 1, 3

Crystal structure analysis, 65, 80, 85, 131

Crystal surface, 279

Crystal surface, 279

Crystal symmetry, 36, 47, 61, 105, 111, 114, 120, 140, 146, 149, 340, 363, 376, 378, 393, 395, 401

Cube texture, 1

Cubic body-centred lattice, 67, 69, 240

Cubic face-centred lattice, 68, 69, 227, 258

Cubic polynomial, 390

Cubic spherical harmonics, 384, 390, 527, 531, 564

Cubic symmetry, 62, 67, 80, 91, 131, 141, 194, 213, 226, 240, 258, 263, 268, 274, 308, 316, 321, 332, 344, 384, 389, 390, 395, 403

Cut surface, 279

Cylindrical symmetry, *see* Rotational symmetry

Deformation

elastic, 321

plastic, 330

Deformation resistance, 331

Deformation tensor, 321, 330

Deformation texture, 227, 240, 244, 247, 250, 251, 263, 268, 272 (*see also* Drawing texture; Rolling texture)

Deformation work, 330

Degree

of harmonics, 351, 365

rolling, 228, 232, 235, 236, 238, 243

of series expansion, 47, 62

Density, *see* Orientation density

Determinants, functional, 33

Difference integral, 79

Diffracting power, 338 (*see also* Reflectivity)

Diffraction, *see* Neutron diffraction;

X-ray diffraction

Dimension of a texture, 178

Direction cosines, 19

Distance, *see* Orientation distance

Displacement vector, 333

Distribution

of the crystallographic planes, 280

Gaussian, 180, 277

of the grain boundaries, 281, 283, 288

of the grain edges, 290, 292

of the grain surfaces, 279

of the number, 42, 274

orientation, 42, 53, 122, 262

of the orientation differences, 282

random, 1, 49, 58, 91, 120, 123, 324

special, 169

of the structural elements, 279

Distribution function

angular, 73

axis, 53, 122

orientation, 42, 47, 208, 482

Dot for characterization of symmetry, 47, 363

Drawing texture, 268

Earing, 1

Edge, *see* Grain edge

Elastic anisotropy, 321

Elastic compliances, 321

Elastic constants, 321

Elasticity, 321

Elasticity tensor, 321

Electron diffraction, 155, 227

Element

of a group, 36

of the structure, 279

(*see also* Identity element; Orientation element; Symmetry element)

Elementary pole figures, 161

Energy dispersive method, 54

Envelope, *see* Convex envelope

Equal area projection, 35

Equal physical properties, 343

Error, 212 (*see also* Indetermination error;

Integration error; Mathematical error; Numerical error; Statistical error; Systematical error; Truncation error)

Error curve, 214, 217

Error integral, 182

Error measure, *see* Accuracy measure

EULER angles, 4

EULER space, 5, 8, 392

Even orders, 62, 104, 145

Example, *see* Numerical example

Expansion, *see* Series expansion; Thermal expansion

Experimental error, 215

Experimental pole figure, 79, 86, 130, 135, 219, 258, 424

Explicit representation, 387

External coordinate system, 307

Extrapolation, 83, 133, 222

Extremal procedure, 96

Face-centred cubic lattice, 68, 69, 227, 258

Factor, *see* Adaption factor; Matching factor; Phase factor; Structure factor; TAYLOR factor; Temperature factor

Ferrite, 261

Ferromagnetism, *see* Magnetic anisotropy; Magnetic remanence

Fibre axis, 176

Fibre texture, 119, 268, 310, 319, 344, 346 cone, 173

ring, 173

(*see also* Rotational symmetry)

Figures (of the functions), 560

Flow stress, 338

Foil, 45

FORTRAN, 195

FOURIER coefficients, 359, 456, 494, 498

FOURIER expansion, 359

FRIEDEL's law, 106, 146

Function values of the cubic-cubic generalized harmonics, 550, 555, 556

of the cubic-orthorhombic generalized harmonics, 533, 543

of the cubic-spherical harmonics, 527, 531

of the generalized LEGENDRE functions,

519

Functional determinant, 33

Fundamental equation

for fibre textures, 126

of texture analysis, 53

Fundamental integral, 371

FUNE program, 200, 449

Gaussian distribution, 180, 277

General axis distribution function, *see* Axis distribution function

Generalized LEGENDRE functions, 352, 519, 560

Generalized spherical harmonics, 351, 533, 543, 550, 555, 556

Germanium, 270

Glide system, 240

Gold, 270

Grain, *see* Crystallite

Grain boundary, 283

Grain boundary energy, 44

Grain boundary line, 283

Grain boundary surface, 283

Grain coarsening, continuous, 44

Grain corner, 290

Grain cut surface, 279

Grain edge, 290

Grain size, 42, 274
distribution, 42
Grain statistics, 213
Graphite, 180, 319
Ground cylinder, 287
Ground sphere, 285
Ground surface, 285, 287
Group, *see* Black-white symmetry;
Orthonormalization; Rotation group;
Space group; Subgroup; Symmetry
group
Growth rate, 45

HARRIS, method of, 77, 218
Hexagonal symmetry, 62, 251, 272, 314,
365, 379, 383, 395
High symmetry, 384
HILL approximation, 302, 326

Icosahedral symmetry, 384
Ideal orientation, 50, 60, 71, 121, 124, 169
Identity element, 36
Identity matrix, 354
Identity rotation, 36
IMHOF, method of, 167
Incomplete pole figure, 85, 135, 225
Indetermination error, 212, 225 (*see also*
Maximum resolving power)
Index, *see* Texture index
Individual orientation measurement, 50,
121, 227
Inhomogeneity of texture, 244
Instrumental symmetry, 297, 340
Integral, *see* Convolution integral; Difference
integral; Error integral; Funda-
mental integral
Integral relation, 76
Integration error, 222
Interchange relation, 354, 360, 363, 402
Intermediate coordinate system, 53, 371
Interpolation, 51, 54, 122
INVA program, 197, 446
Invariant measure, 31
INVE program, 200, 449
Inverse matrix, 17, 79, 130, 157, 163
Inverse pole figure, 15, 69, 71, 126, 197,
200, 207, 218, 270, 273, 432
Inverse rotation, 36, 354

Inversion centre, *see* Centre of inversion
Inversion formula, 118
Iron, 240, 261, 336, 350 (*see also* Steel)
Iron-silicon alloy, 266, 310, 312, 346
Irradiation, *see* Neutron irradiation
Isotropy, 1, 323, 345 (*see also* Quasi-isotropy; Random distribution)

JACOBI polynomials, 97, 352
JETTER, MCHARGUE and WILLIAMS,
method of, 157

KURDJUMOV-SACHS relation, 191, 555

LANKFORD parameter, *see* R-value
Lattice constant, 66
Lattice plane, 57, 63, 67, 250, 254
LAUE photograph, 50
Least-squares method, 78, 129
Left-handed coordinate system, 100, 142
Left-handed crystal, 102, 143
Left-handed symmetry, 48, 369 (*see also*
Crystal symmetry)
LEGENDRE function
associated, 356
normalized, 356
generalized, 352, 519, 560 (*see also*
JACOBI polynomials)
LEGENDRE polynomial, 357
LIBRARY program, 194, 200, 450
Light reflection, 342
Linear combination, 48, 63, 384
Line texture, 178
Listings of programs, 210, 439
Low index orientations, 23, 26
Low symmetry, 382

Magnesium, 254
Magnetic anisotropy, 308, 313, 344, 346, 350
Magnetic remanence, 313
Magnetization energy, 45, 308, 311
Magnetization, saturation, 308, 311, 313
Mainline program, 200, 449
Marble, 154
Matching factor, 82 (*see also* Accommodation
factor; Adaption factor)
Mathematical aids, 351
Mathematical error, 213

Matrix, *see* Identity matrix; Inverse matrix;
Orientation matrix
Matrix representation, 16, 351
Maximum resolving power, 66, 342
Mean value, 302 (*see also* Average value)
Measure, *see* Accuracy measure; Invariant
measure
Metastable phase, 270
Method
of HARRIS, 77, 218
of IMHOF, 167
of JETTER, MCHARGUE and WILLIAMS,
157
least squared errors, 78, 129
of PERLWITZ, LÜCKE and PITSCH, 154
of RUER and BARR, 161 (*see also* Vector
method)
MILLER indices, 15
Mirror plane, 380, 394
Monoclinic symmetry, 62, 365, 379, 395
Multiplication coefficients, 363, 402
Multiplicity of coincidences, 63

Negative values, 321
Neutron diffraction, 214, 229, 241, 245, 310
Neutron irradiation, 320
NISHIYAMA-WASSERMANN relation, 190,
261, 555
Non-negativity condition, 91, 116, 152
(*see also* Positivity condition)
Normal direction, 16
Normalization, 49, 58, 70, 97, 120, 123
(*see also* Orthonormalization; Pseudo-
normalization)
Normalization factor, 54, 58, 86, 135
Normalized associated LEGENDRE func-
tions, 356
Number of crystallites, 154, 212, 227, 274
Numerical error, 213
Numerical example, 205, 423
Numerical tables, 405, 455

Oblique section technique, 214
Octahedral symmetry, 385
Odd order, 104, 116, 145, 152, 365, 392
ODF, *see* Orientation distribution function
ODF program, 194, 423, 439
Order of a property, 340

Orientation, 1, 3
crystal, 1, 3
ideal, 50, 60, 71, 121, 124, 169
low-index, 23, 26
preferred, *see* Ideal orientation; *see under*
Texture
surface, 45, 279

Orientation correlation, 44
Orientation density, 42, 231, 269
Orientation difference, 44, 282
Orientation distance, 38
Orientation distribution, 42, 53, 122, 262
special, 169
Orientation distribution function, 42, 47,
208, 432
Orientation element, 42, 49
Orientation matrix, 16
Orientation parameter, 3, 19
Orientation path, 158
Orientation point, 7, 9, 13, 23, 38, 154,
162, 168
Orientation relation, 188 (*see also* BAIN
relation; KURDJUMOV-SACHS relation;
NISHIYAMA-WASSERMANN relation)
Orientation space, 7, 9, 13, 23, 154,
162, 166, 168, 210
cylindrical, 8, 9
Eulerian, 7, 392
spherical, 10
Orientation transformation, 188 (*see also*
Orientation relation)
Orientation transformation function, 188
Orientation tube, 179, 228
Orthogonality, *see* Orthonormalization
Orthonormalization, 352, 357, 358, 368
Orthorhombic symmetry, 62, 114, 140,
195, 205, 227, 247, 272, 328, 365,
379, 383, 389, 391, 395, 399

Parameter, *see* Orientation parameter
Path, *see* Orientation path
PERLWITZ, PITSCH and LÜCKE, method of, 154
Permutation of indices, 297
Phase factor, 356
Phase, metastable, 270
Phase transformation, 188
Physical meaning (of the coefficients), 348
Physical property, 294

Physical quantity, 295
 PING program, 200, 449
 Plane strain, 332
 Plastic anisotropy, 330
 Plotter deformation, 330 (*see also* Deformation textures)
 Plotter program, 194
 Point, *see* Orientation point
 Polar coordinates, *see* Coordinates
 Pole figure, 14, 57, 123, 206, 424
 biaxial, 157
 calculated, 79, 86, 130, 135, 219, 258, 428
 elementary, 161
 experimental, 79, 86, 130, 135, 219,
 258, 424
 generalized inverse, *see* Axis distribution function
 incomplete, 85, 135, 225
 inverse, 15, 69, 71, 126, 197, 200, 207,
 218, 270, 273, 432
 of the number, 275
 POLF program, 200, 449
 POLO program, 197, 443
 POLV program, 197, 444
 Polycrystal, 1
 structure of, 279
 Polyethylene, 250
 Polyethylene terephthalate, 274
 Polynomial (cubic), 390
 LEGENDRE, 357
 approximation, 183 (*see also* Interpolation; Truncation error)
 Position coordinates of the crystallites, 42
 Positivity condition, 91, 152, 161 (*see also* Non-negativity condition)
 Powder, 281
 Power losses, 312
 Power product, 390
 Preferred orientation, *see* Ideal orientation;
 see under Texture
 Principal axes, 330
 Proceedings of texture conferences, 405
 Program, 194, 439
 library, 194, 200, 450
 mainline, 200, 449
 plotter, 194
 supplementary, 204
 (*see also* Computer program)

Projection
 equal area, 35
 stereographic, 35
 two-dimensional, 71, 345
 Property
 physical, 294
 special, 308
 Property tensor, 295
 Proportion, 43, 171 (*see also* Volume fraction)
 Pseudonormalization, 88
 Pulse statistics, 213
 Quantity, physical, 295
 Quartz, 254
 Quasi-isotropy, 346 (*see also* Isotropy; Random distribution)
 Random comparative sample, 87, 128
 Random distribution, 1, 49, 58, 91, 120,
 123, 234
 Reciprocal pole figure, *see* Inverse pole figure
 Recrystallization, 188, 274
 Recursion relation, 354
 Refinement (method, procedure), 93, 274
 Reflection
 light, 342
 X-ray, 338
 Reflection angle, 63, 338
 Reflection condition, 338
 Reflection plane, *see* Mirror plane
 Reflection region, *see* Back-reflection region
 Reflectivity, 338
 Region, *see* Back-reflection region; Single crystal region; Texture region;
 Transmission region; Zero region
 Relation, *see* Fundamental equation;
 Integral relation; Interchange relation;
 Orientation relation
 Reliability criterion, 213
 Remanence, 313
 Representation
 explicit, 387
 irreducible, 351
 matrix, 16, 351
 of a physical property, 294
 of the rotation group, 352
 spatial, 26, 271, 397

stereoscopic, 154
 surface, 295, 303
 tensor, 295, 302
 Resolving power
 angular, 66, 183
 maximum, 66, 342
 REUSS approximation, 302, 322
 Right-handed coordinate system, 1, 100, 142
 Right-handed crystal, 102, 143
 Right-handed symmetry, 48, 363 (*see also* Sample symmetry)
 Ring fibre texture, 173
 Roe's terminology, 7, 97, 220, 248, 251,
 252, 259, 261, 262
 Rolling degree, 228, 232, 235, 236, 238, 243
 Rolling direction, 16
 Rolling texture, 227, 240, 247, 253, 264
 (*see also* Deformation texture)
 Rotation, 3
 amount of, 36
 conjugate, 36, 354
 identity, 36
 inverse, 36, 354
 Rotational symmetry, 39, 119, 169, 268, 305,
 315, 319, 320, 341, 344, 346, 365, 383
 (*see also* Cylindrical symmetry; Fibre axis; Fibre texture)
 Rotation angle, 8, 264
 Rotation axis, 8, 264
 Rotation group, 36
 RVER and BARO, method of, 161
 R-value, 336 (*see also* LANKFORD parameter; Strain ratio)
 Sample coordinate system, 1, 3, 283, 290
 Sample direction, 10, 40, 101
 Sample, random, 87, 128
 Sample symmetry, 48, 363, 393 (*see also* Right-hand symmetry)
 Saturation magnetization, 308, 311, 313
 Selection rule, 382
 Series development, *see* Series expansion
 Series expansion, 47, 119
 SETS program, 198, 448
 Sharpness measure, *see* Texture index
 Shear spinning, 325
 Sheet symmetry, *see* Orthorhombic symmetry
 grain, 213
 pulse, 213

Steel, 241, 261, 337, 350
(see also Iron)
 Stereographic projection, 35
 Stereoscopic representation, 154
 Storage, 204
 Strain, plane, 332
 Strain ratio, 336 (*see also LANKFORD parameter; R-value*)
 Stress tensor, 321
 Structure analysis, *see Crystal structure analysis*
 of a polycrystal, 279
 Structure analysis factor, 64, 255
 Sub-group, 386
 Sub-routine, 195, 440
 Supplementary programs, 204
 Surface, 45, 279
 cut, 279
 grain boundary, 283
 ground, 285, 287
 Surface normal, 45, 279
 Surface orientation, 45, 279
 Surface representation, 295, 303
 Surface tension (in the grain boundary), 45
 Surface texture, 178
 Surveys on textures, 305
 Symmetric CLEBSCH—GORDAN coefficients, 407
 Symmetric generalized spherical harmonics, 363, 533
 Symmetric spherical harmonics, 376, 527
 Symmetry
 axial, *see Rotational symmetry*
 black—white, 107, 147
 central, 100, 142
 crystal, 36, 47, 61, 105, 111, 114, 120, 140, 146, 149, 340, 363, 376, 378, 393, 395, 401 (*see also Left-handed symmetry*)
 cubic, 62, 67, 80, 91, 131, 141, 194, 213, 226, 240, 258, 263, 268, 274, 308, 321, 332, 344, 384, 389, 390, 395, 403
 cylindrical, *see Rotational symmetry*
 hexagonal, 62, 251, 272, 314, 365, 379, 383, 395
 high, 384

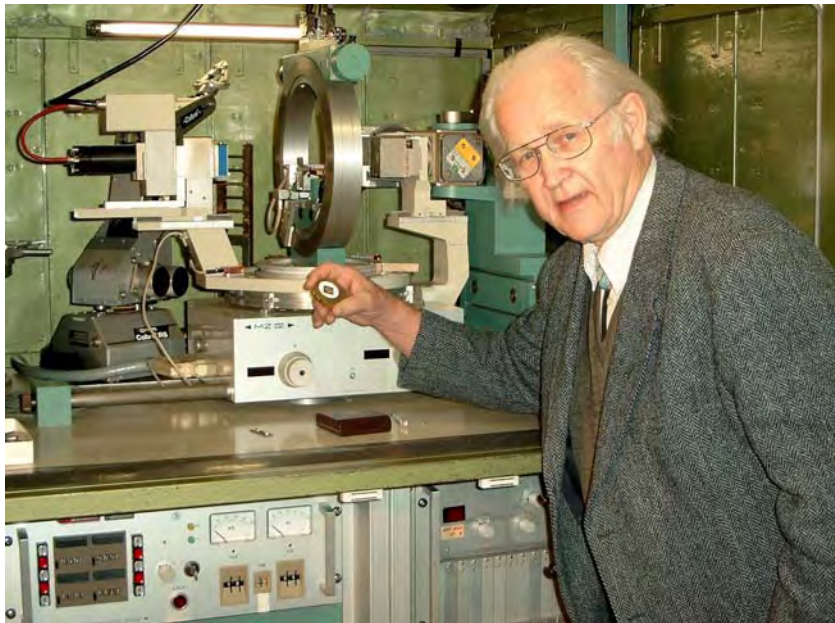
icosahedral, 384
 instrumental, 297, 340
 left-handed, 48, 369 (*see also Crystal symmetry*)
 low, 382
 monoclinic, 62, 365, 379, 395
 octahedral, 385
 orthorhombic, 62, 114, 195, 205, 227, 247, 272, 328, 365, 379, 383, 389, 391, 395, 399
 right-handed, 48, 363 (*see also Sample symmetry*)
 rotational, 39, 119, 169, 268, 305, 315, 319, 320, 341, 344, 346, 365, 383
 sample, 48, 363, 393
 sheet, *see Orthorhombic symmetry*
 spherical, *see Random distribution*
 tetragonal, 62, 365, 379, 383
 tetrahedral, 385
 triclinic, 62, 274, 365
 trigonal, 62, 254, 365
 Symmetry centre, 100, 142
 Symmetry coefficients, 48, 363, 383, 501, 505, 509, 515
 Synthesis, 194
 Systematical error, 215
 Tables (*see Numerical tables*)
 TAYLOR factor, 332
 TAYLOR factor coefficient, 334
 TAYLOR factor curve, 336
 TAYLOR theory, 239, 332
 TAYLOR wire, 270
 Temperature factor, 85, 133
 Tensor, 295, 303
 fourth-order, 328
 second-order, 316
 (*see also Deformation tensor; Elasticity tensor; Property tensor; Texture tensor*)
 Tensor representation, 295, 302
 Tetragonal symmetry, 62, 365, 379, 383
 Tetrahedral symmetry, 385
 Texture
 cone fibre, 173
 deformation 227, 240, 244, 247, 250, 251, 263, 268, 272 (*see also Drawing texture; Rolling texture*)

fibre (wire), 119, 268, 310, 319, 344, 346
 general, 47, 226
 line, 178
 recrystallization, 188, 274
 ring fibre, 173
 rolling, 227, 240, 247, 251, 263 (*see also Deformation texture*)
 rotationally symmetric, *see Fibre texture*
 sheet, 47, 226
 spherical, 176
 surface, 178
 wire, *see Fibre texture*
 Texture conferences (proceedings), 305
 Texture index, 88, 137
 Texture region, 345
 Texture tensor, 326
 Texture transformation, 188, 258, 270
 Thermal expansion, 319
 Three-dimensional orientation distribution function, *see Orientation distribution function*
 Time of calculation, 204
 Titanium, 251, 271
 Torque curve, 310
 Transformation, *see Orientation transformation; Phase transformation; Texture transformation*
 Transformation coefficients, 298, 369
 Transformation texture, 188, 258, 270
 Transmission region, 86, 196, 424
 Triclinic symmetry, 62, 274, 365
 Trigonal symmetry, 62, 254, 365
 Truncation error, 82, 132, 221
 Truncation undulations, 186
 Tube, 244 (*see also Orientation tube*)
 Twinning (mechanical), 236

TWODIM program, 197, 440
 Two-dimensional projection, 71, 345
 Unit element, 36
 Unit vector, 17
 UNKC program, 197, 445
 Uranium, 247, 320
 Value, *see Amount of rotation; Mean value; Negative value*
 Variable coordinate system, 371
 Vector method, 161 (*see also RUER and BARO, method of*)
 VOIGT approximation, 322
 Volume fraction, 43, 171 (*see also Proportion*)
 Volume fraction function, 183
 WASSERMANN limit, 235
 WASSERMANN theory, 236
 Weight factor, 52, 55, 60, 63, 71, 78, 86, 122, 125, 128, 129, 135
 Wire, 268
 TAYLOR, 270
 Wire texture, *see Fibre texture*
 X-DATA program, 198, 448
 X-ray beam, 338
 X-ray diffraction, 338
 X-ray reflection, 338
 YOUNG's modulus, 297, 325, 348, 350
 (*see also Elasticity*)
 Zero range, 116, 152 (*see also Zero region*)
 Zero region, 179

Hans Joachim Bunge

(1929 – 2004)



Hans Joachim Bunge demonstrating a specimen at the ATEMA texture goniometer.

Hans Joachim Bunge was born on July 29, 1929, in Zerbst, a small town situated between Magdeburg and Dessau in East Germany. After having finished high-school in 1946, he was a precision mechanic apprentice. In 1947 he enrolled at the Martin-Luther-University at Halle as a student of physics. In 1955 he received the Dr. rer. nat. degree from the same university for his Ph. D. Thesis "Magnetic Anisotropy of Cold Rolled Iron-Nickel Alloys". From then on his scientific interests have been centered on crystal texture. In 1964 he was awarded his Dr. habil. degree from the Humboldt University of Berlin for the Habilitation Thesis "On the Representation of Textures".

Hans Joachim Bunge was research scientist at the Physics Department of the University of Traffic, Dresden, from 1953 to 1955 where he investigated hard magnetic materials. From 1955 to 1968 followed a fruitful period of scientific work at the Institute of Crystal Structure Research of the (East) German Academy of Sciences in Berlin, tackling polycrystal X-ray diffraction, texture analysis and technological applications. In 1968 he returned to Dresden to the Central Institute of Solid State Physics and Materials Research of the German Academy of Sciences, where he was engaged in texture analysis and neutron diffraction. His promising career as a scientist in East Germany came to an abrupt halt when he and his family tried, in vain, to

escape from ideological persecution. They were imprisoned and kept apart from each other from 1974 to 1975 until they were finally allowed to leave East Germany. From 1975 to 1976 he was DFG fellow (German Research Foundation) at Clausthal-Zellerfeld University of Technology and at University of California Berkeley. In 1976 he succeeded Prof. Dr. Günther Wassermann as Professor and Head of the Institute of Physical Metallurgy of the Clausthal University of Technology. From 1989 to 1991 he was Dean of the Department of Metallurgy and Materials Science of this university.

After his retirement in 1997 he found a supportive new scientific home at the Institute of Physics and Physical Technology of the Clausthal University of Technology. Until his last days he supervised, with great enthusiasm, a research project at the HASYLAB facilities in Hamburg, financially supported by the German Research Foundation (DFG), on texture analysis with hard synchrotron radiation.

Hans Joachim Bunge has achieved an outstanding scientific work. In 1965 he managed to solve, independently of R. J. Roe, one of the greatest challenges of quantitative texture research – the pole figure inversion – by developing the harmonic series expansion method. In 1969 he published the basic treatise on mathematical methods of pole figure inversion "Mathematische Methoden der Texturanalyse". The extended and revised English edition of this book was published in 1982 under the title "Texture Analysis in Materials Science – Mathematical Methods". It is still considered the comprehensive standard handbook in this field of materials science. He is the author or editor of 10 more books on quantitative texture analysis and on anisotropic materials properties. He has published more than 460 contributions to scientific journals and conference proceedings. From 1986 to 2003 Hans Joachim Bunge was the editor of the journal "Textures and Microstructures". Since 1978 he was a member of the International Committee of the International Conference of Textures and Anisotropy (ICOTOM). From 1985 to 2004 he was speaker of the Special Committee for Textures of the German Society of Materials (FA Texturen der DGM).

In recognition of his scientific achievements in materials science, Hans Joachim Bunge received a number of honors. He was awarded, for instance, the degree of a Doctor Honorary of the University of Metz (France) in 1979, the degree of a Professor Honorary of the Beijing Polytechnic University (China) in 1993, the Honorary Membership of the Czech Metal Science Society in 1995, and the Honorary Membership of the Texture Society of India in 2000. In 2003, he received the Carl-Hermann Medal of the German Society for Crystallography.

Hans Joachim Bunge died on November 28, 2004, at the age of 75 years from a brain stroke. He is survived by his wife Helga and his son Hans-Peter. He was a mild-mannered man of a uniformly cheerful and gentle disposition. His life was committed to science. Even in the course of his numerous activities he always had time for students and his colleagues. He still had many plans for the future, both at work and personal.

Robert A. Schwarzer